frontiers | Research Topics

Immune response to SARS-CoV-2 and implications for clinical outcome

Edited by
Edwin Bölke, Martijn van Griensven, E. Marion Schneider and Torsten Feldt

Published in
Frontiers in Immunology

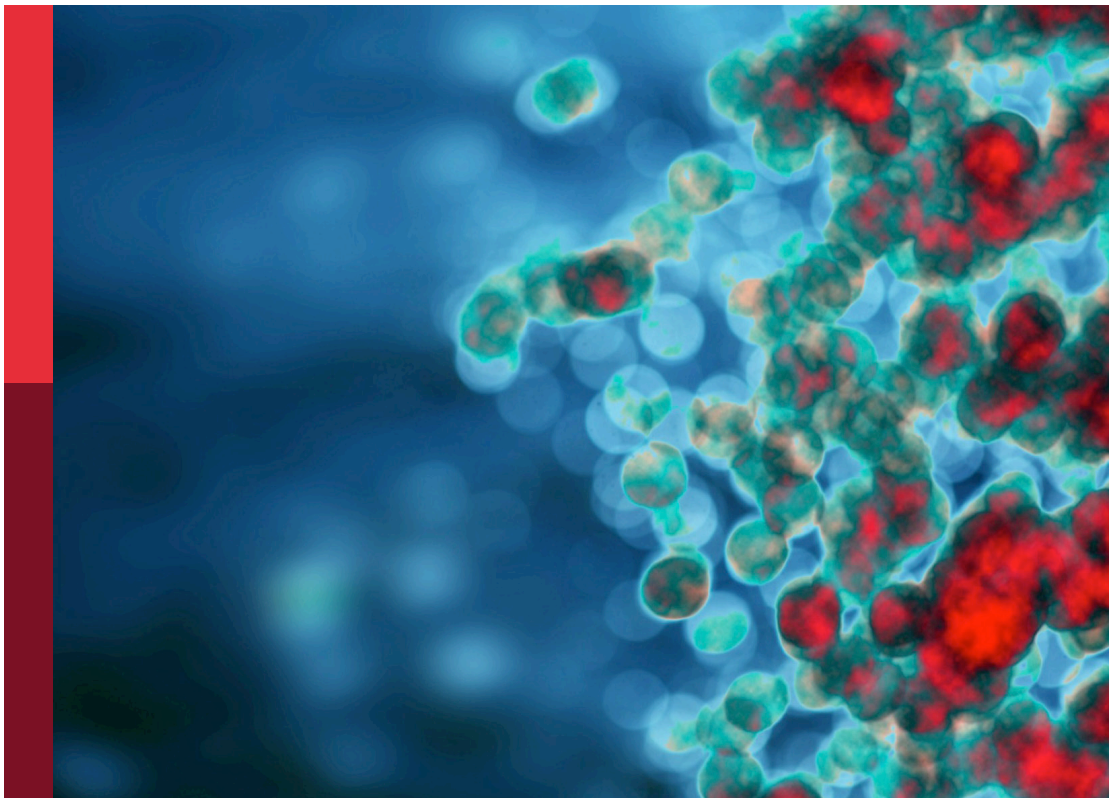

FRONTIERS EBOOK COPYRIGHT STATEMENT

The copyright in the text of individual articles in this ebook is the property of their respective authors or their respective institutions or funders. The copyright in graphics and images within each article may be subject to copyright of other parties. In both cases this is subject to a license granted to Frontiers.

The compilation of articles constituting this ebook is the property of Frontiers.

Each article within this ebook, and the ebook itself, are published under the most recent version of the Creative Commons CC-BY licence. The version current at the date of publication of this ebook is CC-BY 4.0. If the CC-BY licence is updated, the licence granted by Frontiers is automatically updated to the new version.

When exercising any right under the CC-BY licence, Frontiers must be attributed as the original publisher of the article or ebook, as applicable.

Authors have the responsibility of ensuring that any graphics or other materials which are the property of others may be included in the CC-BY licence, but this should be checked before relying on the CC-BY licence to reproduce those materials. Any copyright notices relating to those materials must be complied with.

Copyright and source acknowledgement notices may not be removed and must be displayed in any copy, derivative work or partial copy which includes the elements in question.

All copyright, and all rights therein, are protected by national and international copyright laws. The above represents a summary only. For further information please read Frontiers' Conditions for Website Use and Copyright Statement, and the applicable CC-BY licence.

ISSN 1664-8714
ISBN 978-2-8325-3073-3
DOI 10.3389/978-2-8325-3073-3

About Frontiers

Frontiers is more than just an open access publisher of scholarly articles: it is a pioneering approach to the world of academia, radically improving the way scholarly research is managed. The grand vision of Frontiers is a world where all people have an equal opportunity to seek, share and generate knowledge. Frontiers provides immediate and permanent online open access to all its publications, but this alone is not enough to realize our grand goals.

Frontiers journal series

The Frontiers journal series is a multi-tier and interdisciplinary set of open-access, online journals, promising a paradigm shift from the current review, selection and dissemination processes in academic publishing. All Frontiers journals are driven by researchers for researchers; therefore, they constitute a service to the scholarly community. At the same time, the *Frontiers journal series* operates on a revolutionary invention, the tiered publishing system, initially addressing specific communities of scholars, and gradually climbing up to broader public understanding, thus serving the interests of the lay society, too.

Dedication to quality

Each Frontiers article is a landmark of the highest quality, thanks to genuinely collaborative interactions between authors and review editors, who include some of the world's best academicians. Research must be certified by peers before entering a stream of knowledge that may eventually reach the public - and shape society; therefore, Frontiers only applies the most rigorous and unbiased reviews. Frontiers revolutionizes research publishing by freely delivering the most outstanding research, evaluated with no bias from both the academic and social point of view. By applying the most advanced information technologies, Frontiers is catapulting scholarly publishing into a new generation.

What are Frontiers Research Topics?

Frontiers Research Topics are very popular trademarks of the *Frontiers journals series*: they are collections of at least ten articles, all centered on a particular subject. With their unique mix of varied contributions from Original Research to Review Articles, Frontiers Research Topics unify the most influential researchers, the latest key findings and historical advances in a hot research area.

Find out more on how to host your own Frontiers Research Topic or contribute to one as an author by contacting the Frontiers editorial office: frontiersin.org/about/contact

Immune response to SARS-CoV-2 and implications for clinical outcome

Topic editors

Edwin Bölke — Heinrich Heine University of Düsseldorf, Germany
Martijn van Griensven — Maastricht University, Netherlands
E. Marion Schneider — University of Ulm, Germany
Torsten Feldt — University Hospital of Düsseldorf, Germany

Citation

Bölke, E., van Griensven, M., Schneider, E. M., Feldt, T., eds. (2023). *Immune response to SARS-CoV-2 and implications for clinical outcome*. Lausanne: Frontiers Media SA. doi: 10.3389/978-2-8325-3073-3

Table of contents

08 Editorial: Immune response to SARS-CoV-2 and implications for clinical outcome
Edwin Bölke, Martijn van Griensven, E. Marion Schneider, Johannes C. Fischer, Torsten Feldt, Verena Keitel, Wilfried Budach, Jan Haussmann, Danny Jazmati and Christiane Matuschek

11 Serum soluble Fas ligand is a severity and mortality prognostic marker for COVID-19 patients
Kiarash Saleki, Moein Shirzad, Mostafa Javanian, Sheyda Mohammadkhani, Mohammad Hossein Alijani, Niloufarsadat Miri, Morteza Oladnabi and Abbas Azadmehr

31 Serial infection with SARS-CoV-2 Omicron BA.1 and BA.2 following three-dose COVID-19 vaccination
Hope R. Lapointe, Francis Mwimanzi, Peter K. Cheung, Yurou Sang, Fatima Yaseen, Rebecca Kalikawe, Sneha Datwani, Rachel Waterworth, Gisele Umviligihozo, Siobhan Ennis, Landon Young, Winnie Dong, Don Kirkby, Laura Burns, Victor Leung, Daniel T. Holmes, Mari L. DeMarco, Janet Simons, Nancy Matic, Julio S.G. Montaner, Chanson J. Brumme, Natalie Prystajecky, Masahiro Niikura, Christopher F. Lowe, Marc G. Romney, Mark A. Brockman and Zabrina L. Brumme

41 COVID-19 patients exhibit unique transcriptional signatures indicative of disease severity
Andrea R. Daamen, Prathyusha Bachali, Catherine A. Bonham, Lindsay Somerville, Jeffrey M. Sturek, Amrie C. Grammer, Alexandra Kadl and Peter E. Lipsky

57 Prospects of animal models and their application in studies on adaptive immunity to SARS-CoV-2
Xiaohui Wei, Na Rong and Jiangning Liu

75 Potential of conserved antigenic sites in development of universal SARS-like coronavirus vaccines
Siling Wang, Dinghui Wu, Hualong Xiong, Juan Wang, Zimin Tang, Zihao Chen, Yizhen Wang, Yali Zhang, Dong Ying, Xue Lin, Chang Liu, Shaoqi Guo, Weikun Tian, Yajie Lin, Xiaoping Zhang, Quan Yuan, Hai Yu, Tianying Zhang, Zizheng Zheng and Ningshao Xia

91 Blood gene expression predicts intensive care unit admission in hospitalised patients with COVID-19
Rebekah Penrice-Randal, Xiaofeng Dong, Andrew George Shapanis, Aaron Gardner, Nicholas Harding, Jelmer Legebeke, Jenny Lord, Andres F. Vallejo, Stephen Poole, Nathan J. Brendish, Catherine Hartley, Anthony P. Williams, Gabrielle Wheway, Marta E. Polak, Fabio Strazzeri, James P. R. Schofield, Paul J. Skipp, Julian A. Hiscox, Tristan W. Clark and Diana Baralle

105 Kynurenine serves as useful biomarker in acute, Long- and Post-COVID-19 diagnostics
Daniel Alexander Bizjak, Manfred Stangl, Nikolaus Börner, Florian Bösch, Joachim Durner, Gergana Drunin, Jasmine-Leonike Buhl and Dietmar Abendroth

116 Lymphocyte–C-reactive protein ratio can differentiate disease severity of COVID-19 patients and serve as an assistant screening tool for hospital and ICU admission
Jian-Nan Zhang, Yang Gao, Xin-Tong Wang, Na-Na Li, Xue Du, Yu-Jia Tang, Qi-Qi Lai, Peng-Fei Chen, Chuang-Shi Yue, Ji-Han Wu, Kai Kang and Ming-Yan Zhao

127 Severity of SARS-CoV-2 infection is associated with high numbers of alveolar mast cells and their degranulation
Olga Krysko, Joshua H. Bourne, Elena Kondakova, Elena A. Galova, Katharine Whitworth, Maddy L. Newby, Claus Bachert, Harriet Hill, Max Crispin, Zania Stamataki, Adam F. Cunningham, Matthew Pugh, Abdullah O. Khan, Julie Rayes, Maria Vedunova, Dmitri V. Krysko and Alexander Brill

140 Low baseline IFN-γ response could predict hospitalization in COVID-19 patients
Marion Cremoni, Jonathan Allouche, Daisy Graça, Kevin Zorzi, Céline Fernandez, Maxime Teisseyre, Sylvia Benzaken, Caroline Ruetsch-Chelli, Vincent L. M. Esnault, Jean Dellamonica, Michel Carles, Jérôme Barrière, Michel Ticchioni, Vesna Brglez and Barbara Seitz-Polski

152 Maternal and neonatal immune response to SARS-CoV-2, IgG transplacental transfer and cytokine profile
Rocío Rubio, Ruth Aguilar, Mariona Bustamante, Erica Muñoz, Miquel Vázquez-Santiago, Rebeca Santano, Marta Vidal, Natalia Rodrigo Melero, Daniel Parras, Pau Serra, Pere Santamaria, Carlo Carolis, Luis Izquierdo, Maria Dolores Gómez-Roig, Carlota Dobaño, Gemma Moncunill and Edurne Mazarico

167 Phosphate and IL-10 concentration as predictors of long-covid in hemodialysis patients: A Brazilian study
Hugo L. Corrêa, Lysleine A. Deus, Thaís B. Araújo, Andrea L. Reis, Carlos E. N. Amorim, André B. Gadelha, Rafael L. Santos, Fernando S. Honorato, Daisy Motta-Santos, Carmen Tzanno-Martins, Rodrigo V. P. Neves and Thiago S. Rosa

176 Long-term cellular immune response in immunocompromised unvaccinated COVID-19 patients undergoing monoclonal antibody treatment
Laura Thümmler, Margarethe Konik, Monika Lindemann, Neslinur Fisenkci, Michael Koldehoff, Anja Gäckler, Peter A. Horn, Fotis Theodoropoulos, Christian Taube, Markus Zettler, Olympia Evdoxia Anastasiou, Peer Braß, Sarah Jansen, Oliver Witzke, Hana Rohn and Adalbert Krawczyk

183 Increased prevalence of clonal hematopoiesis of indeterminate potential in hospitalized patients with COVID-19
Judith Schenz, Katharina Rump, Benedikt Hermann Siegler, Inga Hemmerling, Tim Rahmel, Jan N. Thon, Hartmuth Nowak, Dania Fischer, Anna Hafner, Lucas Tichy, Katharina Bomans, Manja Meggendorfer, Björn Koos, Thilo von Groote, Alexander Zarbock, Mascha O. Fiedler, Johanna Zemva, Jan Larmann, Uta Merle, Michael Adamzik, Carsten Müller-Tidow, Torsten Haferlach, Florian Leuschner and Markus A. Weigand

198 MUC22, HLA-A, and HLA-DOB variants and COVID-19 in resilient super-agers from Brazil
Erick C. Castelli, Mateus V. de Castro, Michel S. Naslavsky, Marilia O. Scliar, Nayane S. B. Silva, Raphaela N. Pereira, Viviane A. O. Ciriaco, Camila F. B. Castro, Celso T. Mendes-Junior, Etiele de S. Silveira, Iuri M. de Oliveira, Eduardo C. Antonio, Gustavo F. Vieira, Diogo Meyer, Kelly Nunes, Larissa R. B. Matos, Monize V. R. Silva, Jaqueline Y. T. Wang, Joyce Esposito, Vivian R. Cória, Jhosiene Y. Magawa, Keity S. Santos, Edecio Cunha-Neto, Jorge Kalil, Raul H. Bortolin, Mário Hiroyuki Hirata, Luiz P. Dell'Aquila, Alvaro Razuk-Filho, Pedro B. Batista-Júnior, Amaro N. Duarte-Neto, Marisa Dolhnikoff, Paulo H. N. Saldiva, Maria Rita Passos-Bueno and Mayana Zatz

213 Differential activation of human neutrophils by SARS-CoV-2 variants of concern
Samuel Lebourgeois, Ambroise David, Houssem Redha Chenane, Vanessa Granger, Reyene Menidjel, Nadhira Fidouh, Benoît Noël, Olivier Delelis, Clémence Richetta, Charlotte Charpentier, Sylvie Chollet-Martin, Diane Descamps, Benoit Visseaux and Luc de Chaisemartin

222 Differential effects of age, sex and dexamethasone therapy on ACE2/TMPRSS2 expression and susceptibility to SARS-CoV-2 infection
Shima Shahbaz, Olaide Oyegbami, Suguru Saito, Mohammed Osman, Wendy Sligl and Shokrollah Elahi

237 Development and evaluation of low-volume tests to detect and characterize antibodies to SARS-CoV-2
Alice Halliday, Anna E. Long, Holly E. Baum, Amy C. Thomas, Kathryn L. Shelley, Elizabeth Oliver, Kapil Gupta, Ore Francis, Maia Kavanagh Williamson, Natalie Di Bartolo, Matthew J. Randell, Yassin Ben-Khoud, Ilana Kelland, Georgina Mortimer, Olivia Ball, Charlie Plumptre, Kyla Chandler, Ulrike Obst, Massimiliano Secchi, Lorenzo Piemonti, Vito Lampasona, Joyce Smith, Michaela Gregorova, Lea Knezevic, Jane Metz, Rachael Barr, Begonia Morales-Aza, Jennifer Oliver, Lucy Collingwood, Benjamin Hitchings, Susan Ring, Linda Wooldridge, Laura Rivino, Nicholas Timpson, Jorgen McKernon, Peter Muir, Fergus Hamilton, David Arnold, Derek N. Woolfson, Anu Goenka, Andrew D. Davidson, Ashley M. Toye, Imre Berger, Mick Bailey, Kathleen M. Gillespie, Alistair J. K. Williams and Adam Finn

257 Innate and adaptive immune response in SARS-CoV-2 infection-Current perspectives
Qiugang Zhu, Yan Xu, Ting Wang and Feiting Xie

272 Single-cell multiomics revealed the dynamics of antigen presentation, immune response and T cell activation in the COVID-19 positive and recovered individuals
Partha Chattopadhyay, Kriti Khare, Manish Kumar, Pallavi Mishra, Alok Anand, Ranjeet Maurya, Rohit Gupta, Shweta Sahni, Ayushi Gupta, Saruchi Wadhwa, Aanchal Yadav, Priti Devi, Kishore Tardalkar, Meghnad Joshi, Tavpritesh Sethi and Rajesh Pandey

290 Determinants of long COVID among adults hospitalized for SARS-CoV-2 infection: A prospective cohort study
Mattia Bellan, Daria Apostolo, Alice Albè, Martina Crevola, Nicolò Errica, Giacomo Ratano, Stelvio Tonello, Rosalba Minisini, Davide D'Onghia, Alessio Baricich, Filippo Patrucco, Patrizia Zeppegno, Carla Gramaglia, Piero Emilio Balbo, Giuseppe Cappellano, Sara Casella, Annalisa Chiocchetti, Elisa Clivati, Mara Giordano, Marcello Manfredi, Giuseppe Patti, David James Pinato, Chiara Puricelli, Davide Raineri, Roberta Rolla, Pier Paolo Sainaghi, Mario Pirisi and the No-More COVID study group

302 Distinct systemic immune networks define severe *vs*. mild COVID-19 in hematologic and solid cancer patients
Flávio Pignataro-Oshiro, Amanda B. Figueiredo, Nayane A. L. Galdino, Katia L. P. Morais, Walderez O. Dutra, Bianca Grassi de Miranda Silva, Diego Feriani, Flávia de Azevedo Abrantes, Ivan Leonardo Avelino França e Silva, Jayr Schmidt Filho, Juliana Valéria de Souza Framil, Marcelle Goldner Cesca, Rachel Simões Pimenta Riechelmann, Marjorie V. Batista and Kenneth J. Gollob

321 Analysis of neutralizing antibodies to COVID-19 inactivated or subunit recombinant vaccines in hospitalized patients with liver dysfunction
Hu Li, Shiyin Li, Pan Xu, Xiaohao Wang, Huan Deng, Yu Lei and Shan Zhong

328 Immune responses in mildly versus critically ill COVID-19 patients
Hamid Nasrollahi, Atefe Ghamar Talepoor, Zahra Saleh, Mahsa Eshkevar Vakili, Paria Heydarinezhad, Narges Karami, Maryam Noroozi, Seppo Meri and Kurosh Kalantar

346 Predictors for reactogenicity and humoral immunity to SARS-CoV-2 following infection and mRNA vaccination: A regularized, mixed-effects modelling approach
Erin C. Williams, Alexander Kizhner, Valerie S. Stark, Aria Nawab, Daniel D. Muniz, Felipe Echeverri Tribin, Juan Manuel Carreño, Dominika Bielak, Gagandeep Singh, Michael E. Hoffer, Florian Krammer, Suresh Pallikkuth and Savita Pahwa

356 SARS-COV-2 viroporins activate the NLRP3-inflammasome by the mitochondrial permeability transition pore
Joseph W. Guarnieri, Alessia Angelin, Deborah G. Murdock, Patrick Schaefer, Prasanth Portluri, Timothy Lie, Jessica Huang and Douglas C. Wallace

367 Differential regulatory T cell signature after recovery from mild COVID-19
Pedro Henrique de Sousa Palmeira, Rephany Fonseca Peixoto, Bárbara Guimarães Csordas, Isac Almeida de Medeiros, Fátima de Lourdes Assunção Araújo de Azevedo, Robson Cavalcante Veras, Daniele Idalino Janebro, Ian P.G. Amaral and Tatjana Souza Lima Keesen

384 Architecture of the SARS-CoV-2-specific T cell repertoire
Ksenia V. Zornikova, Saveliy A. Sheetikov, Alexander Yu Rusinov, Rustam N. Iskhakov and Apollinariya V. Bogolyubova

393 Abnormal thrombosis and neutrophil activation increase hospital-acquired sacral pressure injuries and morbidity in COVID-19 patients
Jatin Narang, Samreen Jatana, András K. Ponti, Ryan Musich, Joshua Gallop, Angela H. Wei, Sokhna Seck, Jessica Johnson, Lynne Kokoczka, Amy S. Nowacki, Jeffrey D. McBride, Eduardo Mireles-Cabodevila, Steven Gordon, Kevin Cooper, Anthony P. Fernandez and Christine McDonald

frontiers | Frontiers in Immunology

TYPE Editorial
PUBLISHED 10 July 2023
DOI 10.3389/fimmu.2023.1233291

Check for updates

OPEN ACCESS

EDITED AND REVIEWED BY
Pei-Hui Wang,
Shandong University, China

*CORRESPONDENCE
Edwin Bölke
boelke@med.uni-duesseldorf.de

RECEIVED 01 June 2023
ACCEPTED 23 June 2023
PUBLISHED 10 July 2023

CITATION
Bölke E, van Griensven M, Schneider EM, Fischer JC, Feldt T, Keitel V, Budach W, Haussmann J, Jazmati D and Matuschek C (2023) Editorial: Immune response to SARS-CoV-2 and implications for clinical outcome.
Front. Immunol. 14:1233291.
doi: 10.3389/fimmu.2023.1233291

COPYRIGHT
© 2023 Bölke, van Griensven, Schneider, Fischer, Feldt, Keitel, Budach, Haussmann, Jazmati and Matuschek. This is an open-access article distributed under the terms of the Creative Commons Attribution License (CC BY). The use, distribution or reproduction in other forums is permitted, provided the original author(s) and the copyright owner(s) are credited and that the original publication in this journal is cited, in accordance with accepted academic practice. No use, distribution or reproduction is permitted which does not comply with these terms.

Editorial: Immune response to SARS-CoV-2 and implications for clinical outcome

Edwin Bölke[1]*, Martijn van Griensven[2], E. Marion Schneider[3], Johannes C. Fischer[4], Torsten Feldt[5], Verena Keitel[5], Wilfried Budach[1], Jan Haussmann[1], Danny Jazmati[1] and Christiane Matuschek[1]

[1]Department of Radiation Oncology, University of Dusseldorf, Dusseldorf, Germany, [2]Department cBITE, Institute for Technology-Inspired Regenerative Medicine, Martijn van Griensven Maastricht University, MERLN, Maastricht, Netherlands, [3]Division of Experimental Anesthesiology, University Hospital Ulm, Ulm, Germany, [4]Institute for Transplantation Diagnostics and Cell Therapeutics, Medical Faculty, Heinrich-Heine-University, Dusseldorf, Germany, [5]Clinic of Gastroenterology, Hepatology and Infectious Diseases University Hospital Dusseldorf, Medical Faculty, Heinrich-Heine-University Dusseldorf, Dusseldorf, Germany

KEYWORDS

COVID - 19, cytokine, sepsis, inflammation, pandemic

Editorial on the Research Topic
Immune response to SARS-CoV-2 and implications for clinical outcome

Since the outbreak of the SARS-CoV-2 pandemic in 2019, our understanding of the disease and its pathophysiology has evolved, paving the way to more effective therapeutic and prophylactic approaches (Krysko et al.). As a result of the global vaccination campaign, improved management of severe COVID-19 patients, but also due to decreased pathogenicity of the currently prevailing SARS-CoV-2 variants, mortality and hospitalization due to COVID-19 have been significantly reduced, especially in developed countries increasing natural immunity. Since recently, a major view addresses organ dysfunction in COVID-19 patients leading to improved outcome (1) Nevertheless, the precise nature of an efficient immune response to SARS-CoV-2 remains ill-defined. Inflammation and immune activation are essential but hyperinflammation may turn into a detrimental condition (Krysko et al.). As a consequence, the immune response to SARS-CoV-2 is responsible for a significant proportion of multiple faces of the pathogenicity spectrum (Krysko et al.). SARS-CoV-2 is continuously mutating and poses a major challenge to cellular and humoral immunity, as well as vaccination. On the other hand. The goal of this Research Topic was to present new data regarding the immune response to SARS-CoV-2 and its implication for the clinical outcome.

Saleki et al. showed in this Research Topic that Fas/FasL pathways could play a major role in the mediation of hyperinflammatory cytokine response in COVID-19. According to their results, Fas/FasL pathways are consumed through an interaction with MMPs, and the novel triangle of viral entry, cytokine storm, and multi-system injury. They detected in their investigation that the role of Fas/FasL may depend on the stage of the disease and the severity of COVID-19. By in silico analysis they showed that alterations in the blood of COVID-19 patients influence Fas/FasL interactions at the molecular level. Preclinical and clinical research by antibodies directed against sFAS for COVID-19 treatment could be an option attenuate COVID-19 pandemic severity.

Daamen et al. detected unique transcriptional signatures as surrogate parameters for disease severity. They found immune profiles of severe COVID-19 patients to be of prognostic value for the outcome of the infection. Such alterations in COVID patients could be engineered to better allocate healthcare resources and help to develop targeted treatment plans for i) better care and ii) to combat the worse outcomes.

Lapointe et al. fully characterized humoral responses in a laboratory-confirmed case of serial infection by SARS-CoV-2 Omicron subvariants BA.1 and BA.2 in a patient who showed typical immune responses to three vaccination doses of a COVID-19 mRNA vaccine. Whereas data on repeat Omicron infections are still limited, a recent genomics-based trial from Denmark described 47 cases of BA.2 reinfection that happened between 20 and 60 days following BA.1 infection (24). The authors hypothesize that such events were rare (<0.1% of cases during the brief window of analysis) and would more likely happen among unvaccinated individuals, but additional evaluation of the data shows that most reinfection cases were due to BA.2 following BA.1.

Halliday et al. presented in their trial that low-volume in-house antibody assays are of sufficient diagnostic value. Their study demonstrates the importance of using well-characterized samples and controls for all stages of assay development and evaluation. These cost-effective assays may turn out to be predominantly valuable for seroprevalence studies in developing countries.

Krysko et al. indicated that the severity of SARS-CoV-2 infection correlates with high numbers of alveolar mast cells and their degranulation. Accordingly, SARS-CoV-2 correlated with activation of mast cells, significantly. Mast cell activation appears to be due to indirect effects related to the overall inflammation. Their data recommend that proteases from mast cells might forecast the clinical outcome and sequelae of severe COVID-19 infections. As a consequence, patients might profit from including mast cell stabilizing drugs in their novel treatment scheme.

Penrice-Randal et al. suggest that blood gene expression profiles predict intensive care unit admission in hospitalized patients with COVID-19. Their team demonstrated a "best gene" with its expression signature would be predictive for ICU admission. For this aim, they applied topological data analysis with an accuracy of 0.72 (ROC AUC: 0.76). The gene signature describes herein targeted differentially activated pathways controlling epidermal growth factor receptor (EGFR) presentation, Peroxisome proliferator-activated receptor alpha (PPAR-α) signaling and Transforming growth factor beta (TGF-β) signaling.

Rubio et al. demonstrated that SARS-CoV-2 infection during the third trimester of pregnancy leads to a robust antibody and cytokine response at delivery and causes a significant reduction of the SARS-CoV-2-specific IgGs transplacental transfer, with a significant negative effect when the infection is closer to delivery.

Bizjak et al. emphasized the biomarker, Kynurenine in serum and saliva. Kynurenine may play a role in acute and long-term pathophysiology of the SARS-CoV-2 disease. Specifically, Kynurenine is induced by interferon-g (IFN-g) by innate immune cells (NK-effectors), but also by TH17/IFN-g inflammatory T cells (ref.). The most prevalent pathway of induction in both Long- and Post-COVID for diagnostics and syndrome monitoring needs to be addressed in further studies.

Castelli et al. from Brazil assumed that MUC22, (a member of the mucins' family), may play an important protective part against severe Covid-19. They think that MUC22 might reduce the overactive immune responses in the senior population. Interestingly, the resilient super elderly group showed a higher frequency of some missense variants in the MUC22 gene as one of the most robust signaling elements in the MHC region. These results are based on comparison of the severe Covid-19 group to a general elderly control population.

Schenz et al. from Germany showed an elevated occurrence of clonal hematopoiesis of indeterminate potential in hospitalized patients with COVID-19. Their results indicate an increased exposure to a severe course of COVID-19 requiring hospitalization related with CHIP. Furthermore, they relate it to a differentially regulated cellular immune reply under the pressure of SARS-CoV-2 infection.

Therefore, a better understanding of the immunological background of the disease is of utmost importance in order to develop more effective prevention and treatment strategies.

Author contributions

EB, MvG, EMS, JCF, TF, WB, JH, DJ, VK, CM contributed to drafting and writing the article. All authors contributed to the article and approved the submitted version.

Funding

Res-Q-HR funding was obtained from the German Ministry of Health for CM, EB, JF, TF and VK regarding SARS-CoV-2.

Acknowledgments

This Research Topic is dedicated to Soldano Ferrone and Kurt Zänker.

Conflict of interest

The authors declare that the research was conducted in the absence of any commercial or financial relationships that could be construed as a potential conflict of interest.

Publisher's note

All claims expressed in this article are solely those of the authors and do not necessarily represent those of their affiliated organizations, or those of the publisher, the editors and the reviewers. Any product that may be evaluated in this article, or claim that may be made by its manufacturer, is not guaranteed or endorsed by the publisher.

Reference

1. Borlotti A, Thomaides-Brears H, Georgiopoulos G, Banerjee R, Robson MD, Fusco DN, et al. The additive value of cardiovascular magnetic resonance in convalescent COVID-19 patients. *Front Cardiovasc Med* (2022) 9. doi: 10.3389/fcvm.2022.854750

frontiers | Frontiers in Immunology

TYPE Original Research
PUBLISHED 31 August 2022
DOI 10.3389/fimmu.2022.947401

Check for updates

OPEN ACCESS

EDITED BY
Torsten Feldt,
University Hospital of Düsseldorf, Germany

REVIEWED BY
Luminița-Smaranda Iancu,
Grigore T. Popa University of Medicine and Pharmacy, Romania
Chang Hu,
Zhongnan Hospital of Wuhan University, China
Srikanth Mairpady Shambat,
University Hospital Zürich, Switzerland

*CORRESPONDENCE
Abbas Azadmehr
azadmehr2010@gmail.com

SPECIALTY SECTION
This article was submitted to Viral Immunology, a section of the journal Frontiers in Immunology

RECEIVED 18 May 2022
ACCEPTED 04 August 2022
PUBLISHED 31 August 2022

CITATION
Saleki K, Shirzad M, Javanian M, Mohammadkhani S, Alijani MH, Miri N, Oladnabi M and Azadmehr A (2022) Serum soluble Fas ligand is a severity and mortality prognostic marker for COVID-19 patients.
Front. Immunol. 13:947401.
doi: 10.3389/fimmu.2022.947401

COPYRIGHT
© 2022 Saleki, Shirzad, Javanian, Mohammadkhani, Alijani, Miri, Oladnabi and Azadmehr. This is an open-access article distributed under the terms of the Creative Commons Attribution License (CC BY). The use, distribution or reproduction in other forums is permitted, provided the original author(s) and the copyright owner(s) are credited and that the original publication in this journal is cited, in accordance with accepted academic practice. No use, distribution or reproduction is permitted which does not comply with these terms.

Serum soluble Fas ligand is a severity and mortality prognostic marker for COVID-19 patients

Kiarash Saleki[1,2,3,4], Moein Shirzad[1,2,4], Mostafa Javanian[5], Sheyda Mohammadkhani[2], Mohammad Hossein Alijani[2], Niloufarsadat Miri[1], Morteza Oladnabi[6] and Abbas Azadmehr[1,4,7]*

[1]Cellular and Molecular Biology Research Center, Health Research Institute, Babol University of Medical Sciences, Babol, Iran, [2]Student Research Committee, Babol University of Medical Sciences, Babol, Iran, [3]USERN Office, Babol University of Medical Sciences, Babol, Iran, [4]National Elite Foundation, Mazandaran Province Branch, Mazandaran, Iran, [5]Infectious Diseases and Tropical Medicine Research Center, Health Research Institute, Babol University of Medical Sciences, Babol, Iran, [6]Ischemic Disorders Research Center, Golestan University of Medical Sciences, Gorgan, Iran, [7]Immunology Department, Babol University of Medical Sciences, Babol, Iran

Finding cytokine storm initiator factors associated with uncontrolled inflammatory immune response is necessary in COVID-19 patients. The aim was the identification of Fas/Fas Ligand (FasL) role in lung involvement and mortality of COVID-19 patients. In this case-control study, mild (outpatient), moderate (hospitalized), and severe (ICU) COVID-19 patients and healthy subjects were investigated. RNA isolated from PBMCs for cDNA synthesis and expression of mFas/mFasL mRNA was evaluated by RT-PCR. Serum sFas/sFasL protein by ELISA and severity of lung involvement by CT-scan were evaluated. Also, we docked Fas and FasL *via* Bioinformatics software (*in silico*) to predict the best-fit Fas/FasL complex and performed molecular dynamics simulation (MDS) in hyponatremia and fever (COVID-19 patients), and healthy conditions. mFasL expression was increased in moderate and severe COVID-19 patients compared to the control group. Moreover, mFas expression showed an inverse correlation with myalgia symptom in COVID-19 patients. Elevation of sFasL protein in serum was associated with reduced lung injury and mortality. Bioinformatics analysis confirmed that blood profile alterations of COVID-19 patients, such as fever and hyponatremia could affect Fas/FasL complex interactions. Our translational findings showed that decreased sFasL is associated with lung involvement; severity and mortality in COVID-19 patients. We think that sFasL is a mediator of neutrophilia and lymphopenia in COVID-19. However, additional investigation is suggested. This is the first report describing that the serum sFasL protein is a severity and mortality prognostic marker for the clinical management of COVID-19 patients.

KEYWORDS

COVID-19, hyperinflammation, Fas, viral Immunology, immunoinformatics

Introduction

Coronaviruses (CoVs) created two pandemics in the world by the Severe Acute Respiratory Syndrome (SARS)-CoV (1) and Middle-East respiratory syndrome (MERS)-CoV (2) variants, respectively. Recently, SARS-CoV2 initiated a third pandemic called Coronavirus disease-2019 (COVID-19). This pandemic is a major cause of mortality in the world (3).

On the other hand, COVID-19 is commonly accompanied by a harmful inflammatory response, and overactivation of neutrophils which leads to the formation of Neutrophil Extracellular Traps (NETs), sepsis, and cytokine storm (4, 5). Cytokine storm is one of immunopathological reactions in COVID-19 patients, which is an aggressive inflammatory response with excessive release of cytokines and elements, including interleukin (IL)-2, IL-6, IL-7, IL-10, tumor necrosis factor (TNF), granulocyte colony-stimulating factor (G-CSF), monocyte chemoattractant protein-1 (MCP1; or CCL2), macrophage inflammatory protein 1 alpha (MIP1α; or CCL3), CXC-chemokine ligand 10 (CXCL10), C-reactive protein (CRP), ferritin, and D-dimers (6–8). In addition to cytokine storm, other inflammatory factors such as sFasL increase disease severity and inflammation in COVID-19 patients (9).

We recently proposed a novel triangle in COVID-19, comprising viral infection, cytokine storm, and multi-system damage, such as respiratory and CNS. We described how this triangle dysregulates immune response through Fas/Fas Ligand (FasL) in COVID-19 patients (10–13). Soluble FasL (sFasL) is produced by the cleavage of membrane-attached FasL (mFasL) *via* a zinc-regulated matrix metalloprotease (MMP). mFas/mFasL and sFas/sFasL interactions could induce hyperinflammation and recruit immune cells playing a possible role in the multi-system injury in COVID-19 patients (12).

A new study showed that raised serum sFasL in severe burn is associated with pro-inflammatory cytokine production, organ injury, lymphopenia, and predicts mortality (14). André et al. showed that T-lymphocytes death in COVID-19 patients could be mediated by sFasL and CXCL10, that leads to hyperinflammation in this condition (15). Moreover, mFasL and sFasL lead the inflammaging processes, that are related to viral lung disorders (16). Kessel et al. explained that sFasL is a discriminating factor that can lead to a dysregulated immune response and amplify inflammation in COVID-19 patients (17). Finally, evidence suggests that sFasL may be distinctly implicated in COVID-19 as an important factor in the inflammatory response and contribute to mortality.

In this study, we evaluated mFas/mFasL expression by RT-PCR, sFas/sFasL serum level by ELISA, severity of disease by computed tomography (CT)-scan in COVID-19 patients and utilized *in silico* (Bioinformatics) software to study Fas/FasL interactions.

Methods

Sample selection and data collection

This study enrolled 120 subjects in four groups in 2020-2021; including healthy controls, COVID-19 out-patients (mild), hospitalized COVID-19 (moderate), and ICU COVID-19 (severe). The inclusion criteria for healthy controls were I; no history of any major condition that is associated with hyperinflammation, such as obesity (BMI>30), diabetes, severe cardiovascular, renal, cerebrovascular, or autoimmune disorders, II; not being vaccinated for COVID-19, III; not being infected with or recovering from a recent COVID-19 infection. COVID-19 patients were included without age limitation. Demographic information, clinical symptoms of COVID-19, and past medical history were obtained for COVID-19 patients. Additional laboratory data, such as CBC, C-reactive protein (CRP), ESR, electrolytes, as well as vital signs and O2 saturations were collected for hospitalized and ICU COVID-19 patients. COVID-19 diagnosis was confirmed by serological rapid IgM assay and real-time polymerase chain reaction (RT-PCR). Furthermore, hospitalization or admission of patients to ICU was carried out according to different clinical parameters, including SpO_2, lung computed tomography (CT)-scan, heart rate, and various blood parameters such as LDH, CPK, Ferritin, Troponin, C-reactive protein (CRP) and interleukin-6 (IL-6), similar to criteria provided by the National Institutes of Health (NIH) (https://www.covid19treatmentguidelines.nih.gov) and National Guidelines of the Diagnosis and Treatment Committee for COVID-19. Also, COVID-19 mortality was followed by the medical record center of referred hospital as well as *via* phone calls (the patients him/herself or through patients' family members).

PBMCs isolation, RNA extraction, and cDNA synthesis

Venous whole blood specimens (5 cc) were transferred to collection tubes with EDTA. Peripheral blood mononuclear cells (PBMCs) were isolated *via* lymphocyte separation media. The blood samples by Ficoll as the lymphocyte separation media, were centrifuged at 800 ×g for 20 min. Then, the PBMCs were washed twice by phosphate buffered saline (PBS), at pH 7.4. RNA was extracted from PBMCs by Total RNA Extraction Kit (Yekta tajhiz Azma, Tehran, Iran) based on the manufacturer's instructions. The Easy^{TM} cDNA Reverse Transcription kit (ParsTous, Iran) was used to perform reverse transcription of total RNA into cDNA. Briefly, the template RNA (total RNA or Poly (A) mRNA) and other kit components in RNase-free tube were mixed. Next, the mixture was rapidly vortexed and then, incubation was performed for 10 min at 25°C and 1 hour at 47°C, respectively. The reaction

was stopped by heating at 85°C for 5 minutes. At the end, cDNA products were stored at -80°C.

Serum isolation

Venous whole blood samples from COVID-19 cases and normal participants were obtained in Falcon collection tubes without EDTA. The blood specimens were then centrifuged at 1000 xg for 10 min to remove the clots. The supernatant was collected and stored at -80°C and used for enzyme-linked immunosorbent assay (ELISA) experiment.

Expression analysis of Fas and FasL by real-time PCR

Primer sequences that were used are mentioned in Table 1 (18–20). The used sequences were oligonucleotide primers for the recognition of Fas and FasL. NCBI blast was also used to check the primer against human genome. Glyceraldehyde 3-phosphate dehydrogenase (GAPDH) was selected as reference housekeeping gene, with same primers as our recent previous study (20). These sequences were re-analyzed for suitability by Oligo7. In order to assess relative mRNA expression RT-PCR was performed.

After amplifying cDNAs using PCR with SYBR Green qPCR Master Mix 2X (ParsTous Biotechnology, Mashhad, Iran), we performed real-time PCR test using Applied Biosystems 7300 real-time thermocycler (Applied Biosystems, MA, USA).

We assessed the expression level of Fas and FasL mRNA in mild, moderate, and severe COVID-19 cases, and control subjects, as expression ratios normalized to the expression of the house keeping gene, GAPDH.

Analysis of Fas and FasL protein concentrations by ELISA

Serum of patients was used to measure Fas and FasL proteins. Their levels were quantified for 88 subjects by the BIOTECH ELISA kit for human Fas and FasL (SHANGHAICRYSTAL DAY BIOTECH CO., Shanghai, China), respectively. Concentrations were measured at 450 nm by Synergy HTX multi-mode microplate reader (BioTek Instruments, Winooski, VT, USA) according to the color shade of each plate. We assessed the concentration of Fas and FasL proteins in mild, moderate and severe COVID-19 patients as well as the control group.

Correlation analysis of lung injury CT scan and sFas/sFasL protein levels

Lung has two right and lobes, that includes upper, middle, and lower lobes. Each lobe is about one-sixth of lung area, and percent of involvement is determined by this method in our department. We collected the lung CT-scan results that were available for COVID-19 patients. Correlation analysis was performed between lung injury and sFas/sFasL protein levels that were detected by ELISA.

The *in silico* molecular dynamics study of Fas/FasL interaction in blood

Immunoinformatics is carried using various software that extend our knowledge of molecular findings by facilitating processes such as simulating complex reactions and screening compounds for experimental evaluation of drugs (21). Therefore, we evaluated Fas/FasL interactions *in silico* by simulating the blood profile condition of COVID-19 patients, such as fever and hyponatremia which is responsible for inflammation in this condition.

We modelled Fas and FasL by homology modelling and assessed structure quality. We used the best complex according to docking results. Molecular dynamics simulation (MDS) is a computational simulation method that is utilized for analysis of the physical movement of atoms and molecules. In MDS, a biological system is virtually set up and equilibrated, and is allowed a limited time to evolve. Then, the evolution of the system within the MDS trajectory can be analyzed. One of the most recognized and versatile programs for MDS is GRoningen MAchine for Chemical Simulations (GROMACS). This software package enables rapid and precise simulations (22).

We simulated the best docked Fas/FasL complex in blood *via* GROMACS. Visual Molecular Dynamics (VMD) (23) and UCSF

TABLE 1 Primer sequences.

Gene	Direction	Sequence 5' to 3'	Reference
Fas	Forward	TGAAGGACATGGCTTAGAAGTG	(18)
Fas	Reverse	GGTGCAAGGGTCACAGTGTT	
FasL	Forward	GCAGCCCTTCAATTACCCAT	(19)
FasL	Reverse	CAGAGGTTGGACAGGGAAGAA	
GAPDH	Forward	ACAGTCAGCCGCATCTTC	(20)
GAPDH	Reverse	CTCCGACCTTCACCTTCC	

chimera were employed to assess the simulation box during all MDS steps. Also, OPLS-AA force field was selected to produce topology of proteins (24, 25). Then, the Fas/FasL complex was centered in a triclinic box with edges separated by a minimum of 1 nm from the edges and also the simulation box enclosed the Fas/FasL complex. The box size was set to 6.2, 7.1, 5.2 nm. We used spce16 water for solvation. Moreover, we added Na^+ and Cl^- ions to neutralize the system, and to reach a concentration of 150 mM similar to blood of healthy cases. Previous studies demonstrated that hyponatremia and fever are important pathophysiological findings in COVID-19 patients (26–31). Therefore, for COVID-19 groups; hyponatremia and fever, the simulation setting was modified to 130 mM/37°C and 150 Mm/38.4°C, respectively.

Binding energy analysis of the contact area of the Fas/FasL complex

We selected protein binding energy prediction (PRODIGY) (https://wenmr.science.uu.nl/prodigy/), a novel tool that assesses the binding strength in biological molecules interactions. This algorithm has the ability to utilize alternative atomic radii and various nonpolar solvation modes (32). By this approach, we interconnected MDS with binding energy analysis for contact area of the Fas/FasL complex for all MDS groups. Negative energies were considered an indicator of favorable binding.

Statistical analysis

Statistical Packages for Social Sciences (SPSS), (SPSS Inc., Chicago, USA) and GraphPad Prism version 8.4 (GraphPad Software Inc., La Jolla, CA, USA) were utilized to analyze RT-PCR and ELISA data. Moreover, data normality was evaluated *via* the Kolmogorov-Smirnov test for sample size (n ≥50) or Shapiro-Wilk for sample size (n ≤50) (33). ELISA data were assessed through one-way ANOVA with *post-hoc* Tukey analyses. Results were plotted as mean ± SEM. Moreover, *t* tests or non-parametric tests (e.g., Mann-Whitney) were used where appropriate. For all tests, threshold of significance was considered $p = 0.05$. For Bioinformatics analyses, suitable software packages and servers were used.

Results

Subject's information and demographics

In this study, 120 individuals were enrolled, including mild (n=31), moderate (n=31), and severe (n=31) COVID-19 patients as well as healthy subjects (n=27), for whom gene expression analysis was performed. In the next step, the patients were followed-up for mortality and ELISA study. For follow-up subjects, age of participants was 48.59 ± 17.54, and 43 patients (48.86%) were male and 45 patients (51.14%) were female. As shown in detail in Table 2, clinical findings of COVID-19 patients included fever in 38 patients (57.57%), cough in 36 patients (54.55%), weakness in 31 patients (46.7%), myalgia in 30 patients (45.45%), nervous system symptoms in 22 patients (33.33%), along with GI symptoms such as nausea, vomiting, and diarrhea in 18 patients (27.27%). Inflammatory markers such as CRP and IL-6 as well as demographic information are provided in Table 2.

Expression of mFas and mfasL are attenuated in mild COVID-19 patients

Expression of mFas and mFasL mRNA was evaluated for all groups. COVID-19 patients in the moderate and severe COVID-19 groups showed significantly higher mFas expression

TABLE 2 Patient's clinical characteristics.

Characteristic		COVID-19	Mild COVID-19	Moderate COVID-19	Severe COVID-19	Control group
Gender (Male/Female); n (percentage)		32/34 (48.5%/51.5%)	13/9 (59.1%/40.9%)	12/10 (54.4%/45.5%)	7/15 (31.8%/68.2%)	11/11 (50%/50%)
Age (Mean)		52.37	39.55	57.22	60.36	37.68
IL-6 (pg/mL); mean (SD)		57.49 (35.15)	16.40 (5.05)	67.06 (12.64)	89.01 (27.08)	5.15 (1.45)
CRP (mg/L) mean (SD)		51.20 (42.86)	14.97 (2.60)	65.42 (36.06)	73.21 (47.79)	NA
Symptoms	Fever n (percentage)	38 (57.6%)	15 (68.2%)	14 (63.6%)	9 (40.9%)	0 (0%)
	Cough n (percentage)	26 (39.4%)	10 (45.5%)	7 (31.8%)	9 (40.9%)	0 (0%)
	Myalgia n (percentage)	30 (45.5%)	13 (59.1%)	9 (40.9%)	8 (36.4%)	0 (0%)
	Gastrointestinal n (percentage)	18 (27.3%)	5 (22.7%)	8 (36.4%)	5 (22.7%)	0 (0%)
	Neurological n (percentage)	19 (28.8%)	9 (40.9%)	3 (13.6%)	7 (31.8%)	0 (0%)

NA, Not Applicable.

compared to the mild COVID-19 group ($p < 0.0001$). Further, mild COVID-19 group had lower mFasL expression in comparison with the control group ($p < 0.01$) as well as moderate and severe COVID-19 groups ($p < 0.0001$). Overall, mFasL expression was higher in COVID-19 cases compared to the control group. mFasL expression was significantly elevated in moderate ($p < 0.05$) and severe ($p < 0.001$) COVID-19 groups compared to the control group. PCR results for mFas and mFasL are provided in Figures 1A–F. Also, correlation analysis of mFas/mFasL expression and clinical COVID-19 symptoms are provided in Figure 2.

sFas and sFasL proteins are increased in mild COVID-19

ELISA analysis of serum samples from mild COVID-19 patients displayed an increase in both sFas and sFasL proteins compared to all other subgroups. sFas levels were significantly higher in mild COVID-19 group, compared to the control group ($p < 0.05$) and severe COVID-19 group ($p < 0.01$). sFasL levels were significantly higher in mild COVID-19 compared to moderate COVID-19 group ($p < 0.05$). Also, sFasL levels were lower in severe COVID-19 group compared to control and mild COVID-19 groups. ELISA results for sFas and sFasL are provided in Figures 3A–D.

Correlation analysis of CT scan lung injury and sFas/sFasL protein level in patients with COVID-19

In CT-scan, the normal lung appears clear with low attenuation area and normal vascularity, but inflamed/injured areas appear with ground glass opacity (GGO) and abnormal vascularity. Lung CT-scan of COVID-19 cases representing mild, moderate, and severe respiratory involvement are provided in Figure 4. Analysis of the lung CT-scan in COVID-19 patients showed that a decrease in sFas and sFasL levels was significantly correlated with severity of respiratory injury ($r= -0.3485$, $p= 0.0085$; $r= -0.3388$, $p= 0.0106$), respectively. These results are indicated in Figure 5.

sFasL protein level predicts mortality in COVID-19 patients

In this study, ten patients died, comprising five patients in each of moderate and severe COVID-19 groups. However, none of patients died in the mild COVID-19 group. We performed logistic regression to evaluate the sFas and sFasL levels for prediction of mortality in COVID-19 patients. We found that lower sFasL levels are associated with a significantly increased risk for mortality (OR $\beta1 = 0.940$; 95% CI= 0.881-0.991, $p = 0.038$). Regression analysis and Receiver operating characteristic (ROC) curve are also shown in Figures 6A, B. Area under curve (AUC) was 0.70 ($p = 0.042$). As well, the cut-off value of sFasL was determined 19.65 ng/ml for predicting of COVID-19 patients' mortality. Finally, we performed statistical analysis to compare the mean sFasL levels in dead vs. alive COVID-19 patients. Our results showed that the mean sFasL levels were significantly ($p < 0.05$) lower in the dead group compared to the alive group (Figure 6C).

Homology modelling of Fas and FasL structures

In the present study, homology modelling is defined as the prediction of a protein structure (Fas/FasL) based on experimental data. Single template modelling using 4MSV achieved for FasL. Align 2D algorithm showed an alignment score of 123061.55. molpdf and DOPE score are 865.61 and 15026.96. Furthermore, multiple template modelling using 3TJE and 3X3F was achieved for Fas. molpdf score for the best structure is 2547.91. GA341, a MODELLER tool used to rule out bad models, for generated models was higher than 0.6, confirming that the models had good quality.

Protein structure refinement

In this work, protein structure refinement is defined as the determination and optimizing of protein structure properties, such as amino acid angles, protein Z-score, alignment of beta-sheets, alpha-helices, and coils. The initial models were refined by GalaxyRefine server, through Refine2 tool set to conservative mode. As shown in Figures 7A–F for Fas, RMSD, MolProbity, clash analysis, poor rotamers, Ramachandran preferred, and GALAXY energy for the initial model and the top refined model were 0.000, 3.580, 117.8, 4.9, 90.9, and 1039.44; 8.682, 1.560, 2.7, 1.4, 94.2, and -2838.07, respectively. Also as shown in Figures 8A–F for FasL, RMSD, MolProbity, clash analysis, poor rotamers, Ramachandran preferred, and GALAXY energy for the initial model and the top refined model were 0.000, 2.833, 55.3, 4.4, 97.3, and -1184.28; 6.043, 0.887, 1.5, 0.0, 99.3, and -3912.69, respectively. In this step, we refined the Fas and FasL structure.

Protein structure quality assessment

Protein quality assessment is defined as evaluating of quality of the final target protein, based on the previous steps and Bioinformatics analysis rules, for example, the number of amino acids located in most favorable regions should be maximized.

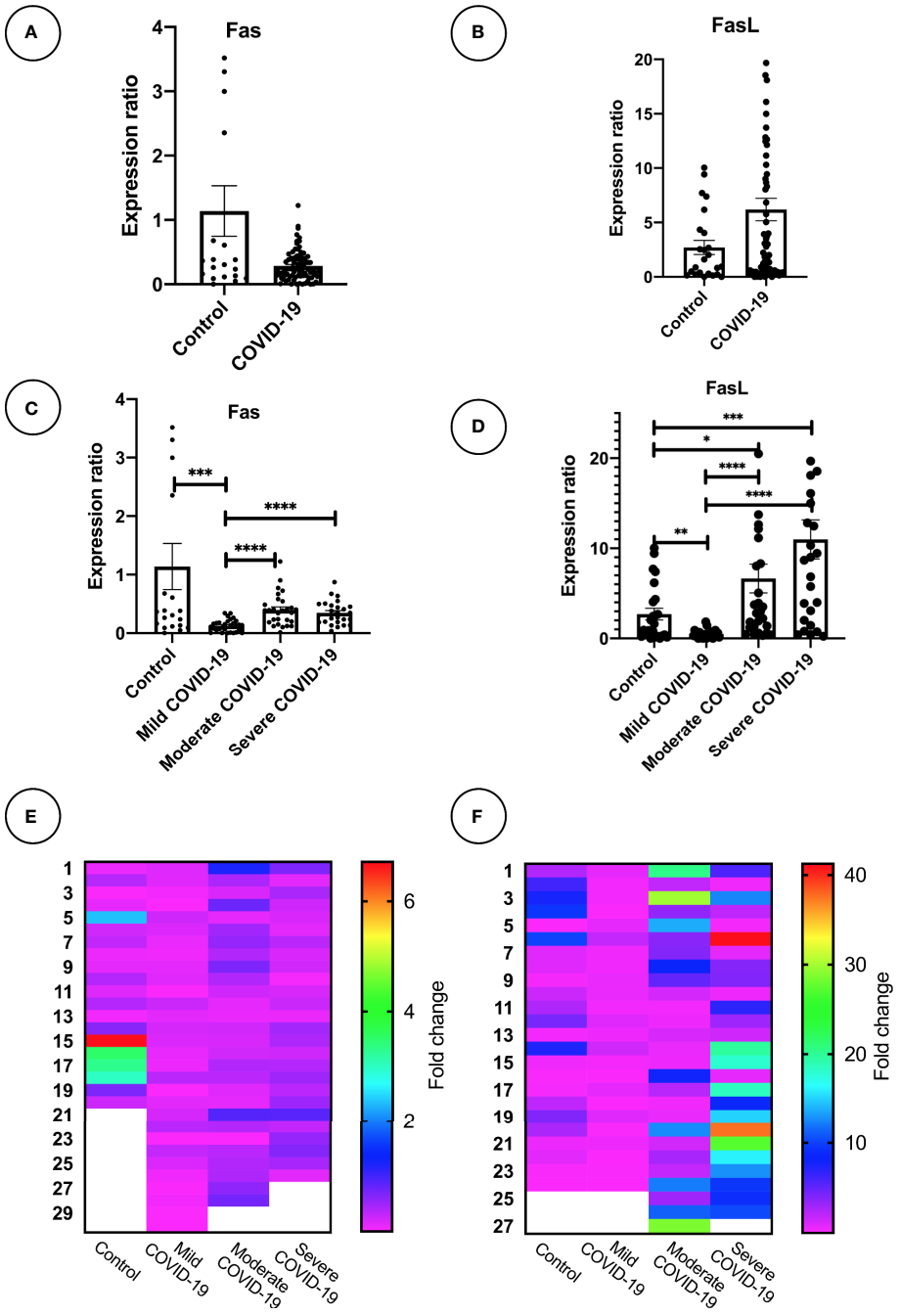

FIGURE 1
Fas and FasL mRNA expression in PBMC samples mRNA expression of Fas and FasL is shown for **(A, B)** COVID-19 (n = 93) and control group (n = 27). **(C, D)**, mild, moderate, and severe COVID-19 (n = 31 per group), and control group (n = 27). **(E, F)** Heatmaps graphically demonstrate expression level; *p<0.05, **p< 0.01, ***p<0.001, ****p< 0.0001. Outlier data which were abnormal were excluded for each gene expression analysis. *Outlier values are displayed as blanked in heatmaps. Higher values than graph range exceed the plot and may not be shown.

For both Fas and FasL, we refined the structures to accomplish a structure that is verified as good quality by various tools, such as Ramachandran plot, ERRAT, and ProSA. For Fas, Ramachandran analysis showed 93.431%, 4.380%, and 2.190% of elements were positioned in the most favored, allowed, and questionable areas. After refinement, mentioned scores were further enhanced, reaching 94.891%, 2.920%, and 2.190%, respectively. For FasL, initial structure showed values of

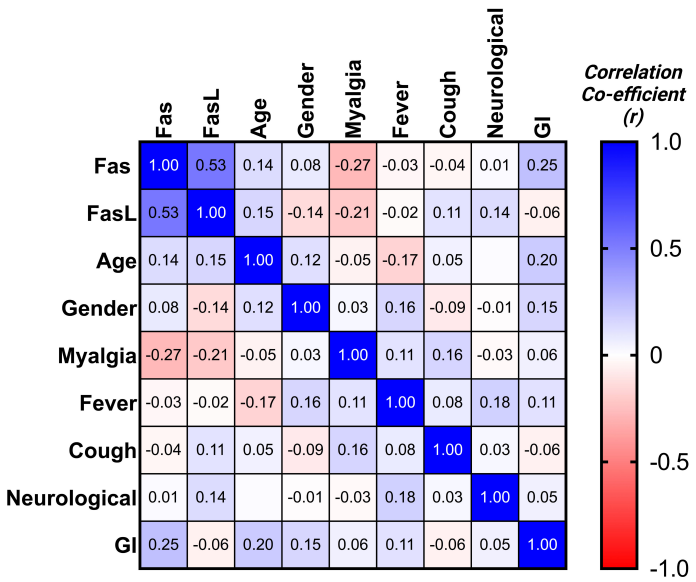

FIGURE 2
Correlation matrix for Fas/FasL and clinical disease properties.

98.473%, 0.763%, and 0.763%. After refinement, these results were further improved to 99.237%, 0.763%, and 0.000%, respectively. Also, ERRAT scores showed the scores of 36.296% and 85.849% for initial and refined Fas structures, respectively. This analysis showed the scores of 70.833% and 88.696% for initial and refined FasL structures, respectively. These results indicate that the refined structures passed the ERRAT analysis. ProSA analysis of protein Z-score showed values that were within the range of experimentally-verified structures of sequences with the same amino acid length. For Fas, Z-scores for initial and refined structures were -3.41 and -4.08, respectively. Also, for FasL, Z-scores for initial and refined structures were -4.3 and -4.93. These results are shown in Figures 7–9.

Docking analysis for Fas/FasL complex

Molecular docking is the evaluation of the way that two or more molecular structures such as protein, enzyme and drugs fit together (34). The final protein structures for best docked complex showed docking score, area, ACE, and transformation of 12864, 1594.40, 137.01, 0.57, and -0.48 -0.04 84.68 -20.55 42.63. After refinement by FireDock, energy (global), attractive VdW, repulsive VdW, ACE, and HB -22.15, -24.02, 4.16, 8.64, and -2.93. The contact residues were detected by UCSF Chimera and default contact criteria. Additionally, 118 contacts were detected in the Fas/FasL complex which are provided in Table 3 and highlighted in yellow within the docked complex in Figure 10.

Molecular dynamics simulation study of Fas/FasL complex for COVID-19 patients

MDS is explained as a computational simulation method that allows the prediction of time-related evolutions of a particular interacting system (35). In our research, the Fas/FasL system was converged to F_{max} < 1000 by the steepest descents algorithm, in 1027 steps, reaching the potential energy of -9.3472875e+05 (Figure 11A). After the NVT equilibration, temperature reached 309.782 °K (Figure 11B), and after NPT equilibration, the pressure of the system reached 0 bar (Figure 11C) and the density was 1027 kg/m3 (Figure 11D). For all studied conditions, gyration, RMSF, and visual evaluation of the MDS trajectory did not show denaturation of the protein (Figure 11E). RMSD of the Fas, FasL, and Fas-FasL complex stabilized after 5-6 ns (Figure 11F). Results for the normal conditions are shown in Figures 11A–F.

Final binding analysis of Fas/FasL interactions in COVID-19

Regarding the PRODIGY analysis, in the control conditions, the average Fas-FasL binding energy was -9.8 kcal.mol^{-1}. In the COVID-19 fever condition, the average Fas-FasL binding energy

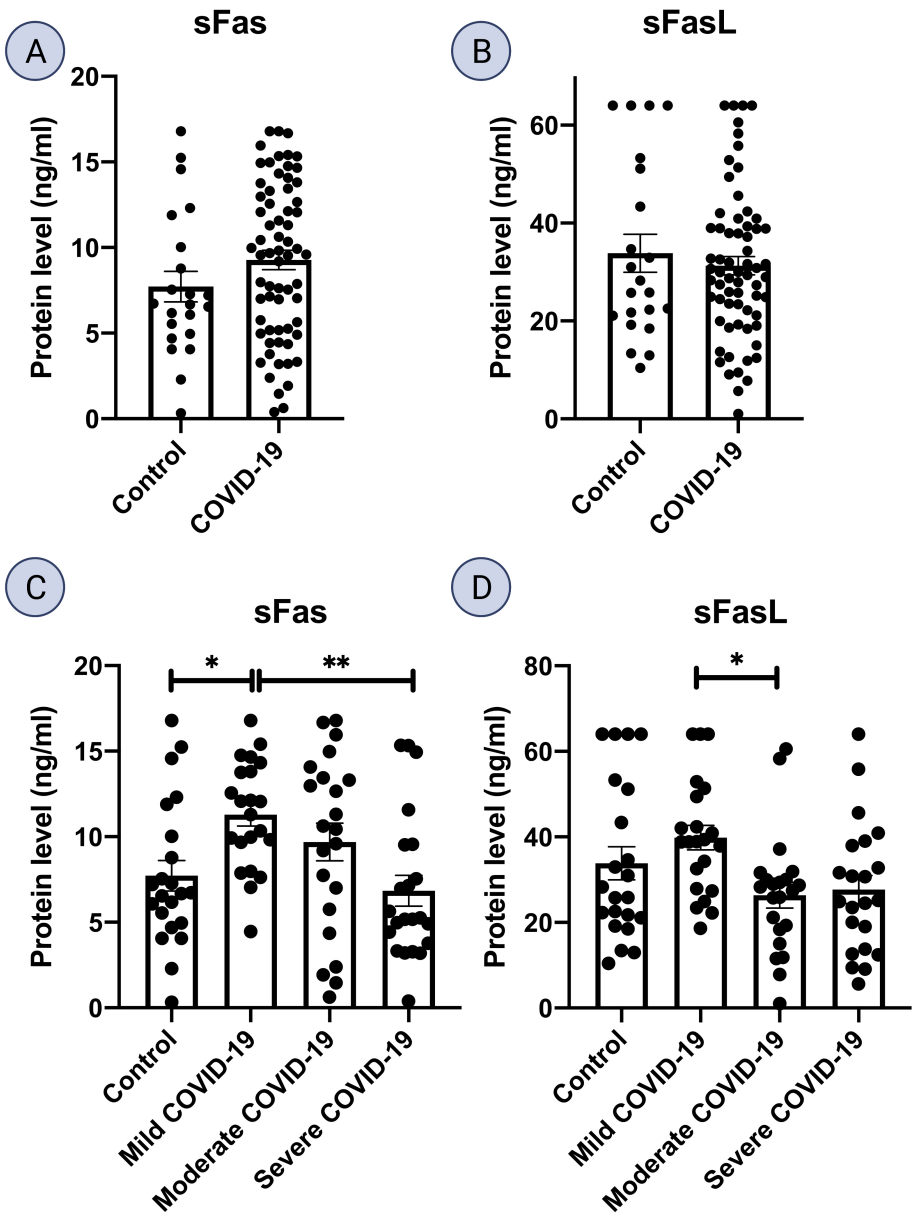

FIGURE 3
Fas and FasL protein level in serum samples. Serum levels of Fas and FasL is shown for **(A, B)** COVID-19 (n = 66) and control group (n = 22). **(C, D)**, mild, moderate, and severe COVID-19, and control group (n = 22 per group); *p<0.05, **p< 0.01, ***p<0.001, ****p< 0.0001.

was -8.11 kcal.mol^{-1}, showing a stable binding. Also, in COVID-19 hyponatremia condition the binding energy was -10.71 kcal.mol^{-1}, which showed a more stable binding state. These results may indicate that a mild increase in temperature can result in slightly less favorable binding while lower Na^+ levels could enhance binding energies. Nonetheless, binding for all group showed a stable negative ΔG, confirming our experimental data. Binding results for all groups are provided in Table 4.

Discussion

Several studies have shown that Fas and FasL activate inflammatory cells, particularly neutrophils, through the release of pro-inflammatory cytokines (4, 36, 37). These molecules lead to neutrophils' and macrophages' recruitment to injury area (12, 38–41). Uncontrolled inflammation mediated by Fas/FasL plays an immunopathological dysregulated immune response and increased neutrophil counts in various tissue

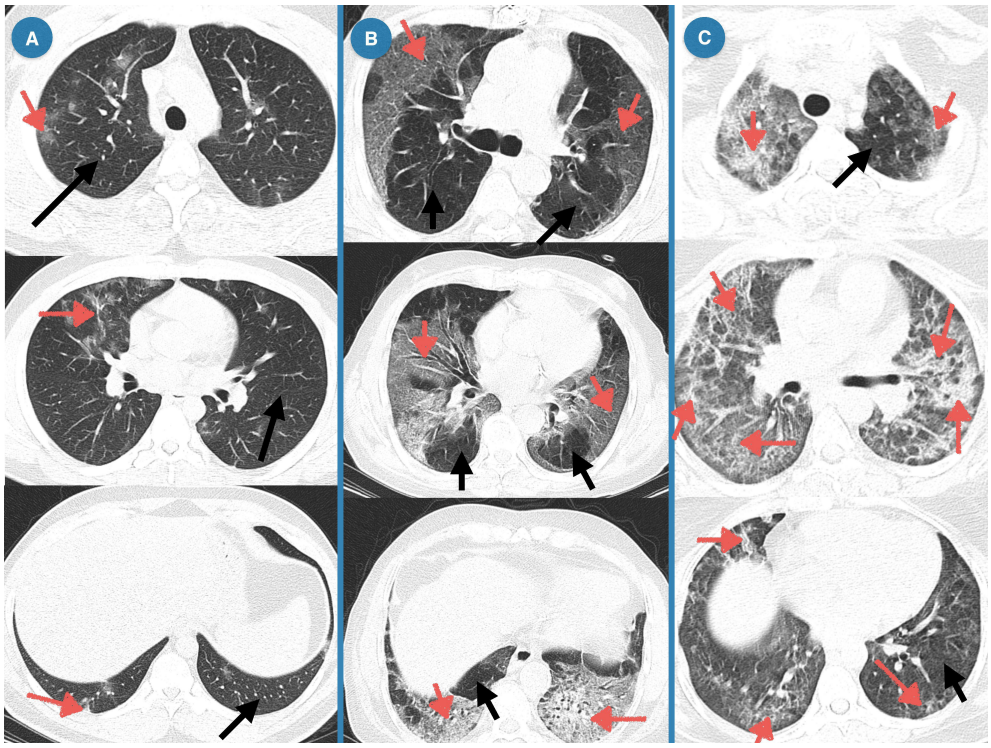

FIGURE 4
Lung CT of COVID-19 patients representing mild, moderate, and severe respiratory injury. **(A)** Mild, Multiple peripheral and central ground glass opacities (GGOs) in right upper lobe and left lower lobe; Band atelectasis in left lower lobe; **(B)** Moderate, Subpleural GGOs near costal and mediastinal pleura of both lungs, Consolidation with air-bronchogram in lower lobes of both lungs, multiple observations of band atelectasis; **(C)** Severe, Peripheral patchy GGOs, Diffuse and mostly peripheral GGOs, Multiple fibrotic bands.

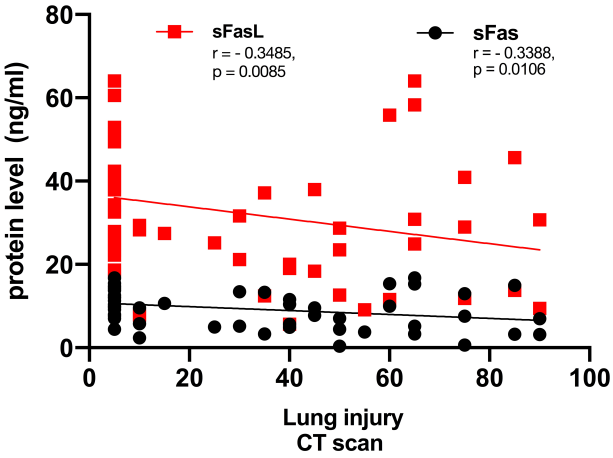

FIGURE 5
Correlation of lung involvement CT scan and sFas/sFasL in COVID-19 patients. Lung has two right and lobes, that includes upper, middle, and lower lobes. Each lobe is about one-sixth of lung area, and percent of involvement is determined by this method in our department.

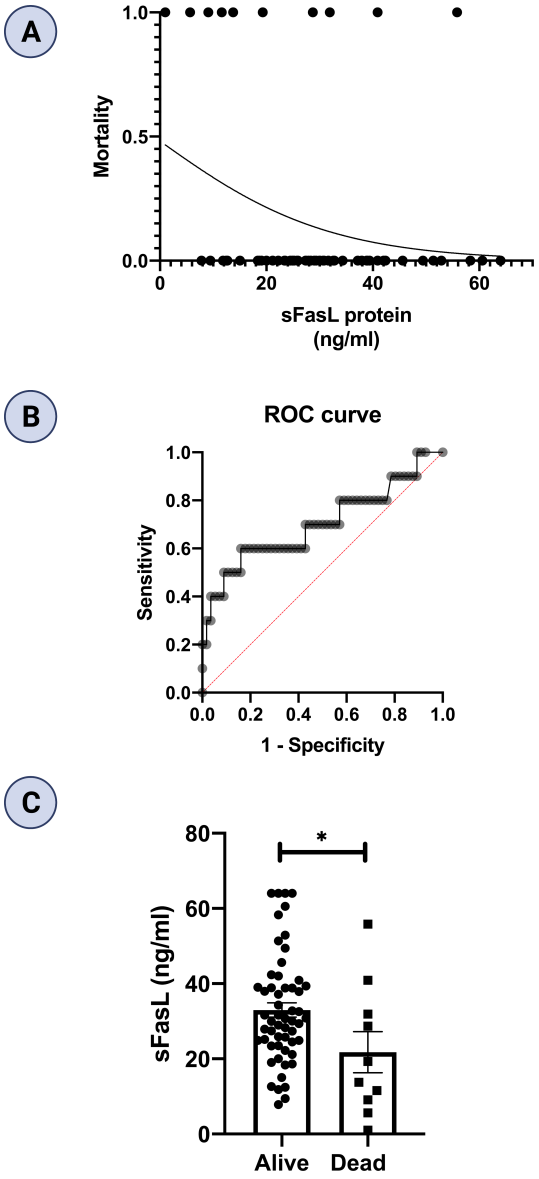

FIGURE 6
Regression analysis and prognostic performance of sFasL for COVID-19 mortality. **(A)** Regression analysis showed lower sFasL is associated with an increased risk for mortality (n =66). **(B)** AUC in ROC was 0.70. **(C)** sFasL levels were lower in dead compared to alive COVID-19 patients. *p<0.05, **p< 0.01, ***p<0.001, ****p< 0.0001.

injuries, including respiratory and neurological disorders (12, 42–46). An important adverse effect of hyperinflammation and cell apoptosis in COVID-19 patients is lymphopenia, that is affected by Fas/FasL (47). A recent investigation demonstrated that increased expression of Fas (CD95) in $CD4^+$ and $CD8^+$ lymphocytes was associated with a reduced proportion of naive events. The findings of their study indicated apoptosis and exhaustion of lymphocytes during COVID-19 infection (10). Also, in our experiment, moderate and severe COVID-19 groups showed higher mFas expression in comparison with the mild COVID-19 group in PBMCs samples, that consist of lymphocytes, monocytes, and immature neutrophils. Additionally, mFasL expression in PBMCs was higher in COVID-19 group in comparison with the control group. Findings of the present study support our hypothesis that mFas/mFasL is converted to sFas/sFasL. This event in the initial inflammatory phase in the mild COVID-19 patients may be mediated through additional mechanisms such as cleavage by MMPs (12). Further studies are recommended to explore these factors in the inflammatory phase of COVID-19.

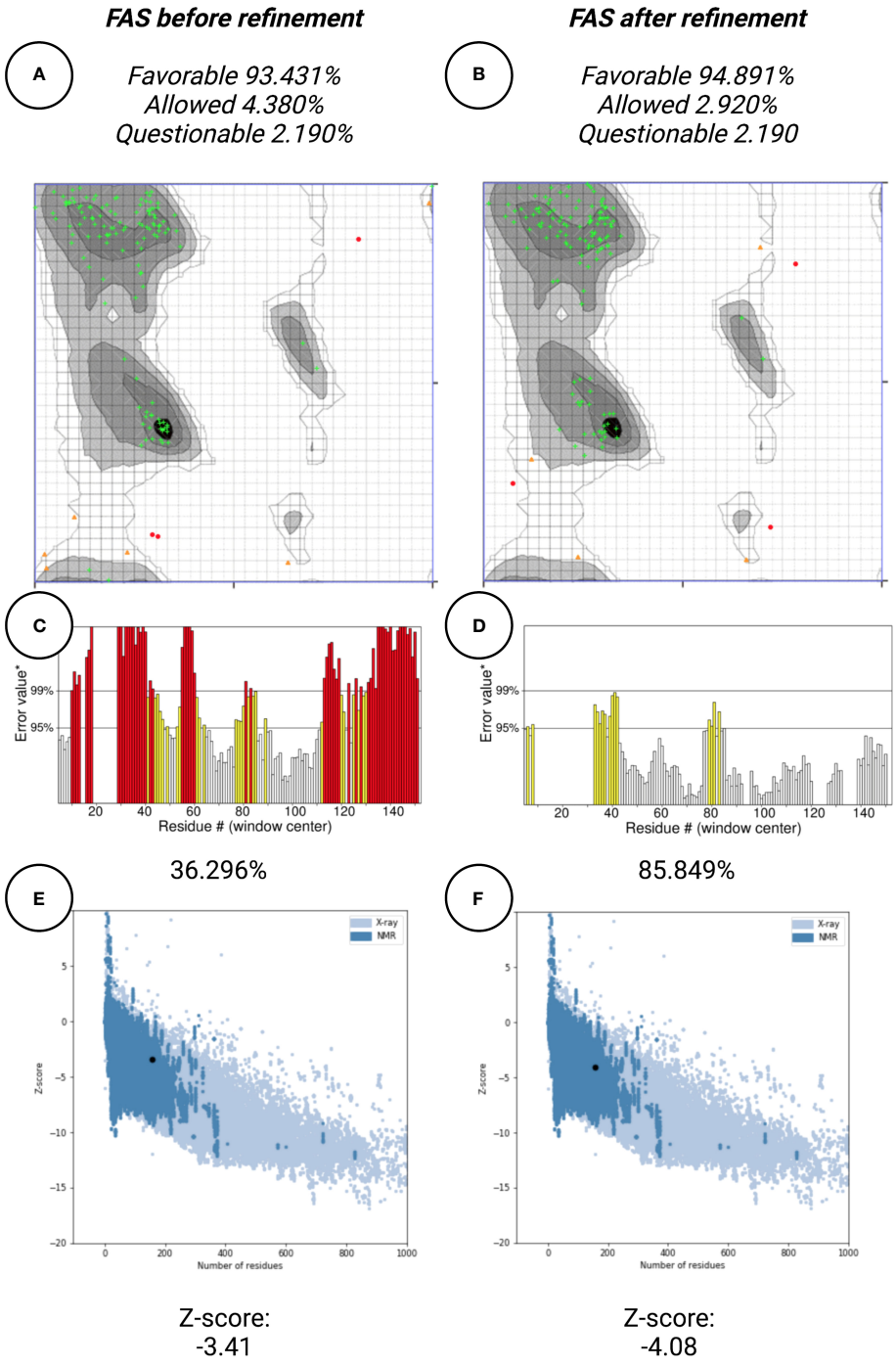

FIGURE 7
Protein quality verification for Fas tertiary structure. In this illustration, the proteins (Fas/FasL) are evaluated based on structural Bioinformatics rules. After refinement, Fas structures was favorable. **(A, B)** In the Ramachandran plot, more residues are located in favorable regions. **(C, D)** ERRAT score was improved from 36.296% to 85.849%. A score over 80% shows the refined structure has good quality. **(E, F)** ProSA Z-score was improved from -3.41 to -4.08 which is within the acceptable range for structures with the same aminoacid length.

Our data confirmed an increase in sFas and sFasL protein production in the initial-stage mild COVID-19 patients. Moreover, we found sFas and sFasL levels were reduced in later-stage more severe COVID-19 groups compared to the mild COVID-19 group. Interestingly, a recent work demonstrated that serum sFasL levels in ICU COVID-19 patients were lower compared to controls at the time of admission (9). Therefore, we suggest that the decrease in sFas/

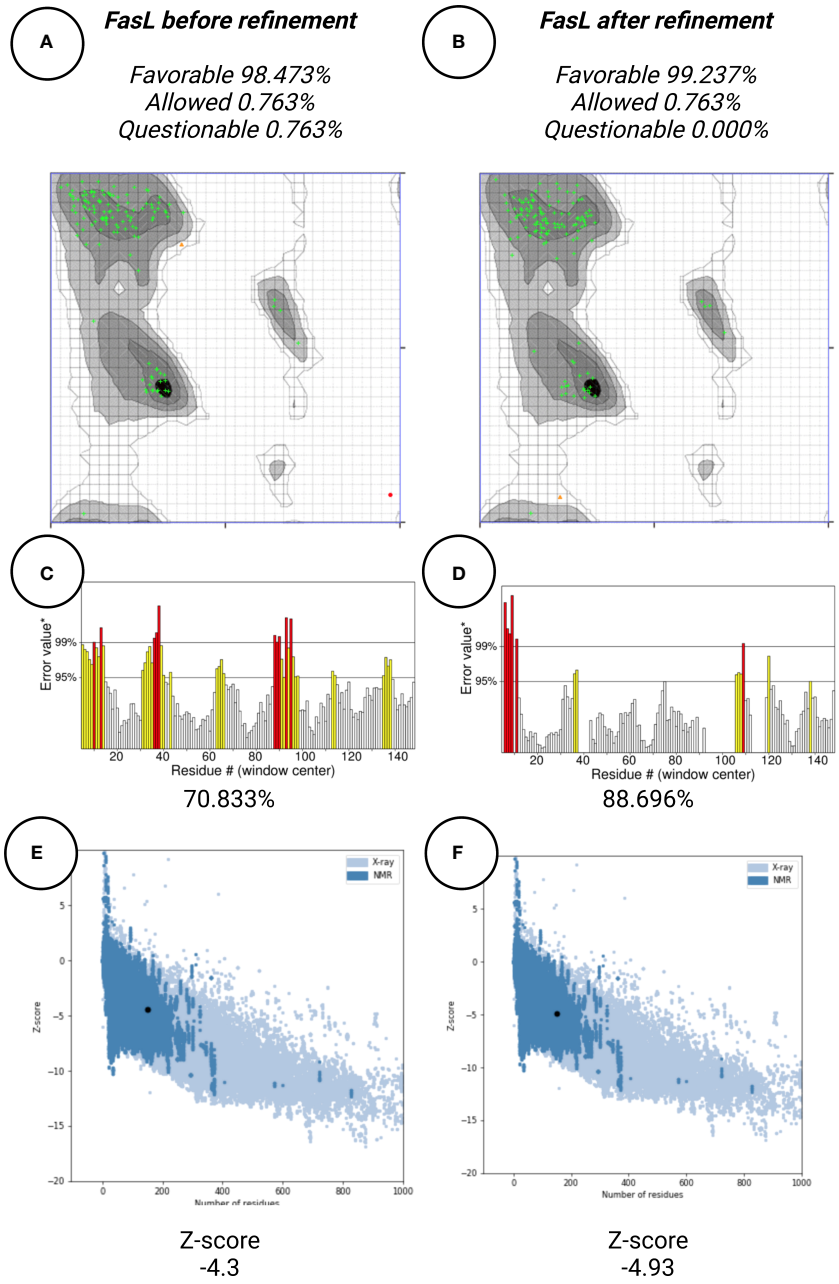

FIGURE 8
Protein quality verification for FasL tertiary structure. After refinement, FasL structure was favorable **(A, B)** In the Ramachandran plot, more residues are located in favorable regions. **(C, D)** ERRAT score was improved from 70.833% to 88.696%. A score over 80% shows the refined structure has good quality. **(E, F)** ProSA Z-score was improved from -4.3 to -4.93 which is within the acceptable range for structures with the same aminoacid length.

sFasL levels could be due to their consumption in the inflammatory phase of COVID-19 for neutrophil activity and recruitment in particular in the lungs. This phenomenon may indicate the increased activity of proteolytic enzymes such as MMPs or the alternative splicing of full-length Fas mRNA on receptor induction. However, further study is suggested (48).

On the other hand, lymphopenia and neutrophilia are found in patients with COVID-19. A previous study showed that neutrophils release sFasL, that activates apoptosis in some cellular subtypes expressing Fas (49, 50). sFasL promotes inflammatory feedback and overactivation of neutrophils from Type 2 Diabetes Mellitus (T2DM) patients without inducing

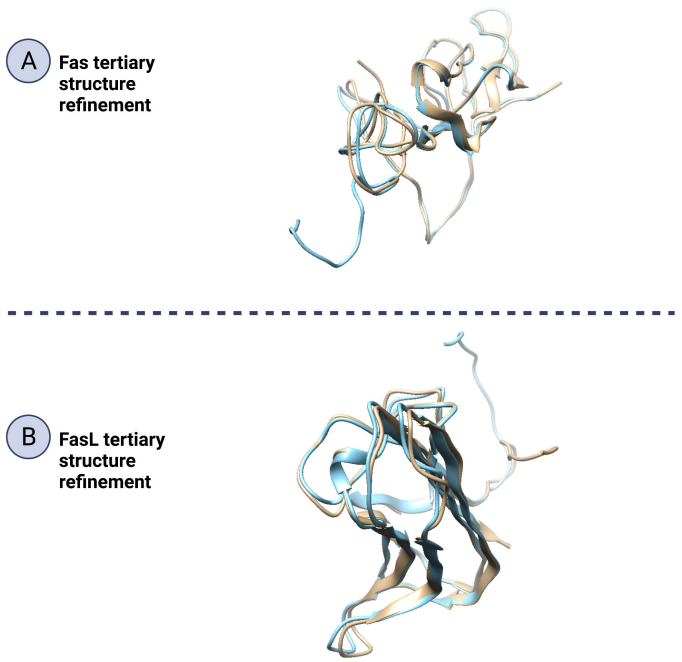

FIGURE 9
Refinement of Fas and FasL tertiary structure. Protein structure refinement is the determination and improving of a protein's structural properties. In this figure (**A**; Fas and **B**; FasL), by beige/blue colors, the initial and refined structure have been matched to show how the 3D structures, such as beta-sheets, alpha-helices and coils have been altered to improve the protein quality. Also, a significant portion of the refined structure is made of beta-sheets or alpha-helices indicating good structural stability.

apoptosis in these cells (4). Another research by Bellesi et al. showed that increased expression of Fas (CD95) in $CD4^+$ and $CD8^+$ lymphocytes was associated with a reduced proportion of naive events. The findings of their study indicated apoptosis and exhaustion of lymphocytes is induced by Fas during COVID-19 infection (10). Moreover, next-generation anti-sFasL therapy through inhalation can be used more specifically and directly in future studies. Interestingly, a previous study showed therapy by anti-FasL antibody preserves lymphocytes and virus-exclusive cellular immune feedback, confirming our suggestion (51). According to results of the present work, we think that neutrophilia and lymphopenia in severe-stage COVID-19 patients is related to the role of sFasL.

In addition, it has been demonstrated that Fas/FasL interactions play a role in immune cytotoxicity, affecting peripheral nerve damage and pain (52). Another study found that the concentration of sFasL was significantly associated with the neuropathy severity (53). Findings of the present work indicated that mFas expression has an inverse correlation with myalgia in patients with COVID-19. A recent work showed that serum sFas production is related to a higher risk of nerve injury in Guillain-Barré syndrome (GBS) patients. Also, other studies indicated that myalgia is the most prevalent pain-related symptom after COVID-19–induced GBS (54, 55). Taken together, we believe that Fas/FasL signaling may affect myalgia in COVID-19 cases. Also, analysis of disease severity in COVID-19 patients by lung CT-scan showed that sFas and sFasL proteins are negatively correlated with respiratory injury. Notably, previous research has demonstrated that Fas/FasL pathways and their common genetic variants are related to lung injury and an inflammatory response, which are in line with our findings (56, 57). This is the first evidence supporting a role for sFas and sFasL proteins in respiratory injury in COVID-19 patients.

Strength of this study is that, for the first time, we employed an interdisciplinary approach comprising various clinical findings, laboratory molecular tests, and Bioinformatics simulation (*in silico*) to evaluate Fas/FasL role in COVID-19 patients. We found that sFasL is a prognostic factor for mortality and severity of COVID-19 patients. Another major strength is the confirmation of previous findings regarding sFasL levels in COVID-19 (9) and the potential relation of sFasL levels to lung injury.

A limitation of this research was that it was a single-center study. Therefore, multi-center research with a larger sample size and age-matched participants may be needed to assess these results in COVID-19. Sampling for this study was performed at the beginning of the COVID-19 pandemic. Thus, our study does not include newer variants such as Omicron and delta. We suggest that future research evaluates these results by including

10.3389/fimmu.2022.947401

TABLE 3 Contact area for Fas/FasL complex.

Atom1	Atom2	Overlap	Distance
LEU 21.A CD2	SER 43.A CB	1.032	2.728
ARG 22.A CD	LYS 46.A CD	0.943	2.817
LEU 19.A CD1	LYS 16.A CE	0.934	2.826
THR 24.A OG1	ASP 35.A CG	0.917	2.423
LYS 17.A CD	GLU 13.A CG	0.887	2.873
ARG 22.A NH1	TYR 47.A N	0.826	2.454
SER 154.A OG	THR 36.A CG2	0.825	2.515
SER 156.A CB	TYR 37.A OH	0.817	2.523
LYS 17.A CE	GLU 13.A CG	0.803	2.957
ARG 22.A N	LEU 42.A O	0.709	2.351
LEU 21.A CD2	SER 43.A OG	0.702	2.638
ARG 22.A NH1	TYR 47.A CB	0.667	2.853
LYS 17.A CG	GLU 13.A CG	0.667	3.093
LYS 110.A CE	PRO 9.A CD	0.642	3.118
ARG 22.A NE	LYS 46.A CD	0.629	2.891
THR 24.A CB	ASP 35.A CG	0.609	3.151
THR 24.A OG1	ASP 35.A OD2	0.595	2.285
LYS 150.A CE	PRO 9.A CG	0.591	3.169
ARG 22.A O	LEU 42.A CB	0.591	2.709
LYS 110.A NZ	PRO 9.A CD	0.573	2.947
LYS 150.A NZ	PRO 9.A CG	0.545	2.975
THR 24.A CB	ASP 35.A CB	0.543	3.217
GLU 152.A OE2	THR 36.A O	0.446	2.394
ARG 22.A NH1	TYR 47.A CA	0.443	3.077
THR 24.A CB	ASP 35.A OD2	0.441	2.859
THR 122.A OG1	ILE 39.A CG2	0.414	2.926
LYS 17.A CD	GLU 13.A CD	0.362	3.398
GLU 152.A CG	THR 36.A CG2	0.352	3.408
ARG 22.A NH1	LEU 42.A CD2	0.335	3.185
THR 122.A CB	ILE 39.A CG2	0.323	3.437
THR 24.A OG1	ASP 35.A CB	0.303	3.037
GLU 152.A CD	THR 36.A O	0.298	3.002
LYS 110.A NZ	PRO 9.A CG	0.277	3.243
LYS 17.A CG	GLU 13.A CD	0.263	3.497
LYS 17.A CD	GLU 13.A OE2	0.23	3.07
THR 122.A OG1	ILE 39.A CD1	0.225	3.115
ARG 22.A CD	LYS 46.A CA	0.223	3.537
ARG 22.A O	LEU 42.A CD2	0.212	3.088
THR 122.A CB	ILE 39.A CG1	0.195	3.565
LEU 21.A CD2	SER 43.A CA	0.191	3.569
LEU 19.A CD1	LYS 16.A NZ	0.178	3.342
ARG 22.A CG	LEU 42.A CD2	0.156	3.604
ARG 22.A CZ	TYR 47.A N	0.136	3.114
ARG 22.A NH2	TYR 47.A O	0.129	2.931
ARG 22.A O	LEU 42.A CG	0.12	3.18
THR 122.A CG2	ILE 39.A CG2	0.115	3.645
SER 154.A CB	THR 36.A CG2	0.111	3.649
GLU 152.A CB	THR 36.A CG2	0.096	3.664

(Continued)

10.3389/fimmu.2022.947401

TABLE 3 Continued

Atom1	Atom2	Overlap	Distance
THR 122.A CB	ILE 39.A CD1	0.082	3.678
ARG 22.A CB	LEU 42.A CG	0.054	3.706
ARG 22.A CB	LEU 42.A CD2	0.053	3.707
ARG 22.A CA	LEU 42.A O	0.048	3.252
LEU 19.A CD2	ASN 55.A ND2	0.013	3.507
LEU 19.A CD1	GLY 44.A O	-0.008	3.308
LYS 17.A CB	GLU 13.A CD	-0.008	3.768
GLU 152.A CG	THR 36.A O	-0.008	3.308
GLU 152.A CG	THR 36.A CA	-0.01	3.77
GLU 152.A CD	THR 36.A CG2	-0.022	3.782
LEU 21.A CD2	LEU 14.A CD1	-0.04	3.8
SER 154.A CB	THR 36.A OG1	-0.043	3.383
ARG 22.A CD	LYS 46.A CE	-0.046	3.806
THR 24.A CG2	ASP 35.A OD2	-0.056	3.356
LEU 21.A CA	LEU 42.A O	-0.067	3.367
ARG 22.A CD	LEU 42.A CD2	-0.072	3.832
LYS 110.A CE	PRO 9.A CG	-0.08	3.84
THR 122.A OG1	ILE 39.A CG1	-0.093	3.433
THR 24.A OG1	ASP 35.A OD1	-0.094	2.974
LYS 17.A CB	GLU 13.A OE2	-0.099	3.399
LEU 19.A CB	GLY 44.A CA	-0.105	3.865
SER 154.A OG	THR 36.A CB	-0.113	3.453
ARG 22.A CD	LYS 46.A NZ	-0.114	3.634
LYS 148.A CE	PRO 8.A CG	-0.116	3.876
LYS 17.A CG	GLU 13.A OE2	-0.119	3.419
ARG 22.A CD	VAL 45.A O	-0.141	3.441
ARG 22.A CD	LYS 46.A CG	-0.147	3.907
ARG 22.A O	LEU 42.A O	-0.157	2.997
LYS 148.A CD	SER 6.A O	-0.171	3.471
ARG 22.A NH1	LYS 46.A CA	-0.189	3.709
LYS 148.A NZ	SER 6.A O	-0.19	3.25
LEU 21.A C	LEU 42.A O	-0.191	3.221
ARG 22.A CD	LYS 46.A CB	-0.198	3.958
LEU 19.A CD1	GLY 44.A CA	-0.206	3.966
ARG 22.A NH1	LYS 46.A C	-0.206	3.456
LYS 17.A NZ	GLU 13.A CG	-0.207	3.727
LYS 17.A CB	GLU 13.A CG	-0.209	3.969
SER 156.A OG	TYR 37.A OH	-0.214	3.134
LYS 17.A CE	GLU 13.A CB	-0.223	3.983
ARG 22.A CB	LEU 42.A O	-0.227	3.527
ARG 22.A NH1	TYR 47.A O	-0.238	3.298
SER 154.A OG	THR 36.A OG1	-0.247	3.167
THR 24.A N	ASP 35.A CB	-0.249	3.769
ARG 22.A NE	LYS 46.A CB	-0.251	3.771
ARG 22.A NE	LYS 46.A CA	-0.255	3.775
LEU 21.A CA	SER 43.A CA	-0.266	4.026
LYS 17.A CE	GLU 13.A CD	-0.271	4.031
THR 24.A O	THR 36.A OG1	-0.297	3.177

(Continued)

10.3389/fimmu.2022.947401

TABLE 3 Continued

Atom1	Atom2	Overlap	Distance
ARG 22.A N	LEU 42.A C	-0.299	3.549
SER 156.A CB	TYR 37.A CZ	-0.305	3.795
THR 24.A CA	ASP 35.A CB	-0.307	4.067
LYS 150.A NZ	PRO 9.A CB	-0.32	3.84
ARG 22.A C	LEU 42.A CD2	-0.321	3.811
THR 122.A CB	ILE 39.A CB	-0.33	4.09
ARG 22.A CZ	LYS 46.A CA	-0.345	3.835
GLU 152.A CG	THR 36.A CB	-0.35	4.11
LYS 150.A CE	PRO 9.A CD	-0.352	4.112
THR 24.A CG2	ASP 35.A CG	-0.352	4.112
LYS 148.A CE	PRO 8.A CD	-0.353	4.113
ARG 22.A C	LEU 42.A CB	-0.356	3.846
ARG 22.A NE	LYS 46.A CG	-0.368	3.888
LEU 21.A CD1	LEU 14.A CD1	-0.375	4.135
LEU 19.A CD1	LYS 16.A CD	-0.377	4.137
ARG 22.A CZ	LYS 46.A CD	-0.383	3.873
ARG 22.A NH1	TYR 47.A C	-0.393	3.643
ARG 22.A NH2	TYR 47.A N	-0.393	3.673
SER 154.A CB	THR 36.A CB	-0.395	4.155
ARG 22.A O	LEU 42.A CA	-0.396	3.696
ARG 22.A CG	LEU 42.A CG	-0.398	4.158

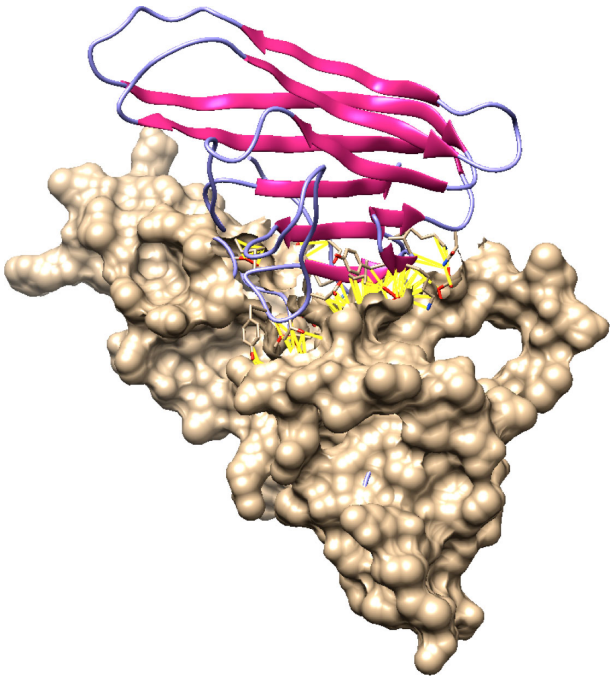

FIGURE 10
Docked Fas/FasL complex. In this figure, molecular docking has been shown. Docking is the Bioinformatics assessment of how two proteins (Fas and FasL) fit best as a complex. Fas and FasL are shown with distinct colors (purple and beige). Fas/FasL complex contacts are highlighted with yellow lines.

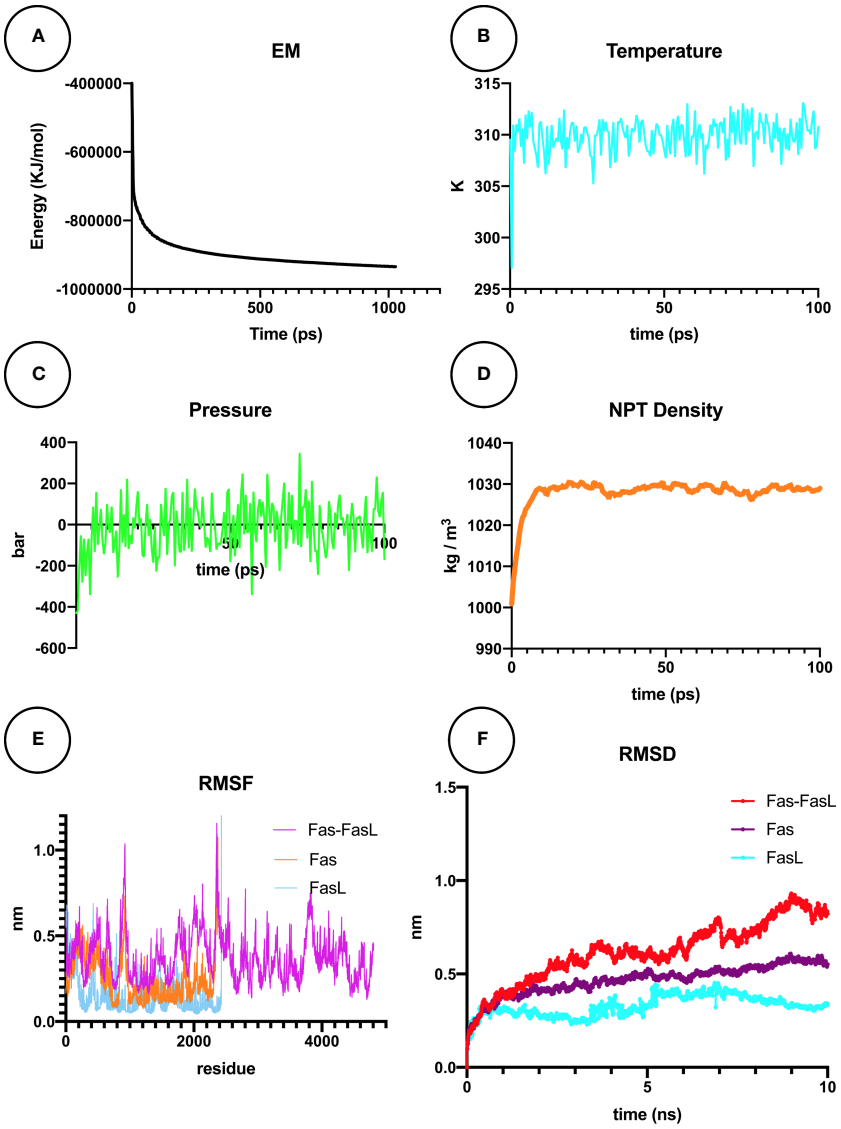

FIGURE 11
Molecular dynamics simulation (MDS) analyses for Fas/FasL in blood MDS is a simulation approach for analysis of the physical movement of atoms. Here, a biological system of Fas/FasL was virtually set up and equilibrated in blood-like conditions, and was allowed a limited time to evolve. **(A)** Energy minimization (EM) was set-up for the Fas/FasL system. **(B)** During the NVT equilibration, the temperature was matched to blood-like conditions. **(C)** During the NPT equilibration, the pressure reached 0 bar. **(D)** Density of the Fas/FasL system was also equilibrated in this step. After production MDS of the Fas/FasL system: **(E)** Root-mean square fluctuation (RMSF) analysis did not show fluctuation in the Fas/FasL system and the proteins did not denature. **(F)** Root-mean square deviation (RMSD) values shows that the Fas/FasL complex reached stability within the blood-like simulation conditions.

TABLE 4 Binding analysis for molecular dynamics study of Fas/FasL.

Time (ns)	1	2	3	4	5	6	7	8	9	10	Average binding energy (kcal.mol^{-1})
Normal	-8.8	-8.9	-8.8	-9.1	-10.2	-9.9	-10.4	-11.0	-10.2	-10.7	-9.8
Fever	-7.9	-7.4	-7.2	-7.7	-8.7	-9.2	-8.4	-8.3	-8.4	-7.9	-8.11
Hyponatremia	-10.1	-9.8	-9.5	-10.3	-11.6	-11.2	-10.9	-10.8	-11.0	-11.9	-10.71

other variants of COVID-19. Another restriction of our work was that we could not obtain bronchoalveolar lavage (BAL) fluid. Exploring of sFasL in the BAL fluid in future studies could lead to major advancements. Overall, these limitations do not significantly impact the results of the present study, and our study provides an essential clue for further studies in the absence of possible disruptive factors such as multiple vaccinations. We recommend that future research evaluates the role of sFasL in different variants of COVID-19 to further confirm these results.

COVID-19 presents itself through complicated multi-system symptoms, affecting a wide range of body systems (3). Although different vaccines have been shown to be effective in slowing the COVID-19 pandemic, they have not been adequately successful in providing a permanent immunoprotection. Therefore, pharmacotherapy of COVID-19, in particular by targeting novel inflammation mediators, such as Fas/FasL, should still be studied (8, 58).

Conclusions

Fas/FasL pathways could play a role in the mediation of hyperinflammatory cytokine response in COVID-19 by being consumed through an interaction with MMPs, and the novel triangle of viral entry, cytokine storm, and multi-system damage. We found the role of Fas/FasL may depend on the disease stage and severity of COVID-19. Our *in silico* analysis confirmed that, alterations in the blood of COVID-19 patients could change Fas/FasL interactions at the molecular level. Preclinical and clinical research testing Fas/FasL-mediating drugs such as anti-sFasL for COVID-19 treatment may aid vaccination efforts to eradicate the COVID-19 pandemic. The findings of the present study indicate that sFasL prognostics severity and mortality in COVID-19 patients. This is the first report describing that the serum sFasL protein is a severity and mortality prognostic marker for the clinical management and therapy of COVID-19 patients.

Data availability statement

Data are available from corresponding author only on reasonable request.

Ethics statement

This work was approved by Ethics Committee of Babol University of Medical Sciences, Babol, Iran (IR.MUBABOL.REC.1399.198, IR.MUBABOL.REC.1399.433, IR.MUBABOL.HRI.REC.1399.102). The patients/participants provided their written informed consent to participate in this study.

Author contributions

AA designed and supervised the study, and prepared the initial and final manuscript. KS and AA conceptualized the study and prepared the initial draft. KS, MS, and MA collected samples. KS, MS, and SM performed the PCR and ELISA experiments. KS performed *in silico* molecular dynamics simulation and docking experiments. AA and KS prepared the final draft. NM and M O critically appraised the manuscript. MJ helped with diagnosis of COVID-1 9 patients. All authors contributed to the article and approved the submitted version.

Funding

This work was supported by National Elite Foundation of Iran (Grant NO. 1640/151). Also, the present study was funded by the Deputy of Research and Technology (Grant NO. 9909808), Babol University of Medical Sciences, Babol, Iran.

Acknowledgments

We thank the National Elite Foundation, Mazandaran Province Branch from Iran. We appreciate the assistance of Dr. Ahmad Ghasemi, (MD., Radiologist) in interpreting the lung CT scan of COVID-19 patients in this manuscript. Figures created with BioRender.com.

Conflict of interest

The authors declare that the research was conducted in the absence of any commercial or financial relationships that could be construed as a potential conflict of interest.

Publisher's note

All claims expressed in this article are solely those of the authors and do not necessarily represent those of their affiliated organizations, or those of the publisher, the editors and the reviewers. Any product that may be evaluated in this article, or claim that may be made by its manufacturer, is not guaranteed or endorsed by the publisher.

Supplementary material

The Supplementary Material for this article can be found online at: https://www.frontiersin.org/articles/10.3389/fimmu.2022.947401/full#supplementary-material

References

1. Leduc JW, Barry MA. SARS, the first pandemic of the 21st century. *Emerg Infect Dis* (2004) 10:e26–6. doi: 10.3201/eid1011.040797_02

2. Da Costa VG, Moreli ML, Saivish MV. The emergence of SARS, MERS and novel SARS-2 coronaviruses in the 21st century. *Arch Virol* (2020) 165:1517–26. doi: 10.1007/s00705-020-04628-0

3. Saleki K, Banazadeh M, Saghazadeh A, Rezaei N. The involvement of the central nervous system in patients with COVID-19. *Rev Neurosci* (2020) 31:453–6. doi: 10.1515/revneuro-2020-0026

4. Margaryan S, Witkowicz A, Arakelyan A, Partyka A, Karabon L, Manukyan G. sFasL-mediated induction of neutrophil activation in patients with type 2 diabetes mellitus. *PloS One* (2018) 13:e0201087. doi: 10.1371/journal.pone.0201087

5. Tomar B, Anders H-J, Desai J, Mulay SR. Neutrophils and neutrophil extracellular traps drive necroinflammation in COVID-19. *Cells* (2020) 9:1383. doi: 10.3390/cells9061383

6. Chen G, Wu D, Guo W, Cao Y, Huang D, Wang H, et al. Clinical and immunological features of severe and moderate coronavirus disease 2019. *J Clin Invest* (2020) 130:2620–9. doi: 10.1172/JCI137244

7. Chen N, Zhou M, Dong X, Qu J, Gong F, Han Y, et al. Epidemiological and clinical characteristics of 99 cases of 2019 novel coronavirus pneumonia in wuhan, China: a descriptive study. *Lancet* (2020) 395:507–13. doi: 10.1016/S0140-6736(20)30211-7

8. Saleki K, Yaribash S, Banazadeh M, Hajihosseinlou E, Gouravani M, Saghazadeh A, et al. Interferon therapy in patients with SARS, MERS, and COVID-19: A systematic review and meta-analysis of clinical studies. *Eur J Pharmacol* (2021) 906:174248. doi: 10.1016/j.ejphar.2021.174248

9. Schweizer TA, Mairpady Shambat S, Vulin C, Hoeller S, Acevedo C, Huemer M, et al. Blunted sFasL signalling exacerbates TNF-driven neutrophil necroptosis in critically ill COVID-19 patients. *Clin Transl Immunol* (2021) 10:e1357. doi: 10.1002/cti2.1357

10. Bellesi S, Metafuni E, Hohaus S, Maiolo E, Marchionni F, D'innocenzo S, et al. Increased CD95 (Fas) and PD-1 expression in peripheral blood T lymphocytes in COVID-19 patients. *Br J Haematol* (2020) 191:207–11. doi: 10.1111/bjh.17034

11. Giamarellos-Bourboulis EJ, Netea MG, Rovina N, Akinosoglou K, Antoniadou A, Antonakos N, et al. Complex immune dysregulation in COVID-19 patients with severe respiratory failure. *Cell Host Microbe* (2020) 27:992–1000.e1003. doi: 10.1016/j.chom.2020.04.009

12. Saleki K, Banazadeh M, Miri NS, Azadmehr A. Triangle of cytokine storm, central nervous system involvement, and viral infection in COVID-19: The role of sFasL and neuropilin-1. *Rev Neurosci* (2022) 33:147–60. doi: 10.1515/revneuro-2021-0047

13. Mairpady Shambat S, Gómez-Mejia A, Schweizer TA, Huemer M, Chang CC, Acevedo C, et al. Hyperinflammatory environment drives dysfunctional myeloid cell effector response to bacterial challenge in COVID-19. *PloS Pathog* (2022) 18:e1010176. doi: 10.1371/journal.ppat.1010176

14. Lin J-C, Chen Z-H, Chen X-D, Wang S-B. Circulating sFasL levels predict the severity and outcome of burn injury: A prospective observational study. *J Surg Res* (2021) 265:1–10. doi: 10.1016/j.jss.2021.01.012

15. André S, Picard M, Cezar R, Roux-Dalvai F, Alleaume-Butaux A, Soundaramourty C, et al. T Cell apoptosis characterizes severe covid-19 disease. *Cell Death Differ* (2022) 29:1486–99. doi: 10.1038/s41418-022-00936-x

16. Wallach-Dayan SB, Petukhov D, Ahdut-Hacohen R, Richter-Dayan M, Breuer R. sFasL–the key to a riddle: Immune responses in aging lung and disease. *Int J Mol Sci* (2021) 22:2177. doi: 10.3390/ijms22042177

17. Kessel C, Vollenberg R, Masjosthusmann K, Hinze C, Wittkowski H, Debaugnies F, et al. Discrimination of COVID-19 from inflammation-induced cytokine storm syndromes using disease-related blood biomarkers. *Arthritis Rheumatol* (2021) 73:1791–9. doi: 10.1002/art.41763

18. Albertoni G, Arnoni CP, Latini FRM, Andrade SS, Araújo PRB, Rodrigues FK, et al. Altered of apoptotic markers of both extrinsic and intrinsic pathways induced by hepatitis c virus infection in peripheral blood mononuclear cells. *Virol J* (2012) 9:1–8. doi: 10.1186/1743-422X-9-314

19. Coppola A, Tomasello L, Pitrone M, Cillino S, Richiusa P, Pizzolanti G, et al. Human limbal fibroblast-like stem cells induce immune-tolerance in autoreactive T lymphocytes from female patients with hashimoto's thyroiditis. *Stem Cell Res Ther* (2017) 8:154. doi: 10.1186/s13287-017-0611-5

20. Oladnabi M, Bagheri A, Kanavi MR, Azadmehr A, Kianmehr A. Extremely low frequency-pulsed electromagnetic fields affect proangiogenic-related gene expression in retinal pigment epithelial cells. *Iranian J Basic Med Sci* (2019) 22:128. doi: 10.22038/IJBMS.2018.25023.6214

21. Abraham MJ, Murtola T, Schulz R, Páll S, Smith JC, Hess B, et al. GROMACS: High performance molecular simulations through multi-level parallelism from laptops to supercomputers. *SoftwareX* (2015) 1:19–25. doi: 10.1016/j.softx.2015.06.001

22. Van Der Spoel D, Lindahl E, Hess B, Groenhof G, Mark AE, Berendsen HJC. GROMACS: Fast, flexible, and free. *J Comput Chem* (2005) 26:1701–18. doi: 10.1002/jcc.20291

23. Humphrey W, Dalke A, Schulten K. VMD: Visual molecular dynamics. *J Mol Graphics* (1996) 14:33–8. doi: 10.1016/0263-7855(96)00018-5

24. Kaminski GA, Friesner RA, Tirado-Rives J, Jorgensen WL. Evaluation and reparametrization of the OPLS-AA force field for proteins *via* comparison with accurate quantum chemical calculations on peptides. *J Phys Chem B* (2001) 105:6474–87. doi: 10.1021/jp003919d

25. Sambasivarao SV, Acevedo O. Development of OPLS-AA force field parameters for 68 unique ionic liquids. *J Chem Theory Comput* (2009) 5:1038–50. doi: 10.1021/ct900009a

26. De La Flor J, Marshall A, Biscotti B. Hyponatremia in COVID-19 infection-should only think about SIADH. *J Clin Nephrol Ren Care* (2020) 6:057. doi: 10.23937/2572-3286.1510057

27. Jin A, Yan B, Hua W, Feng D, Xu B, Liang L, et al. Clinical characteristics of patients diagnosed with COVID-19 in Beijing. *Biosafety Health* (2020) 2:104–11. doi: 10.1016/j.bsheal.2020.05.003

28. Ruiz-Sánchez JG, Núñez-Gil IJ, Cuesta M, Rubio MA, Maroun-Eid C, Arroyo-Espliguero R, et al. Prognostic impact of hyponatremia and hypernatremia in COVID-19 pneumonia. A HOPE-COVID-19 (Health outcome predictive evaluation for COVID-19) registry analysis. *Front Endocrinol* (2020) 11. doi: 10.3389/fendo.2020.599255

29. Akbar MR, Pranata R, Wibowo A, Irvan, Sihite TA, Martha JW. The prognostic value of hyponatremia for predicting poor outcome in patients with COVID-19: A systematic review and meta-analysis. *Front Med* (2021) 8:1486–1499. doi: 10.3389/fmed.2021.666949

30. Gheorghe G, Ilie M, Bungau S, Stoian AMP, Bacalbasa N, Diaconu CC. Is there a relationship between COVID-19 and hyponatremia? *Medicina (Kaunas Lithuania)* (2021) 57:55. doi: 10.3390/medicina57010055

31. Machiraju PK, Alex NM, Safinaaz, Vadamalai V. Hyponatremia in coronavirus disease-19 patients: A retrospective analysis. *Can J Kidney Health Dis* (2021) 8:20543581211067069. doi: 10.1177/20543581211067069

32. Xue LC, Rodrigues JP, Kastritis PL, Bonvin AM, Vangone A. PRODIGY: a web server for predicting the binding affinity of protein–protein complexes. *Bioinformatics* (2016) 32:3676–8. doi: 10.1093/bioinformatics/btw514

33. Mishra P, Pandey CM, Singh U, Gupta A, Sahu C, Keshri A. Descriptive statistics and normality tests for statistical data. *Ann Cardiac Anaesth* (2019) 22:67–72. doi: 10.4103/aca.ACA_157_18

34. Roy K, Kar S, Das RN. "Chapter 10 - other related techniques,". In: K Roy, S Kar and RN Das, editors. *Understanding the basics of QSAR for applications in pharmaceutical sciences and risk assessment*. Boston: Academic Press (2015). p. 357–425.

35. Roy K, Kar S, Das RN. "Chapter 5 - computational chemistry,". In: K Roy, S Kar and RN Das., editors. *Understanding the basics of QSAR for applications in pharmaceutical sciences and risk assessment*. Boston: Academic Press (2015). p. 151–89.

36. Kang S-M, Hofmann A, Le D, Springer ML, Stock PG, Blau HM, et al. Immune response and myoblasts that express fas ligand. *Science* (1997) 278:1322–4. doi: 10.1126/science.278.5341.1322

37. Seino K, Kayagaki N, Takeda K, Fukao K, Okumura K, Yagita H. Contribution of fas ligand to T cell-mediated hepatic injury in mice. *Gastroenterology* (1997) 113:1315–22. doi: 10.1053/gast.1997.v113.pm9322527

38. Kennedy NJ, Kataoka T, Tschopp J, Budd RC. Caspase activation is required for T cell proliferation. *J Exp Med* (1999) 190:1891–6. doi: 10.1084/jem.190.12.1891

39. Matsushita K, Wu Y, Qiu J, Lang-Lazdunski L, Hirt L, Waeber C, et al. Fas receptor and neuronal cell death after spinal cord ischemia. *J Neurosci* (2000) 20:6879–87. doi: 10.1523/JNEUROSCI.20-18-06879.2000

40. Casha S, Yu W, Fehlings M. Oligodendroglial apoptosis occurs along degenerating axons and is associated with FAS and p75 expression following spinal cord injury in the rat. *Neuroscience* (2001) 103:203–18. doi: 10.1016/S0306-4522(00)00538-8

41. Desbarats J, Birge RB, Mimouni-Rongy M, Weinstein DE, Palerme J-S, Newell MK. Fas engagement induces neurite growth through ERK activation and p35 upregulation. *Nat Cell Biol* (2003) 5:118–25. doi: 10.1038/ncb916

42. Parra B, Lin MT, Stohlman SA, Bergmann CC, Atkinson R, Hinton DR. Contributions of fas-fas ligand interactions to the pathogenesis of mouse hepatitis virus in the central nervous system. *J Virol* (2000) 74:2447–50. doi: 10.1128/JVI.74.5.2447-2450.2000

43. Bortolami M, Kotsafti A, Cardin R, Farinati F. Fas/FasL system, IL-1β expression and apoptosis in chronic HBV and HCV liver disease. *J Viral Hepat* (2008) 15:515–22. doi: 10.1111/j.1365-2893.2008.00974.x

44. Schulte-Schrepping J, Reusch N, Paclik D, Baßler K, Schlickeiser S, Zhang B, et al. Severe COVID-19 is marked by a dysregulated myeloid cell compartment. *Cell* (2020) 182:1419–1440.e1423. doi: 10.1016/j.cell.2020.08.001

45. Zhu L, Yang P, Zhao Y, Zhuang Z, Wang Z, Song R, et al. Single-cell sequencing of peripheral mononuclear cells reveals distinct immune response landscapes of COVID-19 and influenza patients. *Immunity* (2020) 53:685–696.e683. doi: 10.1016/j.immuni.2020.07.009

46. Zakaria MM, Derbala SA, Salem AE, El-Agroudy AE, El-Tantawy FM. Inflammatory markers in chronic kidney disease and end stage renal disease patients. *Mol Biol Rep* (2021) 48:6857–62. doi: 10.1007/s11033-021-06684-4

47. Leonardi AJ, Proenca RB. Akt-fas to quell aberrant T cell differentiation and apoptosis in covid-19. *Front Immunol* (2020) 11:600405–5. doi: 10.3389/fimmu.2020.600405

48. Felderhoff-Mueser U, Bührer C, Groneck P, Obladen M, Bartmann P, Heep A. Soluble fas (CD95/Apo-1), soluble fas ligand, and activated caspase 3 in the cerebrospinal fluid of infants with posthemorrhagic and nonhemorrhagic hydrocephalus. *Pediatr Res* (2003) 54:659–64. doi: 10.1203/01.PDR.0000084114.83724.65

49. Serrao KL, Fortenberry JD, Owens ML, Harris FL, Brown L. Neutrophils induce apoptosis of lung epithelial cells via release of soluble fas ligand. *Am J Physiol.-Lung Cell Mol Physiol* (2001) 280:L298–305. doi: 10.1152/ajplung.2001.280.2.L298

50. Yamamoto TN, Lee P-H, Vodnala SK, Gurusamy D, Kishton RJ, Yu Z, et al. T Cells genetically engineered to overcome death signaling enhance adoptive cancer immunotherapy. *J Clin Invest* (2019) 129:1551–65. doi: 10.1172/JCI121491

51. Poonia B., Salvato M.S., Yagita H., Maeda T., Okumura K., Pauza C.D., et al. Treatment with anti-FasL antibody preserves memory lymphocytes and virus-specific cellular immunity in macaques challenged with simian immunodeficiency virus. *Blood* (2009) 114:1196–1204. doi: 10.1002/rmv.2273

52. Davies AJ, Rinaldi S, Costigan M, Oh SB. Cytotoxic immunity in peripheral nerve injury and pain. *Front Neurosci* (2020) 14. doi: 10.3389/fnins.2020.00142

53. Mondal A, Sen S, Chanda D, Kundu S, Chatterjee M, Mukherjee S. Evaluation of diabetic polyneuropathy in type 2 diabetes mellitus by nerve conduction study and association of severity of neuropathy with serum sFasL level. *Indian J Endocrinol Metab* (2012) 16:S465–7. doi: 10.4103/2230-8210.104133

54. Islam Z, Jahan I, Ahammad RU, Shahnaij M, Nahar S, Mohammad QD. FAS promoter polymorphisms and serum sFas level are associated with increased risk of nerve damage in Bangladeshi patients with Guillain-Barré syndrome. *PloS One* (2018) 13:e0192703–e0192703. doi: 10.1371/journal.pone.0192703

55. Paliwal VK, Garg RK, Gupta A, Tejan N. Neuromuscular presentations in patients with COVID-19. *Neurol Sci* (2020) 41:3039–56. doi: 10.1007/s10072-020-04708-8

56. Glavan BJ, Holden TD, Goss CH, Black RA, Neff MJ, Nathens AB, et al. Genetic variation in the FAS gene and associations with acute lung injury. *Am J Respir Crit Care Med* (2011) 183:356–63. doi: 10.1164/rccm.201003-0351OC

57. Nagamine Y, Tojo K, Yazawa T, Takaki S, Baba Y, Goto T, et al. Inhibition of prolyl hydroxylase attenuates fas ligand–induced apoptosis and lung injury in mice. *Am J Respir Cell Mol Biol* (2016) 55:878–88. doi: 10.1165/rcmb.2015-0266OC

58. Mohseni Afshar Z, Babazadeh A, Janbakhsh A, Afsharian M, Saleki K, Barary M, et al. Vaccine-induced immune thrombotic thrombocytopenia after vaccination against covid-19: A clinical dilemma for clinicians and patients. *Rev Med Virol* (2022) 32:e2273. doi: 10.1002/rmv.2273

frontiers | Frontiers in Immunology

TYPE Original Research
PUBLISHED 06 September 2022
DOI 10.3389/fimmu.2022.947021

Check for updates

OPEN ACCESS

EDITED BY
Edwin Bölke,
Heinrich Heine University of Düsseldorf, Germany

REVIEWED BY
Jean-Pierre Routy,
McGill University, Canada
Pinkus Tober-Lau,
Charité University Medicine Berlin, Germany

*CORRESPONDENCE
Zabrina L. Brumme
zbrumme@sfu.ca

†These authors have contributed equally to this work

‡These authors have contributed equally to this work and share senior authorship

SPECIALTY SECTION
This article was submitted to Viral Immunology, a section of the journal Frontiers in Immunology

RECEIVED 18 May 2022
ACCEPTED 16 August 2022
PUBLISHED 06 September 2022

CITATION
Lapointe HR, Mwimanzi F, Cheung PK, Sang Y, Yaseen F, Kalikawe R, Datwani S, Waterworth R, Umviligihozo G, Ennis S, Young L, Dong W, Kirkby D, Burns L, Leung V, Holmes DT, DeMarco ML, Simons J, Matic N, Montaner JSG, Brumme CJ, Prystajecky N, Niikura M, Lowe CF, Romney MG, Brockman MA and Brumme ZL (2022) Serial infection with SARS-CoV-2 Omicron BA.1 and BA.2 following three-dose COVID-19 vaccination.
Front. Immunol. 13:947021.
doi: 10.3389/fimmu.2022.947021

Serial infection with SARS-CoV-2 Omicron BA.1 and BA.2 following three-dose COVID-19 vaccination

Hope R. Lapointe[1†], Francis Mwimanzi[2†], Peter K. Cheung[1,2], Yurou Sang[2], Fatima Yaseen[3], Rebecca Kalikawe[2], Sneha Datwani[2], Rachel Waterworth[2], Gisele Umviligihozo[2], Siobhan Ennis[2], Landon Young[4], Winnie Dong[1], Don Kirkby[1], Laura Burns[5], Victor Leung[4,5,6], Daniel T. Holmes[5,6], Mari L. DeMarco[5,6], Janet Simons[5,6], Nancy Matic[4,5,6], Julio S.G. Montaner[1,7], Chanson J. Brumme[1,7], Natalie Prystajecky[6,8], Masahiro Niikura[2], Christopher F. Lowe[4,5,6], Marc G. Romney[4,5,6‡], Mark A. Brockman[1,2,3‡] and Zabrina L. Brumme[1,2*‡]

[1]British Columbia Centre for Excellence in HIV/AIDS, Vancouver, BC, Canada, [2]Faculty of Health Sciences, Simon Fraser University, Burnaby, BC, Canada, [3]Department of Molecular Biology and Biochemistry, Simon Fraser University, Burnaby, BC, Canada, [4]Division of Medical Microbiology and Virology, St. Paul's Hospital, Vancouver, BC, Canada, [5]Department of Pathology and Laboratory Medicine, Providence Health Care, Vancouver, BC, Canada, [6]Department of Pathology and Laboratory Medicine, University of British Columbia, Vancouver, BC, Canada, [7]Department of Medicine, University of British Columbia, Vancouver, BC, Canada, [8]British Columbia Centre for Disease Control Public Health Laboratory, Vancouver, BC, Canada

SARS-CoV-2 Omicron infections are common among individuals who are vaccinated or have recovered from prior variant infection, but few reports have immunologically assessed serial Omicron infections. We characterized SARS-CoV-2 humoral responses in an individual who acquired laboratory-confirmed Omicron BA.1.15 ten weeks after a third dose of BNT162b2, and BA.2 thirteen weeks later. Responses were compared to 124 COVID-19-naive vaccinees. One month post-second and -third vaccine doses, the participant's wild-type and BA.1-specific IgG, ACE2-displacement and virus neutralization activities were average for a COVID-19-naive triple-vaccinated individual. BA.1 infection boosted the participant's responses to the cohort ≥95th percentile, but even this strong "hybrid" immunity failed to protect against BA.2. Reinfection increased BA.1 and BA.2-specific responses only modestly. Though vaccines clearly protect against severe disease, results highlight the continued importance of maintaining additional protective measures to counteract the immune-evasive Omicron variant, particularly as vaccine-induced immune responses naturally decline over time.

KEYWORDS

COVID-19, vaccine, Omicron variant, reinfection, humoral immunity

Introduction

SARS-CoV-2 infections, predominantly fueled by the Omicron (B.1.1.529) variant, are increasingly common among individuals who are vaccinated and/or have recovered from prior infections (1–3). Globally, the highly transmissible and immune-evasive Omicron variant has rapidly overtaken the previously dominant Delta variant (3–7), and the original Omicron BA.1 strain is being outcompeted by newer Omicron sub-lineages BA.2, BA.3, BA.4 and BA.5 (8, 9). In British Columbia (BC), Canada, Omicron BA.1 had overtaken Delta by December 2021, and BA.2 had largely outcompeted BA.1 by March 2022 (10, 11).

COVID-19 vaccine coverage in BC is relatively high, with 93%, 90% and 57% of individuals aged 12 years or older having received one, two and three COVID-19 immunizations, respectively, by May 2022 (12). Persons at elevated risk of severe COVID-19 were also eligible for fourth doses at this time (13). Despite this, the province experienced fifth and sixth waves of COVID-19, dominated by BA.1 and BA.2, respectively, as public health measures were gradually relaxed (10, 11). Indeed, it is estimated that between December 2021 and March 2022, nearly half of British Columbians experienced a SARS-CoV-2 infection, likely due to Omicron (14, 15).

Several reports have examined post-vaccination Omicron infections, or Omicron reinfections following exposure to prior variants (16–23), but we are aware of only one study that assessed repeat Omicron infection incidence through viral genomic surveillance (24). The prior study however did not measure immune responses (24). In fact, at the time of writing, no studies to our knowledge appear to have investigated vaccine- and infection-induced immune responses after serial Omicron infections. Here, we longitudinally characterize SARS-CoV-2 humoral responses in an individual who experienced serial BA.1 and BA.2 Omicron infections following three-dose COVID-19 mRNA vaccination. Responses were compared to those of 124 COVID-19-naive vaccinees over the same period. Taken together with existing literature, our results suggest that vaccination provides limited protection against infection and/or reinfection by Omicron variants, though the fact that the individual's symptoms were not serious enough to require hospitalization demonstrates that vaccination was nevertheless effective in its primary goal of preventing severe disease.

Methods

Observational COVID-19 vaccine cohort and SARS-CoV-2 infection monitoring

In December 2020, we established a prospective longitudinal study in Vancouver, Canada, to examine SARS-CoV-2 specific humoral immune responses following vaccination with BNT162b2 (Comirnaty; BioNTech/Pfizer) or mRNA-1273 (Spikevax; Moderna) in a cohort of adults aged 24-98 years [described in (25, 26)]. Serum and plasma were collected longitudinally up to 6 months following the third dose (Figure 1A). At each visit, serum was tested for the presence of SARS-CoV-2 anti-nucleocapsid (N) antibodies, which indicate seroconversion following infection, using the Elecsys Anti-SARS-CoV-2 assay on a Cobas e601 module analyzer (Roche Diagnostics). In addition to the case participant, immune measures from a comparison group of 124 participants of this cohort, who remained anti-N seronegative up until at least one month post-third vaccine dose, are included for context.

Ethics approval

All participants or their authorized substitute decision makers provided written informed consent. This study was approved by the University of British Columbia/Providence Health Care and Simon Fraser University Research Ethics Boards (protocol H20-03906).

SARS-CoV-2 diagnostics and lineage confirmation

Diagnostic samples from the case participant's two SARS-CoV-2 infections were tested at the St. Paul's Hospital Virology Laboratory using the cobas® SARS-CoV-2 Test which targets conserved regions within the Orf1a/b and E genes (Roche Diagnostics) followed by screening using a real-time reverse transcription (RT)-PCR based algorithm for SARS-CoV-2 lineage classification that is frequently updated to detect emerging variants (27, 28). Following this, the diagnostic samples were subjected to full-genome SARS-CoV-2 sequencing in two independent laboratories: the BC Centre for Disease Control, the provincial laboratory that performs all SARS-CoV-2 sequencing for epidemiological surveillance, and the BC Centre for Excellence in HIV/AIDS. Both laboratories use the Illumina platform. The SARS-CoV-2 full genome sequences for the participant's BA.1.15 and subsequent BA.2 infections are available in GISAID (Accession IDs EPI_ISL_12767799 and EPI_ISL_12662303, respectively) and in Genbank (Accession Numbers OP237526 and OP237527).

Binding antibody assays

We quantified anti-Spike Receptor Binding Domain (RBD) binding IgG concentrations in serum using the V-plex SARS-CoV-2 (IgG) ELISA kit (Panel 22, Meso Scale Diagnostics), which features wild-type and Omicron BA.1 RBD antigens. For a subset of participants, Anti-Spike binding IgG concentrations in serum were also quantified using the V-plex SARS-CoV-2 (IgG)

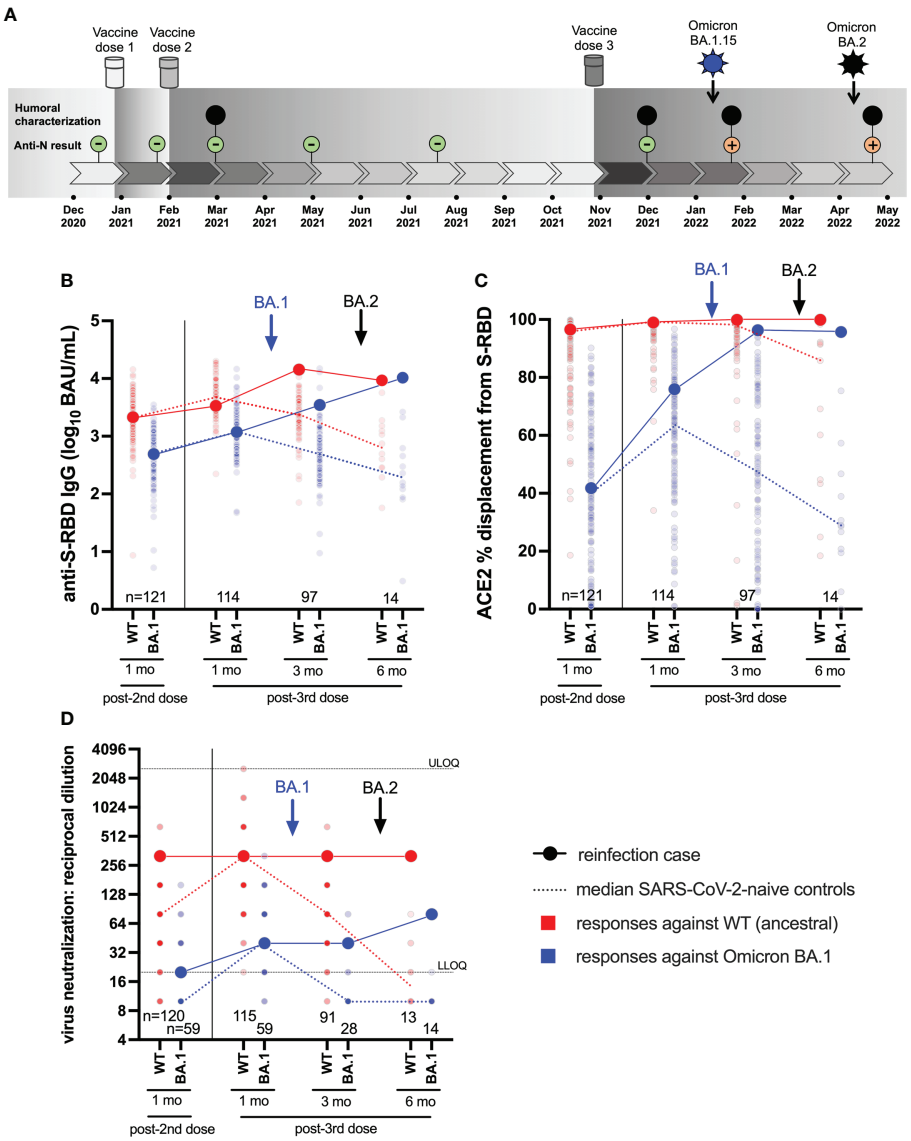

FIGURE 1
Case participant history and longitudinal humoral responses against wild-type and Omicron BA.1 SARS-CoV-2. Panel **(A)** Case participant timeline. Immunizations and SARS-CoV-2 Omicron infection history are shown at the top. Longitudinal SARS-CoV-2 anti-N serology results are shown in small green (anti-N negative) or orange (anti-N positive) circles. Large black circles denote time points where additional humoral functions, shown in panels below, were measured. Panel **(B)** Longitudinal anti-S-RBD IgG concentrations, expressed in $\log_{10}$ BAU/mL, in the case participant (large circles) versus the comparison group of SARS-CoV-2-naive individuals (small circles) at various time points following two- and three-dose COVID-19 vaccination. Wild-type (WT) specific anti-S-RBD responses are shown in red; Omicron BA.1-specific ones are shown in blue. Matching solid lines connect the participant's longitudinal values, while dotted lines connect the median values for the comparison group. Approximate times of BA.1 and BA.2 infections are shown with arrows. Total Ns are shown at the bottom of the plot. Later time points have smaller Ns because some control participants were censored due to post-vaccination SARS-CoV-2 infection or had not yet completed the visit. Panel **(C)** same as **(B)**, but for longitudinal ACE2% displacement function from wild-type (red) and BA.1 (blue) S-RBDs. Panel **(D)** same as **(B)**, but for longitudinal live virus neutralization function against wild-type (red) and BA.1 (blue) strains. ULOQ/LLOQ: upper/lower limit of quantification.

ELISA kit (Panel 25, Meso Scale Diagnostics), which features full-length S antigens from wild-type, Omicron BA.1 and Omicron BA.2. This panel was used because, at the time of analysis, no reagents featuring Omicron BA.2 RBD were offered by the manufacturer. Both assays were performed on a Meso QuickPlex SQ120 instrument, with sera diluted 1:10000. Results are reported as WHO International Standard Units (BAU/mL), using the manufacturer-provided conversion factors.

ACE2 competition assays

We assessed the ability of serum antibodies to block the wild-type and Omicron BA.1 RBD-ACE2 receptor interaction by competition ELISA (Panel 22 V-plex SARS-CoV-2 [ACE2]; Meso Scale Diagnostics). For a subset of 28 participants, we also assessed the ability of serum antibodies to block the wild-type, BA.1 and BA.2 Spike-ACE2 receptor interaction using the same methods (Panel 25 V-plex SARS-CoV-2 [ACE2]). Both assays were performed on a Meso QuickPlex SQ120 instrument, with sera diluted 1:40. Results are reported as % ACE2 displacement.

Live virus neutralization assays

Neutralizing activity in plasma was examined in live SARS-CoV-2 assays using a wild-type isolate (USA-WA1/2020; BEI Resources) and a local Omicron BA.1 isolate (GISAID Accession # EPI_ISL_9805779) on VeroE6-TMPRSS2 (JCRB-1819) target cells. Viral stock was adjusted to 50 TCID50/200 µl in Dulbecco's Modified Eagle Medium in the presence of serial 2-fold plasma dilutions (from 1/20 to 1/2560), incubated at 4°C for 1 hour and added to target cells in 96-well plates in triplicate. Cultures were maintained at 37°C with 5% CO2 and the appearance of viral cytopathic effect (CPE) was recorded three days post-infection. Neutralizing activity is reported as the reciprocal of the highest plasma dilution able to prevent CPE in all triplicate wells. Samples exhibiting partial or no neutralization at 1/20 dilution were defined as below the limit of quantification (BLOQ).

Data analysis

Data visualization and analysis was conducted in Prism v9.2.0 (GraphPad). As this is a report of a single case where immune response data are contrasted to those observed in a COVID-19-naive comparison group, response magnitudes are characterized in detail, but no formal statistical tests were applied.

Results

Case participant SARS-CoV-2 vaccination and infection timeline

The participant was a frontline health care worker, approximately 30 years of age. The participant had no major health conditions, but did take medications for hypothyroidism and familial hypercholesterolemia, both of which were well-controlled. The participant received three doses of mRNA vaccine (all BNT162b2; 30 mcg) in late December 2020, early February 2021 and late October 2021 (Figure 1A). All blood samples collected up to one month following the third immunization were anti-N seronegative.

In early January 2022, ten weeks after the third immunization, the participant experienced moderate COVID-19 symptoms including sore throat, fatigue, congestion, body aches, severe headaches, loss of taste and smell, coughing, shortness of breath and nausea. Symptoms, primarily cough, intensified in the second week after diagnosis requiring corticosteroid therapy. By the third week, symptoms had subsided except for shortness of breath and fatigue, with minimal improvement from short- and long-acting bronchodilating agents. A saline gargle collected on January 10, 2022 tested positive on the cobas® SARS-CoV-2 Test with a cycle threshold (Ct) value of 21 for both Orf1a/b and E gene targets. Real-time RT-PCR-based molecular screening identified the infection as Omicron BA.1, with subsequent full-genome viral sequencing confirming the specific lineage as BA.1.15.

In early April 2022, 13 weeks following the BA.1 infection (and 23 weeks following the third immunization) the participant experienced a profile of milder COVID-19 symptoms that differed compared to the first infection, consisting of a sore throat, fever, body aches, headaches, and diarrhea. No change in sense of taste or smell was noted. The participant noted persisting weakness, fatigue and mental fog, as well as severe long-term, treatment-resistant shortness of breath triggered by mild activities or exercises. A nasopharyngeal swab collected on April 9, 2022 tested positive on the cobas® SARS-CoV-2 Test with Ct values of 24 (Orf1a/b) and 23 (E). This infection was identified as BA.2 by molecular screening and confirmed by full-genome viral sequencing.

Longitudinal humoral responses to wild-type and Omicron BA.1 variants

We began by investigating the magnitude of the participant's humoral immune responses following immunization, in context of a control group of 124 COVID-naïve individuals who were vaccinated during the same period. The comparison group was 74% female with a median age of 57 (Interquartile Range [IQR] 38-76) years. We quantified antibody responses to wild-type and Omicron BA.1 strains in the participant and the comparison group at one month after the second and third vaccine doses, as these time points should capture peak responses post-vaccination (Figures 1B–D).

One month post-second dose, the participant's wild-type and BA.1-specific RBD IgG concentrations were 3.34 and 2.70 $\log_{10}$ BAU/mL respectively, which were equivalent to the 53rd and 50th percentile values of the comparator cohort (Figure 1B). One month post-third dose, the participant's wild-type and BA.1-specific RBD IgG concentrations had increased to 3.51 and 3.06 $\log_{10}$ BAU/mL respectively, equivalent to the 30th and

50th percentile values of the cohort. Similarly, one month post-second dose, the participant's ability to disrupt the interaction between the ACE2 receptor and the wild-type and BA.1 RBDs were 97% (57th percentile) and 42% (55th percentile) respectively (Figure 1C). At one month post-third dose, the participant's wild-type- and BA.1-specific RBD-ACE2 displacement activities had increased to 99% (74th percentile) and 76% (73rd percentile) respectively. Finally, at one month post-second dose, the participant's plasma neutralized wild-type and BA.1 SARS-CoV-2 at reciprocal dilutions of 320 and 20, which were equivalent to the 97th and 76th percentile values of the cohort. At one month post-third dose, the participant's wild-type and BA.1 neutralization titers were 320 (78th percentile) and 40 (59th percentile) respectively. These results indicate that the participant's overall vaccine responses were typical of the cohort, but nevertheless insufficient to prevent infection by BA.1 approximately six weeks later.

Seventeen days after testing positive with BA.1 (which coincided with a three-month post-third-dose study visit), the participant's wild-type and BA.1-specific responses were boosted substantially, reaching the cohort 95th percentile for most measures at this time when immune responses had begun to decline in the comparator cohort (Figures 1B–D). The participant's wild-type RBD IgG concentration increased to 4.15 $\log_{10}$ BAU/mL, while their BA.1-specific RBD IgG concentration increased to 3.55 $\log_{10}$ BAU/mL (Figure 1B). For context, these values would have placed the participant in the 94th and 91st percentiles of "peak" cohort values, measured at one month post-third vaccine dose. Similarly, the participant's wild-type-specific RBD-ACE2 competition activity remained high at 99.9%, while their BA.1-specific RBD-ACE2 competition activity increased to 96.3%. For context, these values would be equivalent to the 99th percentiles of peak cohort values one month post-third vaccine dose (Figure 1C). The participant's wild-type and BA.1-specific neutralization values held at 320 and 40, respectively, equivalent to the 78th and 59th percentiles of peak cohort values (Figure 1D). These results indicate that BA.1 infection boosted the participant's humoral response, particularly in terms of binding antibody concentrations and ACE2 displacement activity. Nevertheless, this boost was insufficient to prevent reinfection by BA.2 approximately 10 weeks later.

Sixteen days after testing positive with BA.2 (which coincided with a six-month post-third-dose study visit), the participant's wild-type-specific responses remained steady or declined slightly (*e.g.* RBD IgG) from prior measurements (Figures 1B–D). Nevertheless, most of the participant's wild-type-specific responses remained at the cohort 100th percentile at this time point, which is unsurprising given that vaccine-induced responses had declined substantially over this time in the COVID-19 naive comparison group. For context, the participant's wild-type-specific responses at this time point would have represented the 84th (RBD IgG), 99th (ACE2 competition) and 78th (neutralization) percentiles of peak cohort values measured at one month post-third vaccine dose.

By contrast, the BA.2 reinfection had mixed effects on BA.1 responses. While the participant's BA.1-specific RBD IgG concentration rose substantially to 4.01 $\log_{10}$ BAU/mL (whereas the cohort median at this time point was nearly 2 $\log_{10}$ lower), no change was seen for BA.1-specific RBD-ACE2 competition, and BA.1 neutralization increased only modestly (Figures 1B–D). The more pronounced impact of BA.2 reinfection was to extend the duration of BA.1-specific responses in the participant, who maintained an RBD-ACE2 competition activity of 95.7% (compared to the cohort median 29% at this time point) and a neutralization activity of 80 (compared to the cohort median BLOQ at this time point). For further context, the participant's BA.1-specific responses at this time point would represent the 99th (RBD IgG), 99th (ACE2 competition) and 83rd (neutralization) percentiles of peak cohort values measured at one month post-third vaccine dose. Nevertheless, despite BA.1 infection and BA.2 reinfection, the participant's virus neutralization activity against BA.1 at this time point, which represented the highest activity measured during the study, remained 4-fold lower compared to that against the wild-type strain one month post-third vaccine dose (Figure 1D). The substantially weaker ability of even "hybrid" (vaccine and dual-infection induced) immune responses to neutralize Omicron compared to wild-type suggests that the participant may remain at risk of additional Omicron infection.

Longitudinal humoral responses to Omicron BA.2

We next characterized BA.2-specific Spike IgG and ACE2 competition activities in the participant, compared to a subset of 28 control vaccinees (79% Female, median age 59 years) beginning one month following the third vaccine dose (Figure 2). As these analyses focus on whole Spike (rather than RBD antigen), the corresponding wild-type and BA.1 Spike-specific responses are also shown for context (Figure 2). We additionally confirmed the (strong) correlations between wild-type- and BA.1-specific RBD and Spike responses in these individuals (all $p<0.0001$; Figure S1). At one month post-third vaccine dose, the participant displayed wild-type, BA.1 and BA.2-specific Spike IgG concentrations of 3.76, 3.14 and 3.41 $\log_{10}$ BAU/mL respectively (Figure 2A), and ACE2 competition activities of 99.4%, 50.6% and 64.3% respectively (Figure 2B). The participant's wild-type and BA.2-specific Spike-specific IgG concentrations and ACE2 competition activities were broadly average compared to control vaccinees at this time (54th and 68th percentiles for IgG, respectively; 46th and 54th percentiles for ACE2 competition, respectively). The participant's values for BA.1-specific IgG and BA.1 Spike-specific ACE2 competition

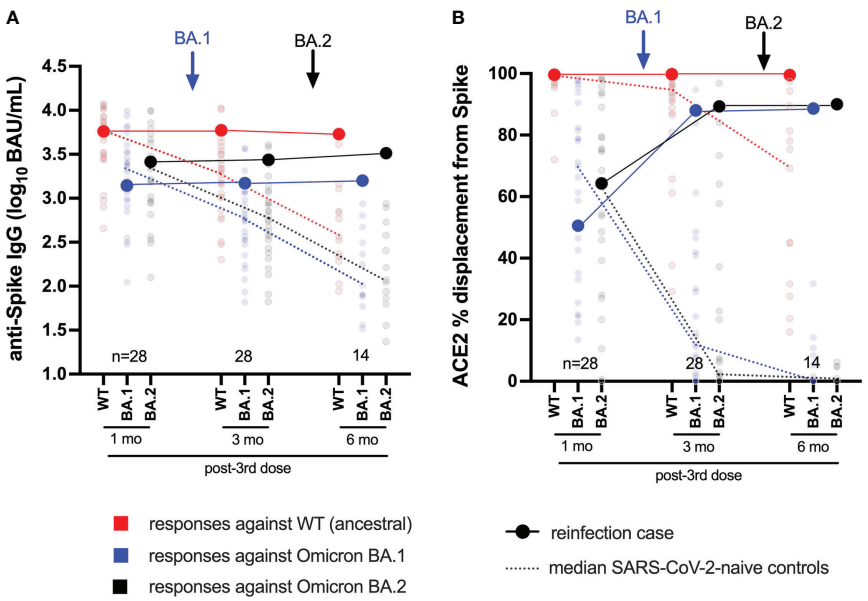

FIGURE 2
Longitudinal humoral responses against wild-type, BA.1 and BA.2 Spike antigens. Panel **(A)** Anti-Spike IgG concentrations, expressed in $\log_{10}$ BAU/mL, in the case participant (large circles) versus a subset of the comparison group of SARS-CoV-2-naive individuals (small circles) at one, three and six months following three-dose COVID-19 vaccination. Wild-type-specific (WT) anti-Spike responses are in red; BA.1-specific ones are in blue; BA.2-specific ones are in black. Matching solid lines connect the participant's longitudinal values; dotted lines connect the median values for the comparison group. Approximate times of BA.1 and BA.2 infections are shown with arrows. Total Ns are shown at the bottom of the plot; the final time point has a smaller N because some control participants were censored due to post-vaccination SARS-CoV-2 infection or had not yet completed the visit. Panel **(B)** same as **(A)**, but for longitudinal ACE2% displacement function from wild-type (red), BA.1 (blue) and BA.2 (black) Spike protein.

however were slightly lower than the averages of the control group (37th and 39th percentiles, respectively).

Following BA.1 infection, the participant's wild-type, BA.1 and BA.2-specific Spike IgG concentrations increased modestly, to 3.77, 3.17 and 3.44 $\log_{10}$ BAU/mL, respectively (Figure 2A). Though the magnitude of these increases was not as pronounced as those observed in the RBD-based assays (shown in Figure 1B), these values nevertheless placed the participant at or above the 85th percentile compared to control vaccinees at this time point, when immune responses had begun to decline in the broader cohort. For context, these values would place the participant in the 57th, 39th, and 68th percentile of peak cohort values measured at one month post-third vaccine dose. Similar to the ACE2 competition activities measured using RBD antigens (shown in Figure 1C), the participant's wild-type Spike-ACE2 competition activities remained high at 99.7%, while BA.1 and BA.2 Spike-ACE2 activities rose substantially to 87.9% and 89.3%, respectively (Figure 2B); values that represented the 71st, 75th, and 79th percentiles of peak values for the control vaccinees at one month post-third vaccine dose.

Following BA.2 infection, the participant's wild-type Spike IgG concentration declined slightly to 3.73 $\log_{10}$ BAU/mL, whereas their BA.1 and BA.2-specific values increased slightly to 3.20 and 3.51 $\log_{10}$ BAU/mL, respectively (Figure 2A). These trends were consistent with the anti-RBD IgG concentrations measured in the primary analysis (shown in Figure 1B), though of a smaller magnitude. Similar to the ACE2 competition activities measured using RBD antigens (shown in Figure 1C), the participant's wild-type Spike-ACE2 competition activity remained high (99.5%) after BA.2 infection. BA.1 and BA.2 Spike-ACE2 activities increased, though only marginally, to 88.6% and 90% respectively (Figure 2B).

Together, these results confirm that the participant's humoral responses to wild-type and Omicron variants were broadly average for a COVID-19-naive individuals one month post-third vaccine dose. While subsequent BA.1 infection boosted Omicron-specific immune responses (highlighted by an increase in BA.1 and BA.2 Spike-ACE2 competition activities), BA.2 reinfection did not substantially augment these activities further, but rather extended the duration of these responses.

Discussion

This study provides a detailed characterization of humoral responses in a laboratory-confirmed case of serial infection by SARS-CoV-2 Omicron subvariants BA.1 and BA.2 in an individual who had mounted typical immune reactivity to

three doses of COVID-19 mRNA vaccine. While data on repeat Omicron infections remain limited, a recent genomics-based study from Denmark identified 47 cases of BA.2 reinfection that occurred between 20 and 60 days following BA.1 infection (24). The authors concluded that such events were rare (<0.1% of cases during the brief window of analysis) and more likely to occur among unvaccinated individuals, but further evaluation of the data indicates that most reinfection cases were due to BA.2 following BA.1. The fact that the present case participant was one of only 151 original enrollees of our observational COVID-19 vaccine study (25, 26), which would translate into an Omicron serial infection prevalence of 0.7%, suggests that the risk of serial infection with Omicron subvariants may be higher than existing estimates. We note however that the participant's status as a frontline healthcare worker may have resulted in an increased risk of exposure and infection over the general population (29). The potential influence of the participant's hypothyroidism and familial hypercholesterolemia (though well-controlled by medication) on the symptoms profile following infection is also unknown.

Acknowledging that our ability to generalize from a single case is limited, we note that initial vaccine-induced IgG, ACE2 competition and virus neutralization response magnitudes against wild-type and Omicron BA.1 in the participant were comparable to the median values observed in diverse COVID-19-naive controls who were vaccinated along the same timeline. The observation that average humoral responses to three-dose vaccination failed to protect the participant against Omicron BA.1 infection is consistent with the extremely high rates of community transmission observed in many regions during recent Omicron-driven pandemic waves. Given that third vaccine doses substantially boost humoral responses in individuals of all ages (30–33), the relative risk of Omicron breakthrough infection is likely to be even higher among individuals who have received fewer than three doses (18, 34). Relative risk is also likely to increase with time following vaccination due to natural declines in antibody responses (26, 35–38), which, combined with natural Spike antigenic drift, may lead to ongoing risk of periodic re-infection (39). Additional studies are needed to assess these factors, as well as to investigate the impact of Omicron (re)infections following three-dose vaccination in larger numbers of individuals.

While it is perhaps unsurprising that COVID-19 vaccines based on ancestral SARS-CoV-2 sequences will not generate sterilizing immunity against Omicron strains that have evolved to evade host immune responses (4, 40–44), various lines of evidence suggest that "hybrid" immunity resulting from vaccination plus infection nevertheless provides enhanced protection against SARS-CoV-2 variants (5, 45), due in part to maturation of Spike-specific antibodies (46–48) and expansion of antiviral T cells (49–54). In light of this, we note that symptomatic BA.1 infection boosted the case participant's vaccine-induced humoral responses against both BA.1 and BA.2. The heightened response nevertheless failed to prevent subsequent symptomatic infection by BA.2 ten weeks later, suggesting that these responses were insufficient to block infection, or that they had already declined to below-protective levels in this relatively short timeframe. Moreover, even after vaccination plus two Omicron infections, the participant's ACE2 competition and virus neutralization responses against BA.1 (as well as ACE2 competition activity against BA.2) plateaued at levels substantially lower than those seen against the wild-type strain, suggesting that the participant will remain at risk of new Omicron infections. A limitation of our study is that it did not assess T cell responses, which can reduce disease severity but may have less impact on virus transmission (55, 56), and thus we may be underestimating the protection that results from infection and reinfection in this case.

Despite documentation of this case, it is important to keep in perspective that the participant's symptoms following both infections were not severe enough to require hospitalization. This clearly demonstrates that vaccination was nevertheless effective in its primary goal of preventing severe disease. Results of our study should therefore not be mis-interpreted to suggest that COVID-19 vaccines (including booster doses) are not effective at their primary goal - indeed, substantial evidence clearly indicates that a third COVID-19 dose significantly reduces the risk of severe disease outcomes, including against Omicron (40, 57–59). Rather, our observation that "typical" antibody responses to vaccination failed to prevent Omicron infection in the case participant, and that the resulting enhanced "hybrid" immunity also failed to prevent Omicron re-infection, are consistent with the potentially limited ability of current vaccines to prevent recurrent symptomatic Omicron infections. Our study thus highlights the importance of additional preventive measures to reduce transmission, including masking, pre-exposure prophylaxis [*e.g* (60)], and potentially variant-specific immunizations (61–64), particularly as vaccine-induced immune responses naturally decline over time.

Data availability statement

The datasets presented in this study can be found in online repositories. The names of the repository/repositories and accession number(s) can be found below: NCBI Genbank, accession numbers OP237526 and OP237527.

Ethics statement

The studies involving human participants were reviewed and approved by University of British Columbia/Providence Health Care and Simon Fraser University Research Ethics Boards (protocol H20-03906). The participants or their authorized substitute decision makers provided their written informed consent to participate in this study.

Author contributions

HL and FM contributed equally as first authors. MR, MB, and ZB obtained project funding and contributed equally as senior authors. HL, FM, MB, and ZB designed the study. HL, FM, PC, YS, FY, RK, SD, RW, GU, SE, LY, WD, DK, and LB contributed to specimen collection and data analysis. HL, YS, VL, DH, MD, JS, NM, JM, CB, NP, MN, CL, MR, MB, and ZB supervised the research, laboratory assays and/or contributed to project or cohort management. HL, MB, and ZB wrote the original manuscript draft. All authors contributed to the article and approved the submitted version.

Funding

This work was supported by the Public Health Agency of Canada through a COVID-19 Immunology Task Force COVID-19 "Hot Spots" Award (2020-HQ-000120 to MR, ZB, MB). Additional funding was received from the Canadian Institutes for Health Research (GA2-177713 and the Coronavirus Variants Rapid Response Network (FRN-175622) to MB) and the Canada Foundation for Innovation through Exceptional Opportunities Fund - COVID-19 awards (to MB, MD, MN, RP, CL, ZB). MD and ZB hold Scholar Awards from the Michael Smith Foundation for Health Research. FM is supported by a fellowship from the CIHR Canadian HIV Trials Network. FY was supported by an SFU Undergraduate Student Research Award. GU holds a Ph.D. fellowship from the Sub-Saharan African Network for TB/HIV Research Excellence (SANTHE), a DELTAS Africa Initiative [grant # DEL-15-006]. The DELTAS Africa Initiative is an independent funding scheme of the African Academy of Sciences (AAS)'s Alliance for Accelerating Excellence in Science in Africa (AESA) and supported by the New Partnership for Africa's Development Planning and Coordinating Agency (NEPAD Agency) with funding from the Wellcome Trust [grant # 107752/Z/15/Z] and the UK government.

Acknowledgments

We thank the leadership and staff of Providence Health Care for their support of this study. We thank the phlebotomists and laboratory staff at St. Paul's Hospital, the BC Centre for Excellence in HIV/AIDS, the Hope to Health Research and Innovation Centre, and Simon Fraser University for assistance. Above all, we thank the participants, without whom this study would not have been possible.

Conflict of interest

The authors declare that the research was conducted in the absence of any commercial or financial relationships that could be construed as a potential conflict of interest.

Publisher's note

All claims expressed in this article are solely those of the authors and do not necessarily represent those of their affiliated organizations, or those of the publisher, the editors and the reviewers. Any product that may be evaluated in this article, or claim that may be made by its manufacturer, is not guaranteed or endorsed by the publisher.

Author disclaimer

The views expressed in this publication are those of the authors and not necessarily those of the funders, including AAS, NEPAD Agency, Wellcome Trust or the UK government.

Supplementary material

The Supplementary Material for this article can be found online at: https://www.frontiersin.org/articles/10.3389/fimmu.2022.947021/full#supplementary-material

SUPPLEMENTARY FIGURE 1
Correlations between wild-type (WT) and BA.1-specific anti-S-RBD and anti-Spike humoral responses measured following three COVID-19 vaccine doses using Meso Scale Diagnostics V-plex panels 22 and 25. All participants who were evaluated for BA.2 responses (i.e. those shown in Figure 2) are included in this analysis. Symbols are colored based on post-vaccination time point, though the Spearman's rho (ρ) and p-value reported are for the combined data.

References

1. Pulliam JRC, van Schalkwyk C, Govender N, von Gottberg A, Cohen C, Groome MJ, et al. Increased risk of SARS-CoV-2 reinfection associated with emergence of omicron in south Africa. *Science* (2022) 376(6593):eabn4947. doi: 10.1126/science.abn4947

2. Bastard J, Taisne B, Figoni J, Mailles A, Durand J, Fayad M, et al. Impact of the omicron variant on SARS-CoV-2 reinfections in France, march 2021 to February 2022. *Euro Surveill* (2022) 27(13):pii=2200247. doi: 10.2807/1560-7917.ES.2022.27.13.2200247

3. Altarawneh HN, Chemaitelly H, Hasan MR, Ayoub HH, Qassim S, AlMukdad S, et al. Protection against the omicron variant from previous SARS-CoV-2 infection. *N Engl J Med* (2022) 386(13):1288–90. doi: 10.1056/NEJMc2200133

4. Cele S, Jackson L, Khoury DS, Khan K, Moyo-Gwete T, Tegally H, et al. Omicron extensively but incompletely escapes pfizer Bnt162b2 neutralization. *Nature* (2022) 602(7898):654–6. doi: 10.1038/s41586-021-04387-1

5. Smid M, Berec L, Pribylova L, Majek O, Pavlik T, Jarkovsky J, et al. Protection by vaccines and previous infection against the omicron variant of SARS-CoV-2. *J Infect Dis* (2022). doi: 10.1093/infdis/jiac161

6. Ahava MJ, Jarva H, Jaaskelainen AJ, Lappalainen M, Vapalahti O, Kurkela S. Rapid increase in SARS-CoV-2 seroprevalence during the emergence of omicron variant, Finland. *Eur J Clin Microbiol Infect Dis* (2022) 41:997–9. doi: 10.1007/s10096-022-04448-x

7. Chaguza C, Coppi A, Earnest R, Ferguson D, Kerantzas N, Warner F, et al. Rapid emergence of SARS-CoV-2 omicron variant is associated with an infection advantage over delta in vaccinated persons. *Med (NY)* (2022) 3(5):325–34. doi: 10.1016/j.medj.2022.03.010

8. Viana R, Moyo S, Amoako DG, Tegally H, Scheepers C, Althaus CL, et al. Rapid epidemic expansion of the SARS-CoV-2 omicron variant in Southern Africa. *Nature* (2022) 603(7902):679–86. doi: 10.1038/s41586-022-04411-y

9. Khan K, Karim F, Ganga Y, Bernstein M, Jule Z, Reedoy K, et al. Omicron Sub-lineages Ba.4/Ba.5 escape Ba.1 infection elicited neutralizing immunity. *medRxiv* (2022). doi: 10.1101/2022.04.29.22274477

10. BC Centre for Disease Control. *Weekly update on variants of concern*. Available at: http://www.bccdc.ca/health-info/diseases-conditions/covid-19/data.

11. BC Centre for Disease Control. *Weekly reporting of covid-19 cases, hospitalizations, and deaths* (2022). Available at: http://www.bccdc.ca/health-info/diseases-conditions/covid-19/data.

12. Public Health Agency of Canada. *Canadian Covid-19 vaccination coverage report* (2022). Available at: https://health-infobase.canada.ca/covid-19/vaccination-coverage/.

13. Government of British Columbia. *Get a booster dose - province of British Columbia* (2022). Available at: https://www2.gov.bc.ca/gov/content/covid-19/vaccine/booster.

14. Steacy LBC. *Covid news: Omicron infected half of British columbians, Henry says Vancouver, Canada* (2022). Available at: https://bc.ctvnews.ca/omicron-wave-exposed-infected-50-per-cent-of-british-columbians-henry-1.5850076.

15. Miller A. *Almost half of canadians may have caught covid: CBC news* (2022). Available at: https://www.cbc.ca/news/health/omicron-immunity-canada-covd19-vaccines-1.6428536.

16. Paterson SBC. *Doctors seeing covid-19 reinfection in patients who recently had omicron Vancouver, Canada* (2022). Available at: https://bc.ctvnews.ca/b-c-doctors-seeing-covid-19-reinfection-in-patients-who-recently-had-omicron-1.5846079.

17. Chang MR, Ke H, Coherd CD, Wang Y, Mashima K, Kastrunes GM, et al. Analysis of a SARS-CoV-2 convalescent cohort identified a common strategy for escape of vaccine-induced anti-rbd antibodies by beta and omicron variants. *EBioMedicine* (2022) 80:104025. doi: 10.1016/j.ebiom.2022.104025

18. Curlin ME, Bates TA, Guzman G, Schoen D, McBride SK, Carpenter SD, et al. Omicron neutralizing antibody response following booster vaccination compared with breakthrough infection. *medRxiv* (2022). doi: 10.1101/2022.04.11.22273694

19. Servellita V, Syed AM, Morris MK, Brazer N, Saldhi P, Garcia-Knight M, et al. Neutralizing immunity in vaccine breakthrough infections from the SARS-CoV-2 omicron and delta variants. *Cell* (2022) 185(9):1539–48.e5. doi: 10.1016/j.cell.2022.03.019

20. Glatman-Freedman A, Bromberg M, Hershkovitz Y, Sefty H, Kaufman Z, Dichtiar R, et al. Effectiveness of Bnt162b2 vaccine booster against SARS-CoV-2 infection and breakthrough complications, Israel. *Emerg Infect Dis* (2022) 28 (5):948–56. doi: 10.3201/eid2805.220141

21. Seaman MS, Siedner MJ, Boucau J, Lavine CL, Ghantous F, Liew MY, et al. Vaccine breakthrough infection with the SARS-CoV-2 delta or omicron (Ba.1) variant leads to distinct profiles of neutralizing antibody responses. *medRxiv* (2022). doi: 10.1101/2022.03.02.22271731

22. Evans JP, Zeng C, Carlin C, Lozanski G, Saif LJ, Oltz EM, et al. Neutralizing antibody responses elicited by SARS-CoV-2 mrna vaccination wane over time and are boosted by breakthrough infection. *Sci Transl Med* (2022) 14(637):eabn8057. doi: 10.1126/scitranslmed.abn8057

23. Kuhlmann C, Mayer CK, Claassen M, Maponga T, Burgers WA, Keeton R, et al. Breakthrough infections with SARS-CoV-2 omicron despite mrna vaccine booster dose. *Lancet* (2022) 399(10325):625–6. doi: 10.1016/S0140-6736(22)00090-3

24. Stegger M, Edslev SM, Sieber RN, Cäcilia Ingham A, Ng KL, Tang M-HE, et al. Occurrence and significance of omicron Ba.1 infection followed by Ba.2 reinfection. *medRxiv* (2022). doi: 10.1101/2022.02.19.22271112

25. Brockman MA, Mwimanzi F, Lapointe HR, Sang Y, Agafitei O, Cheung P, et al. Reduced magnitude and durability of humoral immune responses to covid-19 mrna vaccines among older adults. *J Infect Dis* (2022) 225(7):1129–40. doi: 10.1093/infdis/jiab592

26. Mwimanzi F, Lapointe HR, Cheung PK, Sang Y, Yaseen F, Umviligihozo G, et al. Older adults mount less durable humoral responses to two doses of covid-19 mrna vaccine, but strong initial responses to a third dose. *J Infect Dis* (2022). doi: 10.1093/infdis/jiac199

27. Matic N, Lowe CF, Ritchie G, Stefanovic A, Lawson T, Jang W, et al. Rapid detection of SARS-CoV-2 variants of concern, including B.1.1.28/P.1, British Columbia, Canada. *Emerg Infect Dis* (2021) 27(6):1673–6. doi: 10.3201/eid2706.210532

28. Matic N, Lowe CF, Ritchie G, Young M, Lawson T, Romney MG. Omicron (B.1.1.529) SARS-CoV-2 viral load among nasopharyngeal and oral samples compared to other variants of concern and impact on diagnostic testing strategy. *Clin Microbiol Infect* (2022). doi: 10.1016/j.cmi.2022.04.022

29. Nguyen LH, Drew DA, Graham MS, Joshi AD, Guo CG, Ma W, et al. Risk of covid-19 among front-line health-care workers and the general community: A prospective cohort study. *Lancet Public Health* (2020) 5(9):e475–e83. doi: 10.1016/S2468-2667(20)30164-X

30. Lustig Y, Gonen T, Meltzer L, Gilboa M, Indenbaum V, Cohen C, et al. Superior immunogenicity and effectiveness of the third compared to the second Bnt162b2 vaccine dose. *Nat Immunol* (2022) 23:940–6. doi: 10.1038/s41590-022-01212-3

31. Liu X, Munro APS, Feng S, Janani L, Aley PK, Babbage G, et al. Persistence of immunogenicity after seven covid-19 vaccines given as third dose boosters following two doses of Chadox1 ncov-19 or Bnt162b2 in the uk: Three month analyses of the cov-boost trial. *J Infect* (2022) 84(6):795–813. doi: 10.1016/j.jinf.2022.04.018

32. Moreira EDJr., Kitchin N, Xu X, Dychter SS, Lockhart S, Gurtman A, et al. Safety and efficacy of a third dose of Bnt162b2 covid-19 vaccine. *N Engl J Med* (2022) 386(20):1910–21. doi: 10.1056/NEJMoa2200674

33. Yoon SK, Hegmann KT, Thiese MS, Burgess JL, Ellingson K, Lutrick K, et al. Protection with a third dose of mrna vaccine against SARS-CoV-2 variants in frontline workers. *N Engl J Med* (2022) 386(19):1855–7. doi: 10.1056/NEJMc2201821

34. Goel RR, Painter MM, Lundgreen KA, Apostolidis SA, Baxter AE, Giles JR, et al. Efficient recall of omicron-reactive b cell memory after a third dose of SARS-CoV-2 mrna vaccine. *Cell* (2022) 185 (11):1875–87. doi: 10.1016/j.cell.2022.04.009

35. Mantus G, Nyhoff LE, Edara VV, Zarnitsyna VI, Ciric CR, Flowers MW, et al. Pre-existing SARS-CoV-2 immunity influences potency, breadth, and durability of the humoral response to SARS-CoV-2 vaccination. *Cell Rep Med* (2022) 3(4):100603. doi: 10.1016/j.xcrm.2022.100603

36. Tartof SY, Slezak JM, Puzniak L, Hong V, Xie F, Ackerson BK, et al. Durability of Bnt162b2 vaccine against hospital and emergency department admissions due to the omicron and delta variants in a Large health system in the USA: A test-negative case-control study. *Lancet Respir Med* (2022) 10(7):689–99. doi: 10.1016/S2213-2600(22)00101-1

37. Bonnet B, Chabrolles H, Archimbaud C, Brebion A, Cosme J, Dutheil F, et al. Decline of humoral and cellular immune responses against SARS-CoV-2 6 months after full Bnt162b2 vaccination in hospital healthcare workers. *Front Immunol* (2022) 13:842912. doi: 10.3389/fimmu.2022.842912

38. Sogaard OS, Reekie J, Johansen IS, Nielsen H, Benfield T, Wiese L, et al. Characteristics associated with serological covid-19 vaccine response and durability in an older population with significant comorbidity: The Danish nationwide enforce study. *Clin Microbiol Infect* (2022) 28(8):1126–33. doi: 10.1016/j.cmi.2022.03.003

39. Yewdell JW. Antigenic drift: Understanding covid-19. *Immunity* (2021) 54 (12):2681–7. doi: 10.1016/j.immuni.2021.11.016

40. Andrews N, Stowe J, Kirsebom F, Toffa S, Rickeard T, Gallagher E, et al. Covid-19 vaccine effectiveness against the omicron (B.1.1.529) variant. *New Engl J Med* (2022) 386(16):1532–46. doi: 10.1056/NEJMoa2119451

41. Bjork J, Bonander C, Moghaddassi M, Rasmussen M, Malmqvist U, Inghammar M, et al. Covid-19 vaccine effectiveness against severe disease from SARS-CoV-2 omicron Ba.1 and Ba.2 subvariants - surveillance results from southern Sweden, December 2021 to march 2022. *Euro Surveill* (2022) 27(18): pii=2200322. doi: 10.2807/1560-7917.ES.2022.27.18.2200322

42. Collie S, Champion J, Moultrie H, Bekker LG, Gray G. Effectiveness of Bnt162b2 vaccine against omicron variant in south Africa. *N Engl J Med* (2022) 386 (5):494–6. doi: 10.1056/NEJMc2119270

43. Yu J, Collier AY, Rowe M, Mardas F, Ventura JD, Wan H, et al. Neutralization of the SARS-CoV-2 omicron Ba.1 and Ba.2 variants. *N Engl J Med* (2022) 386(16):1579–80. doi: 10.1056/NEJMc2201849

44. Pedersen RM, Bang LL, Madsen LW, Sydenham TV, Johansen IS, Jensen TG, et al. Serum neutralization of SARS-CoV-2 omicron Ba.1 and Ba.2 after Bnt162b2 booster vaccination. *Emerg Infect Dis* (2022) 28(6):1274–5. doi: 10.3201/eid2806.220503

45. Nordstrom P, Ballin M, Nordstrom A. Risk of SARS-CoV-2 reinfection and covid-19 hospitalisation in individuals with natural and hybrid immunity: A retrospective, total population cohort study in Sweden. *Lancet Infect Dis* (2022) 22(6):781–90. doi: 10.1016/S1473-3099(22)00143-8

46. Chen Y, Tong P, Whiteman N, Moghaddam AS, Zarghami M, Zuiani A, et al. Immune recall improves antibody durability and breadth to SARS-CoV-2 variants. *Sci Immunol* (2022):eabp8328. doi: 10.1126/sciimmunol.abp8328

47. Cho A, Muecksch F, Schaefer-Babajew D, Wang Z, Finkin S, Gaebler C, et al. Anti-SARS-CoV-2 receptor-binding domain antibody evolution after mrna vaccination. *Nature* (2021) 600(7889):517–22. doi: 10.1038/s41586-021-04060-7

48. Muecksch F, Weisblum Y, Barnes CO, Schmidt F, Schaefer-Babajew D, Wang Z, et al. Affinity maturation of SARS-CoV-2 neutralizing antibodies confers potency, breadth, and resilience to viral escape mutations. *Immunity* (2021) 54 (8):1853–68 e7. doi: 10.1016/j.immuni.2021.07.008

49. Rodda LB, Morawski PA, Pruner KB, Fahning ML, Howard CA, Franko N, et al. Imprinted SARS-CoV-2-Specific memory lymphocytes define hybrid immunity. *Cell* (2022) 185(9):1588–601.e14. doi: 10.1016/j.cell.2022.03.018

50. Riou C, Keeton R, Moyo-Gwete T, Hermanus T, Kgagudi P, Baguma R, et al. Escape from recognition of SARS-CoV-2 variant spike epitopes but overall preservation of T cell immunity. *Sci Transl Med* (2022) 14(631):eabj6824. doi: 10.1126/scitranslmed.abj6824

51. Keeton R, Richardson SI, Moyo-Gwete T, Hermanus T, Tincho MB, Benede N, et al. Prior infection with SARS-CoV-2 boosts and broadens Ad26.Cov2.S immunogenicity in a variant-dependent manner. *Cell Host Microbe* (2021) 29 (11):1611–9.e5. doi: 10.1016/j.chom.2021.10.003

52. Keeton R, Tincho MB, Ngomti A, Baguma R, Benede N, Suzuki A, et al. T Cell responses to SARS-CoV-2 spike cross-recognize omicron. *Nature* (2022) 603 (7901):488–92. doi: 10.1038/s41586-022-04460-3

53. Gao Y, Cai C, Grifoni A, Muller TR, Niessl J, Olofsson A, et al. Ancestral SARS-CoV-2-Specific T cells cross-recognize the omicron variant. *Nat Med* (2022) 28(3):472–6. doi: 10.1038/s41591-022-01700-x

54. Goel RR, Painter MM, Apostolidis SA, Mathew D, Meng W, Rosenfeld AM, et al. Mrna vaccines induce durable immune memory to SARS-CoV-2 and variants of concern. *Science* (2021) 374(6572):abm0829. doi: 10.1126/science.abm0829

55. Pollard AJ, Bijker EM. A guide to vaccinology: From basic principles to new developments. *Nat Rev Immunol* (2021) 21(2):83–100. doi: 10.1038/s41577-020-00479-7

56. Jeyanathan M, Afkhami S, Smaill F, Miller MS, Lichty BD, Xing Z. Immunological considerations for covid-19 vaccine strategies. *Nat Rev Immunol* (2020) 20(10):615–32. doi: 10.1038/s41577-020-00434-6

57. Abu-Raddad LJ, Chemaitelly H, Ayoub HH, AlMukdad S, Yassine HM, Al-Khatib HA, et al. Effect of mrna vaccine boosters against SARS-CoV-2 omicron infection in Qatar. *N Engl J Med* (2022) 386(19):1804–16. doi: 10.1056/NEJMoa2200797

58. Chemaitelly H, Ayoub HH, AlMukdad S, Coyle P, Tang P, Yassine HM, et al. Duration of mrna vaccine protection against SARS-CoV-2 omicron Ba.1 and Ba.2 subvariants in Qatar. *Nat Commun* (2022) 13(1):3082. doi: 10.1038/s41467-022-30895-3

59. Link-Gelles R, Levy ME, Gaglani M, Irving SA, Stockwell M, Dascomb K, et al. Effectiveness of 2, 3, and 4 covid-19 mrna vaccine doses among immunocompetent adults during periods when SARS-CoV-2 omicron Ba.1 and Ba.2/Ba.2.12.1 sublineages predominated - vision network, 10 states, December 2021-June 2022. *MMWR Morb Mortal Wkly Rep* (2022) 71(29):931–9. doi: 10.15585/mmwr.mm7129e1

60. Levin MJ, Ustianowski A, De Wit S, Launay O, Avila M, Templeton A, et al. Intramuscular Azd7442 (Tixagevimab-cilgavimab) for prevention of covid-19. *N Engl J Med* (2022) 386(23):2188–200. doi: 10.1056/NEJMoa2116620

61. Hawman DW, Meade-White K, Clancy C, Archer J, Hinkley T, Leventhal SS, et al. Replicating rna platform enables rapid response to the SARS-CoV-2 omicron variant and elicits enhanced protection in naive hamsters compared to ancestral vaccine. *EBioMedicine* (2022) 83:104196. doi: 10.1016/j.ebiom.2022.104196

62. Lam JY, Ng YY, Yuen CK, Wong WM, Yuen KY, Kok KH. A nasal omicron vaccine booster elicits potent neutralizing antibody response against emerging SARS-CoV-2 variants. *Emerg Microbes Infect* (2022) 11(1):964–7. doi: 10.1080/22221751.2022.2053365

63. Ying B, Scheaffer SM, Whitener B, Liang CY, Dmytrenko O, Mackin S, et al. Boosting with variant-matched or historical mrna vaccines protects against omicron infection in mice. *Cell* (2022) 185(9):1572–87.e11. doi: 10.1016/j.cell.2022.03.037

64. Choi A, Koch M, Wu K, Chu L, Ma L, Hill A, et al. Safety and immunogenicity of SARS-CoV-2 variant mrna vaccine boosters in healthy adults: An interim analysis. *Nat Med* (2021) 27(11):2025–31. doi: 10.1038/s41591-021-01527-y

COPYRIGHT

© 2022 Lapointe, Mwimanzi, Cheung, Sang, Yaseen, Kalikawe, Datwani, Waterworth, Umviligihozo, Ennis, Young, Dong, Kirkby, Burns, Leung, Holmes, DeMarco, Simons, Matic, Montaner, Brumme, Prystajecky, Niikura, Lowe, Romney, Brockman and Brumme. This is an open-access article distributed under the terms of the Creative Commons Attribution License (CC BY). The use, distribution or reproduction in other forums is permitted, provided the original author(s) and the copyright owner(s) are credited and that the original publication in this journal is cited, in accordance with accepted academic practice. No use, distribution or reproduction is permitted which does not comply with these terms.

frontiers | Frontiers in Immunology

TYPE Original Research
PUBLISHED 15 September 2022
DOI 10.3389/fimmu.2022.989556

Check for updates

OPEN ACCESS

EDITED BY
Edwin Bölke,
Heinrich Heine University of Düsseldorf, Germany

REVIEWED BY
Rebekah Penrice-Randal,
University of Liverpool, United Kingdom
Alsamman M. Alsamman,
Mohammed VI Polytechnic University, Morocco
Georgia Damoraki,
National and Kapodistrian University of Athens, Greece

*CORRESPONDENCE
Andrea R. Daamen
andrea.daamen@ampelbiosolutions.com
Peter E. Lipsky
peterlipsky@comcast.net

†These authors contributed equally to this work and share last authorship

SPECIALTY SECTION
This article was submitted to Viral Immunology, a section of the journal Frontiers in Immunology

RECEIVED 08 July 2022
ACCEPTED 29 August 2022
PUBLISHED 15 September 2022

CITATION
Daamen AR, Bachali P, Bonham CA, Somerville L, Sturek JM, Grammer AC, Kadl A and Lipsky PE (2022) COVID-19 patients exhibit unique transcriptional signatures indicative of disease severity.
Front. Immunol. 13:989556.
doi: 10.3389/fimmu.2022.989556

COPYRIGHT
© 2022 Daamen, Bachali, Bonham, Somerville, Sturek, Grammer, Kadl and Lipsky. This is an open-access article distributed under the terms of the Creative Commons Attribution License (CC BY). The use, distribution or reproduction in other forums is permitted, provided the original author(s) and the copyright owner(s) are credited and that the original publication in this journal is cited, in accordance with accepted academic practice. No use, distribution or reproduction is permitted which does not comply with these terms.

COVID-19 patients exhibit unique transcriptional signatures indicative of disease severity

Andrea R. Daamen[1*], Prathyusha Bachali[1], Catherine A. Bonham[2], Lindsay Somerville[2,3], Jeffrey M. Sturek[2], Amrie C. Grammer[1], Alexandra Kadl[2,4†] and Peter E. Lipsky[1*†]

[1]AMPEL BioSolutions LLC, Charlottesville, VA, United States, [2]Department of Medicine, Division of Pulmonary and Critical Care Medicine, Charlottesville, VA, United States, [3]Beirne B. Carter Center for Immunology Research, University of Virginia, Charlottesville, VA, United States, [4]Department of Pharmacology, University of Virginia, Charlottesville, VA, United States

COVID-19 manifests a spectrum of respiratory symptoms, with the more severe often requiring hospitalization. To identify markers for disease progression, we analyzed longitudinal gene expression data from patients with confirmed SARS-CoV-2 infection admitted to the intensive care unit (ICU) for acute hypoxic respiratory failure (AHRF) as well as other ICU patients with or without AHRF and correlated results of gene set enrichment analysis with clinical features. The results were then compared with a second dataset of COVID-19 patients separated by disease stage and severity. Transcriptomic analysis revealed that enrichment of plasma cells (PCs) was characteristic of all COVID-19 patients whereas enrichment of interferon (IFN) and neutrophil gene signatures was specific to patients requiring hospitalization. Furthermore, gene expression results were used to divide AHRF COVID-19 patients into 2 groups with differences in immune profiles and clinical features indicative of severe disease. Thus, transcriptomic analysis reveals gene signatures unique to COVID-19 patients and provides opportunities for identification of the most at-risk individuals.

KEYWORDS

COVID-19, severity, classification, transcriptomics, bioinformatics

Introduction

Coronavirus Disease 2019 (COVID-19) is caused by the RNA virus severe acute respiratory syndrome coronavirus 2 (SARS-CoV-2), which mediates respiratory infections and lung pathology of varying severity (1–3). Infected individuals may be asymptomatic or present with a range of mild symptoms that can be treated at home

to severe manifestations requiring hospitalization (4–8). Among hospitalized patients, there remain differences in the degree of respiratory distress and the need for mechanical ventilation. This heterogeneity in COVID-19 patients necessitates the ability to identify risk factors for severe disease and the development of acute hypoxic respiratory failure (AHRF). Currently accepted risk factors for worse clinical prognosis of COVID-19 patients include age, male gender, obesity, pre-existing diabetes, viral load, and pre-existing respiratory conditions or immunodeficiencies (9–11). However, these factors are not predictive of disease severity in all cases and young individuals in good health may still succumb to AHRF.

In addition to demographic statistics, the immune response of COVID-19 patients has been linked to disease severity and presents an opportunity for utilizing immune profiles to predict patient outcomes. To date, several groups have used a combination of flow cytometry, transcriptome data, cytokine levels, and clinical data to categorize COVID-19 patients and to associate particular immune profiles with disease severity (12–30). Immune cells and inflammatory molecules have been implicated in COVID-19 progression, including type I interferon (IFN) (22, 25, 27, 29), innate immune cells (12–14, 16, 18, 28), antibodies (31, 32), autoantibodies (33, 34), and pro-inflammatory cytokines (14, 17, 21, 23, 26, 35). However, these studies often describe conflicting associations of immune profiles with disease, emphasizing the need to better understand the heterogeneity in responses to SARS-CoV-2 infection. Furthermore, little work has focused on the classification of severe COVID-19 patients and the immune profiles associated with greater risk of death as a way to tailor treatment plans to each individual.

We previously utilized publicly available gene expression data to characterize the trajectory of the host immune response to SARS-CoV-2 in the blood, postmortem lung tissue, and bronchoalveolar lavage fluid (BALF) of COVID-19 patients (36). We have now employed a similar bioinformatic approach, combining gene expression and clinical feature data, to classify severe COVID-19 patients with AHRF upon admission to the intensive care unit (ICU) and to differentiate mild from severe patients at different timepoints after disease onset based on their immune profiles. In addition, we used longitudinal gene expression analysis from the same ICU patients to assess the stability of immune signatures over time. As a result, we identified two groups of AHRF COVID-19 patients with distinct enrichment of gene signatures of innate and adaptive immune cells and inflammatory pathways linked with differences in clinical outcomes. This classification of severe COVID-19 patients based on differences in immune profiles offers opportunities for identification of individuals with heightened disease severity and enables a targeted therapeutic approach to employ the most effective therapy for each individual COVID-19 patient.

Materials and methods

Patient population

We included patients who consented to donate blood to the University of Virginia (UVA) Intensive Care Unit (ICU) Biorepository. We then selected patients with confirmed COVID-19 respiratory failure, viral, non-COVID-19 respiratory failure, and patients with non-viral causes of respiratory failure (presumed bacterial infections) in the UVA ICU Biorepository to serve as a comparison cohort. Control patients were patients admitted on mechanical ventilation without respiratory failure (usually intubated for airway protection). We followed the Strengthening the Reporting of Observational Studies in Epidemiology (STROBE) guidelines (37) and our study complied with all principles outlined in the Declaration of Helsinki. All study protocols were approved by the UVA Institutional Review Board for Health Sciences Research (Protocol #21101). Respiratory failure was defined as patients with acute respiratory distress syndrome (ARDS) using Berlin criteria (38) who were on mechanical ventilation in the ICU. COVID-19 diagnoses were confirmed by RealTime SARS-CoV-2 assay performed on the m2000 system (Abbott Molecular Inc.; Des Plaines, IL).

Serum cytokine and chemokine analysis

Serum cytokine and chemokine levels were measured by Merck Millipore MILLIPLEX Human Cytokine/Chemokine/Growth Factor Panel A (HCYTA-60K) and Panel II (HCYP2MAG) assays.

Sample collection

Blood was collected into PAXgene® Blood RNA tubes upon admission to the ICU, and after 24 and 72 hours. RNA was prepared and sequenced by Genewiz (Azenta Life Sciences). RNA was isolated using a Qiagen total RNA isolation kit, followed by RNA-seq library preparation using standard Illumina protocols with rRNA and globin depletion. RNA was sequenced on an Illumina HiSeq 4000.

RNA-seq data analysis

Three independent whole blood datasets were analyzed. In the first dataset of patients from the UVA ICU Biorepository, RNA-seq data was obtained from 13 COVID-19 AHRF patients, 8 viral AHRF, 5 non-viral AHRF, and 5 control ICU patients. COVID-19 patients were subdivided into 2 groups (COVID Group 1 and COVID Group 2) based on separation by PCA of the top 500 variable genes. Additional publicly available RNA-seq datasets (GSE161731; GSE172114), were obtained and analyzed as confirmation studies. Additional dataset details can be found in Supplementary Table 1.

For RNA-seq analysis, the quality of raw FASTQ reads was analyzed using FASTQC (39) to identify the poor-quality reads and the adaptor contamination. Adaptors and low-quality sequencing reads were trimmed using Trimmomatic (40) and reads before 14bp were discarded. The clean raw sequencing reads were aligned to human reference genome (Gencode hg38) using STAR(v2) (41). The SAM files were converted into BAM files using sambamba (42). The aligned BAM files were fed to read summarization program featureCounts (43), to assign the sequencing reads to genomic features. The differential gene expression between COVID-19 and normal patients was carried out using the R/Bioconductor package DESeq2. The raw counts were normalized within the DESeq2 analysis pipeline using the median of ratios method and genes with low expression were filtered using HTSFilter (44). The p-values and adjusted p-values (FDR) were calculated for each gene. Genes with FDR < 0.05 were determined as significant differentially expressed genes. PCA plots of $\log_2$ transformed gene expression values were generated using the plotPCA function from the DESeq2 package.

Gene set variation analysis (GSVA)

The R/Bioconductor package GSVA (45) (v1.25.0) was used as a non-parametric, unsupervised method to estimate the variation in enrichment of pre-defined gene sets in RNA-seq dataset samples as previously described (36) (www.bioconductor.org/packages/release/bioc/html/GSVA.html). In brief, a matrix of $\log_2$ transformed gene expression values for each sample and pre-defined gene sets were used as inputs for the GSVA algorithm. Then enrichment scores (GSVA scores) for each gene set were calculated using a Kolmogorov Smirnoff (KS)-like random walk statistic. GSVA scores for each patient and control were calculated and normalized to scores between -1 (no enrichment) and +1 (enriched). Significance of gene set enrichment between cohorts was calculated using a Welch's t-test and p-value < 0.05 was considered significant.

Input gene sets used for GSVA analysis were previously used for the analysis of COVID-19 patient datasets (36) and can be found in Supplementary Table 4.

Linear regression analysis

Multivariable linear regression analysis was performed with MaAsLin 2 (46), a Bioconductor R package that helps to determine the association between gene expression and complex metadata features. MaAsLin 2 is a statistical method that relies on general linear regression models which can test for the association between various functional and cell specific modules versus individual discrete and categorical clinical variables. Computed GSVA scores and patient metadata were used as input for the MaAsLin 2 function in R with normalization method and transformation method applied "NONE", analysis method "LM", and correction method "BH". The significant associations with clinical variables were visualized using scatterplots and box plots.

Additional linear regression analyses for individual patient cohorts and between PC GSVA scores and $\log_2$ expression of Ig heavy chain transcripts were performed in GraphPad Prism (v 9.1.0; www.graphpad.com). For each analysis, the r^2 value indicating the Goodness of Fit and the p-value testing the significance of the slope are displayed.

Statistical analysis

Patient demographic data from COVID Group 1 and Group 2 were compared using an unpaired t-test with Welch's correction for continuous variables. Pearson's chi-squared tests were used to analyze count data between groups. Cytokine data for COVID Group 1, COVID Group 2, and control ICU patients was compared using Brown-Forsythe and Welch ANOVA tests with Dunnett T3 test for multiple comparisons. Significant differences in gene set enrichment between COVID-19 patients and non-COVID-19 patient cohorts were calculated using Brown-Forsythe and Welch ANOVA tests with Dunnett T3 test for multiple comparisons.

All statistical analyses were performed in GraphPad Prism (v 9.1.0; www.graphpad.com) and a two-tailed p-value of 0.05 was used for statistical significance.

Data and materials availability

The RNA-seq data generated in the current study are publicly available through the National Center for Biotechnology Information (NCBI) under SRA project number PRJNA777938. The confirmation study datasets are publicly available under accessions GSE161731 and GSE172114.

10.3389/fimmu.2022.989556

Results

Transcriptomic analysis differentiates critically ill COVID-19 patients from other patients with AHRF and control patients in the ICU

To identify differences in immune pathology among severe COVID-19 patients, we analyzed whole blood transcriptomes from 13 individuals with COVID-19-induced AHRF, 6 with other viral and 7 with non-viral-induced AHRF, and 5 controls, who were patients admitted to the ICU on mechanical ventilation but without evidence of AHRF (Supplementary Table 1, Supplementary Table 2). Out of 18,130 total transcripts, we found 344 differentially expressed genes (DEGs) between control and COVID-19 ICU patients, 248 DEGs between viral AHRF and COVID-19 patients, and 650 DEGs between non-viral AHRF and COVID-19 patients (Supplementary Table 3 and Figure 1A). Notably, expression of none of the genes previously associated with severe disease or increased mortality and reported as therapeutic targets for treatment of COVID-19 was significantly changed between controls and COVID-19 patients in the ICU (Supplementary Figure 1B) (47–49).

To examine differences in inflammatory pathways between COVID-19 patients and control ICU patients, we carried out Gene Set Variation Analysis (GSVA) (45) using a set of immune cell and pathway gene signatures (Figure 1B). Gene expression from COVID-19 patients was enriched for signatures of granulocytes, including inflammatory neutrophils and low-

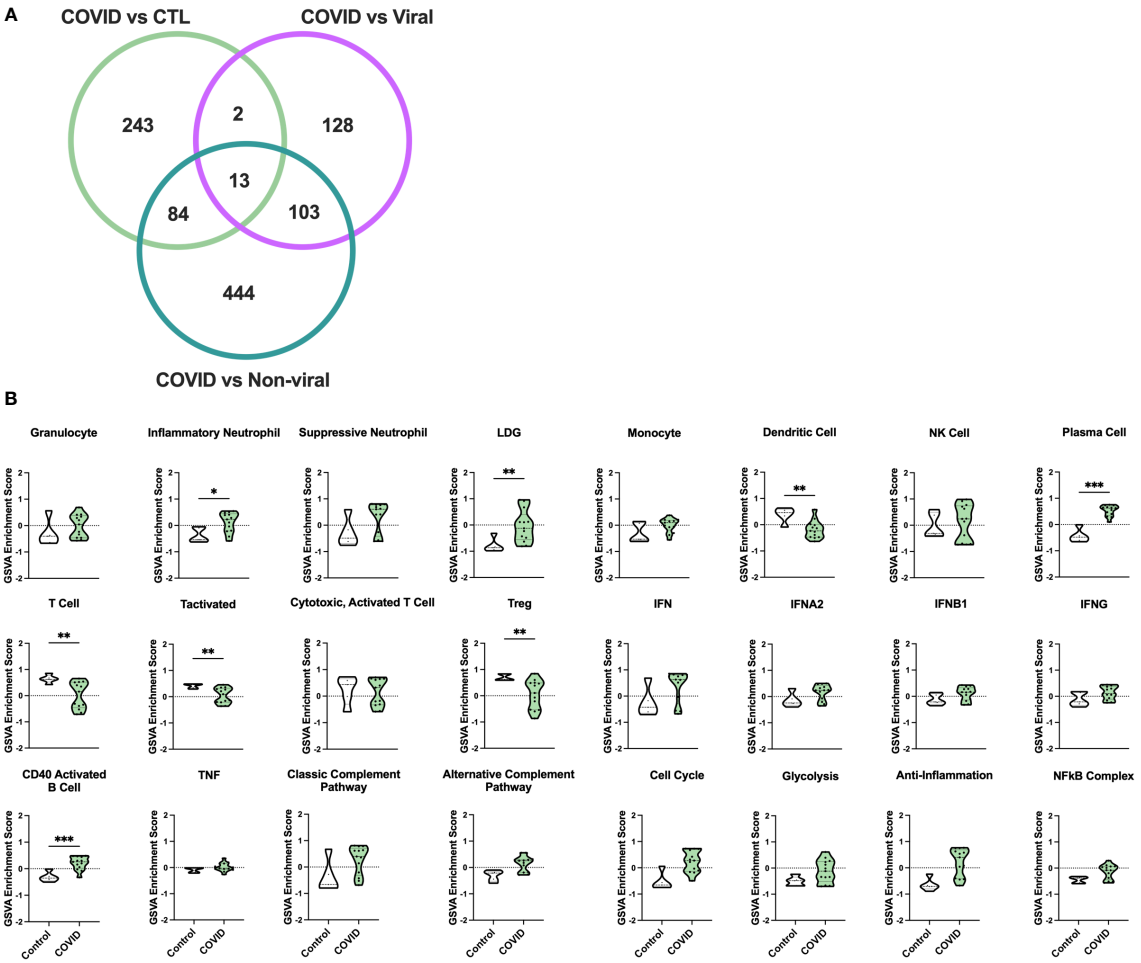

FIGURE 1
Gene signature analysis differentiates COVID-19 AHRF patients and control ICU patients. **(A)** Venn diagram of differentially expressed genes between COVID-19 patients and other ICU cohorts. **(B)** Individual sample gene expression from COVID-19 and control ICU patients was analyzed by GSVA for enrichment of immune cell and pathway gene signatures. Enrichment scores are shown as violin plots. *p < 0.05, **p < 0.01, ***p < 0.001.

density granulocytes (LDGs) as well as plasma cells (PCs) and CD40 activated B cells. In addition, as compared to controls, COVID-19 patients exhibited decreased enrichment for signatures of dendritic cells (DCs), activated T cells, and Tregs.

Enrichment of inflammatory cell types and pathway gene signatures separates COVID-19 ICU patients into two groups

Principal component analysis (PCA) using the $\log_2$ transformed gene expression values differentiating COVID-19 and control ICU patients indicated a division among COVID-19 patients into two groups (Figure 2A). Notably, the two COVID-19 groups differed in expression of specific COVID-19 associated genes (Supplementary Figure 1C). COVID Group 1 patients tended to show an increase in the innate immune checkpoint molecule CD24, whereas COVID Group 2 patients had increased expression of the anti-viral response genes OAS1, OAS2, and OAS3.

We then utilized GSVA to examine inflammatory pathways in the two gene expression-derived COVID-19 patient groups in greater detail (Figure 2B). Enrichment of PCs and de-enrichment of DCs was conserved between both COVID-19 groups compared to controls. However, the majority of signatures were differentially enriched in the two groups, revealing distinct immune profiles. Specific granulocyte population signatures were enriched in the COVID-19 patient

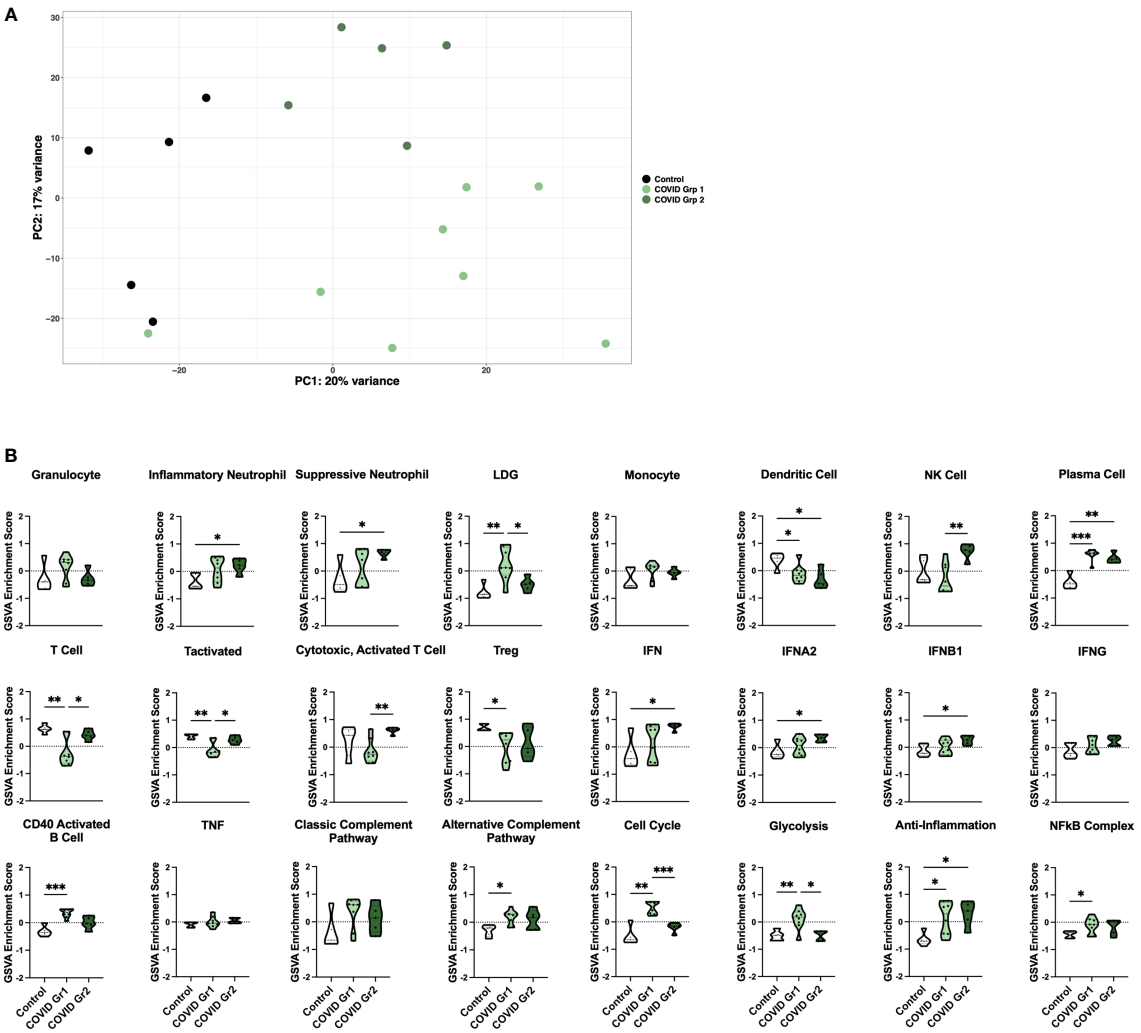

FIGURE 2
Enrichment of inflammatory cell types and pathway gene signatures in gene expression-derived COVID-19 AHRF patient groups. **(A)** Principle component analysis of the top 500 variable genes between control (black) and COVID-19 (green) ICU patients. COVID-19 patients were further separated into COVID Group 1 (light green) and COVID Group 2 (dark green). **(B)** Individual sample gene expression from **(A)** was analyzed by GSVA for enrichment of immune cell and pathway gene signatures. Enrichment scores are shown as violin plots. *p < 0.05, **p < 0.01, ***p < 0.001.

groups with increased LDGs in COVID Group 1 and increased inflammatory and suppressive neutrophils in COVID Group 2. In addition, COVID Group 1 was uniquely enriched for signatures of CD40 activated B cells, the alternative complement pathway, the cell cycle, glycolysis, and the NFkB complex and de-enriched for activated T cell signatures. In COVID Group 2, natural killer (NK) cell, general interferon (IFN), IFNA2, and IFNB1, but not IFNG signatures were significantly increased, whereas no inflammatory signatures were decreased compared to controls.

Conserved and unique immune signatures identify ICU patients with different causes of AHRF

We also compared gene signature enrichment from ICU patients with COVID-19-induced AHRF to patients admitted to the ICU with respiratory failure from other non-SARS-CoV-2 viral infections or non-viral causes (Figure 3A). The PC gene signature was consistently enriched in both COVID Group 1 and 2 compared with the non-viral and viral AHRF cohorts. Numerous differences in gene set enrichment patterns were noted between the COVID-19 groups and those with other causes of AHRF. Many of the differences in immune cell and pathway enrichment between COVID Group 1 and 2 and non-viral AHRF patients were consistent with the differences from control ICU patients, whereas, in general, viral and COVID-19 AHRF were more similar. In COVID Group 1, CD40 activated B cells and the cell cycle were increased over the non-viral AHRF group. In COVID Group 2, suppressive neutrophils, NK cells, T cells, IFN, IFNA2, and IFNB1 were increased, whereas granulocytes and glycolysis were decreased. as compared to non-viral AHRF. The most consistent difference between COVID Group 1 or COVID Group 2 and viral AHRF patients was the increased PC signature in the COVID patients.

To correlate GSVA gene signature enrichment with AHRF patient cohort and clinical features, we performed multivariable linear regression analysis using MaAsLin 2 and plotted relationships with significant correlations (46) (Figure 3B; Supplementary Table 2). As a result, we found the TNF, IFNG, inflammatory neutrophil, and suppressive neutrophil signatures had significant positive correlations with length of stay. In addition, the LDG signature had a significant positive correlation and the activated T cell signature a significant negative correlation with length of intubation. However, when linear regression analysis was carried out individually for each cohort, we found that the gene signature to clinical feature correlations were not significant for all patient cohorts (Figure 3B). None of these gene signature to clinical feature correlations were significant when considering the control ICU patients or non-viral AHRF patients alone, indicating that these relationships were specific for patients with virus-induced respiratory failure. Among viral and COVID AHRF cohorts, the positive correlation between inflammatory neutrophils and length of stay was significant for both COVID and viral AHRF patients while the correlations between TNF, IFNG, or suppressive neutrophils and length of stay were only significant for COVID but not viral AHRF cohorts. Furthermore, the negative correlation between activated T cells and length of intubation was only significant for the viral AHRF cohort, but not for the COVID groups. Therefore, subsets of ICU patients exhibit differences in immune signatures indicative of a worse clinical prognosis, but this is not unique for COVID-19 patients.

Specific plasma cell populations are characteristic of COVID-19-induced AHRF

COVID-19 patients, whether Group 1 or Group 2, had a significant increase in PCs over all other ICU patients. This result was further probed by multivariable linear regression analysis, in which the most significant correlation between GSVA enrichment score and patient cohort was for the PC signature, which was uniquely associated with COVID-19 patient groups (Figure 4A). To investigate the immunoglobulin (Ig) heavy chain(s) expressed by AHRF COVID-19 patient PCs, we carried out linear regression using PC GSVA scores and Ig heavy chain gene expression (Figures 4B, C). As a whole, COVID-19 patient PC GSVA scores were significantly correlated with IGHG3 and IGHA1 Ig heavy chain isotypes (Figure 4B). However, when the COVID groups were analyzed separately, only COVID Group 1 showed a significant correlation with expression of IgHA1 ($r^2 = 0.8$, p=0.004). This was not found with COVID group 2 (Figure 4C).

Clinical features and serum cytokines are indicative of differential disease severity in gene expression-derived COVID-19 patient groups

To determine whether gene expression-derived groups of hospitalized COVID-19 patients also differed in the level of disease severity, we compared clinical feature and cytokine data of COVID Group 1 and Group 2 patients (Figure 5; Supplementary Table 3). We found that baseline demographic data as well as length of stay in ICU and length of intubation were similar between COVID Group 1 and 2 (Figures 5A, B). Notably, however, these cohorts varied widely in a number of clinical features indicating that COVID Group 2 had more severe disease (Figure 5B). On average, COVID Group 2 had two fewer days of symptoms before admission to the ICU and thus had accelerated disease onset. Upon admission, ferritin and AST levels were over 2X and 1.5X higher, respectively, in Group

10.3389/fimmu.2022.989556

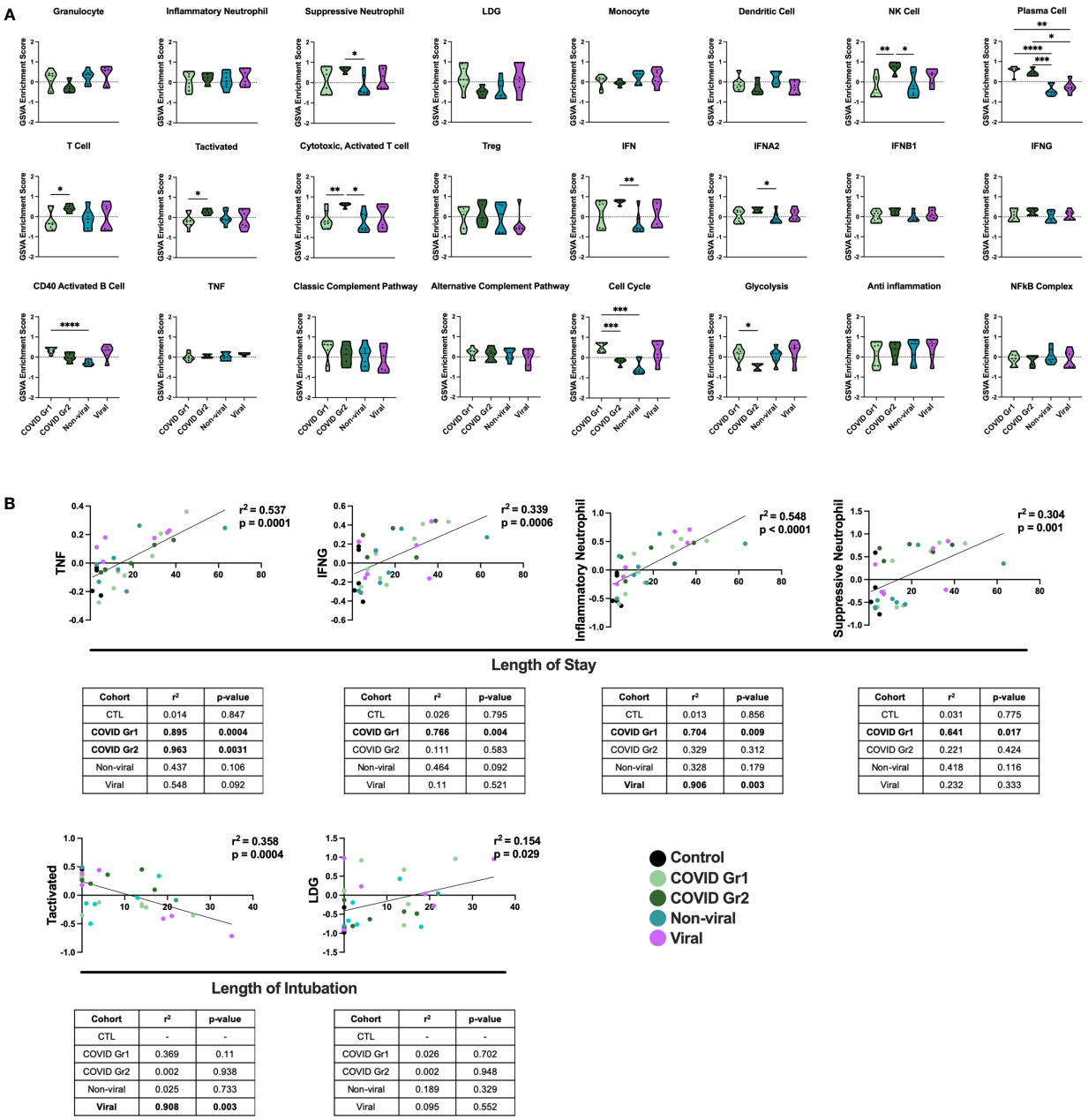

Cohort	r²	p-value
CTL	0.014	0.847
COVID Gr1	**0.895**	**0.0004**
COVID Gr2	**0.963**	**0.0031**
Non-viral	0.437	0.106
Viral	0.548	0.092

Cohort	r²	p-value
CTL	0.026	0.795
COVID Gr1	**0.766**	**0.004**
COVID Gr2	0.111	0.583
Non-viral	0.464	0.092
Viral	0.11	0.521

Cohort	r²	p-value
CTL	0.013	0.856
COVID Gr1	**0.704**	**0.009**
COVID Gr2	0.329	0.312
Non-viral	0.328	0.179
Viral	**0.906**	**0.003**

Cohort	r²	p-value
CTL	0.031	0.775
COVID Gr1	**0.641**	**0.017**
COVID Gr2	0.221	0.424
Non-viral	0.418	0.116
Viral	0.232	0.333

Cohort	r²	p-value
CTL	-	-
COVID Gr1	0.369	0.11
COVID Gr2	0.002	0.938
Non-viral	0.025	0.733
Viral	**0.908**	**0.003**

Cohort	r²	p-value
CTL	-	-
COVID Gr1	0.026	0.702
COVID Gr2	0.002	0.948
Non-viral	0.189	0.329
Viral	0.095	0.552

FIGURE 3
Conserved and unique immune signatures identify ICU patients with different sources of AHRF and vary in correlations with clinical data. **(A)** Individual sample gene expression from COVID Group 1, COVID Group 2, Viral, or Non-viral AHRF ICU patient cohorts was analyzed by GSVA for enrichment of immune cell and pathway gene signatures. Enrichment scores are shown as violin plots. *p < 0.05, **p < 0.01, ***p < 0.001, ****p < 0.0001. **(B)** Multivariable linear regression analysis of immune cell gene signatures significantly correlated with clinical data from Control, COVID Group 1, COVID Group 2, Viral, and Non-viral AHRF ICU patient cohorts. Combined cohort correlations and p-values are displayed in the linear regression plots while individual cohort correlations and p-values are displayed in the tables below. Correlations with p < 0.05 were considered significant.

2 patients whereas their lung function, as measured by mean PF ratio, was lower. Furthermore, maximum ferritin and aspartate aminotransferase (AST) levels were even more elevated in COVID Group 2 than at admission, indicative of rapid disease progression in these patients. In contrast to clinical features, pro-inflammatory cytokines were only modestly elevated in COVID Group 1 and 2 over controls and in COVID Group 2 over Group 1 (Figure 5C). COVID Group 1 and 2 exhibited modest increases

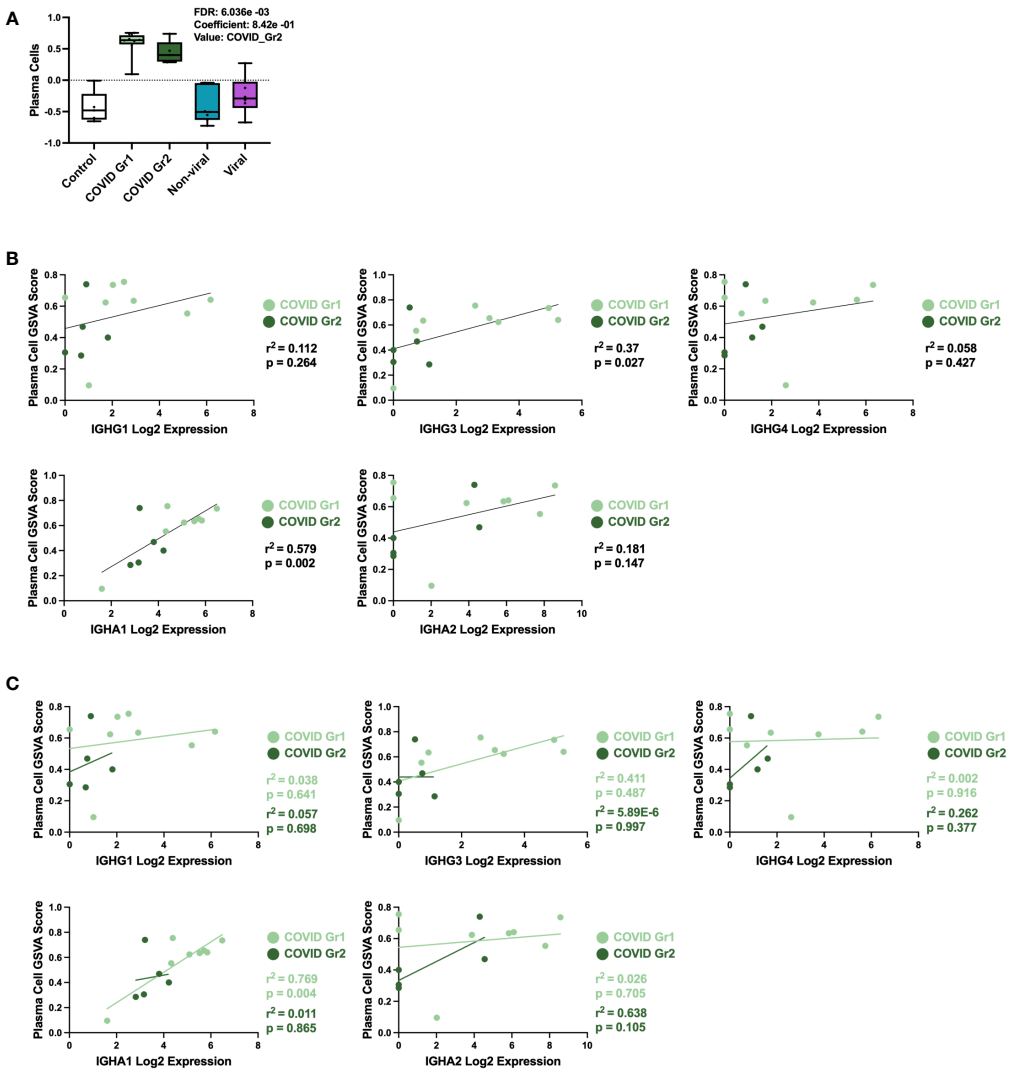

FIGURE 4
Specific plasma cell populations are characteristic of COVID-19-induced AHRF. **(A)** Multivariable linear regression analysis boxplots depicting significant correlation of the PC gene signature GSVA scores with ICU patient cohort. **(B, C)** Linear regression between PC GSVA scores and Ig heavy chain isotype $\log_2$ gene expression values for COVID Group 1 and COVID Group 2 ICU patient cohorts. Combined cohort correlations and p-values are depicted in **(B)** and individual cohort correlations and p-values are depicted in **(C)**. Correlations with $p < 0.05$ were considered significant.

in IL6, IL8, and TNF, although these differences did not reach statistical significance. In addition, COVID Group 1 had slightly elevated CD40L and VEGF and COVID Group 2 had significantly elevated levels of the myeloid chemokines CCL2 and CXCL10 as well as IFNA2 and IFNG. In many cases, severe COVID-19 patients are thought to have had greater viral exposure and thus greater viral load in relation to mild cases (50, 51). However, we found no significant differences in viral loads between the COVID-19 patient groups despite their clear differences in clinical features and gene expression profiles (Figure 5D).

Longitudinal sampling reveals persistence of immune cell and pathway gene signatures in AHRF ICU patients over time

To examine the persistence of gene signature enrichment over time in the ICU, several COVID-19 AHRF, Viral AHRF, and Non-viral AHRF patients were also sampled at 24- and 72-hours post-admission and individualized trajectories of gene expression were assessed (Figure 6 and Supplementary Figure 2). Gene signatures for all AHRF cohorts remained

10.3389/fimmu.2022.989556

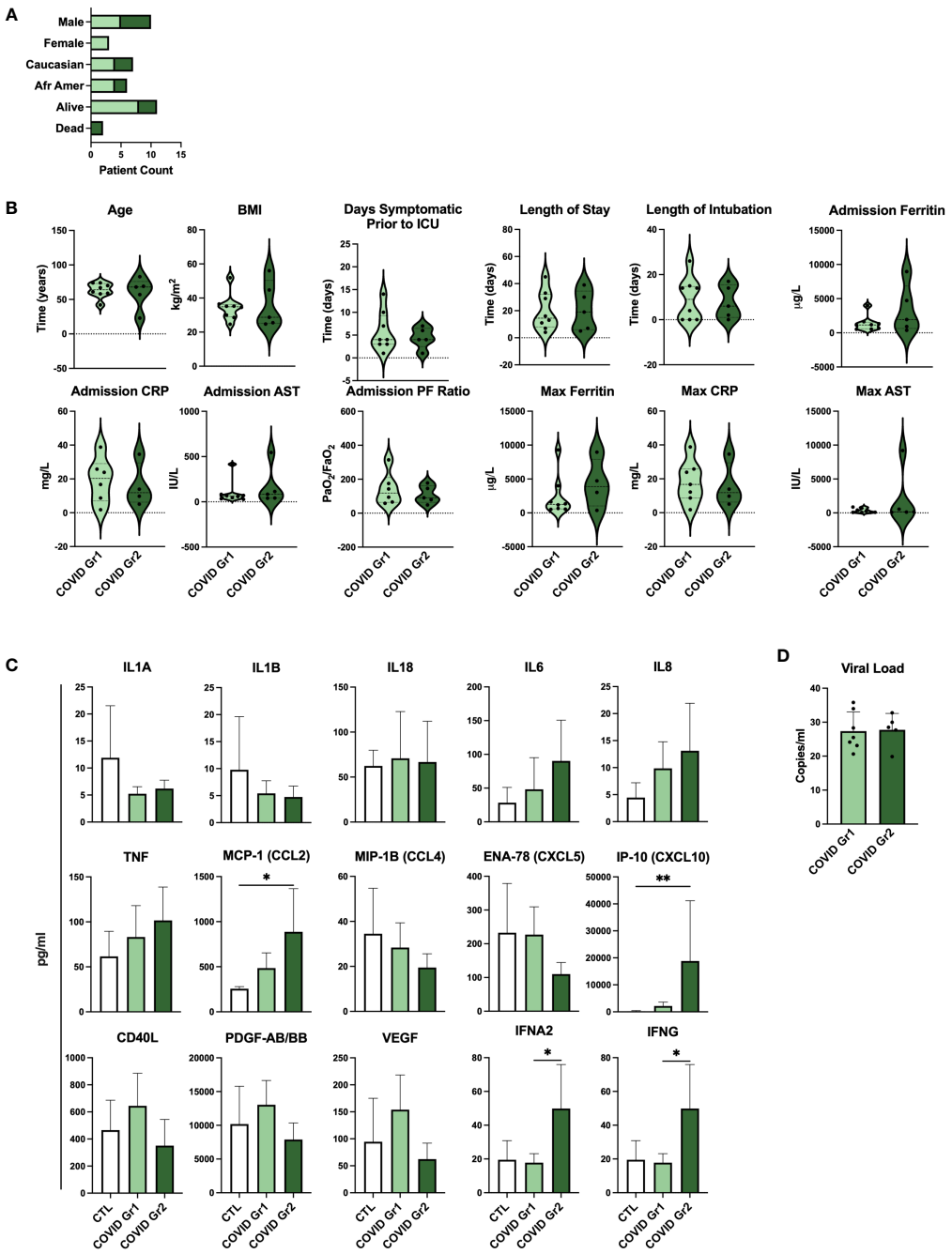

FIGURE 5
Serum cytokines, but not viral load, are indicative of differential disease severity in gene expression-derived COVID-19 patient groups. **(A)** Demographic data and **(B)** clinical feature data from COVID Group and COVID Group 2 patient cohorts. **(C)** Serum cytokine measurements from Control, COVID Group 1, and COVID Group 2 ICU patient cohorts. **(D)** SARS-CoV-2 viral load CT values of nasal swabs from COVID-19 ICU patient cohorts. *p < 0.05, **p < 0.01.

largely stable over time, but among individuals with COVID-19, Group 1 patients appeared to have greater variation than Group 2 patients. In particular, the IFN and neutrophil signatures that were uniquely enriched in COVID Group 2 were decreased in Group 1 patients over time, whereas the LDG signature was increased. Importantly, Group 2 patient 142, who succumbed, displayed very little change in gene expression over the 72 hours.

10.3389/fimmu.2022.989556

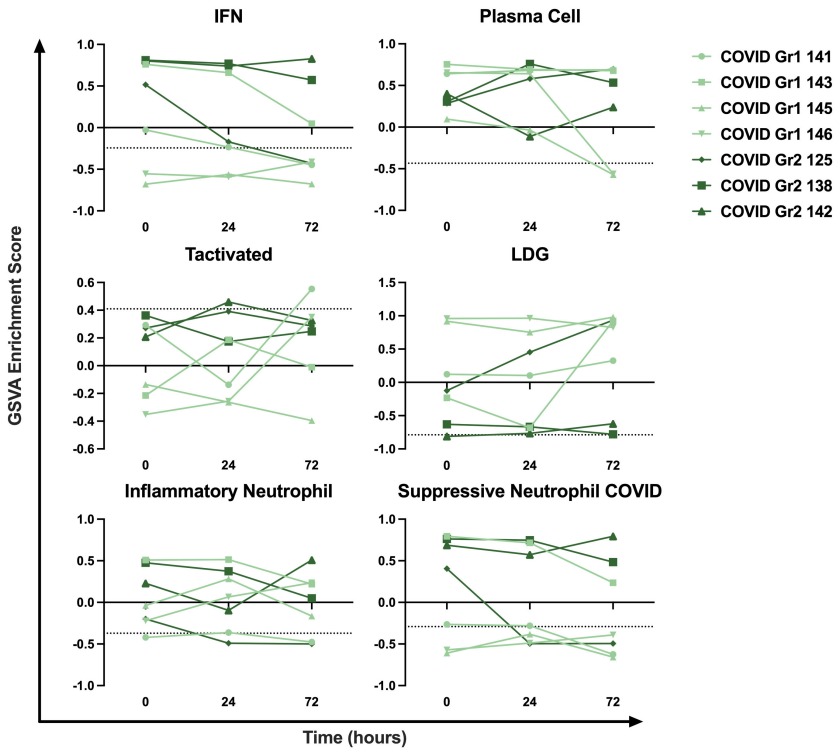

FIGURE 6
Longitudinal sampling reveals persistence of immune cell and pathway gene signatures over time. Trajectory plots of select immune cell and pathway GSVA enrichment scores from individual COVID-19 ICU patients at baseline, 24 hours, and 72 hours post-admission.

Non-hospitalized COVID-19 patient gene expression profiles resemble healthy controls, particularly at later stages of disease

Our initial dataset of COVID-19 patients consisted entirely of severe AHRF cases admitted to the ICU. Therefore, we wanted to characterize the immune profiles of COVID-19 patients at different stages of diseases and severity (non-hospitalized vs hospitalized) as compared to healthy controls. To do this, we analyzed a second publicly available COVID-19 transcriptomic dataset (GSE161731, Supplementary Table 1), which sampled 16 COVID-19 patients at early-stage (< 10 days), 30 at mid-stage (11-21 days), and 17 at late-stage (> 21 days) disease (52). In total, there were 82 common DEGs between individuals with COVID-19 and healthy controls in this study and our analysis of COVID-19 ICU patients compared to controls in the ICU (Supplementary Figure 3). GSVA analysis revealed that many gene signatures enriched in AHRF COVID-19 patients were selectively enriched in the early and mid-stage, but not late-stage disease cohorts (Figure 7A). Furthermore, early-stage patients most resembled the COVID Group 2 cohort, whereas mid-stage disease patients resembled COVID Group 1. Early stage COVID-19 patients were enriched for suppressive neutrophil, monocyte, PC, IFN, CD40 activated B cell, cell cycle, and NFkB gene signatures. Mid-stage patients were enriched for PC, CD40 activated B cell, alternative complement pathway, and cell cycle gene signatures. Late-stage patients were de-enriched for all of these signatures as compared to the early and mid-stage disease cohorts and had no significant differences from healthy controls. Notably, while early and mid-stage cohorts included both mild, non-hospitalized and severe, hospitalized patients, none of the patients with late-stage disease required hospitalization.

Immune cell and pathway gene signature enrichments are conserved between hospitalized COVID-19 patients

In addition to differences in disease stage, patients with early and mid-stage disease were further differentiated by disease severity based on whether they were hospitalized. Comparing 35 non-hospitalized and 11 hospitalized COVID-19 patients (Figure 7B) revealed that a few signatures were commonly enriched in all COVID-19 patients regardless of disease

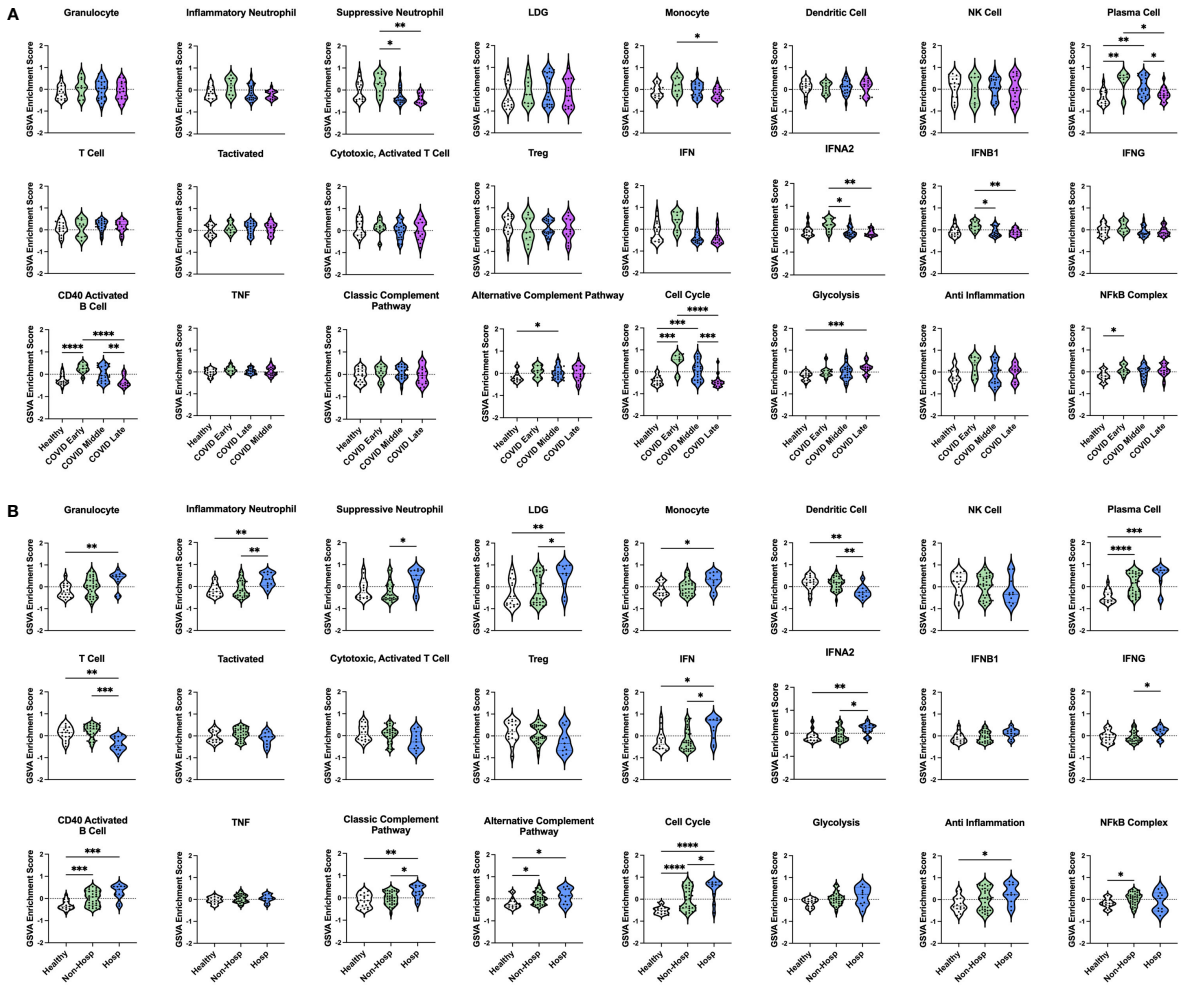

FIGURE 7
Enrichment of immune cell and pathway gene signatures in non-hospitalized and hospitalized COVID-19 patients at different stages of disease. **(A)** Individual sample gene expression from non-hospitalized COVID-19 patients with early-, mid-, or late-stage disease and healthy controls was analyzed by GSVA for enrichment of immune cell and pathway gene signatures. **(B)** Individual sample gene expression from non-hospitalized and hospitalized COVID-19 patients and healthy controls was analyzed by GSVA for enrichment of immune cell and pathway gene signatures. Enrichment scores are shown as violin plots. *p < 0.05, **p < 0.01, ***p < 0.001, ****p < 0.0001.

severity, including PCs, CD40 activated B cells, the alternative complement pathway, and the cell cycle. Interestingly, linear regression analysis of PC GSVA scores with IgH chain gene expression revealed that both non-hospitalized and hospitalized COVID-19 patients had significant correlations with IgG and IgA chain genes, although the non-hospitalized patient correlations were stronger than those of hospitalized patients (Supplementary Figure 4). The NFkB complex signature was the only one uniquely enriched in non-hospitalized COVID-19 patients as compared to healthy controls. In contrast, many inflammatory signatures were specific to hospitalized COVID-19 patients, including increased granulocyte, inflammatory neutrophil, suppressive neutrophil, LDG, monocyte, IFN, classic complement pathway, and anti-inflammation signatures. In addition, only hospitalized patients had decreased DC and T cell gene signatures. To provide further support for these results, we analyzed a third publicly available dataset (GSE172114) of 23 non-critical and 46 critical COVID-19 patients. Critical COVID-19 patients from this study shared 103 and 2573 DEGs with our previous analyses of COVID-19 ICU patients and COVID-19 patients with varying disease severity respectively (Supplementary Figure 3). Notably, the enriched gene signatures previously noted in hospitalized compared to non-hospitalized COVID-19 patients were also enriched in this group of critical compared with non-critical COVID-19 patients (Supplementary Figure 5). Therefore, severe cases of COVID-19, which require hospitalization, have conserved immune profiles as measured by inflammatory gene

signatures, but upon further dissection reveal patient heterogeneity indicative of risk for more severe disease.

Discussion

Bioinformatic analysis of gene expression data from COVID-19 patients of varying disease stage and severity was used to identify immune signatures common to COVID-19 as well as immune signatures that differentiate patients with severe disease requiring hospitalization. Shared enrichment of the PC gene signature was the one constant feature of COVID-19 patients in comparison to healthy controls, regardless of the length of time since symptom onset or whether their disease was severe enough to require hospitalization, which is consistent with previous work from our group and others (3, 19, 36, 53). This rapid increase in the PC signature suggests that SARS-CoV-2 infection initiates a robust generation of antibody secreting cells (ASCs), potentially through an extrafollicular response, which are capable of producing virus-specific neutralizing antibodies (54, 55). These ASCs are presumably generated in secondary immune organs and migrate to the bone marrow as a normal feature of immunization. However, as fully mature PCs are rare to find in the blood, this enrichment likely represents an increase in short-lived plasmablasts (PBs), which are still capable of producing neutralizing antibodies, but may not have undergone somatic hypermutation to increase their specificity for SARS-CoV-2 viral antigens (56). Thus, the increased PC signature may be largely COVID, but not severity -specific and could account for conflicting reports as to whether antibody production in COVID-19 is helpful or harmful (53).

The pathogenic gene signatures associated with hospitalized COVID-19 patients were conserved across multiple datasets, suggesting that these enrichments represent a common immune profile of severe COVID-19 (52). This profile was characterized by increased enrichment of neutrophil subsets and IFN accompanied by de-enrichment of T cells and was specific to patients with early and mid-stage disease (< 21 days since symptom onset). Notably, the greatest inflammatory signature enrichment was observed in early-stage patients (< 10 days since symptom onset). In contrast, the immune profiles of patients who reached late-stage disease (> 21 days since symptom onset) were no different than healthy controls and none of these individuals were hospitalized indicating that they would fully recover. Thus, this result stresses the importance of early identification of infected individuals and provides critical insight into the pathologic immune signatures that are risk factors for the development of severe disease and need for hospitalization.

Analysis of longitudinal gene expression data from patients admitted to the ICU was utilized to decode the heterogeneity among severe COVID-19 patients and to differentiate them from others with AHRF based on their immune profiles. As a result, we identified and characterized 2 groups of COVID-19 patients (COVID Group 1 and COVID Group 2), with conserved and differential enrichment of immune cell and pathway gene signatures. COVID Group 1 was characterized by a lack of activated T cells, increased LDGs, increased CD40-activated B cells, and a general increase in cell proliferation and metabolism pathways. COVID Group 2 was characterized by increased expression of neutrophil subsets, markedly increased IFN gene signatures, and the absence of IgA1 expressing PCs. Aggregated clinical feature data and cytokine profiles for each COVID-19 patient cohort revealed that COVID Group 2 appeared to have more severe disease outcomes and indicated that patients with a similar immune profile would warrant a more targeted and aggressive therapeutic approach to mitigate risk of mortality.

Both COVID Group 1 and 2 shared enrichment of the PC signature, which consistently differentiated COVID-19 patients from control ICU patients as well as patients exhibiting respiratory failure from other viral or non-viral sources. However, it is possible that the IgH heavy chain isotype of PCs is indicative of whether a robust and early PC expansion is beneficial to COVID-19 patients and certain PC isotypes have been linked with severe disease (19). In line with this, we found evidence of differing PC specificities in COVID Group 1 and 2 patients as Group 2 patients, who exhibited more severe clinical features, also appeared to fail to generate an IgA1 PC response. This suggests that Group 2 patients may have a defect in T-B cell collaboration and the ability to produce class-switched IgA1 PCs. The IgA response is important to clear virus from mucosal surfaces, such as the lung and, therefore, a lack of IgA in COVID Group 2 may compromise SARS-CoV-2 clearance in these patients (57). Furthermore, production of autoantibodies of varying specificities has been reported in COVID-19 patients and could represent an non-specific PC response that contributes to systemic inflammation in infected individuals (33, 58). Therefore, a better characterization of the nature of PC generation and function following SARS-CoV-2 infection could be a critical factor in understanding the host immune response and how it differs among individuals.

COVID Group1 patients appeared to have less severe disease as compared to COVID Group 2. Whereas all presented with AHRF, all Group 1 patients recovered, whereas 2 of Group 2 patients died during their hospitalization. Although our data set is limited by the number of patients analyzed, it suggests that the Group 2 gene signature could serve as prognostic marker and warrant individualized intervention. Lymphopenia is an established feature of COVID-19 and, in particular, a lack of T cell responses has been associated with worse clinical outcome (14, 28, 53, 59, 60). However, COVID Group 1 patients had differential enrichment of B and T cell populations with enrichment of CD40 activated B cells and de-enrichment of activated and cytotoxic T cells. In addition, unlike non-viral and viral AHRF patient cohorts, lack of activated T cells failed to correlate with clinical data. This would indicate that a lack of T

cell activation and function is detrimental to patient outcome, but not essential for patient recovery and also that a robust activated B cell response may be able to compensate in some capacity.

COVID Group 1 patients also exhibited an increase in genes associated with LDGs, neutrophil-like granulocytes with enhanced capacity for production of Type I IFNs and formation of neutrophil extracellular traps (NETs) that have been identified in severe COVID-19 patients (61, 62). In agreement with reports that NET formation contributes to enhanced pathogenesis in COVID-19 patients, it is likely that enrichment of LDGs contributes to the development of AHRF (63, 64). However, the lack of LDG enrichment in COVID Group 2 patients suggests that enrichment of LDGs does not increase the risk of death. In fact, the absence of an extreme IFN response and eventual recovery of all COVID Group 1 patients, suggests that the increased LDG signature reflects an appropriate antiviral innate immune response that will eventually subside as the virus is cleared. This was supported by the elevated expression of CD24 observed in COVID Group 1 patients, as the CD24-SIGLEC10 signaling axis serves as an important regulator of innate immune. Notably, CD24Fc was effective in protection against viral pneumonia in a simian model and has been proposed for the treatment of COVID-19 (49).

In contrast to COVID Group 1, the immune response of COVID Group 2 patients appeared to be associated with increased risk of mortality. The primary immune signatures enriched in COVID Group 2 resembled a dysregulated antiviral innate immune response. In particular, Group 2 exhibited enrichment of neutrophil populations expressing pro-inflammatory and suppressive genes that were previously identified in blood from severe COVID-19 patients (13, 18). Furthermore, levels of cytokines and chemokines with roles in myeloid cell activation and recruitment were significantly elevated and could contribute to aberrant expansion of these pathogenic neutrophils and disease progression. COVID Group 2 patients also had significant enrichment of Type I IFN gene signatures and increased serum levels of IFN proteins compared to COVID Group 1. To date, there have been conflicting reports claiming that severe COVID-19 cases exhibit increased (29) or impaired (27) Type I IFN responses. However, our results would suggest that severe COVID-19 patients exhibit a range of IFN responses, but that extreme early IFN production ultimately increases risk of death.

In addition to IFNs, a number of pro-inflammatory cytokines, including members of the IL-1 family, IL-6, IL-8, and TNF have been implicated in COVID-19 pathogenesis and linked to severe disease (14, 24, 35). We also observed that severe COVID-19 patients in the ICU had a trend toward increases in IL-6, IL-8, and TNF over control ICU patients and this increase was even greater in COVID Group 2 over Group 1. However, there was considerable heterogeneity and none of these comparisons reached statistical significance. This result corroborates a number of reports that have questioned the notion that "cytokine storm" is a prominent contributor to COVID-19 pathogenesis (17, 21). Viral load has also had conflicting associations with disease severity (50, 51). However, we found no difference in viral load between our COVID-19 patient cohorts suggesting that greater mortality risk is not necessarily associated with greater viral exposure. One caveat to this is that our viral load measurements were taken from nasal swabs and it is possible that increased viral presence in the lower airway may lead to worse disease outcomes. The lack of a clear association between more severe clinical manifestations and accentuated gene expression profiles and viral load suggests that genetic control of host defense may play a prominent role in disease outcome, as has been suggested (47, 48, 65).

Longitudinal gene expression analysis over 72 hours after admission to the ICU revealed that the immune profiles of COVID and non-COVID AHRF patients remained largely unchanged over time. However, among the COVID-19-induced AHRF patients, profiles of COVID Group 1 patients appeared to exhibit greater changes than COVID Group 2. Strikingly, gene signatures of COVID-associated neutrophil subsets and IFN were decreased, whereas the LDG gene signature was increased in COVID Group 1 patients, further supporting the conclusion that the innate immune response in Group 1 patients contributes to viral clearance whereas the response in Group 2 patients contributes to enhanced inflammation and fatal disease.

We have applied a combination of bioinformatics approaches to characterize COVID-19 patients based on disease stage and severity using gene expression data, but must acknowledge the limitations of the data. Our initial dataset of ICU patients contained up to 13 patients per cohort and COVID-19 patients were also sub-divided into groups, which reduced the statistical power of our analyses. To mitigate this, we designed the study to solely include patients in the ICU, including non-AHRF controls, and thus reduce patient heterogeneity. In addition, a larger publicly available dataset including both hospitalized and non-hospitalized COVID-19 patients with healthy controls was utilized for validation. However, additional studies comparing ICU patients with more patients per cohort and more uniform inclusion criteria are warranted.

Overall, we have identified immune profiles of severe COVID-19 patients associated with full recovery from disease or increased risk of mortality. We propose that these differences in COVID Group 1 and Group 2 patients could be employed to better allocate healthcare resources and design targeted treatment plans to better care for individuals who are at the greatest risk of worse outcomes. Whereas optimal medical care and appropriate ventilator management may be sufficient in patients with immune profiles similar to COVID Group 1, patients with immune profiles similar to COVID Group 2

could benefit from more aggressive therapeutic intervention targeting the dysregulated innate immune response. In particular, drugs targeting Type I IFNs, cytokines, such as IL6 or TNF, or myeloid chemokines such as IP-10 or MCP1 could be effective treatments for these individuals. Our work highlights the heterogeneity among severe cases of COVID-19 and the need for better characterization of hospitalized individuals to determine effective strategies to mitigate pathogenic immune processes that are dysregulated in the most at-risk patients. Furthermore, infected individuals with the potential to progress to severe disease should be identified as early as possible to allow for better resource allocation and early individualized therapies.

Data availability statement

Data deposited in NCBI under BioProject accession PRJNA777938.

Ethics statement

The studies involving human participants were reviewed and approved by UVA Institutional Review Board for Health Sciences Research. The patients/participants provided their written informed consent to participate in this study.

Author contributions

Conceptualization: CB, LS, JS, AG, AK, and PL. Methodology: CB, LS, JS, AK, and PL. Software: PB. Formal Analysis: AD and PB. Data Curation: PB, CB, LS, JS, and AK. Writing – Original Draft: AD. Writing – Review & Editing, AD, CB, LS, JS, AK, and PL. Visualization: AD. Supervision: AD, AG, AK, and PL. Project Administration: AG, AK, and PL. Funding Acquisition: AK and AG. All authors contributed to the article and approved the submitted version.

Funding

NIH NHLBI K23 HL143135 (CB). NIH NIAID 1R21AI160334 (CB). COVID-19 Rapid Response Initiative by the Global Infectious Disease Institute, University of Virginia (CB, LS, AK). The RILITE Foundation (AG, PL).

Acknowledgments

We thank the patients who provided samples for this study as well as the authors of previous studies who made their data publicly available and facilitated our analyses.

Conflict of interest

Authors AD, PB, AG and PL were employed by company AMPEL BioSolutions LLC.

The remaining authors declare that the research was conducted in the absence of any commercial or financial relationships that could be construed as a potential conflict of interest.

Publisher's note

All claims expressed in this article are solely those of the authors and do not necessarily represent those of their affiliated organizations, or those of the publisher, the editors and the reviewers. Any product that may be evaluated in this article, or claim that may be made by its manufacturer, is not guaranteed or endorsed by the publisher.

Supplementary material

The Supplementary Material for this article can be found online at: https://www.frontiersin.org/articles/10.3389/fimmu.2022.989556/full#supplementary-material

References

1. Brodin P. Immune determinants of COVID-19 disease presentation and severity. *Nat Med* (2021) 27:28–33. doi: 10.1038/s41591-020-01202-8

2. Hu B, Guo H, Zhou P, Shi ZL. Characteristics of SARS-CoV-2 and COVID-19. *Nat Rev Microbiol* (2021) 19:141–54. doi: 10.1038/s41579-020-00459-7

3. Tay MZ, Poh CM, Rénia L, MacAry PA, Ng LFP. The trinity of COVID-19: immunity, inflammation and intervention. *Nat Rev Immunol.* (2020) 20(6):363-374. doi: 10.1038/s41577-020-0311-8

4. Berlin DA, Gulick RM, Martinez FJ. Severe covid-19. *N Engl J Med* (2020) 383:2451–60. doi: 10.1056/nejmcp2009575

5. Gandhi RT, Lynch JB, del Rio C. Mild or moderate covid-19. *N Engl J Med* (2020) 383:1757–66. doi: 10.1056/nejmcp2009249

6. Chen G, Wu D, Guo W, Cao Y, Huang D, Wang H, et al. Clinical and immunologic features in severe and moderate coronavirus disease 2019. *J Clin Invest* (2020) 130(5):2620–9. doi: 10.1172/JCI137244

7. Huang C, Wang Y, Li X, Ren L, Zhao J, Hu Y, et al. Clinical features of patients infected with 2019 novel coronavirus in wuhan, China. *Lancet* (2020) 395:497–506. doi: 10.1016/S0140-6736(20)30183-5

8. Wang D, Hu B, Hu C, Zhu F, Liu X, Zhang J, et al. Clinical characteristics of 138 hospitalized patients with 2019 novel coronavirus-infected pneumonia in wuhan, China. *J Am Med Assoc* (2020) 323:1061–9. doi: 10.1001/jama.2020.1585

9. Williamson EJ, Walker AJ, Bhaskaran K, Bacon S, Bates C, Morton CE, et al. Factors associated with COVID-19-related death using OpenSAFELY. *Nature* (2020) 584:430–6. doi: 10.1038/s41586-020-2521-4

10. Yang X, Yu Y, Xu J, Shu H, Xia J, Liu H, et al. Clinical course and outcomes of critically ill patients with COVID19 in wuhan China. *Lancet Respir Med* (2020) 8:475–81. doi: 10.1016/S2213-2600(20)30079-5

11. Zhou F, Yu T, Du R, Fan G, Liu Y, Liu Z, et al. Clinical course and risk factors for mortality of adult inpatients with COVID-19 in wuhan, China: A

retrospective cohort study. *Lancet (London England)* (2020) 395:1054–62. doi: 10.1016/S0140-6736(20)30566-3

12. Arunachalam PS, Wimmers F, Mok CKP, Perera RAPM, Scott M, Hagan T, et al. Systems biological assessment of immunity to mild versus severe COVID-19 infection in humans. *Science* (2020) 369:1210–20. doi: 10.1126/SCIENCE.ABC6261

13. Aschenbrenner AC, Mouktaroudi M, Krämer B, Oestreich M, Antonakos N, Nuesch-Germano M, et al. Disease severity-specific neutrophil signatures in blood transcriptomes stratify COVID-19 patients. *Genome Med* (2021) 13:7. doi: 10.1186/s13073-020-00823-5

14. Lucas C, Wong P, Klein J, Castro TBR, Silva J, Sundaram M, et al. Longitudinal analyses reveal immunological misfiring in severe COVID-19. *Nature* (2020) 584:463–9. doi: 10.1038/s41586-020-2588-y

15. Mathew D, Giles JR, Baxter AE, Oldridge DA, Greenplate AR, Wu JE, et al. Deep immune profiling of COVID-19 patients reveals distinct immunotypes with therapeutic implications. *Science* (2020) 369(6508):eabc8511. doi: 10.1126/SCIENCE.ABC8511

16. Meizlish ML, Pine AB, Bishai JD, Goshua G, Nadelmann ER, Simonov M, et al. A neutrophil activation signature predicts critical illness and mortality in COVID-19. *Blood Adv* (2021) 5:1164–77. doi: 10.1182/bloodadvances.2020003568

17. Mudd PA, Crawford JC, Turner JS, Souquette A, Reynolds D, Bender D, et al. Distinct inflammatory profiles distinguish COVID-19 from influenza with limited contributions from cytokine storm. *Sci Adv* (2020) 6:16–8. doi: 10.1126/sciadv.abe3024

18. Schulte-Schrepping J, Reusch N, Paclik D, Baßler K, Schlickeiser S, Zhang B, et al. Severe COVID-19 is marked by a dysregulated myeloid cell compartment. *Cell* (2020) 182:1419–40.e23. doi: 10.1016/j.cell.2020.08.001

19. Stephenson E, Reynolds G, Botting RA, Calero-Nieto FJ, Morgan MD, Tuong ZK, et al. Single-cell multi-omics analysis of the immune response in COVID-19. *Nat Med* (2021) 27(5):904–16. doi: 10.1038/s41591-021-01329-2

20. Su Y, Chen D, Yuan D, Lausted C, Choi J, Dai CL, et al. Multi-omics resolves a sharp disease-state shift between mild and moderate COVID-19. *Cell* (2020) 183:1479–1495.e20. doi: 10.1016/j.cell.2020.10.037

21. Wilk AJ, Rustagi A, Zhao NQ, Roque J, Martínez-Colón GJ, McKechnie JL, et al. A single-cell atlas of the peripheral immune response in patients with severe COVID-19. *Nat Med* (2020) 26:1070–6. doi: 10.1038/s41591-020-0944-y

22. Zhang JY, Wang XM, Xing X, Xu Z, Zhang C, Song JW, et al. Single-cell landscape of immunological responses in patients with COVID-19. *Nat Immunol* (2020) 21:1107–18. doi: 10.1038/s41590-020-0762-x

23. Blanco-Melo D, Nilsson-Payant BE, Liu W-C, Uhl S, Hoagland D, Møller R, et al. Imbalanced host response to SARS-CoV-2 drives development of COVID-19. *Cell* (2020) 181:1036–1045.e9. doi: 10.1016/j.cell.2020.04.026

24. Del Valle DM, Kim-Schulze S, Huang HH, Beckmann ND, Nirenberg S, Wang B, et al. An inflammatory cytokine signature predicts COVID-19 severity and survival. *Nat Med* (2020) 26:1636–43. doi: 10.1038/s41591-020-1051-9

25. Galani IE, Rovina N, Lampropoulou V, Triantafyllia V, Manioudaki M, Pavlos E, et al. Untuned antiviral immunity in COVID-19 revealed by temporal type I/III interferon patterns and flu comparison. *Nat Immunol* (2021) 22:32–40. doi: 10.1038/s41590-020-00840-x

26. Giamarellos-Bourboulis EJ, Netea MG, Rovina N, Akinosoglou K, Antoniadou A, Antonakos N, et al. Complex immune dysregulation in COVID-19 patients with severe respiratory failure clinical and translational report complex immune dysregulation in COVID-19 patients with severe respiratory failure. *Cell Host Microbe* (2020) 27:992–1000. doi: 10.1016/j.chom.2020.04.009

27. Hadjadj J, Yatim N, Barnabei L, Corneau A, Boussier J, Smith N, et al. Impaired type I interferon activity and inflammatory responses in severe COVID-19 patients. *Science* (2020) 369:718–24. doi: 10.1126/science.abc6027

28. Laing AG, Lorenc A, del Molino del Barrio I, Das A, Fish M, Monin L, et al. A dynamic COVID-19 immune signature includes associations with poor prognosis. *Nat Med* (2020) 26:1623–35. doi: 10.1038/s41591-020-1038-6

29. Lee JS, Park S, Jeong HW, Ahn JY, Choi SJ, Lee H, et al. Immunophenotyping of covid-19 and influenza highlights the role of type i interferons in development of severe covid-19. *Sci Immunol* (2020) 5(49): eabd1554. doi: 10.1126/sciimmunol.abd1554

30. Liu C, Martins AJ, Lau WW, Rachmaninoff N, Chen J, Imberti L, et al. Time-resolved systems immunology reveals a late juncture linked to fatal COVID-19. *Cell* (2021) 184:1836–1857.e22. doi: 10.1016/j.cell.2021.02.018

31. French MA, Moodley Y. The role of SARS-CoV-2 antibodies in COVID-19: Healing in most, harm at times. *Respirology* (2020) 25:680–2. doi: 10.1111/resp.13852

32. Scourfield DO, Reed SG, Quastel M, Alderson J, Bart VMT, Teijeira Crespo A, et al. The role and uses of antibodies in COVID-19 infections: a living review. *Oxford Open Immunol* (2021) 2:1–13. doi: 10.1093/oxfimm/iqab003

33. Bastard P, Rosen LB, Zhang Q, Michailidis E, Hoffmann HH, Zhang Y, et al. Autoantibodies against type I IFNs in patients with life-threatening COVID-19. *Science* (2020) 370(6515):eabd4585. doi: 10.1126/science.abd4585

34. Chang SE, Feng A, Meng W, Apostolidis SA, Mack E, Artandi M, et al. New-onset IgG autoantibodies in hospitalized patients with COVID-19. *medRxiv Prepr Serv Heal Sci* (2021) 12:5417. doi: 10.1101/2021.01.27.21250559

35. Jamilloux Y, Henry T, Belot A, Viel S, Fauter M, El Jammal T, et al. Should we stimulate or suppress immune responses in COVID-19? cytokine and anti-cytokine interventions. *Autoimmun Rev* (2020) 19:102567. doi: 10.1016/j.autrev.2020.102567

36. Daamen AR, Bachali P, Owen KA, Kingsmore KM, Hubbard EL, Labonte AC, et al. Comprehensive transcriptomic analysis of COVID-19 blood, lung, and airway. *Sci Rep* (2021) 11:7052. doi: 10.1038/s41598-021-86002-x

37. von Elm E, Altman DG, Egger M, Pocock SJ, Gøtzsche PC, Vandenbroucke JP. Strengthening the reporting of observational studies in epidemiology (STROBE) statement: Guidelines for reporting observational studies. *BMJ* (2007) 335:806–8. doi: 10.1136/bmj.39335.541782.AD

38. Ranieri VM, Rubenfeld GD, Thompson BT, Ferguson ND, Caldwell E, Fan E, et al. Acute respiratory distress syndrome: The Berlin definition. *JAMA* (2012) 307:2526–33. doi: 10.1001/jama.2012.5669

39. Andrews S. *FastQC: A quality control tool for high throughput sequence data* (2010). Available at: http://www.bioinformatics.babraham.ac.uk/projects/fastqc/.

40. Bolger AM, Lohse M, Usadel B. Trimmomatic: A flexible trimmer for illumina sequence data. *Bioinformatics* (2014) 30:2114–20. doi: 10.1093/bioinformatics/btu170

41. Dobin A, Davis CA, Schlesinger F, Drenkow J, Zaleski C, Jha S, et al. STAR: ultrafast universal RNA-seq aligner. *Bioinformatics* (2013) 29:15–21. doi: 10.1093/bioinformatics/bts635

42. Tarasov A, Vilella AJ, Cuppen E, Nijman IJ, Prins P. Sambamba: Fast processing of NGS alignment formats. *Bioinformatics* (2015) 31:2032–4. doi: 10.1093/bioinformatics/btv098

43. Liao Y, Smyth GK, Shi W. featureCounts: an efficient general purpose program for assigning sequence reads to genomic features. *Bioinformatics* (2014) 30:923–30. doi: 10.1093/bioinformatics/btt656

44. Rau A, Gallopin M, Celeux G, Jaffrézic F. Data-based filtering for replicated high-throughput transcriptome sequencing experiments. *Bioinformatics* (2013) 29:2146–52. doi: 10.1093/bioinformatics/btt350

45. Hänzelmann S, Castelo R, Guinney J. GSVA: Gene set variation analysis for microarray and RNA-seq data. *BMC Bioinf* (2013) 14:7. doi: 10.1186/1471-2105-14-7

46. Mallick H, Rahnavard A, McIver LJ, Ma S, Zhang Y, Tickle TL, et al. Multivariable association discovery in population-scale meta-omics studies. *PLoS Comput Biol.* (2021) 17(11):e1009442. doi: 10.1371/journal.pcbi.1009442

47. Hu J, Li C, Wang S, Li T, Zhang H. Genetic variants are identified to increase risk of COVID-19 related mortality from UK biobank data. *Hum Genomics* (2021) 15:1–10. doi: 10.1186/s40246-021-00306-7

48. Pairo-Castineira E, Clohisey S, Klaric L, Bretherick AD, Rawlik K, Pasko D, et al. Genetic mechanisms of critical illness in covid-19. *Nature* (2020) 591 (7848):92–8. doi: 10.1038/s41586-020-03065-y

49. Tian RR, Zhang MX, Liu M, Fang X, Li D, Zhang L, et al. CD24Fc protects against viral pneumonia in simian immunodeficiency virus-infected Chinese rhesus monkeys. *Cell Mol Immunol* (2020) 17:887–8. doi: 10.1038/s41423-020-0452-5

50. Pujadas E, Chaudhry F, McBride R, Richter F, Zhao S, Wajnberg A, et al. SARS-CoV-2 viral load predicts COVID-19 mortality. *Lancet Respir Med* (2020) 8: e70. doi: 10.1016/S2213-2600(20)30354-4

51. Fajnzylber J, Regan J, Coxen K, Corry H, Wong C, Rosenthal A, et al. SARS-CoV-2 viral load is associated with increased disease severity and mortality. *Nat Commun* (2020) 11:1–9. doi: 10.1038/s41467-020-19057-5

52. McClain MT, Constantine FJ, Henao R, Liu Y, Tsalik EL, Burke TW, et al. Dysregulated transcriptional responses to SARS-CoV-2 in the periphery. *Nat Commun* (2021) 12:1–8. doi: 10.1038/s41467-021-21289-y

53. Rydyznski Moderbacher C, Ramirez SI, Dan JM, Grifoni A, Hastie KM, Weiskopf D, et al. Antigen-specific adaptive immunity to SARS-CoV-2 in acute COVID-19 and associations with age and disease severity. *Cell* (2020) 183:996–1012.e19. doi: 10.1016/j.cell.2020.09.038

54. Nutt SL, Hodgkin PD, Tarlinton DM, Corcoran LM. The generation of antibody-secreting plasma cells. *Nat Rev Immunol* (2015) 15:160–71. doi: 10.1038/nri3795

55. Carter MJ, Mitchell RM, Sauteur PMM, Kelly DF, Trück J. The antibody-secreting cell response to infection: Kinetics and clinical applications. *Front Immunol* (2017) 8:630. doi: 10.3389/fimmu.2017.00630

56. Boulanger M, Molina E, Wang K, Kickler T, Xu Y, Garibaldi BT. Peripheral Plasma Cells Associated with Mortality Benefit in Severe COVID-19: A Marker of Disease Resolution. *Am J Med.* (2021) 134(8):1029-1033. doi: 10.1016/j.amjmed.2021.01.040

57. Sterlin D, Mathian A, Miyara M, Mohr A, Anna F, Claër L, et al. IgA dominates the early neutralizing antibody response to SARS-CoV-2. *Sci Transl Med* (2021) 13:eabd2223. doi: 10.1126/scitranslmed.abd2223

58. Wang EY, Mao T, Klein J, Dai Y, Huck JD, Jaycox JR, et al. Diverse functional autoantibodies in patients with COVID-19. *Nature* (2021) 595 (7866):283–8. doi: 10.1038/s41586-021-03631-y

59. Chen Z, John Wherry E. T Cell responses in patients with COVID-19. *Nat Rev Immunol* (2020) 20:529–36. doi: 10.1038/s41577-020-0402-6

60. Wen W, Su W, Tang H, Le W, Zhang X, Zheng Y, et al. Immune cell profiling of COVID-19 patients in the recovery stage by single-cell sequencing. *Cell Discovery* (2020) 6:31. doi: 10.1038/s41421-020-0168-9

61. Carmona-Rivera C, Kaplan MJ. Low-density granulocytes: a distinct class of neutrophils in systemic autoimmunity. *Semin Immunopathol* (2013) 35:455–63. doi: 10.1007/s00281-013-0375-7

62. Morrissey SM, Geller AE, Hu X, Tieri D, Ding C, Klaes CK, et al. A specific low-density neutrophil population correlates with hypercoagulation and disease severity in hospitalized COVID-19 patients. *JCI Insight* (2021) 6(9):e148435. doi: 10.1172/jci.insight.148435

63. Barnes BJ, Adrover JM, Baxter-Stoltzfus A, Borczuk A, Cools-Lartigue J, Crawford JM, et al. Targeting potential drivers of COVID-19: Neutrophil extracellular traps. *J Exp Med* (2020) 217:1–7. doi: 10.1084/jem.20200652

64. Thierry AR, Roch B. Neutrophil Extracellular Traps and By-Products Play a Key Role in COVID-19: Pathogenesis, Risk Factors, and Therapy. *J Clin Med.* (2020) 9(9):2942. doi: 10.3390/jcm9092942

65. Carter-Timofte ME, Jørgensen SE, Freytag MR, Thomsen MM, Brinck Andersen N-S, Al-Mousawi A, et al. Deciphering the role of host genetics in susceptibility to severe COVID-19. *Front Immunol* (2020) 11:1606. doi: 10.3389/fimmu.2020.01606

frontiers | Frontiers in Immunology

TYPE Review
PUBLISHED 16 September 2022
DOI 10.3389/fimmu.2022.993754

Check for updates

OPEN ACCESS

EDITED BY
Edwin Bölke,
Heinrich Heine University of Düsseldorf, Germany

REVIEWED BY
Rongbao Gao,
Chinese Center For Disease Control and Prevention, China
Jincun Zhao,
Guangzhou Medical University, China

*CORRESPONDENCE
Xiaohui Wei
xiaohui-wei@foxmail.com
Jiangning Liu
liujn@cnilas.org

SPECIALTY SECTION
This article was submitted to Viral Immunology, a section of the journal Frontiers in Immunology

RECEIVED 14 July 2022
ACCEPTED 05 September 2022
PUBLISHED 16 September 2022

CITATION
Wei X, Rong N and Liu J (2022) Prospects of animal models and their application in studies on adaptive immunity to SARS-CoV-2. *Front. Immunol.* 13:993754. doi: 10.3389/fimmu.2022.993754

COPYRIGHT
© 2022 Wei, Rong and Liu. This is an open-access article distributed under the terms of the Creative Commons Attribution License (CC BY). The use, distribution or reproduction in other forums is permitted, provided the original author(s) and the copyright owner(s) are credited and that the original publication in this journal is cited, in accordance with accepted academic practice. No use, distribution or reproduction is permitted which does not comply with these terms.

Prospects of animal models and their application in studies on adaptive immunity to SARS-CoV-2

Xiaohui Wei*, Na Rong and Jiangning Liu*

National Health Commission Key Laboratory of Human Disease Comparative Medicine, Beijing Key Laboratory for Animal Models of Emerging and Remerging Infectious Diseases, Institute of Laboratory Animal Science, Chinese Academy of Medical Sciences and Comparative Medicine Center, Peking Union Medical College, Beijing, China

The adaptive immune response induced by SARS-CoV-2 plays a key role in the antiviral process and can protect the body from the threat of infection for a certain period of time. However, owing to the limitations of clinical studies, the antiviral mechanisms, protective thresholds, and persistence of the immune memory of adaptive immune responses remain unclear. This review summarizes existing research models for SARS-CoV-2 and elaborates on the advantages of animal models in simulating the clinical symptoms of COVID-19 in humans. In addition, we systematically summarize the research progress on the SARS-CoV-2 adaptive immune response and the remaining key issues, as well as the application and prospects of animal models in this field. This paper provides direction for in-depth analysis of the anti-SARS-CoV-2 mechanism of the adaptive immune response and lays the foundation for the development and application of vaccines and drugs.

KEYWORDS

SARS-CoV-2, animal model, adaptive immunity, cross-immune response, tissue-resident immune response, immune memory

Abbreviations: SARS-CoV-2, severe acute respiratory syndrome coronavirus 2; COVID-19, coronavirus disease 2019; SARS-CoV, severe acute respiratory syndrome coronavirus; MERS-CoV, Middle East respiratory syndrome coronavirus; NHP, nonhuman primate; ACE2, angiotensin-converting enzyme 2; hACE2, human ACE2; URT, upper respiratory tract; TMPRSS2, transmembrane serine protease 2; cTfh, circulating T follicular helper cells; CTL, cytotoxic T lymphocyte; B_{RM}, tissue-resident memory B; T_{RM}, tissue-resident memory T; RBD, receptor-binding domain.

Introduction

Severe acute respiratory syndrome coronavirus 2 (SARS-CoV-2) has been circulating since the end of 2019 and has infected more than five hundred million people and killed more than six million people (https://coronavirus.jhu.edu/map.html), which has had an impact on global public security and the global economy (1, 2). Although the development of vaccines and drugs has hindered the spread and pathogenic process of the virus, the emergence of a tremendous number of mutant strains (more than eight million), especially the delta and omicron strains, has reduced the protection afforded by existing vaccines and drugs, resulting in breakthrough infection (3–6). In response to the rapid spread of SARS-CoV-2, some countries, such as Ireland, Denmark, Sweden, the United Kingdom, and Iceland, hope to prevent infection and spread by raising the threshold of "herd immunity", gradually regarding SARS-CoV-2 as similar to influenza and even implementing open-ended nonquarantine precautions. However, it cannot be ignored that we still know very little about SARS-CoV-2. Unlike severe acute respiratory syndrome coronavirus (SARS-CoV) and Middle East respiratory syndrome coronavirus (MERS-CoV) which were rapidly contained (7, 8), it remains to be investigated whether SARS-CoV-2 can be treated as influenza-like for prevention. Moreover, whether the emergence of new variants will increase the harm to public health safety remains worth exploring. Furthermore, how protective the existing vaccines and drugs are against the new variants and the durability of vaccine protection remain to be studied.

SARS-CoV-2 infection can initiate innate and adaptive immune responses. However, early studies have shown that patients with coronavirus disease 2019 (COVID-19) have extensive innate immune dysfunction (9–11), regarding type I and type III IFN responses, which are impaired and delayed, further increasing the clinical risk of patients (12, 13). At present, there is no evidence that the innate immune response can directly and completely control the early infection by SARS-CoV-2. The initiation of an adaptive immune response is critical for controlling SARS-CoV-2 infection and protecting the body from reinfection over time. Despite the uneven data cohort, overall, virus-specific antibody titers in people recovering from SARS-CoV-2 infection can be maintained for at least 4-6 months (14–16), and specific cellular immune responses last longer (17–19). The protective effect of SARS-CoV-2 primary infection on reinfection has received special attention. Follow-up studies on clinical patients have found that primary infection has a certain protective effect on the secondary infection (20).

The animal model is a very useful tool for clinical research on COVID-19. Various animal models of SARS-CoV-2 infection, including nonhuman primates (NHPs), rodents, etc. (21–30), have been developed and used to simulate the clinical pathology of the disease observed in humans and to test the preclinical effects of vaccines and drugs (31–35). Although animal models may not be able to recapitulate all the characteristics of human infection (36), they have more human-like characteristics than *in vitro* cell models and organoid models and can be used to indicate the pathogenesis of virus pathogenesis and immune protection mechanisms and can be used in other related research. In this study, we elaborated the research progress on SARS-CoV-2 *in vitro* and *in vivo* research models and adaptive immunology. In addition, we further summarized the application, advantages, and prospects of existing animal models in SARS-CoV-2 adaptive immunology research.

Classification and application of SARS-CoV-2 infection models

An in-depth understanding of SARS-CoV-2-related immunology is inseparable from the establishment and use of infection models. To date, three types of models have been established and applied in SARS-CoV-2-related research, including cells and organoids as well as animal models. They have different application scopes and advantages in related research (Figure 1), which are elaborated on in this section.

Cell lines

As a classic method to study viruses *in vitro*, cell lines are crucial for understanding the biology, growth kinetics, and

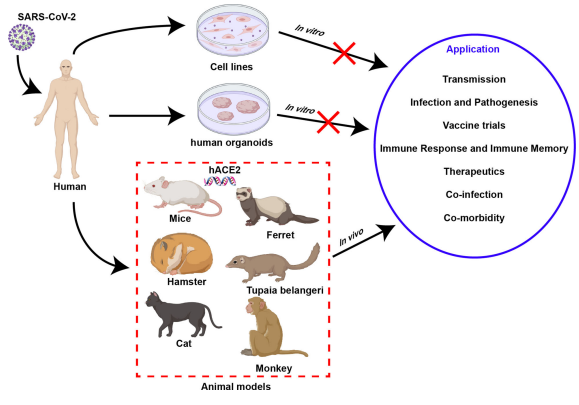

FIGURE 1
Models of SARS-CoV-2 infection. Three kinds of model can be used to study SARS-CoV-2, including *in vitro* model cell line, organoid, and *in vivo* animal models. In contrast with *in vitro* models, animal models can simulate virus-host interactions observed in human clinical research and have unique advantages in their application.

tropism of SARS-CoV-2 infection. Compared with primary human bronchial epithelial cells, which can better reflect the characteristics of infection (37), passaged cell lines have a series of advantages such as infinite proliferation, high stability, low cost, and simple operation, and can be applied to virus infection and replication research. Human angiotensin-converting enzyme 2 (ACE2) has been identified as a key receptor for SARS-CoV-2 to bind and invade cells (38), so a variety of cell lines expressing ACE2 receptors have become effective tools for the study of SARS-CoV-2 (Figure 1), such as Vero E6 cells (39), HEK-293T cells (39), Huh7 cells (40), Caco-II cells (41), and Calu3 cells (40). Especially in Vero E6 cells, the lack of type I interferon (IFN-I) and the high expression of the receptor ACE2 make it a cell line widely used to obtain high titers of virus particles of SARS-CoV-2 (42, 43). The cytopathic effects produced in virus-infected cell lines can be monitored for preclinical *in vitro* drug screening. However, the reliability of cell-based experimental results remains to be further investigated. For example, the antimalarial compounds chloroquine and hydroxychloroquine (HCQ) are effective in inhibiting the virus in cell lines, but less effective in primary cells and animal models (44–47). Therefore, although cell lines are convenient for studying SARS-CoV-2 *in vitro*, the obtained results still need to be further validated in primary cells and animal models. More importantly, deficiency immune-mediated or multicellular interactions are key factors limiting the application of cellular infection models.

Human organoids

Compared with cell lines with good homogeneity, human organoids are more complex 3D structures composed of a variety of cells, which can better simulate the physiological state of normal human organs, so they are more suitable for the study of SARS-CoV-2 infection and tropism and drug screening *in vitro* (48). To date, a large number of human organoids have been developed and used in SARS-CoV-2-related research (Figure 1), including lung organoids (49), bronchial organoids (50), kidney organoids (51), liver ductal organoids (52), intestinal organoids (53) and blood vessel organoids (54). Human organoids may allow observation of viral cell tropism, while exhibiting the accumulation of inflammatory cells and antiviral factors, reproducing the pathological symptoms after SARS-CoV-2 infection, which is crucial for understanding the pathogenesis of COVID-19 (55). Inevitably, the limitations of organoids prevent a deep understanding of severe COVID-19, possibly due to their lack of modulation of relevant immune components, including macrophages and natural killer cells. Furthermore, similar to the cell model, although neither can reproduce the pathogenic process of viral infection seen *in vivo* and the systemic antiviral infection process of the human body, they are good models for the convenient study of SARS-CoV-2 *in vitro*.

Animal models

Compared with *in vitro* models, animal models for SARS-CoV-2 are more complex, but they can yield more reliable clinical data on virus-host interactions (Figure 1). In detail, research on transmission routes, investigation of infection and pathogenic mechanisms, clinical evaluation of vaccines and drugs, elucidation of the host immune response and immune memory, the study of coinfection, and evaluation of complications, etc., requires the use of animal models (Figure 1) (56). Therefore, the rational development of animal models is crucial for gaining an in-depth understanding of SARS-CoV-2. To date, animal infection models that have been developed and are suitable for SARS-CoV-2-related research fall into five categories: small rodents, ferrets, cats, *Tupaia belangeris*, and NHPs.

Small rodents, including hamsters and genetically engineered mice, have many advantages such as easy operation, fast reproduction, and low cost, so they are widely used in research on the efficacy of antiviral drugs, vaccines, and immunotherapy. In particular, hamsters can be naturally infected by SARS-CoV-2 and show typical clinical symptoms, such as weight loss and multiple tissue and organ damage (57–59). Based on these characteristics, the hamster model has been applied to a series of studies, including transmission route (58), variant strain pathogenicity (60), and antibody therapy (61). Due to the limited specificity of the ACE2 receptor, wild-type mice are less sensitive to most variants of SARS-CoV-2, and only to the beta variant (62). Sensitization of mice by adenovirus expressing human ACE2 (Ad5-hACE2) is a fast and efficient method for susceptibility modeling and has been widely applied (63–66). Furthermore, genetically engineering mice to express the human ACE2 (hACE2) receptor is an effective way to increase their susceptibility to other variants of SARS-CoV-2. However, different genetically engineered mice have different clinical manifestations of disease due to differences in the modification and expression of the hACE2 receptors. For example, humanized mice expressing hACE2 under the epithelial cell-specific cytokeratin-18 (Krt 18) promoter (67), a universal chicken beta-actin (β-actin) promoter (68), or the human hepatocyte nuclear factor-3/forkhead homolog 4 (HFH4) promoter (25) are highly susceptible to SARS-CoV-2, develop severe pathological damage resembling COVID-19 symptoms in human lungs, and die rapidly. However, mouse models with only ACE2 replaced show only mild pathology and are confined to the lungs and intestine (24). Other nonprimate model animals, including cats (69, 70), ferrets (71), and *Tupaia belangeris* (72, 73), are susceptible to SARS-CoV-2 but do not produce severe clinical symptoms, so they may be potential intermediate hosts and ideal models for studying transmission in the absence of severe clinical symptoms.

The gold standard animal model that is closest to human genetics, anatomy, and immunology and is suitable for SARS-CoV-2 is the NHP model, mainly including African green monkeys (74), marmosets (23, 26, 75), baboons (75), cynomolgus macaques (23, 26) and rhesus macaques (26, 29, 30). They play a very important role in the study of the pathogenesis of COVID-19 and the development of vaccines and antiviral drugs. At present, it has been confirmed that the immune response of the NHP model after SARS-CoV-2 infection recapitulates the key features of COVID-19 in humans (76, 77). Therefore, the NHP model is the best model for evaluating drugs (78), neutralizing antibodies (79), and multiple vaccines (adenovirus, DNA, mRNA, inactivated, and subunit vaccines) (31, 80–85).

Animal models mimic the clinical features and pathogenesis of COVID-19

COVID-19 is a series of clinical syndromes caused by SARS-CoV-2 in humans, including asymptomatic infection, mild-to-moderate upper respiratory tract infection, pneumonia, acute respiratory distress syndrome (ARDS), hyperinflammatory disease, and long-term neurological and cognitive dysfunction (86). The pathogenesis of COVID-19 is complex and its severity and pathogenicity are closely related to various factors, such as age, complications, and genetic or acquired factors (87–90). Evidence suggests that SARS-CoV-2 is highly persistent and dangerous to those with weakened immune systems, especially elderly patients with cardiovascular disease, diabetes, hypertension, and some other serious chronic diseases (86, 88, 91–93). In particular, elderly individuals >65 years old showed similar lymphopenia, neutropenia, inflammation, and coagulation-related index elevation (90, 94–98). While most young and pediatric patients are asymptomatic or have mild symptoms, many of them experience persistent fatigue, anhedonia, muscle weakness, sleep problems, anxiety and even depression, difficulty concentrating, myalgia, and arthralgia, autonomic function obstacles, etc. (89, 99–101). Although the mechanism remains unclear, SARS-CoV-2 may cause irreversible damage to the brain, based on the evidence that SARS-CoV-2 can infect the central nervous system and brain cells (102–104).

Viral tropism depends on the susceptibility and permissiveness of specific host cells. Some studies suggest that SARS-CoV-2 induces an inflammatory response in the lower respiratory tract leading to lung injury (Figure 2), confirming that the lung is the main site of infection by SARS-CoV-2 (105, 106). Unlike SARS-CoV, SARS-CoV-2 can efficiently infect the upper respiratory tract (URT), such as nasopharyngeal and oropharyngeal tissues, increasing its infectivity and pathogenicity (Figure 2) (107–110). In addition, the gut is another target of SARS-CoV-2, and patients with COVID-19 often report suffering from gastrointestinal diseases (Figure 2) (111, 112). It is generally believed that the classical mechanism of SARS-CoV-2 infection targeting host cells occurs through the interaction between the viral surface structural protein Spike and the cell surface protein ACE2 (38). In addition, the function of the Spike protein requires the assistance of transmembrane serine protease 2 (TMPRSS2) (38, 113). Although it has been reported that other receptors or cofactors are also involved, such as the endosome/lysosomal cysteine proteases cathepsin B and L (CTSB, CTSL) (38), CD147 (114, 115), Neuropilin 1 (116, 117) and DPP4 (118, 119), whether these factors are necessary for SARS-CoV-2 invasion remains to be further confirmed. At least at the level of host protein expression, it has been determined that ACE2/TMPRSS2 are coexpressed in multiple tissues, including nasal epithelial cells (120), the alveolar epithelium (mainly type 2 alveolar cells), the bronchial branch epithelium (120, 121), the intestinal tract (122, 123) and the nervous system (124). This finding is also in line with the infection characteristics of SARS-CoV-2 and the clinical characteristics of patients.

Animal models can mimic the clinical symptoms of COVID-19 in humans and are good models for studying the pathogenesis caused by SARS-CoV-2. A study showed that hACE2-HB-01 transgenic mice exhibited significant weight loss, supported viral replication, and displayed lymphocyte and monocyte infiltration in the alveolar interstitium and macrophage accumulation in the alveolar space after infection with SARS-CoV-2 (24), which

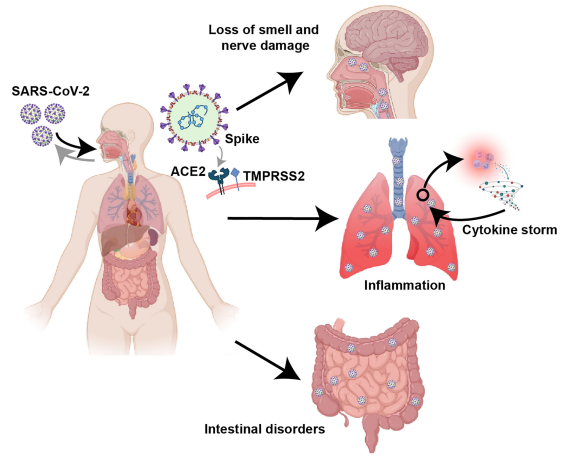

FIGURE 2
Clinical features of COVID-19. Based on the receptor (ACE2/TMPRSS2) binding specificity of the Spike protein, SARS-CoV-2 can infect multiple tissues and organs, especially the respiratory tract, lung and intestine. COVID-19 can cause significant lung inflammation, intestinal disturbances, and nerve damage, including loss of smell.

recapitulate clinical patient findings (125). Furthermore, many studies have shown that Krt18-hACE2, β-actin-hACE2, and HFH4-ACE2 transgenic mice die rapidly after infection with SARS-CoV-2. Their lungs have high viral loads and severe interstitial lesions caused by inflammatory immune cell infiltration, with marked thrombosis and anosmia and neuroinvasive symptoms, consistent with human COVID-19 (25, 68, 126–128).

In the hamster model, SARS-CoV-2 infection has been found to cause weight loss, ruffled fur, postural changes, and symptoms similar to those of human COVID-19, such as dyspnea, olfactory epithelial cell and neuron damage, severe lung pathology, and lymphopenia (59, 129, 130). Furthermore, older hamsters exhibit more pronounced weight loss than younger hamsters (131). Although virus titers are higher in young mice, rapid clearance of the virus can be observed (131). In addition, SARS-CoV-2 infection can occur in hamsters through direct contact, aerosol transmission, and oral transmission, so this model is often used to evaluate the airtightness of surgical masks (58, 132, 133). Moreover, hamsters can be a valuable tool to study the correlation between SARS-CoV-2 pathogenicity and age.

Ferrets are considered the best model for asymptomatic or mild diseases in humans and are frequently used in transmission studies. Multiple studies have shown that ferrets infected with SARS-CoV-2 experience rapid transmission before peak viral load and body temperature, while the virus replicates primarily in the upper respiratory tract of ferrets without causing severe disease, which is consistent with the characteristics of individuals during asymptomatic periods (21, 134, 135). Multiple additional studies showed that ferrets can mimic both direct and indirect transmission of COVID-19 in humans (71, 134, 135). A profile of inflammatory cytokines similar to that in humans, including the expression of genes encoding IL-6, IL-1β, CCL2, and CCL8, was observed in the airways of ferrets after infection (136). In addition, compared with juvenile and adult ferrets, aged ferrets have higher viral loads, longer shedding times, more severe inflammatory cell infiltration in the lungs, and more clinical symptoms (137). In another model animal, *Tupaia belangeri*, higher titers were also observed early after infection in young tree shrews but for a longer duration in elderly tree shrews (73). In addition, evidence of an inflammatory process in the lungs was found in all age groups, and infiltration was similar to that observed in humans and monkeys (72).

The NHP model is the closest model to humans. At present, NHP models applied to SARS-CoV-2 research mainly include African green monkeys (74), marmosets (23, 26, 75), baboons (75), cynomolgus macaques (23, 26), and rhesus macaques (26, 29, 30). Among them, rhesus monkeys showed clinical symptoms similar to COVID-19 patients after infection, including increased expression of inflammatory cytokines and chemokines, decreased blood oxygen levels, and decreased white blood cell and lymphocyte counts (26, 29, 30, 75, 77). Meanwhile, several studies have also shown that lower doses of SARS-CoV-2 infection in African green monkeys than those infected with rhesus monkeys can still cause significant viral replication and lung lesions, which indicates that SARS-CoV-2 also has pathogenic potential in African green monkeys (74, 138). In addition, although there are fewer studies on baboons, one study showed that baboons are sensitive to SARS-CoV-2 infection and develop extensive pathological changes after infection (75). For marmosets and cynomolgus monkeys, the clinical symptoms of SARS-CoV-2 infection were mild and manifested as mild pneumonia (23, 26, 75). Although different monkey species in the NHP model differed in susceptibility and pathogenicity to SARS-CoV-2, overall they did not develop the characteristic cytokine storm syndrome and respiratory distress or even death similar to severe COVID-19 patients (23, 29, 139). In summary, NHP models, especially rhesus monkeys, African green monkeys and baboons, play a very important role in the testing of vaccines and antiviral drugs and the study of virus mechanisms.

The adaptive immune response and immune memory against SARS-CoV-2

Dysregulation of the innate immune response is closely associated with failure to control primary SARS-CoV-2 infection and a high risk of fatal COVID-19 (9–11). Although the adaptive immune response develops slower than the innate immune response, it responds to pathogens in an antigen-specific manner to generate protective immunity capable of protecting the host from reinfection with SARS-CoV-2 (140–142). This indicates that the adaptive immune response, including the action of B cells, $CD4^+$ T cells, and $CD8^+$ T cells, plays a key role in the antiviral process (Figure 3). This subsection will elaborate on the adaptive immune response elicited by SARS-CoV-2 and the key role of animal models in facilitating related research.

Humoral immune response against SARS-CoV-2

Neutralizing antibodies produced by adaptive humoral immune responses play a unique role in inhibiting virus invasion and killing target cells (143). Studies have shown that approximately 90% of the sera collected from COVID-19 patients on the 10th day after infection carry specific antibodies against the Spike and N proteins (Figure 3) (144–148), and specific antibodies against the Spike protein, especially the receptor-binding domain (RBD), can exert a significant neutralizing effect (61, 148, 149). Neutralizing antibody levels

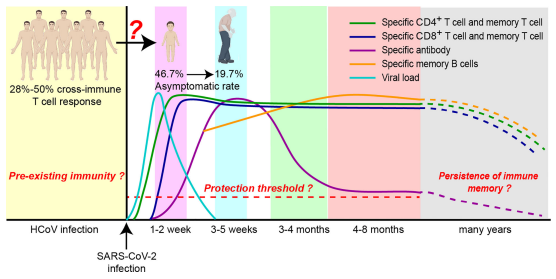

FIGURE 3
Persistence of adaptive immune responses to SARS-CoV-2. Following infection with SARS-CoV-2, an adaptive immune response is initiated. The viral load peaks at one week, $CD4^+$ and $CD8^+$ T cells peak at 1-2 weeks, and antibody levels peak at 3-5 weeks. The persistence and protective thresholds of immune memory in cellular and humoral immune responses are currently unknown. The association of preexisting immunity elicited by cross-reactive T-cell immune responses with asymptomatic infection remains to be further investigated.

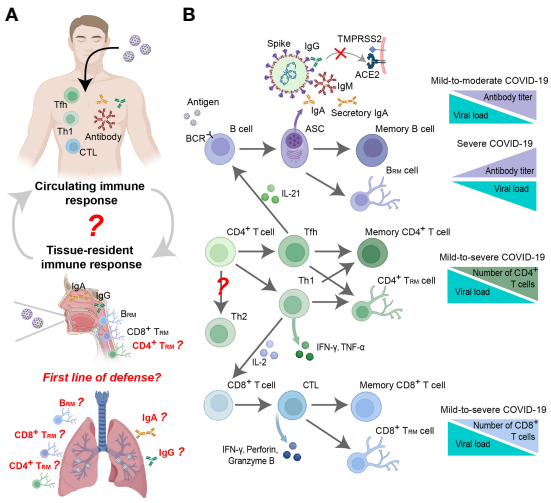

FIGURE 4
Antiviral mechanism of the adaptive immune response to SARS-CoV-2. **(A)** *In vivo* distribution of virus-specific adaptive immune responses, including circulating and tissue-resident adaptive immune responses. The relationship between circulating immune responses and tissue-resident immune responses remains to be further investigated. The role of lung tissue-resident immune responses in the fight against SARS-CoV-2 infection is worth investigating. **(B)** Mechanisms of adaptive immune responses against SARS-CoV-2 and their relationship to disease severity.

peak within the next 3-5 weeks and then decrease, reaching the lower threshold of detection within months (Figure 3) (14, 16, 150–152). Although neutralizing antibody titers drop rapidly, these antibodies still act immediately when the virus re-enters the host. Residual neutralizing antibodies on the mucosal surface can directly block the initial infection of host cells while circulating neutralizing antibodies can further prevent the occurrence of infection (Figures 4A, B). One study showed that a neutralizing titer equivalent to 20% of the mean titer during the recovery period was sufficient to provide 50% protection (153). In addition, non-neutralizing virus-specific antibodies may contribute to immune control of infection by increasing clearance of free virus or by targeting infected cells for immune clearance (through antibody-dependent cytotoxicity and other mechanisms) (154–156), although this phenomenon is difficult to quantify (157, 158). The mechanism may occur through Fc receptor-related functions in serum. Previous studies have confirmed that neutralizing antibodies with Fc receptor-binding ability are more protective in mice, while Fc-dependent antibody effector activity in non-surviving humans has been found to be reduced (82, 154, 159). Moreover, non-neutralizing antibody Fc effector functions such as complement activation, cytotoxicity, and phagocytosis have also been shown to protect model animals (154, 156).

The specific antiviral effects exerted by neutralizing antibodies make them potential therapeutic drugs in the clinic. One study demonstrated that administration of SARS-CoV-2-specific monoclonal antibodies in the early stages of infection in patients with mild-to-moderate COVID-19 accelerated the virus clearance and reduced clinical risk (Figure 4B) (160, 161). It has also been found in animal models that human neutralizing antibodies can protect hamsters and mice, reduce clinical symptoms and even prevent infection (59, 61, 154, 162). In addition, the administration of neutralizing antibodies in NHP models can yield prophylactic and protective effects (79, 162, 163). However, the clinical manifestations of specific monoclonal antibodies administered to critically ill patients are quite different, and some studies have shown that increasing antibody levels can improve clinical outcomes (164, 165), while other studies have reported poorer clinical outcomes (Figure 4B) (166, 167). This discrepancy may be related to the antibody-dependent enhancement of COVID-19 (168), which is supported by *in vitro* and animal experiments (169–175). Interestingly, SARS-CoV-2 neutralizing antibody titers are independent of primary COVID-19 disease severity (145, 176, 177). Based on various animal models, neutralizing antibody titers (and total anti-Spike antibody titers) were further confirmed to be positively correlated with COVID-19 disease severity (Figure 4B) (149, 178). One possible reason is that high neutralizing antibody titers are associated with severe disease and underlying extrafollicular B-cell responses (179).

Neutralizing antibody is a double-edged sword, but whether they are necessary to control SARS-CoV-2 infection remains controversial. One study showed that COVID-19 patients with agammaglobulinemia and no circulating B cells still fully recovered from infection (180), and B-cell depletion therapy in COVID-19 cases have also shown some efficacy (181–183). Furthermore, some convalescent patients have not had

detectable neutralizing antibodies against the virus throughout the disease course (18, 145, 184, 185), which supports the view that a humoral immune response may not be necessary to control SARS-CoV-2 infection.

Nonetheless, most of the current COVID-19 vaccine efforts are still focused on the induction of the production of neutralizing antibodies (186–188). The favorable therapeutic effect of neutralizing antibodies in clinical and animal models (59, 160, 162) and the increase in the number of B cells in convalescent patients (189) make the development of vaccines more promising. However, SARS-CoV-2 has a high level of genetic variability, producing mutant strains such as the alpha strain, beta strain, gamma strain, delta strain, zeta strain, and omicron strain, and the total number of mutants has exceeded 11 million (https://ngdc.cncb.ac.cn/ncov/release_genome). Among them, the number of omicron strains has reached nearly 4 million, and the number is growing continuously. Mutations focused on the Spike protein, especially the RBD, have received widespread attention, as they can allow immune evasion by reducing or even failure of the protection afforded by neutralizing antibodies (190–194). In addition, the high glycosylation level of Spike proteins promotes this effect (195–197). Notably, there are reports that partially neutralizing antibodies can cross-protect against multiple variants (198, 199), providing some promising reports for vaccine development. However, the absence of neutralizing antibodies does not mean that immunity is invalid, and the antiviral effects of neutralizing antibodies at different stages of the disease still need to be further confirmed by clinical data. Specifically, when the neutralizing antibodies produced during primary infection or vaccine immunization disappear, will the neutralizing antibodies secreted by immune memory B cells in a short period during reinfection provide timely effective protection? Furthermore, whether neutralizing antibodies are sufficient to provide complete protection in the absence of a cellular immune response remains to be supported by data. At present, such data are lacking in clinical practice, and it is also difficult to perform targeted research, so the corresponding clinical data must be obtained only *via* animal models with insufficient T-cell immune responses.

Cellular immune response against SARS-CoV-2

As an important part of the adaptive immune response, the cellular immune response also plays an important role in countering SASR-CoV-2 infection. Neutralizing antibody titers are independent of the severity of primary COVID-19 (16, 145, 149, 176–178), while the magnitude of virus-specific T-cell responses is highly correlated with disease severity (Figure 4B) (18, 145, 200, 201). In addition, T-cell responses have been detected in almost all COVID-19 patients (18, 19, 145, 202), suggesting that T-cell responses may be the key to the control and resolution of primary SARS-CoV-2 infection.

Although the data are not completely consistent, some studies have confirmed that $CD4^+$ T cells exhibit a more prominent response and detection rate to SARS-CoV-2 than $CD8^+$ T cells (18, 19, 203) and are associated with the control of primary SARS-CoV-2 infection (145, 177), especially circulating T follicular helper cells (cTfhs) (145). This may be related to the function of cTfhs, which play a key role in the development of long-term humoral immunity through the germinal center response and are essential for the development of most neutralizing antibody responses as well as memory B cells and long-term humoral immunity (Figure 4B) (203–205). At present, many studies have shown a correlation between the intensity of the SARS-CoV-2-specific antibody response and the $CD4^+$ T-cell response (19, 206). In addition, $CD4^+$ T cells can also differentiate into other effector cells with more direct antipathogen activity, Th1 cells, which function mainly by secreting IFNγ (Figure 4B) (19, 145, 207, 208). CD4-cytotoxic T lymphocytes (CTLs) are a related cell type with direct cytotoxic activity, and although some studies have observed CD4-CTL transcriptional signatures (209), their function remains unclear. Notably, Th2 cells are extremely rare in patients with COVID-19 (18, 19, 145) and appear only in critically ill patients (210). Whether this is related to the aggravation of disease in critically ill patients remains to be explored.

SARS-CoV-2-specific $CD4^+$ T-cell responses can be detected as early as 2-4 days after infection (Figure 3) (145, 177, 208) and can produce specific responses to almost all viral proteins, especially the Spike, M, and N proteins, during the recovery period, which are correlated with protein expression levels (19). This finding is very promising, as most of the current vaccine candidates focus on Spike (211). In addition, studies based on earlier animal models of SARS-CoV and MERS-CoV infection confirmed that in the absence of antibodies or $CD8^+$ T cells, adoptive transfer of $CD4^+$ T-cells has a protective effect (212). This finding suggests that the cellular immune response, especially the $CD4^+$ T-cell immune response, may be the key to controlling SARS-CoV-2. In addition, in-depth studies of CD4+ T cell responses based on the NHP model also reconfirmed that SARS-CoV-2 was able to induce a robust germinal center $CD4^+$ T follicular helper cell response (213).

$CD8^+$ T cells can kill infected cells and are also critical for clearing viral infections. Studies have shown that $CD8^+$ T cells in patients with COVID-19 are usually observed within 7 days of symptom onset, with level peaking at 14 days (Figure 3) (210, 214), and are more activated than $CD4^+$ T cells (142, 215, 216). Furthermore, some studies have demonstrated that CTL reactivity is associated with improved clinical outcomes in COVID-19 patients (Figure 4B) (145, 203, 210, 214, 217). Similar to SARS-CoV-2-specific $CD4^+$ T-cells, $CD8^+$ T cells develop rapidly in the acute phase (145) and produce good

antigen specificity against the Spike, N, M, and ORF3a proteins of SARS-CoV-2 (18, 19, 185, 202, 218). Moreover, several studies have reported that intensive care unit (ICU) patients have significantly fewer $CD8^+$ T cells than $CD4^+$ T cells, which appears to be associated with COVID-19-related disease severity and mortality (91, 219–222). Therefore, many vaccines are devoted to stimulating T cell responses and achieving good anti-SARS-CoV-2 infection effects in animal models, including mRNA vaccines (223–225), lentiviral vaccines (226), adenovirus vaccines (83, 227, 228), etc.

Although the T-cell response may be the key to controlling and resolving primary SARS-CoV-2 infection, it is worrisome that approximately 82.1% of SARS-CoV-2 patients develop lymphopenia (229), and the degree of reduction of circulating T-cell levels is as high as 80% (11, 230). This finding suggests that the cellular immune response is suppressed, affecting the clinical recovery process (91, 222, 231). The mechanism leading to lymphopenia in SARS-CoV-2 patients is still unclear and remains to be explored *via* animal model studies. Nonetheless, SARS-CoV-2 variant strains do not escape T-cell immunity as they escape humoral immunity (190–193) because the T-cell epitopes of SARS-CoV-2 are very extensive and involve almost all viral proteins (19, 232–235). In addition, several studies have also shown that T-cell immunity induced by the SARS-CoV-2 vaccine can cross-recognize multiple mutant strains (236, 237), which may be promising for vaccine design and development. Based on the above results, we are optimistic about the relevant research on T-cell epitope vaccines in animal models and determining whether they can achieve the immune protection effect across variant strains. In addition, the current direction should also advance research on antibody-independent T-cell immune protection and immune memory. From previous experience, the adoptive transfer of $CD4^+$ T cells has a protective effect against SARS-CoV and MERS-CoV infection (212), but data on SARS-CoV-2 are very scarce. It is urgent to study the immune protection and immune memory of $CD4^+$ T cells or $CD8^+$ T cells alone or in combination using genetically engineered mouse models lacking humoral immune responses or other models based on short-term antibody clearance of humoral immune responses.

Cross-immune response against SARS-CoV-2

Large-scale survey studies have shown that approximately 20-40% of SARS-CoV-2-infected people suffer from the asymptomatic disease (238–240), and asymptomatic disease is linked to age (Figure 3). The incidence of asymptomatic manifestations was 19.7% in elderly individuals and 46.7% in children (Figure 3) (241). However, the mechanism of this discrepancy remains unclear but may be related to preexisting cross-reactive immune responses. SARS-CoV-2 is a member of the coronavirus family that also includes the human coronaviruses (HCoVs) HCoV-OC43, HCoV-HKU1, HCoV-229E, and HCoV-NL63, which cause the common cold, as well as SARS-CoV-1 and MERS-CoV. Studies on cross-reactive humoral immune responses confirm that cross-neutralizing antibodies to Spike proteins are extremely rare (148, 242–245). Surprisingly, cross-reactive memory T cells are frequently present, detectable in 28%–50% of the population (Figure 3) (19, 207, 208, 218, 246, 247), and the vast majority are cross-reactive $CD4^+$ memory T cells (19). Their recognition epitopes are mostly located in common cold-causing coronaviruses. Although cross-reactive memory $CD8^+$ T cells have been observed less frequently (19), they are still biologically relevant (184). The marked differences in cross-reactive $CD4^+$ T-cell and $CD8^+$ T-cell responses may be related to the restricted presentation pattern of major histocompatibility complex class I and II molecules (248, 249). Interestingly, some studies have shown that cross-reactive $CD8^+$ T-cell responses are mainly localized in tissues but are rarely detected in the circulatory system and may represent the first line of defense in adaptive immune responses (Figure 4A) (250, 251). In a mouse model, studies have also confirmed the existence of cross-reactive T cells after SARS-CoV-2 infection, and mainly cross-reacted with SARS-CoV but not MERS-CoV (65).

Currently, the clinical importance of preexisting cross-reactive T-cell responses in the control of SARS-CoV-2 infection and the impact on herd immunity thresholds are controversial, as the protective mechanisms remain unclear (246, 252). Some studies, after controlling for age and other factors, have found that SARS-CoV-2 patients with a confirmed HCoV infection in the past 3 years had a significantly lower risk of being admitted to the ICU (253). In addition, individuals with strong HCoV-specific T cells may acquire excellent protective cellular immunity after exposure to SARS-CoV-2 (253). Other studies argue that HCoV-specific T cells generally have a low affinity for SARS-CoV-2 peptides (254, 255), making it difficult to play a role in controlling SARS-CoV-2 infection. Regardless of which perspective is correct, further research is urgently needed to map the cross-reactive memory T cells against SARS-CoV-2 induced by different coronaviruses based on animal models under strictly controlled conditions to evaluate their cross-protection efficiency. This research direction has important implications for the control of disease spread and the potential for herd immunity.

Tissue-resident immune response against SARS-CoV-2

The circulating adaptive immune response plays a key role in the body's defense against SARS-CoV-2 infection, but there are very limited reports on the functions of tissue-resident immune cells residing in nonlymphoid tissues including the

lung and URT. Compared with circulating central memory cells and effector memory cells, tissue-resident memory cells respond faster, so the presence of tissue-resident memory cells may be critical for efficient target recognition and immune recall (256, 257). For SARS-CoV-2 infection, some studies have shown that circulating immune responses largely reflect local immune responses, and IgG and IgA antibodies against Spike in saliva have been found to correlate with antibodies in the blood (Figure 4A) (258). However, the neutralizing ability of secretory IgA produced by tissue-resident memory B (B_{RM}) cells is stronger than that of circulating IgA, which may be related to its function and dimeric structure (Figure 4A) (259, 260). The respiratory tract is the main tissue invaded by SARS-CoV-2, so it is urgent to confirm the protective effect of B_{RM} cells in respiratory tissues against reinfection. Intranasal lentiviral vector-mediated antibody delivery reduces SARS-CoV-2 infection in aged and immunocompromised mice, further confirming that antibodies play a non-negligible role in mucosal immunity (261). Over the years, intranasal vaccination has been shown to induce airway IgA and reduce viral load in the early stages of viral infection (262). Therefore, several SARS-CoV-2 intranasal vaccines including lentiviral vaccine (226), adenovirus vaccine (83, 227, 228), and adjuvant-assisted subunit vaccines (263, 264) were developed. Based on animal models, it can elicit systemic and pulmonary antibody responses and significantly reduce pulmonary viral load and local lung inflammation (83, 226–228, 263).

Tissue-resident memory T (T_{RM}) cells may also play a key role locally against SARS-CoV-2 viral infection. Studies have shown that SARS-CoV-2 infection can stimulate the production of T_{RM} cells in local tissues (nasal cavity and lung), and their quantity and degree of activation are associated with clinical protection (265, 266); these cells can last for at least 10 months or more (Figure 4) (267). Another study based on bronchoalveolar lavage samples from COVID-19 patients showed that there were more T cells in the lungs in moderate cases than in severe cases (201), which may be related to the degree of T-cell response impairment and the number of infiltrating cells (268). Studies based on cross-reactive T_{RM} cells have also reported that $CD8^+$ T_{RM} cells may act as the first line of defense in the adaptive immune response against SARS-CoV-2 infection (Figure 4A) (250, 251). Other studies have presented the opposite view, arguing that T_{RM} cells in lung tissue are not sufficient to produce anti-infective protection against SARS-CoV-2 (269, 270). A study based on the NHP model demonstrated that vaccine-induced strong neutralizing antibody and $CD8^+$ T-cell responses can protect the lungs from SARS-CoV-2 infection and viral replication early in infection (days 2-4) (271). The same results were also confirmed in mice (83, 226, 263). These findings suggest that local tissue-resident memory cells are beneficial in antiviral responses (Figure 4A). However, the relationship between tissue-resident and circulating memory cells and their migration during SARS-CoV-2 infection remains unclear. Although some studies have shown that tissue-resident memory $CD8^+$ T cells can shape local and systemic secondary T-cell responses (272, 273), more evidence related to SARS-CoV-2 is still needed.

However, studies on the actual protective effects of B_{RM} and T_{RM} cells are difficult to perform in the clinical setting because it is difficult to separate pulmonary B_{RM} and T_{RM} cells and the interference of many uncontrollable external factors cannot be excluded. Therefore, the animal model of SARS-CoV-2 infection has become a good model for studying tissue-resident immune responses, which can provide conditions for investigating the protective effect and immune memory of tissue (including nasal cavity and lung)-resident immune responses. Notably, tissue-resident immune responses and immune memory can be initiated only by natural infection and nasal vaccination, while other vaccination routes are difficult to efficiently initiate such responses. We are optimistic about research on the immunoprotective effect of the tissue-resident immune response in the initial stage of SARS-CoV-2 infection. This aspect is important because if the tissue-resident immune response is sufficient to protect the body from infection in the early stages of SARS-CoV-2 infection, the vaccine should be replaced and the nasal route is recommended. On the one hand, this route of vaccination is expected to prevent the introduction of pathogens and damage, and on the other hand, it can effectively hinder viral spread. However, evaluation of the effectiveness of the corresponding vaccine has higher requirements for the animal models of simulated infection, such as the need for sensitivity to aerosol or low-dose nasal infection, while animal models of high-dose infection and intratracheal infection cannot be used to evaluate nasal inoculation vaccines. Krt18-hACE2, β-actin-hACE2, or HFH4-ACE2 transgenic mice, golden hamsters, etc., are good animal models for studying tissue-resident immune responses.

Immune memory and protection against reinfection

Immune memory is the source of protective immunity against SARS-CoV-2 reinfection, and it is one of the issues that has been widely studied. Therefore, in addition to measuring circulating antibody levels, evaluating specific memory B- and T-cell persistence may be critical for understanding and predicting the persistence of protection against SARS-CoV-2 infection.

Multiple studies have shown that the frequency of circulating memory B cells in COVID-19 patients continued to increase during the first few months, peaking at 6 months (Figure 3) (16, 274). Moreover, the generated memory B-cell pool for Spike proteins is predominantly IgG and more potent (16, 274). The measurement of T-cell immune memory at 6 months post-infection showed that the positive ratios of

memory $CD4^+$ T cells and memory $CD8^+$ T cells were 90% and 70%, respectively, and the proportion of memory $CD4^+$ T cells was nearly double that of memory $CD8^+$ T cells (16, 150, 275). However, the half-lives of both may be 3-5 months. Through long-term follow-up monitoring of recovered patients, it has been found that the persistence of SARS-CoV-2-specific T-cell responses is better than that of humoral immunity (17). Virus-specific memory T cells can still be detected when the serum antibodies of patients with asymptomatic infection and mild disease are negative (18, 275). In fact, based on previous studies on SARS-CoV (218, 276, 277) and MERS-CoV (278), memory T cells specific for SARS-CoV-2 are expected to be maintained for many years (150). Although the impact of specific immune responses mediated by memory T cells on the pathogenesis of COVID-19 is unclear, based on the results of the assessment of cross-reactive T cells (19, 279), preexisting cross-immune memory may confer resistance to asymptomatic infected individuals. This information will help guide the design of broad-spectrum protective vaccines.

Indeed, whether the immune memory of patients recovering from COVID-19 can protect against reinfection with SARS-CoV-2 remains an open question. It is worrisome that some studies have reported secondary infections. In a comprehensive analysis of more than 133,000 cases, 54 were thought to be reinfections with SARS-CoV-2 at least 45 days after initial infection, and only four were infections with a different variant (280). Another survey study of more than 43,000 participants found that the reinfection rate in seropositive individuals was only 5%. In addition, by examining more than 500,000 people, it was found that patients after recovery from COVID-19 had 80.5%protection for up to 7 months, although protection was observed in only 47% of patients over 65 years of age (281). Although the infection rate is low, a seroepidemiological study also suggested that reinfection is possible 6 to 8 months after infection (282–284), especially since the rapid mutation of the virus may further increase the risk of reinfection (284, 285).

SARS-CoV-2 has been spreading continuously for nearly 3 years since it was first reported, and it has been regarded as influenza in many countries, with no preventative measures. Therefore, it may not be eliminated as quickly as SARS-CoV and MERS-CoV (7, 8). The maintenance time and protection threshold of vaccines and immune memory generated after infection need to be further studied. Although it is difficult to perform relevant experimental studies in clinical practice, because animal models simulate the main clinical symptoms of COVID-19 patients (36), they have become a good tool to study the SARS-CoV-2 immune response and immune memory. The NHP model, in particular, has unique advantages in clinical research (29). Studies have found that primary infection with SARS-CoV-2 in the NHP model protects against high-dose viral challenge for at least 28-35 days, and re-exposure drives memory immune responses that include high levels of binding neutralizing antibodies (29, 30). Furthermore, depletion of $CD8^+$ T cells resulted in a partial loss of protection against rechallenge, including protection against reinfection by $CD8^+$ T_{RM} cells in the URT (Figure 4A) (286). However, the role of antigen-specific $CD4^+$ T memory cells in anti-SARS-CoV-2 function still deserves further study in animal models.

The study of the SARS-CoV-2 vaccine based on animal models can not only mitigate clinical risks but also provide conditions for the *in vivo* testing of vaccines and the design of immunization programs. Therefore, a variety of vaccines, including adenovirus vector vaccines (84, 85), DNA vaccines (84), mRNA vaccines (81), inactivated vaccines (31), and subunit vaccines (80), have been validated in animal models. However, whether vaccine-induced immune responses and immune memory are more effective in controlling infection than natural immunity remains a matter of concern (287). Current studies have demonstrated that both vaccination and infection produce up to 95% protection (288–292); however, peak neutralizing antibody responses produced by the vaccine ranged from approximately 1/2 to four times those in convalescent patients (153, 233, 293). Antibody decay rates did not differ significantly between vaccinated and naturally infected patients, with half-lives around 60 days (153). Repeated boosting with the vaccine may be beneficial to generate a longer period of protection than natural immunity. Although SARS-CoV-2 can evade immunity and reduce vaccine-induced protection by altering the epitopes recognized by neutralizing antibodies (190–193), omicron strains have evolved to exert low pathogenicity and high transmissibility (4–6, 294). This creates a complex situation, and it remains to be seen whether a new and more pathogenic SARS-CoV-2 will emerge in the future. Therefore, expanding protection against different variant strains may be an important requirement for next-generation vaccines.

Conclusions and future perspectives

The global COVID-19 pandemic has caused a global recession and tremendous casualties. Although preventive vaccines for COVID-19 are being developed at an unprecedented rate, we still face many challenges owing to the large genome and high levels of genetic variation of SARS-CoV-2. Currently, there is no evidence that the innate immune response can control primary SARS-CoV-2 infection. Conversely, the loss of control of the innate immune response caused by SARS-CoV-2 immune escape and immune hijacking may correlate with severe clinical disease (9–11). Adaptive immune responses have demonstrated unique advantages in controlling SARS-CoV-2 infection and clinical disease severity (140–142). However, there are still many mysteries regarding the role of adaptive immunity in controlling SARS-CoV-2 infection. The rapid development of SARS-CoV-2 animal models has provided us with a good platform to simulate human clinical studies to understand the mechanism of virus infection and host immune effects, which play an irreplaceable key role in testing the effectiveness of vaccines and drugs.

At present, a variety of animal models ranging from rodents to NHPs have shown clinical symptoms similar to those of human COVID-19 when infected with SARS-CoV-2. However, there is still a gap between animal models and humans in terms of clinical characteristics, and it is difficult to comprehensively summarize the clinical symptoms of COVID-19 patients. However, the application of animal models provides a wealth of insights into SARS-CoV-2 pathogenesis, especially as the NHP model can faithfully reproduce COVID-19 pathology in humans. Although much research has been devoted to the adaptive immune response to SARS-CoV-2, there are still many unanswered questions that need to be further explored using animal models.

- What is the mechanism of lymphopenia caused by SARS-CoV-2 infection? Are there certain viral proteins that antagonize adaptive immune responses?
- Are neutralizing antibodies, $CD4^+$ T cells, or $CD8^+$ T cells necessary for the control of primary viral infection?
- What are the immune protection thresholds and persistence of humoral and cellular immune responses induced by vaccines and infections?
- How does aging affect resistance to SARS-CoV-2 through adaptive immunity?
- Is preexisting cross-immunity sufficiently effective against infection and high pathogenicity caused by SARS-CoV-2?
- What is the antiviral mechanism at play in asymptomatic patients? Is it related to preexisting cross-immunity?
- What is the role of tissue, especially lung-resident, immune responses in anti-SARS-CoV-2 activity and their relationship to circulating immune responses?

In conclusion, although the pathogenicity of omicron variants has been greatly reduced, the long-term existence and high mutation frequency of SARS-CoV-2 require constant attention to its threat to humans. Even though both SARS-CoV-2 and influenza virus can cause respiratory diseases, SARS-CoV-2 far exceeds influenza virus in many aspects, such as mutation rate, transmission characteristics, and induction of mortality. We need a better understanding of SARS-CoV-2 to better prevent the establishment of future novel variants of SARS-CoV-2.

Author contributions

XW and JL conceived, wrote, and revised the study. NR drew the figures. All authors contributed to the article and approved the submitted version.

Funding

This work was supported financially by grants from the National Natural Science Foundation of China (NSFC) (92169210 and 32200752).

Conflict of interest

The authors declare that the research was conducted in the absence of any commercial or financial relationships that could be construed as a potential conflict of interest.

Publisher's note

All claims expressed in this article are solely those of the authors and do not necessarily represent those of their affiliated organizations, or those of the publisher, the editors and the reviewers. Any product that may be evaluated in this article, or claim that may be made by its manufacturer, is not guaranteed or endorsed by the publisher.

References

1. Hu B, Guo H, Zhou P, Shi Z-L. Characteristics of SARS-CoV-2 and COVID-19. *Nat Rev Microbiol* (2021) 19:141–54. doi: 10.1038/s41579-020-00459-7

2. Tao K, Tzou PL, Nouhin J, Gupta RK, de Oliveira T, Kosakovsky Pond SL, et al. The biological and clinical significance of emerging SARS-CoV-2 variants. *Nat Rev Genet* (2021) 22:757–73. doi: 10.1038/s41576-021-00408-x

3. Fisman DN, Tuite AR. Evaluation of the relative virulence of novel SARS-CoV-2 variants: A retrospective cohort study in Ontario, Canada. *CMAJ* (2021) 193:E1619–E25. doi: 10.1503/cmaj.211248

4. Callaway E, Ledford H. How bad is omicron? what scientists know so far. *Nature* (2021) 600:197–9. doi: 10.1038/d41586-021-03614-z

5. Dyer O. Covid-19: South africa's surge in cases deepens alarm over omicron variant. *Bmj* (2021) 375:n3013. doi: 10.1136/bmj.n3013

6. Modes ME, Directo MP, Melgar M, Johnson LR, Yang H, Chaudhary P, et al. Clinical characteristics and outcomes among adults hospitalized with laboratory-confirmed SARS-CoV-2 infection during periods of B.1.617.2 (Delta) and B.1.1.529 (Omicron) variant predominance - one hospital, California, July 15-September 23, 2021, and December 21, 2021-January 27, 2022. *MMWR Morbidity mortality weekly Rep* (2022) 71:217–23. doi: 10.15585/mmwr.mm7106e2

7. Peiris JSM, Lai ST, Poon LLM, Guan Y, Yam LYC, Lim W, et al. Coronavirus as a possible cause of severe acute respiratory syndrome. *Lancet* (2003) 361:1319–25. doi: 10.1016/s0140-6736(03)13077-2

8. Raj VS, Osterhaus ADME, Fouchier RAM, Haagmans BL. MERS: Emergence of a novel human coronavirus. *Curr Opin Virol* (2014) 5:58–62. doi: 10.1016/j.coviro.2014.01.010

9. Lee S, Channappanavar R, Kanneganti T-D. Coronaviruses: Innate immunity, inflammasome activation, inflammatory cell death, and cytokines. *Trends Immunol* (2020) 41:1083–99. doi: 10.1016/j.it.2020.10.005

10. Tay MZ, Poh CM, Rénia L, MacAry PA, Ng LFP. The trinity of COVID-19: Immunity, inflammation and intervention. *Nat Rev Immunol* (2020) 20:363–74. doi: 10.1038/s41577-020-0311-8

11. Kuri-Cervantes L, Pampena MB, Meng W, Rosenfeld AM, Ittner CAG, Weisman AR, et al. Comprehensive mapping of immune perturbations associated with severe COVID-19. *Sci Immunol* (2020) 5:eabd7114. doi: 10.1126/sciimmunol.abd7114

12. Galani IE, Rovina N, Lampropoulou V, Triantafyllia V, Manioudaki M, Pavlos E, et al. Untuned antiviral immunity in COVID-19 revealed by temporal type I/III interferon patterns and flu comparison. *Nat Immunol* (2021) 22:32–40. doi: 10.1038/s41590-020-00840-x

13. Hadjadj J, Yatim N, Barnabei L, Corneau A, Boussier J, Smith N, et al. Impaired type I interferon activity and inflammatory responses in severe COVID-19 patients. *Sci (New York NY)* (2020) 369:718–24. doi: 10.1126/science.abc6027

14. Gudbjartsson DF, Norddahl GL, Melsted P, Gunnarsdottir K, Holm H, Eythorsson E, et al. Humoral immune response to SARS-CoV-2 in Iceland. *N Engl J Med* (2020) 383:1724–34. doi: 10.1056/NEJMoa2026116

15. Turner JS, Kim W, Kalaidina E, Goss CW, Rauseo AM, Schmitz AJ, et al. SARS-CoV-2 infection induces long-lived bone marrow plasma cells in humans. *Nature* (2021) 595:421–5. doi: 10.1038/s41586-021-03647-4

16. Dan JM, Mateus J, Kato Y, Hastie KM, Yu ED, Faliti CE, et al. Immunological memory to SARS-CoV-2 assessed for up to 8 months after infection. *Science* (2021) 371:eabf4063. doi: 10.1126/science.abf4063

17. Kaneko N, Kuo HH, Boucau J, Farmer JR, Allard-Chamard H, Mahajan VS, et al. Loss of bcl-6-Expressing T follicular helper cells and germinal centers in COVID-19. *Cell* (2020) 183:143–57.e13. doi: 10.1016/j.cell.2020.08.025

18. Sekine T, Perez-Potti A, Rivera-Ballesteros O, Stralin K, Gorin JB, Olsson A, et al. Robust T cell immunity in convalescent individuals with asymptomatic or mild COVID-19. *Cell* (2020) 183:158–68 e14. doi: 10.1016/j.cell.2020.08.017

19. Grifoni A, Weiskopf D, Ramirez SI, Mateus J, Dan JM, Moderbacher CR, et al. Targets of T cell responses to SARS-CoV-2 coronavirus in humans with COVID-19 disease and unexposed individuals. *Cell* (2020) 181:1489–501.e15. doi: 10.1016/j.cell.2020.05.015

20. To KK, Hung IF, Ip JD, Chu AW, Chan WM, Tam AR, et al. Coronavirus disease 2019 (COVID-19) re-infection by a phylogenetically distinct severe acute respiratory syndrome coronavirus 2 strain confirmed by whole genome sequencing. *Clin Infect Dis* (2021) 73:e2946–e51. doi: 10.1093/cid/ciaa1275

21. Shi J, Wen Z, Zhong G, Yang H, Wang C, Huang B, et al. Susceptibility of ferrets, cats, dogs, and other domesticated animals to SARS-coronavirus 2. *Sci (New York NY)* (2020) 368:1016–20. doi: 10.1126/science.abb7015

22. Sun S-H, Chen Q, Gu H-J, Yang G, Wang Y-X, Huang X-Y, et al. A mouse model of SARS-CoV-2 infection and pathogenesis. *Cell Host Microbe* (2020) 28:124–33.e4. doi: 10.1016/j.chom.2020.05.020

23. Rockx B, Kuiken T, Herfst S, Bestebroer T, Lamers MM, Oude Munnink BB, et al. Comparative pathogenesis of COVID-19, MERS, and SARS in a nonhuman primate model. *Sci (New York NY)* (2020) 368:1012–5. doi: 10.1126/science.abb7314

24. Bao L, Deng W, Huang B, Gao H, Liu J, Ren L, et al. The pathogenicity of SARS-CoV-2 in hACE2 transgenic mice. *Nature* (2020) 583:830–3. doi: 10.1038/s41586-020-2312-y

25. Jiang R-D, Liu M-Q, Chen Y, Shan C, Zhou Y-W, Shen X-R, et al. Pathogenesis of SARS-CoV-2 in transgenic mice expressing human angiotensin-converting enzyme 2. *Cell* (2020) 182:50–8.e8. doi: 10.1016/j.cell.2020.05.027

26. Lu S, Zhao Y, Yu W, Yang Y, Gao J, Wang J, et al. Comparison of nonhuman primates identified the suitable model for COVID-19. *Signal Transduct Target Ther* (2020) 5:157–. doi: 10.1038/s41392-020-00269-6

27. Gu H, Chen Q, Yang G, He L, Fan H, Deng Y-Q, et al. Adaptation of SARS-CoV-2 in BALB/c mice for testing vaccine efficacy. *Sci (New York NY)* (2020) 369:1603–7. doi: 10.1126/science.abc4730

28. Speranza E, Williamson BN, Feldmann F, Sturdevant GL, Pérez-Pérez L, Meade-White K, et al. Single-cell RNA sequencing reveals SARS-CoV-2 infection dynamics in lungs of African green monkeys. *Sci Trans Med* (2021) 13(578): eabe8146. doi: 10.1126/scitranslmed.abe8146

29. Chandrashekar A, Liu J, Martinot AJ, McMahan K, Mercado NB, Peter L, et al. SARS-CoV-2 infection protects against rechallenge in rhesus macaques. *Science* (2020) 369:812–7. doi: 10.1126/science.abc4776

30. Deng W, Bao L, Liu J, Xiao C, Liu J, Xue J, et al. Primary exposure to SARS-CoV-2 protects against reinfection in rhesus macaques. *Science* (2020) 369:818–23. doi: 10.1126/science.abc5343

31. Gao Q, Bao L, Mao H, Wang L, Xu K, Yang M, et al. Development of an inactivated vaccine candidate for SARS-CoV-2. *Science* (2020) 369:77–81. doi: 10.1126/science.abc1932

32. Wang H, Zhang Y, Huang B, Deng W, Quan Y, Wang W, et al. Development of an inactivated vaccine candidate, BBIBP-CorV, with potent protection against SARS-CoV-2. *Cell* (2020) 182:713–21.e9. doi: 10.1016/j.cell.2020.06.008

33. Dai L, Zheng T, Xu K, Han Y, Xu L, Huang E, et al. A universal design of betacoronavirus vaccines against COVID-19, MERS, and SARS. *Cell* (2020) 182:722–33.e11. doi: 10.1016/j.cell.2020.06.035

34. Du S, Cao Y, Zhu Q, Yu P, Qi F, Wang G, et al. Structurally resolved SARS-CoV-2 antibody shows high efficacy in severely infected hamsters and provides a potent cocktail pairing strategy. *Cell* (2020) 183:1013–23.e13. doi: 10.1016/j.cell.2020.09.035

35. Sheahan TP, Sims AC, Zhou S, Graham RL, Pruijssers AJ, Agostini ML, et al. An orally bioavailable broad-spectrum antiviral inhibits SARS-CoV-2 in human airway epithelial cell cultures and multiple coronaviruses in mice. *Sci Trans Med* (2020) 12(541):eabb5883. doi: 10.1126/scitranslmed.abb5883

36. Khoury DS, Wheatley AK, Ramuta MD, Reynaldi A, Cromer D, Subbarao K, et al. Measuring immunity to SARS-CoV-2 infection: Comparing assays and animal models. *Nat Rev Immunol* (2020) 20:727–38. doi: 10.1038/s41577-020-00471-1

37. Zhu N, Zhang D, Wang W, Li X, Yang B, Song J, et al. A novel coronavirus from patients with pneumonia in China, 2019. *N Engl J Med* (2020) 382:727–33. doi: 10.1056/NEJMoa2001017

38. Hoffmann M, Kleine-Weber H, Schroeder S, Krüger N, Herrler T, Erichsen S, et al. SARS-CoV-2 cell entry depends on ACE2 and TMPRSS2 and is blocked by a clinically proven protease inhibitor. *Cell* (2020) 181:271–80.e8. doi: 10.1016/j.cell.2020.02.052

39. Harcourt J, Tamin A, Lu X, Kamili S, Sakthivel SK, Murray J, et al. Isolation and characterization of SARS-CoV-2 from the first US COVID-19 patient. *bioRxiv preprint server Biol* (2020) 2020.03.02.972935. doi: 10.1101/2020.03.02.972935. 2020.03.02.972935.

40. Ou X, Liu Y, Lei X, Li P, Mi D, Ren L, et al. Characterization of spike glycoprotein of SARS-CoV-2 on virus entry and its immune cross-reactivity with SARS-CoV. *Nat Commun* (2020) 11:1620–. doi: 10.1038/s41467-020-15562-9

41. Kim J-M, Chung Y-S, Jo HJ, Lee N-J, Kim MS, Woo SH, et al. Identification of coronavirus isolated from a patient in Korea with COVID-19. *Osong Public Health Res Perspect* (2020) 11:3–7. doi: 10.24171/j.phrp.2020.11.1.02

42. Desmyter J, Melnick JL, Rawls WE. Defectiveness of interferon production and of rubella virus interference in a line of African green monkey kidney cells (Vero). *J Virol* (1968) 2:955–61. doi: 10.1128/JVI.2.10.955-961.1968

43. Zhou P, Yang X-L, Wang X-G, Hu B, Zhang L, Zhang W, et al. A pneumonia outbreak associated with a new coronavirus of probable bat origin. *Nature* (2020) 579:270–3. doi: 10.1038/s41586-020-2012-7

44. Cavalcanti AB, Zampieri FG, Rosa RG, Azevedo LCP, Veiga VC, Avezum A, et al. Hydroxychloroquine with or without azithromycin in mild-to-Moderate covid-19. *N Engl J Med* (2020) 383:2041–52. doi: 10.1056/NEJMoa2019014

45. Maisonnasse P, Guedj J, Contreras V, Behillil S, Solas C, Marlin R, et al. Hydroxychloroquine use against SARS-CoV-2 infection in non-human primates. *Nature* (2020) 585:584–7. doi: 10.1038/s41586-020-2558-4

46. Liu J, Cao R, Xu M, Wang X, Zhang H, Hu H, et al. Hydroxychloroquine, a less toxic derivative of chloroquine, is effective in inhibiting SARS-CoV-2 infection. *vitro Cell Discovery* (2020) 6:16–. doi: 10.1038/s41421-020-0156-0

47. Wang M, Cao R, Zhang L, Yang X, Liu J, Xu M, et al. Remdesivir and chloroquine effectively inhibit the recently emerged novel coronavirus (2019-nCoV). *vitro Cell Res* (2020) 30:269–71. doi: 10.1038/s41422-020-0282-0

48. Ranga A, Gjorevski N, Lutolf MP. Drug discovery through stem cell-based organoid models. *Adv Drug Delivery Rev* (2014) 69-70:19–28. doi: 10.1016/j.addr.2014.02.006

49. Han Y, Duan X, Yang L, Nilsson-Payant BE, Wang P, Duan F, et al. Identification of SARS-CoV-2 inhibitors using lung and colonic organoids. *Nature* (2021) 589:270–5. doi: 10.1038/s41586-020-2901-9

50. Suzuki T, Itoh Y, Sakai Y, Saito A, Okuzaki D, Motooka D, et al. Generation of human bronchial organoids for SARS-CoV-2 research. *bioRxiv* (2020) 2020.05.25.115600. doi: 10.1101/2020.05.25.115600. 2020.05.25.115600.

51. Sano E, Suzuki T, Hashimoto R, Itoh Y, Sakamoto A, Sakai Y, et al. Cell response analysis in SARS-CoV-2 infected bronchial organoids. *Commun Biol* (2020) 5(1):516. doi: 10.1038/s42003-022-03499-2

52. Fan Z, Chen L, Li J, Cheng X, Yang J, Tian C, et al. Clinical features of COVID-19-Related liver functional abnormality. *Clin Gastroenterol Hepatol* (2020) 18:1561–6. doi: 10.1016/j.cgh.2020.04.002

53. Zhou J, Li C, Liu X, Chiu MC, Zhao X, Wang D, et al. Infection of bat and human intestinal organoids by SARS-CoV-2. *Nat Med* (2020) 26:1077–83. doi: 10.1038/s41591-020-0912-6

54. Zheng Y-Y, Ma Y-T, Zhang J-Y, Xie X. COVID-19 and the cardiovascular system. *Nat Rev Cardiol* (2020) 17:259–60. doi: 10.1038/s41569-020-0360-5

55. Varga Z, Flammer AJ, Steiger P, Haberecker M, Andermatt R, Zinkernagel AS, et al. Endothelial cell infection and endotheliitis in COVID-19. *Lancet* (2020) 395:1417–8. doi: 10.1016/S0140-6736(20)30937-5

56. Pandey K, Acharya A, Mohan M, Ng CL, Reid SP, Byrareddy SN. Animal models for SARS-CoV-2 research: A comprehensive literature review. *Transbound Emerg Dis* (2021) 68:1868–85. doi: 10.1111/tbed.13907

57. Chan JF-W, Zhang AJ, Yuan S, Poon VK-M, Chan CC-S, Lee AC-Y, et al. Simulation of the clinical and pathological manifestations of coronavirus disease 2019 (COVID-19) in a golden Syrian hamster model: Implications for disease pathogenesis and transmissibility. *Clin Infect Dis* (2020) 71:2428–46. doi: 10.1093/cid/ciaa325

58. Sia SF, Yan L-M, Chin AWH, Fung K, Choy K-T, Wong AYL, et al. Pathogenesis and transmission of SARS-CoV-2 in golden hamsters. *Nature* (2020) 583:834–8. doi: 10.1038/s41586-020-2342-5

59. Imai M, Iwatsuki-Horimoto K, Hatta M, Loeber S, Halfmann PJ, Nakajima N, et al. Syrian Hamsters as a small animal model for SARS-CoV-2 infection and countermeasure development. *Proc Natl Acad Sci United States America* (2020) 117:16587–95. doi: 10.1073/pnas.2009799117

60. Zhou B, Thao TTN, Hoffmann D, Taddeo A, Ebert N, Labroussaa F, et al. SARS-CoV-2 spike D614G change enhances replication and transmission. *Nature* (2021) 592:122–7. doi: 10.1038/s41586-021-03361-1

61. Rogers TF, Zhao F, Huang D, Beutler N, Burns A, He W-T, et al. Isolation of potent SARS-CoV-2 neutralizing antibodies and protection from disease in a small animal model. *Sci (New York NY)* (2020) 369:956–63. doi: 10.1126/science.abc7520

62. Chen Q, Huang XY, Sun MX, Li RT, Gu H, Tian Y, et al. Transient acquisition of cross-species infectivity during the evolution of SARS-CoV-2. *Natl Sci Rev* (2021) 8:nwab167. doi: 10.1093/nsr/nwab167

63. Sun J, Zhuang Z, Zheng J, Li K, Wong RL, Liu D, et al. Generation of a broadly useful model for COVID-19 pathogenesis, vaccination, and treatment. *Cell* (2020) 182:734–43.e5. doi: 10.1016/j.cell.2020.06.010

64. Ge J, Wang R, Ju B, Zhang Q, Sun J, Chen P, et al. Antibody neutralization of SARS-CoV-2 through ACE2 receptor mimicry. *Nat Commun* (2021) 12:250. doi: 10.1038/s41467-020-20501-9

65. Zhuang Z, Lai X, Sun J, Chen Z, Zhang Z, Dai J, et al. Mapping and role of T cell response in SARS-CoV-2-infected mice. *J Exp Med* (2021) 218(4):e20202187. doi: 10.1084/jem.20202187

66. Wong LR, Li K, Sun J, Zhuang Z, Zhao J, McCray PBJr., et al. Sensitization of non-permissive laboratory mice to SARS-CoV-2 with a replication-deficient adenovirus expressing human ACE2. *STAR Protoc* (2020) 1:100169. doi: 10.1016/j.xpro.2020.100169

67. McCray PBJr., Pewe L, Wohlford-Lenane C, Hickey M, Manzel L, Shi L, et al. Lethal infection of K18-hACE2 mice infected with severe acute respiratory syndrome coronavirus. *J Virol* (2007) 81:813–21. doi: 10.1128/JVI.02012-06

68. Tseng C-TK, Huang C, Newman P, Wang N, Narayanan K, Watts DM, et al. Severe acute respiratory syndrome coronavirus infection of mice transgenic for the human angiotensin-converting enzyme 2 virus receptor. *J Virol* (2007) 81:1162–73. doi: 10.1128/JVI.01702-06

69. Bosco-Lauth AM, Hartwig AE, Porter SM, Gordy PW, Nehring M, Byas AD, et al. Experimental infection of domestic dogs and cats with SARS-CoV-2: Pathogenesis, transmission, and response to reexposure in cats. *Proc Natl Acad Sci United States America* (2020) 117:26382–8. doi: 10.1073/pnas.2013102117

70. Gaudreault NN, Trujillo JD, Carossino M, Meekins DA, Morozov I, Madden DW, et al. SARS-CoV-2 infection, disease and transmission in domestic cats. *Emerg Microbes Infect* (2020) 9:2322–32. doi: 10.1080/22221751.2020.1833687

71. Richard M, Kok A, de Meulder D, Bestebroer TM, Lamers MM, Okba NMA, et al. SARS-CoV-2 is transmitted *via* contact and *via* the air between ferrets. *Nat Commun* (2020) 11:3496–. doi: 10.1038/s41467-020-17367-2

72. Xu L, Yu D-D, Ma Y-H, Yao Y-L, Luo R-H, Feng X-L, et al. COVID-19-like symptoms observed in Chinese tree shrews infected with SARS-CoV-2. *Zool Res* (2020) 41:517–26. doi: 10.24272/j.issn.2095-8137.2020.053

73. Zhao Y, Wang J, Kuang D, Xu J, Yang M, Ma C, et al. Susceptibility of tree shrew to SARS-CoV-2 infection. *Sci Rep* (2020) 10:16007–. doi: 10.1038/s41598-020-72563-w

74. Woolsey C, Borisevich V, Prasad AN, Agans KN, Deer DJ, Dobias NS, et al. Establishment of an African green monkey model for COVID-19 and protection against re-infection. *Nat Immunol* (2021) 22:86–98. doi: 10.1038/s41590-020-00835-8

75. Singh DK, Singh B, Ganatra SR, Gazi M, Cole J, Thippeshappa R, et al. Responses to acute infection with SARS-CoV-2 in the lungs of rhesus macaques, baboons and marmosets. *Nat Microbiol* (2021) 6:73–86. doi: 10.1038/s41564-020-00841-4

76. Fahlberg MD, Blair RV, Doyle-Meyers LA, Midkiff CC, Zenere G, Russell-Lodrigue KE, et al. Cellular events of acute, resolving or progressive COVID-19 in SARS-CoV-2 infected non-human primates. *Nat Commun* (2020) 11:6078–. doi: 10.1038/s41467-020-19967-4

77. Zheng H, Li H, Guo L, Liang Y, Li J, Wang X, et al. Virulence and pathogenesis of SARS-CoV-2 infection in rhesus macaques: A nonhuman primate model of COVID-19 progression. *PloS Pathog* (2020) 16:e1008949–e. doi: 10.1371/journal.ppat.1008949

78. Williamson BN, Feldmann F, Schwarz B, Meade-White K, Porter DP, Schulz J, et al. Clinical benefit of remdesivir in rhesus macaques infected with SARS-CoV-2. *Nature* (2020) 585:273–6. doi: 10.1038/s41586-020-2423-5

79. Baum A, Ajithdoss D, Copin R, Zhou A, Lanza K, Negron N, et al. REGN-COV2 antibodies prevent and treat SARS-CoV-2 infection in rhesus macaques and hamsters. *Sci (New York NY)* (2020) 370:1110–5. doi: 10.1126/science.abe2402

80. Guebre-Xabier M, Patel N, Tian J-H, Zhou B, Maciejewski S, Lam K, et al. NVX-CoV2373 vaccine protects cynomolgus macaque upper and lower airways against SARS-CoV-2 challenge. *Vaccine* (2020) 38:7892–6. doi: 10.1016/j.vaccine.2020.10.064

81. Corbett KS, Flynn B, Foulds KE, Francica JR, Boyoglu-Barnum S, Werner AP, et al. Evaluation of the mRNA-1273 vaccine against SARS-CoV-2 in nonhuman primates. *N Engl J Med* (2020) 383:1544–55. doi: 10.1056/NEJMoa2024671

82. Yu J, Tostanoski LH, Peter L, Mercado NB, McMahan K, Mahrokhian SH, et al. DNA Vaccine protection against SARS-CoV-2 in rhesus macaques. *Sci (New York NY)* (2020) 369:806–11. doi: 10.1126/science.abc6284

83. Feng L, Wang Q, Shan C, Yang C, Feng Y, Wu J, et al. An adenovirus-vectored COVID-19 vaccine confers protection from SARS-COV-2 challenge in rhesus macaques. *Nat Commun* (2020) 11:4207. doi: 10.1038/s41467-020-18077-5

84. van Doremalen N, Lambe T, Spencer A, Belij-Rammerstorfer S, Purushotham JN, Port JR, et al. ChAdOx1 nCoV-19 vaccine prevents SARS-CoV-2 pneumonia in rhesus macaques. *Nature* (2020) 586:578–82. doi: 10.1038/s41586-020-2608-y

85. Mercado NB, Zahn R, Wegmann F, Loos C, Chandrashekar A, Yu J, et al. Single-shot Ad26 vaccine protects against SARS-CoV-2 in rhesus macaques. *Nature* (2020) 586:583–8. doi: 10.1038/s41586-020-2607-z

86. Huang C, Wang Y, Li X, Ren L, Zhao J, Hu Y, et al. Clinical features of patients infected with 2019 novel coronavirus in wuhan, China. *Lancet* (2020) 395:497–506. doi: 10.1016/S0140-6736(20)30183-5

87. Wiersinga WJ, Rhodes A, Cheng AC, Peacock SJ, Prescott HC. Pathophysiology, transmission, diagnosis, and treatment of coronavirus disease 2019 (COVID-19): A review. *Jama* (2020) 324:782–93. doi: 10.1001/jama.2020.12839

88. Zhou F, Yu T, Du R, Fan G, Liu Y, Liu Z, et al. Clinical course and risk factors for mortality of adult inpatients with COVID-19 in wuhan, China: A retrospective cohort study. *Lancet* (2020) 395:1054–62. doi: 10.1016/S0140-6736(20)30566-3

89. Wu Z, McGoogan JM. Characteristics of and important lessons from the coronavirus disease 2019 (COVID-19) outbreak in China: Summary of a report of 72 314 cases from the Chinese center for disease control and prevention. *Jama* (2020) 323:1239–42. doi: 10.1001/jama.2020.2648

90. Wu C, Chen X, Cai Y, Ja X, Zhou X, Xu S, et al. Risk factors associated with acute respiratory distress syndrome and death in patients with coronavirus disease 2019 pneumonia in wuhan, China. *JAMA Intern Med* (2020) 180:934–43. doi: 10.1001/jamainternmed.2020.0994

91. Chen G, Wu D, Guo W, Cao Y, Huang D, Wang H, et al. Clinical and immunological features of severe and moderate coronavirus disease 2019. *J Clin Invest* (2020) 130:2620–9. doi: 10.1172/JCI137244

92. Garg S, Kim L, Whitaker M, O'Halloran A, Cummings C, Holstein R, et al. Hospitalization rates and characteristics of patients hospitalized with laboratory-confirmed coronavirus disease 2019 - COVID-NET, 14 states, march 1-30, 2020. *MMWR Morbidity mortality weekly Rep* (2020) 69:458–64. doi: 10.15585/mmwr.mm6915e3

93. Wang L, He W, Yu X, Hu D, Bao M, Liu H, et al. Coronavirus disease 2019 in elderly patients: Characteristics and prognostic factors based on 4-week follow-up. *J Infect* (2020) 80:639–45. doi: 10.1016/j.jinf.2020.03.019

94. Yang X, Yu Y, Xu J, Shu H, Ja X, Liu H, et al. Clinical course and outcomes of critically ill patients with SARS-CoV-2 pneumonia in wuhan, China: A single-centered, retrospective, observational study. *Lancet Respir Med* (2020) 8:475–81. doi: 10.1016/S2213-2600(20)30079-5

95. Tabata S, Imai K, Kawano S, Ikeda M, Kodama T, Miyoshi K, et al. Clinical characteristics of COVID-19 in 104 people with SARS-CoV-2 infection on the diamond princess cruise ship: a retrospective analysis. *Lancet Infect Dis* (2020) 20:1043–50. doi: 10.1016/S1473-3099(20)30482-5

96. Liu K, Chen Y, Lin R, Han K. Clinical features of COVID-19 in elderly patients: A comparison with young and middle-aged patients. *J Infect* (2020) 80:e14–e8. doi: 10.1016/j.jinf.2020.03.005

97. Chen N, Zhou M, Dong X, Qu J, Gong F, Han Y, et al. Epidemiological and clinical characteristics of 99 cases of 2019 novel coronavirus pneumonia in wuhan, China: A descriptive study. *Lancet* (2020) 395:507–13. doi: 10.1016/S0140-6736(20)30211-7

98. Wang D, Hu B, Hu C, Zhu F, Liu X, Zhang J, et al. Clinical characteristics of 138 hospitalized patients with 2019 novel coronavirus-infected pneumonia in wuhan, China. *Jama* (2020) 323:1061–9. doi: 10.1001/jama.2020.1585

99. Ottestad W, Søvik S. COVID-19 patients with respiratory failure: What can we learn from aviation medicine? *Br J Anaesth* (2020) 125:e280–e1. doi: 10.1016/j.bja.2020.04.012

100. Lu X, Zhang L, Du H, Zhang J, Li YY, Qu J, et al. SARS-CoV-2 infection in children. *N Engl J Med* (2020) 382:1663–5. doi: 10.1056/NEJMc2005073

101. Guan W-J, Ni Z-Y, Hu Y, Liang W-H, Ou C-Q, He J-X, et al. Clinical characteristics of coronavirus disease 2019 in China. *N Engl J Med* (2020) 382:1708–20. doi: 10.1056/NEJMoa2002032

102. Costello F, Dalakas MC. Cranial neuropathies and COVID-19: Neurotropism and autoimmunity. *Neurology* (2020) 95:195–6. doi: 10.1212/wnl.0000000000009921

103. Lucchese G, Flöel A. Molecular mimicry between SARS-CoV-2 and respiratory pacemaker neurons. *Autoimmun Rev* (2020) 19:102556–. doi: 10.1016/j.autrev.2020.102556

104. Alquisiras-Burgos I, Peralta-Arrieta I, Alonso-Palomares LA, Zacapala-Gómez AE, Salmerón-Bárcenas EG, Aguilera P. Neurological complications associated with the blood-brain barrier damage induced by the inflammatory response during SARS-CoV-2 infection. *Mol Neurobiol* (2021) 58:520–35. doi: 10.1007/s12035-020-02134-7

105. Contini C, Caselli E, Martini F, Maritati M, Torreggiani E, Seraceni S, et al. COVID-19 is a multifaceted challenging pandemic which needs urgent public health interventions. *Microorganisms* (2020) 8:1228. doi: 10.3390/microorganisms8081228

106. Peiris JSM, Chu CM, Cheng VCC, Chan KS, Hung IFN, Poon LLM, et al. Clinical progression and viral load in a community outbreak of coronavirus-associated SARS pneumonia: A prospective study. *Lancet* (2003) 361:1767–72. doi: 10.1016/s0140-6736(03)13412-5

107. Ziegler CGK, Allon SJ, Nyquist SK, Mbano IM, Miao VN, Tzouanas CN, et al. SARS-CoV-2 receptor ACE2 is an interferon-stimulated gene in human airway epithelial cells and is detected in specific cell subsets across tissues. *Cell* (2020) 181:1016–35.e19. doi: 10.1016/j.cell.2020.04.035

108. Wölfel R, Corman VM, Guggemos W, Seilmaier M, Zange S, Müller MA, et al. Virological assessment of hospitalized patients with COVID-2019. *Nature* (2020) 581:465–9. doi: 10.1038/s41586-020-2196-x

109. Xu H, Zhong L, Deng J, Peng J, Dan H, Zeng X, et al. High expression of ACE2 receptor of 2019-nCoV on the epithelial cells of oral mucosa. *Int J Oral Sci* (2020) 12:8–. doi: 10.1038/s41368-020-0074-x

110. Kujawski SA, Wong KK, Collins JP, Epstein L, Killerby ME, Midgley CM, et al. Clinical and virologic characteristics of the first 12 patients with coronavirus disease 2019 (COVID-19) in the united states. *Nat Med* (2020) 26:861–8. doi: 10.1038/s41591-020-0877-5

111. Cholankeril G, Podboy A, Aivaliotis VI, Tarlow B, Pham EA, Spencer SP, et al. High prevalence of concurrent gastrointestinal manifestations in patients with severe acute respiratory syndrome coronavirus 2: Early experience from California. *Gastroenterology* (2020) 159:775–7. doi: 10.1053/j.gastro.2020.04.008

112. Xiao F, Tang M, Zheng X, Liu Y, Li X, Shan H. Evidence for gastrointestinal infection of SARS-CoV-2. *Gastroenterology* (2020) 158:1831–3.e3. doi: 10.1053/j.gastro.2020.02.055

113. Lan J, Ge J, Yu J, Shan S, Zhou H, Fan S, et al. Structure of the SARS-CoV-2 spike receptor-binding domain bound to the ACE2 receptor. *Nature* (2020) 581:215–20. doi: 10.1038/s41586-020-2180-5

114. Qiao J, Li W, Bao J, Peng Q, Wen D, Wang J, et al. The expression of SARS-CoV-2 receptor ACE2 and CD147, and protease TMPRSS2 in human and mouse brain cells and mouse brain tissues. *Biochem Biophys Res Commun* (2020) 533:867–71. doi: 10.1016/j.bbrc.2020.09.042

115. Zamorano Cuervo N, Grandvaux N. ACE2: Evidence of role as entry receptor for SARS-CoV-2 and implications in comorbidities. *Elife* (2020) 9:e61390. doi: 10.7554/eLife.61390

116. Mayi BS, Leibowitz JA, Woods AT, Ammon KA, Liu AE, Raja A. The role of neuropilin-1 in COVID-19. *PloS Pathog* (2021) 17:e1009153–e. doi: 10.1371/journal.ppat.1009153

117. Kyrou I, Randeva HS, Spandidos DA, Karteris E. Not only ACE2-the quest for additional host cell mediators of SARS-CoV-2 infection: Neuropilin-1 (NRP1) as a novel SARS-CoV-2 host cell entry mediator implicated in COVID-19. *Signal Transduct Target Ther* (2021) 6:21–. doi: 10.1038/s41392-020-00460-9

118. Krejner-Bienias A, Grzela K, Grzela T. DPP4 inhibitors and COVID-19-Holy grail or another dead end? *Arch Immunol Ther Exp (Warsz)* (2021) 69:1–. doi: 10.1007/s00005-020-00602-5

119. Pinheiro MM, Fabbri A, Infante M. Cytokine storm modulation in COVID-19: A proposed role for vitamin d and DPP-4 inhibitor combination therapy (VIDPP-4i). *Immunotherapy* (2021) 13:753–65. doi: 10.2217/imt-2020-0349

120. Sungnak W, Huang N, Bécavin C, Berg M, Queen R, Litvinukova M, et al. SARS-CoV-2 entry factors are highly expressed in nasal epithelial cells together with innate immune genes. *Nat Med* (2020) 26:681–7. doi: 10.1038/s41591-020-0868-6

121. Lukassen S, Chua RL, Trefzer T, Kahn NC, Schneider MA, Muley T, et al. SARS-CoV-2 receptor ACE2 and TMPRSS2 are primarily expressed in bronchial transient secretory cells. *EMBO J* (2020) 39:e105114–e. doi: 10.15252/embj.20105114

122. Zhang H, Kang Z, Gong H, Xu D, Wang J, Li Z, et al. Digestive system is a potential route of COVID-19: an analysis of single-cell coexpression pattern of key proteins in viral entry process. *Gut* (2020) 69:1010–8. doi: 10.1136/gutjnl-2020-320953

123. Lamers MM, Beumer J, van der Vaart J, Knoops K, Puschhof J, Breugem TI, et al. SARS-CoV-2 productively infects human gut enterocytes. *Sci (New York NY)* (2020) 369:50–4. doi: 10.1126/science.abc1669

124. Zhou Z, Kang H, Li S, Zhao X. Understanding the neurotropic characteristics of SARS-CoV-2: From neurological manifestations of COVID-19 to potential neurotropic mechanisms. *J Neurol* (2020) 267:2179–84. doi: 10.1007/s00415-020-09929-7

125. Xu Z, Shi L, Wang Y, Zhang J, Huang L, Zhang C, et al. Pathological findings of COVID-19 associated with acute respiratory distress syndrome. *Lancet Respir Med* (2020) 8:420–2. doi: 10.1016/S2213-2600(20)30076-X

126. Song E, Zhang C, Israelow B, Lu-Culligan A, Prado AV, Skriabine S, et al. Neuroinvasion of SARS-CoV-2 in human and mouse brain. *J Exp Med* (2021) 218:e20202135. doi: 10.1084/jem.20202135

127. Winkler ES, Bailey AL, Kafai NM, Nair S, McCune BT, Yu J, et al. SARS-CoV-2 infection of human ACE2-transgenic mice causes severe lung inflammation and impaired function. *Nat Immunol* (2020) 21:1327–35. doi: 10.1038/s41590-020-0778-2

128. Carossino M, Kenney D, O'Connell AK, Montanaro P, Tseng AE, Gertje HP, et al. Fatal neurodissemination and SARS-CoV-2 tropism in K18-hACE2 mice is only partially dependent on hACE2 expression. *Viruses* (2022) 14(3):535. doi: 10.3390/v14030535

129. Zhang AJ, Lee AC-Y, Chu H, Chan JF-W, Fan Z, Li C, et al. Severe acute respiratory syndrome coronavirus 2 infects and damages the mature and immature olfactory sensory neurons of hamsters. *Clin Infect Dis* (2021) 73:e503–e12. doi: 10.1093/cid/ciaa995

130. Kaptein SJ, Jacobs S, Langendries L, Seldeslachts L, ter Horst S, Liesenborghs L, et al. Antiviral treatment of SARS-CoV-2-infected hamsters reveals a weak effect of favipiravir and a complete lack of effect for hydroxychloroquine. *bioRxiv* (2020) 2020.06.19.159053. doi: 10.1101/2020.06.19.159053

131. Osterrieder N, Bertzbach LD, Dietert K, Abdelgawad A, Vladimirova D, Kunec D, et al. Age-dependent progression of SARS-CoV-2 infection in Syrian hamsters. *Viruses* (2020) 12:779. doi: 10.3390/v12070779

132. Lee AC-Y, Zhang AJ, Chan JF-W, Li C, Fan Z, Liu F, et al. Oral SARS-CoV-2 inoculation establishes subclinical respiratory infection with virus shedding in golden Syrian hamsters. *Cell Rep Med* (2020) 1:100121–. doi: 10.1016/j.xcrm.2020.100121

133. Chan JF-W, Yuan S, Zhang AJ, Poon VK-M, Chan CC-S, Lee AC-Y, et al. Surgical mask partition reduces the risk of noncontact transmission in a golden Syrian hamster model for coronavirus disease 2019 (COVID-19). *Clin Infect Dis* (2020) 71:2139–49. doi: 10.1093/cid/ciaa644

134. Kim Y-I, Kim S-G, Kim S-M, Kim E-H, Park S-J, Yu K-M, et al. Infection and rapid transmission of SARS-CoV-2 in ferrets. *Cell Host Microbe* (2020) 27:704–9.e2. doi: 10.1016/j.chom.2020.03.023

135. Everett HE, Lean FZX, Byrne AMP, van Diemen PM, Rhodes S, James J, et al. Intranasal infection of ferrets with SARS-CoV-2 as a model for asymptomatic human infection. *Viruses* (2021) 13:113. doi: 10.3390/v13010113

136. Blanco-Melo D, Nilsson-Payant BE, Liu W-C, Uhl S, Hoagland D, Møller R, et al. Imbalanced host response to SARS-CoV-2 drives development of COVID-19. *Cell* (2020) 181:1036–45.e9. doi: 10.1016/j.cell.2020.04.026

137. Kim Y-I, Yu K-M, Koh J-Y, Kim E-H, Kim S-M, Kim EJ, et al. Age-dependent pathogenic characteristics of SARS-CoV-2 infection in ferrets. *Nat Commun* (2022) 13:21–. doi: 10.1038/s41467-021-27717-3

138. Yuan L, Tang Q, Zhu H, Guan Y, Cheng T, Xia N. SARS-CoV-2 infection and disease outcomes in non-human primate models: Advances and implications. *Emerg Microbes Infect* (2021) 10:1881–9. doi: 10.1080/22221751.2021.1976598

139. Munster VJ, Feldmann F, Williamson BN, van Doremalen N, Pérez-Pérez L, Schulz J, et al. Respiratory disease in rhesus macaques inoculated with SARS-CoV-2. *Nature* (2020) 585:268–72. doi: 10.1038/s41586-020-2324-7

140. Chowdhury MA, Hossain N, Kashem MA, Shahid MA, Alam A. Immune response in COVID-19: A review. *J Infect Public Health* (2020) 13:1619–29. doi: 10.1016/j.jiph.2020.07.001

141. Mazzoni A, Maggi L, Capone M, Spinicci M, Salvati L, Colao MG, et al. Cell-mediated and humoral adaptive immune responses to SARS-CoV-2 are lower in asymptomatic than symptomatic COVID-19 patients. *Eur J Immunol* (2020) 50:2013–24. doi: 10.1002/eji.202048915

142. Yang X, Dai T, Zhou X, Qian H, Guo R, Lei L, et al. Naturally activated adaptive immunity in COVID-19 patients. *J Cell Mol Med* (2020) 24:12457–63. doi: 10.1111/jcmm.15771

143. Lu LL, Suscovich TJ, Fortune SM, Alter G. Beyond binding: antibody effector functions in infectious diseases. *Nat Rev Immunol* (2018) 18:46–61. doi: 10.1038/nri.2017.106

144. Long QX, Liu BZ, Deng HJ, Wu GC, Deng K, Chen YK, et al. Antibody responses to SARS-CoV-2 in patients with COVID-19. *Nat Med* (2020) 26:845–8. doi: 10.1038/s41591-020-0897-1

145. Rydyznski Moderbacher C, Ramirez SI, Dan JM, Grifoni A, Hastie KM, Weiskopf D, et al. Antigen-specific adaptive immunity to SARS-CoV-2 in acute COVID-19 and associations with age and disease severity. *Cell* (2020) 183:996–1012.e19. doi: 10.1016/j.cell.2020.09.038

146. Premkumar L, Segovia-Chumbez B, Jadi R, Martinez DR, Raut R, Markmann A, et al. The receptor binding domain of the viral spike protein is an immunodominant and highly specific target of antibodies in SARS-CoV-2 patients. *Sci Immunol* (2020) 5:eabc8413. doi: 10.1126/sciimmunol.abc8413

147. Ripperger TJ, Uhrlaub JL, Watanabe M, Wong R, Castaneda Y, Pizzato HA, et al. Orthogonal SARS-CoV-2 serological assays enable surveillance of low-prevalence communities and reveal durable humoral immunity. *Immunity* (2020) 53:925–33.e4. doi: 10.1016/j.immuni.2020.10.004

148. Suthar MS, Zimmerman MG, Kauffman RC, Mantus G, Linderman SL, Hudson WH, et al. Rapid generation of neutralizing antibody responses in COVID-19 patients. *Cell Rep Med* (2020) 1:100040–. doi: 10.1016/j.xcrm.2020.100040

149. Robbiani DF, Gaebler C, Muecksch F, Lorenzi JCC, Wang Z, Cho A, et al. Convergent antibody responses to SARS-CoV-2 in convalescent individuals. *Nature* (2020) 584:437–42. doi: 10.1038/s41586-020-2456-9

150. Wheatley AK, Juno JA, Wang JJ, Selva KJ, Reynaldi A, Tan H-X, et al. Evolution of immune responses to SARS-CoV-2 in mild-moderate COVID-19. *Nat Commun* (2021) 12:1162–. doi: 10.1038/s41467-021-21444-5

151. Wajnberg A, Amanat F, Firpo A, Altman DR, Bailey MJ, Mansour M, et al. Robust neutralizing antibodies to SARS-CoV-2 infection persist for months. *Sci (New York NY)* (2020) 370:1227–30. doi: 10.1126/science.abd7728

152. Röltgen K, Powell AE, Wirz OF, Stevens BA, Hogan CA, Najeeb J, et al. Defining the features and duration of antibody responses to SARS-CoV-2 infection associated with disease severity and outcome. *Sci Immunol* (2020) 5:eabe0240. doi: 10.1126/sciimmunol.abe0240

153. Khoury DS, Cromer D, Reynaldi A, Schlub TE, Wheatley AK, Juno JA, et al. Neutralizing antibody levels are highly predictive of immune protection from symptomatic SARS-CoV-2 infection. *Nat Med* (2021) 27:1205–11. doi: 10.1038/s41591-021-01377-8

154. Schäfer A, Muecksch F, Lorenzi JCC, Leist SR, Cipolla M, Bournazos S, et al. Antibody potency, effector function, and combinations in protection and therapy for SARS-CoV-2 infection. *vivo J Exp Med* (2021) 218:e20201993. doi: 10.1084/jem.20201993

155. Lee WS, Selva KJ, Davis SK, Wines BD, Reynaldi A, Esterbauer R, et al. Decay of fc-dependent antibody functions after mild to moderate COVID-19. *Cell Rep Med* (2021) 2:100296–. doi: 10.1016/j.xcrm.2021.100296

156. Winkler ES, Gilchuk P, Yu J, Bailey AL, Chen RE, Chong Z, et al. Human neutralizing antibodies against SARS-CoV-2 require intact fc effector functions for optimal therapeutic protection. *Cell* (2021) 184:1804–20.e16. doi: 10.1016/j.cell.2021.02.026

157. Bartsch YC, Fischinger S, Siddiqui SM, Chen Z, Yu J, Gebre M, et al. Discrete SARS-CoV-2 antibody titers track with functional humoral stability. *Nat Commun* (2021) 12:1018–. doi: 10.1038/s41467-021-21336-8

158. Earle KA, Ambrosino DM, Fiore-Gartland A, Goldblatt D, Gilbert PB, Siber GR, et al. Evidence for antibody as a protective correlate for COVID-19 vaccines. *Vaccine* (2021) 39:4423–8. doi: 10.1016/j.vaccine.2021.05.063

159. Zohar T, Loos C, Fischinger S, Atyeo C, Wang C, Slein MD, et al. Compromised humoral functional evolution tracks with SARS-CoV-2 mortality. *Cell* (2020) 183:1508–19.e12. doi: 10.1016/j.cell.2020.10.052

160. Weinreich DM, Sivapalasingam S, Norton T, Ali S, Gao H, Bhore R, et al. REGN-COV2, a neutralizing antibody cocktail, in outpatients with covid-19. *N Engl J Med* (2021) 384:238–51. doi: 10.1056/NEJMoa2035002

161. Chen P, Nirula A, Heller B, Gottlieb RL, Boscia J, Morris J, et al. SARS-CoV-2 neutralizing antibody LY-CoV555 in outpatients with covid-19. *N Engl J Med* (2021) 384:229–37. doi: 10.1056/NEJMoa2029849

162. Zost SJ, Gilchuk P, Case JB, Binshtein E, Chen RE, Nkolola JP, et al. Potently neutralizing and protective human antibodies against SARS-CoV-2. *Nature* (2020) 584:443–9. doi: 10.1038/s41586-020-2548-6

163. Shi R, Shan C, Duan X, Chen Z, Liu P, Song J, et al. A human neutralizing antibody targets the receptor-binding site of SARS-CoV-2. *Nature* (2020) 584:120–4. doi: 10.1038/s41586-020-2381-y

164. Libster R, Pérez Marc G, Wappner D, Coviello S, Bianchi A, Braem V, et al. Early high-titer plasma therapy to prevent severe covid-19 in older adults. *N Engl J Med* (2021) 384:610–8. doi: 10.1056/NEJMoa2033700

165. Joyner MJ, Carter RE, Senefeld JW, Klassen SA, Mills JR, Johnson PW, et al. Convalescent plasma antibody levels and the risk of death from covid-19. *N Engl J Med* (2021) 384:1015–27. doi: 10.1056/NEJMoa2031893

166. Group A-TL-CS, Lundgren JD, Grund B, Barkauskas CE, Holland TL, Gottlieb RL, et al. A neutralizing monoclonal antibody for hospitalized patients with covid-19. *N Engl J Med* (2021) 384:905–14. doi: 10.1056/NEJMoa2033130

167. Cohen MS. Monoclonal antibodies to disrupt progression of early covid-19 infection. *N Engl J Med* (2021) 384:289–91. doi: 10.1056/NEJMe2034495

168. Mohamed Khosroshahi L, Rokni M, Mokhtari T, Noorbakhsh F. Immunology, immunopathogenesis and immunotherapeutics of COVID-19; an overview. *Int Immunopharmacol* (2021) 93:107364–. doi: 10.1016/j.intimp.2020.107364

169. Zhao J, Yuan Q, Wang H, Liu W, Liao X, Su Y, et al. Antibody responses to SARS-CoV-2 in patients with novel coronavirus disease 2019. *Clin Infect Dis* (2020) 71:2027–34. doi: 10.1093/cid/ciaa344

170. Cao X. COVID-19: Immunopathology and its implications for therapy. *Nat Rev Immunol* (2020) 20:269–70. doi: 10.1038/s41577-020-0308-3

171. Tetro JA. Is COVID-19 receiving ADE from other coronaviruses? *Microbes Infect* (2020) 22:72–3. doi: 10.1016/j.micinf.2020.02.006

172. Zhang B, Zhou X, Zhu C, Song Y, Feng F, Qiu Y, et al. Immune phenotyping based on the neutrophil-to-Lymphocyte ratio and IgG level predicts disease severity and outcome for patients with COVID-19. *Front Mol Biosci* (2020) 7:157. doi: 10.3389/fmolb.2020.00157

173. Wen J, Cheng Y, Ling R, Dai Y, Huang B, Huang W, et al. Antibody-dependent enhancement of coronavirus. *Int J Infect Dis* (2020) 100:483–9. doi: 10.1016/j.ijid.2020.09.015

174. Bournazos S, Gupta A, Ravetch JV. The role of IgG fc receptors in antibody-dependent enhancement. *Nat Rev Immunol* (2020) 20:633–43. doi: 10.1038/s41577-020-00410-0

175. Li D, Edwards RJ, Manne K, Martinez DR, Schäfer A, Alam SM, et al. *In vitro* and *in vivo* functions of SARS-CoV-2 infection-enhancing and neutralizing antibodies. *Cell* (2021) 184:4203–19.e32. doi: 10.1016/j.cell.2021.06.021

176. Baumgarth N, Nikolich-Žugich J, Lee FE-H, Bhattacharya D. Antibody responses to SARS-CoV-2: Let's stick to known knowns. *J Immunol (Baltimore Md 1950)* (2020) 205:2342–50. doi: 10.4049/jimmunol.2000839

177. Tan AT, Linster M, Tan CW, Le Bert N, Chia WN, Kunasegaran K, et al. Early induction of functional SARS-CoV-2-specific T cells associates with rapid viral clearance and mild disease in COVID-19 patients. *Cell Rep* (2021) 34:108728–. doi: 10.1016/j.celrep.2021.108728

178. Piccoli L, Park Y-J, Tortorici MA, Czudnochowski N, Walls AC, Beltramello M, et al. Mapping neutralizing and immunodominant sites on the SARS-CoV-2 spike receptor-binding domain by structure-guided high-resolution serology. *Cell* (2020) 183:1024–42.e21. doi: 10.1016/j.cell.2020.09.037

179. Woodruff MC, Ramonell RP, Nguyen DC, Cashman KS, Saini AS, Haddad NS, et al. Extrafollicular b cell responses correlate with neutralizing antibodies and morbidity in COVID-19. *Nat Immunol* (2020) 21:1506–16. doi: 10.1038/s41590-020-00814-z

180. Soresina A, Moratto D, Chiarini M, Paolillo C, Baresi G, Focà E, et al. Two X-linked agammaglobulinemia patients develop pneumonia as COVID-19 manifestation but recover. *Pediatr Allergy Immunol* (2020) 31:565–9. doi: 10.1111/pai.13263

181. Safavi F, Nourbakhsh B, Azimi AR. B-cell depleting therapies may affect susceptibility to acute respiratory illness among patients with multiple sclerosis during the early COVID-19 epidemic in Iran. *Mult Scler Relat Disord* (2020) 43:102195–. doi: 10.1016/j.msard.2020.102195

182. Novi G, Mikulska M, Briano F, Toscanini F, Tazza F, Uccelli A, et al. COVID-19 in a MS patient treated with ocrelizumab: Does immunosuppression have a protective role? *Mult Scler Relat Disord* (2020) 42:102120–. doi: 10.1016/j.msard.2020.102120

183. Montero-Escribano P, Matías-Guiu J, Gómez-Iglesias P, Porta-Etessam J, Pytel V, Matias-Guiu JA. Anti-CD20 and COVID-19 in multiple sclerosis and related disorders: A case series of 60 patients from Madrid, Spain. *Mult Scler Relat Disord* (2020) 42:102185–. doi: 10.1016/j.msard.2020.102185

184. Schulien I, Kemming J, Oberhardt V, Wild K, Seidel LM, Killmer S, et al. Characterization of pre-existing and induced SARS-CoV-2-specific CD8(+) T cells. *Nat Med* (2021) 27:78–85. doi: 10.1038/s41591-020-01143-2

185. Nelde A, Bilich T, Heitmann JS, Maringer Y, Salih HR, Roerden M, et al. SARS-CoV-2-derived peptides define heterologous and COVID-19-induced T cell recognition. *Nat Immunol* (2021) 22:74–85. doi: 10.1038/s41590-020-00808-x

186. Amanat F, Krammer F. SARS-CoV-2 vaccines: Status report. *Immunity* (2020) 52:583–9. doi: 10.1016/j.immuni.2020.03.007

187. Corey L, Mascola JR, Fauci AS, Collins FS. A strategic approach to COVID-19 vaccine R&D. *Science* (2020) 368:948–50. doi: 10.1126/science.abc5312

188. Thanh Le T, Andreadakis Z, Kumar A, Gómez Román R, Tollefsen S, Saville M, et al. The COVID-19 vaccine development landscape. *Nat Rev Drug Discovery* (2020) 19:305–6. doi: 10.1038/d41573-020-00073-5

189. Quast I, Tarlinton D. B cell memory: Understanding COVID-19. *Immunity* (2021) 54:205–10. doi: 10.1016/j.immuni.2021.01.014

190. Deng X, Garcia-Knight MA, Khalid MM, Servellita V, Wang C, Morris MK, et al. Transmission, infectivity, and neutralization of a spike L452R SARS-CoV-2 variant. *Cell* (2021) 184:3426–37.e8. doi: 10.1016/j.cell.2021.04.025

191. Thomson EC, Rosen LE, Shepherd JG, Spreafico R, da Silva Filipe A, Wojcechowskyj JA, et al. Circulating SARS-CoV-2 spike N439K variants maintain fitness while evading antibody-mediated immunity. *Cell* (2021) 184:1171–87.e20. doi: 10.1016/j.cell.2021.01.037

192. Wang P, Casner RG, Nair MS, Wang M, Yu J, Cerutti G, et al. Increased resistance of SARS-CoV-2 variant P.1 to antibody neutralization. *Cell Host Microbe* (2021) 29:747–51.e4. doi: 10.1016/j.chom.2021.04.007

193. Hoffmann M, Arora P, Groß R, Seidel A, Hörnich BF, Hahn AS, et al. SARS-CoV-2 variants B.1.351 and P.1 escape from neutralizing antibodies. *Cell* (2021) 184:2384–93.e12. doi: 10.1016/j.cell.2021.03.036

194. Cao Y, Wang J, Jian F, Xiao T, Song W, Yisimayi A, et al. Omicron escapes the majority of existing SARS-CoV-2 neutralizing antibodies. *Nature* (2022) 602:657–63. doi: 10.1038/s41586-021-04385-3

195. Walls AC, Park Y-J, Tortorici MA, Wall A, McGuire AT, Veesler D. Structure, function, and antigenicity of the SARS-CoV-2 spike glycoprotein. *Cell* (2020) 181:281–92.e6. doi: 10.1016/j.cell.2020.02.058

196. Walls AC, Tortorici MA, Frenz B, Snijder J, Li W, Rey FA, et al. Glycan shield and epitope masking of a coronavirus spike protein observed by cryo-electron microscopy. *Nat Struct Mol Biol* (2016) 23:899–905. doi: 10.1038/nsmb.3293

197. Watanabe Y, Allen JD, Wrapp D, McLellan JS, Crispin M. Site-specific glycan analysis of the SARS-CoV-2 spike. *Sci (New York NY)* (2020) 369:330–3. doi: 10.1126/science.abb9983

198. Saunders KO, Lee E, Parks R, Martinez DR, Li D, Chen H, et al. Neutralizing antibody vaccine for pandemic and pre-emergent coronaviruses. *Nature* (2021) 594:553–9. doi: 10.1038/s41586-021-03594-0

199. Jalkanen P, Kolehmainen P, Häkkinen HK, Huttunen M, Tähtinen PA, Lundberg R, et al. COVID-19 mRNA vaccine induced antibody responses against three SARS-CoV-2 variants. *Nat Commun* (2021) 12:3991. doi: 10.1038/s41467-021-24285-4

200. Zhou R, To KK-W, Wong Y-C, Liu L, Zhou B, Li X, et al. Acute SARS-CoV-2 infection impairs dendritic cell and T cell responses. *Immunity* (2020) 53:864–77.e5. doi: 10.1016/j.immuni.2020.07.026

201. Liao M, Liu Y, Yuan J, Wen Y, Xu G, Zhao J, et al. Single-cell landscape of bronchoalveolar immune cells in patients with COVID-19. *Nat Med* (2020) 26:842–4. doi: 10.1038/s41591-020-0901-9

202. Peng Y, Mentzer AJ, Liu G, Yao X, Yin Z, Dong D, et al. Broad and strong memory CD4(+) and CD8(+) T cells induced by SARS-CoV-2 in UK convalescent individuals following COVID-19. *Nat Immunol* (2020) 21:1336–45. doi: 10.1038/s41590-020-0782-6

203. Sette A, Crotty S. Adaptive immunity to SARS-CoV-2 and COVID-19. *Cell* (2021) 184:861–80. doi: 10.1016/j.cell.2021.01.007

204. Crotty S. T Follicular helper cell biology: A decade of discovery and diseases. *Immunity* (2019) 50:1132–48. doi: 10.1016/j.immuni.2019.04.011

205. Koutsakos M, Nguyen THO, Kedzierska K. With a little help from T follicular helper friends: Humoral immunity to influenza vaccination. *J Immunol* (2019) 202:360–7. doi: 10.4049/jimmunol.1800986

206. Ni L, Ye F, Cheng M-L, Feng Y, Deng Y-Q, Zhao H, et al. Detection of SARS-CoV-2-Specific humoral and cellular immunity in COVID-19 convalescent individuals. *Immunity* (2020) 52:971–7.e3. doi: 10.1016/j.immuni.2020.04.023

207. Braun J, Loyal L, Frentsch M, Wendisch D, Georg P, Kurth F, et al. SARS-CoV-2-reactive T cells in healthy donors and patients with COVID-19. *Nature* (2020) 587:270–4. doi: 10.1038/s41586-020-2598-9

208. Weiskopf D, Schmitz KS, Raadsen MP, Grifoni A, Okba NMA, Endeman H, et al. Phenotype and kinetics of SARS-CoV-2-specific T cells in COVID-19 patients with acute respiratory distress syndrome. *Sci Immunol* (2020) 5:eabd2071. doi: 10.1126/sciimmunol.abd2071

209. Meckiff BJ, Ramírez-Suástegui C, Fajardo V, Chee SJ, Kusnadi A, Simon H, et al. Imbalance of regulatory and cytotoxic SARS-CoV-2-Reactive CD4(+) T cells in COVID-19. *Cell* (2020) 183:1340–53.e16. doi: 10.1016/j.cell.2020.10.001

210. Notarbartolo S, Ranzani V, Bandera A, Gruarin P, Bevilacqua V, Putignano AR, et al. Integrated longitudinal immunophenotypic, transcriptional and repertoire analyses delineate immune responses in COVID-19 patients. *Sci Immunol* (2021) 6(62):eabg5021. doi: 10.1126/sciimmunol.abg5021

211. Krammer F. SARS-CoV-2 vaccines in development. *Nature* (2020) 586:516–27. doi: 10.1038/s41586-020-2798-3

212. Zhao J, Zhao J, Mangalam AK, Channappanavar R, Fett C, Meyerholz DK, et al. Airway memory CD4(+) T cells mediate protective immunity against emerging respiratory coronaviruses. *Immunity* (2016) 44:1379–91. doi: 10.1016/j.immuni.2016.05.006

213. Shaan Lakshmanappa Y, Elizaldi SR, Roh JW, Schmidt BA, Carroll TD, Weaver KD, et al. SARS-CoV-2 induces robust germinal center CD4 T follicular helper cell responses in rhesus macaques. *Nat Commun* (2021) 12:541. doi: 10.1038/s41467-020-20642-x

214. Bergamaschi L, Mescia F, Turner L, Hanson AL, Kotagiri P, Dunmore BJ, et al. Longitudinal analysis reveals that delayed bystander CD8+ T cell activation and early immune pathology distinguish severe COVID-19 from mild disease. *Immunity* (2021) 54:1257–75.e8. doi: 10.1016/j.immuni.2021.05.010

215. Qin C, Zhou L, Hu Z, Zhang S, Yang S, Tao Y, et al. Dysregulation of immune response in patients with coronavirus 2019 (COVID-19) in wuhan, China. *Clin Infect Dis* (2020) 71:762–8. doi: 10.1093/cid/ciaa248

216. Thevarajan I, Nguyen THO, Koutsakos M, Druce J, Caly L, van de Sandt CE, et al. Breadth of concomitant immune responses prior to patient recovery: A case report of non-severe COVID-19. *Nat Med* (2020) 26:453–5. doi: 10.1038/s41591-020-0819-2

217. Su Y, Chen D, Yuan D, Lausted C, Choi J, Dai CL, et al. Multi-omics resolves a sharp disease-state shift between mild and moderate COVID-19. *Cell* (2020) 183:1479–95.e20. doi: 10.1016/j.cell.2020.10.037

218. Le Bert N, Tan AT, Kunasegaran K, Tham CYL, Hafezi M, Chia A, et al. SARS-CoV-2-specific T cell immunity in cases of COVID-19 and SARS, and uninfected controls. *Nature* (2020) 584:457–62. doi: 10.1038/s41586-020-2550-z

219. Zhou Y, Fu B, Zheng X, Wang D, Zhao C, Qi Y, et al. Pathogenic T-cells and inflammatory monocytes incite inflammatory storms in severe COVID-19 patients. *Natl Sci Rev* (2020) 7:998–1002. doi: 10.1093/nsr/nwaa041

220. Zeng Q, Y-z Li, Huang G, Wu W, Dong S-y, Xu Y. Mortality of COVID-19 is associated with cellular immune function compared to immune function in Chinese han population. *medRxiv* (2020) 2020.03.08.20031229. doi: 10.1101/2020.03.08.20031229. 2020.03.08.20031229.

221. Wang F, Nie J, Wang H, Zhao Q, Xiong Y, Deng L, et al. Characteristics of peripheral lymphocyte subset alteration in COVID-19 pneumonia. *J Infect Dis* (2020) 221:1762–9. doi: 10.1093/infdis/jiaa150

222. Diao B, Wang C, Tan Y, Chen X, Liu Y, Ning L, et al. Reduction and functional exhaustion of T cells in patients with coronavirus disease 2019 (COVID-19). *Front Immunol* (2020) 11:827. doi: 10.3389/fimmu.2020.00827

223. Laczkó D, Hogan MJ, Toulmin SA, Hicks P, Lederer K, Gaudette BT, et al. A single immunization with nucleoside-modified mRNA vaccines elicits strong cellular and humoral immune responses against SARS-CoV-2 in mice. *Immunity* (2020) 53:724–32.e7. doi: 10.1016/j.immuni.2020.07.019

224. Erasmus JH, Khandhar AP, O'Connor MA, Walls AC, Hemann EA, Murapa P, et al. An alphavirus-derived replicon RNA vaccine induces SARS-CoV-2 neutralizing antibody and T cell responses in mice and nonhuman primates. *Sci Trans Med* (2020) 12(555):eabc9396. doi: 10.1126/scitranslmed.abc9396

225. DiPiazza AT, Leist SR, Abiona OM, Moliva JI, Werner A, Minai M, et al. COVID-19 vaccine mRNA-1273 elicits a protective immune profile in mice that is not associated with vaccine-enhanced disease upon SARS-CoV-2 challenge. *Immunity* (2021) 54:1869–82.e6. doi: 10.1016/j.immuni.2021.06.018

226. Ku MW, Bourgine M, Authié P, Lopez J, Nemirov K, Moncoq F, et al. Intranasal vaccination with a lentiviral vector protects against SARS-CoV-2 in preclinical animal models. *Cell Host Microbe* (2021) 29:236–49.e6. doi: 10.1016/j.chom.2020.12.010

227. Hassan AO, Kafai NM, Dmitriev IP, Fox JM, Smith BK, Harvey IB, et al. A single-dose intranasal ChAd vaccine protects upper and lower respiratory tracts against SARS-CoV-2. *Cell* (2020) 183:169–84.e13. doi: 10.1016/j.cell.2020.08.026

228. King RG, Silva-Sanchez A, Peel JN, Botta D, Dickson AM, Pinto AK, et al. Single-dose intranasal administration of AdCOVID elicits systemic and mucosal immunity against SARS-CoV-2 and fully protects mice from lethal challenge. *Vaccines (Basel)* (2021) 9(8):881. doi: 10.3390/vaccines9080881

229. Wu D, Wu T, Liu Q, Yang Z. The SARS-CoV-2 outbreak: What we know. *Int J Infect Dis* (2020) 94:44–8. doi: 10.1016/j.ijid.2020.03.004

230. Laing AG, Lorenc A, Del Molino Del Barrio I, Das A, Fish M, Monin L, et al. A dynamic COVID-19 immune signature includes associations with poor prognosis. *Nat Med* (2020) 26:1623–35. doi: 10.1038/s41591-020-1038-6

231. Fei J, Fu L, Li Y, Xiang H-X, Xiang Y, Li M-D, et al. Reduction of lymphocyte at early stage elevates severity and death risk of COVID-19 patients: A hospital-based case-cohort study. *medRxiv* (2020) 2020.04.02.20050955. doi: 10.1101/2020.04.02.20050955

232. Tarke A, Sidney J, Kidd CK, Dan JM, Ramirez SI, Yu ED, et al. Comprehensive analysis of T cell immunodominance and immunoprevalence of SARS-CoV-2 epitopes in COVID-19 cases. *Cell Rep Med* (2021) 2:100204. doi: 10.1016/j.xcrm.2021.100204

233. Sahin U, Muik A, Derhovanessian E, Vogler I, Kranz LM, Vormehr M, et al. COVID-19 vaccine BNT162b1 elicits human antibody and T(H)1 T cell responses. *Nature* (2020) 586:594–9. doi: 10.1038/s41586-020-2814-7

234. Grifoni A, Sidney J, Vita R, Peters B, Crotty S, Weiskopf D, et al. SARS-CoV-2 human T cell epitopes: Adaptive immune response against COVID-19. *Cell Host Microbe* (2021) 29:1076–92. doi: 10.1016/j.chom.2021.05.010

235. Saini SK, Hersby DS, Tamhane T, Povlsen HR, Amaya Hernandez SP, Nielsen M, et al. SARS-CoV-2 genome-wide T cell epitope mapping reveals immunodominance and substantial CD8(+) T cell activation in COVID-19 patients. *Sci Immunol* (2021) 6:eabf7550. doi: 10.1126/sciimmunol.abf7550

236. Tarke A, Coelho CH, Zhang Z, Dan JM, Yu ED, Methot N, et al. SARS-CoV-2 vaccination induces immunological T cell memory able to cross-recognize variants from alpha to omicron. *Cell* (2022) 185:847–59.e11. doi: 10.1016/j.cell.2022.01.015

237. Keeton R, Tincho MB, Ngomti A, Baguma R, Benede N, Suzuki A, et al. T Cell responses to SARS-CoV-2 spike cross-recognize omicron. *Nature* (2022) 603:488–92. doi: 10.1038/s41586-022-04460-3

238. Kronbichler A, Kresse D, Yoon S, Lee KH, Effenberger M, Shin JI. Asymptomatic patients as a source of COVID-19 infections: A systematic review and meta-analysis. *Int J Infect Dis* (2020) 98:180–6. doi: 10.1016/j.ijid.2020.06.052

239. Buitrago-Garcia D, Egli-Gany D, Counotte MJ, Hossmann S, Imeri H, Ipekci AM, et al. Occurrence and transmission potential of asymptomatic and presymptomatic SARS-CoV-2 infections: A living systematic review and meta-analysis. *PloS Med* (2020) 17:e1003346–e. doi: 10.1371/journal.pmed.1003346

240. Tsitsilonis OE, Paraskevis D, Lianidou E, Terpos E, Akalestos A, Pierros V, et al. SARS-CoV-2 infection is asymptomatic in nearly half of adults with robust anti-spike protein receptor-binding domain antibody response. *Vaccines (Basel)* (2021) 9:207. doi: 10.3390/vaccines9030207

241. Sah P, Fitzpatrick MC, Zimmer CF, Abdollahi E, Juden-Kelly L, Moghadas SM, et al. Asymptomatic SARS-CoV-2 infection: A systematic review and meta-analysis. *Proc Natl Acad Sci United States America* (2021) 118:e2109229118. doi: 10.1073/pnas.2109229118

242. Amanat F, Stadlbauer D, Strohmeier S, Nguyen THO, Chromikova V, McMahon M, et al. A serological assay to detect SARS-CoV-2 seroconversion in humans. *Nat Med* (2020) 26:1033–6. doi: 10.1038/s41591-020-0913-5

243. Tan CW, Chia WN, Qin X, Liu P, Chen MI, Tiu C, et al. A SARS-CoV-2 surrogate virus neutralization test based on antibody-mediated blockage of ACE2-spike protein-protein interaction. *Nat Biotechnol* (2020) 38:1073–8. doi: 10.1038/s41587-020-0631-z

244. Okba NMA, Müller MA, Li W, Wang C, GeurtsvanKessel CH, Corman VM, et al. Severe acute respiratory syndrome coronavirus 2-specific antibody responses in coronavirus disease patients. *Emerg Infect Dis* (2020) 26:1478–88. doi: 10.3201/eid2607.200841

245. Wec AZ, Wrapp D, Herbert AS, Maurer DP, Haslwanter D, Sakharkar M, et al. Broad neutralization of SARS-related viruses by human monoclonal antibodies. *Sci (New York NY)* (2020) 369:731–6. doi: 10.1126/science.abc7424

246. Sette A, Crotty S. Pre-existing immunity to SARS-CoV-2: The knowns and unknowns. *Nat Rev Immunol* (2020) 20:457–8. doi: 10.1038/s41577-020-0389-z

247. Lineburg KE, Grant EJ, Swaminathan S, Chatzileontiadou DSM, Szeto C, Sloane H, et al. CD8(+) T cells specific for an immunodominant SARS-CoV-2 nucleocapsid epitope cross-react with selective seasonal coronaviruses. *Immunity* (2021) 54:1055–65.e5. doi: 10.1016/j.immuni.2021.04.006

248. Rock KL, Reits E, Neefjes J. Present yourself! by MHC class I and MHC class II molecules. *Trends Immunol* (2016) 37:724–37. doi: 10.1016/j.it.2016.08.010

249. Purcell AW, Ramarathinam SH, Ternette N. Mass spectrometry-based identification of MHC-bound peptides for immunopeptidomics. *Nat Protoc* (2019) 14:1687–707. doi: 10.1038/s41596-019-0133-y

250. Niessl J, Sekine T, Lange J, Konya V, Forkel M, Maric J, et al. Identification of resident memory CD8(+) T cells with functional specificity for SARS-CoV-2 in unexposed oropharyngeal lymphoid tissue. *Sci Immunol* (2021) 6:eabk0894. doi: 10.1126/sciimmunol.abk0894

251. Flemming A. Cross-reactive tissue-resident CD8(+) T cells may provide first line of defence against SARS-CoV-2. *Nat Rev Immunol* (2021) 21:693–. doi: 10.1038/s41577-021-00638-4

252. Doshi P. Covid-19: Do many people have pre-existing immunity? *Bmj* (2020) 370:m3563. doi: 10.1136/bmj.m3563

253. Sagar M, Reifler K, Rossi M, Miller NS, Sinha P, White LF, et al. Recent endemic coronavirus infection is associated with less-severe COVID-19. *J Clin Invest* (2021) 131:e143380. doi: 10.1172/JCI143380

254. Bacher P, Rosati E, Esser D, Martini GR, Saggau C, Schiminsky E, et al. Low-avidity CD4(+) T cell responses to SARS-CoV-2 in unexposed individuals and humans with severe COVID-19. *Immunity* (2020) 53:1258–71.e5. doi: 10.1016/j.immuni.2020.11.016

255. Dykema AG, Zhang B, Woldemeskel BA, Garliss CC, Cheung LS, Choudhury D, et al. Functional characterization of CD4+ T cell receptors crossreactive for SARS-CoV-2 and endemic coronaviruses. *J Clin Invest* (2021) 131(10):e146922. doi: 10.1172/jci146922

256. Pizzolla A, Nguyen THO, Smith JM, Brooks AG, Kedzieska K, Heath WR, et al. Resident memory CD8(+) T cells in the upper respiratory tract prevent pulmonary influenza virus infection. *Sci Immunol* (2017) 2(12):eaam6970. doi: 10.1126/sciimmunol.aam6970

257. Allie SR, Bradley JE, Mudunuru U, Schultz MD, Graf BA, Lund FE, et al. The establishment of resident memory b cells in the lung requires local antigen encounter. *Nat Immunol* (2019) 20:97–108. doi: 10.1038/s41590-018-0260-6

258. Isho B, Abe KT, Zuo M, Jamal AJ, Rathod B, Wang JH, et al. Persistence of serum and saliva antibody responses to SARS-CoV-2 spike antigens in COVID-19 patients. *Sci Immunol* (2020) 5:eabe5511. doi: 10.1126/sciimmunol.abe5511

259. Wang Z, Lorenzi JCC, Muecksch F, Finkin S, Viant C, Gaebler C, et al. Enhanced SARS-CoV-2 neutralization by secretory IgA *in vitro*. *bioRxiv* (2020) 2020.09.09.288555. doi: 10.1101/2020.09.09.288555

260. Corthésy B. Role of secretory IgA in infection and maintenance of homeostasis. *Autoimmun Rev* (2013) 12:661–5. doi: 10.1016/j.autrev.2012.10.012

261. Du Y, Zhang S, Zhang Z, Miah KM, Wei P, Zhang L, et al. Intranasal lentiviral vector-mediated antibody delivery confers reduction of SARS-CoV-2 infection in elderly and immunocompromised mice. *Front Immunol* (2022) 13:819058. doi: 10.3389/fimmu.2022.819058

262. Lavelle EC, Ward RW. Mucosal vaccines - fortifying the frontiers. *Nat Rev Immunol* (2022) 22:236–50. doi: 10.1038/s41577-021-00583-2

263. Lin Y, Sun J, Cao X, Wang X, Chen X, Xu H, et al. Non-adjuvanted interferon-armed RBD protein nasal drops protect airway infection from SARS-CoV-2. *Cell Discovery* (2022) 8:43. doi: 10.1038/s41421-022-00411-4

264. An X, Martinez-Paniagua M, Rezvan A, Sefat SR, Fathi M, Singh S, et al. Single-dose intranasal vaccination elicits systemic and mucosal immunity against SARS-CoV-2. *iScience* (2021) 24:103037. doi: 10.1016/j.isci.2021.103037

265. Szabo PA, Dogra P, Gray JI, Wells SB, Connors TJ, Weisberg SP, et al. Longitudinal profiling of respiratory and systemic immune responses reveals myeloid cell-driven lung inflammation in severe COVID-19. *Immunity* (2021) 54:797–814.e6. doi: 10.1016/j.immuni.2021.03.005

266. Roukens AHE, Pothast CR, König M, Huisman W, Dalebout T, Tak T, et al. Prolonged activation of nasal immune cell populations and development of tissue-resident SARS-CoV-2-specific CD8(+) T cell responses following COVID-19. *Nat Immunol* (2022) 23:23–32. doi: 10.1038/s41590-021-01095-w

267. Grau-Expósito J, Sánchez-Gaona N, Massana N, Suppi M, Astorga-Gamaza A, Perea D, et al. Peripheral and lung resident memory T cell responses against SARS-CoV-2. *Nat Commun* (2021) 12:3010. doi: 10.1038/s41467-021-23333-3

268. Oja AE, Saris A, Ghandour CA, Kragten NAM, Hogema BM, Nossent EJ, et al. Divergent SARS-CoV-2-specific T- and b-cell responses in severe but not mild COVID-19 patients. *Eur J Immunol* (2020) 50:1998–2012. doi: 10.1002/eji.202048908

269. Roberts LM, Jessop F, Wehrly TD, Bosio CM. Cutting edge: Lung-resident T cells elicited by SARS-CoV-2 do not mediate protection against secondary infection. *J Immunol* (2021) 207:2399–404. doi: 10.4049/jimmunol.2100608

270. Nguyen TH, McAuley JL, Kim Y, Zheng MZ, Gherardin NA, Godfrey DI, et al. Influenza, but not SARS-CoV-2, infection induces a rapid interferon response that wanes with age and diminished tissue-resident memory CD8(+) T cells. *Clin Trans Immunol* (2021) 10:e1242. doi: 10.1002/cti2.1242

271. Routhu NK, Cheedarla N, Gangadhara S, Bollimpelli VS, Boddapati AK, Shiferaw A, et al. A modified vaccinia Ankara vector-based vaccine protects macaques from SARS-CoV-2 infection, immune pathology, and dysfunction in the lungs. *Immunity* (2021) 54:542–56.e9. doi: 10.1016/j.immuni.2021.02.001

272. Behr FM, Parga-Vidal L, Kragten NAM, van Dam TJP, Wesselink TH, Sheridan BS, et al. Tissue-resident memory CD8(+) T cells shape local and systemic secondary T cell responses. *Nat Immunol* (2020) 21:1070–81. doi: 10.1038/s41590-020-0723-4

273. Qian Y, Zhu Y, Li Y, Li B. Legend of the sentinels: Development of lung resident memory T cells and their roles in diseases. *Front Immunol* (2021) 11:624411. doi: 10.3389/fimmu.2020.624411

274. Gaebler C, Wang Z, Lorenzi JCC, Muecksch F, Finkin S, Tokuyama M, et al. Evolution of antibody immunity to SARS-CoV-2. *Nature* (2021) 591:639–44. doi: 10.1038/s41586-021-03207-w

275. Zuo J, Dowell AC, Pearce H, Verma K, Long HM, Begum J, et al. Robust SARS-CoV-2-specific T cell immunity is maintained at 6 months following primary infection. *Nat Immunol* (2021) 22:620–6. doi: 10.1038/s41590-021-00902-8

276. Guo X, Guo Z, Duan C, Chen Z, Wang G, Lu Y, et al. Long-term persistence of IgG antibodies in SARS-CoV infected healthcare workers. *medRxiv* (2020) 2020.02.12.20021386. doi: 10.1101/2020.02.12.20021386

277. Ng OW, Chia A, Tan AT, Jadi RS, Leong HN, Bertoletti A, et al. Memory T cell responses targeting the SARS coronavirus persist up to 11 years post-infection. *Vaccine* (2016) 34:2008–14. doi: 10.1016/j.vaccine.2016.02.063

278. Sariol A, Perlman S. Lessons for COVID-19 immunity from other coronavirus infections. *Immunity* (2020) 53:248–63. doi: 10.1016/j.immuni.2020.07.005

279. Mateus J, Grifoni A, Tarke A, Sidney J, Ramirez SI, Dan JM, et al. Selective and cross-reactive SARS-CoV-2 T cell epitopes in unexposed humans. *Sci (New York NY)* (2020) 370:89–94. doi: 10.1126/science.abd3871

280. Abu-Raddad LJ, Chemaitelly H, Malek JA, Ahmed AA, Mohamoud YA, Younuskunju S, et al. Assessment of the risk of severe acute respiratory syndrome coronavirus 2 (SARS-CoV-2) reinfection in an intense reexposure setting. *Clin Infect Dis* (2021) 73:e1830–e40. doi: 10.1093/cid/ciaa1846

281. Hansen CH, Michlmayr D, Gubbels SM, Mølbak K, Ethelberg S. Assessment of protection against reinfection with SARS-CoV-2 among 4 million PCR-tested individuals in Denmark in 2020: A population-level observational study. *Lancet* (2021) 397:1204–12. doi: 10.1016/S0140-6736(21)00575-4

282. Buss LF, Prete CAJr., Abrahim CMM, Mendrone AJr., Salomon T, de Almeida-Neto C, et al. Three-quarters attack rate of SARS-CoV-2 in the Brazilian Amazon during a largely unmitigated epidemic. *Sci (New York NY)* (2021) 371:288–92. doi: 10.1126/science.abe9728

283. Sridhar D, Gurdasani D. Herd immunity by infection is not an option. *Science* (2021) 371:230–1. doi: 10.1126/science.abf7921

284. Sabino EC, Buss LF, Carvalho MPS, Prete CAJr., Crispim MAE, Fraiji NA, et al. Resurgence of COVID-19 in manaus, Brazil, despite high seroprevalence. *Lancet* (2021) 397:452–5. doi: 10.1016/S0140-6736(21)00183-5

285. Chen RE, Zhang X, Case JB, Winkler ES, Liu Y, VanBlargan LA, et al. Resistance of SARS-CoV-2 variants to neutralization by monoclonal and serum-derived polyclonal antibodies. *Nat Med* (2021) 27:717–26. doi: 10.1038/s41591-021-01294-w

286. McMahan K, Yu J, Mercado NB, Loos C, Tostanoski LH, Chandrashekar A, et al. Correlates of protection against SARS-CoV-2 in rhesus macaques. *Nature* (2021) 590:630–4. doi: 10.1038/s41586-020-03041-6

287. Burton DR, Topol EJ. Toward superhuman SARS-CoV-2 immunity? *Nat Med* (2021) 27:5–6. doi: 10.1038/s41591-020-01180-x

288. Sadoff J, Le Gars M, Shukarev G, Heerwegh D, Truyers C, de Groot AM, et al. Interim results of a phase 1-2a trial of Ad26.COV2.S covid-19 vaccine. *N Engl J Med* (2021) 384:1824–35. doi: 10.1056/NEJMoa2034201

289. Baden LR, El Sahly HM, Essink B, Kotloff K, Frey S, Novak R, et al. Efficacy and safety of the mRNA-1273 SARS-CoV-2 vaccine. *N Engl J Med* (2021) 384:403–16. doi: 10.1056/NEJMoa2035389

290. Polack FP, Thomas SJ, Kitchin N, Absalon J, Gurtman A, Lockhart S, et al. Safety and efficacy of the BNT162b2 mRNA covid-19 vaccine. *N Engl J Med* (2020) 383:2603–15. doi: 10.1056/NEJMoa2034577

291. Lumley SF, O'Donnell D, Stoesser NE, Matthews PC, Howarth A, Hatch SB, et al. Antibody status and incidence of SARS-CoV-2 infection in health care workers. *N Engl J Med* (2021) 384:533–40. doi: 10.1056/NEJMoa2034545

292. Abu-Raddad LJ, Chemaitelly H, Coyle P, Malek JA, Ahmed AA, Mohamoud YA, et al. SARS-CoV-2 antibody-positivity protects against reinfection for at least seven months with 95% efficacy. *EClinicalMedicine* (2021) 35:100861. doi: 10.1016/j.eclinm.2021.100861

293. Walsh EE, Frenck RWJr., Falsey AR, Kitchin N, Absalon J, Gurtman A, et al. Safety and immunogenicity of two RNA-based covid-19 vaccine candidates. *N Engl J Med* (2020) 383:2439–50. doi: 10.1056/NEJMoa2027906

294. Halfmann PJ, Iida S, Iwatsuki-Horimoto K, Maemura T, Kiso M, Scheaffer SM, et al. SARS-CoV-2 omicron virus causes attenuated disease in mice and hamsters. *Nature* (2022) 603(7902):687–92. doi: 10.1038/s41586-022-04441-6

frontiers | Frontiers in Immunology

TYPE Original Research
PUBLISHED 20 September 2022
DOI 10.3389/fimmu.2022.952650

Check for updates

OPEN ACCESS

EDITED BY
Edwin Bölke,
Heinrich Heine University of Düsseldorf, Germany

REVIEWED BY
Anna Hryniewicz,
Medical University of Bialystok, Poland
Jianwei Wang,
Chinese Academy of Medical Sciences and Peking Union Medical College, China

*CORRESPONDENCE
Tianying Zhang
zhangtianying@xmu.edu.cn
Zizheng Zheng
zhengzizheng@xmu.edu.cn
Ningshao Xia
nsxia@xmu.edu.cn

†These authors have contributed equally to this work

SPECIALTY SECTION
This article was submitted to Viral Immunology, a section of the journal Frontiers in Immunology

RECEIVED 25 May 2022
ACCEPTED 05 September 2022
PUBLISHED 20 September 2022

CITATION
Wang S, Wu D, Xiong H, Wang J, Tang Z, Chen Z, Wang Y, Zhang Y, Ying D, Lin X, Liu C, Guo S, Tian W, Lin Y, Zhang X, Yuan Q, Yu H, Zhang T, Zheng Z and Xia N (2022) Potential of conserved antigenic sites in development of universal SARS-like coronavirus vaccines.
Front. Immunol. 13:952650.
doi: 10.3389/fimmu.2022.952650

COPYRIGHT
© 2022 Wang, Wu, Xiong, Wang, Tang, Chen, Wang, Zhang, Ying, Lin, Liu, Guo, Tian, Lin, Zhang, Yuan, Yu, Zhang, Zheng and Xia. This is an open-access article distributed under the terms of the Creative Commons Attribution License (CC BY). The use, distribution or reproduction in other forums is permitted, provided the original author(s) and the copyright owner(s) are credited and that the original publication in this journal is cited, in accordance with accepted academic practice. No use, distribution or reproduction is permitted which does not comply with these terms.

Potential of conserved antigenic sites in development of universal SARS-like coronavirus vaccines

Siling Wang[1†], Dinghui Wu[2†], Hualong Xiong[1†], Juan Wang[1†], Zimin Tang[1], Zihao Chen[1], Yizhen Wang[1], Yali Zhang[1], Dong Ying[1], Xue Lin[1], Chang Liu[1], Shaoqi Guo[1], Weikun Tian[1], Yajie Lin[1], Xiaoping Zhang[1], Quan Yuan[1], Hai Yu[1], Tianying Zhang[1*], Zizheng Zheng[1*] and Ningshao Xia[1*]

[1]State Key Laboratory of Molecular Vaccinology and Molecular Diagnostics, National Institute of Diagnostics and Vaccine Development in Infectious Diseases, School of Life Sciences, School of Public Health, Xiamen University, Xiamen, China, [2]Department of Pulmonary Medicine, The First Affiliated Hospital of Xiamen University, Xiamen, China

Given pandemic risks of zoonotic SARS-CoV-2 variants and other SARS-like coronaviruses in the future, it is valuable to perform studies on conserved antigenic sites to design universal SARS-like coronavirus vaccines. By using antibodies obtained from convalescent COVID-19 patients, we succeeded in functional comparison of conserved antigenic sites at multiple aspects with each other, and even with SARS-CoV-2 unique antigenic sites, which promotes the cognition of process of humoral immune response to the conserved antigenic sites. The conserved antigenic sites between SARS-CoV-2 and SARS-CoV can effectively induce affinity maturation of cross-binding antibodies, finally resulting in broadly neutralizing antibodies against multiple variants of concern, which provides an important basis for universal vaccine design, however they are subdominant, putatively due to their lower accessibility relative to SARS-CoV-2 unique antigenic sites. Furthermore, we preliminarily design RBDs to improve the immunogenicity of these conserved antigenic sites. Our study focusing on conserved antigenic sites provides insights for promoting the development of universal SARS-like coronavirus vaccines, thereby enhancing our pandemic preparedness.

KEYWORDS

SARS-CoV-2, COVID-19, convalescent individual, conserved antigenic sites, cross-neutralizing antibodies, universal vaccine

Introduction

Severe acute respiratory syndrome coronavirus 2 (SARS-CoV-2) is the cause of the ongoing outbreak of coronavirus disease 2019 (COVID-19), resulting in a global pandemic (1, 2). As of March 14, 2022, SARS-CoV-2 has caused more than 450 million human infections around the world, including approximately 6 million deaths, which has led to unprecedented enormous global health and economic damage. The ~30 kb RNA genome of SARS-CoV-2 encodes four structural proteins including the spike (S), membrane (M), envelope (E) and nucleocapsid (N) proteins, nonstructural proteins, and a number of accessory proteins (3). The transmembrane S glycoprotein is divided into S1, comprising a receptor-binding domain (RBD) and an N-terminal domain (NTD), and S2 promoting membrane fusion *via* a fusion peptide. As most neutralizing monoclonal antibodies (mAbs) isolated from convalescent COVID-19 patients target the RBD (4–8), by which the S protein binds to receptor angiotensin-converting enzyme 2 (ACE2) and promotes the exposure of the fusion peptides within the S2 component to contribute to viral membrane fusion with host cells, this domain is the main target for the design of therapeutics and vaccines (9, 10).

Human coronaviruses (HCoVs) include HCoV-OC43, HCoV-HKU1, HCoV-229E and HCoV-NL63, as well as highly pathogenic Middle East respiratory syndrome coronavirus (MERS-CoV), SARS-CoV and SARS-CoV-2. SARS-CoV-2, which is phylogenetically close to SARS-CoV, is classified in the *Betacoronavirus* genus, which includes another highly pathogenic virus, MERS-CoV, as well as HCoV-OC43 and HCoV-HKU1 variants leading to endemic disease (11, 12). Historically, there have been three HCoV infection outbreaks causing a severe syndrome, including the SARS outbreak that was initially identified as an exotic infection in coronavirus evolution, the MERS-CoV outbreak that was the second most severe outbreak, and the current COVID-19 pandemic (13–16). Studies reveal that it is reasonable to speculate on the possibility of emergence of other SARS-like coronaviruses in the future. Hence, it is certainly valuable to promote the development of more universal coronavirus vaccines and broader therapeutic agents by characterizing conserved antigenic sites in SARS-CoV-2 RBD to enhance our preparedness against the possible pandemic risk of SARS-like coronaviruses in the future. Moreover, as the duration of the SARS-CoV-2 pandemic extends, multiple variants of concern (VOCs) have emerged around the world. Although the D614G mutation in the S protein significantly promotes corresponding variant infectivity in susceptible cells, this residue substitution fails to cause immune escape (17–21). Conversely, multiple studies support that the Beta, Gamma, Delta and Omicron variants could decrease the therapeutic efficacy of neutralizing antibodies (NAbs) and even compromise the protective efficacy of approved SARS-CoV-2 vaccines targeting the initial SARS-CoV-2 strain that emerged in 2019 (20, 22–26). Hence, universal SARS-like coronavirus vaccines based on the conserved antigenic sites in the RBD also have potential in preventing highly pathogenic SARS-CoV-2 variants that could escape established specific immune memory.

Although SARS-CoV-2 and SARS-CoV share 90% amino acid identity in the S2 domain, the SARS-CoV-2 RBD shows only 73% amino acid identity with the SARS-CoV RBD (12), implying that there may be fewer conserved antigenic sites within the RBD. Nevertheless, some highly conserved epitopes in the SARS-CoV RBD have been identified by the mAbs CR3022 (27), S309 (28) and ADI-56046 (6), cross-binding mAbs that were originally isolated from SARS patients, among which S309 and ADI-56046 could efficiently neutralize infection by SARS-CoV-2 and SARS-CoV. In addition, many human mAbs targeting the SARS-CoV-2 S protein isolated from convalescent COVID-19 patients have been reported; however, cross-binding mAbs, especially cross-neutralizing mAbs, are rarely reported (29–31), indicating that the conserved antigenic sites within the RBD may be subdominant compared to the unique sites. While some conserved antigenic sites have been identified by cross-binding mAbs, including CR3022 (27), S309 (28) and ADI-56046 (6) from SARS-CoV infection survivors and COVA1-16 (5), EY6A (8) and 2-36 (32) from COVID-19 patients, no studies have been performed to quantitatively define an antigenic map of conserved sites in the SARS-CoV-2 RBD.

In this study, 77 SARS-CoV-2 RBD-specific antibodies were isolated from a cohort of 10 convalescent COVID-19 patients for further biophysical characterization, by which we succeeded in defining a quantitative antigenic map of neutralizing sites within the SARS-CoV-2 RBD. We identified multiple conserved antigenic sites with weaker immunogenicity, due to their inaccessibility. To improve immune response to conserved antigenic sites, we tried to design RBDs, which might contribute to the development of universal SARS-like coronavirus vaccines.

Materials and methods

Collection of blood samples

In this study, a total of 10 convalescent COVID-19 individuals infected with SARS-CoV-2 were enrolled, and the peripheral bloods were collected. The study was approved by the institutional review board of the School of Public Health in

accordance with the Declaration of Helsinki, and written informed consent was obtained.

Detection of plasma antibody titer against SARS-CoV-2 RBD

To detect the plasma titers of total antibodies (Ab), IgG and IgM against SARS-CoV-2 RBD, we performed commercial enzyme-linked immunosorbent assay (ELISA) kits (Beijing Wantai Biological Pharmacy Enterprise), according to the manufacturer's instructions. The Ab-ELISA kit is based recombinant viral antigen using a double-sandwich reaction form. The IgG-ELISA kit is an indirect ELISA assay, and the IgM-ELISA kit is based on μ-chain capture method. The samples were initially tested undiluted, and the positive samples with the signal to a cutoff ratio (S/CO) >=10 were further diluted (1:10, 1:100, 1:1,000 and 1:10,000) by PBS buffer containing 20% newborn bovine serum (NBS) and tested again. The titers for Ab, IgG and IgM antibody were calculated *via* S/CO multiplied by the maximum dilution factors.

Recombinant expression and purification of SARS-CoV S protein, SARS-CoV-2 S protein and diverse SARS-CoV-2 RBD protein

For SARS-CoV and SARS-CoV-2 S protein, a gene encoding the ectodomain of a prefusion conformation-stabilized S protein was synthesized, composed of SARS-CoV gene sequence (GenBank: ABF65836) or SARS-COV-2 gene sequence (GenBank: MN908947), a C-terminal T4 fibritin trimerization motif, an HRV3C protease and 8xHisTag. To determine the blocking capacity of mAbs, we also synthesized gene of SARS-CoV-2 S fluorescin probe comprising SARS-COV-2 gene sequence, a C-terminal T4 fibritin trimerization motif, an HRV3C protease, 8xHisTag and a C-terminal green fluorescent protein (mGamillus). Moreover, to express mutate, wildtype SARS-CoV-2 RBD, residues 319-518 fused to mouse IgG1 Fc domain. For mutate RBDs, different selected amino acid of RBD were substituted by alanine or arginine on purpose (Table S3). Recombinant expressions of these proteins were performed by the ExpiCHO^{TM} expression system (Thermo Scientific, A29133). Briefly, plasmids encoding targeted proteins were transiently transfected into ExpiCHO cells by using ExpiFectamine^{TM} CHO transfection kit (Thermo Scientific, A29129). The cell-free supernatants were obtained 7 days after transfection by centrifugation and filtration with a 0.22 μm filter. Subsequently, the S-related proteins (SARS-CoV S, SARS-CoV-2 S and SARS-CoV-2 S fluorescin probe) were purified by Ni Sepharose Excel resin, and RBD fused to mouse IgG1 Fc domain by Protein A column, and the S and RBD proteins were stored in the PBS buffer.

Specific memory B cell response and single B cell sorting

RBD specific B cells were obtained in the same way as previously reported. PBMCs collected from 10 individuals were incubated with a cocktail containing live/dead-Aqua, CD3-PE-Cy7, CD19-BV786, CD27-BV650, anti-human IgM-PerCP-Cy5.5, anti-human IgG-BV421, RBD-FITC and biotinylated RBD, followed with Streptavidin-APC binding to biotinylated RBD. The RBD-specific memory B cells were identified as live+CD19+CD3-CD27+IgG+RBD+, and then the single specific memory B cells were sorted by fluorescence activated cell sorting on an Aria III sorter (BD Biosciences) into 96-well PCR plates containing 20 μL per well of lysis buffer [5 μL of 5×first strand buffer (Invitrogen), 1.25 μL dithiothreitol (Invitrogen), 0.5 μL RNase Out (Invitrogen), 0.0625 μL Igepal (Sigma)]. Plates were stored at -80°C prior to reverse transcription reaction.

Single B cell PCR, cloning and expression of antibody

Antibody variable genes (IgH, Igλ and Igκ) were amplified by RT-PCR and nested PCR reactions as previously described (33). The paired heavy and light chains were then cloned into expression vectors containing the constant regions of human IgG1 and light chain. The paired heavy and light chain expression cassettes were then transiently co-transfected into ExpiCHO cells with equal amounts of plasmids according to the manufacturer's instructions (Life Technologies), and antibodies were purified from culture supernatant 5-7 days after transfection, using a recombinant protein-A column (GE Healthcare).

Antibody germline usage and phylogenetic analysis

Antibody gene repertoire was analyzed for the variable region of IgG heavy and light chains using the IMGT V-quest webserver (http://www.imgt.org/IMGT/vquest). Phylogenetic analysis of antibody gene was performed by ggtree R package (34).

Binding activity assay for mAbs by indirect ELISA

The binding activity of the mAbs against SARS-CoV-2 S protein were determined using an indirect ELISA. The mAbs were added to antigen-coated microwell plates, and incubated at 37°C for 30 min. Then, incubation of HRP-conjugated anti-human antibody at 37°C for 30 min to detect the bound mAbs, followed by washing five times. Finally, substrate solution was added to the wells for 15 min at 37°C, and reaction was stopped by adding 50 μL of 2 M H_2SO_4. The optical density (OD) was measured at 450 nm with a reference wavelength of 630 nm. In addition, binding activity of the mAbs against SARS-CoV-2 RBD and SARS-CoV S protein were determined by same method.

Identification of SARS-CoV-2 RBD critical residues recognized by mAbs

To determine the critical residues, mAbs were conjugated with horse radish peroxidase (HRP). Microwell plates were pre-coated with mutate SARS-CoV-2 RBD and wildtype RBD at 100 ng per well. mAbs-HRP were performed two times gradient dilution with 4 μg/mL begin and incubated at 37°C for 30 min followed by washing five times. Substrate solution was incubated for 15 min at 37°C and stopped by 50 μL of 2 M H_2SO_4. OD was determined at 450 nm with a reference wavelength of 630 nm. The binding activity of mAbs against wildtype and mutated RBD was calculated by area under the curve (AUC), and the influence of residues was assessed by binding activity reduction against corresponding mutate SARS-CoV-2 RBD. Residues reducing binding activity by more than 75% are identified as critical residues.

Blocking capacity of mAbs against SARS-CoV-2 S protein

For SARS-CoV-2 S protein-blocking assay, mAbs were pre-made as 2-fold serial dilutions using DMEM containing 10% FBS. Aliquots (44 μL per well) of diluted samples and S protein probes (11 μL per well) were mixed in a 96-well plate with U shaped bottom. Half of the culture medium (50 μL) of 293T-ACE2iRb3 cell plate were gently removed, and 50 μL of sample/probe mixtures were added to each well. Cell image acquisitions performed with Opera Phenix (green, red and near-infrared channels in confocal mode) using a 20x water immersion objective at 1-hour after probe incubation in wash-free and live-cell conditions.

All quantitative image analyses were based on images that acquired by Opera Phenix. All image data were transfer to Columbus system (version 2.5.0, PerkinElmer Inc) for analysis. Multiparametric image analysis was performed as described in the following. The signals of blue channel or near-infrared channel were used to detect the nucleus. As the ACE2 is a membrane protein, the signals of ACE2-mRuby3 (red channel) were used to determine the cell boundary. Then, the cells were further segment into the regions of membrane (outer border: 0%, inner border: 15%), cytoplasm (outer border: 20%, inner border: 45%), and nucleus (outer border: 55%, inner border: 100%). The MFI of probe channel (Ex488/Em525) in the cytoplasmic region (cMFI). The MFI of ACE2-mRuby3 (Ex561/Em590) on the membrane were also calculated for inter-well normalization. The cMFI inhibition ratio (%) of the test sample was calculated using the following equation: [(cMFIpc-cMFItst)/(cMFIpc-cMFIblk)]×100%. In this formula, the cMFIpc is the cMFI value of probe-only well (as positive control), the cMFItst is the cMFI value of test well and the cMFIblk is the cMFI value of cell-only well. For each plate, five replicates of probe-only well and one cell-only well were included. The blocking capacity of mAbs were expressed as IC50.

Neutralization capacity of mAbs determined by SARS-CoV and SARS-CoV-2 pseudovirus

SARS-CoV-2 pseudovirus using VSV carrying the SARS-CoV-2 spike protein were produced according to our previous study. Briefly, SARS-CoV-2 S gene was codon optimized for expression in human cells and truncated with 18 amino acids at the C-terminal, then was cloned into the eukaryotic expression vector pCAG to obtain pCAG-nCoVSde18. The plasmid pCAG-nCoVSde18 was transfected into Vero-E6. VSVdG-EGFP-G (Addgene, 31842) virus was inoculated into cells expressing SARS-CoV-2 Sde18 truncated protein and incubated for 1 hour. Then the VSVdG-EGFP-G virus was removed from the supernatant and anti-VSV-G rat serum was added to block the remaining VSVdG-EGFP-G infection. The progeny virus will carry SARS-CoV-2 Sde18 truncated protein. After VSVdG-EGFP-G infection, supernatant was collected, centrifuged and filtered (Millipore, SLHP033RB) to obtain the SARS-CoV-2 pseudovirus without debris. SARS-CoV pseudovirus was constructed by the same method. Finally, pseudovirus was stored for use at -80°C.

To determine the neutralizing capacity, mAbs with 2-fold serial dilutions with 10% FBS-DMEM from 2 μg/mL were mixed with diluted SARS-CoV or SARS-CoV-2 pseudovirus (MOI = 0.05), incubated at 37°C for 1 hour. A mixture of 80 μL was added to the precoated BHK21-hACE2 cells. After incubation for 12 hours, post-infection cells were fluorescently imaged using Opera phenix or Operetta CLS (Perkinelmer), and quantitatively analyzed by Columbus image management analysis software to detect the number of green, fluorescent positive cells. The

inhibition rate was calculated by reduction of GFP positive cells with presence of mAbs compared with the untreated control wells.

Competition binding assay for neutralizing antibodies by ELISA and cluster analysis

Briefly, the unlabeled mAbs (50 μg per well) or PBS were added to RBD-coated 96-well microplates and then incubated for 30 min at 37°C. Next, HRP-conjugated mAbs were added at selected dilutions, at which OD readings was ~1.5 with PBS present. After incubation for 30 min at 37°C, the microplates were rinsed, and the color was developed. The competitive ability was measured quantitatively by comparing OD in the presence and absence of competitor mAbs and transformed using the formula $\log_2$ ($OD_{inhibited}/OD_{original}$). For mAbs to be clustered by competitive ability, clustering distance was calculated by Euclidean, and mAbs were clustered by ward. D2 method using pheatmap R package (version: 1.0.12).

Mouse immunization

For antibody response evaluation of $RBD_{Glycan420,475}$, $RBD_{Glycan458,475}$, $RBD_{Trucation455-491}$ and $RBD_{Trucation470-491}$, BALB/c mice were immunized with various RBD proteins at 20 μg/dose with FH002C through intramuscular injection. Serum samples were collected at Week 0 and 2 *via* retro-orbital bleeding to measure the antibody titers.

Measurement of mouse sera IgG titer against SARS-CoV and SARS-CoV-2 S protein

Microplates were pre-coated with recombinant antigens of SARS-CoV or SARS-CoV-2 S protein. For detections, serial-diluted (2-fold) serum samples (100 μL per well) were added into the wells, and the plates were incubated at 37°C for 30 min, followed by washing with PBST buffer (20 mM PB7.4, 150 mM NaCl and 0.05% Tween 20). Then, HRP-conjugated anti-mouse IgG solutions (100 μL per well) were added. After a further 30 min incubation followed by washing, TMB chromogen solution (100 μL per well) was added into the well. 15 min later, the chromogen reaction was stopped by adding 50 μL of 2 M H_2SO_4, and the OD450-630 was measured. The IgG titer of each serum was defined as the dilution limit to achieve a positive result (>median+3×SD of ODs of negative controls).

Statistical analysis

To compare continuous variables, the Mann-Whitney U test and non-paired t test were performed. Linear regression model and Spearman test were used for correlation analyses. For difference analysis, p values less than 0.05 are considered statistically significant. GraphPad Prism (version 8.0.1) was used for all statistical calculations. Analysis of protein structure was performed by PyMOL Molecular Graphics System (version 2.3.0).

Results

Seroconversion of antibodies against SARS-CoV-2 in convalescent COVID-19 patients and isolation of SARS-CoV-2 RBD-specific antibodies

We collected blood samples from 10 convalescent COVID-19 patients (Table S1). The humoral immune response was efficiently elicited in these convalescent individuals, as indicated by high plasma titers of RBD-specific IgG with differences of less than an order of magnitude (Table S2). Since the plasma neutralizing capacity strongly correlates with RBD-specific total antibody and IgG titers, indicating that the RBD of the S protein is the dominant target of nAbs elicited by SARS-CoV-2 infection (Figure S1). The proportion of RBD-specific B cells in memory B cells ranged from 0.03% to 0.18%, and RBD-specific memory B cells contained a higher percentage of the IgG subtype than the IgM subtype, revealing that SARS-CoV-2 infection efficiently promoted B cell receptor (BCR) class switching and affinity maturation in convalescent individuals, thus eliciting strong humoral immune response against SARS-CoV-2 (Figures S2A–C). Then, 77 RBD-specific monoclonal antibodies (mAbs) were obtained from the 10 convalescent individuals for comprehensive feature description (Figure S2D).

Characterization of SARS-CoV-2 RBD-specific mAbs obtained from convalescent COVID-19 patients

To characterize SARS-CoV-2 RBD-specific mAb repertoire usage, we compared sequences with the well-defined naïve repertoire of the IMGT database to obtain the assigned germline V region. Based on the exclusion of clonal expansion in P01, P03 and P04, 67 unique clonotypes were identified. Notably, 7 out of 8 antibody sequences obtained from P03 were highly conserved, except for P03-3B1, illustrating that this BCR clonotype was the immunodominant clone in P03 induced by SARS-CoV-2

infection (Figure 1A and Figure S3). Furthermore, enrichment of multiple VH and VK/VL sequences was observed. In addition, VK1-39-derived light chains were most often combined with the heavy chain of various types of VHs to form antibodies, accounting for 22.4% (15/67) (Figure S4 and Figure 1A). The mean somatic hypermutation (SHM) rate of the heavy chain V region was similar among individuals, and the mean levels (2%) were comparable to those detected in the context of infections with other respiratory viruses (Figure 1B) (35–37). Additionally, even though the average length of CDRH3 of RBD-specific mAbs was consistent with that of the naïve repertoire (~15 amino acids), we observed significant enrichment of shorter CDRH3 sequences (11 amino acids) in VH3-53/66-derived mAbs, differing from influenza virus and human immunodeficiency virus (HIV)-1 mAbs (Figure 1C and Figure S8A) (38–40).

Subsequently, we assessed the binding activity of these mAbs to recombinant S protein and RBD protein fragment of SARS-CoV-2 using enzyme-linked immunosorbent assay (ELISA). mAbs presented diverse binding activity to SARS-CoV-2 S protein, of which 61.0% showed strong binding activity (EC_{50}< 1 μg/mL); this result suggested that infection with SARS-CoV-2 can effectively stimulate humoral immune response to produce a large number of specific high-affinity mAbs (Figure S2A and Figure 1D). Interestingly, while there was a correlation between binding activity to SARS-CoV-2 RBD and to S protein, some mAbs bound more strongly to the RBD, implying that their target epitopes were poorly presented in S protein to be recognized, due to coverage by another RBD monomer or the NTD domain (Figure 1E) (41). Next, we assessed the neutralizing activity of these mAbs using a vesicular stomatitis virus (VSV) pseudovirus model carrying the SARS-CoV-2 S protein, and the neutralization IC_{50} potencies are shown in Figure S5C. In total, 80.5% (62/77) of these mAbs displayed neutralization of SARS-CoV-2, characterized as nAbs, among which 16 were identified as potent neutralizers with an IC_{50}< 0.1 μg/mL, 22 as moderate neutralizers with an IC_{50} of 0.1-1 μg/mL, and 24 as weak neutralizers with an IC_{50} of 1-100 μg/mL (Figure 1F). Surprisingly, none of the antibodies isolated from the convalescent individual P03 had a potent neutralizing capacity, although clonal expansion was efficiently elicited (Figure S6).

Next, we investigate whether blocking S protein binding to ACE2 is the key neutralizing mechanism. The results showed that 61.0% of the specific mAbs had the ability to block entrance of the S protein into cells, with IC_{50} values ranging from 4 ng/mL to 100 μg/mL (Figure S5D and Figure 1G). These blocking and neutralizing capacities were well correlated with the binding capacity (Figures 1H, I). In terms of the neutralization and blocking data, we found a good correlation, indicating that blocking the attachment of the SARS-CoV-2 S protein to receptor ACE2 was critical for the inhibition of SARS-CoV-2 infection by nAbs targeting RBD (Figure 1J and Figure S7). However, some nAbs neutralized SARS-CoV-2 with weak blockade of SARS-CoV-2 S protein binding to ACE2 (28). Although the corresponding neutralizing mechanism has not been explained clearly, it is putative that binding of these nAbs may impede sequential conformational changes in the S protein.

To determine whether the affinity of SARS-CoV-2 RBD-specific mAbs efficiently evolves, we analyzed the association between the binding activity of mAbs and the duration of the immune response. The binding activity and neutralizing capacity of specific mAbs correlated with days after symptom onset, illustrating that the affinity of these specific mAbs can continuously evolve (Figures 1K, L and Figure S9). However, the plasma anti-RBD IgG titer did not correlate with days after symptom onset for individuals, which might resulted from the limitation of the plasma samples (Figure S1A) (42). Taken together, humoral immune response is efficiently elicited by SARS-CoV-2 infection, and affinity of functional mAbs is constantly evolving.

Profile of cross-binding antibodies between SARS-CoV and SARS-CoV-2

Due to the 76% sequence identity between SARS-CoV S protein and SARS-CoV-2 S protein, there may be conserved epitopes. Accordingly, humoral immunity could utilize these conserved epitopes to produce cross-reactive mAbs response. In this study, 50.6% of SARS-CoV-2-specific antibodies also bound to SARS-CoV S protein, of which 11 (14.3%) recognized SARS-CoV S protein with strong binding activity (EC_{50}< 1 μg/mL) (Figure 2A and Figure S5B). As expected, these cross-binding mAbs also showed continuous affinity maturation (Figure 2B). In terms of genetic characteristics, it was observed that mAbs encoded by some VH germline genes, such as VH1-69, VH3-13, VH3-30 and VH4-46, had a tendency to broadly react with SARS-CoV and SARS-CoV-2 (Figure 2C). Additionally, cross-binding mAbs showed a tendency for lower SHM in the VH and JH regions, which might limit their affinity maturation, putatively due to the lower exposure of corresponding conserved antigenic sites (Figures 2D, E). Overall, these results confirmed an efficient cross-binding antibody response during SARS-CoV-2 infection and the presence of conserved antigenic sites inducing the maturation of cross-reactive mAbs.

Notably, the majority of mAbs with potent neutralizing activity against SARS-CoV-2 showed no reactivity with SARS-CoV, confirming that the unique antigenic sites in SARS-CoV-2 RBD, as immunodominant sites, more efficiently elicit high-affinity mAbs with potent neutralizing capacity than the conserved sites (Figure 2F). Subsequently, cross-binding mAbs were tested for their ability to neutralize SARS-CoV. Our results indicated that only P10-6G3, P07-4D10, P05-6H7 and P05-5B6 were identified as cross-neutralizing mAbs against both SARS-CoV and SARS-CoV-2, and P10-6G3 displayed higher binding activity to the SARS-CoV-2 S protein than the SARS-CoV S protein (Figures 2F, G). Combined with the weak binding activity, low affinity for SARS-CoV S protein is likely to be the

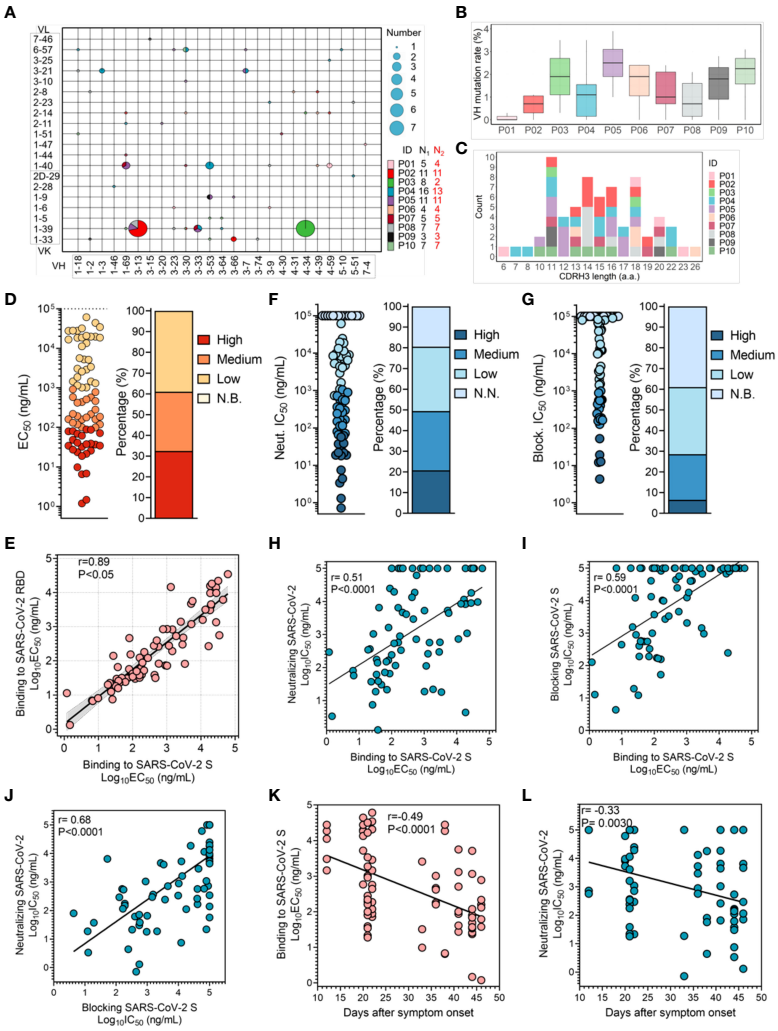

FIGURE 1
Characterization of SARS-CoV-2 RBD-specific mAbs obtained from convalescent COVID-19 patients. **(A)** V gene frequencies for the heavy and light chains of SARS-CoV-2 RBD-specific antibodies. The size corresponding to the number of heavy and light chain pairs in the repertoires is also denoted. Color indicates different convalescent individuals. N_1 indicates the number of SARS-CoV-2 RBD-specific antibodies for different individuals, and N_2 indicates the number of SARS-CoV-2 RBD-specific antibodies with unique clonotypes for different individuals. **(B)** The V region SHM of the heavy chain of specific antibodies from different individuals (N=67). **(C)** Distribution of the CDR3 length of the heavy chain. Antibodies are colored by each individual (N=67). V region germline genes and SHM and CDR3 length were determined using immunogenetics (IMGT). **(D)** The binding activity of specific antibodies to the SARS-CoV-2 S protein was determined by ELISA. Color corresponds to binding activity; high (EC_{50} <100 ng/mL), medium (EC_{50} between 100 ng/mL and 1 µg/mL), low (EC_{50} between 1 µg/mL and 100 µg/mL) and N.B. (EC_{50} >100 µg/mL). **(E)** Correlation between the binding capacities to the SARS-CoV-2 RBD and S protein (N=77). The 95% confidence interval of the regression line is shown in light gray, and the r and P values of the correlation are also indicated. **(F, G)** Neutralizing capacity was determined with a SARS-CoV-2 pseudovirus, and blocking capacity was determined by an S protein binding model. IC50 values are shown in the left panel, and the percentage of mAbs within the indicated IC_{50} range is shown in the right panel. Color represents different neutralizing and blocking capacities; high (IC_{50} <100 ng/mL), medium (IC_{50} between 100 ng/mL and 1 µg/mL), low (IC_{50} between 1 µg/mL and 100 µg/mL), and N.N. or N.B. (IC_{50} >100 µg/mL). **(H, I)** The correlation between binding activity and neutralization or blocking capacity. For the blocking assay, mAbs were pre-made as 2-fold serial dilutions and incubated with S protein probe. The mixture was input into each well coated with 293T-ACE2iRb3 cell. After 1-hour S probe incubation, cell image acquisitions were performed with Opera Phenix. The r and P values of the correlation are also indicated. **(J)** The correlation between neutralization and blocking capacities. The r and P values of the correlation are indicated. **(K)** Correlation between the binding activity of specific antibodies and duration of the immune response in convalescent individuals (N=77). **(L)** The change in neutralization potency of specific mAbs over days after symptom onset. The r and P values of the correlation are indicated. All correlation analyses were performed using the Spearman test.

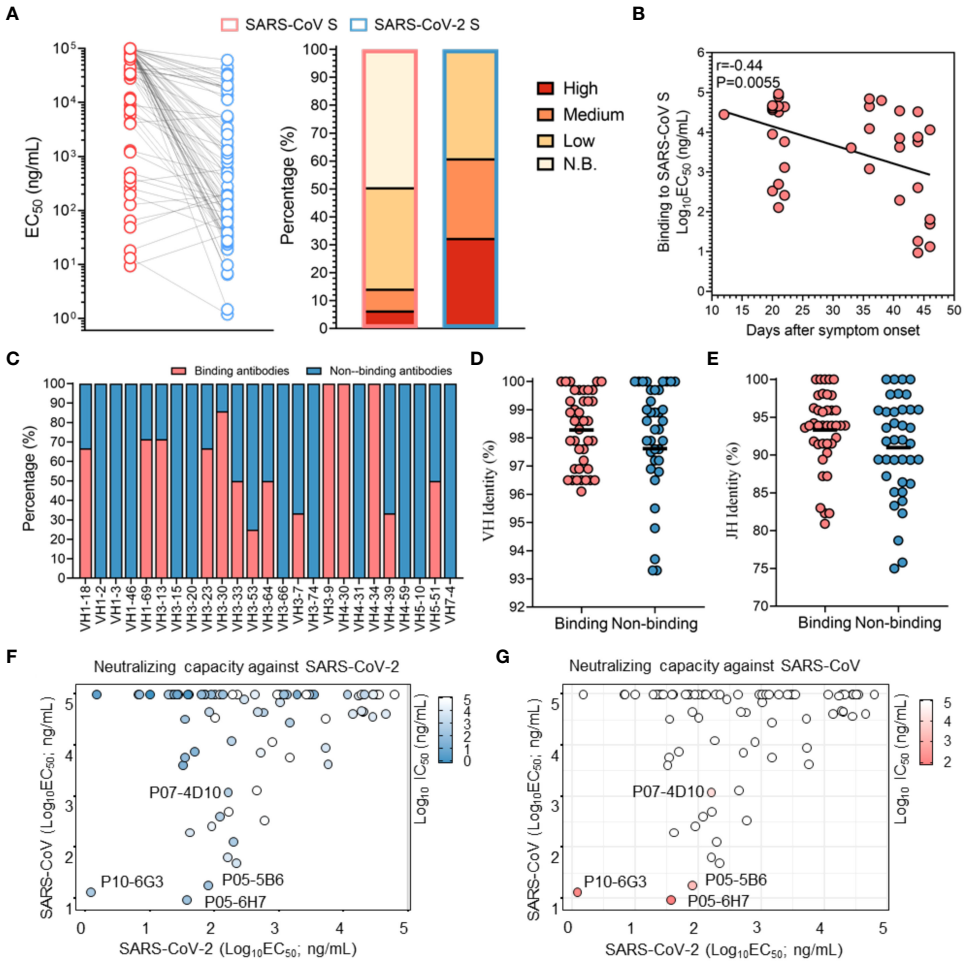

FIGURE 2
Profile of cross-binding SARS-CoV-2 RBD-specific mAbs. **(A)** The binding activity of antibodies specific for the SARS-CoV S protein and SARS-CoV-2 S protein were determined by ELISA. Color corresponds to binding activity; high (EC_{50} <100 ng/mL), moderate (EC_{50} between 100 ng/mL and 1 μg/mL), low (EC_{50} between 1 μg/mL and 100 μg/mL) and N.B. (EC_{50} >100 μg/mL). **(B)** Correlation between binding activity to the SARS-CoV S protein and duration of the immune response. Correlation analysis was performed using the Spearman test, and the r and P values of the correlation are indicated. **(C)** Distribution of SARS-CoV binding mAbs in the VH region (germline). **(D, E)** Comparison of VH and JH mutations between SARS-CoV S protein-binding mAbs and non-SARS-CoV S protein-binding mAbs. The black line denotes the mean value. **(F, G)** Neutralizing capacities against a SARS-CoV pseudovirus and SARS-CoV-2 pseudovirus are shown in the context of binding activity. Color varies with the neutralizing capability, with deep blue and deep red indicating a strong neutralizing capability.

reason why a large number of cross-binding antibodies could not neutralize SARS-CoV (Figure 2G). As the antigenic sites recognized by these cross-neutralizing mAbs were common between SARS-CoV and SARS-CoV-2, they could become the key targets for design of universal vaccines against SARS-like coronaviruses and selection of broad therapeutic antibodies.

Functional characterization of nAbs recognizing multiple antigenic sites

In order to further explore the function of each antigenic sites in RBD, nAbs were classified into six clusters (C1-6) using competition binding assay, and the antigenic sites for C1-6 nAbs were termed as sites S1-6, respectively (Figures S10, S11 and Figure 3A). Site S1 should be immunodominant antigenic sites, because the C1 nAbs accounted for relatively higher proportion (Figure 3A). Notably, nAbs in different clusters were efficiently induced for majority of convalescent SARS-CoV-2 patients, which embodied common immunogenic characteristics of these antigenic sites in RBD and indicated that SARS-CoV-2 infection can elicit antibody response using similar model (Figure 3B).

To determine the functional characteristics of nAbs targeting different sites, we analyzed the biochemical properties of these nAbs. The C1, C2, C4, C5 and C6 nAbs bound to SARS-CoV-2 S protein with comparable EC_{50} values; however, the nAbs elicited

10.3389/fimmu.2022.952650

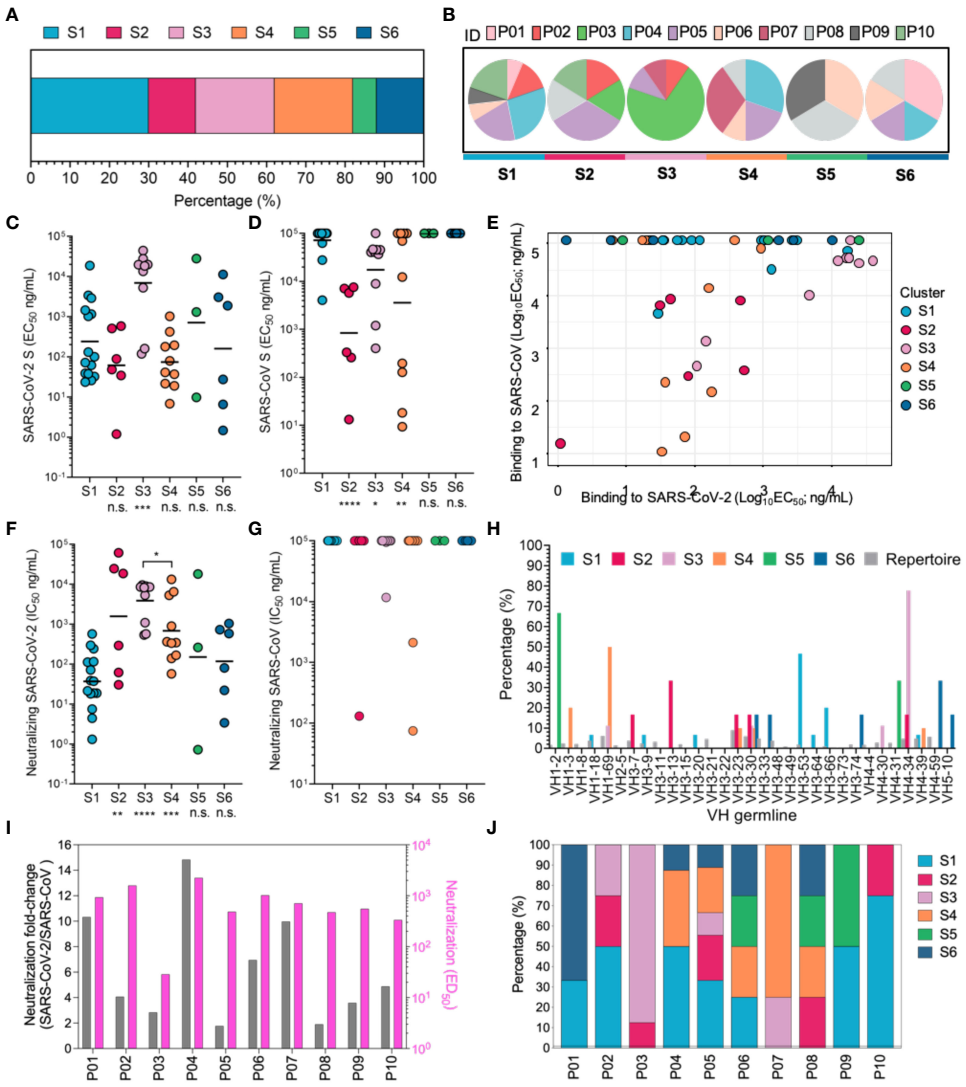

FIGURE 3
Mapping of multiple neutralizing epitopes recognized by mAbs by cluster analysis and functional characterization. **(A)** Based on cluster analysis of competitive ELISA data for nAbs, nAbs were classified into six clusters targeting six different RBD antigenic sites (S1-6). The percentages of nAbs recognizing different antigenic sites were calculated and are displayed. Colors indicate different individuals. **(B)** Individual composition analysis of nAbs targeting different antigenic sites. ID denotes different convalescent individuals marked by colors. **(C, D)** The binding activity to the SARS-CoV and SARS-CoV-2 S proteins were determined by ELISA and are denoted as EC_{50} values. **(E)** Analysis of antigenic sites recognized by cross-binding nAbs. **(F, G)** Neutralizing capacity against a SARS-CoV-2 pseudovirus **(F)** and SARS-CoV pseudovirus **(G)**, with comparison of nAbs targeting S2-6 and S1-directed nAbs. **(H)** The VH germline genes of each cluster of neutralizing antibodies were analyzed. Different colors are used to indicate each neutralizing cluster. **(I)** Fold increase in ED_{50} of plasma against SARS-CoV-2 pseudoviruses, relative to SARS-CoV-2 pseudoviruses, presented as a pink histogram, and gray histogram indicates neutralization against SARS-CoV-2 pseudoviruses. **(J)** Composition of antibodies targeting different antigenic sites in convalescent COVID-19 patients. Different colors indicated antigenic sites targeted by mAbs of convalescent COVID-19 patients. For panels **(C, D, F, G)**, data are plotted as the geometric mean. n.s., no significant difference; *P < 0.05; **P< 0.01; ***P < 0.001. The black line indicates the mean value. Statistical significance in **(C, D, F, G)** was determined using the Mann-Whitney U test. ****P < 0.0001.

by site S3 displayed lower binding activity to SARS-CoV-2 S protein (Figure 3C). Furthermore, the majority of C2, C3 and C4 nAbs showed cross-reactivity with SARS-CoV S protein and SARS-CoV-2 S protein, suggesting that these sites were conserved between SARS-CoV and SARS-CoV-2 (Figures 3D, E). Nevertheless, these conserved sites in the context of natural infection of SARS-CoV-2 just induced four potent cross-neutralizing mAbs (P10-6G3 targeting site S2, P07-4D10 targeting site S3, and P05-5B6 and P05-6H7 targeting site S4) against SARS-CoV and SARS-CoV-2, since most cross-binding nAbs showed obviously weaker affinity for SARS-CoV S protein than SARS-CoV-2 S protein, leading to inability to achieve cross-

neutralization (Figures 3C–G). Notably, the conserved sites-directed nAbs showed lower neutralization capacity against SARS-CoV-2 than nAbs recognizing SARS-CoV-2 unique antigenic sites (sites S1, S5 and S6), except those targeting conserved site S3; based on the premise that all nAbs possess similar binding activity to the SARS-CoV-2 S protein, these nAbs targeting conserved sites are implied to have a disadvantage in blocking S protein binding to receptor ACE2, putatively due to less overlap between their antigenic sites and ACE2 footprint (Figures 3C, F). Markedly, C1 nAbs isolated from the overwhelming majority of convalescent individuals recognized antigenic site S1, and potently and specifically inhibited SARS-CoV-2 infection by blocking S protein attachment to ACE2, revealing that site S1 is an immunodominant antigenic site in SARS-CoV-2 RBD that efficiently elicits a strong NAb response during natural SARS-CoV-2 infection (Figures 3B, F and Figure S12A). The immunodominance of site S1 may result from either its accessibility in different conformations of SARS-CoV-2 S protein or the innate affinity of the corresponding C1 nAbs derived from the naïve B cell repertoire (VH 3-53/66 germline) (Figure 3H); the latter factor would lead to rapid affinity maturation of C1 mAbs without the need for a high level of SHM (31, 43, 44). In contrast, while large amplification of the same antibody clone against site S3 was exhibited in the convalescent individual P03, the nAbs derived from this antibody clone poorly inhibited SARS-CoV-2 infection, revealing that site S3 is possibly an immunodominant, but weakly neutralizing site (Figure 3F, Figure S6, Figure 1A and Figure S4). The characteristics of nAbs targeting different antigenic sites is further mapped to plasma neutralizing function. nAbs recognizing conserved antigenic site S3 showed significant clonal amplification in P03, which resulted in weaker plasma neutralization compared to the other COVID-19 patients. High proportion of specific antibodies against site S1 can ensure stronger neutralization activity against SARS-CoV-2 in COVID-19 patient plasma, but its cross-neutralization potency decreased significantly, and P04 was the most representative among these convalescent patients (Figures 3I, J). On the contrary, P05 and P08 plasma showed higher cross-neutralization potency, which might result from the numerous cross-neutralizing mAbs binding to the conserved antigenic sites. Thus, our findings confirm that conserved antigenic sites can broadly induce antibody response in COVID-19 patients, while cross-neutralization potency varies for different patients.

Taken together, sites S2, S3 and S4 were identified as conserved antigenic sites between SARS-CoV-2 and SARS-CoV that could induce cross-neutralizing antibody response and should be considered in the rational design of universal SARS-like coronavirus vaccines, and the remaining sites were unique antigenic sites for SARS-CoV-2. The difference in binding location possibly confer nAbs elicited by conserved antigenic sites might show weaker neutralization of SARS-CoV-2 than those elicited by unique antigenic sites.

Identification of antigenic sites S1-6 in RBD

It is more helpful to understand the functional characteristics of corresponding antibodies by analyzing the structural characteristics of each antigenic site. To determine the spatial position of sites S1-6, we performed a mutagenesis study by substituting ACE2-interactive and noninteractive residues with alanine or arginine in RBD, and then assessed the decreased binding activity of representative nAbs to mutant RBDs compared to the reference RBD (45). The reduction in binding activity to each mutant RBD is shown in Figure S14. The spatial positions of all antigenic sites in RBD were simultaneously displayed to demonstrate their relative locations, which is critical to elucidate the functional characteristics of all neutralizing antigenic sites in RBD (Figure S15A and Figure 4A). Fortunately, numerous key epitopes in RBD have been identified by antigen-antibody complex structure and could be classified into five classes, which provides an important reference for this study (4, 28, 46). Site S1, S2 (and S3), S4 and S5 (and S6) sites are similar to Class 1, Class 4, Class 5 and Class 2/3 sites, respectively, according to their interactive residues and neutralizing characteristics of corresponding mAbs (Figures 4A, B).

SARS-CoV-2 unique sites S1, S5 and S6 largely overlapped with ACE2 footprint, supporting potent neutralizing activities of corresponding nAbs by efficiently blocking S protein binding to receptor, whereas conserved sites S2, S3 and S4 distant from ACE2 footprint is not conducive for neutralization (Figure S15A). However, site S4-specific nAbs, similar to broadly neutralizing mAb S2H97, might neutralize SARS-CoV-2 and SARS-CoV by promoting direct shed of S1 subunit, rather than blocking RBD attachment to ACE2. Site S2, S3 and S4 are highly conserved among SARS-CoV, SARS-CoV-2 and even other SARS-related viruses (Figure 4C and Figure S15B). Thus, nAbs targeting these antigenic sites retain strong neutralization potency against SARS-CoV-2 variants (B.1.1.7, B.1.351, B.1.1.28 and B.1.617.2), nevertheless, these variants escape neutralization of representative nAbs targeting SARS-CoV-2 unique sites (Figure 4D). As some neutralizing antigenic sites are hidden by the RBD in the lying-down state, this masking becomes an important immune escape mechanism of SARS-CoV-2 (41). The conserved sites, especially site S3, were highly concealed in the RBD lying-down state by adjacent RBD monomers. Even when the RBD was in the standing-up state, site S3 was not sufficiently exposed, and this inadequate exposure failed to improve the affinity maturation of S3-directed mAbs (Figure S16). Similarly, insufficient space for nAbs binding to conserved site S4 was found on the closed S protein, and only the RBD in the standing-up state could improve the accessibility of site S4.

Thus, our findings indicate that conserved antigenic sites display less accessibility than SARS-CoV-2 unique epitopes and that poor accessibility hinders the affinity maturation of site S3-

10.3389/fimmu.2022.952650

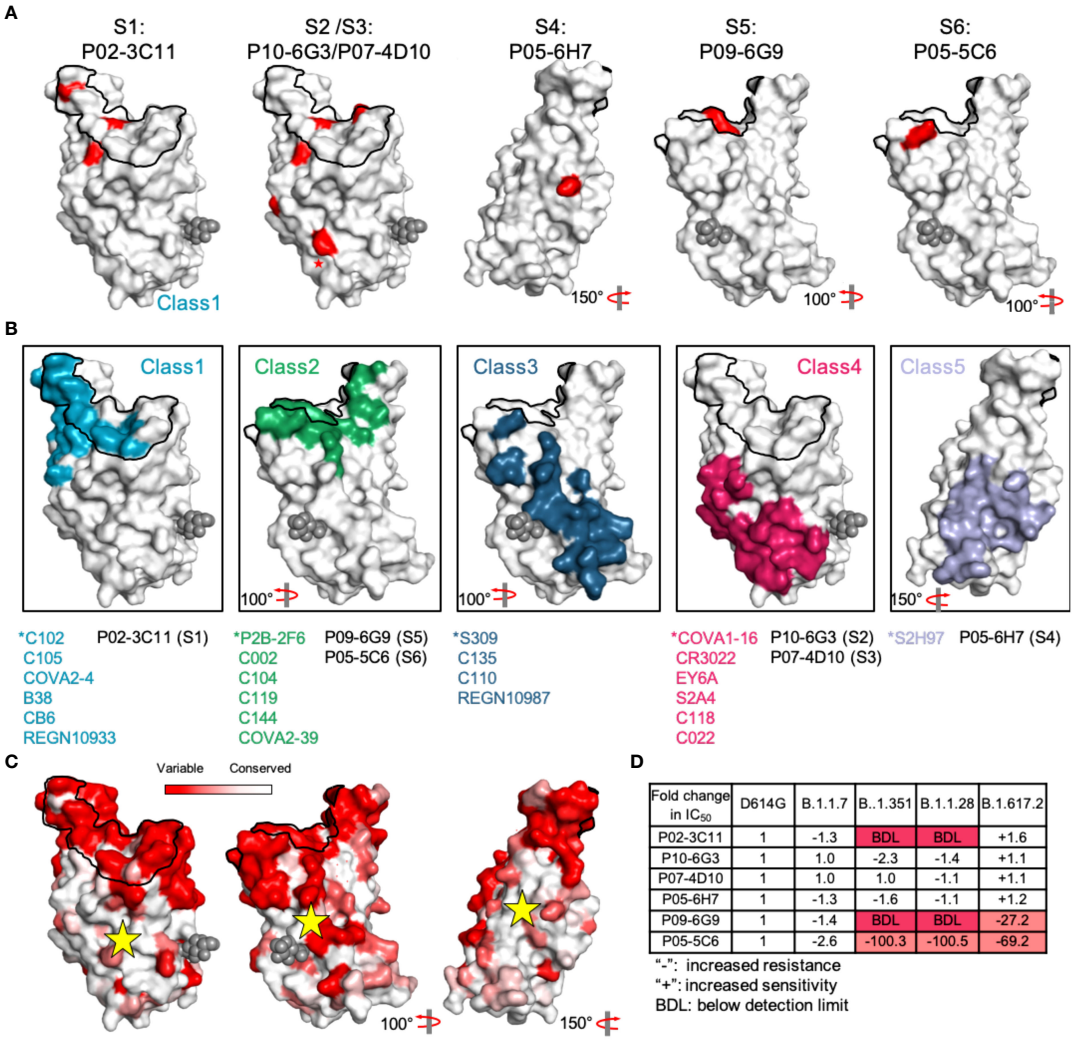

FIGURE 4
Dynamic analysis of site S1-6 accessibility. **(A)** Relative positions of sites S1-6 in the RBD. Red indicates the critical residues interfering the binding activity of representative nAbs. **(B)** Some SARS-CoV-2 RBD-specific mAbs reported in other studies are displayed in different colors, and cyan, green, blue, claret and purple indicate the mAbs C102, P2B-2F6, S309, COVA1-16 and S2H97, respectively. These mAbs were identified as representative mAbs for Classes 1-5. ACE2 footprint is outlined in black line. The glycan at position N343 is rendered as black spheres. **(C)** Conservation analysis of antigenic sites-directed by candidate mAbs using sequences including SARS-CoV-2 (n = 2216,010) and other Sarbecoviruses (n = 80). Deeper white indicates the more conserved region that was marked by a yellow star. **(D)** The fold change of mAbs neutralization potency against SARS-CoV-2 variants (B.1.1.7, B.1.351, B.1.1.28 and B.1.617.2), compared to that against the D614G variant.

directed mAbs in natural infection and even might decrease the cross-neutralizing antibody response after SARS-CoV-2 vaccination.

Rational design of SARS-CoV-2 RBD to enhance the immunodominance of conserved antigenic sites

The majority of mAbs recognizing antigenic site S1 were VH3-53/66 mAbs with a short (mostly 11 residues) CDRH3 sequence. Moreover, many studies have also reported the same enrichment of VH3-53/66 mAbs targeting antigenic sites similar to site S1 and found that they share structural similarities with each other (8, 29, 46–48). These VH3-53/66 mAbs showed native binding to SARS-CoV-2 RBD residues using CDRH1 and CDRH2 by forming many hydrogen bonds (L455, Y473, A475 and N487 bound by CDRH1, and D420, Y421 and R457 bound by CDRH2) (Figure 5A and Figure S17). Therefore, the native binding advantage between antigenic site S1 and VH3-53/66 was the cardinal cause of site S1 immunodominance, which could result in massive amplification of antigenic site S1-specific B cells and competition to inhibit the proliferation of B cells directed against conserved antigenic sites. To indirectly enhance

the competitiveness of conserved antigenic sites in the immune response, it is essential to decrease the immunodominance of site S1. To this end, we designed a variety of SARS-CoV-2 RBD variants with antigenic site S1 silencing using either protein truncation or glycan modification (Figures 5B–E). Glycan modification at positions K458 and A475 within site S1, termed $RBD_{Glycan458,475}$, was successful in destroying the binding of S1-directed mAbs, including P02-3C11 derived from VH3-66 and P05-5C4 derived from VH3-53, and could maintain conserved antigenic sites S2, S3 and S4 (Figure 5F). To preliminarily investigate whether $RBD_{Glycan458,475}$ could improve the cross-binding antibody response, BALB/c mice were immunized with 20 μg/dose $RBD_{Glycan458,475}$. Two weeks after immunization, the mice receiving $RBD_{Glycan458,475}$ or the reference RBD all presented detectable serum anti-SARS-CoV S IgG and anti-SARS-CoV-2 S IgG; however, $RBD_{Glycan458,475}$ induced a significantly higher cross-binding IgG titer than the reference RBD (Figure 5G). Additionally, the results also revealed that $RBD_{Glycan458,475}$ could induce higher cross-binding IgG titer against SARS-CoV-2 and the Omicron variant (BA.1) than the reference RBD (Figure 5G). Hence, universal vaccines based on such glycan modification of the SARS-CoV-2 RBD have the potential to induce a stronger cross-binding antibody response that could efficiently protect against

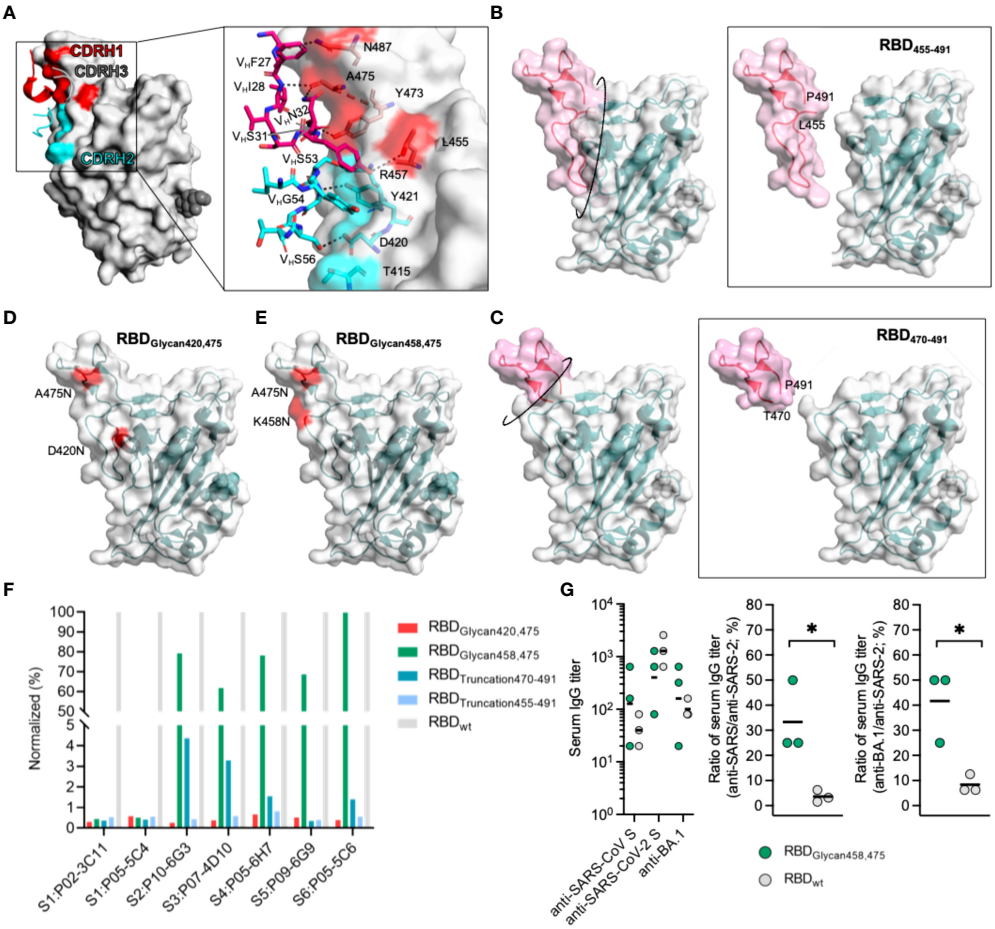

FIGURE 5
Design of SARS-CoV-2 RBD variants to improve the competitiveness of subdominant conserved antigenic sites. **(A)** Interaction between CDRH1 and CDRH2 residues and the SARS-CoV-2 RBD. Residues of mAbs constructing hydrogen bonds with CDRH1 and CDRH2 in the RBD are rendered as red and cyan sticks. **(B–E)** Design of a SARS-COV-2 RBD with an enhanced capability to elicit cross-reactive antibodies. A truncated SARS-CoV-2 RBD was produced by removing T455-P491 and termed $RBD_{Truncation455-491}$ in **(B)**, and the RBD produced by removing T470-P491 was termed $RBD_{Truncation470-491}$ in **(C)**. A SARS-CoV-2 RBD glycosylated at positions 420 and 475 was termed $RBD_{Glycan420,475}$ in **(D)**, and an RBD glycosylated at positions 458 and 475 was termed $RBD_{Glycan458,475}$ in **(E)**. **(F)** Influence of designed RBDs on the binding activity of representative nAbs targeting different antigenic sites. **(G)** Antibody response against the SARS-CoV S protein and SARS-CoV-2 S protein induced by $RBD_{Glycan458,475}$ in mice (N=3). BALB/c mice were immunized with 20 μg/dose at week 0, and specific IgG titers in the serum were tested at week 2. The ratio of the serum IgG titer against the SARS-CoV S protein to that against the SARS-CoV-2 S protein was calculated. For panel **(G)**, data are plotted as the geometric mean or mean. Statistical significance in **(G)** was determined using a nonpaired t test, and * indicates $P < 0.05$.

infection by SARS-like coronaviruses and emerging SARS-CoV-2 variants.

Discussion

RBD is defined as the immunodominant domain within the SARS-CoV-2 S protein (4), which was supported by its few glycosylation sites compared with the other S protein domains and higher accessibility within the S protein with variable conformations, as well as by S1 domain shedding (6, 28). Structural studies have proven that the S protein possesses conformational dynamics, in which different prefusion conformations expose a variety of crucial antigenic sites, including conserved antigenic sites between SARS-CoV and SARS-CoV-2 (31, 49). Although some conserved antigenic sites identified by cross-binding mAbs have been reported, a systematic analysis is still lacking, which is prejudicial to rational design of universal vaccines (4–8). We used information obtained from neutralizing mAbs isolated from convalescent SARS-CoV-2 patients to develop a quantitative antigenic map of SARS-CoV-2 RBD neutralizing sites that demonstrates immunodominance, neutralization properties and conserved properties. Six dominant antigenic sites were identified, of which sites, S2, S3 and S4 are conserved antigenic sites and can elicit cross-neutralizing antibody response to SARS-CoV and SARS-CoV-2. Analysis of difference in plasma neutralization capacity from the perspective of mAbs is more conducive to the cognition of the process of humoral immune response to SARS-CoV-2, so as to promote the directional induction of functional immune response. This study demonstrates that, although similar plasma neutralization against SARS-CoV-2 was determined among convalescent COVID-19 patients, there was significant difference in cross-neutralization activity against SARS-CoV, which was probably caused by the diverse strength of antibody response to different antigenic sites. High proportion of conserved antigenic sites-specific antibodies will significantly decrease plasma neutralization titer, but accompanied by strong cross-neutralization capacity, which gives us the hope of developing universal vaccine based on the conserved antigenic sites, but also presents a serious test of how to effectively enhance the corresponding immune response.

These conserved antigenic sites are subdominant, and S3 induces a lower-affinity mAb response than unique antigenic site S1 that is immunodominant and coincides with the ACE2 footprint; this hierarchy is putatively related to the lower accessibility of conserved antigenic sites in a variety of conformations. Nevertheless, conserved antigenic sites can still effectively induce affinity maturation of specific antibodies, which provides an important basis for vaccine design based on conserved antigenic sites. SARS-CoV-2 unique antigenic sites (S1, S5 and S6) efficiently induce a specific antibody response and inhibit the production of cross-binding antibodies. Additionally, antigenic site S1 with native binding advantage of antibodies derived from VH3-53/66 might further suppress the humoral immune response to conserved antigenic sites through the depletion of a large number of B cells. Therefore, these antigenic sites, especially site S1, should be silenced for universal vaccine design. Moreover, some predominant SARS-CoV-2 variants, including B.1.351 and B.1.1.28 with K417N, E484K and N501Y mutations causing changes in antigenic sites overlapping with unique antigenic sites S1, S5 and S6, promote evasion of antibody-mediated immunity obtained by natural infection or vaccination; however, no cross-binding mAbs displaying decreased binding activity to these variants have been reported (20, 22–24). These findings prove that it is difficult for universal vaccines based on unique antigenic sites in the RBD to induce conserved antibody responses to prevent the possible pandemic risks of persistent SARS-CoV-2 variants with antigenic drift or SARS-like coronaviruses in the future; nevertheless, focusing on conserved antigenic sites might have great potential for universal SARS-like coronavirus vaccines (50).

Similar strategies for universal vaccine design have been proposed for the development of universal influenza virus vaccines that protect against infection with seasonal drift and novel pandemic influenza virus strains (51, 52). Candidates for universal influenza vaccines are mainly based on the conserved antigenic sites in the stalk domain of hemagglutinin, for example, headless hemagglutinin structures and display of conserved stalk epitopes on nanoparticles, which has shown promising results in animal models and has great reference significance for SARS-CoV-2 vaccines (53–56). To indirectly enhance the competitiveness of conserved sites in the mAb response by decreasing the immunodominance of site S1, we designed a variety of SARS-CoV-2 RBD proteins with site S1 silencing by either removal of a peptide fragment or glycan modification. In this study, the designed protein $RBD_{Glycan458,475}$ with a glycan modification destroying site S1 and maintaining the remaining conserved sites induced stronger cross-binding antibody response, revealing that such a SARS-CoV-2 RBD design could promote the development of universal vaccines against SARS-like coronaviruses. To further enhance the immunogenicity, the modified RBD could be display on particle, such as ferritin (57), mi3 (58) and I53 (59).

In summary, our studies defined a quantitative antigenic map of neutralizing sites within SARS-CoV-2 RBD and completed the characterization of conserved antigenic sites, which is required for rational design of universal vaccines. Moreover, we tried to design RBD proteins to enhance the immune competitiveness of conserved antigenic sites. Although SARS-CoV-2 vaccines have been developed and approved, our long-term efforts aimed at preparing universal vaccines for other human epidemics caused by SARS-CoV-2 VOCS and SARS-like coronaviruses that may become prevalent in the future are still necessary.

Data availability statement

The original contributions presented in the study are included in the article/Supplementary Material. Further inquiries can be directed to the corresponding authors.

Ethics statement

The studies involving human participants were reviewed and approved by School of Public Health. The patients/participants provided their written informed consent to participate in this study.

Author contributions

SW, QY, HY, TZ, ZZ, and NX contributed to the experimental design. SW, DW, QY, HX, JW, TZ, ZZ, and NX participated in discussion and interpretation of the results. SW, DW, HX, JW, TZ, ZZ, and NX contributed to the manuscript preparation. SW, HX, JW, ZT, ZC, YZ, DY, XL, CL, SG, YL, and XZ contributed to the preparation and *in vitro* characterization of antibody. YW and WT performed the animal experiments. All authors contributed to the article and approved the submitted version.

Funding

This work was supported by the National Natural Science Foundation of China (81993149041 for NX; 81871316 for QY). The Science and Technology Major Project of Fujian Province (grant number 2020YZ014001). Xiamen Science and Technology Major Project (grant number 3502Z2020YJ02).

Conflict of interest

The authors declare that the research was conducted in the absence of any commercial or financial relationships that could be construed as a potential conflict of interest.

Publisher's note

All claims expressed in this article are solely those of the authors and do not necessarily represent those of their affiliated organizations, or those of the publisher, the editors and the reviewers. Any product that may be evaluated in this article, or claim that may be made by its manufacturer, is not guaranteed or endorsed by the publisher.

Supplementary material

The Supplementary Material for this article can be found online at: https://www.frontiersin.org/articles/10.3389/fimmu.2022.952650/full#supplementary-material

SUPPLEMENTARY FIGURE 1
Characteristics analysis of humoral immune response by COVID-19 convalescent plasma. **(A)** Correlation between days after symptom onset and plasma antibody titer including anti-RBD antibody, anti-RBD IgG and anti-RBD IgM, using Spearman correlation test. **(B)** Correlation test between anti-RBD titers and PSV SARS-CoV-2 neutralizing capacity are determined by Spearman correlation test. r and P values of the correlation are indicated.

SUPPLEMENTARY FIGURE 2
Identification of SARS-CoV-2 RBD-specific memory B cells and isolation of SARS-CoV-2 RBD-specific antibodies. **(A)** SARS-CoV-2 RBD-specific memory B cells are identified as CD3-/CD19+/CD27+/SARS-CoV-2 RBD+, and the percentage of RBD-specific B cells is indicated. **(B, C)** The BCR (B cell receptor) subtypes of RBD-specific memory B cells are analyzed by goat anti-human IgG and goat anti-human IgM, then are statistically analyzed. **(D)** Recombinant monoclonal antibodies with SARS-CoV-2 RBD specificity are identified by ELISA. Gray line indicates limitation of anti-RBD antibodies detection.

SUPPLEMENTARY FIGURE 3
Phylogenetic analysis of heavy chain gene of SARS-CoV-2 RBD-specific mAbs. Maximum-likelihood phylogenetic tree of fully heavy chain of RBD-specific antibodies (N=77). Each color represents heavy chain sequence of SARS-CoV-2 RBD-specific mAbs from different convalescent individuals.

SUPPLEMENTARY FIGURE 4
Gene repertoire analysis of SARS-CoV-2 RBD-specific mAbs. V gene frequencies for heavy chain **(A)** and light chain **(B)** of SARS-CoV-2 RBD-specific antibodies. Colors indicate different convalescent individuals. Germline of VH is determined using the Immunogenetics (IMGT).

SUPPLEMENTARY FIGURE 5
Binding activity to S protein and neutralizing capacity against SARS-CoV-2 pseudovirus of SARS-CoV-2 RBD-specific mAbs. **(A, B)** Binding activity of mAbs to SARS-CoV S protein are compared among individual in B, and to SARS-CoV-2 S protein in C. Black line indicates mean value of EC_{50}. **(C, D)** Neutralizing capacity of mAbs against SARS-CoV-2 are compared among individual in **(C)** and blocking capacity of mAbs in **(D)**. Neutralizing capacity are tested by SARS-CoV-2 pseudovirus. Blocking assay is performed by incubating mixture of antibodies and SARS-CoV-2 S protein with ACE2-expressing cells. Black line indicates mean IC_{50}.

SUPPLEMENTARY FIGURE 6
Neutralization of SARS-CoV-2 RBD-specific mAbs against SARS-CoV-2 pseudovirus. Red indicates mAbs obtained from P03 convalescent individual.

SUPPLEMENTARY FIGURE 7
The correlation between neutralization potency and blocking capability of SARS-CoV-2 RBD-specific mAbs. The scatter plot depicting neutralizing capacity and blocking capacity of specific mAbs from different individuals annotated by colors.

SUPPLEMENTARY FIGURE 8
Analysis of CDRH3 length of antibodies derived from VH 3-53/66. **(A)** Repertoire information of RBD-specific antibodies composed of VH 3-53/66. **(B)** Length distribution of CDRH3 for RBD-specific antibodies derived from VH 3-53/66 by comparison with the remaining VH germline encoding antibodies. **(C)** Correlation of CDRH3 length and binding activity to SARS-CoV-2 S protein is performed for specific antibodies derived from of VH 3-53/66.

SUPPLEMENTARY FIGURE 9
Correlation analysis for days after symptom onset and mean binding activity of SARS-CoV-2 RBD-specific mAbs from corresponding convalescent individuals using Spearman correlation test. r and P values of the correlation are indicated.

SUPPLEMENTARY FIGURE 10
Competition ELISA for neutralizing mAbs. Competition ELISA is performed by using naked mAbs to block HRP-coupled mAbs, and ELISA signal for each HRP-coupled mAb is normalized to the signal in the absence of naked mAbs. The heat map of competition ELISA data is shown, with parameters colored continuously from white (0, corresponding to 0% inhibition) to red (4, corresponding to 93.7% inhibition) in the scale bar.

SUPPLEMENTARY FIGURE 11
Epitope mapping of mAbs by clustering analysis and functional characterization. By competition ELISA data, neutralizing mAbs are clustered into six group, Cluster1-6, and corresponding epitopes to each mAb cluster are defined as Site1-6. The color ranging from red to blue represented blocking potency against other antibodies (4.321 corresponding to 95% blocking rate and 0.074 corresponding to 5% blocking rate). The source of information and neutralization potency of each mAb are also indicated by different colors.

SUPPLEMENTARY FIGURE 12
Analysis of blocking capability against SARS-CoV-2 S protein binding to ACE2. **(A)** Blocking capacity of nAbs targeting sites S2-6 are compared with that of nAbs recognizing S1. **(B)** The neutralizing capacity and blocking capacity of nAbs recognizing site S4 are analyzed, and nAbs ID are indicated in figure.

SUPPLEMENTARY FIGURE 13
Neutralization capacity of a combination of representative nAbs targeting sites S1-6 against the SARS-CoV-2 pseudovirus and SARS-CoV-2 pseudovirus.

SUPPLEMENTARY FIGURE 14
Identification of SARS-CoV-2 RBD critical residues recognized by nAbs using selected amino acid substitution. **(A)** Mutate residues of SARS-CoV-2 RBD shown in pink. **(B)** Mutation of residues leading to damaging effect on SARS-CoV-2 RBD activity. Dash line indicates 25% binding activity of mutant RBD relative to wild type RBD. **(C)** The selected amino acid of RBD is mutated to alanine or arginine on purpose. Binding activity of sites S1-6 representative mAbs to wild-type (WT) and mutant RBD was measured by ELISA. The binding capacity to mutate RBD is normalized by binding to wild type RBD. Lines denote 10% binding activity relative to wild type RBD and 25% binding activity relative to wild type RBD. Residues reducing binding activity by more than 75% are identified critical residues for representative nAbs.

SUPPLEMENTARY FIGURE 15
Identification of sites S1-6 spatial position. **(A)** Structure of the RBD highlighting the critical residues interfering binding activity of representative nAbs, red denotes residues reducing binding activity by more than 75%. **(B)** Conservative analysis of sites S1-6, carmine denotes different residues between SARS-CoV-2 RBD and SARS-CoV RBD.

SUPPLEMENTARY FIGURE 16
CDRH1-3 sequence analysis of mAbs derived from IGHV3-53/66, including P05-5C4 derived from IGHV3-53 and P02-3C11 derived from IGHV3-66 targeting site S1.

SUPPLEMENTARY TABLE 1
Information of COVID-19 convalescent individuals. F, female; M, male.

SUPPLEMENTARY TABLE 2
Plasma anti-RBD antibody titers and neutralization capacity for COVID-19 convalescent individuals.

SUPPLEMENTARY TABLE 3
Amino acid sequence of diverse SARS-CoV-2 RBD variants expressed.

References

1. Wu F, Zhao S, Yu B, Chen YM, Wang W, Song ZG, et al. A new coronavirus associated with human respiratory disease in China.. *Nature* (2020) 579 (7798):265–9. doi: 10.1038/s41586-020-2008-3

2. Zhou G, Zhao Q. Perspectives on therapeutic neutralizing antibodies against the novel coronavirus SARS-CoV-2. *Int J Biol Sci* 16(10):1718–23. doi: 10.7150/ijbs.45123

3. Kim D, Lee JY, Yang JS, Kim JW, Kim VN, Chang H. The architecture of sars-cov-2 transcriptome. *Cell* 181(4):914–21. doi: 10.1016/j.cell.2020.04.011

4. Piccoli L, Park YJ, Tortorici MA, Czudnochowski N, Walls AC, Beltramello M, et al. Mapping neutralizing and immunodominant sites on the Sars-Cov-2 spike receptor-binding domain by structure-guided high-resolution serology. *Cell* 183 (4):1024–42. doi: 10.1016/j.cell.2020.09.037

5. Liu H, Wu NC, Yuan M, Bangaru S, Torres JL, Caniels TG, et al. Cross-neutralization of a sars-cov-2 antibody to a functionally conserved site is mediated by avidity. *Immunity* 53(6):1272–80. doi: 10.1016/j.immuni.2020.10.023

6. Wec AZ, Wrapp D, Herbert AS, Maurer DP, Haslwanter D, Sakharkar M, et al. Broad neutralization of sars-related viruses by human monoclonal antibodies. *Science* (2020) 369(6504):731–6. doi: 10.1126/science.abc7424

7. Yuan MA-O, Wu NA-O, Zhu XA-O, Lee CA-O, So RA-O, Lv HA-O, et al. A highly conserved cryptic epitope in the receptor binding domains of sars-cov-2 and sars-cov. *Science* (2020) 368(6491):630–3. doi: 10.1126/science.abb7269

8. Zhou D, Duyvesteyn HME, Chen CP, Huang CG, Chen TH, Shih SR, et al. Structural basis for the neutralization of sars-cov-2 by an antibody from a convalescent patient. *Nat Struct Mol Biol* (2020) 27(10):950–8. doi: 10.1038/s41594-020-0480-y

9. Hoffmann M, Kleine-Weber H, Schroeder S, Krüger N, Herrler T, Erichsen S, et al. Sars-Cov-2 Ccell entry depends on ace2 and tmprss2 and is blocked by a clinically proven protease inhibitor. *Cell* (2020) 181(2):271–80. doi: 10.1016/j.cell.2020.02.052

10. Walls AC, Park YJ, Tortorici MA, Wall A, McGuire AT, Veesler D. Structure, function, and antigenicity of the sars-cov-2 spike glycoprotein. *Cell* (2020) 181(2):281–92. doi: 10.1016/j.cell.2020.02.058

11. Ar Gouilh M, Puechmaille SJ, Diancourt L, Vandenbogaert M, Serra-Cobo J, Lopez Roïg M, et al. Sars-Cov related betacoronavirus and diverse alphacoronavirus members found in western old-world. *Virology* (2018) 517 (10):88–97. doi: 10.1016/j.virol.2018.01.014

12. Zhou P, Yang XL, Wang XG, Hu B, Zhang L, Zhang W, et al. A pneumonia outbreak associated with a new coronavirus of probable bat origin. *Nature* (2020) 579(7798):270–3. doi: 10.1038/s41586-020-2012-7

13. Chan-Yeung M, Xu RH. Sars: Epidemiology. *Respirology* (2003) 8(10):9–14. doi: 10.1046/j.1440-1843.2003.00518.x

14. Lam WK, Zhong Ns Fau - Tan WC, Tan WC. Overview on sars in asia and the world. *Respirology* (2003) 8(10):2–5. doi: 10.1046/j.1440-1843.2003.00516.x

15. Mackay IM, Arden KE. Mers coronavirus: Diagnostics, epidemiology and transmission. *Virol J* (2015) 12(11):222–8. doi: 10.1186/s12985-015-0439-5

16. de Wit E, van Doremalen N, Falzarano D, Munster VJ. Sars and mers: recent insights into emerging coronaviruses. *Nat Rev Microbiol* (2016) 14(8):523–34. doi: 10.1038/nrmicro.2016.81

17. Plante JA, Liu Y, Liu J, Xia H, Johnson BA, Lokugamage KG, et al. Spike mutation d614g alters sars-cov-2 fitness. *Nature* (2020) 592(7852):116–21. doi: 10.1038/s41586-020-2895-3

18. Shi PY, Plante J, Liu Y, Liu J, Xia H, Johnson B, et al. Spike mutation d614g alters sars-cov-2 fitness and neutralization susceptibility. *Res Sq* (2020) 10(8):121–9. doi: 10.21203/rs.3.rs-70482/v1

19. Plante JA, Liu Y, Liu J, Xia H, Johnson BA, Lokugamage KG, et al. Spike mutation d614g alters sars-cov-2 fitness and neutralization susceptibility. *bioRxiv* (2020). doi: 10.1101/2020.09.01.278689

20. Li QQ, Wu JJ, Nie JH, Zhang L, Hao H, Liu S, et al. The impact of mutations in sars-cov-2 spike on viral infectivity and antigenicity. *Cell* (2020) 182(5):1284–94. doi: 10.1016/j.cell.2020.07.012

21. Weissman D, Alameh MG, de Silva T, Collini P, Hornsby H, Brown R, et al. D614g spike mutation increases sars cov-2 susceptibility to neutralization. *Cell Host Microbe* (2021) 29(1):23–31. doi: 10.1016/j.chom.2020.11.012

22. Thomson EC, Rosen LE, Shepherd JG, Spreafico R, da Silva Filipe A, Wojcechowskyj JA, et al. Circulating sars-cov-2 spike n439k variants maintain fitness while evading antibody-mediated immunity. *Cell* (2021) 184(5):1171–87. doi: 10.1016/j.cell.2021.01.037

23. Zhou D, Dejnirattisai W, Supasa P, Liu C, Mentzer AJ, Ginn HM, et al. Evidence of escape of escape of sars-cov-2 variant b.1.351 from natural and vaccine induced sera. *Cell* (2021) 184(9):2348–61. doi: 10.1016/j.cell.2021.02.037

24. Li Q, Nie J, Wu J, Zhang L, Ding R, Wang H, et al. No higher infectivity but immune escape of sars-cov-2 501y.v2 variants. *Cell* (2021) 184(9):2362–71. doi: 10.1016/j.cell.2021.02.042

25. Wang P, Nair MS, Liu L, Iketani S, Luo Y, Guo Y, et al. Antibody resistance of sars-cov-2 variants b.1.351 and b.1.1.7. *Nature* (2021) 593(7857):130–5. doi: 10.1038/s41586-021-03398-2

26. He X, He C, Hong W, Zhang K, Wei X. The challenges of covid-19 delta variant: prevention and vaccine development. *MedComm* (2020) 2021) 2(4):846–54. doi: 10.1002/mco2.95

27. Tian X, Li C, Huang A, Xia S, Lu S, Shi Z, et al. Potent binding of 2019 novel coronavirus spike protein by a sars coronavirus-specific human monoclonal antibody. *Emerg Microbes Infect* (2020) 9(1):382–5. doi: 10.1080/22221751.2020.1729069

28. Pinto D, Park YJ, Beltramello M, Walls AC, Tortorici MA, Bianchi S, et al. Cross-neutralization of sars-cov-2 by a human monoclonal sars-cov antibody. *Nature* (2020) 583(7815):290–5. doi: 10.1038/s41586-020-2349-y

29. Brouwer PA-O, Caniels TA-OX, van der Straten KA-O, Snitselaar JL, Aldon YA-O, Bangaru S, et al. Potent neutralizing antibodies from covid-19 patients define multiple targets of vulnerability. *Science* (2020) 369(6504):643–50. doi: 10.1126/science.abc5902

30. Lv H, Wu NC, Tsang OT, Yuan M, Perera R, Leung WS, et al. Cross-reactive antibody response between sars-cov-2 and sars-cov infections. *Cell Rep* 31 (9):17725–9. doi: 10.1016/j.celrep.2020.107725

31. Rogers TA-OX, Zhao FA-O, Huang DA-OX, Beutler NA-O, Burns A, He WA-O, et al. Isolation of potent sars-cov-2 neutralizing antibodies and protection from disease in a small animal model. *Science* (2020) 369(6506):956–63. doi: 10.1126/science.abc7520

32. Liu LH, Wang PF, Nair MS, Yu J, Rapp M, Wang Q, et al. Potent neutralizing antibodies against multiple epitopes on sars-cov-2 spike. *Nature* (2020) 584(7821):450–6. doi: 10.1038/s41586-020-2571-7

33. Tiller T, Meffre E Fau - Yurasov S, Yurasov S Fau - Tsuiji M, Tsuiji M Fau - Nussenzweig MC, Nussenzweig Mc Fau - Wardemann H, Wardemann H. Efficient generation of monoclonal antibodies from single human b cells by single cell rt-pcr and expression vector cloning. *J Immunol Methods* (2008) 329(1):112–24. doi: 10.1016/j.jim.2007.09.017

34. Yu G, Smith DK, Zhu H, Guan Y, Lam TT-Y. Ggtree: An R package for visualization and annotation of phylogenetic trees with their covariates and other associated data. *Methods Ecol Evol* (2017) 8(1):28–36. doi: 10.1111/2041-210X.12628

35. Goodwin E, Gilman MSA, Wrapp D, Chen M, Ngwuta JO, Moin SM, et al. Infants infected with respiratory syncytial virus generate potent neutralizing antibodies that lack somatic hypermutation. *Immunity* (2018) 48(2):339–49. doi: 10.1016/j.immuni.2018.01.005

36. Wrammert J, Smith K Fau - Miller J, Miller J Fau - Langley WA, Langley Wa Fau - Kokko K, Kokko K Fau - Larsen C, Larsen C Fau - Zheng N-Y, et al. Rapid cloning of high-affinity human monoclonal antibodies against influenza virus. *Nature* (2008) 453(7195):667–71. doi: 10.1038/nature06890

37. Gilman MS, Castellanos CA, Chen M, Ngwuta JO, Goodwin E, Moin SM, et al. Rapid profiling of rsv antibody repertoires from the memory b cells of naturally infected adult donors. *Sci Immunol* (2016) 1(6):1–8. doi: 10.1126/sciimmunol.aaj1879

38. Wu NA-O, Grande G, Turner HL, Ward AB, Xie J, Lerner RA, et al. *In vitro* evolution of an influenza broadly neutralizing antibody is modulated by hemagglutinin receptor specificity. *Nat Commun* (2017) 8(10):15371–9. doi: 10.1038/ncomms15371

39. Yu L, Guan Y. Immunologic basis for long hcdr3s in broadly neutralizing antibodies against hiv-1. *Front Immunol* (2014) 5(250):1–8.

40. Briney B, Inderbitzin A, Joyce C, Burton DR. Commonality despite exceptional diversity in the baseline human antibody repertoire. *Nature* (2019) 566(7744):393–7. doi: 10.1038/s41586-019-0879-y

41. Shang J, Wan Y, Luo C, Ye G, Geng Q, Auerbach A, et al. Cell entry mechanisms of sars-cov-2. *Proc Natl Acad Sci USA* (2020) 117(21):11727–34. doi: 10.1073/pnas.2003138117

42. Long Q-X, Tang X-J, Shi Q-L, Li Q, Deng H-J, Yuan J, et al. Clinical and immunological assessment of asymptomatic sars-cov-2 infections. *Nat Med* (2020) 26(8):1200–4. doi: 10.1038/s41591-020-0965-6

43. Barnes CO, West APJr., Huey-Tubman KE, Hoffmann MAG, Sharaf NG, Hoffman PR, et al. Structures of human antibodies bound to sars-cov-2 spike reveal common epitopes and recurrent features of antibodies. *Cell* (2020) 182(4):828–42. doi: 10.1016/j.cell.2020.06.025

44. Cao Y, Su B, Guo X, Sun W, Deng Y, Bao L, et al. Potent neutralizing antibodies against sars-cov-2 identified by high-throughput single-cell sequencing of convalescent patients' b cells. *Cell* (2020) 182(1):73–84. doi: 10.1016/j.cell.2020.05.025

45. Zost Sj Fau - Gilchuk P, Gilchuk P Fau - Case JB, Case Jb Fau - Binshtein E, Binshtein E Fau - Chen RE, Chen Re Fau - Reidy JX, Reidy Jx Fau - Trivette A, et al. Potently eutralizing human antibodies that block sars-cov-2 receptor binding and protect animals. *Nature* (2020) 584(7821):443–9. doi: 10.1038/s41586-020-2548-6

46. Barnes CO, Jette CA, Abernathy ME, Dam KA-O, Esswein SA-O, Gristick HB, et al. Sars-Cov-2 neutralizing antibody structures inform therapeutic strategies. *Nature* (2020) 588(7839):682–7. doi: 10.1038/s41586-020-2852-1

47. Yuan M, Liu H, Wu NC, Lee CD, Zhu X, Zhao F, et al. Structural basis of a shared antibody response to sars-cov-2. *Science* (2020) 369(6507):1119–23. doi: 10.1126/science.abd2321

48. Wu NC, Yuan M, Liu HJ, Lee CCD, Zhu XY, Bangaru S, et al. An alternative binding mode of ighv3-53 antibodies to the sars-cov-2 receptor binding domain. *Cell Rep* (2020) 33(3). doi: 10.1016/j.celrep.2020.108274

49. Wrapp DA-O, Wang NA-OX, Corbett KA-O, Goldsmith JA, Hsieh CL, Abiona OA-O, et al. Cryo-em structure of the 2019-ncov spike in the prefusion conformation. *Science* (2020) 367(6483):1260–3. doi: 10.1126/science.abb2507

50. Weiss SR. Forty years with coronaviruses. *J Exp Med* (2020) 217(5):1–4. doi: 10.1084/jem.20200537

51. Gerdil C. The annual production cycle for influenza vaccine. *Vaccine* (2003) 21(16):1776–9. doi: 10.1016/s0264-410x(03)00071-9

52. Krammer F, Palese P. Influenza virus hemagglutinin stalk-based antibodies and vaccines. *Curr Opin Virol* (2013) 3(5):521–30. doi: 10.1016/j.coviro.2013.07.007

53. Graves PN, Schulman JL, Young JF, Palese P. Preparation of influenza virus subviral particles lacking the ha1 subunit of hemagglutinin: unmasking of cross-reactive ha2 determinants. *Virology* (1983) 126(1):106–16. doi: 10.1016/0042-6822(83)90465-8

54. Bommakanti G, Citron MP, Hepler RW, Callahan C, Heidecker GJ, Najar TA, et al. Design of an ha2-based escherichia coli expressed influenza immunogen that protects mice from pathogenic challenge. *P Natl Acad Sci USA* (2010) 107 (31):13701–6. doi: 10.1073/pnas.1007465107

55. Schneemann A, Speir Ja Fau - Tan GS, Tan Gs Fau - Khayat R, Khayat R Fau - Ekiert DC, Ekiert Dc Fau - Matsuoka Y, Matsuoka Y Fau - Wilson IA, et al. A virus-like particle that elicits cross-reactive antibodies to the conserved stem of influenza virus hemagglutinin. *J Virol* (2012) 86(21):11686–97. doi: 10.1128/JVI.01694-12

56. Kanekiyo M, Wei Cj Fau - Yassine HM, Yassine Hm Fau - McTamney PM, McTamney Pm Fau - Boyington JC, Boyington Jc Fau - Whittle JRR, Whittle SSJr Fau - Rao, et al. Self-assembling influenza nanoparticle vaccines elicit broadly neutralizing h1n1 antibodies. *Nature* (2013) 499(7456):102–6. doi: 10.1038/nature12202

57. Kang YF, Sun C, Zhuang Z, Yuan RY, Zheng QB, Li JP, et al. Rapid development of sars-cov-2 spike protein receptor-binding domain self-assembled nanoparticle vaccine candidates. *ACS Nano* (2021) 15(2):2738–52. doi: 10.1021/acsnano.0c08379

58. Bruun TUJ, Andersson AMC, Draper SJ, Howarth M. Engineering a rugged nanoscaffold to enhance plug-and-display vaccination. *ACS Nano* (2018) 12 (9):8855–66. doi: 10.1021/acsnano.8b02805

59. Brouwer PJM, Antanasijevic A, Berndsen Z, Yasmeen A, Fiala B, Bijl TP, et al. Enhancing and shaping the immunogenicity of native-like hiv-1 envelope trimers with a two-component protein nanoparticle. *Nat Commun* (2019) 10 (1):4272–9. doi: 10.1038/s41467-019-12080-1

frontiers | Frontiers in Immunology

TYPE Original Research
PUBLISHED 20 September 2022
DOI 10.3389/fimmu.2022.988685

Check for updates

OPEN ACCESS

EDITED BY
Martijn van Griensven,
Maastricht University, Netherlands

REVIEWED BY
Diane Marie Del Valle,
Icahn School of Medicine at Mount Sinai, United States
Mattia Bellan,
Università del Piemonte Orientale, Italy

*CORRESPONDENCE
Rebekah Penrice-Randal
R.Penrice-Randal@liverpool.ac.uk

†These authors share senior authorship

SPECIALTY SECTION
This article was submitted to Viral Immunology, a section of the journal Frontiers in Immunology

RECEIVED 07 July 2022
ACCEPTED 29 August 2022
PUBLISHED 20 September 2022

CITATION
Penrice-Randal R, Dong X, Shapanis AG, Gardner A, Harding N, Legebeke J, Lord J, Vallejo AF, Poole S, Brendish NJ, Hartley C, Williams AP, Wheway G, Polak ME, Strazzeri F, Schofield JPR, Skipp PJ, Hiscox JA, Clark TW and Baralle D (2022) Blood gene expression predicts intensive care unit admission in hospitalised patients with COVID-19. *Front. Immunol.* 13:988685. doi: 10.3389/fimmu.2022.988685

COPYRIGHT
© 2022 Penrice-Randal, Dong, Shapanis, Gardner, Harding, Legebeke, Lord, Vallejo, Poole, Brendish, Hartley, Williams, Wheway, Polak, Strazzeri, Schofield, Skipp, Hiscox, Clark and Baralle. This is an open-access article distributed under the terms of the Creative Commons Attribution License (CC BY). The use, distribution or reproduction in other forums is permitted, provided the original author(s) and the copyright owner(s) are credited and that the original publication in this journal is cited, in accordance with accepted academic practice. No use, distribution or reproduction is permitted which does not comply with these terms.

Blood gene expression predicts intensive care unit admission in hospitalised patients with COVID-19

Rebekah Penrice-Randal[1,2*], Xiaofeng Dong[1], Andrew George Shapanis[3], Aaron Gardner[2], Nicholas Harding[2], Jelmer Legebeke[3,4], Jenny Lord[3], Andres F. Vallejo[5], Stephen Poole[4,5], Nathan J. Brendish[4,5], Catherine Hartley[1], Anthony P. Williams[6], Gabrielle Wheway[3], Marta E. Polak[5,7], Fabio Strazzeri[2], James P. R. Schofield[2], Paul J. Skipp[2,8], Julian A. Hiscox[1,9,10], Tristan W. Clark[4,5†] and Diana Baralle[3,4†]

[1]Institute of Infection, Veterinary and Ecological Sciences, University of Liverpool, Liverpool, United Kingdom, [2]TopMD Precision Medicine Ltd, Southampton, United Kingdom, [3]School of Human Development and Health, Faculty of Medicine, University of Southampton, Southampton, United Kingdom, [4]National Institute for Health Research (NIHR) Southampton Biomedical Research Centre, University Hospital Southampton National Health Service (NHS) Foundation Trust, University of Southampton, Southampton, United Kingdom, [5]School of Clinical and Experimental Sciences, Faculty of Medicine, University of Southampton, Southampton, United Kingdom, [6]Cancer Sciences Division, Faculty of Medicine, University Hospital Southampton, Southampton, United Kingdom, [7]Institute for Life Sciences, University of Southampton, Southampton, United Kingdom, [8]Centre for Proteomic Research, School of Biological Sciences, University of Southampton, Southampton, United Kingdom, [9]NIHR Health Protection Research Unit in Emerging and Zoonotic Infections, Liverpool, United Kingdom, [10]ASTAR Infectious Diseases Laboratories (ASTAR ID Labs), Agency for Science, Technology and Research (ASTAR) Singapore, Singapore, Singapore

Background: The COVID-19 pandemic has created pressure on healthcare systems worldwide. Tools that can stratify individuals according to prognosis could allow for more efficient allocation of healthcare resources and thus improved patient outcomes. It is currently unclear if blood gene expression signatures derived from patients at the point of admission to hospital could provide useful prognostic information.

Methods: Gene expression of whole blood obtained at the point of admission from a cohort of 78 patients hospitalised with COVID-19 during the first wave was measured by high resolution RNA sequencing. Gene signatures predictive of admission to Intensive Care Unit were identified and tested using machine learning and topological data analysis, TopMD.

Results: The best gene expression signature predictive of ICU admission was defined using topological data analysis with an accuracy: 0.72 and ROC AUC: 0.76. The gene signature was primarily based on differentially activated pathways controlling epidermal growth factor receptor (EGFR) presentation,

Peroxisome proliferator-activated receptor alpha (PPAR-α) signalling and Transforming growth factor beta (TGF-β) signalling.

Conclusions: Gene expression signatures from blood taken at the point of admission to hospital predicted ICU admission of treatment naïve patients with COVID-19.

KEYWORDS

COVID-19, Critical Care, biomarkers, prognosis, topology, transcriptome, RNA-seq - RNA sequencing

Introduction

Severe acute respiratory syndrome coronavirus 2 (SARS-CoV-2) is a *betacoronavirus* responsible for coronavirus disease-19 (COVID-19) resulting in a global pandemic with over 6.3 million deaths by June 2022. SARS-CoV-2 causes a spectrum of symptoms in humans, from asymptomatic to severe disease, where the latter requires continuous and intensive care and is associated with extensive pulmonary immunopathology (1, 2). The nature of severe coronavirus disease has caused a strain on healthcare systems across the world (3). Biomarkers predictive of outcome in patients with Ebola virus disease have been identified (4), highlighting that prognostic biomarkers could be useful in outbreak and clinical settings. There is an urgent need for tools which can stratify patients according to prognosis to better manage healthcare resources and improve patient outcomes, particularly in resource poor or limited settings.

There have been many attempts to define prognostic biomarkers in COVID-19 (5–10). However, these have focused on predicting mortality, which is primarily associated with older age groups. The ability to predict, at admission to hospital, the trajectory of a patient towards intensive care unit (ICU) admission will allow for more efficient triaging and improve outcomes through early targeted interventions. The decision to admit individuals to ICU is a result of applying standard clinical and physiological metrics with clinical oversight and scoring tools such as NEWS2 (11). Leveraging host response data from an accessible sample (e.g., peripheral blood) to predict and inform ICU admission is therefore an exciting continuation of previous work to define the host response in patients with COVID-19 (12).

Several studies in different disease contexts, including COVID-19, have been conducted to predict in-hospital mortality and ICU admission (11, 13–17). For sepsis, NEWS, was assessed for the prediction of in-hospital death with an AUROC of 0.65 (0.61 to 0.68) and ICU admission with an AUROC of 0.64 (0.57 to 0.71), however, the authors highlight that no scoring system has both high sensitivity and specificity for predicting adverse outcomes in sepsis at admission (13). A retrospective analysis of data available at the time of admission, including heart rate, supplementary oxygen, abnormal sodium, and amount of time spent in the emergency department, was used to build a logistic regression model to predict early ICU admission which produced a AUROC of 0.70 (0.67-0.72), and was able to identify 10% of early ICU transfers (14). Some attempts in predicting COVID-19 ICU admission have not performed well (16). However, a model based on age, sex and comorbidities did predict ICU mortality and ICU admission in COVID-19 patients, generating a c-statistic of 0.876 (0.864-0.886) (11). Others have found that CURB-65 scores perform well in predicting in-hospital mortality with an AUC of 0.781, and the qCSI score performed well in predicting ICU admission with an AUC of 0.761 (15). Models with AUC values between 0.86 – 0.88 have been developed for predicting hospitalisation, ICU care and mechanical ventilation (18). Age and BMI were important predictors for hospitalisation, whereas for ICU admission male sex, opacities in chest scans and age were important variables (17). Routine laboratory values predictive of ICU admission and mechanical ventilation included elevated serum lactate dehydrogenase (LDH), C-reactive protein (CRP), anion gap and glucose, in addition to decreased serum calcium, sodium and albumin (17).

Using gene expression signatures to predict clinical outcome or care trajectories, from a sample such as blood, have been infrequently reported in the literature. Previously, an 11-gene host response score was found to perform similarly to SAPS3 and APACHE II as a stand-alone test, from whole blood collected within 30 days of admission when predicting 60-day mortality (AUC: 0.68), in-hospital mortality (AUC: 0.75), shock patients (AUC: 77) and primary MODS or ARDS (AUC: 0.98) (19). In sepsis, 20 and 10 gene panels have been trialed with AUCs between 0.723 to 0.956 being achieved depending on the cohort and the number of genes included in the panel (20).

Genomic analyses such as RNAseq are routinely used to inform clinical decisions (21–24). Turnaround times from sampling to actionable data are continually improving, making their potential

use as point-of-care tools more feasible. In addition, the cost of sequencing continues to decrease and many sequencing platforms are becoming more accessible. In this study, using blood gene expression profiles from 78 SARS-CoV-2 infected patients, machine learning and an emerging topological data analysis approach (25, 26) was used to identify and validate gene signatures that were predictive of ICU admission of patients with COVID-19 disease. This predictive model, demonstrates potential as a valuable tool for personalised treatment and assist in the clinical decision making for hospitalised COVID-19 patients, and provide a point of comparison for evaluating the effects of medical countermeasures.

Materials and methods

Patient cohort and study design

In this study, a cohort of 78 patients presenting hospitalised with COVID-19 were analysed. Samples were collected as part of the CoV-19POC study (ISRCTN trial registry: ISRCTN14966673) as previously described (12). In brief, blood samples were collected in PAXgene tubes within 24 hours of admission to hospital between March and April 2020. All patients were sampled and RNAseq data generated. Detailed patient characteristics and demographics collected at time of admission from medical records, are included in Table 1, generated by gtsummary (27).

Extraction of RNA from clinical samples and Illumina sequencing

Total RNA was extracted from PAXgene BRT using the PAXgene Blood RNA Kit (PreAnalytix), according to the manufactures protocol at Containment Level 3 in a Tripass Class I hood. Libraries were sequenced using 150 bp paired-end reads on an Illumina® NovaSeq 6000.

Data processing and machine learning

Raw paired-end fastq files generated by the NovaSeq were trimmed for the presence of adapter sequences using cutadapt (v.1.2.1), with the -O 3 parameter (28). The fastq files were further trimmed using sickle (v.1.200) with a minimum window quality score of 20 and reads shorter than 15bp are removed from analysis (18). Hisat2 v2.1.0 (29) was used to map the trimmed reads on the reference Homo sapiens genome assembly (release-94) downloaded from the Ensembl FTP site. The resultant alignment files were processed by featureCounts v2.0.0 (30) with the default setting to generate raw read counts per gene. Before further analysis, outlier samples in the hierarchical clustering were removed and low-expression genes (at least 1 read per million in smallest groups) were filtered. The decision trees models to classify ICU admission in COVID-19 samples were built according to the random forest classifier based on gene expression or traits of hospital assay by using randomForest() function in R package "randomForest" (31) with "ntree=500, proximity=TRUE, mtry=5". Variable importance in the random forest models were measured through mean decrease in accuracy and the Gini Index.

Topological data analysis (TDA)

To determine reliability and accuracy of the TDA method presented here, the cohort was divided randomly in two not-overlapping sets, one for training (48 samples) and another for statistical testing (30 samples). Patient demographics and characteristics are presented in Table 2 for the test and training datasets. The average gene expression of ICU samples within the training set was also calculated and its topology of the global differential gene expression was measured by Topological Pathway Mapping, TopMD, without filtering. Such topology was then used as a reference with respect to the topology of global differential gene expression of each sample. Highly modulated pathways are large features of the TopMD Maps; gene pathways of high importance. When performing the regression analysis, *via* Logistic Regression with ElasticNet penalty (see formula below), we stress that the TopMD ICU profile used as reference was computed only on the training set.

To define a gene signature, TopMD profiles were computed for both each patient blood sample and the ICU average gene expression within the training set, relative to the average of all training set samples. From the training ICU profile, a panel of m genes taken from N TopMD-pathways of highest importance was selected and subsequently a feature matrix was constructed to perform the linear regression analysis, as follows.

From the training ICU profile, a reference panel is constructed using the most important N TopMD-pathways and, per each of them, the m most abundant genes. The feature matrix was then constructed associating each sample to a row and each reference gene to a column, that is, the entry (i, j) referred to sample Pi and gene gj. Any matrix entry (i, j) was defined to be 0 whenever the gene gj was not within the TopMD-defined sample panel, that is, gj was not one of the m most abundant genes within the N most important TopMD-pathways for the Pi TopMD-profile. Otherwise, such entry was the relative gene expression of gj for sample Pi.

For the statistical analysis, the Logistic Regression model, with ElasticNet penalty, was used, defined by the following formula:

$$\min_{w,c} \frac{1-p}{2} w^T w + p||w||_1 + C\sum_{i=1}^{n} \log\left(\exp\left(-y_i(X_i^T w + c)\right) + 1\right)$$

Where X is the feature matrix, y the binary classification vector and w is the weights vector. Parameters for this model are C,

TABLE 1 Patient characteristics and demographics grouped by ICU admission status.

Characteristic	N	Overall, N = 78[1]	Not admitted to ICU, N = 51[1]	Admitted to ICU, N = 27[1]	p-value[2]
Dataset split	78				0.43
Test		48 (62%)	33 (65%)	15 (56%)	
Training		30 (38%)	18 (35%)	12 (44%)	
Symptom duration days	78	7 (5, 10)	7 (4, 10)	8 (6, 10)	0.43
LOS (hours)	75	198 (100, 332)	147 (59, 256)	296 (214, 546)	<0.001
Age	78	61 (46, 74)	70 (49, 80)	56 (45, 61)	0.006
Sex	78				0.61
F		26 (33%)	18 (35%)	8 (30%)	
M		52 (67%)	33 (65%)	19 (70%)	
Smoking status	78				0.91
Ex-smoker		31 (40%)	21 (41%)	10 (37%)	
Never		36 (46%)	22 (43%)	14 (52%)	
Unknown		7 (9.0%)	5 (9.8%)	2 (7.4%)	
Yes		4 (5.1%)	3 (5.9%)	1 (3.7%)	
Ethnicity	78				0.037
White - British		47 (60%)	33 (65%)	14 (52%)	
White – Any other white background		6 (7.7%)	6 (12%)	0 (0%)	
Asian or Asian British - Indian		3 (3.8%)	2 (3.9%)	1 (3.7%)	
Asian or Asian British – Any other Asian background		13 (17%)	5 (9.8%)	8 (30%)	
Black or Black British - Caribbean		2 (2.6%)	2 (3.9%)	0 (0%)	
Black or Black British - African		6 (7.7%)	2 (3.9%)	4 (15%)	
Unknown		1 (1.3%)	1 (2.0%)	0 (0%)	
Clinical Metrics					
Hypertension	78				0.72
No		45 (58%)	29 (57%)	16 (59%)	
Unknown		4 (5.1%)	2 (3.9%)	2 (7.4%)	
Yes		29 (37%)	20 (39%)	9 (33%)	
CV disease	78				0.17
No		59 (76%)	37 (73%)	22 (81%)	
Unknown		3 (3.8%)	1 (2.0%)	2 (7.4%)	
Yes		16 (21%)	13 (25%)	3 (11%)	
Resp Disease other	78				0.47
No		54 (69%)	35 (69%)	19 (70%)	
Unknown		3 (3.8%)	1 (2.0%)	2 (7.4%)	
Yes		21 (27%)	15 (29%)	6 (22%)	
Asthma	78				0.51
No		62 (79%)	41 (80%)	21 (78%)	
Unknown		3 (3.8%)	1 (2.0%)	2 (7.4%)	
Yes		13 (17%)	9 (18%)	4 (15%)	
COPD	78				0.49
No		68 (87%)	45 (88%)	23 (85%)	
Unknown		3 (3.8%)	1 (2.0%)	2 (7.4%)	
Yes		7 (9.0%)	5 (9.8%)	2 (7.4%)	
CKD	78				0.53
No		69 (88%)	46 (90%)	23 (85%)	
Unknown		3 (3.8%)	1 (2.0%)	2 (7.4%)	
Yes		6 (7.7%)	4 (7.8%)	2 (7.4%)	
CLD	78				0.55

(Continued)

TABLE 1 Continued

Characteristic	N	Overall, N = 78[1]	Not admitted to ICU, N = 51[1]	Admitted to ICU, N = 27[1]	p-value[2]
No		72 (92%)	48 (94%)	24 (89%)	
Unknown		3 (3.8%)	1 (2.0%)	2 (7.4%)	
Yes		3 (3.8%)	2 (3.9%)	1 (3.7%)	
Diabetes	78				0.50
No		56 (72%)	38 (75%)	18 (67%)	
Unknown		3 (3.8%)	1 (2.0%)	2 (7.4%)	
Yes		19 (24%)	12 (24%)	7 (26%)	
Active malignancy	78				0.11
No		69 (88%)	44 (86%)	25 (93%)	
Unknown		3 (3.8%)	1 (2.0%)	2 (7.4%)	
Yes		6 (7.7%)	6 (12%)	0 (0%)	
Dementia	78				0.048
No		67 (86%)	42 (82%)	25 (93%)	
Unknown		3 (3.8%)	1 (2.0%)	2 (7.4%)	
Yes		8 (10%)	8 (16%)	0 (0%)	
Immunosuppressed[+]	78				0.16
No		70 (90%)	48 (94%)	22 (81%)	
Unknown		4 (5.1%)	1 (2.0%)	3 (11%)	
Yes		4 (5.1%)	2 (3.9%)	2 (7.4%)	
Abx during admission	78	72 (92%)	46 (90%)	26 (96%)	0.66
Blood chemistry					
Haemoglobin	77	132 (124, 148)	132 (122, 140)	144 (128, 151)	0.20
White blood cells	77	7.8 (5.7, 11.5)	6.2 (4.9, 10.7)	9.4 (6.8, 11.5)	0.026
Platelets	77	236 (184, 291)	227 (182, 280)	255 (186, 294)	0.45
Neutrophils	77	6.0 (4.0, 9.6)	4.8 (3.6, 8.1)	8.2 (5.2, 9.7)	0.012
Lymphocytes	77	1.00 (0.80, 1.20)	1.00 (0.80, 1.18)	1.00 (0.75, 1.30)	0.72
Sodium	77	135 (133, 138)	136 (133, 138)	135 (132, 136)	0.091
Potassium	71	4.00 (3.65, 4.40)	3.90 (3.65, 4.35)	4.00 (3.75, 4.43)	0.44
Urea	77	6.3 (4.7, 9.9)	6.4 (4.3, 10.1)	6.3 (4.8, 8.9)	0.95
Creatine	77	86 (67, 110)	84 (67, 109)	88 (66, 108)	0.79
Albumin	73	34 (30, 35)	34 (31, 36)	31 (28, 34)	0.009
Bilirubin	73	11 (8, 13)	10 (8, 12)	11 (10, 14)	0.063
Alanine Aminotransferase	70	34 (24, 70)	28 (21, 56)	37 (32, 77)	0.050
Alkaline Phosphatase	73	89 (61, 115)	80 (56, 110)	96 (62, 124)	0.12
Total Protein	72	70 (66, 73)	70 (67, 73)	71 (66, 74)	0.85
LDH	52	766 (561, 1,133)	650 (506, 776)	1,130 (850, 1,382)	<0.001
Ferritin	61	678 (354, 1,693)	521 (203, 750)	1,427 (908, 2,073)	<0.001
D-dimer	45	469 (320, 942)	456 (298, 1,426)	535 (385, 812)	0.53
Trop	60	12 (5, 46)	11 (4, 28)	12 (8, 63)	0.25
CRP	77	120 (52, 164)	80 (22, 131)	168 (128, 254)	<0.001
Cytokines/Chemokines					
IL-6 (pg/mL)	78	52 (32, 106)	43 (30, 85)	82 (43, 132)	0.030
TNFα (pg/mL)	78	20 (17, 25)	20 (16, 25)	22 (19, 25)	0.27
IL-8 (pg/mL)	78	35 (26, 59)	34 (25, 53)	49 (34, 64)	0.10
IL-1β9 (pg/mL)	78	0.39 (0.26, 0.56)	0.35 (0.24, 0.48)	0.47 (0.31, 0.66)	0.056
GM-CSF (pg/mL)	78	1.30 (0.80, 1.86)	1.20 (0.77, 2.28)	1.49 (1.01, 1.79)	0.43
IFNg (pg/mL)	78	12 (4, 27)	9 (2, 27)	16 (8, 35)	0.072

(Continued)

TABLE 1 Continued

Characteristic	N	Overall, N = 78[1]	Not admitted to ICU, N = 51[1]	Admitted to ICU, N = 27[1]	p-value[2]
IL-10 (pg/mL)	78	16 (10, 28)	15 (8, 27)	17 (13, 29)	0.22
IL-33 (pg/mL)	78	0.35 (0.17, 0.61)	0.28 (0.15, 0.39)	0.46 (0.35, 0.91)	0.009
Physiological Metrics					
Heart Rate	78	98 (85, 109)	92 (82, 107)	102 (94, 110)	0.064
Systolic Blood Pressure	78	132 (122, 143)	135 (122, 145)	128 (124, 134)	0.14
Respiration rate	78	26 (20, 32)	24 (20, 28)	28 (23, 34)	0.054
Oxygen Saturation	78	95 (92, 96)	96 (93, 97)	95 (90, 96)	0.047
Temperature (°C)	76	37.20 (36.60, 38.20)	37.20 (36.65, 38.10)	37.20 (36.60, 38.40)	0.61
O2	78	37 (47%)	17 (33%)	20 (74%)	<0.001
NEWS2	76	6 (4, 7)	5 (2, 6)	6 (5, 8)	0.012
CXR	78	77 (99%)	50 (98%)	27 (100%)	>0.99
Consolidation or infiltrates	77	66 (86%)	39 (78%)	27 (100%)	0.007
CT	78	8 (10%)	5 (9.8%)	3 (11%)	>0.99
ICU specific metrics					
Duration O2	78	19 (5, 112)	9 (1, 17)	161 (110, 397)	<0.001
NIV duration	78	0 (0, 13)	0 (0, 0)	25 (6, 49)	<0.001
IV duration	78	0 (0, 0)	0 (0, 0)	114 (0, 277)	<0.001
Optiflow duration	78	7 (9.0%)	0 (0%)	7 (26%)	<0.001
ECMO	75	1 (1.3%)	0 (0%)	1 (4.2%)	0.32
Died within 30 days of admission	77	15 (19%)	12 (24%)	3 (12%)	0.21

[1]n (%); Median (IQR) [2] arson's Chi-squared test; Wilcoxon rank sum test; Fisher's exact test.
[+]Immunosuppressed definition derived from UKHSA Influenza treatment guidance.
ICU, Intensive Care Unit; CV, Cardiovascular; COPD, Chronic obstructive pulmonary disease; CKD, Chronic kidney disease; CLD, Chronic liver disease; LDH, Lactate dehydrogenase; IL, Interleukin; TNF, Tumour necrosis factor; GMCSF, Granulocyte-macrophage colony-stimulating factor; IFN, Interferon; NEWS2, National early warning score 2; O2, administration of supplementary oxygen; CXR, Chest x-ray; CT, Computational tomography; NIV, Non-invasive ventilation; IV, Invasive ventilation; ECMO, Extracorporeal membrane oxygenation.

a regularisation parameter (improving numerical stability), and ρ which controls the strength of l1 and l2 regularisation, respectively the first and second member in the formula. The best performing panel of genes was selected, among all the combination of N and m with value ranging from 1 to 100, given that $m \leq N$. The best performing model, with respect to predictive error, was obtained using N=10 TopMD-pathways and m=5 genes. The regression model allows naturally to define the belongingness probability to the positive class, the ICU class in this case. For statistical testing purposes, each patient blood sample in the test set is predicted to be ICU when such probability is higher than 0.5.

Statistical analysis

Statistical testing was performed including a Shapiro-Wilk test to assess for data normality followed with either an unpaired parametric T-test (Shapiro-Wilk test p-value > 0.05) or an unpaired non-parametric Wilcoxon test (Shapiro-Wilk test p-value< 0.05) for continuous data, or a Chi-square test for categorical data.

Results

To identify transcripts that were predictive of ICU admission for those with COVID-19 disease, the transcriptome of blood samples from infected patients was analysed.

Patient characteristics

These samples were collected through the CoV-POC trial in early 2020. Out of the 78 samples included in this study, 48 were included in the training dataset and 30 in the test dataset. The median age of the study population was 61 (IQR: 46-74) 52 were male (67%) and 26 were female (33%). The most common comorbidities were hypertension (37%), chronic respiratory disease (27%) and diabetes mellitus (24%) (Table 1). 27 were admitted to ICU of which 15 died within 30 days of admission. In this dataset there was no difference in sex between those admitted to ICU and those not admitted to ICU, p = 0.61. Age was different between those admitted to ICU and those not admitted to ICU, p 0.006, median age of 56 and 70 years respectively. Table 1 shows that data points from blood

TABLE 2 Patient characteristics and demographics grouped by test or train status.

Characteristic	N	Overall, N = 78[1]	Test, N = 48[1]	Training, N = 30[1]	p-value[2]
Symptom duration days	78	7 (5, 10)	8 (6, 10)	6 (2, 10)	0.076
Length of stay (hours)	75	198 (100, 332)	206 (104, 331)	186 (80, 376)	0.98
Age (years)	78	61 (46, 74)	56 (41, 72)	66 (58, 76)	0.028
Sex	78				0.62
F		26 (33%)	15 (31%)	11 (37%)	
M		52 (67%)	33 (69%)	19 (63%)	
Smoking status	78				0.90
Ex-smoker		31 (40%)	19 (40%)	12 (40%)	
Never		36 (46%)	21 (44%)	15 (50%)	
Unknown		7 (9.0%)	5 (10%)	2 (6.7%)	
Yes		4 (5.1%)	3 (6.2%)	1 (3.3%)	
Ethnicity	78				0.034
White - British		47 (60%)	27 (56%)	20 (67%)	
White – Any other white background		6 (7.7%)	5 (10%)	1 (3.3%)	
Asian or Asian British - Indian		3 (3.8%)	1 (2.1%)	2 (6.7%)	
Asian or Asian British – Any other Asian background		13 (17%)	11 (23%)	2 (6.7%)	
Black or Black British - Caribbean		2 (2.6%)	2 (4.2%)	0 (0%)	
Black or Black British - African		6 (7.7%)	1 (2.1%)	5 (17%)	
Unknown		1 (1.3%)	1 (2.1%)	0 (0%)	
Clinical Metrics					
Hypertension	78				0.008
No		45 (58%)	34 (71%)	11 (37%)	
Unknown		4 (5.1%)	2 (4.2%)	2 (6.7%)	
Yes		29 (37%)	12 (25%)	17 (57%)	
CV disease	78				0.55
No		59 (76%)	38 (79%)	21 (70%)	
Unknown		3 (3.8%)	1 (2.1%)	2 (6.7%)	
Yes		16 (21%)	9 (19%)	7 (23%)	
Resp Disease other	78				0.39
No		54 (69%)	32 (67%)	22 (73%)	
Unknown		3 (3.8%)	1 (2.1%)	2 (6.7%)	
Yes		21 (27%)	15 (31%)	6 (20%)	
Asthma	78				0.71
No		62 (79%)	39 (81%)	23 (77%)	
Unknown		3 (3.8%)	1 (2.1%)	2 (6.7%)	
Yes		13 (17%)	8 (17%)	5 (17%)	
COPD	78				0.22
No		68 (87%)	41 (85%)	27 (90%)	
Unknown		3 (3.8%)	1 (2.1%)	2 (6.7%)	
Yes		7 (9.0%)	6 (12%)	1 (3.3%)	
CKD	78				0.018
No		69 (88%)	46 (96%)	23 (77%)	
Unknown		3 (3.8%)	1 (2.1%)	2 (6.7%)	
Yes		6 (7.7%)	1 (2.1%)	5 (17%)	
CLD	78				0.80
No		72 (92%)	45 (94%)	27 (90%)	
Unknown		3 (3.8%)	1 (2.1%)	2 (6.7%)	
Yes		3 (3.8%)	2 (4.2%)	1 (3.3%)	

(Continued)

TABLE 2 Continued

Characteristic	N	Overall, N = 78[1]	Test, N = 48[1]	Training, N = 30[1]	p-value[2]
Diabetes	78				0.048
No		56 (72%)	39 (81%)	17 (57%)	
Unknown		3 (3.8%)	1 (2.1%)	2 (6.7%)	
Yes		19 (24%)	8 (17%)	11 (37%)	
Active malignancy	78				0.48
No		69 (88%)	44 (92%)	25 (83%)	
Unknown		3 (3.8%)	1 (2.1%)	2 (6.7%)	
Yes		6 (7.7%)	3 (6.2%)	3 (10%)	
Dementia	78				0.45
No		67 (86%)	43 (90%)	24 (80%)	
Unknown		3 (3.8%)	1 (2.1%)	2 (6.7%)	
Yes		8 (10%)	4 (8.3%)	4 (13%)	
Immunosuppressed[+]	78				0.004
No		70 (90%)	47 (98%)	23 (77%)	
Unknown		4 (5.1%)	1 (2.1%)	3 (10%)	
Yes		4 (5.1%)	0 (0%)	4 (13%)	
Abx during admission	78	72 (92%)	44 (92%)	28 (93%)	>0.99
Blood Chemistry					
Haemoglobin	77	132 (124, 148)	132 (124, 152)	132 (127, 144)	0.39
White blood cells	77	7.8 (5.7, 11.5)	7.1 (5.6, 11.2)	9.0 (6.0, 11.7)	0.32
Platelets	77	236 (184, 291)	228 (181, 289)	260 (191, 291)	0.45
Neutrophils	77	6.0 (4.0, 9.6)	4.9 (3.8, 8.5)	7.4 (4.4, 9.7)	0.14
Lymphocytes	77	1.00 (0.80, 1.20)	1.00 (0.80, 1.20)	1.00 (0.70, 1.20)	0.56
Sodium	77	135 (133, 138)	136 (134, 138)	134 (133, 136)	0.011
Potassium	71	4.00 (3.65, 4.40)	3.95 (3.75, 4.40)	4.00 (3.65, 4.35)	0.94
Urea	77	6.3 (4.7, 9.9)	5.8 (4.3, 9.5)	7.2 (5.8, 9.9)	0.20
Creatine	77	86 (67, 110)	84 (66, 102)	87 (76, 125)	0.47
Albumin	73	34 (30, 35)	34 (31, 36)	31 (28, 34)	0.012
Bilirubin	73	11 (8, 13)	11 (8, 14)	10 (8, 13)	0.71
Alanine Aminotransferase	70	34 (24, 70)	34 (26, 65)	36 (22, 75)	0.57
Alkaline Phosphatase	73	89 (61, 115)	93 (61, 117)	84 (62, 106)	0.54
Total Protein	72	70 (66, 73)	70 (67, 75)	69 (66, 72)	0.41
LDH	52	766 (561, 1,133)	698 (540, 932)	1,022 (661, 1,380)	0.061
Ferritin	61	678 (354, 1,693)	638 (421, 1,291)	970 (339, 1,978)	0.51
D-dimer	45	469 (320, 942)	448 (350, 886)	535 (300, 884)	0.89
Trop	60	12 (5, 46)	10 (5, 50)	13 (9, 34)	0.33
CRP	77	120 (52, 164)	92 (44, 155)	135 (108, 185)	0.046
Cytokines/Chemokines					
IL-6 (pg/ml)	78	52 (32, 106)	41 (25, 85)	82 (44, 174)	0.002
TNFα (pg/ml)	78	20 (17, 25)	20 (15, 24)	21 (18, 28)	0.090
IL-8(pg/ml)	78	35 (26, 59)	34 (21, 52)	49 (32, 72)	0.006
IL-1β9 (pg/ml)	78	0.39 (0.26, 0.56)	0.36 (0.24, 0.49)	0.46 (0.29, 0.61)	0.20
GM-CSF (pg/ml)	78	1.30 (0.80, 1.86)	1.21 (0.76, 1.65)	1.47 (0.82, 2.58)	0.20
IFNg (pg/ml)	78	12 (4, 27)	13 (2, 27)	11 (6, 28)	0.73
IL-10 (pg/ml)	78	16 (10, 28)	14 (8, 24)	20 (14, 31)	0.052
IL-33(pg/ml)	78	0.35 (0.17, 0.61)	0.34 (0.17, 0.51)	0.36 (0.17, 0.69)	0.50
Physiological Metrics					
Heart Rate	78	98 (85, 109)	102 (88, 110)	90 (85, 100)	0.034

(Continued)

TABLE 2 Continued

Characteristic	N	Overall, N = 78[1]	Test, N = 48[1]	Training, N = 30[1]	p-value[2]
Systolic Blood Pressure	78	132 (122, 143)	130 (120, 138)	134 (126, 145)	0.20
Respiration Rate	78	26 (20, 32)	24 (20, 32)	26 (22, 33)	0.17
Oxygen Saturation	78	95 (92, 96)	96 (93, 97)	94 (91, 96)	0.051
Temperature (°C)	76	37.20 (36.60, 38.20)	37.20 (36.60, 38.23)	37.20 (36.68, 38.12)	0.88
O2	78	37 (47%)	18 (38%)	19 (63%)	0.026
NEWS2	76	6 (4, 7)	6 (3, 7)	6 (5, 6)	0.62
CXR	78	77 (99%)	48 (100%)	29 (97%)	0.38
Consolidation or infiltrates	77	66 (86%)	40 (83%)	26 (90%)	0.52
CT	78	8 (10%)	6 (12%)	2 (6.7%)	0.70
ICU Specific Metrics					
Duration O2*	78	19 (5, 112)	16 (4, 88)	24 (14, 179)	0.091
ICU admission	78	27 (35%)	15 (31%)	12 (40%)	0.43
NIV duration*	78	0 (0, 13)	0 (0, 16)	0 (0, 9)	0.93
IV duration*	78	0 (0, 0)	0 (0, 0)	0 (0, 151)	0.030
Optiflow duration*	78	7 (9.0%)	3 (6.2%)	4 (13%)	0.42
ECMO*	75	1 (1.3%)	1 (2.1%)	0 (0%)	>0.99
Died within 30 days of admission*	77	15 (19%)	6 (12%)	9 (31%)	0.047

[1]Median (IQR); n (%) [2]Wilcoxon rank sum test; Pearson's Chi-squared test; Fisher's exact test.
* Metric excluded from machine learning analysis.
[†]Immunosuppressed definition derived from UKHSA Influenza treatment guidance.
ICU, Intensive Care Unit; CV, Cardiovascular; COPD, Chronic obstructive pulmonary disease; CKD, Chronic kidney disease; CLD, Chronic liver disease; LDH, Lactate dehydrogenase; IL, Interleukin; TNF, Tumour necrosis factor; GMCSF, Granulocyte-macrophage colony-stimulating factor; IFN, Interferon; NEWS2, National early warning score 2; O2, administration of supplementary oxygen; CXR, Chest x-ray; CT, Computational tomography; NIV, Non-invasive ventilation; IV, Invasive ventilation; ECMO, Extracorporeal membrane oxygenation.

chemistry, cytokine/chemokine assessment and physiological metrics are significantly different between the patients admitted to ICU and not admitted to ICU. Including white blood cell count, neutrophil count, albumin, LDH, ferritin, CRP, IL-6, IL-33, Oxygen saturation, administration of oxygen, NEWS and consolidation of infiltrates. Patient characteristics and demographics are also shown for the test and training split (Table 2).

Machine learning

Combinations of the top 30 important genes were identified by Random Forest analysis predictive of ICU admission in the test dataset (Figure 1), achieving good accuracy (0.73) and a ROC of 0.68. The higher the value of importance of the variable (mean decrease gini score), the higher the importance of the genes in the model. In this analysis, the gene that was most associated with the decision to admit to ICU was family with sequence similarity 219 member A (FAM219A) gene.

Topological data analysis

TopMD Pathway Biomarker Analysis defined a model with 79 genes identified from TopMD clusters predictive of ICU admission in the test dataset with accuracy: 0.72 and ROC AUC: 0.76 (Figure 2). The genes of this predictive signature were features of the top 10 pathways with top 10 genes for a total of 79 genes overall; differentially activated gene pathways between patients admitted to ICU or not admitted to ICU in the training dataset.

The top 3 identified pathways predictive of ICU admission are involved in EGFR, PPAR-α and TGFβ signalling pathways

TopMD analysis identified pathways associated with ICU admission by defining and ranking pathways by their topological volume, the sum of normalised differential expression. The gene with the largest fold change was termed the peak-gene of the identified pathway. The top pathway had peak gene SNX2, associated with epidermal growth factor receptor (EGFR) signalling, followed by ACAA1, associated with Peroxisome proliferator-activated receptor alpha (PPAR-α) signalling and finally, FAM89B associated with Transforming growth factor beta (TGF-β) signalling (Figure 3). Additional peak genes and pathways are presented in Supplementary Figure 1. These consist of peak genes PHETA1, KEAP1, BAIAP2, TRAPPC6A, AGXT, HES1 and CDK5R1. Highlighting pathways such as phosphatidylinositol signalling, and glyoxylate and dicarboxylate metabolism (Supplementary Figure 1).

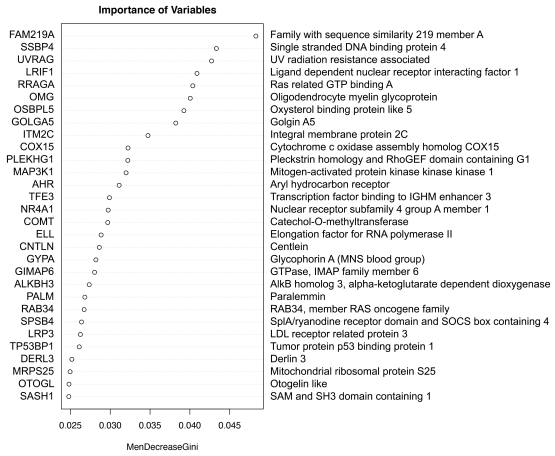

FIGURE 1
The importance of genes in a classification of ICU admission with Random Forest. The higher the value of importance of the variable (mean decrease gini score), the higher the importance of the gene(s) in the model.

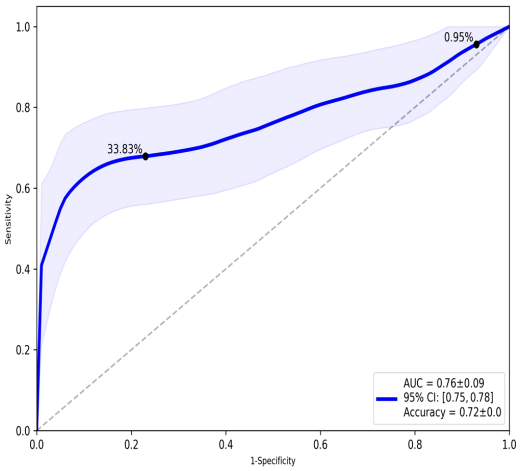

FIGURE 2
ROC analysis of the overall performance of the TopMD-defined gene signature predictive of ICU admission. ROC curve with split 62/38, using top 10 pathways with top 10 genes for a total of 79 genes overall.

Discussion

The emergence of the novel infectious agent SARS-CoV-2 has had a huge impact on healthcare systems worldwide and highlighted the importance of pandemic preparedness and management of limited healthcare resources. Here we demonstrate using retrospective analysis of gene expression data from patients hospitalised with COVID-19, at the point of admission, that there are markers that can predict the patient's clinical outcome.

Like many other studies have previously identified, there were significant differences between clinical observations and physiological metrics for those who were and were not admitted to the ICU. In this study population, this included white blood cell count, neutrophil count, albumin, LDH, ferritin, CRP, IL-6, IL-33, oxygen saturation, NEWS, and consolidation of infiltrates (Table 1). This is in line with previous studies (17, 32). To further understand the host response in this study population and to determine whether mRNA signatures were able to predict ICU admission, a combination of topological analysis and machine learning was employed to identify genes and related pathways that predict disease.

To test the predictive nature of the model, data was split randomly into training and test datasets. There were differences in variables between the training and test cohorts (Table 2). Differences in measured variables are expected with high dimensional profiling of randomly split cohorts. The results of this study represent biological mechanisms which are consistent across the training and test cohorts, however, they are likely to be not the only mechanisms at play in driving COVID-19 disease severity, including those related to variables not balanced between the training and test cohorts.

COVID-19 gene expression prognosis studies are limited (33, 34). Scoring algorithm of molecular subphenotypes (SAMS) have been used to identify 50-gene risk profiles for COVID-19 which discriminate between mild and severe disease (33). Such

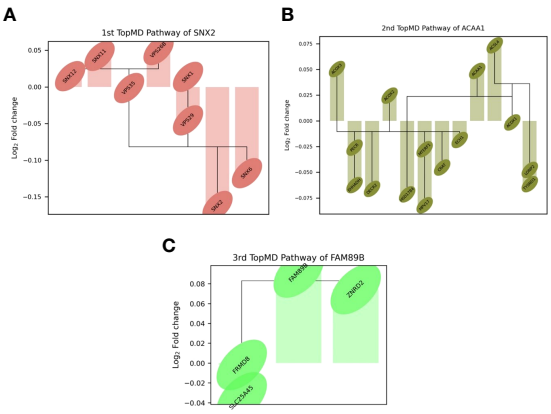

FIGURE 3
Differential expression of top genes in the top 3 pathways between patients admitted to ICU and not admitted to ICU of the training set. Connections represent known gene interactions according to STRING-db. **(A)** SNX2 - controlling epidermal growth factor receptor (EGFR) presentation, **(B)** ACAA1-peak pathway, representing peroxisome proliferator-activated receptor alpha (PPAR-α) signalling, **(C)** FAM89B-peak pathway, mediating transforming growth factor beta (TGF-β) signalling. Pathways and genes identified by topological data analysis, TopMD.

profiles were able to predict ICU admission, the need for mechanical ventilation and mortality with an AUC of 0.77, 0.75 and 0.74 respectively. Immunophenotyping in addition to transcriptomic analysis on data derived from COVID-19 patients has led to the discovery of molecules that were associated with more severe disease, however, no AUC values were presented (34). In our analysis we ranked the top 30 most important genes with random forest, achieving an accuracy of 0.73 and ROC of 0.68, where FAM219A was identified as the most important variable for predicting ICU admission. FAM219A has been identified as a potential interactor with the SARS-CoV-2 M protein (35), however, the transcripts function is unknown.

TopMD analysis is an emerging topological data analysis (TDA) technology. When using high dimensional and noisy biological data sets, such as gene expression data, TDA approaches are particularly advantageous and have been successful in disease sub-phenotyping studies (25, 36–40). These approaches facilitate measurement of genes relative to their networks in disease context as opposed to the conventional differential abundance analysis, traditionally utilised in biomarker discovery. The TopMD algorithm was applied to gene expression data from COVID-19 patients at point of admission, with varying care trajectories. Our analysis shows that gene expression signatures in blood predict ICU admission. Gene expression signatures predictive of ICU admission were defined by machine learning and TopMD with accuracy: 0.73 and ROC: 0.68 and accuracy: 0.72 and ROC: 0.76 respectively. Topological analysis with TopMD improved the predictive model in comparison to the machine learning approach, demonstrating the advantages of considering the shape of data relative to underlying biological mechanisms above standard bioinformatic approaches which rely on statistical analysis of abundances of isolated molecules in vastly reduced, noisy, 'omics datasets.

The TDA analysis of gene expression relative to pathways by TopMD acts as a global pathway analysis tool, defining patterns of differentially expressed genes with evidenced interactions. The top pathways differentially modulated between patients admitted to ICU and not admitted to ICU were 1st, SNX2-peak pathway, controlling epidermal growth factor receptor (EGFR) presentation, 2nd, ACAA1-peak pathway, representing peroxisome proliferator-activated receptor alpha (PPAR-α) signalling and 3rd, FAM89B-peak pathway, mediating transforming growth factor beta (TGF-β) signalling. (Figure 2). SNX2 was the top peak gene identified through TopMD analysis and is associated with EGFR signalling pathways. Dysfunctional EGFR signalling has been identified as a contributing factor to pulmonary fibrotic-like illness during SARS-CoV infections in animal models following the SARS-CoV pandemic in 2002, where authors speculated that inhibiting EGFR pathways would prevent fibrotic disease (41, 42). This is further supported by similar findings in SARS-CoV-2 infected patients, whereby EGFR was again found to be a regulator of pulmonary fibrosis (43). Inhibiting this pathway with nimotuzumab, a monoclonal antibody against EGFR, was found to decrease inflammatory markers and fibrosis associated with COVID-19 (44, 45). ACAA1; the peak gene of the second top pathway; is representative of PPAR-α signalling. PPAR-α signalling is a key mediator of inflammation, and like EGFR a potential marker for acute lung injury. Modulation of PPAR-α signalling by SARS-CoV-2 may alter lipid metabolism in the lung epithelial cells, contributing to lipotoxicity, inflammation and untoward respiratory effects (46). Therapeutics such as fenofibrate that target PPAR-α have been recommended to enter clinical trials (47). Where others have proposed that oleoylethanolamide (OEA), a high-affinity agonist to PPAR-α and ultramicronised palmitoylethanolamide (PEA), may have therapeutic effects by suppressing inflammatory responses (48, 49). Where PEA is also able to inhibit SARS-CoV-2 entry and replication (50). Interestingly, others have identified PPAR-α as a potential mediator neuroinflammation in COVID-19 (51). The third Top pathway had peak gene FAM89B, representing TGFβ signalling pathway, which is also associated with pulmonary fibrosis (52). TGFβ is a known regulator of immune reactions and its signalling is associated with fibrosis (53, 54). In the context of COVID-19, TGFβ gene signatures are observed in plasmablasts following seroconversion and is associated with a chronic immune reaction and severe disease (52). Within the ten pathways, peak gene KEAP1 was identified as a biomarker for ICU admission. KEAP1 is most well-known for its interaction with Nrf2 facilitating its ubiquitination, where exploiting this interaction to manage cytokine storms has been discussed in the context of COVID-19 (55, 56).

A key limitation of this study is that only one time point was considered in this analysis, although this was at the point of admission to hospital, which demonstrates its potential value as a POC tool, it does not consider the dynamic element of disease-course, future studies would benefit from gene expression measured at multiple time points. RNA sequencing can take a long time, however, with the third-generation sequencing platforms, rapid biomarker discovery and implementation at POC may be possible in the future. RNA sequencing at the bedside for personalised and precision medicine may not be an accessible solution for healthcare systems at this point in time, however, our data and analysis shows the potential use of sequencing data for prognosis. As sequencing costs continue to fall and accessibility to sequencing increases, this concept could progress to the bedside. In the case of retrospective analysis, useful pathways can also be identified informing future research and thus our understanding of disease.

Prognostic gene expression signatures identified here, upon further validation in independent cohorts, could be used to

inform management of healthcare resources and improve outcomes of patients with COVID-19. Gene expression signatures measured in global RNAseq transcriptomics data could be applied across health and disease for precision medicine.

Data availability statement

The datasets presented in this study can be found in online repositories. The names of the repository/repositories and accession number(s) can be found below: European Genome-Phenome Archive, EGAS00001005971.

Ethics statement

The studies involving human participants were reviewed and approved by South Central Hampshire A Research Ethics Committee. The patients/participants provided their written informed consent to participate in this study.

Author contributions

TC and DB conceptualised the study. SP and NB screened and recruited the patients and collected the data in the CoV-19POC trials. RP-R and CH sample processing and experiments. RP-R, XD, AG, JS, and JH performed data analysis. RP-R, AG, JS, and JH drafted the article, and editing. All authors read and approved the final manuscript.

Funding

The author(s) disclosed receipt of the following financial support for the research, authorship, and/or publication of this article: the CoV-19POC trial was funded by University Hospital Southampton Foundation Trust (UHSFT). In addition, the CoV-19POC trials were supported by the NIHR Southampton Clinical Research Facility and NIHR Southampton Biomedical Research Centre (BRC). JLe was supported by a PhD studentship from the NIHR Southampton BRC (no. NIHR-INF-0932). NB was supported by the NIHR Clinical Lecturer scheme. JH, RP-R, CH, and XD were supported by the US Food and Drug Administration Medical Countermeasures Initiative (no 75F40120C00085) awarded to JH. MP was supported by a Sir Henry Dale Fellowship from Welcome Trust and The Royal Society (no. 109377/Z/15/Z). TC was supported by a NIHR Post-Doctoral Fellowship (no. 2016-09-061). DB and her laboratory are supported by a NIHR Research Professorship (no. RP-2016-07-011). TopMD, the University of Southampton and the University of Liverpool are members of the DRAGON consortium, which received funding from the Innovative Medicines Initiative 2 Joint Undertaking (JU) under grant agreement no 101005122. The funders had no role in study design, data collection and analysis, decision to publish, or preparation of the manuscript.

Acknowledgments

The authors would like to acknowledge and gives thanks to the patients who kindly participated in this study and to all the clinical staff at University Hospital Southampton Foundation Trust who cared for them. The DRAGON consortium is a group of high-tech SMEs, academic research institutes, biotech and pharma partners, affiliated patient-centered organisations and professional societies aiming to apply artificial intelligence for improved and more rapid diagnosis and prognosis in COVID-19.) Further details may be found at https://www.imi.europa.eu/projects-results/project-factsheets/dragon.

Conflict of interest

TC has received speaker fees, honoraria, travel reimbursement, and equipment and consumables free of charge for the purposes of research from BioFire diagnostics LLC and BioMerieux. TC has received discounted equipment and consumables for the purposes of research from QIAGEN. TC has received consultancy fees from Biofire diagnostics LLC, BioMerieux, Synairgen research Ltd, Randox laboratories Ltd and Cidara therapeutics. TC has been a member of advisory boards for Roche and Janssen and has received reimbursement for these. TC is member of two independent data monitoring committees for trials sponsored by Roche. TC has previously acted as the UK chief investigator for trials sponsored by Janssen. TC is currently a member of the NHSE COVID-19 Testing Technologies Oversight Group and the NHSE COVID-19 Technologies Validation Group. JS is a founding director, CEO, employee, and shareholder in TopMD Precision Medicine Ltd. FS is a founding director, CTO, employee, and shareholder in TopMD Precision Medicine Ltd. PS is a founding director, employee and shareholder in TopMD Precision Medicine Ltd. AG is an employee

and shareholder in TopMD Precision Medicine Ltd. RP-R is an employee at TopMD Precision Medicine Ltd.

The remaining authors declare that the research was conducted in the absence of any commercial or financial relationships that could be construed as a potential conflict of interest.

Publisher's note

All claims expressed in this article are solely those of the authors and do not necessarily represent those of their affiliated organizations, or those of the publisher, the editors and the reviewers. Any product that may be evaluated in this article, or claim that may be made by its manufacturer, is not guaranteed or endorsed by the publisher.

Supplementary material

The Supplementary Material for this article can be found online at: https://www.frontiersin.org/articles/10.3389/fimmu.2022.988685/full#supplementary-material

References

1. Dorward DA, Russell CD, Um IH, Elshani M, Armstrong SD, Penrice-Randal R, et al. Tissue-specific immunopathology in fatal COVID-19. *Am J Respir Crit Care Med* (2021) 203(2):192–201. doi: 10.1164/rccm.202008-3265OC

2. Russell CD, Valanciute A, Gachanja NN, Stephen J, Penrice-Randal R, Armstrong SD, et al. Tissue proteomic analysis identifies mechanisms and stages of immunopathology in fatal COVID-19. *Am J Respir Cell Mol Biol* (2022) 66 (2):196–205. doi: 10.1165/rcmb.2021-0358OC

3. Lal A, Erondu NA, Heymann DL, Gitahi G, Yates R. Fragmented health systems in COVID-19: rectifying the misalignment between global health security and universal health coverage. *Lancet* (2021) 397(10268):61–7. doi: 10.1016/S0140-6736(20)32228-5

4. Liu X, Speranza E, Muñoz-Fontela C, Haldenby S, Rickett NY, Garcia-Dorival I, et al. Transcriptomic signatures differentiate survival from fatal outcomes in humans infected with Ebola virus. *Genome Biol* (2017) 18(1):4. doi: 10.1186/s13059-016-1137-3

5. Ye W, Chen G, Li X, Lan X, Ji C, Hou M, et al. Dynamic changes of d-dimer and neutrophil-lymphocyte count ratio as prognostic biomarkers in COVID-19. *Respir Res* (2020) 21(1):169. doi: 10.1186/s12931-020-01428-7

6. Aboughdir M, Kirwin T, Abdul Khader A, Wang B. Prognostic value of cardiovascular biomarkers in COVID-19: A review. *Viruses* (2020) 12(5):527. doi: 10.3390/v12050527

7. Danlos FX, Grajeda-Iglesias C, Durand S, Sauvat A, Roumier M, Cantin D, et al. Metabolomic analyses of COVID-19 patients unravel stage-dependent and prognostic biomarkers. *Cell Death Dis* (2021) 12(3):258. doi: 10.1038/s41419-021-03540-y

8. Ponti G, Maccaferri M, Ruini C, Tomasi A, Ozben T. Biomarkers associated with COVID-19 disease progression. *Crit Rev Clin Lab Sci* (2020) 57(6):389–99. doi: 10.1080/10408363.2020.1770685

9. Kermali M, Khalsa RK, Pillai K, Ismail Z, Harky A. The role of biomarkers in diagnosis of COVID-19 - a systematic review. *Life Sci* (2020) 254:117788. doi: 10.1016/j.lfs.2020.117788

10. Zahran AM, El-Badawy O, Ali WA, Mahran ZG, Mahran E, Rayan A. Circulating microparticles and activated platelets as novel prognostic biomarkers in COVID-19; relation to cancer. *PloS One* (2021) 16(2):e0246806. doi: 10.1371/journal.pone.0246806

11. Carr E, Bendayan R, Bean D, Stammers M, Wang W, Zhang H, et al. Evaluation and improvement of the national early warning score (NEWS2) for COVID-19: A multi-hospital study. *BMC Med* (2021) 19(1):23. doi: 10.1186/s12916-020-01893-3

12. Legebeke J, Lord J, Penrice-Randal R, Vallejo AF, Poole S, Brendish NJ, et al. Evaluating the immune response in treatment-naive hospitalised patients with influenza and COVID-19. *Front Immunol* (2022) 13. doi: 10.3389/fimmu.2022.853265

13. Goulden R, Hoyle MC, Monis J, Railton D, Riley V, Martin P, et al. qSOFA, SIRS and NEWS for predicting inhospital mortality and ICU admission in emergency admissions treated as sepsis. *Emerg Med J* (2018) 35(6):345–9. doi: 10.1136/emermed-2017-207120

14. Glass G, Hartka TR, Keim-Malpass J, Enfield KB, Clark MT. Dynamic data in the ED predict requirement for ICU transfer following acute care admission. *J Clin Monit Comput* (2021) 35(3):515–23. doi: 10.1007/s10877-020-00500-3

15. Rodriguez-Nava G, Yanez-Bello MA, Trelles-Garcia DP, Chung CW, Friedman HJ, Hines DW. Performance of the quick COVID-19 severity index and the brescia-COVID respiratory severity scale in hospitalized patients with COVID-19 in a community hospital setting. *Int J Infect Dis* (2021) 102:571–6. doi: 10.1016/j.ijid.2020.11.003

16. Wang AZ, Ehrman R, Bucca A, Croft A, Glober N, Holt D, et al. Can we predict which COVID-19 patients will need transfer to intensive care within 24 hours of floor admission? *Acad Emerg Med* (2021) 28(5):511–8. doi: 10.1111/acem.14245

17. Hao B, Sotudian S, Wang T, Xu T, Hu Y, Gaitanidis A, et al. Early prediction of level-of-care requirements in patients with COVID-19. *Elife* (2020) 9:e60519. doi: 10.7554/eLife.60519

18. Joshi N, Fass J. *Sickle: A sliding-window, adaptive, quality-based trimming tool for FastQ files* (2011). Available at: https://github.com/najoshi/sickle.

19. Moore AR, Roque J, Shaller BT, Asuni T, Remmel M, Rawling D, et al. Prospective validation of an 11-gene mRNA host response score for mortality risk stratification in the intensive care unit. *Sci Rep* (2021) 11(1):13062. doi: 10.1038/s41598-021-91201-7

20. Banerjee S, Mohammed A, Wong HR, Palaniyar N, Kamaleswaran R. Machine learning identifies complicated sepsis course and subsequent mortality based on 20 genes in peripheral blood immune cells at 24 h post-ICU admission. *Front Immunol* (2021) 12:592303. doi: 10.3389/fimmu.2021.592303

21. Oberg JA, Glade Bender JL, Sulis ML, Pendrick D, Sireci AN, Hsiao SJ, et al. Implementation of next generation sequencing into pediatric hematology-oncology practice: Moving beyond actionable alterations. *Genome Med* (2016) 8(1):133. doi: 10.1186/s13073-016-0389-6

22. Qiao B, Zhao M, Wu J, Wu H, Zhao Y, Meng F, et al. A novel RNA-Seq-Based model for preoperative prediction of lymph node metastasis in oral squamous cell carcinoma. *BioMed Res Int* (2020) 2020:4252580. doi: 10.1155/2020/4252580

23. Schieffer KM, Choi CS, Emrich S, Harris L, Deiling S, Karamchandani DM, et al. RNA-Seq implicates deregulation of the immune system in the pathogenesis of diverticulitis. *Am J Physiol Gastrointest Liver Physiol* (2017) 313(3):G277–g84. doi: 10.1152/ajpgi.00136.2017

24. Seco-Cervera M, González-Rodríguez D, Ibáñez-Cabellos JS, Peiró-Chova L, Pallardó FV, García-Giménez JL. Small RNA-seq analysis of circulating miRNAs to identify phenotypic variability in friedreich's ataxia patients. *Sci Data* (2018) 5:180021. doi: 10.1038/sdata.2018.21

25. Bigler J, Boedigheimer M, Schofield JPR, Skipp PJ, Corfield J, Rowe A, et al. A severe asthma disease signature from gene expression profiling of peripheral blood from U-BIOPRED cohorts. *Am J Respir Crit Care Med* (2017) 195(10):1311–20. doi: 10.1164/rccm.201604-0866OC

26. Nicolau M, Levine AJ, Carlsson G. Topology based data analysis identifies a subgroup of breast cancers with a unique mutational profile and excellent survival. *Proc Natl Acad Sci U.S.A.* (2011) 108(17):7265–70. doi: 10.1073/pnas.1102826108

27. Sjoberg DD, Whiting K, Curry M, Lavery JA, Larmarange J. Reproducible summary tables with the gtsummary package. *R J* (2021) 13:570–80. doi: 10.32614/RJ-2021-053

28. Martin M. Cutadapt removes adapter sequences from high-throughput sequencing reads. *EMBnetjournal* (2011) 17. doi: 10.14806/ej.17.1.200

29. Kim D, Langmead B, Salzberg SA-O. HISAT: a fast spliced aligner with low memory requirements. *Nat Methods* (2015) 12(4):357–60. doi: 10.1038/nmeth.3317

30. Liao Y, Smyth GK, Shi W. featureCounts: an efficient general purpose program for assigning sequence reads to genomic features. *Bioinformatics* (2014) 30(7):923–30. doi: 10.1093/bioinformatics/btt656

31. Breiman L. Bagging predictors. *Mach Learn* (1996) 24(2):123–40. doi: 10.1007/BF00058655

32. Henry BM, MHSd O, Benoit S, Plebani M, Lippi G. Hematologic, biochemical and immune biomarker abnormalities associated with severe illness and mortality in coronavirus disease 2019 (COVID-19): A meta-analysis. *Clin Chem Lab Med (CCLM)* (2020) 58(7):1021–8. doi: 10.1515/cclm-2020-0369

33. Juan Guardela BM, Sun J, Zhang T, Xu B, Balnis J, Huang Y, et al. 50-gene risk profiles in peripheral blood predict COVID-19 outcomes: A retrospective, multicenter cohort study. *EBioMedicine* (2021) 69:103439. doi: 10.1016/j.ebiom.2021.103439

34. Russick J, Foy PE, Josseaume N, Meylan M, Hamouda NB, Kirilovsky A, et al. Immune signature linked to COVID-19 severity: A SARS-score for personalized medicine. *Front Immunol* (2021) 12:701273. doi: 10.3389/fimmu.2021.701273

35. Chen Z, Wang C, Feng X, Nie L, Tang M, Zhang H, et al. Interactomes of SARS-CoV-2 and human coronaviruses reveal host factors potentially affecting pathogenesis. *EMBO J.* 40(17):e107776. doi: 10.15252/embj.2021107776

36. Schofield JPR, Burg D, Nicholas B, Strazzeri F, Brandsma J, Staykova D, et al. Stratification of asthma phenotypes by airway proteomic signatures. *J Allergy Clin Immunol* (2019) 144(1):70–82. doi: 10.1016/j.jaci.2019.03.013

37. Tariq K, Schofield JPR, Nicholas BL, Burg D, Brandsma J, Bansal AT, et al. Sputum proteomic signature of gastro-oesophageal reflux in patients with severe asthma. *Respir Med* (2019) 150:66–73. doi: 10.1016/j.rmed.2019.02.008

38. De Meulder B, Lefaudeux D, Bansal AT, Mazein A, Chaiboonchoe A, Ahmed H, et al. A computational framework for complex disease stratification from multiple large-scale datasets. *BMC Syst Biol* (2018) 12(1):60. doi: 10.1186/s12918-018-0556-z

39. Östling J, van Geest M, Schofield JPR, Jevnikar Z, Wilson S, Ward J, et al. IL-17-high asthma with features of a psoriasis immunophenotype. *J Allergy Clin Immunol* (2019) 144(5):1198–213. doi: 10.1016/j.jaci.2019.03.027

40. Schofield JPR, Strazzeri F, Bigler J, Boedigheimer M, Adcock IM, Chung KF, et al. Morse-Clustering of a topological data analysis network identifies phenotypes of asthma based on blood gene expression profiles. *bioRxiv* (2020) 516328. doi: 10.1101/516328

41. Venkataraman T, Coleman CM, Frieman MB. Overactive epidermal growth factor receptor signaling leads to increased fibrosis after severe acute respiratory syndrome coronavirus infection. *J Virol* (2017) 91(12):e00182-17. doi: 10.1128/JVI.00182-17

42. Venkataraman T, Frieman MB. The role of epidermal growth factor receptor (EGFR) signaling in SARS coronavirus-induced pulmonary fibrosis. *Antiviral Res* (2017) 143:142–50. doi: 10.1016/j.antiviral.2017.03.022

43. Vagapova ER, Lebedev TD, Prassolov VS. Viral fibrotic scoring and drug screen based on MAPK activity uncovers EGFR as a key regulator of COVID-19 fibrosis. *Sci Rep* (2021) 11(1):11234. doi: 10.1038/s41598-021-90701-w

44. Londres HD, Armada JJ, Martínez AH, Abdo Cuza AA, Sánchez YH, Rodríguez AG, et al. Blocking EGFR with nimotuzumab: A novel strategy for COVID-19 treatment. *Immunotherapy* (2022) 14(7):521–30. doi: 10.2217/imt-2022-0027

45. Abdo Cuza AA, Ávila JP, Martínez RM, González JJ, Aspuro GP, Gutiérrez Martínez JA, et al. Nimotuzumab for COVID-19: Case series. *Immunotherapy* (2022) 14(3):185–93. doi: 10.2217/imt-2021-0269

46. Heffernan KS, Ranadive SM, Jae SY. Exercise as medicine for COVID-19: On PPAR with emerging pharmacotherapy. *Med Hypotheses* (2020) 143:110197. doi: 10.1016/j.mehy.2020.110197

47. Buschard K. Fenofibrate increases the amount of sulfatide which seems beneficial against covid-19. *Med Hypotheses* (2020) 143:110127. doi: 10.1016/j.mehy.2020.110127

48. Del Re A, Corpetti C, Pesce M, Seguella L, Steardo L, Palenca I, et al. Ultramicronized palmitoylethanolamide inhibits NLRP3 inflammasome expression and pro-inflammatory response activated by SARS-CoV-2 spike protein in cultured murine alveolar macrophages. *Metabolites* (2021) 11(9):592. doi: 10.3390/metabo11090592.

49. Akbari N, Ostadrahimi A, Tutunchi H, Pourmoradian S, Farrin N, Najafipour F, et al. Possible therapeutic effects of boron citrate and oleoylethanolamide supplementation in patients with COVID-19: A pilot randomized, double-blind, clinical trial. *J Trace Elem Med Biol* (2022) 71:126945. doi: 10.1016/j.jtemb.2022.126945

50. Fonnesu R, Thunuguntla V, Veeramachaneni GK, Bondili JS, La Rocca V, Filipponi C, et al. Palmitoylethanolamide (PEA) inhibits SARS-CoV-2 entry by interacting with s protein and ACE-2 receptor. *Viruses* (2022) 14(5):1080. doi: 10.3390/v14051080.

51. Flannery LE, Kerr DM, Hughes EM, Kelly C, Costello J, Thornton AM, et al. N-acylethanolamine regulation of TLR3-induced hyperthermia and neuroinflammatory gene expression: A role for PPARα. *J Neuroimmunol* (2021) 358:577654. doi: 10.1016/j.jneuroim.2021.577654

52. Ferreira-Gomes M, Kruglov A, Durek P, Heinrich F, Tizian C, Heinz GA, et al. SARS-CoV-2 in severe COVID-19 induces a TGF-β-dominated chronic immune response that does not target itself. *Nat Commun* (2021) 12(1):1961. doi: 10.1038/s41467-021-22210-3

53. Beller A, Kruglov A, Durek P, von Goetze V, Werner K, Heinz GA, et al. Specific microbiota enhances intestinal IgA levels by inducing TGF-β in T follicular helper cells of peyer's patches in mice. *Eur J Immunol* (2020) 50(6):783–94. doi: 10.1002/eji.201948474

54. Lee CG, Homer RJ, Zhu Z, Lanone S, Wang X, Koteliansky V, et al. Interleukin-13 induces tissue fibrosis by selectively stimulating and activating transforming growth factor beta(1). *J Exp Med* (2001) 194(6):809–21. doi: 10.1084/jem.194.6.809

55. Singh E, Matada GSP, Abbas N, Dhiwar PS, Ghara A, Das A. Management of COVID-19-induced cytokine storm by Keap1-Nrf2 system: A review. *Inflammopharmacology* (2021) 29(5):1347–55. doi: 10.1007/s10787-021-00860-5

56. Ulasov AV, Rosenkranz AA, Georgiev GP, Sobolev AS. Nrf2/Keap1/ARE signaling: Towards specific regulation. *Life Sci* (2022) 291:120111. doi: 10.1016/j.lfs.2021.120111

frontiers | Frontiers in Immunology

TYPE Original Research
PUBLISHED 23 September 2022
DOI 10.3389/fimmu.2022.1004545

Check for updates

OPEN ACCESS

EDITED BY
Edwin Bölke,
Heinrich Heine University of Düsseldorf, Germany

REVIEWED BY
Michael Maes,
Chulalongkorn University, Thailand
George Anderson,
CRC Scotland & London, United Kingdom

*CORRESPONDENCE
Dietmar Abendroth
dietmar.abendroth@t-online.de

†These authors have contributed equally to this work

SPECIALTY SECTION
This article was submitted to Viral Immunology, a section of the journal Frontiers in Immunology

RECEIVED 27 July 2022
ACCEPTED 06 September 2022
PUBLISHED 23 September 2022

CITATION
Bizjak DA, Stangl M, Börner N, Bösch F, Durner J, Drunin G, Buhl J-L and Abendroth D (2022) Kynurenine serves as useful biomarker in acute, Long- and Post-COVID-19 diagnostics. *Front. Immunol.* 13:1004545. doi: 10.3389/fimmu.2022.1004545

COPYRIGHT
© 2022 Bizjak, Stangl, Börner, Bösch, Durner, Drunin, Buhl and Abendroth. This is an open-access article distributed under the terms of the Creative Commons Attribution License (CC BY). The use, distribution or reproduction in other forums is permitted, provided the original author(s) and the copyright owner(s) are credited and that the original publication in this journal is cited, in accordance with accepted academic practice. No use, distribution or reproduction is permitted which does not comply with these terms.

Kynurenine serves as useful biomarker in acute, Long- and Post-COVID-19 diagnostics

Daniel Alexander Bizjak[1†], Manfred Stangl[2†], Nikolaus Börner[2], Florian Bösch[2], Joachim Durner[3], Gergana Drunin[3], Jasmine-Leonike Buhl[1] and Dietmar Abendroth[4*]

[1]Division of Sports and Rehabilitation Medicine, Ulm University Hospital, Ulm, Germany, [2]Division of General, Visceral and Transplant Surgery, Hospital Großhadern, Ludwig-Maximilians-University, Munich, Germany, [3]Neurology Department, Special Medical Clinic Ichenhausen, Ichenhausen, Germany, [4]Division of Surgery, Ulm University Hospital, Ulm, Germany

Introduction: In patients with SARS-CoV-2, innate immunity is playing a central role, depicted by hyperinflammation and longer lasting inflammatory response. Reliable inflammatory markers that cover both acute and long-lasting COVID-19 monitoring are still lacking. Thus, we investigated one specific inflammatory marker involved as one key player of the immune system, kynurenine (Kyn), and its use for diagnosis/detection of the Long-/Post-COVID syndrome in comparison to currently used markers in both serum and saliva samples.

Material and methods: The study compromised in total 151 inpatients with a SARS-CoV-2 infection hospitalized between 03/2020 and 09/2021. The group NC (normal controls) included blood bank donors (n=302, 144f/158m, mean age 47.1 ± 18.3 years (range 18-75)). Two further groups were generated based on Group A (n=85, 27f/58m, mean age 63.1 ± 18.3 years (range 19-90), acute admission to the hospital) and Group B (n=66, 22f/44m, mean age 66.6 ± 17.6 years (range 17-90), admitted either for weaning or for rehabilitation period due to Long-COVID symptoms/syndrome). Plasma concentrations of Kyn, C-Reactive Protein (CRP) and interleukin-6 (IL-6) were measured on admission. In Group B we determined Kyn 4 weeks after the negative PCR-test. In a subset of patients (n=11) concentrations of Kyn and CRP were measured in sera and saliva two, three and four months after dismission. We identified 12 patients with Post-COVID symptoms >20 weeks with still significant elevated Kyn-levels.

Results: Mean values for NC used as reference were 2.79 ± 0.61 µM, range 1.2-4.1 µM. On admission, patients showed significantly higher concentrations of Kyn compared to NC (p-values < 0.001). Kyn significantly correlated with IL-6 peak-values (r=0.411; p-values <0.001) and CRP (r=0.488, p-values<0.001). Kyn values in Group B (Long-/Post-COVID) showed still significant higher values (8.77 ± 1.72 µM, range 5.5-16.6 µM), whereas CRP values in Group B were in the normal range.

Conclusion: Serum and saliva Kyn are reflecting the acute and long-term pathophysiology of the SARS-CoV-2 disease concerning the innate immune

10.3389/fimmu.2022.1004545

response and thus may serve a useful biomarker for diagnosis and monitoring both Long- and Post-COVID syndrome and its therapy.

KEYWORDS

kynurenine reference values, inflammation diagnostics, COVID-19 monitoring, Long-COVID biomarkers, innate immunity

Introduction

The mutual reaction of host defense against pathogens generally exhibit an initial tissue injury mediated by various generated pathogen-associated molecular patterns (PAMPs) and by any injurious nonpathogenic factors that includes the generation and appearance of damage-associated molecular patterns (DAMPs) (1).

There is evidence that in the center of tissue injury, reactive oxygen species (ROS) play a dominant role and that its origin (e.g., infectious, toxic, physical, or other injurious events) has only a minor effect (2). Oral gingival epithelium as well as the airway epithelium are predisposed as a sentinel system to detect pathogens and nonpathogenic agents and to initiate a host innate defense response (3–5).

The innate immune responses and respective involved cell types play a vital role in the origin of clinical symptoms and severity of COVID-19 disease. This assumption is in agreement with previous studies on the SARS-CoV, which is the closest relative to SARS-CoV-2, and that predominantly infects airway and alveolar epithelial cells, vascular endothelial cells, and macrophages (6). It has been demonstrated that SARS-CoV can influence and trigger various innate recognition and response pathways (6).

The prevailing evidence suggests that patients with severe COVID-19 seem to have an overreaction of the innate immune system demonstrating exacerbated levels of inflammation caused by a so-called "cytokine storm" (6). Although COVID-19 has been closely examined in the last two years regarding acute and long-term mental and physiological health consequences, the versatile mechanisms that underpin COVID-19 are still intensely studied with regard to possible symptoms and health outcome (6, 7).

Inside the tryptophan metabolism, the kynurenine pathway (KP) plays a critical role in generating cellular energy in the form of nicotinamide adenine dinucleotide (NAD^+). Especially during an immune response, energy requirements are substantially increased and the KP acts a key regulator of the immune system (8). This key regulator is of utmost importance especially in the line of first defense in the innate immune activation (9).

Kynurenine is known to signal through the aryl hydrocarbon receptor (Ahr) with the possibility for modulation of ROS levels (10). The Ahr promoter region contains several sites for NF-kB binding, indicating that inflammation is a key factor modulating Ahr expression. Furthermore, kynurenine activation of Ahr stimulate expression of the enzyme Indoleamine 2,3-dioxygenase 1 (IDO1), which generates kynurenine by degrading tryptophan (11). On the one hand, this positive feedback loop may link inflammation with ROS production, whereas on the other hand, the antioxidant Nrf2 can be stimulated by Ahr, and Nrf2 can itself activate Ahr expression. The balance between pro- and anti-oxidative functions of Ahr mediated by kynurenine may therefore regulate healthy versus unhealthy aging in different tissues and organ systems (11).

Kynurenine is metabolized by IDO-1 in the brain. Prolonged exposure by chemokines due to increased kynurenine levels may result in long-term brain impairment. Kynurenine metabolites itself are producing pro-oxidative and pro-inflammatory effects, resulting in impairment of cognitive function, enhanced oxidative stress and decreased brain-derived neurotrophic factor. The place of action is located in the microglia cells, responsible as innate immune cells (9, 12).

The mechanistic pathways especially in the brain through which the kynurenines interact with these systems are well known, and the subsequent inflammation and inflammatory events induced by e.g., virus-driven diseases can negatively affect emotion, cognition, pain, metabolic function, and aging (8). In doing so, abnormal concentrations or a disbalance of kynurenine metabolites have the potential for increasing the risk of developing psychiatric disorders (13, 14).

The currently most prominent example of the virus-driven activation and not successfully downregulated innate immune response together or alone with a cytokine storm event is the so-called Long-COVID syndrome in adults, or the PIMS (pediatric inflammatory multiorgan syndrome) in children (15). These syndromes include long-term health consequences including impaired healing in the brain (depression), in the lung (fibrosis), in the cardiovascular system (loss of heart function, endothelial reaction) and in the kidney (loss of renal function). The disease exhibits symptoms like severe pneumonia, associated to a severe inflammatory reaction including high C-reactive protein (CRP) and interleukin-6 (IL-6) levels, low albumin and eosinophils, but high sedimentation rate and lymphopenia. Hospitalized individuals also have increased lactate dehydrogenase (LDH), a marker of cellular death, often associated with altered coagulation (16, 17). With more than

90% accuracy, high concentrations of high-sensitivity CRP and LDH as well as a low lymphocyte count can predict mortality of individual patients more than 10 days in advance (18). Several meta-analyses also associated IL-6 levels with the severity of COVID-19 syndrome (19–21).

The Long-COVID syndrome is a longer lasting subclinical inflammation in different parts of the body yet, leading in some individuals to chronic manifestations called Post-COVID syndrome (> 12 weeks), but the diversity of symptoms and individual disease progression indicates that there is no main clinical denominator of biomarkers so far (22–24). The duration and kind of predictive forecasting of the COVID-19 infection by measuring this sustained subclinical inflammation might thus be a valuable asset for clinical diagnostics.

This asset might be the aforementioned aromatic amino acid kynurenine. It has been observed that in some cases, SARS-CoV-2 elicits a reaction like the cytokine storm syndrome seen in sepsis. During sepsis, dendritic cells showing an "overproduction"of IDO, leading to a powerful counter-regulatory, anti-inflammatory reaction characterized by apoptosis of immune effector cell and cellular (especially T cell) exhaustion. The resulting consequence is often seen by immunosuppression and increased susceptibility to secondary infections (25–28). Recently, a meta-analysis showed that the kynurenine pathway is extremely active in acute COVID-19, accompanied by reduced tryptophan and elevated kynurenine, and much more active in severe COVID-19 patients compared to mild or moderate patients (29).

All these patterns are related to the tryptophan-metabolism and its central molecule, kynurenine. The ongoing elevation of the tryptophan metabolism downstream including kynurenine and kynurenic acid is thus of utmost importance.

The main purpose of this proof-of-concept study was 1) to examine if kynurenine is able to depict the inflammatory situation during the acute phase of the disease and 2) if so, if there will be the theoretically developed prognosis of an ongoing subclinical inflammatory situation in patients with the Long-/Post-COVID syndrome.

Material and methods

Study population

The study compromised in total 151 inpatients with a SARS-CoV-2 infection hospitalized between 03/2020 and 09/2021 in LMU Munich (Großhadern). The group NC (normal controls) included blood bank donors (n=302, 144f/158m, mean age 47.1 ± 18.3 years (range 18-75)). Detailed NC characteristic can be found in Kaden et al. (2015) and Abendroth et al. (2014) (30, 31).

Two further groups were generated based on acute admission at the hospital:

Group **A** (n=85, 27 f/58 m, mean age 63.1 ± 18.3 years (range 19-90), admitted LMU Großhadern) was treated either on the infection ward (n=67) or the Intensive care Unit (ICU) (n=18), whereas Group **B** was admitted either for weaning or for rehabilitation period due to Long-COVID symptoms/syndrome (n= 66, 22 f/44 m, mean age 66.6 ± 17.6 years (range 17-90), admitted Rehabilitation Hospital Ichenhausen). Plasma concentrations of kynurenine, CRP and interleukin-6 (IL-6) were measured on admission (Table 1).

In Group **B** kynurenine concentrations were determined 4 weeks after the negative PCR-test. In a subset of patients (n=11) concentrations of kynurenine and CRP were measured in sera and saliva 2, 3 and 4 months after dismission in a pilot-like sub study. The same protocol was used for saliva measurements withdrawn for PCR-Analysis for detection of COVID-19 antibodies (n=11). Figure 1 illustrates the different groups with the experimental determined biomarkers at the respective time points.

As has been shown earlier, there exists a linear correlation ($r^{2=}$ 0.902) between the measurement of kynurenine in serum and in saliva (24).

Ethics

The study was released and signed by the ethics committee of the University of Ulm (4/2011, 312/2015, 19/2020) and ethics committee of the Ludwigs-Maximilians-University Munich (CORKUM, associated research project) and performed in accordance with the current Declaration of Helsinki. Each patient signed a letter of informed consent for the leave of blood and saliva samples.

Biosampling

We established a biobank by collecting leftovers of blood samples from patients suffering from COVID-19 whenever sent to the central laboratory of our university hospital.

Blood for routine monitoring of the patients was normally withdrawn every Monday, Wednesday and Friday between 7:00 and 8:00 o'clock a.m. After measurement of routine parameters, the remaining serum was stored at -30°C until further measurements. Saliva sampling was performed by using the Salivette™ tube (Sarstedt, Nümbrecht, Germany).

10.3389/fimmu.2022.1004545

TABLE 1 Demographic and biochemical data of group NC, A, B.

Group	NC, Normal Controls n = 302	A, Acute COVID-19 n = 85	B, Long-COVID-19 n = 66	p-value
Age (years)	48.3 ± 18.3	63.1 ± 16.5	66.6 ± 17.6	B-C
	(Range 18-75)	(Range 19-90)	(Range 17-90)	n.s.
Gender (f/m)	144/158	27/58	22/44	
ICU (n/%)	n.a.	18/22%	6/9%	
Ventilation (days)	n.a.	12 (3 – 131 days)	Weaning	n.a.
Biochemical Parameter				
Kynurenine (µM)	2.79 ± 0.61	10.18 ± 8.88	9.01 ± 3.62	NC vs. A/B p<0.001 A vs. B p=0.182
CRP (mg/L)	< 5	69.2 ± 14.9	Admission: Month 2: 4.14 ± 2.1 Month 3: 1.88 ± 0.8 > Month 5: 1.28 ± 0.5	n.a.
IL-6 pg/ml (peak)	<1.0	58.8 ± 17.4	n.d.	n.a.

All three groups were comparable concerning age and gender distribution. There was a significant difference concerning kynurenine between the normal controls and patients with COVID-19 infections or with Long-COVID syndrome. All data are given as mean ± standard deviation if not otherwise stated. The respective range is presented in parentheses. (ICU, intensive care unit; n.a., not applicable; n.d., not done; n.s., not significant).

Kynurenine, IL-6 and CRP measurement

The method of kynurenine measurement was already published in detail (30). In short, serum samples were deproteinized with acetic acid trichloride, followed by consecutive proton-dominant hydrolysis. The stable metabolite kynurenine is reacting under the use of 4-dimethylamino-benzaldehyde (Ehrlich's reagent) into a yellow product. Said coloring reagent serves for the detection of primary amino groups, pyrrole and indole derivatives as well. The colorimetric determination of the concentration is performed with monochromatic light. The standard solution of kynurenine was prepared by using L-kynurenine sulfate. Equal amounts of sample were mixed with 100 ml trichloroacetic acid (30%) thoroughly. Absorption was measured with 492 nm wavelength in a linear sector from 0.5–100 µM of the concentration of N-formylkynurenine, proportional to the activity of the enzyme indoleamine-2,3-dioxygenase. The absorbents of each sample at 492 nm were compared with the absorbents at 650 nm or 690 nm of the same sample. Then the absorbents of the controls were

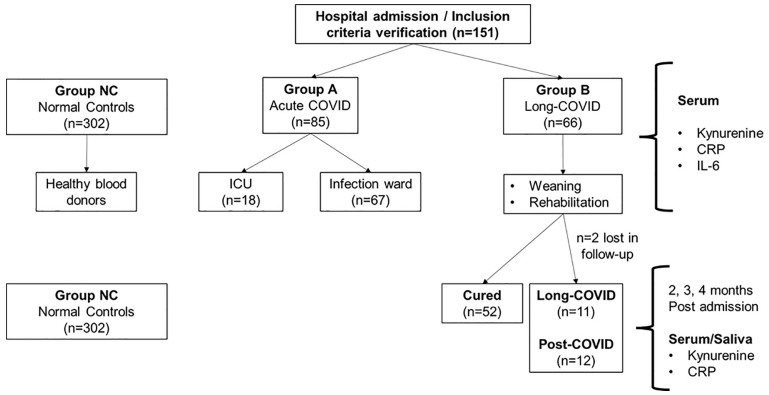

FIGURE 1
Overview of the different study populations and the respective experimental biomarkers. Group NC (normal controls) consisted of healthy blood donors (30, 31) where kynurenine concentrations were measured and taken as reference values for the Sars-CoV-2 infected individuals (Group A and Group B). ICU = Intensive Care Unit; CRP = C-Reactive Protein; IL-6 = Interleukin 6.

subtracted from the absorbents of each well. By preparing a standard curve the concentration of kynurenine in each sample could be determined.

Kynurenine concentration stability of stored samples for NC and the COVID-groups were observed (31). Thus, a reliable comparison of reference samples (NC) and the study groups A and B can be assumed.

IL-6 and CRP were measured with commercial immunoassays on a COBAS 8000 analyzer™ (Roche Diagnostics, Rotkreuz, Switzerland).

Statistical analysis

Descriptive data analysis and analysis of variance methods were used to characterize the data. All p-values are two-sided and considered to be descriptive. For a formal statement of descriptive significance, a nominal type I error level of α=0.05 (two-sided) was assumed.

The exact Mann-Whitney U test was performed for comparison of two groups with not normally distributed continuous variables. Spearman's rho (ρ) was performed to assess correlations between parameters of tryptophan metabolism and IL-6.

If not otherwise stated, all values are given as mean ± standard deviation. The analyses were performed using Sigma Plot 14™ from Systat Software Inc. (San Jose, CA, USA).

Results

In this pilot-study, including n=85 patients infected with COVID-19 (mean age 52.8 ± 30.0 years) and n=302 NC, we first measured kynurenine in serum and subsequently in saliva (n=11).

Serum kynurenine, IL-6 and CRP in group A and B on first admission

On admission, serum kynurenine was significantly elevated in COVID-19 patients Group A compared to NC (10.81 ± 8.8 µM vs. 2.79 ± 0.61 µM; p<0.001) (Figure 2). Samples in Group A were taken by starting clinical treatment in the first week. For better graphical demonstration, we left out two results in the COVID-19 positive group (43 and 58 µM) with a hyperinflammatory syndrome.

Kynurenine significantly correlated positively with IL-6 peak-values (r=0.411; p<0.001) and CRP (r=0.488, p<0.001) (Table 1).

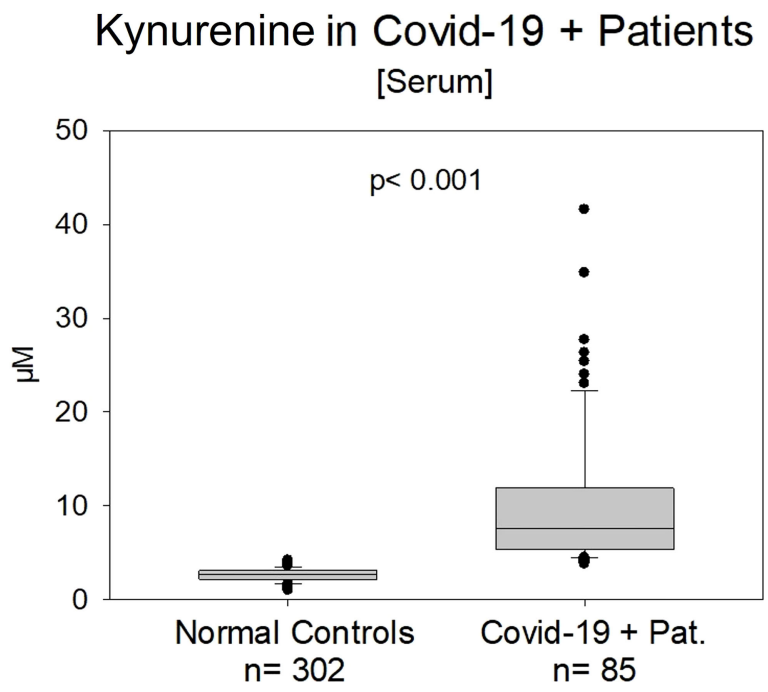

FIGURE 2
Kynurenine in normal controls (n=302) vs. COVID-19 patients in the early acute clinical state (n=85). The difference was significant (p< 0.001). We left out two results (58 and 43 µM) with an extreme hyperinflammatory syndrome in the COVID-19 positive group A.

Kynurenine values in Group B (Long-COVID) showed still significantly higher values (8.77 ± 1.72 µM, range 5.5-24.6 µM, p<0.001 (Figure 3).

Serum vs saliva kynurenine

Kynurenine was measured not only in serum. In Figure 4 the measurements of kynurenine of NC and COVID-19 positive patients (n=11) either measured in serum or saliva were compared according to the previous publication data of our group (30, 31). Serum and saliva values in the previously COVID-19 positive patients were significantly higher compared to NC (p<0.001).

Serum kynurenine, IL-6 and CRP in group A and B on follow-up admission

Looking in the follow-up of a starting group of patients (n=11) with the diagnosis of Long-COVID syndrome, we could observe the sustained elevated level of kynurenine compared to NC from month 2 until month 4, the end of the follow up monitoring period so far. This was not found for CRP (Figures 5A, B). We compared 11 patients with positive infection and patients after COVID-19 positive infection without signs of a Long-COVID syndrome.

CRP, described in the literature as a good biomarker in COVID-19 patients (17), was not suitable to identify the Long-COVID syndrome. CRP at 2 months after positive testing was near the normal range of >5 mg/L or 5 µg/ml (Figure 5A). These findings are showing the difference between the Long-COVID (4-12 weeks) and Post-COVID syndrome (> 12 weeks).

12 patients with Post-COVID symptoms >20 weeks (range 20-42 weeks) with still elevated serum kynurenine-levels (8.73 ± 3.19 µM, range 5.4-16.5 µM) were identified (Figure 6).

Discussion

Long-COVID is a chronic illness with a wide variety of symptoms, of which many are not explainable using conventional laboratory tests. There still are existing difficulties in detecting the illness. Researchers looking more deeply at Long-COVID patients have found visible dysfunctions throughout the body (22, 32).

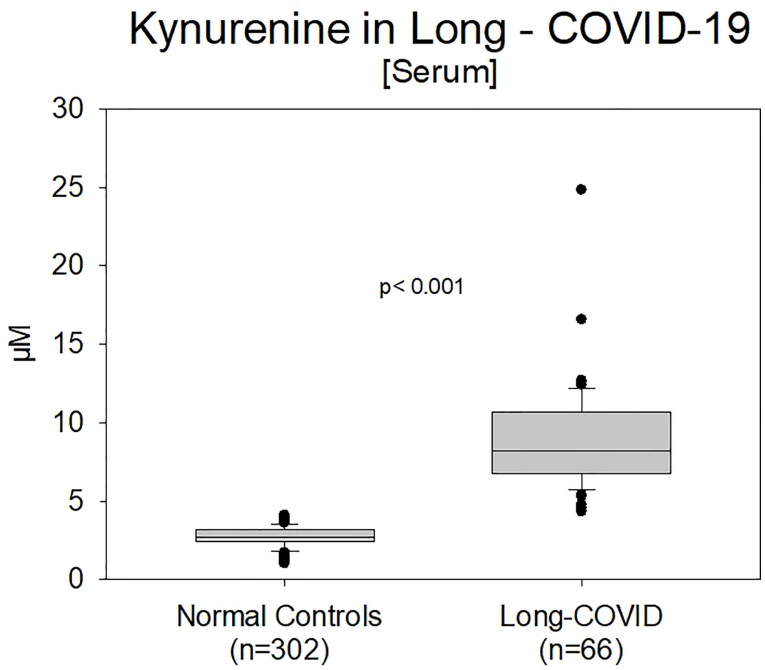

FIGURE 3
Comparison of kynurenine values between normal controls (n=302) and previously positive COVID-19 patients (Group B, n=66) with an existing Long-COVID syndrome (p<0.001). Patients with the LCS were currently under therapeutic management.

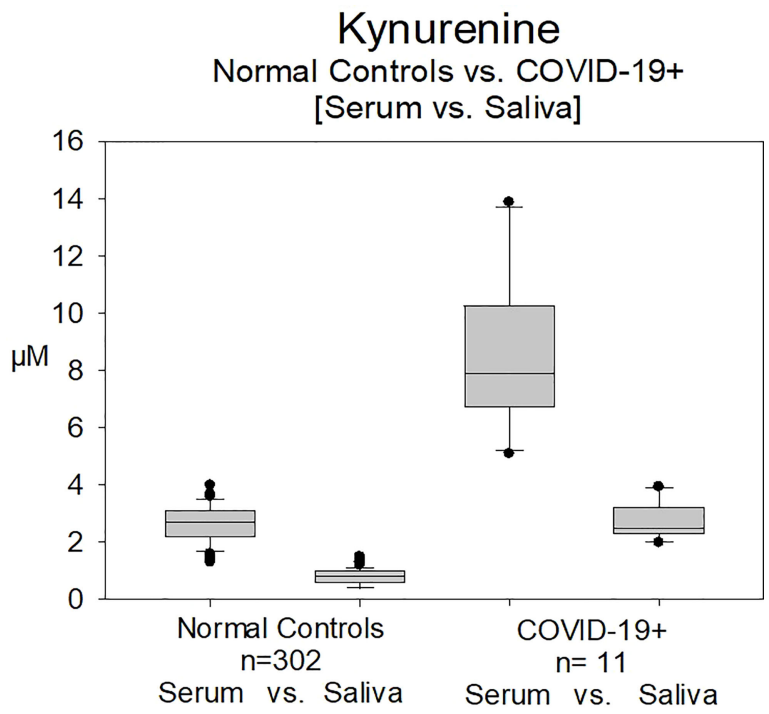

FIGURE 4
Measurement of Kynurenine in serum and in saliva in normal controls (n=302) and in patients with COVID-19 infection (Group B, n=11). Serum and saliva values in the previously COVID-19 positive patients were significantly higher compared to normal controls (p<0.001).

Although it was shown that the marker CRP might be helpful during the acute phase of the disease (16, 17), the long-term value remains questionable. Our data underline the appropriate use of CRP in the acute phase, while CRP concentrations in Long-COVID are comparable with normal controls and thus do not reflect the long-term inflammation. This was supported by previous results of our group in renal transplanted patients, where the diagnosis of rejection could not be estimated by CRP-monitoring (30).

In contrast, kynurenine was still increased up to four months in patients suffering from Long- and Post-COVID compared to

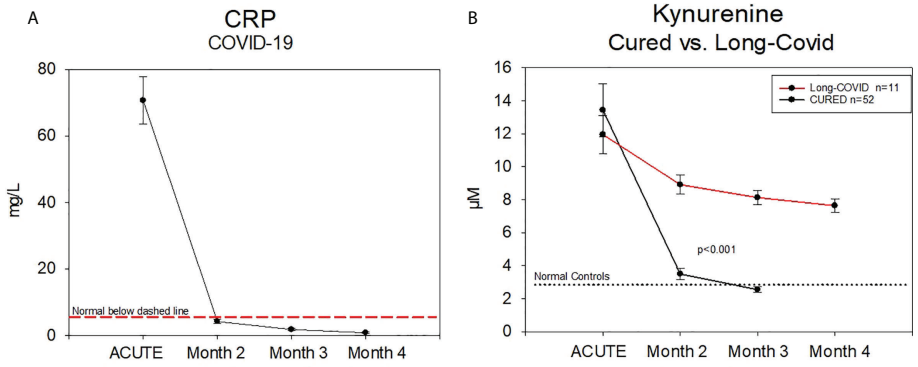

FIGURE 5
(A) Follow up of C–Reactive Protein and Kynurenine–measurement in patients either cured (n=11) or with a Long-COVID-syndrome (n=11) from a subset of Group B CRP was in a normal range after month 2 post infection (verified by a positive PCR-Test). **(B)** Kynurenine was still significantly increased.

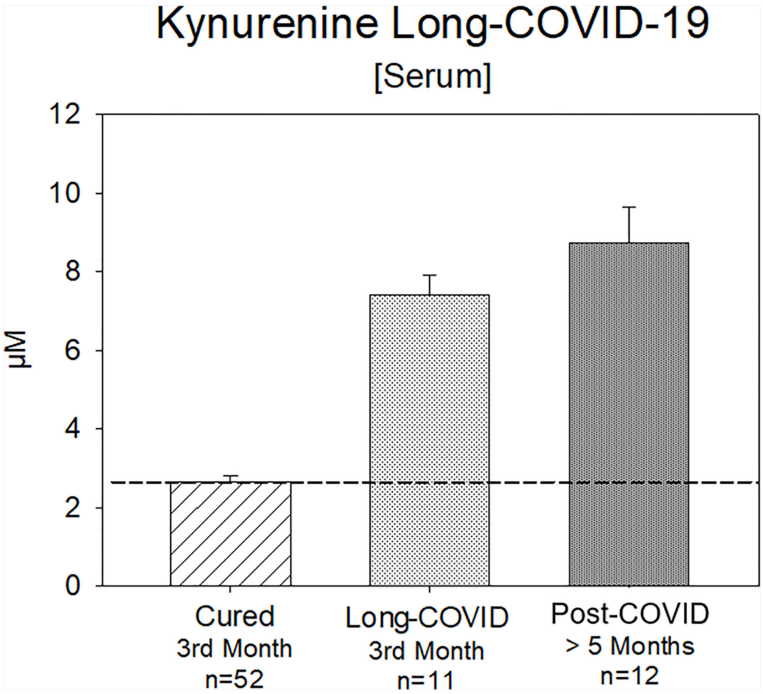

FIGURE 6
Kynurenine (Serum) in the 3rd month after positive PCR-testing: either cured or with a Long-COVID syndrome for 3 months or Post-COVID syndrome more than 5 months in a subset of Group B Kynurenine is still significantly increased, whereas the values of the cured patients are in a normal range.

cured COVID-patients without developing Long-/Post-COVID (subpopulation of Group B) or NC. In addition, the picture of hyperinflammation with extraordinary high levels of kynurenine was solely found in COVID-19 patients, especially in those on the ICU with kynurenine concentrations up to 79.4 µM (data not shown).

Furthermore, the accumulative evidence of the COVID-19 specific studies published in the last year suggests that SARS-CoV-2 infection induces a powerful, and apparently uncontrolled inflammatory response. This inflammation can be assumed to contribute to the tissue damage already caused by the viral infection towards the COVID-19 underlying pathology. The short- and long-term sequalae following recovery of COVID-19 suggests that these syndromes lead to an accelerated state of chronic subclinical systemic inflammation. Thus, a reliable immunological marker to support prognosis in the acute and long-term phase of the COVID-19 disease and which reflects the current inflammatory status would be a valuable asset.

Studies estimate that around 10-30% of people infected with SARS-CoV-2 may develop long-term symptoms. Four different risk factors were identified for a more severe development: a) the presence of having Type 2 diabetes, b) reactivation of Epstein-Barr virus (EBV) c) presence of certain autoantibodies and d) high levels of viral RNA early during an infection (16, 24).

The interdependence of virus infection with kynurenine and the activation of the kynurenine pathway in SARS-CoV-2 positive patients has been examined by fellow working groups. Lawler et al. evaluated indicators of the tryptophan metabolism by quantitative metabolic phenotyping and found that especially the neurotoxic metabolites kynurenine, quinolinic acid and 3-hydroxykynurenine were increased in ten SARS-CoV-2 positive subjects (33). This finding was confirmed by the metabolomic study of Thomas et al., who observed a profound alteration of the kynurenine pathway in patients with SARS-CoV-2 infection (34). In their study population of 33 SARS-CoV-2 positive subjects, a significant decrease of tryptophan with concomitant increases of kynurenine, kynurenic acid and picolinic acid was observed.

Furthermore, the association between the disease outcome and the plasma levels of kynurenine pathway metabolites demonstrates that indicators of tryptophan metabolism - especially but not limited to kynurenine - may have the potential as prognostic biomarkers in individuals with SARS-CoV-2 infection. Kynurenine levels of patients compromised by virus-infections (Cytomegalovirus vs. COVID-19) are comparable, but much more pronounced in COVID-19 (30). In addition, we already showed that kynurenine is elevated in patients suffering from overtraining symptom and associated

chronic fatigue (35), which is also a common side effect of Long- and Post Covid, compared to healthy individuals.

Post-COVID patients appear to have a disrupted immune system to Long-COVID patients who fully recover. One reason is that the body is still fighting remnants of SARS-CoV-2. Other groups found that the virus spreads widely during an initial infection, while SARS-CoV-2 specific genetic remnants can remain in tissues for many months (i.a., in the intestines and lymph nodes) (36). A further possibility is that the initial viral infection induces chronic inflammatory processes, possibly by reactivating other viruses in the patient's body that are normally dormant. Most individuals are infected during their childhood and adolescence, and its reactivation might help predict whether a person will develop Long-COVID.

Beside CRP, we found correlations between kynurenine and peak IL-6 values in the acute infection phase. Long-term assessments are still undergoing, but recent studies point to a link between Long-COVID and elevated IL-6 concentrations (37). Hence, the simultaneous determination of EBV, IL-6 and kynurenine may therefore complement each other in a "Long-COVID-Panel" for the clinical assessment and monitoring, as all three can reliably be measured non-invasive in saliva (38), and might provide even higher prognosis accuracy.

Thus, our results are demonstrating the relevance concerning diagnosis and monitoring of a Long- and Post-COVID syndrome and PIMS in children and the potential for other virus induced inflammation monitoring. Furthermore, recent data indicates that the maintenance of gut dysbiosis and increased gut permeability, evident in acute COVID patients, may underpin Long-COVID (39). Given that alterations in gut dysbiosis/permeability impact on systemic mitochondrial function, including in immune and glial cells (40) as well as increasing the pro-inflammatory cytokines driving IDO and the conversion of tryptophan to kynurenine, the role of gut dysbiosis/permeability interactions with kynurenine, serotonin and melatonin may be important to examine. It should also be noted that the kynurenine activation of the AhR will actively suppress natural killer cells, and therefore the capacity of the body to detect and eliminate virus-infected cells as well as cancer cells (41).

Above that, our pilot experiment of determining kynurenine in serum and subsequently in saliva demonstrates the additional usefulness of clinical kynurenine monitoring. The non-invasive kynurenine measurement in saliva is a safe and fast approach of assessing the disease status of COVID-19 patients that is not biased by blood-thinning medications or other therapy targeting the cardiovascular or blood system.

Taken together, our data supports the following possible theory behind the Long-COVID syndrome: the longer lasting activation of the innate immunity, triggered additionally by genetic material of the virus in tissue, induce DAMP-like inflammatory reactions, which may end up in a subclinical chronic inflammation. This subclinical chronic inflammation could be detected by measuring kynurenine that opens a window for new therapeutical approaches which could be easy monitored.

Strengths and limitations

Nevertheless, some limitations of this study must be considered. Due to the retrospective study design, only the routinely measured parameters were available for statistical analysis. Furthermore, kynurenine concentrations in saliva and serum of Long- and Post-COVID patients were only determined in a limited subsample of the whole cohort, which limits the statistical effect size.

A strength of the study is that none of the patients in Group A or B was under hemodialysis. Therefore, an influence on the kynurenine level by this treatment is unlikely. Above that, this pilot study was partly designed as a "proof-of-concept" study to show the prognostic value of kynurenine monitoring. Although the preliminary results are promising, higher participant numbers are needed for still higher validity and reliability of the presented data.

Another source of bias may be the parenteral substitution of amino acids in ICU patients. We do not have information about the exact nutritional program of the included ICU patients. Hence, we cannot rule out an influence on the measurements of the tryptophan metabolites, although the effect might be supposedly weak (42). Considering a normal diet, the daily uptake is nearly five times higher than the need. Lack of supply for tryptophan is only existent in heavenly starving people and not in the western hemisphere, so an influence on the kynurenine level is again unlikely. Additionally there are a few more mechanisms regulating the tryptophan pathway (43) which need to be considered in interpreting the observed results.

Conclusion and future perspectives

Kynurenine can be regarded as a useful biomarker in detection of the inflammatory and hyperinflammatory character of the SARS-CoV-2 disease in the acute as well as the long-term progression. Furthermore, kynurenine is able to detect the chronic subclinical systemic inflammation typical for the Long-COVID- and more pronounced for Post-COVID syndrome.

In addition, we could demonstrate in a sub study with pilot character that in a subpopulation of previously COVID-19 positive patients, kynurenine could be the first time measured additionally in saliva and serum with comparable results. We are working on a test (ELISA as well as a LFA-format) to translate this biomarker testing in a new format either concerning the matrix (saliva) and the technique. Measurements in saliva opens the opportunity for self-monitoring of the patients and noninvasive therapy control.

Given the wider alterations arising from the conversion of tryptophan to kynurenine, including suppressed levels of serotonergic and melatonergic pathway activation (44), it will be important to determine the relevance of such coordinated changes together with kynurenine monitoring in acute, Long- and Post-COVID. Further pathway studies including the different sides of kynurenine pathways (hepatocytes, muscle cells, gut lumen) may shed additional light on the involvement of kynurinen and its metabolites in virus driven disease like COVID-19 and assist in clinical monitoring and disease outcome. Investigations on such processes will allow for better integration of the role of raised kynurenine levels in both Acute and Long-COVID.

Data availability statement

The original contributions presented in the study are included in the article/supplementary material. Further inquiries can be directed to the corresponding author.

Ethics statement

The studies involving human participants were reviewed and approved by ethics committee of the University of Ulm (4/2011, 312/2015, 19/2020) and ethics committee of the Ludwigs-Maximilians-University Munich (CORKUM, associated research project). The patients/participants provided their written informed consent to participate in this study.

Author contributions

DB, MS, DA, and J-LB contributed to conception and design of the study. DA and MS organized the database. DB, MS, JD, GD, J-LB, and DA performed the statistical analysis. DB, MS, and DA wrote the first draft of the manuscript. JD and GD wrote sections of the manuscript. All authors contributed to the article and approved the submitted version.

Acknowledgments

We gratefully acknowledge the continuous support of Prof. Dr. Jürgen M. Steinacker (Head of the Division of Sports and Rehabilitation Medicine Ulm) by allowing to use his laboratory and his intellectual input as well as B.Sc. Lucas John for the experimental analysis. We thank our collaboration partners JC Hellmuth (Department of Medicine III, University Hospital Munich, Bavaria, Germany), Clemens Scherer (Department of Medicine I, University Hospital Munich, Munich, Bavaria, Germany) and Maximilian Muenchhoff (Virology, Ludwig Maximilians University of Munich, Munich, Bavaria, Germany).

Conflict of interest

The authors declare that the research was conducted in the absence of any commercial or financial relationships that could be construed as a potential conflict of interest.

Publisher's note

All claims expressed in this article are solely those of the authors and do not necessarily represent those of their affiliated organizations, or those of the publisher, the editors and the reviewers. Any product that may be evaluated in this article, or claim that may be made by its manufacturer, is not guaranteed or endorsed by the publisher.

References

1. Land WG. *Innate alloimmunity. Part 2: Innate immunity and allograft rejection*. Lengerich: Pabst Science Publishers (2011). Available at: https://www.lehmanns.de/shop/medizin-pharmazie/21802432-9783899677386-innate-alloimmunity-part-2-innate-immunity-and-allograft-rejection.

2. Mittal M, Siddiqui MR, Tran K, Reddy SP, Malik AB. Reactive oxygen species in inflammation and tissue injury. *Antioxid Redox Signal* (2014) 20:1126–67. doi: 10.1089/ars.2012.5149

3. Sugawara Y, Uehara A, Fujimoto Y, Kusumoto S, Fukase K, Shibata K, et al. Toll-like receptors, NOD1, and NOD2 in oral epithelial cells. *J Dent Res* (2006) 85:524–9. doi: 10.1177/154405910608500609

4. Hippenstiel S, Opitz B, Schmeck B, Suttorp N. Lung epithelium as a sentinel and effector system in pneumonia–molecular mechanisms of pathogen recognition and signal transduction. *Respir Res* (2006) 7:97. doi: 10.1186/1465-9921-7-97

5. Greene CM, Carroll TP, Smith SG, Taggart CC, Devaney J, Griffin S, et al. TLR-induced inflammation in cystic fibrosis and non-cystic fibrosis airway epithelial cells. *J Immunol* (2005) 174:1638–46. doi: 10.4049/jimmunol.174.3.1638

6. Bektas A, Schurman SH, Franceschi C, Ferrucci L. A public health perspective of aging: do hyper-inflammatory syndromes such as COVID-19, SARS, ARDS, cytokine storm syndrome, and post-ICU syndrome accelerate short- and long-term inflammaging? *Immun Ageing* (2020) 17:23. doi: 10.1186/s12979-020-00196-8

7. Gu J, Gong E, Zhang B, Zheng J, Gao Z, Zhong Y, et al. Multiple organ infection and the pathogenesis of SARS. *J Exp Med* (2005) 202:415–24. doi: 10.1084/jem.20050828

8. Savitz J. The kynurenine pathway: A finger in every pie. *Mol Psychiatry* (2020) 25:131–47. doi: 10.1038/s41380-019-0414-4

9. Cervenka I, Agudelo LZ, Ruas JL. Kynurenines: Tryptophan's metabolites in exercise, inflammation, and mental health. *Science* (2017) 357:34. doi: 10.1126/science.aaf9794

10. Wirthgen E, Hoeflich A, Rebl A, Günther J. Kynurenic acid: The janus-faced role of an immunomodulatory tryptophan metabolite and its link to pathological conditions. *Front Immunol* (2017) 8:1957. doi: 10.3389/fimmu.2017.01957

11. Lee S-M, Park HY, Suh Y-S, Yoon EH, Kim J, Jang WH, et al. Inhibition of acute lethal pulmonary inflammation by the IDO-AhR pathway. *Proc Natl Acad Sci U.S.A.* (2017) 114:E5881–90. doi: 10.1073/pnas.1615280114

12. Chen Y, Guillemin GJ. Kynurenine pathway metabolites in humans: Disease and healthy states. *Int J Tryptophan Res* (2009) 2:1–19. doi: 10.4137/ijtr.s2097

13. Bouças AP, Rheinheimer J, Lagopoulos J. Why severe COVID-19 patients are at greater risk of developing depression: A molecular perspective. *Neuroscientist* (2022) 28:11–9. doi: 10.1177/1073858420967892

14. Vénéreau E, Ceriotti C, Bianchi ME. DAMPs from cell death to new life. *Front Immunol* (2015) 6:422. doi: 10.3389/fimmu.2015.00422

15. Harwood R, Allin B, Jones CE, Whittaker E, Ramnarayan P, Ramanan AV, et al. A national consensus management pathway for paediatric inflammatory multisystem syndrome temporally associated with COVID-19 (PIMS-TS): results of a national Delphi process. *Lancet Child Adolesc Health* (2021) 5:133–41. doi: 10.1016/S2352-4642(20)30304-7

16. Zhou F, Yu T, Du R, Fan G, Liu Y, Liu Z, et al. Clinical course and risk factors for mortality of adult inpatients with COVID-19 in wuhan, China: A retrospective cohort study. *Lancet* (2020) 395:1054–62. doi: 10.1016/S0140-6736(20)30566-3

17. Zhang Z-L, Hou Y-L, Li D-T, Li F-Z. Laboratory findings of COVID-19: A systematic review and meta-analysis. *Scand J Clin Lab Invest* (2020) 80:441–7. doi: 10.1080/00365513.2020.1768587

18. Liang W, Liang H, Ou L, Chen B, Chen A, Li C, et al. Development and validation of a clinical risk score to predict the occurrence of critical illness in hospitalized patients with COVID-19. *JAMA Intern Med* (2020) 180:1081–9. doi: 10.1001/jamainternmed.2020.2033

19. Yan L, Zhang H-T, Goncalves J, Xiao Y, Wang M, Guo Y, et al. An interpretable mortality prediction model for COVID-19 patients. *Nat Mach Intell* (2020) 2:283–8. doi: 10.1038/s42256-020-0180-7

20. Aziz M, Fatima R, Assaly R. Elevated interleukin-6 and severe COVID-19: A meta-analysis. *J Med Virol* (2020) 92:2283–5. doi: 10.1002/jmv.25948

21. Zhu J, Pang J, Ji P, Zhong Z, Li H, Li B, et al. Elevated interleukin-6 is associated with severity of COVID-19: A meta-analysis. *J Med Virol* (2021) 93:35–7. doi: 10.1002/jmv.26085

22. Sudre CH, Murray B, Varsavsky T, Graham MS, Penfold RS, Bowyer RC, et al. Attributes and predictors of long COVID. *Nat Med* (2021) 27:626–31. doi: 10.1038/s41591-021-01292-y

23. Mendelson M, Nel J, Blumberg L, Madhi SA, Dryden M, Stevens W, et al. Long-COVID: An evolving problem with an extensive impact. *S Afr Med J* (2020) 111:10–2. doi: 10.7196/SAMJ.2020.v111i11.15433

24. Maglietta G, Diodati F, Puntoni M, Lazzarelli S, Marcomini B, Patrizi L, et al. Prognostic factors for post-COVID-19 syndrome: A systematic review and meta-analysis. *J Clin Med* (2022) 11:1541–56. doi: 10.3390/jcm11061541

25. Herridge MS, Tansey CM, Matté A, Tomlinson G, Diaz-Granados N, Cooper A, et al. Functional disability 5 years after acute respiratory distress syndrome. *N Engl J Med* (2011) 364:1293–304. doi: 10.1056/NEJMoa1011802

26. Boomer JS, Green JM, Hotchkiss RS. The changing immune system in sepsis: is individualized immuno-modulatory therapy the answer? *Virulence* (2014) 5:45–56. doi: 10.4161/viru.26516

27. Davies MG, Hagen PO. Systemic inflammatory response syndrome. *Br J Surg* (1997) 84:920–35. doi: 10.1002/bjs.1800840707

28. Hotchkiss RS, Monneret G, Payen D. Immunosuppression in sepsis: a novel understanding of the disorder and a new therapeutic approach. *Lancet Infect Dis* (2013) 13:260–8. doi: 10.1016/S1473-3099(13)70001-X

29. Almulla AF, Supasitthumrong T, Tunvirachaisakul C, Algon AA, Al-Hakeim HK, Maes M. The tryptophan catabolite or kynurenine pathway in COVID-19 and critical COVID-19: A systematic review and meta-analysis. *BMC Infect Dis* (2022) 22:615. doi: 10.1186/s12879-022-07582-1

30. Kaden J, Abendroth D, Völp A, Marzinzig M. Dynamics and diagnostic relevance of kynurenine serum level after kidney transplantation. *Ann Transplant* (2015) 20:327–37. doi: 10.12659/AOT.893721

31. Abendroth D, Stangl MJ, Marzinzig M. *WO2014177680 - in vitro method for the early detection of a potential inflammation, in particular associated with rejection of a transplant, a neurodegenerative disorder or a depression (WO/2014/177680)* (2014). Available at: https://www.mysciencework.com/patent/download/vitro-method-early-detection-potential-inflammation-associated-rejection-transplant-EP2992332B1/EP2992332B1 (Accessed cited 2022 Aug 18).

32. García LF. Immune response, inflammation, and the clinical spectrum of COVID-19. *Front Immunol* (2020) 11:1441. doi: 10.3389/fimmu.2020.01441

33. Lawler NG, Gray N, Kimhofer T, Boughton B, Gay M, Yang R, et al. Systemic perturbations in amine and kynurenine metabolism associated with acute SARS-CoV-2 infection and inflammatory cytokine responses. *J Proteome Res* (2021) 20:2796–811. doi: 10.1021/acs.jproteome.1c00052

34. Thomas T, Stefanoni D, Reisz JA, Nemkov T, Bertolone L, Francis RO, et al. COVID-19 infection alters kynurenine and fatty acid metabolism, correlating with IL-6 levels and renal status. *JCI Insight* (2020) 5. doi: 10.1172/jci.insight.140327

35. Bizjak DA, Treff G, Zügel M, Schumann U, Winkert K, Schneider M, et al. Differences in immune response during competition and preparation phase in elite rowers. *Front Physiol* (2021) 12:803863. doi: 10.3389/fphys.2021.803863

36. Chertow D, Stein S, Ramelli S, Grazioli A, Chung J-Y, Singh M, et al. SARS-CoV-2 infection and persistence throughout the human body and brain. (2021). doi: 10.21203/rs.3.rs-1139035/v1

37. Phetsouphanh C, Darley DR, Wilson DB, Howe A, Munier CM, Patel SK, et al. Immunological dysfunction persists for 8 months following initial mild-to-moderate SARS-CoV-2 infection. *Nat Immunol* (2022) 23:210–6. doi: 10.1038/s41590-021-01113-x

38. Perkins E, Davison G. Epstein-Barr Virus (EBV) DNA as a potential marker of *in vivo* immunity in professional footballers. *Res Q Exerc Sport* (2021), 1–8. doi: 10.1080/02701367.2021.1932707

39. Giannos P, Prokopidis K. Gut dysbiosis and long COVID-19: Feeling gutted. *J Med Virol* (2022) 94:2917–8. doi: 10.1002/jmv.27684

40. Anderson G, Maes M. Gut dysbiosis dysregulates central and systemic homeostasis *via* suboptimal mitochondrial function: Assessment, treatment and classification implications. *Curr Top Med Chem* (2020) 20:524–39. doi: 10.2174/1568026620666200131094445

41. Anderson G. Tumour microenvironment: Roles of the aryl hydrocarbon receptor, O-GlcNAcylation, acetyl-CoA and melatonergic pathway in regulating dynamic metabolic interactions across cell types-tumour microenvironment and metabolism. *Int J Mol Sci* (2020) 22:141–71. doi: 10.3390/ijms22010141

42. Fernández-Castañeda A, Lu P, Geraghty AC, Song E, Lee M-H, Wood J, et al. Mild respiratory SARS-CoV-2 infection can cause multi-lineage cellular dysregulation and myelin loss in the brain. (2022). doi: 10.1101/2022.01.07.475453

43. Tanaka M, Vécsei L. Monitoring the kynurenine system: Concentrations, ratios or what else? *Adv Clin Exp Med* (2021) 30:775–8. doi: 10.17219/acem/139572

44. Anderson G, Carbone A, Mazzoccoli G. Tryptophan metabolites and aryl hydrocarbon receptor in severe acute respiratory syndrome, coronavirus-2 (SARS-CoV-2) pathophysiology. *Int J Mol Sci* (2021) 22:1597–1613. doi: 10.3390/ijms22041597

frontiers | Frontiers in Immunology

TYPE Original Research
PUBLISHED 23 September 2022
DOI 10.3389/fimmu.2022.957407

Check for updates

OPEN ACCESS

EDITED BY
Edwin Bölke,
Heinrich Heine University of Düsseldorf, Germany

REVIEWED BY
Mehmet Ağirbaşli,
Istanbul Medeniyet University, Turkey
Jian Zhou,
Second Xiangya Hospital, Central South University, China

*CORRESPONDENCE
Kai Kang
janekk79@126.com
Ming-Yan Zhao
mingyan0927@126.com

†These authors have contributed equally to this work

SPECIALTY SECTION
This article was submitted to Viral Immunology, a section of the journal Frontiers in Immunology

RECEIVED 31 May 2022
ACCEPTED 05 September 2022
PUBLISHED 23 September 2022

CITATION
Zhang J-N, Gao Y, Wang X-T, Li N-N, Du X, Tang Y-J, Lai Q-Q, Chen P-F, Yue C-S, Wu J-H, Kang K and Zhao M-Y (2022) Lymphocyte–C-reactive protein ratio can differentiate disease severity of COVID-19 patients and serve as an assistant screening tool for hospital and ICU admission. *Front. Immunol.* 13:957407. doi: 10.3389/fimmu.2022.957407

COPYRIGHT
© 2022 Zhang, Gao, Wang, Li, Du, Tang, Lai, Chen, Yue, Wu, Kang and Zhao. This is an open-access article distributed under the terms of the Creative Commons Attribution License (CC BY). The use, distribution or reproduction in other forums is permitted, provided the original author(s) and the copyright owner(s) are credited and that the original publication in this journal is cited, in accordance with accepted academic practice. No use, distribution or reproduction is permitted which does not comply with these terms.

Lymphocyte–C-reactive protein ratio can differentiate disease severity of COVID-19 patients and serve as an assistant screening tool for hospital and ICU admission

Jian-Nan Zhang[1†], Yang Gao[2,3†], Xin-Tong Wang[1†], Na-Na Li[1†], Xue Du[1†], Yu-Jia Tang[1], Qi-Qi Lai[1], Peng-Fei Chen[1], Chuang-Shi Yue[1], Ji-Han Wu[1], Kai Kang[1,3*] and Ming-Yan Zhao[1*]

[1]Department of Critical Care Medicine, The First Affiliated Hospital of Harbin Medical University, Harbin, China, [2]Department of Critical Care Medicine, The Sixth Affiliated Hospital of Harbin Medical University, Harbin, China, [3]Institute of Critical Care Medicine, The Sino Russian Medical Research Center of Harbin Medical University, Harbin, China

In this study, we aimed to explore whether lymphocyte–C-reactive protein ratio (LCR) can differentiate disease severity of coronavirus disease 2019 (COVID-19) patients and its value as an assistant screening tool for admission to hospital and intensive care unit (ICU). A total of 184 adult COVID-19 patients from the COVID-19 Treatment Center in Heilongjiang Province at the First Affiliated Hospital of Harbin Medical University between January 2020 and March 2021 were included in this study. Patients were divided into asymptomatic infection group, mild group, moderate group, severe group, and critical group according to the Diagnosis and Treatment of New Coronavirus Pneumonia (ninth edition). Demographic and clinical data including gender, age, comorbidities, severity of COVID-19, white blood cell count (WBC), neutrophil proportion (NEUT%), lymphocyte count (LYMPH), lymphocyte percentage (LYM%), red blood cell distribution width (RDW), platelet (PLT), C-reactive protein (CRP), alanine aminotransferase (ALT), aspartate aminotransferase (AST), serum creatinine (SCr), albumin (ALB), total bilirubin (TB), direct bilirubin (DBIL), indirect bilirubin (IBIL), and D-dimer were obtained and collated from medical records at admission, from which sequential organ failure assessment (SOFA) score and LCR were calculated, and all the above indicators were compared among the groups. Multiple clinical parameters, including LYMPH, CRP, and LCR, showed significant differences among the groups. The related factors to classify COVID-19 patients into moderate, severe, and critical groups included age, number of comorbidities, WBC, LCR, and AST. Among these factors, the number of comorbidities showed the greatest effect, and only WBC and LCR were protective factors. The area under the receiver operating characteristic (ROC) curve of LCR to classify COVID-19 patients into moderate, severe, and critical groups was 0.176. The cutoff value

of LCR and the sensitivity and specificity of the ROC curve were 1,780.7050 and 84.6% and 66.2%, respectively. The related factors to classify COVID-19 patients into severe and critical groups included the number of comorbidities, PLT, LCR, and SOFA score. Among these factors, SOFA score showed the greatest effect, and LCR was the only protective factor. The area under the ROC curve of LCR to classify COVID-19 patients into severe and critical groups was 0.106. The cutoff value of LCR and the sensitivity and specificity of the ROC curve were 571.2200 and 81.3% and 90.0%, respectively. In summary, LCR can differentiate disease severity of COVID-19 patients and serve as a simple and objective assistant screening tool for hospital and ICU admission.

KEYWORDS

lymphocyte–C-reactive protein ratio, disease severity, COVID-19, SARS-CoV-2 infection, screening tool, hospital admission, ICU admission

Background

Although it has been more than 2 years since the first outbreak of coronavirus disease 2019 (COVID-19) in Wuhan, this highly pathogenic disease has so far shown no signs of abating, suggesting that severe acute respiratory syndrome coronavirus type 2 (SARS-CoV-2) may coexist with humans for a long time to come (1). As the epidemic spreads, rapid recombination and successive mutation of SARS-CoV-2 make its variants more pathogenic and transmissible, which in turn possess the ability to continue spreading in the face of rising population immunity (2–5). Without predictable preparation and effective medical management, the rapid outbreak and surge of COVID-19 patients in a short period will overwhelm limited medical resources (6). Under these new circumstances, China's response must strike a balance between epidemic prevention and management and economic development, making the need for China to adopt a unique anti-epidemic path in the near future, rather than copying the models in other countries.

The latest Diagnosis and Treatment of New Coronavirus Pneumonia (ninth edition) has pointed out that mild COVID-19 cases, let alone asymptomatic infection cases, only need centralized isolation without hospitalization. The timely detection of COVID-19 patients with disease progression to severe and critical illness and their transfer to intensive care unit (ICU) for appropriate organ support are expected to eventually improve prognosis (7). There is an urgent need to explore an easy-to-implement and high-accuracy clinical objective parameter as an assistant screening tool to identify COVID-19 patients who need hospitalization and detect severe and critical COVID-19 patients who need timely transfer to ICU. The pathogenesis of COVID-19 may be complex and related to inflammation, immunity, blood coagulation, multiple organ functions, and their interactions (8–10). Therefore, the ideal candidate clinical variables should contain some parameters reflecting these aspects but should not be too complicated and difficult to implement as an assistant screening tool for hospital and ICU admission.

To address the above issue, we aimed to explore whether the lymphocyte–C-reactive protein ratio (LCR) can differentiate disease severity of COVID-19 patients and its value as an assistant screening tool for hospital and ICU admission. Our findings will provide a solid basis for the rational allocation and utilization of limited medical resources in the ongoing pandemic.

Methods

Study design

A total of 184 adult COVID-19 patients from the COVID-19 Treatment Center in Heilongjiang Province at the First Affiliated Hospital of Harbin Medical University between January 2020 and March 2021 were included in this single-center retrospective study. These patients were divided into asymptomatic infection group (n = 16), mild group (n = 23), moderate group (n = 105), severe group (n = 33), and critical group (n = 7) according to the Diagnosis and Treatment of New Coronavirus Pneumonia (ninth edition). Demographic and clinical data including gender, age, comorbidities, severity of COVID-19, white blood cell count (WBC), neutrophil proportion (NEUT%), lymphocyte count (LYMPH), lymphocyte percentage (LYM%), red blood cell distribution width (RDW), platelet (PLT), C-reactive protein (CRP), alanine aminotransferase (ALT), aspartate aminotransferase (AST), serum creatinine (SCr), albumin (ALB), total bilirubin (TB), direct bilirubin (DBIL), indirect bilirubin (IBIL), and D-dimer were obtained and collated from medical

records at admission. From these data, sequential organ failure assessment (SOFA) score and LCR were calculated, and all the above indicators were compared among the groups. This study was reviewed and approved by the Ethics Committee of the First Affiliated Hospital of Harbin Medical University (IRB number: IRB-AF/SC-04/01.0).

Study population

In this study, the inclusion criteria were age ≥18 years old and confirmed COVID-19 patients. COVID-19 patients who met the following criteria were excluded: uncontrolled malignant tumors with multiple metastases, leukemia, acquired immunodeficiency syndrome (AIDS), chronic organ failure, immunotherapy or organ transplant within 6 months, autoimmune disorder, pregnant or breastfeeding women, and incomplete medical records (Figure 1).

Diagnosis and classification of COVID-19

All enrolled adult COVID-19 patients were confirmed by detection of SARS-CoV-2 nucleic acids on oropharyngeal swabs, nasopharyngeal swabs, or lower respiratory tract specimens. These patients were then classified into asymptomatic infection group, mild group, moderate group, severe group, and critical group according to the Diagnosis and Treatment of New Coronavirus Pneumonia (ninth edition).

Data collection

Demographic data, involving gender, age, comorbidities, and clinical data, including the severity of COVID-19, SOFA score, WBC, NEUT%, LYMPH, LYM%, RDW, PLT, CRP, LCR, ALT, AST, SCr, ALB, TB, DBIL, IBIL, and D-dimer were obtained and collated from medical records at admission by dedicated personnel in our research team. None of the other members of our research team was privy to the enrolled patient's personal information beyond what was required for this study.

Statistical analyses

SPSS 23.0 (SPSS, Inc., Chicago, IL, USA) was used for statistical analyses. Continuous data with normal distribution are expressed as mean ± standard deviation (SD), while those with non-normal distribution are described as median (P25, P75). One-way analysis of variance (ANOVA) was adopted for three-group comparisons of continuous data with normal distribution. If there was a significant difference, the least significant difference (LSD) method was used for further pairwise comparison. The Kruskal–Wallis rank-sum test was employed for three-group comparisons and further pairwise comparisons of continuous data with non-normal distribution. Independent-samples *t*-test was used to perform intergroup comparisons of continuous data with normal distribution, while the Mann–Whitney *U* test was adopted for intergroup comparisons of continuous data with non-

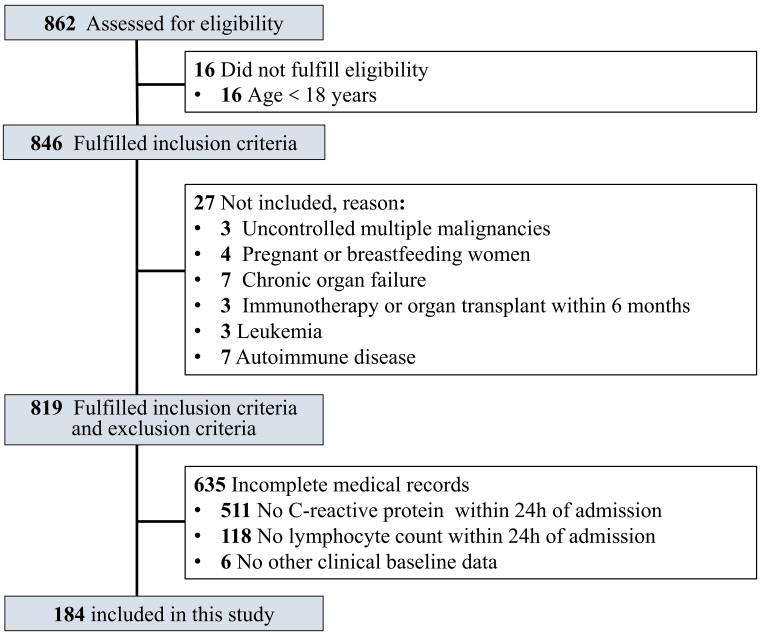

FIGURE 1
Flowchart of the study participants.

normal distribution. On the basis of intergroup comparisons, multiple logistic regression analysis was conducted with significant variables as independent variables and groups as dependent variables. The independent variables were screened by the Wald backward method. The receiver operating characteristic (ROC) curve of LCR was analyzed, and the area under the ROC curve, the sensitivity and specificity of the ROC curve, and the cutoff value of LCR were calculated. *P*-values <0.05 were considered to indicate statistical significance.

Results

Comparison of demographic and clinical baseline data among asymptomatic infection and mild groups combined, moderate group, and severe and critical groups combined

A total of 184 adult COVID-19 patients from the COVID-19 Treatment Center in Heilongjiang Province at the First Affiliated Hospital of Harbin Medical University between January 2020 and March 2021 were included and divided into asymptomatic infection group (n = 16), mild group (n = 23), moderate group (n = 105), severe group (n = 33), and critical group (n = 7) according to the Diagnosis and Treatment of New Coronavirus Pneumonia (ninth edition). Age, number of comorbidities, WBC, NEUT%, LYMPH, LYM%, PLT, CRP, AST, ALB, TB, IBIL, D-dimer, LCR, and SOFA score showed significant differences among the groups (P = 0.000, P = 0.000, P = 0.021, P = 0.000, P = 0.000, P = 0.000, P = 0.000, P = 0.000, P = 0.000, P = 0.000, P = 0.014, P = 0.000, P = 0.000, P = 0.000, respectively). No significant differences were observed in the remaining demographic and clinical baseline data, including gender, hypertension, diabetes, RDW, ALT, SCr, and DBIL (Table 1).

Comparison of demographic and clinical baseline data between asymptomatic infection and mild groups combined and moderate, severe, and critical groups combined

Age, hypertension, diabetes, number of comorbidities, WBC, LYMPH, PLT, CRP, AST, ALB, DBIL, D-dimer, LCR, and SOFA

TABLE 1 Comparison of demographic and clinical baseline data among asymptomatic infection and mild groups combined, moderate group, and severe and critical groups combined.

	Asymptomatic infection and mild groups combined	Moderate group	Severe and critical groups combined	$Z/F/\chi^2$	P
Age	42.00 (31.00, 56.00)	62.00 (48.00, 67.00) a	68.00 (58.25, 75.75) ab	37.382	0.000
Gender (F/M)	19/20	61/44	22/18	1.016	0.602
Hypertension (Y/N)	6/33	38/67	14/26	5.989	0.052
Diabetes (Y/N)	1/38	15/90	8/32	5.626	0.060
Number of comorbidities	0 (0, 1)	1 (1, 3) a	3 (1, 4.75) ab	36.277	0.000
WBC	6.38 ± 2.04	5.29 ± 2.03 a	5.36 ± 2.47 a	3.930	0.021
NEUT%	62.37 ± 10.40	61.40 ± 11.92	73.63 ± 17.25 ab	13.397	0.000
LYMPH	1.50 (1.19, 1.83)	1.24 (0.89, 1.63)	0.65 (0.42, 0.99) ab	45.062	0.000
LYM%	25.37 ± 9.27	27.37 ± 9.85	15.85 ± 8.99 ab	21.281	0.000
RDW	40.20 (38.70, 42.20)	41.00 (38.40, 43.15)	41.55 (38.00, 43.93)	0.282	0.868
PLT	228.00 (177.00, 271.00)	174.00 (140.00, 228.00) a	148.00 (121.50, 209.25) a	16.799	0.000
CRP	4.57 ± 8.03	21.23 ± 38.73 a	52.76 ± 47.98 ab	17.474	0.000
ALT	23.60 (17.70, 36.89)	25.60 (17.50, 36.75)	28.61 (18.15, 38.70)	0.660	0.791
AST	19.50 (16.80, 24.83)	25.60 (19.36, 37.65) a	32.94 (20.50, 51.67) a	20.579	0.000
SCr	61.20 (48.99, 73.88)	62.25 (53.20, 73.75)	63.79 (51.10, 86.28)	0.376	0.829
ALB	42.93 ± 4.63	39.74 ± 5.00 a	34.85 ± 5.75 ab	25.551	0.000
TB	8.80 (4.55, 10.80)	7.80 (6.13, 11.71)	11.00 (7.74, 16.41) ab	15.929	0.000
DBIL	1.70 (0.00, 2.30)	2.00 (0.00, 3.10)	2.65 (0.00, 4.68)	5.685	0.058
IBIL	7.00 (3.13, 8.80)	6.74 (4.30, 8.81)	8.46 (5.67, 12.48) ab	8.519	0.014
D-dimer	0.56 (0.47, 0.72)	0.74 (0.54, 1.01) a	1.17 (0.67, 3.01) ab	27.192	0.000
LCR	9,554.14 (2,560.61, 27,000.00)	1,404.96 (575.52, 4,941.62) a	140.42 (71.32, 420.27) ab	76.498	0.000
SOFA score	0 (0, 0)	0 (0, 1)	3 (2, 5) ab	80.893	0.000

a and b represent significant differences compared to asymptomatic infection and mild groups combined and moderate group, respectively.

10.3389/fimmu.2022.957407

score showed significant differences between the groups ($P = 0.000$, $P = 0.015$, $P = 0.029$, $P = 0.000$, $P = 0.001$, $P = 0.000$, $P = 0.000$, $P = 0.000$, $P = 0.000$, $P = 0.033$, $P = 0.000$, $P = 0.000$, $P = 0.000$, respectively), while no significant differences were seen in the remaining demographic and clinical baseline data, including gender, NEUT%, LYM%, RDW, ALT, SCr, TB, and IBIL (Table 2).

Analysis of the related factors to classify COVID-19 patients into moderate, severe, and critical groups

The related factors to classify COVID-19 patients into moderate, severe, and critical groups included age, number of comorbidities, WBC, LCR, and AST. With every unit change in age, number of comorbidities, WBC, LCR, and AST, the possibility of classifying COVID-19 patients into moderate, severe, and critical groups was 1.054, 1.814, 0.719, 0.9999, and 1.064 of the original rates, respectively. Among these factors, the number of comorbidities showed the greatest effect, and only WBC and LCR were protective factors (Table 3). The area under the ROC curve of LCR to classify COVID-19 patients into moderate, severe, and critical groups was 0.176 (Figure 2 and Table 4). The cutoff value of LCR and the sensitivity and specificity of the ROC curve were 1,780.7050 and 84.6% and 66.2%, respectively.

Comparison of demographic and clinical baseline data between asymptomatic infection, mild, and moderate groups combined and severe and critical groups combined

Significant differences were obtained in age, number of comorbidities, NEUT%, LYMPH, LYM%, PLT, CRP, AST, ALB, TB, IBIL, D-dimer, LCR, and SOFA score between the groups ($P = 0.000$, $P = 0.000$, $P = 0.000$, $P = 0.000$, $P = 0.000$, $P = 0.008$, $P = 0.000$, $P = 0.004$, $P = 0.000$, $P = 0.000$, $P = 0.004$, $P = 0.000$, $P = 0.000$, $P = 0.000$, respectively), while no significant differences were observed in the remaining demographic and clinical baseline data, including gender, hypertension, diabetes, WBC, RDW, ALT, SCr, and DBIL (Table 5).

TABLE 2 Comparison of demographic and clinical baseline data between asymptomatic infection and mild groups combined and moderate, severe, and critical groups combined.

	Asymptomatic infection and mild groups combined	Moderate, severe, and critical groups combined	$Z/t/\chi^2$	P
Age	42.00 (31.00, 56.00)	64.00 (50.50, 70.00)	−5.335	0.000
Gender (F/M)	19/20	83/62	0.904	0.342
Hypertension (Y/N)	6/33	52/93	5.970	0.015
Diabetes (Y/N)	1/38	23/122	4.792	0.029
Number of comorbidities	0 (0, 1)	2 (1, 3)	−5.058	0.000
WBC	5.98 (4.92, 7.46)	5.00 (3.85, 6.26)	−3.302	0.001
NEUT%	62.37 ± 10.40	64.77 ± 14.61	−0.963	0.337
LYMPH	1.50 (1.19, 1.83)	1.07 (0.67, 1.59)	−3.688	0.000
LYM%	25.37 ± 9.27	24.19 ± 10.89	0.619	0.537
RDW	40.20 (38.70, 42.20)	41.00 (38.35, 43.15)	−0.422	0.673
PLT	228.00 (177.00, 271.00)	168.00 (138.00, 224.00)	−3.722	0.000
CRP	1.68 (0.50, 6.02)	13.98 (3.94, 34.87)	−6.137	0.000
ALT	23.60 (17.70, 36.89)	27.00 (17.63, 36.90)	−0.608	0.543
AST	19.50 (16.80, 24.83)	27.30 (19.80, 42.04)	−4.162	0.000
SCr	62.20 (48.99, 73.88)	62.30 (52.35, 74.20)	−0.097	0.923
ALB	42.93 ± 4.63	38.39 ± 5.64	4.623	0.000
TB	8.80 (4.55, 10.80)	8.80 (6.55, 13.35)	−1.690	0.091
DBIL	1.70 (0.00, 2.30)	2.10 (0.00, 3.35)	−2.138	0.033
IBIL	7.00 (3.13, 8.80)	7.09 (4.40, 9.69)	−1.128	0.259
D-dimer	0.56 (0.47, 0.72)	0.80 (0.56, 1.24)	−4.031	0.000
LCR	9,554.14 (2,560.61, 27,000.00)	733.77 (241.72, 3,629.01)	−6.211	0.000
SOFA score	0 (0, 0)	1 (0, 2)	−4.500	0.000

10.3389/fimmu.2022.957407

TABLE 3 Analysis of the related factors to classify COVID-19 patients into moderate, severe, and critical groups.

	B	SE	Wald	*P*-value	OR	95% CI	
						Lower bound	Upper bound
Age	0.052	0.017	9.088	0.003	1.054	1.019	1.090
Number of comorbidities	0.595	0.265	5.038	0.025	1.814	1.078	3.051
WBC	−0.331	0.129	6.609	0.010	0.719	0.558	0.924
LCR	−0.00089	0.00025	12.359	0.000	0.9999	0.99986	0.99996
AST	0.062	0.027	5.335	0.021	1.064	1.009	1.122
Constant	−1.081	1.169	0.855	0.355	0.339		

Analysis of the related factors to classify COVID-19 patients into severe and critical groups

The related factors to classify COVID-19 patients into severe and critical groups included the number of comorbidities, PLT, LCR, and SOFA score. With every unit change in the number of comorbidities, PLT, LCR, and SOFA score, the possibility of classifying COVID-19 patients into severe and critical groups was 1.466, 1.009, 0.9996, and 3.56 of the original rates, respectively. Among these factors, SOFA score showed the greatest effect, and only LCR was a protective factor (Table 6). The area under the ROC curve of LCR to classify COVID-19 patients into severe and critical groups was 0.106 (Figure 3 and Table 7). The cutoff value of LCR and the sensitivity and specificity of the ROC curve were 571.2200 and 81.3% and 90.0%, respectively.

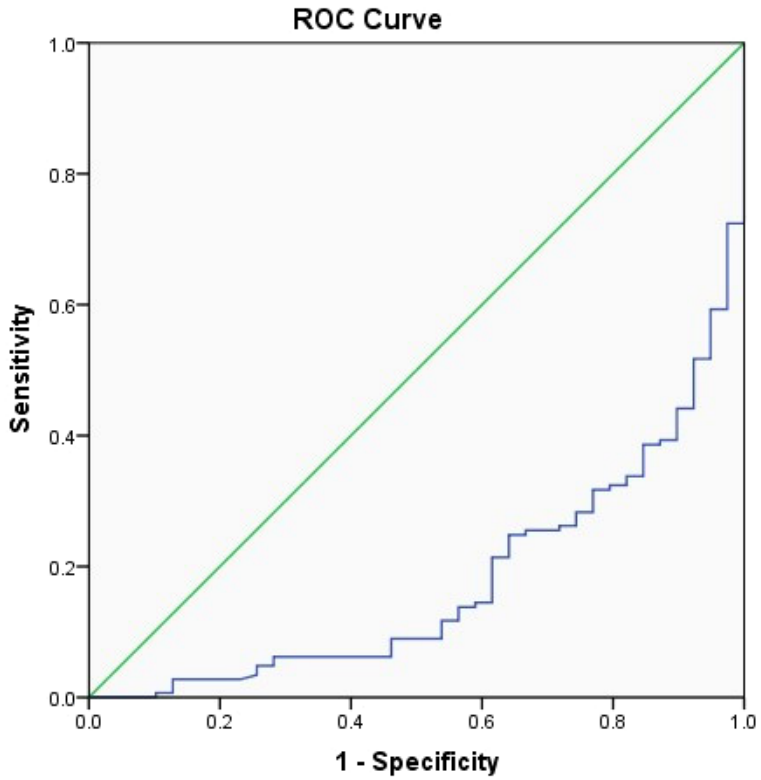

FIGURE 2
The receiver operating characteristic (ROC) curve of LCR to classify COVID-19 patients into moderate, severe, and critical groups.

TABLE 4 Area under the receiver operating characteristic curve.

Area	SE	Asymptotic, *P*-value	Lower bound	Asymptotic 95% CI
				Upper bound
0.176	0.034	0.000	0.108	0.243

Discussion

SARS-CoV-2, a novel highly pathogenic human coronavirus (hCoV), has posed an unprecedented and persistent threat to the global health system due to rapid evolution resulting in constant emergence of variants with spike protein mutations. Mutations in SARS-CoV-2 enable it to facilitate antigenic shifting for escaping the host antiviral defense and the humoral immune system. This makes it possible to break through the protection of vaccination and then increases the risk of infection in vaccinated populations and reinfection in those previously infected with different variants and even leads to repeated outbreaks of the epidemic (3, 11–13). Although human-to-human transmission is still the main pathway of COVID-19 spread, SARS-CoV-2 infections caused by indirect transmission from the contamination of inert/inanimate surfaces are increasingly common (14). It is important to note that environmental contamination caused by infected animals, especially domestic pets, constitutes a potential virus reservoir and may be one of the pathways of SARS-CoV-2 transmission during COVID-19 outbreaks, despite the lack of direct evidence of human–animal–human transmission (15, 16). A small blind spot in epidemic prevention and management will lead to a total loss of the epidemic response (17).

COVID-19 patients with different disease severity should be triaged to ensure the rational allocation and utilization of limited medical resources, such as centralized isolation and treatment for asymptomatic infection and mild patients, hospitalization for moderate patients, and timely transfer to ICU for severe and critical cases. Therefore, an easy-to-implement and high-accuracy clinical objective parameter as an assistant screening tool to classify COVID-19 patients is required. Multiple candidate clinical parameters, including LYMPH and CRP involved in this study, have been shown to be closely

TABLE 5 Comparison of demographic and clinical baseline data between asymptomatic infection, mild, and moderate groups combined and severe and critical groups combined.

	Asymptomatic infection, mild, and moderate groups combined	Severe and critical groups combined	$Z/t/\chi^2$	*P*
Age	55.50 (42.25, 66.00)	68.00 (58.25, 75.75)	−4.331	0.000
Gender (F/M)	80/64	22/18	0.004	0.950
Hypertension (Y/N)	44/100	14/26	0.286	0.592
Diabetes (Y/N)	16/128	8/32	2.181	0.140
Number of comorbidities	1 (0, 2)	3 (1, 4.75)	−4.529	0.000
WBC	5.27 (3.99, 6.78)	4.85 (3.79, 5.87)	−1.225	0.221
NEUT%	61.55 (53.95, 69.33)	75.8 (66.95, 85.08)	−5.249	0.000
LYMPH	1.35 (0.99, 1.69)	0.65 (0.42, 0.99)	−6.403	0.000
LYM%	26.82 ± 9.71	15.85 ± 8.99	6.424	0.000
RDW	40.8 (38.50, 42.88)	41.55 (38.00, 43.93)	−0.426	0.670
PLT	198.00 (149.75, 238.75)	148.00 (121.50, 209.25)	−2.668	0.008
CRP	6.30 (1.70, 14.48)	35.49 (20.90, 68.05)	−7.012	0.000
ALT	25.37 (17.55, 36.78)	28.61 (18.15, 38.70)	−0.685	0.494
AST	23.36 (18.00, 34.17)	32.94 (20.50, 51.67)	−2.873	0.004
SCr	62.08 (52.45, 73.16)	63.79 (51.10, 86.28)	−0.609	0.542
ALB	40.60 ± 5.09	34.85 ± 5.75	6.152	0.000
TB	8.10 (5.93, 10.98)	11.00 (7.74, 16.41)	−3.940	0.000
DBIL	1.85 (0.00, 3.00)	2.65 (0.00, 4.68)	−1.600	0.110
IBIL	6.77 (4.20, 8.78)	8.455 (5.67, 12.48)	−2.898	0.004
D-dimer	0.69 (0.52, 0.94)	1.17 (0.67, 3.01)	−4.284	0.000
LCR	2,407.47 (640.31, 8,755.06)	140.42 (71.32, 420.27)	−7.621	0.000
SOFA score	0 (0, 1)	3 (2, 5)	−8.721	0.000

10.3389/fimmu.2022.957407

TABLE 6 Analysis of the related factors to classify COVID-19 patients into severe and critical groups.

	B	SE	Wald	*df*	*P*-value	OR	95% CI	
							Lower bound	Upper bound
Number of comorbidities	0.382	0.180	4.527	1.000	0.033	1.466	1.031	2.084
PLT	0.009	0.004	4.002	1.000	0.045	1.009	1.000	1.018
LCR	−0.00039	0.00020	3.847	1.000	0.049	0.99960	0.99920	0.99999
SOFA score	1.270	0.256	24.542	1.000	0.000	3.560	2.154	5.884
Constant	−4.881	1.107	19.438	1.000	0.000	0.008		

associated with disease severity, rapid progression, and clinical prognosis in COVID-19 patients (10, 18–21).

Lymphocytes are a type of white blood cell, accounting for about 20%–40% of all white blood cells. They are mainly produced by lymphoid organs and reflect the body's protective immune ability against infection. Related studies showed that lymphopenia at the time of admission was strongly associated with organ damage, disease severity, need for intensive therapy, and poor prognosis in COVID-19 patients, especially in younger cases (22, 23). Redistribution of T cells, termination of T-cell activation by proinflammatory cytokines, and direct destruction of T cells induced by SARS-CoV-2 might be the main causes of lymphopenia (21, 24–26). Likewise, CRP, as a non-specific acute-phase reactant and representative marker of systemic inflammatory response syndrome (SIRS), was found to be significantly elevated at the initial and progression stages of SARS-CoV-2 infection and could be an early clinical predictor for disease severity and adverse outcomes (18, 27, 28). CRP could also activate complement and co-induce the production and release of proinflammatory cytokines, which were involved in the pathogenesis of COVID-19 (29). This further suggested that uncontrolled systemic inflammatory response to SARS-CoV-2 invasion, rather than the fatal virus

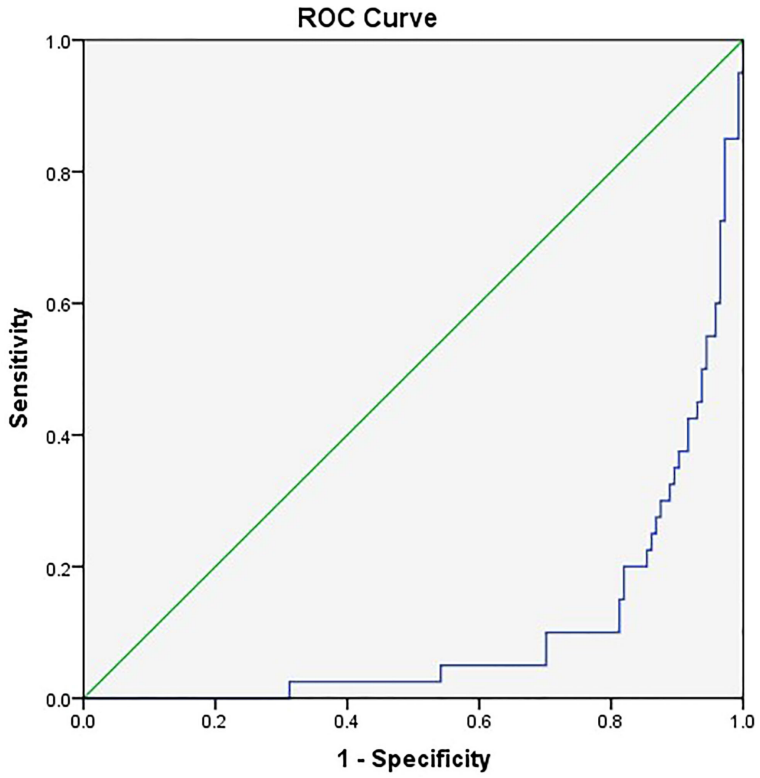

FIGURE 3
The receiver operating characteristic (ROC) curve of LCR to classify COVID-19 patients into severe and critical groups.

TABLE 7 Area under the receiver operating characteristic curve.

Area	SE	Asymptotic, *P*-value	Asymptotic 95% CI	
			Lower bound	Upper bound
0.106	0.026	0.000	0.054	0.157

infection itself, is a driver behind disease deterioration and poor prognosis in COVID-19 patients (8).

It is self-evident that imbalanced immune responses and uncontrolled systemic inflammatory responses intertwine, interacting and influencing each other in the pathogenesis of COVID-19 (30). LCR, as the ratio of the above two clinical parameters, represents both the protective immune activation status and the degree of systemic inflammatory response of the body after SARS-CoV-2 invasion. Perioperative LCR was first utilized as a promising novel biomarker for assessing disease development and the risk of recurrence. It was used in predicting postoperative complications and short-term and long-term prognoses and determining individualized therapeutic strategies in patients with malignant diseases and then extended to many other areas (31–34). A declined level of LCR in COVID-19 patients suggests compromised immune responses and/or an enhancement of systemic inflammatory responses, either of which can be fatal after SARS-CoV-2 invasion. Several lines of evidence demonstrated that the level of LCR could provide pivotal information for evaluating disease severity and predicting prognosis in COVID-19 patients, but its value proposed in our study as an assistant screening tool for admission to hospital and ICU had not been further explored (35, 36).

To our knowledge, our study was the first to explore the value of LCR as an assistant screening tool for COVID-19-related hospital and ICU admission. Our results showed that LCR exhibited significant differences among the groups regardless of grouping. LCR was a protective factor in moderate, severe, and critical groups combined, as well as severe and critical groups combined. The cutoff values of LCR to classify COVID-19 patients into moderate, severe, and critical groups and severe and critical groups were 1,780.7050 and 571.2200, respectively, proving that it can be utilized as an assistant screening tool to triage COVID-19 patients. That is, when the level of LCR in COVID-19 patients is greater than 1,780.7050, between 178.7050 and 571.2200, and less than 571.2200, centralized isolation and treatment, hospitalization, and timely transfer to ICU can be considered, respectively.

Several limitations in the present study should be noted. First of all, the reliability and generalizability of our conclusion were limited by the nature of a single-center retrospective study. Second, due to the lack of LYMPH and CRP within 24 h of admission in a large number of asymptomatic infection and mild patients with COVID-19, the final sample size of our study was relatively small, and thus the results need to be interpreted with caution. Finally, the clinical value of dynamic monitoring of LCR was not further discussed.

Conclusion

The present study is the first pilot study showing that LCR, as the ratio of lymphocyte to CRP, can differentiate disease severity of COVID-19 patients and serve as a simple and objective assistant screening tool for admission to hospital and ICU. Our findings need to be further validated with a larger sample size.

Data availability statement

The raw data supporting the conclusions of this article will be made available by the authors, without undue reservation.

Ethics statement

The study was reviewed and approved by the Ethics Committee of the First Affiliated Hospital of Harbin Medical University (IRB-AF/SC-04/01.0). Written informed consent for participation was not required for this study in accordance with national legislation and institutional requirements.

Author contributions

J-NZ, YG, X-TW, N-NL, XD, KK, and M-YZ took part in the literature search, conception, study design, statistical analysis, analysis and discussion of results, and manuscript preparation, editing, and review. Y-JT, Q-QL, P-FC, C-SY, and J-HW assisted in the literature search, data acquisition and collation, statistical analysis, analysis and discussion of results, and manuscript preparation. All authors read and approved the final article. J-NZ, YG, X-TW, N-NL and XD contributed equally to this work.

Funding

This study was supported by the Key Research and Development Project of Heilongjiang Province (GA21C011),

the National Natural Science Foundation of China (Nos. 81772045, 81902000, and 82172164), Heilongjiang Province Postdoctoral Start-up Fund (LBH-Q20037), and Scientific Research Innovation Fund of The First Affiliated Hospital of Harbin Medical University (Nos. 2021M08).

Acknowledgments

The authors are grateful to all colleagues who worked with them in the COVID-19 Treatment Center of Heilongjiang Province and all those who provided selfless advice and help for this article. We pay tribute to the medical staff who lost their lives in the national fight against the COVID-19 epidemic.

Conflict of interest

The authors declare that the research was conducted in the absence of any commercial or financial relationships that could be construed as a potential conflict of interest.

Publisher's note

All claims expressed in this article are solely those of the authors and do not necessarily represent those of their affiliated organizations, or those of the publisher, the editors and the reviewers. Any product that may be evaluated in this article, or claim that may be made by its manufacturer, is not guaranteed or endorsed by the publisher.

References

1. Chen Q, Gao Y, Wang CS, Kang K, Yu H, Zhao MY, et al. Exploration of transmission chain and prevention of the recurrence of coronavirus disease 2019 in heilongjiang province due to in-hospital transmission. *World J Clin cases* (2021) 9:5420–6. doi: 10.12998/wjcc.v9.i20.5420

2. Saito A, Irie T, Suzuki R, Maemura T, Nasser H, Uriu K, et al. Enhanced fusogenicity and pathogenicity of SARS-CoV-2 delta P681R mutation. *Nature* (2022) 602:300–6. doi: 10.1038/s41586-021-04266-9

3. Tao K, Tzou PL, Nouhin J, Gupta RK, de Oliveira T, Kosakovsky Pond SL, et al. The biological and clinical significance of emerging SARS-CoV-2 variants. *Nat Rev Genet* (2021) 22:757–73. doi: 10.1038/s41576-021-00408-x

4. Meo SA, Meo AS, Al-Jassir FF, Klonoff DC. Omicron SARS-CoV-2 new variant: global prevalence and biological and clinical characteristics. *Eur Rev Med Pharmacol Sci* (2021) 25:8012–8. doi: 10.26355/eurrev_202112_27652

5. Chen J, Wang R, Wang M, Wei GW. Mutations strengthened SARS-CoV-2 infectivity. *J Mol Biol* (2020) 432:5212–26. doi: 10.1016/j.jmb.2020.07.009

6. Yang B, Gao Y, Kang K, Li J, Wang L, Wang H, et al. Holistic care model of time-sharing management for severe and critical COVID-19 patients. *World J Clin cases* (2020) 8:5513–7. doi: 10.12998/wjcc.v8.i22.5513

7. Wang CS, Gao Y, Kang K, Fei DS, Meng XL, Liu HT, et al. Standardization of critical care management of non-critically ill patients with COVID-19. *World J Clin cases* (2021) 9:2696–702. doi: 10.12998/wjcc.v9.i12.2696

8. Gao Y, Wang C, Kang K, Peng Y, Luo Y, Liu H, et al. Cytokine storm may not be the Chief culprit for the deterioration of COVID-19. *Viral Immunol* (2021) 34:336–41. doi: 10.1089/vim.2020.0243

9. Kang K, Gao Y, Zhao M, Fei D, Ye M, Gao Y, et al. Cytokine levels and pathological characteristics of a patient with severe coronavirus disease 2019: A case report. *Chin Med J (Engl)* (2021) 135:101–3. doi: 10.1097/CM9.0000000000001540

10. Henry BM, de Oliveira MHS, Benoit S, Plebani M, Lippi G. Hematologic, biochemical and immune biomarker abnormalities associated with severe illness and mortality in coronavirus disease 2019 (COVID-19): A meta-analysis. *Clin Chem Lab Med* (2020) 58:1021–8. doi: 10.1515/cclm-2020-0369

11. Kirtipal N, Bharadwaj S, Kang SG. From SARS to SARS-CoV-2, insights on structure, pathogenicity and immunity aspects of pandemic human coronaviruses. *Infect Genet Evol* (2020) 85:104502. doi: 10.1016/j.meegid.2020.104502

12. Bakhshandeh B, Jahanafrooz Z, Abbasi A, Goli MB, Sadeghi M, Mottaqi MS, et al. Mutations in SARS-CoV-2; consequences in structure, function, and pathogenicity of the virus. *Microb Pathog* (2021) 154:104831. doi: 10.1016/j.micpath.2021.104831

13. Lipsitch M, Krammer F, Regev-Yochay G, Lustig Y, Balicer RD. SARS-CoV-2 breakthrough infections in vaccinated individuals: Measurement, causes and impact. *Nat Rev Immunol* (2022) 22:57–65. doi: 10.1038/s41577-021-00662-4

14. Xie C, Zhao H, Li K, Zhang Z, Lu X, Peng H, et al. The evidence of indirect transmission of SARS-CoV-2 reported in guangzhou, China. *BMC Public Health* (2020) 20:1202. doi: 10.1186/s12889-020-09296-y

15. Kang K, Chen Q, Gao Y, Yu KJ. Detection of SARS-CoV-2 B.1.617.2 (Delta) variant in three cats owned by a confirmed COVID-19 patient in Harbin, China. *Vet Med Sci* (2022) 8:945–6. doi: 10.1002/vms3.715

16. Kim YI, Kim SG, Kim SM, Kim EH, Park SJ, Yu KM, et al. Infection and rapid transmission of SARS-CoV-2 in ferrets. *Cell Host Microbe* (2020) 27:704–709.e2. doi: 10.1016/j.chom.2020.03.023

17. Larsen HD, Fonager J, Lomholt FK, Dalby T, Benedetti G, Kristensen B, et al. Preliminary report of an outbreak of SARS-CoV-2 in mink and mink farmers associated with community spread, Denmark, June to November 2020. *Euro Surveill* (2021) 26:2100009. doi: 10.2807/1560-7917.ES.2021.26.5.210009

18. Ponti G, Maccaferri M, Ruini C, Tomasi A, Ozben T. Biomarkers associated with COVID-19 disease progression. *Crit Rev Clin Lab Sci* (2020) 57:389–99. doi: 10.1080/10408363.2020.1770685

19. Tjendra Y, Al Mana AF, Espejo AP, Akgun Y, Millan NC, Gomez-Fernandez C, et al. Predicting disease severity and outcome in COVID-19 patients: A review of multiple biomarkers. *Arch Pathol Lab Med* (2020) 144:1465–74. doi: 10.5858/arpa.2020-0471-SA

20. Ruan Q, Yang K, Wang W, Jiang L, Song J. Clinical predictors of mortality due to COVID-19 based on an analysis of data of 150 patients from wuhan, China. *Intensive Care Med* (2020) 46:846–8. doi: 10.1007/s00134-020-05991-x

21. Akbari H, Tabrizi R, Lankarani KB, Aria H, Vakili S, Asadian F, et al. The role of cytokine profile and lymphocyte subsets in the severity of coronavirus disease 2019 (COVID-19): A systematic review and meta-analysis. *Life Sci* (2020) 258:118167. doi: 10.1016/j.lfs.2020.118167

22. Huang I, Pranata R. Lymphopenia in severe coronavirus disease-2019 (COVID-19): Systematic review and meta-analysis. *J Intensive Care* (2020) 8:36. doi: 10.1186/s40560-020-00453-4

23. Pan F, Yang L, Li Y, Liang B, Li L, Ye T, et al. Factors associated with death outcome in patients with severe coronavirus disease-19 (COVID-19): A case-control study. *Int J Med Sci* (2020) 17:1281–92. doi: 10.7150/ijms.46614

24. Xu J, Liu Z, Liu H, Luo Y, Kang K, Li X, et al. Decreased T cell levels in critically ill coronavirus patients: Single-center, prospective and observational study. *J Inflammation Res* (2021) 14:1331–40. doi: 10.2147/JIR.S303117

25. Merad M, Martin JC. Pathological inflammation in patients with COVID-19: a key role for monocytes and macrophages. *Nat Rev Immunol* (2020) 20:355–62. doi: 10.1038/s41577-020-0331-4

26. Xu Z, Shi L, Wang Y, Zhang J, Huang L, Zhang C, et al. Pathological findings of COVID-19 associated with acute respiratory distress syndrome. *Lancet Respir Med* (2020) 8:420–2. doi: 10.1016/S2213-2600(20)30076-X

27. Tan C, Huang Y, Shi F, Tan K, Ma Q, Chen Y, et al. C-reactive protein correlates with computed tomographic findings and predicts severe COVID-19 early. *J Med Virol* (2020) 92:856–62. doi: 10.1002/jmv.25871

28. Luo X, Zhou W, Yan X, Guo T, Wang B, Xia H, et al. Prognostic value of c-reactive protein in patients with coronavirus 2019. *Clin Infect Dis* (2020) 71:2174–9. doi: 10.1093/cid/ciaa641

29. Mosquera-Sulbaran JA, Pedreañez A, Carrero Y, Callejas D. C-reactive protein as an effector molecule in covid-19 pathogenesis. *Rev Med Virol* (2021) 31: e2221. doi: 10.1002/rmv.2221

30. Qin C, Zhou L, Hu Z, Zhang S, Yang S, Tao Y, et al. Dysregulation of immune response in patients with coronavirus 2019 (COVID-19) in wuhan, China. *Clin Infect Dis* (2020) 71:762–8. doi: 10.1093/cid/ciaa248

31. Okugawa Y, Toiyama Y, Yamamoto A, Shigemori T, Ide S, Kitajima T, et al. Lymphocyte-c-reactive protein ratio as promising new marker for predicting surgical and oncological outcomes in colorectal cancer. *Ann Surg* (2020) 272:342–51. doi: 10.1097/SLA.0000000000003239

32. Lu LH, Zhong C, Wei W, Li SH, Mei J, Zou JW, et al. Lymphocyte-c-reactive protein ratio as a novel prognostic index in intrahepatic cholangiocarcinoma: A multicentre cohort study. *Liver Int* (2021) 41:378–87. doi: 10.1111/liv.14567

33. Yildirim M, Koca B. Lymphocyte c-reactive protein ratio: A new biomarker to predict early complications after gastrointestinal oncologic surgery. *Cancer biomark* (2021) 31:409–17. doi: 10.3233/CBM-210251

34. Yamamoto A, Toiyama Y, Okugawa Y, Ichikawa T, Imaoka H, Yasuda H, et al. Clinical implications of the preoperative lymphocyte c-reactive protein ratio in esophageal cancer patients. *Surg Today* (2021) 51:745–55. doi: 10.1007/s00595-020-02166-5

35. Erdogan A, Can FE, Gönüllü H. Evaluation of the prognostic role of NLR, LMR, PLR, and LCR ratio in COVID-19 patients. *J Med Virol* (2021) 93:5555–9. doi: 10.1002/jmv.27097

36. Lagunas-Rangel FA. Neutrophil-to-lymphocyte ratio and lymphocyte-to-C-reactive protein ratio in patients with severe coronavirus disease 2019 (COVID-19): A meta-analysis. *J Med Virol* (2020) 92:1733–4. doi: 10.1002/jmv.25819

frontiers | Frontiers in Immunology

TYPE Original Research
PUBLISHED 26 September 2022
DOI 10.3389/fimmu.2022.968981

Check for updates

OPEN ACCESS

EDITED BY
Martijn van Griensven,
Maastricht University, Netherlands

REVIEWED BY
Benoît Ho-Tin-Noé,
Institut National de la Santé et de la Recherche Médicale (INSERM), France
Makoto Kurano,
The University of Tokyo, Japan
Valentina Gentili,
University of Ferrara, Italy

*CORRESPONDENCE
Dmitri V. Krysko
Dmitri.Krysko@ugent.be
Alexander Brill
A.Brill@bham.ac.uk

†These authors share first authorship

‡These authors share senior authorship

SPECIALTY SECTION
This article was submitted to Viral Immunology, a section of the journal Frontiers in Immunology

RECEIVED 14 June 2022
ACCEPTED 05 September 2022
PUBLISHED 26 September 2022

CITATION
Krysko O, Bourne JH, Kondakova E, Galova EA, Whitworth K, Newby ML, Bachert C, Hill H, Crispin M, Stamataki Z, Cunningham AF, Pugh M, Khan AO, Rayes J, Vedunova M, Krysko DV and Brill A (2022) Severity of SARS-CoV-2 infection is associated with high numbers of alveolar mast cells and their degranulation. *Front. Immunol.* 13:968981. doi: 10.3389/fimmu.2022.968981

COPYRIGHT
© 2022 Krysko, Bourne, Kondakova, Galova, Whitworth, Newby, Bachert, Hill, Crispin, Stamataki, Cunningham, Pugh, Khan, Rayes, Vedunova, Krysko and Brill. This is an open-access article distributed under the terms of the Creative Commons Attribution License (CC BY). The use, distribution or reproduction in other forums is permitted, provided the original author(s) and the copyright owner(s) are credited and that the original publication in this journal is cited, in accordance with accepted academic practice. No use, distribution or reproduction is permitted which does not comply with these terms.

Severity of SARS-CoV-2 infection is associated with high numbers of alveolar mast cells and their degranulation

Olga Krysko[1†], Joshua H. Bourne[2†], Elena Kondakova[3], Elena A. Galova[4], Katharine Whitworth[2], Maddy L. Newby[5], Claus Bachert[1], Harriet Hill[6], Max Crispin[5], Zania Stamataki[6], Adam F. Cunningham[6], Matthew Pugh[6], Abdullah O. Khan[2], Julie Rayes[2], Maria Vedunova[3‡], Dmitri V. Krysko[3,7,8*‡] and Alexander Brill[2*‡]

[1]Upper Airways Research Laboratory, Department of Head and Skin, Ghent University, Ghent, Belgium, [2]Institute of Cardiovascular Sciences, College of Medical and Dental Sciences, University of Birmingham, Birmingham, United Kingdom, [3]Institute of Biology and Biomedicine, Department of Basic and Medical Genetics, National Research Lobachevsky State University of Nizhniy Novgorod, Nizhniy Novgorod, Russia, [4]University Clinic of Privolzhsky Research Medical University, Nizhny Novgorod, Russia, [5]School of Biological Sciences, University of Southampton, Southampton, United Kingdom, [6]Institute of Immunology and Immunotherapy, University of Birmingham, Birmingham, United Kingdom, [7]Department of Pathophysiology, Sechenov First Moscow State Medical University (Sechenov University), Moscow, Russia, [8]Cell Death Investigation and Therapy Laboratory, Department of Human Structure and Repair, Ghent University and Cancer Research Institute Ghent (CRIG), Ghent, Belgium

Background: The systemic inflammatory response post-SARS-CoV-2 infection increases pro-inflammatory cytokine production, multi-organ damage, and mortality rates. Mast cells (MC) modulate thrombo-inflammatory disease progression (*e.g.*, deep vein thrombosis) and the inflammatory response post-infection.

Objective: To enhance our understanding of the contribution of MC and their proteases in SARS-CoV-2 infection and the pathogenesis of the disease, which might help to identify novel therapeutic targets.

Methods: MC proteases chymase (CMA1), carboxypeptidase A3 (CPA3), and tryptase beta 2 (TPSB2), as well as cytokine levels, were measured in the serum of 60 patients with SARS-CoV-2 infection (30 moderate and 30 severe; severity of the disease assessed by chest CT) and 17 healthy controls by ELISA. MC number and degranulation were quantified by immunofluorescent staining for tryptase in lung autopsies of patients deceased from either SARS-CoV-2 infection or unrelated reasons (control). Immortalized human FcεR1$^+$c-Kit$^+$ LUVA MC were infected with SARS-CoV-2, or treated with its viral proteins, to assess direct MC activation by flow cytometry.

Results: The levels of all three proteases were increased in the serum of patients with COVID-19, and strongly correlated with clinical severity. The density of degranulated MC in COVID-19 lung autopsies was increased compared to control lungs. The total number of released granules and the number of granules per each MC were elevated and positively correlated with von Willebrand factor levels in the lung. SARS-CoV-2 or its viral proteins spike and nucleocapsid did not induce activation or degranulation of LUVA MC *in vitro*.

Conclusion: In this study, we demonstrate that SARS-CoV-2 is strongly associated with activation of MC, which likely occurs indirectly, driven by the inflammatory response. The results suggest that plasma MC protease levels could predict the disease course, and that severe COVID-19 patients might benefit from including MC-stabilizing drugs in the treatment scheme.

KEYWORDS

COVID-19, mast cells, protease, LUVA cells, von Willebrand factor

Introduction

As of January 2022, the coronavirus disease (COVID-19) has resulted in over 343 million confirmed cases and 5,6 million deaths. The morbidity and mortality in COVID-19 patients is a result of a high virus transmission rate, inadequate anti-viral immune response, and a high incidence of life-threatening complications, such as acute respiratory distress syndrome (ARDS), extrapulmonary organ dysfunction and uncontrolled thrombosis (1–7). Understanding the mechanisms driving the development of tissue damage, ARDS and multiple organ failure in patients with severe COVID-19 is critical to develop targeted therapeutic approaches.

Mast cells (MC) are bone marrow-derived myeloid cells, which possess pleiotropic functions in allergy, asthma, anaphylactic reactions, and gastrointestinal disorders (8, 9). In healthy lung tissue, they express low levels of angiotensin converting enzyme (ACE)-2 and transmembrane serine protease 2 (TMPRSS2), two molecules involved in cellular entry of SARS-CoV-2 (10). Thus, it could be speculated that MC contribute to the severe inflammatory response and subsequent thrombosis in patients with COVID-19.

Recent studies provide increasing evidence for a role of MC in host defense. They are widely distributed in peripheral tissues and are activated in an antigen-dependent manner *via* crosslinking FcεRI in IgE-mediated allergic reactions (11, 12). In addition, MC recognize and become activated by viral and bacterial pathogens through pattern-recognition receptors (PRRs) including toll like receptors (TLRs), nucleotide oligomerization domain-like binding receptors (NLR), and retinoic acid-inducible gene-I (RIG-I)- like receptors (RIG), Mas-related G protein-coupled receptors and C-type lectin binding receptors (13, 14). Their activation induces rapid degranulation leading to the release of inflammatory mediators such as histamine, proteases, TNF-α, serotonin, heparin, bioactive lipids, cytokines and chemokines (15, 16). MC-derived mediators cause increased vascular permeability, edema and innate and adaptive immune cell recruitment (17, 18). The effects of MC on endothelial cell activation and vascular integrity could be potentiated by MC release of TNF-α and proteases. This provides a link between inflammation and blood coagulation, complement pathway, and kallikrein-kinin system (19). The mediators released during MC degranulation, including proteases and histamine, could contribute to inflammatory cell infiltration in the airways, increase of vascular permeability, and activation of airway epithelial cells (20).

MC-derived pro-inflammatory substances, such as histamine and TNF-α, can activate endothelium and stimulate its degranulation. Von Willebrand factor (VWF) is one of the mediators stored in Weibel-Palade bodies of the endothelium. This is a large protein capable of binding platelet surface glycoprotein Ibα (GPIbα) and strongly potentiating platelet adhesion and aggregation. VWF is implicated in thromboembolic events in the setting of COVID-19 (21). In the current study, we aimed to explore MC and their biomarkers in SARS-CoV-2 infection. In particular, we demonstrate increased numbers and degree of degranulation of lung MC in patients, and positive correlation of MC degranulation with lung VWF, which reflects local prothrombotic potential. We have also revealed elevated levels of MC-derived proteases in the serum of these

patients, which correlates with disease severity. Finally, we report that MC are not directly activated by the whole virus or its membrane proteins. Thus, prevention of MC recruitment and degranulation may dampen the inflammatory environment and be therefore a promising therapeutic strategy in COVID-19 infection.

Methods

Patients

This study complies with the principles of the Declaration of Helsinki. The patients for the measurement of serum MC markers were enrolled at the University Clinic of Privolzhsky Research Medical University, Nizhny Novgorod, Russia; an approval for this research project was obtained from the local ethics committee of the Nizhny Novgorod State University. SARS-CoV-2 infection was confirmed in pharyngeal swabs by real-time reverse-transcription polymerase chain reaction (RT-PCR). The patients in the control group were age-matched healthy volunteers without any acute respiratory symptoms. A detailed description of the study cohort is provided in our earlier report (22). The patients were grouped into moderate and severe illness according to the COVID-19 treatment guidelines (23). Patients with moderate disease severity (7 males and 23 females) were admitted to hospital, but not the intensive care unit (ICU), whereas severe COVID-19 cases (11 male and 19 female) were both admitted to hospital and ICU. Postmortem MC staining in the lungs was performed at the University of Birmingham. Collection of post-mortem FFPE tissue was approved (IRAS: 197937) and the samples were received by a prospective consent and retrospective acquisition of tissue, for which consent for use in research had already been obtained. Ethical approval for the use of patient tissue was provided by the Health Research Authority with a National Health Service Research Ethics Committee; approval issued by North East-Newcastle and North Tyneside 1 (19/NE/0336). A written consent was obtained for all patients. Patient (n = 8) lung samples were taken from individuals deceased from COVID-19 infection, aged between 59 and 89, of both sexes. Controls (n = 3) were individuals died from non-COVID-19-related reasons. Detailed information about both patient and control cohorts can be found in (24). Patient lung damage was quantified by a semi-quantitative scale for the evaluation of lesion volume in lungs based on a chest CT scan, applied according to the national guidelines (25, 26) as follows: chest CT grade 0 (no low abnormalities on the chest CT), chest CT grade 1 (25% of the lungs were affected), chest CT grade 2 (50% of the lungs were affected), chest CT grade 3 (75% of the lungs were affected), chest CT grade 4 (100% of the lungs were affected).

MC staining in the lungs

FFPE sections were deparaffinized and rehydrated, followed by antigen retrieval by heating in a microwave (10 min) in citrate buffer (pH 6). Autofluorescence was quenched using 3% hydrogen peroxide and sections blocked by PBS-Tween 0.05% containing 3% bovine serum albumin (BSA) and 5% goat serum for 1h at room temperature. Monoclonal primary antibody against tryptase (1:1000, clone G3, Merck) was applied overnight at 4°C. Then, the sections were washed, incubated with secondary antibody conjugated with Alexa-Fluor 647 (Invitrogen), washed again and autofluorescence was quenched again by Vector® TrueVIEW® Autofluorescence Quenching Kit (Vector Laboratories, CA, USA). After mounting, sections were analyzed by an epifluorescent microscope. Tryptase-positive objects with the area of >50 µm were considered MC, whereas objects with the area of <50 µm were regarded as released granules. The numbers of lung MC and cell-free granules as well as MC area were averaged from 15 random fields per patient/control using ImageJ (National Institute of Health, USA) (27).

VWF staining in lung sections

FFPE lung sections from COVID-19 patients and controls were rehydrated and underwent antigen retrieval and blocking with PBS containing 5% BSA and 10% goat serum for 1h at room temperature. Next, sections were incubated overnight with rabbit anti human VWF antibody (Agilent) at 4°C and then secondary antibody (goat anti rabbit, conjugated to Alexa Fluor 647, Invitrogen, 1 h, RT). Nuclei were counterstained by DAPI. Lung autofluorescence was quenched using commercial kit (Vector laboratories) and slides mounted using ProLong Gold Antifade Mountant (Life Technologies). VWF analysis was performed as described (28). Briefly, images were acquired using a Zeiss Axio Scan.Z1 Epi Fluorescence system and quantified using Fiji (29) by manually designating ROIs and measuring intensity after background subtraction and denoising.

Enzyme-linked immunosorbent assays

On the day of admission to the hospital, peripheral blood samples were collected by venipuncture, centrifuged for 10 min at 845 g, and sera were stored at −80°C until further analysis. The levels of MC proteases in sera of the patients were analyzed by commercial ELISAs for human tryptase beta-2 (TPSB2, ELH-TPSB2-1, RayBio, Peachtree Corners, GA, USA), chymase 1 (CMA1, ELK3058, ELK Biotech, Wuhan, P.R.C), and carboxypeptidase 3 (CPA3, LS -F52226, LSBio, Seattle, WA, USA).

Biochemical parameters

The analysis of creatinine, glucose, alanine aminotransferase (ALT), aspartate aminotransferase (AST), C-reactive protein (CRP), were done by an Indiko automatic biochemical analyzer (ThermoScientific, Finland) using the manufacturer's reagents. Control materials were produced by RANDOX (Randox Laboratories, UK). Lactate dehydrogenase activity in serum was analyzed using a kinetics method according to the manufacturer's instructions (DDS *in vitro* Solutions, Pushchino, Russia). The levels of fibrinogen and D-dimer were analyzed using a coagulation analyzer ACL TOP 500 (Instrumentation Laboratory, USA).

Cell culture

Immortalized human mast cell line, LUVA (Kerafast, USA), was used to model lung-resident mast cell response to SARS-CoV-2 infection. We and others (Laidlaw et al., 2011) have shown that LUVA cells express FcεRI and c-Kit similarly to normal human MC. Cells were cultured in StemPro-34 SFM media (Gibco, USA) with L-glutamine (2 mM) and Penicillin-Streptomycin (10 U/ml) in a humidified incubator at 5% CO_2 and 37°C. Cells were maintained at $5x10^5$/ml and passaged up to 15 times; FcεRI and c-Kit expression the cell surface of LUVA cells was maintained throughout passaging.

Antigen generation and virus

SARS-CoV-2 England 2 virus (Wuhan strain) was a kind gift from Christine Bruce, Public Health England. Recombinant trimeric spike glycoprotein (S) was produced in human embryonic kidney (HEK) 293F cells as previously described (30). Nucleocapsid (N) protein was produced in *E.coli* bacteria and purified as described (31). The levels of endotoxin in the protein preparations were lower than 0.005 EU/mg.

MC stimulation

LUVA cells were either naive or primed using the presence or absence of native human IgE (1 μg/ml; Abcam, UK) for 24 h, before thrice washing with HEPES buffer. Cells were plated at $3x10^5$/ml, and stimulated with a vehicle control, Compound 48/80 (50 μg/ml; Sigma) or SARS-CoV-2-related antigens (1-10 μM) for 1 h at 37°C in a CO_2-free incubator; CO_2 has been shown to limit MC degranulation (32). The stimulation of LUVA cells by SARS-CoV-2 (2,500 IU/ml) were performed as above, but at 5% CO_2 due to limitations by Biosafety level 3.

Flow cytometry

LUVA cells were blocked in 10% serum (20 min on ice), prior to an incubation in the conjugated antibody cocktail, or company recommended isotype control (30 min on ice): hAce-2-AF405 (#535919; 1:300; R&D, USA), Avidin-fluorescein (#A821; 1:5,000; Invitrogen, USA), FcεRIα-PE (#AER-37; 1:300; Invitrogen, USA), CD63C-PECy5.5 (#H5C6; 1:300, BioLegend, USA), CD203c-PECy7 (#NP4D6, 1:300, Invitrogen), c-Kit-APC (#104D2; 1:300; BD Bioscience, USA). Cells were fixed with 10% formalin, and acquired using a CytoFLEX flow cytometer (Beckman, USA). At least 10,000 events were recorded, and gating strategy is outlined in Figure S1. Data was analyzed using FlowJo v10 and presented using GraphPad Prism v9.

Statistical analysis

The difference between the healthy controls, moderate and severe patients was analyzed by one-way ANOVA and Kruskal-Wallis test for multiple comparisons. Following analysis for Gaussian distribution, Pearson's correlation coefficient and two-tailed p values were calculated for the selected datasets using GraphPad Prism 9.0. The numbers of lung MC, cell-free granules, and MC area were compared by two-tail student's t-test. The p-value of less than 0.05 was considered significant.

Results

Clinical characteristics of the COVID-19 patient cohort

Patients were classified based on the severity of SARS-CoV-2-infection as described in the Methods. Patients with severe disease were significantly older than moderate cases (59.1 ±15.9 *vs.* 47.7 ±16.2 years, $p < 0.02$) with mildly increased body mass index (31.6 ±4.9 *vs.* 27.8 ±4.7, p=0.003) (Table 1). No marked difference in the symptoms was seen on admission between patient groups while severely affected patients had several comorbidities as described in our earlier report (22). On admission, severely ill patients with COVID-19 had a higher breathing rate than moderately ill patients. Peripheral capillary oxygen saturation (SpO_2) reached 95.2 ±1.9% in moderate cases and was lower in severe cases (89.9 ±5.3%, p<0.0001). Fifteen patients with severe COVID-19 received non-invasive oxygen support, while those with a moderate severity did not require oxygen support.

Fifty-six percent of the patients with severe COVID-19 and only 16% of patients with moderate disease had thromboembolic

10.3389/fimmu.2022.968981

TABLE 1 Demographics and baseline characteristics of patients included in the study.

	controls	moderate	severe
	(n=17)	(n=30)	(n=30)
Age, years	54,7±19,7	47,7±16,2	59,1 ±15,9
Gender	7M/10F	7M/23F	11M/19F
Body mass index	25,09±3,6	27,8±4,7	31,6±4,9
Hypertension (n,%)	4 (23%)	16 (53%)	24 (80%)
Diabetes (n,%)	1 (6%)	1 (3%)	13 (43%)
Cardiovascular disease (n,%)	3 (17%)	4 (13%)	14 (46%)
Malignancy (n,%)	0 (0)	4 (13%)	5 (16%)
Stroke (n,%)	0 (0)	1 (3%)	3 (10%)
Chronic lung diseases (n,%)	0 (0)	2 (6%)	2 (6%)
Arrhythmia (n,%)	0 (0)	4 (13%)	1 (3%)
Rheumatoid arthritis (n,%)	1 (6%)	0 (0%)	1 (3%)

The number (n) of the patients in each group is provided with description of their age, gender, and comorbidities. For demographic characteristics data are presented as median ± standard deviation.

events such as stroke and myocardial infarction. A chest CT scan performed upon patient admission revealed pneumonia in 27 out of 30 severely ill COVID-19 patients. Ten percent of the patients with moderate disease severity had 75% lung damage accompanied by moderate clinical symptoms, 63% had lung damage between 25 and 50%, and 27% had below 25%. Only one patient in the group with moderate COVID-19 had reported current tobacco smoking. The patients were hospitalized for a median of 9.1 ±6 days to 9 ±3.6 days for severely and moderately ill COVID-19 patients, respectively. Four patients in a group of severely affected patients were mechanically ventilated and eventually died from ARDS and endotoxic shock.

MC proteases are elevated in patient serum relative to the clinical severity of COVID-19

The MC protease levels were analyzed in the serum of patients on the day of admission. All tested MC proteases, CMA1, CPA3, and TPSB2, were increased in the serum of patients compared to healthy controls (Figure 1), and in severe patients compared to moderate individuals. The levels of the proteases in four patients subsequently deceased from COVID-19 were comparable to the levels in the patients with severe COVID-19: CPA3 (21.54 ±6.6 *vs.* 22.25 ±5.7 ng/ml, p = 0.72); CMA1 (2426 ±1113 *vs.* 2387 ±720 ng/ml, p = 0.73) and for TPSB2 (27.5 ±17 *vs.* 30.04 ±17 ng/ml, p=0.95). Fifteen patients with severe COVID-19 that required oxygen support had levels of MC proteases comparable to other patients with severe disease (Figure S1).

A strong positive correlation was observed between the degree of lung damage (4 grades assessed by chest CT scan) and the serum levels of CMA1 (Pearson's r= 0.591, p<0.0001), CPA3 (Pearson's r= 0.577, p<0.0001), and TPSB2 (Pearson's r= 0.503, p<0.0001) (Table 2). Levels of MC proteases in serum of patients with COVID-19 strongly correlated with the severity grade of the disease (Table 2). Patients with severe COVID-19 showed higher levels of proteases than individuals with moderate severity. Thus, MC protease activity is associated with lung damage and subsequent poor clinical outcome post SARS-CoV-2 infection although certain contribution of other comorbidities in SARS-CoV-2 patients cannot be ruled out.

MC numbers and degranulation are increased in the lungs of COVID-19 patients

We next assessed MC accumulation and degranulation in lung autopsies by immunofluorescence staining for MC marker, tryptase. These sections were collected from a separate cohort of patients who died of COVID-19, as well as from patients who died from non-COVID-19-related reasons as a control. The numbers of tryptase-positive MC (Figures 2A, B) were dramatically increased in patients with COVID-19 *vs.* non-COVID-19 controls (26.4 ±9.85 *vs.* 13 ±1.32 per view field, p < 0.009). The amount of secreted MC granules was also elevated as well as the granule/MC ratio, which reflects the average number of released granules per one MC (226.7 ±154.5 *vs.* 47.1 ±7.28 per view field, p < 0.02 and 7.3 ±3.4 *vs.* 4 ±0.63 per view field, p < 0.04, respectively; Figures 2C–E). There was a strong correlation between the numbers of MC and secreted granules (r = 0.84, p < 0.02;

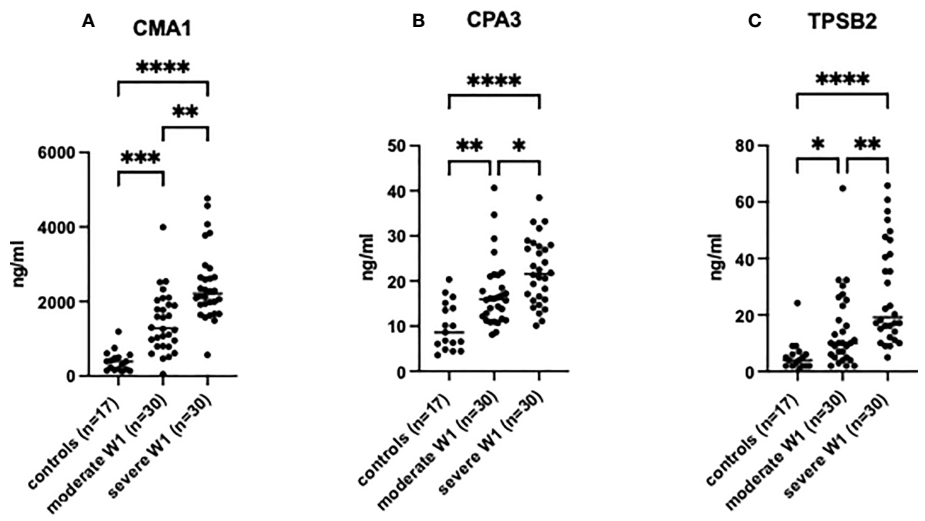

FIGURE 1
MC degranulation markers in patient serum are increased relative to clinical severity of patients post-SARS-CoV-2 infection. The presence of **(A)** CMA1, **(B)** CPA3 and **(C)** TPSB2 in patient serum was determined by ELISA. Healthy controls (n=17) were used to compare to patients post-SARS-CoV-2 infection with moderate (admission to hospital; n=30), or severe (admission to ICU; n=30) clinical outcome. Statistical significance was determined using a one-way ANOVA with Kruskal-Wallis multiple comparison test. *p<0.05, **p<0.01, ***p<0.001, ****p<0.0001.

Figure 2F). Enhanced release of granular content could be expected to reduce the volume of MC; hence we next calculated the average area of MC in the lung sections, however this parameter did not differ between COVID-19 patients and controls (Figure 2G). The increased numbers of MC and their granules in the lungs post-infection may suggest their contribution to the immune response in patients with COVID-19.

Neither live SARS-CoV-2 nor its viral proteins directly activate MC *in vitro*

To test whether SARS-CoV-2 can directly activate MC, we next performed experiments using human immortalized MC line, LUVA, initially derived from CD34$^+$ mononuclear cells (33). Prior to the experiments, we confirmed that the cells express high levels of both CD117 (c-kit) and FcεRI, typical for a regular MC phenotype (Figure S2). Incubation of LUVA cells with increasing concentrations of SARS-CoV-2 viral proteins nucleocapsid or spike protein for 1 h, as well as live SARS-CoV-2, did not change the expression of both FcεRI and CD117 (data not shown). The proteins also did not affect MC degranulation as assessed by granule staining using fluorescently-labeled avidin (Figure 3A), which rapidly binds heparin in MC granules (34). The membrane expression of CD203c or CD63 (Figures 3B, C) as well as by β-hexosaminidase secretion were unchanged (data not shown). Stimulation of MCs with compound 48/80, a potent MC

TABLE 2 Correlation analysis of MC protease levels in serum with demographical and clinical characteristics of patients with COVID-19.

	CMA1		CPA3		TPSB2	
	Pearson's r	p-value	Pearson's r	p-value	Pearson's r	p-value
Age, year	0.147	0.261	0.209	0.11	0.127	0.335
Body mass index	0.109	0.417	0.121	0.368	0.281	0,033
Intensive care unit	0.187	0.153	0.244	0.06	0.3	0,020
Oxygen support	0.174	0.183	0.3	0,020	0.125	0.341
Severity grade	0.561	<0,0001	0.452	<0,0001	0.465	<0,0001
Chest CT at admission (grade)	0.591	<0,0001	0.577	<0,0001	0.503	<0,0001
Chest CT at day 7-10 (grade)	0.586	<0,0001	0.561	<0,0001	0.472	<0,0001
SpO2 at admission	-0.076	0.564	-0.214	0.102	-0.399	0,002

Pearson correlation coefficient and two-tailed p values were calculated for the selected datasets using GraphPad Prism 9.0.

10.3389/fimmu.2022.968981

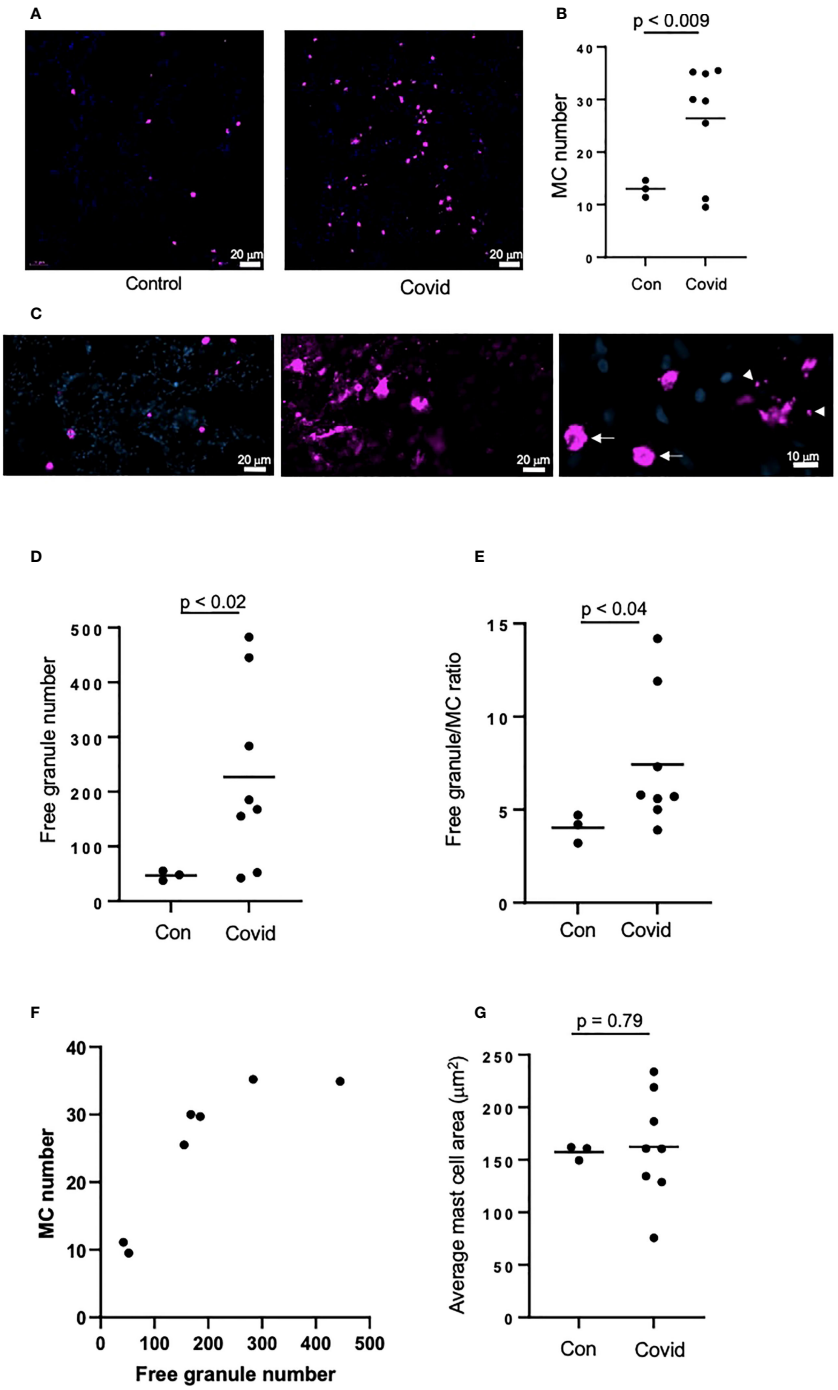

FIGURE 2
MC recruitment and degranulation is increased in the lungs of patients post-SARS-CoV-2 infection. The lungs of patients deceased post-SARS-CoV-2 infection were frozen, sectioned to 6 µm and labelled by immunofluorescence, before imaging using an epifluorescence microscope. Lungs of non-SARS-CoV-2-linked deaths were used as a control. **(A)** MCs were identified by tryptase (magenta) in the lungs of deceased non-SARS-CoV-2 (n=3) or COVID-19 patients (n=8); **(B)** Quantification of MC numbers; **(C)** Non-degranulated (controls, left panel) and degranulated (COVID-19, middle panel) MCs; right panel represents non-degranulated MC (arrows) and granules (arrowheads) releasing from a MC in the process of degranulation; **(D)** Quantification of MC granules identified as tryptase-positive objects with the area of <50 µm^2; **(E)** Ratio between the numbers of cell-free granules and MCs; **(F)** Correlation between the numbers of MCs and cell-free granules; **(G)** Quantification of the average of MC area. Images were analyzed using ImageJ. Horizontal lines represent mean. Statistical significance was determined using the unpaired Student's t-test.

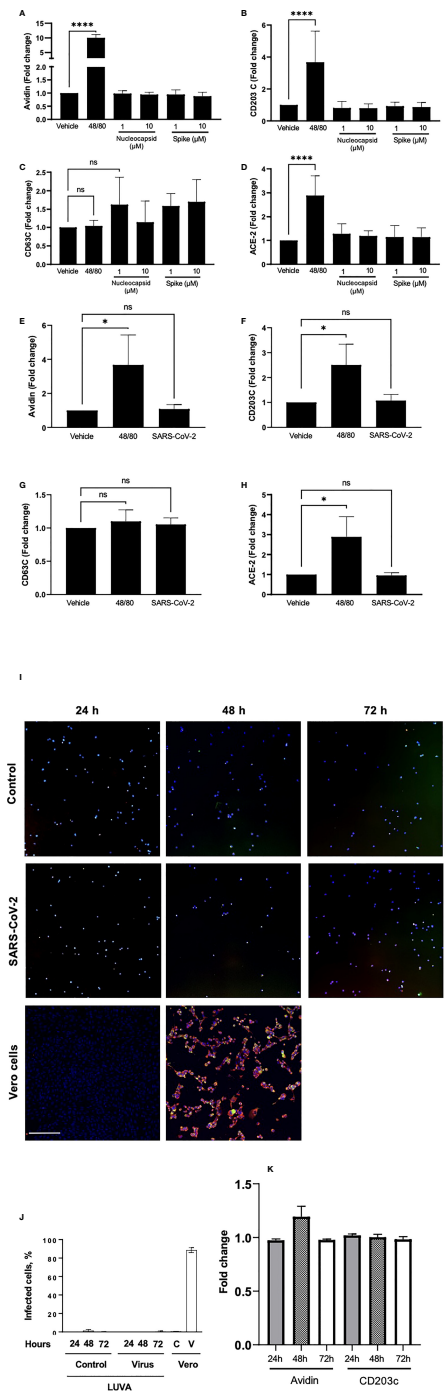

FIGURE 3
Neither viral proteins nor the SARS-CoV-2 virus directly induce MC degranulation, and SARS-CoV-2 virus does not penetrates MC. LUVA cells were cultured in the presence or absence of compound 48/80 (10 μg/ml) or spike protein or nucleocapsid protein (1-10 μM; **A–D**), or SARS-CoV-2 **(E–H)** for 1 h in a CO_2-free humidified atmosphere at 37°C. Cells were analyzed for the expression of **(A, E)** avidin, **(B, F)** CD203c, **(C, G)** CD63, or ACE-2 **(D, H)** using a CytoFlex flow cytometer and quantified using FlowJo v10. Statistical significance was determined using a one-way ANOVA with Tukey's multiple comparisons test. *p<0.05, ****p<0.0001. ns, not significant. LUVA cells were incubated without or with (first and second rows, respectively) ARS-CoV-2 virus for 24 h, 48 h or 72 h, after which cells were seeded on a polylysine-coated polystyrene wells and stained for nuclei (blue), nucleocapsid protein (red), and spike protein (green) to evaluate virus entry into the cells **(I)**. Vero cells (third row) served as a control of both virus penetration and quality of the antibodies. No dissemination of the virus inside cells was observed at all time points, which is confirmed by quantitation of the fluorescence **(J)**; C and V designate control and virus for Vero cells. Staining of cell samples for avidin and CD203c revealed no degranulation **(K)**. Scale bar 200 um, n = 3 for each time point.

secretagogue, upregulated the surface expression of ACE-2, whereas its expression remained unchanged in the presence of the viral proteins (Figure 3D). Expression of CD63, CD203c, ACE-2, and avidin binding remained unaffected also after exposure of the cells to the live virus (Figures 3E–H). The same results were obtained also in all described experiments using MCs primed with native human IgE (data not shown). Incubation of LUVA cells with the virus for longer periods of time (24 - 72 h) also resulted in neither virus penetration into the cells, nor their activation (Figure 3I–K). Thus, degranulation of MCs post-SARS-CoV-2 infection is unlikely to be through a direct activation by the virus but could occur through mechanisms different from a direct contact with viral epitopes.

MC granule release positively correlates with lung VWF levels in COVID-19 patients

COVID-19 infection frequently leads to thrombotic complications. To address whether MCs could be implicated in the development of local pro-thrombotic conditions we assessed the correlation of VWF levels in the lung sections (Figures 4A, B) with MC-related parameters. No correlation of lung VWF with MCs numbers was observed in the lungs of patients with COVID-19 ($p = 0.27$; Figure 4C). In contrast, the number of secreted granules moderately correlated with the VWF levels ($r = 0.5311$, $p < 0.03$) whereas correlation with granule/MC ratio was strong ($r = 0.7348$, $p < 0.004$; Figures 4D, E). Thus, the degree of MC degranulation rather than their total numbers is associated with the pro-thrombotic phenotype typical of SARS-CoV-2 infection.

Discussion

In the current study, we have analyzed the role of MC activation post-SARS-CoV-2 infection by measuring the levels of three MC-specific proteases, TPSB2, CMA-1, and CPA3, in serum of patients with moderate and severe clinical severity. We report (i) increased levels of MC proteases in serum of patients with COVID-19, and (ii) enhanced infiltration of MCs and their degranulation in lung tissue post-mortem, which may imply MC involvement in the pathogenesis of the disease. The degree of degranulation of each MC was increased and positively correlated with lung VWF levels; (iii) the live SARS-CoV-2 virus or its protein components did not degranulate MCs *in vitro*, suggesting that an indirect mechanism of MC activation could be involved.

Our studies show the simultaneous increase in CMA1, CPA3, and TPSB2 in COVID-19 patients, which are indicative of the MC_{TC} subset of MCs (the most common subset in human airways) in the lungs of patients with COVID-19 (35). Eosinophil and MC activation has previously been reported in patients with COVID-19, whereby MC proteases in serum and lungs of COVID-19 patients were elevated (36). TPSB2 and CMA-1 have been demonstrated to induce vascular leakage in response to viral infection, which may explain the increased lung damage observed in CT scans (37). Moreover, other mediators released during MC degranulation, including proteases and histamine, could contribute to inflammatory cell infiltration in the airways, increase of vascular permeability, and activation of airway epithelial cells (20). Moreover, increased CMA1 in patients with severe COVID-19 contributes directly to destabilization of cellular contacts *via* degradation of MMPs, laminin, fibronectin (38, 39) and to the generation of pro-inflammatory cytokines IL-6, IL-1β, IL-18, IL-33, and TNF-α (40–43). This has been supported by *in vivo* data, whereby the administration of MC stabilizers reduced SARS-CoV-2-induced production of pro-inflammatory factors and the degree of lung injury (20). This outlines a clear role for MCs and their proteases in the modulation of the inflammatory response to SARS-CoV-2 through cytokine production and regulation of vascular permeability.

We here demonstrated that MC numbers increase in the lungs of patients with COVID-19. These findings corroborate previously reported accumulation of MCs in the perivascular spaces and alveolar septa next to alveolar capillaries (44) as well as recently demonstrated MC-mediated lung tissue damage (45). In the setting of SARS-CoV-2 infection, MCs accrued in the lungs had a connective tissue phenotype, which is untypical of non-COVID-related lung infections (45). In our samples, MCs were apparently activated as large amounts of cell-free tryptase-rich granules were observed in the lung tissues. Moreover, the total amount of the released MC content was apparently defined not only by the elevated numbers of MCs *per se*, but also by increased numbers of granules released by each MC as judged by the ratio between the quantities of MCs cell-free granules.

The nature of the factors recruiting MCs into the lungs is still to be defined. The "cytokine storm" observed during SARS-CoV-2 infection includes multiple pro-inflammatory agents that can chemoattract MC, such as components of the coagulation system (*e.g.*, fibrinogen) or TGF-β, shown to contribute to pulmonary fibrosis (46–48). Multiple agents found in the plasma of COVID-19 patients, such as TNF-α and IL-8, can induce chemotaxis of MC. VWF is one of the key prothrombotic proteins capable of recruiting platelets, which in turn can stimulate MC degranulation through platelet-activating factor (49). VWF is stored in the Weibel-Palade bodies of the

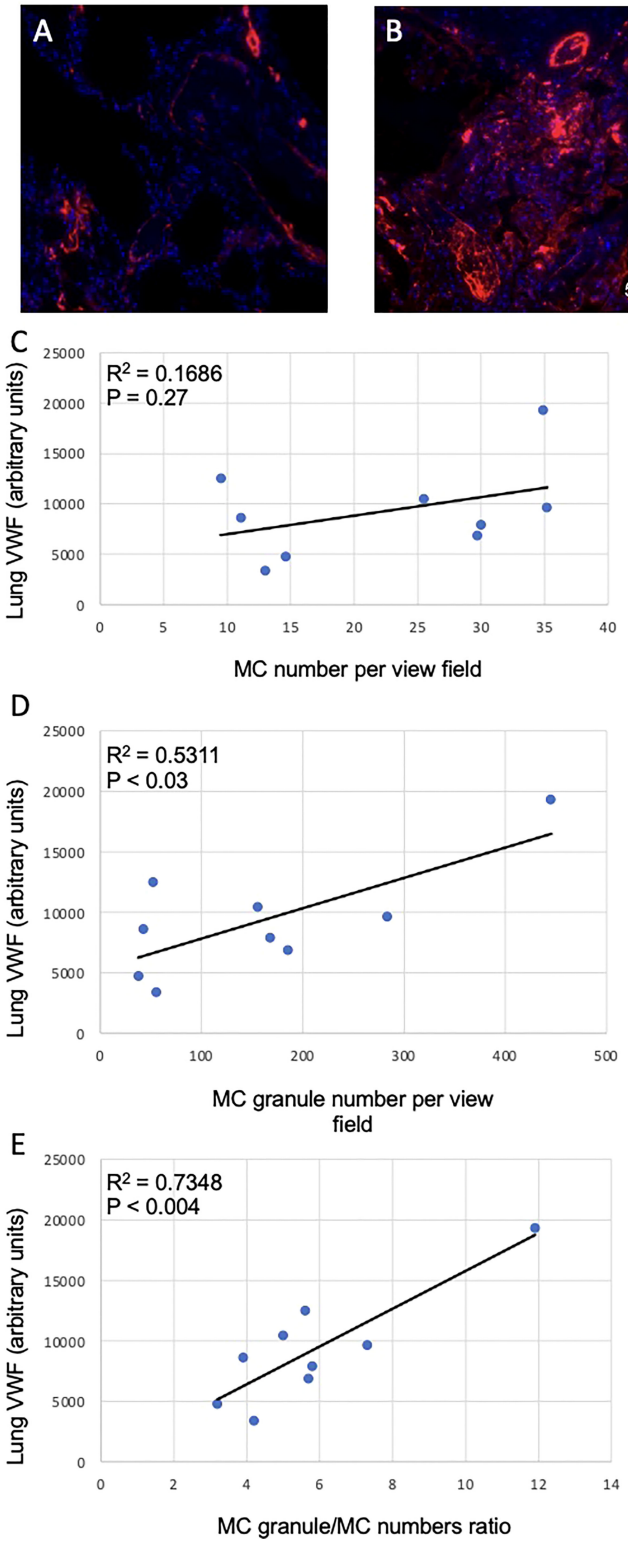

FIGURE 4
Correlation between MC-related parameters and lung VWF levels. The levels of VWF in the lungs were determined as fluorescence intensity in arbitrary units. **(A)** and **(B)**, representative images of VWF staining in the lungs of non-COVID-19 and COVID-19 patients, respectively. Correlations of VWF levels with **(C)** MC numbers, **(D)** cell-free granule numbers and **(E)** granule/MC number ratio are presented. Pearson r coefficient was calculated using MS Excel.

endothelium, and it is likely that MC-derived histamine, one of the most potent Weibel-Palade bodies secretagogues, stimulates its release in the COVID-19 setting. It has recently been shown that thrombi in the pulmonary artery can develop *in situ* (50), a process, in which VWF could be involved in the COVID-19 setting. Immuno-thrombosis mediated by MC accumulated in the lung septa has recently been reported using histopathology of post-mortem lung biopsies of patients with COVID-19 (44). This could represent a "vicious circle" underlying massive pulmonary thrombosis, a leading cause of SARS-Cov-2-induced mortality.

It is reasonable to hypothesize that MC degranulation is directly induced by viral proteins. Several viruses were shown to induce MC degranulation, including influenza A, Zika virus, herpes simplex virus and respiratory syncytial virus (51–56). Despite previous reports that the SARS-CoV-2 virus induces degranulation of MC line, LAD2, and in humanized ACE-2 mice (20), we did not observe direct LUVA MC activation by the virus or its proteins. Exposure of LUVA cells to live virus for longer periods of time (days) resulted in neither virus replication in the cells nor cell degranulation. This finding suggests that, in COVID-19 infection, MC are likely activated indirectly, potentially by certain elements of the "cytokine storm" typical for this infection, which are obviously absent in the cell culture experiments. It cannot also be ruled out that specific microenvironment in the lungs renders MC more susceptible to direct interactions with viral components than in the *in vitro* model. MC activation by a secondary mediator likely facilitates its binding to the virus, as judged by elevated expression of ACE-2 induced by compound 48/80, although the consequences of such binding are still to be determined. MC activating agents could originate from immune cells such as macrophages, which are considered critical for cytokine storm, COVID-19 severity and eventually death (57, 58). It is conceivable that MC degranulation can further accelerate lung inflammation and eventual dysfunction through release of histamine, myeloid chemoattractant CCL3 and prostaglandins (11). Therefore, MC could be a key point for the positive feedback, in which they are activated by a strong systemic pro-inflammatory milieu and then further enhance local inflammatory response.

In conclusion, our study shows that activation and degranulation of MC in the lungs of patients with COVID-19 correlates with the degree of disease severity, lung damage and local pro-thrombotic potential. An increase in MC protease levels is more pronounced in severe COVID-19, which could potentially contribute to their detrimental role in disease progression by increasing vessel permeability and contributing to the progression of ARDS and cytokine storm *via* secretion of inflammatory mediators. Therefore, the use of MC stabilizers might be beneficial in dampening the inflammatory response in patients at risk of developing severe COVID-19.

Data availability statement

The raw data supporting the conclusions of this article will be made available by the authors, without undue reservation.

Ethics statement

The studies involving human participants were reviewed and approved by the Health Research Authority (HRA) with an NHS (National Health Service) REC (Research Ethics Committee); approval issued by North East-Newcastle and North Tyneside 1 (19/NE/0336). The patients for the measurement of serum MC markers were enrolled at the University Clinic of Privolzhsky Research Medical University, Nizhny Novgorod, Russia; an approval for this research project was obtained from the local ethics committee of the Nizhny Novgorod State University. The patients/participants provided their written informed consent to participate in this study.

Author contributions

OK, AB, MV, and DK designed experiments, analyzed data, supervised the study, and wrote and revised the manuscript; JB performed experiments, collected and analyzed data and revised the manuscript; KW, AB, HH, and ZS performed experiments; EG enrolled patients in the study, collected clinical information and peripheral blood; AK analyzed data; JR performed experiments, and revised the manuscript. MC, MN, MP, and AC provided reagents and revised the manuscript. EK performed ELISA's, analyzed data and revised the manuscript; CB revised the manuscript. All authors contributed to the article and approved the submitted version.

Funding

The research was supported by FWO-Flanders 3G065319N to OK and CB. DK lab is supported by FWO-Flanders (G043219N, G016221), Ghent University BOF (Special Research Fund 01/O3618 and BOF/IOP/2022/033) and the project (40007488) from the FWO and F.R.S.-FNRS under the "Excellence of Science" program. MV acknowledges the Ministry of Science and Higher Education of the Russian Federation, agreement No. 075-15-2020-808. JR is a British Heart Foundation Intermediate Fellow (FS/IBSRF/20/25039). AK is a Henry Wellcome fellow (218649/Z/19/Z). The study was supported by the British Heart Foundation Senior Basic Science Research Fellowship (FS/19/30/34173) and a BHF Project Grant (PG/18/46/33817) to AB.

Conflict of interest

The authors declare that the research was conducted in the absence of any commercial or financial relationships that could be construed as a potential conflict of interest.

Publisher's note

All claims expressed in this article are solely those of the authors and do not necessarily represent those of their affiliated organizations, or those of the publisher, the editors and the reviewers. Any product that may be evaluated in this article, or claim that may be made by its manufacturer, is not guaranteed or endorsed by the publisher.

Supplementary material

The Supplementary Material for this article can be found online at: https://www.frontiersin.org/articles/10.3389/fimmu.2022.968981/full#supplementary-material

References

1. da Silva SR, Ju EG, Meng W, Mondolfi AEP, Dacic S, Green A, et al. Broad severe acute respiratory syndrome coronavirus 2 cell tropism and immunopathology in lung tissues from fatal coronavirus disease 2019. *J Infect Dis* (2021) 223(11):1842–54. doi: 10.1093/infdis/jiab195

2. Ferrando C, Suarez-Sipmann F, Mellado-Artigas R, Hernandez M, Gea A, Arruti E, et al. Clinical features, ventilatory management, and outcome of ARDS caused by COVID-19 are similar to other causes of ARDS. *Intensive Care Med* (2020) 46(12):2200–11. doi: 10.1007/s00134-020-06192-2

3. Wu J, Shi YH, Pan XY, Wu S, Hou RX, Zhang Y, et al. SARS-CoV-2 ORF9b inhibits RIG-I-MAVS antiviral signaling by interrupting K63-linked ubiquitination of NEMO. *Cell Reports* (2021) 34(7):108761. doi: 10.1016/j.celrep.2021.108761

4. Serato AC, Gaglia MM. All hands on deck: SARS-CoV-2 proteins that block early anti-viral interferon responses. *Curr Res Virol Sci* (2021) 2:100015. doi: 10.1016/j.crviro.2021.100015

5. Berlin DA, Gulick RM, Martinez FJ. Severe covid-19. *New Engl J Med* (2020) 383(25):2451–60. doi: 10.1056/NEJMcp2009575

6. Attaway AH, Scheraga RG, Bhimraj A, Biehl M, Hatipoglu U. Severe covid-19 pneumonia: pathogenesis and clinical management. *Bmj-British Med Journal* (2021) 372:n436. doi: 10.1136/bmj.n436

7. Qadeer A, Bannon F, Dimitrios A, Dolan E, Cormican L. Tocilizumab use in 44 hospitalized patient with severe covid-19 pneumonia, a single centre observational study. *Irish J Med Sci* (2021) 190(Suppl 5):199–200. doi: 10.1007/s11845-020-02450-w

8. Bischoff SC. Mast cells in gastrointestinal disorders. *Eur J Pharmacol* (2016) 778:139–45. doi: 10.1016/j.ejphar.2016.02.018

9. Murphy RC, Hallstrand TS. Exploring the origin and regulatory role of mast cells in asthma. *Curr Opin Allergy Clin Immunol* (2021) 21(1):71–8. doi: 10.1097/Aci.0000000000000703

10. Hoffmann M, Kleine-Weber H, Schroeder S, Kruger N, Herrler T, Erichsen S, et al. SARS-CoV-2 cell entry depends on ACE2 and TMPRSS2 and is blocked by a clinically proven protease inhibitor. *Cell* (2020) 181(2):271–280.e8. doi: 10.1016/j.cell.2020.02.052

11. Krystel-Whittemore M, Dileepan KN, Wood JG. Mast cell: A multi-functional master cell. *Front Immunol* (2016) 6:620. doi: 10.3389/fimmu.2015.00620

12. Sibilano R, Frossi B, Pucillo CE. Mast cell activation: A complex interplay of positive and negative signaling pathways. *Eur J Immunol* (2014) 44(9):2558–66. doi: 10.1002/eji.201444546

13. Hermans MAW, van Stigt AC, van de Meerendonk S, Schrijver B, van Daele PLA, van Hagen PM, et al. Human mast cell line HMC1 expresses functional mas-related G-protein coupled receptor 2. *Front Immunol* (2021) 12:625284. doi: 10.3389/fimmu.2021.625284

14. Jimenez M, Cervantes-Garcia D, Cordova-Davalos LE, Perez-Rodriguez MJ, Gonzalez-Espinosa C, Salinas E. Responses of mast cells to pathogens: Beneficial and detrimental roles. *Front Immunol* (2021) 12:685865. doi: 10.3389/fimmu.2021.685865

15. Marshall JS. Mast-cell responses to pathogens. *Nat Rev Immunol* (2004) 4(10):787–99. doi: 10.1038/nri1460

16. Wernersson S, Pejler G. Mast cell secretory granules: armed for battle. *Nat Rev Immunol* (2014) 14(7):478–94. doi: 10.1038/nri3690

17. Morimoto K, Shirata N, Taketomi Y, Tsuchiya S, Segi-Nishida E, Inazumi T, et al. Prostaglandin e-2-EP3 signaling induces inflammatory swelling by mast cell activation. *J Immunol* (2014) 192(3):1130–7. doi: 10.4049/jimmunol.1300290

18. Hackler Y, Siebenhaar F, Lohning M, Maurer M, Munoz M. Mast cells modulate antigen-specific CD8(+) T cell activation during LCMV infection. *Front Immunol* (2021) 12:688347. doi: 10.3389/fimmu.2021.688347

19. Scharfstein J. Subverting bradykinin-evoked inflammation by co-opting the contact system: lessons from survival strategies of trypanosoma cruzi. *Curr Opin Hematol* (2018) 25(5):347–57. doi: 10.1097/Moh.0000000000000444

20. Wu ML, Liu FL, Sun J, Li X, He XY, Zheng HY, et al. SARS-CoV-2-triggered mast cell rapid degranulation induces alveolar epithelial inflammation and lung injury. *Signal Transduction Targeted Ther* (2021) 6(1):428. doi: 10.1038/s41392-021-00849-0

21. Huisman A, Beun R, Sikma M, Westerink J, Kusadasi N. Involvement of ADAMTS13 and von willebrand factor in thromboembolic events in patients infected with SARS-CoV-2. *Int J Lab Hematol* (2020) 42(5):E211–2. doi: 10.1111/ijlh.13244

22. Krysko O, Kondakova E, Vershinina O, Galova E, Blagonravova A, Gorshkova E, et al. Artificial intelligence predicts severity of COVID-19 based on correlation of exaggerated monocyte activation, excessive organ damage and hyperinflammatory syndrome: A prospective clinical study. *Front Immunol* (2021) 12:715072. doi: 10.3389/fimmu.2021.715072

23. Bethesda (MD). Coronavirus Disease 2019 (COVID-19) Treatment Guidelines. US: National Institutes of Health (2021). Available at: https://www.ncbi.nlm.nih.gov/books/NBK570371/

24. Khan AO, Reyat JS, Hill H, Bourne JH, Colicchia M, Newby ML, et al. Preferential uptake of SARS-CoV-2 by pericytes potentiates vascular damage and permeability in an organoid model of the microvasculature. *Cardiovasc Res* (2022) cvac097. doi: 10.1093/cvr/cvac097

25. Morozov S, Gombolevskiy V, Chernina V, Blokhin I, Mokienko O, Vladzimirskiy A, et al. Prediction of lethal outcomes in covid-19 cases based on the results chest computed tomography. *In: Tuberculosis Lung Dis* (2020) 98(6):7–14. doi: 10.21292/2075-1230-2020-98-6-7-14

26. Goncharov M, Pisov M, Shevtsov A, Shirokikh B, Kurmukov A, Blokhin I, et al. CT-based COVID-19 triage: Deep multitask learning improves joint identification and severity quantification. *In: Med Image Anal* (2020) 71:102054. doi: 10.1016/j.media.2021.102054

27. Schneider CA, Rasband WS, Eliceiri KW. NIH Image to ImageJ: 25 years of image analysis. *Nat Methods* (2012) 9(7):671–5. doi: 10.1038/nmeth.2089

28. Khan AO, Reyat JS, Bourne JH, Colicchia M, Newby ML, Allen JD, et al. Stimulation of vascular organoids with SARS-CoV-2 antigens increases endothelial permeability and regulates vasculopathy. *medRxiv* (2022) 2021.04.25.21255890. doi: 10.1101/2021.04.25.21255890

29. Schindelin J, Arganda-Carreras I, Frise E, Kaynig V, Longair M, Pietzsch T, et al. Fiji: an open-source platform for biological-image analysis. *Nat Methods* (2012) 9(7):676–82. doi: 10.1038/Nmeth.2019

30. Chawla H, Jossi SE, Faustini SE, Samsudin F, Allen JD, Watanabe Y, et al. Glycosylation and serological reactivity of an expression-enhanced SARS-CoV-2 viral spike mimetic. *J Mol Biol* (2022) 434(2):167332. doi: 10.1016/j.jmb.2021.167332

31. Faustini S, Jossi S, Perez-Toledo M, Allen J, Watanabe Y, Newby ML, et al. Detection of antibodies to the SARS-CoV-2 spike glycoprotein in both serum and

saliva enhances detection of infection. *MedRxiv* (2020) 18:2020.06.16.20133025. doi: 10.1101/2020.06.16.20133025

32. Strider JW, Masterson CG, Durham PL. Treatment of mast cells with carbon dioxide suppresses degranulation *via* a novel mechanism involving repression of increased intracellular calcium levels. *Allergy* (2011) 66(3):341–50. doi: 10.1111/j.1398-9995.2010.02482.x

33. Laidlaw TM, Steinke JW, Tinana AM, Feng CL, Xing W, Lam BK, et al. Characterization of a novel human mast cell line that responds to stem cell factor and expresses functional fc is an element of RI. *J Allergy Clin Immunol* (2011) 127 (3):815–U499. doi: 10.1016/j.jaci.2010.12.1101

34. Joulia R, Gaudenzio N, Rodrigues M, Lopez J, Blanchard N, Valitutti S, et al. Mast cells form antibody-dependent degranulatory synapse for dedicated secretion and defence. *Nat Commun* (2015) 6:6174. doi: 10.1038/ncomms7174

35. Dwyer DF, Ordovas-Montanes J, Allon SJ, Buchheit KM, Vukovic M, Derakhshan T, et al. Human airway mast cells proliferate and acquire distinct inflammation-driven phenotypes during type 2 inflammation. *Sci Immunol* (2021) 6(56):eabb7221. doi: 10.1126/sciimmunol.abb7221

36. Gebremeskel S, Schanin J, Coyle KM, Butuci M, Luu T, Brock EC, et al. Mast cell and eosinophil activation are associated with COVID-19 and TLR-mediated viral inflammation: Implications for an anti-Siglec-8 antibody. *Front Immunol* (2021) 12:650331. doi: 10.3389/fimmu.2021.650331

37. St John AL, Rathore APS, Raghavan B, Ng ML, Abraham SN. Contributions of mast cells and vasoactive products, leukotrienes and chymase, to dengue virus-induced vascular leakage. *Elife* (2013) 2:e00481. doi: 10.7554/eLife.00481

38. Dell'Italia LJ, Collawn JF, Ferrario CM. Multifunctional role of chymase in acute and chronic tissue injury and remodeling. *Circ Res* (2018) 122(2):319–36. doi: 10.1161/Circresaha.117.310978

39. Pejler G. Novel insight into the *in vivo* function of mast cell chymase: Lessons from knockouts and inhibitors. *J Innate Immun* (2020) 12(5):357–72. doi: 10.1159/000506985

40. Fu ZR, Thorpe M, Alemayehu R, Roy A, Kervinen J, de Garavilla L, et al. Highly selective cleavage of cytokines and chemokines by the human mast cell chymase and neutrophil cathepsin G. *J Immunol* (2017) 198(4):1474–83. doi: 10.4049/jimmunol.1601223

41. Mizutani H, Schechter N, Lazarus G, Black RA, Kupper TS. Rapid and specific conversion of precursor interleukin-1-Beta (Il-1-Beta) to an active il-1 species by human mast-cell chymase. *J Exp Med* (1991) 174(4):821–5. doi: 10.1084/jem.174.4.821

42. Piliponsky AM, Chen CC, Rios EJ, Treuting PM, Lahiri A, Abrink M, et al. The chymase mouse mast cell protease 4 degrades TNF, limits inflammation, and promotes survival in a model of sepsis. *Am J Pathol* (2012) 181(3):875–86. doi: 10.1016/j.ajpath.2012.05.013

43. Teufelberger AR, Van Nevel S, Hulpiau P, Nordengrun M, Savvides SN, De Graeve S, et al. Mouse strain-dependent difference toward theStaphylococcus aureusAllergen serine protease-like protein d reveals a novel regulator of IL-33. *Front Immunol* (2020) 11:582044. doi: 10.3389/fimmu.2020.582044

44. Motta JD, Miggiolaro AFRD, Nagashima S, de Paula CBV, Baena CP, Scharfstein J, et al. Mast cells in alveolar septa of COVID-19 patients: A pathogenic pathway that may link interstitial edema to immunothrombosis. *Front Immunol* (2020) 11:574862. doi: 10.3389/fimmu.2020.574862

45. Schaller T, Markl B, Claus R, Sholl L, Hornick JL, Giannetti MP, et al. Mast cells in lung damage of COVID-19 autopsies: A descriptive study. *Allergy* (2022) 77 (7):2237–9. doi: 10.1111/all.15293

46. Halova I, Department L, Draber P. Mast cell chemotaxis - chemoattractants and signaling pathways. *Front Immunol* (2012) 3:119. doi: 10.3389/fimmu.2012.00119

47. Afzali B, Noris M, Lambrecht BN, Kemper C. The state of complement in COVID-19. *Nat Rev Immunol* (2022) 22(2):77–84. doi: 10.1038/s41577-021-00665-1

48. de Paula CBV, Nagashima S, Liberalesso V, Collete M, da Silva FPG, Oricil AGG, et al. COVID-19: Immunohistochemical analysis of TGF-beta signaling pathways in pulmonary fibrosis. *Int J Mol Sci* (2022) 23(1):168. doi: 10.3390/ijms23010168

49. Karhausen J, Choi HW, Maddipati KR, Mathew JP, Ma Q, Boulaftali Y, et al. Platelets trigger perivascular mast cell degranulation to cause inflammatory responses and tissue injury. *Sci Adv* (2020) 6(12):eaay6314. doi: 10.1126/sciadv.aay6314

50. Porembskaya O, Zinserling V, Tomson V, Toropova Y, Starikova EA, Maslei VV, et al. Neutrophils mediate pulmonary artery thrombosis in situ. *Int J Mol Sci* (2022) 23(10):5829. doi: 10.3390/ijms23105829

51. Aoki R, Kawamura T, Goshima F, Ogawa Y, Nakae S, Nakao A, et al. Mast cells play a key role in host defense against herpes simplex virus infection through TNF-alpha and IL-6 production. *J Invest Dermatol* (2013) 133(9):2170–9. doi: 10.1038/jid.2013.150

52. Reeves SR, Barrow KA, Rich LM, White MP, Shubin NJ, Chan CK, et al. Respiratory syncytial virus infection of human lung fibroblasts induces a hyaluronan-enriched extracellular matrix that binds mast cells and enhances expression of mast cell proteases. *Front Immunol* (2020) 10:3159. doi: 10.3389/fimmu.2019.03159

53. Hu YX, Jin Y, Han DP, Zhang GZ, Cao SP, Xie JJ, et al. Mast cell-induced lung injury in mice infected with H5N1 influenza virus. *J Virol* (2012) 86(6):3347–56. doi: 10.1128/Jvi.06053-11

54. Graham AC, Hilmer KM, Zickovich JM, Obar JJ. Inflammatory response of mast cells during influenza a virus infection is mediated by active infection and RIG-I signaling. *J Immunol* (2013) 190(9):4676–84. doi: 10.4049/jimmunol.1202096

55. Graham AC, Temple RM, Obar JJ. Mast cells and influenza a virus: association with allergic responses and beyond. *Front Immunol* (2015) 6:238. doi: 10.3389/fimmu.2015.00238

56. Belser JA, Gustin KM, Pearce MB, Maines TR, Zeng H, Pappas C, et al. Pathogenesis and transmission of avian influenza a (H7N9) virus in ferrets and mice. *Nature* (2013) 501(7468):556. doi: 10.1038/nature12391

57. Xu JM, Shi GP. Emerging role of mast cells and macrophages in cardiovascular and metabolic diseases. *Endocrine Rev* (2012) 33(1):71–108. doi: 10.1210/er.2011-0013

58. Meidaninikjeh S, Sabouni N, Marzouni HZ, Bengar S, Khalili A, Jafari R. Monocytes and macrophages in COVID-19: Friends and foes. *Life Sci* (2021) 269:119010. doi: 10.1016/j.lfs.2020.119010

frontiers | Frontiers in Immunology

TYPE Original Research
PUBLISHED 26 September 2022
DOI 10.3389/fimmu.2022.953502

Check for updates

OPEN ACCESS

EDITED BY
E. Marion Schneider,
University of Ulm, Germany

REVIEWED BY
Tomabu Adjobimey,
University Hospital Bonn, Germany
Ken Shirato,
Kyorin University, Japan

*CORRESPONDENCE
Barbara Seitz-Polski
seitz-polski.b@chu-nice.fr

SPECIALTY SECTION
This article was submitted to Viral Immunology, a section of the journal Frontiers in Immunology

RECEIVED 26 May 2022
ACCEPTED 30 August 2022
PUBLISHED 26 September 2022

CITATION
Cremoni M, Allouche J, Graça D, Zorzi K, Fernandez C, Teisseyre M, Benzaken S, Ruetsch-Chelli C, Esnault VLM, Dellamonica J, Carles M, Barrière J, Ticchioni M, Brglez V and Seitz-Polski B (2022) Low baseline IFN-γ response could predict hospitalization in COVID-19 patients. *Front. Immunol.* 13:953502. doi: 10.3389/fimmu.2022.953502

COPYRIGHT
© 2022 Cremoni, Allouche, Graça, Zorzi, Fernandez, Teisseyre, Benzaken, Ruetsch-Chelli, Esnault, Dellamonica, Carles, Barrière, Ticchioni, Brglez and Seitz-Polski. This is an open-access article distributed under the terms of the Creative Commons Attribution License (CC BY). The use, distribution or reproduction in other forums is permitted, provided the original author(s) and the copyright owner(s) are credited and that the original publication in this journal is cited, in accordance with accepted academic practice. No use, distribution or reproduction is permitted which does not comply with these terms.

Low baseline IFN-γ response could predict hospitalization in COVID-19 patients

Marion Cremoni[1,2], Jonathan Allouche[3], Daisy Graça[2], Kevin Zorzi[1], Céline Fernandez[1], Maxime Teisseyre[1], Sylvia Benzaken[2], Caroline Ruetsch-Chelli[1,2], Vincent L. M. Esnault[1], Jean Dellamonica[1,4,5], Michel Carles[6], Jérôme Barrière[7], Michel Ticchioni[2], Vesna Brglez[1,2] and Barbara Seitz-Polski[1,2]*

[1]Clinical Research Unit Côte d'Azur (UR2CA), University Côte d'Azur, Nice, France, [2]Immunology Laboratory, Archet 1 Hospital, Nice University Hospital, Nice, France, [3]Department of Public Health, Archet 1 Hospital, Nice University Hospital, Nice, France, [4]Intensive Care Medicine Department, Archet 1 Hospital, Nice University Hospital, Nice, France, [5]Medical ICU, Archet 1 Hospital, Nice University Hospital, Nice, France, [6]Infectious Diseases Department, Archet 1 Hospital, Nice University Hospital, Nice, France, [7]Department of Medical Oncology, Polyclinique Saint-Jean, Cagnes-sur-mer, France

The SARS-CoV-2 infection has spread rapidly around the world causing millions of deaths. Several treatments can reduce mortality and hospitalization. However, their efficacy depends on the choice of the molecule and the precise timing of its administration to ensure viral clearance and avoid a deleterious inflammatory response. Here, we investigated IFN-γ, assessed by a functional immunoassay, as a predictive biomarker for the risk of hospitalization at an early stage of infection or within one month prior to infection. Individuals with IFN-γ levels below 15 IU/mL were 6.57-times more likely to be hospitalized than those with higher values ($p<0.001$). As confirmed by multivariable analysis, low IFN-γ levels, age >65 years, and no vaccination were independently associated with hospitalization. In addition, we found a significant inverse correlation between low IFN-γ response and high level of IL-6 in plasma (Spearman's rho=-0.38, $p=0.003$). Early analysis of the IFN-γ response in a contact or recently infected subject with SARS-CoV-2 could predict hospitalization and thus help the clinician to choose the appropriate treatment avoiding severe forms of infection and hospitalization.

KEYWORDS

SARS-CoV-2, viral infection, IFN-γ, functional immunoassay, predictive biomarker, personalized medicine

Introduction

The severe acute respiratory syndrome coronavirus 2 (SARS-CoV-2) infection that emerged in China in late 2019 has spread rapidly around the world, causing millions of deaths, overwhelming public health services, and resulting in severe economic and social crisis. Individuals who are male, older than 60 years, and have comorbidities are at higher risk for severe COVID-19, requiring hospitalization and more frequently presenting with complications such as multivisceral failure or death (1–4). The implementation of preventive measures such as lockdown, social distancing (5, 6) and vaccination (7–9) have limited its spread. Although no curative treatment has unequivocally demonstrated its effectiveness (10), the administration of antiviral drugs in the early phase of the disease appears to decrease viral replication and pathogenesis (11–13), interferon (IFN) therapy reduces the duration and severity of symptoms, as well as mortality, if administered early (14–20), and the treatment with monoclonal antibodies results in fewer hospitalizations and deaths in immunocompromised patients (21–23).

The immune response to a viral agent, including SARS-CoV-2, involves both the innate and adaptative response. Innate immunity induced by Toll-like receptors 3 (TLR3) and TLR7/8 signaling activates effector cells to mediate viral clearance, induces inflammation through secretion of proinflammatory cytokines (e.g., IL-6 and IL-1β), produces antiviral cytokines and stimulates the adaptative immune response by activating antigen-specific T cells. Type I and II IFN (i.e., IFN-α/β and IFN-γ, respectively) are the first-line cytokines against viral infections. While many studies have focused on type I and III IFN alteration in severe forms of COVID-19 (24–34), less research has been conducted on type II IFN deficiency (35–38). However, if type I IFN is a component of innate immunity, type II IFN is involved in both innate and adaptative immune responses. Indeed, IFN-γ is produced by natural killer cells and macrophages, effector cells in innate immunity, as well as by $CD4^+$ T cells of the Th1 type and $CD8^+$ T cells that participate in the adaptative response.

Moreover, rapidly after the beginning of the pandemic, many authors highlighted that an excessive pro-inflammatory innate immune response could be deleterious in the defense against the virus, leading to a cytokine storm responsible for acute respiratory distress syndrome, multivisceral failure and even death. Interleukin-6 (IL-6) is one of the main cytokines involved in the cytokine storm (35, 39–43). This observation made anti-IL-6 and corticosteroids first-line treatments for severe COVID-19. However, the evidence of excessive secretion of pro-inflammatory cytokines, including IL-6, is often late in the infection and does not allow the implementation of preventive measures. It is likely that a deficiency in interferons, responsible for a persistence of the virus by defect of clearance, can support the overexpression of pro-inflammatory cytokines at the origin of the cytokine storm (35, 41).

To our knowledge, no study has investigated the IFN response at an early stage of SARS-CoV-2 infection, or even before contamination, to detect preexistent immune dysfunction in subjects who may subsequently progress to a severe form of the disease. Thus, we hypothesize that dysregulation of the basal IFN-γ response, as assessed by an easy to perform functional immunoassay, promotes severe forms of COVID-19 requiring hospitalization. A clinically applicable blood biomarker identifying patients with dysregulated IFN-γ response could optimize management by directing the prescription of antivirals and/or IFN and/or monoclonal antibodies to patients likely to benefit from them, thus reducing the number of hospitalizations, while avoiding deleterious over-prescription and potential associated adverse effects in those for whom the treatment would not be of interest.

Materials and methods

Participants, data collection and ethics statement

We performed a prospective monocentric longitudinal and ancillary study at the Nice University Hospital, France. The participants included were extracted from three prospective monocentric cohorts: (i) patients recruited during an infectious diseases or emergency room consultation following COVID-19 symptoms, or a contact case between March 2020 and January 2022 (CovImmune 1 study, NCT04355351); (ii) patients recruited by partner laboratories during a positive RT-PCR for SARS-CoV-2, performed in the context of suggestive symptomatology, contact case, or health pass, between August 2021 and November 2021 (CovImmune 1 study, NCT04355351); (iii) voluntary participants from the general population monitored systematically and periodically since July 2020 as part of an epidemiological study in the context of COVID-19 (CovImmune 2 study, NCT04429594). COVID-19 positive participants for whom we had a stimulated blood sample either a) within one month prior to infection or b) within five days after the first symptoms of the disease or after a close contact with a COVID-19 case, were enrolled in this study. Demographic, clinical, biological, and outcome data were collected by the study investigators and then centralized in an anonymized database. Written informed consent was obtained from all study participants.

Blood collection and immunoassays

Blood samples were collected between 8am and 12pm by nurses or physicians in tubes containing lithium heparinate. After receipt in the laboratory, one milliliter of whole blood was stimulated with immune agents that mimic the pathogen-associated molecular patterns that activate immune cells (R848 as TLR7/8 agonist and anti-CD3 as T-cell stimulant) in QuantiFERON-Monitor® specific tubes (Qiagen®, Germany) within eight hours from blood collection. To measure IFN-γ levels produced by SARS-CoV-2-specific T cells, we used the QuantiFERON® SARS-CoV-2 test (Qiagen®, Germany) in which one milliliter of whole blood was collected in tubes containing a mixture of SARS-CoV-2 peptides. Blood samples stimulated with SARS-CoV-2 specific and nonspecific immune agents were then incubated for 16 to 18 hours at 37°C and then centrifugated at 2000-3000 x g for 15 minutes to harvest the plasmas. Plasmas were then stored at –80°C until analysis and freeze-thaw cycles were minimized to preserve the quality of the samples. Plasma IFN-γ levels after stimulation were measured by enzyme-linked immunosorbent assay (ELISA). The procedure with nonspecific response is summarized in Figure 1. To note, when IFN-γ values obtained after a nonspecific response were above the limit of detection range (e.g., IFN-γ >1000 IU/mL), the values were arbitrarily scored as 1000 IU/mL. This functional test is simple to implement for both clinical and laboratory staff, making it applicable for routine use. In addition, for patients included *via* hospital consultations (CovImmune 1 study), we also measured plasma IL-6 by ELISA without cellular stimulation with custom-designed cartridges Ella (ProteinSimple™).

The proportions and numbers of CD4+ T cells, CD8+ T cells, NK cells and B cells, as well as their IFN-γ production with no stimulation or after nonspecific stimulation, were assessed in three healthy volunteers by flow cytometry. Eight milliliters of blood were collected: 2 mL with unstimulated cells, including 1 mL to measure IFN-γ by ELISA and 1 mL to identify IFN-γ-producing cells by flow cytometry, 2 mL with cells stimulated with TLR7/8 agonist, 2 mL with cells stimulated with anti-CD3, and 2 mL with cells stimulated with both TLR7/8 agonist and anti-CD3. After 4 hours of incubation, BD GolgiStopTM (0.66µL/mL) was added to the samples for flow cytometry, followed by an additional incubation time of 12 hours. Finally, cells were fixed and stained using fluorochrome-conjugated antibodies against surface molecules (CD45 BV786, CD5 PerCP-Cy5.5, CD2 FITC, CD7 BV711, CD3 BV510, CD8 PE, CD4 BV605, CD19 PE-Cy7, CD16 BV510, CD56-BV510, CD64 APC-H7) and intracellular molecules (CD3 APC, IFN-γ R718). All antibodies used are commercially available. Flow cytometry data were acquired on a BD FACSLyric™ and analyzed using BD FACSuite™ software. The gating strategy is depicted in Supplementary Figure 1.

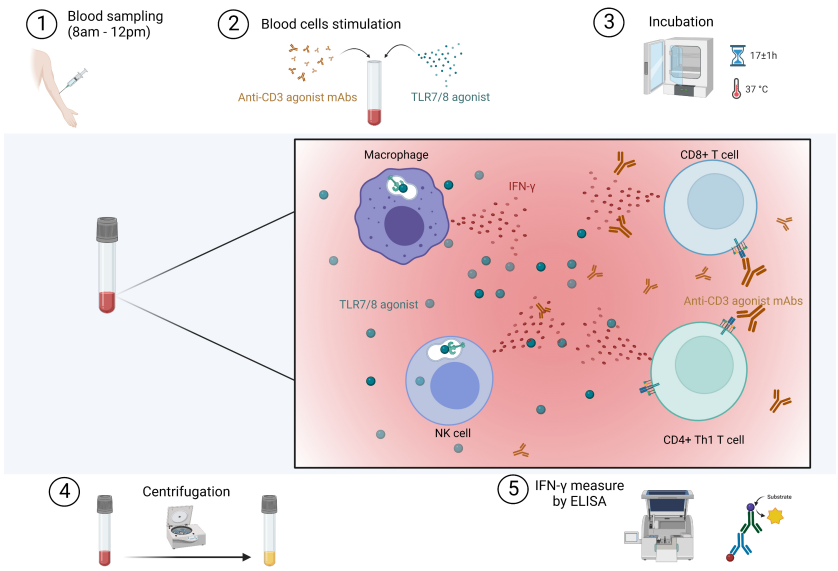

FIGURE 1
Procedure for the *in vitro* stimulation of immune cells in whole blood. Immune ligands mimic pathogen-associated molecular patterns that activate innate immune cells through TLR7/8 and T cells through CD3. IFN, interferon; mAbs, monoclonal antibodies; TLR, toll-like receptor. Created with BioRender.com.

Statistical analyses

Data are presented as mean and standard deviation for quantitative variables with Gaussian distribution, as median and interquartile range [25th percentile; 75th percentile] for quantitative variables with non-Gaussian distribution, or as numbers and percentages for qualitative variables. The Shapiro-Wilk normality test was used to verify the distribution of data. Comparisons were performed using the unpaired two-sided Student's t-test or Wilcoxon-Mann-Whitney U test according to data distribution for quantitative variables, and the Chi-square test for qualitative variables. The associations between specific and nonspecific IFN-γ responses, and between nonspecific IFN-γ response and plasma IL-6 values were compared using Spearman rank correlation coefficient. Multivariable logistic regression model was used to investigate independent factors that influence hospitalization. Receiver Operating Characteristic (ROC) curve was used to define an IFN-γ threshold below which patients would be considered at risk for hospitalization. Kaplan-Meier analysis was used to estimate the probability of hospitalization based on IFN-γ response. Statistical analyses were performed using GraphPad Prism 8 (GraphPad Software, Inc., San Diego, CA) for unadjusted analysis and Jamovi (version 1.8.4.0) for multivariable analysis. All comparisons were two-tailed, and the differences were considered significant when p value < 0.05.

Results

Interferon-γ production after nonspecific stimulation of innate and adaptive immune cells in healthy volunteers

Immune cells of seven healthy donors were stimulated with immune ligands: TLR7/8 agonist as a stimulant of innate immune cells, anti-CD3 as T cells stimulant, both TLR7/8 agonist and anti-CD3, or no stimulation. As shown in Figure 2A, a very low level of IFN-γ was detected in plasma without cell stimulation. TLR7/8 agonist and anti-CD3 stimulations significantly increased IFN-γ production (p=0.0006 and p=0.03, respectively). Stimulation with the combination of a TLR7/8 agonist and an anti-CD3 significantly increased IFN-γ production (p=0.0006), but without a significant increase compared to the TLR7/8 agonist alone, probably due to a too small sample size.

The immune cells involved in IFN-γ production after nonspecific stimulation were innate immune cells, particularly NK cells, $CD4^+$ T and $CD8^+$ T cells (Figure 2B). Interestingly, we showed that the TLR7/8 agonist also activated $CD8^+$ T cells (44, 45) and that the action of the two immune agents together seemed to be synergistic. There are probably large variations in the proportions and cell types activated after nonspecific stimulation from one individual to another (Supplementary Figure 2).

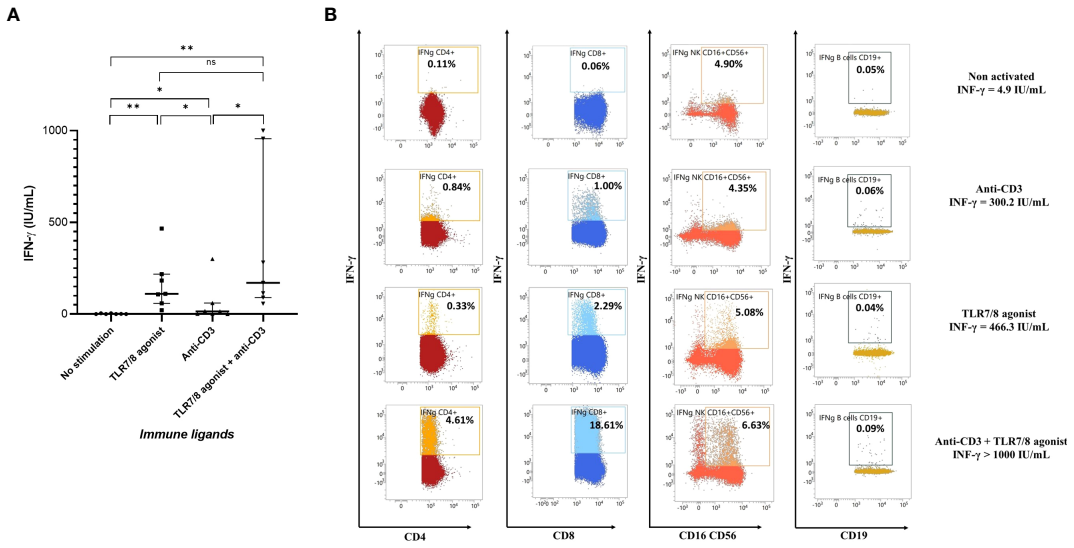

FIGURE 2
Evaluation of IFN-γ production after stimulation or not of circulating peripheral blood cells in healthy donors. **(A)** Plasma cytokine levels in seven healthy donors after *in vitro* nonspecific stimulation of immune cells by anti-CD3, or TLR7/8 agonist, or both anti-CD3 and TLR7/8 agonist, or no stimulation. IFN-γ production was mainly increased after TLR7/8 agonist stimulation and partially after anti-CD3 stimulation. **(B)** Representative plots of IFN-γ production by $CD4^+$ T cells, $CD8^+$ T cells, NK cells and B cells after stimulation or not with TL7/8 agonist and/or anti-CD3. As expected, after nonspecific stimulation $CD4^+$ T, $CD8^+$ T and NK cells produce more IFN-γ, but not B cells. The level of IFN-γ measured on the same individual and in the same conditions with no stimulation and after nonspecific stimulation with anti-CD3, TLR7/8 agonist, or both was 4.9, 300.2, 466.3 and >1000.0 IU/mL, respectively. *p<0.05; **p<0.01; ns, not significant. IFN, interferon; TLR, Toll-like receptor.

Characteristics of the population and outcomes

We included 115 individuals infected with SARS-CoV-2 for whom we obtained a blood sample with nonspecific cell stimulation within one month prior to infection or within five days after the first symptoms during the period from March 2020 to January 2022 (Figure 3). The population's characteristics are shown in Table 1. Sixty-six (57.4%) of the subjects were women, and the average age of the cohort was 53.9 (± 17.2) years. Sixty-three (54.8%) participants had at least one comorbidity. The most frequent comorbidities were hypertension (26.1%), immunosuppressive therapy (13.9%) and respiratory diseases (13.0%). Seventy-eight (67.8%) individuals were completely vaccinated. Common symptoms, including cough (47.0%), fever (39.1%) and dyspnea (26.1%), were reported by many individuals. Only five of them (4.3%) received antiviral treatment. Among the 115 individuals included in this study, twenty-eight (24.3%) subsequently progressed to severe pneumonia requiring hospitalization, 24 (20.9%) and 16 (13.9%) required oxygen therapy and corticosteroids, respectively, 11 (9.6%) were transferred to an intensive care unit, and five (4.3%) died. To note, among the 24 who required corticosteroids, 22 were hospitalized and two were outpatients.

Factors associated with the risk of hospitalization for COVID-19 patients

As shown in previous studies (1–3, 46–49), unadjusted analysis of this cohort (Table 2) confirmed that the risk of hospitalization was significantly higher with increased age ($p<0.001$), male gender ($p<0.001$), and the existence of at least one comorbidity ($p<0.001$). No significant difference was found with body mass index (BMI) ($p=0.083$). As expected, the proportion of patients vaccinated was significantly lower in the group of patients requiring hospitalization ($p<0.001$). There was no difference in the lymphocytes count between the two groups ($p=0.212$), but a significant difference in the ability of immune

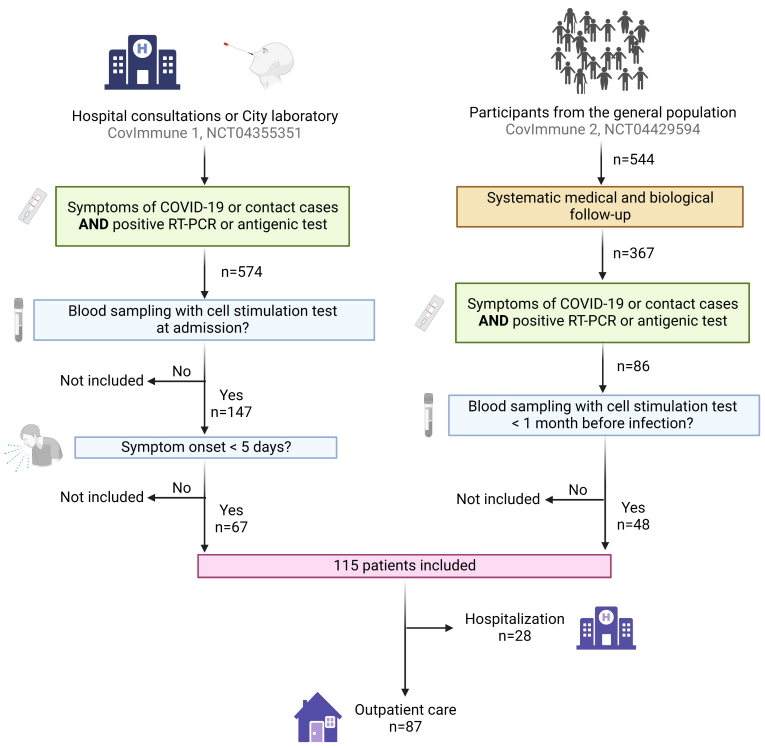

FIGURE 3
Flow chart showing participants enrollment. The participants were included from three cohorts: (i) patients recruited during a hospital consultation following COVID-19 symptoms, or as contact of a diagnosed COVID-19 case (CovImmune 1 study, NCT04355351); (ii) patients recruited by partner laboratories during a positive RT-PCR for SARS-CoV-2 (CovImmune 1 study, NCT04355351); (iii) participants monitored periodically since July 2020 as part of an epidemiological study in the context of COVID-19 (CovImmune 2 study, NCT04429594) and developing a SARS-CoV-2 infection. COVID-19 positive participants for whom we had a stimulated blood sample either a) within one month prior to infection or b) within five days after the first symptoms of the disease or after a close contact with a COVID-19 case, were enrolled in this study. COVID-19, coronavirus disease 2019; RT-PCR, reverse transcription-polymerase chain reaction. Created with BioRender.com.

10.3389/fimmu.2022.953502

TABLE 1 Population's characteristics.

Population's characteristics	Patients, n = 115
Baseline characteristics	
Sex	
Male	49 (42.6%)
Female	66 (57.4%)
Age, years	53.9 (± 17.2)
Comorbidities	
BMI (kg/m²)	24.9 [21.5-28.3]
Type 2 diabetes	11 (9.6%)
Cardiovascular diseases*	11 (9.6%)
Hypertension	30 (26.1%)
Respiratory diseases (COPD, asthma)	15 (13.0%)
Active cancer	9 (7.8%)
Immunosuppressive therapy	16 (13.9%)
SARS-CoV-2 vaccination**	78 (67.8%)
Presentation at diagnosis	
Symptoms	
Fever (>38·0°C)	45 (39.1%)
Cough	54 (47.0%)
Dyspnea	30 (26.1%)
Headache	27 (23.5%)
Myalgia	27 (23.5%)
Diarrhea	11 (9.6%)
Anosmia	19 (16.5%)
None	9 (7.8%)
Laboratory data	
Lymphocytes count (G/L)	1.1 [0.8-1.6]
Neutrophils count (G/L)	4.4 [2.9-6.3]
Hematocrit (L/L)	0.39 (± 0.64)
CRP (mg/L)	28.9 [6.4-106.6]
Serum creatinine (µmol/L)	77.0 [57.8-114.3]
IFN-γ levels after *in vitro* cell stimulation (IU/mL)	58.0 [15.0-234.0]
Outcomes	
Hospitalization	28 (24.3%)
Oxygen therapy	24 (20.9%)
Corticosteroids	16 (13.9%)
Intensive care unit	11 (9.6%)
Death	5 (4.3%)

The number (and percentage) are indicated for categorical variables, mean (and standard deviation) are shown for continuous variables with Gaussian distribution and median (and interquartile range) for continuous variable with non-Gaussian distribution. Lymphocyte and neutrophil counts, CRP and creatinine values were available for 59 patients. Hematocrit was available for 62 patients.
*heart failure or coronary artery disease.
**complete scheme (two or more injections of an mRNA vaccine, one or more injection of Janssen vaccine).
BMI, body mass index; COPD, chronic obstructive pulmonary disease; CRP, C-reactive protein; IFN-γ, interferon-gamma.

cells to respond to a nonspecific stimulus, as measured by IFN-γ production, in those who were subsequently hospitalized (97.0 [interquartile range (IQR), 23.6-332.0] IU/mL vs 11.6 [IQR, 3.3-53.9] IU/mL, p<0.001) (Figure 4). Because we found a difference in hematocrit values between the two groups (p=0.022), we corrected for IFN-γ levels by performing a ratio with hematocrit values: again, patients who were subsequently hospitalized had a lower ability of immune cells to respond to a nonspecific stimulus (p<0.001). We then compared IFN-γ production between COVID-19 patients and 544 uninfected volunteers from the general population: we found no difference between outpatients and uninfected individuals (p=0.52) but a significant difference between hospitalized patients and uninfected individuals (p<0.001) (Figure 4). Of note, three patients in the outpatient group and ten uninfected individuals had IFN-γ above the limit of detection and the value was considered to be 1000 IU/mL. For information, the IFN-γ responses of volunteers from the general population, by age group and sex, are available as additional data (Supplementary Table 1).

Of the 115 patients, we performed IFN-γ assay after specific stimulation with SARS-CoV-2 peptides for 84 (73%) of them, of which ten were hospitalized and 74 were outpatients. Although there is a correlation between specific and nonspecific cellular responses (Spearman's rho=0.246 [0.027; 0.443], p=0.024), we did not find an altered specific cellular response in patients who will subsequently be hospitalized (p=0.149). The data are shown in Supplementary Figure 3.

As confirmed by multivariable analysis, low stimulated IFN-γ levels were an independent predictor of hospitalization in COVID-19 patients (p=0.023), as were no vaccination (p<0.001) and being over the age of 65 (p=0.037). These results are detailed in Table 3.

A low IFN-γ response correlates with hospitalization in COVID-19 patients

We then examined the utility of measuring IFN-γ response as a biomarker of hospitalization in the early phase of COVID-19 infection. We found a significant inverse correlation between IFN-γ response and hospitalization (odds ratio=0.990 [0.981; 0.996], p=0.007). Next, we evaluated the relevance of using IFN-γ response as a biomarker of hospitalization in COVID-19 patients using a receiver-operating characteristic (ROC) curve: the area under the ROC curve (AUC) was 87.9%, revealing a good performance of IFN-γ response in predicting hospitalization in COVID-19 patients. Using this ROC curve, we defined an IFN-γ cut-off value at 15 IU/mL to identify patients at risk of hospitalization (sensitivity: 67.9%, specificity: 94.3%, p<0.001). In univariable analysis, individuals with less than 15 IU/mL of IFN-γ after nonspecific stimulation were 6.57-times more likely to be subsequently hospitalized (odds ratio=6.57 [2.55; 16.95], p<0.001) (Figure 5). We then sought to clarify the predictive impact of the IFN-γ response by adjusting for variables independently associated with hospitalization in the multivariable model. We found that IFN-γ level was more predictive when the subject was older

10.3389/fimmu.2022.953502

TABLE 2 Clinical and biological presentation of COVID-19 patients according to clinical course.

	Outpatient care n = 87	Hospitalization n = 28	Univariable p value
Demographic data			
Age	50.1 (± 15.4)	65.5 (± 17.5)	<0.001
Sex (Male)	29 (33.3%)	20 (71.4%)	<0.001
BMI (kg/m²)	23.8 [21.2-27.6]	26.3 [24.7-29.4]	0.083
One or more comorbidities	38 (45.2%)	25 (89.3%)	<0.001
Vaccine schedule			
SARS-CoV-2 vaccination*	68 (59.1%)	10 (35.7%)	<0.001
Biological data at presentation			
Lymphocytes count (G/L)	1.2 [0.8-1.7]	1.0 [0.6-1.5]	0.212
Neutrophils count (G/L)	3.9 [2.9-5.0]	4.9 [3.2-7.4]	0.788
Hematocrit (L/L)	0.41 (± 0.52)	0.37 (± 0.69)	0.022
IFN-γ levels after *in vitro* cell stimulation (IU/mL)	97.0 [23.6-332.0]	11.6 [3.3-53.9]	<0.001
IFN-γ/hematocrit ratio (IU/mL)	270.5 [47.0-542.4]	36.3 [9.2-134.9]	<0.001

The number (and percentage) are indicated for categorical variables, mean (and standard deviation) are shown for continuous variables with Gaussian distribution and median (and interquartile range) for continuous variable with non-Gaussian distribution. Comparisons were performed using the unpaired two-sided Student's t-test or Wilcoxon-Mann-Whitney U test according to data distribution for quantitative variables, and the Chi-square test for qualitative variables. Significant associations are highlighted.
*complete scheme (two or more injections of an mRNA vaccine, one or more injection of Janssen vaccine).
BMI, body mass index; IFN-γ, interferon-gamma. Bold value = p > 0.05.

than 65 years, male, had at least one comorbidity and was not vaccinated (Figure 6). In other words, the risk of hospitalization in a young, healthy, vaccinated subject is low even if his or her IFN-γ is less than 15 IU/mL, whereas the risk is major in an individual with one or more associated factors who would have the same IFN-γ level. Thus, our data suggest that IFN-γ response, assessed by functional immunoassay, may be a tool for predicting the risk of hospitalization for early or subsequent SARS-CoV-2 infection.

A low IFN-γ response correlates with a high level of IL-6 in plasma

For the 56 (48.7%) patients included *via* hospital consultations, we also had a plasma IL-6 assay without cell stimulation. Among them, 30 (53.6%) were outpatients and 26 (46.4%) were hospitalized. As expected, hospitalized patients exhibited more IL-6 levels than outpatients (40.70 [9.50; 71.60] vs 7.00 [0.99; 35.70] pg/mL respectively, p<0.001). Significant

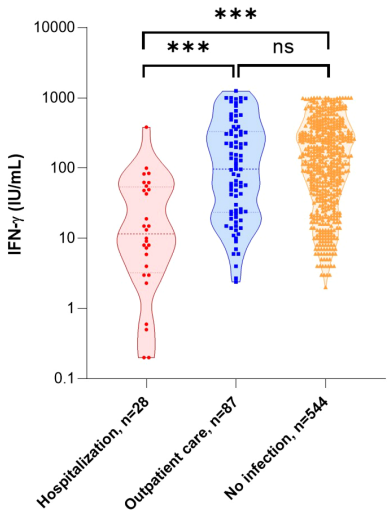

FIGURE 4
IFN-γ response and the risk of hospitalization after SARS-CoV-2 infection. Comparison of IFN-γ secretion by stimulated blood cells in relation to subsequent care for infection management and compared with no infection. Statistical significance of difference between groups was assessed using Mann-Whitney non-parametric test. ***p<0.001; ns, not significant. IFN, interferon.

10.3389/fimmu.2022.953502

TABLE 3 Factors independently associated with hospitalization for COVID-19.

	Adjusted odds ratio [95% CI]	Multivariable p value
Demographic data		
Age < 45 vs > 65 years	0.340 [0.043-2.694]	0.307
Age 45-65 vs > 65 years	0.129 [0.019-0.886]	0.037
Sex (Male)	3.424 [0.686-17.095]	0.134
One or more comorbidities	3.041 [0.567-16.302]	0.194
Vaccine schedule		
SARS-CoV-2 vaccination*	0.098 [0.025-0.390]	<0.001
Biological data at presentation		
IFN-γ ≤ 15 IU/mL	4.623 [1.231-17.361]	0.023

Multivariable logistic regression model was used to investigate independent factors that influence hospitalization. Significant associations are highlighted. Overall test model: p<0.001, R^2=43.8%.
*complete scheme (two or more injections of an mRNA vaccine, one or more injection of Janssen vaccine).
CI, confidence interval; IFN-γ, interferon-gamma. Bold value = p > 0.05.

inverse correlation was found between IFN-γ response and plasma IL-6 (Spearman's rho=-0.38 [-0.59; -0.13], p=0.003).

Discussion

In this ancillary study of several prospective cohorts, we investigated whether an individual's IFN-γ response, as assessed by a functional immunoassay, could predict the risk of hospitalization after SARS-CoV-2 infection. We found that participants with IFN-γ levels below 15 IU/mL were 6.57-times more likely to be hospitalized for COVID-19 than those with higher values. This risk was even higher if participants also had an associated factor such as age >65 years, male gender, presence of at least one comorbidity, or lack of vaccination. Probably due to a lack of statistical power, in the overall multivariable analysis, the relative risk of those under 45 years was not significantly associated with a lower risk of hospitalization than those over 65 years (Table 3), although it was in the logistic regression considering only the IFN-γ response and the age group (Figure 6A). Unlike other studies (4, 50), obesity was not found to be a risk factor for hospitalization, probably because few subjects were overweight in this cohort of individuals from southern France. In addition, we found a significant inverse correlation between IFN-γ response and plasma IL-6 in a subgroup of 56 patients, supporting data from other teams (24, 35, 41). This association supports the hypothesis that interferon deficiency may promote excess secretion of proinflammatory cytokines, probably due in part to the deficit in viral clearance. However, this result must be tempered by the fact that it is derived from a subgroup of patients and that the number of patients who have progressed to a severe form of

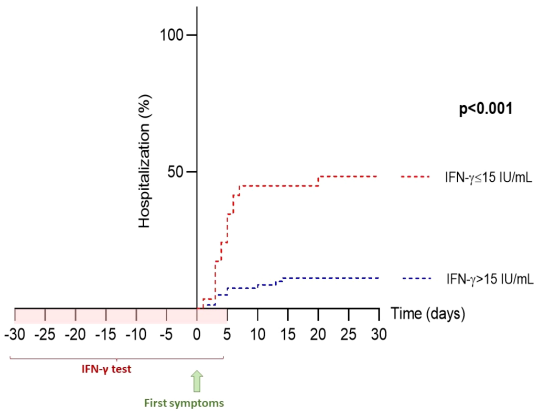

FIGURE 5
Hospitalization-free survival rate based on IFN-γ response. The IFN-γ threshold of 15 IU/mL, determined by ROC curve (sensitivity 67.9% and specificity 94.3%), was used for Kaplan-Meier analysis. Of the 32 patients with IFN-γ ≤15 IU/mL, 17 (53%) were subsequently hospitalized, whereas only 11 of 72 (15%) patients with IFN-γ >15 IU/mL were hospitalized. IFN, interferon; ROC, receiver operating characteristics.

COVID-19 requiring intensive care management is low. Further studies, including preclinical studies, are needed to demonstrate the impact of interferon variations on the inflammatory response in the context of SARS-CoV-2.

In this study, the SARS-CoV-2 specific cellular response was not associated with the risk of hospitalization. This result is not surprising given the study design. Indeed, in addition to the fact that the specific cellular tests were performed in only 84 patients, they were also performed very early after the infection, even before the contact with the infectious agent for almost half of the patients, including non-vaccinated patients for whom the specific response was necessarily non-existent without presaging their subsequent antiviral response. In our opinion, the evaluation of the specific cellular response is of particular interest in the evaluation of the post-vaccination immune response.

We believe that this simple to use functional measure of nonspecific cellular response could help clinicians identify patients who would benefit from early antiviral or IFN therapy, allowing for more personalized prescription. Moreover, the immune response must be maintained in a balanced manner and some recent data suggest that long COVID-19 may be due to an excessive IFN response (51). Thus, the choice of the molecule and the precise timing of its administration seem necessary both to induce viral clearance and prevent immunopathology. It could therefore be detrimental to prescribe IFN-based therapies in patients whose immunological balance is already dysregulated in favor of this pathway. Here again, this functional immunological test could help optimize management for a tailored prescription. Clinical trials could be considered: IFN or antiviral treatment if IFN-γ after cell stimulation <15 IU/mL in a patient with one or more associated factors but not within the indications of these therapies, to be compared to a standard-of-care arm.

The originality of this study is the analysis of the individual functional cellular response, at the early phase of the infection, and even before the infection for nearly half of the individuals included. If performed too late after the contamination, the results of the test would probably be modified by the ongoing anti-infectious response in various proportions: IFN-γ secretion increased at the peak of the antiviral response, decreased at the time of immune reconstitution and even more so in case of cell exhaustion, or even increased persistently in case of long COVID. As suggested by other teams, but without a functional approach (30, 38), a functional immunoassay performed early during the infection, or even before contamination, could predict the antiviral response against SARS-CoV-2, but also the response against other viruses or intracellular pathogens (52). This hypothesis is partly confirmed by our work but requires further studies.

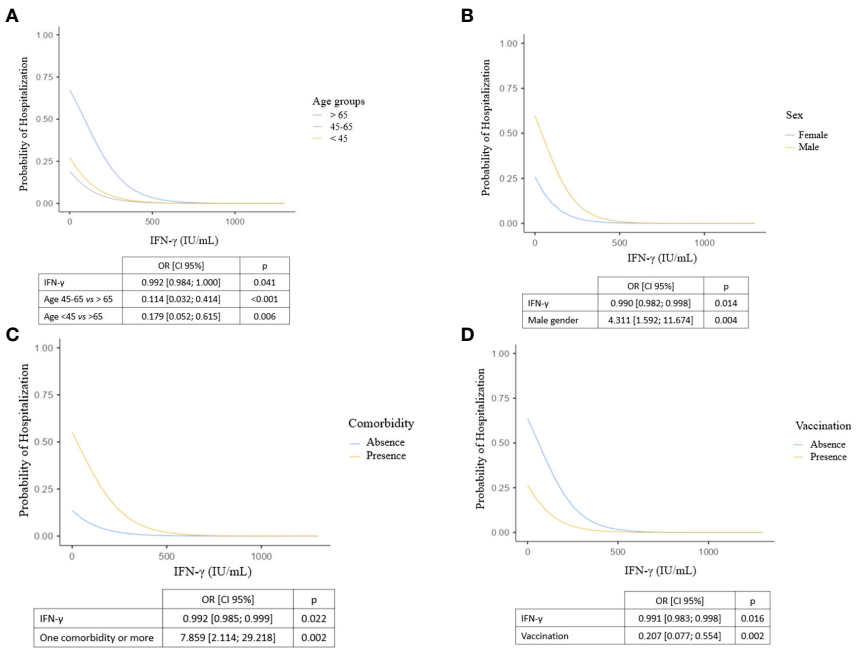

FIGURE 6
Probability of hospitalization according to IFN-γ levels, adjusted for **(A)** age class, **(B)** sex, **(C)** presence of at least one comorbidity and **(D)** vaccination. Logistic regression models including explanatory variables associated with hospitalization in multivariable analysis. We show here four representations of the model adjusted on the explanatory variables: each of them represents the impact of a factor and IFN-γ production on hospitalization after adjustment. CI, confidence interval; IFN, interferon; OR, odds ratio.

Nevertheless, our study has several limitations. First, the inclusion period is long, extending from the beginning of the pandemic to a more recent period. It therefore covers infections with various variants of SARS-CoV-2 and pre- and post-vaccination periods. However, we are not studying the specific immune response to SARS-CoV-2 but the antiviral response in general, so the strain of virus should not influence the results. Also, vaccination was included in the multivariable model, which limits this bias. Secondly, the ability of immune cells to respond to stimulation also depends on an individual's age, comorbidities, and infectious and immunological history (53). It is therefore difficult to disentangle these variables and establish IFN-γ standards. Finally, although the cohort size is reasonable given its prospective design and its biological assays with strict pre-analytical procedures, the sample size remains small, and the results need to be confirmed on a larger cohort.

Although many questions remain, early analysis of the IFN-γ response in a contact or recently infected subject could help the clinician choose the appropriate molecule for management and thus avoid severe forms of infection and hospitalization.

Data availability statement

The raw data supporting the conclusions of this article will be made available by the authors, without undue reservation.

Ethics statement

The studies involving human participants were reviewed and approved by Comités de Protection des Personnes Sud-Ouest et Outre-Mer 1 et 2, Agence Régionale de Santé - 10 Chemin du Raisin - 31050 TOULOUSE CEDEX 9. The patients/participants provided their written informed consent to participate in this study.

Author contributions

BS-P designed the study; DG, VB, and MCr carried out experiments; MCr, BS-P, CF, KZ, JA, and CR-C collected data; MCr, KZ, JA, CR-C, MTi, and BS-P analyzed and interpreted the data; MCr and BS-P drafted and revised the manuscript. All authors contributed to the article and approved the submitted version.

Funding

This research was supported by grants from the Agence Nationale de la Recherche (Flash-COVID ANR- 20-COVI-000) and Conseil Départemental des Alpes-Maritimes (CD06).

Acknowledgments

We thank the medical and paramedical staff involved in the care of patients and all the participants.

Conflict of interest

The authors declare that the research was conducted in the absence of any commercial or financial relationships that could be construed as a potential conflict of interest.

Publisher's note

All claims expressed in this article are solely those of the authors and do not necessarily represent those of their affiliated organizations, or those of the publisher, the editors and the reviewers. Any product that may be evaluated in this article, or claim that may be made by its manufacturer, is not guaranteed or endorsed by the publisher.

Supplementary material

The Supplementary Material for this article can be found online at: https://www.frontiersin.org/articles/10.3389/fimmu.2022.953502/full#supplementary-material

References

1. Wang D, Hu B, Hu C, Zhu F, Liu X, Zhang J, et al. Clinical characteristics of 138 hospitalized patients with 2019 novel coronavirus–infected pneumonia in wuhan, China. *JAMA* (2020) 323(11):1061. doi: 10.1001/jama.2020.1585

2. Guan Wj, Liang Wh, Zhao Y, Liang Hr, Chen Zs, Li Ym, et al. Comorbidity and its impact on 1590 patients with COVID-19 in China: a nationwide analysis. *Eur Respir J* (2020) 55(5):2000547. doi: 10.1183/13993003.00547-2020

3. Jin JM, Bai P, He W, Wu F, Liu XF, Han DM, et al. Gender differences in patients with COVID-19: Focus on severity and mortality. *Front Public Health* (2020) 8:152. doi: 10.3389/fpubh.2020.00152

4. Lighter J, Phillips M, Hochman S, Sterling S, Johnson D, Francois F, et al. Obesity in patients younger than 60 years is a risk factor for COVID-19 hospital admission. *Clin Infect Dis* (2020) doi: 10.1093/cid/ciaa415/5818333

5. Chu DK, Akl EA, Duda S, Solo K, Yaacoub S, Schünemann HJ. Physical distancing, face masks, and eye protection to prevent person-to-person transmission of SARS-CoV-2 and COVID-19: a systematic review and meta-analysis. *Lancet Lond Engl* (2020) 395(10242):1973–87. doi: 10.1016/S0140-6736(20)31142-9

6. Talic S, Shah S, Wild H, Gasevic D, Maharaj A, Ademi Z, et al. Effectiveness of public health measures in reducing the incidence of covid-19, SARS-CoV-2 transmission, and covid-19 mortality: systematic review and meta-analysis. *BMJ*. (2021) 375:e068302. doi: 10.1136/bmj-2021-068302

7. Polack FP, Thomas SJ, Kitchin N, Absalon J, Gurtman A, Lockhart S, et al. Safety and efficacy of the BNT162b2 mRNA covid-19 vaccine. *N Engl J Med* (2020) 383(27):2603–15. doi: 10.1056/NEJMoa2034577

8. Munro APS, Janani L, Cornelius V, Aley PK, Babbage G, Baxter D, et al. Safety and immunogenicity of seven COVID-19 vaccines as a third dose (booster) following two doses of ChAdOx1 nCov-19 or BNT162b2 in the UK (COV-BOOST): a blinded, multicentre, randomised, controlled, phase 2 trial. *Lancet* (2021) 398(10318):2258–76. doi: 10.1016/S0140-6736(21)02717-3

9. Arbel R, Hammerman A, Sergienko R, Friger M, Peretz A, Netzer D, et al. BNT162b2 vaccine booster and mortality due to covid-19. *N Engl J Med* (2021) 385 (26):2413–20. doi: 10.1056/NEJMoa2115624

10. WHO Solidarity Trial Consortium, Pan H, Peto R, Henao-Restrepo AM, Preziosi MP, Sathiyamoorthy V, et al. Repurposed antiviral drugs for covid-19 - interim WHO solidarity trial results. *N Engl J Med* (2021) 384(6):497–511. doi: 10.1056/NEJMoa2023184

11. Torneri A, Libin P, Vanderlocht J, Vandamme AM, Neyts J, Hens N. A prospect on the use of antiviral drugs to control local outbreaks of COVID-19. *BMC Med* (2020) 18(1):191. doi: 10.1186/s12916-020-01636-4

12. Wang Y, Zhang D, Du G, Du R, Zhao J, Jin Y, et al. Remdesivir in adults with severe COVID-19: a randomised, double-blind, placebo-controlled, multicentre trial. *Lancet Lond Engl* (2020) 395(10236):1569–78. doi: 10.1016/S0140-6736(20)31022-9

13. Wen W, Chen C, Tang J, Wang C, Zhou M, Cheng Y, et al. Efficacy and safety of three new oral antiviral treatment (molnupiravir, fluvoxamine and paxlovid) for COVID-19:a meta-analysis. *Ann Med* (2022) 54(1):516–23. doi: 10.1080/07853890.2022.2034936

14. Hung IFN, Lung KC, Tso EYK, Liu R, Chung TWH, Chu MY, et al. Triple combination of interferon beta-1b, lopinavir-ritonavir, and ribavirin in the treatment of patients admitted to hospital with COVID-19: an open-label, randomised, phase 2 trial. *Lancet Lond Engl* (2020) 395(10238):1695–704. doi: 10.1016/S0140-6736(20)31042-4

15. Rahmani H, Davoudi-Monfared E, Nourian A, Khalili H, Hajizadeh N, Jalalabadi NZ, et al. Interferon β-1b in treatment of severe COVID-19: A randomized clinical trial. *Int Immunopharmacol nov* (2020) 88:106903. doi: 10.1016/j.intimp.2020.106903

16. Wang N, Zhan Y, Zhu L, Hou Z, Liu F, Song P, et al. Retrospective multicenter cohort study shows early interferon therapy is associated with favorable clinical responses in COVID-19 patients. *Cell Host Microbe* (2020) 28 (3):455–464.e2. doi: 10.1016/j.chom.2020.07.005

17. Zhou Q, Chen V, Shannon CP, Wei XS, Xiang X, Wang X, et al. Interferon-α2b treatment for COVID-19. *Front Immunol* (2020) 11:1061/full?utm_source=fweb&utm_medium=nblog&utm_campaign=ba-sci-fimmu-covid-interferon-treatment. doi: 10.3389/fimmu.2020.01061/full?utm_source=fweb&utm_medium=nblog&utm_campaign=ba-sci-fimmu-covid-interferon-treatment

18. Feld JJ, Kandel C, Biondi MJ, Kozak RA, Zahoor MA, Lemieux C, et al. Peginterferon lambda for the treatment of outpatients with COVID-19: a phase 2, placebo-controlled randomised trial. *Lancet Respir Med* (2021) 9(5):498–510. doi: 10.1016/S2213-2600(20)30566-X

19. Monk PD, Marsden RJ, Tear VJ, Brookes J, Batten TN, Mankowski M, et al. Safety and efficacy of inhaled nebulised interferon beta-1a (SNG001) for treatment of SARS-CoV-2 infection: a randomised, double-blind, placebo-controlled, phase 2 trial. *Lancet Respir Med* (2021) 9(2):196–206. doi: 10.1016/S2213-2600(20)30511-7

20. Pandit A, Bhalani N, Bhushan BLS, Koradia P, Gargiya S, Bhomia V, et al. Efficacy and safety of pegylated interferon alfa-2b in moderate COVID-19: A phase II, randomized, controlled, open-label study. *Int J Infect Dis* (2021) 105:516–21. doi: 10.1016/j.ijid.2021.03.015

21. Dougan M, Nirula A, Azizad M, Mocherla B, Gottlieb RL, Chen P, et al. Bamlanivimab plus etesevimab in mild or moderate covid-19. *N Engl J Med* (2021) 385(15):1382–92. doi: 10.1056/NEJMoa2102685

22. Klein EJ, Hardesty A, Vieira K, Farmakiotis D. Use of anti-spike monoclonal antibodies in kidney transplant recipients with COVID-19: Efficacy, ethnic and racial disparities. *Am J Transplant* (2021) 22(2):640–5. doi: 10.1111/ajt.16843

23. Gueguen J, Colosio C, Bello AD, Scemla A, N'Guyen Y, Rouzaud C, et al. Early administration of anti-SARS-CoV-2 monoclonal antibodies prevents severe covid-19 in kidney transplant patients. *Kidney Int Rep* (2022) 7(6):1241–7. doi: 10.1016/j.ekir.2022.03.020

24. Hadjadj J, Yatim N, Barnabei L, Corneau A, Boussier J, Smith N, et al. Impaired type I interferon activity and inflammatory responses in severe COVID-19 patients. *Science* (2020) 369(6504):718–24. doi: 10.1101/2020.04.19.20068015

25. Bastard P, Rosen LB, Zhang Q, Michailidis E, Hoffmann HH, Zhang Y, et al. Auto-antibodies against type I IFNs in patients with life-threatening COVID-19. *Science*. (2020) 370(6515):eabd4585. doi: 10.1126/science.abd4585

26. Zhang Q, Bastard P, Liu Z, Pen JL, Moncada-Velez M, Chen J, et al. Inborn errors of type I IFN immunity in patients with life-threatening COVID-19. *Science* (2020) 370(6517):eabd4570. doi: 10.1126/science.abd4570

27. Acharya D, Liu G, Gack MU. Dysregulation of type I interferon responses in COVID-19. *Nat Rev Immunol* (2020) 20(7):397–8. doi: 10.1038/s41577-020-0346-x

28. Andreakos E, Tsiodras S. COVID-19: lambda interferon against viral load and hyperinflammation. *EMBO Mol Med* (2020) 12(6):e12465. doi: 10.15252/emmm.202012465

29. Troya J, Bastard P, Planas-Serra L, Ryan P, Ruiz M, de Carranza M, et al. Neutralizing autoantibodies to type I IFNs in >10% of patients with severe COVID-19 pneumonia hospitalized in Madrid, Spain. *J Clin Immunol* (2021) 41(5):914–22. doi: 10.1007/s10875-022-01241-5

30. Lopez J, Mommert M, Mouton W, Pizzorno A, Brengel-Pesce K, Mezidi M, et al. Early nasal type I IFN immunity against SARS-CoV-2 is compromised in patients with autoantibodies against type I IFNs. *J Exp Med* (2021) 218(10): e20211211. doi: 10.1084/jem.20211211

31. Cheemarla NR, Watkins TA, Mihaylova VT, Wang B, Zhao D, Wang G, et al. Dynamic innate immune response determines susceptibility to SARS-CoV-2 infection and early replication kinetics. *J Exp Med* (2021) 218(8):e20210583. doi: 10.1084/jem.20210583

32. Hatton CF, Botting RA, Dueñas ME, Haq IJ, Verdon B, Thompson BJ, et al. Delayed induction of type I and III interferons mediates nasal epithelial cell permissiveness to SARS-CoV-2. *Nat Commun* (2021) 12:7092. doi: 10.1038/s41467-021-27318-0

33. Blanco-Melo D, Nilsson-Payant BE, Liu WC, Uhl S, Hoagland D, Møller R, et al. Imbalanced host response to SARS-CoV-2 drives development of COVID-19. *Cell* (2020) 181(5):1036–45. doi: 10.1016/j.cell.2020.04.026

34. Vanderheiden A, Ralfs P, Chirkova T, Upadhyay AA, Zimmerman MG, Bedoya S, et al. Type I and type III interferons restrict SARS-CoV-2 infection of human airway epithelial cultures. *J Virol* (2020) 94(19):e00985-20. doi: 10.1128/JVI.00985-20

35. Chen G, Wu D, Guo W, Cao Y, Huang D, Wang H, et al. Clinical and immunological features of severe and moderate coronavirus disease 2019. *J Clin Invest* (2020) 13(5):2620–9. doi: 10.1172/JCI137244

36. Cremoni M, Ruetsch C, Zorzi K, Fernandez C, Boyer-Suavet S, Benzaken S, et al. Humoral and cellular response of frontline health care workers infected by SARS-CoV-2 in nice, France: A prospective single-center cohort study. *Front Med* (2021) 7:608804/full. doi: 10.3389/fmed.2020.608804/full

37. Ruetsch C, Brglez V, Crémoni M, Zorzi K, Fernandez C, Boyer-Suavet S, et al. Functional exhaustion of type I and II interferons production in severe COVID-19 patients. *Front Med* (2021) 7:603961/full. doi: 10.3389/fmed.2020.603961/full

38. Rouchka EC, Chariker JH, Alejandro B, Adcock RS, Singhal R, Ramirez J, et al. Induction of interferon response by high viral loads at early stage infection may protect against severe outcomes in COVID-19 patients. *Sci Rep* (2021) 11 (1):15715 doi: 10.1038/s41598-021-95197-y.

39. Del Valle DM, Kim-Schulze S, Huang HH, Beckmann ND, Nirenberg S, Wang B, et al. An inflammatory cytokine signature predicts COVID-19 severity and survival. *Nat Med* (2020) 26(10):1636–43. doi: 10.1038/s41591-020-1051-9

40. Fajgenbaum DC, June CH, Cytokine Storm. Longo DL. Cytokine storm. *N Engl J Med* (2020) 383(23):2255–73. doi: 10.1056/NEJMra2026131

41. Diao B, Wang C, Tan Y, Chen X, Liu Y, Ning L, et al. Reduction and functional exhaustion of T cells in patients with coronavirus disease 2019 (COVID-19). *Front Immunol* (2020) 11:827/full. doi: 10.3389/fimmu.2020.00827/full

42. Chen X, Zhao B, Qu Y, Chen Y, Xiong J, Feng Y, et al. Detectable serum severe acute respiratory syndrome coronavirus 2 viral load (RNAemia) is closely correlated with drastically elevated interleukin 6 level in critically ill patients with coronavirus disease 2019. *Clin Infect Dis Off Publ Infect Dis Soc Am* (2020) 71 (8):1937–42. doi: 10.1093/cid/ciaa449

43. Miossec P. Understanding the cytokine storm during COVID-19: Contribution of preexisting chronic inflammation. *Eur J Rheumatol* (2020) 7 (Suppl 2):S97–8. doi: 10.5152/eurjrheum.2020.2062

44. Caron G, Duluc D, Frémaux I, Jeannin P, David C, Gascan H, et al. Direct stimulation of human T cells *via* TLR5 and TLR7/8: Flagellin and r-848 up-regulate proliferation and IFN-γ production by memory CD4+ T cells. *J Immunol* (2005) 175(3):1551–7. doi: 10.4049/jimmunol.175.3.1551

45. Smits ELJM, Ponsaerts P, Berneman ZN, Van Tendeloo VFI. The use of TLR7 and TLR8 ligands for the enhancement of cancer immunotherapy. *Oncologist* (2008) 13(8):859–75. doi: 10.1634/theoncologist.2008-0097

46. Guan Wj, Ni Z, Hu Y, Liang Wh, Ou Cq, He Jx, et al. Clinical characteristics of coronavirus disease 2019 in China. *N Engl J Med* (2020) 382(18):1708–20. doi: 10.1056/NEJMoa2002032

47. Zhou F, Yu T, Du R, Fan G, Liu Y, Liu Z, et al. Clinical course and risk factors for mortality of adult inpatients with COVID-19 in wuhan, China: a retrospective cohort study. *Lancet* (2020) 395(10229):1054–62. doi: 10.1016/S0140-6736(20)30566-3

48. Chen N, Zhou M, Dong X, Qu J, Gong F, Han Y, et al. Epidemiological and clinical characteristics of 99 cases of 2019 novel coronavirus pneumonia in wuhan, China: a descriptive study. *Lancet Lond Engl* (2020) 395(10223):507–13. doi: 10.1016/S0140-6736(20)30211-7

49. Scully EP, Haverfield J, Ursin RL, Tannenbaum C, Klein SL. Considering how biological sex impacts immune responses and COVID-19 outcomes. *Nat Rev Immunol* (2020) 20(7):442–7. doi: 10.1038/s41577-020-0348-8

50. Simonnet A, Chetboun M, Poissy J, Raverdy V, Noulette J, Duhamel A, et al. High prevalence of obesity in severe acute respiratory syndrome coronavirus-2 (SARS-CoV-2) requiring invasive mechanical ventilation. *Obesity*. (2020) 28 (7):1195–9. doi: 10.1002/oby.22831

51. Phetsouphanh C, Darley DR, Wilson DB, Howe A, Munier CML, Patel SK, et al. Immunological dysfunction persists for 8 months following initial mild-to-moderate SARS-CoV-2 infection. *Nat Immunol* (2022) 23(2):210–6. doi: 10.1038/s41590-021-01113-x

52. Boyer-Suavet S, Cremoni M, Dupeyrat T, Zorzi K, Brglez V, Benzaken S, et al. Functional immune assay using interferon-gamma could predict infectious events in end-stage kidney disease. *Clin Chim Acta* (2020) 502:287–92. doi: 10.1016/j.cca.2019.11.018

53. Sattler A, Angermair S, Stockmann H, Heim KM, Khadzhynov D, Treskatsch S, et al. SARS–CoV-2–specific T cell responses and correlations with COVID-19 patient predisposition. *J Clin Invest* 130(12):6477–89. doi: 10.1172/JCI140965

frontiers | Frontiers in Immunology

TYPE Original Research
PUBLISHED 27 September 2022
DOI 10.3389/fimmu.2022.999136

Check for updates

OPEN ACCESS

EDITED BY
E. Marion Schneider,
University of Ulm, Germany

REVIEWED BY
Miguel de Mulder Rougvie,
Cornell University, United States
Rakesh Kumar,
Askham Bryan College,
United Kingdom

*CORRESPONDENCE
Gemma Moncunill
gemma.moncunill@isglobal.org
Carlota Dobaño
carlota.dobano@isglobal.org

†These authors have contributed equally to this work and share first authorship

‡These authors have contributed equally to this work and share senior authorship

SPECIALTY SECTION
This article was submitted to Viral Immunology, a section of the journal Frontiers in Immunology

RECEIVED 20 July 2022
ACCEPTED 05 September 2022
PUBLISHED 27 September 2022

CITATION
Rubio R, Aguilar R, Bustamante M, Muñoz E, Vázquez-Santiago M, Santano R, Vidal M, Melero NR, Parras D, Serra P, Santamaria P, Carolis C, Izquierdo L, Gómez-Roig MD, Dobaño C, Moncunill G and Mazarico E (2022) Maternal and neonatal immune response to SARS-CoV-2, IgG transplacental transfer and cytokine profile.
Front. Immunol. 13:999136.
doi: 10.3389/fimmu.2022.999136

Maternal and neonatal immune response to SARS-CoV-2, IgG transplacental transfer and cytokine profile

Rocío Rubio[1†], Ruth Aguilar[1†], Mariona Bustamante[2], Erica Muñoz[3], Miquel Vázquez-Santiago[1], Rebeca Santano[1], Marta Vidal[1], Natalia Rodrigo Melero[4], Daniel Parras[5], Pau Serra[5], Pere Santamaria[5,6], Carlo Carolis[4], Luis Izquierdo[1,7], Maria Dolores Gómez-Roig[3], Carlota Dobaño[1,7*‡], Gemma Moncunill[1,7*‡] and Edurne Mazarico[3‡]

[1]Barcelona Institute for Global Health, Hospital Clínic - Universitat de Barcelona, Barcelona, Spain, [2]Barcelona Institute for Global Health, Spanish Consortium for Research on Epidemiology and Public Health (CIBERESP), Center for Genomic Regulation (CRG), Barcelona Institute of Science and Technology (BIST), Barcelona, Spain, [3]Barcelona Center for Maternal-Fetal and Neonatal Medicine (BCNatal), Hospital Sant Joan de Déu and Hospital Clínic, Institut de Recerca Sant Joan de Déu (IR-SJD), Barcelona, Spain, [4]Biomolecular screening and Protein Technologies Unit, Centre for Genomic Regulation (CRG), The Barcelona Institute of Science and Technology, Barcelona, Spain, [5]Pathogenesis and treatment of autoimmunity department, Institut D'Investigacions Biomèdiques August Pi i Sunyer (IDIBAPS), Barcelona, Spain, [6]Julia McFarlane Diabetes Research Centre (JMDRC), and Department of Microbiology, Immunology and Infectious Diseases, Snyder Institute for Chronic Diseases, Cumming School of Medicine, University of Calgary, Calgary, AB, Canada, [7]Barcelona Institute for Global Health, CIBER de Enfermedades Infecciosas (CIBERINFEC), Barcelona, Spain

SARS-CoV-2 infected pregnant women are at increased risk of severe COVID-19 than non-pregnant women and have a higher risk of adverse pregnancy outcomes like intrauterine/fetal distress and preterm birth. However, little is known about the impact of SARS-CoV-2 infection on maternal and neonatal immunological profiles. In this study, we investigated the inflammatory and humoral responses to SARS-CoV-2 in maternal and cord blood paired samples. Thirty-six pregnant women were recruited at delivery at Hospital Sant Joan de Déu, Barcelona, Spain, between April-August 2020, before having COVID-19 available vaccines. Maternal and pregnancy variables, as well as perinatal outcomes, were recorded in questionnaires. Nasopharyngeal swabs and maternal and cord blood samples were collected for SARS-CoV-2 detection by rRT-PCR and serology, respectively. We measured IgM, IgG and IgA levels to 6 SARS-CoV-2 antigens (spike [S], S1, S2, receptor-binding domain [RBD], nucleocapsid [N] full-length and C-terminus), IgG to N from 4 human coronaviruses (OC43, HKU1, 229E and NL63), and the concentrations of 30 cytokines, chemokines and growth factors by Luminex. Mothers were classified as infected or non-infected based on the rRT-PCR and serology results. Sixty-four % of pregnant women were infected with SARS-CoV-2 (positive by rRT-PCR during the third trimester and/or serology just after delivery). None of the

newborns tested positive for rRT-PCR. SARS-CoV-2 infected mothers had increased levels of virus-specific antibodies and several cytokines. Those with symptoms had higher cytokine levels. IFN-α was increased in cord blood from infected mothers, and in cord blood of symptomatic mothers, EGF, FGF, IL-17 and IL-15 were increased, whereas RANTES was decreased. Maternal IgG and cytokine levels showed positive correlations with their counterparts in cord blood. rRT-PCR positive mothers showed lower transfer of SARS-CoV-2-specific IgGs, with a stronger effect when infection was closer to delivery. SARS-CoV-2 infected mothers carrying a male fetus had higher antibody levels and higher EGF, IL-15 and IL-7 concentrations. Our results show that SARS-CoV-2 infection during the third trimester of pregnancy induces a robust antibody and cytokine response at delivery and causes a significant reduction of the SARS-CoV-2-specific IgGs transplacental transfer, with a stronger negative effect when the infection is closer to delivery.

KEYWORDS

SARS-CoV-2, maternal and neonatal immunity, antibodies, cytokines, transplacental transfer

Introduction

Coronavirus 2019 (COVID-19) pandemic caused by the severe acute respiratory syndrome coronavirus 2 (SARS-CoV-2), has resulted in more than six million deaths and has infected over 500 million people as of July 19, 2022 (1). The most severe outcomes of COVID-19 have been documented in geriatric individuals and pregnant women with chronic diseases, including hypertension, diabetes, and cardiopulmonary problems, or with some other respiratory viral infections (2).

The immune status of pregnant women adapts to ensure tolerance to the fetus by changing the cellular composition and the functions of immune cells. T cell-mediated immunity and humoral responses are suppressed particularly during the third trimester (3), production of IL-4 and IL-10 are increased while IL-2 and IFN-γ are reduced in peripheral blood mononuclear cells (4, 5). As a consequence, pregnant women are at increased risk of morbidity and mortality from respiratory viral infections (6–9). Several studies show that pregnant women with COVID-19 are more likely to be hospitalized and have increased rates of ICU admissions and mechanical ventilation compared with non-pregnant women with COVID-19, resulting in a higher risk of mortality (10–15).

The maternal inflammatory response induced by SARS-CoV-2 infection may also have deleterious effects on the offspring. Although vertical transmission has been hardly observed in SARS-CoV-2 to date (16), with a rate of around 3% (17), pregnant women with COVID-19 are at increased risk of adverse pregnancy outcomes like intrauterine/fetal distress and preterm birth (11, 18). The pro-inflammatory cytokines induced during infection may enter the amniotic cavity and interfere with normal fetal development (19–21) causing short- and long-term damage (22–24) such as miscarriage, restricted fetal growth, or still-birth (25) and neurodevelopmental affection as seen in other viral infections ranging from autism spectrum disorder, attention deficit hyperactivity disorder, and cognitive dysfunction, to anxiety, depression, and schizophrenia (26). Recent studies evidence that SARS-CoV-2 infection during pregnancy results in offspring neurodevelopmental morbidity (26). Maternal infection may also alter the ability of antibodies to transfer across the placenta as has been shown for other infections like HIV (27), malaria (28), dengue (29) or Zika (30) and recently in COVID-19 (31–34). Vaccination of pregnant women with an mRNA COVID-19 vaccine resulted in a significantly greater antibody persistence in infants than infection at 20 to 32 weeks gestation. At 6 months, 57% of infants born to vaccinated mothers had detectable antibodies compared with 8% of infants born to infected mothers (35).

However, our knowledge is limited regarding the immune response in pregnant women infected by SARS-CoV-2 and the immunopathological mechanisms in maternal and neonatal outcomes. Studying the maternal immune response after infection and the *in-utero* antibody transfer can help understand neonatal vulnerability to infection and protection.

In this study, we investigated the inflammatory and humoral responses to SARS-CoV-2 in maternal and cord blood samples collected from pregnant women who had tested positive during the third trimester of pregnancy, and their neonates, by measuring antibody levels against SARS-CoV-2 antigens, their IgG transplacental transfer, and cytokine concentrations.

10.3389/fimmu.2022.999136

Materials and methods

Study design, participants and sample collection

This is a prospective case-control study in which pregnant women were recruited at delivery at Hospital Sant Joan de Déu (HSJD), Barcelona (Spain) between April and August 2020, before having COVID-19 available vaccines. Women approached were those visited at the hospital, or who arrived in labor or with a programmed induction of labor. To capture the maximum number of SARS-CoV-2 infected mothers inclusion criteria were: i) women with a positive SARS-CoV-2 rRT-PCR; and/or ii) symptoms consistent with SARS-CoV-2 infection (high temperature, fatigue, muscular pain, diarrhea, taste and smell loss, cough, difficulty breathing, pneumonia); and/or iii) direct contact (more than 15 min and less than 2 m distance) with someone diagnosed with COVID-19 by rRT-PCR during the third trimester. Pregnant women who did not meet any of the inclusion criteria were recruited for the control group. Women with multiple gestations, aged <18 or >45 years, with a fetus affected by abnormal karyotype, structural abnormalities, congenital infections, or who did not communicate in Catalan, Spanish or English, were excluded from the study. Thirty-six mother-newborn pairs were enrolled in the study. The study protocol was approved by the Ethics Committee for Clinical Research of the HSJD with the approval code number PIC 48-20, and informed consent was obtained from each participant.

Maternal (age, parity, ethnic group and pathologies) and pregnancy (high blood pressure, gestational diabetes, fetal growth retardation, preterm delivery or other pregnancy complications) variables as well as perinatal outcomes (type of delivery or any newborn complications), were recorded in a questionnaire or obtained from medical records.

Maternal and neonatal nasopharyngeal swabs, and maternal peripheral and cord blood samples, were collected just after delivery. Nasopharyngeal swabs were used for SARS-CoV-2 detection by rRT-PCR. Blood samples were processed to isolate serum that was stored at -80˚C until the analysis of antibody levels and cytokines. Data from the rRT-PCR and serology tests performed with the samples collected just after delivery was used to reallocate mothers to the case (infected) or control (not infected) groups, for the subsequent analyses.

Antibody luminex assays

IgM, IgG and IgA antibodies to six SARS-CoV-2 antigens were measured in mother and cord serum samples by Luminex as previously described (36). SARS-CoV-2 antigens included in the panel were: the spike full-length protein (S), its subunits S1 and S2, the receptor-binding domain (RBD), the nucleocapsid full-length protein (N FL) and its C-terminus region (N CT) (37). The full-length N proteins from the four HuCoVs OC43, HKU1, 229E and NL63 (37) were also included in the IgG panel. A positive control curve and four blanks were included in each assay plate for QA/QC purposes, and 129 pre-pandemic samples as negative controls to estimate the seropositivity cutoffs. To quantify IgM, test samples and controls were pre-treated with anti-human IgG (Gullsorb) to avoid IgG interferences. Paired mother-cord samples were tested in the same assay plate. At least 50 microspheres per analyte/well were acquired, and the median fluorescence intensity (MFI) was reported for each analyte. Assay positivity cutoffs specific for each isotype and antigen were calculated as 10 to the mean plus 3 standard deviations (SD) of $\log_{10}$-transformed MFI of the 129 pre-pandemic controls. A more detailed description of the antigens and the assay are included in the Supplementary Material.

Cytokine luminex assay

The Cytokine Human Magnetic 30-Plex Panel from Invitrogen™ was used to measure the concentrations of 30 analytes in serum from mothers and cord blood samples. Samples were tested using half of the reagents following a modification of the manufacturer's protocol (38–40). Paired mother-cord samples were tested in the same assay plate. Each plate included 16 serial dilutions (2-fold) of a standard curve, two blank controls and three positive controls of high, medium and low concentrations for QA/QC purposes. Samples were acquired on a Luminex® 100/200. The interpolation of concentrations and imputation of missing data was done using the R package drLumi (41). A more detailed description of the analytes and the assay are included in the Supplementary Material.

Groups definitions and statistical analysis

SARS-CoV-2 infected mother groups were reallocated using serological data from the antibody Luminex assay. Thus, mothers were classified as infected when having a SARS-CoV-2 positive rRT-PCR during the third trimester and/or being seropositive just after delivery, and non-infected when not having reported any SARS-CoV-2 rRT-PCR positive during the third trimester and being seronegative just after delivery. Pregnant women were considered seropositive if positive for one or more isotype-antigen pairs. Time since the infection was estimated as the time since positive rRT-PCR or symptoms onset to delivery. This variable was not available for three mothers who were seropositive just after delivery but did not report any positive rRT-PCR or symptoms.

A comparison of clinical and demographic characteristics between infected and non-infected mothers was performed by the Wilcoxon-rank-sum-test for age (continuous) and by Fisher's exact

test for the rest of the variables (categorical). Antibody and cytokine data were log_{10}-transformed to perform the statistical analysis and non-parametric tests were used. The IgG transplacental transfer was calculated as the log_{10}-transformed ratio of antibody levels (MFI) in cord vs. mother in paired samples. Comparisons of antibody and cytokine levels between the study groups were performed by the Wilcoxon-rank-sum-test. Correlations between analytes were assessed with Spearman's rank correlation coefficient ρ (rho) and p-values were computed *via* the asymptotic t approximation. Univariable linear regression models were performed to assess the associations between IgG transplacental transfer (ratio MFI Cord/MFI Mother) as the outcome variable and SARS-CoV-2 infection, infection during the third trimester or just after delivery, time since infection, gestational age, and birth weight as predictor variables. Nominal p-values (not adjusted for multiple testing due to small sample size) of <0.05 were considered statistically significant. All data processing and statistical analyses were performed using the R software version 4.1.1.

Results

Pregnancy outcomes in SARS-CoV-2 infected mothers

Our study included 36 pregnant women, 23 SARS-CoV-2 infected and 13 non-infected. No differences were observed between these two groups regarding parity, maternal age at delivery, ethnicity or pathologies (Table 1). Among the non-infected women, two reported COVID-19 compatible symptoms probably from another viral infection. Although having symptoms consistent with COVID-19 was an inclusion criterion for those infected or possibly infected with SARS-CoV-2, we included these two cases in the non-infected group because they were neither rRT-PCR positive nor seropositive. Thirty-nine % (9/23) of the infected women showed pregnancy complications vs. 15% (2/13) of the non-infected, although differences were not statistically significant (p=0.086). Pregnancy complications were of different etiologies

TABLE 1 Characteristics of the study population.

Variable N (%)		All 36	SARS-CoV-2 Non-infected 13 (36.1%)	SARS-CoV-2 Infected 23 (63.9%)	p-value
Maternal age at delivery (median (IQR))		34 (7.5)	33 (5.5)	35 (10)	0.960
Ethnic group N					
African		3 (8.3%)	0	3 (13.1%)	0.473
European		23 (63.9%)	10 (76.9%)	13 (56.5%)	
South American		8 (22.2%)	3 (23.1%)	5 (21.7%)	
South Asiatic		2 (5.6%)	0	2 (8.7%)	
Any maternal pathology*	yes	7 (19.4%)	3 (23.1%)	4 (17.4%)	0.686
Parity: Nulliparous		21 (58.3%)	8 (61.5%)	13 (56.5%)	0.385
COVID-19 compatible symptoms					
asymptomatic		23 (63.8%)	11 (84.6%)	12 (52.2%)	0.054
mild		10 (27.7%)	2 (15.5%)	8 (34.8%)	
moderate		1 (2.7%)	0	1 (4.3%)	
severe		2 (5.5%)	0	2 (8.7%)	
Pregnancy complications†	yes	11 (30.6%)	2 (15.4%)	9 (39.1%)	0.086
High blood pressure	yes	1 (2.8%)	0	1 (4.3%)	0.639
Gestational diabetes	yes	4 (11.1%)	1 (7.7%)	3 (13.1%)	0.541
Other pregnancy complications‡	yes	6 (16.7%)	0	6 (26.1%)	0.052
Delivery type					
cesarean		15 (41.6%)	4 (30.8%)	11 (47.8%)	0.261
vaginal		21 (58.4%)	9 (69.2%)	12 (52.2%)	
Newborn complications§	yes	5 (13.9%)	0	5 (21.7%)	0.089
Preterm delivery	yes	4 (11.1%)	1 (7.7%)	3 (13.1%)	0.541
Fetal growth retardation	yes	3 (8.3%)	1 (7.7%)	2 (8.7%)	0.708
Low birth weight	yes	6 (16.7%)	2 (15.4%)	4 (17.4%)	0.631
Child SARS-CoV-2 rRT-PCR	positive	0	0	0	1

*N = 3 hypothyroidism; 1 hyperthyroidism; 1 celiac disease; 1 asthma; 1 hypothyroidism and eating disorder.
†N = 1 high blood pressure; 4 gestational diabetes; 3 fetal growth retardations; 4 preterm deliveries.
‡N = 2 gestational cholestasis; 2 membranes rupture 31.5 weeks and 22 weeks; 1 carbohydrates intolerance; 1 genital herpes.
§N = 3 premature; 1 hyperbilirubinemia phototherapy; 1 lymphopenia.
For numerical variables, the median and interquartile range , in brackets, are given. For the categorical variables, the number of individuals for each group and percentages, in parentheses, are given. For the age variable, the Wilcoxon-rank-sum-test was used to compare differences between median values. For the categorical variables, the Fisher exact test was used.

without a predominant one (Table 1). Twenty-two % (5/23) of the newborns from infected women had complications vs. none of the 13 born from non-infected mothers, although differences were not statistically significant (p=0.089). Newborn complications consisted of three premature, one with hyperbilirubinemia and one with lymphopenia. None of the newborns tested positive for SARS-CoV-2 rRT-PCR just after delivery, and neither showed detectable levels of IgM or IgA in cord blood, which are indicative of fetal infection (data not shown).

Antibody response in SARS-CoV-2 infected mothers

From the infected group (N=23), 11 were rRT-PCR positive in the third trimester and seropositive just after delivery; eight did not report any rRT-PCR positive during pregnancy but were seropositive just after delivery (5 reported symptoms during the third trimester and 3 were asymptomatic), and 4 were rRT-PCR positive but seronegative just after delivery, denoting recent infections or deficiency in producing antibodies. Anti-SARS-CoV-2 antibody levels did not differ between infected rRT-PCR positive (N=15) and negative (N=8) mothers during the third trimester (Figure 1). Infected mothers showed higher antibody levels compared to non-infected mothers (p≤0.01) regardless of the rRT-PCR status, except for IgM against N antigen (Figure 1). Among the infected mothers, those with symptoms showed an overall trend of higher antibody levels compared to asymptomatic mothers although not statistically significant except for IgA to RBD (p=0.049) (Figure S1).

Effect of time since infection on SARS-CoV-2 antibody levels

We evaluated the association of antibody levels with time since infection in paired infected mother-cord samples. Anti-SARS-CoV-2 IgG levels in cord blood showed moderate positive associations with time since infection (ρ=0.3-0.54) for all antigens, being lower when the infection was closer to delivery, as expected, and the associations were statistically significant for S, S1 and RBD (Figure 2). However, only IgG levels to S1 and RBD showed moderate positive associations with time since infection in maternal samples (ρ=0.3) and were not statistically significant (Figure 2).

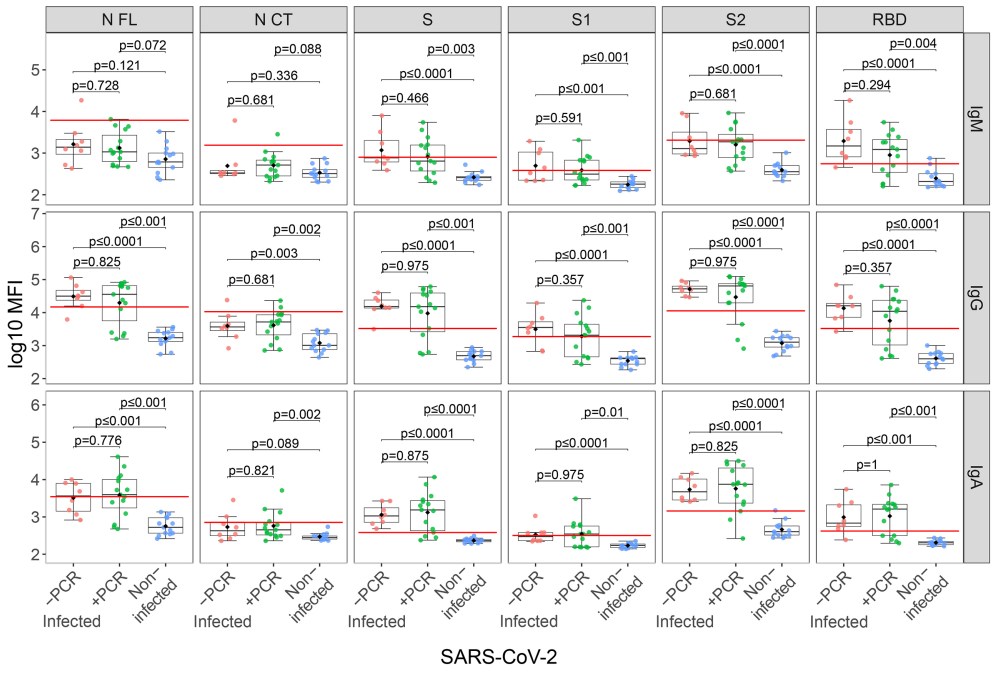

FIGURE 1
Anti-SARS-CoV-2 antibody levels in mothers stratified by infection and rRT-PCR (PCR) results. Comparison of anti-SARS-CoV-2 IgM, IgG and IgA serum levels (log_{10} median fluorescence intensity, MFI) between infected mothers who tested COVID-19 positive by rRT-PCR during the third trimester (+PCR, N=15, in green), those that tested negative (-PCR, N=8, in red) and non-infected mothers (N=13, in blue). The boxplots represent the median (bold line), the mean (black diamond), the 1st and 3rd quartiles (box) and the largest and smallest values within 1.5 times the inter-quartile range (whiskers). Groups were compared by the Wilcoxon-rank-sum-test. The red line indicates the seropositivity cutoff calculated as 10 to the mean plus 3 standard deviations (SD) of log_{10}-transformed MFI of 129 pre-pandemic controls. Antigens: nucleocapsid full-length (N FL) and C-terminus (N CT), spike full-length (S), S1 and S2 subunits, and receptor-binding domain (RBD).

IgG transplacental transfer in SARS-CoV-2 infected mothers

Among infected mothers, antigen-specific IgG levels in serum showed moderate to strong positive correlations with levels in cord blood (ρ=0.54-0.8, p<0.05, Figure 3A). Contrary to what was observed in mother samples, IgG levels to S antigens in cord blood showed significant differences depending on the the maternal rRT-PCR status during the third trimester (p<0.05), being higher in the infected but rRT-PCR negative (Figure 3B), suggesting a negative effect of infection during the third trimester in the IgG transfer. To confirm this observation, we assessed the effect of the SARS-CoV-2 infection on the IgG transplacental transfer by linear regression models in paired seropositive infected mothers and cord blood. The rRT-PCR positive mothers just after the delivery or during the third trimester transferred fewer anti-SARS-CoV-2 IgGs to cord blood compared to rRT-PCR negative, except for N FL antigen when tested positive during the third trimester (Figures 4A and S2A, p<0.01). Then, we investigated if this IgG transplacental transfer reduction was extensible to HuCoVs antigens by linear regression models in all study population. Being infected with SARS-CoV-2 reduced the transference of IgG to 229E N antigen (p<0.05) and having a positive rRT-PCR, either during the third trimester or just after delivery, to OC43 N antigen (p<0.05) (Figures 4B and S2B). This suggests a most noticeable negative effect for anti-SARS-CoV-2 antibodies. Gestational age and birth weight, two variables strongly associated with antibody transfer, did not affect the SARS-CoV-2 IgG transplacental transfer in seropositive infected mothers (Figure S3).

According to the lower anti-SARS-CoV-2 IgG levels observed in cord blood in recent compared to past infections (Figure 2), there was a positive effect of time since infection on anti-SARS-CoV-2 IgG transplacental transfer (Figures 4A and S4). This observation together with the lack of correlation of maternal antibody levels with time since infection, confirms the impact of SARS-CoV-2 infection on IgG transplacental transfer and suggests a stronger negative effect when the infection is closer to delivery. Time since infection did not affect the HuCoVs IgG transference (Figure 4B).

Fetus sex effect on SARS-CoV-2 antibody response

SARS-CoV-2 infected mothers with a male fetus had higher SARS-CoV-2 antibody levels in serum compared to those with a female fetus (Figure 5A), specifically IgM against S, S1 and RBD (p<0.05); IgA against N antigens and S1 (p<0.05); and IgG to all antigens (p<0.05). However, no differences were found in cord blood samples (data not shown). Also, no differences were found by fetus sex in antibody levels against the N antigen of the HuCoVs, neither in the mother nor cord blood (data not shown). Interestingly, there was a trend of lower anti-SARS-CoV-2 IgG transplacental transfer in mothers carrying a male fetus compared to mothers carrying a female (Figure 5B), but not statistically significant. The same trend, not statistically significant, by fetus sex was observed for the transfer of IgG to N of the HuCoVs in SARS-CoV-2 infected mothers (Figure S5).

Cytokine profile in SARS-CoV-2 infected mothers

SARS-CoV-2 infected mothers had higher serum concentrations of the growth factor EGF, the Th2 cytokine IL-13, the pro-inflammatory marker IL-2R, the anti-inflammatory cytokine IL-17, and the chemokines IP-10, MIG and MIP-1β (p<0.05) compared to non-infected mothers (Figures 6A and S6). Those with symptoms at any time during the third trimester showed higher levels of growth factors EGF, G-CSF and HGF,

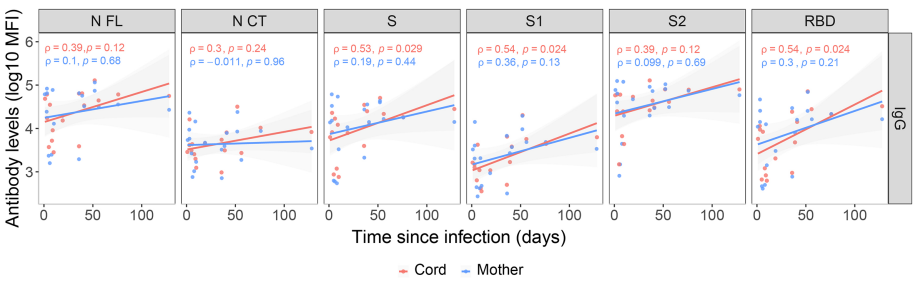

FIGURE 2
Correlations between anti-SARS-CoV-2 IgG levels and time since infection. Correlations of anti-SARS-CoV-2 IgG levels (log_{10} median fluorescence intensity, MFI) in infected mothers (blue) and cord blood (red) with time since infection (days since positive rRT-PCR or symptoms onset), represented as a linear model with standard error as confidence interval (shaded areas) and assessed by the Spearman test, showing the rho (ρ) and p-values. Only data from SARS-CoV-2 infected mothers and their newborns are included (N=20). Antigens: nucleocapsid full-length (N FL) and C-terminus (N CT), spike full-length (S), S1 and S2 subunits, and receptor-binding domain (RBD).

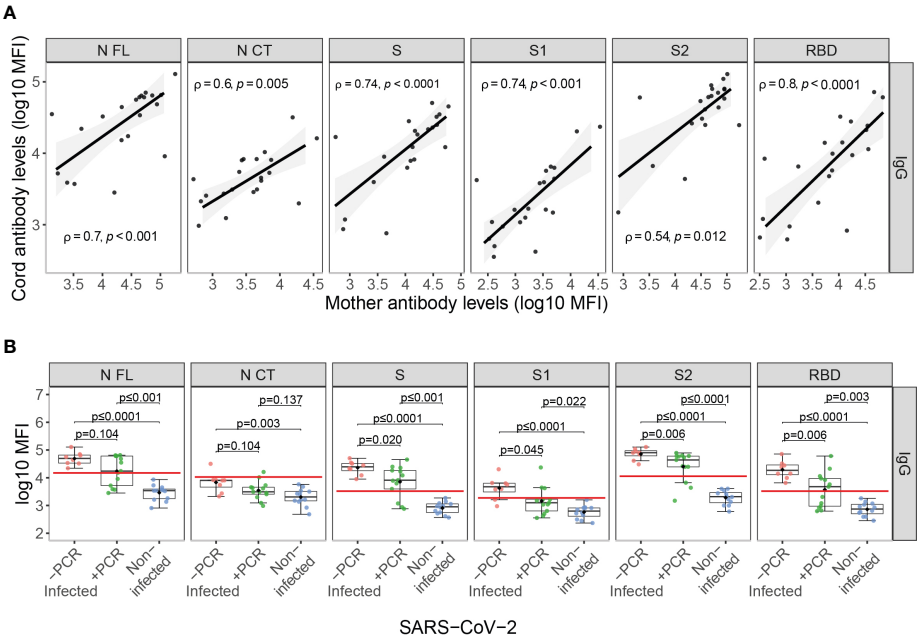

FIGURE 3
Anti-SARS-CoV-2 antibody levels in cord blood. **(A)** Correlations of anti-SARS-CoV-2 IgG levels (log_{10} median fluorescence intensity, MFI) in paired infected mothers and cord blood samples represented as a linear model with standard error as confidence interval (shaded areas) and assessed by the Spearman test, showing the rho (ρ) and p-values. **(B)** Comparison of anti-SARS-CoV-2 IgG cord blood levels (log_{10} MFI) between infected mothers who tested COVID-19 rRT-PCR positive (+PCR, N=13, in green) during the third trimester, those that tested rRT-PCR negative (-PCR, N=8, in red) and from non-infected mothers (N=12, in blue). The boxplots represent the median (bold line), the mean (black diamond), the 1st and 3rd quartiles (box) and the largest and smallest values within 1.5 times the inter-quartile range (whiskers). Groups were compared by the Wilcoxon-rank-sum-test. The red line indicates the seropositivity cutoff calculated as 10 to the mean plus 3 standard deviations (SD) of log_{10}-transformed MFI of 129 pre-pandemic controls. Antigens: nucleocapsid full-length (N FL) and C-terminus (N CT), spike full-length (S), S1 and S2 subunits, and receptor-binding domain (RBD).

the pro-inflammatory cytokines IL-1β and IL-6, and the chemokines IP-10, MCP-1 and MIG ($p<0.05$) compared to the asymptomatic ones (Figures 6B and S7); and when the symptoms were at delivery, FGF, the anti-inflammatory cytokine IL-15, the Th1 markers IL-2, IL-2R, MIP-1α, MIP-1β and the pro-inflammatory cytokine TNF-α ($p<0.05$) were also increased (Figures 6C and S8).

Newborns from infected mothers showed higher concentrations of the pro-inflammatory cytokine IFN-α ($p=0.044$) in cord blood than those from non-infected mothers (Figures 7A and S9). Newborns from mothers with symptoms at any time during the third trimester presented higher levels of EGF, FGF and IL-17 ($p<0.05$) in cord blood compared to those from asymptomatic ones (Figures 7B and S10); and when symptoms were at delivery IL-15 was also increased while the chemokine RANTES was decreased ($p<0.05$) (Figures 7C and S11). Infected mothers showed positive significant correlations for EGF, HGF, IL-13, IL-17, IL-1β, IL-1RA, IL-5, IL-7 and IL-8, and MIP-1β ($ρ=0.44$-0.77, $p<0.05$) concentrations in serum and cord blood (Figures 8 and S12).

Fetus sex effect on SARS-CoV-2 cytokine response

SARS-CoV-2 infected women carrying a male fetus had higher concentrations of EGF, IL-15 and the regulatory cytokine IL-7 in serum compared to women carrying a female fetus (Figure S13, $p<0.05$). There were no differences in any of the analytes tested by the sex of the fetus in cord samples (data not shown).

Discussion

The SARS-CoV-2 infection during the third trimester induced a robust antibody and cytokine response detected at delivery in the mother and cord blood. Symptomatic mothers induced higher levels of cytokines and SARS-CoV-2 specific antibodies than asymptomatic women, and maternal levels correlated with cord blood levels. However, the infection during the third trimester caused an impairment of the IgG

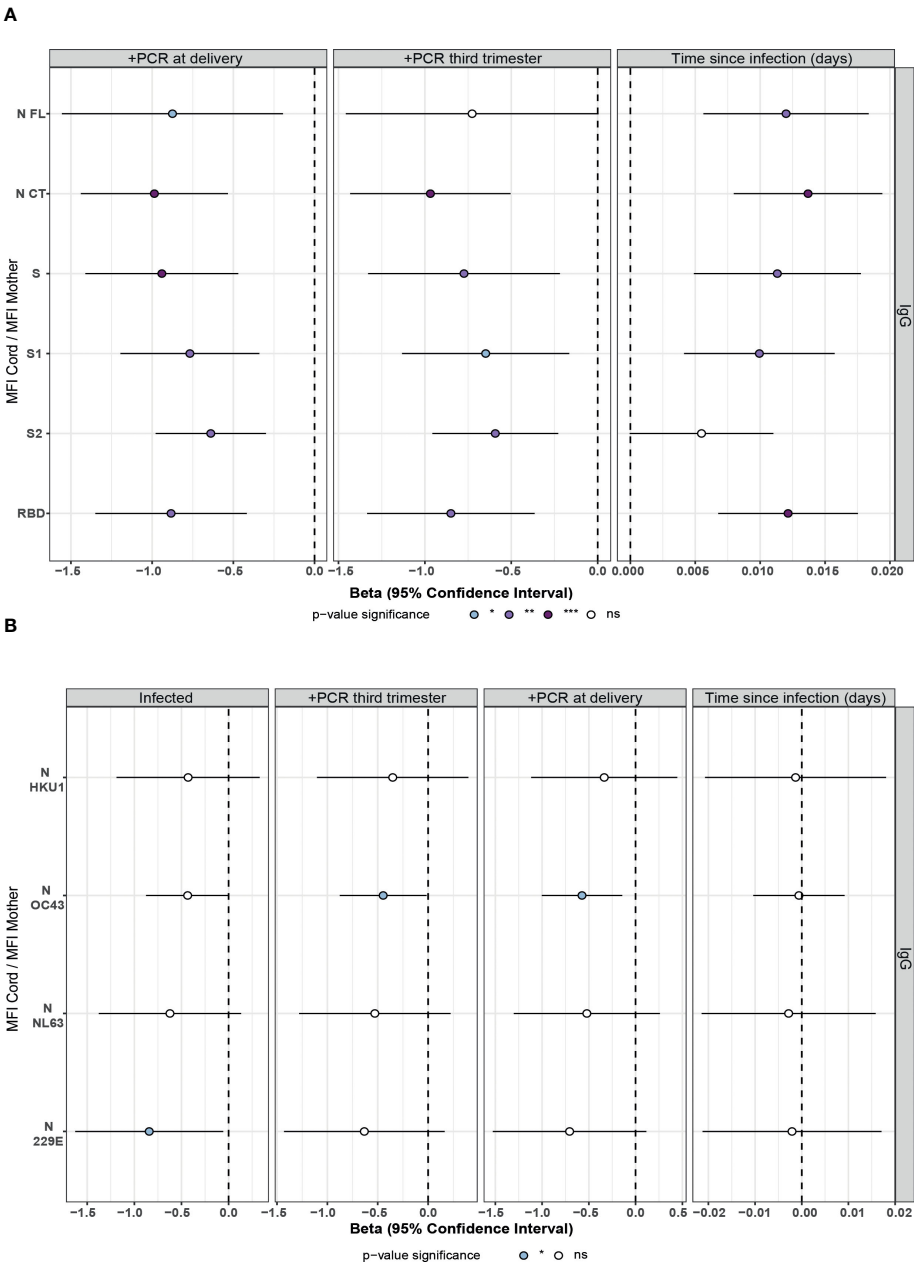

FIGURE 4
Association of SARS-CoV-2 infection and time since infection on IgG transfer from mother to the newborn in univariable linear regression models. Forest plots show the effect of SARS-CoV-2 infection, positive rRT-PCR (+PCR) during the third trimester or at delivery, and the time since infection (days since positive rRT-PCR or symptoms onset) on IgG transfer from mother to the newborn (MFI Cord/MFI Mother) for **(A)** SARS-CoV-2 antigens in seropositive paired infected mothers and cord blood and **(B)** HuCoVs N proteins in all study population. Univariable linear regression models were fitted to calculate the betas (dots) and 95% confidence intervals (CI) (lines). The color of the dots represents the p-value significance, where *p-value ≤ 0.05, **p-value ≤ 0.01 and ***p-value ≤ 0.001, ns, not significant. Antigens: nucleocapsid full-length (N FL) and C-terminus (N CT), spike full-length (S), S1 and S2 subunits, and receptor-binding domain (RBD).

transplacental transfer that was stronger when the infection was closer to delivery. Furthermore, we observed that mothers carrying a male fetus induced higher anti-SARS-CoV-2 antibody levels and had higher EGF, IL-15 and IL-7 concentrations than mothers carrying a female fetus.

Among the infected pregnant women, those with symptoms had higher anti-SARS-CoV-2 antibody levels, especially IgA and IgM to RBD. Higher RBD-IgA levels in symptomatic infections in non-pregnant adults have been previously reported (42–44). Two recent studies have also reported higher RBD-IgG levels at

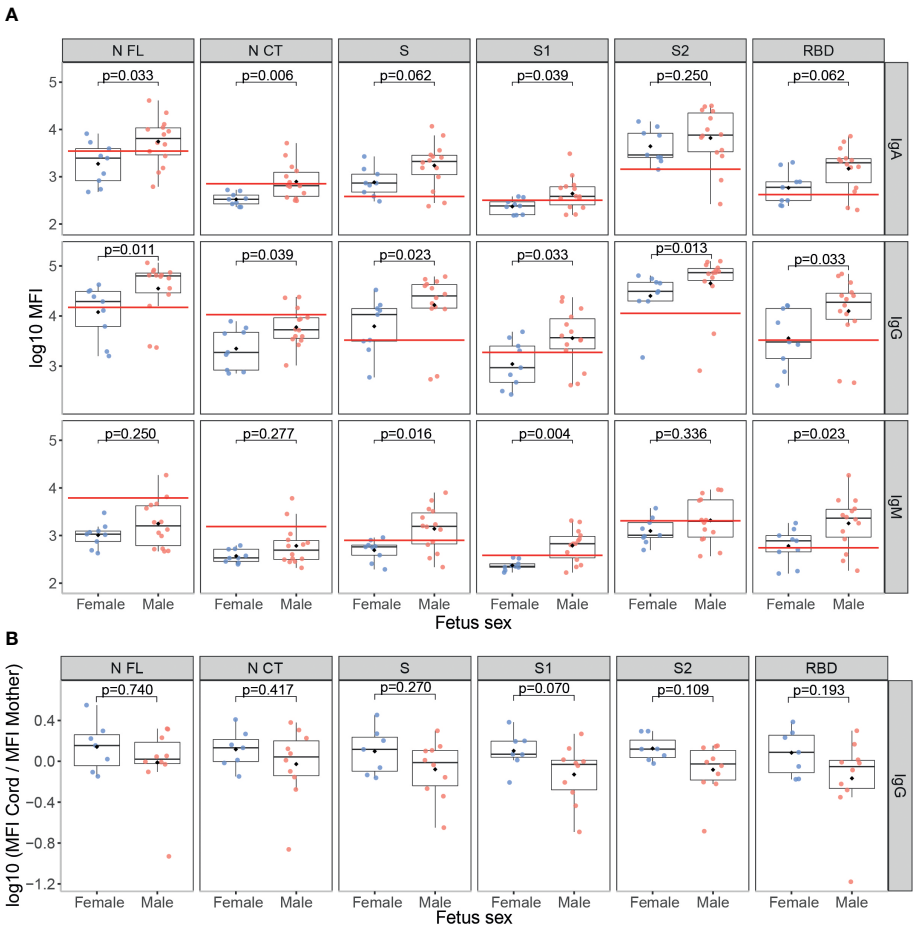

FIGURE 5
Anti-SARS-CoV-2 antibody levels by fetus sex. **(A)** Comparison of anti-SARS-CoV-2 levels (log_{10} median fluorescence intensity, MFI) in infected mothers between those who had a male fetus (N=14, in red) and those who had a female fetus (N=9, in blue). **(B)** Comparison of the ratios of IgG levels (log_{10} MFI) to SARS-CoV-2 antigens in cord blood vs. mother peripheral blood from seropositive mothers who had a male fetus (N=10, in red) and those that had a female fetus (N=7, in blue). The boxplots represent the median (bold line), the mean (black diamond), the 1st and 3rd quartiles (box) and the largest and smallest values within 1.5 times the inter-quartile range (whiskers). Groups were compared by the Wilcoxon-rank-sum-test. The red line indicates the seropositivity cutoff calculated as 10 to the mean plus 3 standard deviations (SD) of log_{10}-transformed MFI of 129 pre-pandemic controls. Antigens: nucleocapsid full-length (N FL) and C-terminus (N CT), spike full-length (S), S1 and S2 subunits, and receptor-binding domain (RBD).

delivery in pregnant patients with symptomatic infections compared to the asymptomatic ones (31, 45), and it probably impacts the passive transfer of protective IgA through breast milk.

SARS-CoV-2 infected mothers with symptoms presented increased levels of several cytokines compared to the asymptomatic ones, and cytokine serum levels correlated with cord blood levels. In a SARS-CoV-2 infection, inflammatory cytokine storms are an important cause of severe manifestations of COVID-19. This is critically important in the case of pregnant women because of the consequences for the fetus. We observed higher levels of IL-1β, IL-6 and TNF in symptomatic mothers, and of IFN-α in cord blood from SARS-CoV-2 infected mothers. Elevated levels of these cytokines may affect fetal development, increase the risk of neurological diseases, and lead to abortion in the first and second trimesters and preterm birth in the third trimester (46). We also observed increased levels of IL-17 in cord blood from infected symptomatic mothers. High levels of IL-17 can lead to cortical dysplasia and behavioral abnormalities in fetuses and increase the probability that offspring develop mental illness in adulthood (46). However, cytokine data have to be considered with caution due to the dramatic fluctuation of cytokines intrapartum. Normal delivery is pro-inflammatory and women with pregnancy complications, such as preterm delivery or fetal growth retardation, have an ever more pro-inflammatory profile (47), making it difficult to disentangle what is due to COVID-19 or to inflammatory changes in the labor process.

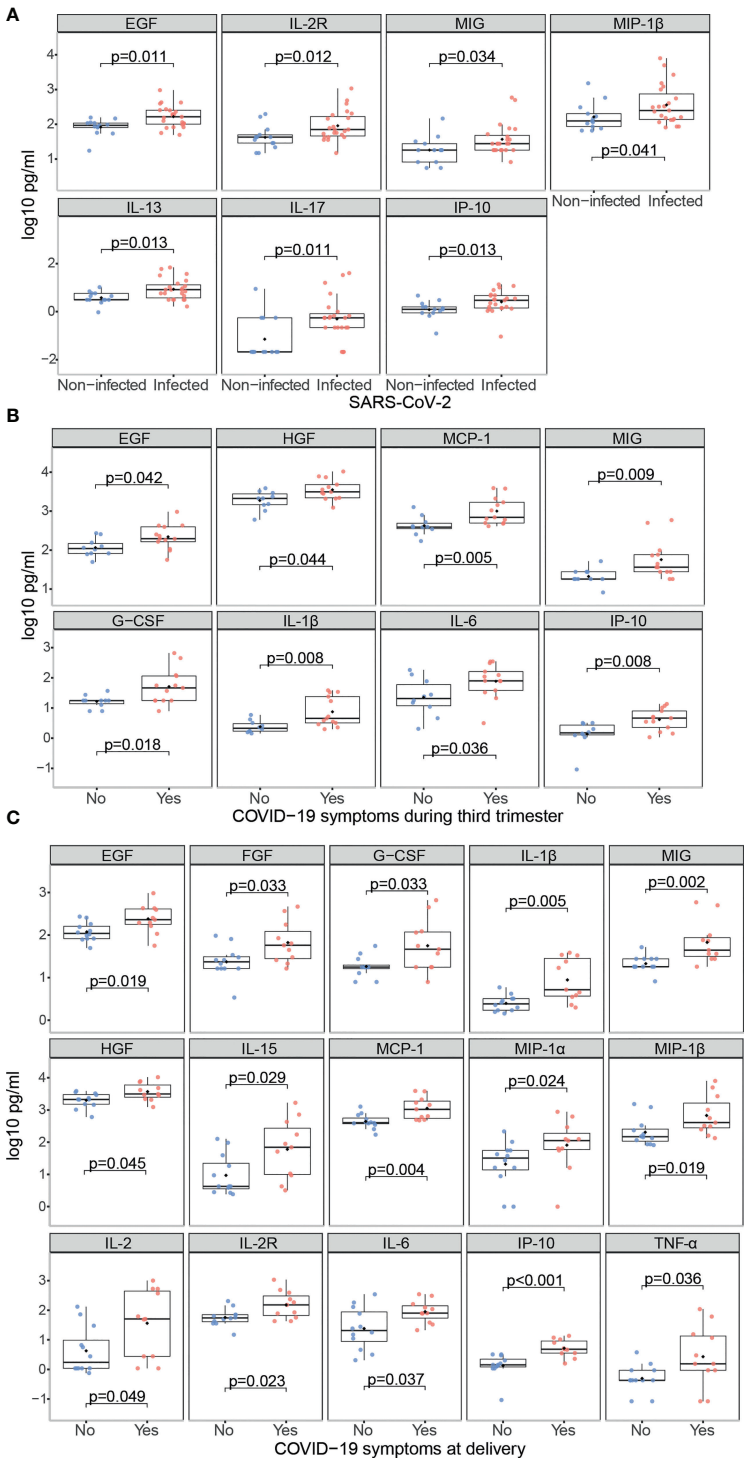

FIGURE 6
Cytokine, chemokine and growth factor concentrations in SARS-CoV-2 infected mothers. Comparison of inflammatory markers concentrations (log_{10} pg/ml) in serum between **(A)** Infected (N=23, in red) vs. non-infected (N=13, in blue) mothers; **(B)** Infected symptomatic (N=13, in red) vs. asymptomatic (N=10, in blue) mothers during the third trimester; **(C)** Infected symptomatic (N=11, in red) vs. asymptomatic (N=12, in blue) mothers at delivery. Groups were compared by the Wilcoxon-rank-sum-test. Only significant comparisons are shown, the remaining are in Figures S6–8.

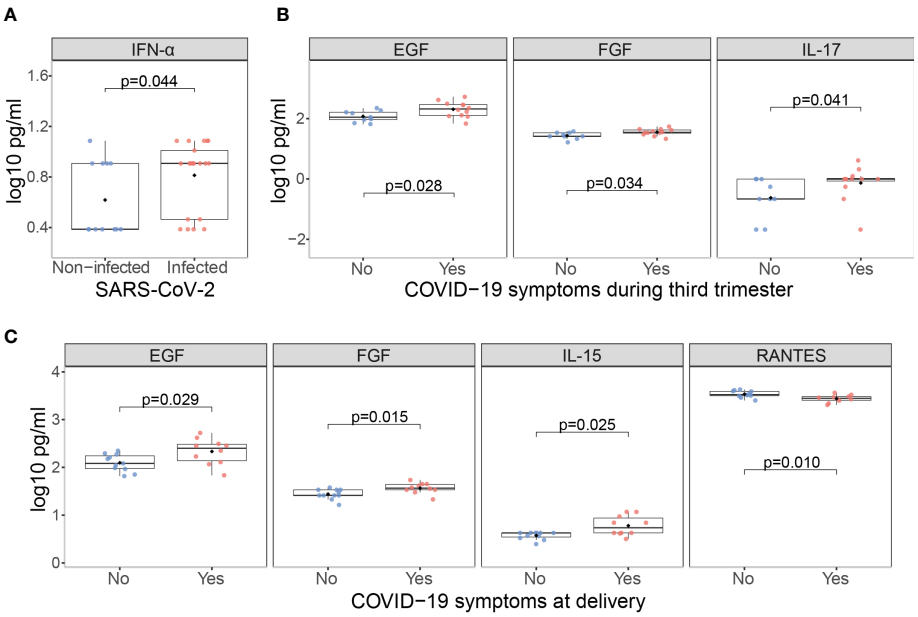

FIGURE 7
Cytokine, chemokine and growth factor concentrations in cord blood from children born from SARS-CoV-2 infected mothers. Comparison of inflammatory markers concentrations (log_{10} pg/ml) in cord blood between **(A)** Infected (N=21, in red) vs. non-infected (N=12, in blue) mothers; **(B)** Infected symptomatic (N=12, in red) vs. asymptomatic (N=9, in blue) mothers during the third trimester; **(C)** Infected symptomatic (N=11, in red) vs. asymptomatic (N=12, in blue) mothers at delivery. Groups were compared by the Wilcoxon-rank-sum-test. Only significant comparisons are shown, the remaining are in Figures S9–11.

We observed that maternal antibody levels highly correlated to cord blood levels, similar to previous studies (31, 45). However, rRT-PCR positive mothers during the third trimester of pregnancy had a reduction in the IgG transplacental transfer, also observed in previous studies (31–34). We also found that the negative effect of the infection on the IgG transfer was stronger as the infection was closer to delivery. Previous studies have reported that the IgG transfer ratio at birth is significantly lower for third trimester as compared to second-trimester infections (48–50). This could be because the mother has been seropositive for a shorter period, therefore maternal antibody levels may have not reached the peak response and there has been less time for transfer of antibodies. However, we did not detect an effect of antibody levels in the mother by time since infection. Moreover, in the transfer ratio, the IgG levels in cord blood we corrected by the IgG levels in the mother. In addition, although it has been previously documented that preterm newborns have reduced IgG transplacental transfer (51, 52), prematurity was ruled out as the cause of the reduction of SARS-CoV-2 IgG transfer because neither gestational age nor birth weight were associated. All together suggest that SARS-CoV-2 infections closer to term have a stronger negative impact on the IgG transplacental transfer. Interestingly, the reduction in IgG transfer was more marked for the anti-SARS-CoV-2 IgGs than for the anti-HuCoV IgGs. This stronger effect on the transfer of anti-SARS-CoV-2 IgGs vs. other IgGs has also been observed in the studies by Edlow et al. (34) and Atyeo et al. (49). They suggest a potential alteration in the Fc region glycosylation of SARS-CoV-2–specific antibodies probably mediated by the inflammation (34, 49), which may result in a compromised transfer by the Fc receptors (53). Neonatal transferred anti-SARS-CoV-2 antibodies may also be of lower activity (49) and short-lived (54), which raises further concern.

Mothers carrying a male fetus had higher concentrations of EGF, IL-15 and IL-7 cytokines, and induced higher antibody levels against SARS-CoV-2 than those carrying a female, but IgG transfer to the fetus was less efficient in the first ones. Previous studies have shown that fetal sex influences maternal serum cytokine and antibody profiles (55–57). In the context of SARS-CoV-2 infection, a recent study has reported similar results to ours, and a more pronounced SARS-CoV-2-specific antibody glycosylation in mothers carrying a male fetus, which would explain the reduced transplacental transfer (58).

In line with previous studies, SARS-CoV-2 infected pregnant women and their newborns showed more gestational complications than the non-infected women, although differences did not reach statistical significance. An increased risk of adverse birth outcomes, preterm birth, preeclampsia, cesarean section, and even stillbirth, neonatal death and maternal mortality has been reported in

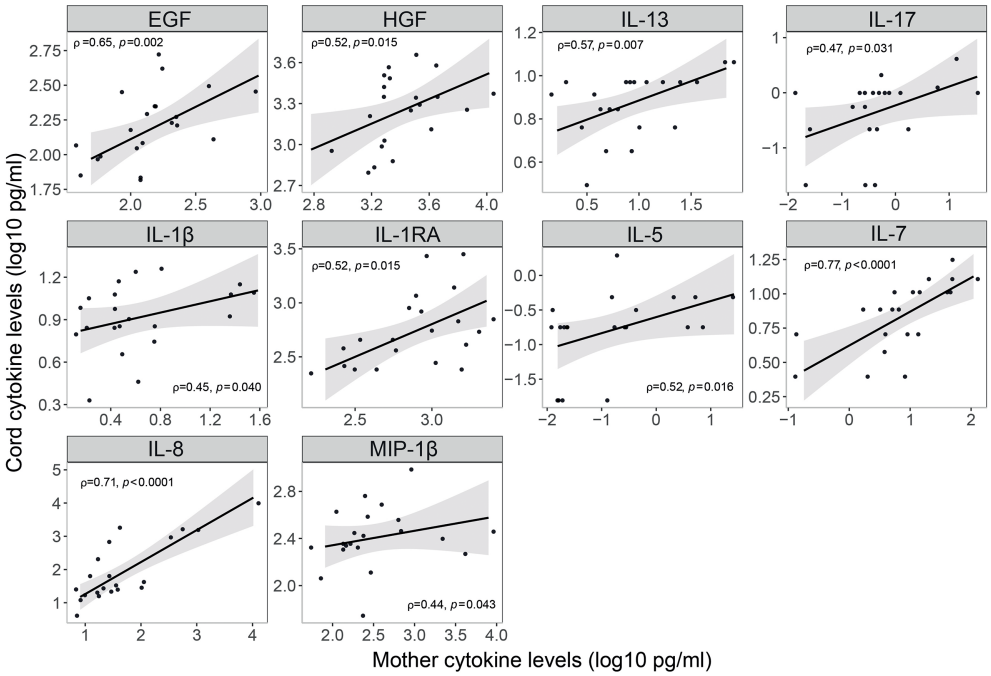

FIGURE 8
Correlations of cytokine, chemokine and growth factor concentrations in serum and cord blood from SARS-CoV-2 infected mothers. Correlations of inflammatory markers concentrations (log_{10} pg/ml) in serum blood and cord blood from SARS-CoV-2 infected mothers are represented as a linear model with standard error as a confidence interval (shaded areas). Correlations were assessed by the Spearman test, and the rho (ρ) and p-values are shown. Only significant correlations are shown, the remaining are in Figure S12.

COVID-19 positive pregnant women (59–63). A surveillance study by the CDC also showed that pregnant women suffer a greater clinical burden due to COVID-19 than their non-pregnant counterparts (10). A meta-analysis of 86 studies reported a high proportion of pregnant women with COVID-19 who had preterm birth (22%) and cesarean delivery (48%), and higher estimated rates of admission to the ICU (7% vs. 4% of non-pregnant women) (64).

One of the main strengths of the study is the broad panel of antigen-specific antibodies of three isotypes, including SARS-CoV-2 and HuCoVs, and cytokines measured, which allows having a very comprehensive picture of the humoral immune response in SARS-CoV-2 infected pregnant women and their newborns. However, the study has some limitations. The main one is the small sample size. Also, we did not adjust the p-values for multiple comparisons due to the small sample size, and therefore results should be taken with caution and require further validation. Larger sample size would have increased the statistical power to detect additional differences. It would have also been interesting to have histological data on placental samples to assess associations with the humoral response, the antibody transfer, and the delivery outcomes.

Results from this study indicate that we should pay greater attention to women infected with SARS-CoV-2 and their newborns. Children born to mothers with SARS-CoV-2 during pregnancy should be longitudinally observed to assess long-term outcomes. In addition, the vaccination of pregnant women should be highly recommended. Safety data on COVID-19 vaccines in pregnancy are rapidly accumulating without safety concerns being detected (65–68). However, additional longitudinal studies of vaccinated pregnant women at different trimesters and information on vaccine breakthroughs are necessary to inform maternally, pregnancy, and infant outcomes.

Future studies should further address the impact of SARS-CoV-2 infection in vaccinated and unvaccinated mothers along with gestational age on immune responses, how those affect fetal development, antibody mammary transfer, and the mechanisms underlying them. This knowledge may provide insights for vaccination strategies to assure the greatest protection for both mother and neonate.

Data availability statement

The raw data supporting the conclusions of this article will be made available by the authors upon request.

Ethics statement

The study was reviewed and approved by the Ethics Committee for Clinical Research of the Hospital Sant Joan de Déu. The patients/participants provided their written informed consent to participate in this study.

Author contributions

EMa, GM, and CD designed the study. EMu processed the samples at HSJD. MB managed the database. RR and RA developed and performed the serological and cytokines assays, the analysis and interpretation of the results. MV-S, RS, and MV gave support with the assays and analysis. LI, CC, PSa, PSe, DP, and NM produced the antigens. GM and CD supervised the assays and data analyses. RA and RR wrote the draft of the manuscript and GM, CD, MG-R, MB, and EMa reviewed the manuscript. All authors contributed to the article and approved the submitted version.

Funding

This work was supported by the Fundació Privada Daniel Bravo Andreu. RR had the support of the Health Department, Catalan Government (PERIS SLT017/20/000224). LI work was supported by the PID2019-110810RB-I00 grant from the Spanish Ministry of Science & Innovation. We acknowledge support from the Spanish Ministry of Science and Innovation and State Research Agency through the "Centro de Excelencia Severo Ochoa 2019-2023" Program (CEX2018-000806-S), and support from the Generalitat de Catalunya through the CERCA Program.

Acknowledgments

We are grateful to the participants of the study. Special thanks to the team members from ISGlobal, specifically Laura Puyol for the organization and coordination of shipment of samples and materials, Diana Barrios and Alfons Jiménez for the technical support in the lab, Gemma Ruiz-Olalla for the statistical support and Jordi Chi for the production of N antigens.

Conflict of interest

The authors declare that the research was conducted in the absence of any commercial or financial relationships that could be construed as a potential conflict of interest.

Publisher's note

All claims expressed in this article are solely those of the authors and do not necessarily represent those of their affiliated organizations, or those of the publisher, the editors and the reviewers. Any product that may be evaluated in this article, or claim that may be made by its manufacturer, is not guaranteed or endorsed by the publisher.

Supplementary material

The Supplementary Material for this article can be found online at: https://www.frontiersin.org/articles/10.3389/fimmu.2022.999136/full#supplementary-material

References

1. WHO. *WHO coronavirus disease (COVID-19) dashboard* . Available at: https://covid19whoint/ (Accessed 11 April 2021).

2. Kumar R, Yeni CM, Utami NA, Masand R, Asrani RK, Patel SK, et al. SARS-CoV-2 infection during pregnancy and pregnancy-related conditions: Concerns, challenges, management and mitigation strategies-a narrative review. *J Infect Public Health [Internet]* (2021) 14(7):863–75. doi: 10.1016/j.jiph.2021.04.005

3. Aghaeepour N, Ganio EA, Mcilwain D, Tsai AS, Tingle M, van Gassen S, et al. An immune clock of human pregnancy. *Sci Immunol* (2017) 2(15):eaan2946. doi: 10.1126/sciimmunol.aan2946

4. Marzi M, Vigano A, Trabattoni D, Villa ML, Salvaggio A, Clerici E, et al. Characterization of type 1 and type 2 cytokine production profile in physiologic and pathologic human pregnancy. *Clin Exp Immunol* (1996) 106(1):127–33. doi: 10.1046/j.1365-2249.1996.d01-809.x

5. Robinson DP, Klein SL. Pregnancy and pregnancy-associated hormones alter immune responses and disease pathogenesis. *Horm Behav* (2012) 62(3):263–71. doi: 10.1016/j.yhbeh.2012.02.023

6. Jamieson DJ, Honein MA, Rasmussen SA, Williams JL, Swerdlow DL, Biggerstaff MS, et al. H1N1 2009 influenza virus infection during pregnancy in the USA. *Lancet.* (2009) 374(9688):451–8. doi: 10.1016/S0140-6736(09)61304-0

7. Rasmussen SA, Jamieson DJ, Uyeki TM. Effects of influenza on pregnant women and infants. *Am J Obstet Gynecol* (2012) 207(3 Suppl):S3–8. doi: 10.1016/j.ajog.2012.06.068

8. Liu H, Wang LL, Zhao SJ, Kwak-Kim J, Mor G, Liao AH. Why are pregnant women susceptible to COVID-19? an immunological viewpoint. *J Reprod Immunol* (2020) 139:103122. doi: 10.1016/j.jri.2020.103122

9. Mullins E, Evans D, Viner RM, O'Brien P, Morris E. Coronavirus in pregnancy and delivery: rapid review. *Ultrasound obstetrics gynecology* (2020) 55 (5):586–92. doi: 10.1002/uog.22014

10. Ellington S, Strid P, Tong VT, Woodworth K, Galang RR, Zambrano LD, et al. Characteristics of women of reproductive age with laboratory-confirmed SARS-CoV-2 infection by pregnancy status - united states, January 22-June 7, 2020. *MMWR Morb Mortal Wkly Rep* (2020) 69(25):769–75. doi: 10.15585/mmwr.mm6925a1

11. CDC. Investigating the impact of COVID-19 during pregnancy. (2021). Available at: https://www.cdc.gov/coronavirus/2019-ncov/cases-updates/special-populations/pregnancy-data-on-covid-19/what-cdc-is-doing.html (Accessed 8 July 2022)

12. Lokken EM, Huebner EM, Taylor GG, Hendrickson S, Vanderhoeven J, Kachikis A, et al. Disease severity, pregnancy outcomes, and maternal deaths

among pregnant patients with severe acute respiratory syndrome coronavirus 2 infection in Washington state. *Am J Obstet Gynecol* (2021) 225(1):77.e1–77.e14. doi: 10.1016/j.ajog.2020.12.1221

13. Lokken EM, Taylor GG, Huebner EM, Vanderhoeven J, Hendrickson S, Coler B, et al. Higher severe acute respiratory syndrome coronavirus 2 infection rate in pregnant patients. *Am J Obstetrics Gynecol* (2021) 225(1):75.e1–75.e16. doi: 10.1016/j.ajog.2021.02.011

14. Zambrano LD, Ellington S, Strid P, Galang RR, Oduyebo T, Tong VT, et al. Update: Characteristics of symptomatic women of reproductive age with laboratory-confirmed SARS-CoV-2 infection by pregnancy status - united states, January 22-October 3, 2020. *MMWR Morb Mortal Wkly Rep* (2020) 69(44):1641–7. doi: 10.15585/mmwr.mm6944e3

15. WAPM. Maternal and perinatal outcomes of pregnant women with SARS-CoV-2 infection. *Ultrasound Obstet Gynecol* (2021) 57(2):232–41. doi: 10.1002/uog.23107

16. Perlman JM, Salvatore C. Coronavirus disease 2019 infection in newborns. *Clin Perinatol* (2022) 49(1):73–92. doi: 10.1016/j.clp.2021.11.005

17. Yuan J, Qian H, Cao S, Dong B, Yan X, Luo S, et al. Is there possibility of vertical transmission of COVID-19: a systematic review. *Transl Pediatr* (2021) 10 (2):423–34. doi: 10.21037/tp-20-144

18. Akhtar H, Patel C, Abuelgasim E, Harky A. COVID-19 (SARS-CoV-2) infection in pregnancy: A systematic review. *Vol 85 Gynecologic obstetric Invest* (2020) p:295–306. doi: 10.1159/000509290

19. Yockey LJ, Iwasaki A. Interferons and proinflammatory cytokines in pregnancy and fetal development. (2018) 49(3):397–412. doi: 10.1016/j.immuni.2018.07.017

20. Racicot K, Mor G. Risks associated with viral infections during pregnancy. *J Clin Invest* (2017) 127(5):1591–9. doi: 10.1172/JCI87490

21. Chudnovets A, Liu J, Narasimhan H, Liu Y, Burd I. Role of inflammation in virus pathogenesis during pregnancy. *J Virol* (2020) 95(2):e01381–19. doi: 10.1128/JVI.01381-19

22. Prochaska E, Jang M, Burd I. COVID-19 in pregnancy: Placental and neonatal involvement. *Am J Reprod Immunol* (2020) 84(5):e13306. doi: 10.1111/aji.13306

23. Estes ML, McAllister AK. Maternal immune activation: Implications for neuropsychiatric disorders. *Science*. (2016) 353(6301):772–7. doi: 10.1126/science.aag3194

24. Mor G, Cardenas I. The immune system in pregnancy: a unique complexity. *Am J Reprod Immunol* (2010) 63(6):425–33. doi: 10.1111/j.1600-0897.2010.00836.x

25. Rad HS, Röhl J, Stylianou N, Allenby MC, Bazaz SR, Warkiani ME, et al. The effects of COVID-19 on the placenta during pregnancy. *Front Immunol* (2021) 12:743022. doi: 10.3389/fimmu.2021.743022

26. Shook LL, Sullivan EL, Lo JO, Perlis RH, Edlow AG. COVID-19 in pregnancy: implications for fetal brain development. *Trends Mol Med* (2022) 28 (4):319–30. doi: 10.1016/j.molmed.2022.02.004

27. Cumberland P, Shulman CE, Maple PAC, Bulmer JN, Dorman EK, Kawuondo K, et al. Maternal HIV infection and placental malaria reduce transplacental antibody transfer and tetanus antibody levels in newborns in Kenya. *J Infect Dis* (2007) 196(4):550–7. doi: 10.1086/519845

28. Ogolla S, Daud II, Asito AS, Sumba OP, Ouma C, Vulule J, et al. Reduced transplacental transfer of a subset of Epstein-Barr virus-specific antibodies to neonates of mothers infected with plasmodium falciparum malaria during pregnancy. *Clin Vaccine Immunol* (2015) 22(11):1197–205. doi: 10.1128/CVI.00270-15

29. Perret C, Chanthavanich P, Pengsaa K, Limkittikul K, Hutajaroen P, Bunn JEG, et al. Dengue infection during pregnancy and transplacental antibody transfer in Thai mothers. *J Infect* (2005) 51(4):287–93. doi: 10.1016/j.jinf.2004.10.003

30. Castanha PMS, Souza W v, Braga C, de Araújo TVB, Ximenes RAA, Albuquerque MdeFPM, et al. Perinatal analyses of zika- and dengue virus-specific neutralizing antibodies: A microcephaly case-control study in an area of high dengue endemicity in Brazil. *PLoS Negl Trop Dis* (2019) 13(3):e0007246. doi: 10.1371/journal.pntd.0007246

31. Kubiak JM, Murphy EA, Yee J, Cagino KA, Friedlander RL, Glynn SM, et al. Severe acute respiratory syndrome coronavirus 2 serology levels in pregnant women and their neonates. *Am J Obstet Gynecol* (2021) 225(1):73.e1–7. doi: 10.1016/j.ajog.2021.01.016

32. Sherer ML, Lei J, Creisher PS, Jang M, Reddy R, Voegtline K, et al. Pregnancy alters interleukin-1 beta expression and antiviral antibody responses during severe acute respiratory syndrome coronavirus 2 infection. *Am J Obstet Gynecol* (2021) 225(3):301.e1–301.e14. doi: 10.1016/j.ajog.2021.03.028

33. Flannery DD, Gouma S, Dhudasia MB, Mukhopadhyay S, Pfeifer MR, Woodford EC, et al. Assessment of maternal and neonatal cord blood SARS-CoV-2 antibodies and placental transfer ratios. *JAMA Pediatr* (2021) 175(6):594–600. doi: 10.1001/jamapediatrics.2021.0038

34. Edlow AG, Li JZ, Collier ARY, Atyeo C, James KE, Boatin AA, et al. Assessment of maternal and neonatal SARS-CoV-2 viral load, transplacental antibody transfer, and placental pathology in pregnancies during the COVID-19 pandemic. *JAMA Netw Open* (2020) 3(12):e2030455. doi: 10.1001/jamanetworkopen.2020.30455

35. Shook LL, Atyeo CG, Yonker LM, Fasano A, Gray KJ, Alter G, et al. Durability of anti-spike antibodies in infants after maternal COVID-19 vaccination or natural infection. *JAMA* (2022) 327(11):1087–1089. doi: 10.1001/jama.2022.1206

36. Dobaño C, Ramírez-Morros A, Alonso S, Vidal-Alaball J, Ruiz-Olalla G, Vidal M, et al. Persistence and baseline determinants of seropositivity and reinfection rates in health care workers up to 12.5 months after COVID-19. *BMC Med* (2021) 19(1):155. doi: 10.1186/s12916-021-02032-2

37. Dobaño C, Santano R, Jiménez A, Vidal M, Chi J, Rodrigo Melero N, et al. Immunogenicity and crossreactivity of antibodies to the nucleocapsid protein of SARS-CoV-2: utility and limitations in seroprevalence and immunity studies. *Trans Res* (2021) 232:60–74. doi: 10.1016/j.trsl.2021.02.006

38. Aguilar R, Campo JJ, Chicuecue S, Cisteró P, Català A, Luis L, et al. Changing plasma cytokine, chemokine and growth factor profiles upon differing malaria transmission intensities. *Malaria J* (2019) 18(1):406. doi: 10.1186/s12936-019-3038-x

39. Ballart C, Torrico MC, Vidal G, Torrico F, Lozano D, Gállego M, et al. Clinical and immunological characteristics of tegumentary leishmaniasis cases in Bolivia. *PLoS Negl Trop Dis* (2021) 15(3):e0009223. doi: 10.1371/journal.pntd.0009223

40. Natama HM, Moncunill G, Rovira-Vallbona E, Sanz H, Sorgho H, Aguilar R, et al. Modulation of innate immune responses at birth by prenatal malaria exposure and association with malaria risk during the first year of life. *BMC Med* (2018) 16(1):198. doi: 10.1186/s12916-018-1187-3

41. Sanz H, Aponte JJ, Harezlak J, Dong Y, Ayestaran A, Nhabomba A, et al. drLumi: An open-source package to manage data, calibrate, and conduct quality control of multiplex bead-based immunoassays data analysis. *PLoS One* (2017) 12 (11):1:e018790. doi: 10.1371/journal.pone.0187901

42. Garcia-Basteiro AL, Moncunill G, Tortajada M, Vidal M, Guinovart C, Jiménez A, et al. Seroprevalence of antibodies against SARS-CoV-2 among health care workers in a large Spanish reference hospital. *Nat Commun* (2020) 11(1):3500. doi: 10.1038/s41467-020-17318-x

43. Moncunill G, Mayor A, Santano R, Jiménez A, Vidal M, Tortajada M, et al. SARS-CoV-2 seroprevalence and antibody kinetics among health care workers in a Spanish hospital after three months of follow-up. *J Infect Dis* (2020) 223(1):62–71. doi: 10.1093/infdis/jiaa696

44. Shields AM, Faustini SE, Perez-Toledo M, Jossi S, Allen JD, Al-Taei S, et al. Serological responses to SARS-CoV-2 following non-hospitalised infection: clinical and ethnodemographic features associated with the magnitude of the antibody response. *BMJ Open Respir Res* (2021) 8(1):e000872. doi: 10.1136/bmjresp-2020-000872

45. Joseph NT, Dude CM, Verkerke HP, Irby LS, Dunlop AL, Patel RM, et al. Maternal antibody response, neutralizing potency, and placental antibody transfer after severe acute respiratory syndrome coronavirus 2 (SARS-CoV-2) infection. *Obstet Gynecol* (2021) 138(2):189–97. doi: 10.1097/AOG.0000000000004440

46. Dang D, Wang L, Zhang C, Li Z, Wu H. Potential effects of SARS-CoV-2 infection during pregnancy on fetuses and newborns are worthy of attention. *J Obstet Gynaecol Res* (2020) 46(10):1951–7. doi: 10.1111/jog.14406

47. Denney JM, Nelson E, Wadhwa P, Waters T, Mathew L, Goldenberg RL, et al. Cytokine profiling: Variation in immune modulation with preterm birth vs. uncomplicated term birth identifies pivotal signals in pathogenesis of preterm birth. *J Perinatal Med* (2021) 49(3):299–309. doi: 10.1515/jpm-2020-0025/html

48. Beharier O, Plitman Mayo R, Raz T, Nahum Sacks K, Schreiber L, Suissa-Cohen Y, et al. Efficient maternal to neonatal transfer of antibodies against SARS-CoV-2 and BNT162b2 mRNA COVID-19 vaccine. *J Clin Invest* (2021) 131(13): e154834. doi: 10.1172/JCI150319

49. Atyeo C, Pullen KM, Bordt EA, Fischinger S, Burke J, Michell A, et al. Compromised SARS-CoV-2-specific placental antibody transfer. *Cell.* (2021) 184 (3):628–42.e10. doi: 10.1016/j.cell.2020.12.027

50. Palmeira P, Quinello C, Silveira-Lessa AL, Zago CA, Carneiro-Sampaio M. IgG placental transfer in healthy and pathological pregnancies. *Salumets A editor Clin Dev Immunol* (2012) 2012:985646. doi: 10.1155/2012/985646

51. Okoko BJ, Wesumperuma HL, Fern J, Yamuah LK, Hart CA. The transplacental transfer of IgG subclasses: influence of prematurity and low birthweight in the Gambian population. *Ann Trop Paediatr* (2002) 22(4):325–32. doi: 10.1179/027249302125001985

52. Costa-Carvalho BT, Vieria HM, Dimantas RB, Arslanian C, Naspitz CK, Solé D, et al. Transfer of IgG subclasses across placenta in term and preterm newborns. *razilian J Med Biol Res = Rev Bras pesquisas medicas e biologicas* (1996) 29(2):201–4.

53. Jennewein MF, Abu-Raya B, Jiang Y, Alter G, Marchant A. Transfer of maternal immunity and programming of the newborn immune system. *Semin Immunopathol* (2017) 39(6):605–13. doi: 10.1007/s00281-017-0653-x

54. Gao J, Li W, Hu X, Wei Y, Wu J, Luo X, et al. Disappearance of SARS-CoV-2 antibodies in infants born to women with COVID-19, wuhan, China. *Emerging Infect diseases* (2020) Vol. 26:2491–4. doi: 10.3201/eid2610.202328

55. Ramiro-Cortijo D, de la Calle M, Böger R, Hannemann J, Lüneburg N, López-Giménez MR, et al. Male Fetal sex is associated with low maternal plasma anti-inflammatory cytokine profile in the first trimester of healthy pregnancies. *Cytokine.* (2020) 136:155290. doi: 10.1016/j.cyto.2020.155290

56. Mitchell AM, Palettas M, Christian LM. Fetal sex is associated with maternal stimulated cytokine production, but not serum cytokine levels, in human pregnancy. *Brain Behav Immun* (2017) 60:32–7. doi: 10.1016/j.bbi.2016.06.015

57. Moncunill G, Dobaño C, González R, Smolen KK, Manaca MN, Balcells R, et al. Association of maternal factors and HIV infection with innate cytokine responses of delivering mothers and newborns in Mozambique. *Front Microbiol* (2020) 11:1452. doi: 10.3389/fmicb.2020.01452

58. Bordt EA, Shook LL, Atyeo C, Pullen KM, de Guzman RM, Meinsohn MC, et al. Maternal SARS-CoV-2 infection elicits sexually dimorphic placental immune responses. *Sci Transl Med* (2021) 13(617):eabi7428. doi: 10.1126/scitranslmed.abi7428

59. Yang R, Mei H, Zheng T, Fu Q, Zhang Y, Buka S, et al. Pregnant women with COVID-19 and risk of adverse birth outcomes and maternal-fetal vertical transmission: a population-based cohort study in wuhan, China. *BMC Med* (2020) 18(1):330. doi: 10.1186/s12916-020-01798-1

60. Carrasco I, Muñoz-Chapuli M, Vigil-Vázquez S, Aguilera-Alonso D, Hernández C, Sánchez-Sánchez C, et al. SARS-COV-2 infection in pregnant women and newborns in a Spanish cohort (GESNEO-COVID) during the first wave. *BMC Pregnancy Childbirth* (2021) 21(1):326. doi: 10.1186/s12884-021-03784-8

61. Villar J, Ariff S, Gunier RB, Thiruvengadam R, Rauch S, Kholin A, et al. Maternal and neonatal morbidity and mortality among pregnant women with and without COVID-19 infection: The INTERCOVID multinational cohort study. *JAMA Pediatr [Internet]* (2021) 175(8):817–26. doi: 10.1001/jamapediatrics.2021.1050

62. Laresgoiti-Servitje E, Cardona-Pérez JA, Hernández-Cruz RG, Helguera-Repetto AC, Valdespino-Vázquez MY, Moreno-Verduzco ER, et al. COVID-19 infection in pregnancy: PCR cycle thresholds, placental pathology, and perinatal outcomes. *Viruses* (2021) 13(9):1884. doi: 10.3390/v13091884

63. Chamseddine RS, Wahbeh F, Chervenak F, Salomon LJ, Ahmed B, Rafii A. Pregnancy and neonatal outcomes in SARS-CoV-2 infection: A systematic review. *Marozio L editor J Pregnancy* (2020) 2020:4592450. doi: 10.1155/2020/4592450

64. Khalil A, Kalafat E, Benlioglu C, O'Brien P, Morris E, Draycott T, et al. SARS-CoV-2 infection in pregnancy: A systematic review and meta-analysis of clinical features and pregnancy outcomes. *EClinicalMedicine.* (2020) 25:100446. doi: 10.1016/j.eclinm.2020.100446

65. Goldshtein I, Nevo D, Steinberg DM, Rotem RS, Gorfine M, Chodick G, et al. Association between BNT162b2 vaccination and incidence of SARS-CoV-2 infection in pregnant women. *JAMA [Internet]* (2021) 326(8):728–35. doi: 10.1001/jama.2021.11035

66. Adhikari EH, Spong CY. COVID-19 vaccination in pregnant and lactating women. *JAMA.* (2021) 325(11):1039–40. doi: 10.1001/jama.2021.1658

67. Theiler RN, Wick M, Mehta R, Weaver AL, Virk A, Swift M. Pregnancy and birth outcomes after SARS-CoV-2 vaccination in pregnancy. *Am J Obstet Gynecol MFM* (2021) 3(6):100467. doi: 10.1016/j.ajogmf.2021.100467

68. Dagan N, Barda N, Biron-Shental T, Makov-Assif M, Key C, Kohane IS, et al. Effectiveness of the BNT162b2 mRNA COVID-19 vaccine in pregnancy. *Nat Med* (2021) 27(10):1693–1695. doi: 10.1038/s41591-021-01490-8

COPYRIGHT

© 2022 Rubio, Aguilar, Bustamante, Muñoz, Vázquez-Santiago, Santano, Vidal, Melero, Parras, Serra, Santamaria, Carolis, Izquierdo, Gómez-Roig, Dobaño, Moncunill and Mazarico. This is an open-access article distributed under the terms of the Creative Commons Attribution License (CC BY). The use, distribution or reproduction in other forums is permitted, provided the original author(s) and the copyright owner(s) are credited and that the original publication in this journal is cited, in accordance with accepted academic practice. No use, distribution or reproduction is permitted which does not comply with these terms.

frontiers | Frontiers in Immunology

TYPE Original Research
PUBLISHED 30 September 2022
DOI 10.3389/fimmu.2022.1006076

Check for updates

OPEN ACCESS

EDITED BY
Martijn van Griensven,
Maastricht University, Netherlands

REVIEWED BY
Pedro Paulo Gattai Gomes,
University of São Paulo, Brazil
Fernando Mafra,
University of Mogi das Cruzes, Brazil

*CORRESPONDENCE
Thiago S. Rosa
thiagoacsdkp@yahoo.com.br

SPECIALTY SECTION
This article was submitted to Viral Immunology, a section of the journal Frontiers in Immunology

RECEIVED 28 July 2022
ACCEPTED 15 September 2022
PUBLISHED 30 September 2022

CITATION
Corrêa HL, Deus LA, Araújo TB, Reis AL, Amorim CEN, Gadelha AB, Santos RL, Honorato FS, Motta-Santos D, Tzanno-Martins C, Neves RVP and Rosa TS (2022) Phosphate and IL-10 concentration as predictors of long-covid in hemodialysis patients: A Brazilian study. *Front. Immunol.* 13:1006076. doi: 10.3389/fimmu.2022.1006076

COPYRIGHT
© 2022 Corrêa, Deus, Araújo, Reis, Amorim, Gadelha, Santos, Honorato, Motta-Santos, Tzanno-Martins, Neves and Rosa. This is an open-access article distributed under the terms of the Creative Commons Attribution License (CC BY). The use, distribution or reproduction in other forums is permitted, provided the original author(s) and the copyright owner(s) are credited and that the original publication in this journal is cited, in accordance with accepted academic practice. No use, distribution or reproduction is permitted which does not comply with these terms.

Phosphate and IL-10 concentration as predictors of long-covid in hemodialysis patients: A Brazilian study

Hugo L. Corrêa[1], Lysleine A. Deus[1], Thaís B. Araújo[1], Andrea L. Reis[1], Carlos E. N. Amorim[2], André B. Gadelha[1,5,6], Rafael L. Santos[1], Fernando S. Honorato[1], Daisy Motta-Santos[3], Carmen Tzanno-Martins[4], Rodrigo V. P. Neves[1] and Thiago S. Rosa[1*]

[1]Department of Physical Education, Catholic University of Brasília, Brasília, DF, Brazil, [2]Physical Education Department, Federal University of Maranhão, Maranhão, Brazil, [3]Pontifical Catholic University of Minas Gerais and Sports Department, EEFFTO, UFMG, Belo, Horizonte, Brazil, [4]Clinical Group Home Dialysis Center and RenalClass, São Paulo, Brazil, [5]Serviço de Preparação Física/COPSA/COSAU/DIGEP/SA/SG/Presidência da República, Brasília, Brazil, [6]Seção de Educação Física do Colégio Militar de Brasília, Brasília, Brazil

Background: The global burden of persistent COVID-19 in hemodialysis (HD) patients is a worrisome scenario worth of investigation for the critical care of chronic kidney disease (CKD). We performed an exploratory *post-hoc* study from the trial U1111-1237-8231 with two specific aims: i) to investigate the prevalence of COVID-19 infection and long COVID symptoms from our Cohort of 178 Brazilians HD patients. ii) to identify whether baseline characteristics should predict long COVID in this sample.

Methods: 247 community-dwelling older (>60 years) patients (Men and women) undergoing HD (glomerular filtration rate < 15 mL/min/1.73m^2) with arteriovenous fistula volunteered for this study. All patients presented hypertension and diabetes. Patients were divided in two groups: without long-COVID and with long-COVID. Body composition, handgrip strength, functional performance, iron metabolism, phosphate, and inflammatory profile were assessed. Patients were screened for 11-months after COVID-19 infection. Results were considered significant at $P < 0.05$.

Results: We found that more than 85% of the COVID-19 infected patients presented a severe condition during the infection. In our sample, the mortality rate over 11-month follow was relatively low (8.4%) when compared to worldwide (approximately 36%). Long COVID was highly prevalent in COVID-19 survivors representing more than 80% of all cases. Phosphate and IL-10 were higher in the long COVID group, but only phosphate higher than 5.35 mg/dL appears to present an increased prevalence of long COVID, dyspnea, and fatigue.

Conclusion: There was a high prevalence of COVID-19 infection and long COVID in HD patients from the Brazilian trial 'U1111-1237-8231'. HD clinics should be aware with phosphate range in HD patients as a possible target for adverse post-COVID events.

KEYWORDS

inflammation, phosphate, post-COVID, nephrology, hemodialysis

Introduction

Coronavirus disease 2019 (COVID-19), caused by the severe acute respiratory syndrome coronavirus-2 (SARS-CoV-2) has impacted worldwide public health (1, 2). More than 6 million deaths were registered by May 2022, being more evident in Europe and Americas (https://covid19.who.int/; assessed 30 May 2022). Recent studies suggest that are several risk factors for severe or fatal COVID-19 that differs according to pre-existing diseases status (1, 3).

Chronic kidney disease (CKD) has emerged as an independent risk factor for the severeness of COVID-19 illness (1, 3–5). Such adverse condition appears to be related with impaired immune function, low-grade chronic inflammation, cardiovascular diseases, frailty, and endothelial dysfunction, which are enhanced according to the severity of CKD, especially in patients undergoing maintenance hemodialysis (HD) (6–8). The Centre for the Mathematical Modeling of Infectious Diseases COVID-19 working group (1) suggested CKD as an important risk factor for severe COVID-19. Furthermore, the ERA-EDTA Council (European Renal Association and European Dialysis and Transplantation Association) and the ERACODA Working Group demonstrated that HD (2021) (9), organ transplantation, and low renal function (estimated glomerular filtration rate < 30 mL/min/1.73m^2) are associated with highest mortality risk from COVID-19. Carriazo et al. (7) showed that the increased mortality rate persists during the one-year after COVID-19 diagnosis in HD patients. Therefore, it is recommended that patients undergoing HD that were infected with COVID-19 should be monitored continuously to avoid future complications, especially in the first three months (8).

The long-term of new, returning, or ongoing health issues after the first infection with SARS-CoV-2 is recognized as post-acute COVID-19 syndrome conditions or long COVID (10–12). This scenario can last ranging from weeks to years. Post-COVID symptoms mostly reported are fatigue, fever, shortness of breath, cough, body aches, heart palpitations, neurological symptoms, diarrhea, stomach pain, and body aches (13). Noteworthy, subjects with underlying health conditions, including HD patients are likely to develop long-COVID (8, 11–14). Considering the global interest on how COVID-19 symptoms might persist in HD patients, as well as possible targets to avoid this condition, we performed an exploratory *post-hoc* study from the trial U1111-1237-8231 (15) with two specific aims: i) to characterize COVID-19 infection and long COVID symptoms from our Cohort of 178 Brazilians HD patients. ii) to identify whether baseline characteristics should predict long COVID in this sample. This study provides relevant information regarding the prevalence of COVID-19 and long COVID in HD patients and suggested phosphate and interleukin (IL-10) as possible targets associated with post-COVID conditions.

Methods

This study is a follow-up study of data from the trial U1111-1237-8231. This study has been conducted prospectively in hemodialysis clinics from Brazil and has been previous described (15). It is worth to state that this manuscript presents additional data from the study of 15. Briefly, this study covered 247 (two hundred and forty-seven) community-dwelling older patients undergoing HD (glomerular filtration rate < 15 mL/min/1.73m^2) with arteriovenous fistula who volunteered for this study. All patients presented hypertension and diabetes. Eligibility criteria for participants were: (i) age equal to or older than 60 years; (ii) hemodialysis for at least 3 months; (iii) dialysis at least three times per week; and (iv) no significant medical complications in the last 3 months, except for vascular access correction. Exclusion criteria were: (i) systemic lupus erythematosus; (ii) congenital kidney malformation or some auto-immune disease that affects the kidneys; (iii) severe decompensated diabetes. Participants were informed about the procedures and possible risks of participation in the study. Before participation in the research project, each participant completed a medical history questionnaire and voluntarily signed a written informed consent form. The study was conducted according to the Declaration of Helsinki (1975). All methods and procedures were approved by the Local Human Research Ethics Committee, Brazil (no 08856012.6.0000.5505

and updated 23007319.0.0000.0029). Furthermore, a new protocol register number was made and approved for conducting the study with COVID-19 patients (no 47011221.2.0000.5086). After 11-month follow-up only 178 patients were analyzed for COVID-19 and long-COVID. All patients' selection can be found in Figure 1.

Anthropometric assessment

All subjects were weighed on a mechanical scale (Filizola®, São Paulo, Brazil), and height was measured with a stadiometer built into the scale (precision: 0.5 cm). Waist circumference was assessed at the level of umbilicus using an anthropometric tape (Sanny®, São Paulo, Brazil). Body composition was measured using a Prodigy Advance Plus (LUNAR,Corp/General Electric; Madison, Wisconsin, USA) dual-energy X-ray absorptiometry (DXA) according to previously specified procedures (16). All measurements were carried out by the same experienced researcher.

Handgrip strength and functional performance

Handgrip strength was measured with a hydraulic hand dynamometer (Jamar® - Sammons Preston, Bolingbrook, USA). According to the recommendations of the American Society of Hand Therapists, measurements were performed with participants in a sitting position, elbow joint at 90°, forearm in a neutral position, and wrist between 0° and 30° of extension. The best performance of three trials in the contralateral arm to the arteriovenous fistula was recorded and used for the present analyses (17, 18). Functional performance was evaluated by the Timed Up-and-Go (TUG) test and six-minute walking test (6MWT). Procedures were fully explained before the assessment, followed by a familiarization attempt as described elsewhere (19).

Medications in use

All patients had similar medication regimen. Briefly, for glucose control the most common treatment was long-acting insulin. Erythropoietin was administered raging from 50 to 100 UI/kg three times/week with constant adjustments for anemia control. Simvastatin, Pravastatin, Fluvastatin, and Rosuvastatin with the following doses/day: 5 – 20mg, 10 – 40mg, 80mg, 10 – 20mg, respectively. Phosphate binder Sevelamer was administered 800mg three times/day to control phosphate levels between 5.5 and 7.5mg/dL.

Blood collection

Venous blood samples were obtained from all patients to measure biochemical variables using dry and EDTA containing tubes. All blood was obtained before COVID infection. Samples were obtained in the morning (8 to 12 h of fasting) and all patients were instructed not to practice any physical activity for 48 h before. Samples were centrifuged at 1500 x g for 15 min; after processing, the specimens were aliquoted into cryovials and stored at -80° C.

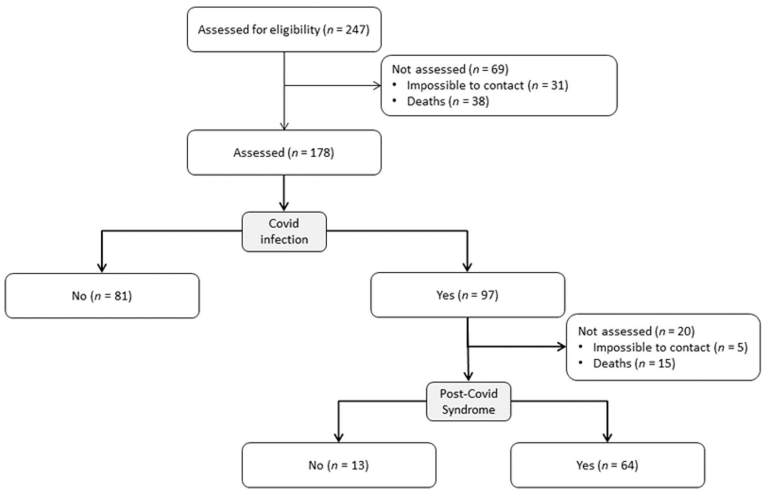

FIGURE 1
Participant's flow-chart.

Inflammatory profile

The systemic TNF-α, IL-6, and IL-10 levels were measured in triplicate by enzyme-linked immunosorbent assay (ELISA) kits from R&D Systems (Minneapolis, MN, USA) according to the manufacturer's instructions. The detectable limits for TNF-α, IL-6, and IL-10 were 10, 18, and 0.2 pg,mL^{-1}, respectively. The overall intra- and inter-assay CVs for inflammatory markers and hepcidin were in a range from 2.3 to 10%.

COVID and post-acute COVID-19 syndrome assessment

Covid diagnostic by PCR and severity, including hospitalizations, deaths, nursery, intensive care unit, and supplementary O_2 was obtained through the 11-months follow-up by checking the medical records from the HD clinic. Long COVID symptoms were recorded by performing a semi-structured telephone call, conducted through all 11-months follow-up. During the interviews patients were asked if they are feeling dyspnea, dizziness, headache, myalgia, cognitive deficits, and fatigue. After that, the interviewer checked with the responsible person for the patient if all the symptoms are corrected recorded and if they were not evident before COVID infection. At least ten contact attempts were made to each volunteer with missed calls. All telephone calls were made by the same person, who had experience with telephone interviews (20). The long-term of new, returning, or ongoing health issues after the first infection with SARS-CoV-2 recognized as post-acute COVID-19 syndrome conditions or long COVID (10–12).

Statistical analysis

Descriptive characteristics are presented as means and standard deviations unless otherwise noted. The Shapiro–Wilk test and Levene were used to verify data distribution nature and homogeneity, respectively. X^2 tests were performed to compare categorical variables, while continuous variables were tested for significance by performing a student t test to compare groups (with and without post-covid syndrome. The Receiver Operating Characteristic (ROC) curve was generated plotting sensitivity (y-axis) as a function of 1-specificity (x-axis). Sensitivity or true-positive points to the individual that was correctly diagnosed with the outcome by an indicator. 1-specificity or true-negative refers to the subjects that were wrongly diagnosed with the outcome by an indicator. In the present study, to be considered an indicator, the area under the ROC curve should be higher than 0.50 and lower than 1.00. Therefore, a larger area indicates a greater discriminatory power of the respective indicator. Herein the two elected indicators were phosphate and IL-10. To establish the cut-off point, was considered the closest value between sensitivity and 1-specificity not lower than 0.60. Furthermore, the odds ratio (95% confidence interval [CI]) were obtained for phosphate and IL-10 to verify the likelihood to present post-covid syndrome according to the cut-off points established for both variables.

After performing the aforementioned analysis, phosphate was elected as a possible predictor of the post-covid syndrome. Therefore, the subjects were subgrouped according to the cut-off points established by the ROC curve (group 1: phosphate <5.35; group 2: phosphate >5.35). For that purpose, the groups were than compared using a chi-squared test. Results were considered significant at $P < 0.05$, and all analysis were performed using *IBM Corp. Released 2013. IBM SPSS Statistics for Windows, version 22.0. Armonk, NY: IBM Corp. And GraphPad Prism version 8.0.0 to Windows, GraphPad Software, San Diego, california, EUA, www.graphpad.com* ".

Results

COVID infection occurs raging from April to December of 2020. The prevalence of COVID-19 in our Cohort was 54.5%. 87% were hospitalized, 91.6% needed nursery, 98.8% used supplementary O_2, and 91.6% were hospitalized in an intensive care unit. Time of hospitalization ranged from 1 to 11 days (mean ± SD: 5.95 ± 3). Furthermore, patients were not vaccinated yet. As observed on Figure 1, there were 15 deaths (8.4%) from the patients infected with COVID-19 in an eleven-months follow-up. From the 77 survivors (79.38%), 64 developed long covid (83.12%). Approximately 30% of the patients presented at least four post-covid symptoms, which the most prevalent were dyspnea and fatigue (78 and 77%, respectively). No differences were found between men and women related to post-covid syndrome ($P > 0.05$). See Figure 2

Baselines characteristics stratified by the long covid diagnosis are described on Table 1. Patients that developed long covid demonstrated higher values of phosphate and IL-10 when compared to patients without long covid. In this context, a ROC curve was generated to verify the cut-off points of the aforementioned variables as possible risk factors for long covid (Table 2).

The cut-off point stablished by the ROC curve for phosphate and IL-10 was 5.35 mg/dL and 9.75 pg/mL, respectively. Both variables seem to predict long covid in maintenance HD patients (area under the ROC curve higher than 0.50 and lower than 1.00). However, only phosphate presented a significant odds ratio (11.118%CI: 1.279 – 96.661). See Table 2. Noteworthy, IL-10 and phosphate levels from patients who did not survive were higher than the cut points proposed in the study: 11.25 ± 3.73 and 5.63 ± 0.87, respectively.

Patients with phosphate ≥ 5.35 mg/dL presented higher prevalence of long covid. Analyzing every symptom separately,

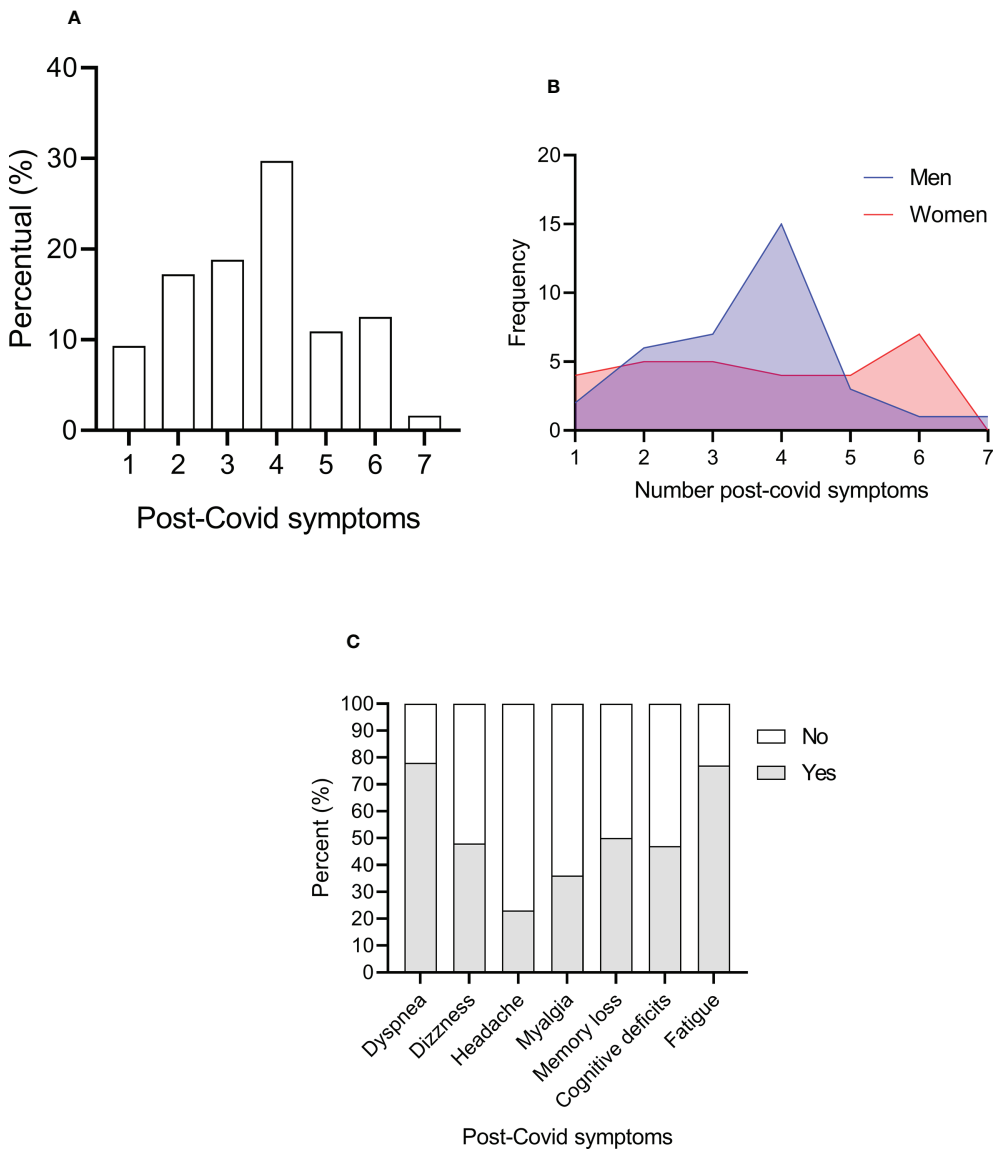

FIGURE 2
Percent of long covid symptoms **(A)**, frequency of men and women for each number of post-covid symptoms, and frequency of each symptom in hemodialysis patients **(B)**. Percent of each post-covid symptoms **(C)**.

it seems that subjects with higher values of phosphate are likely to present a higher prevalence of dyspnea and fatigue. See Table 3 and Figure 3. Correlation matrix between these variables is presented on Figure 2.

Discussion

This study sought to characterize COVID-19 infection and long COVID symptoms from our cohort of 178 Brazilians HD patients, and to identify whether baseline characteristics should predict long COVID in this sample. We found that more than 85% of the COVID-19 infected patients presented a severe condition during the infection (hospitalized, needed supplementary O_2, nursery or hospitalized in an intensity unit care). In our sample, the mortality rate over 11-month follow was relatively low (8.4%) when compared to the present literature (approximately 36%) (7). However, long COVID was highly prevalent in COVID-19 survivors representing more than 80% of all cases. A key finding of the study was the association of baseline phosphate and IL-10 with long COVID, demonstrating that higher levels of these two variables might be a risk factor for post-COVID complications. We suggested that patients with phosphate higher than 5.35 mg/dL may present an increased

10.3389/fimmu.2022.1006076

TABLE 1 Baseline characteristics stratified by the presence of long COVID.

Variables	Total (n=64)	Long COVID		*P* Value
		No (n=13)	Yes (n=64)	
Age (years)	66.8 ± 3.34	65.31 ± 4.77	67.11 ± 2.99	0.211
Body mass (kg)	75.2 ± 13.91	73.97 ± 18.49	75.82 ± 12.97	0.735
BMI (kg/m2)	26.85 ± 3	26.42 ± 3.78	27.08 ± 2.77	0.826
Waist circumference (cm)	95.66 ± 11.31	96.78 ± 14.77	95.82 ± 10.75	0.353
Fat-free mass (kg)	44.82 ± 5.07	43.23 ± 6.84	45.13 ± 4.55	0.995
Body fat (kg)	30.22 ± 9.48	30.74 ± 12.37	30.71 ± 9.18	0.842
Handgrip (kgf)	24.06 ± 6.45	22.54 ± 6.5	23.86 ± 6.73	0.519
TUG (s)	8.55 ± 2.54	9.12 ± 2.35	8.53 ± 2.47	0.432
6MWT (m)	495.34 ± 102.33	498.08 ± 128.29	491.92 ± 96.91	0.844
Hemoglobin (g/dl)	12.14 ± 1.29	11.48 ± 1.18	12.06 ± 1.41	0.242
Iron (µg/dl)	77.69 ± 20.81	81.28 ± 20.37	74.99 ± 23.65	0.447
Ferritin (ng/ml)	404.79 ± 145.58	389.39 ± 179.46	428.77 ± 151.3	0.484
Hepcidin (ng/mL)	39.76 ± 10.58	42.11 ± 10.64	37.47 ± 10.6	0.225
Phosphate (mg/dl)	5.25 ± 0.91	**4.28 ± 0.67**	**5.26 ± 0.91**	**0.003**
TNF (pg/mL)	16.46 ± 6.38	17.62 ± 6.62	17.35 ± 6.37	0.908
IL 10 (pg/mL)	9.76 ± 3.21	**6.84 ± 1.92**	**9.77 ± 3.13**	**0.007**
IL 6 (pg/mL)	3.24 ± 1	3.55 ± 1.27	3.09 ± 1.03	0.243

Independent Students T test was applied to compare groups. BMI, body mass index; TUG, timed up and go; 6MWT, six-minute walking test; TNF, tumor necrosis factor, IL, interleukin. Data expressed by mean and standard deviation. Bold values highlight statistical significances.

prevalence of long COVID, dyspnea, and fatigue. Although our sample size was not robust, these results may motivate further prospective and randomized trial to investigate deepest this relation between increased phosphate and long COVID.

In COVID-19-infected patients without CKD, higher levels of phosphate appear to be a protective factor against pulmonary damage, COVID severity, and mortality (21–24). Javdani et al. (25) suggests that hypophosphatemia is associated with severe lung injures, while increased serum phosphate may be associated with better CT scan of lung outcomes. Wang et al. (24) verified that hypophosphatemia at admission may be associated with increased mortality. Xue et al. (22) indicated that the severity of COVID-19 might be linked with lower phosphate levels. By this scenario, it would be rationale to infer those higher levels of phosphate would protect HD patients from long COVID since post-covid symptoms are likely related to COVID severity and organ damage (1, 4, 12). However, due to the decreased number of nephrons, CKD patients develop a compensate mechanism for phosphate balance characterized by the increase of fibroblast growth factor – 23 (FGF-23), parathormone, and decreased Vitamin D (Kuro-o, 2013; 26, 27). This mechanism precedes a hyperphosphatemia since the residual renal function are insufficient to excrete phosphate, leading to bone mineral disorders, inflammation, and interstitial fibrosis in HD patients (Kuro-o, 2013; 26, 27).

McGovern et al. (28) verified that higher serum phosphate concentrations (>1.5 mmol/L or >4.65 mg/dL) is associated with increased cardiovascular risk in CKD stages 3-5 (odds ratio = 2.34; 95% confidence interval = 1.64 – 3.32). This same study demonstrated that subjects without CKD could also present increased cardiovascular risk related to phosphate. Furthermore, even in normal ranges, greater serum phosphate is associated with vascular and valvular calcification in CKD patients (29). Noteworthy, HD patients hospitalized with COVID-19 seems to present hyperphosphatemia (30). Taken together, all this evidence underpins the results of the present study, suggesting higher serum phosphate as a possible predictors of persistence COVID symptoms. In this regard, further studies should address the impact of phosphate on COVID-19 prognosis, and long COVID prevalence among HD patients. Although our study did not present mechanistic insights, the role of phosphate in a worst prognosis of COVID patients with HD, might be related to an increased systemic inflammation (21, 31).

A striking feature of COVID-19 severity is the 'citokine storm' (32, 33). This phenomenon has been attributed as a clinical condition caused by an hyperactivation of immune system associated with several diseases (32). It is known that some cytokines are elevated on cytokine storm, including IL-10, TNF, and IL-6 (32, 33). Furthermore, these cytokines appear to be higher on patients infected with COVID-19 hospitalized in intensive care units (2). Although IL-10 acts as an anti-inflammatory cytokine inhibiting TNF and IL-6, it increased concentrations in cytokine storm might be likely due to insufficient counterregulatory action to the proinflammatory proteins (32). However, another hypothesis was made based on recent studies rising IL-10 as a possible proinflammatory cytokine in COVID-19 burden, but this concept must be further tested in detail (34, 35). These findings support the

10.3389/fimmu.2022.1006076

TABLE 2 Area under the ROC curve and odds ratio in presenting post-covid syndrome.

Variables	AUC ROC	95% CI	Cut-off point	Sensitivity/1-especificity	Odds ratio	95% CI
Phosphate	0.804	0.656 - 0.952	5.35 (mg/dL)	0.900/0.632	11.118	1.279 - 96.661
IL-10	0.795	0.661 - 0.929	9.75 (pg/mL)	0.900/0.600	7.286	0.838 - 63.345

TABLE 3 Long COVID according with phosphate concentrations.

Variables	Phosphate		X^2	P value
	<5.35mg/dL	≥5.35 mg/dL		
Long covid	**17 (65.4)**	**21 (95.5)**	**6.533**	**0.011**
Dyspnea	**12 (46.2)**	**20 (90.9)**	**10.741**	**0.001**
Dizziness	8 (30.8)	11 (50)	1.843	0.175
Headache	5 (50)	5 (50)	0,088	0,766
Myalgia	6 (23.1)	10 (45.5)	2.685	0.101
Cognitive deficits	7 (26.9)	8 (36.4)	0.494	0.482
Fatigue	**11 (42.3)**	**17 (77.3)**	**5.994**	**0.014**

Data expressed by n (%).
Chi-squared test was performed to compare groups. Bold values highlight statistical significances.

elevated concentrations of serum IL-10 in patients that developed long COVID presented in the present study. Suggesting that baseline IL-10 levels might be associated with post COVID symptoms. These results should encourage further researchers in identifying whether IL-10 levels could predict COVID-19 complications and long COVID.

This study presents several limitations that should be considered: first, this is a follow-up study which were not designed to analyze COVID-19 or long COVID *a priori*. However, considering the global burden of persistent COVID-19 in HD patients, this is a topic worth of investigation in the critical care of CKD patients. Second, the small sample size limits

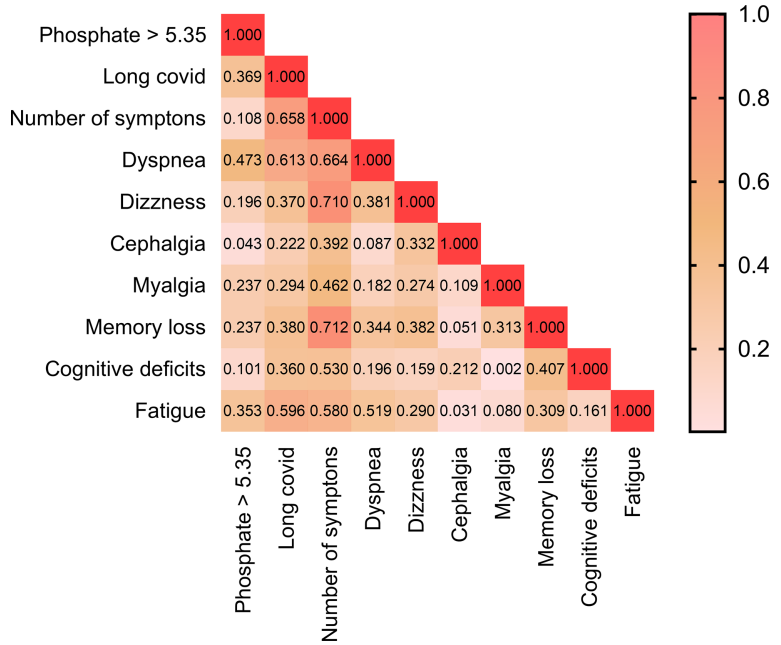

FIGURE 3
Heat map of the correlation matrix between phosphate ≥ 5.35 with each post COVID symptoms.

our inference in the general population with HD. Third, the lack of more time points of analysis limits our observation of the phenomenon. Finally, the lack of nutrition control limit our results, and we encourage further studies to control this variable. Nonetheless, to our knowledge, this is the first study that screened COVID and long COVID in HD patients and identified two possible targets (phosphate and IL10) of post-covid symptoms in this population.

In sum, there was a high prevalence of COVID-19 infection and long COVID in HD patients from the Brazilian trial 'U1111-1237-8231'. Further studies should give a special look on serum phosphate and IL-10 levels in HD patients as possible targets of persistent COVID symptoms and severity.

Data availability statement

The raw data supporting the conclusions of this article will be made available by the authors, without undue reservation.

Ethics statement

The studies involving human participants were reviewed and approved by Ethic committee of Catholic University of Brasília. The patients/participants provided their written informed consent to participate in this study.

Author contributions

HC, RN, LD, TA, AG, AR, RS, and TR: Conceptualization; HC, RN, LD, TA, AG, AR, RS, and TR: Data curation; HC: Formal analysis; CT-M and TR: Funding acquisition; HC, FH, RS, TA, DM-S, and TR: Investigation; Project administration; HC, DM-S, CT-M, CA, and TR: Roles/Writing - original draft; HC, DM-S, CA, and TR: Writing - review and editing. All authors contributed to the article and approved the submitted version.

Funding

TSR, HLC, TBA, and LAD were supported by a grant provided by the Coordenação de Aperfeiçoamento de Pessoal de Nível Superior – Brazil (CAPES) – Finance Code 001 and National Council for Scientific and Technological Development (CNPq).

Conflict of interest

The authors declare that the research was conducted in the absence of any commercial or financial relationships that could be construed as a potential conflict of interest.

Publisher's note

All claims expressed in this article are solely those of the authors and do not necessarily represent those of their affiliated organizations, or those of the publisher, the editors and the reviewers. Any product that may be evaluated in this article, or claim that may be made by its manufacturer, is not guaranteed or endorsed by the publisher.

References

1. Clark A, Jit M, Warren-Gash C, Guthrie B, Wang HHX, Mercer SW, et al. Global, regional, and national estimates of the population at increased risk of severe COVID-19 due to underlying health conditions in 2020: A modelling study. *Lancet Glob Health* (2020) 8:e1003–17. doi: 10.1016/S2214-109X(20)30264-3

2. Huang C, Wang Y, Li X, Ren L, Zhao J, Hu Y, et al. Clinical features of patients infected with 2019 novel coronavirus in Wuhan, China. *Lancet* (2020) 395:497–506. doi: 10.1016/S0140-6736(20)30183-5

3. Williamson EJ, Walker AJ, Bhaskaran K, Bacon S, Bates C, Morton CE, et al. Factors associated with COVID-19-related death using OpenSAFELY. *Nature* (2020) 584:430–6. doi: 10.1038/s41586-020-2521-4

4. Cai R, Zhang J, Zhu Y, Liu L, Liu Y, He Q. Mortality in chronic kidney disease patients with COVID-19: A systematic review and meta-analysis. *Int Urol Nephrol* (2021) 53:1623–9. doi: 10.1007/s11255-020-02740-3

5. Flythe JE, Assimon MM, Tugman MJ, Chang EH, Gupta S, Shah J, et al. Characteristics and outcomes of individuals with pre-existing kidney disease and COVID-19 admitted to intensive care units in the United States. *Am J Kidney Dis* (2021) 77:190–203.e191. doi: 10.1053/j.ajkd.2020.09.003

6. Wang R, Liao C, He H, Hu C, Wei Z, Hong Z, et al. COVID-19 in hemodialysis patients: A report of 5 cases. *Am J Kidney Dis* (2020) 76:141–3. doi: 10.1053/j.ajkd.2020.03.009

7. Carriazo S, Mas-Fontao S, Seghers C, Cano J, Goma E, Avello A, et al. Increased 1-year mortality in haemodialysis patients with COVID-19: A prospective, observational study. *Clin Kidney J* (2022) 15:432–41. doi: 10.1093/ckj/sfab248

8. Demiray A, Kanbay A, Kanbay M. Long-term effect of COVID-19 infection on hemodialysis patients: Should we follow hemodialysis patients more closely? *Clin Kidney J* (2022) 15:369–71. doi: 10.1093/ckj/sfab265

9. Ortiz A, Cozzolino M, Fliser D, Fouque D, Goumenos D, Massy ZA, et al. Chronic kidney disease is a key risk factor for severe COVID-19: A call to action by the ERA-EDTA. *Nephrol Dial Transplant* (2021) 36:87–94. doi: 10.1093/ndt/gfaa314

10. Maestre-Muñiz MM, Arias Á., Mata-Vázquez E, Martín-Toledano M, López-Larramona G, Ruiz-Chicote AM, et al. Long-term outcomes of patients with coronavirus disease 2019 at one year after hospital discharge. *J Clin Med* (2021) 10:1–15. doi: 10.3390/jcm10132945

11. Och A, Tylicki P, Polewska K, Puchalska-Reglińska E, Parczewska A, Szabat K, et al. Persistent post-COVID-19 syndrome in hemodialyzed patients-a longitudinal cohort study from the north of Poland. *J Clin Med* (2021) 10:1–10. doi: 10.3390/jcm10194451

12. Willi S, Lüthold R, Hunt A, Hänggi NV, Sejdiu D, Scaff C, et al. COVID-19 sequelae in adults aged less than 50 years: A systematic review. *Travel Med Infect Dis* (2021) 40:101995. doi: 10.1016/j.tmaid.2021.101995

13. Shah W, Hillman T, Playford ED, Hishmeh L. Managing the long term effects of covid-19: Summary of NICE, SIGN, and RCGP rapid guideline. *Bmj* (2021) 372:n136. doi: 10.1136/bmj.n136

14. Ozturk S, Turgutalp K, Arici M, Gorgulu N, Tonbul HZ, Eren N, et al. The longitudinal evolution of post-COVID-19 outcomes among hemodialysis patients in Turkey. *Kidney Int Rep* (2022) 7, 1393–1405. doi: 10.1016/j.ekir.2022.03.017

15. Gadelha AB, Cesari M, Corrêa HL, Neves RVP, Sousa CV, Deus LA, et al. Effects of pre-dialysis resistance training on sarcopenia, inflammatory profile, and anemia biomarkers in older community-dwelling patients with chronic kidney disease: a randomized controlled trial. *Int Urol Nephrol* (2021) 53:2137–47. doi: 10.1007/s11255-021-02799-6

16. Neves RVP, Corrêa HL, Deus LA, Reis AL, Souza MK, Simões HG, et al. Dynamic not isometric training blunts osteo-renal disease and improves the sclerostin/FGF23/Klotho axis in maintenance hemodialysis patients: a randomized clinical trial. *J Appl Physiol (1985)* (2021) 130:508–16. doi: 10.1152/japplphysiol.00416.2020

17. Mathiowetz V, Weber K, Volland G, Kashman N. Reliability and validity of grip and pinch strength evaluations. *J Handb Surg Am* (1984) 9:222–6. doi: 10.1016/S0363-5023(84)80146-X

18. Corrêa HL, Rosa TDS, Dutra MT, Sales MM, Noll M, Deus LA, et al. Association between dynapenic abdominal obesity and inflammatory profile in diabetic older community-dwelling patients with end-stage renal disease. *Exp Gerontol* (2021) 146:111243. doi: 10.1016/j.exger.2021.111243

19. De Luca Corrêa H, Neves RVP, Deus LA, Reis AL, Raab ATO, Rodrigues-Silva PL, et al. MicroRNA levels in hemodialysis patients following resistance training: Associations with functional performance, inflammatory profile, sestrins-2, and nitric oxide. *Exp Gerontol* (2022) 162:111761. doi: 10.1016/j.exger.2022.111761

20. Frontera JA, Yang D, Lewis A, Patel P, Medicherla C, Arena V, et al. A prospective study of long-term outcomes among hospitalized COVID-19 patients with and without neurological complications. *J Neurol Sci* (2021) 426:117486. doi: 10.1016/j.jns.2021.117486

21. Yamada S, Tokumoto M, Tatsumoto N, Taniguchi M, Noguchi H, Nakano T, et al. Phosphate overload directly induces systemic inflammation and malnutrition as well as vascular calcification in uremia. *Am J Physiol Renal Physiol* (2014) 306:F1418–1428. doi: 10.1152/ajprenal.00633.2013

22. Xue X, Ma J, Zhao Y, Zhao A, Liu X, Guo W, et al. Correlation between hypophosphatemia and the severity of corona virus disease 2019 patients. *MedRxiv.* (2020). doi: 10.1101/2020.03.27.20040816

23. Van Kempen T, Deixler E. SARS-CoV-2: influence of phosphate and magnesium, moderated by vitamin d, on energy (ATP) metabolism and on severity of COVID-19. *Am J Physiol Endocrinol Metab* (2021) 320:E2–e6. doi: 10.1152/ajpendo.00474.2020

24. Wang R, He M, Kang Y. Hypophosphatemia at admission is associated with increased mortality in COVID-19 patients. *Int J Gen Med* (2021) 14:5313–22. doi: 10.2147/IJGM.S319717

25. Javdani F, Parsa S, Shakeri H, Hatami N, Kalani N, Haghbeen M, et al. Phosphate levels and pulmonary damage in COVID-19 patients based on CO-RADS scheme: Is there any link between parathyroid gland and COVID-19? *MedRxiv.* (2020). doi: 10.1101/2020.08.25.20181453

26. Kuro OM. The klotho proteins in health and disease. *Nat Rev Nephrol* (2019) 15:27–44. doi: 10.1038/s41581-018-0078-3

27. Kuro-O M. Klotho, phosphate and FGF-23 in ageing and disturbed mineral metabolism. *Nat Rev Nephrol* (2013) 9:650–60. doi: 10.1038/nrneph.2013.111

28. Mcgovern AP, De Lusignan S, Van Vlymen J, Liyanage H, Tomson CR, Gallagher H, et al. Serum phosphate as a risk factor for cardiovascular events in people with and without chronic kidney disease: A large community based cohort study. *PloS One* (2013) 8:e74996. doi: 10.1371/journal.pone.0074996

29. Adeney KL, Siscovick DS, Ix JH, Seliger SL, Shlipak MG, Jenny NS, et al. Association of serum phosphate with vascular and valvular calcification in moderate CKD. *J Am Soc Nephrol* (2009) 20:381–7. doi: 10.1681/ASN.2008040349

30. Malieckal DA, Uppal NN, Ng JH, Jhaveri KD, Hirsch JS. Electrolyte abnormalities in patients hospitalized with COVID-19. *Clin Kidney J* (2021) 14:1704–7. doi: 10.1093/ckj/sfab060

31. Komaba H, Fukagawa M. Phosphate-A poison for humans? *Kidney Int* (2016) 90:753–63. doi: 10.1016/j.kint.2016.03.039

32. Fajgenbaum DC, June CH. Cytokine storm. *N Engl J Med* (2020) 383:2255–73. doi: 10.1056/NEJMra2026131

33. Karki R, Kanneganti TD. The 'cytokine storm': Molecular mechanisms and therapeutic prospects. *Trends Immunol* (2021) 42:681–705. doi: 10.1016/j.it.2021.06.001

34. Lu L, Zhang H, Zhan M, Jiang J, Yin H, Dauphars DJ, et al. Preventing mortality in COVID-19 patients: Which cytokine to target in a raging storm? *Front Cell Dev Biol* (2020) 8:677. doi: 10.3389/fcell.2020.00677

35. Lu L, Zhang H, Dauphars DJ, He YW. A potential role of interleukin 10 in COVID-19 pathogenesis. *Trends Immunol* (2021) 42:3–5. doi: 10.1016/j.it.2020.10.012

frontiers | Frontiers in Immunology

TYPE Original Research
PUBLISHED 13 October 2022
DOI 10.3389/fimmu.2022.980698

Check for updates

OPEN ACCESS

EDITED BY
Torsten Feldt,
University Hospital of
Düsseldorf, Germany

REVIEWED BY
Barbara Seitz-Polski,
University of Nice Sophia
Antipolis, France
Stephen Rawlings,
Maine Health, United States

*CORRESPONDENCE
Adalbert Krawczyk
Adalbert.krawczyk@uk-essen.de
Hana Rohn
Hana.rohn@uk-essen.de

†These authors have contributed equally to this work and share first authorship

‡These authors have contributed equally to this work and share last authorship

SPECIALTY SECTION
This article was submitted to Viral Immunology, a section of the journal Frontiers in Immunology

RECEIVED 28 June 2022
ACCEPTED 26 September 2022
PUBLISHED 13 October 2022

CITATION
Thümmler L, Konik M, Lindemann M, Fisenkci N, Koldehoff M, Gäckler A, Horn PA, Theodoropoulos F, Taube C, Zettler M, Anastasiou OE, Braß P, Jansen S, Witzke O, Rohn H and Krawczyk A (2022) Long-term cellular immune response in immunocompromised unvaccinated COVID-19 patients undergoing monoclonal antibody treatment. *Front. Immunol.* 13:980698. doi: 10.3389/fimmu.2022.980698

Long-term cellular immune response in immunocompromised unvaccinated COVID-19 patients undergoing monoclonal antibody treatment

Laura Thümmler[1,2†], Margarethe Konik[1†], Monika Lindemann[2], Neslinur Fisenkci[2], Michael Koldehoff[3,4], Anja Gäckler[5], Peter A. Horn[2], Fotis Theodoropoulos[6], Christian Taube[6], Markus Zettler[1], Olympia Evdoxia Anastasiou[7], Peer Braß[1], Sarah Jansen[1], Oliver Witzke[1], Hana Rohn[1*‡] and Adalbert Krawczyk[1,7*‡]

[1]Department of Infectious Diseases, West German Centre of Infectious Diseases, University Medicine Essen, University Hospital Essen, University Duisburg-Essen, Essen, Germany, [2]Institute for Transfusion Medicine, University Medicine Essen, University Hospital Essen, University Duisburg-Essen, Essen, Germany, [3]Department of Hematology and Stem Cell Transplantation, University Medicine Essen, University Hospital Essen, University of Duisburg-Essen, Essen, Germany, [4]Department of Hygiene and Environmental Medicine, University Medicine Essen, University Hospital Essen, University of Duisburg-Essen, Essen, Germany, [5]Department of Nephrology, University Medicine Essen, University Hospital Essen, University of Duisburg-Essen, Essen, Germany, [6]Department of Pneumology, University Medicine Essen-Ruhrlandklinik, University Duisburg- Essen, Essen, Germany, [7]Institute for Virology, University Medicine Essen, University Hospital Essen, University Duisburg-Essen, Essen, Germany

Immunocompromised patients are at increased risk for a severe course of COVID-19. Treatment of severe acute respiratory syndrome coronavirus-2 (SARS-CoV-2) infection with anti-SARS-CoV-2 monoclonal antibodies (mAbs) has become widely accepted. However, the effects of mAb treatment on the long-term primary cellular response to SARS-CoV-2 are unknown. In the following study, we investigated the long-term cellular immune responses to SARS-CoV-2 Spike S1, Membrane (M) and Nucleocapsid (N) antigens using the ELISpot assay in unvaccinated, mAb-treated immunocompromised high-risk patients. Anti-SARS-CoV-2 mAb untreated though vaccinated COVID-19 immunocompromised patients, vaccinated SARS-CoV-2 immunocompromised patients without COVID-19 and vaccinated healthy control subjects served as control groups. The cellular immune response was determined at a median of 5 months after SARS-CoV-2 infection. Our data

suggest that immunocompromised patients develop an endogenous long-term cellular immune response after COVID-19, although at low levels. A better understanding of the cellular immune response will help guide clinical decision making for these vulnerable patient cohorts.

KEYWORDS

COVID-19, immunosuppression, SARS-CoV-2, monoclonal antibody treatment, cellular immune response

Introduction

The severe acute respiratory syndrome coronavirus 2 (SARS-CoV-2) has caused a pandemic of coronavirus disease 2019 (COVID-19), resulting in more than 530 million infected people and 6.3 million deaths (June 2022). Despite the availability of vaccines, the pandemic remains a global health burden (1). Many risk factors for the progression of COVID-19 to a severe and critical stage have been identified, including age, underlying comorbidities such as diabetes, obesity, chronic lung diseases, and immunodeficiency (2–4). Primary SARS-CoV-2 infections as well as breakthrough infections represent a potential risk for these vulnerable groups (5) resulting in a high burden of morbidity and mortality (6). During the early pandemic, COVID-19 patients were treated with SARS-CoV-2 convalescent plasma. Numerous studies were conducted, indicating that early onset of antiviral treatment is necessary to improve the course of disease and protect against a severe outcome (7–10). Later, monoclonal antibodies (mAb) against SARS-CoV-2 became available (11). Early treatment of SARS-CoV-2 infections with mAbs such as bamlanivimab (12) or a combination of the monoclonal antibodies casirivimab and imdevimab (11) has been shown to markedly reduce the risk of hospitalization or death among high-risk patients with COVID-19 (11, 12). However, the occurrence of novel SARS-CoV-2 variants of concern (VOCs) such as Alpha (Pango nomenclature B.1.1.7), Beta (B.1.351), Gamma (P1, B.1.1.28), Delta (B.1.617.2) and Omicron (B.1.1.529) led to an increase in the frequency of reinfection and vaccination breakthrough SARS-CoV-2 infections (3, 13, 14). Some of the mutations within the SARS-CoV-2 spike antigen are associated with immune escape, and thus a reduced effectivity of monoclonal antibodies against SARS-CoV-2 spike protein variants (15, 16). However, a recent study suggests that monoclonal antibody treatment, with respect to available antibody formulations and circulating viral variants, may provide favorable outcomes for mild to moderate COVID-19 in vulnerable patients, such as solid organ recipients (17).

Although the role of antibodies induced by immunization or additionally administrated early upon infection in those patients was already described, less is known about the cellular immune response in immunocompromised patients with primary or breakthrough infections and antibody treatment (18).

In the present study, we investigated the long-term cellular immune response in severely immunocompromised unvaccinated patients suffering from a SARS-CoV-2 infection and treated with the mAb bamlanivimab or a combination of the mAbs casirivimab and imdevimab in the early phase of infection. We compared the cellular immune response of these patients with those of vaccinated immunocompromised patients with a SARS-CoV-2 infection but without antibody treatment as well as vaccinated immunocompromised patients and immunocompetent volunteers without SARS-CoV-2 infection.

Methods

Study subjects and sampling

In the present study, we investigate the long-term cellular immune response against SARS-CoV-2 spike (S), Membrane (M) and Nucleocapsid (N) antigens in immunocompromised patients with primary SARS-CoV-2 infection after early mAb treatment (group 1) up to 5 months after COVID-19. Vaccinated immunocompromised patients with COVID-19 (group 2), as well as vaccinated immunocompromised patients (group 3) and vaccinated healthy volunteers (group 4) without COVID-19 served as controls. All immunocompromised patients (group 1-3) had a medical condition associated with secondary severe immunodeficiency. Patients suffering from a primary SARS-CoV-2 infection (group 1) were treated early with monoclonal antibodies (mAbs) bamlanivimab (LY-CoV555, Eli Lilly) or casirivimab/imdevimab (Ronapreve, Roche and Regeneron), which both bind to the SARS-CoV-2 spike protein. Group 1 included 12 non-vaccinated patients. Of the 12 patients, 8 were treated with 700 mg bamlanivimab (concentration 35 mg/ml) and 4 with a combination of 1200 mg casirivimab/imdevimab (concentration of 120 mg/ml each). Antibodies were administrated intravenously. The group consisted of 2 men and 10 women, and the median age was 57 years (range 31-78). The cellular immune response in the first

group was examined at a median of 146 days (range 74-182) after mAb therapy. One of the patients had breast cancer, three had a kidney transplantation (median since transplantation 5.6 years, range 4 months – 10 years), seven had a lung transplantation (median since transplantation 10.2 months, range 4 - 25 months), one prostate cancer and one cachexia. In this first group, the three kidney transplant patients had concomitant arterial hypertension and an impaired renal function. In the lung transplant recipient group, one patient had coronary artery disease as an additional risk factor for a severe COVID-19 course. Except for one patient, all solid organ transplant patients had triple immunosuppressive therapy containing prednisone, the calcineurin inhibitor (CNI) tacrolimus, and mycophenolic acid (MMF) or the mTOR inhibitor everolimus. One renal transplant patient had triple immunosuppressive therapy containing prednisolone, MMF, and belatacept.

Group 2 included 10 immunocompromised, vaccinated patients with a SARS-CoV-2 infection. All patients were vaccinated with an mRNA vaccine (BioNTech or Moderna). The group was composed of seven men and three women and the median age was 59 years (range 20-69) after hematopoietic stem cell transplantation (HSCT). HSCT took place at a median of 2.9 years (range 0.9-17) prior to blood collection and all patients achieve complete remission of their underlying hematologic malignancy. Three patients had coronary artery disease as additional COVID-19 risk factor, one patient had grade I obesity, and one had a history of chronic obstructive pulmonary disease and splenectomy. 7 patients had developed graft versus host disease (GVHD) after HSCT and were treated immunosuppressive with steroids with or without CNI for this purpose. One patient received an mTor inhibitor plus steroids. The cellular immune response was explored at a median of 145 days (range 61-230) after infection.

Group 3 included 14 immunocompromised, vaccinated patients without SARS-CoV-2 infection. All patients were vaccinated with an mRNA vaccine (n=13 Comirnaty, BioNTech/Pfizer; n=1 Spikevax, Moderna). The group contained six men and eight women with a median age of 55 years (range 21-64). Of the 14 patients, four had a HSCT a median of 4.3 years (range 1.3-16.1) prior to testing and ten had a kidney transplant at a median of 3.1 years (range 0.09-10.5) prior to blood collection. The cellular immune response in this group was examined at a median of 87 days (range 16-238) after vaccination. 3 HSCT patients were on dual immunosuppressive therapy (steroid, with CNI or MMF) because of persistent GVHD; one patient had additional arterial hypertension and diabetes mellitus as risk factors for severe COVID-19 progression. All except one kidney transplant recipients had concomitant arterial hypertension and impaired renal function and received triple immunosuppressive therapy with prednisolone, MMF, and CNI. One patient received triple immunosuppressive therapy with prednisolone, MMF, and belatacept.

Group 4 included 14 healthy volunteers after the third SARS-CoV-2 vaccination with an mRNA SARS-CoV-2 vaccine (n=3 Comirnaty, BioNTech/Pfizer; n=11 Spikevax, Moderna). The group was composed of six men and eight women and the median age was 50 years (range 29-65). They were tested at a median of 47 days (range 30-72) after the third vaccination.

There were no significant differences between the different cohorts with respect to the known COVID-19 related risk factors being sex, age, and lymphocyte count (Table 1).

The study was conducted according to the Helsinki principles and was approved by the local ethics committee of the University Hospital Essen, Germany (20-9225-BO, 20-9254-BO, and 20-9374-BO). All subjects provided informed consent to participate in the study.

T cell ELISpot assays for S1-, M-, and N-derived SARS-CoV-2 peptides

To analyze SARS-CoV-2 specific cellular immune responses, we performed interferon gamma (IFN-γ) enzyme-linked immunospot (ELISpot) assays as previously described (19). 250,000 peripheral blood mononuclear cells (PBMC) were cultured in the presence or absence of the PepTivator® SARS-CoV-2 membrane (M) protein, nucleocapsid (N) protein (600 pmol/mL of each peptide, Miltenyi Biotec, Bergisch Gladbach, Germany) or the S1 protein (4 µg/ml, Sino Biological, Wayne, PA, USA) (each in single cell culture) in 150 µL of AIM-V®. The peptide mixes corresponding to the M and N proteins cover the complete sequence of the glycoproteins. The S1 protein is a recombinant protein expressed in HEK293 cells and covers the sequence of aa 1 to aa 692 of the spike protein subunit 1. The peptide pools consisted of 15-mer sequences with an overlap of 11 amino acids. After 19 h of incubation at 37°C, IFN-γ production was measured as previously described (19). The spot numbers were evaluated by an ELISpot reader (AID Fluorospot; Autoimmun Diagnostika GmbH, Strassberg, Germany). From duplicate cell cultures, the mean value was considered. SARS-CoV-2 specific spots were determined as stimulated minus non-stimulated values (spot increment). The negative controls had an average of 0.21 spots (range 0-3) and their three-fold standard deviation was 3 x 0.67 spots = 2.01 spots (which we considered as background for the negative controls). As we used increment values, a three-fold higher value versus background means 3 x 2.01 spots minus 1 x 2.01 spots, which is 4.02 spots increment. We therefore chose a cut-off point of 4 as positivity.

Statistical analysis

Statistical analysis was performed using GraphPad Prism 9.3.1 software (San Diego, CA, USA). We used the Kruskal-

10.3389/fimmu.2022.980698

TABLE 1 Overview of the study cohort.

group	1	2	3	4	p-value
Antibody therapy? (Y: yes, N: no)	Y	N	N	N	
Infected? (Y: yes, N: no)	Y	Y	N	N	
Vaccinated? (Y: yes, N: no)	N	Y	Y	Y	
Severely Immunocompromised? (Y: yes, N: no)	Y	Y	Y	N	
Total number	12	10	14	14	
number of women	10	3	8	8	$p = 0.09$
number of men	2	7	6	6	
median age [years] (range)	57 (31-78)	59 (20-69)	55 (21-64)	50 (29-65)	$p = 0.23$
Count of lymphocytes [x103/µl] Mean (SD)	8.8 (6.4)	9.6 (13.0)	14.1 (5.8)	12.1 (5.0)	$p = 0.29$
Interval infection/vaccination – blood collection Mean (range)	146 days (74-182)	145 days (61-230)	87 days (16-238)	47 days (30-72)	$p< 0.001$
SARS-CoV-2 vairant or SARS-CoV-2 vaccine	SARS-CoV- 2 D614G (wild type)	SARS-CoV- 2 D614G (wild type) 8x Comirnaty® (BioNTech/ Pfizer) 2x Spikevax® (Moderna)	13x Comirnaty® (BioNTech/ Pfizer) 1x Spikevax® (Moderna)	3x Comirnaty® (BioNTech/ Pfizer) 11x Spikevax® (Moderna)	
Number of SARS-CoV-2 vaccinations	0	2	2	3	

Characteristics of the four different study groups. Groups 1-3 include the different cohorts of patients in terms of monoclonal antibody treatment, SARS-CoV-2 infection, and SARS-CoV-2 vaccination; group 4 represents the healthy control group (SARS-CoV-2 vaccination, without SARS-CoV-2 infection). Comparison between COVID-19 related risk factors sex, age and lymphocyte counts was performed using the Kruskal Wallis test. Statistical significance was set at the level of $p < 0.05$.

Wallis-test and the Mann-Whitney U test for numerical variables. Fisher's exact test was used for categorical variables. Two-sided p values < 0.05 were considered significant.

Results

In the present study, we examined the long-term cellular immune response unvaccinated severely immunocompromised patients suffering from a SARS-CoV-2 infection after treatment with bamlanivimab or a combination of the monoclonal antibodies casirivimab and imdevimab early after infection using ELISpot assay. We also investigated the cellular immune response in vaccinated immunocompromised patients after SARS-CoV-2 infection as well as in vaccinated immunocompromised patients and immunocompetent volunteers without a history of SARS-CoV-2 infection.

Unvaccinated immunocompromised patients with SARS-CoV-2 infection and early mAb treatment (group 1) showed a similar cellular immune response to all stimuli in the ELISpot assay to vaccinated immunocompromised patients with a SARS-CoV-2 infection (group 2) (Figures 1A–C). The measured mean values of spots increment after stimulation with spike S1 protein were 2.1 in group 1 and 2.8 in group 2 ($p = 0.2$) (Figure 1A), after stimulation with M protein 2.0 in group 1 and 7.9 in group 2 ($p = 0.09$) (Figure 1B) and after stimulation with N protein 6.1 in group 1 and 6.2 in group 2 ($p = 0.2$) (Figure 1C). In particular, the cellular immune response in group 1 and 2 was higher than in vaccinated immunocompromised patients (group 3) (Figures 1A–C). Significant differences in spots increment were observed between group 2 and 3 after stimulation with S1 protein (2.8 in group 2 and 1.1 in group 3 ($p = 0.04$)) (Figure 1A) and N protein (6.2 in group 2 and 0.6 in group 3 ($p = 0.002$)) (Figure 1C). As expected, healthy immunocompetent vaccinated volunteers (group 4) showed a higher cellular immune response than vaccinated immunocompromised patients (group 3) (Figure 1A). The spots increment after stimulation with the spike S1 protein were 1.1 in group 3 and 3.8 in group 4 ($p = 0.01$) (Figure 1A). No significant differences between groups 3 and 4 could be observed after stimulation with M protein (3.7 in group 3 and 1.1 in group 4 ($p = 0.5$) or N protein (0.6 in group 3 and 0.9 in group 4 ($p = 0.6$) (Figures 1B, C).

Interestingly, after mAb treatment (group 1), the frequency of single and combined positive cellular response to S1, M, or N proteins was lower than in the vaccinated cohort with SARS-CoV-2 infection (group2) (S1: 14% vs. 30%; M: 21% vs. 50%; N: 14% vs. 30%, combined: 33% vs. 60% statistically not significant as calculated with the Fischer´s exact test). In the groups

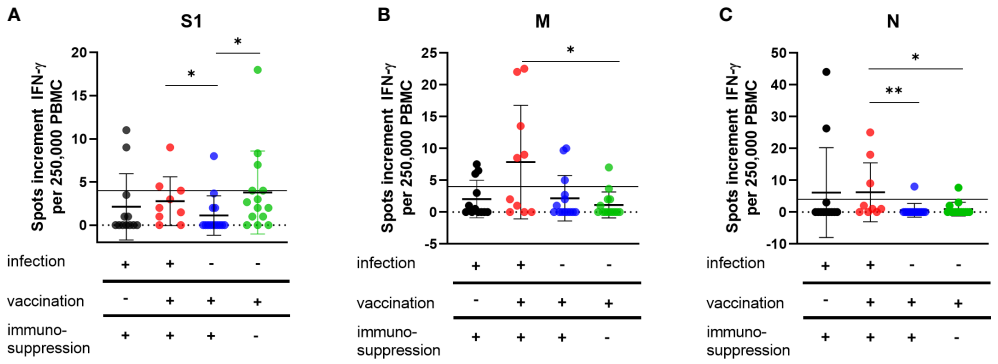

FIGURE 1
Cellular immunity to SARS-CoV-2 antigens in vaccinated and/or recovered immunosuppressed individuals. Cellular immune responses towards SARS-CoV-2 S1 **(A)**, M **(B)** and N **(C)** antigens were determined by IFN-γ ELISpot assay. Please note that the scales differ. Horizontal lines indicate mean values, error bars indicate the standard deviation (SD). The dotted gray line represents the assay cut-off. Differences between the groups were compared by Mann-Whitney U test (*$p < 0.05$).

vaccinated against SARS-CoV-2 without COVID-19, only one of 14 immunocompromised patients (group 3) developed a positive response to S1 (7%), compared with 5 of 14 (35%) in the volunteer group (group 4). Immune responses against the M antigen could be detected in three volunteers from group 3 and two from group 4 and against the N antigen in one volunteer from group 3 and 4, respectively. All of these volunteers had no documented SARS-CoV-2 infection.

Discussion

In this paper, we present the profiling of cellular immunity in a cohort of immunocompromised, unvaccinated patients who developed COVID-19 and thus were treated with bamlanivimab or with the combination therapy casirivimab and indevimab. A cohort of immunocompromised patients vaccinated against SARS-CoV-2 who developed COVID-19, as well as immunized immunocompromised patients or healthy participants without COVID-19, served as controls. Our data suggest that immunocompromised patients may develop an endogenous long-term cellular immune response after COVID-19. The observed T cell-mediated immunity against the spike protein in unvaccinated immunocompromised patients after mAb therapy, seems to be blunted compared to vaccinated and mAb untreated immunocompromised patients with COVID-19. Consistent with this finding, cellular immune responses in our patient cohort were lower after mAb treatment compared with previously published results from immunosuppressed cohorts after COVID-19 but without mAb treatment (20–24).

Early treatment of SARS-CoV-2 infection in high-risk cohorts with mAbs is widely accepted, and mAbs clinical trials have reported overall reduced hospitalization rates in patients with mild to moderate COVID-19 (25–29). While many studies focused on the clinical efficacy of the treatment, its effects on long-term immunologic responses to the virus are largely unknown (12, 17, 30–33). The optimal use of these therapeutic options requires a sophisticated understanding of their effects on both the virus and the host immune system. For a long time, anti-SARS-CoV-2 T cell immunity was considered less important than specific antibodies as a parameter for immune protection in patients at risk of severe COVID-19 (34). However, the humoral anti-SARS-CoV-2 response declines over time, whereas SARS-CoV-2-specific T cell immunity appears to persist longer, even in seronegative convalescents (35–38). To our knowledge, no study has explored the effect of mAb treatment on cellular immunity in severely immunocompromised patients at risk for severe COVID-19 and only two studies explored the effect of treatment on humoral immunity (39, 40). Both studies demonstrated that passive immunization of COVID-19 patients with anti-S monoclonal IgG preparations profoundly suppressed the induction of the endogenous anti-S IgM response and, to a lesser extent, the anti-N IgG response. It is noteworthy that not only immunosuppressed patients were included in those analyses, as these patients would likely exhibit a reduced immune response due to immunosuppression (41–45). Anti-SARS-CoV-2 mAb preparations are reportedly able to reduce viral load (46, 47). Reduction of viral load in the early stage of infection might be expected to result in reduced immune responses. Additionally, stronger SARS-CoV-2 specific T cell responses are well documented in patients who had recovered from more severe symptoms of COVID-19 (48–51). Therefore, it seems possible that after mAbs treatment, the improvement in COVID-19 course is causative of the decreased immunologic response.

Conclusion

Most of the immunosuppressed, non-vaccinated COVID-19 patients treated with monoclonal antibodies within the present study developed no SARS-CoV-2 specific T-cell response. The adaptive immune response is an important factor in the clinical course after SARS-CoV-2 infection and may protect from reinfections. Deeper immunophenotyping of immunocompromised patients after mAb therapy will be important in expanding knowledge about long-term immunity to SARS-CoV-2. Its understanding is not only essential to evaluate the potential effect of COVID-19 treatment on future reinfection but also crucial for further risk assessment especially in the high-risk cohort of immunocompromised patients.

Data availability statement

The raw data supporting the conclusions of this article will be made available by the authors, without undue reservation.

Ethics statement

The study was conducted according to the Helsinki principles and was approved by the local ethics committee of the University Hospital Essen, Germany (20-9225-BO, 20-9254-BO, and 20-9374-BO). All subjects provided informed consent to participate in the study.

Author contributions

Conceptualization, MaK, ML, HR, OW, PAH, and AK; methodology, LT, MaK, AG, FT, and CT; validation, AK, HR, and OW; investigation, LT, NF, PB, and SJ; resources, MaK, MiK, AG, CT, and MZ; data curation, LT, MZ, OA, and OW; writing—original draft preparation, LT, HR, and AK; writing—review and editing, LT, HR, ML, and AK; visualization, LT, HR, and AK; supervision, HR and AK; funding acquisition, OW, HR, and AK. All authors have read and agreed to the published version of the manuscript.

Funding

OW received funding from the Rudolf Ackermann-Stiftung, AK and HR received funding from the Stiftung Universitätsmedizin Essen. The publication is support by the Open Access Publication Fund of the University of Duisburg-Essen.

Acknowledgments

We feel deep gratitude to the patients who donated their blood samples and clinical data for this project.

Conflict of interest

The authors declare that the research was conducted in the absence of any commercial or financial relationships that could be construed as a potential conflict of interest.

Publisher's note

All claims expressed in this article are solely those of the authors and do not necessarily represent those of their affiliated organizations, or those of the publisher, the editors and the reviewers. Any product that may be evaluated in this article, or claim that may be made by its manufacturer, is not guaranteed or endorsed by the publisher.

References

1. Gebru AA, Birhanu T, Wendimu E, Ayalew AF, Mulat S, Abasimel HZ, et al. Global burden of COVID-19: Situational analyis and review. *Hum Antibodies* (2021) 29:139–48. doi: 10.3233/HAB-200420

2. Gao YD, Ding M, Dong X, Zhang JJ, Kursat Azkur A, Azkur D, et al. Risk factors for severe and critically ill COVID-19 patients: A review. *Allergy* (2021) 76:428–55. doi: 10.1111/all.14657

3. Van Der Straten K, Van Gils MJ, De Taeye SW, De Bree GJ. Optimization of anti-SARS-CoV-2 neutralizing antibody therapies: Roadmap to improve clinical effectiveness and implementation. *Front Med Technol* (2022) 4:867982. doi: 10.3389/fmedt.2022.867982

4. Wunsch K, Anastasiou OE, Alt M, Brochhagen L, Cherneha M, Thummler L, et al. COVID-19 in elderly, immunocompromised or diabetic patients-from immune monitoring to clinical management in the hospital. *Viruses* (2022) 14:1–17. doi: 10.3390/v14040746

5. Lipsitch M, Krammer F, Regev-Yochay G, Lustig Y, Balicer RD. SARS-CoV-2 breakthrough infections in vaccinated individuals: measurement, causes and impact. *Nat Rev Immunol* (2022) 22:57–65. doi: 10.1038/s41577-021-00662-4

6. Caillard S, Chavarot N, Francois H, Matignon M, Greze C, Kamar N, et al. Is COVID-19 infection more severe in kidney transplant recipients? *Am J Transplant* (2021) 21:1295–303. doi: 10.1111/ajt.16424

7. Duan K, Liu B, Li C, Zhang H, Yu T, Qu J, et al. Effectiveness of convalescent plasma therapy in severe COVID-19 patients. *Proc Natl Acad Sci USA* (2020) 117:9490–6. doi: 10.1073/pnas.2004168117

8. Fischer JC, Zanker K, Van Griensven M, Schneider M, Kindgen-Milles D, Knoefel WT, et al. The role of passive immunization in the age of SARS-CoV-2: an update. *Eur J Med Res* (2020) 25:16. doi: 10.1186/s40001-020-00414-5

9. Liu STH, Lin HM, Baine I, Wajnberg A, Gumprecht JP, Rahman F, et al. Convalescent plasma treatment of severe COVID-19: a propensity score-matched control study. *Nat Med* (2020) 26:1708–13. doi: 10.1038/s41591-020-1088-9

10. Lindemann M, Lenz V, Knop D, Klump H, Alt M, Aufderhorst UW, et al. Convalescent plasma treatment of critically ill intensive care COVID-19 patients. *Transfusion* (2021) 61, 1394–403. doi: 10.1111/trf.16392

11. O'brien MP, Forleo-Neto E, Musser BJ, Isa F, Chan KC, Sarkar N, et al. Subcutaneous REGEN-COV antibody combination to prevent covid-19. *N Engl J Med* (2021) 385:1184–95. doi: 10.1056/NEJMoa2109682

12. Chen P, Nirula A, Heller B, Gottlieb RL, Boscia J, Morris J, et al. SARS-CoV-2 neutralizing antibody LY-CoV555 in outpatients with covid-19. *N Engl J Med* (2021) 384:229–37. doi: 10.1056/NEJMoa2029849

13. Klompas M. Understanding breakthrough infections following mRNA SARS-CoV-2 vaccination. *JAMA* (2021) 326:2018–20. doi: 10.1001/jama.2021.19063

14. Townsend JP, Hassler HB, Wang Z, Miura S, Singh J, Kumar S, et al. The durability of immunity against reinfection by SARS-CoV-2: a comparative evolutionary study. *Lancet Microbe* (2021) 2:e666–75. doi: 10.1016/S2666-5247(21)00219-6

15. Weisblum Y, Schmidt F, Zhang F, Dasilva J, Poston D, Lorenzi JCC, et al. Escape from neutralizing antibodies by SARS-CoV-2 spike protein variants. *eLife* (2020) 9:1–31. doi: 10.7554/eLife.61312.sa2

16. Harvey WT, Carabelli AM, Jackson B, Gupta RK, Thomson EC, Harrison EM, et al. SARS-CoV-2 variants, spike mutations and immune escape. *Nat Rev Microbiol* (2021) 19:409–24. doi: 10.1038/s41579-021-00573-0

17. Sarrell BA, Bloch K, El Chediak A, Kumm K, Tracy K, Forbes RC, et al. Monoclonal antibody treatment for COVID-19 in solid organ transplant recipients. *Transpl Infect Dis* (2022) 24:e13759. doi: 10.1111/tid.13759

18. Al Jurdi A, Gassen RB, Borges TJ, Solhjou Z, Hullekes FE, Lape IT, et al. Non-invasive monitoring for rejection in kidney transplant recipients after SARS-CoV-2 mRNA vaccination. *Front Immunol* (2022) 13:838985. doi: 10.3389/fimmu.2022.838985

19. Schwarzkopf S, Krawczyk A, Knop D, Klump H, Heinold A, Heinemann FM, et al. Cellular immunity in COVID-19 convalescents with PCR-confirmed infection but with undetectable SARS-CoV-2-Specific IgG. *Emerg Infect Dis* (2021) 27:122–9. doi: 10.3201/2701.203772

20. Bertrand D, Hamzaoui M, Drouot L, Lamulle J, Hanoy M, Edet S, et al. SARS-CoV-2-specific humoral and cellular immunities in kidney transplant recipients and dialyzed patients recovered from severe and nonsevere COVID-19. *Transplant Direct* (2021) 7:e792. doi: 10.1097/TXD.0000000000001230

21. Candon S, Guerrot D, Drouot L, Lemoine M, Lebourg L, Hanoy M, et al. T Cell and antibody responses to SARS-CoV-2: Experience from a French transplantation and hemodialysis center during the COVID-19 pandemic. *Am J Transplant* (2021) 21:854–63. doi: 10.1111/ajt.16348

22. Fava A, Donadeu L, Sabe N, Pernin V, Gonzalez-Costello J, Llado L, et al. SARS-CoV-2-specific serological and functional T cell immune responses during acute and early COVID-19 convalescence in solid organ transplant patients. *Am J Transplant* (2021) 21:2749–61. doi: 10.1111/ajt.16570

23. Qiu L, Zhang J, Huang Y, Chen G, Chen Z, Ming C, et al. Long-term clinical and immunological impact of severe COVID-19 on a living kidney transplant recipient - a case report. *Front Immunol* (2021) 12:741765. doi: 10.3389/fimmu.2021.741765

24. Thieme CJ, Anft M, Paniskaki K, Blazquez-Navarro A, Doevelaar A, Seibert FS, et al. The magnitude and functionality of SARS-CoV-2 reactive cellular and humoral immunity in transplant population is similar to the general population despite immunosuppression. *Transplantation* (2021) 105:2156–64. doi: 10.1097/TP.0000000000003755

25. Chen X, Li R, Pan Z, Qian C, Yang Y, You R, et al. Human monoclonal antibodies block the binding of SARS-CoV-2 spike protein to angiotensin converting enzyme 2 receptor. *Cell Mol Immunol* (2020) 17:647–9. doi: 10.1038/s41423-020-0426-7

26. Chen P, Datta G, Grace Li Y, Chien J, Price K, Chigutsa E, et al. First-in-Human study of bamlanivimab in a randomized trial of hospitalized patients with COVID-19. *Clin Pharmacol Ther* (2021) 110:1467–77. doi: 10.1002/cpt.2405

27. Kreuzberger N, Hirsch C, Chai KL, Tomlinson E, Khosravi Z, Popp M, et al. SARS-CoV-2-neutralising monoclonal antibodies for treatment of COVID-19. *Cochrane Database Syst Rev* (2021) 9:CD013825. doi: 10.1002/14651858.CD013825.pub2

28. Taylor PC, Adams AC, Hufford MM, de la Torre I, Winthrop K, Gottlieb RL. Neutralizing monoclonal antibodies for treatment of COVID-19. *Nat Rev Immunol* (2021) 21:382–93. doi: 10.1038/s41577-021-00542-x

29. Yetmar ZA, Beam E, O'horo JC, Ganesh R, Bierle DM, Brumble L, et al. Monoclonal antibody therapy for COVID-19 in solid organ transplant recipients. *Open Forum Infect Dis* (2021) 8:ofab255. doi: 10.1093/ofid/ofab255

30. Weinreich DM, Sivapalasingam S, Norton T, Ali S, Gao H, Bhore R, et al. REGN-COV2, a neutralizing antibody cocktail, in outpatients with covid-19. *N Engl J Med* (2021) 384:238–51. doi: 10.1056/NEJMoa2035002

31. Bachmann F, Budde K, Suttorp N, Lingscheid T, Stegemann MS, Osmanodja B, et al. Initial experience with SARS-CoV-2-Neutralizing monoclonal antibodies in kidney or combined kidney-pancreas transplant recipients. *Transpl Int* (2022) 35:10109. doi: 10.3389/ti.2022.10109

32. Roberts SC, Foppiano Palacios C, Grubaugh ND, Alpert T, Ott IM, Breban MI, et al. An outbreak of SARS-CoV-2 on a transplant unit in the early vaccination era. *Transpl Infect Dis* (2022) 24:e13782. doi: 10.1111/tid.13782

33. Wang AX, Busque S, Kuo J, Singh U, Roeltgen K, Pinsky BA, et al. SARS-CoV-2 neutralizing monoclonal antibodies for the treatment of COVID-19 in kidney transplant recipients. *Kidney360* (2022) 3:133–43. doi: 10.34067/KID.0005732021

34. Manothummetha K, Chuleerarux N, Sanguankeo A, Kates OS, Hirankarn N, Thongkam A, et al. Immunogenicity and risk factors associated with poor humoral immune response of SARS-CoV-2 vaccines in recipients of solid organ transplant: A systematic review and meta-analysis. *JAMA Netw Open* (2022) 5: e226822. doi: 10.1001/jamanetworkopen.2022.6822

35. Le Bert N, Tan AT, Kunasegaran K, Tham CYL, Hafezi M, Chia A, et al. SARS-CoV-2-specific T cell immunity in cases of COVID-19 and SARS, and uninfected controls. *Nature* (2020) 584:457–62. doi: 10.1038/s41586-020-2550-z

36. Breton G, Mendoza P, Hagglof T, Oliveira TY, Schaefer-Babajew D, Gaebler C, et al. Persistent cellular immunity to SARS-CoV-2 infection. *J Exp Med* (2021) 218:1–11. doi: 10.1084/jem.20202515

37. Mohn KG, Bredholt G, Zhou F, Madsen A, Onyango TB, Fjelltveit EB, et al. Durable T-cellular and humoral responses in SARS-CoV-2 hospitalized and community patients. *PloS One* (2022) 17:e0261979. doi: 10.1371/journal.pone.0261979

38. Moss P. The T cell immune response against SARS-CoV-2. *Nat Immunol* (2022) 23:186–93. doi: 10.1038/s41590-021-01122-w

39. Zhang L, Poorbaugh J, Dougan M, Chen P, Gottlieb RL, Huhn G, et al. Endogenous antibody responses to SARS-CoV-2 in patients with mild or moderate COVID-19 who received bamlanivimab alone or bamlanivimab and etesevimab together. *Front Immunol* (2021) 12:790469. doi: 10.3389/fimmu.2021.790469

40. Kim PS, Dimcheff DE, Siler A, Schildhouse RJ, Chensue SW. Effect of monoclonal antibody therapy on the endogenous SARS-CoV-2 antibody response. *Clin Immunol* (2022) 236:108959. doi: 10.1016/j.clim.2022.108959

41. Eckerle I, Rosenberger KD, Zwahlen M, Junghanss T. Serologic vaccination response after solid organ transplantation: a systematic review. *PloS One* (2013) 8: e56974. doi: 10.1371/journal.pone.0056974

42. Boyarsky BJ, Werbel WA, Avery RK, Tobian A, Massie AB, Segev DL, et al. Immunogenicity of a single dose of SARS-CoV-2 messenger RNA vaccine in solid organ transplant recipients. *JAMA* (2021) 325:1784–6. doi: 10.1001/jama.2021.4385

43. Chavarot N, Ouedrani A, Marion O, Leruez-Ville M, Vilain E, Baaziz M, et al. Poor anti-SARS-CoV-2 humoral and T-cell responses after 2 injections of mRNA vaccine in kidney transplant recipients treated with belatacept. *Transplantation* (2021) 105:e94–5. doi: 10.1097/TP.0000000000003784

44. Woodle ES, Gebel HM, Montgomery RA, Maltzman JS. SARS-CoV-2 vaccination, immune responses, and antibody testing in immunosuppressed populations: Tip of the iceberg. *Transplantation* (2021) 105:1911–3. doi: 10.1097/TP.0000000000003859

45. Furian L, Russo FP, Zaza G, Burra P, Hartzell S, Bizzaro D, et al. Differences in humoral and cellular vaccine responses to SARS-CoV-2 in kidney and liver transplant recipients. *Front Immunol* (2022) 13:853682. doi: 10.3389/fimmu.2022.853682

46. Gottlieb RL, Nirula A, Chen P, Boscia J, Heller B, Morris J, et al. Effect of bamlanivimab as monotherapy or in combination with etesevimab on viral load in patients with mild to moderate COVID-19: A randomized clinical trial. *JAMA* (2021) 325:632–44. doi: 10.1001/jama.2021.0202

47. Vellas C, Del Bello A, Debard A, Steinmeyer Z, Tribaudeau L, Ranger N, et al. Influence of treatment with neutralizing monoclonal antibodies on the SARS-CoV-2 nasopharyngeal load and quasispecies. *Clin Microbiol Infect* (2022) 28139: e135–139 e138. doi: 10.1016/j.cmi.2021.09.008

48. Li T, Qiu Z, Zhang L, Han Y, He W, Liu Z, et al. Significant changes of peripheral T lymphocyte subsets in patients with severe acute respiratory syndrome. *J Infect Dis* (2004) 189:648–51. doi: 10.1086/381535

49. Channappanavar R, Zhao J, Perlman S. T Cell-mediated immune response to respiratory coronaviruses. *Immunol Res* (2014) 59:118–28. doi: 10.1007/s12026-014-8534-z

50. Peng Y, Mentzer AJ, Liu G, Yao X, Yin Z, Dong D, et al. Broad and strong memory CD4(+) and CD8(+) T cells induced by SARS-CoV-2 in UK convalescent individuals following COVID-19. *Nat Immunol* (2020) 21:1336–45. doi: 10.1038/s41590-020-0782-6

51. Konik M, Lindemann M, Zettler M, Meller L, Dolff S, Rebmann V, et al. Long-term SARS-CoV-2 specific immunity is affected by the severity of initial COVID-19 and patient age. *J Clin Med* (2021) 10:1–17. doi: 10.3390/jcm10194606

COPYRIGHT

© 2022 Thümmler, Konik, Lindemann, Fisenkci, Koldehoff, Gäckler, Horn, Theodoropoulos, Taube, Zettler, Anastasiou, Braß, Jansen, Witzke, Rohn and Krawczyk. This is an open-access article distributed under the terms of the Creative Commons Attribution License (CC BY). The use, distribution or reproduction in other forums is permitted, provided the original author(s) and the copyright owner(s) are credited and that the original publication in this journal is cited, in accordance with accepted academic practice. No use, distribution or reproduction is permitted which does not comply with these terms.

frontiers | Frontiers in Immunology

TYPE Original Research
PUBLISHED 14 October 2022
DOI 10.3389/fimmu.2022.968778

Check for updates

OPEN ACCESS

EDITED BY
E. Marion Schneider,
University of Ulm, Germany

REVIEWED BY
Ionna Galani,
Biomedical Research Foundation of the Academy of Athens (BRFAA), Greece
Ilnaz Rahimmanesh,
Isfahan University of Medical Sciences, Iran

*CORRESPONDENCE
Judith Schenz
judith.schenz@med.uni-heidelberg.de

†These authors have contributed equally to this work

SPECIALTY SECTION
This article was submitted to Viral Immunology, a section of the journal Frontiers in Immunology

RECEIVED 14 June 2022
ACCEPTED 05 September 2022
PUBLISHED 14 October 2022

CITATION
Schenz J, Rump K, Siegler BH, Hemmerling I, Rahmel T, Thon JN, Nowak H, Fischer D, Hafner A, Tichy L, Bomans K, Meggendorfer M, Koos B, von Groote T, Zarbock A, Fiedler MO, Zemva J, Larmann J, Merle U, Adamzik M, Müller-Tidow C, Haferlach T, Leuschner F and Weigand MA (2022) Increased prevalence of clonal hematopoiesis of indeterminate potential in hospitalized patients with COVID-19.
Front. Immunol. 13:968778.
doi: 10.3389/fimmu.2022.968778

Increased prevalence of clonal hematopoiesis of indeterminate potential in hospitalized patients with COVID-19

Judith Schenz[1*†], Katharina Rump[2,3†], Benedikt Hermann Siegler[1], Inga Hemmerling[4], Tim Rahmel[2], Jan N. Thon[1], Hartmuth Nowak[2,3], Dania Fischer[1], Anna Hafner[1], Lucas Tichy[1], Katharina Bomans[1], Manja Meggendorfer[5], Björn Koos[2,3], Thilo von Groote[3,6], Alexander Zarbock[3,6], Mascha O. Fiedler[1], Johanna Zemva[7], Jan Larmann[1], Uta Merle[8], Michael Adamzik[2,3], Carsten Müller-Tidow[9], Torsten Haferlach[5], Florian Leuschner[4] and Markus A. Weigand[1,10]

[1]Department of Anesthesiology, Heidelberg University Hospital, Heidelberg, Germany, [2]Klinik für Anästhesiologie, Intensivmedizin und Schmerztherapie, Universitätsklinikum, Knappschaftskrankenhaus Bochum, Ruhr-University Bochum, Bochum, Germany, [3]CovidDataNet.NRW, Germany, [4]Department of Medicine, Cardiology, Heidelberg University Hospital, Heidelberg, Germany, [5]MLL Munich Leukemia Laboratory, Munich, Germany, [6]Department of Anesthesiology, Intensive Care and Pain Medicine, University Hospital Münster, Münster, Germany, [7]Department of Endocrinology, Diabetology, Metabolic Diseases and Clinical Chemistry, Heidelberg University Hospital, Heidelberg, Germany, [8]Department of Gastroenterology and Infectious Diseases, Heidelberg University Hospital, Heidelberg, Germany, [9]Department of Medicine, Hematology, Oncology and Rheumatology, Heidelberg University Hospital, Heidelberg, Germany, [10]University Center for ARDS and Weaning, Heidelberg University Hospital, Heidelberg, Germany

Clonal hematopoiesis of indeterminate potential (CHIP) leads to higher mortality, carries a cardiovascular risk and alters inflammation. All three aspects harbor overlaps with the clinical manifestation of COVID-19. This study aimed to identify the impact of CHIP on COVID-19 pathophysiology. 90 hospitalized patients were analyzed for CHIP. In addition, their disease course and outcome were evaluated. With a prevalence of 37.8%, the frequency of a CHIP-driver mutation was significantly higher than the prevalence expected based on median age (17%). CHIP increases the risk of hospitalization in the course of the disease but has no age-independent impact on the outcome within the group of hospitalized patients. Especially in younger patients (45 – 65 years), CHIP was associated with persistent lymphopenia. In older patients (> 65 years), on the other hand, CHIP-positive patients developed neutrophilia in the long run. To what extent increased values of cardiac biomarkers are caused by CHIP independent of age could not be elaborated solely based on this study. In conclusion, our results indicate an increased susceptibility to a severe course of COVID-19 requiring hospitalization associated with CHIP. Secondly, they link it to a differentially regulated cellular immune response under the pressure of SARS-CoV-2 infection.

10.3389/fimmu.2022.968778

Hence, a patient's CHIP-status bears the potential to serve as biomarker for risk stratification and to early guide treatment of COVID-19 patients.

KEYWORDS

cardiac function, CHIP, critically ill, immune system, SARS-CoV-2

Introduction

Clonal hematopoiesis of indeterminate potential (CHIP) is defined as the occurrence of an expanded proportion of mature blood cells derived from a single mutant hematopoietic precursor without evidence of hematological malignancies (1, 2). The principle behind the manifestation of CHIP is that the somatic mutation confers a certain predominance to the affected cell (3, 4). Different clinical consequences are linked to this expansion. Early reports have already described an association of clonal hematopoiesis with a higher mortality risk compared to individuals without CHIP-driver mutations (5, 6). Interestingly, this is not related to increased rates of cancer but associated in particular with increased cardiovascular mortality (7). Mechanistically, the development of clonal hematopoiesis is not only related to inflammatory processes, but it has even been identified as a driver of inflammation (8–12). In COVID-19, both inflammatory (13–15) and cardiac-associated processes (16–18) have been described. They are involved in the pathophysiology of the complex extra-pulmonary manifestations occurring in affected patients alongside pulmonary symptoms (19–21). Chronic infections with the human immunodeficiency virus and the thereby impacted inflammatory regulation have been linked already to an increased risk of age-related clonal hematopoiesis (22). Furthermore, it is known that the risk of numerous infections is increased by hematopoietic mosaic chromosomal alterations (23). Regarding CHIP and COVID-19 there is contradictory evidence. On the one hand, a stable CHIP prevalence and no outcome-relevant influence was described in a cohort including both hospitalized patients and outpatients with COVID-19 (24, 25). On the other hand, CHIP was reported being a risk factor for severe courses (26). With the aim of comprehensively assessing the impact of clonal hematopoiesis on the pathophysiology of COVID-19, hospitalized patients were evaluated for the presence of CHIP-driver mutations and an association between CHIP and disease progression.

Materials and methods

Study cohort

Patient recruitment was conducted at Heidelberg University Hospital, University Hospital Knappschaftskrankenhaus Ruhr University Bochum, and University Hospital Münster (all three: Germany). The ethics committees of the Medical Faculties of Heidelberg University (reference: S-176/2020), the Ruhr University Bochum (reference: 19-6606_6-BR), and the University of Münster (reference: SepsisDataNet.NRW: 2107-513-b-S, substantial amendment: CovidDataNet.NRW) approved this prospective observational clinical study. Patients were enrolled between October 2020 and August 2021. Written informed consent was obtained from all patients. If patients were incapable to give their consent, it was obtained from their legal representatives. All patients had a positive SARS-CoV-2 PCR test, were not vaccinated against SARS-CoV-2, and were admitted to the hospital due to COVID-19. Study inclusion was conducted within a maximum of 48 hours after initial admission to an intensive care unit (ICU) or general ward (time point: admission). Exclusion criteria were pregnancy, enrolment in an interventional study, preexisting immunosuppression, hematologic malignancies, or anemia.

Whole blood was drawn at enrolment. Upon centrifugation (2,000x*g*), the plasmatic fraction was removed and stored at -80°C for cytokine quantification. Peripheral blood mononuclear cells (PBMC) were separated directly by density gradient centrifugation and stored at -80°C until DNA extraction.

DNA isolation

DNA isolation from PBMC was performed either with the DNeasy Blood & Tissue Kit (Qiagen, Hilden, Germany) or the Roche MagNA Pure System with the MagNAPure96 DNA and Viral NA LV Kit (Roche LifeScience, Mannheim, Germany).

Sequencing, bioinformatics, and variant interpretation

Next-Generation Sequencing was performed for all samples by MLLSEQ - MLL Dx GmbH (Munich, Germany). The library preparation for enrichment was performed with 150ng DNA per sample with the Illumina TruSeq DNA Nano Kit (Illumina, San Diego, CA, USA) using Unique Dual Indices. Within the protocol, the DNA was fragmented to a length of 150bp using the Covaris LE220-plus ultrasonicator (Covaris, Woburn, MA, USA). Subsequently, the DNA target regions were enriched using the IDT Hybridization Capture Protocol and a corresponding custom lockdown gene panel (IDT Integrated DNA Technologies, Coralville, IA, USA). Sequencing of the libraries was performed on Illumina NovaSeq 6000 instruments (Illumina, San Diego, CA, USA) with paired end sequencing mode (2x101 cycles) and a target coverage of 4,000x.

The lockdown panel covered following genes: *ABL1, ASXL1, ATRX, BCOR, BCORL1, BRAF, CALR, CBL, CBLB, CBLC, CDKN2A, CEBPA, CSF3R, CUX1, DNMT3A, ETV6, EZH2, FBXW7, FLT3, GATA1, GATA2, GNAS, GNB1, HRAS, IDH1, IDH2, IKZF1, JAK2, JAK3, KDM6A, KIT, KRAS, KMT2A, MPL, MYD88, NOTCH1, NPM1, NRAS, PDGFRA, PHF6, PPM1D, PTEN, PTPN11, RAD21, RUNX1, SETBP1, SF3B1, SMC1A, SMC3, SRSF2, STAG2, TET2, TP53, U2AF1, WT1, ZRSR2.*

Ilumina's BaseSpace Enrichment app (v3.1.1) was used to align the raw reads to hg19 reference sequence (Isaac Aligner v03.16.02.20). Subsequently, variants were called using PISCES (v5.1.3.60) somatic variant caller with 1% variant allele frequency (VAF) cutoff and 29 base quality filter and PCR duplicate flagging. In addition, the same data was processed through Illumina's Dragen Enrichment app (v3.6.3) with 1% VAF, 1% VAF filter threshold and duplicate marking. We combined calls from both result files (VCF) for tertiary analysis.

The classification of the variants in mutated, variant of uncertain significance (VUS), or polymorphism was done using the public databases ClinVar, COSMIC, dbSNP, gnomAD, as well as the MLL in-house variant data base. Variants with a VAF <5% were validated in a subsequent amplicon-based assay.

Flow cytometry

For quantification of HLA-DR expression on monocytes, 50µL freshly drawn whole blood was stained with 20µL BD Quantibrite anti-HLA-DR/anti-Monocyte PerCP-Cy5.5 reagent (clone: L243/MwP9) (BD Biosciences, Franklin Lakes, NJ, USA) for 30 minutes in the dark. For erythrocyte lysis, 450µL lysing solution (BD Biosciences, Franklin Lakes, NJ, USA) were added. Measurement was done immediately after incubation (15 minutes, in darkness). BD Quantibrite PE tubes (BD Biosciences, Franklin Lakes, NJ, USA) were used for quantifying the average number of HLA-DR molecules per monocyte as indicated by the manufacturer.

For quantification of lymphocyte subsets and monocytes, 50µL freshly drawn whole blood was stained with 20µL BD Multitest 6-color TBNK reagent and 5µL anti-Human CD14-V450 (clone: MφP9) using BD Trucount tubes to determine absolute counts (all BD Biosciences, Franklin Lakes, NJ, USA). After 30 minutes incubation in the dark, 450µL lysing solution (BD Biosciences, Franklin Lakes, NJ, USA) were added and measurement was performed immediately after 15 minutes incubation in darkness.

To identify T_{reg} cells and monocyte subsets, 100µL whole blood each were incubated (10 minutes) with 5µL Human TruStain FcX (BioLegend, San Diego, CA, USA) for Fc receptor blocking and stained by the addition of the appropriate antibodies (all from BD Biosciences, Franklin Lakes, NJ, USA) for 30 minutes at 4°C in the dark (T_{reg}: 5µL anti-Human CD3-FITC (clone: UCHT1), 5µL anti-Human CD4-V500 (clone: RPA-T4), 20µL anti-Human CD25-PE (clone: M-A251), 20µL anti-Human CD127-Alexa Fluor 647 (clone: HIL-7R-M21); monocytes: 5µL anti-Human CD14-V450 [clone: MφP9), 5µL anti-Human CD16-FITC (clone: B73.1)]. Lysing of erythrocytes was done by adding 2mL lysing solution and incubation for 15 minutes at room temperature in darknes. Afterwards, the suspension was centrifuged (250x*g*, 5 minutes), the supernatant discarded, the cells washed (250x*g*, 5 minutes) once with 2mL CellWASH, and resuspended in FACSFlow (all from BD Biosciences, Franklin Lakes, NJ, USA).

A FACSLyric flow cytometer was used for all measurement. Results were analyzed using BD FACSuite software (both from BD Biosciences, Franklin Lakes, NJ, USA). Representative gating strategy is shown in Supplementary Figure S1.

PBMC stimulation

$1.5x10^5$ freshly isolated PBMC were resuspended in 300µL of RPMI 1640 (Thermo Fisher Scientific Inc, Waltham, MA, USA), containing GlutaMAX, 100units/mL penicillin, 100µg/mL streptomycin and 10% heat-inactivated fetal bovine serum ultra-low endotoxin (Cell Concepts, Umkirch, Germany). Stimulation was performed with 3µL Dynabeads Human T-Activator CD3/CD28 (Thermo Fisher Scientific, Waltham, MA, USA). Prior to use, Dynabeads were washed and resuspended in culture medium according to the manufacturer's instruction. Control cells were incubated without a stimulating agent. Following a 24h incubation (37°C, 5% CO_2), supernatants were collected by centrifugation (1,000x*g*, 5 minutes) and stored at -80°C until cytokine quantification.

Cytokine quantification

Cytokine levels in plasma or supernatants were measured using colorimetric enzyme-linked immunosorbent assay (ELISA) according to the respective manufacturer's instructions. For CXCL10/IP-10 (limit of detection (LOD): 31.2pg/mL), TGF-β1 (LOD: 31.2pg/mL), and IL-6 (LOD: 9.4pg/mL) the respective human Duo-Set ELISA (all from R&D Systems, Minneapolis, MN, USA) were used. IFN-γ (LOD: 0.06pg/mL) was measured using the IFN gamma Human ELISA Kit, High Sensitivity (Invitrogen, Thermo Fisher Scientific Inc, Waltham, MA, USA).

Statistical analyses

All statistical analyses were performed using SPSS Statistics (Version 27.0.1.0, IBM®, Armonk, NY, USA). Continuous variables are presented as median (interquartile range (IQR)). Two-sided Mann–Whitney U-test or Kruskal-Wallis test were used for comparison, as appropriate. Categorical variables are shown as absolute number (frequency) and compared using Chi-square test or Fisher's exact test, as appropriate. Binomial test was used to compare an observed prevalence against an expected. Figures were created using GraphPad Prism (V9.3.1 for Windows, GraphPad software, La Jolla, CA, USA).

Results

Patient characteristics

In total, 90 patients hospitalized due to COVID-19 were included in the study (Table 1). 72 of these patients were critically ill and treated in an ICU at the time of inclusion. The other 18 patients were admitted to general wards. Two of them were transferred to an ICU at a later stage. Patients had a median age of 60.5 (52.0 – 69.3) years and were overweight (body mass index: 28.4 (24.4 – 32.6) kg/m^2). 35.6% of the cohort were female. At admission, only 35.6% of the patients were spontaneously breathing and without supplemental oxygen demand or respiratory support.

Prevalence of CHIP-associated mutations

With a VAF ≥ 1%, at least one CHIP-driver mutation was detected in 34 out of the 90 patients included in the study, corresponding to a prevalence of 37.8% (Figure 1A). According to modeling by Watson et al. including ~50,000 unselected individuals, 1% VAF cutoff at the median age of our cohort would be expected to result in a prevalence of single-mutant clones of 17% (P<0.001) (4). Thus, the frequency of a CHIP-driver mutation is significantly higher in hospitalized COVID-19 patients than in the general population adjusted for age.

Among the 34 CHIP-positive patients, 25 patients (73.5%) showed one single gene mutation, seven patients (20.6%) had two mutations, and two cases (5.9%) showed five mutations (Figure 1B). Most frequently mutated genes were *DNMT3A* (16/90 = 17.8%), *PPM1D* (8/90 = 8.9%), *TET2* (6/90 = 6.7%), *SF3B1* (3/90 = 3.3%), and *ZRSR2* (3/90 = 3.3%) (Figure 1C). Of the 49 single mutations identified, 32 (65.3%) were single nucleotide variants, nine (18.4%) were deletion mutants, seven (14.3%) were duplication mutants, and one (2.0%) was an insertion mutant (Supplementary Table S1).

Prognostic relevance of CHIP-driver mutations for disease progression

The occurrence of at least one CHIP-driver mutation was associated with a significantly inferior clinical outcome in terms of survival within a 60-day follow-up period (Figure 2A). Since both groups significantly differed for age (CHIP-positive: 66.5 years (56.8 – 74.8); CHIP-negative: 55.5 years (50.3 – 65.8); P=0.003) (Table 1), Cox proportional regression analysis was performed to account for the potential effect of age: Only age was independently associated with survival, whereas carrying a CHIP-driver mutation was not (Table 2). Therefore, three subgroups were defined according to age (<45 years: n=8, 45-65 years: n=50, >65 years: n=32). Again, with these subgroups, it was confirmed that older patients had a significantly worse survival (Figure 2B). It is therefore not surprising that within these subgroups there is no difference in survival between patients with and without CHIP-driver mutation (Supplementary Figure S2A). There were no differences in age between CHIP-positive and -negative patients, within the age groups (Supplementary Figure S2B).

In the group of patients younger than 45 years (median: 36.0 (26.3 – 42.5) years), no CHIP-driver mutation was detected (Figure 2C). In patients aged 45 to 65 years (median: 55.0 (52.0 – 61.3) years), 32% harbored a mutation (Figure 2D). According to Watson et al. (4), the expected prevalence at the subgroup's median age would be only 10% (P<0.001). A similar result was revealed for patients older than 65 years (Figure 2E). With a median age of 75.0 (68.3 – 80.8) years in this subgroup, 40% prevalence would be expected according to the modeling. In contrast, among the hospitalized COVID-19 patients the prevalence was 56.3% (P=0.046).

Beyond age, the groups of CHIP-positive and -negative patients notably did not differ in terms of sex (Table 1), SOFA score at admission (Figure 2F), length of hospitalization and ICU stay (Figures 2G, H), or concerning other baseline characteristics (Table 1). This is also true when comparing the two groups

TABLE 1 Baseline characteristics.

	Total cohort (n=90)	CHIP-positive (n=34)	CHIP-negative (n=56)	P-value
Age, years				0.003
Median (IQR)	60.5 (52.0 – 69.3)	66.5 (56.8 – 74.8)	55.5 (50.3 – 65.8)	
Range	24 – 95	45 – 95	24 – 87	
Sex, no. (%)				1.000
Female	32 (35.6%)	12 (35.3%)	20 (35.7%)	
Male	58 (64.4%)	22 (64.7%)	36 (64.3%)	
Body mass index, kg/m^2				0.188
Median (IQR)	28.4 (24.4 – 32.8)	29.7 (25.7 – 34.6)	28.3 (24.1 – 31.5)	
Range	17.3 – 45.2	23.4 – 45.2	17.3 – 39.9	
	n=48	n=14	n=34	
SOFA score at ICU admission				0.311
Media (IQR)	4.0 (2.0 – 10.0)	5.0 (3.0 – 10.0)	4.0 (2.0 – 9.8)	
Range	0 – 17	0 – 17	0 – 16	
Hospitalization, days				0.962
Media (IQR)	18.5 (10.8 – 39.0)	20.5 (11.8 – 34.0)	18.0 (10.0 – 40.8)	
Range	3 – 84	3 – 61	3 – 84	
Length of ICU stay, days				0.582
Media (IQR)	10.0 (3.0 – 27.0)	10.0 (3.8 – 21.0)	10.5 (3.0 – 30.8)	
Range	0 – 83	0 – 39	0 – 83	
Discharge status, no. (%)				0.145
Deceased	24 (26.7%)	13 (38.2%)	11 (19.6%)	
Home	46 (51.1%)	16 (47.1%)	30 (53.6%)	
Rehabilitation clinic	5 (5.6.%)	1 (2.9%)	4 (7.1%)	
Transfer to peripheral hospital	14 (15.6%)	3 (8.2%)	11 (19.3%)	
Other	1 (1.1%)	1 (2.9%)	0 (0.0%)	
Ventilation at admission, no. (%)				0.926
Extracorporeal membrane oxygenation	3 (3.3%)	1 (2.9%)	2 (3.3%)	
Invasive ventilation	17 (18.9%)	5 (14.7%)	12 (21.4%)	
Non-invasive ventilation	21 (23.3%)	9 (26.5%)	12 (21.4%)	
Nasal high flow therapy	17 (18.9%)	6 (17.6%)	11 (19.6%)	
Spontaneously breathing	32 (35.6%)	13 (38.2%)	19 (33.9%)	

P-values from two-sided Fisher's exact test for sex, Chi-square test for discharge status and ventilation at admission, and from two-sided Mann–Whitney U-test for comparison of continuous variables.

based on age (Supplementary Figures S3A, B) or comparing the three age groups with each other (Supplementary Figure S3C).

Association between clonal hematopoiesis and organ function

At admission, CHIP-positive and -negative patients had comparable supplemental oxygen demand and required invasive or non-invasive ventilation to a comparable extent (Table 1). Besides, there were no differences regarding Horovitz index (Supplementary Table S2). Therefore, a similar degree of lung injury can be assumed in both groups. The infection-related parameters C-reactive protein (Figure 3A) and procalcitonin (Figure 3B) likewise did not vary between CHIP-positive and CHIP-negative patients. Surprisingly, investigating biomarkers for organ functions (Supplementary Table S2), at admission, the two groups differed only, but significantly regarding the cardiac biomarkers NT-proBNP (Figure 3C) and Troponin T (Figure 3D). Both markers already showed a clinically relevant increase in the CHIP-negative group (NT-proBNP: 347.0 (133.8 – 1217.0) pg/ml; Troponin T: 15.0 (5. – 28.5) pg/ml). Yet, the increase was markedly higher in the group carrying a CHIP-driver mutation (NT-proBNP: 991.9 (270.5 – 3726.0) pg/ml; Troponin T: 23.0 (16.0 – 44.3) pg/ml). High levels of cardiac markers were not related to poorer survival (Supplementary Figure S4). However, when both NT-proBNP and Troponin T were compared in relation to age, significantly higher values were again found in older patients (Figure 4A). Within the age groups, no differences were found between CHIP-positive and -negative patients regarding these cardiac markers, neither for

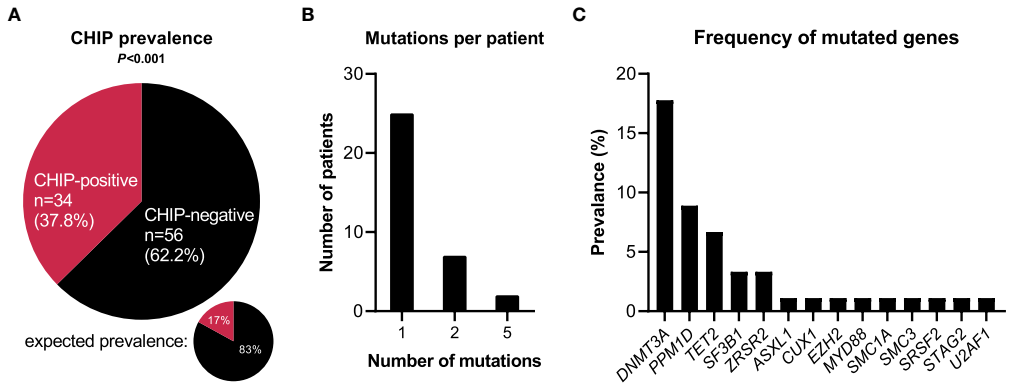

FIGURE 1
CHIP-associated mutations in hospitalized patients with COVID-19. **(A)** Prevalence of clonal hematopoiesis in hospitalized patients with COVID-19. CHIP-positive = patients carrying at least one CHIP-driver mutation with a VAF≥0.01. Expected prevalence according to Watson et al. (4). Observed and expected prevalence were compared using binomial test. Statistically significant results ($P \leq 0.05$) are highlighted by bold print. **(B)** Number of individual mutations per CHIP-positive patient. **(C)** Prevalence broken down by affected genes.

those aged 45 – 65 years (Figure 4B) nor for those over 65 years (Figure 4C). Normal values for serum creatinine were found in patients with and without a CHIP-driver mutation (Figure 3E). D-dimer levels did not differ between both groups (Figure 3F).

Association between clonal hematopoiesis and peripheral immune parameters

At admission, immune parameters were comprehensively determined from whole blood from a 42-patient subcohort to provide evidence of the mechanistic link between clonal hematopoiesis, immune function, and poorer patient outcome (Supplementary Table S3). No differences were found between CHIP-positive and CHIP-negative patients concerning their absolute numbers of different lymphocytic populations and monocyte subpopulations or HLA-DR expression on monocytes. Plasma cytokine levels for IFN-γ, IP-10, TGF-β, and IL-6 also did not differ. Moreover, the cytokine response to *ex vivo* stimulation (αCD3/αCD28) of freshly isolated PBMC was found to be comparable.

Since the immune parameters at admission did not differ between CHIP-positive and CHIP-negative patients, parameters of the differential blood count routinely determined during treatment were used for comparison over time from the entire cohort (Supplementary Table S4). As expected, there were no differences between the groups at admission. However, at discharge, differences were found for lymphocytes, neutrophils, and eosinophils. Patients with a CHIP-driver mutation had higher neutrophil counts than patients without such a mutation (8.0 (5.4 – 13.2) vs. 5.5 (3.6 – 9.8) cells/nL; P=0.024)) (Figure 5A). These values indicate that especially CHIP-positive patients show neutrophilia (>7.7 cells/nL). Since the timepoint "discharge" has a very variable time lag to the timepoint "admission" depending on the course of the disease, these parameters were also compared at day 7 [total cohort: 64/90 (71.1%), CHIP-positive: 24/34 (70.6%), CHIP-negative: 40/56 (71.4%)] and day 14 (total cohort: 43/90 (47.8%), CHIP-positive: 13/34 (38.2%), CHIP-negative: 30/56 (53.6%)) after admission, including all patients who were still treated in the original hospital at that time. At day 7, both groups showed no significant alterations (Supplementary Table S4). The difference in neutrophil counts only became apparent at day 14 after admission (Figure 5B). The still more pronounced neutrophilia at this timepoint compared to "discharge" seems to be causative for the leukocytosis occurring in patients with mutation (Figure 5C). Albeit the group over 65 years of age tended to have higher leukocyte (Figure 5D) and neutrophil (Figure 5E) counts compared to the younger patients, the significant difference between CHIP-positive and -negative patients was maintained in this age group (Figures 5F, G). Among those aged 45 – 65 years, however, no difference was found (Figures 5H, I).

While both groups were lymphopenic (<1.0 cells/nL) at admission (0.8 (0.4 – 1.3) vs. 0.8 (0.6 – 1.0); P=0.907) (Figure 6A), patients with a CHIP-driver mutation recovered worse and had significantly lower lymphocyte counts at discharge than patients without a mutation (1.1 (0.6 – 1.4) vs. 1.6 (1.1 – 2.0); P=0.002) (Figure 6B). Here again, differences between the age groups were apparent. Especially in the group of 45 – 65-year-olds, CHIP-positive patients poorly overcame lymphopenia and had significantly lower lymphocyte counts at discharge compared to patients without clonal hematopoiesis

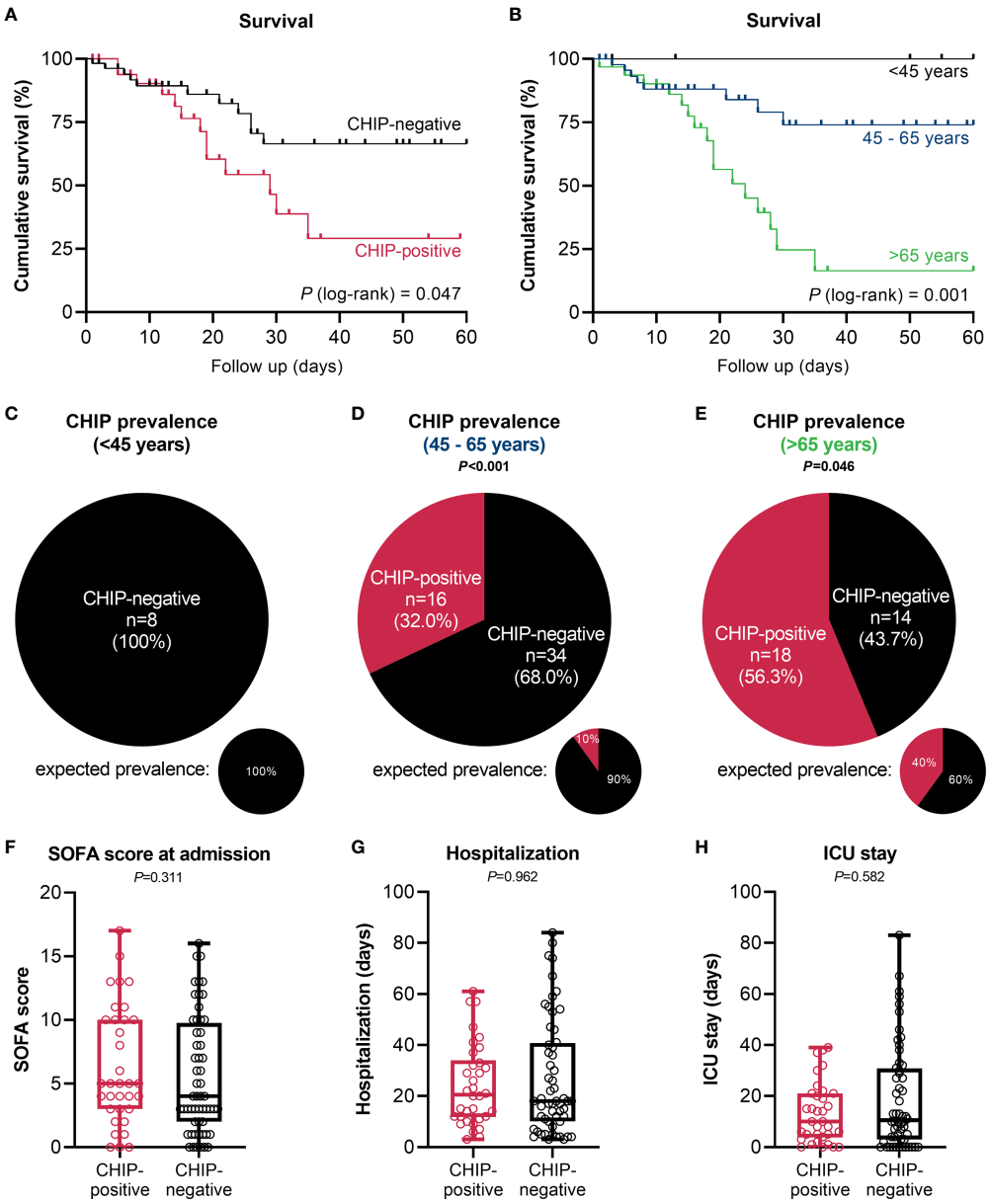

FIGURE 2
Impact of clonal hematopoiesis on patient outcome. **(A)** Kaplan-Meier survival curve for overall survival of CHIP-positive (n=34) vs. CHIP-negative (n=56) patients within a 60-day period. **(B)** Kaplan-Meier survival curve for overall survival of patients <45 years (n=8), 45 – 65 years (n=50), and >65 years (n=32) within a 60-day follow-up period. Statistical evaluations were done using log-rank Mantel-Cox test. CHIP prevalence in patients **(C)** <45 years, **(D)** 45 – 65 years, and **(E)** >65 years. Expected prevalences according to Watson et al. (4). Observed and expected prevalence were compared using binomial test. **(F)** SOFA score at admission, and length of **(G)** hospitalization and **(H)** ICU stay. Each data point represents an individual patient (CHIP-positive n=34; CHIP-negative n=56). Horizontal line within the box marks the median, boxes depict the IQR, and whiskers indicate the total range. Group comparisons were performed by two sided Mann–Whitney U-test. Statistically significant results ($P \leq 0.05$) are highlighted by bold print.

(Figure 6C). CHIP-negative patients older than 65 years were less efficient in controlling their lymphopenia, thus presenting with similarly low lymphocyte levels as CHIP-positive patients (Figure 6D). When comparing the age groups with each other, the lymphocyte counts were comparable (Figure 6E). Surprisingly, patients without a mutation had higher eosinophil granulocyte counts but without clinical relevance (eosinophilia >0.5 cells/nL) (Supplementary Table S4). Although not statistically significant, a

TABLE 2 Cox proportional regression with age and CHIP status included as covariates.

Overall survival	HR	95% CI	P-value
Age	1.093	1.052 – 1.135	<0.001
CHIP status (CHIP-positive vs. CHIP-negative)	1.254	0.547 – 2.877	0.593

trend in both lymphocytes and eosinophils might also be seen when comparing patients at day 14 (Supplementary Table S4).

Discussion

Investigating the impact of CHIP in patients with COVID-19, we demonstrate here that CHIP prevalence in patients hospitalized due to COVID-19 is significantly higher than in the general population. Hence, and in line with Bolton et al. (26), CHIP increases the risk of a severe course of the disease. This also holds true when subgroups are evaluated separately according to age. Remarkably, Petzer et al. reported lower prevalences and no link with severe courses (24). This dichotomy might be explained by a higher VAF cutoff of 2% compared to 1% in our study. Intriguingly, based on our data, we reveal that CHIP leads to a differentially regulated cellular immune response under the pressure of SARS-CoV-2 infection. This becomes apparent with age-dependent differences especially in neutrophils and lymphocytes only in the later course. Furthermore, the presence of a respective driver mutation seems to be mechanistically related to the COVID-19 risk factor age. Thus, the results of our study provide novel insights into the group of nonmalignant diseases in which clonal hematopoiesis is closely linked to adverse courses or outcome.

Within our cohort, the group harboring a CHIP-driver mutation was significantly older than the group without a corresponding mutation. This is consistent with previous studies analyzing patients hospitalized for COVID-19 (25, 27) and with the fact that clonal hematopoiesis is an age-associated process (7). However, for COVID-19, age itself is a well-known risk factor for mortality (28, 29) and only age remained independently associated with survival in our cohort. Thus, for patients hospitalized for COVID-19, CHIP alone does not impact survival. The markedly higher prevalence of CHIP in these patients compared with an overall population, however, was still observed within the subgroups formed according to age. CHIP is, therefore, a risk factor for COVID-19 courses requiring hospitalization but does not directly affect outcome within the hospitalized group. The cohort unintentionally includes mainly overweight patients. Obesity is a well-described risk factor for COVID-19-related hospitalization (30). Against this background, it is to be expected that a large proportion of the cohort is overweight. However, since CHIP-positive and -negative patients did not differ with respect to their body mass index, this factor can be excluded as an influencing factor in our study. However, it should be mentioned that a possible link between obesity and CHIP is the subject of current investigations. Especially in the context of cardiovascular diseases, which correlates with both CHIP and obesity, a direct mechanistic link between CHIP and obesity is discussed (31, 32). In addition, our study did not analyze other risk factors or preexisting conditions associated with a high risk of COVID-19-related hospitalization.

CHIP-positive and -negative patients had a comparable disease severity at the time of admission to ICU or general ward, respectively, underscoring the role of CHIP as a risk factor for severe courses. Particularly their SOFA scores, as an established measure to predict clinical outcome at an early stage, especially in critically ill patients, did not differ. Severity of SARS-CoV-2-induced lung injury was also comparable in both groups. Moreover, both groups showed no differences in further infection- or organ function-related biomarkers, with exception of the cardiac marker NT-proBNP and Troponin T. The increase in both parameters was significantly greater in the CHIP-positive patients. Cardiac involvement in the pathophysiological appearance of severe COVID-19 has been described in detail previously (33, 34) and might be the underlying reason for the comparatively slight increase in CHIP-negative patients compared to standard values. Concurrent with the effect on survival, the observed difference equalizes in age-adjusted subgroups. Several studies revealed CHIP bearing an excessive cardiovascular risk and linked it, among others, to atherosclerosis, coronary artery diseases, or degenerative aortic valve stenosis (35–37). Based on our data, we cannot distinguish whether the tremendous increase in the CHIP-positive cohort can be related to clonal hematopoiesis or is simply a consequence of cardiac risk increasing with age. The interrelation and mutually reinforcing effect of all these factors, nevertheless, is unequivocal. Furthermore, it is in line with a modeling-based proposition formulated in June 2020 that COVID-19 mortality is linear correlated with CHIP frequency (38). Further investigations are needed to provide evidence if a CHIP-related higher, possibly previously unknown cardiac burden leads to deteriorated courses of COVID-19 or if CHIP fuels cardiac involvement in the manifestations of COVID-19.

Mas-Peiro et al. recently detected higher levels of proinflammatory subsets of circulating T cells and monocytes in patients with degenerative aortic valve stenosis carrying DNMT3A- or TET2-CHIP mutations (39). Avagyan et al. provided evidence, that clonal fitness is related to upregulation of anti-inflammatory signaling pathways in the mutant progenitor cells, leading to resistance to inflammatory

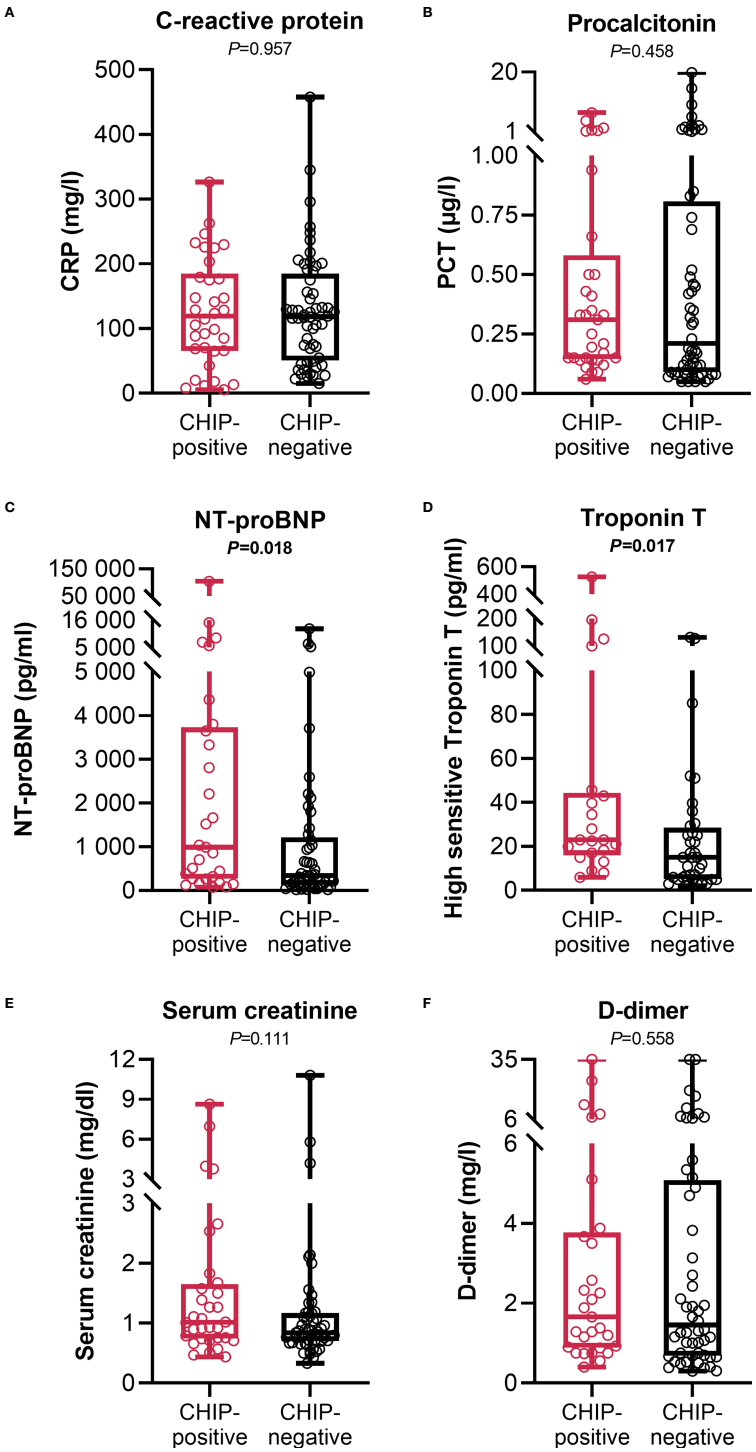

FIGURE 3
Infection and organ function related clinical parameters at admission. **(A)** C-reactive protein (CHIP-positive: n=34; CHIP-negative: n=56), **(B)** procalcitonin (CHIP-positive: n=33; CHIP-negative: n=56), **(C)** NT-proBNP (CHIP-positive: n=29; CHIP-negative: n=49), **(D)** high sensitive Troponin T (CHIP-positive: n=21; CHIP-negative: n=36), **(E)** serum creatinine (CHIP-positive: n=32; CHIP-negative: n=55), and **(F)** D-dimer (CHIP-positive: n=29; CHIP-negative: n=52) levels at admission. Each data point represents an individual patient. Horizontal line within the box marks the median, boxes depict the IQR, and whiskers indicate the total range. Group comparisons were performed by two sided Mann–Whitney U-test. Statistically significant results ($P \leq 0.05$) are highlighted by bold print.

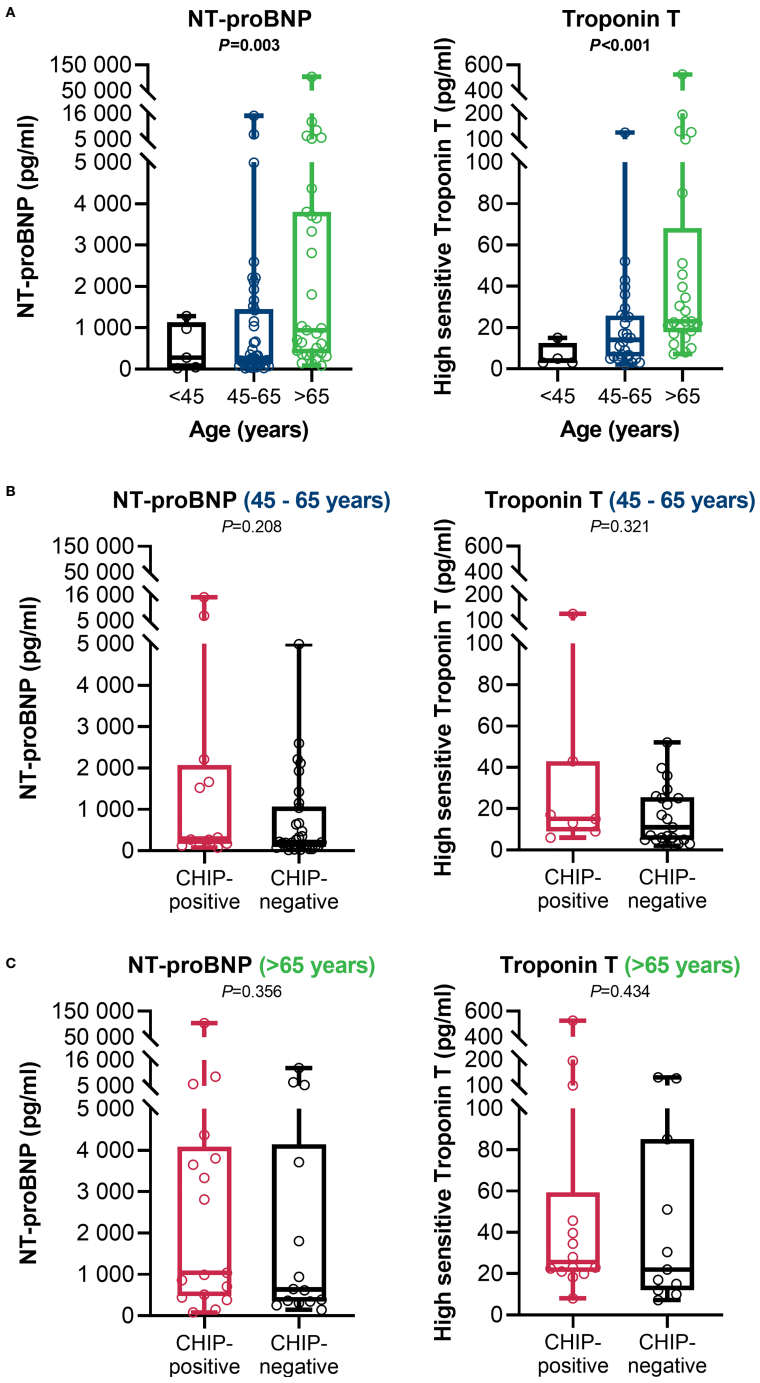

FIGURE 4
Age-adjusted cardiac function related clinical parameters at admission. **(A)** NT-proBNP (< 45: n=5; 45 – 65: n=42; > 65: n=31) and high sensitive Troponin T (<45: n=4; 45 – 65: n=28; >65: n=25) in comparison between the age groups. Group comparisons were done using Kruskal-Wallis test. **(B)** NT-proBNP (CHIP-positive: n=12; CHIP-negative: n=30) and Troponin T (CHIP-positive: n=7; CHIP-negative: n=21) in the 45 – 65 age group. **(C)** NT-proBNP (CHIP-positive: n=17; CHIP-negative: n=14) and Troponin T (CHIP-positive: n=14; CHIP-negative: n=11) for the > 65-year-olds. Group comparisons were performed by two sided Mann–Whitney U-test. Each data point represents an individual patient. Horizontal line within the box marks the median, boxes depict the IQR, and whiskers indicate the total range. Statistically significant results ($P \leq 0.05$) are highlighted by bold print.

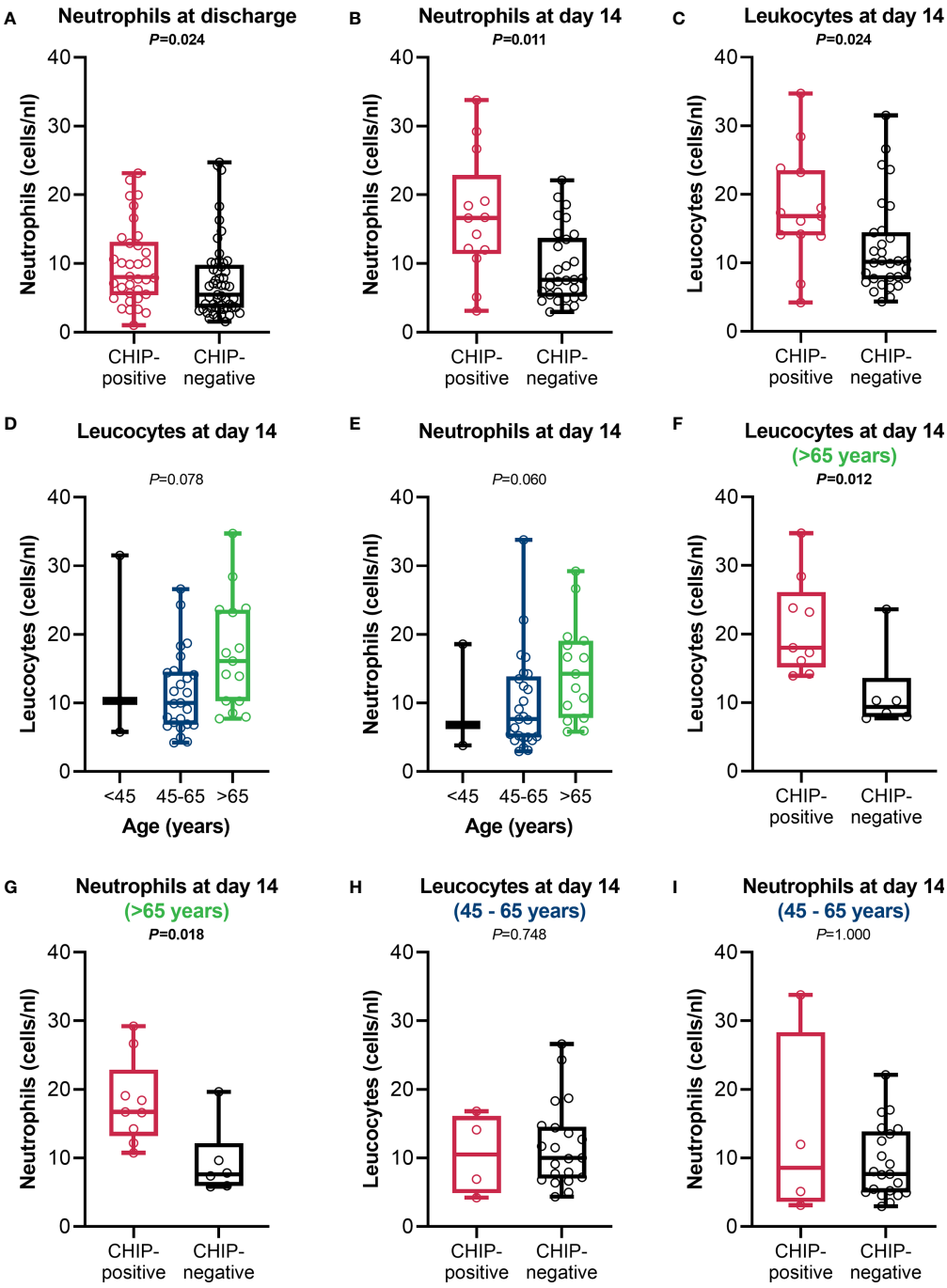

FIGURE 5
Leucocyte and neutrophil counts. Neutrophil counts at **(A)** discharge (CHIP-positive: n=34; CHIP-negative: n=53), **(B)** day 14 after admission, and **(C)** leucocyte counts at day 14 after admission (CHIP-positive: n=13; CHIP-negative: n=30). **(D)** Leucocyte and **(E)** neutrophil counts in comparison between the different age groups at day 14 after admission (<45: n=3; 45-65: n=25; >65: n=15).**(F)** Leucocyte and **(G)** neutrophil counts for patients aged >65 years (CHIP-positive: n=9; CHIP-negative: n=6) and **(H, I)** 45 – 65 years (CHIP-positive: n=4; CHIP-negative: n=21) at day 14 after admission. Group comparisons were performed by two sided **(A–C, F–I)** Mann–Whitney U-test or **(D, E)** Kruskal-Wallis test. Each data point represents an individual patient. Horizontal line within the box marks the median, boxes depict the IQR, and whiskers indicate the total range. Statistically significant results ($P \leq 0.05$) are highlighted by bold print.

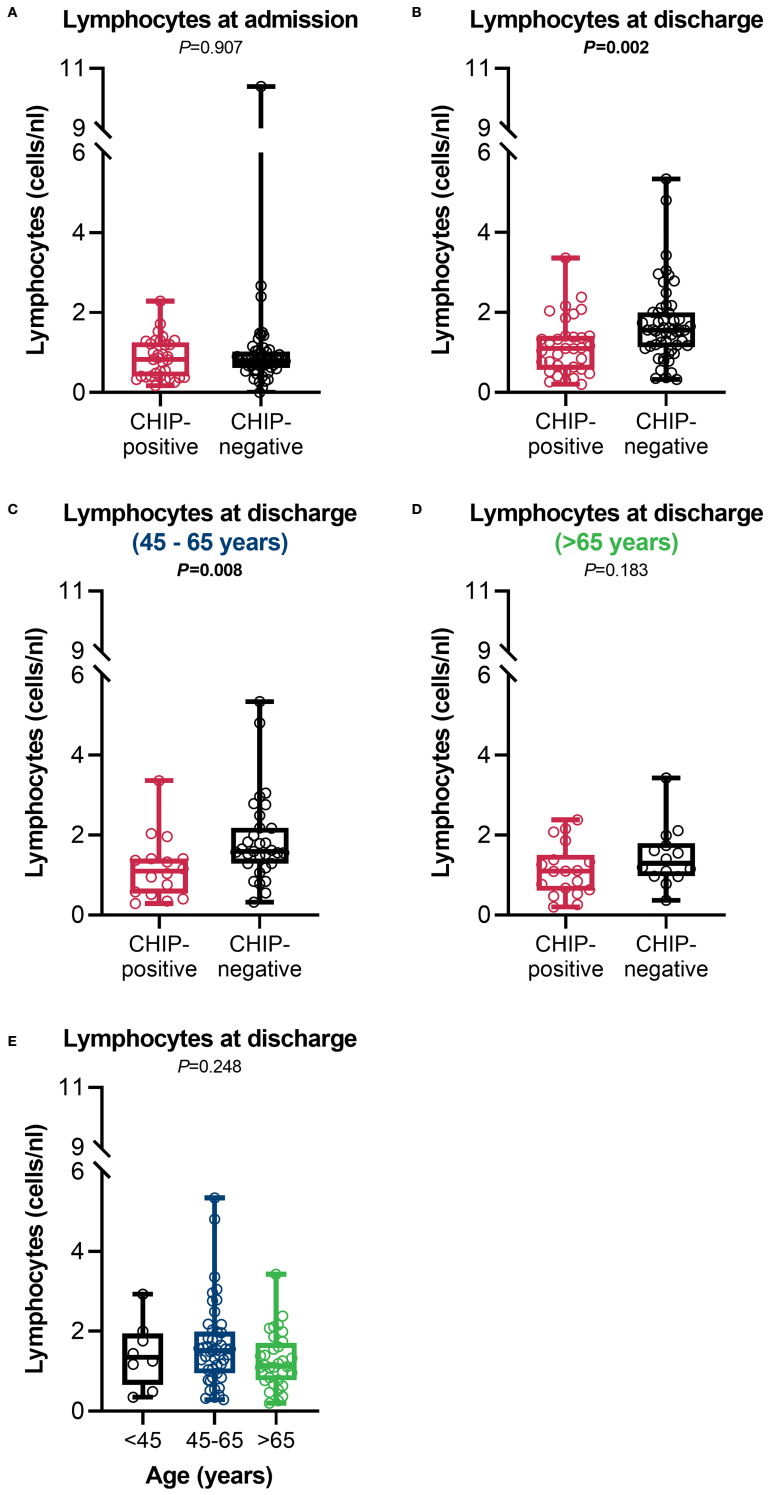

FIGURE 6
Lymphocyte counts. Lymphocyte counts at **(A)** admission (CHIP-positive: n=34; CHIP-negative: n=53) and **(B)** discharge (CHIP-positive: n=34; CHIP-negative: n=53). Lymphocyte counts at discharge for patients aged **(C)** 45 – 65 years (CHIP-positive: n=16; CHIP-negative: n=31) and **(D)** > 65 years (CHIP-positive: n=18; CHIP-negative: n=14). **(E)** Lymphocyte counts at discharge in comparison between the different age groups (<45: n=8; 45-65: n=47; >65: n=32). Group comparisons were performed by two sided **(A–D)** Mann–Whitney U-test or **(E)** Kruskal-Wallis test. Each data point represents an individual patient. Horizontal line within the box marks the median, boxes depict the IQR, and whiskers indicate the total range. Statistically significant results ($P \leq 0.05$) are highlighted by bold print.

signaling in their mature cellular progeny (40). Hence, it can be assumed that alongside with changes in cardiac function, immune response related differences are contributing to the higher disease severity in CHIP-positive patients. To our surprise, this only became detectable in the prolonged clinical course. At the time of admission, only lymphopenia, typical of severe COVID-19 (41, 42), as well as a weak T-cell response to *ex vivo* stimulation were apparent in both CHIP-positive and -negative patients, while there were no differences related to the immune response between the two groups. Patients without CHIP-driver mutations were able to overcome the lymphopenia, whereas in patients with such a mutation, long lasting neutrophilia may indicate persistent inflammation. Remarkably, these two, immune system-related, effects of CHIP do not appear to be necessarily linked but rather to vary in strength age-dependently. Protracted lymphopenia is most evident in the younger (45 – 65-years-old) patients. The contrast between CHIP-positive and CHIP-negative patients is hardly noticeable in the older ones, as here the CHIP-negative ones recover less well. However, there is persistent neutrophilia in this age group of over 65 years, which is not even a trend in the younger patients.

Taken together, our study substantiates the findings that harboring acquired somatic mutations in hematopoietic cells linked with CHIP amplifies the risk for hospitalization over the course of COVID-19. Additionally, we provide evidence that CHIP leads to distinct, late-occurring alterations of circulating immune cells in an age-dependent manner. Therefore, our data imply a CHIP-associated higher susceptibility to a sever course of COVID-19 on the one hand, and under the pressure of SARS-CoV-2 infection, an altered immune regulation in the long run. Based on this study, it is not possible to establish a direct, sole impact on the survival of hospitalized COVID-19 patients. Albeit the question remains to what extent CHIP, whose prevalence increases exponentially with age, indirectly contributes to the risk of death, which also increases depending on age. Our data at least propose that CHIP may be a hidden mechanistic link. Future studies are required to unravel these interconnections as well as the contribution of cardiac injury, as cardiac biomarkers were significantly elevated in the total cohort but not age-dependent and without an impact on survival. Another limitation of our study is the comparatively small number of patients, especially in each age-related subgroup. In view of this, our results need to be validated in further studies including substantially more patients. Finally, the mechanistic link between the different mutations on the one hand and the differently regulated immune response as well as its age dependence, on the other hand, appears worthy of further investigations. Yet, the findings we present here strongly support clonal hematopoiesis being a potent biomarker for early risk stratification and might be used to early guide clinical treatment of patients with COVID-19.

Data availability statement

The sequence data presented in the study are deposited at the European Genome-phenome Archive (EGA), which is hosted by the EBI and the CRG, under accession number EGAS00001006218: https://ega-archive.org/studies/EGAS00001006218.

Ethics statement

The studies involving human participants were reviewed and approved by the ethics committees of the Medical Faculties of Heidelberg University, the Ruhr University Bochum, and the University of Münster. The patients/participants provided their written informed consent to participate in this study.

Author contributions

JS, IH, CM-T, FL, and MW designed the study. KR, BS, JT, HN, AZ, MA, and MW obtained ethics approval. BS, JT, HN, DF, AH, TG, AZ, MF, JZ, JL, UM, MA and MW performed patient recruitment and obtained informed consent. JS, KR, BS, JT, LT, KB, and BK carried out the experiments. MM and TH performed sequencing, bioinformatic analysis and variant interpretation. JS, KR, BS, JT, HN, DF, BK, and TG performed data collection. JS, KR, BS, IH, TR, DF, AH, BK, AZ, JL, MA, FL, and MW performed data interpretation. JS wrote the manuscript. All authors critically revised and drafted the manuscript. All authors read and approved the final manuscript.

Funding

Parts of this work were supported by grants from the German Research Foundation [KFO342-1, ZA428/18-1, and ZA428/21-1 to AZ] and from the Government of North-Rhine Westphalia [CovidDataNet.NRW to KR, TR, HN, BK, MA].

Acknowledgments

The authors thank Sabine Stegmaier, Jan Pfister, and Ute Krauser from Heidelberg for their comprehensive and excellent technical support.

Conflict of interest

Author TH declares part ownership of MLL Munich Leukemia Laboratory. Author MM is employed by MLL.

The remaining authors declare that the research was conducted in the absence of any commercial or financial relationships that could be construed as a potential conflict of interest.

Publisher's note

All claims expressed in this article are solely those of the authors and do not necessarily represent those of their affiliated organizations, or those of the publisher, the editors and the reviewers. Any product that may be evaluated in this article, or claim that may be made by its manufacturer, is not guaranteed or endorsed by the publisher.

Supplementary material

The Supplementary Material for this article can be found online at: https://www.frontiersin.org/articles/10.3389/fimmu.2022.968778/full#supplementary-material

References

1. McKerrell T, Park N, Moreno T, Grove CS, Ponstingl H, Stephens J, et al. Leukemia-associated somatic mutations drive distinct patterns of age-related clonal hemopoiesis. *Cell Rep* (2015) 10:1239–45. doi: 10.1016/j.celrep.2015.02.005

2. Steensma DP, Bejar R, Jaiswal S, Lindsley RC, Sekeres MA, Hasserjian RP, et al. Clonal hematopoiesis of indeterminate potential and its distinction from myelodysplastic syndromes. *Blood* (2015) 126:9–16. doi: 10.1182/blood-2015-03-631747

3. Arends CM, Galan-Sousa J, Hoyer K, Chan W, Jäger M, Yoshida K, et al. Hematopoietic lineage distribution and evolutionary dynamics of clonal hematopoiesis. *Leukemia* (2018) 32:1908–19. doi: 10.1038/s41375-018-0047-7

4. Watson CJ, Papula AL, Poon GY, Wong WH, Young AL, Druley TE, et al. The evolutionary dynamics and fitness landscape of clonal hematopoiesis. *Science* (2020) 367:1449–54. doi: 10.1126/science.aay9333

5. Biernaux C, Loos M, Sels A, Huez G, Stryckmans P. Detection of major bcr-abl gene expression at a very low level in blood cells of some healthy individuals. *Blood* (1995) 86:3118–22. doi: 10.1182/blood.V86.8.3118.3118

6. Genovese G, Kähler AK, Handsaker RE, Lindberg J, Rose SA, Bakhoum SF, et al. Clonal hematopoiesis and blood-cancer risk inferred from blood DNA sequence. *N Engl J Med* (2014) 371:2477–87. doi: 10.1056/NEJMoa1409405

7. Jaiswal S, Fontanillas P, Flannick J, Manning A, Grauman PV, Mar BG, et al. Age-related clonal hematopoiesis associated with adverse outcomes. *N Engl J Med* (2014) 371:2488–98. doi: 10.1056/NEJMoa1408617

8. Chavakis T, Wielockx B, Hajishengallis G. Inflammatory modulation of hematopoiesis: Linking trained immunity and clonal hematopoiesis with chronic disorders. *Annu Rev Physiol* (2022) 84:183–207. doi: 10.1146/annurev-physiol-052521-013627

9. Cook EK, Luo M, Rauh MJ. Clonal hematopoiesis and inflammation: Partners in leukemogenesis and comorbidity. *Exp Hematol* (2020) 83:85–94. doi: 10.1016/j.exphem.2020.01.011

10. Jaiswal S, Libby P. Clonal haematopoiesis: connecting ageing and inflammation in cardiovascular disease. *Nat Rev Cardiol* (2020) 17:137–44. doi: 10.1038/s41569-019-0247-5

11. Svensson EC, Madar A, Campbell CD, He Y, Sultan M, Healey ML, et al. TET2-driven clonal hematopoiesis and response to canakinumab: An exploratory analysis of the CANTOS randomized clinical trial. *JAMA Cardiol* (2022) 7(5):521–8. doi: 10.1001/jamacardio.2022.0386

12. Asada S, Kitamura T. Clonal hematopoiesis and associated diseases: A review of recent findings. *Cancer Sci* (2021) 112:3962–71. doi: 10.1111/cas.15094

13. Hadjadj J, Yatim N, Barnabei L, Corneau A, Boussier J, Smith N, et al. Impaired type I interferon activity and inflammatory responses in severe COVID-19 patients. *Science* (2020) 369:718–24. doi: 10.1126/science.abc6027

14. Bernardes JP, Mishra N, Tran F, Bahmer T, Best L, Blase JI, et al. Longitudinal multi-omics analyses identify responses of megakaryocytes, erythroid cells, and plasmablasts as hallmarks of severe COVID-19. *Immunity* (2020) 53:1296–314.e9. doi: 10.1016/j.immuni.2020.11.017

15. Zhu L, Yang P, Zhao Y, Zhuang Z, Wang Z, Song R, et al. Single-cell sequencing of peripheral mononuclear cells reveals distinct immune response landscapes of COVID-19 and influenza patients. *Immunity* (2020) 53:685–96.e3. doi: 10.1016/j.immuni.2020.07.009

16. Lindner D, Fitzek A, Bräuninger H, Aleshcheva G, Edler C, Meissner K, et al. Association of cardiac infection with SARS-CoV-2 in confirmed COVID-19 autopsy cases. *JAMA Cardiol* (2020) 5:1281–5. doi: 10.1001/jamacardio.2020.3551

17. Siripanthong B, Nazarian S, Muser D, Deo R, Santangeli P, Khanji MY, et al. Recognizing COVID-19-related myocarditis: The possible pathophysiology and proposed guideline for diagnosis and management. *Heart Rhythm* (2020) 17:1463–71. doi: 10.1016/j.hrthm.2020.05.001

18. Guzik TJ, Mohiddin SA, Dimarco A, Patel V, Savvatis K, Marelli-Berg FM, et al. COVID-19 and the cardiovascular system: implications for risk assessment, diagnosis, and treatment options. *Cardiovasc Res* (2020) 116:1666–87. doi: 10.1093/cvr/cvaa106

19. Osuchowski MF, Aletti F, Cavaillon J-M, Flohé SB, Giamarellos-Bourboulis EJ, Huber-Lang M, et al. SARS-CoV-2/COVID-19: Evolving reality, global response, knowledge gaps, and opportunities. *Shock* (2020) 54:416–37. doi: 10.1097/SHK.0000000000001565

20. Li H, Liu L, Zhang D, Xu J, Dai H, Tang N, et al. SARS-CoV-2 and viral sepsis: observations and hypotheses. *Lancet* (2020) 395:1517–20. doi: 10.1016/S0140-6736(20)30920-X

21. Varga Z, Flammer AJ, Steiger P, Haberecker M, Andermatt R, Zinkernagel AS, et al. Endothelial cell infection and endotheliitis in COVID-19. *Lancet* (2020) 395:1417–8. doi: 10.1016/S0140-6736(20)30937-5

22. Dharan NJ, Yeh P, Bloch M, Yeung MM, Baker D, Guinto J, et al. HIV Is associated with an increased risk of age-related clonal hematopoiesis among older adults. *Nat Med* (2021) 27:1006–11. doi: 10.1038/s41591-021-01357-y

23. Zekavat SM, Lin S-H, Bick AG, Liu A, Paruchuri K, Wang C, et al. Hematopoietic mosaic chromosomal alterations increase the risk for diverse types of infection. *Nat Med* (2021) 27:1012–24. doi: 10.1038/s41591-021-01371-0

24. Petzer V, Schwendinger S, Haschka D, Vogi V, Tymoszuk P, Burkert F, et al. Clonal hematopoiesis in patients with covid-19 is stable and not linked to an aggravated clinical course. *Am J Hematol* (2021) 96:E331–3. doi: 10.1002/ajh.26251

25. Duployez N, Demonchy J, Berthon C, Goutay J, Caplan M, Moreau A-S, et al. Clinico-biological features and clonal hematopoiesis in patients with severe COVID-19. *Cancers (Basel)* (2020) 12, 1992. doi: 10.3390/cancers12071992

26. Bolton KL, Koh Y, Foote MB, Im H, Jee J, Sun CH, et al. Clonal hematopoiesis is associated with risk of severe covid-19. *Nat Commun* (2021) 12:5975. doi: 10.1038/s41467-021-26138-6

27. Hameister E, Stolz SM, Fuhrer Y, Thienemann F, Schaer DJ, Nemeth J, et al. Clonal hematopoiesis in hospitalized elderly patients with COVID-19. *Hemasphere* (2020) 4:e453. doi: 10.1097/HS9.0000000000000453

28. Zheng Z, Peng F, Xu B, Zhao J, Liu H, Peng J, et al. Risk factors of critical & mortal COVID-19 cases: A systematic literature review and meta-analysis. *J Infect* (2020) 81:e16–25. doi: 10.1016/j.jinf.2020.04.021

29. Liu B, Spokes P, He W, Kaldor J. High risk groups for severe COVID-19 in a whole of population cohort in Australia. *BMC Infect Dis* (2021) 21:685. doi: 10.1186/s12879-021-06378-z

30. Rommel A, von der LE, Treskova-Schwarzbach M, Scholz S. Population with an increased risk of severe COVID-19 in germany. analyses from GEDA 2019/2020-EHIS. *J Health Monit* (2021) 6:2–15. doi: 10.25646/7859

31. Haring B, Reiner AP, Liu J, Tobias DK, Whitsel E, Berger JS, et al. Healthy lifestyle and clonal hematopoiesis of indeterminate potential: Results from the women's health initiative. *J Am Heart Assoc* (2021) 10:e018789. doi: 10.1161/JAHA.120.018789

32. Thom CS, Wilken MB, Chou ST, Voight BF. Body mass index and adipose distribution have opposing genetic impacts on human blood traits. *Elife* (2022) 11:e75317. doi: 10.7554/eLife.75317

33. Pranata R, Huang I, Lukito AA, Raharjo SB. Elevated n-terminal pro-brain natriuretic peptide is associated with increased mortality in patients with COVID-19: systematic review and meta-analysis. *Postgrad Med J* (2020) 96:387–91. doi: 10.1136/postgradmedj-2020-137884

34. Peiris S, Ordunez P, DiPette D, Padwal R, Ambrosi P, Toledo J, et al. Cardiac manifestations in patients with COVID-19: A scoping review. *Glob Heart* (2022) 17:2. doi: 10.5334/gh.1037

35. Abplanalp WT, Mas-Peiro S, Cremer S, John D, Dimmeler S, Zeiher AM. Association of clonal hematopoiesis of indeterminate potential with inflammatory gene expression in patients with severe degenerative aortic valve stenosis or chronic postischemic heart failure. *JAMA Cardiol* (2020) 5:1170–5. doi: 10.1001/jamacardio.2020.2468

36. Jaiswal S, Natarajan P, Silver AJ, Gibson CJ, Bick AG, Shvartz E, et al. Clonal hematopoiesis and risk of atherosclerotic cardiovascular disease. *N Engl J Med* (2017) 377:111–21. doi: 10.1056/NEJMoa1701719

37. Fuster JJ, MacLauchlan S, Zuriaga MA, Polackal MN, Ostriker AC, Chakraborty R, et al. Clonal hematopoiesis associated with TET2 deficiency accelerates atherosclerosis development in mice. *Science* (2017) 355:842–7. doi: 10.1126/science.aag1381

38. Shivarov V, Ivanova M. Clonal haematopoiesis and COVID-19: A possible deadly liaison. *Int J Immunogenet* (2020) 47:329–31. doi: 10.1111/iji.12503

39. Mas-Peiro S, Hoffmann J, Fichtlscherer S, Dorsheimer L, Rieger MA, Dimmeler S, et al. Clonal haematopoiesis in patients with degenerative aortic valve stenosis undergoing transcatheter aortic valve implantation. *Eur Heart J* (2020) 41:933–9. doi: 10.1093/eurheartj/ehz591

40. Avagyan S, Henninger JE, Mannherz WP, Mistry M, Yoon J, Yang S, et al. Resistance to inflammation underlies enhanced fitness in clonal hematopoiesis. *Science* (2021) 374:768–72. doi: 10.1126/science.aba9304

41. Tan AT, Linster M, Tan CW, Le Bert N, Chia WN, Kunasegaran K, et al. Early induction of functional SARS-CoV-2-specific T cells associates with rapid viral clearance and mild disease in COVID-19 patients. *Cell Rep* (2021) 34:108728. doi: 10.1016/j.celrep.2021.108728

42. Mathew D, Giles JR, Baxter AE, Oldridge DA, Greenplate AR, Wu JE, et al. Deep immune profiling of COVID-19 patients reveals distinct immunotypes with therapeutic implications. *Science* (2020) 369:eabc8511. doi: 10.1126/science.abc8511

COPYRIGHT

© 2022 Schenz, Rump, Siegler, Hemmerling, Rahmel, Thon, Nowak, Fischer, Hafner, Tichy, Bomans, Meggendorfer, Koos, von Groote, Zarbock, Fiedler, Zemva, Larmann, Merle, Adamzik, Müller-Tidow, Haferlach, Leuschner and Weigand. This is an open-access article distributed under the terms of the Creative Commons Attribution License (CC BY). The use, distribution or reproduction in other forums is permitted, provided the original author(s) and the copyright owner(s) are credited and that the original publication in this journal is cited, in accordance with accepted academic practice. No use, distribution or reproduction is permitted which does not comply with these terms.

frontiers | Frontiers in Immunology

TYPE Original Research
PUBLISHED 25 October 2022
DOI 10.3389/fimmu.2022.975918

Check for updates

OPEN ACCESS

EDITED BY
Martijn van Griensven,
Maastricht University, Netherlands

REVIEWED BY
Pierre-Antoine Gourraud,
Université de Nantes,
France
Shabnam Salimi,
University of Washington,
United States

*CORRESPONDENCE
Mayana Zatz
mayazatz@usp.br
Erick C. Castelli
erick.castelli@unesp.br
Mateus V. de Castro
mateusvidigal@hotmail.com

†These authors have contributed equally to this work

SPECIALTY SECTION
This article was submitted to Viral Immunology, a section of the journal Frontiers in Immunology

RECEIVED 22 June 2022
ACCEPTED 15 September 2022
PUBLISHED 25 October 2022

CITATION
Castelli EC, de Castro MV, Naslavsky MS, Scliar MO, Silva NSB, Pereira RN, Ciriaco VAO, Castro CFB, Mendes-Junior CT, Silveira ES, de Oliveira IM, Antonio EC, Vieira GF, Meyer D, Nunes K, Matos LRB, Silva MVR, Wang JYT, Esposito J, Cória VR, Magawa JY, Santos KS, Cunha-Neto E, Kalil J, Bortolin RH, Hirata MH, Dell'Aquila LP, Razuk-Filho A, Batista-Júnior PB, Duarte-Neto AN, Dolhnikoff M, Saldiva PHN, Passos-Bueno MR and Zatz M (2022) MUC22, HLA-A, and HLA-DOB variants and COVID-19 in resilient super-agers from Brazil. *Front. Immunol.* 13:975918. doi: 10.3389/fimmu.2022.975918

MUC22, HLA-A, and HLA-DOB variants and COVID-19 in resilient super-agers from Brazil

Erick C. Castelli[1,2*†], Mateus V. de Castro[3*†], Michel S. Naslavsky[3,4], Marilia O. Scliar[3], Nayane S. B. Silva[2], Raphaela N. Pereira[2], Viviane A. O. Ciriaco[2], Camila F. B. Castro[2,5], Celso T. Mendes-Junior[6], Etiele de S. Silveira[7], Iuri M. de Oliveira[7], Eduardo C. Antonio[7], Gustavo F. Vieira[7,8], Diogo Meyer[4], Kelly Nunes[4], Larissa R. B. Matos[3], Monize V. R. Silva[3], Jaqueline Y. T. Wang[3], Joyce Esposito[3], Vivian R. Cória[3], Jhosiene Y. Magawa[9,10,11], Keity S. Santos[9,10,11], Edecio Cunha-Neto[9,10,11], Jorge Kalil[9,10,11], Raul H. Bortolin[12], Mário Hiroyuki Hirata[12], Luiz P. Dell'Aquila[13], Alvaro Razuk-Filho[13], Pedro B. Batista-Júnior[13], Amaro N. Duarte-Neto[14], Marisa Dolhnikoff[14], Paulo H. N. Saldiva[14], Maria Rita Passos-Bueno[3,4] and Mayana Zatz[3,4*]

[1]Department of Pathology, School of Medicine, São Paulo State University (UNESP), Botucatu, Brazil, [2]Molecular Genetics and Bioinformatics Laboratory, Experimental Research Unit (Unipex), School of Medicine, São Paulo State University (UNESP), Botucatu, Brazil, [3]Human Genome and Stem Cell Research Center, University of São Paulo, São Paulo, Brazil, [4]Department of Genetics and Evolutionary Biology, Biosciences Institute, University of São Paulo, São Paulo, Brazil, [5]Centro Universitário Sudoeste Paulista, Avaré, Brazil, [6]Departamento de Química, Faculdade de Filosofa, Ciências e Letras de Ribeirão Preto, Universidade de São Paulo, Ribeirão Preto, Brazil, [7]Programa de Pós-Graduação em Genética e Biologia Molecular, Universidade Federal do Rio Grande do Sul (UFRGS), Porto Alegre, Brazil, [8]Laboratório de Saúde Humana *In Silico*, Programa de Pós-Graduação em Saúde e Desenvolvimento Humano, Universidade La Salle, Canoas, Brazil, [9]Departamento de Clínica Médica, Disciplina de Alergia e Imunologia Clínica, Faculdade de Medicina da Universidade de São Paulo, São Paulo, Brazil, [10]Laboratório de Imunologia, Instituto do Coração (InCor), LIM19, Hospital das Clínicas da Faculdade de Medicina da Universidade de São Paulo, (HCFMUSP), São Paulo, Brazil, [11]Instituto de Investigação em Imunologia, Instituto Nacional de Ciências e Tecnologia-iii (INCT), São Paulo, Brazil, [12]Department of Clinical and Toxicological Analyses, School of Pharmaceutical Sciences, University of São Paulo, São Paulo, Brazil, [13]Prevent Senior Institute, São Paulo, Brazil, [14]Department of Pathology, School of Medicine, University of Sao Paulo, Sao Paulo, Brazil

Background: Although aging correlates with a worse prognosis for Covid-19, super elderly still unvaccinated individuals presenting mild or no symptoms have been reported worldwide. Most of the reported genetic variants responsible for increased disease susceptibility are associated with immune response, involving type I IFN immunity and modulation; *HLA* cluster genes; inflammasome activation; genes of interleukins; and chemokines receptors. On the other hand, little is known about the resistance mechanisms against SARS-CoV-2 infection. Here, we addressed polymorphisms in the MHC region

associated with Covid-19 outcome in super elderly resilient patients as compared to younger patients with a severe outcome.

Methods: SARS-CoV-2 infection was confirmed by RT-PCR test. Aiming to identify candidate genes associated with host resistance, we investigated 87 individuals older than 90 years who recovered from Covid-19 with mild symptoms or who remained asymptomatic following positive test for SARS-CoV-2 as compared to 55 individuals younger than 60 years who had a severe disease or died due to Covid-19, as well as to the general elderly population from the same city. Whole-exome sequencing and an in-depth analysis of the MHC region was performed. All samples were collected in early 2020 and before the local vaccination programs started.

Results: We found that the resilient super elderly group displayed a higher frequency of some missense variants in the *MUC22* gene (a member of the mucins' family) as one of the strongest signals in the MHC region as compared to the severe Covid-19 group and the general elderly control population. For example, the missense variant rs62399430 at *MUC22* is two times more frequent among the resilient super elderly (p = 0.00002, OR = 2.24).

Conclusion: Since the pro-inflammatory basal state in the elderly may enhance the susceptibility to severe Covid-19, we hypothesized that *MUC22* might play an important protective role against severe Covid-19, by reducing overactive immune responses in the senior population.

KEYWORDS

human leukocyte antigens, immune response, major histocompatibility complex (MCH), HLA, SARS-CoV-2, MUC22, COVID-19, resistant genetic variants

Introduction

Although a diverse clinical spectrum has been described among patients with Covid-19, robust data show that increasing age correlates with more severe disease and a higher frequency of deaths worldwide (1). While the elderly have a higher prevalence of comorbidities such as cardiovascular diseases, diabetes, and cancer - which are also independently associated with a higher risk of severe Covid-19 (2), increasing age is still the most significant risk factor for Covid-19 mortality (3). To yield clues about this infection susceptibility, the comparison of extremely older people presenting mild symptoms and young adults with a very severe outcome may contribute with relevant observations.

Covid-19 severity among the elderly may be related to immunosenescence, changes in cytokine patterns, activation of inflammatory pathways, and impaired innate and adaptive immune responses (4–6). Also, comorbidities in older individuals are strongly associated with an increased risk of Covid-19 complications (7, 8). Alternatively, older individuals are more likely to have been exposed to other corona and influenza viruses during their lifespan, even by vaccination, increasing their odds of defeating SARS-CoV-2 (9). For instance, centenarians exposed to the 1918 H1N1 influenza virus might present some protection against SARS-CoV-2 infection (10).

The MHC (Major Histocompatibility Complex) region contains more than 200 genes, many of them related to immunity. Therefore, it is a natural candidate for influencing infectious disease susceptibility and severity. MHC genes influence different levels of the immune response against viruses, such as genes encoding cytokines and molecules of the complement system, which may influence Covid-19 severity and cytokine storm (11, 12), genes encoding membrane-associated mucins (*MUC22*) (13), and genes encoding molecules that mediate NK cell responses (*HLA-G*, *HLA-E*, *MICA*, and *MICB*) (14–17). Some of the MHC genes are particularly important to the antigen presentation pathway. *HLA-A*, *HLA-B*, and *HLA-C* encode the heavy chain of the MHC-I molecule, responsible for binding the intracellular antigens and presenting

them on the cell surface to the T cell receptor (TCR) of CD8 T lymphocytes. Likewise, *HLA-DRA*, *HLA-DRB1*, *HLA-DQA1*, *HLA-DQB1*, *HLA-DPA1*, *HLA-DPB1*, and others, encode the MHC-II molecule, responsible for binding the exogenous antigens, usually internalized by antigen-presenting cells such as macrophages, and presenting them on the cell surface to CD4 T lymphocytes. These genes are highly polymorphic, with hundreds to thousands of alleles for each locus (18). Such diversity influences antigen presentation since different MHC molecules may present a different subset of antigens (19).

Because of the unusually high polymorphism and extensive paralogy of the MHC region, particularly at the HLA classical class I and II genes, the MHC region requires specialized tools to align short reads correctly and, thus, call genotypes and haplotypes properly (20, 21). Additionally, allele frequencies vary across populations, as clearly documented in previous studies focusing on HLA genes and Covid-19 (22–26). Associations between HLA genotype and disease severity extend to other unrelated viruses, such as HIV and dengue (27, 28). Some MHC variants have already been reported to be associated with Covid-19 severity. *HLA-G* variant rs9380142 was associated with Covid-19 critical illness (29) and *HLA-E* allele E*01:01 with Covid-19 severity, particularly in patients requiring intensive care (30). The *CCHCR1* locus was associated with critical illness in Covid-19 (29).

We hypothesized that differences in MHC can predispose to a severe or mild clinical course in Covid-19 despite age. Therefore, aiming to verify the existence of MHC differences between extreme opposed outcomes for Covid-19, we have analyzed exomes of Brazilian convalescents by SARS-COV-2 grouped according to Covid-19 clinical status and age: a group of super elderly patients (>= 94 yo) recovered from Covid-19 with mild to moderate symptoms (without ventilation support) as compared to younger adults (mean age <= 52) with severe disease (with ventilation support). We also compared patients with a previously whole-genome sequenced (WGS) census-based sample of elderly individuals from the same city (São Paulo, Brazil), sampled before the current pandemic (31). Brazilians are a highly admixed population composed of tri-hybrid proportions of European (average 73%), African (18%), and Native American (9%) ancestries (31). This was taken into account and therefore global genomic ancestry was controlled when performing the association study.

Materials and methods

Definition of the groups

This survey included 225 patients with Covid-19, as illustrated in Figure 1. Diagnostic tests (RT-PCR) confirmed the positive SARS-CoV-2 infection in all individuals. The samples were collected between June and October 2020, before new SARS-CoV-2 variants were reported in Brazil (especially Gamma) and before the onset of the Brazilian vaccination program against Covid-19.

Covid-19 severity was classified according to the clinical spectrum of the World Health Organization's updated guideline

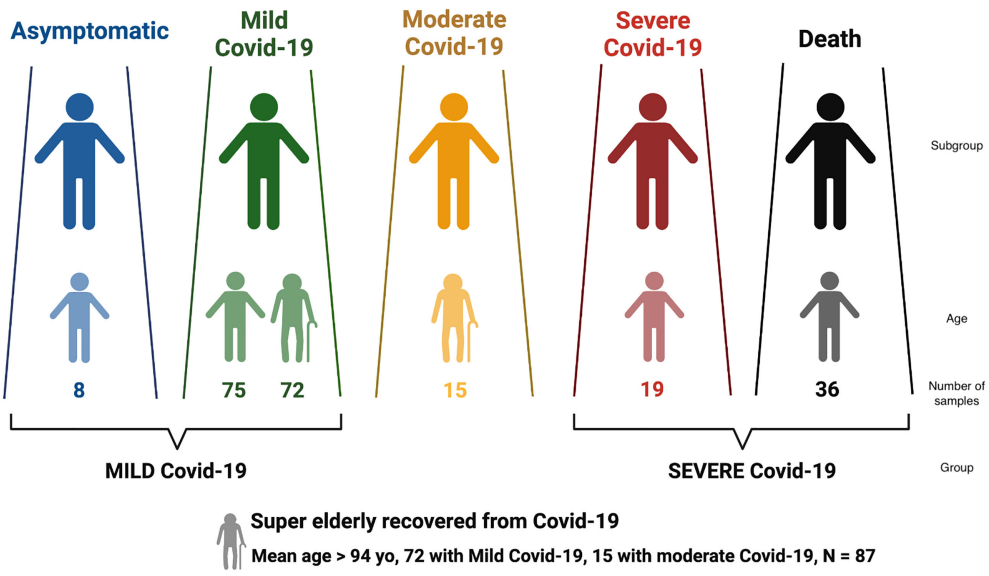

FIGURE 1
Distribution of Brazilian individuals with SARS-CoV-2 infection according to Covid-19 severity, and the definition of the larger groups MILD and SEVERE Covid-19.

for Covid-19 treatment (https://www.covid19treatmentguidelines.nih.gov/overview/clinical-spectrum/). Patients that were asymptomatic or presented mild symptoms were grouped into MILD Covid-19; deceased and/or hospitalized in ICU requiring ventilation support were grouped into SEVERE Covid-19 (Figure 1). The SEVERE group is significantly younger than the MILD group (Supplementary Table S1, $p< 10^{-5}$).

We also considered a special group named super elderly (>= 94 yo) who recovered from Covid-19, with 72 super elderly with mild Covid-19 and 15 with moderate symptoms. We retrieved clinical data regarding the progression of Covi-19 and diagnostic test results.

These Covid-19 groups were compared with MHC data from a previously whole-genome sequenced (WGS) sample of Brazilian elderly individuals (>= 65 yo), known as the SABE cohort (31), collected before the SARS-CoV-2 outbreak and representative of the general elderly population in the same city. Age, sex, and mean genetic ancestry distributions for each group are displayed in Supplementary Table S1 and were used as co-variables in regression models.

Exome and whole-genome sequencing

We obtained full exomes from DNA extracted from patients' samples with SARS-CoV-2 infection. We used the Nextera Rapid Capture Custom Enrichment Kit or the Nextera Flex Kit (Illumina, San Diego, CA, USA) for library preparation and the IDT xgen-V1 kit for capture following manufacturer protocols. Whole-exome sequencing was performed on the NovaSeq 6000 equipment (Illumina, USA) with a 150-base paired-end dual index read format. Reads were aligned to the human reference GRCh38 using Burrow–Wheeler Aligner (BWA), algorithm MEM (https://github.com/lh3/bwa/tree/master/bwakit). We also called genotypes using GATK HaplotypeCaller (version 4.0.9). We used the genotypes obtained in this step to infer the genetic ancestry. The pipeline used for alignment, variant calling, variant refinement, and genetic ancestry assessment is detailed elsewhere (22).

For the general elderly population (SABE), whole-genome sequencing was performed previously (31). Although SARS-Cov-2 infection is unknown for this cohort, this data provides a baseline for the frequency of each polymorphism in the general elderly population from São Paulo.

MHC genotyping and haplotyping

The MHC region is prone to genotyping errors because of alignment bias in paralogous and highly polymorphic genes (20, 21, 32). The HLA classical class I and II genes are the most impacted ones by alignment bias, and conventional NGS analysis workflows are not suitable for genotyping them. We used a customized workflow to circumvent this issue and get reliable genotypes and haplotypes in the MHC region. We used HLA-mapper (version 4) (20) to optimize read alignment along the MHC region (Supplementary Figure S1). The input for HLA-mapper is the BAM file obtained in the previous step (for exomes or whole-genomes). After applying HLA-mapper to correct the alignments, we called genotypes using GATK 4 HaplotypeCaller. Then, we selected only the variants that overlapped the region captured by the Exome, with no more than 5% of missing alleles in the Exomes. After, we refined the variants using the standard Variant Quality Score Recalibration (VQSR) supplemented with known variants from HLA genes. To obtain phased variants for each gene, we first phased closely located variants using WhatsHap (33). Then, we combined phase sets using Shapeit 4 (34). The final product is a phased VCF with SNPs throughout the MHC.

HLA allele calling

For *HLA-A*, *HLA-B*, *HLA-C*, *HLA-E*, *HLA-F*, *HLA-G*, *MICA*, *MICB*, *HLA-DOA*, *HLA-DOB*, *HLA-DMA*, *HLA-DMB*, *HLA-DRA*, *HLA-DPA1*, *HLA-DPB1*, *TAP1*, and *TAP2*, we obtained the complete exonic sequences for each individual by converting the phased VCF obtained in the previous step into complete CDS sequences using vcfx transcript (www.castelli-lab.net/apps/vcfx). We also translated these sequences into protein sequences (the allotypes) using Emboss transeq. We called HLA alleles (3-field and 2-field resolution) directly from these CDS and predicted protein sequences, comparing them with the ones reported in the IPD-IMGT/HLA database (35). Because of exome probe-capturing bias in some MHC regions, we imputed *HLA-DRB1*, *HLA-DQA1*, and *HLA-DQB1* 2-field alleles instead of calling alleles directly from the VCF data, as discussed in the next section.

Quality control for MHC variants and HLA imputation for *HLA-DRB1*, *HLA-DQA1*, and HLA-*DQB1*

For exomes, we noticed a probe-capturing bias in some MHC regions, which is not an unexpected issue, especially for HLA genes (32, 36). This bias is quite strong for *HLA-DRB1*, *HLA-DQA1*, and *HLA-DQB1*, as illustrated in Supplementary Figure S2. Although the HLA-mapper optimization corrects most of the alignment errors in HLA genes, the absence of sequences from one chromosome (the capture bias) led to genotyping bias and allele call errors. This is particularly problematic when comparing exomes and whole genomes because this error occurs only in the former.

To circumvent this issue, we only selected from the exomes the variants with an average proportion of reads among alleles in

heterozygous sites (i.e., the allele balance) over 0.3, represented as a red line in Supplementary Figure S2. This procedure might have eliminated some important variants, but it allowed us to compare exomes and whole genomes by avoiding variants prone to genotyping errors. In addition, we selected only variants with a frequency of at least 1%, either among patients or among the general elderly population. Accordingly, 2,346 SNPs were selected across the MHC and were considered for all subsequent analyses.

The capture bias discussed above prevented the direct call of HLA alleles for *HLA-DRB1*, *HLA-DQA1*, and *HLA-DQB1*. We applied an imputation method with HIBAG 1.5 (37) to call 2-field resolution alleles (Supplementary Figure S1). First, we built a reference panel based on whole-genome data from Brazilians, the 1000Genomes, and HGDP datasets, using the same pipeline as presented in Supplementary Figure S1. The selected variants for the imputation model are bi-allelic variants present in both the reference panel and exomes and show an average proportion of reads among alleles in heterozygous sites over 0.30 in exomes (Supplementary Figure S2). After imputation, the incompatibility between imputed HLA alleles and direct calls was as follows: HLA-A (4.1%), HLA-B (2.8%), HLA-C (2.2%), HLA-DRB1 (20.9%), HLA-DQA1 (23%), and HLA-DQB1 (28.4%). Because of that, we opted to consider only the direct calls for *HLA-A*, *HLA-B*, and *HLA-C*, and only the imputed alleles from *HLA-DRB1*, *HLA-DQA1*, and *HLA-DQB1*.

Statistical analyses for association

The usual threshold for genome-wide significance in GWAS studies is $P< 10^{-8}$, defined based on the average number of segregation blocks in European genomes. However, here, we are focusing on 2,346 SNPs across the MHC (not the full genome), in a different population (admixed Brazilians), and in a region with different LD patterns than the rest of the genome. Therefore, we calculated the number of different segregation blocks observed across our data by using Haploview and the confidence intervals algorithm (38). We detected exactly 100 segregation blocks with all bi-allelic markers with minimum allele frequencies of 2%. Therefore, we set alpha = 0.05/100 = 0.0005 as the threshold for detecting an associated variant despite multiple tests (the red lines in the Manhattan plots). We also report candidates that reach a 10-fold higher threshold, alpha < 0.005 (the blue line in the Manhattan plots) to avoid missing potential variants associated with Covid 19 severity.

We used plink2 to fit a logistic regression that considers each variable site, allotype, or amino acid residue as an independent marker. We created a plink-format table file containing a column for each allele of a SNP, every allotype, each amino acid in a specific position, and the dosage observed for the samples (from 0 to 2). The regression analysis, performed in R, considered sex and genetic ancestry as covariables in all comparisons. We did not include age as covariable to adjust *P*-values because of the super elderly. To evaluate the amino acid residues, we first aligned the predicted protein sequence of all individuals. While we considered all SNPs that have passed the filter described above, for the allotype and amino acid residues, we considered only the following genes: *HLA-A*, *HLA-B*, *HLA-C*, *HLA-E*, *HLA-F*, *HLA-G*, *MICA*, *MICB*, *HLA-DRA*, *HLA-DRB1*, *HLA-DQA1*, *HLA-DQB1*, *HLA-DPA1*, *HLA-DPB1*, *HLA-DOA*, *HLA-DOB*, *HLA-DMA*, *HLA-DMB*, *TAP1*, and *TAP2*.

Modeling of HLA structures and analysis of immunogenic regions and spike epitopes

Aiming to enhance our understanding of underlying mechanisms for HLA alleles associated with disease severity and the mechanisms underlying the associations, we have predicted the HLA molecule structure and the SARS-CoV-2 peptides that can bind to these HLA versions. The detailed methods are in the supplementary material.

Results

Covid-19 demographic data

Supplementary Table S1 presents demographic data and mean genome-wide genetic ancestry for each group. The mean age for the MILD group (66.9 years) is significantly higher than the SEVERE group (51.3 years), $p < 10^{-5}$. There are more women in the MILD group (58.3%) and among the super elderly (74.7%) than in the SEVERE Covid-19 (43.6%).

All groups present similar proportions of genetic ancestry, except the SEVERE group which has a greater African and Native American ancestry than the MILD or the general elderly population from the same city (Supplementary Table S1). On one hand, ancestry might be related to Covid-19 severity, as observed for some Covid-19 comorbidities. For example, diabetes is a risk factor for severe Covid-19 (39) and is more frequent in individuals with higher African and Native-American ancestry in some populations (40). On the other hand, the lower socioeconomic status of a Brazilian citizen is correlated with a higher African and Native American ancestry. Most of the severe cases came from public hospitals, which, on average, are of poorer quality and lower efficiency, and then enriched for individuals with lower socioeconomic status (41). Nevertheless, the reported association results were controlled for genetic ancestry, which allowed adjustment to some extent for the socioeconomic scores.

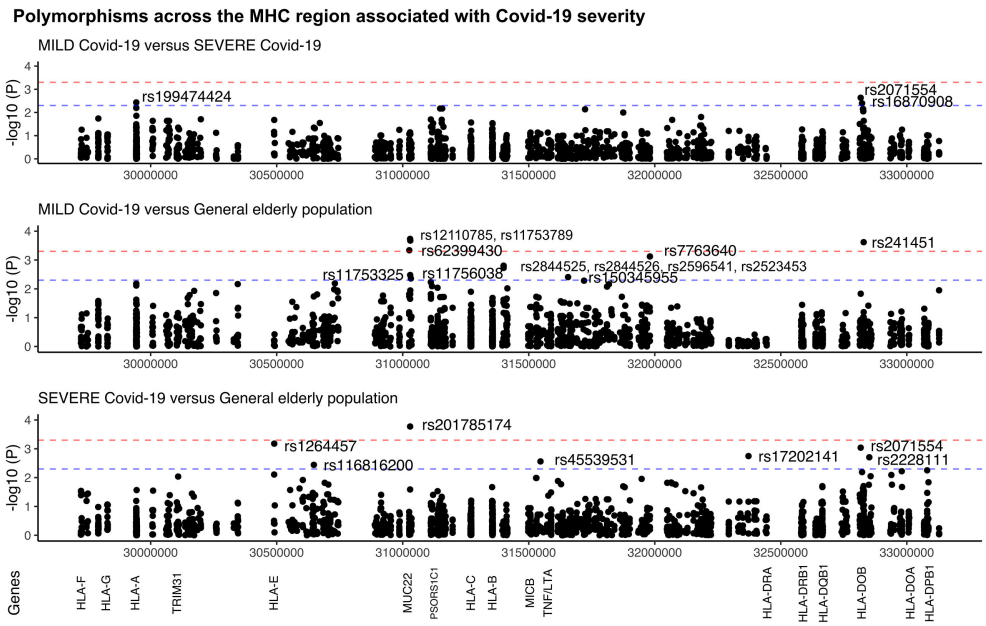

FIGURE 2
Manhattan plot illustrating differences among patients with MILD and SEVERE Covid-19, and the general elderly population from the same city. The general elderly population consists of whole-genomes (WGS) of 1,170 elders from São Paulo city, with unknown status regarding Covid-19. We considered only variants with a minor allele frequency of 1% in at least one of the groups, with no more than 5% of missing alleles in both groups, and with a ratio between read depth for each allele in heterozygous sites ranging from 0.3 to 0.5 for Exomes (the MILD and SEVERE groups). The red line marks the threshold for detecting a variant associated with the phenotype by calculating the number of segregation blocks observed in our data. The blue line marks the suggestive threshold for a candidate variant, $p < 0.005$. Most *MUC22* variants are in Linkage Disequilibrium ($r^2 > 0.8$).

Extreme outcomes for Covid-19 severity

The comparison between the SEVERE and MILD groups revealed three missense candidate variants that are 2-3 times more frequent in the SEVERE group than in MILD, coinciding with genes *HLA-A*, *HLA-DOB*, and *TAP2* (Figure 2 and Table 1). The *HLA-A* variant is also significantly less frequent in the MILD group than in the general elderly population ($p = 0.0066$), and *HLA-DOB* and *TAP2* variants are also significantly overrepresented in the SEVERE group compared to the general elderly population ($p = 0.0009$ and $p = 0.0064$, respectively), according with Table 1.

Probably because of the relatively small and different sample size of both the MILD and SEVERE groups, some variants are highlighted when compared to the general elderly population but not when comparing the Covid-19 groups, as, the susceptibility missense variants rs1264457 at *HLA-E* and rs2228111 at *TAP1*, among others. On the other hand, the protective missense variants at *MUC22* are significantly overrepresented among patients with MILD Covid-19 (Figure 2 and Table 1).

We also evaluated whether variants are associated with Covid-19 severity in younger patients by removing the super elderly from the MILD group. The resulting smaller sample size did not allow the identification of candidate variants in this comparison. However, the pattern observed in Table 1 was maintained.

We explored the allotypes and amino acid frequencies in different groups (Table 2). DOB*01:02 and the amino acid that defines this allotype, 18Q, are overrepresented in the SEVERE group compared to the MILD and the general elderly population. This amino acid exchange is related to the rs2071554 variant described in Table 1. HLA-E*01:03 and the main amino acid exchange that composes this allotype, 128G, is significantly overrepresented in the SEVERE group when compared to the general elderly population ($p < 0.005$) and the MILD group ($p < 0.05$). This amino acid exchange is related to rs1264457 (Table 1). All variants that define the allotype MICA*008 are overrepresented in the MILD group when compared to the general population (Table 2).

Two amino acid residues at HLA-A, 86R and 87N (full-length protein) or 62R and 63N (mature protein), are

TABLE 1 Polymorphisms across the MHC region (SNPs and indels) that are associated with Covid-19 severity in Brazilian patients.

Position (Chr6, hg38)	SNP	Allele	Gene	LD group	Type	Severe (N = 55)	Mild (N = 163)	General population (N = 1.170)	Severe vs mild (p)	Severe vs general population (p)	Mild vs general population (p)
29942944	rs199474424	C	*HLA-A*	none	missense	0.2091	0.0890	0.1543	0.0037	0.1135	0.0066
30490287	rs1264457	G	*HLA-E*	none	missense	0.5545	0.4540	0.4325	0.0210	0.0007	0.6720
30647507	rs116816200	A	*C6orf136*	none	intronic	0.0545	0.0337	0.0175	0.2926	0.0036	0.1671
31026089	rs62399430	T	*MUC22*	A	missense	0.1273	0.2362	0.1449	0.0849	0.5381	0.0005*
31029301	rs11753789	C	*MUC22*	A	synonymous	0.1182	0.2393	0.1436	0.0720	0.4688	0.0002*
31029557	rs11756038	G	*MUC22*	A	missense	0.1182	0.2025	0.1299	0.1659	0.6488	0.0033
31030047	rs12110785	C	*MUC22*	none	missense	0.1636	0.2577	0.1778	0.0867	0.6170	0.0002*
31032362	rs11753325	T	*MUC22*	A	synonymous	0.1182	0.2025	0.1278	0.2361	0.7307	0.0044
31399930	rs2844526	C	*MICA*	B	upstream	0.4364	0.3712	0.4692	0.4112	0.6266	0.0016
31400061	rs2596541	A	*MICA*	B	upstream	0.4364	0.3712	0.4692	0.4113	0.6266	0.0016
31400348	rs2523453	G	*MICA*	B	upstream	0.4455	0.3742	0.4718	0.3335	0.7015	0.0019
31400377	rs2844525	C	*MICA*	B	upstream	0.4364	0.3712	0.4697	0.4112	0.5952	0.0016
31546626	rs45539531	A	*ATP6V1G2/ DDX39B*	none	upstream	0.0727	0.0337	0.0282	0.0841	0.0027	0.7841
31656057	rs150345955	G	*APOM*	none	missense	0.0000	0.0184	0.0034	0.5197	0.9881	0.0039
31980631	rs7763640	C	*STK19/C4A*	none	intronic/ upstream	0.0182	0.0123	0.0667	0.4561	0.1179	0.0008
32371721	rs17202141	G	*TSBP1*	none	downstream	0.0364	0.0031	0.0047	0.1123	0.0018	0.6683
32816899	rs2071554	T	*HLA-DOB*	none	missense	0.1364	0.0552	0.0607	0.0023	0.0009	0.7990
32822312	rs16870908	A	*TAP2*	none	missense	0.1364	0.0521	0.0697	0.0040	0.0064	0.5050
32851137	rs2228111	A	*TAP1*	none	missense	0.0364	0.0061	0.0056	0.2484	0.0020	0.3688

The SABE cohort represents the general population frequencies in the same city as the Covid-19 patients.
*These variants achieved the threshold for a variant associated with mild Covid-19 infection. All others are candidate variants. LD (Linkage Disequilibrium) groups, A: $r^2 > 0.8$, B: $r^2 > 0.98$.

significantly overrepresented in the SEVERE group when compared to the MILD group ($p < 0.005$), and overrepresented in the general elderly population when compared to the MILD group ($p < 0.01$). Likewise, HLA-A residue 156/W is less frequent in the MILD group compared to the SEVERE ($p < 0.05$) and the general elderly population ($p < 0.005$). Residues 62R and 63N are associated with many HLA-A allotypes, including A*25, A*26, A*33, A*34, A*66, A*68, and A*69. Residue 156/W is associated with allotypes A*25, A*26, A*34, A*43, A*66, and A*68.

The linkage disequilibrium (LD) pattern in Figure S7 indicates that most Covid-19-associated *MUC22* polymorphisms are in strong LD. Likewise, the MICA variants (all associated with MICA*008) are in strong LD. *MUC22* and

TABLE 2 MHC allotypes and amino acid residues associated with Covid-19 disease severity in Brazil.

Allotype	Severe covid-19 (*N* = 55)	Mild covid-19 (*N* = 163)	General population (*N* = 1170)	Severe vs mild (*P*)	Severe vs general population (*P*)	Mild vs general population (*P*)
DOB*01:02 or 18Q	0.1364	0.0552	0.0607	0.0005	0.0007	0.7951
E*01:03	0.5455	0.4356	0.4137	0.0173	0.0001	0.7079
HLA-E^G	0.5545	0.4324	0.4539	0.0227	0.0008	0.7176
MICA*008	0.2727	0.3221	0.2436	0.1758	0.6026	0.0039
Amino Acid exchanges that define MICA*008	0.2727	0.3220	0.2444	0.1759	0.6332	0.0044
HLA-A 62R/63N	0.2090	0.0889	0.1542	0.0017	0.1345	0.0055
HLA-A 156W	0.1636	0.0797	0.1380	0.0254	0.3280	0.0027
TAP1 286F	0.0363	0.0061	0.0055	0.2133	0.0001	0.4647

*adjusted for sex and genetic ancestry.

MICA are independent signals. The signals from *HLA-DOB* and TAP2 might not be independent. There is no LD between the *HLA-A* variant and other relevant variants across the MHC.

Super elderly patients recovered from Covid-19 as compared to the elderly general population

The strongest signal coincides with gene *MUC22*, rs62399430, two times more frequent among the super elderly than in the SEVERE group (p = 0.0057, OR=0.30). Moreover, when super elderly are compared to the general elderly population from the same city, we detected candidate variants in two genes, *MUC22 and PSORS1C1/CDSN* (Figure 3). Most of the signals coincide with gene *MUC22*. Variants rs62399430, rs11753789, and rs12110785 (p < 0.0002, OR > 2.0) are, in general, two times more frequent among super elderly recovered from Covid-19. Two of these are missense variants. Most *MUC22* variants are in Linkage Disequilibrium (r^2> 0.8, Figure S7). These variants are also overrepresented in the MILD Covid-19 group, which includes most of the super elderly patients and younger patients with mild Covid-19. Another candidate variant for protection is rs145583110, an intronic variant from *PSORS1C1* or exonic for *CDSN*, which is 3 times more frequent among the super elderly than in the general population (p = 0.0018, OR = 3.85).

The allotype and amino acid residue frequencies reveal no relevant association when comparing super elderly with MILD Covid-19 and younger patients with SEVERE Covid-19, or when super elderly are compared to the general elderly population.

Discussion

Here we investigated the polymorphisms across the MHC region associated with Covid-19 disease severity in patients with extreme phenotypes: young adults with severe Covid-19, and super elderly individuals with mild Covid-19. All the samples were collected between June and October 2020, before new SARS-CoV-2 variants were reported in Brazil (especially Gamma) and before the onset of the Brazilian vaccination program against Covid-19. This data may shed some light on the mechanisms underlying SARS-CoV-2 resistance, particularly for the earlier SARS-CoV-2 strains in unvaccinated individuals. All samples from the control elderly Brazilian population were collected before the SARS-CoV-2 outbreak.

We applied a bioinformatics pipeline to correct alignments and call reliable genotypes and HLA alleles and detected some associated and candidate variants that influence infection severity, some related to genes from the antigen presentation pathway and others from different pathways. This section will focus on the strongest hits and the frequent candidate variants associated with the phenotypes, particularly *MUC22*, *HLA-A*, and *HLA-DOB*.

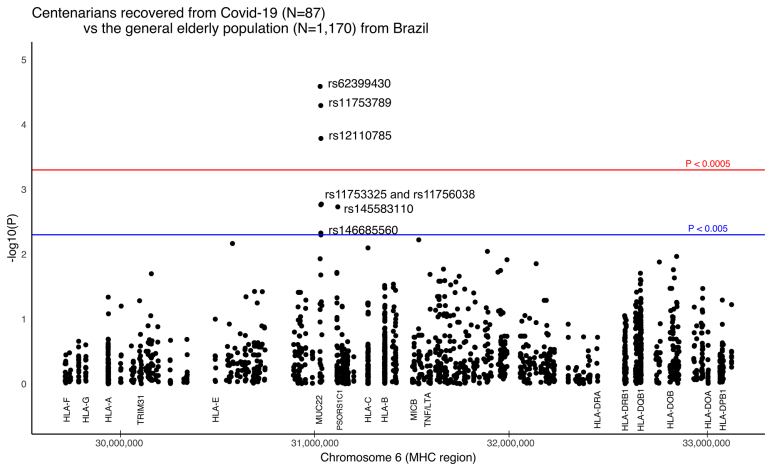

FIGURE 3
Manhattan plot illustrating differences between Brazilian centenarians (>90 y) recovered from Covid-19 and the general elderly population. The general population consists of whole-genomes (WGS) of 1,170 elders from São Paulo city (> 65 y), with unknown status regarding Covid-19. The centenarian group includes exomes of 87 patients more than 90 years old that presented mild Covid-19 symptoms. We considered only variants with a minor allele frequency of 1% in at least one of the groups, with no more than 5% of missing alleles in both groups, and with a ratio between read depth for each allele in heterozygous sites ranging from 0.3 to 0.5 for Exomes. The red line marks the threshold for detecting a variant associated with the phenotype by calculating the number of segregation blocks observed in our data. The blue line marks the suggestive threshold for a candidate variant, p < 0.005. Most *MUC22* variants are in Linkage Disequilibrium (r^2 > 0.8).

MUC22 variants and mild Covid-19

We detected missense *MUC22* variants associated with mild Covid-19 when evaluating all patients with mild symptoms, and the super elderly recovered from Covid-19. MUC genes encode mucins, and 16 different mucins have been identified in the lung (42). Mucins are high-molecular-weight glycoproteins that can be secreted or anchored to the cell membrane (transmembrane mucins) (42). *MUC22* is a member of the mucins' family. It encodes transmembrane mucins expressed in the bronchi of the lungs and participates in the inflammatory and innate immune response (43, 44). Airway mucus comprises water, antimicrobial proteins, serum protein transudates, and mucus glycoproteins. It protects and lubricates the respiratory tract. However, excessive mucus production is related to inflammatory lung diseases (45), which are found in severe cases of Covid-19. Overexpression of MUC1 and MUC5AC mucins, for instance, play a key role in Covid-19 symptoms and may contribute to the high viscosity of airway mucus, leading to airflow obstruction and respiratory distress (46).

MUC22 is up-regulated in infections with respiratory syncytial vírus (47). Some studies have been pointing to mucin´s role in Covid-19 (48, 49). The outcome of SARS-CoV-2 infection may be correlated with a signature of shed mucins in circulation from infected lung or respiratory tract epithelial cells (48). *MUC22* polymorphisms have been associated with diffuse panbronchiolitis (43) and asthma in Latinos (50).

One may argue that these variants are related to longevity and not with protection against severe Covid-19. However, this variant is not correlated with longevity because (a) the SABE sample refers to a census-based cohort of elderly Brazilians with an average age of 75, and thus variant associated with longevity would already be more frequent, and (b) their frequency in SABE is very similar to frequencies observed in European and Latin American populations (https://www.ncbi.nlm.nih.gov/snp/rs62399430#frequency_tab).

Except for rs146685560, all *MUC22* protective variants are correlated with higher expression of miR-6891 in many tissues, including the esophagus and lung (gtexportal.org). miR-6891 is co-expressed with *MUC22* in the alveolus (pneumocyte type II). Interestingly, miR-6891 is encoded in the MHC, and targets the ORF3a gene from SARS-CoV-2 (51), which encodes a sodium or calcium ion channel protein involved in replication and pathogenesis (52). Most importantly, miR-6891-5p is upregulated in Calu3 cells infected with SARS-CoV-2 (53). During the early stages of SARS-CoV-2 infection, ORF3a directs the host's immune response (54), may induce lysosomal evasion (55, 56) and could promote cytokine storms by activating the NF-kB signaling and NLRP3 inflammasomes pathways (57). Therefore, we can hypothesize that a higher expression of miR-6891-5p, associated with all *MUC22* protective variants, may contribute to less severe symptoms during SARS-CoV-2 infection.

One possible explanation for higher miR-6891-5p expression is linkage with *HLA-B* since the *MIR6891* gene coincides with an *HLA-B* intron. In the present study, there is a clear association between the protective variant rs62399430/T and some *HLA-B* alleles, such as B*35:01, B*35:03, B*48:02, and B*51:01. All of these *HLA-B* alleles are listed as high mRNA expressing alleles (58–60). Thus, higher *HLA-B* mRNA expression might be correlated with higher miR-6891 expression, and *MUC22* variants are tagging this phenotype.

Also, *MUC22* is approximately 100 kb from *CCHCR1* gene, the most important signal in the MHC region for Covid-19 susceptibility, according to the Covid-19 Host Genetics Consortium (Covid19hg - https://app.covid19hg.org/). All *CCHCR1* variants associated with Covid-19 (29, 61) are intronic and were not captured by our genotyping method (whole-exome sequencing). The exomic *CCHCR1* variants included in our survey do not correlate with Covid-19 severity. This is expected since the meta-analysis provided by Covid19hg indicates that *CCHCR1* is associated with Covid-19 susceptibility but not with severity when comparing hospitalized and non-hospitalized patients (as performed here). Moreover, studying LD among the most relevant variants from *MUC22* and *CCHCR1*, we detected a weak LD ($r2 < 0.3$, $D' < 0.7$). Covid19hg effort detected no relevant signal from *MUC22*, including the SNPs described here. Although our *MUC22* findings are not cross-validated by the Covid19hg, we must consider that we are evaluating a very different cohort, aged and super elderly individuals with mild Covid-19 and younger patients with severe Covid-19. The signal from *MUC22* is much stronger in the super elderly group. The frequency of rs62399430 among the super elderly with mild Covid-19 is 2x higher than the observed among Europeans and in the general elderly populations and 3.8x higher than in Africa. Therefore, considering study designs and cohort ancestries, the *MUC22* signal might be ancestry-specific and independent of *CCHCR1*.

*HLA-DOB*01:02*/rs2071554 and severe Covid-19

The HLA-DO molecule is a heterodimer formed by two heavy chains, HLA-DOA and HLA-DOB. HLA-DO is a non-classical MHC-II molecule that does not present peptides on the cell surface, but it is required to efficiently load endosomal peptides onto MHC-II molecules (62–66). Thus, modifications in *HLA-DOB* may directly influence antigen presentation in the MHC class II pathway.

The HLA-DOB*01:02 allele has also been associated with an increased risk of death in patients with non-small cell lung cancer; reduced median survival time (67, 68), with type 1

diabetes (69), which is a major comorbidity related to severe Covid-19 (39), and with resistance to SARs-CoV-2 infection (22). DOB*01:02 has a different signal peptide, which may influence cellular localization and trafficking of the protein (15), possibly leading to inadequate antigen presentation.

HLA-DOB*01:02 is rare (0.6%) among SARs-CoV-2 resistant individuals (22), has similar frequencies of around 6% among patients with mild Covid-19 or the control elderly population, and reaches 13.6% in patients with severe Covid-19 (Table 1). The frequency of DOB*01:02 among the super elderly is similar to the general elderly population.

DOB*01:02 is frequent in Africa (reaching the same frequency as the SEVERE group) and less frequent in Europe. Although the percentage of Native-American and African ancestries are much higher in the SEVERE group than others, the associations described here are adjusted for genetic ancestry and sex. Because DOB*01:02 frequencies vary among different biogeographic regions, other studies are unlikely to find similar results unless addressing African or admixed populations comparable to the Brazilian one.

HLA-A, *TAP1*, and *TAP2* polymorphisms and severe Covid-19

We detected three different associations involving genes from the class I antigen presentation pathway. These associations involve *TAP1* and *TAP2*, which participate in the peptide pumping from the cytoplasm to the endoplasmic reticulum, and gene *HLA-A*, which will present these peptides on the cell surface to T CD8 lymphocytes (Tables 1, 2). High expression levels of TAP1 and TAP2 are correlated with the amount of virus in lung tissue (70). The *TAP2* signal might be a hitchhiking association due to linkage with HLA-DOB*01:02 (Figure S7).

For HLA-A, the amino acid residues at positions 62 and 63 (mature protein) depend on the haplotype formed by four different variants, rs1059455, rs1064588, rs2230991, and rs199474424. Their presence is associated with severe Covid-19. The fact that (a) this combination of amino acids only occurs when there is a specific haplotype, (b) this haplotype occurs in many different *HLA-A* alleles, and (c) allele frequencies vary in different populations, may explain why we did not detect any association between *HLA-A* allotypes with Covid-19 severity and why previous surveys described different results or no association (23, 71–77).

One possible mechanism for these associations is different binding affinities to SARs-CoV-2 peptides coupled with the subset of peptides pumped by TAP. The higher frequency of 62R-63N in the SEVERE group is related to alleles A*33:03, A*68:01, and A*68:02. A*68 alleles are among the strong binders for SARs-CoV-2 peptides (78, 79) and among the best binders for respiratory viruses (70).

To investigate whether residues 62R/63N could be interfering with the subset of antigens presented by *HLA-A*, we performed an *in silico* prediction of the antigen processing pathway impact on the presentation ability of the alleles carrying 62R/63N. Since the set of MHC alleles that an individual presents defines the ligandome on its cell surface, we predicted the peptidome of inspected alleles and compared them with the corresponding immunogenic regions from the SARS-CoV-2 spike protein. The comparison did not provide evidence that the investigated alleles lack the potential to present T cell epitopes already described for SARS-CoV-2 sequences (Supplementary Figures S3, S4). Additionally, we extracted the frequency of response for each predicted peptide from each 62R/63N sample alleles to compare their average values of immunogenicity frequencies with other alleles associated with good and bad outcomes in Covid-19. Again, the alleles carrying 62R/63N and overrepresented in the severe group exhibited similar numbers, indicating that the presentation ability was not responsible for the impaired response (Supplementary Figure S5).

To infer if the mutations could be interfering with immunogenicity triggering, we also looked for alterations present in the 62R/63N alleles that could impact the TCR interaction surface of the MHC cleft. The HLA structural models were screened, looking for shared features in regions usually contacted by complementarity-determining region 3 (CDR3) loops (Supplementary Figure S6). Hierarchical clustering analysis showed that four out of eight investigated alleles presented an electrostatic potential distribution fingerprint in the probed area. This physicochemical element was already described as pivotal to cytotoxicity elicitation, as described previously (80).

Interestingly, the clustered alleles were HLA-A*33:01, A*33:03, A*68:01, and A*68:02, the ones with higher frequencies among patients with Severe Covid-19 (Figure 4). These analyses emphasize the need for a deeper investigation when we are dealing with HLA alleles and their involvement with immunogenic issues. Only looking for ligandome predictions can underestimate the whole importance of these structures in T cell stimulation.

Among the alleles with increased frequency in the SEVERE group, A*68:02 is particularly frequent in Africa, A*62:01 among Native Americans, and A*33:03 in Asia (www.allelefrequencies.net). Although the SEVERE group from Brazil presents a higher African and Native American ancestry than the MILD group (Supplementary Table S1), the associations presented here (62R/63N, $p = 0.0017$, OR=2.7) are adjusted for ancestry and sex.

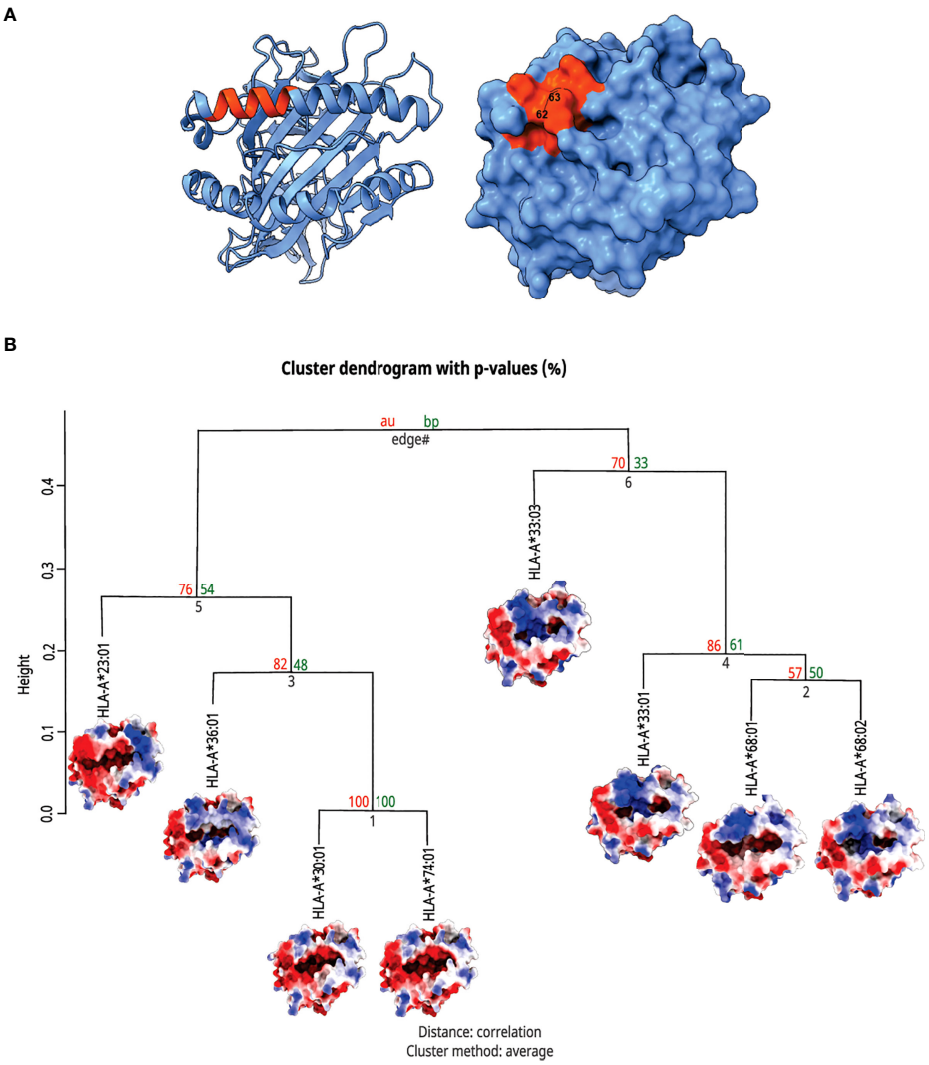

FIGURE 4
Top view of HLA-A molecules and hierarchical clusterization of HLA-A alleles. In **(A)** there is a MHC structure in both the ribbon and surface visualizations from the region that interacts with the TCR, respectively. The area in orange represents the zone proximal about the residues 62 and 63. In **(B)** we can see the cluster dendrogram of the analyzed MHCs. Under each allele name, there is the surface image that was generated for electrostatic potential distribution. In the right branch, we can see the cluster of alleles carrying rs199474424 (please refer to Figure 2), HLA-A*33:01, A*33:03, A*68:01, and A*68:02, with their respective shared molecular fingerprint.

This *p*-value is much lower, 0.0003, and significant even after correction for multiple tests within the *HLA-A* locus when not adjusted for ancestry. Therefore, population stratification should be ruled out as the main issue leading to these results. Since the associated alleles are most frequent in non-European populations, particularly Native Americans and Africans, it is unlikely that any study addressing European ancestry samples (23, 25, 74, 75, 77, 81–83) would find similar results. In fact, most of the previous studies evaluate European patients and find different results than the one presented here. Nevertheless, a frequency analysis of HLA alleles among Covid-19 infected patients from Saudi Arabia found HLA-A*68 among the most common alleles associated with severe disease (84), and A*68 is relatively common in Saudi Arabia (www.allelefrequencies.net). These results demonstrate the importance of addressing admixed populations such as Brazilians and other less-studied population samples.

Conclusions

In short, here, we performed an in-depth analysis of the MHC region in a cohort of unvaccinated super elderly individuals with Covid-19 that presented mild, or no symptoms compared with a group of younger patients with severe Covid-19 and/or a lethal

outcome. We used a method to call genotypes and haplotypes in the MHC that minimizes alignment and genotyping errors. Interestingly, the strongest signals in the MHC region for candidate variants protecting against severe Covid-19 coincide with gene *MUC22*. Missense variants at *MUC22* are more frequent among the super elderly and in the MILD group than in the SEVERE group and the general elderly population. We hypothesized that *MUC22* might play an important protective role against severe Covid-19. Functional studies must be placed to evaluate the true impact of such variants on *MUC22* function.

Data availability statement

The datasets presented in this study can be found in online repositories. The names of the repository/repositories and accession number(s) can be found below: European Genome-phenome Archive (EGA), under accession number EGAS0000100637.

Ethics statement

This study was approved by the Committee for Ethics in Research of the Institute of Biosciences at the University of São Paulo (CAAE 34786620.2.0000.5464). The patients/participants provided their written informed consent to participate in this study.

Author contributions

EC, MC, MN, and MZ contributed to the conceptualization. MC, LM, and MVRS contributed to data curation. EC, MN, MOS, NS, KN, IO, EA, ES, and GV contributed to the formal analysis. MZ contributed to funding acquisition. MC, MN, MOS, EC-N, and KS contributed to the investigation. EC, MN, MOS, and KN contributed to the methodology. MZ contributed to the project administration. EC, MN, and MOS contributed the software. EC, MN, MOS, and KN contributed to visualization. EC, MZ, MC, MN, KS, and MOS contributed to writing–original draft. NS, RP, VAOC, CC, CM-J, GV, DM, LM, MVRS, JW, JE, VRC, JM, EN, JK, RB, MH, LD'A, AR-F, PB, AD, MD, PS, MP-B, and MZ contributed to writing–review, and editing. All authors contributed to the article and approved the submitted version.

Funding

This work was supported by the São Paulo Research Foundation (FAPESP/Brazil) (grant numbers 2013/08028-1, 2014/50931-3, 2019/19998-8, and 2020/09702-1), the National Council for Scientific and Technological Development (CNPq) (grant number 465355/2014-5), and JBS S.A. (grant number 69004). FAPESP/Brazil (Grant numbers 2013/17084-0 and 2017/19223-0) and the United States National Institutes of Health (NIH) (R01 GM075091) supported the development of the HLA and KIR pipeline and the genetic ancestry approach. This study was also supported by the Coordenação de Aperfeiçoamento de Pessoal de Nível Superior-Brasil (CAPES)-Finance Code 001 and Fleury Group (Project NP-565). The funders were not involved in the study design, collection, analysis, interpretation of data, the writing of this article, or the decision to submit it for publication.

Acknowledgments

The authors are extremely grateful to all volunteers for their participation and collaboration, the nurses for sample collection, the technical team for the material process and data analysis, and the Fleury Laboratory for serology tests. Special thanks to Brazilian Senator Mara Gabrilli for financial support and to JBS S.A. for the additional funding. The funders were not involved in the study design, collection, analysis, interpretation of data, the writing of this article, or the decision to submit it for publication.

Conflict of interest

The authors declare that the research was conducted in the absence of any commercial or financial relationships that could be construed as a potential conflict of interest.

Publisher's note

All claims expressed in this article are solely those of the authors and do not necessarily represent those of their affiliated organizations, or those of the publisher, the editors and the reviewers. Any product that may be evaluated in this article, or claim that may be made by its manufacturer, is not guaranteed or endorsed by the publisher.

Supplementary material

The Supplementary Material for this article can be found online at: https://www.frontiersin.org/articles/10.3389/fimmu.2022.975918/full#supplementary-material

References

1. Dhama K, Patel SK, Natesan S, Vora KS, Iqbal Yatoo M, Tiwari R, et al. COVID-19 in the elderly people and advances in vaccination approaches. *Hum Vaccines Immunother* (2020) 16(12):2938–43. doi: 10.1080/21645515.2020.1842683

2. Bajgain KT, Badal S, Bajgain BB, Santana MJ. Prevalence of comorbidities among individuals with COVID-19: A rapid review of current literature. *Am J Infect Control* (2021) 49(2):238–46. doi: 10.1016/j.ajic.2020.06.213

3. Ho FK, Petermann-Rocha F, Gray SR, Jani BD, Katikireddi SV, Niedzwiedz CL, et al. Is older age associated with COVID-19 mortality in the absence of other risk factors? general population cohort study of 470,034 participants. *PloS One* (2020) 15(11):e0241824. doi: 10.1371/journal.pone.0241824

4. López-Otín C, Blasco MA, Partridge L, Serrano M, Kroemer G. The hallmarks of aging. *Cell* (2013) 153(6):1194–217. doi: 10.1016/j.cell.2013.05.039

5. Fuentes E, Fuentes M, Alarcón M, Palomo I. Immune system dysfunction in the elderly. *Acad Bras Ciênc* (2017) 89:285–99. doi: 10.1590/0001-3765201720160487

6. Amore S, Puppo E, Melara J, Terracciano E, Gentili S, Liotta G. Impact of COVID-19 on older adults and role of long-term care facilities during early stages of epidemic in Italy. *Sci Rep* (2021) 11(1):12530. doi: 10.1038/s41598-021-91992-9

7. Yuki K, Fujiogi M, Koutsogiannaki S. COVID-19 pathophysiology: A review. *Clin Immunol Orlando Fla* (2020) 215:108427. doi: 10.1016/j.clim.2020.108427

8. Parasher A. COVID-19: Current understanding of its pathophysiology, clinical presentation and treatment. *Postgrad Med J* (2021) 97(1147):312–20. doi: 10.1136/postgradmedj-2020-138577

9. Debisarun PA, Gössling KL, Bulut O, Kilic G, Zoodsma M, Liu Z, et al. Induction of trained immunity by influenza vaccination - impact on COVID-19. *PloS Pathog* (2021) 17(10):e1009928. doi: 10.1371/journal.ppat.1009928

10. Poulain M, Chambre D, Pes GM. Centenarians exposed to the Spanish flu in their early life better survived to COVID-19. *Aging* (2021) 13(18):21855–65. doi: 10.18632/aging.203577

11. Charitos P, Heijnen IAFM, Egli A, Bassetti S, Trendelenburg M, Osthoff M. Functional activity of the complement system in hospitalized COVID-19 patients: A prospective cohort study. *Front Immunol* (2021) 12:765330. doi: 10.3389/fimmu.2021.765330

12. Karki R, Kanneganti TD. The "cytokine storm": molecular mechanisms and therapeutic prospects. *Trends Immunol* (2021) 42(8):681–705. doi: 10.1016/j.it.2021.06.001

13. Linden SK, Sutton P, Karlsson NG, Korolik V, McGuckin MA. Mucins in the mucosal barrier to infection. *Mucosal Immunol* (2008) 1(3):183–97. doi: 10.1038/mi.2008.5

14. Castelli EC, de Almeida BS, Muniz YCN, Silva NSB, Passos MRS, Souza AS, et al. HLA-G genetic diversity and evolutive aspects in worldwide populations. *Sci Rep* (2021) 11(1):23070. doi: 10.1038/s41598-021-02106-4

15. Hervier B, Russick J, Cremer I, Vieillard V. NK cells in the human lungs. *Front Immunol* (2019) 10:1263. doi: 10.3389/fimmu.2019.01263

16. Raulet DH, Gasser S, Gowen BG, Deng W, Jung H. Regulation of ligands for the NKG2D activating receptor. *Annu Rev Immunol* (2013) 31:413–41. doi: 10.1146/annurev-immunol-032712-095951

17. Borst L, van der Burg SH, van Hall T. The NKG2A-HLA-E axis as a novel checkpoint in the tumor microenvironment. *Clin Cancer Res Off J Am Assoc Cancer Res* (2020) 26(21):5549–56. doi: 10.1158/1078-0432.CCR-19-2095

18. Radwan J, Babik W, Kaufman J, Lenz TL, Winternitz J. Advances in the evolutionary understanding of MHC polymorphism. *Trends Genet TIG* (2020) 36(4):298–311. doi: 10.1016/j.tig.2020.01.008

19. Wieczorek M, Abualrous ET, Sticht J, Álvaro-Benito M, Stolzenberg S, Noé F, et al. Major histocompatibility complex (MHC) class I and MHC class II proteins: Conformational plasticity in antigen presentation. *Front Immunol* (2017) 8:292. doi: 10.3389/fimmu.2017.00292

20. Castelli EC, Paz MA, Souza AS, Ramalho J, Mendes-Junior CT. Hla-mapper: An application to optimize the mapping of HLA sequences produced by massively parallel sequencing procedures. *Hum Immunol* (2018) 79(9):678–84. doi: 10.1016/j.humimm.2018.06.010

21. Brandt DYC, Aguiar VRC, Bitarello BD, Nunes K, Goudet J, Meyer D. Mapping bias overestimates reference allele frequencies at the HLA genes in the 1000 genomes project phase I data. *G3 Bethesda Md* (2015) 5(5):931–41. doi: 10.1534/g3.114.015784

22. Castelli EC, de Castro MV, Naslavsky MS, Scliar MO, Silva NSB, Andrade HS, et al. MHC variants associated with symptomatic versus asymptomatic SARS-CoV-2 infection in highly exposed individuals. *Front Immunol* (2021) 12:742881. doi: 10.3389/fimmu.2021.742881

23. Iturrieta-Zuazo I, Rita CG, García-Soidán A, de Malet Pintos-Fonseca A, Alonso-Alarcón N, Pariente-Rodríguez R, et al. Possible role of HLA class-I genotype in SARS-CoV-2 infection and progression: A pilot study in a cohort of covid-19 Spanish patients. *Clin Immunol Orlando Fla* (2020) 219:108572. doi: 10.1016/j.clim.2020.108572

24. Nguyen A, David JK, Maden SK, Wood MA, Weeder BR, Nellore A, et al. Human leukocyte antigen susceptibility map for severe acute respiratory syndrome coronavirus 2. *J Virol* (2020) 94(13):e00510–20. doi: 10.1128/JVI.00510-20

25. Schetelig J, Heidenreich F, Baldauf H, Trost S, Falk B, Hoßbach C, et al. Individual HLA-a, -b, -c, and -DRB1 genotypes are no major factors which determine COVID-19 severity. *Front Immunol* (2021) 12:698193. doi: 10.3389/fimmu.2021.698193

26. Fischer JC, Schmidt AG, Bölke E, Uhrberg M, Keitel V, Feldt T, et al. Association of HLA genotypes, AB0 blood type and chemokine receptor 5 mutant CD195 with the clinical course of COVID-19. *Eur J Med Res* (2021) 26(1):107. doi: 10.1186/s40001-021-00560-4

27. Stephens H a. F, Klaythong R, Sirikong M, Vaughn DW, Green S, Kalayanarooj S, et al. HLA-a and -b allele associations with secondary dengue virus infections correlate with disease severity and the infecting viral serotype in ethnic thais. *Tissue Antigens* (2002) 60(4):309–18. doi: 10.1034/j.1399-0039.2002.600405.x

28. MacDonald KS, Fowke KR, Kimani J, Dunand VA, Nagelkerke NJ, Ball TB, et al. Influence of HLA supertypes on susceptibility and resistance to human immunodeficiency virus type 1 infection. *J Infect Dis* (2000) 181(5):1581–9. doi: 10.1086/315472

29. Pairo-Castineira E, Clohisey S, Klaric L, Bretherick AD, Rawlik K, Pasko D, et al. Genetic mechanisms of critical illness in COVID-19. *Nature* (2021) 591(7848):92–8. doi: 10.1038/s41586-020-03065-y

30. Vietzen H, Zoufaly A, Traugott M, Aberle J, Aberle SW, Puchhammer-Stöckl E. Deletion of the NKG2C receptor encoding KLRC2 gene and HLA-e variants are risk factors for severe COVID-19. *Genet Med* (2021) 23(5):963–7. doi: 10.1038/s41436-020-01077-7

31. Naslavsky MS, Scliar MO, Yamamoto GL, Wang JYT, Zverinova S, Karp T, et al. Whole-genome sequencing of 1,171 elderly admixed individuals from são paulo, Brazil. *Nat Commun* (2022) 13(1):1004. doi: 10.1038/s41467-022-28648-3

32. Kiyotani K, Mai TH, Nakamura Y. Comparison of exome-based HLA class I genotyping tools: identification of platform-specific genotyping errors. *J Hum Genet* (2017) 62(3):397–405. doi: 10.1038/jhg.2016.141

33. Martin M, Patterson M, Garg S, Fischer SO, Pisanti N, Klau GW, et al. WhatsHap: fast and accurate read-based phasing. *bioRxiv* (2016), 085050. doi: 10.1101/085050

34. Delaneau O, Zagury JF, Robinson MR, Marchini JL, Dermitzakis ET. Accurate, scalable and integrative haplotype estimation. *Nat Commun* (2019) 10(1):5436. doi: 10.1038/s41467-019-13225-y

35. Robinson J, Barker DJ, Georgiou X, Cooper MA, Flicek P, Marsh SGE. IPD-IMGT/HLA database. *Nucleic Acids Res* (2020) 48(D1):D948–55. doi: 10.1093/nar/gkq998

36. Wang VG, Kim H, Chuang JH. Whole-exome sequencing capture kit biases yield false negative mutation calls in TCGA cohorts. *PloS One* (2018) 13(10):e0204912. doi: 10.1371/journal.pone.0204912

37. Zheng X, Shen J, Cox C, Wakefield JC, Ehm MG, Nelson MR, et al. HIBAG–HLA genotype imputation with attribute bagging. *Pharmacogenomics J* (2014) 14(2):192–200. doi: 10.1038/tpj.2013.18

38. Gabriel SB, Schaffner SF, Nguyen H, Moore JM, Roy J, Blumenstiel B, et al. The structure of haplotype blocks in the human genome. *Science.* (2002) 296(5576):2225–9. doi: 10.1126/science.1069424

39. Hartmann-Boyce J, Rees K, Perring JC, Kerneis SA, Morris EM, Goyder C, et al. Risks of and from SARS-CoV-2 infection and COVID-19 in people with diabetes: A systematic review of reviews. *Diabetes Care* (2021) 44(12):2790–811. doi: 10.2337/dc21-0930

40. Chande AT, Rishishwar L, Conley AB, Valderrama-Aguirre A, Medina-Rivas MA, Jordan IK. Ancestry effects on type 2 diabetes genetic risk inference in Hispanic/Latino populations. *BMC Med Genet* (2020) 21(Suppl 2):132. doi: 10.1186/s12881-020-01068-0

41. da Silva NN, Favacho VBC, Boska Gde A, Andrade Eda C, das Merces NP, de Oliveira MAF. Access of the black population to health services: integrative review. *Rev Bras Enferm* (2020) 73:1–9. doi: 10.1590/0034-7167-2018-0834

42. Ballester B, Milara J, Cortijo J. Mucins as a new frontier in pulmonary fibrosis. *J Clin Med* (2019) 8(9):1447. doi: 10.3390/jcm8091447

43. Hijikata M, Matsushita I, Tanaka G, Tsuchiya T, Ito H, Tokunaga K, et al. Molecular cloning of two novel mucin-like genes in the disease-susceptibility locus for diffuse panbronchiolitis. *Hum Genet* (2011) 129(2):117–28. doi: 10.1007/s00439-010-0906-4

44. Rose MC, Voynow JA. Respiratory tract mucin genes and mucin glycoproteins in health and disease. *Physiol Rev* (2006) 86(1):245–78. doi: 10.1152/physrev.00010.2005

45. Evans CM, Koo JS. Airway mucus: the good, the bad, the sticky. *Pharmacol Ther* (2009) 121(3):332–48. doi: 10.1016/j.pharmthera.2008.11.001

46. Lu W, Liu X, Wang T, Liu F, Zhu A, Lin Y, et al. Elevated MUC1 and MUC5AC mucin protein levels in airway mucus of critical ill COVID-19 patients. *J Med Virol* (2021) 93(2):582–4. doi: 10.1002/jmv.26406

47. Baños-Lara MDR, Piao B, Guerrero-Plata A. Differential mucin expression by respiratory syncytial virus and human metapneumovirus infection in human epithelial cells. *Mediators Inflamm* (2015) 2015:347292. doi: 10.1155/2015/347292

48. Bose M, Mitra B, Mukherjee P. Mucin signature as a potential tool to predict susceptibility to COVID-19. *Physiol Rep* (2021) 9(1):e14701. doi: 10.14814/phy2.14701

49. Smet A, Breugelmans T, Michiels J, Lamote K, Arras W, De Man JG, et al. A dynamic mucin mRNA signature associates with COVID-19 disease presentation and severity. *JCI Insight* (2021) 6(19):e151777. doi: 10.1172/jci.insight.151777

50. Galanter JM, Gignoux CR, Torgerson DG, Roth LA, Eng C, Oh SS, et al. Genome-wide association study and admixture mapping identify different asthma-associated loci in latinos: the genes-environments & admixture in Latino americans study. *J Allergy Clin Immunol* (2014) 134(2):295–305. doi: 10.1016/j.jaci.2013.08.055

51. Saçar Demirci MD, Adan A. Computational analysis of microRNA-mediated interactions in SARS-CoV-2 infection. *PeerJ* (2020) 8:e9369. doi: 10.7717/peerj.9369

52. Castaño-Rodriguez C, Honrubia JM, Gutiérrez-Álvarez J, DeDiego ML, Nieto-Torres JL, Jimenez-Guardeño JM, et al. Role of severe acute respiratory syndrome coronavirus viroporins e, 3a, and 8a in replication and pathogenesis. *mBio* (2018) 9(3):e02325–17. doi: 10.1128/mBio.02325-17

53. Demirci YM, Saçar Demirci MD. Circular RNA-MicroRNA-MRNA interaction predictions in SARS-CoV-2 infection. *J Integr Bioinforma* (2021) 18(1):45–50. doi: 10.1515/jib-2020-0047

54. Silvas JA, Vasquez DM, Park JG, Chiem K, Allué-Guardia A, Garcia-Vilanova A, et al. Contribution of SARS-CoV-2 accessory proteins to viral pathogenicity in K18 human ACE2 transgenic mice. *J Virol* (2021) 95(17):e0040221. doi: 10.1128/JVI.00402-21

55. Chen D, Zheng Q, Sun L, Ji M, Li Y, Deng H, et al. ORF3a of SARS-CoV-2 promotes lysosomal exocytosis-mediated viral egress. *Dev Cell* (2021) 56(23):3250–63. doi: 10.1016/j.devcel.2021.10.006

56. Miao G, Zhao H, Li Y, Ji M, Chen Y, Shi Y, et al. ORF3a of the COVID-19 virus SARS-CoV-2 blocks HOPS complex-mediated assembly of the SNARE complex required for autolysosome formation. *Dev Cell* (2021) 56(4):427–442.e5. doi: 10.1016/j.devcel.2020.12.010

57. Siu KL, Yuen KS, Castaño-Rodriguez C, Ye ZW, Yeung ML, Fung SY, et al. Severe acute respiratory syndrome coronavirus ORF3a protein activates the NLRP3 inflammasome by promoting TRAF3-dependent ubiquitination of ASC. *FASEB J Off Publ Fed Am Soc Exp Biol* (2019) 33(8):8865–77. doi: 10.1096/fj.201802418R

58. Yamamoto F, Suzuki S, Mizutani A, Shigenari A, Ito S, Kametani Y, et al. Capturing differential allele-level expression and genotypes of all classical HLA loci and haplotypes by a new capture RNA-seq method. *Front Immunol* (2020) 11:941. doi: 10.3389/fimmu.2020.00941

59. Johansson T, Yohannes DA, Koskela S, Partanen J, Saavalainen P. HLA RNA sequencing with unique molecular identifiers reveals high allele-specific variability in mRNA expression. *Front Immunol* (2021) 12:629059. doi: 10.3389/fimmu.2021.629059

60. Aguiar VRC, César J, Delaneau O, Dermitzakis ET, Meyer D. Expression estimation and eQTL mapping for HLA genes with a personalized pipeline. *PloS Genet* (2019) 15(4):e1008091. doi: 10.1371/journal.pgen.1008091

61. Pathak GA, Karjalainen J, Stevens C, Neale BM, Daly M, Ganna A, et al. A first update on mapping the human genetic architecture of COVID-19. *Nature.* (2022) 608(7921):E1–10. doi: 10.1038/s41586-022-04826-7

62. Poluektov Y, Kim A, Sadegh-Nasseri S. HLA-DO and its role in MHC class II antigen presentation. *Front Immunol* (2013) 4:260. doi: 10.3389/fimmu.2013.00260

63. van Ham M, van Lith M, Griekspoor A, Neefjes J. What to do with HLA-DO? *Immunogenetics* (2000) 51(10):765–70. doi: 10.1007/s002510000208

64. Liljedahl M, Kuwana T, Fung-Leung WP, Jackson MR, Peterson PA, Karlsson L. HLA-DO is a lysosomal resident which requires association with HLA-DM for efficient intracellular transport. *EMBO J* (1996) 15(18):4817–24. doi: 10.1002/j.1460-2075.1996.tb00862.x

65. Naruse TK, Kawata H, Inoko H, Isshiki G, Yamano K, Hino M, et al. The HLA-DOB gene displays limited polymorphism with only one amino acid substitution. *Tissue Antigens* (2002) 59(6):512–9. doi: 10.1034/j.1399-0039.2002.590608.x

66. Denzin LK, Sant'Angelo DB, Hammond C, Surman MJ, Cresswell P. Negative regulation by HLA-DO of MHC class II-restricted antigen processing. *Science* (1997) 278(5335):106–9. doi: 10.1126/science.278.5335.106

67. Wang H, Zhao S, Zhang X, Jia K, Deng J, Zhou C, et al. Major histocompatibility complex class II molecule in non-small cell lung cancer diagnosis, prognosis and treatment. *OncoTargets Ther* (2019) 12:7281–8. doi: 10.2147/OTT.S214231

68. Pu X, Hildebrandt MA, Lu C, Roth JA, Stewart DJ, Zhao Y, et al. Inflammation-related genetic variations and survival in patients with advanced non-small cell lung cancer receiving first-line chemotherapy. *Clin Pharmacol Ther* (2014) 96(3):360–9. doi: 10.1038/clpt.2014.89

69. He C, Hamon S, Li D, Barral-Rodriguez S, Ott J. MHC fine mapping of human type 1 diabetes using the T1DGC data. *Diabetes Obes Metab* (2009) 11(Suppl 1):53–9. doi: 10.1111/j.1463-1326.2008.01003.x

70. Desterke C, Turhan AG, Bennaceur-Griscelli A, Griscelli F. HLA-dependent heterogeneity and macrophage immunoproteasome activation during lung COVID-19 disease. *J Transl Med* (2021) 19(1):290. doi: 10.1186/s12967-021-02965-5

71. Shkurnikov M, Nersisyan S, Jankevic T, Galatenko A, Gordeev I, Vechorko V, et al. Association of HLA class I genotypes with severity of coronavirus disease-19. *Front Immunol* (2021) 12. doi: 10.3389/fimmu.2021.641900

72. Wang W, Zhang W, Zhang J, He J, Zhu F. Distribution of HLA allele frequencies in 82 Chinese individuals with coronavirus disease-2019 (COVID-19). *HLA* (2020) 96(2):194–6. doi: 10.1111/tan.13941

73. Littera R, Campagna M, Deidda S, Angioni G, Cipri S, Melis M, et al. Human leukocyte antigen complex and other immunogenetic and clinical factors influence susceptibility or protection to SARS-CoV-2 infection and severity of the disease course. *Sardinian Experience. Front Immunol* (2020) 11:605688. doi: 10.3389/fimmu.2020.605688

74. The Severe Covid-19 GWAS Group, Ellinghaus D., Degenhardt F., Bujanda L., Buti M., Albillos A., et al. Genomewide association study of severe covid-19 with respiratory failure. *N Engl J Med* (2020) 383(16):1522–34. doi: 10.1056/NEJMoa2020283

75. Novelli A, Andreani M, Biancolella M, Liberatoscioli L, Passarelli C, Colona VL, et al. HLA allele frequencies and susceptibility to COVID-19 in a group of 99 Italian patients. *HLA.* (2020) 96(5):610–4. doi: 10.1111/tan.14047

76. Nguyen A, Yusufali T, Hollenbach JA, Nellore A, Thompson RF. Minimal observed impact of HLA genotype on hospitalization and severity of SARS-CoV-2 infection. *HLA* (2022). doi: 10.1101/2021.12.22.21268062

77. Langton DJ, Bourke SC, Lie BA, Reiff G, Natu S, Darlay R, et al. The influence of HLA genotype on the severity of COVID-19 infection. *HLA* (2021) 98(1):14–22. doi: 10.1111/tan.14284

78. Barquera R, Collen E, Di D, Buhler S, Teixeira J, Llamas B, et al. Binding affinities of 438 HLA proteins to complete proteomes of seven pandemic viruses and distributions of strongest and weakest HLA peptide binders in populations worldwide. *HLA* (2020) 96(3):277–98. doi: 10.1111/tan.13956

79. Balz K, Chen M, Kaushik A, Cemic F, Heger V, Renz H, et al. Homologies between SARS-CoV-2 and allergen proteins may direct T cell-mediated heterologous immune responses. *Res Sq* (2020) 86873. rs.3.rs-. doi: 10.21203/rs.3.rs-86873/v1

80. Vianna P, Mendes MFA, Bragatte MA, Ferreira PS, Salzano FM, Bonamino MH, et al. pMHC structural comparisons as a pivotal element to detect and validate T-cell targets for vaccine development and immunotherapy-a new methodological proposal. *Cells* (2019) 8(12):E1488. doi: 10.3390/cells8121488

81. Lorente L, Martín MM, Franco A, Barrios Y, Cáceres JJ, Solé-Violán J, et al. [HLA genetic polymorphisms and prognosis of patients with COVID-19]. *Med Intensiva* (2021) 45(2):96–103. doi: 10.1016/j.medin.2020.08.004

82. Amoroso A, Magistroni P, Vespasiano F, Bella A, Bellino S, Puoti F, et al. HLA and AB0 polymorphisms may influence SARS-CoV-2 infection and COVID-19 severity. *Transplantation* (2021) 105(1):193–200. doi: 10.1097/TP.0000000000003507

83. Ben Shachar S, Barda N, Manor S, Israeli S, Dagan N, Carmi S, et al. MHC haplotyping of SARS-CoV-2 patients: HLA subtypes are not associated with the presence and severity of COVID-19 in the Israeli population. *J Clin Immunol* (2021) 41(6):1154–61. doi: 10.1007/s10875-021-01071-x

84. Naemi FMA, Al-Adwani S, Al-Khatabi H, Al-Nazawi A. Frequency of HLA alleles among COVID-19 infected patients: Preliminary data from Saudi Arabia. *Virology* (2021) 560:1–7. doi: 10.1016/j.virol.2021.04.011

COPYRIGHT

© 2022 Castelli, de Castro, Naslavsky, Scliar, Silva, Pereira, Ciriaco, Castro, Mendes-Junior, Silveira, de Oliveira, Antonio, Vieira, Meyer, Nunes, Matos, Silva, Wang, Esposito, Cória, Magawa, Santos, Cunha-Neto, Kalil, Bortolin, Hirata, Dell'Aquila, Razuk-Filho, Batista-Júnior, Duarte-Neto, Dolhnikoff, Saldiva, Passos-Bueno and Zatz. This is an open-access article distributed

under the terms of the Creative Commons Attribution License (CC BY). The use, distribution or reproduction in other forums is permitted, provided the original author(s) and the copyright owner(s) are credited and that the original publication in this journal is cited, in accordance with accepted academic practice. No use, distribution or reproduction is permitted which does not comply with these terms.

frontiers | Frontiers in Immunology

TYPE Original Research
PUBLISHED 27 October 2022
DOI 10.3389/fimmu.2022.1010140

Check for updates

OPEN ACCESS

EDITED BY
Edwin Bölke,
Heinrich Heine University of Düsseldorf, Germany

REVIEWED BY
Chaitanya Kurhade,
University of Texas Medical Branch at Galveston, United States
Jose Arturo Molina Mora,
University of Costa Rica, Costa Rica

*CORRESPONDENCE
Samuel Lebourgeois
samuel.lebourgeois@inserm.fr

SPECIALTY SECTION
This article was submitted to Viral Immunology, a section of the journal Frontiers in Immunology

RECEIVED 02 August 2022
ACCEPTED 14 October 2022
PUBLISHED 27 October 2022

CITATION
Lebourgeois S, David A, Chenane HR, Granger V, Menidjel R, Fidouh N, Noël B, Delelis O, Richetta C, Charpentier C, Chollet-Martin S, Descamps D, Visseaux B and de Chaisemartin L (2022) Differential activation of human neutrophils by SARS-CoV-2 variants of concern. *Front. Immunol.* 13:1010140. doi: 10.3389/fimmu.2022.1010140

COPYRIGHT
© 2022 Lebourgeois, David, Chenane, Granger, Menidjel, Fidouh, Noël, Delelis, Richetta, Charpentier, Chollet-Martin, Descamps, Visseaux and de Chaisemartin. This is an open-access article distributed under the terms of the Creative Commons Attribution License (CC BY). The use, distribution or reproduction in other forums is permitted, provided the original author(s) and the copyright owner(s) are credited and that the original publication in this journal is cited, in accordance with accepted academic practice. No use, distribution or reproduction is permitted which does not comply with these terms.

Differential activation of human neutrophils by SARS-CoV-2 variants of concern

Samuel Lebourgeois[1]*, Ambroise David[2], Houssem Redha Chenane[1], Vanessa Granger[2,3], Reyene Menidjel[1], Nadhira Fidouh[4], Benoît Noël[3], Olivier Delelis[5], Clémence Richetta[5], Charlotte Charpentier[1,4], Sylvie Chollet-Martin[2,3], Diane Descamps[1,4], Benoit Visseaux[1,4] and Luc de Chaisemartin[2,3]

[1]Université Paris Cité, Infection Antimicrobials Modelling Evolution (IAME), Institut National de la Santé et de la Recherche Médicale (INSERM), Paris, France, [2]Assistance Publique - Hôpitaux de Paris (AP-HP), University Hospital Bichat-Claude Bernard, Laboratoire d'Immunologie, Paris, France, [3]Inflammation, Microbiome and Immunosurveillance, Université Paris-Saclay, Institut National de la Santé et de la Recherche Médicale (INSERM), Châtenay-Malabry, France, [4]Assistance Publique - Hôpitaux de Paris (AP-HP), University Hospital Bichat-Claude Bernard, Laboratoire de Virologie, Paris, France, [5]LBPA-Laboratoire Biologie Pharmacologie Appliquée, Ecole Normal Supérieur (ENS) Paris-Saclay, Centre National de la Recherche Scientifique (CNRS) Unité Mix de Recherche (UMR), Université Paris-Saclay, Gif-sur-yvette, France

The emerging SARS-CoV-2 virus has affected the entire world with over 600 million confirmed cases and 6.5 million deaths as of September 2022. Since the beginning of the pandemic, several variants of SARS-CoV-2 have emerged, with different infectivity and virulence. Several studies suggest an important role of neutrophils in SARS-Cov-2 infection severity, but data about direct activation of neutrophils by the virus is scarce. Here, we studied the *in vitro* activation of human neutrophils by SARS-CoV-2 variants of concern (VOCs). In our work, we show that upon stimulation with SARS-Cov-2 infectious particles, human healthy resting neutrophils upregulate activation markers, degranulate IL-8, produce Reactive Oxygen Species and release Neutrophil Extracellular Traps. Neutrophil activation was dependent on TLR7/8 and IRF3/STING. We then compared the activation potential of neutrophils by SARS-CoV-2 variants and showed a significantly increased activation by the Delta variant and a decreased activation by the Omicron variant as compared to the initial strain. In this study, we demonstrate that the SARS-Cov-2 virus can directly activate neutrophils in COVID-19 and that the different VOCs had differences in neutrophil activation intensity that mirror the differences of clinical severity. These data highlight the need to address neutrophil-virus interactions as a potential target for therapeutic intervention in SARS-CoV-2 infection.

KEYWORDS

human neutrophils, SARS-CoV-2, variant of concerns, netosis, IL-8

10.3389/fimmu.2022.1010140

Introduction

The emerging SARS-CoV-2 virus was first identified in Wuhan City, China, on 31 December 2019 as the etiological agent of coronavirus infectious disease 2019 (COVID-19). It was subsequently declared pandemic by the World Health Organization (WHO) on 11 March 2020 (1). Until 15 September, 2022, the entire world has been affected by this virus with over 600 million confirmed cases and over 6.5 million deaths.

Since the beginning of the pandemic, several variants of SARS-CoV-2 have emerged. The first successful emergence was observed between March and April 2020 with the spread of the D614G mutation. This mutation was associated with higher viral loads and improved adhesion to the cellular angiotensin-converting enzyme 2 (ACE2) receptor (2). Since the late 2020s, several new variants of concern (VOC) have been identified, including the Alpha (B.1.1.7), Beta (B.1.351), Gamma (P.1) and then Delta (B.1.617.2) variants, which have rapidly and widely dominated in Europe and worldwide. More recently, the Omicron variant (B.1.1.526) has come to the forefront of global concern. However, this variant, which is thought to have a much higher adhesion capacity than other VOCs (3), seem to induce a less severe disease (4).

In humans, coronavirus infection generally causes mild respiratory infections such as common cold, including fever, cough and shortness of breath (5). Several clinical profiles have been described, but none of them was associated to a specific risk factor (6). Most people infected are only mildly symptomatic, but approximately 20% of patients may progress to severe disease with a risk of acute respiratory distress syndrome (ARDS), sepsis, multiorgan dysfunction and ultimately death (5). The overactivation of the innate immune response against SARS-CoV-2, including production of pro-inflammatory cytokines (TNFα, IL-6, IL-1β and IFN-γ/α) is thought to play a major role in the pathophysiology (7).

Among the first immune cells to be recruited and activated in infections are neutrophils. Neutrophils possess formidable anti-infectious weaponry including secretion of proteases and cytokines, production of reactive oxygen species (ROS), and even expulsion of extracellular DNA filaments called neutrophil extracellular traps, or NETs (8). Although neutrophils are more studied in bacterial or fungal infections, they are now recognized to be of importance during viral infections as well (8, 9). In COVID-19 infection, increased circulating neutrophil numbers and neutrophil recruitment to lungs have been described and linked to severity (10). Additionally, elevated NETs have been measured in blood and tissues and associated to lung injury, thrombosis, and severity (11, 12).

However, despite the large amount of data available on the activation status of neutrophils in COVID-19, there is still little information on how the neutrophils respond to the SARS-CoV-2 itself, and particularly to the different VOCs of the virus. In this study, we explored the neutrophil activation potential of all the major VOCs of SARS-CoV-2 *in vitro*, and demonstrated a significant disparity in neutrophil activation intensity depending on the variant.

Material and methods

Viral strains

The viral strains of human SARS-CoV-2 VOCs were obtained from a positive nasopharyngeal PCR sample. The viruses have been treated in biosafety level-3 laboratory (BSL-3). The SARS-CoV-2 primo-culture stocks used as B (EPI_ISL_4537783), Alpha (EPI_ISL_4536454 and EPI_ISL_4536996), Beta (EPI_ISL_4537125 and EPI_ISL_4537284), Gamma (EPI_ISL_4536760), Delta (EPI_ISL_4536228) and Omicron (EPI_ISL_13017139) were produced in Vero E6 cells. The infected Vero E6 cells were incubated at 37°C in a humidified atmosphere with 5% of CO2. The supernatants were purified and concentrated in Amicon®Ultra-15 diafiltration devices (Merck Milipore Ltd). Then, supernatants were quantified for viral RNA levels by RT-qPCR (Altona ®, Roche) and viral infectivity by lysis plaque assay titration (13) (see below). Supernatants were then aliquoted and stored at −80°C until use. All sequences of culture strains have been sequenced with Nanopore technology (Agilent technologies®) using the Artic protocol.

Viral titration

SARS-CoV-2 infectious titers were obtained by a lysis-plaque assay as previously described (13). Briefly, Vero E6 cells were seeded onto a 12-well plate at a density of 100,000 in DMEM with 10% FBS. The next day, cells were infected by 10 to 10 serial viral dilutions with the same infection protocol than for our viral infection assays (13). After the viral adsorption period of 1 h at 37°C, 500 µl of an agarose medium mix was added. After 3-day incubation at 37°C with 5% of CO2, the supernatant was removed and cells were fixed with 1 ml of a 6% formalin solution for 30 min. The formalin solution was then removed, and cells were colored with a 10% crystal violet solution for 15 min. All wells were then washed with distilled water and dried on bench-coat paper.

SARS-CoV-2 pseudovirus assay

To compare the differences in neutrophil activation as a function of SARS-CoV-2 VOCs, lentiviral particles pseudotyped with spike proteins encoded for B, Delta and Omicron have been used. We used a NLENG1-ES-IRES plasmid coding for a derived HIV-1 virus NL4-3 (14). The virus produced by this plasmid are all defective carrying two stop codons in the reading frame of the

envelope and expressing a fluorescent reporter gene GFP. Also, we used spike SARS-CoV-2 and VOCs expression plasmid (B, Delta and Omicron)(pLV-Spike, *In vivo*gen). Briefly, pseudoviruses were produced in HEK293T cells by lipofectamine co-transfection of NLENG1-ES-IRES and pLV-Spike plasmids. The virus production have been concentrated and purified using a 100kDa specific filter (Amicon®, Milipore). Viruses' productions were stored at -80°C until use. A measure of the viral load was performed on all purified viruses suspensions as previously described (15).

Neutrophil surface activation markers

Heparinized whole blood neutrophils were counted on an automated hematometer (Sysmex) and the blood was adjusted to a concentration of $4x10^6$ millions neutrophils/mL. Alternatively, neutrophils were magnetically isolated (see below). Neutrophils were incubated with virus at multiplicity of infection (MOI) ranging from 0.1 to 500 or medium for 90 min at 37°C, CO_2, H_20. Anti-CD62L and anti-CD11b fluorescent antibodies (Becton-Dickinson) were added for 15 min at 4°C. Whole blood samples were then subjected to red blood cell (RBC) lysis (BD FACS Lysing Solution, Becton-Dickinson). After washing, cells were acquired on a FACS Lyrics cytometer (Becton-Dickinson). Results were expressed as percentage of activated $CD62L^{low}/CD11b^{bright}$ neutrophils. When indicated, whole blood was pre-incubated for 30 min with 10µM cytochalasin D (Sigma), 50nM TLR7/8 inhibitor ODN 2088 (Miltenyi), or 1µM IRF-3 inhibitor BX795 (*In vivo*gen).

IL-8 measurement

Degranulated IL-8 was measured in supernatants from virus-activated neutrophils after 90 min of contact (short incubation to avoid measuring neosynthesized cytokines) using Human IL-8 Duoset ELISA kit (Bio-techne) according to manufacturers' recommendations.

ROS measurement

Heparinized whole blood was pre-incubated with 600ng/ml dihydroethidium (DHE, Sigma-Aldrich) ROS probe for 15 min at 37°C under agitation in a water bath before adding the virus at MOI 0.1-500 or medium for 45min at 37°C, CO_2, H_20. Samples were then subjected to RBC lysis and washing before acquisition on a FACS Lyrics cytometer. Results were expressed in mean fluorescence intensity (MFI) of the probe.

Apoptosis measurement

Apoptosis was measured on virus-treated neutrophils at MOI 100 using Apoptosis staining kit I (BD Biosciences) according to manufacturer's recommendations. Alternatively, neutrophils were fixed and permeabilized using Cytofix/Cytoperm kit (BD Biosciences) according to manufacturer's recommendations, and stained for 30 min with anti-activated Caspase-3 antibody (Clone C92-605 BD Pharmingen).

NETosis assay

Neutrophils were purified from EDTA-treated whole blood using MACSXpress Neutrophil isolation kit (Miltenyi Biotech) which allowed a purity routinely over 98%. Purified neutrophils were suspended at $1x10^6$ cells/mL and seeded in 12-well plates. Virus at MOI 100 or medium was added and the plates were incubated at 37°C, CO_2, H_20 for 3h. The supernatant was then collected and DNA-MPO complexes were measured by an in-house ELISA as previously described (16). Additionally, DNA-MPO complexes were measured in sera from COVID-infected patients using the same in-house method.

Patients

Whole blood and neutrophils used for *in vitro* stimulation experiments were collected from healthy volunteers from Etablissement Français du Sang. Samples from 35 SARS-Cov-2 infected patients used to measure NETs were collected upon admission to Bichat Hospital in the context of a clinical study approved by an Ethics committee with consent of patients (National Ethics committee "Ile de France 8"n°2020-A02676-33).

Statistics

Comparison between paired data set was done with paired Wilcoxon signed-rank test or Friedman test for comparison of more than two groups. Comparison of unpaired data sets was done with Mann-Whitney test or Kruskal-Wallis test for comparison of more than two groups followed by Dunn post-test. Analyses were done in Graphpad Prism v9.3.1 (GraphPad Software, LLC.). A p-value <0.05 was considered significant.

Results

Neutrophil activation by SARS-CoV-2 virus requires actin polymerization, TRL7/8 and IRF-3

A significant increase in $CD11b^{hi}/CD62L^{low}$ activated neutrophils from whole blood could be seen after 90 min of incubation at relatively high MOI (100 to 500, p=0.0002 for both compared to medium) with the ancestral Wuhan strain (B.) of

10.3389/fimmu.2022.1010140

SARS-CoV-2 (Figure 1A). A similar activation could be observed on magnetically isolated neutrophils at the same MOIs (Figure S1). To confirm this activation, we additionally measured degranulated IL-8 (Figure 1B) and ROS production (Figure 1C). Both IL-8 and ROS were significantly increased in virus-treated neutrophil supernatants as compared to medium at MOI 500 (333 ± 102 *vs* 8.2 ± 1.9pg/mL, p=0.0001; and 1551 ± 155 *vs* 683 ± 78 relative fluorescence units (RFU), p=0.0012, respectively). After 18h of incubation, late apoptotic cells were dramatically reduced in neutrophils incubated with SARS-CoV-2 compared to the medium alone (13.6% *vs* 57.0%, p<0.0001) (Figure 1D), in line with a strongly reduced active caspase 3 expression (3% *vs* 55%, P=0.0022) indicating that SARS-CoV-2 is able to delay neutrophil spontaneous apoptosis (Figure 1E).

To decipher neutrophil activation pathways, neutrophils were preincubated with several inhibitors prior to stimulation with the virus (Figure 1F). Neutrophil activation could be effectively reduced by inhibition of actin polymerization (52.7 ± 7.9% inhibition, p<0.0001), suggesting endocytosis is necessary for virus-induced neutrophil activation. In line with this, we found that neutrophil activation could also be reduced by inhibition of endosomal RNA-sensing pattern recognition receptors (PRR) TLR7/8 (45% ± 9, p<0.0001). Intriguingly, inhibition of IRF-3, a transcription factor downstream of nucleic acid sensors TLR3 and STING, could also significantly inhibit neutrophil activation (36.7% ± 7, p<0.0001). Since neutrophils do not possess TLR3, this suggests that the cytoplasmic receptor STING could also participate in neutrophil activation. Similarly, RIG-I and MDA-5, known to recognize viral

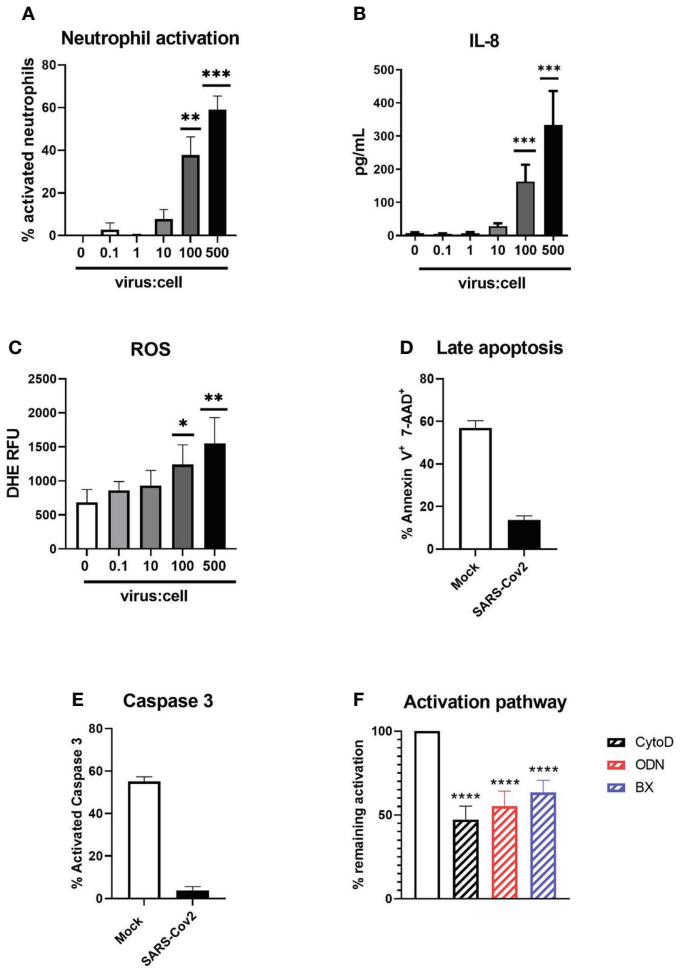

FIGURE 1
Activation of neutrophils by SARS-CoV-2 infectious particles. **(A)** Percentage of CD11bhigh/CD62Llow activated neutrophils after 90 min incubation of whole blood with SARS-CoV-2 ("Wuhan" B. strain)(n=12). **(B)** Concentration of IL-8 in supernatant after incubation with SARS-CoV-2 (n=12). **(C)** ROS production of neutrophils after incubation with SARS-CoV-2 virus. RFU, relative fluorescence units (n=12). **(D, E)** Percentage of (d) annexin V+/ 7-AAD+ late apoptotic neutrophils and (e) neutrophil expressing active caspase 3 after 18h of incubation of SARS-CoV-2 virus or medium (Mock)(n=12). **(F)** Percentage of inhibition of neutrophil activation by actin polymerization inhibitor cytochalasin D, TLR7 and TLR8 inhibitor ODN 2088 and STING/TLR3 signalling inhibitor BX795 (n=12). Data are mean ± SEM, *p<0.05; **p<0.01; ***p<0.001, ****p<0.0001.

double-stranded RNA, could also induce activation of IRF3. However, this would need cytoplasmic replication of SARS-Cov2 in neutrophils, which has not been observed so far.

Thus, our data show that human neutrophils can be directly activated by SARS-CoV-2 virus in an actin- and PRR-dependent manner.

SARS-CoV-2 variants have distinct activating properties of neutrophils

SARS-CoV-2 VOCs were cultivated from clinical isolates and used after infectious titration in neutrophil activation experiments in comparison with the original "Wuhan" (B) strain (Figures 2A–C). For a same MOI, incubation with the Delta variant induced a significantly higher percentage of neutrophil activation compared to the ancestral strain (84 ± 4% vs 44 ± 8%, p=0.03), while the Omicron variant induced a much lower activation than all other strains, in particular compared to the Delta strain (11.3 ± 3% vs 87 ± 4%, p<0.0001, Figure 2A). To confirm these results in a different model, we used lentiviral pseudotyped viruses expressing the spike protein from Delta and Omicron. In line with our results with the full virus, we found a significantly higher neutrophil activation with the Delta spike than with the Omicron spike (p<0.001; Figure S3). Next, we measured degranulated IL-8 in full virus-treated neutrophil supernatants, which showed an even larger difference for Delta variant compared to the Omicron variant (1914± 408 vs 87 ± 11 pg/mL, p<0.0001; Figure 2B). Since NETosis seems to be a prominent feature of neutrophil contribution to COVID-19 pathogeny, we tested NET generating capacity of SARS-CoV-2 variants circulating at the time of the study (Delta and Omicron) on isolated neutrophils. We show that the supernatants of neutrophils stimulated with the B. strain or the Delta strain contain higher NETs concentrations than those stimulated with the Omicron

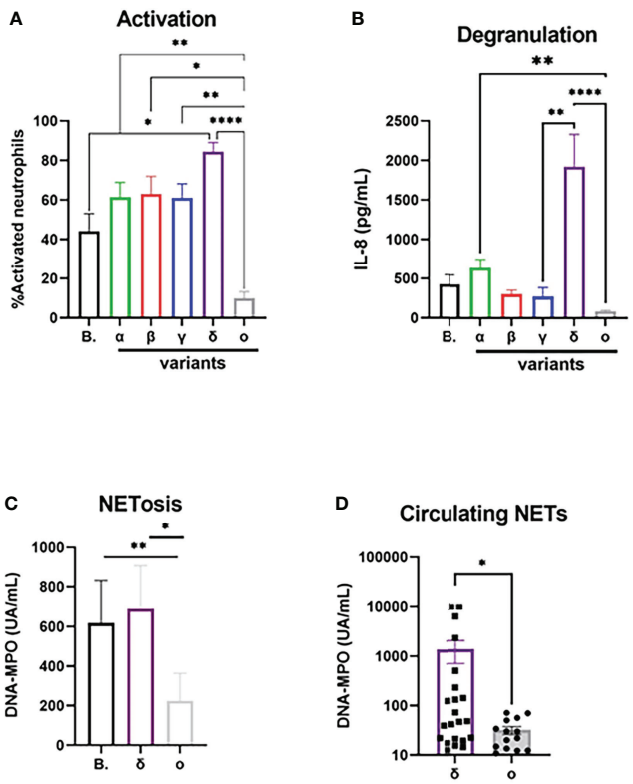

FIGURE 2
Activation potential of neutrophils differ between SARS-CoV-2 variants. **(A)** Percentage of CD11bhigh/CD62Llow activated neutrophils after 90 min incubation with SARS-CoV-2 "Wuhan" strain B and its major VOCs after normalization for medium (n=12). **(B)** Concentration of IL-8 in supernatant after 90 min incubation with SARS-CoV-2 after normalization for medium (n=12). **(C)** Concentration of DNA-MPO complexes in supernatant of isolated neutrophils after 3h of incubation with SARS-CoV-2 virus after normalization for medium (n=12). **(D)** Circulating concentration of DNA-MPO complexes in patients infected with Delta (n=22) or Omicron strain (n=14). Data are mean ± SEM, *p<0.05; **p<0.01; ****p<0.0001.

strain (618 ± 213 and 690 ± 217 vs 224 ± 139 UA/mL, p=0.0005 for both, Figure 2C). To confirm the impact *in vivo*, we measured circulating NET concentrations at diagnosis in patients infected with Delta or Omicron variants (Table 1), and found a higher concentration in patients with the Delta strain (1359 ± 658 *vs* 31.7 ± 5 UA/mL, p=0.027, Figure 2D) although blood neutrophil concentrations were similar in both groups (Supplemental Figure 2)

Discussion

Neutrophils are major players in SARS-CoV-2 infection and neutrophil activation has been linked to severity and poor prognosis (12, 17, 18). Therefore, understanding neutrophil activation pathways in COVID-19 is of paramount importance to design neutrophil-targeted therapeutic interventions. In this study, we demonstrate that one of the neutrophil activation pathways could be direct activation by infectious viral particles. We show that, *in vitro*, human healthy resting neutrophils can sense SARS-CoV-2 by TLR7/8 and STING activation, upregulate membrane activation markers, degranulate IL-8 and produce ROS and NETs. Additionally, we show that SARS-Cov2 is able to delay neutrophil apoptosis *via* downregulation of active caspase 3 expression, which could participate to a sustained pro-inflammatory effect. We then compared the activation potential of neutrophil by SARS-CoV-2 variants and showed a significantly increased activation by the Delta variant compared to the ancestral strain and a decreased activation by the Omicron variant.

We and other have described early neutrophil activation in blood and tissue neutrophils from COVID-19 patients (12, 17, 18). This activation is mostly believed to be due to pro-inflammatory cytokine released in particular by macrophages and monocytes (19, 20). Indeed, plasma from severe patients can activate neutrophils from healthy donors (21–23). However, a study suggested this could be dependent on circulating immune complexes rather than cytokines (24). Here, we show that direct

TABLE 1 Patients sera: These table contain age and gender of patients used to Netosis assay.

Delta sera			Omicron sera		
Patient	**Age**	**Gender**	**Patient**	**Age**	**Gender**
1	62	M	1	73	M
2	69	M	2	69	M
3	63	F	3	74	F
4	59	M	4	94	M
5	64	F	5	86	F
6	65	M	6	73	M
7	83	M	7	82	M
8	88	M	8	60	M
9	78	F	9	70	M
10	73	M	10	87	M
11	69	M	11	71	F
12	58	F	12	73	M
13	78	M	13	76	F
14	74	F	14	64	F
15	47	M	*Average age*		73
16	64	F	*Median age*		75
17	51	M	*Percentage of Men (%)*		64.3
18	64	M	*Percentage of Women (%)*		35.7
19	108	F			
20	80	M			
21	72	M			
22	64	M			
Average age		67			
Median age		70			
Percentage of Men (%)		68.2			
Percentage of Women (%)		31.8			

activation by the virus itself could contribute to neutrophil activation at infection sites. While a direct neutrophil activation would seem a counterproductive strategy for a virus, it has been shown that neutrophil proteases could participate in the maturation of the spike protein and thus facilitate infection (25, 26). More intriguing, it was recently suggested that the SARS-CoV-2 could use the histones on NETs as a hook to facilitate infection of neighboring cells *via* sialic acid binding (27).

The quantity of virus necessary to activate neutrophils seemed relatively large as compared to what is usually necessary to infect epithelial cells (28). However, at infection sites there is a huge amplification of viral particles due to viral replication. Moreover, we used untouched resting neutrophils from healthy donors that are less responsive to weak stimuli. Indeed, it is well described that neutrophil activation is a multistep process and that a priming step is necessary to get a full response (29). In an infectious context, neutrophils recruited to tissues are primed by the chemotaxis and diapedesis process and arrive in an inflammatory environment, making them likely to respond to much lower quantities of free viral particles.

Some studies have already shown activation of neutrophils by SARS-CoV-2 (8, 9), but none have compared the activation potential of all major variants so far. In doing so, we demonstrated a significant difference between Delta and Omicron variants, the latter being much less active on neutrophils. Interestingly, we were able to link this finding to clinical data since patients with Omicron presented less NETs in their serum, a fact recently confirmed by a preliminary study (30). Clinically, it is now well established that infection with the Omicron variant causes less severe disease that infection with Delta with a significantly lower hospitalization and lethality rate (31, 32). Since neutrophils are believed to be instrumental in disease severity, one may speculate this could participate to the less severe disease phenotype.

In addition, our results with spike-expressing pseudoviruses strongly suggests that the spike protein plays an important role in neutrophil activation. Indeed, it has been shown that the spike protein alone can induce neutrophil activation and NETosis (33). Additionally, one team has recently demonstrated that the Omicron spike protein presented a new cleavage site for neutrophil Cathepsin G protease (25), a feature which might interfere with its neutrophil activation properties.

The main limitation of this study is the *in vitro* experiments that do not reproduce accurately the inflamed setting in which the neutrophil meets the virus. However, this bias was necessary to be able to distinguish the signal induced by the virus itself from the one induced by the inflammatory background. In the future, studies on more elaborate models including infected epithelial cells will allow to explore further the virus-neutrophil interactions in a more physiological setting. Additionally, we did not explore the effect of co-infection with several VOCs. Indeed, co-infections with several VOCs have been described (34). While the clinical significance of such occurrence is not yet well known, in light of our data, it would be interesting to study their effect on innate immune response.

In conclusion, we demonstrate that neutrophil activation in COVID-19 patients can be done directly by the virus, and that the differences of clinical severity between the different strains of SARS-CoV-2 could be caused by differences in neutrophil activation potential. These data highlights even more the need to address neutrophil-virus interactions as an additional potential target for therapeutic intervention in SARS-CoV-2 infection.

Data availability statement

The raw data supporting the conclusions of this article will be made available by the authors, without undue reservation.

Ethics statement

The studies involving human participants were reviewed and approved by National Ethics committee Ile de France 8 n°2020-A02676-33. Written informed consent for participation was not required for this study in accordance with the national legislation and the institutional requirements.

Author contributions

LDC and SL contributed to conception and design of the study. LDC and SL organized the database. SL and LDC wrote the first draft of the manuscript. All authors contributed to manuscript revision and read and approved the submitted version. OD and CR contributed to the technical implementation of the revisions. All authors contributed to the article and approved the submitted version.

Funding

This study has been funded in part by grant #AC43 of the French "Agence Nationale de Recherche sur le SIDA et les hépatites virales" (ANRS).

Acknowledgments

We wish to thank the team of the National Reference Center (CNR) of Mycobacteria for their valuable help in this work.

Conflict of interest

The authors declare that the research was conducted in the absence of any commercial or financial relationships that could be construed as a potential conflict of interest.

Publisher's note

All claims expressed in this article are solely those of the authors and do not necessarily represent those of their affiliated organizations, or those of the publisher, the editors and the reviewers. Any product that may be evaluated in this article, or claim that may be made by its manufacturer, is not guaranteed or endorsed by the publisher.

Supplementary material

The Supplementary Material for this article can be found online at: https://www.frontiersin.org/articles/10.3389/fimmu.2022.1010140/full#supplementary-material

References

1. Xiao X, Zhou Q, Zhu J, Sun L, Zhang H, Sun Y, et al. False-positive colloidal gold-based immunochromatographic strip assay reactions for antibodies to SARS-CoV-2 in patients with autoimmune diseases. *Ann Transl Med* (2021) 9:534. doi: 10.21037/atm-20-6509

2. Bhattacharya M, Chatterjee S, Sharma AR, Agoramoorthy G, Chakraborty C. D614G mutation and SARS-CoV-2: impact on s-protein structure, function, infectivity, and immunity. *Appl Microbiol Biotechnol* (2021) 105:9035–45. doi: 10.1007/s00253-021-11676-2

3. Ren S-Y, Wang W-B, Gao R-D, Zhou A-M. Omicron variant (B.1.1.529) of SARS-CoV-2: Mutation, infectivity, transmission, and vaccine resistance. *World J Clin Cases* (2022) 10:1–11. doi: 10.12998/wjcc.v10.i1.1

4. Peacock TP, Brown JC, Zhou J, Thakur N, Newman J, Sukhova K, et al. The SARS-CoV-2 variant, omicron, shows rapid replication in human primary nasal epithelial cultures and efficiently uses the endosomal route of entry. *bioRxiv* (2022) 2021.12.31.474653. doi: 10.1101/2021.12.31.474653

5. Wiersinga WJ, Rhodes A, Cheng AC, Peacock SJ, Prescott HC. Pathophysiology, transmission, diagnosis, and treatment of coronavirus disease 2019 (COVID-19): A review. *JAMA* (2020) 324:782–93. doi: 10.1001/jama.2020.12839

6. Molina-Mora JA, González A, Jiménez-Morgan S, Cordero-Laurent E, Brenes H, Soto-Garita C, et al. Clinical profiles at the time of diagnosis of SARS-CoV-2 infection in Costa Rica during the pre-vaccination period using a machine learning approach. *Phenomics* (2022) 2:312–22. doi: 10.1007/s43657-022-00058-x

7. Anka AU, Tahir MI, Abubakar SD, Alsabbagh M, Zian Z, Hamedifar H, et al. Coronavirus disease 2019 (COVID-19): An overview of the immunopathology, serological diagnosis and management. *Scand J Immunol* (2021) 93:e12998. doi: 10.1111/sji.12998

8. Veras FP, Pontelli MC, Silva CM, Toller-Kawahisa JE, de Lima M, Nascimento DC, et al. SARS-CoV-2-triggered neutrophil extracellular traps mediate COVID-19 pathology. *J Exp Med* (2020) 217:e20201129. doi: 10.1084/jem.20201129

9. Arcanjo A, Logullo J, Menezes CCB, de Souza Carvalho Giangiarulo TC, Dos Reis MC, de Castro GMM, et al. The emerging role of neutrophil extracellular traps in severe acute respiratory syndrome coronavirus 2 (COVID-19). *Sci Rep* (2020) 10:19630. doi: 10.1038/s41598-020-76781-0

10. Barnes BJ, Adrover JM, Baxter-Stoltzfus A, Borczuk A, Cools-Lartigue J, Crawford JM, et al. Targeting potential drivers of COVID-19: Neutrophil extracellular traps. *J Exp Med* (2020) 217:e20200652. doi: 10.1084/jem.20200652

11. Borges L, Pithon-Curi TC, Curi R, Hatanaka E. COVID-19 and neutrophils: The relationship between hyperinflammation and neutrophil extracellular traps. *Mediators Inflamm* (2020) 2020:8829674. doi: 10.1155/2020/8829674

12. Peyneau M, Granger V, Wicky P-H, Khelifi-Touhami D, Timsit J-F, Lescure F-X, et al. Innate immune deficiencies are associated with severity and poor prognosis in patients with COVID-19. *Sci Rep* (2022) 12:638. doi: 10.1038/s41598-021-04705-7

13. Gordon DE, Jang GM, Bouhaddou M, Xu J, Obernier K, White KM, et al. A SARS-CoV-2 protein interaction map reveals targets for drug repurposing. *Nature* (2020) 583:459–68. doi: 10.1038/s41586-020-2286-9

14. Richetta C, Subra F, Malet I, Leh H, Charpentier C, Corona A, et al. Mutations in the 3'-PPT lead to HIV-1 replication without integration. *J Virol* (2022) 96:e0067622. doi: 10.1128/jvi.00676-22

15. Martin C, Gracias S, Charpentier C, Descamps D, Le Hingrat Q, Plantier J-C, et al. HIV-1 non-group m phenotypic susceptibility *in vitro* to bictegravir and cabotegravir. *J Antimicrob Chemother* (2021) 76:2306–9. doi: 10.1093/jac/dkab196

16. Granger V, Taillé C, Roach D, Letuvé S, Dupin C, Hamidi F, et al. Circulating neutrophil and eosinophil extracellular traps are markers of severe asthma. *Allergy* (2019) 75:699–702. doi: 10.1111/all.14059

17. Petito E, Falcinelli E, Paliani U, Cesari E, Vaudo G, Sebastiano M, et al. Association of neutrophil activation, more than platelet activation, with thrombotic complications in coronavirus disease 2019. *J Infect Dis* (2021) 223:933–44. doi: 10.1093/infdis/jiaa756

18. Vanderbeke L, Van Mol P, Van Herck Y, De Smet F, Humblet-Baron S, Martinod K, et al. Monocyte-driven atypical cytokine storm and aberrant neutrophil activation as key mediators of COVID-19 disease severity. *Nat Commun* (2021) 12:4117. doi: 10.1038/s41467-021-24360-w

19. Nicolai L, Leunig A, Brambs S, Kaiser R, Joppich M, Hoffknecht M, et al. Vascular neutrophilic inflammation and immunothrombosis distinguish severe COVID-19 from influenza pneumonia. *J Thromb Haemost* (2020) 19:574–581. doi: 10.1111/jth.15179

20. Morris G, Bortolasci CC, Puri BK, Olive L, Marx W, O'Neil A, et al. The pathophysiology of SARS-CoV-2: A suggested model and therapeutic approach. *Life Sci* (2020) 258:118166. doi: 10.1016/j.lfs.2020.118166

21. Delaveris CS, Wilk AJ, Riley NM, Stark JC, Yang SS, Rogers AJ, et al. Synthetic siglec-9 agonists inhibit neutrophil activation associated with COVID-19. *ACS Cent Sci* (2021) 7:650–7. doi: 10.1021/acscentsci.0c01669

22. Middleton EA, He X-Y, Denorme F, Campbell RA, Ng D, Salvatore SP, et al. Neutrophil extracellular traps contribute to immunothrombosis in COVID-19 acute respiratory distress syndrome. *Blood* (2020) 136:1169–79. doi: 10.1182/blood.2020007008

23. Zuo Y, Yalavarthi S, Shi H, Gockman K, Zuo M, Madison JA, et al. Neutrophil extracellular traps in COVID-19. *JCI Insight* (2020) 5:e138999. doi: 10.1172/jci.insight.138999

24. Mazzitelli I, Bleichmar L, Ludueña MG, Pisarevsky A, Labato M, Chiaradia V, et al. Immunoglobulin G immune complexes may contribute to neutrophil activation in the course of severe coronavirus disease 2019. *J Infect Dis* (2021) 224:575–85. doi: 10.1093/infdis/jiab174

25. Mustafa Z, Kalbacher H, Burster T. Occurrence of a novel cleavage site for cathepsin G adjacent to the polybasic sequence within the proteolytically sensitive activation loop of the SARS-CoV-2 omicron variant: The amino acid substitution N679K and P681H of the spike protein. *PloS One* (2022) 17:e0264723. doi: 10.1371/journal.pone.0264723

26. Mustafa Z, Zhanapiya A, Kalbacher H, Burster T. Neutrophil elastase and proteinase 3 cleavage sites are adjacent to the polybasic sequence within the proteolytic sensitive activation loop of the SARS-CoV-2 spike protein. *ACS Omega* (2021) 6:7181–5. doi: 10.1021/acsomega.1c00363

27. Hong W, Yang J, Zou J, Bi Z, He C, Lei H, et al. Histones released by NETosis enhance the infectivity of SARS-CoV-2 by bridging the spike protein subunit 2 and sialic acid on host cells. *Cell Mol Immunol* (2022) 19:577–87. doi: 10.1038/s41423-022-00845-6

28. Lebourgeois S, Menidjel R, Chenane HR, Ferré VM, Collin G, Damond F, et al. Alpha (B.1.1.7) and delta (B.1.617.2 - AY.40) SARS-CoV-2 variants present strong neutralization decay at M4 post-vaccination and a faster replication rates than D614G (B.1) lineage. *J Infect* (2022) 84:418–67. doi: 10.1016/j.jinf.2021.11.012

29. El-Benna J, Hurtado-Nedelec M, Marzaioli V, Marie J-C, Gougerot-Pocidalo M-A, Dang PM-C. Priming of the neutrophil respiratory burst: role in host defense and inflammation. *Immunol Rev* (2016) 273:180–93. doi: 10.1111/imr.12447

30. Carmona-Rivera C, Zhang Y, Dobbs K, Markowitz TE, Dalgard CL, Oler AJ, et al. Multicenter analysis of neutrophil extracellular trap dysregulation in adult and pediatric COVID-19. *medRxiv* (2022). doi: 10.1101/2022.02.24.22271475

31. Nyberg T, Ferguson NM, Nash SG, Webster HH, Flaxman S, Andrews N, et al. Comparative analysis of the risks of hospitalisation and death associated with SARS-CoV-2 omicron (B.1.1.529) and delta (B.1.617.2) variants in England: a cohort study. *Lancet* (2022) 399:1303–12. doi: 10.1016/S0140-6736(22)00462-7

32. Abdullah F, Myers J, Basu D, Tintinger G, Ueckermann V, Mathebula M, et al. Decreased severity of disease during the first global omicron variant covid-19 outbreak in a large hospital in tshwane, south africa. *Int J Infect Dis* (2022) 116:38–42. doi: 10.1016/j.ijid.2021.12.357

33. Youn Y-J, Lee Y-B, Kim S-H, Jin HK, Bae J-S, Hong C-W. Nucleocapsid and spike proteins of SARS-CoV-2 drive neutrophil extracellular trap formation. *Immune Netw* (2021) 21:e16. doi: 10.4110/in.2021.21.e16

34. Molina-Mora JA, Cordero-Laurent E, Calderón-Osorno M, Chacón-Ramírez E, Duarte-Martínez F. Metagenomic pipeline for identifying co-infections among distinct SARS-CoV-2 variants of concern: study cases from alpha to omicron. *Sci Rep* (2022) 12:9377. doi: 10.1038/s41598-022-13113-4

frontiers | Frontiers in Immunology

TYPE Original Research
PUBLISHED 03 November 2022
DOI 10.3389/fimmu.2022.1021928

Check for updates

OPEN ACCESS

EDITED BY
Pei-Hui Wang,
Shandong University, China

REVIEWED BY
Kathrin Sutter,
University of Duisburg-Essen, Germany
Francesca Cossarini,
Icahn School of Medicine at Mount Sinai, United States

*CORRESPONDENCE
Shokrollah Elahi
elahi@ualberta.ca

SPECIALTY SECTION
This article was submitted to Viral Immunology, a section of the journal Frontiers in Immunology

RECEIVED 17 August 2022
ACCEPTED 21 October 2022
PUBLISHED 03 November 2022

CITATION
Shahbaz S, Oyegbami O, Saito S, Osman M, Sligl W and Elahi S (2022) Differential effects of age, sex and dexamethasone therapy on ACE2/TMPRSS2 expression and susceptibility to SARS-CoV-2 infection. *Front. Immunol.* 13:1021928. doi: 10.3389/fimmu.2022.1021928

COPYRIGHT
© 2022 Shahbaz, Oyegbami, Saito, Osman, Sligl and Elahi. This is an open-access article distributed under the terms of the Creative Commons Attribution License (CC BY). The use, distribution or reproduction in other forums is permitted, provided the original author(s) and the copyright owner(s) are credited and that the original publication in this journal is cited, in accordance with accepted academic practice. No use, distribution or reproduction is permitted which does not comply with these terms.

Differential effects of age, sex and dexamethasone therapy on ACE2/TMPRSS2 expression and susceptibility to SARS-CoV-2 infection

Shima Shahbaz[1], Olaide Oyegbami[1], Suguru Saito[1], Mohammed Osman[2], Wendy Sligl[3,4] and Shokrollah Elahi[1,5,6]*

[1]Department of Dentistry, Division of Foundational Sciences, Edmonton, AB, Canada, [2]Department of Medicine, Division of Rheumatology, University of Alberta, Edmonton, AB, Canada, [3]Department of Critical Care Medicine, University of Alberta, Edmonton, AB, Canada, [4]Department of Medicine, Division of Infectious Diseases, University of Alberta, Edmonton, AB, Canada, [5]Department of Medical Microbiology and Immunology, Li Ka Shing Institute of Virology, Edmonton, AB, Canada, [6]Women and Children Health Research Institute, Faculty of Medicine and Dentistry, University of Alberta, Edmonton, AB, Canada

ACE2 and TMPRSS2 are crucial for SARS-CoV-2 entry into the cell. Although ACE2 facilitates viral entry, its loss leads to promoting the devastating clinical symptoms of COVID-19 disease. Thus, enhanced ACE2/TMPRSS2 expression is likely to increase predisposition of target cells to SARS-CoV-2 infection. However, little evidence existed about the biological kinetics of these two enzymes and whether dexamethasone treatment modulates their expression. Here, we show that the expression of ACE2 at the protein and mRNA levels was significantly higher in the lung and heart tissues of neonatal compared to adult mice. However, the expression of TMPRSS2 was developmentally regulated. Our results may introduce a novel concept for the reduced susceptibility of the young to SARS-CoV-2 infection. Moreover, ACE2 expression but not TMPRSS2 was upregulated in adult female lungs compared to their male counterparts. Interestingly, the ACE2 and TMPRSS2 expressions were upregulated by dexamethasone treatment in the lung and heart tissues in both neonatal and adult mice. Furthermore, our findings provide a novel mechanism for the observed differential therapeutic effects of dexamethasone in COVID-19 patients. As such, dexamethasone exhibits different therapeutic effects depending on the disease stage. This was supported by increased ACE2/TMPRSS2 expression and subsequently enhanced infection of normal human bronchial epithelial cells (NHBE) and Vero E6 cells with SARS-CoV-2 once pre-treated with dexamethasone. Therefore, our results suggest that individuals who take dexamethasone for other clinical conditions may become more prone to SARS-CoV-2 infection.

KEYWORDS

COVID-19, ACE2, TMPRSS2, dexamethasone, age, sex

Introduction

The emergence of the Coronavirus Disease 2019 (COVID-19) has led to a major global pandemic. While severe/critical illness and death are more common in the elderly (1), severe outcomes are uncommon in the young (2, 3). Although infants and children are susceptible to infection, up to 90% of SARS-CoV-2 infected infants/children are asymptomatic or exhibit mild symptoms without a need for hospitalization (4, 5). These observations suggest that there are differences in the immune response to SARS-CoV-2 infection in the young versus the elderly. For instance, it has been proposed that infants respond to micro-organisms through biased immune tolerance rather than resistance strategies – preventing excessive immune response and collateral damage in the young (3). Also, more frequent/recent immunizations in young populations may result in trained immunity and cross-protection against SARS-CoV-2 (5).

Another host factor that may influence the infectivity to SARS-CoV-2 is the differential age-dependent expression of the viral receptor(s) and co-receptor on the target cell (6). Previous studies have indicated that SARS-CoV-2 enters the cell by binding to the Angiotensin-converting enzyme 2 (ACE2) on the cell surface *via* the spike protein (7, 8). Subsequently, the spike protein is cleaved by transmembrane protease serine 2 (TMPRSS2), facilitating target cell entry (7). Thus, SARS-CoV-2 not only gains initial entry *via* ACE2 but also downregulates ACE2, which impairs its protective physiological role (9). The downregulation of ACE2 in the respiratory tract is linked to neutrophil infiltration in response to LPS (10) and may result in angiotensin II accumulation and lung injury in respiratory viral infections (11, 12). Because ACE2 is a carboxypeptidase degrading angiotensin II, B1-bradykinin, and apelin-13, it contributes to cardiovascular physiology (13). Moreover, the enzymatic activity of ACE2 is protective against acute respiratory distress syndrome (ARDS) caused by viral and non-viral lung injury. ACE2 is predominantly expressed in the upper respiratory tract, heart, and other tissues (14, 15).

Therefore, in addition to the respiratory tract, the cardiac tissue could be the target of SARS-CoV-2. For example, it is reported that infected individuals with SARS-CoV-2 could experience cardiovascular disease such as myocarditis (16). A pilot study has reported the detection of SARS-CoV-2 viral RNA in 41% of heart tissues from deceased individuals who died of COVID-19 disease (17).

Although mounting evidence suggests that age and sex may influence ACE2 expression (18), this has been the subject of debate. For example, ACE2 expression in the lung tissue was not different between sexes and age groups in different cohorts of rodents (rats and mice) (19). Similar results were reported for the expression of ACE2 in human lung tissues (19). However, upregulation of ACE2 with age has been seen only in COVID-19 patients requiring mechanical ventilation (20). In contrast, a higher ACE2 expression in the lung of younger compared to older animals, regardless of their sex, has been reported (21). A couple of recent studies reported increased ACE2 gene expression with age in the respiratory tract (22). This discordance illustrates the need for a more unifying explanation as to whether ACE2 and TMPRSS2 are differentially expressed in the young and whether sex influences their expression. Moreover, recent evidence supports a survival advantage with dexamethasone in COVID-19 patients requiring oxygen or invasive mechanical ventilation (23, 24). However, the same treatment has no benefit and may exacerbate disease in patients with milder disease (24).

In the present study, we examined the expression of ACE2 and/or TMPRSS2 in one week old neonatal, 2 and > 6 months old mice at the gene and protein levels. We also examined the effects of dexamethasone treatment on ACE2 and TMPRSS2 expression in lung and heart tissues of both neonatal and adult mice. Finally, as proof of concept, we show that dexamethasone treatment enhances the infectivity of Verso E6 and normal human bronchial epithelial cells (NHBE) to pseudo SARS-CoV-2. Thus, our study may provide a potential and novel explanation for the observed differential effects of dexamethasone in COVID-19 patients.

Material and methods

Animal studies

BALB/c mice at different age groups were used for these studies. Similarly, the effects of dexamethasone (Sigma) on ACE2 and TMPRSS2 expression in the lung and heart tissues were assessed 2 days post intraperitoneal (IP) injection using the physiologically relevant concentration of 1 μg/g body weight (25). The research ethics boards at the University of Alberta approved these studies with the protocol # AUP0001021.

Western blot analyses

Tissues were lysed in lysis buffer supplemented with a protease inhibitor cocktail (Sigma-Aldrich) and protein concentration was determined using a BCA assay kit (Thermo Fisher Scientific). Protein samples were separated by electrophoresis on either 7%, 17%, or 4-15% gradient polyacrylamide gels and then transferred to PVDF membranes. The membranes were blocked with 5% milk and incubated with the anti-ACE2 (Abcam, ab15348), anti-TMPRSS2 (Abcam, ab242384), and anti-β-actin/GAPDH (Sigma) antibodies using 1:1000 dilution.

Next, membranes were incubated with the appropriate HRP-conjugated secondary antibodies and developed using an enhanced chemiluminescence detection kit (Thermo Fisher Scientific).

Protein bands of interest were quantified using Image Lab Software v6.0.1 (Bio-Rad).

Gene expression analysis

RNA was isolated from the lung and heart tissues of mice using RNAeasy mini kit (Qiagen). The concentration of isolated RNA samples was measured using a nanodrop spectrophotometer (ThermoFisher Scientific) and samples with 260/280 ratios between 1.8 and 2.0 were selected for further analysis. RNA (500 ng) was used for cDNA synthesis using the miScript II Reverse Transcription Kit (Qiagen) and the T100 Thermal Cycler (Bio-Rad). The expression of genes was measured by RT-PCR using CFX96 Touch Real-Time PCR Detection System (Bio-Rad). The Quantitect Primer assay (Qiagen) was carried out for the following genes: ACE2, TMPRSS2 with Beta-2-microglobulin used as the reference gene. Data analysis was done using the 2^{-CT} method as we reported elsewhere (26, 27).

Immunofluorescence staining

Tissues were harvested and fixed in 4% PFA overnight. Slides were deparaffinized by washing twice in xylene for 10 min, 2 times in 100% EtOH for 10 min, 1 time in 95% EtOH for 5 min, 1 time in 70% EtOH for 5 min, and finally a 5-min wash in H_2O. Next, slides were incubated in pre-warmed citrate buffer (pH 6.0) in a water bath at 92°C for 10 min, then removed and allowed to cool to room temperature followed by 3 washes with 1x PBS with 5 min intervals. First, slides were incubated in 10% donkey serum in PBST at RT for 1 hour to minimize non-specific antibody binding. After 3 washes with 1x PBS at 5 min intervals, samples were incubated in 100 µL of ACE2 primary antibody (1:200 Abcam ab15348) overnight in a moist chamber at 4°C. For the staining of TMPRSS2, samples were incubated in 100 µL of TMPRSS2 primary antibody (1:200 Abcam ab92323) overnight in a moist chamber at 4°C. For the negative control, samples were incubated with 100 µL PBS overnight in a moist chamber at 4°C. The next day slides were washed 3 times with 1x PBS at 5 min intervals. Finally, 100 µL of Alexa Flour 488 secondary antibody (1:1000 Invitrogen A32790) was added to samples in the dark and incubated for 1 hour at room temperature, and then washed 3 times with 1x PBS for 5 min each wash. The samples were then incubated with 100 µL of DAPI (1:1000 Invitrogen D1306) for 10 min. Slides were then washed 3 times with 1x PBS at 5 min intervals. A drop of ProLong Mountant (Invitrogen P36934) was added to each sample before coverslips were placed.

Infection assay with the pseudo SARS-CoV-2

Vero E6 cells were seeded at 30,000 cells/well in complete RPMI culture media in the presence or absence of dexamethasone (0.5 µg/ml and 1 µg/ml, Sigma) in a 48 well flat-bottomed plate for 24 hr. Similarly, NHBE cells originally purchased from the ATCC but no information was provided for the age/sex of the donor. These cells were seeded at 30,000 cells/well in bronchia epithelial cell growth media (BEGM, Sigma) in the presence or absence of dexamethasone (1 µg/ml) in a 48 well flat-bottomed plate for 24 hr. Then, cells were washed with warm PBS and exposed to the pseudo SARS-CoV-2 spike Delta variant green reporter (Montana Molecular, MT, USA) according to the manufacturers' instruction overnight. Then cells were trypsinized and extensively washed of any extracellular pseudo virus before analysis by imaging and/or flow cytometry.

Flow cytometry

The expression of ACE2/TMPRSS2 was analyzed by using the anti-ACE2 (535919) from R&D, and the anti-TMPRSS2 (EPR3862) from abcam according to our methods (28–30). Besides, Live/dead fixable dead cell stain (ThermoFisher) was used to exclude dead cells in flow cytometry. Paraformaldehyde fixed cells were acquired by flow cytometry using a LSRFORTESSA flow cytometer (BD) and analyzed with FlowJo software (version 10).

Statistical analysis

Statistical analysis was performed using the Prism software. Based on the distribution of data the appropriate test was used. The non-parametric tests such as the Mann-Whitney U-test or Kruskal–Wallis one-way analysis of variance was used. Also, Wilcoxon matched-pairs signed rank test was used for paired studies (e.g. *in vitro* treatment). The *P*-values are shown in the graphs and measures are expressed as mean ± SEM and *P*-value < 0.05 was considered to be statistically significant.

Results

Higher ACE2 but lower TMPRSS2 in lung tissues of neonatal compared to adult mice

To compare the expression levels of ACE2 in the lung of neonatal compared to older mice, we measured total ACE2 protein levels by western blot in lung tissues. We found that neonatal mice (one week old) had significantly higher ACE2 protein levels compared to older adult mice (> 6 months) in bulk lung tissues (Figures 1A, B). A similar pattern was noted at the gene expression level when ACE2 mRNA was quantified in lung tissues of neonatal versus older adult mice (Figure 1C). This was also the case for ACE2 expression at the protein and gene levels in heart tissues of neonatal compared to older adult mice

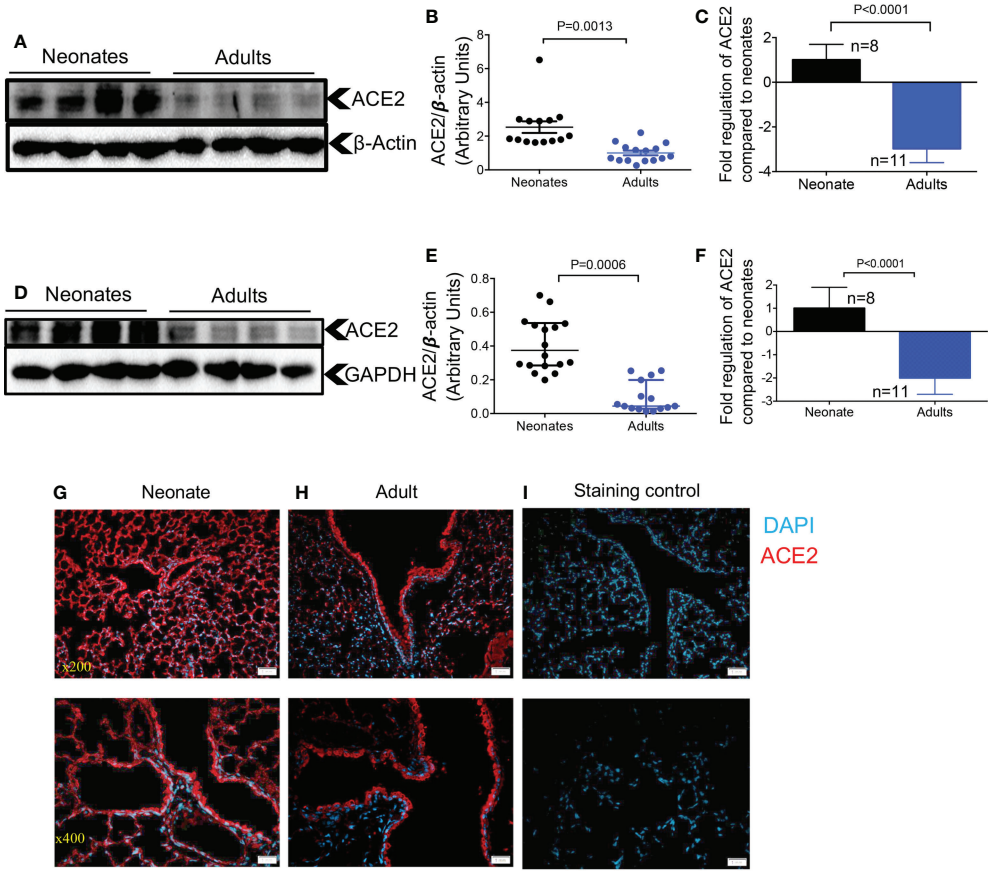

FIGURE 1
Differential expression of ACE2 and TMPRSS2 in the lung and heart tissues of neonatal compared to adult mice. **(A)** Representative western immunoblots, and **(B)** cumulative data of ACE2 protein in the lung tissues of neonatal (1-week-old) versus adult mice (> 6 months). **(C)** Cumulative data showing fold regulation of ACE2 mRNA in the lung tissues of neonatal versus adult mice (> 6 months). **(D)** Representative western immunoblots, and **(E)** cumulative data of ACE2 in the heart tissues of neonatal versus adult mice (> 6 months). **(F)** Cumulative data showing fold regulation of ACE2 mRNA in the heart tissues of neonatal versus adult mice (> 6 months). **(G)** Representative immunofluorescence (IF) images of ACE2 expression in the lung tissue of a neonatal mouse, and **(H)** an adult mouse (5 sections/tissue, n= >3/group). **(I)** IF image of the lung section stained with the secondary antibody as control. Scale bar: 100 µm. Magnification x200 and x400. Sample size (n) is shown for each group. All blots were repeated for reproducibility and lanes were loaded with equal amounts of protein. Quantification of ACE2 (97 KDa) and TMPRSS2 (54 KDa) normalised to the loading control. Error bars indicate mean ± SEM from more than two independent experiments. Each dot represents data from an animal.

(Figures 1D-F). It is worth mentioning that although ACE2 is observed as a single band in most tissues of mice, it is usually observed as double bands in lung tissue as reported elsewhere (29). We further investigated the expression of ACE2 in the lung tissue by immunofluorescence staining (IF). Although we did not quantify the expression level, these observations suggest a more intense and less scattered ACE2 expression in the lung tissue of neonatal versus adult mice (Figures 1G-I). However, our observations did not support a differential expression level for ACE2 in neonatal female/male mice.

In a recent study, the developmental regulation of TMPRSS2 expression in the human lung epithelium was suggested to be the primary determinant of age-related differences in SARS-CoV-2 infection susceptibility (6). To determine whether this was the case in mice, we examined TMPRSS2 expression by western blot and qPCR in the lung tissues of neonatal versus older adult mice. We found that older adult animals, had significantly higher TMPRSS2 expression compared to neonates at the protein and gene levels in their lung tissues (Figures 2A-C). These observations were further confirmed by the IF staining that showed scarce expression of TMPRSS2 in the lung of neonatal versus older adult mice (Figures 2D-F). We further observed that TMPRSS2 expression was developmentally regulated in the lung tissues regardless of the animal sex as noted in female (Figures 2G, H) and male mice (Figures 2I, J). However, we were unable to detect TMPRSS2 expression in heart tissue as reported elsewhere (31). These results confirm the developmental regulation of TMPRSS2 in lung tissues of mice.

10.3389/fimmu.2022.1021928

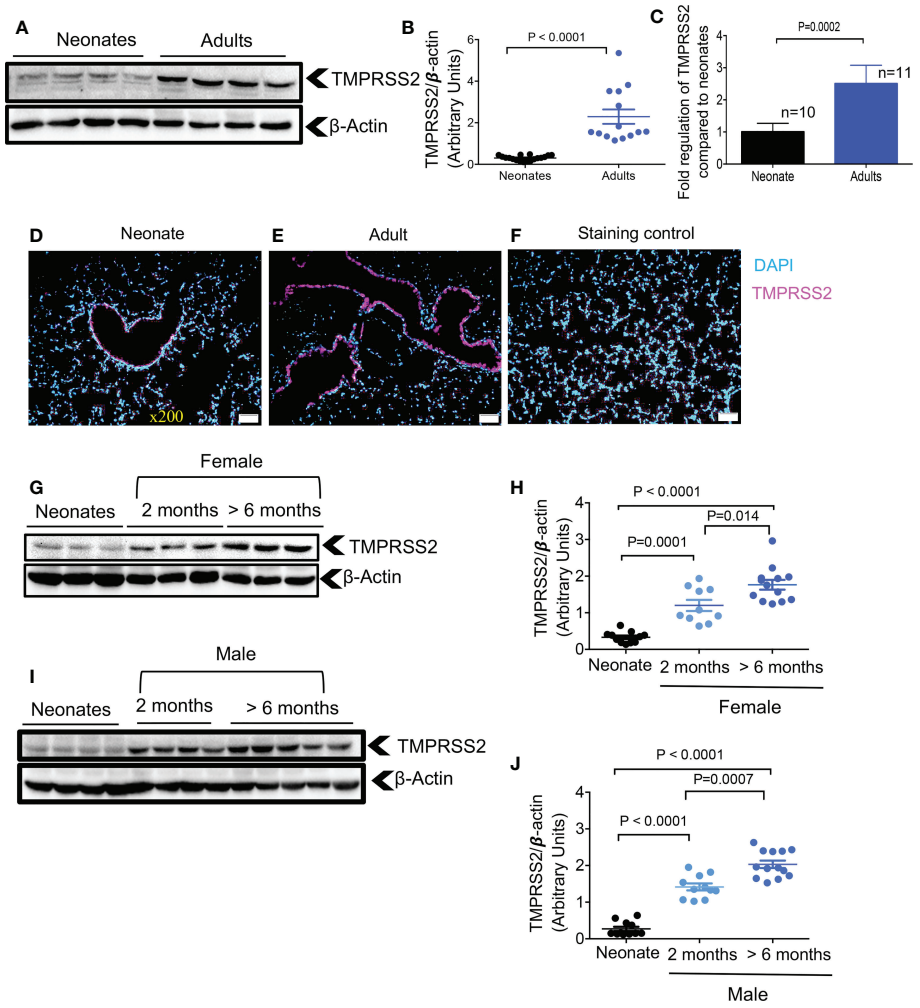

FIGURE 2
Developmental regulation of TMPRSS2 in the lung tissues of mice. **(A)** Representative western immunoblots, and **(B)** cumulative data of TMPRSS2 protein in the lung tissues of neonatal versus adult mice (> 6 months). **(C)** Cumulative data showing fold regulation of TMPRSS2 mRNA in the lung tissues of neonatal versus adult mice (> 6 months). **(D)** Representative immunofluorescence (IF) images of TMPRSS2 expression in the lung tissue of a neonatal mouse, and **(E)** an adult mouse (5 sections/tissue, n= >3/group). **(F)** IF image of the lung section stained with the secondary antibody as control. Scale bar: 100 µm. Magnification x200. **(G)** Representative western immunoblots, and **(H)** cumulative data of TMPRSS2 protein in the lung tissues of neonatal (8 days old), young adults (2 months) versus older adult (> 6 months) female mice. **(I)** Representative western immunoblots, and **(J)** cumulative data of TMPRSS2 protein in the lung tissues of neonatal, young adults (2 months) versus older adult (> 6 months) male mice. All blots were repeated for reproducibility and lanes were loaded with equal amounts of protein. Quantification of ACE2 and TMPRSS2 normalised to the loading control. Error bars indicate mean ± SEM from at least three independent experiments.

Higher expression of ACE2 but not TMPRSS2 in the lung tissue of female mice

Hormonal and genetic factors are reported to result in ACE2 upregulation in females (32), which may, in part, explain differences in COVID-19 outcomes in females versus males. Thus, we analyzed the expression of ACE2 and TMPRSS2 in the lung tissues of older (> 6 months old) female versus male mice. We found that females had significantly higher ACE2 expression at the protein and gene levels in lung tissue compared to males (Figures 3A-C). However, this difference was noted only at the gene level but not at the protein level in the heart tissues of females (Figures 3D-F). When TMPRSS2 expression was analyzed, we did not find any significant differences between males and females at the gene and protein levels in lung tissues (Figures 3G-I). In agreement with another report (31), we were unable to detect TMPRSS2 gene expression in heart tissue. These results highlight the differential effects of sex on ACE2 and TMPRSS2 expression in older mice.

10.3389/fimmu.2022.1021928

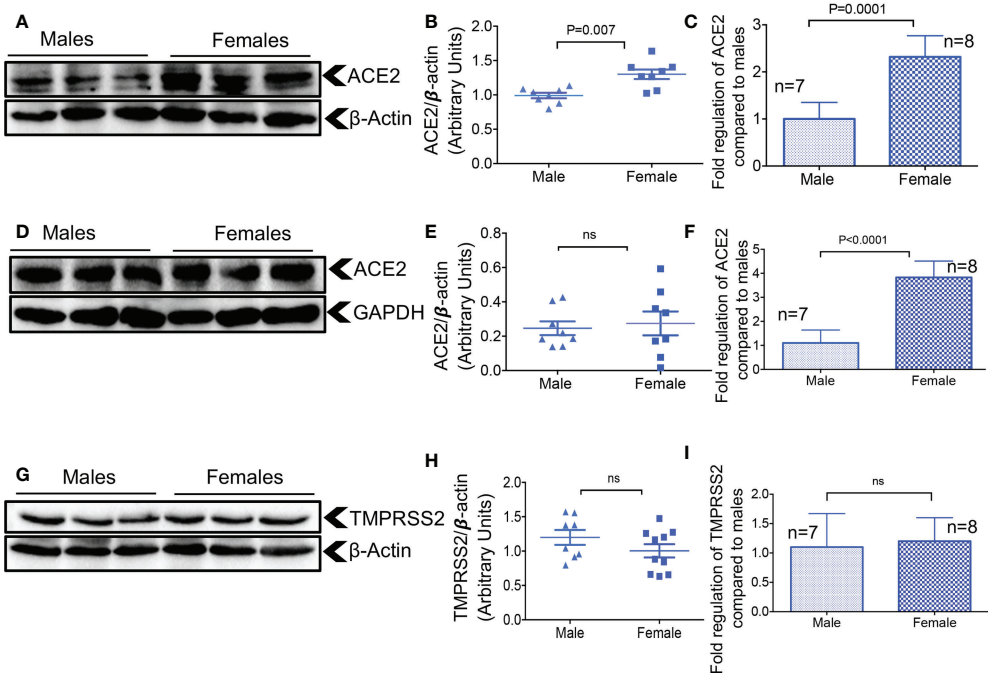

FIGURE 3
Elevated ACE2 at the gene and protein levels in the lungs of female mice. **(A)** Representative western immunoblots, and **(B)** cumulative data of ACE2 protein in the lung tissues of adult male and female mice. **(C)** Cumulative data showing fold regulation of ACE2 mRNA in the lung tissues of male versus female adult mice. **(D)** Representative western immunoblots, and **(E)** cumulative data of ACE2 protein in the heart tissues of adult male and female mice. **(F)** Cumulative data showing fold regulation of ACE2 mRNA in the heart tissues of male versus female adult mice. **(G)** Representative western immunoblots, and **(H)** cumulative data of TMPRSS2 protein in the lung tissues of male versus female older adult mice. **(I)** Cumulative data showing fold regulation of TMPRSS2 mRNA in the lung tissues of male versus female adult mice. All blots were repeated for reproducibility and lanes were loaded with equal amounts of protein. Quantification of ACE2 and TMPRSS2 normalised to the loading control. Error bars indicate mean ± SEM from at least two independent experiments. ns, Not significant.

Dexamethasone upregulates the expression of ACE2 and TMPRSS2 in neonatal mice

Treatment with dexamethasone in hospitalized COVID patients has been shown to reduce mortality among those who require oxygen and/or mechanical ventilation (23). However, there is no evidence, to our knowledge, that dexamethasone may impact the expression of ACE2 and TMPRSS2 in these patients. Therefore, we aimed to determine the effects of dexamethasone on the expression of ACE2 and TMPRSS2 in neonatal mice. One-week old mice were administered intraperitoneal (IP) dexamethasone (1 µg/g body weight) for two consecutive days and their lung and heart tissues were harvested a day later (Figure 4A). Control animals were injected (IP) with phosphate buffered-saline (PBS) because the dexamethasone was water soluble and then was diluted in PBS. We found that dexamethasone treatment resulted in a significant upregulation of ACE2 at the protein and gene levels in the lung tissues of one-week old mice (Figures 4B-D). Furthermore, using the IF staining, we noted a more intense and less scattered ACE2 expression in the lung tissues of treated versus control mice (Figures 4E, F). However, the IF staining was not quantified and only implies a higher ACE2 expression in the treated group. Moreover, the expression of ACE2 at the protein and gene levels in heart tissues confirmed similar results (Figures 4G-I). Next, we assessed the expression of TMPRSS2 in the lungs of neonatal mice after treatment with dexamethasone. These studies yielded results that were consistent with the ACE2 expression (Figures 4J-L). In summary, these findings support the role of dexamethasone in upregulating the expression of ACE2 and TMPRSS2 in the lung and ACE2 in the heart tissues of neonatal mice.

Dexamethasone upregulates the expression of ACE2 and TMPRSS2 in adult mice

Since our results showed differential expression of ACE2 and TMPRSS2 in the lung and heart tissues of neonatal mice (Figure 1), we hypothesized that dexamethasone may also

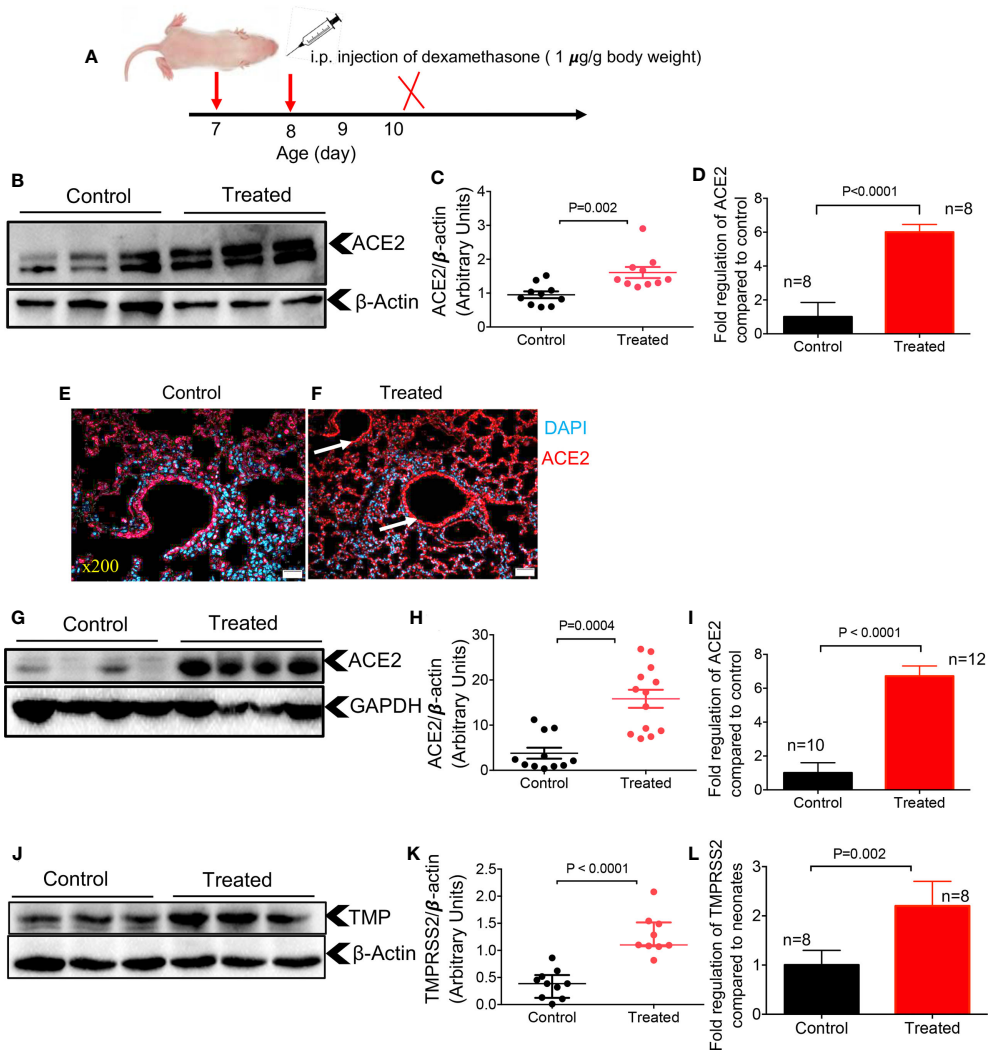

FIGURE 4
Dexamethasone upregulates the expression of ACE2 and TMPRSS2 in the tissues of neonatal mice. **(A)** Dexamethasone treatment strategy. **(B)** Representative western immunoblots, and **(C)** cumulative data of ACE2 protein in the lung tissues of neonatal mice treated with dexamethasone (IP, 1 µg/g body weight for two consecutive days) versus those treated with PBS (control). **(D)** Cumulative data showing fold regulation of ACE2 mRNA in the lung tissues of treated neonates versus control. **(E)** Representative immunofluorescence (IF) images of ACE2 expression in the lung tissue of a control versus **(F)** dexamethasone treated neonatal mouse (5 sections/tissue, n= >3/group). Scale bar: 100 µm. Magnification x200. **(G)** Representative western immunoblots, and **(H)** cumulative data of ACE2 protein in the heart tissues of control versus dexamethasone treated neonatal mice **(I)** Cumulative data showing fold regulation of ACE2 mRNA in the heart tissues of neonatal mice treated with dexamethasone compared to controls. **(J)** Representative western immunoblots, and **(K)** cumulative data of TMPRSS2 (TMP) protein in the lung tissues of control versus dexamethasone treated neonatal mice **(L)** Cumulative data showing fold regulation of TMPRSS2 mRNA in the lung tissues of neonatal mice treated with dexamethasone compared to controls. All blots were repeated for reproducibility and lanes were loaded with equal amounts of protein. Quantification of ACE2 and TMPRSS2 normalised to the loading control. Error bars indicate mean ± SEM from more than three independent experiments.

exhibit differential effects on the expression of ACE2 and TMPRSS2 in older adult mice. Strikingly, we found that dexamethasone treatment (1 µg/g body weight, IP) for two consecutive days increased the expression of ACE2 at the protein level in adult mice (> 6 months) regardless of their sex (Figures 5A, B). We also observed similar effects in 2-month-old mice. To better understand the role of sex following treatment with dexamethasone, we measured the mRNA level for ACE2 in lung tissues of both male and female adult mice. We observed that dexamethasone treatment upregulated the mRNA expression for ACE2 in lung tissues of both female and male adult mice, respectively (Figures 5C, D). Similar observations were made for ACE2 expression at the gene level in the heart tissues of mice once treated with dexamethasone regardless of

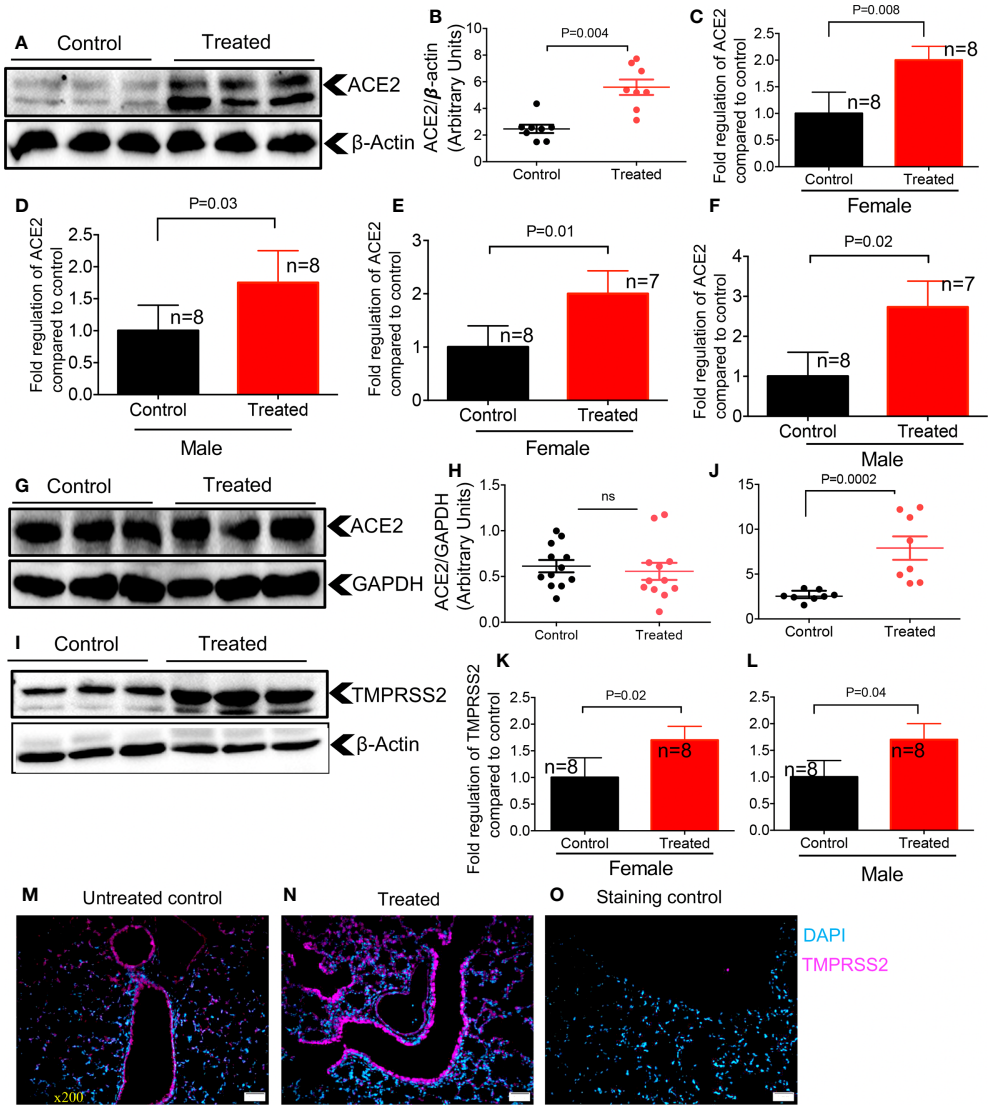

FIGURE 5
Dexamethasone upregulates the expression of ACE2 and TMPRSS2 in the lung and heart tissues of adult mice. **(A)** Representative western immunoblots, and **(B)** cumulative data of ACE2 protein in the lung tissues of adult mice (> 6 months) treated with dexamethasone (IP, 1 µg/g body weight for two consecutive days) versus those treated with PBS (control). **(C)** Cumulative data showing fold regulation of ACE2 mRNA in the lung tissues of treated male, and **(D)** female versus control mice. **(E)** Cumulative data showing fold regulation of ACE2 mRNA in the heart tissues of treated male, and **(F)** female versus control mice. **(G)** Representative western immunoblots, and **(H)** cumulative data of ACE2 protein in the heart tissues of adult mice (> 6 months) treated with dexamethasone versus controls. **(I)** Representative western immunoblots, and **(J)** cumulative data of TMPRSS2 protein in the lung tissues of adult mice (> 6 months) treated with dexamethasone versus controls. **(K)** Cumulative data showing fold regulation of YMPRSS2 mRNA in the lung tissues of treated male, and **(L)** female versus controls. **(M)** IF images of TMPRSS2 expression in the lung tissue of a control versus **(N)** dexamethasone treated adult mouse. **(O)** Stained with the secondary antibody (5 sections/tissue, n= >3/group). Scale bar: 100 µm. Magnification x200. All blots were repeated for reproducibility and lanes were loaded with equal amounts of protein. Quantification of ACE2 and TMPRSS2 normalised to the loading control. Error bars indicate mean ± SEM from more than three independent experiments. ns, Not significant.

their sex (Figures 5E, F). However, we did not find any changes in ACE2 expression at the protein level in heart tissues of adult mice regardless of their sex despite treating additional animals (Figures 5G, H).

Next, we quantified the expression of TMPRSS2 in the lung tissue of animals treated with dexamethasone versus controls, which showed a significantly enhanced TMPRSS2 at the protein level in treated animals (Figures 5I, J). We further found that dexamethasone treatment significantly upregulated TMPRSS2 at the mRNA level in treated versus control female and male mice, respectively (Figures 5K, L). Finally, the IF staining on sections obtained from the lung tissues of control and treated mice

supported the enhanced expression of TMPRSS2 following treatment with dexamethasone (Figures 5M-O). Thus, these observations confirmed that dexamethasone enhances ACE2 and TMPRSS2 expression in the lung tissues of adult mice.

Pre-treatment with dexamethasone enhances susceptibility of NHBE and Vero E6 cells to infection with pseudo SARS-CoV-2

Considering the upregulation of ACE2 and TMPRSS2 in the lung tissues of mice following treatment with dexamethasone, we decided to recapitulate these observations in NHBE cells, as a proof of concept. We found that overnight treatment with dexamethasone (1 µg/ml), significantly increased the expression of ACE2 and TMPRSS2 in NHBE cells (Figures 6A-D). This observation was similar to that seen in animal studies (Figures 4 and 5). As anticipated, upregulation of SARS-CoV-2 receptor and co-receptor, not only increased the proportion of infected NHBE cells to pseudo SARS-CoV-2 infection (Figures 6E, F) but also significantly enhanced the intensity of infection in these cells (Figures 6G, H). This was further confirmed by microscopic examinations (Figures 6I-K). Wells without treatment served as controls. In addition, we performed similar studies on Vero E6 cells to reconfirm and validate our observations in another cell line. Vero E6 cells are widely used for SARS-CoV-2 infection assays *in vitro* (33). We observed that overnight treatment of Vero E6 cells with dexamethasone (0.5 and 1 µg/ml) significantly increased their susceptibility to infection in a dose dependent manner when exposed to pseudo SARS-CoV-2 and analyzed by flow cytometer (Figures 7A, B). Also, the intensity of infection was more pronounced in dexamethasone treated versus untreated Vero E6 cells in a dose dependent manner (Figures 7C, D). Finally, our microscopic examinations further confirmed these observations (Figures 7E-J). Therefore, these results imply that dexamethasone increases NHBE and Vero E6 cells infectivity to SARS-CoV-2 *via* the upregulation of ACE2 and TMPRSS2.

Discussion

Here, we report several notable findings in this basic science study with important clinical implications. First, we find that TMPRSS2 is dynamically and developmentally regulated by age. However, ACE2 is highly expressed at the gene and protein levels in the very young and it is not developmentally regulated in mice. Our results are consistent with an earlier study showing greater expression of ACE2 in the lung of young Rhesus monkeys and mice (21, 34). However, our findings contradict another report showing continued expression of ACE2 in the lung as mice age (35). However, this study only analyzed the expression of ACE2 in the lungs of 2-month-old versus older animals (35). In fact, these findings are consistent with our observations except that this group did not investigate the expression of ACE2 in neonatal mice. Similarly, others have identified increased ACE2 expression by age at the gene and protein levels in human lungs (20). However, these results were based on the expression levels of ACE2 in the lungs of older versus younger adults (20). Our results suggest that differential ACE2 expression may contribute to increased or decreased susceptibility to SARS-CoV-2 infection. The second interesting finding of our study is our observation that ACE2 is highly expressed at the gene and protein levels in the lungs of older female mice compared to their male counterparts. Although ACE2 expression is associated with cellular susceptibility to SARS-CoV-2 infection (7, 29), lower tissue levels are correlated with worse clinical outcomes and lung injury (36).Greater ACE2 expression could enhance viral entry at the cellular level, but may provide protection at the organ/tissue level. It is worth mentioning that despite higher expression of ACE2 in the lung of older female mice, TMPRSS2 expression was unchanged. This suggests that females might not be at a greater risk of infection because of the unchanged expression of the co-receptor in their lungs. Instead, this in part may explain why women are at lower risk of complications and mortality associated with COVID-19 infection (18, 37). An additional observation of our study was changes in ACE2 and TMPRSS2 expression in the heart tissues of neonatal versus older mice. We observed a higher expression of ACE2 in the heart tissues of neonatal that older animals. This may increase the likelihood of infection with SARS-CoV-2, as suggested by others, in the lung (38). Notably, in the present study, we found very low to the undetectable levels of TMPRSS2 in the heart tissues, suggesting the inability of SARS-CoV-2 to enter the myocardium. Our results concur with human studies detecting relatively very low TMPRSS2 expression in myocardium (39, 40). This implies that although ACE2 is highly expressed in the heart, without the presence of a co-receptor (e.g. TMPRSS2), myocardial infectivity of SARS-CoV-2 is low. Emerging data indicate an association between COVID-19 and myocarditis (41, 42). Intriguingly, the association between COVID-19 and myocarditis has been reported to be the highest among those younger than 16 years (43). Although causality is unknown, we suggest that higher expression of ACE2 in the heart of the young could partially explain the observed age-related association.

Another finding was the effects of dexamethasone on ACE2 and TMPRSS2 expression in tissues of neonatal and older mice. Strikingly, our results revealed that dexamethasone treatment enhances the expression of ACE2 and TMPRSS2 at the gene and protein levels in the lung tissues of mice regardless of their age/sex. Based on these observations we speculate that dexamethasone may exhibit the same effects in human subjects resulting in enhanced susceptibility to SARS-CoV-2 infection. This hypothesis was further confirmed when we noted

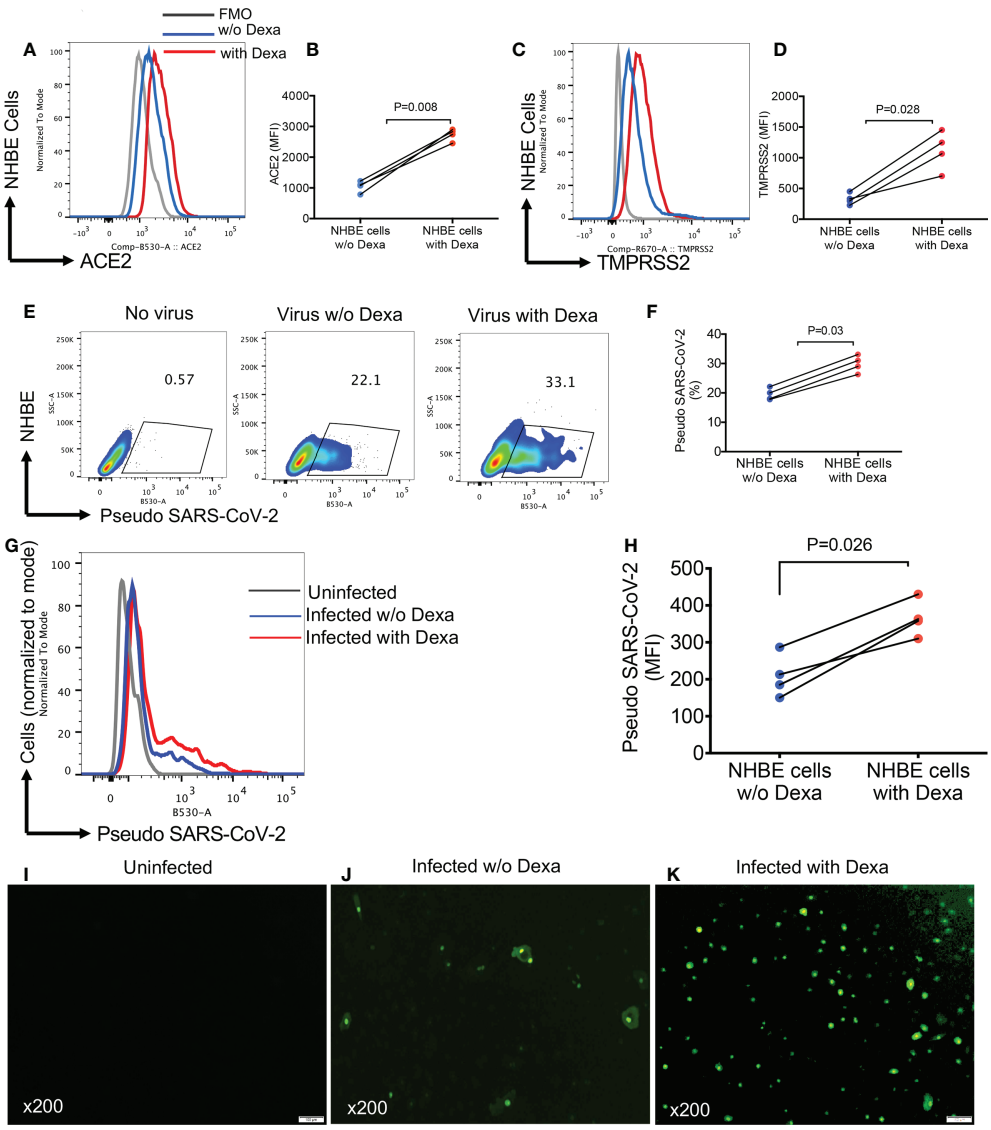

FIGURE 6
Dexamethasone treatment enhances the infectivity of NHBE cells to Pseudo SARS-CoV-2 infection. **(A)** Representative plots, and **(B)** cumulative data of ACE2 expression as measured by the mean fluorescence intensity (MFI) in NHBE cells following overnight treatment with (0.5 μg/ml) or without dexamethasone treatment. **(C)** Representative plots, and **(D)** cumulative data of TMPRSS2 expression (MFI) in NHBE cells following overnight treatment with (0.5 μg/ml) or without dexamethasone treatment. **(E)** Representative flow cytometry plots, and **(F)** cumulative data showing percentages of NHBE cells untreated or treated with dexamethasone (0.5 μg/ml) and infected with the pseudo SARS-CoV-2. **(G)** Representative flow cytometry histogram plots, and **(H)** cumulative data showing the intensity [the mean fluorescence intensity (MFI)] of pseudo SARS-CoV-2 infection in NHBE cells untreated or treated with dexamethasone (0.5 μg/ml). **(I)** Representative image of uninfected NHBE cells. **(J)** Representative images of dexamethasone untreated but infected NHBE cells with pseudo SARS-CoV-2. **(K)** Representative images of dexamethasone treated (0.5 μg/ml) and infected NHBE cells with pseudo SARS-CoV-2, magnification x200. Error bars indicate mean ± SEM from at least two independent experiments. Each dot represents results from a single experiment. Dexamethasone (Dexa), w/o (without). Fluorescence minus one (FMO).

significantly increased ACE2 and TMPRSS2 expression in NHBE cells upon treatment with dexamethasone. This was resulted in enhanced infectivity of NHBE cells with pseudo-SARS-CoV-2 once pre-treated with dexamethasone *in vitro*. However, these are hypotheses generated based on our intriguing animal and *in vitro* results, which require validation in human subjects.

Moreover, viral entry represents just one of several elements involved in SARS-CoV-2 infection, each of which involves different genes and pathways that may potentially be influenced by dexamethasone in the lung/heart and elsewhere. As such, whether dexamethasone modulates other genes and pathways associated with viral replication/infection merits further investigation.

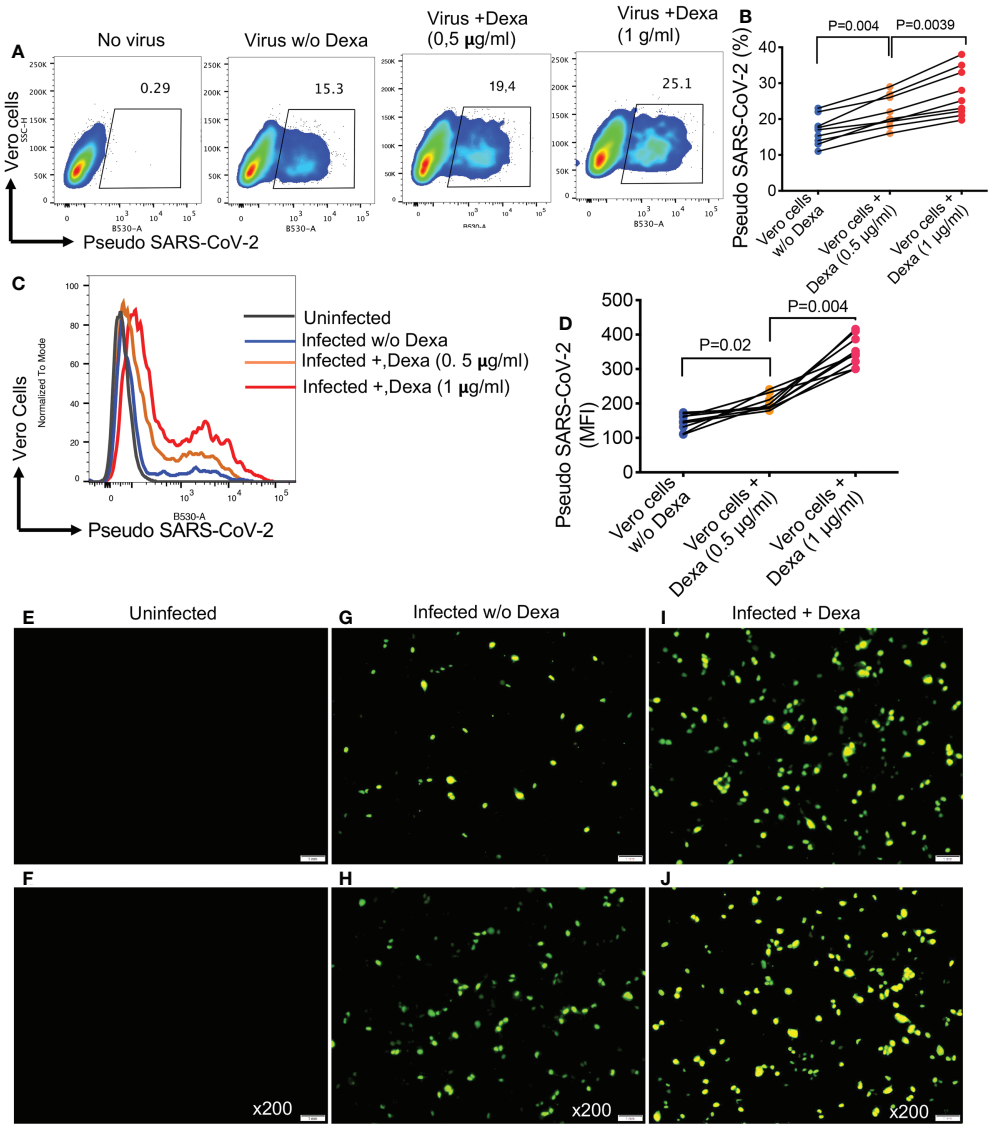

FIGURE 7
Dexamethasone treatment enhances the infectivity of Vero E6 cells to Pseudo SARS-CoV-2 infection. **(A)** Representative flow cytometry plots, and **(B)** cumulative data showing percentages of Vero E6 cells untreated or treated with dexamethasone (0.5 µg/ml and 1 µg/ml) and infected with the pseudo SARS-CoV-2. **(C)** Representative flow cytometry histogram plots, and **(D)** cumulative data showing the MFI of pseudo SARS-CoV-2 infection in Vero E6 cells untreated or treated with dexamethasone (0.5 µg/ml and 1 µg/ml). **(E, F)** Representative images of uninfected Vero E6 cells. **(G, H)** Representative images of dexamethasone untreated but infected Vero E6 cells with pseudo SARS-CoV-2. **(I, J)** Representative images of dexamethasone treated and infected Vero E6 cells with pseudo SARS-CoV-2, magnification x200. Error bars indicate mean ± SEM from at least two independent experiments. Each dot represents results from a single experiment. Dexamethasone (Dexa), Vero E6 cells (Vero cells), virus (pseudo SARS-CoV-2).

Another important discovery of this study is the very low expression of TMPRSS2 in both lungs and heart tissues of neonatal compared to older mice. Similar to our results, very low expression of TMPRSS2 has been reported in the lungs of human infants and prenatal mice (6). Given the very low expression of TMPRSS2 in neonatal mice and humans, this may explain why neonates are relatively protected against infection with SARS-CoV-2. Furthermore, our observations support the notion of developmental regulation of TMPRSS2 (6), which may present a mechanistic reason for the observed relative protection of infants and children from the severe form of COVID-19 disease. Moreover, the tightly regulated neonatal immune system (3, 44, 45) may prevent hyper-immune activation and collateral tissue damage associated with COVID-19 pathogenesis (46).

Lastly, our results provide a potential mechanistic explanation for why COVID-19 patients treated with dexamethasone may have different clinical outcomes. It is reported that dexamethasone provides benefits only to COVID-19 patients receiving oxygen therapy and/or invasive mechanical ventilation (23). These patients are in the inflammatory phase of the disease by the time they require respiratory support. This suggests that at this stage COVID-19 disease is dominated by immunopathological alterations and not by active viral replication. Therefore, we speculate that dexamethasone treatment at this phase of the disease may upregulate ACE2 and TMPRSS2 expression, and subsequently counterbalance the increase in RAS activity by converting pro-inflammatory angiotensin II to anti-inflammatory angiotensin (40). Conversely, our data suggest that dexamethasone treatment in the early stage of COVID-19 may be more harmful than helpful. Treatment given at a time when viral entry and replication are high can be detrimental as the upregulation of ACE2 and TMPRSS2 may enhance infection. In support of this concept, slower clearance of virus has been reported in individuals with influenza, SARS, and the Middle East respiratory syndrome (MERS) treated with systemic glucocorticoids (47–50).

Another explanation for the differential effects of dexamethasone on SARS versus SARS-CoV-2 might be related to differential viral replication phases. In contrary to SARS, in which viral replication peaks in the second week of disease (51), viral replication in SARS-CoV-2 is more pronounced early in the disease and falls rapidly thereafter (52–54). Therefore, our results suggest that dexamethasone may be beneficial only at the right time and in the right patient. We, however, caution against extrapolating these results to COVID-19 patients with other underlying conditions and/or patients with other viral respiratory infections.

The observed increase in expression of ACE2 and TMPRSS2 due to dexamethasone suggests that individuals receiving this treatment for other clinical reasons may be more susceptible to SARS-CoV-2 infection, however, this merits further investigation. Dexamethasone is one of the WHO essential medicines and is readily available, however, our results support its use in the later phase of COVID-19 when viral replication is low and inflammation high. However, in addition to its well-defined anti-inflammatory properties (25), our study provides novel evidence that treatment with dexamethasone can upregulate the expression of ACE2 and TMPRSS2 in lung and heart tissues. Therefore, giving dexamethasone at a time when viral replication is high and viral control is essential could be harmful to the patient.

We are aware of multiple study limitations such as the lack of study on human tissues. Although our studies support the upregulation of ACE2 and TMPRSS2, we were unable to examine the precise effects of dexamethasone treatment on ACE2 and TMPRSS2 localization and different immune/non-immune cells since our studies were performed on bulk tissue. Because dexamethasone may exhibit differential effects on ACE2/TMPRSS2 depending on the target cell (e.g. enhancing the maturation of erythroid progenitors) (29, 55, 56). Also, we did not investigate mechanistically how dexamethasone influences the upregulation of ACE2 and TMPRSS2. Thus, continued investigation into the mechanism associated with enhanced upregulation of ACE2 and TMPRSS2 in the lungs and hearts may shed light on a potential therapeutic approach focused on the modulation of ACE2 and TMPRSS2 expression. Another element that should be taken into consideration is the duration of treatment. Although we examined the effects of dexamethasone following two consecutive days of treatment, human subjects normally receive this medication for a longer period of time (the standard course is 10 days), which may exhibit more pronounced effects. It is also important to acknowledge that the administered dexamethasone dose in animals was higher than that prescribed in COVID-19 patients. However, steroids are usually administered intravenously (IV) in COVID patients, resulting in the highest bioavailability and predictable drug levels. Due to the impracticality in neonatal mice, we administered dexamethasone into animals *via* the IP route. It is well documented that the rate of absorption is much lower by IP versus the IV routes. The rate of absorption after IP injection can be 50% to 25% lower compared with IV administration (57, 58). Another factor that should be taken into consideration is how the administered dexamethasone from the peritoneal cavity gets absorbed. It may face one of two pathways to reach the systemic circulation. It is absorbed through the visceral peritoneum, the mesentery and omentum and is drained into the portal circulation, or the compound may bypass the liver if absorbed through the parietal peritoneum and lymphatics (59). As such it is impossible to assess how much of the drug undergoes hepatic metabolism. Perhaps the systemic dexamethasone bioavailability might be comparable in treated animals in our study to patients, or very close. In support of this hypothesis, we observed significant increase in ACE2 and TMPRSS2 expression levels in NHBE cells following a single treatment with lower dexamethasone concentration (1 μg/ml). Mice are not normally susceptible to SARS-CoV-2 infection and we were unable to conduct such studies in other animal models. Such studies are needed to better investigate the role of dexamethasone *in vivo*. Recently, the effects of dexamethasone treatment in a humanized mouse model of SARS-CoV-2 infection was examined (60). The authors concluded that the initiation of dexamethasone at day 3 post-infection when the viral load is still high was associated with moribund but the same treatment starting at day 7 post infection when the viral load had declined was protective (60). Although the impact of dexamethasone treatment on ACE2 and TMPRSS2 was not examined, it suggests that upregulation of ACE2/TMPRSS2 might be a contributing factor to these observations.

It is intriguing to question whether dexamethasone or other glucocorticoids modulate and upregulate the expression of

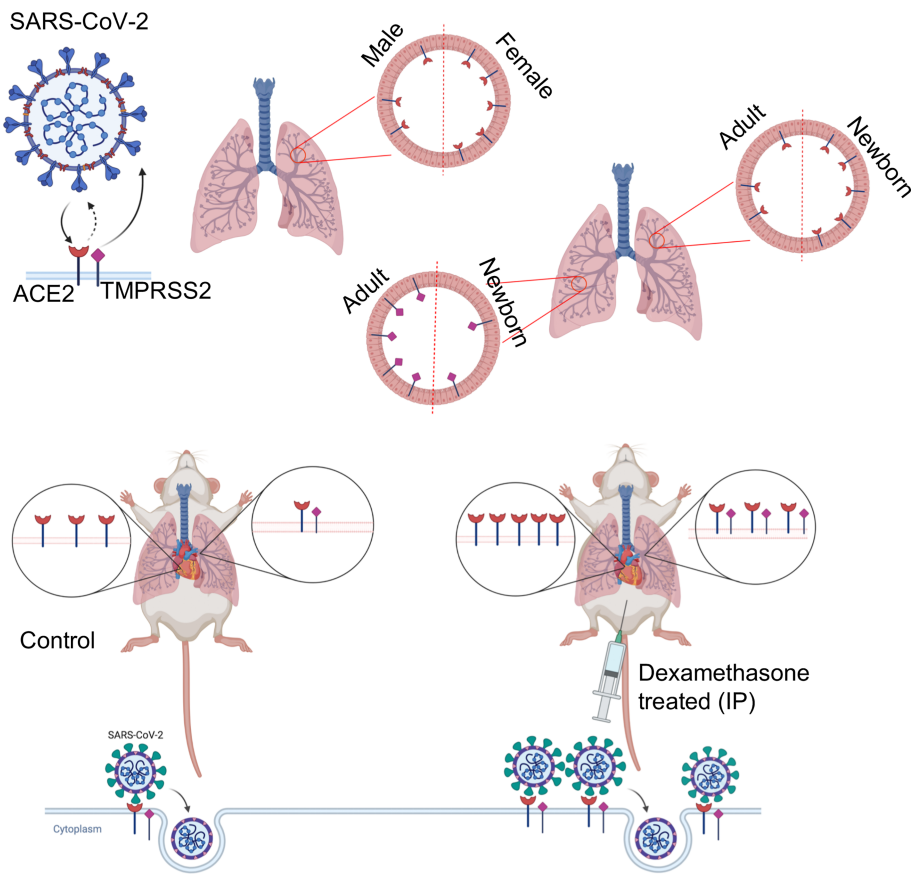

FIGURE 8
The visual summary of the study.

ACE2 in the cilia of the nasal and upper respiratory tract the same as the lung and heart tissues. If this is the case, individuals with other underlying conditions, even children who are on dexamethasone, may be at higher risk of SARS-CoV-2 infection. The higher expression of ACE2 in neonatal hearts and upregulation of ACE2 in the heart of neonatal versus adult mice may suggest a higher affinity of the spike protein for the heart tissues of infants, in particular, when on dexamethasone. However, it's unclear whether other glucocorticoids exhibit similar effects on ACE2 and TMPRSS2 expression in tissues. Moreover, the expression of ACE2 and TMPRSS2 is not restricted to the lung and heart tissues but other organs (e.g. liver and kidney) and different cells (55, 56). Therefore, examining the broader effects of dexamethasone treatment on the expression levels of ACE2 and TMPRSS2 in immune and non-immune cells merits further investigation.

In conclusion, we found that ACE2 expression in the lung and heart varies in relation to sex and age. The identification of developmental regulation of TMPRSS2 expression could partially explain the differential susceptibility of neonates to SARS-CoV-2 infection. Moreover, we reveal *in vivo* evidence that dexamethasone enhances the expression of ACE2 and TMPRSS2 (Figure 8), and subsequently the infectivity of NHBE and Vero E6 cells to pseudo SARS-CoV-2. These observations suggest that this medication might exhibit differential therapeutic effects depending on the phase of COVID-19. Finally, our results suggest that dexamethasone treatment for other clinical purposes may enhance the susceptibility of those patients to SARS-CoV-2 infection.

Data availability statement

The original contributions presented in the study are included in the article/supplementary material. Further inquiries can be directed to the corresponding author.

Ethics statement

The animal study was reviewed and approved by the research ethics boards at the University of Alberta that approved these studies with the protocol # AUP0001021.

Author contributions

ShS performed PCR, flow cytometry related, and *in vitro* infection studies. OO performed western blotting and flow cytometry studies. SS assisted in *in vitro* infection studies. MO and WS provided resources and inputs in experimental design. SE conceptualized the study, designed the study approach, provided resources, supervised the study, designed the figures and wrote the manuscript. All authors contributed to the article and approved the submitted version.

Funding

This work was supported by the Canadian Institutes of Health Research (CIHR, grant #453061) and a LI Ka Shing Institute of Virology Innovation grant (both to SE).

Acknowledgments

The authors would like to thank the University of Alberta, Faculty of Medicine and Dentistry's Flow cytometry facility.

Conflict of interest

The authors declare that the research was conducted in the absence of any commercial or financial relationships that could be construed as a potential conflict of interest.

Publisher's note

All claims expressed in this article are solely those of the authors and do not necessarily represent those of their affiliated organizations, or those of the publisher, the editors and the reviewers. Any product that may be evaluated in this article, or claim that may be made by its manufacturer, is not guaranteed or endorsed by the publisher.

References

1. Wu ZY, McGoogan JM. Characteristics of and important lessons from the coronavirus disease 2019 (COVID-19) outbreak in China summary of a report of 72 314 cases from the Chinese center for disease control and prevention. *Jama-J Am Med Assoc* (2020) 323(13):1239–42. doi: 10.1001/jama.2020.2648

2. Bialek S, Gierke R, Hughes M, McNamara LA, Pilishvili T, Skoff T, et al. Coronavirus disease 2019 in children - united states, February 12-April 2, 2020. *Mmwr-Morbid Mortal W.* (2020) 69(14):422–6. doi: 10.15585/mmwr.mm6914e4

3. Elahi S. Neonatal and children's immune system and COVID-19: Biased immune tolerance versus resistance strategy. *J Immunol* (2020) 205(8):1990–7. doi: 10.4049/jimmunol.2000710

4. Dong YY, Mo X, Hu YB, Qi X, Jiang F, Jiang ZY, et al. Epidemiology of COVID-19 among children in China. *Pediatrics* (2020) 145(6). doi: 10.1542/peds.2020-0702

5. Fidel PLJr., Noverr MC. Could an unrelated live attenuated vaccine serve as a preventive measure to dampen septic inflammation associated with COVID-19 infection? *mBio* (2020) 11(3):e00907-20. doi: 10.1128/mBio.00907-20

6. Schuler BA, Habermann AC, Plosa EJ, Taylor CJ, Jetter C, Negretti NM, et al. Age-determined expression of priming protease TMPRSS2 and localization of SARS-CoV-2 in lung epithelium. *J Clin Invest* (2021) 131(1):e140766. doi: 10.1172/JCI140766

7. Hoffmann M, Kleine-Weber H, Schroeder S, Kruger N, Herrler T, Erichsen S, et al. SARS-CoV-2 cell entry depends on ACE2 and TMPRSS2 and is blocked by a clinically proven protease inhibitor. *Cell* (2020) 181(2):271–+. doi: 10.1016/j.cell.2020.02.052

8. Letko M, Marzi A, Munster V. Functional assessment of cell entry and receptor usage for SARS-CoV-2 and other lineage b betacoronaviruses. *Nat Microbiol* (2020) 5(4):562–9. doi: 10.1038/s41564-020-0688-y

9. Kuba K, Imai Y, Rao S, Gao H, Guo F, Guan B, et al. A crucial role of angiotensin converting enzyme 2 (ACE2) in SARS coronavirus-induced lung injury. *Nat Med* (2005) 11(8):875–9. doi: 10.1038/nm1267

10. Sodhi CP, Wohlford-Lenane C, Yamaguchi Y, Prindle T, Fulton WB, Wang S, et al. Attenuation of pulmonary ACE2 activity impairs inactivation of des-Arg(9) bradykinin/BKB1R axis and facilitates LPS-induced neutrophil infiltration. *Am J Physiol Lung Cell Mol Physiol* (2018) 314(1):L17–31. doi: 10.1152/ajplung.00498.2016

11. Gu H, Xie Z, Li T, Zhang S, Lai C, Zhu P, et al. Angiotensin-converting enzyme 2 inhibits lung injury induced by respiratory syncytial virus. *Sci Rep* (2016) 6:19840. doi: 10.1038/srep19840

12. Yang P, Gu H, Zhao Z, Wang W, Cao B, Lai C, et al. Angiotensin-converting enzyme 2 (ACE2) mediates influenza H7N9 virus-induced acute lung injury. *Sci Rep* (2014) 4:7027. doi: 10.1038/srep07027

13. Lu J, Sun PD. High affinity binding of SARS-CoV-2 spike protein enhances ACE2 carboxypeptidase activity. *J Biol Chem* (2020) 295(52):18579–88. doi: 10.1074/jbc.RA120.015303

14. Hou YJ, Okuda K, Edwards CE, Martinez DR, Asakura T, Dinnon KH3rd, et al. SARS-CoV-2 reverse genetics reveals a variable infection gradient in the respiratory tract. *Cell* (2020) 182(2):429–46 e14. doi: 10.1016/j.cell.2020.05.042

15. Nicin L, Abplanalp WT, Mellentin H, Kattih B, Tombor L, John D, et al. Cell type-specific expression of the putative SARS-CoV-2 receptor ACE2 in human hearts. *Eur Heart J* (2020) 41(19):1804–6. doi: 10.1093/eurheartj/ehaa311

16. Daniels CJ, Rajpal S, Greenshields JT, Rosenthal GL, Chung EH, Terrin M, et al. Prevalence of clinical and subclinical myocarditis in competitive athletes with recent SARS-CoV-2 infection: Results from the big ten COVID-19 cardiac registry. *JAMA Cardiol* (2021) 6(9):1078–87. doi: 10.1001/jamacardio.2021.2065

17. Lindner D, Fitzek A, Brauninger H, Aleshcheva G, Edler C, Meissner K, et al. Association of cardiac infection with SARS-CoV-2 in confirmed COVID-19 autopsy cases. *JAMA Cardiol* (2020) 5(11):1281–5. doi: 10.1001/jamacardio.2020.3551

18. Guan WJ, Ni ZY, Hu Y, Liang WH, Ou CQ, He JX, et al. Clinical characteristics of coronavirus disease 2019 in China. *New Engl J Med* (2020) 382:1708–20. doi: 10.1056/NEJMoa2002032

19. Smith JC, Sausville EL, Girish V, Yuan ML, Vasudevan A, John KM, et al. Cigarette smoke exposure and inflammatory signaling increase the expression of the SARS-CoV-2 receptor ACE2 in the respiratory tract. *Dev Cell* (2020) 53(5):514–29 e3. doi: 10.1016/j.devcel.2020.05.012

20. Baker SA, Kwok S, Berry GJ, Montine TJ. Angiotensin-converting enzyme 2 (ACE2) expression increases with age in patients requiring mechanical ventilation. *PloS One* (2021) 16(2):e0247060. doi: 10.1371/journal.pone.0247060

21. Xie X, Chen J, Wang X, Zhang F, Liu Y. Age- and gender-related difference of ACE2 expression in rat lung. *Life Sci* (2006) 78(19):2166–71. doi: 10.1016/j.lfs.2006.09.028

22. Steinman JB, Lum FM, Ho PP, Kaminski N, Steinman L. Reduced development of COVID-19 in children reveals molecular checkpoints gating pathogenesis illuminating potential therapeutics. *Proc Natl Acad Sci United States America.* (2020) 117(40):24620–6. doi: 10.1073/pnas.2012358117

23. Group RC, Horby P, Lim WS, Emberson JR, Mafham M, Bell JL, et al. Dexamethasone in hospitalized patients with covid-19. *New Engl J Med* (2021) 384 (8):693–704. doi: 10.1056/NEJMoa2021436

24. Sterne JAC, Murthy S, Diaz JV, Slutsky AS, Villar J, Angus DC, et al. Association between administration of systemic corticosteroids and mortality among critically ill patients with COVID-19 a meta-analysis. *Jama-J Am Med Assoc* (2020) 324(13):1330–41. doi: 10.1001/jama.2020.17023

25. Okoye IS, Xu L, Walker J, Elahi S. The glucocorticoids prednisone and dexamethasone differentially modulate T cell function in response to anti-PD-1 and anti-CTLA-4 immune checkpoint blockade. *Cancer Immunol Immunother.* (2020) 69(8):1423–36. doi: 10.1007/s00262-020-02555-2

26. Elahi S, Shahbaz S, Houston S. Selective upregulation of CTLA-4 on CD8+ T cells restricted by HLA-B*35Px renders them to an exhausted phenotype in HIV-1 infection. *PloS Pathog* (2020) 16(8):e1008696. doi: 10.1371/journal.ppat.1008696

27. Shahbaz S, Dunsmore G, Koleva P, Xu L, Houston S, Elahi S. Galectin-9 and VISTA expression define terminally exhausted T cells in HIV-1 infection. *J Immunol* (2020) 204(9):2474–91. doi: 10.4049/jimmunol.1901481

28. Shahbaz S, Jovel J, Elahi S. Differential transcriptional and functional properties of regulatory T cells in HIV-infected individuals on antiretroviral therapy and long-term non-progressors. *Clin Transl Immunol* (2021) 10(5): e1289. doi: 10.1002/cti2.1289

29. Shahbaz S, Xu L, Osman M, Sligl W, Shields J, Joyce M, et al. Erythroid precursors and progenitors suppress adaptive immunity and get invaded by SARS-CoV-2. *Stem Cell Rep* (2021) 16(5):1165–81. doi: 10.1016/j.stemcr.2021.04.001

30. Shahbaz S, Xu L, Sligl W, Osman M, Bozorgmehr N, Mashhouri S, et al. The quality of SARS-CoV-2-Specific T cell functions differs in patients with Mild/Moderate versus severe disease, and T cells expressing coinhibitory receptors are highly activated. *J Immunol* (2021) 207(4):1099–111. doi: 10.4049/jimmunol.2100446

31. Kim TS, Heinlein C, Hackman RC, Nelson PS. Phenotypic analysis of mice lacking the Tmprss2-encoded protease. *Mol Cell Biol* (2006) 26(3):965–75. doi: 10.1128/MCB.26.3.965-975.2006

32. Gagliardi MC, Tieri P, Ortona E, Ruggieri A. ACE2 expression and sex disparity in COVID-19. *Cell Death Discovery* (2020) 6:37. doi: 10.1038/s41420-020-0276-1

33. Essaidi-Laziosi M, Perez Rodriguez FJ, Hulo N, Jacquerioz F, Kaiser L, Eckerle I. Estimating clinical SARS-CoV-2 infectiousness in vero E6 and primary airway epithelial cells. *Lancet Microbe* (2021) 2(11):e571. doi: 10.1016/S2666-5247(21)00216-0

34. Cao B, Zhang L, Liu H, Ma S, Mi K. The dynamic expression of potential mediators of severe acute respiratory syndrome coronavirus 2 cellular entry in fetal, neonatal, and adult rhesus monkeys. *Front Genet* (2020) 11:607479. doi: 10.3389/fgene.2020.607479

35. Yee M, David Cohen E, Haak J, Dylag AM, O'Reilly MA. Neonatal hyperoxia enhances age-dependent expression of SARS-CoV-2 receptors in mice. *Sci Rep* (2020) 10(1):22401. doi: 10.1038/s41598-020-79595-2

36. Zhang HB, Penninger JM, Li YM, Zhong NS, Slutsky AS. Angiotensin-converting enzyme 2 (ACE2) as a SARS-CoV-2 receptor: molecular mechanisms and potential therapeutic target. *Intens Care Med* (2020) 46(4):586–90. doi: 10.1007/s00134-020-05985-9

37. Chen G, Wu D, Guo W, Cao Y, Huang D, Wang H, et al. Clinical and immunological features of severe and moderate coronavirus disease 2019. *J Clin Invest* (2020) 130(5):2620–9. doi: 10.1172/JCI137244

38. Inde Z, Croker BA, Yapp C, Joshi GN, Spetz J, Fraser C, et al. Age-dependent regulation of SARS-CoV-2 cell entry genes and cell death programs correlates with COVID-19 severity. *Sci Adv* (2021) 7(34):eabf8609. doi: 10.1126/sciadv.abf8609

39. Bristow MR, Zisman LS, Altman NL, Gilbert EM, Lowes BD, Minobe WA, et al. Dynamic regulation of SARS-Cov-2 binding and cell entry mechanisms in remodeled human ventricular myocardium. *Jacc-Basic Transl Sc.* (2020) 5(9):871–83. doi: 10.1016/j.jacbts.2020.06.007

40. Lin HB, Liu PP. COVID-19 and the heart: ACE2 level and the company it keeps hold the key. *JACC Basic Transl Sci* (2020) 5(9):884–7. doi: 10.1016/j.jacbts.2020.07.005

41. Murk W, Gierada M, Fralick M, Weckstein A, Klesh R, Rassen JA. Diagnosis-wide analysis of COVID-19 complications: an exposure-crossover study. *CMAJ* (2021) 193(1):E10–E8. doi: 10.1503/cmaj.201686

42. Rathore SS, Rojas GA, Sondhi M, Pothuru S, Pydi R, Kancherla N, et al. Myocarditis associated with covid-19 disease: A systematic review of published case reports and case series. *Int J Clin Pract* (2021) 75(11):e14470. doi: 10.1111/ijcp.14470

43. Boehmer TK, Kompaniyets L, Lavery AM, Hsu J, Ko JY, Yusuf H, et al. Association between COVID-19 and myocarditis using hospital-based administrative data - united states, march 2020-January 2021. *Mmwr-Morbid Mortal W.* (2021) 70(35):1228–32. doi: 10.15585/mmwr.mm7035e5

44. Elahi S, Ertelt JM, Kinder JM, Jiang TT, Zhang X, Xin L, et al. Immunosuppressive CD71+ erythroid cells compromise neonatal host defence against infection. *Nature* (2013) 504(7478):158–62. doi: 10.1038/nature12675

45. Elahi S, Vega-López MA, Herman-Miguel V, Ramírez-Estudillo C, Mancilla-Ramírez J, Motyka B, et al. CD71+ erythroid cells in human neonates exhibit immunosuppressive properties and compromise immune response against systemic infection in neonatal mice. *Front Immunol* (2020) 11(3076). doi: 10.3389/fimmu.2020.597433

46. Bozorgmehr N, Mashhouri S, Perez Rosero E, Xu L, Shahbaz S, Sligl W, et al. Galectin-9, a player in cytokine release syndrome and a surrogate diagnostic biomarker in SARS-CoV-2 infection. *mBio* (2021) 12(3):e00384-21. doi: 10.1128/mBio.00384-21

47. Arabi YM, Mandourah Y, Al-Hameed F, Sindi AA, Almekhlafi GA, Hussein MA, et al. Corticosteroid therapy for critically ill patients with middle East respiratory syndrome. *Am J Respir Crit Care Med* (2018) 197(6):757–67. doi: 10.1164/rccm.201706-1172OC

48. Lansbury LE, Rodrigo C, Leonardi-Bee J, Nguyen-Van-Tam J, Shen Lim W. Corticosteroids as adjunctive therapy in the treatment of influenza: An updated cochrane systematic review and meta-analysis. *Crit Care Med* (2020) 48(2):E98–E106. doi: 10.1097/CCM.0000000000004093

49. Lee N, Allen Chan KC, Hui DS, Ng EK, Wu A, Chiu RW, et al. Effects of early corticosteroid treatment on plasma SARS-associated coronavirus RNA concentrations in adult patients. *J Clin Virol* (2004) 31(4):304–9. doi: 10.1016/j.jcv.2004.07.006

50. Stockman LJ, Bellamy R, Garner P. SARS: Systematic review of treatment effects. *PloS Med* (2006) 3(9):1525–31. doi: 10.1371/journal.pmed.0030343

51. Cheng PK, Wong DA, Tong LK, Ip SM, Lo AC, Lau CS, et al. Viral shedding patterns of coronavirus in patients with probable severe acute respiratory syndrome. *Lancet* (2004) 363(9422):1699–700. doi: 10.1016/S0140-6736(04)16255-7

52. He X, Lau EHY, Wu P, Deng X, Wang J, Hao X, et al. Temporal dynamics in viral shedding and transmissibility of COVID-19. *Nat Med* (2020) 26(5):672–5. doi: 10.1038/s41591-020-0869-5

53. To KK, Tsang OT, Leung WS, Tam AR, Wu TC, Lung DC, et al. Temporal profiles of viral load in posterior oropharyngeal saliva samples and serum antibody responses during infection by SARS-CoV-2: an observational cohort study. *Lancet Infect Dis* (2020) 20(5):565–74. doi: 10.1016/S1473-3099(20)30196-1

54. Wolfel R, Corman VM, Guggemos W, Seilmaier M, Zange S, Muller MA, et al. Virological assessment of hospitalized patients with COVID-2019. *Nature* (2020) 581(7809):465–9. doi: 10.1038/s41586-020-2196-x

55. Elahi S. Hematopoietic responses to SARS-CoV-2 infection. *Cell Mol Life Sci CMLS.* (2022) 79(3):187. doi: 10.1007/s00018-022-04220-6

56. Saito S, Shahbaz S, Sligl W, Osman M, Tyrrell DL, Elahi S. Differential impact of SARS-CoV-2 isolates, namely, the wuhan strain, delta, and omicron variants on erythropoiesis. *Microbiol Spectr.* (2022) 10(4):e0173022. doi: 10.1128/spectrum.01730-22

57. Durk MR, Deshmukh G, Valle N, Ding X, Liederer BM, Liu XR. Use of subcutaneous and intraperitoneal administration methods to facilitate cassette dosing in microdialysis studies in rats. *Drug Metab Dispos* (2018) 46(7):964–9. doi: 10.1124/dmd.118.080697

58. Shimada T, Nomura M, Yokogawa K, Endo Y, Sasaki T, Miyamoto K, et al. Pharmacokinetic advantage of intraperitoneal injection of docetaxel in the treatment for peritoneal dissemination of cancer in mice. *J Pharm Pharmacol* (2005) 57(2):177–81. doi: 10.1211/0022357055380

59. Al Shoyaib A, Archie SR, Karamyan VT. Intraperitoneal route of drug administration: Should it be used in experimental animal studies? *Pharm Res-Dordr.* (2020) 37(1):12. doi: 10.1007/s11095-019-2745-x

60. Sefik E, Israelow B, Mirza H, Zhao J, Qu R, Kaffe E, et al. A humanized mouse model of chronic COVID-19. *Nat Biotechnol* (2022) 40(6):906–20. doi: 10.1038/s41587-021-01155-4

frontiers | Frontiers in Immunology

TYPE Original Research
PUBLISHED 09 November 2022
DOI 10.3389/fimmu.2022.968317

Check for updates

OPEN ACCESS

EDITED BY
E. Marion Schneider,
University of Ulm, Germany

REVIEWED BY
Stephen Crooke,
Centers for Disease Control and Prevention (CDC), United States
Nicole Jane Moreland,
The University of Auckland, New Zealand

*CORRESPONDENCE
Alice Halliday
alice.halliday@bristol.ac.uk

†These authors have contributed equally to this work and share last authorship

SPECIALTY SECTION
This article was submitted to Viral Immunology, a section of the journal Frontiers in Immunology

RECEIVED 13 June 2022
ACCEPTED 30 August 2022
PUBLISHED 09 November 2022

CITATION
Halliday A, Long AE, Baum HE, Thomas AC, Shelley KL, Oliver E, Gupta K, Francis O, Williamson MK, Di Bartolo N, Randell MJ, Ben-Khoud Y, Kelland I, Mortimer G, Ball O, Plumptre C, Chandler K, Obst U, Secchi M, Piemonti L, Lampasona V, Smith J, Gregorova M, Knezevic L, Metz J, Barr R, Morales-Aza B, Oliver J, Collingwood L, Hitchings B, Ring S, Wooldridge L, Rivino L, Timpson N, McKernon J, Muir P, Hamilton F, Arnold D, Woolfson DN, Goenka A, Davidson AD, Toye AM, Berger I, Bailey M, Gillespie KM, Williams AJK and Finn A (2022) Development and evaluation of low-volume tests to detect and characterize antibodies to SARS-CoV-2.
Front. Immunol. 13:968317.
doi: 10.3389/fimmu.2022.968317

Development and evaluation of low-volume tests to detect and characterize antibodies to SARS-CoV-2

Alice Halliday[1*], Anna E. Long[2], Holly E. Baum[1,3], Amy C. Thomas[4,5], Kathryn L. Shelley[3,6], Elizabeth Oliver[1], Kapil Gupta[6], Ore Francis[4], Maia Kavanagh Williamson[1], Natalie Di Bartolo[6], Matthew J. Randell[2], Yassin Ben-Khoud[2], Ilana Kelland[2], Georgina Mortimer[2], Olivia Ball[2], Charlie Plumptre[1], Kyla Chandler[2], Ulrike Obst[3], Massimiliano Secchi[7], Lorenzo Piemonti[7], Vito Lampasona[7], Joyce Smith[1], Michaela Gregorova[1], Lea Knezevic[4], Jane Metz[1,8], Rachael Barr[1,8], Begonia Morales-Aza[1], Jennifer Oliver[5], Lucy Collingwood[5], Benjamin Hitchings[1], Susan Ring[5,9], Linda Wooldridge[4], Laura Rivino[1], Nicholas Timpson[5,9], Jorgen McKernon[10], Peter Muir[10], Fergus Hamilton[9,11], David Arnold[11], Derek N. Woolfson[3,6,12], Anu Goenka[1,8], Andrew D. Davidson[1], Ashley M. Toye[6,12,13], Imre Berger[3,6,12], Mick Bailey[4], Kathleen M. Gillespie[2], Alistair J. K. Williams[2†] and Adam Finn[1,5,8†]

[1]School of Cellular and Molecular Medicine, University of Bristol, Bristol, United Kingdom, [2]Diabetes and Metabolism, Bristol Medical School, University of Bristol, Bristol, United Kingdom, [3]School of Chemistry, University of Bristol, Bristol, United Kingdom, [4]Bristol Veterinary School, University of Bristol, Bristol, United Kingdom, [5]Population Health Sciences, Bristol Medical School, University of Bristol, Bristol, United Kingdom, [6]School of Biochemistry, Biomedical Sciences Building, University Walk, University of Bristol, Bristol, United Kingdom, [7]Diabetes Research Institute, IRCCS San Raffaele Scientific Institute, Milan, Italy, [8]Department of Paediatric Immunology and Infectious Diseases, Bristol Royal Hospital for Children, Bristol, United Kingdom, [9]MRC Integrative Epidemiology Unit at University of Bristol, Bristol, United Kingdom, [10]National Infection Service, UK Health Security Agency, Southmead Hospital, Bristol, United Kingdom, [11]Academic Respiratory Unit, Bristol Medical School, University of Bristol, Bristol, United Kingdom, [12]Bristol BioDesign Institute, University of Bristol, Bristol, United Kingdom, [13]Bristol Institute of Transfusion Sciences, NHS Blood and Transplant Filton, Bristol, United Kingdom

Low-volume antibody assays can be used to track SARS-CoV-2 infection rates in settings where active testing for virus is limited and remote sampling is optimal. We developed 12 ELISAs detecting total or antibody isotypes to SARS-CoV-2 nucleocapsid, spike protein or its receptor binding domain (RBD), 3 anti-RBD isotype specific luciferase immunoprecipitation system (LIPS) assays and a novel Spike-RBD bridging LIPS total-antibody assay. We utilized pre-pandemic (n=984) and confirmed/suspected recent COVID-19 sera taken pre-vaccination rollout in 2020 (n=269). Assays measuring total antibody

10.3389/fimmu.2022.968317

discriminated best between pre-pandemic and COVID-19 sera and were selected for diagnostic evaluation. In the blind evaluation, two of these assays (Spike Pan ELISA and Spike-RBD Bridging LIPS assay) demonstrated >97% specificity and >92% sensitivity for samples from COVID-19 patients taken >21 days post symptom onset or PCR test. These assays offered better sensitivity for the detection of COVID-19 cases than a commercial assay which requires 100-fold larger serum volumes. This study demonstrates that low-volume in-house antibody assays can provide good diagnostic performance, and highlights the importance of using well-characterized samples and controls for all stages of assay development and evaluation. These cost-effective assays may be particularly useful for seroprevalence studies in low and middle-income countries.

KEYWORDS

antibody, diagnostic, ELISA, evaluation, SARS-CoV-2, COVID-19, immunity, luciferase immunoprecipitation system (LIPS)

1 Introduction

The COVID-19 pandemic has caused over 6 million deaths and significant morbidity worldwide and major disruption to many societies (1). Mass testing for antibodies specific for SARS-CoV-2 plays an important role in understanding prevalence and transmission at the population level and has become a pillar of COVID-19 surveillance in many countries including the UK (2). In contrast to tests detecting the virus, antibody assays can confirm previous infection and are particularly useful for identifying undetected, often asymptomatic cases (3). This provides a more sensitive and practical approach to estimating prevalence than repeated testing of symptomatic individuals. Moreover, measuring antibody responses to different antigens and detecting specific antibody isotypes provides insights into levels of immunity in populations and mechanisms of immune-protection. Over time SARS-CoV-2 antibody testing is playing an increasing role in shaping vaccine evaluation and policy (4, 5). In low and middle income countries, less viral antigen/PCR testing is performed, thus data on infection and immunity gathered through simple and affordable tests is essential to guide vaccination rollout (6).

While many approaches to measuring antibodies to SARS-CoV-2 have been reported previously (7, 8), there is considerable variability in reported seropositivity rates determined using different assays/platforms, so that robust conclusions relating to population level exposure and immunity are elusive. Lab-based commercial assays have been widely evaluated in target populations in high income settings, offer good diagnostic performance, and have been deployed effectively to determine serological antibody status as well as to support clinical diagnoses (9). However, these assays are costly, often require dedicated specialist equipment, large sample volumes, and in general do not fully characterize the antibody response in terms of isotype. In contrast, lateral flow antibody assays require very low sample volumes and can be cheaper. These user-facing tests are suitable for large population surveillance and surveys, but have shown sub-optimal performance for detection of SARS-CoV-2 specific antibodies in evaluation studies (10). Sub-optimal performance of antibody assays can lead to uncertainty around persistence of antibodies and associated immune protection. Non-commercial ('in-house') assays have played an essential role in characterizing the antibody responses in various large cohort studies (11, 12), but many lack standardization and have been optimized/evaluated using relatively small numbers of samples making their performance unclear (13). A range of high-performance platforms such as ELISA and Luciferase Immunoprecipitation System (LIPS) assays have been reported and widely used for the measurement of SARS-CoV-2 antibodies (7, 14). Although less well known than ELISA, the LIPS platform offers an alternative method for measuring SARS-CoV-2 specific antibody responses that is more amenable to the use of competition (selecting for high affinity antibodies), and has potential to improve specificity for target antigens/epitopes (14, 15). LIPS also offers a wider dynamic range, allowing quantification of antibody responses using low sample volumes.

We therefore sought to utilize a varied and well characterized set of samples from recent COVID-19 cases (known positives) and pre-pandemic (known negative) individuals to develop and retrospectively evaluate in-house antibody assays for detecting recent infection. Multiple studies have reported differing antibody titers and profiles in groups with varying clinical outcomes (12, 16), as well as varying levels of cross-reactive responses among pre-pandemic samples from individuals of different ages (17). The COVID-19 cases therefore

included severe and mild hospitalized PCR-confirmed and clinically suspected cases as well as PCR-confirmed mild and asymptomatic SARS-CoV-2 community infections (18) using samples collected during the early stages of the pandemic (2020). These were combined with large numbers of pre-pandemic sera from multiple collections (known negatives) and distributed across distinct stages of assay development and evaluation. The assays included total antibody and isotype-specific, standardized, low serum volume assays on two different platforms (ELISA and LIPS) and a novel LIPS bridging format with high throughput potential. To facilitate interpretation of the assays, we also sought to relate the results of our binding antibody assays to functional responses by comparing with two different neutralization assay platforms. Finally, we describe the process of reporting binding antibody in international units and demonstrate the deployment of the assays in a population of healthcare workers with unknown serological and infection status.

2 Materials and methods

2.1 Study approval

This work utilizes various collections of samples collected both before and during the COVID-19 pandemic *via* different approvals and protocols. All samples were used in accordance with the Human Tissue Act (2004) with appropriate consent and ethical approvals in place. Further details are indicated in three sections below.

2.1.1 COVID-19 cases

PCR confirmed and clinically suspected COVID-19 cases were recruited *via* two independent routes in Bristol, United Kingdom between April and November 2020 (prior to roll out of vaccinations). PCR confirmed and clinically suspected severe COVID-19 cases admitted to hospital were recruited into the DISCOVER study at North Bristol NHS Trust for which HRA Approval was granted by the South Yorkshire Research Ethics Committee (20/YH/0121). Clinical and demographic features were recorded during the in-patient stay and subsequently at out-patient follow-up clinics. Respiratory samples were submitted for SARS-CoV-2 PCR testing on admission or first presentation; further samples were tested where initial samples tested negative for SARS-CoV-2 RNA. Serum or plasma samples were collected at various time points during in-patient and out-patient follow-up.

In addition, healthcare workers (HCWs) at University Hospitals Bristol, North Bristol NHS Trust and Weston NHS Foundation Trust who had a previous positive nasopharyngeal swab for SARS-CoV-2 by PCR were invited to donate blood samples into the Bristol Biobank (NHS Research Ethics Committee Ref 20/WA/0273). A clinical data form was used to collect details of symptoms, tests and other information relating to the donor and their COVID-19 status at the point of sampling. A subset of donors were invited back for a repeat donation at >12 weeks post symptom onset.

2.1.2 Pre-pandemic samples

Samples collected prior to December 2019 were sourced from various collections held in Bristol, UK, as detailed in Table 1.

2.1.3 Samples from a longitudinal cohort of hospital-based healthcare workers collected during the pandemic

Patient-facing clinical staff members working in the Children's Emergency Department (CED) of Bristol Royal Hospital for Children, including doctors, nurses and healthcare assistants were invited to take part in the LOGIC (LOnGItudinal Study of COVID-19: Symptoms, Virology & Immunity) study in April 2020; REC reference number 20/YH/0148. In this study, participants donated blood samples over a 12-month period.

2.2 Serum and plasma sample collection

Blood from suspected and proven recent COVID-19 cases was collected into SST vacutainers (BD Biosciences) and serum was separated by centrifugation at 1300g for 10 minutes, before being aliquoted into cryovials and stored at -70°C.

2.3 Heat inactivation

Samples from suspected and proven PCR confirmed COVID-19 cases were heat treated to inactivate live virus, at 56°C for 30 minutes according to local and national health and safety guidance.

2.4 Antigen production

2.4.1 SARS-CoV-2 trimeric spike protein, and receptor binding domain

SARS-CoV-2 Spike ectodomain and RBD were expressed in Hi5 insect cells as previously described (7). The Spike ectodomain construct was comprised of amino acids 1 to 1213 fused with a thrombin cleavage site followed by a T4-foldon trimerization domain and a hexahistidine affinity purification tag at the C-terminus. The polybasic furin cleavage site was mutated (RRAR to A) (7). The construct for RBD was comprised of amino acids 1-14 (secretion signal) and then 319-541 of the Spike ectodomain and was followed by a hexahistidine affinity purification tag at the C-terminus (7, 22). Both Spike protein and RBD were purified using a previously described purification protocol (23). Briefly, supernatant media containing expressed

TABLE 1 Details of pre-pandemic samples collated from various collections including research ethics committee (REC) references, sample types and years of collection, numbers and distribution in sample sets.

Cohort	Donor type	Sample types	Year/s of collection	Ethical approval details of use and/or reference/s	Number of samples and distribution in sample sets
1998 Blood Donors	Healthy adults	Serum	1998	Approved by Wales REC 6, reference 19/WA/0295	Threshold set n = 226; Validation set n = 286
2019 Blood Donors	Healthy adults	Plasma	2019	NHSBT Bioresource samples approved for use by NHSBT internal review and approved by Yorkshire & The Humber - Leeds West Research Ethics Committee reference REC 20/YH/0168	Threshold set n = 27; Validation set n = 171
Avon Longitudinal Study or Pregnant women And Children (ALSPAC) cohort and healthy controls	Longitudinal cohort of children aged 7, 9, 13, 15, 17.	Serum and Plasma	Various between 1998-2017	Ethical approval for the use of these samples was obtained from the ALSPAC Ethics and Law Committee and the Local RECs (19, 20);	Threshold set n = 100
Healthy control adults	Healthy control adults aged 20-60.	Serum and Plasma	2014	Ethical approval obtained from South West Frenchay Proportionate Review Committee, Bristol, UK reference 14/SW/0087 (21).	Threshold set n = 48
Bristol Biobank	Healthy adults and children participating in research studies	Serum	Various between 2006-2015	Samples released under approved Biobank Use application (U-0042). Ethics REC reference 20/WA/0273.	Threshold set n = 2; Validation set n = 106
Pneumonia/pleural cases	Hospitalized adults with pleural empyema or parapneumonic effusion	Serum	Various between 2009-2016	Samples drawn from a prospective observational study with full REC approvals (08/H0102/11)	Validation set n = 20

proteins were harvested from transfected cells 3 days post-transfection and were incubated with HisPur Ni-NTA Superflow Agarose (Thermo Fisher Scientific) for 1h at 4°C. Resin bound with SARS-CoV-2 Spike or RBD protein was separated and extensively washed with wash buffer (65 mM NaH_2PO_4, 300 mM NaCl, 20 mM imidazole, pH 7.5) and finally protein was eluted with buffer (65 mM NaH_2PO_4, 300 mM NaCl, 235 mM imidazole, pH 7.5). Eluted protein was then concentrated, and buffer exchanged to phosphate-buffered saline (PBS) pH 7.5 using 10 kDa (for RBD) and 50 kDa (for Spike) MWCO Amicon centrifugal filter units (EMD Millipore). Concentrated proteins were then aliquoted, flash frozen in liquid nitrogen and stored at -70°C until further use.

2.4.2 Nucleoprotein (ELISA)

The *E. coli* codon optimized nucleotide sequence of full-length nucleoprotein from SARS-CoV-2 was synthesized by GenScript. The sequence was synthesized with an *NdeI* restriction site at the 5' end and the *BamHI* site at the 3' end and cloned into pET28a expression vector. All proteins were expressed with C-terminal His_6-tags to facilitate subsequent purification. The recombinant plasmids (pET28a-NP-FL) were transformed into *E. coli* strain BL21 (DE3). Protein expression was induced by the addition of 1 mM IPTG and then incubated overnight at 20°C. Cells were pelleted by centrifugation and resuspended in 20 mM Tris pH 8, 500 mM NaCl, 10 mM imidazole, 1 mM NaF and 1 mM PMSF. Cells were lysed by passage through a French Press cell (Spectronic Instruments) and the resulting lysates were centrifuged at 39,000g at 4°C for 30 min. The supernatant was applied to a HisTrap HP nickel affinity column (GE Healthcare) and washed with a series of gradient wash buffers (20 mM Tris pH 8, 500 mM NaCl, 10, 20 and 40 mM Imidazole). The protein was eluted in 20 mM Tris pH 8, 500 mM NaCl and 500 mM imidazole and further purified by size exclusion chromatography using a HiLoad 16/600 Superdex 200 ® pg column (GE Healthcare) equilibrated and eluted in 20 mM Tris pH 8 and 500 mM NaCl. Peak fractions were pooled and concentrated in a 10 kDa MWCO Vivaspin ultrafiltration unit. Protein concentration was determined using the Bradford assay. Typical yields of N proteins after Ni-NTA and size exclusion chromatography was approximately 9 mg/L. Purified proteins were analyzed by SDS-PAGE and by Western-blots assays using an anti-His tag antibody (Sigma).

2.4.3 Luciferase tagged RBD for LIPS

RBD antigen tagged with a luciferase reporter (nanoluciferase, Nluc) was generated and provided by Dr Vito Lampasona (Milan) for a Luciferase Immunoprecipitation System (LIPS) assay (14, 23).

2.5 Production of in-house standard and controls

To allow for assay standardization and to monitor quality control of results over time, including intra- and inter- plate

variability, control material was generated from large volume serum samples with known recent infection and well-characterized antibody status. For the pooled standard, (which was used for all ELISA assays, the RBD LIPS Bridging and IgG assays) sera from 3 mildly affected PCR-confirmed cases were combined and aliquoted.

2.6 ELISA

The ELISA protocol is based on the RBD screening and Spike confirmatory ELISA assays described in (7, 24) with some modifications. MaxiSorp high-binding ELISA plates (NUNC) were coated with Spike (10 µg/ml), RBD (20 µg/ml) or N protein (20 µg/ml) in PBS and incubated overnight at 4°C (except for IgM ELISAs, where all antigens were coated at 2 µg/ml). Subsequent steps were all performed at room temperature (RT). Unbound antigen was removed with 3x washes in PBS with 0.1% v/v Tween-20 and plates were blocked for 1 hour with 3% BSA/PBS or 3% milk (Sigma) for IgM assays. Serum samples were diluted in either 1% BSA/PBS or 1% milk (for IgM only) and incubated on the plate (100 µl per well) for 2 hours. After washing, HRP-conjugated anti-human Pan-Immunoglobulin (Pan) (Sigma), IgG (Southern Biotech), IgA (Sigma) or IgM (Sigma) secondary antibody, in the same dilution buffer as the samples, was added (50 µl per well) and incubated for 1 hour. Plates were washed and dried before development with the HRP substrate OPD (SigmaFast; 100 µl per well). The reaction was terminated after 30 minutes by the addition of 3 M HCl (50 µl per well). Optical density was measured at 492 nm and 620 nm on a BMG FLUOstar OMEGA MicroPlate Reader with MARS Data Analysis software. The 620 nm reference wavelength measurements were subtracted from the 492 nm wavelength measurements for each well to give background corrected values. Averaged blank values from wells containing no serum were then subtracted from all experimental values for each plate.

Three read out approaches were explored for test samples: OD values normalized to the internal positive control, an area under the curve (AUC) generated from a 4-point dilution series (where available), and an interpolated value (arbitrary units).

2.7 LIPS

Non-competitive: The Nluc-RBD antigen (5) was diluted in 20 mM Tris, 150 mM NaCl, pH 7.4 with 0.5% v/v Tween-20 (TBST) and 0.05% casein to $4x10^6$+/-5% light units (LU) per 25µl. All steps were carried out at RT, unless specified. Reagents were stored at 4°C, TBST and diluted antigen were used directly from 4°C, Nano-Glo® substrate was equilibrated to RT before use. Serum samples (1µl, 2 replicates) were pipetted into a 96-well plate and incubated with 25µl diluted antigen for 2 hours in a dark area. Immunocomplexes were precipitated using 2.5µl glycine-blocked Protein A Sepharose 4 fast flow (GB-PAS) (GE Healthcare Life Sciences, Chicago, IL, USA) and 2.5µl ethanolamine-blocked Protein G Sepharose (EB-PGS) (GE Healthcare Life Sciences) (washed 4 times in TBST) for 1hr with shaking (~700rpm). Precipitates were washed 5 times with TBST and then transferred to a 96-well Optiplate™ (Perkin-Elmer, Waltham, MA, USA) and excess buffer removed by aspiration. Nano-Glo® substrate (40 µl, Promega) was injected into each well immediately before counting in a Hidex Sense Beta (Hidex, Turku, Finland).

Competitive: To overcome cross reactive responses from non-COVID-19 samples, SARS-CoV-2 RBD protein (as used in ELISA) was used to outcompete the Nluc-RBD label. A range of concentrations of RBD were tested with $8x10^{-8}$ mol/L showing good affinity for RBD specific IgG. Sera (1µl, 4 replicates) were pipetted into a 96 well plate. The Nluc-RBD antigen was diluted in TBST with 0.05% casein to $4x10^6$+/-5% LU per 25µl with or without unlabeled RBD added at a final concentration of $8x10^{-8}$ mol/L. Two replicates of each samples were incubated with Nluc-RBD and two replicates with competition of Nluc-RBD binding with unlabeled RBD. Immunocomplexes were precipitated and measured as outlined above. Where antibodies were of higher affinity unlabeled RBD outcompeted binding of Nluc-RBD, lowering the LU measured. A delta LU was calculated (mean LU of non-competed wells - mean LU of competed wells) and then interpolated from LU by the standard curve, creating LIPS units corrected for non-specific binding.

IgA and IgM measurement: IgA was measured in 1µl serum per replicate, with competitive displacement (as for IgG) and immunoprecipitated using 3.75 µl per well IgA agarose (Sigma), in place of GB-PAS/EB-PGS. IgM was measured in 2µl serum per replicate, without competitive displacement using 5µl per well IgM agarose (Sigma).

2.7.1 Spike-RBD bridging LIPS

To develop a novel LIPS bridging assay format for high throughput requirements, Spike antigen diluted to 2.5ng/µl in 40µl PBS was pipetted into every well of a 96-well high-binding OptiPlate™ (Perkin-Elmer, Waltham, MA, USA) and incubated for 18hrs at 4°C. The plate was washed 4 times with TBST and blocked with 1% Casein in PBS (Thermo Scientific, Waltham, MA, USA). The plate was left to air-dry for 2-3hrs before being stored with a sachet of desiccant in a sealed plastic bag at 4°C and used within three weeks.

The Nluc-RBD antigen was diluted in TBST to $10x10^6$+/-5% LU per 25µl. Sera (1.5µl, 2 replicates) were pipetted into a 96-well plate and incubated with 37.5µl diluted labelled antigen for 2hrs. Of this mixture, 26µl was transferred into the coated OptiPlate and incubated shaking (~700rpm) for 1.5hrs. The plate was washed 8 times with TBST, excess buffer was removed by aspiration, then 40µl of a 1:1 dilution of Nano-Glo® substrate (Promega) and 20mM Tris 150mM NaCl pH 7.4 with 0.15% v/v Tween-20 was injected into each well before counting in a Hidex

Sense Beta Luminometer (Turku, Finland). Units were interpolated from LU through a standard curve.

2.8 Roche SARS-CoV-2 anti-nucleocapsid antibody assay

Serum samples from PCR-confirmed cases were analyzed using the commercial Elecsys® Anti-SARS-CoV-2 (Roche) in the Department of Microbiology, Infection Sciences, Southmead Hospital, North Bristol NHS Trust, Southmead Road, BS10 5NB, UK following manufacturer's instructions. Elecsys® Anti-SARS-CoV-2 is an immunoassay for the *in vitro* detection of total antibodies (including IgG) to SARS-CoV-2 in human serum and plasma. The assay uses a recombinant protein representing the nucleocapsid (N) antigen in a double-antigen sandwich assay format, which favors detection of high affinity antibodies against SARS-CoV-2.

2.9 Microneutralization assay

VeroE6 cells (ATCC) were cultured in Dulbecco's Modified Eagle's medium containing GlutaMAX (Thermo Fisher Scientific) supplemented with 10% fetal calf serum (FCS) (Thermo Fisher Scientific) and 0.1 mM non-essential amino acids (NEAA) (Sigma Aldrich) at 37°C in 5% CO_2. For immunofluorescence analysis, cells were seeded the day prior to infection in appropriate media in µClear 96-well Microplates (Greiner Bio-one). Neutralizing capacity of human serum samples was quantified using a microneutralization assay as previously described (23). Briefly, heat-inactivated serum was serially diluted 2.5-fold from 1:20 for 8 dilutions and incubated with live virus (SARS-CoV-2/human/Liverpool/REMRQ0001/2020) for 60 mins at 37°C. Following incubation, the mixtures of virus and diluted sera were added to VeroE6 cells and incubated for 18 hours before being, fixed and stained with antibodies against the SARS-CoV-2 N protein (1:2000 dilution; 200-401-A50, Rockland) followed by an Alexa Fluor-conjugated secondary antibody (ThermoFisher) and DAPI (Sigma Aldrich). Images were acquired on the ImageXpress Pico Automated Cell Imaging System (Molecular Devices) using a 10X objective and infected cells detected and quantified using Cell ReporterXpress software (Molecular Devices). The percentage of infected cells was calculated relative to control wells which contained virus only, without serum.

2.10 Pseudovirus neutralization assay

Luciferase-expressing vesicular stomatitis virus (VSV*ΔG-FLuc particles) were a gift from Yohei Yamauchi. VSV-G-harboring BHK21 cells were infected with VSV*ΔG-FLuc particles to generate complemented VSV*G-FLuc particles as previously described (25). To generate Spike-harboring pseudovirus (VSV-S-FLuc), 293T cells were seeded and transiently transfected with a plasmid corresponding to the original Wuhan strain Spike protein (pCAGGS-S2-spike) using Turbofect transfection reagent (ThermoFisher R0532) for 16 hours following the manufacturer's instructions. Transfected 293T cells were then infected with VSV*G-FLuc particles for 2 hours, washed with PBS, then incubated with fresh DMEM, supplemented with 10% FBS and 1:2000 (v/v) I1 (anti-VSV-G) antibody (absolute antibody Ab01401-10.3). Optimal pseudotype cell entry was achieved using VeroE6 cells stably expressing the human angiotensin-converting enzyme 2 (ACE2) receptor and the cell surface protease TMPRSS2 (Vero ACE2 TMPRSS2 (VAT) cells, which were a kind gift from Dr Suzannah Rihn, MRC-University of Glasgow Centre for Virus Research (26).

For pseudovirus neutralization assays, 10,000 VAT cells were seeded per well in opaque, white 96-well plates. The following day, serum samples were titrated 2.5-fold, 9 times across 96-well plates from a starting dilution of 1:40. Pseudovirus corresponding to 10,000 RLU was immediately added to each well, mixed and incubated for 1 hour. After aspirating cell media from VAT cells, pseudovirus/serum and control mixtures were added to corresponding wells on VAT cells and incubated at 37°C 5% CO_2 overnight. Luminescence measurements were taken 16 hours after infection, using the ONE-Glo Luciferase Assay System (Promega). Luminescence was measured using a Tecan Infinite 200 plate reader at room temperature.

2.11 Blinding of validation set

The validation set of samples (n=807) were split into multiple aliquots (n=5) for randomization and blinding by assigning a new barcode ID for each aliquot. The 5 sets of samples each had a unique order and the LIPS and ELISA assays were performed one separate sets, such that each lab remained blind to the results of the other. Screening ELISAs were performed on the same samples at the same time. Unblinding took place after all assay were performed and the data had been finalized.

2.12 Statistical analysis

Data analyses were performed using either R software (version 4.2.0) with R Studio (2022.07.1+554), or GraphPad Prism (version 9) as detailed below.

2.12.1 Standardization to serum pool standards

In both ELISA and LIPS assays, each plate or set of 2 plates included a dilution series of the in-house serum pool, to standardize sample values and control samples across plates. For the ELISA assay, sample values are reported as normalized

ODs, where average OD values are divided by the top standard value in the plate. However, sample readouts using other methods including interpolated unit values (from a 4-parameter logistic regression model fit (on Prism or within BMG software) to the 7-point standard pool dilution series) and AUC from sample dilution series were used in the development stage. For LIPS assays, the raw luminescence unit values for the standard pool dilution series across two plates were fitted to a logarithmic curve to allow for interpolation of in-house unit values to average raw light unit values for samples.

The WHO International Standard (First WHO International Standard for anti-SARS-CoV-2 immunoglobulin (human) (NIBSC code 20/136) and the WHO Reference Panel (First WHO Reference Panel for anti-SARS-CoV-2 immunoglobulin) (NIBSC Code 20/268) were both purchased from the National Institute for Biologic Standards and Control (NIBSC), Potters Bar, Hertforshire, UK in 2021.

2.12.2 Diagnostic accuracy estimates and setting of thresholds

Performance of candidate tests for discriminating between pre-pandemic and COVID-19 samples was performed using Receiver Operator Characteristic (ROC) Curve analysis. From such analysis of threshold set samples, thresholds meeting the following criteria were identified (for each assay) and selected for evaluation in the blind evaluation: 99th centile of pre-pandemic levels (to achieve 99% specificity); 98th centile of pre-pandemic samples, and the point at which the highest Youden's index is achieved (Jmax). In selected samples sets based on recommended categorization of COVID-19 cases, sensitivity and specificity at target thresholds were determined using ROC curve analysis and, where appropriate, estimates on sensitivity and specificity were reported at a pre-specified threshold; 95% confidence intervals around these estimates were calculated using the Clopper method without correction for multiple comparisons.

2.12.3 Correlation

Associations between the results of the different assays were assessed using the Kendall's Tau correlation method. Multiple correlations were combined into a correlation matrix and plotted using the corrplot package in R.

2.12.4 Assessing for parallel lines

To assess for parallelism between the in house and international serum standards, a full standard curve (in duplicate) of the in-house pooled standard was ran on the same plate as the WHO international standard (NIBSC code 20/136 as above), at the appropriate dilution range for each assay. This was repeated up to 3 times to ensure robust comparisons and to account for inter-plate variability. Duplicate ODs from each dilution in each series were averaged, and plate replicates were combined as repeats for each standard and fitted to a non-linear regression model (usually 4-parameter logistic) curve. The combined dilution series for each standard (where average ODs from each plate were classed as replicate values) were used to assess for goodness of fit of two nested models: one where the HillSlope of the models is shared, and one where they differ. The resulting F statistic and P value determine whether the Model where HillSlope is shared (i.e. the lines are parallel for the midpoint).

2.12.5 Assigning BAU values to in house standards

For those assays where the international standard and in-house standard were found to be parallel, replicated run values were used to ascertain the IC50 values for each standard, followed by the ratio between the control samples to determine the conversion equation.

2.13 STARD Checklist

This study conforms to the STARD checklist for publishable diagnostic accuracy studies (27), as outlined in Table S1 (Supplementary Material).

3 Results

3.1 Sample collections and study flow for assay evaluation

We collected well characterized plasma and serum samples from multiple sources and distributed them into sets for distinct stages of assay development and evaluation (Figure 1). The 'known negative' samples were pre-pandemic samples from a range of donor types including adult blood donors, and adults and children involved in research studies. A small group of adult hospitalized patients with pneumonia/other pleural conditions were also included (Figure 1A). The cohort of COVID-19 cases were recruited *via* two routes in 2020 (prior to vaccine rollout): 1) convalescent hospital workers identified after receiving a positive PCR test, and 2) patients confirmed and/or clinically suspected to have COVID-19 at the point of recruitment during inpatient/outpatient hospital/secondary care visits in Bristol, UK (Figure 1B). The COVID-19 cohort included the full spectrum of disease (asymptomatic to severe/fatal) and encompassed a range of times since symptom onset or PCR confirmation (those without PCR confirmation were clinically suspected based on symptom presentation in hospital). The sample sets were used for development and evaluation as shown in Figure 1C, with only the optimal screening assays being included in the full diagnostic evaluation process.

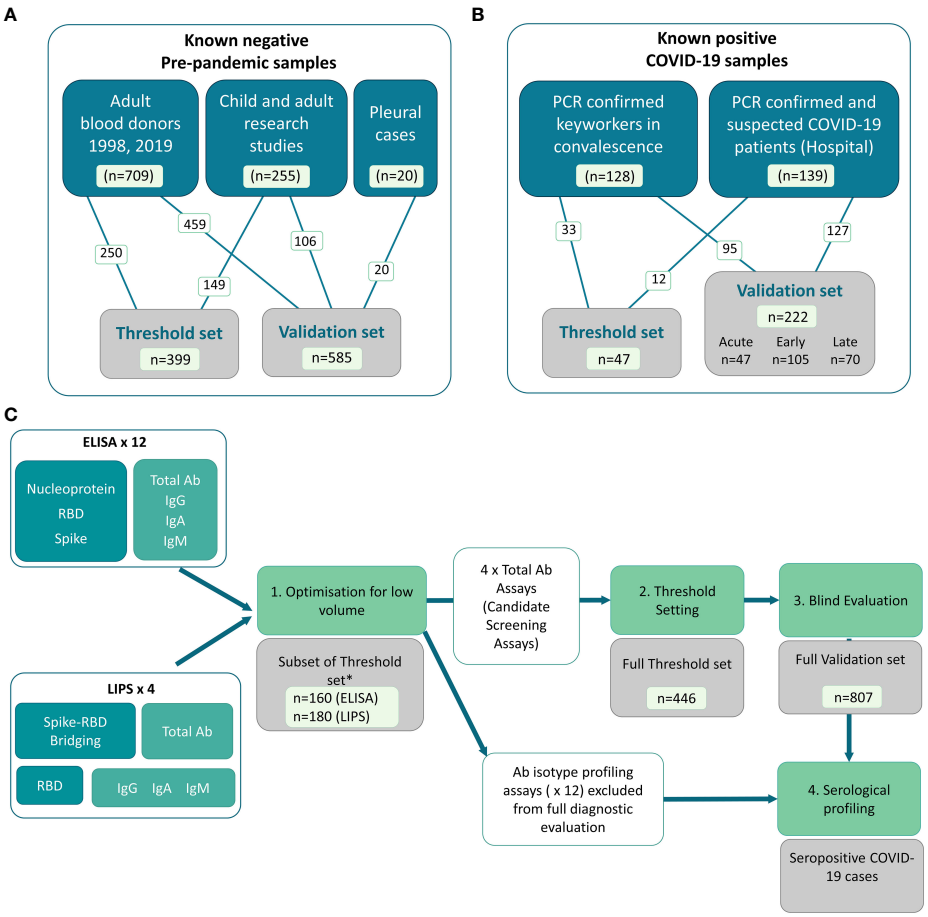

FIGURE 1
Distribution of samples into sets, and flow diagram of assay development and evaluation. In-house COVID-19 antibody assays using pooled controls and a set of well characterized samples to first optimize and then set thresholds for positive and negative. **(A)** Known negative samples were all collected pre-pandemic (i.e. pre-December 2019) from various Biobanks and included adult and child plasma and serum samples from research studies, adult blood donors and a small collection of samples from hospitalized cases of pleurisy. **(B)** Known positive samples were collected from a full spectrum of COVID-19 adult cases, including RT-PCR confirmed COVID-19 cases recruited in convalescence from the community and PCR confirmed and clinically suspected COVID-19 cases recruited in hospitals. **(C)** Flow diagram showing use of sample sets in assay development, selection of screening assays and diagnostic evaluation. A total of 16 assays including isotype-specific and total antibody assays on both ELISA and LIPS platforms were optimized using a subset of the threshold set of these samples (n = 160 or n = 180depending on assay platform) for initial selection of candidate screening assays (Stage 1). * Note that whilst the number of threshold set samples used for optimization was comparable for ELISA and LIPS assays, the exact samples used differed slightly due to low samples volume for use across 16 assays. The assays which performed best for each antigen/platform combination were then taken forward for the full threshold setting to determine optimal thresholds for specificity (stage 2) including the remaining n = ~300 samples for all 4 screening assays (i.e. total of n = 446). Candidate screening assays with pre-defined thresholds were then deployed on a blind validation cohort containing n = 222 samples from COVID-19 cases and n = 585 pre-pandemic samples. The performance characteristics were defined using the validation set to guide utility of deployment. The 12 x non-screening assays were subsequently used only for profiling of seropositive samples (stage 4) and comparing to functional assays.

3.2 Assay optimization and selection of screening assays

By building on an ELISA protocol made widely available at the start of the pandemic, we used a subset of the threshold set of samples (n=160) to optimize assay conditions to measure antibodies specific to three antigens from SARS-CoV-2: the Nucleocapsid (N), the receptor binding domain (RBD) of Spike, and the stabilized trimeric Spike protein, with a focus on achieving discrimination between pre-pandemic and COVID-19 samples using small serum/plasma volumes (<10 µl). For each antigen, a suite of ELISAs was set up to measure either total antibody/Pan Immunoglobulin using a commercially available 'anti human IgG' secondary antiserum which detects the Fab region (i.e., anti-IgG H+L) and therefore detects all isotypes, (hereafter labelled 'Pan'), or IgG, IgA and IgM isotypes (using class-specific secondary antibodies) (Figure S1). We generated a pooled serum 'standard' from donors with high responses to all

antigens that was used to standardize between plates (Figure S2A). The optimal dilutions for the standards, controls and samples to achieve discrimination between pre-pandemic and COVID-19 samples were determined. We found that a single sample dilution, normalized to a top standard control, could provide improved or equivalent discrimination between groups when compared to using AUC calculated from a 4-point dilution series or deriving an interpolated value (respectively) (Figures S2B, C). Since the aim was to optimize assays for discrimination, but also low sample-volume and high throughput, we elected to report ELISA results as normalized ODs which are the simplest to perform. For each antigen, the Pan (total antibody) ELISAs outperformed the isotype specific assays in discriminating between pre-pandemic samples and those from COVID-19 cases, as demonstrated by greater AUCs after receiver operator characteristic (ROC) analysis (Figures 2A, B).

A suite of LIPS assays measuring antibodies specific to the RBD, were developed based on protocols outlined in (14), a

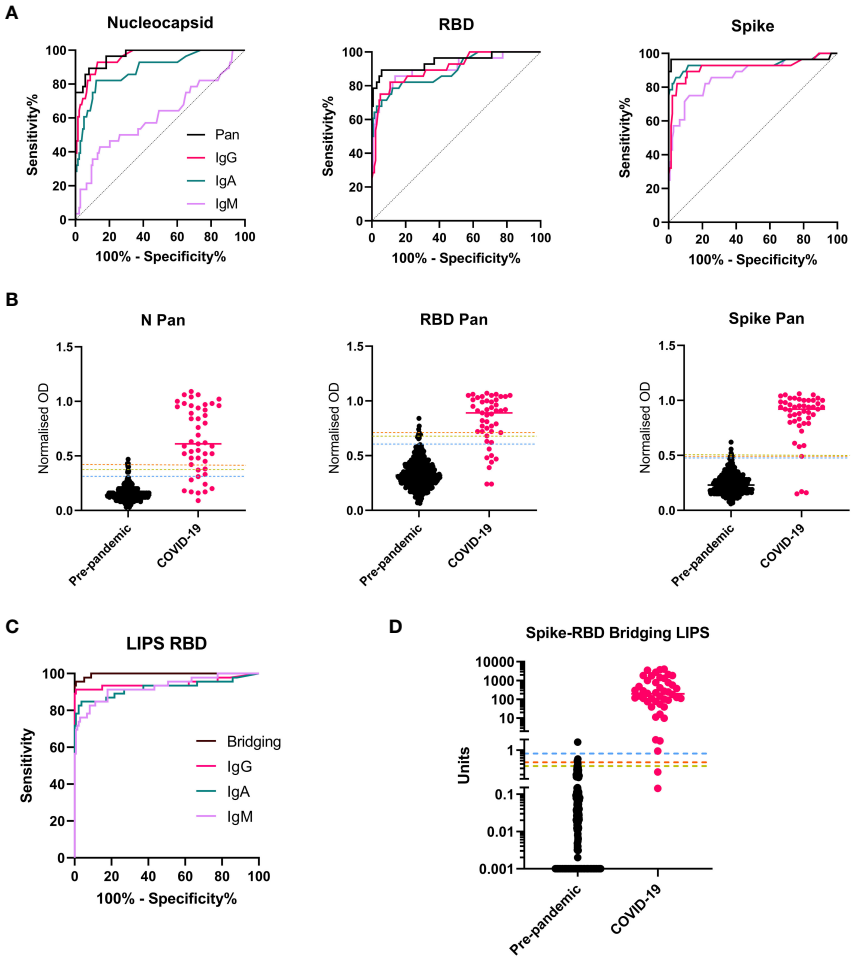

FIGURE 2
Selection of screening assays and threshold setting with the threshold set. A subset of the threshold set samples were used for assay optimization and then to compare performance of isotype/total antibody specific assays for each antigen/platform combination. **(A)** ROC curves showing the relative performance of ELISAs using different secondary antibodies (Pan total antibody (Black); IgG (pink); IgA (green), IgM (purple) in a cohort of n = 27 COVID-19 samples and n = 133 pre-pandemic samples from the threshold set. For all three antigens, the Pan/total antibody assays provided the best performance as evidenced by highest AUCs. **(B)** Scatterplots showing the individual normalized OD readings for all three ELISA screening assays (N Pan, RBD Pan and Spike Pan) in the full threshold set of n = 45 COVID-19 samples and n = 399 pre-pandemic), with the median represented by a line for each group and the three thresholds for each assay indicated with a line across the plot: 1 – the 99th percentile of pre-pandemic levels (orange dashed line); 2 - The 98th percentile (yellow dashed line); 3 – Youden's index (blue dashed line). **(C)** ROC curves for all LIPS assays deployed on a subset of the threshold set (n = 46 COVID-19 cases and n = 134 pre-pandemic) showing optimal performance with the Spike-RBD Bridging LIPS assay, which was therefore taking forward for full threshold setting on the full threshold set (n = 446) with results shown in the scatterplot in **(D)**. (Interpolated unit values shown on y axis with log10 scale and broken axis to allow visualization of thresholds. To ensure all results were plotted, a result of zero units was assigned a value of 0.001 for this graph. The three thresholds are indicated: 1 – the 99th percentile of pre-pandemic levels (orange dashed line); 2 - The 98th percentile (yellow dashed line); 3 – Youden's index (blue dashed line).

study in which detection of serum RBD specific antibodies was found to be associated with survival in hospitalized cases of COVID-19. For measuring IgG and IgA isotypes, using unlabeled RBD in competition with Nluc-labelled RBD was found to improve discrimination between pre-pandemic and COVID-19 cases (Figures S3A, B) whereas no optimal level of competition was identified for IgM. For detection of total antibody with high affinity for RBD, the novel Spike-RBD bridging assay format was adopted in which plates coated with trimeric stabilized Spike could bind samples prelabelled with Nluc-RBD (Figure S1B). All LIPS-based assay results are reported in interpolated units using the internal pooled serum standard. As with the Pan ELISAs, the Spike-RBD bridging assay demonstrated superior AUCs after ROC analysis amongst the LIPS assays for discrimination between COVID-19 cases and pre-pandemic controls when ROC curve analysis was performed (Figures 2C, D). Despite using the same target antigen, the RBD LIPS assays provided higher AUCs than the RBD-specific ELISA assays for all antibody isotypes when the same samples sets were compared (Figure S3).

In summary, we developed 16 antibody assays for detection of COVID-19 antibody responses using <5 µl serum samples in a single dilution, which can be scaled to high throughput. Since the total antibody assays (i.e., N, RBD and Spike Pan ELISAs and the Spike-RBD bridging LIPS) performed best for discrimination in the optimization stage, these were designated as the best candidates for screening assays to identify COVID-19 seropositive individuals.

3.3 Threshold setting

Candidate screening assays (n=4) were run on samples from the full threshold set consisting of 399 pre-pandemic and 47 COVID-19 case samples (Table S2); the predominance of pre-pandemic samples in this cohort highlights the aim to achieve optimal specificity. Thresholds were determined using three distinct criteria: 1) The 99th percentile of the negative (pre-pandemic) controls; 2) The 98th percentile of the negative (pre-pandemic) controls; 3) The highest Youden Index to achieve balanced sensitivity and specificity (Figures 2B, C) and assay performance in the threshold set was determined. In this sample set, all assays provided good discrimination between COVID-19 and pre-pandemic samples (AUCs ranging from 0.95-0.997), with the Spike-RBD bridging LIPS assay providing optimal and almost perfect performance (AUC = 0.997, 95% CI 0.993-1.001) (Table S3). We did not observe differences in pre-pandemic total antibody assay signals between adults, teens and children (Figure S4A). We compared background signal levels in serum and plasma and found no statistical differences in signal between matched plasma/serum from pre-pandemic donors (Figure S4). Thus, using both serum and plasma samples, thresholds for each assay were set which were identical for all age groups.

3.4 Blind evaluation of screening tests to detect confirmed and suspected COVID-19 cases

The 4 screening assays measuring total antibodies were tested on the full validation sample set (n=807) in a blinded fashion. To explore sensitivity of candidate assays for different periods post infection, the COVID-19 samples were divided into 3 time periods for diagnostic evaluation such that no repeat samples were included in each group: Acute (< 21 days post symptom onset (p.s.o) or PCR test), Early Convalescent (3-12 weeks p.s.o), Late Convalescent (>12 weeks p.s.o) (Table 2). Results for the 4 screening assays are presented either as dot plots or ROC curves (Figures 3A, C, D, F). Sensitivity and specificity estimates (and 95% CI) of the assays at each pre-defined threshold are reported (Table 3) and presented in (Figures 3B, E). High specificity for recent COVID-19 infection was maintained from the threshold setting set, with all thresholds providing >96% specificity (and most >98%); for each assay, the threshold providing at least 98% specificity whilst achieving optimal sensitivity was selected (Table 3), except for the Spike Pan ELISA where the highest specificity provided was 97.3% (95% CI 95.9-98.5). Of note, the optimal threshold method differed across the 4 assays, e.g. for the N Pan ELISA the 98th percentile performed optimally, whilst for the Spike-RBD bridging LIPS it was the Jmax value (highest Youden's index). The screening assays generally displayed low levels of intra- and inter-assay variation; coefficients of variation were between 1.8% and 23.4% for QC samples in the positive range (Table S4).

We performed a sensitivity analysis to evaluate whether inclusion of samples from clinically suspected COVID-19 cases, who were not virologically confirmed, and/or those samples collected within 21 days p.s.o (i.e. in the Acute group), was detrimental to diagnostic performance when compared to including only samples from RT-PCR confirmed individuals 3 weeks p.s.o (one sample per donor only) (Figures 3C, F and Table S5). The performance of each assay was best in the RT-PCR confirmed group, suggesting that some of the suspected COVID-19 cases may not have been infected with SARS-CoV-2.

The best performing assays for all groups were the Spike Pan ELISA and the Spike-RBD bridging LIPS assay which provided comparable sensitivities for detection of COVID-19 cases (i.e. between 92.4-95.7% sensitivity for COVID-19 cases >21 days p.s.o, depending on the group of interest (Tables 3, S5 and Figure 3), and good specificity (between 96.7-98.5% depending on the threshold used). It is important to consider that there were differences in the proportions of COVID-19 cases from the two recruitment streams included in the different COVID-19 time periods used to assess assay sensitivity, and that these groups had different clinical/demographic features (Table 2). As such, it is not possible to infer whether differences in

TABLE 2 COVID-19 cases in validation cohort.

	Hospitalized COVID-19 cases	Mild convalescent clinic	Total	Statistical comparison[$]
Number of individuals	96	86	182	–
Sampling dates	March – July 2020	May – August 2020	March – August 2020	–
Method of COVID-19 diagnosis, n (%)				<0.0001
PCR-confirmed	71 (74)	86 (100)	159 (87.4)	
Clinically Suspected	25 (26)	0 (0)	23 (12.6)	
Age (at baseline)				
Median years (range)	59 (19-89)	41.7 (18.4-68.8)	52 (18.4-89)	<0.0001
Unknown, n (%)	0 (0)	2 (2.3)	2 (11.0)	–
Female, number (%)	38 (40.4)	69 (80.2)	107 (58.8)	<0.0001
Time since symptom onset (OR PCR+ test*), days, median (range)	78 (0-126)	48 (11-122)	58.5 (0-133)	0.6881
Severity of infection, n (%)				<0.0001
Asymptomatic	0 (0)	6 (16.7)	6 (3.3)	
Mild (Symptomatic, not hospitalized)	0 (0)	77 (89.5)	77 (42.3)	
Moderate (Hospitalized, no ventilatory support)	14 (14.6)	3 (3.5)	17 (9.3)	
Severe (Hospitalized, required ventilatory support/high care)	76 (79.2)	0 (0)	76 (41.8)	
Died	6 (6.3)	0 (0)	6 (3.3)	
Repeat Samples				0.0112
Total samples, n	127	95	222	
Baseline, n (% of total samples)	96 (75.6)	86 (90.5)	182 (82.0)	
Repeat 1, n (% of total samples)	30 (23.6)	9 (9.5)	39 (17.6)	
Repeat 2, n (% of total samples)	1 (0.8)	0 (0)	1 (0.5)	
Period post infection, n samples (% of total samples)				<0.0001
Acute (0–3 weeks)	43 (33.9)	4 (4.2)	47 (25.8)	
Early convalescent (3–12 weeks)	27 (21.3)	78 (82.1)	105 (57.7)	
Late convalescent (>12 weeks)	57 (44.9)	12 (12.6)	70 (38.5)	

*Where cases were asymptomatic, time since PCR test was used for this variable.
Clinical and demographic features relating to the n = 182 individuals diagnosed with COVID-19 whose samples (n = 222) were included to assess sensitivity of the screening assays. Individuals were recruited *via* two main routes – either as part of secondary care in hospital, or community cases invited to a convalescent clinic at least 14 days after symptom onset. Percentages are from total of individuals unless otherwise stated. [$]The clinical and demographic features of the two groups were compared (either using a Fisher's exact or Chi-Squared test for categorical data, or the Mann-Whitney U test for numerical data); and the p values are reported in the final column.

performance across different time periods relates directly to time since symptoms onset, and is not confounded by other differences between the groups.

3.5 The spike-RBD bridging LIPS assay and spike pan ELISA perform better than a commercial high-volume assay for detection of recent COVID-19 cases

We compared the sensitivity of the commercially available Roche Elecsys serum assay (a high volume test using the nucleocapsid as the target antigen) to the ELISA and LIPS screening assays using samples from n=218 COVID-19 cases from the validation set for which sufficient volume of sample was available. At the time of testing, this assay was the main assay being used in clinical labs in the UK. The Spike-RBD Bridging LIPS assay and the Spike Pan ELISA provided optimal sensitivity for COVID-19 cases, with both providing 93.58% sensitivity for RT-PCR confirmed cases whilst the Roche assay provided 89.30% (Figure 4A and Table S6); the N Pan and RBD Pan ELISAs provided 77.01% and 76.47% sensitivity respectively. Thus, whilst our in-house N Pan ELISA underperformed compared to a commercial assay using the same antigen, the two best performing assays (the Spike Pan ELISA and Spike-RBD Bridging LIPS) were able to provide superior sensitivity for

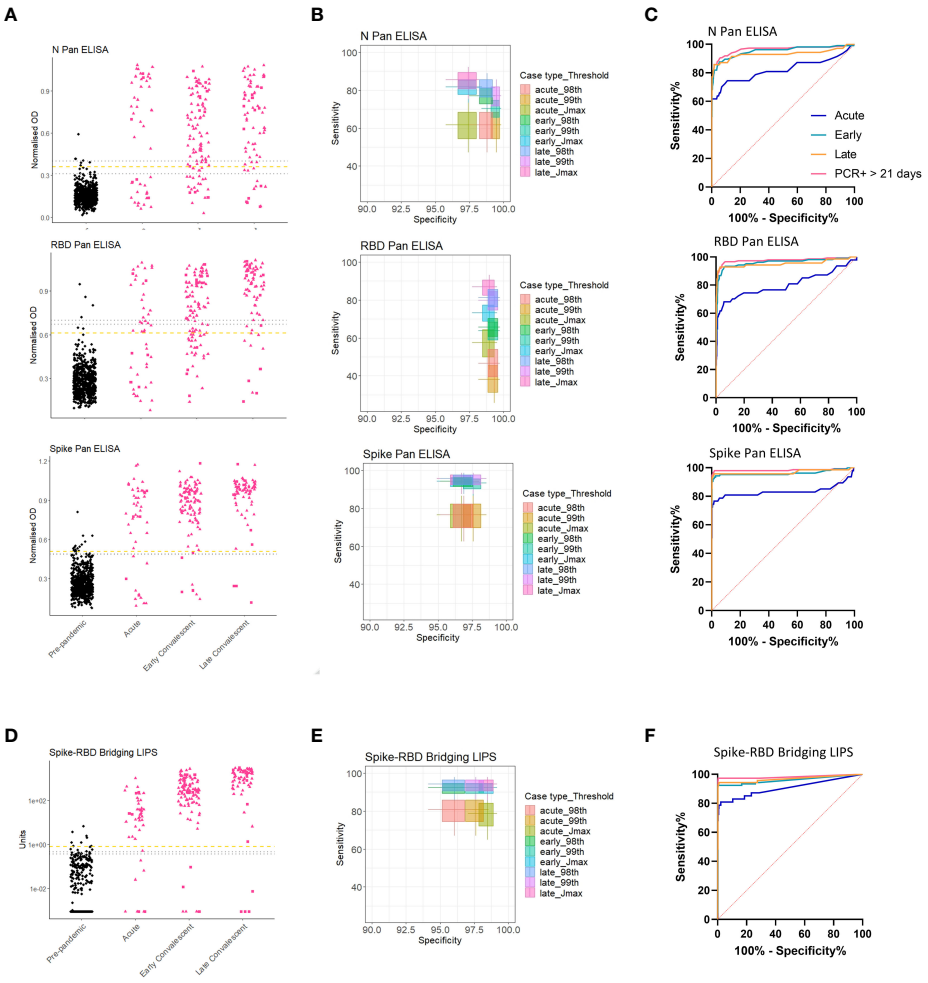

FIGURE 3
Performance of screening assays in validation cohort. Dot plots showing assay results for the 3 screening ELISAs [N, RBD and Spike Pan] **(A)**, and the Spike-RBD Bridging LIPS **(D)**; black dots represent pre-pandemic samples and pink dots represent COVID-19 samples separated by different periods post infection: Acute; Early Convalescent; Late Convalescent. One misrepresentative highly positive pre-pandemic result has been removed from **(D)** as analysis after unblinding indicated it was the result of human error after unmatching (it still is included in the ROC/sensitivity analyses). **(B, E)** Boxplots indicating sensitivity and specificities for COVID-19 performed by each assay at each of the pre-defined thresholds. **(C, F)** ROC curves indicating performance of each assay for differentiating acute (< 21 days p.s.o.; blue), early convalescent (21 days – 12 weeks p.s.o; turquoise) or late convalescent (> 12 weeks p.s.o.; orange) COVID-19 cases from pre-pandemic samples in the blind validation cohort. The performance for detection of the most likely to be 'true seropositive' COVID-19 cases is also included, i.e. those who were sampled after 21 days after a confirmed PCR test (pink).

some COVID-19 samples. Interestingly, the most marked improvement in sensitivity over the Roche assay was shown in the acute COVID-19 group, where the two best performing in-house assays could detect an additional 15% of samples in this group.

A comparison of the Spike Pan ELISA and Spike-RBD bridging LIPS assays revealed very good concordance for the detection of COVID-19 cases, but less so for the responses recorded from pre-pandemic samples, where different individuals were found to be positive on each assay (Figure 4B). Kendall's tau correlations were performed to compare screening assay results (normalized ODs) on the full validation set. Strongest agreement was observed between the Spike and RBD Pan ELISA results (Figure 4C). All isotype specific assays were deployed on the seropositive COVID-19 cases; within this sample set the strongest agreement between assays was for IgG and total antibody (Pan or Bridging) responses on the same platform and with the same antigen (Figure 4D).

3.6 Reporting in international units

To ensure antibody levels measured using the in-house assays can be compared to those generated using other assays,

10.3389/fimmu.2022.968317

TABLE 3 Performance of total antibody screening assays in blind diagnostic evaluation using the validation set (n = 807 samples).

	Specificity at defined thresholds (95% CI)			Sensitivity for Acute COVID-19 at defined thresholds (95% CI)			Sensitivity for Early Convalescent COVID-19 at defined thresholds (95% CI)			Sensitivity for Late COVID-19 at defined thresholds (95% CI)			Optimal Threshold Value (method)
Threshold*	**1**	**2**	**3**	**1**	**2**	**3**	**1**	**2**	**3**	**1**	**2**	**3**	
N Pan ELISA	99.5 (98.4 - 99.8)	98.8 (97.5 - 99.4)	97.4 (95.8 - 98.4)	61.7 (47.2 - 74.4)	61.7 (47.2 - 74.4)	61.7 (47.2 - 74.4)	70.5 (61.1 - 78.4)	77.1 (68.1 - 84.2)	81.9 (73.3 - 88.2)	77.1 (65.9 - 85.5)	81.4 (70.6 - 88.9)	85.7 (75.4 - 92.1)	(2)
RBD Pan ELISA	99.3 (98.2 - 99.7)	99.3 (98.2 - 99.7)	99 (97.7 - 99.5)	38.3 (25.6 - 52.8)	46.8 (33.1 – 61)	57.4 (43.1 - 70.7)	63.8 (54.2 - 72.4)	65.7 (56.1 - 74.2)	73.3 (64.1 - 80.9)	80 (69 - 87.8)	81.4 (70.6 - 88.9)	87.1 (77.1 - 93.2)	(3)
Spike Pan ELISA	97.3 (95.9 - 98.5)	96.7 (95.2 – 98.1)	96.7 (95.2 – 98.1)	76.6 (62.5 - 86.6)	76.6 (62.5 - 86.6)	76.6 (62.5 - 86.6)	93.3 (88.6 – 97.1)	94.3 (87.8 - 98.1)	94.3 (87.8 - 98.1)	95.7 (87.5 - 98.6)	95.7 (87.5 - 98.6)	95.7 (87.5 - 98.6)	(1)
Spike-RBD Bridging LIPS	97.6 (96 - 98.6)	96 (94.1 - 97.4)	98.5 (97.1 - 99.2)	80.9 (67.1 - 89.7)	80.9 (67.1 - 89.7)	78.7 (64.8 - 88.2)	92.4 (85.5 - 96.1)	92.4 (85.5 - 96.1)	92.4 (85.5 - 96.1)	94.3 (85.7 - 97.8)	94.3 (85.7 - 97.8)	94.3 (85.7 - 97.8)	(3)

*Threshold method key: 1 - 99th Percentile; 2 - 98th percentile; 3 - Jmax i.e., highest Youden IndexFigure headings.
For each candidate screening assays, one value for specificity of the assays is reported, and sensitivity estimates are provided for COVID-19 samples taken at different time periods (Acute, Early Convalescent and Late Convalescent) post infection are reported for each of the threshold methods. Confidence intervals (95% CI) are given for each estimate. The optimal threshold methods was determined by finding the value which provided at least (or as near to) 98% specificity, whilst offering the optimal sensitivity.

we compared the WHO international standard to that of our in-house standard pool on a subset of the ELISAs (N Pan and IgG, Spike Pan and IgG). The WHO/NIBSC reference panel was used to compare antibody levels measured with our assays to the summary results using assays with similar antigen and antibody specificity from the inter-lab comparison study (28). Serial dilutions of both standards showed similar shaped curves when fitted to a 4PL regression and parallel lines (i.e. shared HillSlopes) for the two pools in all four assays (Figure 4E) thus allowing for conversion to international binding antibody units (BAU) values from the WHO standard to the in-house assays when using interpolation (Table S7); approximate BAU/ml values could also be assigned to the normalised OD thresholds. Furthermore, BAU/ml values identified on the in-house assay platforms were found to be comparable to the average values reported in the NIBSC inter-lab comparison (28), with the exception of samples with high levels of antibody, where the Spike Pan ELISA showed lower than expected levels, probably due to saturation of signal at this higher end of the assay signal range (Figure 4F).

3.7 Exploring the relationship between binding antibody assay signals and neutralizing activity

To identify any relationship between immunoassay results and the functional activity of antibodies in sera, assays were developed to measure virus neutralization *in vitro* which were then deployed on a subset of our samples. A microneutralization assay using SARS-CoV-2 virus was first used to measure virus neutralization in samples from n=31 RT-PCR confirmed COVID-19 cases and n=17 pre-pandemic samples from the threshold set, with results expressed as half maximal dilutions (ND50) (Figures 5A, B). The pre-pandemic samples included some that had shown high signals in one or more of the immunoassays (i.e. false positives), to explore whether these false positives relate to functional cross-reactive responses. We observed low levels of virus neutralization (ND50 <125) in only 4 of the 17 pre-pandemic samples, two of which displayed above-threshold immunoassay signals (one in the RBD Pan ELISA and another in the bridging assay). Amongst the samples from confirmed COVID-19 cases, samples with reasonable neutralizing capacity (ND50 >125) had results in the high positive range for the Spike and RBD-specific assays (e.g. > 0.72 normalized OD on the Spike Pan assay and >20 units on the Spike-RBD Bridging assay), but with the N Pan assay some strongly neutralizing samples showing normalized ODs around/below the optimal threshold for detection for an N-specific antibody response (Figure 5A). Agreement between the screening assay results and Log10 ND50 for neutralizing samples from individuals with known or unclear status (as measured with the SARS-CoV-2 microneutralization assay) was

10.3389/fimmu.2022.968317

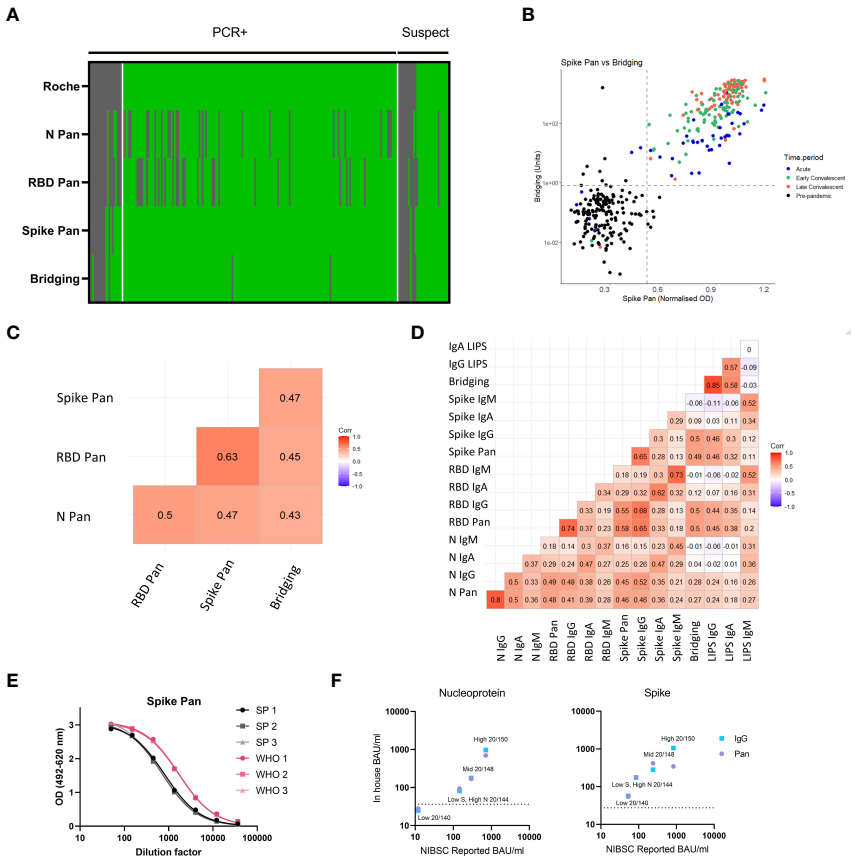

FIGURE 4
Comparing sensitivity of screening assays to a commercial assay (Roche Elecsys nucleocapsid) and correlation/concordance of all antibody assay results in samples within the validation set. **(A)** Heatmap comparing results of the 4 screening assays to the commercially available Roche Elecsys nucleocapsid assay in a cohort n = 218 individuals with RT-PCR confirmed or suspected COVID-19 (from the validation set). Samples are arranged in columns, split first by COVID-19 status followed by Roche Elecsys result. The results of each test assay is indicated in the different rows going downwards. Green indicates above positive threshold, grey negative. **(B)** Scatterplot showing the quantitative readouts from the top performing screening assays – Spike Pan ELISA and Spike-RBD Bridging LIPS assay with their best performing threshold indicated with dashed lines. The colours of point indicate the clinical group as shown in the key. **(C)** Correlogram reporting correlation coefficients using Kendall's tau of all 4 screening assays in full validation set including pre-pandemic samples (n = 806). **(D)** Correlogram showing the relationship between results of all 16 antibody assays in samples from COVID-19 cases (n = 222). **(E)** Comparison of the standard curves generated using either our in-house pooled serum standard, or the WHO/NIBSC international standard, by running these side by side on 3 plates of the N Pan and Spike Pan ELISAs. The curves were found to be parallel. From these plots a ratio could be calculated to allow for conversion to BAU/ml from in house standard. **(F)** BAU/ml values for 4 samples provided in the WHO/NIBSC reference panel, as calculated by a collaborative inter-lab comparison (X axis) compared to calculating using the in-house standard, on the N Pan/IgG and Spike Pan/IgG ELISAs.

determined using Kendall's rank correlation (Figure 5B). There was significant agreement in all cases, with the RBD Pan ELISA showing the highest tau coefficient (0.58). These results suggest agreement between the candidate screening assays results and functional capacity, but more so for the Spike-RBD specific assays that for the N Pan ELISA.

We also developed a pseudotype virus neutralization assay using vesicular stomatitis virus (VSV) expressing SARS-CoV-2 Spike protein and VeroE6 cells expressing ACE2 and TMPRSS2 and deployed this on a larger set of samples from COVID-19 cases from across the sample sets representing a range of antibody responses using the full suite of assays (i.e. total antibody and isotype specific). There was good correlation between the neutralizing titer values reported from the two assay platforms (Figure S5), but the pseudotype assays showed a wider dynamic range. Amongst the neutralizing samples the Spike IgA and IgG ELISA assays showed the strongest correlation with half maximal neutralization titer using this assay (Figure 5C).

3.8 Field testing of screening assays

To field test two of the best-performing screening assays for determining changes in serological status in a population of interest during a time of vaccination rollout, the N and Spike

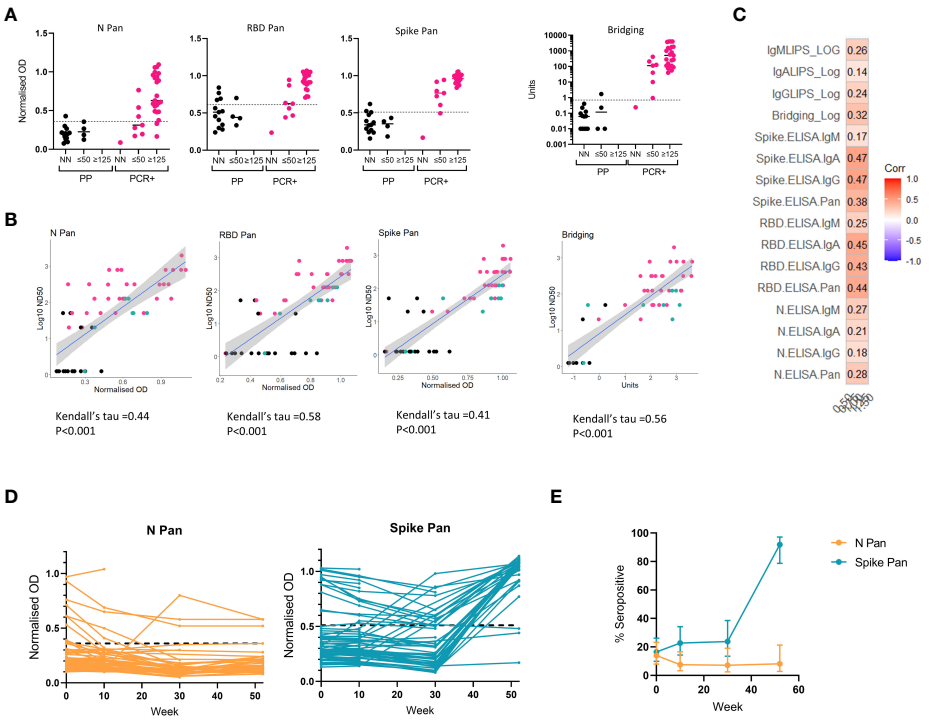

FIGURE 5
Relationship between binding antibody results and neutralization titers and application of screening assay to longitudinal cohort. On a subset of the samples from the threshold and validation sets, we compared screening assay results to neutralizing antibody titers were measured using a microneutralization assay using SARS-CoV-2 and a pseudotype viral neutralization assay using vesicular stomatitis virus (VSV) expressing Spike **(A-C)**. **(A)** A microneutralization assay was performed on 17 pre-pandemic serum samples and 31 from RT-PCR confirmed cases, and stratified the results into 3 groups: non neutralizing (ND); ND50 of 20 or 50 (≤50); ND50 of 125 or above (≥125) and compared these groupings to the screening assay results: N Pan ELISA; RBD Pan ELISA; Spike Pan ELISA; Spike-RBD Bridging LIPS assay (where readouts are normalised OD or Units). **(B)** The relationship between results from each screening assay results and ND50 measured using the microneutralization assay in n = 59 samples displayed in scatterplots from a mixture of pre-pandemic (black), PCR-confirmed COVID-19 cases (pink) and exposed individuals or recent COVID-19 suspects (green). with a line showing the smoothed mean determined using a generalized linear model +/- 95% confidence intervals; and correlation performed using Kendall's tau. **(C)** Correlogram showing the relationship between a novel pseudotype viral neutralization assay (using mouse VSV expressing SARS-CoV-2 Spike and ACE-2 and TMPRSS-2) and all 16 ELISA and LIPS assays (total antibody and isotype specific) in n = 36 samples with neutralising capacity. **(D)** Field testing two screening assays (N Pan and Spike Pan ELISA) on longitudinal samples from a cohort of n = 79 healthcare workers in Bristol in 2020 and 2021. **(E)** Observed seroprevalence/antibody positivity to N and Spike proteins using Pan ELISA assays in a cohort of n = 79 healthcare workers. Total samples collected at each timepoint were as follows: week 0, n=79; week 10, n=66; week 30, n = 42; week 52, n = 37. 95% confidence intervals were calculated using the Wilson method.

Pan ELISAs were deployed on serum samples collected longitudinally from a cohort of n=79 hospital-based healthcare workers over a one-year period from April 2020 – May 2021 (Figure 5D). At baseline the rate of seropositivity with N Pan and Spike Pan was very similar at 13.92% and 16.46% respectively, but then the rate declined for N Pan to around 7% whilst remaining stable for Spike between weeks 10 and 30 (Figure 5E). By week 52 (end of study), we observed a divergence in the proportion of positive cases reported by the 2 assays, with Spike Pan showing up to 91.89% (78.70-97.20%) seropositive against Spike whilst there was negligible change in the proportion found to be seropositive to the nucleocapsid antigen (N) during the same period [8.11% (95%CI 2.80-21.30%)], probably due to responses to vaccination among the majority of the cohort and low rates of new infections.

4 Discussion

We optimized and evaluated a suite of in-house ELISA and LIPS assays for detecting and measuring antibody responses to SARS-CoV-2 by adapting available protocols (7, 14, 24). Whilst such assays have been used widely to explore the heterogeneity of immune responses to SARS-CoV-2 infection and vaccination (11, 12, 29), few have simultaneously and rigorously evaluated two different platforms with shared standards and quality controls using the same well characterized, large sample collections. This approach facilitated accurate threshold setting to determine serological status. The Spike Pan ELISA and Spike-RBD Bridging LIPS assays demonstrated superior performance in a blinded head-to-head comparison with a widely used commercial assay. All assays were optimized for low blood

volume, low cost per sample and require relatively inexpensive laboratory equipment, paving the way for their use in a wide variety of settings and for a range of purposes, including population monitoring.

Initially the total antibody and isotype specific assays were compared for use as screening assays for recent SARS-CoV-2 infection in a subset of the threshold set. On both platforms, the assays measuring total antibody performed better than IgG, IgA or IgM specific assays in discriminating between samples from COVID-19 cases and pre-pandemic donors in the threshold sample set, and thus the four total antibody assays (N Pan, RBD Pan and Spike Pan ELISAs, and the Spike-RBD Bridging LIPS assay) were selected for validation as potential screening assays using a large, blinded validation set from pre-pandemic donors and confirmed/suspected COVID-19 cases. The superiority of the total antibody assays as sensitive tests for recent infection has been observed by others (30) and is unsurprising given the varying kinetics in antibody isotype responses over time, with a predominance of IgM and IgA isotypes in the acute stages followed by a dominant IgG response in most individuals after 21 days post infection (12). Importantly, our COVID-19 validation set included a wide spectrum of cases, including those with no or mild symptoms, who are likely to represent a large proportion of unknown community cases and clinically suspected hospitalized cases who may not have been tested for the virus at the optimal time. All total antibody assays achieved >97% specificity using at least one of the pre-defined thresholds. Sensitivity estimates for detection of recent COVID-19 cases varied but was highest for all assays when samples taken in late convalescence (>12 weeks post symptom onset) were used. The Spike Pan and Spike-RBD Bridging LIPS assays performed the best overall, providing up to 95% sensitivity for COVID-19 cases. Whilst not as sensitive as the two best performing screening assays, the N Pan and RBD Pan ELISAs provided a high level of specificity and could detect up to 82% and 73% of cases respectively. When sensitivities of the candidate screening assays were compared directly to the commercial Roche Elecsys N assay, the Spike Pan ELISA and the Spike-RBD LIPS Bridging assays detected cases missed by the Roche assay and offered improved sensitivity despite using a 100-fold smaller volume of sample. Others have demonstrated that responses to the nucleocapsid wane more quickly than to Spike/RBD and optimal sensitivity for recent COVID-19 cases can be achieved with Spike-based assays (31). However a serology testing consortium (Oxford, UK) also reported a highly sensitive, specific and scalable anti-Spike IgG in-house ELISA which performed comparably to or better than commercial antibody assays in terms of diagnostic accuracy (32). Therefore, in-house assays can offer high diagnostic accuracy and are suitable for population level surveillance.

We directly compared the ELISA and LIPS platforms by focusing on the RBD-specific antibody assays (as the antigen was common). On the ELISA platform, the RBD assays performed less well than the Spike assays. However, the detection of RBD-specific antibodies by the novel Spike-RBD Bridging LIPS assay was better than the RBD Pan ELISA (sensitivities of 92.4% (95% CI 85.5-96.1) and 73.3 (95% CI 64.1-80.9), respectively, for infections confirmed by RT-PCR >21 days previously). As has been reported elsewhere for COVID-19 bridging antibody assays, the Spike-RBD Bridging LIPS assay results showed an upward trend in antibody levels over time since infection (33, 34) compared to a decline in levels observed with the corresponding RBD ELISA assays. It is likely that the bridging antigen format and the use of antigen competition for the IgG and IgA assays, select for higher affinity antibodies resulting in improved accuracy for discriminating between pre-pandemic and COVID-19 samples (34), but potentially also reflects affinity maturation due to somatic hypermutation in the weeks following priming. The bridging antigen format is used in other assays including the commercially available Roche Elecsys S and N assays but has not previously been applied to LIPS assays. LIPS has been found to offer improved diagnostic performance over other immunoassays including ELISA when deployed for detecting specific antibodies involved in identifying cases of autoimmune or infectious diseases (35). When measuring antibody levels in one sample dilution, the LIPS platform also provides a broader dynamic range. In contrast to ELISA, the isotype-specific LIPS assays should not be affected by within-well competition from other antibody isotypes, which may also explain the differences observed in this comparison. In conclusion, we found LIPS assays to be highly sensitive for the measurement of SARS-CoV-2 RBD specific antibodies, which may offer unique information on the affinity of antibody binding when compared to other platforms. Further investigation into why antibody kinetics are profiled differently for the same samples measured using assays from different platforms will inform the optimal use of each platform for a given purpose relating to the measurement of specific antibody (e.g. as a proxy for a functional responses versus accurately quantifing antibody decay rates).

ELISA and LIPS assays measure levels of binding antibody to specific antigens, but these measurements do not necessarily correlate accurately with antibody-mediated protection. Neutralization assays are widely deployed to monitor functional antibody responses to SARS-CoV-2 and nAb levels have been shown to correlate with protection against re-infection and/after vaccination (36). However, in this study and others, binding antibody levels (particularly IgG/total antibody to the RBD and/or Spike antigens) correlated strongly with nAb levels when measured using two different neutralization assays (37), and have been shown to correlate with protection (4). Thus, to some extent, binding antibody assays specific to RBD and Spike can be used as surrogates for functional, protective antibody responses. Further work may lead to the identification of binding antibody thresholds of our candidate assays indicative of protection and/or sufficient levels

of nAbs. We identified some false positive ELISA/LIPS samples in the pre-pandemic sample sets, and 4 samples with low level neutralizing capacity, which could reflect the presence of cross-reactive antibodies in these samples perhaps resulting from other CoV infections. Interestingly, there was little agreement across the different assays in terms of which samples were identified as positive amongst pre-pandemic samples, even among those that were tested by neutralization -i.e. not all with neutralizing capacity demonstrated binding to RBD/Spike. This suggests that false positive pre-pandemic samples were not the result of cross-reactive antibody responses. Unlike Ng et al, who reported that antibodies from pre-pandemic samples had binding capacity to the S2 portion of Spike (17), we did not observe binding to Spike in the 4 pre-pandemic samples with low neutralizing capacity.

We demonstrate the feasibility of assigning international BAU to samples measured with our assays, and report similar levels of antibody to other laboratories who contributed to the development of international reference standards (28, 38), allowing comparison of results from our assays with others. We deployed two of the screening assays (Spike and N Pan ELISA) on samples from a longitudinal cohort of healthcare workers in Bristol, UK (LOGIC). These data suggest comparable sensitivity for recent infection prior to vaccination rollout in the UK but, as expected, an increase in anti-Spike specific responses was observed after vaccination was introduced and the seropositivity rate was very high (>95%) by the end of the 12 month follow up period (31st May 2021), causing a divergence in the relative seropositive rates within the cohort. As such, using a combination of our assays to measure antibody positivity rates in order to estimate recent infection and/or vaccination exposures is feasible. In countries/areas with high vaccination coverage, the nucleocapsid specific assays are therefore increasingly of relevance for seroprevalence studies, whilst Spike/RBD assays (as well as neutralizing antibody assays) are less able to differentiate vaccination-specific from infection-specific immunity, but are probably better correlates of immunity. However, not all vaccines are Spike-only (e.g., the Valneva vaccine contains the whole virion), and the relative rate of seroconversion to nucleocapsid after prior exposure to Spike *via* vaccination (compared to naïve individuals) has not been ascertained. Thus, there are important considerations to bear in mind when using nucleocapsid assays to determine recent infection amongst vaccinated individuals.

Strengths of this study include rigorous development of high performance, low blood volume, cost-effective tests which can be easily deployed in a variety of settings, but our approach also has several limitations. Firstly, whilst samples from pre-pandemic children were included, samples from children with COVID-19 were not available to us and as such, assay performance for detecting recent pediatric infections cannot be reported. However, since widespread vaccination of children is not currently common in many countries while asymptomatic/mild pediatric infections are, antibody assays offer a useful tool for monitoring infection in this age group. The antigens used in the in-house assays were generated using the genetic sequence from the parent Wuhan strain of SARS-CoV-2 first described in 2020 (7) from which several new variants of concern (VOC) have evolved and have caused significant waves of infection globally. Some of these variants, especially Omicron, include multiple mutations in these target antigens and as such, may lead to antibody responses with differential binding to the target antigens. Indeed, antibodies responses raised to antigens from one SARS-CoV-2 variant genetic sequence lead to differential ability to neutralize VOC strains. However, whilst others have shown reduced binding to antigens from sequences of VOCs, rates of seropositivity when using different antigens, and/or from people who were infected with non-Wuhan variants, appear to be relatively unchanged (39, 40). It will be important to monitor changes in antibody assay performance for detecting recent infection as new variants emerge and become dominant.

In summary, we present a blueprint for the development and evaluation of low volume antibody assays for screening for seropositive individuals and/or profiling of serum isotype-specific antibody responses after SARS-CoV-2 infection and/or vaccination. With the use of appropriate controls, these assays offer a low cost and reliable alternative to commercial assays and can be used with simple laboratory equipment, potentially allowing for infection/immunity monitoring in hard-to-reach communities (*via* field or at-home sampling) and in low-income settings where other testing approaches are not feasible. Evaluation of one or more of these assays in areas where epidemiological information on COVID-19 is sparse, could be of great value.

Data availability statement

The majority of the data relating to the analyses/ findings presented in this article are available upon request from the University of Bristol data repository at the following link: https://doi.org/10.5523/bris.3bo7kz80s21fy2oknckvi8xq18. The informed consent obtained from two pre-pandemic cohorts, 'ALSPAC cohort' and 'healthy control adults' (see Table 1), do not allow the data to be made freely available through any third party maintained public repository. However, data from these samples/donors used for this article (all part of the threshold setting aspects of the study) can be made available on request to the ALSPAC Executive. The ALSPAC data management plan describes in detail the policy regarding data sharing, which is through a system of managed open access. Full instructions for applying for data access can be found here: http://www.bristol.ac.uk/alspac/researchers/access/. The ALSPAC study website contains details of all the data that are available (http://www.bristol.ac.uk/alspac/researchers/our-data/).

Ethics statement

This study involved human samples from multiple collections and collected under various ethical approvals. Details of these are found in Section 2.1 and Table 1 in the Methods. Written informed consent for the use of these samples was provided by the participants themselves, or the participants' legal guardian/next of kin.

Author contributions

AH, AL, HB, ACT, AF, DW, MB, AW, and KMG conceived/designed the study. AG, JaM, RB, CP, FH, and DA recruited recently infected SARS-CoV-2 participants/donors and healthcare workers. EO, MG, LK, AH, HB, LC, JO, BM-A, LW, LR, SR, NT, FH, DA, AMT, KC, and KMG sourced, provided, and/or processed samples. KG, NB, AMT, and IB produced antigens. HB, AH, EO, BH, JS, and UO performed the ELISAs. MR, YB-K, IK, GM, OB, and KC performed the LIPS labwork. MS, LP, and VL provided LIPS reagents. JoM and PM performed the Roche Elecsys nucleocapsid bridging assay. OF, MW, LW, and AD developed and performed the pseudo neutralization and neutralization assays. AH, AL, HB, CP, ACT, and KS performed the data analysis. AH, AL, HB, KS, and KMG wrote the manuscript. All authors contributed to the article and approved the submitted version.

Funding

This work was supported by multiple grants to AH, AL, OF, AMT, and IB awarded by the Elizabeth Blackwell Institute, and funded in part by the Wellcome Trust [Grant number 204813/Z/16/Z] with additional support from Bristol Alumni and Friends. AL is funded by a Diabetes UK/JDRF RD Lawrence Fellowship (18/0005778 and 3-APF-2018-591-A-N). The DISCOVER study was supported by donations to Southmead Hospital Charity (Registered Charity Number: 1055900). The LOGIC study was funded by The Grand Appeal (The Official Bristol Children's Hospital Charity; a registered charity in England and Wales (1043603)) through a grant awarded to AF and AG. ACT is supported by the Wellcome Trust (217509/Z/19/Z) and UKRI through the JUNIPER consortium MR/V038613/1 and CoMMinS study MR/V028545/1. The UK Medical Research Council and Wellcome (Grant ref: 217065/Z/19/Z) and the University of Bristol provide core support for ALSPAC. NT is a Wellcome Trust Investigator (202802/Z/16/Z), is the PI of the Avon Longitudinal Study of Parents and Children (MRC & WT 217065/Z/19/Z), is supported by the University of Bristol NIHR Biomedical Research Centre (BRC-1215-2001), the MRC Integrative Epidemiology Unit (MC_UU_00011/1) and works within the CRUK Integrative Cancer Epidemiology Programme (C18281/A29019). LIPS assay development was supported by a joint grant from Diabetes UK/JDRF (20/0006217) to KMG. IB is supported by the Wellcome Trust (106115/Z/14/Z, 221708/Z/20/Z), the ERC (contr. nrs. 834631, 963992) and the EPSRC Impact Acceleration Account EP/R511663/1. We also acknowledge funding from BBSRC/EPSRC Synthetic Biology Research Centre (BB/L01386X/1, to DNW, NB and AMT), NHS Blood and Transplant (WP15-05, to NB and AMT), and the NIHR Blood and Transplant Research Unit in Red Cell Products (IS-BTU-1214-10032, to NB and AMT). This publication is the work of the authors and AH et al. will serve as guarantors for the contents of this paper.

Acknowledgments

We dedicate this manuscript to our colleague and friend, Alistair Williams, who sadly passed away in September 2020 after a brave battle with cancer. Alistair was an expert in autoantibody assay development and used this expertise to guide us through incorporation of optimal standardization and quality control approaches. We are extremely grateful to all the donors (COVID-19 cases and pre-pandemic donors) who provided serum and plasma samples for scientific research; this project highlights the value of Biobank/sample collections for scientific research and development. For those samples from the ALSPAC study, we also thank the midwives for their help in recruiting the study participants, and the whole ALSPAC team, which includes interviewers, computer and laboratory technicians, clerical workers, research scientists, volunteers, managers, receptionists, and nurses. We thank Hayley Jones for guidance on the statistics and analytical approach. We thank Jill King for support in recruitment of Biobank donors, and Helen Thompson for support in coordinating sample donations *via* the Biobank, and for wider administrative support. We thank Leigh Johnson and Douglas Owen for supporting sample collection for the LOGIC study. We are grateful for the Bristol UNCOVER community for advice, guidance and support over the past 2 years. This article was made freely available prior to peer review and publication on medRxiv (41).

Conflict of interest

AF is a member of the Joint Committee on Vaccination and Immunisation, the UK National Immunisation Technical Advisory Group and is chair of the WHO European Regional Technical Advisory Group of Experts (ETAGE) on immunization and *ex officio* a member of the WHO SAGE working group on COVID vaccines. He is investigator COVID-19 vaccine on studies and trials funded by Pfizer, Sanofi, Valneva, the Gates Foundation and the UK government. This manuscript presents independent research funded in part by the National Institute for Health Research (NIHR). The views expressed are those of the

authors and not necessarily those of the NHS, the NIHR, or the Department of Health and Social Care.

The remaining authors declare that the research was conducted in the absence of any commercial or financial relationships that could be construed as a potential conflict of interest.

Publisher's note

All claims expressed in this article are solely those of the authors and do not necessarily represent those of their affiliated organizations, or those of the publisher, the editors and the reviewers. Any product that may be evaluated in this article, or claim that may be made by its manufacturer, is not guaranteed or endorsed by the publisher.

Supplementary material

The Supplementary Material for this article can be found online at: https://www.frontiersin.org/articles/10.3389/fimmu.2022.968317/full#supplementary-material

References

1. *COVID-19 weekly epidemiological update*. World Health Organization (2022). Geneva, Switzerland. Available at: https://www.who.int/emergencies/diseases/novel-coronavirus-2019/situation-reports

2. Hall VJ, Foulkes S, Charlett A, Atti A, Monk EJM, Simmons R, et al. SARS-CoV-2 infection rates of antibody-positive compared with antibody-negative health-care workers in England: A large, multicentre, prospective cohort study (SIREN). *Lancet* (2021) 397(10283):1459–69. doi: 10.1016/S0140-6736(21)00675-9

3. Jonczyk R, Stanislawski N, Seiler LK, Blume H, Heiden S, Lucas H, et al. Combined prospective seroconversion and PCR data of selected cohorts indicate a high rate of subclinical SARS-CoV-2 infections-an open observational study in lower Saxony, Germany. *Microbiol Spectr.* (2022) 10(1):e0151221–e. doi: 10.1128/spectrum.01512-21

4. Earle KA, Ambrosino DM, Fiore-Gartland A, Goldblatt D, Gilbert PB, Siber GR, et al. Evidence for antibody as a protective correlate for COVID-19 vaccines. *Vaccine* (2021) 39(32):4423–8. doi: 10.1016/j.vaccine.2021.05.063

5. Cromer D, Steain M, Reynaldi A, Schlub TE, Wheatley AK, Juno JA, et al. Neutralising antibody titres as predictors of protection against SARS-CoV-2 variants and the impact of boosting: A meta-analysis. *Lancet Microbe* (2022) 3 (1):e52–61. doi: 10.1016/S2666-5247(21)00267-6

6. Hyder AA, Hyder MA, Nasir K, Ndebele P. Inequitable COVID-19 vaccine distribution and its effects. *Bull World Health Organ*. World Health Organization (2021). 99(6):406-406A. doi: 10.2471/BLT.21.285616

7. Amanat F, Stadlbauer D, Strohmeier S, Nguyen THO, Chromikova V, McMahon M, et al. A serological assay to detect SARS-CoV-2 seroconversion in humans. *Nat Med* (2020) 26(7):1033–6. doi: 10.1038/s41591-020-0913-5

8. Grzelak L, Temmam S, Planchais C, Demeret C, Tondeur L, Huon C, et al. A comparison of four serological assays for detecting anti-SARS-CoV-2 antibodies in human serum samples from different populations. *Sci Transl Med* (2020) 12(559). doi: 10.1126/scitranslmed.abc3103

9. Atti A, Ferrari M, Castillo-Olivares J, Monk EJM, Gopal R, Patel M, et al. Serological profile of first SARS-CoV-2 reinfection cases detected within the SIREN study. *J Infection.* (2022) 84(2):248–88. doi: 10.1016/j.jinf.2021.09.019

10. Jones HE, Mulchandani R, Taylor-Phillips S, Ades AE, Shute J, Perry KR, et al. Accuracy of four lateral flow immunoassays for anti SARS-CoV-2 antibodies: a head-to-head comparative study. *EBioMedicine* (2021) 68. doi: 10.1016/j.ebiom.2021.103414

11. Letizia AG, Ge Y, Vangeti S, Goforth C, Weir DL, Kuzmina NA, et al. SARS-CoV-2 seropositivity and subsequent infection risk in healthy young adults: a prospective cohort study. *Lancet Respir Med* (2021) 9(7):712–20. doi: 10.1016/S2213-2600(21)00158-2

12. Dan JM, Mateus J, Kato Y, Hastie KM, Yu ED, Faliti CE, et al. Immunological memory to SARS-CoV-2 assessed for up to 8 months after infection. *Science* (2021) ;371(6529):eabf4063. doi: 10.1126/science.abf4063

13. Haljasmägi L, Remm A, Rumm AP, Krassohhina E, Sein H, Tamm A, et al. LIPS method for the detection of SARS-CoV-2 antibodies to spike and nucleocapsid proteins. *Eur J Immunol* (2020) 50(8):1234–6. doi: 10.1002/eji.202048715

14. Secchi M, Bazzigaluppi E, Brigatti C, Marzinotto I, Tresoldi C, Rovere-Querini P, et al. COVID-19 survival associates with the immunoglobulin response to the SARS-CoV-2 spike receptor binding domain. *J Clin Invest.* (2020) 130 (12):6366–78. doi: 10.1172/JCI142804

15. Kurtz AB, DiSilvio L, Bosi E. The determination of detection limits for insulin antibody assays. *Diabetologia* (1988) 31(6):395–9. doi: 10.1007/BF02341510

16. Garcia-Beltran WF, Lam EC, Astudillo MG, Yang D, Miller TE, Feldman J, et al. COVID-19-neutralizing antibodies predict disease severity and survival. *Cell* (2021) 184(2):476–88.e11. doi: 10.1016/j.cell.2020.12.015

17. Ng KW, Faulkner N, Cornish GH, Rosa A, Harvey R, Hussain S, et al. Preexisting and *de novo* humoral immunity to SARS-CoV-2 in humans. *Science* (2020) 370(6522):1339–43. doi: 10.1126/science.abe1107

18. Deeks JJ, Dinnes J, Takwoingi Y, Davenport C, Spijker R, Taylor-Phillips S, et al. Antibody tests for identification of current and past infection with SARS-CoV-2. *Cochrane Database Syst Rev* (2020) 6(6):Cd013652. doi: 10.1002/14651858.CD013652

19. Boyd A, Golding J, Macleod J, Lawlor DA, Fraser A, Henderson J, et al. Cohort profile: The 'Children of the 90s'–the index offspring of the Avon longitudinal study of parents and children. *Int J Epidemiol* (2012) 42(1):111–27. doi: 10.1093/ije/dys064

20. Fraser A, Macdonald-Wallis C, Tilling K, Boyd A, Golding J, Davey Smith G, et al. Cohort profile: the Avon longitudinal study of parents and children: ALSPAC mothers cohort. *Int J Epidemiol* (2013) 42(1):97–110. doi: 10.1093/ije/dys066

21. Santos Ferreira DL, Maple HJ, Goodwin M, Brand JS, Yip V, Min JL, et al. The effect of pre-analytical conditions on blood metabolomics in epidemiological studies. *Metabolites* (2019) 9(4):64. doi: 10.3390/metabo9040064

22. Berger I, Fitzgerald DJ, Richmond TJ. Baculovirus expression system for heterologous multiprotein complexes. *Nat Biotechnol* (2004) 22(12):1583–7. doi: 10.1038/nbt1036

23. Goenka A, Halliday A, Gregorova M, Milodowski E, Thomas A, Williamson MK, et al. Young infants exhibit robust functional antibody responses and restrained IFN-gamma production to SARS-CoV-2. *Cell Rep Med* (2021) 2 (7):100327. doi: 10.1016/j.xcrm.2021.100327

24. Stadlbauer D, Amanat F, Chromikova V, Jiang K, Strohmeier S, Arunkumar GA, et al. SARS-CoV-2 seroconversion in humans: A detailed protocol for a serological assay, antigen production, and test setup. *Curr Protoc Microbiol* (2020) 57(1):e100. doi: 10.1002/cpmc.100

25. Whitt MA. Generation of VSV pseudotypes using recombinant ΔG-VSV for studies on virus entry, identification of entry inhibitors, and immune responses to vaccines. *J Virological Methods* (2010) 169(2):365–74. doi: 10.1016/j.jviromet.2010.08.006

26. Rihn SJ, Merits A, Bakshi S, Turnbull ML, Wickenhagen A, Alexander AJT, et al. A plasmid DNA-launched SARS-CoV-2 reverse genetics system and coronavirus toolkit for COVID-19 research. *PloS Biol* (2021) 19(2):e3001091. doi: 10.1371/journal.pbio.3001091

27. Cohen JF, Korevaar DA, Altman DG, Bruns DE, Gatsonis CA, Hooft L, et al. STARD 2015 guidelines for reporting diagnostic accuracy studies: Explanation and elaboration. *BMJ Open* (2016) 6(11):e012799. doi: 10.1136/bmjopen-2016-012799

28. Mattiuzzo G, Bentley EM, Hassall M, Routley S, Richardson S, Bernasconi V, et al. Establishment of the WHO International Standard and Reference Panel for anti-SARS-CoV-2 antibody. (2020) WHO Expert Committee on Biological Standardization. Geneva. WHO/BS/2020.2403

29. Ripperger TJ, Uhrlaub JL, Watanabe M, Wong R, Castaneda Y, Pizzato HA, et al. Orthogonal SARS-CoV-2 serological assays enable surveillance of low-

prevalence communities and reveal durable humoral immunity. *Immunity* (2020) 53(5):925–33.e4. doi: 10.1016/j.immuni.2020.10.004

30. Faustini SE, Jossi SE, Perez-Toledo M, Shields AM, Allen JD, Watanabe Y, et al. Development of a high-sensitivity ELISA detecting IgG, IgA and IgM antibodies to the SARS-CoV-2 spike glycoprotein in serum and saliva. *Immunology* (2021). 164:135–147. doi: 10.1111/imm.13349

31. Whitcombe AL, McGregor R, Craigie A, James A, Charlewood R, Lorenz N, et al. Comprehensive analysis of SARS-CoV-2 antibody dynamics in New Zealand. *Clin Transl Immunol* (2021) 10(3):e1261. doi: 10.1002/cti2.1261

32. National SARS-CoV-2 Serology Assay Evaluation Group, Ainsworth M, Auckland K, Baillie JK, Barnes E, Beer S, et al. Performance characteristics of five immunoassays for SARS-CoV-2: A head-to-head benchmark comparison. *Lancet Infect Dis* (2020) 20(12):1390–400. doi: 10.1016/S1473-3099(20)30634-4

33. Harris RJ, Whitaker HJ, Andrews NJ, Aiano F, Amin-Chowdhury Z, Flood J, et al. Serological surveillance of SARS-CoV-2: Six-month trends and antibody response in a cohort of public health workers. *J Infection.* (2021) 82(5):162–9. doi: 10.1016/j.jinf.2021.03.015

34. Theel ES, Johnson PW, Kunze KL, Wu L, Gorsh AP, Granger D, et al. SARS-CoV-2 serologic assays dependent on dual-antigen binding demonstrate diverging kinetics relative to other antibody detection methods. *J Clin Microbiol* (2021) 0(ja): JCM.01231-21. doi: 10.1128/JCM.01231-21

35. Liberati D, Wyatt RC, Brigatti C, Marzinotto I, Ferrari M, Bazzigaluppi E, et al. A novel LIPS assay for insulin autoantibodies. *Acta Diabetol* (2018) 55 (3):263–70. doi: 10.1007/s00592-017-1082-y

36. Khoury DS, Cromer D, Reynaldi A, Schlub TE, Wheatley AK, Juno JA, et al. Neutralizing antibody levels are highly predictive of immune protection from symptomatic SARS-CoV-2 infection. *Nat Med* (2021) 27(7):1205–11. doi: 10.1038/s41591-021-01377-8

37. Castillo-Olivares J, Wells DA, Ferrari M, Chan ACY, Smith P, Nadesalingam A, et al. Analysis of serological biomarkers of SARS-CoV-2 infection in convalescent samples from severe, moderate and mild COVID-19 cases. *Front Immunol* (2021) 12. doi: 10.3389/fimmu.2021.748291

38. Kristiansen PA, Page M, Bernasconi V, Mattiuzzo G, Dull P, Makar K, et al. WHO international standard for anti-SARS-CoV-2 immunoglobulin. *Lancet* (2021) 397(10282):1347–8. doi: 10.1016/S0140-6736(21)00527-4

39. Faustini S, Shields A, Banham G, Wall N, Al-Taei S, Tanner C, et al. Cross reactivity of spike glycoprotein induced antibody against delta and omicron variants before and after third SARS-CoV-2 vaccine dose in healthy and immunocompromised individuals. *J Infection* (2022) 84(4):579–613. doi: 10.1016/j.jinf.2022.01.002

40. Edara VV, Norwood C, Floyd K, Lai L, Davis-Gardner ME, Hudson WH, et al. Infection- and vaccine-induced antibody binding and neutralization of the b. *1.351 SARS-CoV-2 variant. Cell Host Microbe* (2021) 29(4):516–21.e3. doi: 10.1016/j.chom.2021.03.009

41. Halliday A, Long AE, Baum HE, Thomas AC, Shelley KL, Oliver E, et al. Development and evaluation of low-volume tests to detect and characterise antibodies to SARS-CoV-2. *medRxiv* (2022):2022.05.03.22274395. doi: 10.1101/2022.05.03.22274395

COPYRIGHT

© 2022 Halliday, Long, Baum, Thomas, Shelley, Oliver, Gupta, Francis, Williamson, Di Bartolo, Randell, Ben-Khoud, Kelland, Mortimer, Ball, Plumptre, Chandler, Obst, Secchi, Piemonti, Lampasona, Smith, Gregorova, Knezevic, Metz, Barr, Morales-Aza, Oliver, Collingwood, Hitchings, Ring, Wooldridge, Rivino, Timpson, McKernon, Muir, Hamilton, Arnold, Woolfson, Goenka, Davidson, Toye, Berger, Bailey, Gillespie, Williams and Finn. This is an open-access article distributed under the terms of the Creative Commons Attribution License (CC BY). The use, distribution or reproduction in other forums is permitted, provided the original author(s) and the copyright owner(s) are credited and that the original publication in this journal is cited, in accordance with accepted academic practice. No use, distribution or reproduction is permitted which does not comply with these terms.

frontiers | Frontiers in Immunology

TYPE Review
PUBLISHED 22 November 2022
DOI 10.3389/fimmu.2022.1053437

Check for updates

OPEN ACCESS

EDITED BY
Ralf Braun,
Danube Private University, Austria

REVIEWED BY
Stephen Crooke,
Centers for Disease Control and Prevention (CDC), United States
Mariah Hassert,
The University of Iowa, United States

*CORRESPONDENCE
Feiting Xie
xiefeiting@zju.edu.cn

SPECIALTY SECTION
This article was submitted to Viral Immunology, a section of the journal Frontiers in Immunology

RECEIVED 25 September 2022
ACCEPTED 09 November 2022
PUBLISHED 22 November 2022

CITATION
Zhu Q, Xu Y, Wang T and Xie F (2022) Innate and adaptive immune response in SARS-CoV-2 infection-Current perspectives.
Front. Immunol. 13:1053437.
doi: 10.3389/fimmu.2022.1053437

COPYRIGHT
© 2022 Zhu, Xu, Wang and Xie. This is an open-access article distributed under the terms of the Creative Commons Attribution License (CC BY). The use, distribution or reproduction in other forums is permitted, provided the original author(s) and the copyright owner(s) are credited and that the original publication in this journal is cited, in accordance with accepted academic practice. No use, distribution or reproduction is permitted which does not comply with these terms.

Innate and adaptive immune response in SARS-CoV-2 infection-Current perspectives

Qiugang Zhu[1], Yan Xu[2], Ting Wang[3] and Feiting Xie[4]*

[1]Department of Laboratory Medicine, Shangyu People's Hospital of Shaoxing, Shaoxing, China, [2]Department of Respiratory Medicine, Shangyu People's Hospital of Shaoxing, Shaoxing, China, [3]Department of Laboratory Medicine, Affiliated Hospital of Jiangsu University, Zhenjiang, China, [4]Zhejiang Provincial Key Laboratory of Precision Diagnosis and Therapy for Major Gynecological Diseases, Women's Hospital, Zhejiang University School of Medicine, Hangzhou, China

Coronavirus disease 2019 (COVID-19) has been a global pandemic, caused by a novel coronavirus strain with strong infectivity, severe acute respiratory syndrome coronavirus 2 (SARS-CoV-2). With the in-depth research, the close relationship between COVID-19 and immune system has been dug out. During the infection, macrophages, dendritic cells, natural killer cells, $CD8^+$ T cells, Th1, Th17, Tfh cells and effector B cells are all involved in the anti-SARS-CoV-2 responses, however, the dysfunctional immune responses will ultimately lead to the excessive inflammation, acute lung injury, even other organ failure. Thus, a detailed understanding of pertinent immune response during COVID-19 will provide insights in predicting disease outcomes and developing appropriate therapeutic approaches. In this review, we mainly clarify the role of immune cells in COVID-19 and the target-vaccine development and treatment.

KEYWORDS

COVID-19, SARS-CoV-2, immune responses, vaccination, treatment

1 Introduction

In December 2019, severe acute respiratory syndrome coronavirus 2 (SARS-CoV-2) emerged in Wuhan, China, a novel coronavirus that has never been reported before.The disease caused by SARS-CoV-2 is known as coronavirus disease 2019 (COVID-19), has spread rapidly in China and all over the world due to the high transmissibility, threatening human health and public safety (1). Clinical symptoms that patients exhibit include pyrexia, fatigue, cough, and even lead to organ function damage (2). Over the past years, the investigation of the interaction between the "attacker" and the "defender" has provided us more supporting evidences on host immune responses and the plan for therapeutic vaccines and drugs in the future. In this review, we mainly discuss the innate and the adaptive immune responses in COVID-19 to provide a deeper

insight into the disease pathogenesis, thereby providing more information for COVID-19 treatments exploration.

2 Structure, infection and epidemiology of SARS-CoV-2

As a novel coronavirus, 79% and 50% genome sequence identity of SARS-CoV-2 are similar to SARS-CoV and Middle East respiratory syndrome coronavirus (MERS-CoV), respectively (3). There are six functional open reading frames in SARS-CoV-2, including ORF1a/ORF1b, spike (S), envelope (E), membrane (M) and nucleocapsid (N) from 5' to 3' in the genome (4). Up to now, real-time reverse transcriptase-polymerase chain reaction (RT-PCR) assays for SARS-CoV-2 nucleic acid mainly targeting ORF1a/1b, N, E and S genes are considered as the gold standard for confirming SARS-CoV-2 infection in patients (5). In addition, the amino acid identity of structural and non-structural proteins encoded by SARS-CoV-2 is similar to SARS-CoV. Apart from spike, another three structural proteins (envelope-membrane-nucleocapsid) have more than 90% amino acid identity with SARS-CoV, and most non-structural proteins are above 85% (3, 6).

The spike (S)-glycoprotein contains two functional domains, the amino (N)-terminal and carboxyl (C)-terminal named S1 subunit and S2 subunit, respectively (7). S1 subunit includes a receptor-binding domain (RBD), which is a key site in mediating the fusion of SARS-CoV-2 and host cell membrane during the infection. Being different from S1 subunit, the S2 subunit is a coiled helix structurethat contains a hydrophobic fusion loop and two heptad repeat regions. Previous reports have revealed these two domains exist as homo-trimer spikes and bind to the human Angiotensin-converting enzyme 2 (ACE2) host cell receptor in an accessible conformation *via* RBD domain of S1 subunit (8).

ACE2, a well-known receptor of SAR-CoV, has also been revealed to be the receptor of S-glycoprotein in SARS-CoV-2. ACE2 is widely expressed in human, bats, pangolins, pigs, ferrets, rhesus monkeys, civets, cats and dogs, which implies a wide host range of SARS-CoV-2 (9). For humans, the invasion of SARS-CoV-2 was not determined solely by ACE2 expression but also the assist by other factors (such as host proteases). For instance, the expression of ACE2 was limited in the respiratory tract which were favored by SARS-CoV-2 (10).

In the initial stage of infection, S1 protein binds to ACE2 *via* the RBD and then S1 protein shed from the virus surface, prompting the S2 domain membrane fusion with host cell (Figure 1) (11, 12). This process must be activated by cleavage of the S1 protein by the host protease to activate the S protein, including transmembrane protease serine protease 2 (TMPRSS2), cathepsin L and furin (11, 13). The study suggested that TMPRSS2 could be hired for the priming of SARS-CoV-2 S protein, which contributed to the fusion of the virus with the host cell membrane (13). Also, it could cooperate with cathepsin L to generate the cumulative effects in the fusion process (11). Additionally, other membrane proteins have also been confirmed to involve in this process. Interestingly, researchers from Peking University found that LDLRAD3, TMEM30A and CLEC4G effectively mediated virus invasion into cells in an ACE2-independent manner (14).

Similar to other coronaviruses, variants of SARS-CoV-2 have emerged in the past few years, and the main prevalent variant in the world today is Omicron variant (15–17). Variants might influence the epidemiological characteristics and clinical symptoms of COVID-19, even reducing the protection established by neutralizing antibodies and vaccines. Therefore, comprehending the immune responses to SARS-CoV-2 is of great importance for future vaccination and therapy.

Age is one of the main factors affecting the COVID-19 severity. Previous studies showed that every age group was susceptible to SARS-CoV-2, and in contrast to children (0-14 years old), old adults (above 65 years old), especially those with underlying diseases, are prone to develop severe respiratory diseases or even die (2, 18). Notably, some studies reported that SARS-CoV-2 could be transmitted to the fetus from pregnant women with COVID-19 through the placenta (19–21). Thus, all population are susceptible to SARS-CoV-2 through different ways.

3 Immune responses in COVID-19

Along with the deepening of research, the role of immune cells in the anti-SARS-CoV-2 response has increasingly being recognized. In the following description, we will discuss both innate and adaptive immune responses in COVID-19 (Figure 2 and Table 1).

3.1 Innate immune responses in COVID-19

3.1.1 Monocyte/Macrophage

Macrophages are myeloid immune cells that are involve in inflammation and tissue reparation. In lung, macrophages are divided into alveolar macrophages and interstitial macrophages. The former are mainly distributed near type I/II epithelial alveolar cells, while the latter preferentially reside between the microvascular endothelium and alveolar epithelium zone (36, 37). When pathogens and heterologous materials enter into lung, actived macrophages serve as the first line to resist the attackers. It is worth noting that short-lived macrophages can limit the replication of the virus, and once converted into long-lived macrophages, they might become infected resident cells (38).

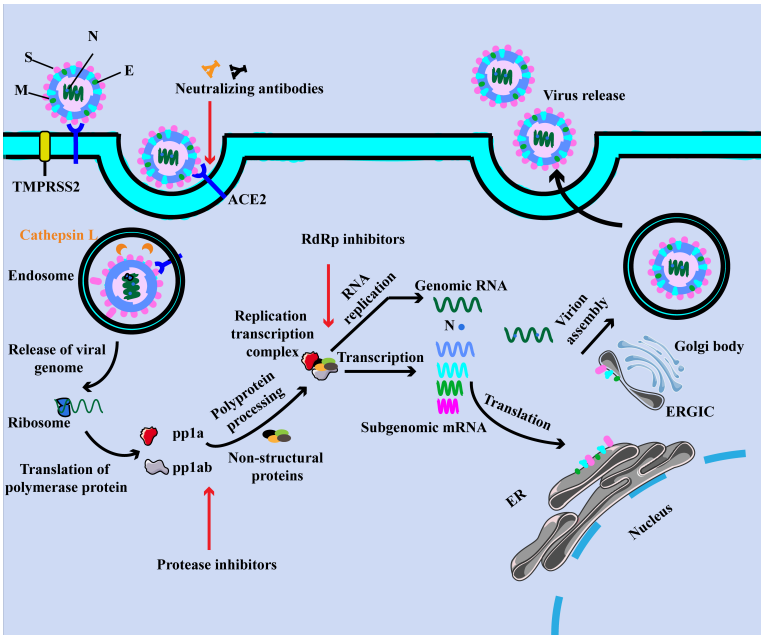

FIGURE 1
The SARS-CoV-2 virion and life cycle. The SARS-CoV-2 virion contains four structural proteins, namely spike (S), envelope (E), membrane (M), and nucleocapsid (N). The positive-sense, single-stranded RNA genome (+ssRNA) is encapsidated by N, whereas M and E ensure its incorporation into the viral particle during the assembly process. The spike (S) protein of SARS-CoV-2 specifically binds to ACE2, together with host factors (such as the cell surface serine protease TMPRSS2), facilitating the uptake and fusion of the virus in the cell or endosomal membrane. Following entry, the release and uncoating of the incoming genomic RNA allow it to the immediate translation of open reading frames. The resulting polyproteins pp1a and pp1ab are co-translated and post-translationally processed into the individual non-structural proteins (NSPs) that form the viral replication and transcription complex. Translated structural proteins translocate into endoplasmic reticulum (ER) membranes and transit through the ER-to-Golgi intermediate compartment (ERGIC), where they interact with N-encapsidated, newly produced genomic RNA and then lead tobudding into the lumen of secretory vesicular compartments. Finally, SARS-CoV-2 are secreted from the infected cell by exocytosis.

Upon SASR-CoV-2 infection, the pro-inflammatory activity of macrophages was enhanced, as indicated by the increased expression of inflammatory cytokines (IL-1β, IL-6) and chemokines (CXCL10) by macrophages (39, 40). Macrophages adjacent to areas of endothelial cell damage were the main producers of IFN-I, which might be elicited by the stimulator of interferon genes (STING) induced-IFN-I production and mtDNA release from adjacent endothelial cells (41). Increased pro-inflammatory factors may led to the occurrence of cytokine storm, which was correlated with the poor prognosis of COVID-19 patients (42, 43). Independent infection experiments in human macrophages also corroborated that the induction of IFN-I, TNF, IL-1β and IL-6 generally resulted in IFN-I-mediated cell death (39). Studies have shown that S-protein in SARS-CoV-2 could elicit inflammasome formation and IL-1β production in macrophages from COVID-19 patients, and further exploration revealed that this process needed non-specific activation of monocytes *in vivo* to trigger NLRP3 inflammatory signaling (40). Macrophages express ACE2, furin and TMPRSS2, whether the three have a synergistic effect in the process of virus infection still need to be explored (44–46). SARS-CoV-2 infection might promote macrophages to adopt a profibrotic phenotype and result in lung fibrosis (22). *In vitro*, SARS-CoV-2 induced profibrotic programs in classical monocytes, as indicated by a profibrotic proteome profile that was also expressed in idiopathic pulmonary fibrosis (22). There were several articles looking at the future of mesenchymal stem cells (MSC) and MSC-derived extracellular vesicles (MSC-EVs) as living anti-inflammatory therapy for COVID-19, including inhalation of MSC-EVs that promoted the macrophages polarization into a M2 phenotype (47, 48). A novel ACE2-overexpressing microparticles (AO-MPs) could adsorb more virus and then deliver them into alveolar macrophages, consequently quenched in alveolar macrophages and ameliorated macrophage-mediated inflammation (49). Accordingly, macrophages are non-negligible players in SARS-CoV-2-elicited inflammation and lung firbrosis, and macrophages might be a target for COVID-19 treatment.

3.1.2 Dendritic cell

A recent study revealed that patients with COVID-19 exhibited a defective DC response (24). In severe COVID-19

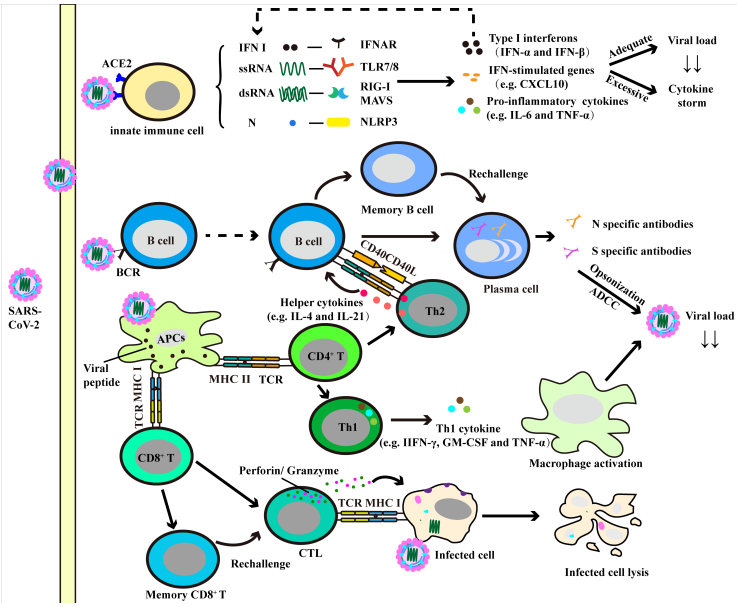

FIGURE 2
Immune response against SARS-CoV-2. The induction of innate immune cells (e.g. neutrophils, monocytes/macrophages and dendritic cells) results in production of various pro-inflammatory cytokines and chemokines. And the adequate production of these factors helps to clear the virus, while over-production can lead to cytokine storm and lung injury. The presentation of antigen by antigen-presenting cells (APCs) can induce humoral and cellular immunity in the human body. Specific $CD4^+$ T cells can be activated and differentiate into Th cells, where Th1 cells promote the activation of macrophage-dependent virus clearance *via* producing macrophage activating factors (e.g. TNF-α and GM-CSF), and Th2 cells facilitate the humoral immunity. With the help of Th2 cells, B cells produce virus specific antibodies and neutralize viruses. $CD8^+$ T cells differentiate into cytotoxic T lymphocyte (CTL), contributing to virus clearance by lysis of infected cells.

cases, plasmacytoid DCs (pDCs, critical effectors of antiviral immunity) exhibited increased pro-apoptotic pathways than those in moderate cases, accompanied by the downregulation of antiviral interferon-stimulated genes (ISGs) and innate sensors, TLR9, IFNAR and DHX36 (23, 24). pDCs are one of the main producers of IFN-I, which might produce more IFN-I than other immune cells or infected cells (50). Infiltration of pDCs (sensing SARS-CoV-2) were positively correlated with IFN-I production, contributing to the macrophage-mediated cytokine storm in the lungs of COVID-19 patients and might

TABLE 1 Roles of immune cells in the pathogenesis of SARS-CoV-2 infection.

Cell	Roles in viral progression	Function	References
Monocyte/Macrophage	Not duplicate	Cell pyrosis and induced profibrotic effects	(22)
pDC	Inhibiting	Mediated by IFN-I	(23)
cDC	Inhibiting	Mediated by IFN-I	(24)
NK cell	Inhibiting	Mediated by IFN-γ and TNF-α	(25)
	Antifibrotic activity	Inhibited expression of profibrotic genes in lung fibroblasts	
Th1 cell	Inhibiting	Mediated by IFN-γ	(26)
senescent Th2 cell	–	independent and significant risk factors for death	(27)
Tfh cell	Inhibiting	Supported GC responses	(28)
Tfr cell	Promoting	Suppressed anti-viral responses	(29)
Treg cell	Promoting	Suppressed the anti-viral responses *via* TGF-β and IL-10	(30)
CTL cell	Inhibiting	Secreted cytotoxic molecules	(31)
Effector B cell	Inhibiting	Secreted nAb against virus	(32–34)
Regulatory B cell	Promoting	Need further exploration	(35)

increase the lung inflammation (51). In detail, IFN-α production following TLR7 sensing of SARS-CoV-2 in pDCs mediated the transcriptional and epigenetic changes in macrophages, which facilitated their hyperactivation upon environmental stimuli (51). Comparing with moderate cases, conventional DCs (cDCs) from patients with severe COVID-19 exhibited decreased IFN signature and MHC II expression, contrary to pro-inflammatory pathways (24). Further exploration suggested that this reduction was correlated with low expression of MHC-II regulators (RFX5, RFXANK and CIITA) in severe cases. This viral inhibition of antigen presentation may explain the disease aggravation in severe cases and provide novel targets to restore the defective antiviral defense (24). Above all, DCs may have the potential to be a target to enhance the protective effects triggered by vaccines.

3.1.3 Natural killer cell

NK cells from healthy individuals showed anti-viral activity, as indicated by the reduced SARS-CoV-2 protein levels in cocultured infected cells (52). In addition to the anti-viral activity, NK cells also exhibited antifibrotic activity by the decreased expression of profibrotic genes COL1A1 and ACTA2 in lung fibroblasts (25). In contrast to the healthy individuals, NK cells from patients with COVID-19 showed limited anti-viral activity with an exhausted phenotype (53, 54). Previous studies have reported that the quantity of NK cells was significantly reduced in COVID-19 patients, displaying an exhausted phenotype by increased expression of NK inhibitory marker NKG2A (53, 55). Nevertheless, increased expression of NKG2A led to the reduced levels of CD107a (degranulation marker), IFN-γ, IL-2, granzyme B, and TNF-α in NK cells from COVID-19 patients (53). COVID-19-associated NK cells display a genetic profile similar to that of pulmonary NK cells from patients with pulmonary fibrosis, accompanied by the decreased ability to suppress the profibrotic gene expression (mentioned above) in lung fibroblasts (25). As an important anti-viral effector molecule, IFN-α suppressed the IFN-γ production by NK cells, but neutralization of IFN-α was unable to rescue the function of NK cells.

Based on the reduced anti-viral activity and antifibrotic activity of NK cells in patients with COVID-19, recovering their activities might be promising therapies against SAR-CoV-2. A recent study revealed that BNT162b1 mRNA vaccine significantly increased the quantity of $CD56^{bright}$, $CD56^{dim}$, and $CD56^{dim}/CD16^{dim}$ NK cells, and with an increase in IFN-γ, perforin and granzyme content (56). This result offered further support to end the SARS-CoV-2 pandemic with worldwide vaccination efforts (56). Therefore, the benefits of NK cell-based immunotherapy in patients with COVID-19 require further study.

Immunity against viral infection mainly begins with the recognition by pattern recognition receptor (PRRs) that are widely distributed on a variety of immune and non-immune cells. Signaling *via* PRRs induce the production of type I/III IFNs and pro-inflammatory cytokines, which trigger the transcription of ISGs to restrict viral infection. Valuable descriptive and correlative information about COVID-19 and innate immune responses (monocytes/macrophages, dendritic cells and NK cells) have been gathered during the pandemic. In addition to the above discussion, other innate immune cells (including neutrophils, eosinophils and epithelial cells) also have an important role in COVID-19 prediction and development. For example, neutrophils responses and neutrophil extracellular traps (NETs, contain nuclear component, microbicidal proteins and oxidative enzymes derived from neutrophils to limit infection) are correlated with the hyperinflammation in COVID-19 patients (57). Thus, targeting innate immunity may become a new strategy for the treatment of COVID-19.

3.2 Adaptive responses to SARS-CoV-2

Virus-specific cellular and humoral responses are the main weapons in protecting patients after SARS-CoV-2 infection. Next, we will comprehensively discuss the role of adaptive immunity in the fight against SARS-CoV-2.

3.2.1 $CD4^+$ T cell

Different $CD4^+$ T cell subsets can play beneficial or detrimental roles in the progression of COVID-19. Highly activated, functional $CD4^+$ T cells and functionally exhausted $CD4^+$ T cells have been detected simultaneously in individuals with severe COVID-19 (58). Previous studies have demonstrated that 83% of $CD4^+$ T cells in patients with COVID-19 were S reactive, which could respond to both N and C terminal of S protein (59). Thus, the interest in studying S protein-specific antiviral immune responses (including T-cell responsive COVID-19 vaccine) has been stimulated (60, 61). SARS-CoV-2-specific $CD4^+$ T cells were associated with ameliorated COVID-19 disease severity, and the induction of SARS-CoV-2-specific $CD4^+$ T cells was correlated with rapid decrease of viral load (62, 63). Another study also confirmed that early viral clearance and less critical illness were correlated with the higher counts of $CD4^+$ T cells, particularly naïve $CD4^+$ T cells (64).

3.2.1.1 Th1, Th2 and Th 17 cells

The disproportionality of T helper type 1 (Th1) or Th2 cells has been well elucidated in patients suffered from COVID-19 pandemic and non-infected people who are at maximum risk of infection (26). In an observational study,COVID-19 patients have been reported to have lower proportion of Th1 and Th17 cells and a higher proportion of activated Th2 cells compared with control population (27). In addition, higher proportion of senescent ($PD1^+/ICOS^-$) Th2 cells in dead patients than in

survivors (27). By evaluating the relationship between Th subsets and mortality, they found that the total lymphocytes and the higher percentages of senescent Th2 cells seem to be independent and significant risk factors for death (27). In the stage of recovery, the proportion of both Th1 and Th2 cells in patients were decreased than in healthy controls (27, 65). Thus, the dynamic change of Th cells might be a tool to monitor the development of COVID-19.

Th17 cells play pivotal roles in tissue damage and excessive inflammation *via* IL-17 and IL-23 (66). Researchers have found that high levels of Th17 cells in the periphery of patients infected with SARS-CoV-2 (30, 67, 68). A new study revealed that IL-17A expression was significantly associated with the severity of the disease (69). The results of studies also suggested that a systemic neutrophil environment may preferentially skew $CD4^+$ T cells toward Th17 and IL-17A promotion, thereby exacerbating inflammation (69, 70). Another study's results were consistent with this phenomenon, further experiment provided the evidence that this Th17 promotion could be reversed by inhibitors of arginase-1 (Arg-1), NO synthase (NOS), and reactive oxygen species (ROS), all produced by myeloid cells under oxidative stress (71). Thus, for clinical benefit, targeting Th17 promotion and blocking IL-17 signaling to manage COVID-19 patients, particularly those presenting with cytokine storm syndrome is promising.

3.2.1.2 Tfh cells

Among $CD4^+$ Th cell subsets, follicular helper T (Tfh) cells participate in humoral immunity *via* interacting with B cells in the germinal center (GC), facilitating the differentiation of B cells into plasma cells to product high-affinity neutralizing antibodies (28). Researchers revealed the absence of GC in thoracic lymph nodes and spleens from COVID-19 patients, accompanied by the reduction of Bcl-6^+ GC B cells in both organs (72). The reduction of $CD4^+CXCR5^+$Bcl-6^+ germinal center Tfh cells might explain the loss of GCs and the accumulation of non-GC-derived activated B cells (72). However, SARS-CoV-2 infection increased the number of peripheral $CD4^+$ Tfh and GC responses in rhesus macaques (73). In clinical studies, convalescent individuals who experienced severe COVID-19 showed a higher induction of $CXCR3^+$ Tfh cells when compared with those non-severe COVID-19-convalescent individuals. And the frequencies of them were positively associated with neutralizing antibody titers in convalescent individuals (74). In addition, they intriguingly found that circulating Tfh cells were S-protein specific and functional in spleen (73, 74). Moreover, researchers found that circulating S-specific Tfh cells could persist in constant numbers in the blood and lymph nodes for more than six months (75). In this study, they highlighted the importance of virus-specific Tfh cell responses in mRNA vaccine-induced robust and durable immune protection against SARS-CoV-2 (75). Furthermore, in Tfh-deleted mice immunized with S protein vaccination, Tfh cells also played an indispensable role for the formation of optimal SARS-CoV-2 Spike-specific B cell in GCs and for somatic hypermutation (SHM) (76).

In addition to the above protective effects, Tfh cells could also accelerate the disease progression in certain cases. Compared to non-hospitalized COVID-19 patients, severe cases showed increased cytotoxic Tfh cells which manifested high levels of IFN-γ, IL-2, and TNF-α (77). In an observational study, the results showed that $CCR4^+$ and $CCR6^+$ Tfh cells could be pathogenic in COVID-19 patients (78). In addition, attention needs to be focused on COVID-19 patients those who have Tfh-associated diseases, such as HIV, autoimmune diseases, who are more likely to develop severe disease (79, 80).

3.2.1.3 Treg cells

Regulatory T cells (Tregs) keep the immune homeostasis *via* multiple mechanisms thus the role of Tregs has not allow to ignore in these processes (81). Flow cytometric analysis showed an increased proportion of Tregs in peripheral blood mononuclear cells (PBMCs) with enhanced expression of FoxP3, which correlated with poor prognosis (82). In mechanically ventilated patients with COVID-19 acute respiratory distress syndrome (ARDS, hypoxemic respiratory failure caused by inflammation within the lung), in sharp contrast to the lymphopenia in both subsets of $CD4^+$ and $CD8^+$ T cells, the proportions of Tregs were increased in the lungs and PBMCs (83). The recruitment of Tregs into the lungs of COVID-19 patients may determine the severity of the disease since patients with more Treg cells experienced the milder disease (84). However, recent clinical studies showed that $CD3^+CD4^+CD25^{hi}CD127^{lo}FoxP3^+$ Tregs in PBMCs markedly reduced in severe COVID-19 patients (77, 85, 86). In ICU patients with COVID-19, the quantity of Tregs in PBMCs and their functional molecules (TGF-β and IL-10) were significantly reduced, accompanied by an increased ratio of Th17/Treg cells, RORγt/FoxP3, and IL-17/IL-10 in patients compared with the controls (30). In adults and children with severe COVID-19, the proportion of Tregs in $CD4^+$ T was also decreased (87). When recovered from mild COVID-19, patients seem to exhibit decreased levels of Tregs compared to themselves during hospitalization, and severe convalescents resulted in perturbances in $CD4^+$ Tregs (88, 89). Moreover, Treg-targeted therapies have been proposed and might be promising, including the adoptive transfer of Tregs and rIL-2 administration (NCT04468971 and NCT04357444, ClinicalTrials.gov) (90). Above all, a comprehensive understanding of the roles of Treg in COVID-19, and identification of the mechanisms regulating the balance between Tregs and other Th subsets may offer therapeutic novelties for COVID-19 infection.

3.2.2 CD8$^+$ T cells

It was reported that SARS-CoV-2-specific CD8$^+$ T-cell responses might be associated with disease severity during the acute phase, and decreased number has been observed in severe cases (31, 62, 91). For example, a study suggested that weak CD8$^+$ T cell responses, despite high antibody titers, might contribute to the pathogenesis of acute COVID-19 (54). Depletion of CD8$^+$ T cells in vaccinated macaques prior to SARS-CoV-2 infection led to the higher levels of peak viral load and day 4 in both the upper and lower respiratory tracts (92). CD8$^+$ T cells from COVID-19 patients exerted enhanced production of IL-2, IL-17, and the expression of degranulation marker CD107a upon anti-CD3/CD28 stimulation when compared to cells from healthy controls (70). In contrast to the previous conclusion, several studies reported that CD8$^+$ T cells from COVID-19 patients exhibited a decreased cytokine-producing capacity (53, 91). However, all this information was not based on SARS-CoV-2 antigen stimulation. There was increasing evidence that circulating CD8$^+$ T cells from severe COVID-19 patients with exhibited an exhausted phenotype characterized by increased expression of PD-1, TIM-3, LAG-3, CTLA-4, NKG2A, and CD39, and there was an inverse relationship between the expression of PD-1 and CD38 (an activation marker) in CD8$^+$ T cells (53, 93–96). Accumulated evidence revealed that the expression of PD-1 in CD8$^+$ T cells from COVID-19 patients was increased, especially ICU patients (95). Moreover, a recent study revealed that SARS-Cov-2-specific CD8$^+$PD-1$^+$ T cells produced more IFN-γ than PD-1-negative populations regardless of disease severity, indicating a functional state of SARS-CoV-2-specific CD8$^+$PD-1$^+$ T cells (96).

In the acute phase of COVID-19, SARS-CoV-2-specific CD8$^+$ T cells expressed activation markers (CD38 and HLA-DR) and secreted cytotoxic molecules (perforins and granzyme B), indicating these cells were activated with cytotoxic functions (31). Nasal-resident SARS-CoV-2-specific CD8$^+$ cells could be detected almost exclusively in vaccinees who experienced SARS-CoV-2 breakthrough infection (persisted for ≥140d) (12). And these CD8$^+$ T cells were predominantly tissue-resident memory T cells which had an elevated proportion of activated cells (97, 98). Moreover, researchers have found that memory CD8$^+$ T cells were required for the clearance of SARS-CoV-2, which was reflected by a delayed decreased of viral loads in the respiratory tract in CD8$^+$ T cells-depleted and SARS-CoV-2 rechallenged convalescent rhesus macaques (99). It's worth noting that memory CD8$^+$ T cells found in a study of UK convalescent individuals following COVID-19 would support an understanding of protective immunity and may contribute to put forward potential immune-based therapeutics (100). Vaccine-induced CD8$^+$ T cells also help to fight against SARS-CoV-2 re-infection (101–103). One week after prime vaccination with BNT162b2, a stable and fully functional CD8$^+$ T cell response was mobilized, as indicated by the increased production of IFN-γ and TNF-α (104). In addition, boost vaccination-induced highly differentiated effector CD8$^+$ T cells and vaccination-induced early memory T cells exhibited similar capacities (104).

3.3 B cells

The alterations of B cell subpopulations in COVID-19 have been reported, either immature or terminally differentiated. Compared to healthy subjects, the frequencies of CD19$^+$ B cells in PBMCs seem to be slightly increased in severe and critical cases (105). The double negative (DN) fraction (CD27$^-$ IgD$^-$) is one of B cell compartments that showed significant alterations in COVID-19 (105). Depending on the disease severity, mean frequencies of DN1 (CD21$^+$CD11c$^-$), DN2 (CD21$^-$CD11c$^+$), and DN3 (CD21$^-$CD11c$^-$) subsets exhibited shifted distributions. DN1 B cells showed a significant reduction in severe and critical cases. DN2 B cells displayed a significant increase in severe cases vs mild/moderate and critical cases while DN3 B cells were significantly increased as disease severity increased. In addition, immature, activated naïve B cells and the DN3 fraction showed a strong correlation with ventilatory parameters, such as respiratory rate, SpO2, and PaO2/FiO2 (105). Another study also revealed similar phenomenon about DN2 B cells in acute patients with COVID-19 (106). This study also revealed that severe patients displayed enhanced extrafollicular B cell activation with accelerated inflammation, while mild patients counteracted the disease through the timely induction of mitochondrial dysfunction in B cells, which suppressed the extrafollicular responses, resulting in increased neutralizing potency index and reduced inflammation (106).

Germinal centers (GCs) are transient microstructures formed within the follicles of secondary lymphoid tissues. Within GCs, activated B cells undergo clonal expansion and affinity maturation and get further help from Tfh cells to differentiate into memory B cells or long-lived plasma cells, which is of vital importance for the generation of humoral immunity (107). In severe SARS-CoV-2 infection, GC responses were suppressed, which inhibited the production of neutralizing antibody (nAb). Multicolor histological assessments revealed that GCs were also largely absent in thoracic lymph nodes and spleens from patients succumbing to COVID-19. There were also the absence of BCL6$^+$ B cells or Tfh cells, both were the contributors to GCs (72). Furthermore, they also speculated that excess TNF-α inhibited the formation of GC responses in COVID-19 *via* blocking Tfh cell differentiation (72, 108, 109).

Following infection with SARS-CoV-2, naïve B cells and existed memory B cells (upon early exposure of other coronaviruses) will be activated and differentiate into antibody-secreting cells (ASCs). Discrete increments of ASCs were seen in patients with mild/moderate COVID-19 and were

significantly amplified with disease severity (105). In contrast to the majority infection, the serum IgG appeared at approximately the same time as serum IgM and IgA responses to SARS-CoV-2 S and N, usually within the first 2 weeks after symptom onset (32–34). Importantly, the memory B cell is the only B cell subset that correlated with a clinical outcome in hospitalization period (105). A recent study revealed that individuals recovered from COVID-19 developed SARS-CoV-2-specific immunoglobulin (IgG) antibodies, neutralizing plasma, and memory B and memory T cells which could persist for at least 3 months. Moreover, SARS-CoV-2-specific IgG memory B cells (MBCs) increased over time (110). S-RBD-specific class-switched MBCs were detected in 13 of 14 participants, failing only in the individual with the lowest plasma levels of anti-S-RBD IgG and neutralizing antibodies. Resting MBCs (rMBCs) made up the largest proportion of S-RBD-specific MBCs patients with mild disease and hospitalized patients with moderate to severe disease (111). Another study found that in mild and severe COVID-19 patients, serum neutralizing antibody (nAb) responses waned rapidly but spike (S)-specific IgG^+ memory B cells (MBCs) remained stable or increased. Analysis of 1,213 monoclonal antibodies (mAbs) isolated from S-specific MBCs displayed increased somatic hypermutation, binding affinity, and neutralization potency over time, indicating prolonged protection *via* humoral immunity (111). A recent study introduced that the effect of MBCs elicited by mRNA vaccines in preventing SARS-CoV-2 variants (including Omicron variants), highlighting the protective roles of MBCs in disease (112).

The adaptive immune system is important for control of most viral infections. We have discussed the roles of Th, Tfh, $CD8^+$ T and B cells in the pathogenesis of COVID-19, and other adaptive immune cells, such as Tfr cells, also contribute to optimize humoral immunity, meaning their importance to avoid the overactivation of immune responses. Whether viral-inhibiting or viral-promoting effects of immune cells in COVID-19, these researches state the importance of them in anti-SARS-CoV-2 and define emergence of new paradigms in anti-viral activity.

4 Vaccine development

Vaccination is considered as one of the greatest successes in the history of medicine, it could decrease the disease incidence, or at least suppress its detrimental or even fatal clinical manifestations. At present, there are mainly five kinds of SARS-CoV-2 vaccines, including inactivated vaccines, recombinant protein vaccines, viral vector-based vaccines, live attenuated vaccines and nucleic acid vaccines (113). As the first inactivated SARS-CoV-2 vaccine, PiCoVacc induced SARS-CoV-2-specific neutralizing antibodies in mice, rats and non-human primates, and these antibodies showed a broader neutralizing ability against other 10 representative SARS-CoV-2 strains (114). *In vivo*, vaccinated macaques related symptom ameliorated, as indicated by the mild and focal histopathological changes and viral load compared with the controls (114). In phase 1/2 clinical trials, CoronaVac has been confirmed to be safe and well-tolerated, inducing humoral responses in children and adolescents aged 3-17 years and healthy adults (≥18 years old) (115–117). The phase 3 trial in Turkey also revealed a vaccine efficacy of 83.5% in the vaccine group with good safety and tolerability profile (118). In phase 4 studies, scientists found that low antibody concentrations 6 months after previous immunisation with two doses of CoronaVac. However, a third dose induced a significant increase of neutralizing antibodies, which could improve protection against infection. Importantly, heterologous boosting produce a more stronger immune response than homologous boosting (119). The BNT162b2 mRNA and mRNA-1273 COVID-19 vaccine are the most widely used mRNA vaccines, and both vaccines showed more than 90% protective efficiency (120, 121). Viral vector-based adenoviral vaccines have also been explored, including adenovirus-vectored vaccines. Exploration conducted by Chen's team showed that the recombinant adenovirus type 5 transmitted COVID-19 vaccine was safe in a single dose, and induced robust immune responses in healthy adults aged 18 years or older and children or adolescents (122–124). Humoral responses peaked at day 28 post-vaccination in healthy adults, and rapid specific T-cell responses were noted from day 14 post-vaccination (122). Another adenovirus-vectored vaccine, ChAdOx1 nCoV-19 vaccine also exerted protective effective against SARS-CoV-2 (125, 126). Recently, recombinant tandem-repeat dimeric RBD-based protein subunit vaccine (such as ZF2001) also have been investigated and showed a good protective effect (127, 128). Scientists evaluated the SARS-CoV-2-spike-specific immune responses to Moderna mRNA-1273, Pfizer/BioNTech BNT162b2, Janssen Ad26.COV2.S, and Novavax NVX-CoV2373 (129). 100% of individuals made memory $CD4^+$ T cells, and cTfh and CD4-CTL highly represented only after mRNA or NVX-CoV2373 vaccination, and a differentiating feature of Ad26.COV2.S immunization was a high frequency of $CXCR3^+$ memory B cells (129). mRNA vaccinees had substantial declines in antibodies, while memory T and B cells were comparatively stable (129). A recent study demonstrated that Omicron infection enhances pre-existing immunity elicited by vaccines and, higher neutralization titres against all variants of concern (VOC) (130). Thus, Omicron infection may confer broad protection against non-Omicron variants in vaccinated individuals (130). Although there are different variants (Beta, Delta, Omicron and others), these vaccines are still effective especially in preventing the occurrence of severe cases (131–134).

Although vaccines can prevent the occurrence of severe diseases, accumulated evidence still showed that additional protective measures should be maintained to fight against

variants with increased infectivity (135–137). In particular, as time goes on, the vaccine induced immune response will naturally decline.

5 Potential treatment of COVID-19

Currently, COVID-19 pandemic is one of the greatest threats to human health with more than 611 million confirmed cases and over 6.51 million deaths reported worldwide (as of September 23, 2022, sources from WHO). Various drugs were proclaimed to be effective against SARS-CoV-2, such as remdesivir, paxlovid, lopinavir/ritonavir, molnupiravir, and some monoclonal antibodies (138).

Monoclonal antibodies are used as a potential therapeutic and preventive drug for viral infection due to its high specificity and the ability to enhance immune response. Bamlanivimab (LY-CoV555, IgG1), a potent anti-spike neutralizing antibody, block the binding and entry to human cells (139). For primary outcomes, no differences were observed in bamlanivimab vs placebo, but bamlanivimab treatment was associated with lower day 3 nasopharyngeal viral levels and faster reductions in inflammatory markers and viral decay (140). One of three doses of bamlanivimab appeared to promote the natural decline in viral load over time (141). Moreover, compared to the placebo group, patients within LY-CoV555 group had a lower ratio of COVID-19-related hospitalization or visit to an emergency department (141). When combined with another monoclonal antibody, Etesevimab, the incidence of COVID-19-related hospitalization and death was decreased than the placebo group, accompanied by the decline of viral load (142). Sotrovimab (IgG1), casirivimab (IgG1-κ) and imdevimab (IgG1-λ), as S protein RBD specific antibodies which could prevent the binding of SARS-CoV-2 to the human ACE-2 receptor, may contribute to COVID-19 patients recover (143–145). Tocilizumab, a monoclonal antibody binds specifically to both soluble and membrane-bound receptors for IL-6and has been explored in the treatment of COVID-19. The results showed that the mortality in the tocilizumab group was lower than not treated with tocilizumab (146).

Remdesivir, an adenosine analogue, can be metabolized to its active metabolite remdesivir triphosphatea (an analogue of ATP), and integrate into the nascent viral RNA *via* RNA polymerase, resulting in delayed chain termination during replication, thereby inhibiting viral replication (147). In 2020, a study reported that patients with severe COVID-19 receiving remdesivir had a numerically faster time to clinical improvement than those patients receiving placebo when the duration of symptoms was 10 days or less (148). The ratio of adverse events was similar in both groups, but the proportion of patients who stopped clinical trial was higher in remdesivir group (12%) than placebo group (5%) (148). A 5 day remdesivir therapy of COVID-19 patients showed greater clinical improvement than patients in placebo group, but not different from a 10 day therapy (149). For cases treated in the ICU, remdesivir use within 9 days from symptom onset reduced mortality risk compared with control group (150).

Janus activated kinase (JAK) inhibitors also have been applied to the treatment of COVID-19 (151, 152). Baricitinib is a selective inhibitor of JAK1 and JAK2, both of which mediate signaling for inflammatory cytokines involved in inflammation and the immune response of COVID-19 (151). The results indicated a lower case fatality rate within 2 weeks in the baricitinib group (0%) than the control (6.4%) (152). In addition, the ICU admission rate was lower in patients receiving baricitinib treatment (0.88%) than controls (17.9%) (152). Tofacitinib is another inhibitor of JAK, which has been shown to inhibit the activity of JAK1, JAK2, JAK3, and to a lesser extent of Tyk2 (153). The results of a clinical trial have demonstrated that tofacitinib led to a lower risk of death or respiratory failure through day 28 than placebo (18.1% vs 29.0%), implying the therapeutic effects of tofacitinib in COVID-19 (154). By day 28, death occurred in 2.8% of patients in the tofacitinib group and in 5.5% of patients in the placebo group (154). Thus, the use of JAK inhibitors in hospitalized patients with COVID-19 should be considered to improve the clinical outcome and prevent death.

Paxlovid is a therapeutic combination consisting of two compounds: nirmatrelvir and ritonavir (155). Ritonavir could inhibit the metabolism of nirmatrelvir and allow the administration of lower doses of this substance (156). A recent study revealed that among patients who received paxlovid treatment within three days of symptom onset, only 0.8% patients were admitted to hospital by day 28 after randomization and no deaths. In comparison, these two values in the control group were 7% and 7 (157). In participants treated within five days of symptom onset, the effect of paxlovid was still significant. In addition, no deaths were reported in the paxlovid group as compared to 10 deaths (1.6%) in the placebo group (157). During the pandemic of COVID-19 in Shanghai (2022), scientists found that unvaccinated, delayed use of paxlovid (started 5 days after diagnosis) and immunosuppressive status were independent risk factors for delayed virus clearance (158). Compared with patients who delayed paxlovid treatment, immunosuppressive patients who began to use paxlovid within 5 days after diagnosis had an earlier virus clearance time of about 6 days. Moreover, correlation analysis showed that the earlier paxlovid was used, the more rapidly the virus was cleared (158). Although the benefit of paxlovid has been confirmed and has been approved in some contries, the furture of paxlovid still need further exploration (159).

Molnupiravir is a new oral antiviral drug that has recently been tested in COVID-19 (160). The results of phase clinical trial (NCT04575597) of molnupiravir showed that it can significantly reduce the risk of hospitalization and mortality in mild to moderate COVID-19 patients. Compared with placebo, patients taking molnupiravir had a 50% lower risk of hospitalization or death. More impressively, no deaths were

reported in the group of patients taking molnupiravir, while there were 8 deaths in the placebo group. In terms of side effects, there was no difference between the two groups (161–163). Also, molnupiravir accelerated SARS-CoV-2 RNA clearance and elimination of infectious virus in patients with COVID-19 (median 14 days vs 15 days, log rank p= 0.013) (164). In this study, molnupiravir was well tolerated across all doses (200/400/800 mg), and the adverse events were mainly low-drade that were similar to those reported by participants in placebo group (164). For SARS-CoV-2 variants, a recent study found that SARS-CoV-2 Omicron variant was highly sensitive to molnupiravir, nirmatrelvir, and the combination (165). These evidence suggest molnupiravir is a promising drug in treating COVID-19.

Azvudine, a nucleoside reverse transcriptase inhibitor that previously been used in HIV-1 infection (166). In recent years, the effects of azvudine in COVID-19 have been revealed (167, 168). A randomized, open-label, controlled clinical trial (ChiCTR2000029853, http://www.chictr.org.cn) contained 20 mild and common COVID-19 patients showed that the mean times of the first nucleic acid negative conversion (NANC) of azvudine group and the control group were 2.6 days and 5.6 days, respectively (p = 0.008) (167). Also, the mean time of the first NANC of newly diagnosed subjects in the azvudine group was shorter (167). Thus, azvudine is an effective anti-SARS-CoV-2 drug in treating COVID-19 patients, and it has been approved to treat COVID-19 in China (169).

Diamidobenzimidazole 4 (diABZI-4), an STING agonist, has been confirmed to induce a rapid short-lived activation of STING, then the transient expression of proinflammatory cytokines and lymphocyte activation (170). *In vitro*, diABZI-4 significantly inhibited SARS-CoV-2 replication in infected cells (170, 171). In mouse model, the results showed that the viral load in both nasal cavity and lung was lower than the control, consequently prevented the disease progression (171). For variants (B.1.351), diABZI-4 showed good antiviral effect as well (171). In this process, attention needs to be taken to avoid excessive production of pro-inflammatory cytokines and cytokine storm.

As an important part of world medicine, Chinese traditional medicine is safe and effective in the treatment of COVID-19. The results showed that after 14 days of treatment with Lianhua Qingwen capsule, the cure rate of main clinical symptoms (fever, fatigue and cough) in the treatment group was significantly higher than the control group, reaching 57.7% on the 7th day, 80.3% on the 10th day and 91.5% on the 14th day. The duration of single symptoms of fever, fatigue and cough was also shortened. In terms of reducing the proportion of patients with severe disease, the treatment group of Lianhua Qingwen capsule was significantly lower than the control group (Lianhua Qingwen treatment group: 2.1%, control group: 4.2%) (172). Another study using network pharmacological strategy revealed that AKT1 is a promising drug target to reduce tissue damage and help eliminate virus infection (173). Practically, Chinese traditional medicine have been written up in COVID-19 diagnosis and treatment plan in China (173).

6 Conclusion

The current knowledge about SASR-CoV-2 indicates that the immune system plays a crucial role in setting the severity of COVID-19. Although an extraordinary amount has been accomplished during the last three years, the relationship between immune responses and the severity of diseases still remains to be explored. Appropriate responses against SARS-CoV-2 could ameliorate the symptoms of COVID-19 and prevent the occurrence of severe diseases, while excessive responses elicited cytokine storm and pathogenic B cell activation, increasing the risk of death. Thus, in immune-based therapeutics, avoiding the excessive activation of immune cells will also be the proposition of our future research. However, understanding heterogeneous disease manifestations of COVID-19 remains a major knowledge gap, and exploring the relationships between COVID-19 and immunity is a priority. The emergence of new mutant strains has also brought unprecedented pressure to vaccine development. With the advent of new technologies such as next-generation sequencing (NGS), CRISPR-based assays and nanotechnology, enhanced the the accuracy and sensitivity of COVID-19 diagnosis and treatments. Furthermore, duration of immune memory and protective immunity to SARS-CoV-2 after infection or vaccination will be a high priority for years to come.

Author contributions

QZ drafted the manuscript. YX and TW discussed and revised the manuscript. FX conceived the topic and revised the manuscript. All authors contributed to the article and approved the submitted version.

Conflict of interest

The authors declare that the research was conducted in the absence of any commercial or financial relationships that could be construed as a potential conflict of interest.

Publisher's note

All claims expressed in this article are solely those of the authors and do not necessarily represent those of their affiliated organizations, or those of the publisher, the editors and the reviewers. Any product that may be evaluated in this article, or claim that may be made by its manufacturer, is not guaranteed or endorsed by the publisher.

References

1. Yang J, Chen X, Deng X, Chen Z, Gong H, Yan H, et al. Disease burden and clinical severity of the first pandemic wave of covid-19 in wuhan, China. *Nat Commun* (2020) 11(1):5411. doi: 10.1038/s41467-020-19238-2

2. Guan WJ, Ni ZY, Hu Y, Liang WH, Ou CQ, He JX, et al. Clinical characteristics of coronavirus disease 2019 in China. *New Engl J Med* (2020) 382 (18):1708–20. doi: 10.1056/NEJMoa2002032

3. Lu R, Zhao X, Li J, Niu P, Yang B, Wu H, et al. Genomic characterisation and epidemiology of 2019 novel coronavirus: Implications for virus origins and receptor binding. *Lancet* (2020) 395(10224):565–74. doi: 10.1016/S0140-6736(20) 30251-8

4. Tsai PH, Wang ML, Yang DM, Liang KH, Chou SJ, Chiou SH, et al. Genomic variance of open reading frames (Orfs) and spike protein in severe acute respiratory syndrome coronavirus 2 (Sars-Cov-2). *J Chin Med Association: JCMA* (2020) 83 (8):725–32. doi: 10.1097/jcma.0000000000000387

5. Rahbari R, Moradi N, Abdi M. Rrt-pcr for sars-Cov-2: Analytical considerations. *Clin Chim Acta* (2021) 516:1–7. doi: 10.1016/j.cca.2021.01.011

6. Chan JF, Kok KH, Zhu Z, Chu H, To KK, Yuan S, et al. Genomic characterization of the 2019 novel human-pathogenic coronavirus isolated from a patient with atypical pneumonia after visiting wuhan. *Emerg Microbes Infect* (2020) 9(1):221–36. doi: 10.1080/22221751.2020.1719902

7. Gui M, Song W, Zhou H, Xu J, Chen S, Xiang Y, et al. Cryo-electron microscopy structures of the sars-cov spike glycoprotein reveal a prerequisite conformational state for receptor binding. *Cell Res* (2017) 27(1):119–29. doi: 10.1038/cr.2016.152

8. Wrapp D, Wang N, Corbett Kizzmekia S, Goldsmith Jory A, Hsieh C-L, Abiona O, et al. Cryo-em structure of the 2019-ncov spike in the prefusion conformation. *Science* (2020) 367(6483):1260–3. doi: 10.1126/science.abb2507

9. Saponaro F, Rutigliano G, Sestito S, Bandini L, Storti B, Bizzarri R, et al. Ace2 in the era of sars-Cov-2: Controversies and novel perspectives. *Front Mol Biosci* (2020) 7:588618. doi: 10.3389/fmolb.2020.588618

10. Hikmet F, Mear L, Edvinsson A, Micke P, Uhlen M, Lindskog C. The protein expression profile of Ace2 in human tissues. *Mol Syst Biol* (2020) 16(7): e9610. doi: 10.15252/msb.20209610

11. Shang J, Wan Y, Luo C, Ye G, Geng Q, Auerbach A, et al. Cell entry mechanisms of sars-Cov-2. *Proc Natl Acad Sci USA* (2020) 117(21):11727–34. doi: 10.1073/pnas.2003138117

12. Lim JME, Tan AT, Le Bert N, Hang SK, Low JGH, Bertoletti A. Sars-Cov-2 breakthrough infection in vaccinees induces virus-specific nasal-resident Cd8+ and Cd4+ T cells of broad specificity. *J Exp Med* (2022) 219(10):e20220780. doi: 10.1084/jem.20220780

13. Hoffmann M, Kleine-Weber H, Schroeder S, Krüger N, Herrler T, Erichsen S, et al. Sars-Cov-2 cell entry depends on Ace2 and Tmprss2 and is blocked by a clinically proven protease inhibitor. *Cell* (2020) 181(2):271–80.e8. doi: 10.1016/ j.cell.2020.02.052

14. Zhu S, Liu Y, Zhou Z, Zhang Z, Xiao X, Liu Z, et al. Genome-wide crispr activation screen identifies candidate receptors for sars-Cov-2 entry. *Sci China Life Sci* (2022) 65(4):701–17. doi: 10.1007/s11427-021-1990-5

15. Tao K, Tzou PL, Nouhin J, Gupta RK, de Oliveira T, Kosakovsky Pond SL, et al. The biological and clinical significance of emerging sars-Cov-2 variants. *Nat Rev Genet* (2021) 22(12):757–73. doi: 10.1038/s41576-021-00408-x

16. Callaway E. Omicron likely to weaken covid vaccine protection. *Nature* (2021) 600(7889):367–8. doi: 10.1038/d41586-021-03672-3

17. Uraki R, Kiso M, Iida S, Imai M, Takashita E, Kuroda M, et al. Characterization and antiviral susceptibility of sars-Cov-2 omicron ba. *2 Nat* (2022) 607(7917):119–27. doi: 10.1038/s41586-022-04856-1

18. Huang C, Wang Y, Li X, Ren L, Zhao J, Hu Y, et al. Clinical features of patients infected with 2019 novel coronavirus in wuhan, China. *Lancet* (2020) 395 (10223):497–506. doi: 10.1016/S0140-6736(20)30183-5

19. Vivanti AJ, Vauloup-Fellous C, Prevot S, Zupan V, Suffee C, Do Cao J, et al. Transplacental transmission of sars-Cov-2 infection. *Nat Commun* (2020) 11 (1):3572. doi: 10.1038/s41467-020-17436-6

20. Chen H, Guo J, Wang C, Luo F, Yu X, Zhang W, et al. Clinical characteristics and intrauterine vertical transmission potential of covid-19 infection in nine pregnant women: A retrospective review of medical records. *Lancet* (2020) 395(10226):809–15. doi: 10.1016/S0140-6736(20)30360-3

21. Bandyopadhyay T, Sharma A, Kumari P, Maria A, Choudhary R. Possible early vertical transmission of covid-19 from an infected pregnant female to her neonate: A case report. *J Trop Pediatr* (2021) 67(1):fmaa094. doi: 10.1093/tropej/ fmaa094

22. Wendisch D, Dietrich O, Mari T, von Stillfried S, Ibarra IL, Mittermaier M, et al. Sars-Cov-2 infection triggers profibrotic macrophage responses and lung fibrosis. *Cell* (2021) 184(26):6243–61.e27. doi: 10.1016/j.cell.2021.11.033

23. Hadjadj J, Yatim N, Barnabei L, Corneau A, Boussier J, Smith N, et al. Impaired type I interferon activity and inflammatory responses in severe covid-19 patients. *Sci (New York NY)* (2020) 369(6504):718–24. doi: 10.1126/science.abc6027

24. Saichi M, Ladjemi MZ, Korniotis S, Rousseau C, Ait Hamou Z, Massenet-Regad L, et al. Single-cell rna sequencing of blood antigen-presenting cells in severe covid-19 reveals multi-process defects in antiviral immunity. *Nat Cell Biol* (2021) 23(5):538–51. doi: 10.1038/s41556-021-00681-2

25. Kramer B, Knoll R, Bonaguro L, ToVinh M, Raabe J, Astaburuaga-Garcia R, et al. Early ifn-alpha signatures and persistent dysfunction are distinguishing features of nk cells in severe covid-19. *Immunity* (2021) 54(11):2650–69.e14. doi: 10.1016/ j.immuni.2021.09.002

26. Supriya R, Gao Y, Gu Y, Baker JS. Role of exercise intensity on Th1/Th2 immune modulations during the covid-19 pandemic. *Front Immunol* (2021) 12:761382. doi: 10.3389/fimmu.2021.761382

27. Gil-Etayo FJ, Suarez-Fernandez P, Cabrera-Marante O, Arroyo D, Garcinuno S, Naranjo L, et al. T-Helper cell subset response is a determining factor in covid-19 progression. *Front Cell Infect Microbiol* (2021) 11:624483. doi: 10.3389/fcimb.2021.624483

28. Crotty S. Follicular helper Cd4 T cells (Tfh). *Annu Rev Immunol* (2011) 29:621–63. doi: 10.1146/annurev-immunol-031210-101400

29. Zahran AM, Abdel-Rahim MH, Nasif KA, Hussein S, Hafez R, Ahmad AB, et al. Association of follicular helper T and follicular regulatory T cells with severity and hyperglycemia in hospitalized covid-19 patients. *Virulence* (2022) 13(1):569–77. doi: 10.1080/21505594.2022.2047506

30. Sadeghi A, Tahmasebi S, Mahmood A, Kuznetsova M, Valizadeh H, Taghizadieh A, et al. Th17 and treg cells function in sars-Cov2 patients compared with healthy controls. *J Cell Physiol* (2021) 236(4):2829–39. doi: 10.1002/jcp.30047

31. Sekine T, Perez-Potti A, Rivera-Ballesteros O, Stralin K, Gorin JB, Olsson A, et al. Robust T cell immunity in convalescent individuals with asymptomatic or mild covid-19. *Cell* (2020) 183(1):158–68.e14. doi: 10.1016/j.cell.2020.08.017

32. Röltgen K, Nielsen SCA, Arunachalam PS, Yang F, Hoh RA, Wirz OF, et al. Mrna vaccination compared to infection elicits an igg-predominant response with greater sars-Cov-2 specificity and similar decrease in variant spike recognition. *medRxiv preprint server Health Sci* [Preprint] (2021). doi: 10.1101/2021.04. 05.21254952

33. Long QX, Liu BZ, Deng HJ, Wu GC, Deng K, Chen YK, et al. Antibody responses to sars-Cov-2 in patients with covid-19. *Nat Med* (2020) 26(6):845–8. doi: 10.1038/s41591-020-0897-1

34. Iyer AS, Jones FK, Nodoushani A, Kelly M, Becker M, Slater D, et al. Persistence and decay of human antibody responses to the receptor binding domain of sars-Cov-2 spike protein in covid-19 patients. *Sci Immunol* (2020) 5 (52):eabe0367. doi: 10.1126/sciimmunol.abe0367

35. Cervantes-Díaz R, Sosa-Hernández VA, Romero-Ramírez S, Torres-Ruiz J, Pérez-Fragoso A, Meza-Sánchez DE, et al. Circulating B10 regulatory cells are decreased in severe and critical covid-19. *J leukocyte Biol* (2022) 112(2):333–7. doi: 10.1002/jlb.5covcra0721-387rr

36. Schneberger D, Aharonson-Raz K, Singh B. Monocyte and macrophage heterogeneity and toll-like receptors in the lung. *Cell Tissue Res* (2011) 343(1):97–106. doi: 10.1007/s00441-010-1032-2

37. Wang C, Xie J, Zhao L, Fei X, Zhang H, Tan Y, et al. Alveolar macrophage dysfunction and cytokine storm in the pathogenesis of two severe covid-19 patients. *EBioMedicine* (2020) 57:102833. doi: 10.1016/j.ebiom.2020.102833

38. Nikitina E, Larionova I, Choinzonov E, Kzhyshkowska J. Monocytes and macrophages as viral targets and reservoirs. *Int J Mol Sci* (2018) 19(9):2821. doi: 10.3390/ijms19092821

39. Zheng J, Wang Y, Li K, Meyerholz DK, Allamargot C, Perlman S. Severe acute respiratory syndrome coronavirus 2-induced immune activation and death of monocyte-derived human macrophages and dendritic cells. *J Infect Dis* (2021) 223 (5):785–95. doi: 10.1093/infdis/jiaa753

40. Theobald SJ, Simonis A, Georgomanolis T, Kreer C, Zehner M, Eisfeld HS, et al. Long-lived macrophage reprogramming drives spike protein-mediated inflammasome activation in covid-19. *EMBO Mol Med* (2021) 13(8):e14150. doi: 10.15252/emmm.202114150

41. Domizio JD, Gulen MF, Saidoune F, Thacker VV, Yatim A, Sharma K, et al. The cgas-sting pathway drives type I ifn immunopathology in covid-19. *Nature* (2022) 603(7899):145–51. doi: 10.1038/s41586-022-04421-w

42. Vaninov N. In the eye of the covid-19 cytokine storm. *Nat Rev Immunol* (2020) 20(5):277. doi: 10.1038/s41577-020-0305-6

43. Fajgenbaum DC, June CH. Cytokine storm. *New Engl J Med* (2020) 383 (23):2255–73. doi: 10.1056/NEJMra2026131

44. Keewan E, Beg S, Naser SA. Anti-Tnf-A agents modulate sars-Cov-2 receptors and increase the risk of infection through notch-1 signaling. *Front Immunol* (2021) 12:641295. doi: 10.3389/fimmu.2021.641295

45. Verdecchia P, Cavallini C, Spanevello A, Angeli F. The pivotal link between Ace2 deficiency and sars-Cov-2 infection. *Eur J Internal Med* (2020) 76:14–20. doi: 10.1016/j.ejim.2020.04.037

46. Zhao G, Yang W, Wu J, Chen B, Yang X, Chen J, et al. Influence of a coronary artery disease-associated genetic variant on furin expression and effect of furin on macrophage behavior. *Arteriosclerosis Thrombosis Vasc Biol* (2018) 38 (8):1837–44. doi: 10.1161/atvbaha.118.311030

47. Cao Y, Wu H, Zhai W, Wang Y, Li M, Li M, et al. A safety consideration of mesenchymal stem cell therapy on covid-19. *Stem Cell Res* (2020) 49:102066. doi: 10.1016/j.scr.2020.102066

48. Zhao R, Wang L, Wang T, Xian P, Wang H, Long Q. Inhalation of msc-evs is a noninvasive strategy for ameliorating acute lung injury. *J Controlled Release* (2022) 345:214–30. doi: 10.1016/j.jconrel.2022.03.025

49. Wang Z, Lv J, Yu P, Qu Y, Zhou Y, Zhou L, et al. Sars-Cov-2 treatment effects induced by Ace2-expressing microparticles are explained by the oxidized cholesterol-increased endosomal ph of alveolar macrophages. *Cell Mol Immunol* (2022) 19(2):210–21. doi: 10.1038/s41423-021-00813-6

50. Fitzgerald-Bocarsly P, Dai J, Singh S. Plasmacytoid dendritic cells and type I ifn: 50 years of convergent history. *Cytokine Growth Factor Rev* (2008) 19(1):3–19. doi: 10.1016/j.cytogfr.2007.10.006

51. Laurent P, Yang C, Rendeiro AF, Nilsson-Payant BE, Carrau L, Chandar V, et al. Sensing of sars-Cov-2 by pdcs and their subsequent production of ifn-I contribute to macrophage-induced cytokine storm during covid-19. *Sci Immunol* (2022) 7(75):eadd4906. doi: 10.1126/sciimmunol.add4906

52. Krämer B, Knoll R, Bonaguro L, ToVinh M, Raabe J, Astaburuaga-García R, et al. Early ifn-A signatures and persistent dysfunction are distinguishing features of nk cells in severe covid-19. *Immunity* (2021) 54(11):2650–69.e14. doi: 10.1016/j.immuni.2021.09.002

53. Zheng M, Gao Y, Wang G, Song G, Liu S, Sun D, et al. Functional exhaustion of antiviral lymphocytes in covid-19 patients. *Cell Mol Immunol* (2020) 17(5):533–5. doi: 10.1038/s41423-020-0402-2

54. Zhou R, To KK, Wong YC, Liu L, Zhou B, Li X, et al. Acute sars-Cov-2 infection impairs dendritic cell and T cell responses. *Immunity* (2020) 53(4):864–77.e5. doi: 10.1016/j.immuni.2020.07.026

55. Wang F, Nie J, Wang H, Zhao Q, Xiong Y, Deng L, et al. Characteristics of peripheral lymphocyte subset alteration in covid-19 pneumonia. *J Infect Dis* (2020) 221(11):1762–9. doi: 10.1093/infdis/jiaa150

56. Saresella M, Piancone F, Marventano I, Hernis A, Trabattoni D, Invernizzi M, et al. Innate immune responses to three doses of the Bnt162b2 mrna sars-Cov-2 vaccine. *Front Immunol* (2022) 13:947320. doi: 10.3389/fimmu.2022.947320

57. Zuo Y, Yalavarthi S, Shi H, Gockman K, Zuo M, Madison JA, et al. Neutrophil extracellular traps in covid-19. *JCI Insight* (2020) 5(11):e138999. doi: 10.1172/jci.insight.138999

58. Adamo S, Chevrier S, Cervia C, Zurbuchen Y, Raeber ME, Yang L, et al. Profound dysregulation of T cell homeostasis and function in patients with severe covid-19. *Allergy* (2021) 76(9):2866–81. doi: 10.1111/all.14866

59. Braun J, Loyal L, Frentsch M, Wendisch D, Georg P, Kurth F, et al. Sars-Cov-2-Reactive T cells in healthy donors and patients with covid-19. *Nature* (2020) 587(7833):270–4. doi: 10.1038/s41586-020-2598-9

60. Krammer F. Sars-Cov-2 vaccines in development. *Nature* (2020) 586 (7830):516–27. doi: 10.1038/s41586-020-2798-3

61. Zhang C, Zhou C, Shi L, Liu G. Perspectives on development of vaccines against severe acute respiratory syndrome coronavirus 2 (Sars-Cov-2). *Hum Vaccin Immunother* (2020) 16(10):2366–9. doi: 10.1080/21645515.2020.1787064

62. Rydyznski Moderbacher C, Ramirez SI, Dan JM, Grifoni A, Hastie KM, Weiskopf D, et al. Antigen-specific adaptive immunity to sars-Cov-2 in acute covid-19 and associations with age and disease severity. *Cell* (2020) 183(4):996–1012 e19. doi: 10.1016/j.cell.2020.09.038

63. Tan AT, Linster M, Tan CW, Le Bert N, Chia WN, Kunasegaran K, et al. Early induction of functional sars-Cov-2-Specific T cells associates with rapid viral clearance and mild disease in covid-19 patients. *Cell Rep* (2021) 34(6):108728. doi: 10.1016/j.celrep.2021.108728

64. Zlei M, Sidorov IA, Joosten SA, Heemskerk MHM, Myeni SK, Pothast CR, et al. Immune determinants of viral clearance in hospitalised covid-19 patients: Reduced circulating naïve Cd4+ T cell counts correspond with delayed viral clearance. *Cells* (2022) 11(17):2743. doi: 10.3390/cells11172743

65. Fathi F, Sami R, Mozafarpoor S, Hafezi H, Motedayyen H, Arefnezhad R, et al. Immune system changes during covid-19 recovery play key role in determining disease severity. *Int J Immunopathol Pharmacol* (2020) 34:2058738420966497. doi: 10.1177/2058738420966497

66. Martonik D, Parfieniuk-Kowerda A, Rogalska M, Flisiak R. The role of Th17 response in covid-19. *Cells* (2021) 10(6):1550. doi: 10.3390/cells10061550

67. Wu D, Yang XO. Th17 responses in cytokine storm of covid-19: An emerging target of Jak2 inhibitor fedratinib. *J microbiol immunol infection = Wei mian yu gan ran za zhi* (2020) 53(3):368–70. doi: 10.1016/j.jmii.2020.03.005

68. Xu Z, Shi L, Wang Y, Zhang J, Huang L, Zhang C, et al. Pathological findings of covid-19 associated with acute respiratory distress syndrome. *Lancet Respir Med* (2020) 8(4):420–2. doi: 10.1016/s2213-2600(20)30076-x

69. Choto TA, Makupe I, Cakana AZ, Sibanda EN, Mduluza T. Excessive neutrophil recruitment promotes typical T-helper 17 responses in coronavirus disease 2019 patients. *PloS One* (2022) 17(8):e0273186. doi: 10.1371/journal.pone.0273186

70. De Biasi S, Meschiari M, Gibellini L, Bellinazzi C, Borella R, Fidanza L, et al. Marked T cell activation, senescence, exhaustion and skewing towards Th17 in patients with covid-19 pneumonia. *Nat Commun* (2020) 11(1):3434. doi: 10.1038/s41467-020-17292-4

71. Parackova Z, Bloomfield M, Klocperk A, Sediva A. Neutrophils mediate Th17 promotion in covid-19 patients. *J Leukocyte Biol* (2021) 109(1):73–6. doi: 10.1002/jlb.4covcra0820-481rrr

72. Kaneko N, Kuo HH, Boucau J, Farmer JR, Allard-Chamard H, Mahajan VS, et al. Loss of bcl-6-Expressing T follicular helper cells and germinal centers in covid-19. *Cell* (2020) 183(1):143–57.e13. doi: 10.1016/j.cell.2020.08.025

73. Shaan Lakshmanappa Y, Elizaldi SR, Roh JW, Schmidt BA, Carroll TD, Weaver KD, et al. Sars-Cov-2 induces robust germinal center Cd4 T follicular helper cell responses in rhesus macaques. *Nat Commun* (2021) 12(1):541. doi: 10.1038/s41467-020-20642-x

74. Zhang J, Wu Q, Liu Z, Wang Q, Wu J, Hu Y, et al. Spike-specific circulating T follicular helper cell and cross-neutralizing antibody responses in covid-19-Convalescent individuals. *Nat Microbiol* (2021) 6(1):51–8. doi: 10.1038/s41564-020-00824-5

75. Mudd PA, Minervina AA, Pogorelyy MV, Turner JS, Kim W, Kalaidina E, et al. Sars-Cov-2 mrna vaccination elicits a robust and persistent T follicular helper cell response in humans. *Cell* (2022) 185(4):603–13.e15. doi: 10.1016/j.cell.2021.12.026

76. Cavazzoni CB, Hanson BL, Podestà MA, Bechu ED, Clement RL, Zhang H, et al. Follicular T cells optimize the germinal center response to sars-Cov-2 protein vaccination in mice. *Cell Rep* (2022) 38(8):110399. doi: 10.1016/j.celrep.2022.110399

77. Meckiff BJ, Ramírez-Suástegui C, Fajardo V, Chee SJ, Kusnadi A, Simon H, et al. Imbalance of regulatory and cytotoxic sars-Cov-2-Reactive Cd4(+) T cells in covid-19. *Cell* (2020) 183(5):1340–53.e16. doi: 10.1016/j.cell.2020.10.001

78. Fenoglio D, Dentone C, Parodi A, Di Biagio A, Bozzano F, Vena A, et al. Characterization of T lymphocytes in severe covid-19 patients. *J Med Virol* (2021) 93(9):5608–13. doi: 10.1002/jmv.27037

79. Picchianti-Diamanti A, Aiello A, Laganà B, Agrati C, Castilletti C, Meschi S, et al. Immunosuppressivetherapies differently modulate humoral- and T-Cell-Specific responses to covid-19 mrna vaccine in rheumatoid arthritis patients. *Front Immunol* (2021) 12:740249. doi: 10.3389/fimmu.2021.740249

80. Riou C, du Bruyn E, Stek C, Daroowala R, Goliath RT, Abrahams F, et al. Relationship of sars-Cov-2-Specific Cd4 response to covid-19 severity and impact of hiv-1 and tuberculosis coinfection. *J Clin Invest* (2021) 131(12):e149125. doi: 10.1172/jci149125

81. Corthay A. How do regulatory T cells work? *Scandinavian J Immunol* (2009) 70(4):326–36. doi: 10.1111/j.1365-3083.2009.02308.x

82. Galvan-Pena S, Leon J, Chowdhary K, Michelson DA, Vijaykumar B, Yang L, et al. Profound treg perturbations correlate with covid-19 severity. *Proc Natl Acad Sci U.S.A.* (2021) 118(37):e2111315118. doi: 10.1073/pnas.2111315118

83. Ronit A, Berg RMG, Bay JT, Haugaard AK, Ahlstrom MG, Burgdorf KS, et al. Compartmental immunophenotyping in covid-19 Ards: A case series. *J Allergy Clin Immunol* (2021) 147(1):81–91. doi: 10.1016/j.jaci.2020.09.009

84. Taefehshokr N, Taefehshokr S, Heit B. Mechanisms of dysregulated humoral and cellular immunity by sars-Cov-2. *Pathog (Basel Switzerland)* (2020) 9(12):1027. doi: 10.3390/pathogens9121027

85. Kratzer B, Trapin D, Ettel P, Kormoczi U, Rottal A, Tuppy F, et al. Immunological imprint of covid-19 on human peripheral blood leukocyte populations. *Allergy* (2021) 76(3):751–65. doi: 10.1111/all.14647

86. Mohebbi SR, Baghaei K, Rostami-Nejad M, Nazemalhosseini Mojarad E, Mirjalali H, Yadegar A, et al. Significant changes of Cd4, Foxp3, Cd25, and Il6 expression level in Iranian covid-19 patients. *Gastroenterol Hepatol bed to bench* (2020) 13(4):388–92.

87. Jia R, Wang X, Liu P, Liang X, Ge Y, Tian H, et al. Mild cytokine elevation, moderate Cd4(+) T cell response and abundant antibody production in children with covid-19. *Virologica Sin* (2020) 35(6):734–43. doi: 10.1007/s12250-020-00265-8

88. Seepathomnarong P, Ongarj J, Sophonmanee R, Seeyankem B, Chusri S, Surasombatpattana S, et al. Regulatory T cells decreased during recovery from mild covid-19. *Viruses* (2022) 14(8):1688. doi: 10.3390/v14081688

89. Wiech M, Chroscicki P, Swatler J, Stepnik D, De Biasi S, Hampel M, et al. Remodeling of T cell dynamics during long covid is dependent on severity of sars-Cov-2 infection. *Front Immunol* (2022) 13:886431. doi: 10.3389/fimmu.2022.886431

90. Stephen-Victor E, Das M, Karnam A, Pitard B, Gautier JF, Bayry J. Potential of regulatory T-Cell-Based therapies in the management of severe covid-19. *Eur Respir J* (2020) 56(3):2002182. doi: 10.1183/13993003.02182-2020

91. Mazzoni A, Salvati L, Maggi L, Capone M, Vanni A, Spinicci M, et al. Impaired immune cell cytotoxicity in severe covid-19 is il-6 dependent. *J Clin Invest* (2020) 130(9):4694–703. doi: 10.1172/jci138554

92. Liu J, Yu J, McMahan K, Jacob-Dolan C, He X, Giffin V, et al. Cd8 T cells contribute to vaccine protection against sars-Cov-2 in macaques. *Sci Immunol* (2022) 7(77):eabq7647. doi: 10.1126/sciimmunol.abq7647

93. Song JW, Zhang C, Fan X, Meng FP, Xu Z, Xia P, et al. Immunological and inflammatory profiles in mild and severe cases of covid-19. *Nat Commun* (2020) 11 (1):3410. doi: 10.1038/s41467-020-17240-2

94. Zheng HY, Zhang M, Yang CX, Zhang N, Wang XC, Yang XP, et al. Elevated exhaustion levels and reduced functional diversity of T cells in peripheral blood may predict severe progression in covid-19 patients. *Cell Mol Immunol* (2020) 17(5):541–3. doi: 10.1038/s41423-020-0401-3

95. Diao B, Wang C, Tan Y, Chen X, Liu Y, Ning L, et al. Reduction and functional exhaustion of T cells in patients with coronavirus disease 2019 (Covid-19). *Front Immunol* (2020) 11:827. doi: 10.3389/fimmu.2020.00827

96. Rha MS, Jeong HW, Ko JH, Choi SJ, Seo IH, Lee JS, et al. Pd-1-Expressing sars-Cov-2-Specific Cd8(+) T cells are not exhausted, but functional in patients with covid-19. *Immunity* (2021) 54(1):44–52.e3. doi: 10.1016/j.immuni.2020.12.002

97. Szabo PA, Dogra P, Gray JI, Wells SB, Connors TJ, Weisberg SP, et al. Longitudinal profiling of respiratory and systemic immune responses reveals myeloid cell-driven lung inflammation in severe covid-19. *Immunity* (2021) 54 (4):797–814.e6. doi: 10.1016/j.immuni.2021.03.005

98. Kuse N, Zhang Y, Chikata T, Nguyen HT, Oka S, Gatanaga H, et al. Long-term memory Cd8(+) T cells specific for sars-Cov-2 in individuals who received the Bnt162b2 mrna vaccine. *Nat Commun* (2022) 13(1):5251. doi: 10.1038/s41467-022-32989-4

99. McMahan K, Yu J, Mercado NB, Loos C, Tostanoski LH, Chandrashekar A, et al. Correlates of protection against sars-Cov-2 in rhesus macaques. *Nature* (2021) 590(7847):630–4. doi: 10.1038/s41586-020-03041-6

100. Peng Y, Mentzer AJ, Liu G, Yao X, Yin Z, Dong D, et al. Broad and strong memory Cd4(+) and Cd8(+) T cells induced by sars-Cov-2 in uk convalescent individuals following covid-19. *Nat Immunol* (2020) 21(11):1336–45. doi: 10.1038/s41590-020-0782-6

101. Kalimuddin S, Tham CYL, Qui M, de Alwis R, Sim JXY, Lim JME, et al. Early T cell and binding antibody responses are associated with covid-19 rna vaccine efficacy onset. *Med (N Y)* (2021) 2(6):682–8.e4. doi: 10.1016/j.medj.2021.04.003

102. Rydyznski Moderbacher C, Kim CJ, Mateus J, Plested JS, Zhu M, Cloney-Clark S, et al. Nvx-Cov2373 vaccination induces functional sars-Cov-2-Specific Cd4+ and Cd8+ T cell responses. *J Clin Invest* (2022) 132(19):e160898. doi: 10.1172/jci160898

103. Reinscheid M, Luxenburger H, Karl V, Graeser A, Giese S, Ciminski K, et al. Covid-19 mrna booster vaccine induces transient Cd8+ T effector cell responses while conserving the memory pool for subsequent reactivation. *Nat Commun* (2022) 13(1):4631. doi: 10.1038/s41467-022-32324-x

104. Oberhardt V, Luxenburger H, Kemming J, Schulien I, Ciminski K, Giese S, et al. Rapid and stable mobilization of Cd8(+) T cells by sars-Cov-2 mrna vaccine. *Nature* (2021) 597(7875):268–73. doi: 10.1038/s41586-021-03841-4

105. Sosa-Hernández VA, Torres-Ruíz J, Cervantes-Díaz R, Romero-Ramírez S, Páez-Franco JC, Meza-Sánchez DE, et al. B cell subsets as severity-associated signatures in covid-19 patients. *Front Immunol* (2020) 11:611004. doi: 10.3389/fimmu.2020.611004

106. Cao T, Liu L, To KK, Lim CY, Zhou R, Ming Y, et al. Mitochondrial regulation of acute extrafollicular b-cell responses to covid-19 severity. *Clin Trans Med* (2022) 12(9):e1025. doi: 10.1002/ctm2.1025

107. Huang C. Germinal center reaction. *Adv Exp Med Biol* (2020) 1254:47–53. doi: 10.1007/978-981-15-3532-1_4

108. Ryg-Cornejo V, Ioannidis LJ, Ly A, Chiu CY, Tellier J, Hill DL, et al. Severe malaria infections impair germinal center responses by inhibiting T follicular helper cell differentiation. *Cell Rep* (2016) 14(1):68–81. doi: 10.1016/j.celrep.2015.12.006

109. Popescu M, Cabrera-Martinez B, Winslow GM. Tnf-A contributes to lymphoid tissue disorganization and germinal center b cell suppression during intracellular bacterial infection. *J Immunol (Baltimore Md 1950)* (2019) 203 (9):2415–24. doi: 10.4049/jimmunol.1900484

110. Rodda LB, Netland J, Shehata L, Pruner KB, Morawski PA, Thouvenel CD, et al. Functional sars-Cov-2-Specific immune memory persists after mild covid-19. *Cell* (2021) 184(1):169–83.e17. doi: 10.1016/j.cell.2020.11.029

111. Ogega CO, Skinner NE, Blair PW, Park HS, Littlefield K, Ganesan A, et al. Durable sars-Cov-2 b cell immunity after mild or severe disease. *J Clin Invest* (2021) 131(7):e145516. doi: 10.1172/jci145516

112. Sokal A, Broketa M, Barba-Spaeth G, Meola A, Fernández I, Fourati S, et al. Analysis of mrna vaccination-elicited rbd-specific memory b cells reveals strong but incomplete immune escape of the sars-Cov-2 omicron variant. *Immunity* (2022) 55(6):1096–104.e4. doi: 10.1016/j.immuni.2022.04.002

113. Awadasseid A, Wu Y, Tanaka Y, Zhang W. Current advances in the development of sars-Cov-2 vaccines. *Int J Biol Sci* (2021) 17(1):8–19. doi: 10.7150/ijbs.52569

114. Gao Q, Bao L, Mao H, Wang L, Xu K, Yang M, et al. Development of an inactivated vaccine candidate for sars-Cov-2. *Science* (2020) 369(6499):77–81. doi: 10.1126/science.abc1932

115. Zhang Y, Zeng G, Pan H, Li C, Hu Y, Chu K, et al. Safety, tolerability, and immunogenicity of an inactivated sars-Cov-2 vaccine in healthy adults aged 18-59 years: A randomised, double-blind, placebo-controlled, phase 1/2 clinical trial. *Lancet Infect Dis* (2021) 21(2):181–92. doi: 10.1016/s1473-3099(20)30843-4

116. Wu Z, Hu Y, Xu M, Chen Z, Yang W, Jiang Z, et al. Safety, tolerability, and immunogenicity of an inactivated sars-Cov-2 vaccine (Coronavac) in healthy adults aged 60 years and older: A randomised, double-blind, placebo-controlled, phase 1/2 clinical trial. *Lancet Infect Dis* (2021) 21(6):803–12. doi: 10.1016/s1473-3099(20)30987-7

117. Han B, Song Y, Li C, Yang W, Ma Q, Jiang Z, et al. Safety, tolerability, and immunogenicity of an inactivated sars-Cov-2 vaccine (Coronavac) in healthy children and adolescents: A double-blind, randomised, controlled, phase 1/2 clinical trial. *Lancet Infect Dis* (2021) 21(12):1645–53. doi: 10.1016/s1473-3099(21)00319-4

118. Tanriover MD, Doganay HL, Akova M, Guner HR, Azap A, Akhan S, et al. Efficacy and safety of an inactivated whole-virion sars-Cov-2 vaccine (Coronavac): Interim results of a double-blind, randomised, placebo-controlled, phase 3 trial in Turkey. *Lancet* (2021) 398(10296):213–22. doi: 10.1016/S0140-6736(21)01429-X

119. Costa Clemens SA, Weckx L, Clemens R, Almeida Mendes AV, Ramos Souza A, Silveira MBV, et al. Heterologous versus homologous covid-19 booster vaccination in previous recipients of two doses of coronavac covid-19 vaccine in Brazil (Rhh-001): A phase 4, non-inferiority, single blind, randomised study. *Lancet* (2022) 399(10324):521–9. doi: 10.1016/S0140-6736(22)00094-0

120. Polack FP, Thomas SJ, Kitchin N, Absalon J, Gurtman A, Lockhart S, et al. Safety and efficacy of the Bnt162b2 mrna covid-19 vaccine. *New Engl J Med* (2020) 383(27):2603–15. doi: 10.1056/NEJMoa2034577

121. Baden LR, El Sahly HM, Essink B, Kotloff K, Frey S, Novak R, et al. Efficacy and safety of the mrna-1273 sars-Cov-2 vaccine. *New Engl J Med* (2021) 384 (5):403–16. doi: 10.1056/NEJMoa2035389

122. Zhu FC, Li YH, Guan XH, Hou LH, Wang WJ, Li JX, et al. Safety, tolerability, and immunogenicity of a recombinant adenovirus type-5 vectored covid-19 vaccine: A dose-escalation, open-label, non-randomised, first-in-Human trial. *Lancet* (2020) 395(10240):1845–54. doi: 10.1016/S0140-6736(20)31208-3

123. Zhu FC, Guan XH, Li YH, Huang JY, Jiang T, Hou LH, et al. Immunogenicity and safety of a recombinant adenovirus type-5-Vectored covid-19 vaccine in healthy adults aged 18 years or older: A randomised, double-blind, placebo-controlled, phase 2 trial. *Lancet* (2020) 396(10249):479–88. doi: 10.1016/S0140-6736(20)31605-6

124. Zhu F, Jin P, Zhu T, Wang W, Ye H, Pan H, et al. Safety and immunogenicity of a recombinant adenovirus type-5-Vectored covid-19 vaccine with a homologous prime-boost regimen in healthy participants aged 6 years and above: A randomised, double-blind, placebo-controlled, phase 2b trial. *Clin Infect Dis* (2021) 75(1):e783–91. doi: 10.1093/cid/ciab845

125. Hung IFN, Poland GA. Single-dose Oxford-astrazeneca covid-19 vaccine followed by a 12-week booster. *Lancet* (2021) 397(10277):854–5. doi: 10.1016/S0140-6736(21)00528-6

126. Folegatti PM, Ewer KJ, Aley PK, Angus B, Becker S, Belij-Rammerstorfer S, et al. Safety and immunogenicity of the Chadox1 ncov-19 vaccine against sars-Cov-2: A preliminary report of a phase 1/2, single-blind, randomised controlled trial. *Lancet* (2020) 396(10249):467–78. doi: 10.1016/S0140-6736(20)31604-4

127. Yang S, Li Y, Dai L, Wang J, He P, Li C, et al. Safety and immunogenicity of a recombinant tandem-repeat dimeric rbd-based protein subunit vaccine (Zf2001) against covid-19 in adults: Two randomised, double-blind, placebo-controlled, phase 1 and 2 trials. *Lancet Infect Dis* (2021) 21(8):1107–19. doi: 10.1016/S1473-3099(21)00127-4

128. Cao Y, Yisimayi A, Bai Y, Huang W, Li X, Zhang Z, et al. Humoral immune response to circulating sars-Cov-2 variants elicited by inactivated and rbd-subunit vaccines. *Cell Res* (2021) 31(7):732–41. doi: 10.1038/s41422-021-00514-9

129. Zhang Z, Mateus J, Coelho CH, Dan JM, Moderbacher CR, Gálvez RI, et al. Humoral and cellular immune memory to four covid-19 vaccines. *Cell* (2022) 185 (14):2434–51.e17. doi: 10.1016/j.cell.2022.05.022

130. Suryawanshi RK, Chen IP, Ma T, Syed AM, Brazer N, Saldhi P, et al. Limited cross-variant immunity from sars-Cov-2 omicron without vaccination. *Nature* (2022) 607(7918):351–5. doi: 10.1038/s41586-022-04865-0

131. Ranzani OT, Hitchings MDT, Dorion M, D'Agostini TL, de Paula RC, de Paula OFP, et al. Effectiveness of the coronavac vaccine in older adults during a gamma variant associated epidemic of covid-19 in Brazil: Test negative case-control study. *BMJ (Clinical Res ed)* (2021) 374:n2015. doi: 10.1136/bmj.n2015

132. Madhi SA, Baillie V, Cutland CL, Voysey M, Koen AL, Fairlie L, et al. Efficacy of the Chadox1 ncov-19 covid-19 vaccine against the b. 1.351 variant. *New Engl J Med* (2021) 384(20):1885–98. doi: 10.1056/NEJMoa2102214

133. Lopez Bernal J, Andrews N, Gower C, Gallagher E, Simmons R, Thelwall S, et al. Effectiveness of covid-19 vaccines against the B.1.617.2 (Delta) variant. *New Engl J Med* (2021) 385(7):585–94. doi: 10.1056/NEJMoa2108891

134. Cheng SMS, Mok CKP, Leung YWY, Ng SS, Chan KCK, Ko FW, et al. Neutralizing antibodies against the sars-Cov-2 omicron variant Ba.1 following homologous and heterologous coronavac or Bnt162b2 vaccination. *Nat Med* (2022) 28(3):486–9. doi: 10.1038/s41591-022-01704-7

135. Lapointe HR, Mwimanzi F, Cheung PK, Sang Y, Yaseen F, Kalikawe R, et al. Serial infection with sars-Cov-2 omicron Ba.1 and Ba.2 following three-dose covid-19 vaccination. *Front Immunol* (2022) 13:947021. doi: 10.3389/fimmu.2022.947021

136. Hajnik RL, Plante JA, Liang Y, Alameh MG, Tang J, Bonam SR, et al. Dual spike and nucleocapsid mrna vaccination confer protection against sars-Cov-2 omicron and delta variants in preclinical models. *Sci Trans Med* (2022) 14(662): eabq1945. doi: 10.1126/scitranslmed.abq1945

137. Barchuk A, Cherkashin M, Bulina A, Berezina N, Rakova T, Kuplevatskaya D, et al. Vaccine effectiveness against referral to hospital after sars-Cov-2 infection in st. Petersburg, Russia, during the delta variant surge: A test-negative case-control study. *BMC Med* (2022) 20(1):312. doi: 10.1186/s12916-022-02509-8

138. Drożdżal S, Rosik J, Lechowicz K, Machaj F, Szostak B, Przybyciński J, et al. An update on drugs with therapeutic potential for sars-Cov-2 (Covid-19) treatment. *Drug resistance updates Rev commentaries antimicrobial Anticancer chemother* (2021) 59:100794. doi: 10.1016/j.drup.2021.100794

139. Kuritzkes DR. Bamlanivimab for prevention of covid-19. *Jama* (2021) 326 (1):31–2. doi: 10.1001/jama.2021.7515

140. Chew KW, Moser C, Daar ES, Wohl DA, Li JZ, Coombs RW, et al. Antiviral and clinical activity of bamlanivimab in a randomized trial of non-hospitalized adults with covid-19. *Nat Commun* (2022) 13(1):4931. doi: 10.1038/s41467-022-32551-2

141. Chen P, Nirula A, Heller B, Gottlieb RL, Boscia J, Morris J, et al. Sars-Cov-2 neutralizing antibody ly-Cov555 in outpatients with covid-19. *New Engl J Med* (2021) 384(3):229–37. doi: 10.1056/NEJMoa2029849

142. Dougan M, Nirula A, Azizad M, Mocherla B, Gottlieb RL, Chen P, et al. Bamlanivimab plus etesevimab in mild or moderate covid-19. *New Engl J Med* (2021) 385(15):1382–92. doi: 10.1056/NEJMoa2102685

143. Gupta A, Gonzalez-Rojas Y, Juarez E, Crespo Casal M, Moya J, Falci DR, et al. Early treatment for covid-19 with sars-Cov-2 neutralizing antibody sotrovimab. *New Engl J Med* (2021) 385(21):1941–50. doi: 10.1056/NEJMoa2107934

144. An eua for sotrovimab for treatment of covid-19. *Med letter Drugs Ther* (2021) 63(1627):97–xx8.

145. RECOVERY Collaborative Group. Casirivimab and imdevimab in patients admitted to hospital with covid-19 (Recovery): A randomised, controlled, open-label, platform trial. *Lancet* (2022) 399(10325):665–76. doi: 10.1016/s0140-6736(22)00163-5

146. Malgie J, Schoones JW, Pijls BG. Decreased mortality in coronavirus disease 2019 patients treated with tocilizumab: A rapid systematic review and meta-analysis of observational studies. *Clin Infect Dis* (2021) 72(11):e742–e9. doi: 10.1093/cid/ciaa1445

147. Lamb YN. Remdesivir: First approval. *Drugs* (2020) 80(13):1355–63. doi: 10.1007/s40265-020-01378-w

148. Wang Y, Zhang D, Du G, Du R, Zhao J, Jin Y, et al. Remdesivir in adults with severe covid-19: A randomised, double-blind, placebo-controlled, multicentre trial. *Lancet* (2020) 395(10236):1569–78. doi: 10.1016/s0140-6736(20)31022-9

149. Lai CC, Chen CH, Wang CY, Chen KH, Wang YH, Hsueh PR. Clinical efficacy and safety of remdesivir in patients with covid-19: A systematic review and network meta-analysis of randomized controlled trials. *J Antimicrobial Chemother* (2021) 76(8):1962–8. doi: 10.1093/jac/dkab093

150. Hanafusa M, Nawa N, Goto Y, Kawahara T, Miyamae S, Ueki Y, et al. Effectiveness of remdesivir with corticosteroids for covid-19 patients in intensive care unit: A hospital-based observational study. *J Med Virol* (2022). doi: 10.1002/jmv.28168

151. Stebbing J, Krishnan V, de Bono S, Ottaviani S, Casalini G, Richardson PJ, et al. Mechanism of baricitinib supports artificial intelligence-predicted testing in covid-19 patients. *EMBO Mol Med* (2020) 12(8):e12697. doi: 10.15252/emmm.202012697

152. Cantini F, Niccoli L, Nannini C, Matarrese D, Natale MED, Lotti P, et al. Beneficial impact of baricitinib in covid-19 moderate pneumonia; multicentre study. *J infection* (2020) 81(4):647–79. doi: 10.1016/j.jinf.2020.06.052

153. Dowty ME, Lin J, Ryder TF, Wang W, Walker GS, Vaz A, et al. The pharmacokinetics, metabolism, and clearance mechanisms of tofacitinib, a janus kinase inhibitor, in humans. *Drug Metab disposition: Biol fate chemicals* (2014) 42 (4):759–73. doi: 10.1124/dmd.113.054940

154. Guimarães PO, Quirk D, Furtado RH, Maia LN, Saraiva JF, Antunes MO, et al. Tofacitinib in patients hospitalized with covid-19 pneumonia. *New Engl J Med* (2021) 385(5):406–15. doi: 10.1056/NEJMoa2101643

155. Extance A. Covid-19: What is the evidence for the antiviral paxlovid? *BMJ (Clinical Res ed)* (2022) 377:o1037. doi: 10.1136/bmj.o1037

156. Halford B. The path to paxlovid. *ACS Cent Sci* (2022) 8(4):405–7. doi: 10.1021/acscentsci.2c00369

157. Mahase E. Covid-19: Pfizer's paxlovid is 89% effective in patients at risk of serious illness, company reports. *BMJ (Clinical Res ed)* (2021) 375:n2713. doi: 10.1136/bmj.n2713

158. Sun F, Lin Y, Wang X, Gao Y, Ye S. Paxlovid in patients who are immunocompromised and hospitalised with sars-Cov-2 infection. *Lancet Infect Dis* (2022) 22(9):1279. doi: 10.1016/s1473-3099(22)00430-3

159. Burki T. The future of paxlovid for covid-19. *Lancet Respir Med* (2022) 10 (7):e68. doi: 10.1016/s2213-2600(22)00192-8

160. Graham F. Daily briefing: Inside merck's covid drug, molnupiravir. *Nature* (2021). doi: 10.1038/d41586-021-02792-0

161. Johnson MG, Puenpatom A, Moncada PA, Burgess L, Duke ER, Ohmagari N, et al. Effect of molnupiravir on biomarkers, respiratory interventions, and medical services in covid-19 : A randomized, placebo-controlled trial. *Ann Internal Med* (2022) 175(8):1126–34. doi: 10.7326/m22-0729

162. Jayk Bernal A, Gomes da Silva MM, Musungaie DB, Kovalchuk E, Gonzalez A, Delos Reyes V, et al. Molnupiravir for oral treatment of covid-19 in nonhospitalized patients. *New Engl J Med* (2022) 386(6):509–20. doi: 10.1056/NEJMoa2116044

163. Mahase E. Covid-19: Molnupiravir reduces risk of hospital admission or death by 50% in patients at risk, msd reports. *BMJ (Clinical Res ed)* (2021) 375: n2422. doi: 10.1136/bmj.n2422

164. Fischer WA2nd, Eron JJJr., Holman W, MS C, Fang L, LJ S, et al. A phase 2a clinical trial of molnupiravir in patients with covid-19 shows accelerated sars-Cov-2 rna clearance and elimination of infectious virus. *Sci Trans Med* (2022) 14 (628):eabl7430. doi: 10.1126/scitranslmed.abl7430

165. Li P, Wang Y, Lavrijsen M, Lamers MM, de Vries AC, Rottier RJ, et al. Sars-Cov-2 omicron variant is highly sensitive to molnupiravir, nirmatrelvir, and the combination. *Cell Res* (2022) 32(3):322–4. doi: 10.1038/s41422-022-00618-w

166. Sun L, Peng Y, Yu W, Zhang Y, Liang L, Song C, et al. Mechanistic insight into antiretroviral potency of 2'-Deoxy-2'-B-Fluoro-4'-Azidocytidine (Fnc) with a long-lasting effect on hiv-1 prevention. *J medicinal Chem* (2020) 63(15):8554–66. doi: 10.1021/acs.jmedchem.0c00940

167. Ren Z, Luo H, Yu Z, Song J, Liang L, Wang L, et al. A randomized, open-label, controlled clinical trial of azvudine tablets in the treatment of mild and common covid-19, a pilot study. *Advanced Sci (Weinheim Baden-Wurttemberg Germany)* (2020) 7(19):e2001435. doi: 10.1002/advs.202001435

168. Yu B, Chang J. Azvudine (Fnc): A promising clinical candidate for covid-19 treatment. *Signal Transduct Target Ther* (2020) 5(1):236. doi: 10.1038/s41392-020-00351-z

169. Zhang JL, Li YH, Wang LL, Liu HQ, Lu SY, Liu Y, et al. Azvudine is a thymus-homing anti-Sars-Cov-2 drug effective in treating covid-19 patients. *Signal Transduct Target Ther* (2021) 6(1):414. doi: 10.1038/s41392-021-00835-6

170. Humphries F, Shmuel-Galia L, Jiang Z, Wilson R, Landis P, Ng SL, et al. A diamidobenzimidazole sting agonist protects against sars-Cov-2 infection. *Sci Immunol* (2021) 6(59):eabi9002. doi: 10.1126/sciimmunol.abi9002

171. Li M, Ferretti M, Ying B, Descamps H, Lee E, Dittmar M, et al. Pharmacological activation of sting blocks sars-Cov-2 infection. *Sci Immunol* (2021) 6(59):eabi9007. doi: 10.1126/sciimmunol.abi9007

172. Hu K, Guan WJ, Bi Y, Zhang W, Li L, Zhang B, et al. Efficacy and safety of lianhua qingwen capsules, a repurposed Chinese herb, in patients with coronavirus disease 2019: A multicenter, prospective, randomized controlled trial [Phytomedicine 85 (2021) 153242]. *Phytomedicine* (2022) 94:153800. doi: 10.1016/j.phymed.2021.153800

173. Xia QD, Xun Y, Lu JL, Lu YC, Yang YY, Zhou P, et al. Network pharmacology and molecular docking analyses on lianhua qingwen capsule indicate Akt1 is a potential target to treat and prevent covid-19. *Cell Prolif* (2020) 53(12):e12949. doi: 10.1111/cpr.12949

frontiers | Frontiers in Immunology

TYPE Original Research
PUBLISHED 02 December 2022
DOI 10.3389/fimmu.2022.1034159

Check for updates

OPEN ACCESS

EDITED BY
Edwin Bölke,
Heinrich Heine University of Düsseldorf, Germany

REVIEWED BY
Kelly Nunes,
University of São Paulo, Brazil
Junliang Fu,
Fifth Medical Center of PLA General Hospital, China

*CORRESPONDENCE
Meghnad Joshi
drmeghnadjoshi@gmai.com
Tavpritesh Sethi
tavpriteshsethi@iiitd.ac.in
Rajesh Pandey
rajesh.p@igib.res.in;
rajeshp@igib.in

†These authors have contributed equally to this work

SPECIALTY SECTION
This article was submitted to Viral Immunology, a section of the journal Frontiers in Immunology

RECEIVED 01 September 2022
ACCEPTED 16 November 2022
PUBLISHED 02 December 2022

CITATION
Chattopadhyay P, Khare K, Kumar M, Mishra P, Anand A, Maurya R, Gupta R, Sahni S, Gupta A, Wadhwa S, Yadav A, Devi P, Tardalkar K, Joshi M, Sethi T and Pandey R (2022) Single-cell multiomics revealed the dynamics of antigen presentation, immune response and T cell activation in the COVID-19 positive and recovered individuals. *Front. Immunol.* 13:1034159. doi: 10.3389/fimmu.2022.1034159

Single-cell multiomics revealed the dynamics of antigen presentation, immune response and T cell activation in the COVID-19 positive and recovered individuals

Partha Chattopadhyay[1,2], Kriti Khare[1,2†], Manish Kumar[2,3†], Pallavi Mishra[1†], Alok Anand[4†], Ranjeet Maurya[1,2], Rohit Gupta[1], Shweta Sahni[3], Ayushi Gupta[4], Saruchi Wadhwa[3], Aanchal Yadav[1,2], Priti Devi[1,2], Kishore Tardalkar[5], Meghnad Joshi[5*], Tavpritesh Sethi[4*] and Rajesh Pandey[1,2*]

[1]Division of Immunology and Infectious Disease Biology, INtegrative GENomics of HOst-PathogEn (INGEN-HOPE) laboratory, CSIR-Institute of Genomics and Integrative Biology (CSIR-IGIB), Delhi, India, [2]Academy of Scientific and Innovative Research (AcSIR), Ghaziabad, India, [3]CSIR-Institute of Genomics and Integrative Biology (CSIR-IGIB), Delhi, India, [4]Indraprastha Institute of Information Technology Delhi, New Delhi, India, [5]Department of Stem Cells and Regenerative Medicine, Dr. D. Y. Patil Medical College, Hospital and Research Institute, Kolhapur, Maharashtra, India

Introduction: Despite numerous efforts to describe COVID-19's immunological landscape, there is still a gap in our understanding of the virus's infections after-effects, especially in the recovered patients. This would be important to understand as we now have huge number of global populations infected by the SARS-CoV-2 as well as variables inclusive of VOCs, reinfections, and vaccination breakthroughs. Furthermore, single-cell transcriptome alone is often insufficient to understand the complex human host immune landscape underlying differential disease severity and clinical outcome.

Methods: By combining single-cell multi-omics (Whole Transcriptome Analysis plus Antibody-seq) and machine learning-based analysis, we aim to better understand the functional aspects of cellular and immunological heterogeneity in the COVID-19 positive, recovered and the healthy individuals.

Results: Based on single-cell transcriptome and surface marker study of 163,197 cells (124,726 cells after data QC) from the 33 individuals (healthy=4, COVID-19 positive=16, and COVID-19 recovered=13), we observed a reduced MHC Class-I-mediated antigen presentation and dysregulated MHC Class-II-mediated antigen presentation in the COVID-19 patients, with restoration of the process in the recovered individuals. B-cell maturation process was also impaired in the positive and the recovered individuals. Importantly, we discovered that a subset of the naive T-cells from the healthy individuals

10.3389/fimmu.2022.1034159

were absent from the recovered individuals, suggesting a post-infection inflammatory stage. Both COVID-19 positive patients and the recovered individuals exhibited a CD40-CD40LG-mediated inflammatory response in the monocytes and T-cell subsets. T-cells, NK-cells, and monocyte-mediated elevation of immunological, stress and antiviral responses were also seen in the COVID-19 positive and the recovered individuals, along with an abnormal T-cell activation, inflammatory response, and faster cellular transition of T cell subtypes in the COVID-19 patients. Importantly, above immune findings were used for a Bayesian network model, which significantly revealed *FOS, CXCL8, IL1β, CST3, PSAP, CD45* and *CD74* as COVID-19 severity predictors.

Discussion: In conclusion, COVID-19 recovered individuals exhibited a hyper-activated inflammatory response with the loss of B cell maturation, suggesting an impeded post-infection stage, necessitating further research to delineate the dynamic immune response associated with the COVID-19. To our knowledge this is first multi-omic study trying to understand the differential and dynamic immune response underlying the sample subtypes.

KEYWORDS

COVID-19, single cell multi-omics, recovered COVID-19 individuals, immune response, bayesian network model, T-cell activation

Introduction

COVID-19 pandemic is into its 3rd year in continuum, and it continues to pose threat to lives, healthcare support, medical infrastructure and livelihoods. This has been compounded by new emerging SARS-CoV-2 variants of concern (VOC) with differential geographical origin and emphasizing the constant need for effective vaccines/dosage. Due to the lack of antibody neutralization along with immune evasion, these emerging variants of SARS-CoV-2 have posed a global threat to human health compounded by the diversity of disease severity symptoms. Therefore, it is important to undertake studies in different population cohorts, especially high population density regions, to understand and elucidate the differential immune response. This will enable mechanistic understanding of the hosts' immune response during COVID-19 disease. Towards this, studying the whole transcriptome along with surface marker expression at the single cell resolution can provide detailed functional insights into the COVID-19 pathology.

Previous evidence suggests that a significant immune dysregulation occurs in severe COVID-19 patients (Su, 2020). In particular, studies on peripheral blood mononuclear cells (PBMCs) have revealed reduced IFN-gamma production (1), expansion of highly cytotoxic effector T cell subsets (2), and increased expression of the exhaustion markers programmed cell death protein 1 and Tim-3 on CD8+ T cells in the severe COVID-19 patients (3). Another study revealed classical monocytes, along with monocyte chemoattractant CCL2 and its receptor CCR2, the neutrophil chemoattractant CXCL8, and TNF-α as the main mechanism of cytokine storm observed in the COVID-19 (4). A significant decrease in the non-classical monocyte genes (*C1AQ, C1BQ*, and *LSTB1* expression) and a corresponding relative increase of classical monocytes genes (*S100A8, S100A9*, and *S100A12* expression) in the critical COVID-19 patients was also observed (5). Upregulation of *IL6R* and *IL6ST* in the COVID-19 patients have been reported, which synergistically promotes increased proinflammatory cytokines during pathogenesis. Several interferon (IFN)-stimulated genes (ISGs; including *ISG15, IFI44, IFI44L*, and *RSAD2*) were also specifically upregulated in the PBMCs from the COVID-19 patients, enhancing antiviral and immune modulatory functions (6). Presence of lymphopenia, immune cell exhaustion, and elevated serum pro-inflammatory cytokines are some of the striking features of COVID-19 disease severity (1, 7, 8). Also, impaired activation of B cell subsets provides evidence to explain the delayed viral clearance in the severely ill COVID-19 patients (9). While several studies have provided a comprehensive atlas of the immune response dynamics in the COVID-19 patients, a few studies have recently highlighted the immune repertoire of the recovered individuals. In one study, neutrophil activation and migration associated genes were reported to be downregulated in the recovered individuals compared to the active infection (10). The monocyte mediated immune response was reported to be restored to normal in the convalescent COVID-19 patients (11). Another study reported a decreased T cell differentiation in the

recovered individuals post severe COVID-19, but an opposite pattern post mild/moderate COVID-19 (12).

Above studies have augmented our understanding of the spectrum of immune response in the COVID-19 patients globally, except India. However, it is also true that most of the studies have reported the immune profile between the healthy and SARS-CoV-2 infected individuals. We think it would also be fruitful to understand and investigate the pathophysiology that drives the SARS-CoV-2 infection by single cell based immune profile post-infection, in the *recovered patients along with the healthy and active infection*. Along with this, in addition to the transcriptomic response, the cell surface markers can also provide vital clues about the pathophysiology, as they not only are cell-type identifiers, but they also represent the cell state as well. Yet, a comprehensive investigation of COVID-19 pathophysiology, across active COVID-19 and recovered patients, including transcriptome as well as cell surface marker is lacking. Here, for the first time, we performed simultaneous single-cell transcriptomics and single-cell Ab-seq across the healthy, COVID-19 positive and recovered individuals.

Our study reports a decreased MHC Class I-mediated antigen presentation as well as dysfunctional MHC Class II-mediated antigen presentation in the COVID-19 positive patients, followed by a restoration of the function in the recovered individuals. We also found a loss of B cell maturation process, reduced cytotoxicity and antibody response in the recovered individuals. Besides, we identified a CD40-CD40 ligand interaction-mediated increased inflammatory, immune and stress response by the monocyte, NK cells, CD4+ TCM, and CD8+ T cell populations in the COVID-19 patients. We observed a faster cellular transition within the T cell subtypes in COVID-19 patients, with a T cell-mediated perturbation of normal cellular functions alongside the immune/inflammatory response. Finally, using a Bayesian Network model, we identified *FOS, CXCL8, IL1β, CST3, PSAP, CD45* and *CD74* as predictors of the COVID-19 disease. The findings will augment the understanding vis-a-vis the heterogeneity and complexity of the immune response in the COVID-19 positive and recovered individuals, as well as provide an integrated multi-omics model for immune response during infection, post-infection and without infection.

Methods and materials

Patient cohort, sampling and data collection

Sample collection

The samples were collected at a tertiary care center (Dr. D. Y. Patil Medical College, Hospital and Research Institute, Kolhapur, Maharashtra, India) from the healthy volunteers, patients with confirmed COVID-19 positive status and patients recovered from COVID-19 (within 4 weeks) based on qRT-PCR results under the ethics oversight of the institution. The samples were matched with respect to age and gender, and the infecting SARS-CoV-2 variant was identified using Oxford Nanopore sequencing. In the COVID-19 positive group, 13 out of 16 individuals were infected with 20B, and the rest three with 20A variant. In the recovered group, 11 out of 13 were infected with 20B and rest two with 20A. The COVID-19 positive and recovered individuals were matched with respect to the disease severity. The blood samples were collected in the BD Vacutainer® CPT™ Cell Preparation Tube with sodium citrate. Peripheral blood mononuclear cells (PBMC) were isolated from whole blood using the manufacturer's recommendation (ref no 362761). The PBMCs were cryopreserved in a cryopreservation media (FBS and DMSO at 9:1 ratio) till further use.

Sample processing and library preparation

The PBMCs were revived and processed using BD Rhapsody single cell analysis system as per Domenico et al. (13). Briefly, 0.2 million cells per sample were taken and labelled using BD™ Single-Cell Multiplexing Kit-Human and 40 BD™ AbSeq Ab-Oligos as per manufacturer's guide (Doc ID: 214419 Rev. 2.0). An average of 30000 pooled cells were loaded in each cartridge on the BD Rhapsody express single cell analysis system for single cell capture followed by the cDNA synthesis as per manufacturer's guideline (Doc ID: 210967 Rev. 1.0). mRNA Whole Transcriptome Analysis (WTA), Ab-Seq, and Sample Tag library were prepared using BD Rhapsody™ WTA Amplification kit as per manufacturer's guideline (Doc ID: 23-21752-00). The libraries were sequenced using NovaSeq 6000 S2 reagent kit at 30000 reads/cell for WTA, 20000 reads/cell for AbSeq, and 120 reads/cell/Sample Tag for sample tag library, with 101 x 2 cycles.

scRNA-seq data processing, clustering and cell-type annotation

The raw sequencing data was demultiplexed and converted to FASTQ format using the bcl2fastq tool. The data was analyzed using BD Rhapsody WTA analysis pipeline as per manufacturer's guideline (Doc ID: 47383 Rev. 9.0). The count matrix with recursive substitution error correction was imported to Seurat R package for downstream analysis and visualization (14). The WTA and Ab-Seq count matrices for all the healthy, active COVID-19 and recovered patients (a total of 163197 cells) were merged for integrated multimodal analysis. Quality parameters were optimized and cells containing >2500 UMI and <20UMI were discarded. Batch effects were normalized and

data was normalized using Seurat SCTransform V2 (15, 16). Finally, cells were clustered using unsupervised clustering at a resolution of 0.4 and visualized with UMAP algorithm (17). Cluster specific genes were identified using FindAllMarker function (Wilcoxon rank sum test, Log2 Fold Change cut-off 1.5). Clusters were comprehensively annotated manually using a combination of CellMarker DB, PanglaoDB, and Azimuth, as well as automatically using scpred, an SVM-based single cell annotation tool. The same pipeline was also applied for a pairwise visualization of the data (healthy vs COVID-19, COVID-19 vs recovered, and healthy vs recovered).

Differential gene expression and gene set enrichment analysis

Differential gene expression analysis was performed on clustered pairwise data (healthy/COVID-19, COVID-19/recovered and healthy/recovered) using Seurat FindMarker function (Wilcoxon rank sum test, Log2FC cut-off 1.5, q value cut-off 0.05). For cluster-wise pseudo-bulk differential gene expression analysis, average gene expression was taken at the sample-level, followed by differential gene expression analysis using DESeq2 r package across the three groups (18). Wald test was applied for the analysis, followed by the visualization using pheatmap R package. Gene set enrichment analysis (GSEA) was performed at the single cell resolution, keeping the cluster and group identity, using the escape R package. Gene set collections were used from built-in Molecular Signature Database to perform the enrichment. The relative enrichment scores for each pathway were represented in the form of a heatmap using dittoSeq R package (19).

Signaling networks interaction inference

The Signaling network analysis was performed using CellDesigner to infer the protein and pathways interaction networks for significantly differentially expressed gene sets. The P values were corrected using the Bonferroni Method.

Single cell pseudotime trajectory analysis

At first, the T cell subtypes were extracted from the Seurat object containing all the 17 cell types. The data was preprocessed as documented by Packer et al. (20). A principal trajectory graph was built within each partition using the learn_graph function in Monocle3 (21). The cells were ordered along with the pseudotime trajectory which follows the shortest path. Naive CD4+/CD8+ T cell was defined as the root node while constructing the trajectory. To find the modules of co-expressed genes, we used the differentially expressed genes across the healthy, COVID-19 positive and recovered individuals (pseudobulk differential expression analysis). We extracted the genes falling in each module and performed GO enrichment using Enrichr (22). GO molecular functions with statistically significant enrichment score (p value < 0.05) were selected and visualized using the ggplot2 r package.

Multi-omics analysis

Multi- omics analysis was performed on the transcriptome, surface marker expression and clinical information. In order to avoid possible bias induced by the unequal number of cells in each sample, three samples from each group i.e., COVID-19 positive, healthy and recovered were sampled to select an equal number of cells from each sample. This stratified sampling approach resulted in 24633 cells from nine patients. Similarity network fusion was used to fuse the multi-omic data into a single matrix of size, 24633 by 24633. tSNE was performed upon the fused data to visualize seven clusters selected by the elbow method using k-means clustering. The clusters were identified manually as described earlier in the "scRNA-seq Data Processing, Clustering and Cell-Type Annotation" section.

Clinical features and an integrated Bayesian network model

The data from stratified random samples of single cell RNA expression, surface marker and SNF cluster membership were integrated with high-resolution CT (HRCT) scores of the COVID-19 patients. The healthy and recovered individuals were assigned an HRCT score of zero, indicating absence of active pneumonia. The integrative modeling analysis was carried out using the wiseR (23) package for end-to-end Bayesian network learning, inference and dashboard deployment. All continuous variables in the integrated data were discretized using the k-means algorithm with k=3 for biological interpretability as low, medium and high. A discrete Bayesian network was learnt from the data using hill climbing optimization for finding the directed acyclic graph encoding the structural dependencies between the variables. Eleven Bayesian network structures were ensembled and averaged to derive the consensus structure. The consensus structure was then parametrized with marginal and conditional probability distributions using Monte Carlo Markov Chain (MCMC) approximate inference method.

10.3389/fimmu.2022.1034159

Results

Spectrum of cellular heterogeneity in healthy, COVID-19 and recovered patients

To understand the spectrum of immune response and cellular heterogeneity before, during and after the SARS-CoV-2 infection, we performed simultaneous single-cell transcriptome and targeted proteome (40 surface markers) sequencing of the PBMCs collected from 33 individuals (healthy = 4, COVID-19 = 16, and recovered = 13) using a microwell-based scRNA-seq platform (BD Rhapsody Express). We sequenced a total of 163197 cells for both the surface proteins and RNA (Figure 1A). The details of the oligo-attached antibodies (list and oligo sequences) are available in the Supplementary File 1; Table S1. Post QC of the data quality (Supplementary File 1; Figure S1A), a total of 124726 cells were retained after removing the low-quality cells. We performed batch effect correction and normalization using Seurat SCTransform v2 (24), followed by dimension reduction and unsupervised clustering using the Louvain algorithm (resolution = 0.4). The cluster specific genes were identified using Seurat FindMarker functions and the clusters were annotated manually using CellMarker, PanglaoDB and Azimuth, as well as using a Support Vector Machine (SVM)-based annotation tool scPred (the ROC, sensitivity and specificity are available at Supplementary File 1; Table S2) (14, 16, 25–27). A total of 17 annotated clusters were identified across the three groups (Figure 1B). Figure 1C represents the frequency of the cell types between the three groups (normalized to the total number of cells in the group).

Decreased professional antigen presenting cells in the COVID-19 patients

Antigens undergo a proteolytic cleavage, followed by presentation to the CD8+ T cells and CD4+ T cells by MHC class I or class II molecule, respectively. B cells, macrophages and the dendritic Cells (DC) are the professional antigen presenting cells (APCs) involved in the T cell mediated immune response. We found that the B cell population was significantly decreased (P-value < 0.00001) in the COVID-19 patients compared to the healthy individuals. Interestingly, recovered patients had a higher number of these cells, although not similar to the healthy. However, the DC population increased in the positive patients which increased further in the recovered individuals. On the other hand, we observed a decrease in the CD8+ T cells and increase in the CD4+ T cell population in the COVID-19 patients. We also observed an increased abundance of activated CD4+ T cells compared to the Naïve CD4+/CD8+ T cells in the COVID-19 patients. Together, these indicate a suboptimal MHC Class I mediated but increased MHC Class II mediated antigen presentation in the COVID-19 patients. On the other hand, the increased abundance of the APCs and the CD8+ T cells in the recovered, possibly indicate recovery of the loss of MHC Class I mediated antigen presentation function.

Increased cytotoxicity in response to COVID-19

The monocytes and NK cells confer the 'killing function' and cytotoxicity. We observed an increased killer cell population (Natural killer or NK and NK T cells) in the infected patients, which subsequently decreased in the recovered. The proliferating NK cells were the highest in recovered individuals, correlating with the half-life of the mature NK cells as well as the infection duration (28). The higher abundance of the proliferating NK cells in the recovered indicates the decrease in IFN-γ production post-infection (29). The classical monocyte population also followed a pattern like the NK cells, while the CD14+/CD16+ Intermediate monocyte, highly abundant in the healthy individuals, decreased significantly in the COVID-19 patients followed by an increase in the recovered individuals. This suggests higher activation of monocytes in the COVID-19 patients, followed by a partial restoration in the recovered individuals. Together, the increased 'killer cell' population and monocyte suggest an increased cytotoxicity in the COVID-19 patients. The statistical significance of the frequency of the cell types across three groups as well as pairwise comparison groups are available as Supplementary File 1; Table S3.

Reduced immune response and increased inflammatory response by naïve CD4+/CD8+ T cells in the recovered individuals

The cell type specific expression of the surface markers and intracellular markers are presented in the Figures 1D, E. Figure 1F shows the expression of the cell type specific markers used for the cell type annotation across groups. We also looked at the cellular heterogeneity in a pairwise comparison (healthy vs COVID-19 positive, COVID-19 positive vs recovered, and healthy vs recovered) (Figure 1G; H, Supplementary File 1, Figures S1B-1E). Surprisingly, we found an unidentified cluster to be present explicitly in the healthy and was absent in the recovered (Figure 1G, H; Supplementary File 1; Figure S1F). Upon annotation using scpred, it was found to be the Naïve CD4+ T Cell population, with reduced expression of *MALAT1, BACH2* and several ribosomal protein coding genes when compared to the existing Naive CD4+/CD8+ T cells of the

10.3389/fimmu.2022.1034159

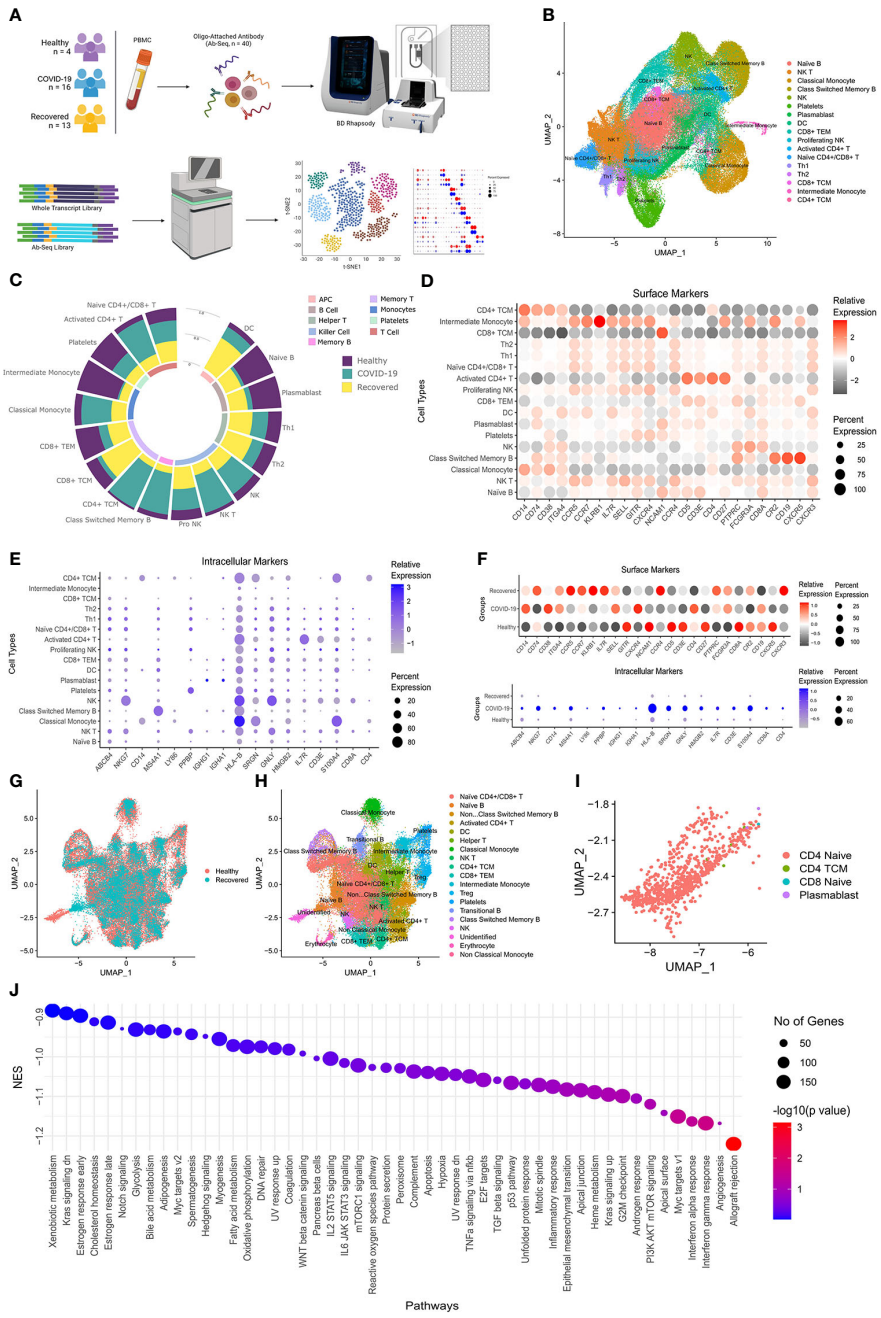

FIGURE 1
Cellular Heterogeneity across Healthy, Infected and Recovered COVID-19 Individuals. **(A)** Sample distribution and schematic workflow for the scRNA-seq, followed by analysis for the cellular heterogeneity and differential expression. **(B)** UMAP visualization of the 124726 cells across the healthy, active COVID-19 and the recovered individuals. **(C)** Frequency of cell types across the three groups, normalized to the total number of cells. **(D, E)** Cell type specific expression of **(D)** Surface markers, and **(E)** RNA level. Color scale denotes the relative expression whereas circle size denotes the percent of cells expressing the marker. **(F)** Expression of cell type specific markers across the three groups. **(G)** UMAP visualization of healthy vs recovered comparison group showing no batch effect between the two groups, the box highlights the cluster absent in the recovered individuals. **(H)** UMAP visualization of healthy vs recovered comparison group with cell type annotation, the box highlights the unidentified cluster. **(I)** UMAP visualization of the unidentified cluster after machine learning-based cell type annotation. **(J)** GSEA of differentially expressed genes between novel subset of the Naive CD4+ T cell and existing Naive CD4+/CD8+ T cells.

healthy/recovered individuals (Figure 1I; Supplementary File 2). Reduced expression of these genes confers increased immune response, reduced cytokine production and inflammatory response (Figure 1J) (30–32). Thus, loss of this Naïve CD4+ T cell population suggests a reduced immune response and increased inflammatory response by the Naïve CD4+/CD8+ T cells in the recovered individuals.

Loss of B cell maturation process in the recovered individuals

To understand the cross-talk across cell types and subsequent regulation of immunological functions, we performed cell-cell communication analysis using the CellChat R package (33). The cell-cell communication analysis revealed a CD22-CD45 signaling between the Class-switched memory B cell and the Activated CD4+ T cells, in healthy but not in the COVID-19 positive or recovered (Supplementary File 1; Figures S1G-1I). It is important to note that the CD45, negatively regulates the CD22 level, which is crucial for B cell maturation and antibody production (34). Absence of CD22-CD45 interaction, thus indicates dysregulated B cell maturation in the COVID-19 patients. On the other side, CD99 signaling in the NK cells and CADM1 signaling in the CD8+ TCM were observed in the COVID-19 patients but not in healthy or recovered individuals. CD99 signaling in NK cells are known to upregulate the IL-6 and TNF-α (35), whereas the CADM1 signaling is known to increase the cytotoxicity and IFN-γ secretion (36). Together, these suggests a NK and CD8+ T cell-mediated elevated immune and inflammatory response in the COVID-19 patients.

Compromised adaptive immunity in COVID-19 patients is mediated by CD40-CD40LG, enriched in the monocyte and T cells

The immune and inflammatory response in the COVID-19 patients, as revealed by the cell-cell communication analysis, is modulated not only by CD22-CD45 interaction, but also CD40 and CD40LG interaction. However, the CD40-CD40LG interaction was not observed in our cell-cell communication analysis. The CD40-CD40 ligand expression and interaction are important not only for the activation of adaptive immune response, but also infection induced inflammation and CD8+ T cell apoptosis (37). Therefore, we looked at the CD40-CD40LG expression between the groups. Figure 2A shows the surface level expression of CD40-CD40LG, wherein we observed a decreased expression of CD40-CD40LG in the COVID-19 patients, with the further decreased expression in the recovered individuals, especially in the professional antigen presenting cells (APC) (Figures 2B, C). This indicates a decreased adaptive immune response during COVID-19, increased infection induced inflammation and CD8+ T cell apoptosis.

Subsequently, we looked at the expression of the FAS receptor, a death receptor expressed during apoptosis. We observed an increased expression in all the CD4+ and CD8+ T cell populations. Surprisingly, we also observed a higher expression of *FAS* in the B cell population (Naïve B cell, Class-switched Memory B cells), indicating an abnormal antigen presentation and antibody response in the COVID-19 patients (Figure 2D). Further, chemokine and cytokine receptors (*CXCR3, CXCR4, CXCR5, CCR4, CCR5*, and *CCR7*) expression was increased in active COVID-19 and recovered patients (Figures 2E, F). Alongside, we observed a high expression of cytokines (*CCL3, CCL4, CCL5, CCL7, CCL18* and *CCL20*) in the CD4+ TCM, Classical monocytes and NK cells in the COVID-19 patients (Figure 2G). A higher expression of chemokines (*CXCL1, CXCL2, CXCL3, CXCL8* and *CXCL16*) were also found in the CD4+ TCM and Classical Monocytes in the COVID-19 patients (Figure 2H). This indicates a CD4+ TCM and monocyte driven increased cytokines and chemokines in the active COVID-19 patients. Also, the interleukins (*IL1B, IL15, IL16*, and *IL32*) were found to be upregulated in the active COVID-19 patients, indicating a T cell and monocyte-mediated proinflammatory response during active COVID-19 (Figure 2I).

We observed increased expression of *TNFRSF1B*, also known as TNF receptor 2 (*TNFR2*) in the Classical monocytes and NK cells during active COVID-19 (Figure 2J). *TNFR2* is involved in the regulation of inflammation in the macrophage and CD8+ T cells. *TNFRSF13C*, a pro-survival receptor for B cells, was found to have increased expressed in the Class-switched memory B cells during active COVID-19 (38). Deficiency of *TNFRSF13C* is characterized by low circulating B cells, serum IgG and IgM but high levels of IgA (39). Thus, the very low expression of *TNFRSF13C* in the Class-switched memory B cells in the recovered individuals lends support to our earlier finding of decreased Class-switched memory B cells in the recovered individuals. It also indicates increased IgA antibody, and not IgG or IgM antibody in the recovered. The increased expression of *TNFRSF14* and *TNFRSF17* in the recovered individuals indicate an increased inflammatory response (Figure 2J). Together, the dysregulation of the CD40-CD40LG caused an increased monocyte and T cell mediated inflammatory response during active COVID-19. The overall differential expression of genes in activated CD4+ T cell, CD8+ TEM, Classical monocytes, NK cells, CD4+ TCM and CD8+ TCM are represented in the Supplementary File 1, 2; Figures S2A-2F. The protein-protein interaction-level network obtained from the differentially expressed genes revealed elevated TNF-α signaling in the Activated CD4+ T cells, IL-6 signaling in the CD8+ TEM cells, which are indicative of elevated inflammatory response during active COVID-19 (Figures 2K, L; Supplementary File 1, Figure S2G).

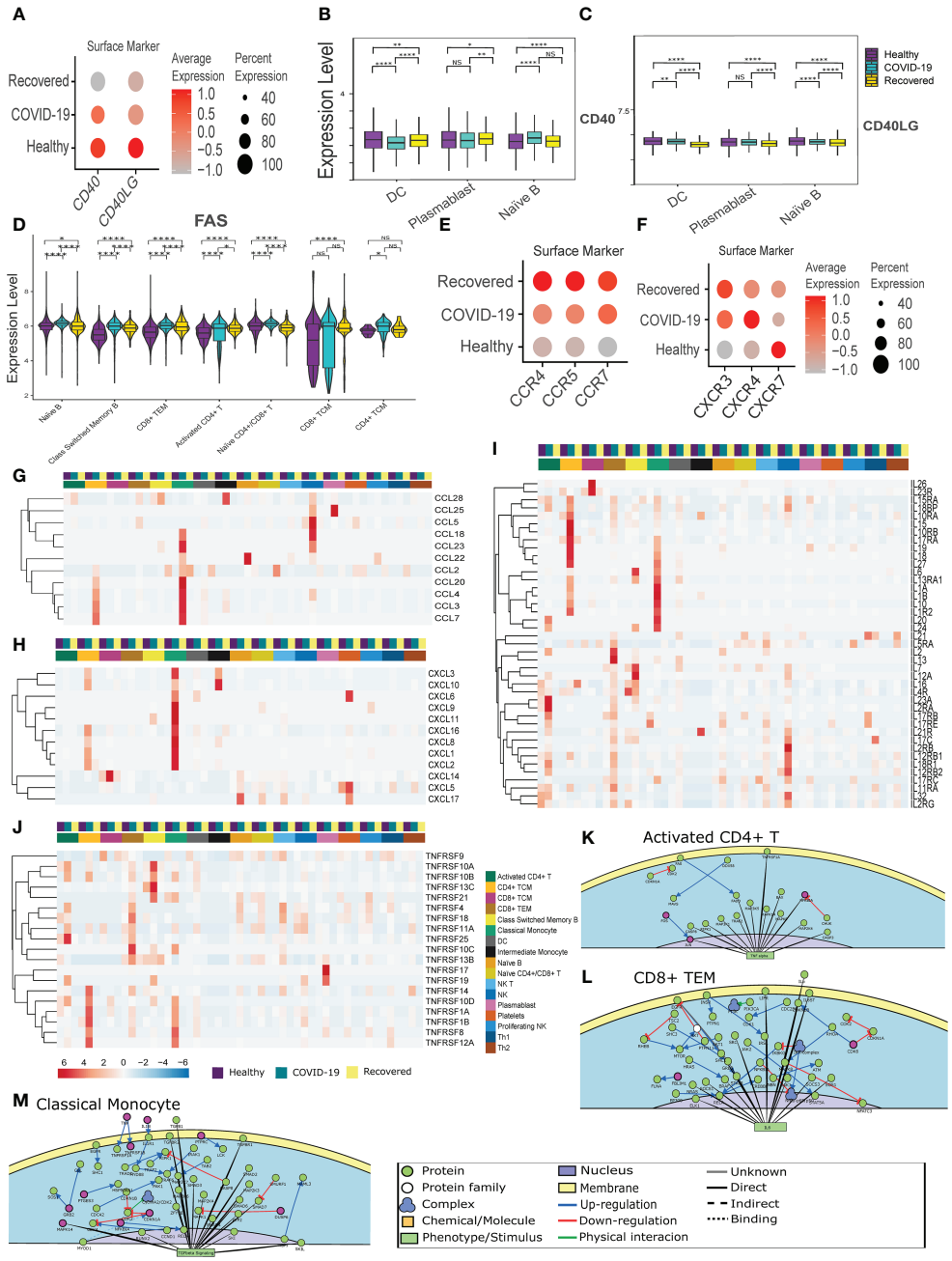

FIGURE 2
CD40-CD40LG mediated Inflammatory response in the COVID-19 patients. **(A)** CD40-CD40LG expression at surface level across the three groups of COVID-19 active infection, healthy and the recovered individuals. Color scale denotes the relative expression whereas circle size denotes the percentage of cells expressing the marker. **(B, C)** Cell- type specific surface expression of CD40-CD40LG across the 3 groups. **(D)** Surface level expression of FAS in the B and T cells. **(E, F)** Chemokine and Chemokine receptor expression at the surface level across the three groups. **(G–J)** RNA level expression of **(G)** Cytokines, **(H)** Chemokines, **(I)** Interleukins and **(J)** TNF Receptor Superfamily across all the cell types. **(K–M)** PPI level interaction network at **(K)** Activated CD4+ T cells, **(L)** CD8+ TCM, and **(M)** monocytes. [NS represents non-significant, *represents p-value < 0.05, **represents p-value < 0.01, **** represents p-value < 0.0001].

Surprisingly, we observed increased TGF-β signaling in the monocytes and NK cells (Figure 2M; Supplementary File 1; Figure S2H), indicating a pro-viral role of these cells (40). Besides, we also observed a decreased immune response and T cell activation in the CD4+ TCM and CD8+ TCM respectively, indicating an abnormal immune response and T cell activation (Supplementary File 1; Figures S2I, J). Besides, these also indicate the dysregulation of antigen presentation in the COVID-19 patients. Together, the results indicate a CD40-CD40 ligand interaction mediated increase of the cytokine response and abnormal T cell activation in the COVID-19 positive individuals.

Immune, stress and antiviral responses are mediated by the T cells, monocytes and NK cells

To understand the cell type specific immune and stress response dynamics, we performed GSEA at single cell resolution using Escape R/Bioconductor package by using molecular signature database (MSigDB-H) (Figure 3A) (41). We found immune response related pathways (TGF-β, IL2-STAT5, IL6-JAK-STAT3, and TNFα signaling, Complement system activation, and Inflammatory response pathway) to be

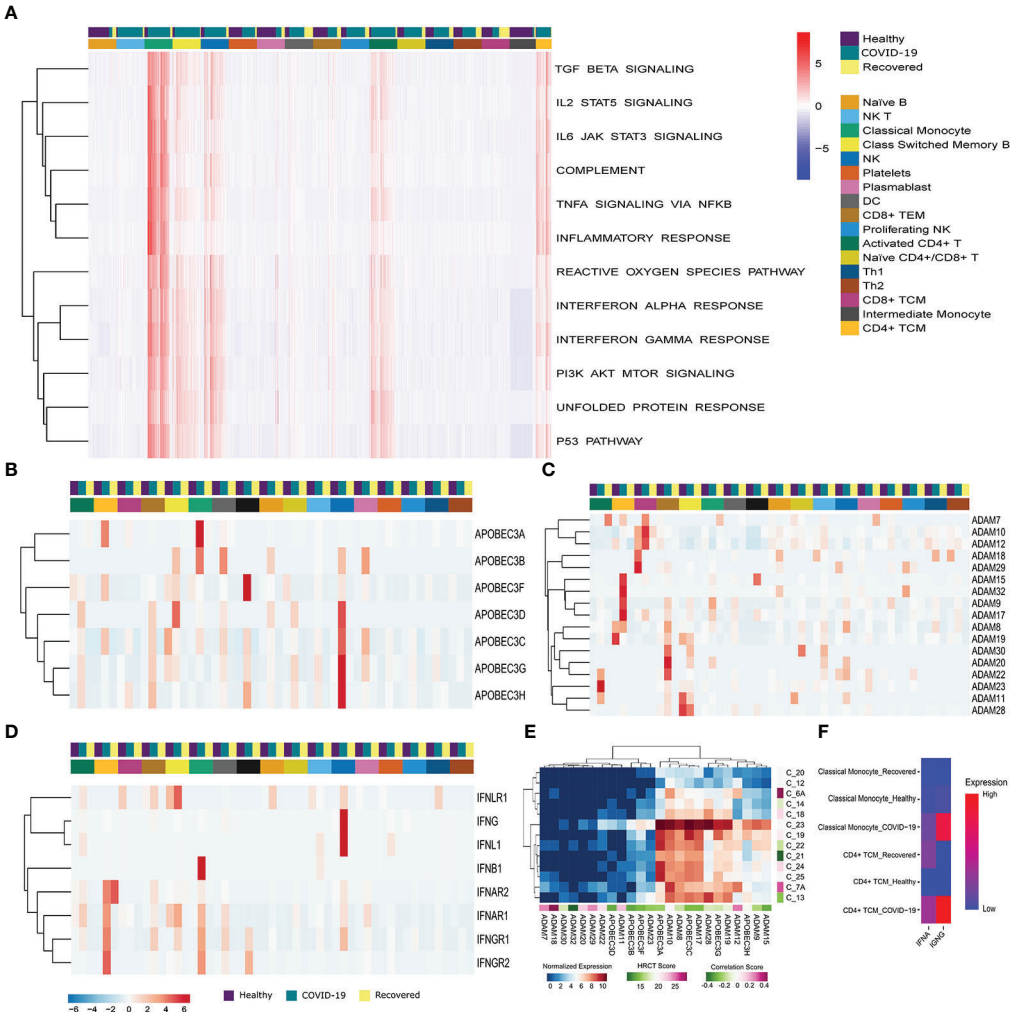

FIGURE 3
Immune, stress and antiviral Response during the SARS-CoV-2 infection. **(A)** G SEA at the single cell resolution across the three groups (COVID-19 patients, healthy and recovered), the row dendrograms distinguish the immune and stress response pathways. The cell types and the groups were highlighted using different color bars. Data is expressed as a relative enrichment score for each pathway. **(B, C)** Expression of **(B)** *ADAM*, and **(C)** *APOBEC3* genes. **(D)** Expression of antiviral genes in the COVID-19 patients and correlation with HRCT score. **(E)** Expression of IFN family genes across all the cell types across the three groups. Cell types and groups were highlighted using different color bars. **(F)** Cumulative expression of type I and type II IFN receptors between the Classical monocyte and CD4+ TCM across the three groups.

upregulated in the classical monocyte, NK cells, activated CD4+ T cells and CD4+ central memory T cells in active COVID-19 patients. TGF-β and IL2 STAT5 signaling, as well as Complement system activation pathways were also upregulated in the Class-switched memory B cells during active COVID-19. On the other hand, the stress response related pathways (ROS pathway, Interferon alpha and gamma response, PI3K–AKT-mTOR signaling, UPR and p53 pathways) were also particularly enriched in the Classical monocyte, NK cells, activated CD4+ T cells, Class-switched memory B cells and CD4+ central memory T cells of the COVID-19 positive patients. Besides, the reactive oxygen species (ROS) and unfolded protein response (UPR) pathway, two major stress response pathways, were also enriched in the plasmablast in the recovered individuals. Together, these indicates T Cells, monocytes and NK cells mediated upregulation of the immune and stress response during active COVID-19.

To understand the dynamics of the antiviral response, we looked at the expression of *ADAM, APOBEC3* and *IFN* family members. We found a high expression of *APOBEC3A, APOBEC3B, APOBEC3C, APOBEC3D, APOBEC3F, APOBEC3G* and *APOBEC3H* in the classical, intermediate monocytes and NK cells of the COVID-19 patients compared to the healthy or recovered individuals (Figure 3B). On the other hand, ADAM family members were upregulated in the T cells (Activated CD4+ T cells, CD4+ TCM, CD8+ TCM, CD8+ TEM) in active COVID-19 compared to the healthy and recovered (Figure 3C). This highlights a T cell, monocyte and NK cell mediated upregulation of antiviral response during the SARS-CoV-2 infection. Within our data, we also checked for the possible association of the increased antiviral response with the disease severity within the COVID-19 positive patients. We found that the expression of the antiviral genes negatively correlated (except *ADAM7, ADAM11, ADAM12, ADAM18, ADAM20*, and *ADAM29*) with the HRCT score of the COVID-19 patients suggesting association of increased antiviral response with decreased disease severity (Figure 3D).

Finally, we found *IFNAR1* and *IFNAR2*, a receptor for type I interferon (IFNα) to be upregulated in the CD4+ TCM and classical monocytes of the COVID-19 patients, compared to the others. Receptors for type II interferon, *IFNGR1* and *IFNGR2* were also upregulated in the CD4+ TCM and classical monocyte (Figure 3E). However, the expression of type II IFN receptors was higher in COVID-19 patients in both the cell types, whereas type I IFN receptors were upregulated in the CD4+ central memory T cells of the recovered individuals (Figure 3F). In summary, inferences from our data suggests that the antiviral response is mediated by the central memory T cells, monocytes and NK cells during the SARS-CoV-2 infection and transcription of proinflammatory cytokines are increased as a result of type II IFN receptor mediated signaling during the SARS-CoV-2 infection.

Aberrant activation of T cells in COVID-19 positive individuals

To understand the T cell dynamics across the three groups, we looked for the expression of the T cell activation and exhaustion markers. We observed higher expression of CD38, CD69 and CD40LG during active COVID-19 infection, indicating an activated phase of T cell population, compared to the healthy and the recovered, where the T cells are at resting phase in comparison to the active infection (Figure 4A). We also observed higher expression of T cell exhaustion markers, i.e., *TIM-3, LAG3, CD152* or *CTLA4* and *CD279* or *PD-1* in the recovered individuals compared to the active COVID-19 and healthy individuals (Figure 4B). *This indicates that a larger population of the T cells are exhausted post recovery from the COVID-19.*

We then looked at the expression of a specific T cell receptor type. Generally, around 95% of the T cell receptor carry αβ chain, and T cells carrying αβ receptor chain respond to the pathogen in an antigen specific manner to induce cytokine productions followed by B cell maturation and antibody secretion. However, a small fraction of T cells carrying γδ receptor chains are essential in the initial immune and inflammatory responses (42). Surprisingly, we observed a gradual shift of TCR from αβ to γδ type across healthy, active COVID-19 and recovered, with highest expression of TCR γδ in the recovered (Figure 4C). Thus, the T cell exhaustion and the abundance of TCR γδ in the recovered individuals indicate an abnormal T cell response during the active COVID-19.

To understand the difference of T cell subtypes across the three groups, we constructed cell trajectory with respect to pseudotime using Monocle 3 (Figures 4D, E) (43). The cells for each cell type were plotted against the pseudotime for all the three groups and a significant difference of median pseudotime was observed (Figures 4F–H; Supplementary File 1; Figure S3). Importantly, we observed a lower pseudotime in the COVID-19 patients (except for the CD8+ TEM and CD4+ TCM), possibly indicating a faster transition from one cell type and/state to another. Finally, to understand the co-expression of genes with respect to pseudotime, we clustered the genes that were differentially expressed across healthy, COVID-19 positive and recovered, in each T cell subtypes, and identified four modules of co-expressed genes. While module 1, 2 and 4 showed significant GO enrichment (p-value <0.05) for the housekeeping cellular functions required for cell growth and development, module 3 showed significant enrichment for the immune and inflammatory response associated molecular functions (Figures 4I–L; Supplementary File 4). This indicates the possible impact of COVID-19 on normal cell functions beyond the conventional immune/inflammatory response.

10.3389/fimmu.2022.1034159

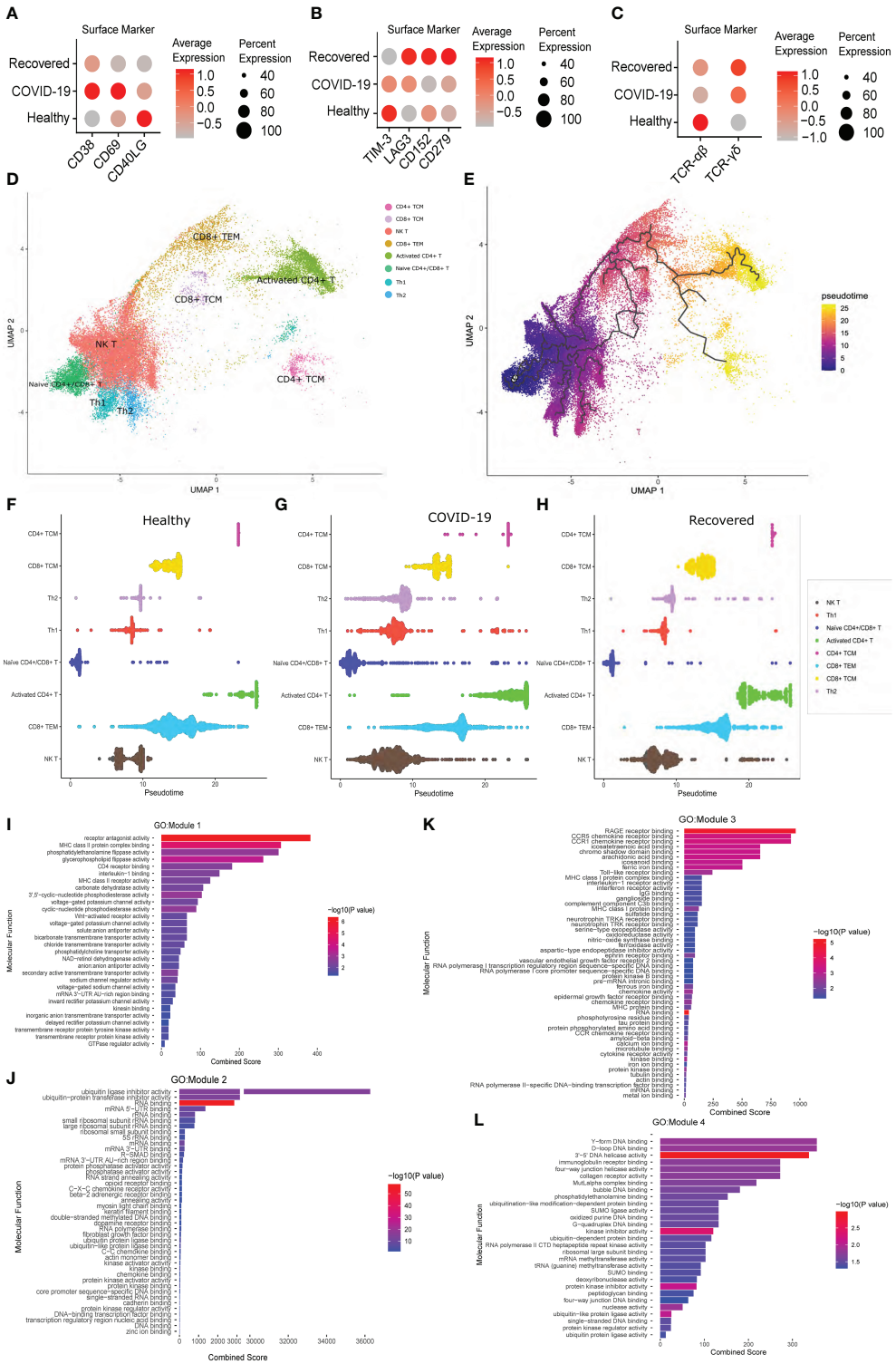

FIGURE 4
T Cell specific surface marker expression and Pseudotime analysis across the healthy, COVID-19 positive and recovered individuals. **(A)** Expression of the T cell activation markers at the surface marker level. **(B)** Expression of T cell exhaustion markers at the surface marker level. **(C)** Expression of TCR αβ and γδ chain at the surface marker level. Color scale denotes the relative expression whereas circle size denotes the percentage of cells expressing the marker. **(D)** UMAP visualization of T cell subtypes. **(E)** UMAP visualization of T cell subtypes with respect to pseudotime. **(F–H)** Distribution of cells against pseudotime for T cell subtypes across **(F)** healthy, **(G)** COVID-19 positive, and **(H)** recovered individuals. **(I–L)** GO enrichment of genes from **(I)** Module 1, **(J)** Module 2, **(K)** Module 3, and **(L)** Module 4.

Distinct immune response signatures as revealed by similarity network fusion and machine learning model

To understand the multiple modalities of the data and their association with the COVID-19 disease, we integrated gene expression, surface marker expression and clinical details of the individuals to perform a similarity network fusion (SNF)-based clustering (Figure 5A). The Dendritic cell population was found to be decreased in the COVID-19 patients and increased in the recovered individuals, reiterating our initial results towards a dysregulated antigen presentation in the infected individuals, followed by recovery of the function, post-infection (Figure 5B). We also observed a decrease in the NK T cells and monocyte populations post-infection, highlighting a reduced cytotoxicity in the recovered individuals. Besides, the upregulation of *S100A8*, *TXNIP* and *MT2A* genes in the monocytes indicate an inflammatory response upregulation in the infected individuals. We also observed an increased CD69+ memory T cell population in the recovered individuals. High expression of CD69 in the memory T cell population indicates higher tissue residence of the memory T cell population in the recovered individuals. Together, these results highlight a dysregulated antigen

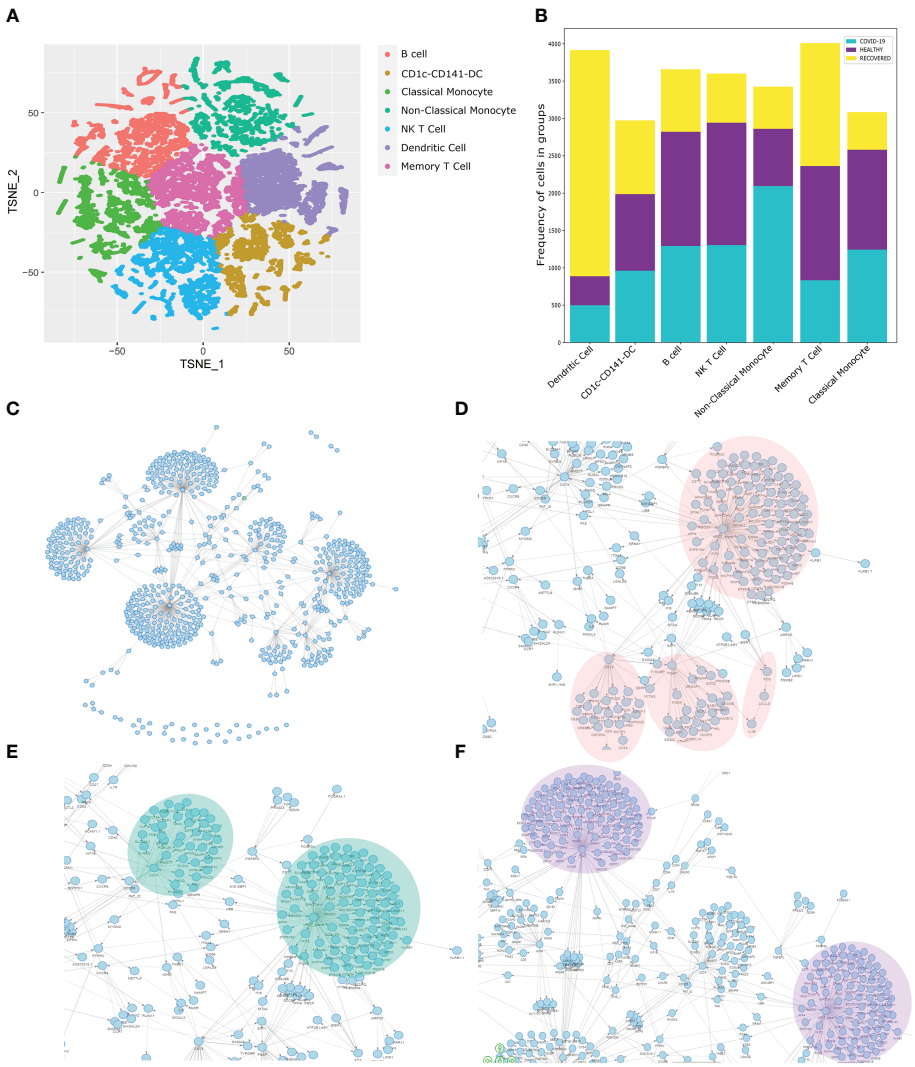

FIGURE 5
Similarity Network Fusion and Bayesian Network Model for Biomarker discovery. **(A)** SNF clustering of cells based on the gene expression, surface marker expression and clinical details of the individuals. **(B)** Distribution of the identified cell types across the healthy, COVID-19 positive and recovered individuals. **(C)** Bayesian Network Model built on the SNF clusters, gene expression, surface marker expression, and clinical data including the HRCT score of the individuals. **(D–F)** Specific highlights from the Bayesian Network Model showing the association of HRCT score with **(D)** *FOS, CST3, PSAP*, **(E)** *CD74*, and **(F)** *CD45*.

presentation and increased cytotoxicity in the infected individuals, and their reversal post-infection.

Towards the quest for the biomarkers associated with COVID-19 in our study cohort, we build a Bayesian Network model (Figure 5C). The complete network is available at Zenodo (https://doi.org/10.5281/zenodo.6583269). Importantly, we observed a strong connection between the HRCT score, *FOS* and *CXCL8* genes (Figure 5D). *FOS* is known to regulate cell death, apoptosis and inflammatory response, (44) which is one of the most significantly differentially expressed genes in the MERS and SARS-CoV-2 infection. The *CXCL8* is a neutrophil chemoattractant which recruits the neutrophil at the site of infection and initiates a proinflammatory response mediated by the *IL-8* and other cytokines (45). We also observed a direct association of *IL1β* with the *CXCL8*. Elevated *IL1β* and *IL6* activity is a feature of COVID-19 disease and dysregulation of the same is associated with disease severity (46). Thus, the association of *FOS, CXCL8* and *IL1β* with HRCT score make them a strong predictor of COVID-19 disease. Besides, we identified a strong association of HRCT score with *CST3*, a marker gene for monocytes. Monocytes, as we have shown earlier, are involved in the inflammatory responses in COVID-19 patients. Besides, the association of CST3 with *S100A9* also indicates a correlation between monocyte-mediated inflammatory response and HRCT score, which supports our previous findings. We also found a strong association between HRCT score and *PSAP*, a gene involved in antigen presentation and male fertility, both are perturbed in severe COVID-19 patients (47, 48).

We observed a strong association of HRCT score with *CD74*, also known as MHC Class-II invariant chain (Figure 5E). *CD74* is involved in MHC Class-II mediated antigen presentation, a process upregulated in the COVID-19 patients. Besides, *CD74* is known to have increased expressed in the severe COVID-19 patients (49). *CD74* also has immune-suppressant role, often observed in severe COVID-19 patients (50). Finally, we observed a strong association of *CD45* with HRCT score though *PDE11A* (Figure 5F). *PDE11A* is known to be involved in inflammatory response and is abundantly expressed in the severe COVID-19 patients (51). Just like *CD74, CD45* is also an immune-suppressant, and therefore enhanced expression in the severe COVID-19 patients. Therefore, the association of *CD74* and *CD45* with the HRCT score suggests the possible role of *CD74* and *CD45* in the COVID-19 disease and can possibly be used as a biomarker for the disease.

Discussion

Although several studies have revealed the dysregulation of the immune system during COVID-19 disease (52, 53), there are still a few critical missing links in our understanding of the mechanisms behind the immune response dysfunction. Using single-cell resolution transcriptomics and targeted proteomics of 33 individuals (healthy, active COVID-19, and recovered), this study highlights major shifts in immune regulation occurring in the COVID-19 disease. While the decrease in B cell and CD8+ T cell population suggest a decreased MHC Class I mediated antigen presentation, the slight increase of DC and CD4+ T cell populations indicate an elevated MHC Class II mediated antigen presentation in the COVID-19 positive individuals. However, the decreased immune response by the CD4+ T cells of the infected individuals, as revealed by the PPI network, highlights suboptimal MHC Class II mediated antigen presentation. The high expression of FAS on the surface of B cells highlights B cell senescence in active COVID-19 cases, further strengthening our finding of diminished MHC Class I mediated antigen presentation. Increase in the B cell and CD8+ T cell population in the recovered group highlights the restoration of the MHC Class I mediated antigen presentation function. While the NK cell and classical monocyte population, the master regulator of the cytokine and chemokine response, were increased in the infected individuals followed by a decrease in the abundance in the recovered individuals, it was interesting to observe the increased abundance of proliferating NK cells in the recovered individuals (Figure 6).

Although not a well-studied cell population, the high abundance of proliferating NK cells in the recovered individuals can be explained with the 7-10 days half-life of the mature/activated NK cells, which then requires proliferation to maintain the desired level (28). NK cell activation is a distinct feature of COVID-19 and the average duration of the infection coincides with the half-life of activated NK cells (54), highlighting the process of restoration of the NK cell pool, post-infection. Besides, proliferating NK cells mediated reversal of the IFN-γ production (55), which increases during active infection, highlights the significance of this particular cell type. The Naïve T cell subset in the healthy individuals have higher immune response and decreased inflammatory response potential compared to the Naïve CD4+/CD8+ T cell population. Loss of this Naïve T cell subtype in the recovered individuals, thus highlights higher inflammatory response potential compared to the healthy. Cell-cell communication analysis reveals intra- and inter-cellular communication based on ligand-receptor interaction.

Our analysis revealed a shift in the intra- and inter- cellular communication between healthy to infected and to recovered individuals. While the CD22-CD45 signaling in the healthy group, involved in the B cell maturation process was absent in the infected and recovered group, the CD99 and CADM1 signaling observed in the infected group were absent post-infection. Thus, although the NK cell and CD8+ T cell mediated cytotoxicity were reversed in the recovered individuals, the B cell maturation process was still impaired in the recovered individuals, despite the increased abundance of B cells in the recovered individuals.

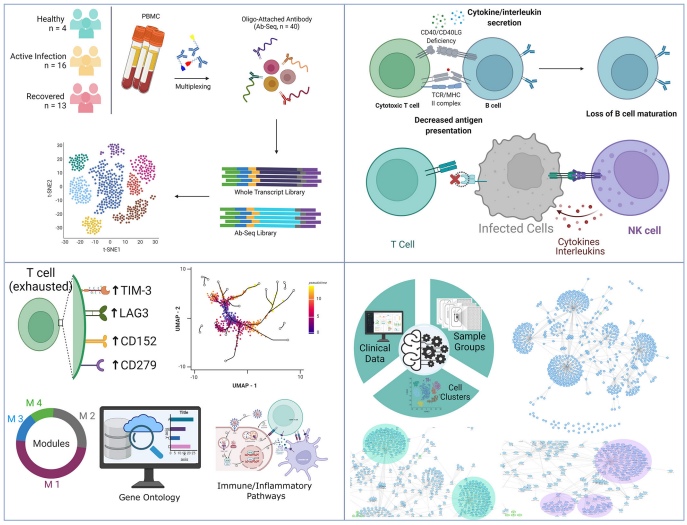

FIGURE 6
Summary of the key findings from the study. It highlights the observed T-cell dynamics within the COVID-19 patients, recovered individuals and healthy, as well as key immune findings harnessing strength of machine learning.

The CD40 and CD40 ligand interaction is known to regulate a wide range of immunological events, including infection-induced inflammatory response, CD8 T cell senescence and increased viral replication (56). The gradual decrease in the expression of CD40 and CD40LG in the COVID-19 positive and recovered groups suggest an enhanced infection-induced inflammation and apoptosis of CD8+ T cells during COVID-19 infection. Indeed, we observed high expression of FAS on CD8+ T cells and decreased abundance of CD8+ T cells in the infected patients. Interestingly, earlier studies also report the T cell depletion caused by the high levels of FAS molecules in the severe COVID-19 disease (57). Disrupted antigen presentation and antibody response were also observed during COVID-19 from an increased expression of FAS receptors (pro-apoptotic molecules) in CD4+ T and CD8+ T cell populations as well as B cell populations (Naïve B cell, class-switched memory B cell) (58).

On the other hand, the chemokines, cytokines, and interleukins were upregulated in the infected individuals, wherein the upregulation was mediated by the CD4+ T cells, CD8+ T cells, NK cells and monocytes. Interestingly, these inflammatory markers were found to be downregulated in the recovered individuals, highlighting the importance of understanding the post infection phase. The cell type specific PPI network revealed elevated TGF-β signaling in the monocyte and NK cells. The TGF-β signaling acts as a double edge sword, wherein on one hand it activates CD8+ T cells, and on other side, it facilitates viral replication, thus revealing another aspect of monocyte and NK cell mediated modulation of COVID-19. Further, this also reiterates the decreased CD40-CD40 ligand interaction-mediated increase of viral replication in the infected patients.

We found several immune responses associated signaling pathways such as IL6-JAK-STAT3, IL2-STAT5, TGF-β, TNFα, Inflammatory response pathway, and Complement system activation, upregulated in the classical monocyte, NK cells, activated CD4+ T cells, and CD4+ central memory T cells during active COVID-19. Other pathways involved in the stress response such as ROS pathway, Interferon alpha and gamma response, PI3K AKT mTOR signaling, UPR pathway and p53 pathways were also elevated in classical monocyte, NK cells, activated CD4+ T cells, Class-switched memory B cells and CD4+ central memory T cells in the active COVID-19 patients. These findings suggest the upregulation of immune pathways and stress pathways mediated *via* T cells, monocytes, and NK cells and fall in concurrence with the previous studies where multiple immune response pathways activate in the COVID-19 patients (59, 60).

The antiviral response during active COVID-19 disease was confirmed with a high expression of APOBEC3 and ADAM family members in the classical monocytes, NK cells, and T cells, respectively. Both APOBEC3 and ADAM family members are known to confer innate immunity (61, 62) and therefore can possibly be responsible for enhancing the antiviral response in active COVID-19 through T cell, NK cell, and monocytes. The upregulated expression of type II interferon receptors (IFNAR1 and IFNAR2) in CD4+ TCM and classical monocytes were more pronounced in active COVID-19 groups compared to recovered, where type I interferon receptor (*IFNGR1* and *IFNGR2*) expression dominated, thereby suggesting a surge of

proinflammatory cytokines mediated *via* type II IFN receptor signaling during the active COVID-19 disease.

Previous studies have reported the dysregulation of T cells during COVID-19 disease (63, 64) which was observed in this study as well. This is particularly important, since lymphopenia is a key feature of COVID-19 disease, and an altered lymphopenia is also observed in convalescent COVID-19 patients (65–67). A sharp decrease in the CD4+ and CD8+ T cell and a delayed T cell response were associated with higher COVID-19severity, and similar to our findings, a restoration of the same in the recovered individuals has been highlighted by limited yet important study (65). Several studies have also highlighted abnormal abundance of helper T cells (Th1/Th2/Th17) and its association with decreased viral clearance and higher disease severity during COVID-19 (68, 69). The lymphopenia observed in the COVID-19 patients is also characterized by the abnormal activation and exhaustion of the T cell. We found a significant increase in the expression of CD38 and CD69 in the active COVID-19 patients compared to the healthy and recovered, suggesting an activated T cell response. A high level of exhaustion markers has been reported in the severe COVID-19 patients (70, 71), however, we observed elevated expression of the T cell exhaustion markers like *LAG3, CTLA4*, and *PD-1* in the recovered individuals. Together, this reveals an active phase of T cells during COVID-19 disease where after recovery the exhausted population of T cells becomes dominant. We further investigated the T cell receptor (TCR) type, where a gradual shift of TCR from αβ to γδ type was observed, with maximum expression in the recovered individuals. As the γδ TCR is responsible for inducing initial immune and inflammatory responses against specific antigens (72), their presence in the recovered individuals reflects aberrant and divergent T cell dynamics during the COVID-19 disease. Through our pseudotime analysis, different cell trajectories for T cell subsets revealed a reduced pseudotime amongst the COVID-19 patients, thereby suggesting a rapid transition between T cell subtypes that might be responsible for inducing aberrant T cell activation. We also observed differences among the constructed modules of co-expressed genes across the healthy, COVID-19 positive, and recovered groups in the T cell subsets where out of 4 modules, 3 of them exhibited significant housekeeping cellular functions that possibly indicate varied consequences of COVID-19 disease.

Finally, our similarity network fusion-based clustering reiterates our findings of dysregulated antigen presentation in the COVID-19 patients, whereas reduced cytotoxicity and higher tissue residence of the memory T cells in the recovered individuals. Our Bayesian network model reveals *FOS, CXCL8* and *IL1β* as important predictors for HRCT scores. While the FOS gene is known to be associated with apoptosis (73), CXCL8-mediated recruitment and activation of neutrophils is responsible for causing pathogenesis of lower respiratory tract infection and if overproduced, leads to cystic fibrosis (74). It is also suspected of playing a role in endothelial dysfunction. SARS-CoV-2 has been known to induce the apoptosis pathway, which has been shown to be intricately connected with inflammation and fibrosis, leading to medical complications (75). Thus, the association of increased levels of *FOS, CXCL8* and *IL1β* in patients with higher HRCT scores in our study using the integrative model provides support to this finding. Furthermore, we also found a strong correlation between *CST3* and *S100A9* and simultaneously with HRCT score. The monocyte markers *CST3* and *S100A9* exhibit monocyte-mediated pro-inflammatory responses (76). Together their association with HRCT score suggests the involvement of monocytes in inflammatory response during the COVID-19 disease. HRCT score was also strongly associated with *CD74* and *CD45*. Both *CD74* and *CD45* are immune-suppressants and are known to be elevated in the severe COVID-19 patients. Therefore, their correlation with HRCT score possibly signifies their role in the COVID-19 disease progression and severity.

Conclusion

Our Single cell based COVID-19 study, highlights a dysregulated antigen presentation, CD40-CD40LG deficiency-mediated heightened immune/inflammatory/stress and antiviral response in the COVID-19 positive and recovered individuals, faster cellular transition in the COVID-19 patients, and COVID-19 disease biomarkers such as *FOS, CD45*, and *CD74*. These findings may further assist in understanding the complexity of immune response heterogeneity that possibly can serve to delineate treatment strategies for SARS-CoV-2 infection. Besides, our study also highlights the importance of understanding the COVID-19 aftereffects in recovered individuals which may be relevant for the re-infection/s. Further, a follow-up study with longitudinal COVID-19 recovered individuals, potentially with differential disease severity, would further the understanding of immune response dynamics in the recovered individuals.

Data availability statement

The data presented in the study are deposited in the NCBI GEO repository, accession number GSE201088.

Ethics statement

The studies involving human participants were reviewed and approved by CSIR-IGIB's Human Ethics Committee Clearance (Ref No: CSIR-IGIB/IHEC/2020-21/01). The patients/participants provided their written informed consent prior to

participation in this study. The patients/participants provided their written informed consent to participate in this study.

Author contributions

PC, formal analysis, investigation, data curation, visualization, and writing - original draft. KK, data curation and writing - original draft. MK, SW, and SS, investigation. PM, formal analysis, visualization, and writing - original draft. AA, formal analysis and writing - original draft. RM, RG, and AG, formal analysis. AY and PD, data curation. KT and MJ, resources. TS, formal analysis, visualization, writing - review and editing, supervision. RP, conceptualization, methodology, supervision, writing - review and editing, funding acquisition. All authors contributed to the article and approved the submitted version.

Funding

This research was funded by Bill and Melinda Gates Foundation, [Grant number - INV-033578 and INV-030592].

Acknowledgments

The authors duly acknowledge all the COVID-19 patients, healthy and recovered individuals who participated in the study. Authors also would like to acknowledge the support of D.Y. Patil Medical College, Hospital and Research Institute, Kolhapur, Maharashtra, India for providing the relevant samples for this study. Authors acknowledge the help and support from Dr. Aradhita Baral towards facilitation as Research manager and coordination with the funders, Dr. Mohd Faruq for experimental facilitation. Authors acknowledge the support of Anil Kumar and Nisha Rawat towards COVID-19 sample transport and sample management. PC, PD, KK and AY acknowledge the CSIR for their research fellowship.

Conflict of interest

The authors declare that the research was conducted in the absence of any commercial or financial relationships that could be construed as a potential conflict of interest.

Publisher's note

All claims expressed in this article are solely those of the authors and do not necessarily represent those of their affiliated organizations, or those of the publisher, the editors and the reviewers. Any product that may be evaluated in this article, or claim that may be made by its manufacturer, is not guaranteed or endorsed by the publisher.

Supplementary material

The Supplementary Material for this article can be found online at: https://www.frontiersin.org/articles/10.3389/fimmu.2022.1034159/full#supplementary-material

SUPPLEMENTARY FILE 1
Details of the oligo-attached antibodies (list and oligo sequences).

SUPPLEMENTARY FILE 2
Table showing differential gene expression between the new Naïve T cell subset vs Naïve CD4+/CD8+ T cell in the healthy vs recovered individuals.

SUPPLEMENTARY FILE 3
Pseudobulk differential gene expression of the cell types highlighted in the study.

SUPPLEMENTARY FILE 4
GO enrichment analysis of the genes from each module.

References

1. Chen G, Wu D, Guo W, Cao Y, Huang Da, Wang H, et al. Clinical and immunological features of severe and moderate coronavirus disease 2019. *J Clin Invest* (2020) 130(5):2620–9. doi: 10.1172/jci137244

2. Zhang J-Y, Wang X-M, Xing X, Xu Z, Zhang C, Song J-W, et al. Single-cell landscape of immunological responses in patients with COVID-19. *Nat Immunol* (2020) 21:1107–18. doi: 10.1038/s41590-020-0762-x

3. Diao B, Wang C, Tan Y, Chen X, Liu Y, Ning L, et al. Reduction and functional exhaustion of T cells in patients with coronavirus disease 2019 (COVID-19). *Front Immunol* (2020) 11:827. doi: 10.3389/fimmu.2020.00827

4. Vanderbeke L, Van Mol P, Van Herck Y, De Smet F, Humblet-Baron S, Martinod K, et al. Monocyte-driven atypical cytokine storm and aberrant neutrophil activation as key mediators of COVID-19 disease severity. *Nat Commun* (2021) 12:4117. doi: 10.1038/s41467-021-24360-w

5. Wong KL, Tai JJ-Y, Wong W-C, Han H, Sem X, Yeap W-H, et al. Gene expression profiling reveals the defining features of the classical, intermediate, and nonclassical human monocyte subsets. *Blood* (2011) 118:e16–31. doi: 10.1182/blood-2010-12-326355

6. Zhu L, Yang P, Zhao Y, Zhuang Z, Wang Z, Song R, et al. Single-cell sequencing of peripheral mononuclear cells reveals distinct immune response landscapes of COVID-19 and influenza patients. *Immunity* (2020) 53:685–696.e3. doi: 10.1016/j.immuni.2020.07.009

7. Tan L, Wang Q, Zhang D, Ding J, Huang Q, Tang Y-Q, et al. Correction: Lymphopenia predicts disease severity of COVID-19: a descriptive and predictive study. *Signal Transduction Targeting Ther* (2020) 5:61. doi: 10.1038/s41392-020-0159-1

8. Zheng M, Gao Y, Wang G, Song G, Liu S, Sun D, et al. Functional exhaustion of antiviral lymphocytes in COVID-19 patients. *Cell Mol Immunol* (2020) 17:533–5. doi: 10.1038/s41423-020-0402-2

9. Yao C, Bora SA, Parimon T, Zaman T, Friedman OA, Palatinus JA, et al. Cell-Type-Specific immune dysregulation in severely ill COVID-19 patients. *Cell Rep* (2021) 34:108590. doi: 10.1016/j.celrep.2020.108590

10. Zhao P, Zou J, Zhou F, Zhu Y, Song Q, Yu D, et al. Immune features of COVID-19 convalescent individuals revealed by a single-cell RNA sequencing. *Int Immunopharmacol.* (2022) 108:108767. doi: 10.1016/j.intimp.2022.108767

11. Rutkowska E, Kwiecień I, Kłos K, Rzepecki P, Chciałowski A. Intermediate monocytes with PD-L1 and CD62L expression as a possible player in active SARS-CoV-2 infection. *Viruses* (2022) 14(4):819. doi: 10.3390/v14040819

12. Li X, Garg M, Jia T, Liao Q, Yuan L, Li M, et al. Single-cell analysis reveals the immune characteristics of myeloid cells and memory T cells in recovered COVID-19 patients with different severities. *Front Immunol* (2022) 12:781432. doi: 10.3389/fimmu.2021.781432

13. De Domenico E, Bonaguro L, Schulte-Schrepping J, Becker M, Händler K, Schultze JL. Optimized workflow for single-cell transcriptomics on infectious diseases including COVID-19. *STAR Protoc* (2020) 1:100233. doi: 10.1016/j.xpro.2020.100233

14. Hao Y, Hao S, Andersen-Nissen E, Mauck WM, Zheng S, Butler A, et al. Integrated analysis of multimodal single-cell data. *Cell* (2021) 184:3573–3587.e29. doi: 10.1016/j.cell.2021.04.048

15. Butler A, Hoffman P, Smibert P, Papalexi E, Satija R. Integrating single-cell transcriptomic data across different conditions, technologies, and species. *Nat Biotechnol* (2018) 36:411–20. doi: 10.1038/nbt.4096

16. Stuart T, Butler A, Hoffman P, Hafemeister C, Papalexi E, Mauck WM, et al. Comprehensive integration of single-cell data. *Cell* (2019) 177:1888–1902.e21. doi: 10.1186/s13059-020-02015-1

17. Zhai Z, Lei YL, Wang R, Xie Y. Supervised capacity preserving mapping: A clustering guided visualization method for scRNAseq data. *Bioinformatics* (2022) 38(9):2496–503. doi: 10.1093/bioinformatics/btac131

18. Love MI, Huber W, Anders S. Moderated estimation of fold change and dispersion for RNA-seq data with DESeq2. *Genome Biol* (2014) 15:550. doi: 10.1186/s13059-014-0550-8

19. Bunis DG, Andrews J, Fragiadakis GK, Burt TD, Sirota M. dittoSeq: Universal user-friendly single-cell and bulk RNA sequencing visualization toolkit. *Bioinformatics* (2020) 36(22-3):5535–6. doi: 10.1093/bioinformatics/btaa1011

20. Packer JS, Zhu Q, Huynh C, Sivaramakrishnan P, Preston E, Dueck H, et al. A lineage-resolved molecular atlas of c. elegans embryogenesis at single-cell resolution. *Science* (2019) 365(6459):eaax1971. doi: 10.1126/science.aax1971

21. Tran TN, Bader GD. Tempora: Cell trajectory inference using time-series single-cell RNA sequencing data. *PloS Comput Biol* (2020) 16:e1008205. doi: 10.1371/journal.pcbi.1008205

22. Kuleshov MV, Jones MR, Rouillard AD, Fernandez NF, Duan Q, Wang Z, et al. Enrichr: a comprehensive gene set enrichment analysis web server 2016 update. *Nucleic Acids Res* (2016) 44:W90–7. doi: 10.1093/nar%2Fgkw377

23. *A shiny application for end-to-End Bayesian decision network analysis and web-deployment [R package wiseR version 1.0.1* (2018). Available at: https://cran.r-project.org/package=wiseR.

24. Chu S-K, Zhao S, Shyr Y, Liu Q. Comprehensive evaluation of noise reduction methods for single-cell RNA sequencing data. *Brief. Bioinf* (2022) 23. doi: 10.1093/bib/bbab565

25. Zhang X, Lan Y, Xu J, Quan F, Zhao E, Deng C, et al. CellMarker: a manually curated resource of cell markers in human and mouse. *Nucleic Acids Res* (2019) 47:D721–8. doi: 10.1093/nar/gky900

26. Franzén O, Gan L-M, Björkegren JLM. PanglaoDB: a web server for exploration of mouse and human single-cell RNA sequencing data. *Database (Oxford)* (2019) 2019. doi: 10.1093/database/baz046

27. Alquicira-Hernandez J, Sathe A, Ji HP, Nguyen Q, Powell JE. scPred: accurate supervised method for cell-type classification from single-cell RNA-seq data. *Genome Biol* (2019) 20:264. doi: 10.1186/s13059-019-1862-5

28. Zhang Y, Wallace DL, de Lara CM, Ghattas H, Asquith B, Worth A, et al. In vivo kinetics of human natural killer cells: the effects of ageing and acute and chronic viral infection. *Immunology* (2007) 121:258–65. doi: 10.1111/j.1365-2567.2007.02573.x

29. Tarrio ML, Lee S-H, Fragoso MF, Sun H-W, Kanno Y, O'Shea JJ, et al. Proliferation conditions promote intrinsic changes in NK cells for an IL-10 response. *J Immunol* (2014) 193:354–63. doi: 10.4049/jimmunol.1302999

30. Huang K, Wang C, Vagts C, Raguveer V, Finn PW, Perkins DL. Long non-coding RNAs (lncRNAs) NEAT1 and MALAT1 are differentially expressed in severe COVID-19 patients: An integrated single-cell analysis. *PloS One* (2022) 17:e0261242. doi: 10.1371/journal.pone.0261242

31. Hipp N, Symington H, Pastoret C, Caron G, Monvoisin C, Tarte K, et al. IL-2 imprints human naive b cell fate towards plasma cell through ERK/ELK1-mediated BACH2 repression. *Nat Commun* (2017) 8:1443. doi: 10.1038/s41467-017-01475-7

32. Chen C, Peng J, Ma S, Ding Y, Huang T, Zhao S, et al. Ribosomal protein S26 serves as a checkpoint of T-cell survival and homeostasis in a p53-dependent manner. *Cell Mol Immunol* (2021) 18:1844–6. doi: 10.1038/s41423-021-00699-4

33. Interlandi M, Kerl K, Dugas M. InterCellar enables interactive analysis and exploration of cell-cell communication in single-cell transcriptomic data. *Commun Biol* (2022) 5:21. doi: 10.1038/s42003-021-02986-2

34. Coughlin S, Noviski M, Mueller JL, Chuwonpad A, Raschke WC, Weiss A, et al. An extracatalytic function of CD45 in b cells is mediated by CD22. *Proc Natl Acad Sci USA* (2015) 112:E6515–24. doi: 10.1073/pnas.1519925112

35. Takheaw N, Earwong P, Laopajon W, Pata S, Kasinrerk W. Interaction of CD99 and its ligand upregulates IL-6 and TNF-α upon T cell activation. *PloS One* (2019) 14:e0217393. doi: 10.1371/journal.pone.0217393

36. Ge Z, Wu S, Zhang Z, Ding S. Mechanism of tumor cells escaping from immune surveillance of NK cells. *Immunopharmacol Immunotoxicol* (2020) 42:187–98. doi: 10.1080/08923973.2020.1742733

37. Chand Dakal T, Dhabhai B, Agarwal D, Gupta R, Nagda G, Meena AR, et al. Mechanistic basis of co-stimulatory CD40-CD40L ligation mediated regulation of immune responses in cancer and autoimmune disorders. *Immunobiol* (2020) 225:151899. doi: 10.1016/j.imbio.2019.151899

38. Smulski CR, Eibel H. BAFF and BAFF-receptor in b cell selection and survival. *Front Immunol* (2018) 9:2285. doi: 10.3389/fimmu.2018.02285

39. Warnatz K, Salzer U, Rizzi M, Fischer B, Gutenberger S, Böhm J, et al. B-cell activating factor receptor deficiency is associated with an adult-onset antibody deficiency syndrome in humans. *Proc Natl Acad Sci USA* (2009) 106:13945–50. doi: 10.1073/pnas.0903543106

40. Denney L, Branchett W, Gregory LG, Oliver RA, Lloyd CM. Epithelial-derived TGF-β1 acts as a pro-viral factor in the lung during influenza a infection. *Mucosal Immunol* (2018) 11:523–35. doi: 10.1038/mi.2017.77

41. Borcherding N, Vishwakarma A, Voigt AP, Bellizzi A, Kaplan J, Nepple K, et al. Mapping the immune environment in clear cell renal carcinoma by single-cell genomics. *Commun Biol* (2021) 4:122. doi: 10.1038/s42003-020-01625-6

42. Hayes SM, Laird RM, Love PE. Beyond alphabeta/gammadelta lineage commitment: TCR signal strength regulates gammadelta T cell maturation and effector fate. *Semin Immunol* (2010) 22:247–51. doi: 10.1016/j.smim.2010.04.006

43. Trapnell C, Cacchiarelli D, Grimsby J, Pokharel P, Li S, Morse M, et al. The dynamics and regulators of cell fate decisions are revealed by pseudotemporal ordering of single cells. *Nat Biotechnol* (2014) 32:381–6. doi: 10.1038/nbt.2859

44. Hop HT, Arayan LT, Huy TXN, Reyes AWB, Vu SH, Min W, et al. The key role of c-fos for immune regulation and bacterial dissemination in brucella infected macrophage. *Front Cell Infect Microbiol* (2018) 8:287. doi: 10.3389/fcimb.2018.00287

45. Russo RC, Garcia CC, Teixeira MM, Amaral FA. The CXCL8/IL-8 chemokine family and its receptors in inflammatory diseases. *Expert Rev Clin Immunol* (2014) 10:593–619. doi: 10.1586/1744666x.2014.894886

46. Bell LCK, Meydan C, Kim J, Foox J, Butler D, Mason CE, et al. Transcriptional response modules characterize IL-1β and IL-6 activity in COVID-19. *IScience* (2021) 24:101896. doi: 10.1016/j.isci.2020.101896

47. Ghosh S, Parikh S, Nissa MU, Acharjee A, Singh A, Patwa D, et al. Semen proteomics of COVID-19 convalescent men reveals disruption of key biological pathways relevant to Male reproductive function. *ACS Omega* (2022) 7:8601–12. doi: 10.1021/acsomega.1c06551

48. Darmoise A, Maschmeyer P, Winau F. The immunological functions of saposins. *Adv Immunol* (2010) 105:25–62. doi: 10.1016/S0065-2776(10)05002-9

49. Huang L, Shi Y, Gong B, Jiang L, Zhang Z, Liu X, et al. Dynamic blood single-cell immune responses in patients with COVID-19. *Signal Transduction Targeting Ther* (2021) 6:110. doi: 10.1038/s41392-021-00526-2

50. Liu N, Jiang C, Cai P, Shen Z, Sun W, Xu H, et al. Single-cell analysis of COVID-19, sepsis, and HIV infection reveals hyperinflammatory and immunosuppressive signatures in monocytes. *Cell Rep* (2021) 37:109793. doi: 10.1016/j.celrep.2021.109793

51. Zhou S, Zhang J, Xu J, Zhang F, Li P, He Y, et al. An epigenome-wide DNA methylation study of patients with COVID-19. *Ann Hum Genet* (2021) 85:221–34. doi: 10.1111/ahg.12440

52. Stephenson E, Reynolds G, Botting RA, Calero-Nieto FJ, Morgan MD, Tuong ZK, et al. Single-cell multi-omics analysis of the immune response in COVID-19. *Nat Med* (2021) 27:904–16. doi: 10.1038/s41591-021-01329-2

53. Unterman A, Sumida TS, Nouri N, Yan X, Zhao AY, Gasque V, et al. Single-cell multi-omics reveals dyssynchrony of the innate and adaptive immune system in progressive COVID-19. *Nat Commun* (2022) 13:440. doi: 10.1038/s41467-021-27716-4

54. Market M, Angka L, Martel AB, Bastin D, Olanubi O, Tennakoon G, et al. Flattening the COVID-19 curve with natural killer cell based immunotherapies. *Front Immunol* (2020) 11:1512. doi: 10.3389/fimmu.2020.01512

55. van Eeden C, Khan L, Osman MS, Cohen Tervaert JW. Natural killer cell dysfunction and its role in COVID-19. *Int J Mol Sci* (2020) 21(17):6351. doi: 10.3390/ijms21176351

56. Elgueta R, Benson MJ, de Vries VC, Wasiuk A, Guo Y, Noelle RJ. Molecular mechanism and function of CD40/CD40L engagement in the immune system. *Immunol Rev* (2009) 229:152–72. doi: 10.1111/j.1600-065x.2009.00782.x

57. Chen Z, John Wherry E. T Cell responses in patients with COVID-19. *Nat Rev Immunol* (2020) 20:529–36. doi: 10.1038/s41577-020-0402-6

58. Vabret N, Britton GJ, Gruber C, Hegde S, Kim J, Kuksin M, et al. Immunology of COVID-19: Current state of the science. *Immunity* (2020) 52:910–41. doi: 10.1016/j.immuni.2020.05.002

59. Catanzaro M, Fagiani F, Racchi M, Corsini E, Govoni S, Lanni C. Immune response in COVID-19: addressing a pharmacological challenge by targeting pathways triggered by SARS-CoV-2. signal transduct. *Targeting Ther* (2020) 5:84. doi: 10.1038/s41392-020-0191-1

60. Farahani M, Niknam Z, Mohammadi Amirabad L, Amiri-Dashatan N, Koushki M, Nemati M, et al. Molecular pathways involved in COVID-19 and potential pathway-based therapeutic targets. *Biomed Pharmacother* (2022) 145:112420. doi: 10.1016/j.biopha.2021.112420

61. Cullen BR. Role and mechanism of action of the APOBEC3 family of antiretroviral resistance factors. *J Virol* (2006) 80:1067–76. doi: 10.1128/jvi.80.3.1067-1076.2006

62. Lambrecht BN, Vanderkerken M, Hammad H. The emerging role of ADAM metalloproteinases in immunity. *Nat Rev Immunol* (2018) 18:745–58. doi: 10.1038/s41577-018-0068-5

63. Luo L, Liang W, Pang J, Xu G, Chen Y, Guo X, et al. Dynamics of TCR repertoire and T cell function in COVID-19 convalescent individuals. *Cell Discovery* (2021) 7:89. doi: 10.1038/s41421-021-00321-x

64. Kalfaoglu B, Almeida-Santos J, Tye CA, Satou Y, Ono M. T-Cell dysregulation in COVID-19. *Biochem Biophys Res Commun* (2021) 538:204–10. doi: 10.1016/j.bbrc.2020.10.079

65. Liu J, Li H, Luo M, Liu J, Wu L, Lin X, et al. Lymphopenia predicted illness severity and recovery in patients with COVID-19: A single-center, retrospective study. *PloS One* (2020) 15(11):e0241659. doi: 10.1371/journal.pone.0241659

66. Fathi N, Rezaei N. Lymphopenia in COVID-19: Therapeutic opportunities. *Cell Biol Int* (2020) 44(9):1792–7. doi: 10.1002/cbin.11403

67. Huang I, Pranata R. Lymphopenia in severe coronavirus disease-2019 (COVID-19): systematic review and meta-analysis. *J Intensive Care* (2020) 8 (1):1–10. doi: 10.1186/s40560-020-00453-4

68. Shahbazi M, Jafari M, Moulana Z, Sepidarkish M, Bagherzadeh M, Rezanejad M, et al. Reduced frequency of T helper 17 and T helper 1 cells and their association with critical coronavirus disease 2019. *Apmis* (2021) 129(5):271–9. doi: 10.1111/apm.13129

69. Gil-Etayo FJ, Suàrez-Fernández P, Cabrera-Marante O, Arroyo D, Garcinuño S, Naranjo L, et al. T-Helper cell subset response is a determining factor in COVID-19 progression. *Front Cell Infect Microbiol* (2021) 11:624483. doi: 10.3389/fcimb.2021.624483

70. Zheng H-Y, Zhang M, Yang C-X, Zhang N, Wang X-C, Yang X-P, et al. Elevated exhaustion levels and reduced functional diversity of T cells in peripheral blood may predict severe progression in COVID-19 patients. *Cell Mol Immunol* (2020) 17:541–3. doi: 10.1038/s41423-020-0401-3

71. Rha M-S, Shin E-C. Activation or exhaustion of CD8+ T cells in patients with COVID-19. *Cell Mol Immunol* (2021) 18:2325–33. doi: 10.1038/s41423-021-00750-4

72. Wo J, Zhang F, Li Z, Sun C, Zhang W, Sun G. The role of gamma-delta T cells in diseases of the central nervous system. *Front Immunol* (2020) 11:580304. doi: 10.3389/fimmu.2020.580304

73. Preston GA, Lyon TT, Yin Y, Lang JE, Solomon G, Annab L, et al. Induction of apoptosis by c-fos protein. *Mol Cell Biol* (1996) 16:211–8. doi: 10.1128/mcb.16.1.211

74. Jundi K, Greene CM. Transcription of interleukin-8: How altered regulation can affect cystic fibrosis lung disease. *Biomolecules* (2015) 5:1386–98. doi: 10.3390/biom5031386

75. Li S, Zhang Y, Guan Z, Li H, Ye M, Chen X, et al. SARS-CoV-2 triggers inflammatory responses and cell death through caspase-8 activation. *Signal Transduction Targeting Ther* (2020) 5:235. doi: 10.1038/s41392-020-00334-0

76. Hu Y, Hu Y, Xiao Y, Wen F, Zhang S, Liang D, et al. Genetic landscape and autoimmunity of monocytes in developing vogt-Koyanagi-Harada disease. *Proc Natl Acad Sci USA* (2020) 117:25712–21. doi: 10.1073/pnas.2002476117

COPYRIGHT

© 2022 Chattopadhyay, Khare, Kumar, Mishra, Anand, Maurya, Gupta, Sahni, Gupta, Wadhwa, Yadav, Devi, Tardalkar, Joshi, Sethi and Pandey. This is an open-access article distributed under the terms of the Creative Commons Attribution License (CC BY). The use, distribution or reproduction in other forums is permitted, provided the original author (s) and the copyright owner(s) are credited and that the original publication in this journal is cited, in accordance with accepted academic practice. No use, distribution or reproduction is permitted which does not comply with these terms.

frontiers | Frontiers in Immunology

TYPE Original Research
PUBLISHED 19 December 2022
DOI 10.3389/fimmu.2022.1038227

Check for updates

OPEN ACCESS

EDITED BY
Edwin Bölke,
Heinrich Heine University of Düsseldorf, Germany

REVIEWED BY
Barbara Ruaro,
University of Trieste, Italy
Riccardo Pozzan,
University of Trieste, Italy

*CORRESPONDENCE
Mattia Bellan
mattia.bellan@med.uniupo.it

SPECIALTY SECTION
This article was submitted to Viral Immunology, a section of the journal Frontiers in Immunology

RECEIVED 06 September 2022
ACCEPTED 25 November 2022
PUBLISHED 19 December 2022

CITATION
Bellan M, Apostolo D, Albè A, Crevola M, Errica N, Ratano G, Tonello S, Minisini R, D'Onghia D, Baricich A, Patrucco F, Zeppegno P, Gramaglia C, Balbo PE, Cappellano G, Casella S, Chiocchetti A, Clivati E, Giordano M, Manfredi M, Patti G, Pinato DJ, Puricelli C, Raineri D, Rolla R, Sainaghi PP, Pirisi M and the No-More COVID study group (2022) Determinants of long COVID among adults hospitalized for SARS-CoV-2 infection: A prospective cohort study. *Front. Immunol.* 13:1038227. doi: 10.3389/fimmu.2022.1038227

COPYRIGHT
© 2022 Bellan, Apostolo, Albè, Crevola, Errica, Ratano, Tonello, Minisini, D'Onghia, Baricich, Patrucco, Zeppegno, Gramaglia, Balbo, Cappellano, Casella, Chiocchetti, Clivati, Giordano, Manfredi, Patti, Pinato, Puricelli, Raineri, Rolla, Sainaghi, Pirisi and the No-More COVID study group. This is an open-access article distributed under the terms of the Creative Commons Attribution License (CC BY). The use, distribution or reproduction in other forums is permitted, provided the original author(s) and the copyright owner(s) are credited and that the original publication in this journal is cited, in accordance with accepted academic practice. No use, distribution or reproduction is permitted which does not comply with these terms.

Determinants of long COVID among adults hospitalized for SARS-CoV-2 infection: A prospective cohort study

Mattia Bellan[1,2]*, Daria Apostolo[1], Alice Albè[1,2], Martina Crevola[1,2], Nicolò Errica[1,2], Giacomo Ratano[1,2], Stelvio Tonello[1], Rosalba Minisini[1], Davide D'Onghia[1], Alessio Baricich[1,2], Filippo Patrucco[1,2], Patrizia Zeppegno[1,2], Carla Gramaglia[1,2], Piero Emilio Balbo[2], Giuseppe Cappellano[1], Sara Casella[1], Annalisa Chiocchetti[1], Elisa Clivati[2], Mara Giordano[1,2], Marcello Manfredi[1], Giuseppe Patti[1,2], David James Pinato[1,3], Chiara Puricelli[1,2], Davide Raineri[1], Roberta Rolla[1], Pier Paolo Sainaghi[1,2], Mario Pirisi[1,2] and the No-More COVID study group

[1]Università del Piemonte Orientale (UPO), Novara, Italy, [2]"AOU Maggiore della Carità", Novara, Italy, [3]Department of Surgery and Cancer, Imperial College London, Hammersmith Hospital, London, United Kingdom, [4]Dipartimento di Scienze della Salute, Novara, Italy

Rationale: Factors associated with long-term sequelae emerging after the acute phase of COVID-19 (so called "long COVID") are unclear. Here, we aimed to identify risk factors for the development of COVID-19 sequelae in a prospective cohort of subjects hospitalized for SARS-CoV-2 infection and followed up one year after discharge.

Methods: A total of 324 subjects underwent a comprehensive and multidisciplinary evaluation one year after hospital discharge for COVID-19. A subgroup of 247/324 who consented to donate a blood sample were tested for a panel of circulating cytokines.

Results: In 122 patients (37.8%) there was evidence of at least one persisting physical symptom. After correcting for comorbidities and COVID-19 severity, the risk of developing long COVID was lower in the 109 subjects admitted to the hospital in the third wave of the pandemic than in the 215 admitted during the first wave, (OR 0.69, 95%CI 0.51-0.93, p=0.01). Univariable analysis revealed female sex, diffusing capacity of the lungs for carbon monoxide (DLCO) value, body mass index, anxiety and depressive symptoms to be positively associated with COVID-19 sequelae at 1 year. Following logistic regression analysis, DLCO was the only independent predictor of residual symptoms (OR 0.98 CI 95% (0.96-0.99), p=0.01). In the subgroup of subjects with normal DLCO (> 80%), for whom residual lung damage was an unlikely explanation for long COVID, the presence of anxiety and depressive symptoms was significantly associated to persistent

symptoms, together with increased levels of a set of pro-inflammatory cytokines: interferon-gamma, tumor necrosis factor-alpha, interleukin (IL)-2, IL-12, IL-1β, IL-17. In logistic regression analysis, depressive symptoms (p=0.02, OR 4.57 [1.21-17.21]) and IL-12 levels (p=0.03, OR 1.06 [1.00-1.11]) 1-year after hospital discharge were independently associated with persistence of symptoms.

Conclusions: Long COVID appears mainly related to respiratory sequelae, prevalently observed during the first pandemic wave. Among patients with little or no residual lung damage, a cytokine pattern consistent with systemic inflammation is in place.

KEYWORDS

long COVID-19, SARS-CoV-2 infection, cytokines, DLCO, depression

1 Introduction

The Severe Acute Respiratory Syndrome Coronavirus-2 (SARS-CoV-2) pandemic continues to have an impact on global health, as a result of acute infection and long-term sequelae. Unfortunately, a significant proportion of Coronavirus Disease (COVID-19) survivors experiences the persistence of symptoms many months after the acute phase of disease (1, 2).

Up to 58% of recovered patients show at least one symptom up to two years after the acute phase of the disease (3). The constellation of symptomatic and functional sequelae arising post-COVID-19 has been dubbed "long COVID", thereby categorizing those patients who have symptoms that persist or develop after the acute phase of SARS-CoV-2 infection and are not explained by alternative diagnoses (4). Long COVID is a multi-systemic condition which encompasses pulmonary, immunological, cardiovascular, neuropsychiatric, gastroenterological, hepatic, renal, endocrine and dermatological sequelae (5–7).

Whereas the pathogenetic mechanisms that determine the acute phase of disease have been quite well elucidated (8), those underlying the long COVID syndrome remain poorly understood (9, 10). Indeed, a dysregulated inflammatory response with a huge release of pro-inflammatory cytokines, including IL-1β, IL-7, IL-8, IL-9, IFN-γ, TNF, has been observed during the acute phase of the disease (11–13). This condition may result in the recruitment of different immune cells at the site of infection leading to inflammatory damage of the alveolar-capillary membrane and vascular barrier damage inducing respiratory failure and the development and progression of acute respiratory distress syndrome (ARDS) (14, 15). Eventually, the uncontrolled immune response may result in extra-pulmonary manifestations with a possible evolution into multi-organ failure (11).

A variety of mechanisms have been claimed as potentially relevant for long COVID, among which the persistence of end organ damage following acute COVID-19, the effect of mood perturbation and the maintenance of a chronic pro-inflammatory state (5, 16, 17). The latter hypothesis belongs to the observation that long COVID shares clinical features with myalgic encephalomyelitis/chronic fatigue syndrome (ME/CFS) (18), a poorly understood clinical condition, which can be elicited by acute viral infections. Indeed, the evidence is growing to suggest the persistence of a pro-inflammatory state in long COVID, months after virus has been cleared from the organism and the convalescence phase has been completed (19, 20).

Further insight into the pathogenesis of long COVID is paramount to pave the way for better tailored treatments and to contain the demand on health systems still under heavy pressure for the pandemic (5). In the present paper, we aimed to evaluate the role of potentially relevant pathogenetic mechanisms in the development of long COVID: more specifically, we evaluated the potential role of residual organ damage, persistent inflammation and psychological impact. This is a novel and multidisciplinary approach allowing us to better verify the relative contribution of these pathogenetic mechanisms to the development of long term sequelae.

2 Materials and methods

This prospective cohort study was approved by the local ethics committee (Comitato Etico Interaziendale Novara, IRB code CE 117/20) and conducted in strict accordance with the principles of the Declaration of Helsinki. All participants signed a written informed consent.

2.1 Study population

We contacted patients discharged between March 1st, 2020 and May 28th, 2021, from the Maggiore della Carità University Hospital of Novara, Piedmont, with a confirmed diagnosis of COVID-19. We included all patients aged 18 years or older who agreed to participate to the study. Patients were divided into two subsets: the first one which included subjects discharged between March 1st and June 29th, 2020, corresponding to the first wave of the pandemic in Italy; the second one, including patients admitted during the third Italian wave (15th March, 28th May 2021).

The patients were contacted by telephone and asked to attend a dedicated clinic for a follow-up visit 12 months after discharge; of them, 324 agreed to participate in the study. Follow-up visits took place from March 15th, 2021 to June 28th, 2022.

2.2 Study procedures

Patients were evaluated with a multidisciplinary approach, which included:

1. Clinical evaluation
2. Lung function assessment
3. Mental health assessment

2.2.1 Clinical evaluation

A survey was carried out aimed at recording: patients' demographic characteristics, symptoms during the acute phase of the disease, severity of the acute phase of the disease classified using an eight-category scale, as previously described (21), home medications and comorbidities which were cumulatively scored using the cumulative illness rating scale (CIRS) (22), patient symptoms at follow-up, vital signs and cardio-pulmonary physical examination.

2.2.2 Lung function assessment

All patients underwent standard pulmonary function tests (PFT) with a Quark PFT with X9 pneumotach (COSMED srl, Rome, Italy) to evaluate forced expiratory volume in 1 second (FEV1), vital capacity, forced vital capacity (FVC), diffusing capacity of the lungs for carbon monoxide (DLCO), DLCO constant, and total lung capacity. DLCO and total lung capacity were determined by the single-breath co technique.

The spirometer was calibrated on the day the test was performed and the barometric pressure and temperature were simultaneously recorded. A trained technician coached the patient, while a pulmonologist was responsible for test validation and interpretation based on the 2005 the American Thoracic Society and European Respiratory Society statements. Appropriate safety measures were adopted (including use of a dedicated spirometer to avoid cross-infection, use of a mouthpiece with a different antimicrobial filter for each patient and use of complete PPE by the staff). At the end of each day, the room underwent disinfection.

2.2.3 Mental health assessment

Patients were interviewed by an experienced psychiatrist, trained in the use of the Mini-International Neuropsychiatric Interview (MINI) (23), using structured and unstructured questions about current mental health status. Information about previous psychiatric history (being already treated by psychiatric services; a history of depression and/or anxiety), presence/absence of depressive and anxiety symptoms (independent of a full-criteria diagnosis of major depressive disorder, panic disorder, and generalized anxiety disorder) was gathered.

2.3 Laboratory analysis

To evaluate the potential role of cytokines, we performed a multipanel assessment of pro-inflammatory cytokines, using a Bio-PlexProTM Human Cytokine Assays (BioRad, Hercules, CA, US CAT.#M500KCAF0Y): interferon (IFN)-γ, interleukin (IL)-1β, IL-2, IL-6, IL-12, IL-17, tumor necrosis factor (TNF)-α were dosed. These studies were performed on 247/324 subjects who agreed to undergo peripheral venous blood sampling at the 12-months follow-up visit; for 73 patients, a blood sample, obtained during the acute phase of disease was also available and was therefore used to assess the potential predictive value of baseline cytokines levels on long COVID development.

Bio-PlexProTM Assays are sandwich immunoassays formatted on magnetic beads. Primitive antibodies directed against the desired biomarker are covalently coupled to the beads. Coupled beads react with the sample containing the biomarker of interest. After a series of washes to remove unbound protein, a biotinylated detection secondary antibody is added to create a sandwich complex. The final detection complex is formed with the addition of streptavidin-phycoerythrin (SA-PE) conjugate. Phycoerythrin serves as a fluorescent indicator, or reporter.

The samples were processed following the steps of the Bio-PlexProTM Assays manual issued by the supplier.

2.4 Statistical analysis

The data collected were recorded in a database and analyzed with MedCalc v.18.10.2 (MedCalc Software, Mariakerke, Belgium). For continuous variables, the measures of centrality and dispersion were medians and interquartile ranges [IQR] and

the differences between groups were evaluated by the Mann-Whitney test. The Pearson χ^2 or the Fisher exact test were used, as appropriate, to analyze the association between categorical variables. The existence of a correlation between continuous variables was verified calculating the corresponding Spearman correlation coefficient ρ. All variables found to have a statistical association with residual symptoms or DLCO impairment were entered into multivariate logistic regression models. The threshold for statistical significance was set at 0.05 (two-tailed).

3 Results

3.1 Impact of the pandemic wave on the development of long COVID

Out of the cohort of 324 subjects (196 males, 60.5%), 215 (66.3%) had been admitted to hospital during the first wave of the pandemic; data about their long-term sequelae have been published previously (18). Conversely, 109 were diagnosed during the third wave of the pandemic. In Supplementary Table 1 we described the main features of the general population, during the acute phase of disease.

After 368 [364-391] days, 37.8% of patients (N. = 122) still complained at least one physical symptom (also see Supplementary Table 2 for more details) and 151 (46.7%) patients reported the persistence of a reduction of their tolerance to physical activity.

Moreover, among the 310 patients who underwent a comprehensive psychiatric evaluation, anxiety symptoms were reported by 54 (17.4%) patients, while depressive symptoms were reported by 66 (21.3%) subjects.

Finally, 317 subjects underwent a pulmonary function test, according to which, the median FEV1 was 100 [89-112] of predicted, the median forced FVC was 80 [70-91] of predicted and the median DLCO was 98 [88-109] of predicted.

One of our research questions was to verify whether the risk of developing persistent symptoms might have changed over time. As shown in Table 1, the proportion of subjects complaining persistent symptoms was similar among those subjects admitted to the hospital during the first wave and those admitted during the third wave. However, in the third wave both the median severity of their condition and CIRS score were higher.

Therefore, to rule out the impact of the different time of hospital admission, we built a logistic regression model, which showed that being admitted to the hospital during the third wave was protective against the development of persistent symptoms (p=0.01, OR 0.69, 95%CI 0.51-0.93). Moreover, CIRS (p=0.22) and disease severity (p=0.13) during the acute phase were not associated to the development of persistent symptoms. However, in a multiple regression analysis model, the 12 months DLCO value was predicted by the wave of pandemic during which the patient was admitted to hospital (p<0.0001), along with disease severity during acute phase (p=0.02) and CIRS (p<0.0001).

TABLE 1 General features of the study population classified according to the wave of hospital admission.

	Patients admitted during the first wave	Patients admitted during the third wave	p
Age, years	61 [50-70]	59 [52-67]	0.51
Sex, M/F	132 (61.4)/83 (38.6)	64 (58.7) /45 (41.3)	0.72
Oxygen supplementation			
None	63 (29.3)	0 (0.0)	<0.0001*
Nasal cannulae or Ventimask	91 (41.3)	24 (22.0)	
Non-invasive ventilation	43 (20.0)	85 (78.0)	
Mechanical ventilation	18 (8.4)	0 (0.0)	
Class of severity			
3	51 (23.7)	1 (0.9)	<0.0001*
4	9 (4.2)	0 (0.0)	
5	86 (40.0)	23 (21.1)	
6	48 (22.3)	85 (78.0)	
7	21 (9.8)	0 (0.0)	
CIRS	2 [1-3]	4 [2-6]	<0.0001*
Residual symptoms, N/Y	126 (58.9)/88 (41.1)	71 (65.1)/34 (31.2)	0.09
Anxiety symptoms, N/Y	163 (81.1)/38 (18.9)	93 (85.3)/16 (14.7)	0.43
Depressive symptoms	161 (80.1)/40 (19.9)	83 (76.1)/26 (23.9)	0.47
FEV1, % of predicted	100 [90-112]	101 [87-111]	0.46
FVC, % of predicted	98 [89-109]	98 [86-108]	0.64
DLCO, % of predicted	78 [68-90]	81 [72-93]	0.02

CIRS, cumulative illness rating scale; DLCO, diffusing capacity of the lungs for carbon monoxide; FEV1, forced expiratory volume in the first second; FVC, forced vital capacity.
*p < 0.05

10.3389/fimmu.2022.1038227

3.2 Evaluation of pathogenetic mechanisms underlying the development of long COVID

To better evaluate the pathogenetic mechanisms underlying the development of long COVID, we analyzed a subgroup of 247 patients (151 males, 61.1%) with a median age of 60 [51-69] years, for whom a blood sample, collected one year after hospital discharge, was available. 155 (62.8%) were admitted during the first wave, while 92 (37.2%) were admitted during the third wave.

The median number of ongoing drugs for routine therapies at admission was 1 [0-4], while the median number of comorbidities was 2 [1-3], among them arterial hypertension (42.9%), obesity (22.2%) and diabetes mellitus (15.1%) were the most frequent ones, and the median CIRS was 2 [1-4].

The median duration of hospital stay during the acute phase was 11 [7-16] days. Disease severity during the acute phase was distributed as follows:

-Class 3, N. 37 (15.0%);
-Class 4, N. 5 (2.0%);
-Class 5, N. 83 (33.6%);
-Class 6, N. 107 (43.3%);
-Class 7, N. 15 (6.1%).

During hospital stay, 44 patients did not require oxygen supplementation (17.8%), 87 received oxygen through nasal cannula or Venturi mask (35.2%), 104 underwent non-invasive ventilation (42.1%) and, finally, 12 (4.9%) were mechanically ventilated. 18 (7.3%) were admitted to an intensive care unit, where they stayed for a median of 7.5 [5.0-20.0] days.

One year after discharge, 93 subjects (37.7%) still complained of at least one symptom (also see Table 2 for more details). Moreover, 111 subjects (44.9%) reported a reduction of their tolerance to physical effort and 64 (25.9%) reported alopecia. The main symptoms and the results of pulmonary function tests are reported in Table 2.

TABLE 2 Main findings at the one year follow-up visit.

Cough	20 (8.1)
Fever	3 (1.2)
Dyspnoea	11 (4.5)
Diarrhoea	13 (5.3)
Arthralgia/Myalgia	41 (16.6)
Dysgeusia	15 (6.1)
Fatigue	38 (15.4)
Anosmia	19 (7.7)
DLCO	81 [70 – 91]
FEV1	102 [94,3 – 113,8]
FVC	98 [89 – 109]

DLCO, diffusing capacity of the lungs for carbon monoxide; FEV1, forced expiratory volume in the first second; FVC, forced vital capacity.

The association between clinical variables and persistence of symptoms is shown in Table 3, which identified DLCO, BMI, the persistence of anxiety and depressive symptoms and female sex as predictors at univariate analysis. We built a logistic regression analysis model including as independent variables all those associated to persistent symptoms at univariate analysis: DLCO emerged as the only independent predictor of residual symptoms (OR 0.98 CI95% (0.96-0.99), p=0.01), suggesting the relevance of residual organ impairment in the development of long COVID (Supplementary Table 3).

This hypothesis is supported by the demonstration that the prevalence of residual symptoms is higher among the 111 subjects with a reduction of DLCO below the threshold of 80% of predicted (N. = 53, 47.7%), than in those with a normal DLCO (N. = 40, 30.1%; p=0.005).

However, this finding also confirms that a consistent proportion of subjects with no significant respiratory function impairment still complains symptoms 1 year after hospital discharge. We therefore investigated other potential pathogenetic factors, firstly focusing our attention on the psychiatric sequelae. To do that, we investigated the association between anxiety/depression symptoms and long COVID among patients with and without a reduction of DLCO (Table 4). As shown in the table, the presence of anxiety or depression symptoms is associated with long COVID only among those subjects who did not show a significant reduction in their DLCO, suggesting that in this subset, mental health may play a key role in the development of long COVID.

We finally aimed to evaluate the potential role of a persistent subclinical inflammation assessed with the dosage of a set of pro-inflammatory cytokines: IL-2, IL-12, IL-1β, IFN-γ, TNF-α and IL-17. In Supplementary Table 4 we report the plasma levels of these cytokines in the study population; moreover, we report the concentrations observed in a subgroup of 73 subjects for whom a baseline blood sample, obtained during the acute phase of disease was available. We then evaluated whether the persistence of symptoms was associated to cytokine levels at baseline or at follow-up visit (Table 5). As reported in the table, none of the assessed cytokines, measured at baseline, predicted the development of persistent symptom. Conversely, patients suffering of long COVID, showed increased values of IL-12, IL-17, IL-1β, IFN-γ and TNF-α, one year after hospital discharge.

In a logistic regression analysis, including clinical variables associated to the persistence of long-term sequelae, DLCO (OR 0.98, 95%CI 0.96-0.99; p=0.04) and IL-12 (OR 1.04, 95%CI 1.00-1.08; p=0.04) were the only variables independently associated with the persistence of symptoms at one year from hospital discharge in this subgroup (see Supplementary Table 5).

Interestingly, when we evaluated only those patients with a DLCO >80% and with no residual organ damage, we confirmed the independent association between residual symptoms and IL-12 plasma concentration (OR 1.06, 95%

TABLE 3 Univariate analysis of clinical variables among patients with and without residual symptoms.

	No residual symptoms	Residual symptoms	p
Age, years	59 [51-68]	61 [50-70]	0.63
Gender, M/F	106 (70.2)/48 (50.0)	45 (29.8)/48 (50.0)	0.002*
Oxygen supplementation			
None	25 (16.2)	19 (20.4)	0.41
Nasal cannulae or Ventimask	60 (39.0)	27 (29.0)	
Non-invasive ventilation	61 (39.6)	43 (46.2)	
Mechanical ventilation	8 (5.2)	4 (4.3)	
Class of severity			
3	22 (14.3)	15 (16.1)	0.79
4	3 (1.9)	2 (2.2)	
5	56 (36.4)	27 (29.0)	
6	65 (42.2)	42 (45.2)	
7	8 (5.2)	7 (7.5)	
Oxygen supplementation			
None	39 (19.4)	24 (19.7)	0.63
Nasal cannula or Venturi mask	76 (37.8)	38 (31.1)	
Non-invasive ventilation	76 (37.8)	52 (42.6)	
Mechanical ventilation	10 (5.0)	8 (6.6)	
Drugs			
Hydroxychloroquine	106 (57.0)	75 (66.4)	0.11
Steroids	87 (46.8)	46 (40.7)	0.34
Antiviral agents	76 (40.9)	52 (46.0)	0.40
Anti-IL6	5 (2.7)	3 (2.7)	1.00
CIRS	2 [1-4]	2 [2-3]	0.45
BMI, kg/m2	27.4 [24.7-31.2]	30.1 [26.2-32.3]	0.02*
Anxiety symptoms, N/Y	136 (89.5)/16 (10.5)	67 (77.0)/20 (23.0)	0.01*
Depressive symptoms, N/Y	128 (84.2)/24 (15.8)	59 (67.8)/28 (32.2)	0.005*
FEV1, %	102 [88-111]	100 [90-114]	0.98
FVC, %	98 [89-109]	97 [87-108]	0.42
DLCO, %	83 [72-91]	77 [68-84]	0.0007*

BMI, body mass index; CIRS, cumulative illness rating scale; DLCO, diffusing capacity of the lungs for carbon monoxide; FEV1, forced expiratory volume in the first second; FVC, forced vital capacity.
*p < 0.05.

TABLE 4 Proportion of patients complaining residual symptoms and mental health impairment categorized according to diffusing capacity of the lungs for carbon monoxide (DLCO) values.

DLCO ≥ 80%

	No residual symptoms	Residual symptoms	p
Anxiety symptoms, No/Yes	84 (91.3)/8 (8.7)	27 (71.1)/11 (28.9)	0.003*
Depressive symptoms, No/Yes	83 (90.2)/9 (9.8)	23 (60.5)/15 (39.5)	0.0002*
DLCO < 80%			
	No residual symptoms	**Residual symptoms**	**p**
Anxiety symptoms, No/Yes	50 (87.7)/7 (12.3)	40 (81.6)/9 (18.4)	0.42
Depressive symptoms, No/Yes	44 (77.2)/13 (22.8)	36 (73.5)/13 (26.5)	0.82

*p < 0.05.

CI 1.00-1.11; p=0.03), which was associated with long COVID along with the persistence of depressive symptoms (OR 4.57, 95%CI 1.21-17.21; p=0.02) see Supplementary Table 6). Taking together these findings, IL-12 seems to be independently associated to the presence of persistent symptoms in patients with no significant organ involvement. Accordingly, IL-12 levels bore no correlation with DLCO (ρ=-0.079, p=0.22).

10.3389/fimmu.2022.1038227

TABLE 5 Levels of pro-inflammatory cytokines in patients with and without residual symptoms.

Cytokine concentration at baseline (N. = 73)	Residual symptoms	No residual symptoms	p
IL-12	3.47 [0.12-5.73]	2.62 [0.00-4.68]	0.47
IL-1ß	0.59 [0.07-2.57]	0.41 [0.00-1.26]	0.38
IL-17	5.43 [2.63-8.72]	3.93 [2.54-5.43]	0.07
IL-6	8.03 [4.92-25.28]	9.12 [5.35-19-51]	0.95
IL-2	2.16 [0.00-6.57]	2.16 [0.00-3.84]	0.49
IFN-γ	6.09 [5.20-12.03]	7.64 [5.20-8.68]	0.87
TNF-α	21.36 [15.61-28.44]	20.15 [16.31-25.97]	0.86
Cytokine concentration at follow-up visit (N. = 247)	**Residual symptoms**	**No residual symptoms**	**p**
IL-12	12,90 [1.75-26.15]	4,40 [0.30-14.19]	0.0003*
IL-1ß	0,61 [0.00-1.69]	0,20 [0.00-0.80]	0.005*
IL-17	10,68 [5.25-25.04]	6,55 [3.24-13.81]	0.0008*
IL-6	0,00 [0.00-1.52]	0,00 [0.00-1.45]	0.65
IL-2	1,11 [0.00-3.43]	0,00 [0.00-1.19]	0.005*
IFN-γ	5,27 [2.03-15.14]	3,33 [1.69-8.71]	0.006*
TNF-α	53,70 [24.28-76.18]	43,57 [11.86-63.98]	0.01*

IFN, interferon; IL, interleukin; TNF, tumor necrosis factor.
*$p < 0.05$.

We finally evaluated whether any of the assayed cytokines may play a role in the development of alopecia; in Table 6 we report the clinical features and the median values of cytokines concentration at baseline and at follow-up. As reported in the table, female sex, anxiety and depressive symptoms were associated with development of alopecia. The baseline levels of pro-inflammatory cytokines did not predict alopecia; in contrast, the concentration of IL-12, IL-2, IL-17, IFN-γ and TNF-α at 1 year was significantly increased in patients complaining alopecia. At logistic regression analysis, female sex and IL-17 plasma concentrations, were independently associated with development of alopecia (Supplementary Table 7).

4 Discussion

The present study shows that the risk of long COVID was significantly greater in the first wave of pandemic, when compared to the third one. Moreover, we confirm that respiratory function impairment, assessed by DLCO measurement, is the main factor associated with the persistence of symptoms. This suggests that residual organ damage plays a key role in the development of residual symptoms; however long COVID may affect also patients with normal lung function. Among those subjects with preserved respiratory function, our results suggest that the development of depressive symptoms and the persistence of a chronic inflammatory state may represent major determinants of long COVID. These novel findings deserve a deeper discussion.

In the present study we firstly considered a large cohort of 324 patients followed-up, with a multidisciplinary approach, one year after their discharge from an Italian hospital. Part of the present cohort had already been described in a previous paper (24). Consistently with our previous findings, around 38% of patients still complained symptoms one year after the acute phase of disease. This is in line with previous papers (25, 26), which reported similar rates of long COVID at the same timepoint. Other authors reported even higher rates of residual symptoms, although differences in clinical assessment and in the definition of long COVID may easily subside the discrepancies with our findings (3, 27).

Our first aim was to evaluate whether being admitted at different waves of the pandemic was associated to a different risk of residual symptoms. Indeed, it is well known that the case fatality rate of the acute phase of disease is decreasing over time (28, 29). However, it is still unclear whether this outcome improvement might also be associated to a reduced risk of developing long COVID. Despite finding a similar proportion of subjects with residual symptoms, the patients admitted during the third wave were more comorbid and showed a higher class of disease severity during the acute phase. Indeed, during the first wave of the pandemic in Italy, when the virus was largely unknown and the number of cases relatively low, there was a local tendency of admitting a larger proportion of patients who tested positive, even when there was no evidence of respiratory failure. Conversely, during the third wave, the huge number of patients testing positive and requiring oxygen supplementation prevented the admission of patients with mild disease.

When we assessed the role of the wave of pandemic on long COVID development, we demonstrated that, being admitted during the third wave was protective against long COVID; this observation, to the best of our knowledge, is novel and probably reflects the improvement of preventive (vaccines) and therapeutic strategies. Although a direct effect related to the

10.3389/fimmu.2022.1038227

TABLE 6 Comparison of clinical features and cytokine levels among patients with or without alopecia.

	Alopecia N = 64	Alopecia N = 180	p
Age, years	61 [50-69]	59 [51-68]	0.36
Sex, M/F	18 (11.9)/46 (47.9)	133 (88.1)/50 (52.1)	<0.0001*
BMI, kg/m^2	28.6 [24.8-32.1]	28.1 [25.5-31.5]	0.92
DLCO, %	76 [68-85]	82 [70-92]	0.04*
CIRS	2 [1-3]	2 [1-4]	0.12
Class of severity, 3/4/5/6/7	11 (17.2)/1 (1.6)/23 (35.9)/22 (34.4)/7 (10.9)	26 (14.2)/4 (2.2)/60 (32.8)/85 (46.4)/8 (4.4)	0.24
Anxiety symptoms, No/Yes	43 (21.2)/16 (44.4)	160 (88.9)/20 (55.6)	0.005*
Depressive symptoms, No/Yes	39 (20.9)/20 (38.5)	148 (79.1)/32 (61.5)	0.02*
IL-12 baseline	3.47 [0.00-4.50]	2.62 [0.12-4.70]	0.66
IL-1β baseline	1.09 [0.15-2.33]	0.35 [0.00-1.43]	0.38
IL-17 baseline	3.33 [2.03-5.05]	4.37 [2.91-6.45]	0.07
IL-6 baseline	5.35[2.13-22.81]	9.12 [5.39-20.62]	0.95
IL-2 baseline	2.46 [0.41-6.17]	2.16 [0.00-4.06]	0.49
IFN-γ baseline	5.60 [5.20-7.68]	7.37 [5.20-11.38]	0.87
TNF-α baseline	25.97 [20.45-27.79]	20.02 [15.42-27.88]	0.33
IL-12 1-y follow-up	12.44 [1.84-25.76]	5.18 [0.48-16.10]	0.007*
IL-1β 1-y follow-up	0.53 [0.00-1.61]	0.20 [0.00-0.84]	0.005*
IL-17 1-y follow-up	13.90 [7.51-25.72]	6.44 [3.24-13.81]	0.0008*
IL-6 1-y follow-up	0,00 [0.00-1.12]	0,00 [0.00-1.70]	0.65
IL-2 1-y follow-up	1,13 [0.00-3.85]	0,00 [0.00-1.52]	0.005*
IFN-γ 1-y follow-up	6.26 [2.76-16.04]	3.29 [1.69-8.71]	0.002*
TNF-α 1-y follow-up	56.95 [46.57-73.66]	41.76[12.68-64.03]	0.0007*

BMI, body mass index; CIRS, cumulative illness rating scale; DLCO, diffusing capacity of the lungs for carbon monoxide; IFN, interferon; IL, interleukin; TNF, tumor necrosis factor.
*p < 0.05.

changes of the virus, with the development of subsequent variants, can only be hypothesized, it should be acknowledged that patients in the third wave were infected when delta variant was the most represented one in Italy. It is well known that this specific variant was burdened by a severity and mortality even greater than alpha variant (30). In this context, a major limitation of our study is that we did not identify the variants affecting our patients. However, based on our findings, it is reasonable to postulate that, beside a reduction of the severity of acute infection, the prevalence of long-term sequelae may reduce over time.

We then moved our attention towards the identification of clinical factors associated with the development of long COVID. In line with previous reports, we found that a decreasing DLCO (31), female gender (32), a higher BMI (33) and the presence of anxiety and depression symptoms (34) were all associated to the persistence of symptoms at univariable analysis; when included in a logistic regression model, the strongest and unique independent predictor of residual symptoms was DLCO, suggesting that the residual organ impairment after acute phase might be the major driver of long COVID. Indeed, residual symptoms are, according to our data, more prevalent among patients with a DLCO<80%. Obviously, our data rely only on post-COVID PFTs; pre-COVID DLCO values were not available and, therefore, we are not able to assess whether this functional impairment should completely be attributed to SARS-CoV-2 infection or, rather, whether this might follow a pre-existing lung condition. Whichever the cause of DLCO impairment, the decrease in lung function remains the most relevant factor associated with long COVID symptoms.

Clearly, DLCO impairment cannot entirely justify the whole spectrum of long COVID; it is a common experience to identify patients with residual symptoms and a fully normal lung function. However, impaired DLCO may act as a surrogate for severe COVID-19, a condition known to be associated with a higher risk of sequelae compared to asymptomatic infection. In this context, other pathogenetic mechanisms should be involved.

First, we demonstrated that mental health impairment is very relevant in this subset of patients. Beside a strong association between anxiety/depressive and organic symptoms in patients with a DLCO > 80%, in those with a normal DLCO, this association was completely lost. This observation suggests that the mental health impact may be a cause, rather than a consequence of long COVID, at least for those patients without long term organ function impairment. It is well known that the prevalence of COVID-19 survivors showing anxiety/depressive symptoms is high (35, 36). The pandemic impacted severely on the mental health of the general population: the effects on persons who required hospital admission, especially if they experienced traumatic events such as mechanical ventilation or

familiar mourns, are conceivably more severe. Our findings suggest that a proper psychological support might be helpful in preventing and/or attenuating long COVID.

We finally explored the hypothesis that a persistent pro-inflammatory state may contribute to long COVID pathogenesis. This idea stems from the observation that long COVID shares common features with other post-acute syndromes following viral infection, which have been linked to persistent chronic inflammation (37). The present paper supports this theory, since patients complaining persistent symptoms were characterized by increased concentration of a plethora of pro-inflammatory cytokines. Interestingly, the only one which was not associated was IL-6, which is known to have a key role during acute infection being a potential target of treatment (38). Conversely, we found that increased levels of IL-1β, IL-2, IL-12, IL-17, IFN-γ and TNF-α are associated with persistent symptoms of disease. Our findings integrate and expand recent data: in a paper by Queiroz et al. (39), IL-17 and IL-2 were reported to be increased in patients with post-acute sequelae. Similarly, Schultheiß recently reported the association of IL-1, IL-6 and TNFα (40). All these contributions point towards the hypothesis that counteracting this derangement of innate immunity might be helpful in the pharmaceutical management of long COVID. A novel finding emerging from our cohort is the central role of IL-12. IL-12 is a key cytokine in innate immunity, which enhances NK cytotoxicity and IFN-γ production (41). The association between IL-12 levels and long COVID has never been reported to date; however, in the past, increased levels of IL-12 have already been reported in patients with a condition bearing similarities with long COVID, i.e., CFS.

We finally focused our attention on a specific long-lasting condition, alopecia, which is unexpectedly reported in a high proportion of COVID-19 survivors (42). Previous data on alopecia areata suggested that cytokines may contribute to hair loss (43). Indeed, drugs counteracting cytokines activity, such as baricitinib are sometime used for alopecia areata treatment (44). However, to the best of our knowledge, the association between pro-inflammatory cytokines and alopecia in long COVID has never been shown before. According to our data, Th1 and Th17 cytokines are increased in patients complaining hair loss; among them, IL-17 seems to be particularly relevant as already reported by previous papers on alopecia areata (45).

Finally, it is relevant to underline that we also tried to evaluate the predictive role of baseline cytokines on the persistence of symptoms; we failed to disclose any association, although the small sample size of patients with the availability of a baseline blood sample might have underpowered our findings.

5 Limitations

We are aware that this study has some limitations. The small number of samples collected during the acute phase of disease prevent us to reliably evaluate the impact of acute inflammatory response on chronic disease. In addition, hospitalized patients represent a small proportion of COVID-19 cases and for this reason, focusing only on discharged hospitalized patients could provide a limited perspective on the experience of long COVID in the broader population. Moreover, we did not have specific information on the variants affecting our study population.

6 Conclusions

In conclusion, our work shades new light on the mechanisms underlying the development of long COVID, suggesting that the persistence of respiratory function impairment is crucial, but even in subjects with a completely normal lung function, symptoms may persist as a result of mental health derangement and/or persistent chronic inflammation, involving Th1 and Th17 cytokines. These findings, if confirmed in larger studies, might provide a rationale for trials with drugs targeting pro-inflammatory cytokines in patients with severe sequelae of SARS-CoV-2 infection.

No-More COVID study group

Mattia Bellan, Università del Piemonte Orientale (UPO), Novara, Italy, "AOU Maggiore della Carità", Novara, Italy; Daria Apostolo, Università del Piemonte Orientale (UPO), Novara, Italy; Alice Albè, Università del Piemonte Orientale (UPO), Novara, Italy, "AOU Maggiore della Carità", Novara, Italy; Martina Crevola, Università del Piemonte Orientale (UPO), Novara, Italy, "AOU Maggiore della Carità", Novara, Italy; Nicolò Errica, Università del Piemonte Orientale (UPO), Novara, Italy, "AOU Maggiore della Carità", Novara, Italy; Giacomo Ratano, Università del Piemonte Orientale (UPO), Novara, Italy, "AOU Maggiore della Carità", Novara, Italy; Acquaviva Antonio, Università del Piemonte Orientale (UPO), Novara, Italy, "AOU Maggiore della Carità", Novara, Italy; Luigi Mario Castello, Università del Piemonte Orientale (UPO), Novara, Italy; Donato Colangelo, Dipartimento di Scienze della Salute, Novara, Italy; Stelvio Tonello, Università del Piemonte Orientale (UPO), Novara, Italy; Rosalba Minisini, Università del Piemonte Orientale (UPO), Novara, Italy; Davide D'Onghia, Università del Piemonte Orientale (UPO), Novara, Italy; Alessio Baricich, Università del Piemonte Orientale (UPO), Novara, Italy, "AOU Maggiore della Carità", Novara, Italy; Filippo Patrucco, Università del Piemonte Orientale (UPO), Novara, Italy, "AOU Maggiore della Carità", Novara, Italy; Patrizia Zeppegno, Università del Piemonte Orientale (UPO), Novara, Italy, "AOU Maggiore della Carità", Novara, Italy; Carla Gramaglia, Università del Piemonte Orientale (UPO), Novara, Italy, "AOU Maggiore della Carità", Novara, Italy; Gian Carlo Avanzi, Università del Piemonte Orientale (UPO), Novara, Italy, "AOU Maggiore della Carità",

Novara, Italy; Piero Emilio Balbo, "AOU Maggiore della Carità", Novara, Italy; Giulia Baldon, Università del Piemonte Orientale (UPO), Novara, Italy, "AOU Maggiore della Carità", Novara, Italy; Michela Barini, Università del Piemonte Orientale (UPO), Novara, Italy; Marco Battaglia, Università del Piemonte Orientale (UPO), Novara, Italy, "AOU Maggiore della Carità", Novara, Italy; Simone Bor, Università del Piemonte Orientale (UPO), Novara, Italy, "AOU Maggiore della Carità", Novara, Italy; Vincenzo Cantaluppi, Università del Piemonte Orientale (UPO), Novara, Italy, "AOU Maggiore della Carità", Novara, Italy; Giuseppe Cappellano, "AOU Maggiore della Carità", Novara, Italy; Alessandro Carriero, Università del Piemonte Orientale (UPO), Novara, Italy, "AOU Maggiore della Carità", Novara, Italy; Sara Casella, Università del Piemonte Orientale (UPO), Novara, Italy; Annalisa Chiocchetti, Università del Piemonte Orientale (UPO), Novara, Italy; Elisa Clivati, "AOU Maggiore della Carità", Novara, Italy; Daria Cuneo, Università del Piemonte Orientale (UPO), Novara, Italy, "AOU Maggiore della Carità", Novara, Italy; Eleonora Gambaro, Università del Piemonte Orientale (UPO), Novara, Italy, "AOU Maggiore della Carità", Novara, Italy; Mara Giordano, Università del Piemonte Orientale (UPO), Novara, Italy, "AOU Maggiore della Carità", Novara, Italy; Luisa Isabella, Università del Piemonte Orientale (UPO), Novara, Italy, "AOU Maggiore della Carità", Novara, Italy; Alberto Loro, Università del Piemonte Orientale (UPO), Novara, Italy, "AOU Maggiore della Carità", Novara, Italy; Marcello Manfredi, Università del Piemonte Orientale (UPO), Novara, Italy; Debora Marangon, "AOU Maggiore della Carità", Novara, Italy; Emanuele Mones, Università del Piemonte Orientale (UPO), Novara, Italy, "AOU Maggiore della Carità", Novara, Italy; Elena Paracchini, "AOU Maggiore della Carità", Novara, Italy; Giuseppe Patti, Università del Piemonte Orientale (UPO), Novara, Italy, "AOU Maggiore della Carità", Novara, Italy; David James Pinato, Università del Piemonte Orientale (UPO), Novara, Italy, Department of Surgery and Cancer, Imperial College London, Hammersmith Hospital, London, United Kingdom; Chiara Puricelli, Università del Piemonte Orientale (UPO), Novara, Italy, "AOU Maggiore della Carità", Novara, Italy; Davide Raineri, Università del Piemonte Orientale (UPO), Novara, Italy; Roberta Rolla, Università del Piemonte Orientale (UPO), Novara, Italy; Pier Paolo Sainaghi, Università del Piemonte Orientale (UPO), Novara, Italy, "AOU Maggiore della Carità", Novara, Italy; Stefano Tricca, Università del Piemonte Orientale (UPO), Novara, Italy; Mario Pirisi, Università del Piemonte Orientale (UPO), Novara, Italy, "AOU Maggiore della Carità", Novara, Italy.

Data availability statement

The raw data supporting the conclusions of this article will be made available by the authors, without undue reservation.

Ethics statement

The studies involving human participants were reviewed and approved by Comitato Etico Interaziendale Novara, IRB code CE 117/20. The patients/participants provided their written informed consent to participate in this study.

Author contributions

MB had full access to all of the data in the study and takes responsibility for the integrity of the data and the accuracy of the data analysis. Study concept and design: MB, AB, FP, PZ, CG, GP, and MP. Acquisition of data: AAl, MC, NE, GR, AAn, AB, FP, PZ, CG, PB, SC, EC, GP, CP, and PS. Analysis and interpretation of data: MB, DA, ST, RM, DD, GC, AC, MG, MM, DR, and RR. Drafting of the manuscript: MB and DP. Critical revision of the manuscript for important intellectual content: All the authors. Statistical analysis: MB and MP. Obtained funding: MB and AC. Administrative, technical, or material support: ST and RM. Study supervision: MP. All authors contributed to the article and approved the submitted version.

Funding

This work has been supported by the Fondazione Cariplo (grant no. 2021-1541) and by the "Piano Riparti Piemonte", Azione n. 173 "INFRA-P. Realizzazione, rafforzamento e ampliamento Infrastrutture di ricerca pubbliche–bando" INFRA-P2-TECHNOMED-HUB n. 378-48.

Conflict of interest

The authors declare that the research was conducted in the absence of any commercial or financial relationships that could be construed as a potential conflict of interest.

Publisher's note

All claims expressed in this article are solely those of the authors and do not necessarily represent those of their affiliated organizations, or those of the publisher, the editors and the reviewers. Any product that may be evaluated in this article, or claim that may be made by its manufacturer, is not guaranteed or endorsed by the publisher.

Supplementary material

The Supplementary Material for this article can be found online at: https://www.frontiersin.org/articles/10.3389/fimmu.2022.1038227/full#supplementary-material

References

1. Mehandru S, Merad M. Pathological sequelae of long-haul COVID. *Nat Immunol* (2022) 23:194–202. doi: 10.1038/s41590-021-01104-y

2. Bellan M, Soddu D, Balbo PE, Baricich A, Zeppegno P, Avanzi GC, et al. Respiratory and psychophysical sequelae among patients with COVID-19 four months after hospital discharge. *JAMA Netw Open* (2021) 4:e2036142. doi: 10.1001/jamanetworkopen.2020.36142

3. Huang L, Li X, Gu X, Zhang H, Ren L, Guo L, et al. Health outcomes in people 2 years after surviving hospitalisation with COVID-19: a longitudinal cohort study. *Lancet Respir Med* (2022) 10(9):863–76. doi: 10.1016/S2213-2600(22)00126-6

4. National Institute for Health and Care Excellence. *COVID-19 rapid guideline: managing the long-term effects of COVID-19 NICE guideline* (2020). Available at: https://www.nice.org.uk/guidance/ng188/chapter/Recommendations.

5. Crook H, Raza S, Nowell J, Young M, Edison P. Long covid-mechanisms, risk factors, and management. *BMJ* (2021) 374:n1648. doi: 10.1136/bmj.n1648

6. Nalbandian A, Sehgal K, Gupta A, Madhavan MV, McGroder C, Stevens JS, et al. Post-acute COVID-19 syndrome. *Nat Med* (2021) 27:601–15. doi: 10.1038/s41591-021-01283-z

7. O'Sullivan O. Long-term sequelae following previous coronavirus epidemics. *Clin Med* (2021) 21:e68–70. doi: 10.7861/clinmed.2020-0204

8. Merad M, Blish CA, Sallusto F, Iwasaki A. The immunology and immunopathology of COVID-19. *Science* (2022) 375:1122–7. doi: 10.1126/science.abm8108

9. Pavli A, Theodoridou M, Maltezou HC. Post-COVID syndrome: Incidence, clinical spectrum, and challenges for primary healthcare professionals. *Arch Med Res* (2021) 52:575–81. doi: 10.1016/j.arcmed.2021.03.010

10. Castanares-Zapatero D, Chalon P, Kohn L, Dauvrin M, Detollenaere J, Maertens de Noordhout C, et al. Pathophysiology and mechanism of long COVID: a comprehensive review. *Ann Med* (2022) 54:1473–87. doi: 10.1080/07853890.2022.2076901

11. Girija ASS, Shankar EM, Larsson M. Could SARS-CoV-2-Induced hyperinflammation magnify the severity of coronavirus disease (CoViD-19) leading to acute respiratory distress syndrome? *Front Immunol* (2020) 11. doi: 10.3389/fimmu.2020.01206

12. Wilson JG, Simpson LJ, Ferreira AM, Rustagi A, Roque J, Asuni A, et al. Cytokine profile in plasma of severe COVID-19 does not differ from ARDS and sepsis. *JCI Insight* (2020) 5:e140289. doi: 10.1172/jci.insight.140289

13. Ghazavi A, Ganji A, Keshavarzian N, Rabiemajd S, Mosayebi G. Cytokine profile and disease severity in patients with COVID-19. *Cytokine* (2021) 137:155323. doi: 10.1016/j.cyto.2020.155323

14. Cardone M, Yano M, Rosenberg AS, Puig M. Lessons learned to date on COVID-19 hyperinflammatory syndrome: Considerations for interventions to mitigate SARS-CoV-2 viral infection and detrimental hyperinflammation. *Front Immunol* (2020) 11. doi: 10.3389/fimmu.2020.01131

15. Salton F, Confalonieri P, Campisciano G, Cifaldi R, Rizzardi C, Generali D, et al. Cytokine profiles as potential prognostic and therapeutic markers in SARS-CoV-2-Induced ARDS. *J Clin Med* (2022) 11:2951. doi: 10.3390/jcm11112951

16. Cortellini A, Gennari A, Pommeret F, Patel G, Newsom-Davis T, Bertuzzi A, et al. COVID-19 sequelae and the host proinflammatory response: An analysis from the OnCovid registry. *J Natl Cancer Inst* (2022) 114:979–87. doi: 10.1093/jnci/djac057

17. Baratella E, Ruaro B, Marrocchio C, Starvaggi N, Salton F, Giudici F, et al. Interstitial lung disease at high resolution ct after sars-cov-2-related acute respiratory distress syndrome according to pulmonary segmental anatomy. *J Clin Med* (2021) 10:3985. doi: 10.3390/jcm10173985

18. Komaroff AL, Lipkin WI. Insights from myalgic encephalomyelitis/chronic fatigue syndrome may help unravel the pathogenesis of postacute COVID-19 syndrome. *Trends Mol Med* (2021) 27:895–906. doi: 10.1016/j.molmed.2021.06.002

19. Phetsouphanh C, Darley DR, Wilson DB, Howe A, Munier C, Patel SK, et al. Immunological dysfunction persists for 8 months following initial mild-to-moderate SARS-CoV-2 infection. *Nat Immunol* (2022) 23:210–6. doi: 10.1038/s41590-021-01113-x

20. Acosta-Ampudia Y, Monsalve DM, Rojas M, Rodríguez Y, Zapata E, Ramírez-Santana C, et al. Persistent autoimmune activation and proinflammatory state in post-coronavirus disease 2019 syndrome. *J Infect Dis* (2022) 225:2155–62. doi: 10.1093/infdis/jiac017

21. Beigel JH, Tomashek KM, Dodd LE, Mehta AK, Zingman BS, Kalil AC, et al. Remdesivir for the treatment of covid-19 - final report. *N Eng J Med* (2020) 383:1813–26. doi: 10.1056/NEJMoa2007764

22. Linn BS, Linn MW, Gurel L. Cumulative illness rating scale. *J Am Geriatr Soc* (1968) 16:622–6. doi: 10.1111/j.1532-5415.1968.tb02103.x

23. Sheehan DV, Lecrubier Y, Sheehan KH, Amorim P, Janavs J, Weiller E, et al. The mini-international neuropsychiatric interview (M.I.N.I.): the development and validation of a structured diagnostic psychiatric interview for DSM-IV and ICD-10. *Clin Psych* (1998) 59 S20:22–57.

24. Bellan M, Baricich A, Patrucco F, Zeppegno P, Gramaglia C, Balbo PE, et al. Long-term sequelae are highly prevalent one year after hospitalization for severe COVID-19. *Sci Rep* (2021) 11:22666. doi: 10.1038/s41598-021-01215-4

25. Xiong Q, Xu M, Li J, Liu Y, Zhang J, Xu Y, et al. Clinical sequelae of COVID-19 survivors in wuhan, China: a single-centre longitudinal study. *Clin Microbiol Infect* (2021) 27:89–95. doi: 10.1016/j.cmi.2020.09.023

26. Fumagalli C, Zocchi C, Tassetti L, Silverii MV, Amato C, Livi L, et al. Factors associated with persistence of symptoms 1 year after COVID-19: A longitudinal, prospective phone-based interview follow-up cohort study. *Eur J Int Med* (2022) 97:36–41. doi: 10.1016/j.ejim.2021.11.018

27. Lombardo M, Foppiani A, Peretti GM, Mangiavini L, Battezzati A, Bertoli S, et al. Long-term coronavirus disease 2019 complications in inpatients and outpatients: A one-year follow-up cohort study. *Open Forum Infect Dis* (2021) 8:ofab384. doi: 10.1093/ofid/ofab384

28. Bellan M, Patti G, Hayden E, Azzolina D, Pirisi M, Acquaviva A, et al. Fatality rate and predictors of mortality in an Italian cohort of hospitalized COVID-19 patients. *Sci Rep* (2020) 10:20731. doi: 10.1038/s41598-020-77698-4

29. Bechman K, Yates M, Mann K, Nagra D, Smith LJ, Rutherford AI, et al. Inpatient COVID-19 mortality has reduced over time: Results from an observational cohort. *PloS One* (2022) 17(1):e0261142. doi: 10.1371/journal.pone.0261142

30. Twohig KA, Nyberg T, Zaidi A, Thelwall S, Sinnathamby MA, Aliabadi S, et al. Hospital admission and emergency care attendance risk for SARS-CoV-2 delta (B.1.617.2) compared with alpha (B.1.1.7) variants of concern: a cohort study. *Lancet Infect Dis* (2022) 22:35–42. doi: 10.1016/S1473-3099(21)00475-8

31. Cortés-Telles A, López-Romero S, Figueroa-Hurtado E, Pou-Aguilar YN, Wong AW, Milne KM, et al. Pulmonary function and functional capacity in COVID-19 survivors with persistent dyspnoea. *Respir Physiol Neurobiol* (2021) 288:103644. doi: 10.1016/j.resp.2021.103644

32. Bai F, Tomasoni D, Falcinella C, Barbanotti D, Castoldi R, Mulè G, et al. Female gender is associated with long COVID syndrome: a prospective cohort study. *Clin Microbiol Infect* (2022) 28:611.e9–611.e16. doi: 10.1016/j.cmi.2021.11.002

33. Vimercati L, De Maria L, Quarato M, Caputi A, Gesualdo L, Migliore G, et al. Association between long COVID and Overweight/Obesity. *J Clin Med* (2021) 10:4143. doi: 10.3390/jcm10184143

34. Islam MS, Ferdous MZ, Islam US, Mosaddek A, Potenza MN, Pardhan S. Treatment, persistent symptoms, and depression in people infected with COVID-19 in Bangladesh. *Int J Environ Res Public Health* (2021) 18:1453. doi: 10.3390/ijerph18041453

35. Gramaglia C, Gambaro E, Bellan M, Balbo PE, Baricich A, Sainaghi PP, et al. Mid-term psychiatric outcomes of patients recovered from COVID-19 from an Italian cohort of hospitalized patients. *Front Psychiatry* (2021) 12:667385. doi: 10.3389/fpsyt.2021.667385

36. Gramaglia C, Gattoni E, Gambaro E, Bellan M, Balbo PE, Baricich A, et al. Anxiety, stress and depression in COVID-19 survivors from an Italian cohort of hospitalized patients: Results from a 1-year follow-up. *Front Psychiatry* (2022) 13:862651. doi: 10.3389/fpsyt.2022.862651

37. Hirschenberger M, Hunszinger V, Sparrer K. Implications of innate immunity in post-acute sequelae of non-persistent viral infections. *Cells* (2021) 10:2134. doi: 10.3390/cells10082134

38. Giannakodimos I, Gkountana GV, Lykouras D, Karkoulias K, Tsakas S. The role of interleukin-6 in the pathogenesis, prognosis and treatment of severe COVID-19. *Curr Med Chem* (2021) 28:5328–38. doi: 10.2174/0929867328666201209100259

39. Queiroz M, Neves P, Lima SS, Lopes J, Torres M, Vallinoto I, et al. Cytokine profiles associated with acute COVID-19 and long COVID-19 syndrome. *Front Cell Infect Microbiol* (2022) 12:922422. doi: 10.3389/fcimb.2022.922422

40. Schultheiß C, Willscher E, Paschold L, Gottschick C, Klee B, Henkes SS, et al. The IL-1β, IL-6, and TNF cytokine triad is associated with post-acute sequelae of COVID-19. *Cell Rep Med* (2022) 3:100663. doi: 10.1016/j.xcrm.2022.100663

41. Tait Wojno ED, Hunter CA, Stumhofer JS. The immunobiology of the interleukin-12 family: Room for discovery. *Immunity* (2019) 50:851–70. doi: 10.1016/j.immuni.2019.03.011

42. Nguyen B, Tosti A. Alopecia in patients with COVID-19: A systematic review and meta-analysis. *JAAD Int* (2022) 7:67–77. doi: 10.1016/j.jdin.2022.02.006

43. Waśkiel-Burnat A, Osińska M, Salińska A, Blicharz L, Goldust M, Olszewska M, et al. The role of serum Th1, Th2, and Th17 cytokines in patients with alopecia areata: Clinical implications. *Cells* (2021) 10:3397. doi: 10.3390/cells10123397

44. Ibrahim O, Bayart CB, Hogan S, Piliang M, Bergfeld WF. Treatment of alopecia areata with tofacitinib. *JAMA Dermatol* (2017) 153:600–2. doi: 10.1001/jamadermatol.2017.0001

45. Aşkın Ö, Yücesoy SN, Coşkun E, Engin B, Serdaroğlu S. Evaluation of the level of serum interleukins (IL-2, IL-4, IL-15 andIL-17) and its relationship with disease severity in patients with alopecia areata. *Bras Dermatol* (2021) 96:551–7. doi: 10.1016/j.abd.2021.03.006

frontiers | Frontiers in Immunology

TYPE Original Research
PUBLISHED 09 January 2023
DOI 10.3389/fimmu.2022.1052104

Check for updates

OPEN ACCESS

EDITED BY
Martijn van Griensven,
Maastricht University, Netherlands

REVIEWED BY
Marzena Lenart,
Jagiellonian University, Poland
Annalisa Chiocchetti,
Università del Piemonte Orientale, Italy

*CORRESPONDENCE
Kenneth J. Gollob
kjgollob.einstein@gmail.com
Marjorie V. Batista
marjorie.batista@accamargo.org.br

SPECIALTY SECTION
This article was submitted to Viral Immunology, a section of the journal Frontiers in Immunology

RECEIVED 23 September 2022
ACCEPTED 20 December 2022
PUBLISHED 09 January 2023

CITATION
Pignataro-Oshiro F, Figueiredo AB, Galdino NAL, Morais KLP, Dutra WO, Silva BGdM, Feriani D, Abrantes FdA, Silva ILAFe, Filho JS, Framil JVdS, Cesca MG, Riechelmann RSP, Batista MV and Gollob KJ (2023) Distinct systemic immune networks define severe *vs*. mild COVID-19 in hematologic and solid cancer patients. *Front. Immunol.* 13:1052104. doi: 10.3389/fimmu.2022.1052104

COPYRIGHT
© 2023 Pignataro-Oshiro, Figueiredo, Galdino, Morais, Dutra, Silva, Feriani, Abrantes, Silva, Filho, Framil, Cesca, Riechelmann, Batista and Gollob. This is an open-access article distributed under the terms of the Creative Commons Attribution License (CC BY). The use, distribution or reproduction in other forums is permitted, provided the original author(s) and the copyright owner(s) are credited and that the original publication in this journal is cited, in accordance with accepted academic practice. No use, distribution or reproduction is permitted which does not comply with these terms.

Distinct systemic immune networks define severe *vs*. mild COVID-19 in hematologic and solid cancer patients

Flávio Pignataro-Oshiro[1], Amanda B. Figueiredo[1], Nayane A. L. Galdino[1], Katia L. P. Morais[1], Walderez O. Dutra[2], Bianca Grassi de Miranda Silva[3], Diego Feriani[3], Flávia de Azevedo Abrantes[3], Ivan Leonardo Avelino França e Silva[3], Jayr Schmidt Filho[4], Juliana Valéria de Souza Framil[3], Marcelle Goldner Cesca[5], Rachel Simões Pimenta Riechelmann[5], Marjorie V. Batista[3*] and Kenneth J. Gollob[1,6*]

[1]International Research Center, Translational Immuno-oncology Group, A.C.Camargo Cancer Center, São Paulo, Brazil, [2]Department of Morphology, Federal University of Minas Gerais, Belo Horizonte, Brazil, [3]Infectious Diseases Department, A.C.Camargo Cancer Center, Sao Paulo, Brazil, [4]Hematology Department, A.C.Camargo Cancer Center, Sao Paulo, Brazil, [5]Clinical Oncology Department, A.C.Camargo Cancer Center, Sao Paulo, Brazil, [6]Hospital Israelita Albert Einstein, Israelite Institute for Education and Research, Translational Immuno-oncology Laboratory, São Paulo, Brazil

Introduction: The COVID-19 pandemic, caused by the coronavirus SARS-CoV-2, has impacted health across all sectors of society. A cytokine-release syndrome, combined with an inefficient response of innate immune cells to directly combat the virus, characterizes the severe form of COVID-19. While immune factors involved in the development of severe COVID-19 in the general population are becoming clearer, identification of the immune mechanisms behind severe disease in oncologic patients remains uncertain.

Methods: Here we evaluated the systemic immune response through the analysis of soluble blood immune factors and anti-SARS-CoV-2 antibodies within the early days of a positive SARS-CoV-2 diagnostic in oncologic patients.

Results: Individuals with hematologic malignancies that went on to die from COVID-19 displayed at diagnosis severe leukopenia, low antibody production against SARS-CoV-2 proteins, and elevated production of innate immune cell recruitment and activation factors. These patients also displayed correlation networks in which IL-2, IL-13, TNF-alpha, IFN-gamma, and FGF2 were the focal points. Hematologic cancer patients that showed highly networked and coordinated anti-SARS-CoV-2 antibody production, with central importance of IL-4, IL-5, IL-12A, IL-15, and IL-17A, presented only mild COVID-19. Conversely, solid tumor patients that had elevated levels of inflammatory

cytokines IL-6, CXCL8, and lost the coordinate production of anti-virus antibodies developed severe COVID-19 and died. Patients that displayed positive correlation networks between anti-virus antibodies, and a regulatory axis involving IL-10 and inflammatory cytokines recovered from the disease. We also provided evidence that CXCL8 is a strong predictor of death for oncologic patients and could be an indicator of poor prognosis within days of the positive diagnostic of SARS-CoV-2 infection.

Conclusion: Our findings defined distinct systemic immune profiles associated with COVID-19 clinical outcome of patients with cancer and COVID-19. These systemic immune networks shed light on potential immune mechanisms involved in disease outcome, as well as identify potential clinically useful biomarkers.

KEYWORDS

SARS-CoV-2, COVID-19, cancer, systemic immune profile, disease severity prediction, cytokine-release syndrome

Introduction

Coronavirus Disease 2019 (COVID-19) is an illness caused by Severe Acute Respiratory Syndrome Coronavirus-2 (SARS-CoV-2), identified following an outbreak of unknown pneumonia cases during 2019. The etiological agent was classified as a betacoronavirus closely related to Severe Respiratory Syndrome Coronavirus (SARS-CoV) and Middle East Respiratory Syndrome Coronavirus (MERS-CoV), associated with outbreaks in 2002 and 2012, respectively (1).

Patients infected by SARS-CoV-2 primarily present with fever, cough, shortness of breath, dyspnea, lung infiltration and possibly respiratory failure, depending on the disease severity (1). The symptoms are partially explained by the virus' biology, which leads to infection of cells *via* proteases and angiotensin-converting enzyme 2 (ACE2), present in respiratory tract tissues (1). The acute respiratory distress syndrome observed in COVID-19 is believed to be due to a cytokine-release syndrome, lack of immune regulation, and may be associated with multiple-organ failure (2).

Typically about 80% of the cases are classified as mild, 15% as severe and 5% as critical (1). Nevertheless, data from May 2020 reported that about 90% of the registered cases in Brazil resulted in hospitalization, of which 30% were admitted to intensive care units (ICU) (3). Later on, in 2021, 99% of the cases reported in the Brazilian Healthcare System database (DATASUS) had resulted in hospitalization, of which 36% needed ICU admissions, culminating in a rate of death approximately 37% (4). By October 2022, Brazil had more than 34 million confirmed cases, and almost 688,000 deaths, reaching a lethality of 2% (5). It is important to take into consideration that that Brazil is a country with a unique healthcare system, an expressive prevalence of comorbidities among its population, and that its national vaccination campaign had a very good coverage once implemented, explaining in parts both the high rates of hospitalization and ICU admissions in 2020 and 2021, and the progressively lower infection and lethality rates by 2022 (4, 6).

In general, male individuals aged 60 or above, with chronic cardiovascular or respiratory conditions, hypertension, obesity or diabetes have increased risk of severe disease and death (1, 2). Individuals with cancer specifically present lower survival rates (7, 8) with case-fatality percentages ranging from 11% to 26% (9), and higher chances of hospitalization and death compared to those from the general population (10). In patients with cancer the risk of developing severe COVID-19 is associated with hematologic malignancies, non-white race, age 65 or above, chronic lymphopenia, use of corticosteroid combined with immune checkpoint inhibitors therapy, former or current smoker status, hypertension, and chronic kidney, cardiac or lung disorders (9, 10). Within the hematological malignancies, acute myeloid leukemia, aggressive non-Hodgkin lymphoma, multiple myeloma and plasma cell malignancies were associated with a greater risk of hospitalization and death (10). Similarly, some solid tumor patients also showed higher risk of severe COVID-19 than the general population (8, 11, 12). In Brazil, a study demonstrated that an increased chance of death in cancer patients was associated with lung and hematological tumors (13).

Oncologic patients, and in particular those with hematologic malignancies, often display immunosuppression as a

10.3389/fimmu.2022.1052104

consequence of cancer progression or of therapeutic interventions (14). We hypothesize that specific systemic immune response profiles in cancer patients may be related to distinct COVID-19 clinical outcomes and that these profiles could potentially be used to predict COVID-19 progression. Thus, we investigated systemic soluble factor immunoregulatory networks in oncologic COVID-19 patients with differential clinical outcomes. We identified specific immune mediators and networks associated with hematologic malignancy patients that maintained mild COVID-19 *vs.* those that develop severe disease and death. These findings advance our understanding of immune imbalances related to severe COVID-19 in oncologic patients and point towards potentially clinically useful immune markers of severity in oncological patients.

Results

Hematologic or solid tumor cancer patients display distinct outcomes of COVID-19

We separated the oncological patient cohorts into hematologic cancers (n = 21) and solid tumors (n = 22) based on previous studies demonstrating distinct clinical outcomes in cancer patients with COVID-19 (8, 11, 12). We further segregated COVID-19 disease severity in Mild, Severe-Recovered, and Severe-Death depending on the use of supplemental oxygen therapy, based on recommendations by the World Health Organization (Figure 1A). A summary of patient characteristics,

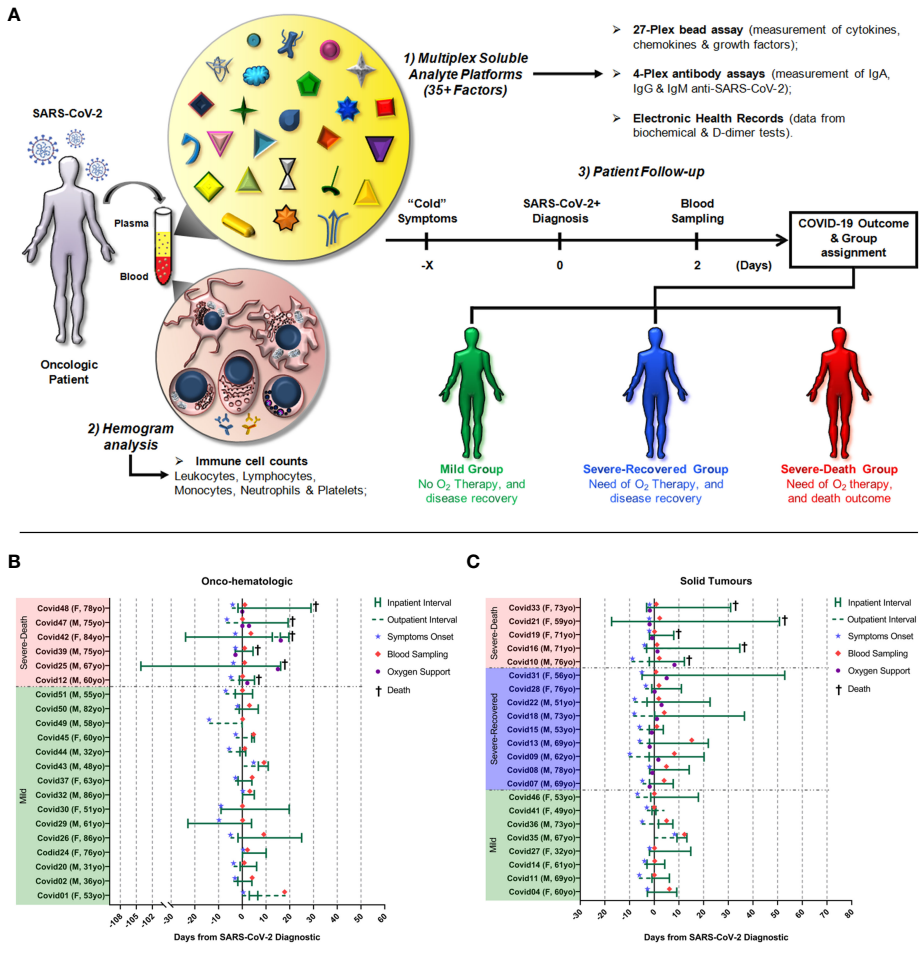

FIGURE 1
Experimental design, cohort clinical characteristics and timeframe of sampling utilized in the study. The first illustration **(A)** represents the experimental design of this study. Briefly, oncologic patients from A.C.Camargo Cancer Center that had a positive diagnostic of SARS-CoV-2 infection were invited to participate in the study. Blood samples were drawn at a median of two days after the confirmed diagnostic and analyzed for the concentrations of soluble factors and cell counts. Then each patient was followed-up and assigned to a group based on the need of supplemental O_2 therapy and outcome of COVID-19. Below, the illustration represents the timeframe of hospitalization, symptoms onset, blood sampling and clinical complications (need of oxygen supplementation and death) observed in hematologic cancer **(B)** or solid tumor **(C)** patients. Time zero was defined as the day of the positive SARS-CoV-2 qPCR positive diagnostic.

including the timeframe of hospitalization, onset of symptoms, blood sampling and clinical complications observed during COVID-19 is shown (Figures 1B, C). Individuals with hematologic malignancies displayed a distinct COVID-19 evolution as compared to patients with solid tumors, showing either mild disease or severe disease with progression to death, whereas 41% of the patients with solid tumors developed severe COVID-19 but recovered. Further epidemiological information, such as age and sex distribution, tumor type, treatments, Eastern Cooperative Oncologic Group (ECOG) performance status score and cancer status is presented in Table 1 and Supplementary Figure 1.

Patients with hematologic malignancies that presented leukopenia, lower anti-SARS-CoV-2 antibody production, and higher expression of inflammatory factors went on to die from COVID-19

To address the potential impact of hematological alterations on COVID-19 progression and outcome, we first evaluated biochemical and hematological parameters assessed at the time of the SARS-CoV-2 infection diagnosis (Figure 2). Patients with hematologic malignancies that presented with leukopenia, which reflected a decrease in lymphocytes and monocytes (Figure 2A), went on to die from COVID-19 (Severe-Death group). In addition, hematocrit and hemoglobin values were also lower in Severe-Death hematologic patients, as compared to Mild (Figure 2B), while neutrophil and platelet numbers did not differ between groups (not shown). Conversely, biochemical analysis showed augmented levels of CRP and D-dimer in the Severe-Death hematologic cancer patients as compared to the Mild group (Figure 2C), whereas none of the hematological or biochemical parameters differed between solid tumor patients with distinct clinical outcomes (Figures 2A–C).

Next, we aimed to better understand the mechanisms related to disease evolution and clinical outcome. To do so we evaluated circulating soluble mediators in plasma sampled within a median of two days of SARS-CoV-2 positive diagnostic (Figure 3).

Within the hematologic cancer patient cohort there was a striking increase in the levels of the chemokines CCL2, CCL3, CCL4, CXCL8, and the cytokine IL-1β, in the Severe-Death group compared to the Mild group (Figure 3A). Levels of VEGFA and most of the cytokines measured (IL-2, IL-5, IL-6, IL-10, IL-13, IL-15, IL-17A and IL-1RN) were also increased or showed similar trends in Severe-Death hematologic patients as compared to Mild, with no differences in FGF2, PDGFB, and TNFα concentrations (Figures 3B, C). No difference was observed for CCL5, CCL11, Colony Stimulating Factor 2 (CSF2), Colony Stimulating Factor 3 (CSF3), IFN-γ, IL-7, IL-9, as well as IL-12A or IL-4, critical for T_H1 and T_H2 subset polarization, respectively (Supplementary Figure 2).

Conversely, patients with solid tumors had fewer changes in the levels of soluble factors than that observed in the hematologic group (Figure 3), displaying higher concentrations of CXCL8 among patients that went to die compared to those who recovered (Figure 3A). The concentration of IL-6 was increased in patients with severe disease that progressed to death as compared to Mild, while a similar trend was observed for CCL3, CXCL8, FGF2, and TNFα (Figures 3A–C). The growth factor PDGFB presented a trend toward a decrease in concentration comparing patients with mild disease and those who would die from COVID-19 (Figure 3B). In addition, IL-15 showed a trend to increase in patients that had severe disease and recovered, as compared to those in the Mild group (Figure 3C).

Lastly, we determined the levels of IgA, IgG and IgM antibodies against SARS-CoV-2 nucleocapsid, spike proteins (spike 1 and spike 2), and receptor binding domain (RBD) in patients with different tumors and COVID-19 outcomes (Figure 4). Interestingly, we observed an overall decrease in levels of IgM and IgG anti-SARS-CoV-2 proteins in the hematologic cancer patients that would die from COVID-19 (Figures 4B, C), while no changes were observed in IgA levels (Figure 4A). We also observed a dramatic decrease in IgM anti-nucleocapsid comparing individuals who progressed to death with those who cured among the solid tumor patients (Figure 4C). An overview of the mean antibody production is represented with radar charts for both hematologic malignancies patients (Figure 4D) and solid tumors patients (Figure 4E), showing a similar pattern of antibody synthesis from different immunoglobulin classes.

Unsupervised cluster and network analysis identifies immunological parameters that segregate death from other clinical outcomes in patients with hematologic tumors

To identify combinations of factors that segregate among distinct COVID-19 clinical outcomes we performed an unsupervised cluster analysis within each cancer group, considering only factors with a p-value of 0.1 or below. Hematologic cancer patients segregated based on a major cluster of high production of immune mediators in the Severe-Death group, together with lower levels of IgG and IgM anti-SARS-CoV-2 proteins and lower counts of leukocyte subpopulations (Figure 5A). The solid tumor groups separated the Severe-Death patients in one branch characterized by higher production of soluble immune factors and lower production of IgM. This branch also contained patients with other outcomes, whereas the remainder of patients that had mild COVID-19 or recovered from the disease grouped in secondary branches (Figure 5B). Categorical patient data, such as chemotherapy one month prior to COVID-19 diagnostic, presence of leukopenia,

10.3389/fimmu.2022.1052104

TABLE 1 Clinical and demographic characteristics of COVID-19 hematologic cancer and solid tumor patients.

	Onco-hematologic (n = 21)		Solid Tumor (n = 22)		
	Mild (n = 15)	Severe-Death (n = 6)	Mild (n = 8)	Severe-Recovered (n = 9)	Severe-Death (n = 5)
Age					
Median	58	75	60.5	69	71
Range	31-86	60-84	32-73	51-78	59-76
p-value (median)*	p = 0.0990		p = 0.1459		
p-value (Fisher)#	**p = 0.0456**		p = 0.9999		
Sex					
Female	6 (40%)	2 (33%)	5 (63%)	2 (22%)	3 (60%)
Male	9 (60%)	4 (67%)	3 (37%)	7 (78%)	2 (40%)
p-value (Fisher)#	p = 0.9999		p = 0.6241		
ECOG Score					
Zero	12 (80%)	3 (50%)	6 (75%)	6 (67%)	2 (40%)
I-II	3 (20%)	2 (33%)	2 (25%)	3 (33%)	2 (40%)
III-IV	0 (0%)	1 (17%)	0 (0%)	0 (0%)	1 (20%)
p-value (Fisher)$	p = 0.2857		p = 0.2273		
Hematological Malignancy					
Lymphoma	9 (60%)	2 (33%)	NA	NA	NA
Leukemia	2 (13%)	1 (17%)	NA	NA	NA
Myeloma	2 (13%)	3 (50%)	NA	NA	NA
Other hematological	2 (12%)	0 (0%)	NA	NA	NA
Solid Tumor					
Breast	NA	NA	3 (38%)	0 (0%)	0 (0%)
Digestive Organs	NA	NA	2 (25%)	1 (11%)	3 (60%)
Prostate	NA	NA	2 (25%)	1 (22%)	0 (0%)
Urinary Tract	NA	NA	0 (0%)	2 (22%)	2 (40%)
Lungs	NA	NA	0 (0%)	2 (22%)	0 (0%)
Reproductive System	NA	NA	0 (0%)	1 (11%)	0 (0%)
Other	NA	NA	1 (12%)	2 (22%)	0 (0%)
Comorbidities					
Diabetes	3 (20%)	2 (33%)	2 (25%)	2 (22%)	2 (40%)
Obesity	1 (7%)	1 (17%)	2 (25%)	2 (22%)	0 (0%)
Cardiac Disease	6 (40%)	6 (100%)	4 (50%)	7 (78%)	2 (40%)
Neurologic Disease	0 (0%)	1 (17%)	0 (0%)	0 (0%)	1 (20%)
Pulmonary Disease	1 (7%)	0 (0%)	1 (12%)	3 (33%)	0 (0%)
Renal Disease	0 (0%)	0 (0%)	0 (0%)	2 (22%)	0 (0%)
Smoker (Current)	1 (7%)	0 (0%)	1 (12%)	1 (11%)	0 (0%)

(Continued)

10.3389/fimmu.2022.1052104

TABLE 1 Continued

	Onco-hematologic (n = 21)		Solid Tumor (n = 22)		
	Mild (n = 15)	Severe-Death (n = 6)	Mild (n = 8)	Severe-Recovered (n = 9)	Severe-Death (n = 5)
Smoker (Former)	2 (13%)	2 (33%)	3 (38%)	2 (22%)	1 (20%)
Former Infection[&]	2 (13%)	2 (33%)	0 (0%)	3 (33%)	0 (0%)
Treatment (Cancer)					
Cell Transplant	3 (20%)	3 (50%)	0 (0%)	0 (0%)	0 (0%)
Chemotherapy	12 (80%)	5 (83%)	5 (63%)	7 (78%)	4 (80%)
Immuno (Anti-CD20)	1 (7%)	1 (17%)	0 (0%)	0 (0%)	0 (0%)
Immuno (Anti-CD38)	1 (7%)	2 (33%)	0 (0%)	0 (0%)	0 (0%)
Immuno (PD-1 Axis)	1 (7%)	0 (0%)	0 (0%)	0 (0%)	1 (20%)
Radiotherapy	2 (13%)	0 (0%)	2 (25%)	5 (56%)	2 (40%)
Surgery	4 (27%)	0 (0%)	5 (63%)	5 (56%)	4 (80%)
Targeted Therapy	0 (0%)	0 (0%)	1 (12%)	2 (22%)	0 (0%)
Cancer Status					
Under Investigation	5 (33%)	2 (33%)	1 (12%)	0 (0%)	1 (20%)
Stable Disease	5 (33%)	1 (17%)	4 (50%)	8 (89%)	3 (60%)
Remission	4 (27%)	1 (17%)	0 (0%)	0 (0%)	1 (20%)
Progression	1 (7%)	2 (33%)	3 (38%)	1 (11%)	0 (0%)

*Considering alive vs. deceased patients (Mann-Whitney test).
[#]Considering alive vs. deceased patients to verify if death outcome is influenced by age (Fisher's exact test).
[$]Considering alive vs. deceased patients, comparing individuals with ECOG scores 0-2 vs. 3-4 (Fisher's exact test).
[&]Refers to pulmonary infections or chronic infections of the urinary system.
Bold values indicate $p<0.05$.

gender, ECOG score, or tumor grade, did not cluster together with disease outcome. A similar segregation of groups was seen using all the factors analyzed in this project (Supplementary Figure 3).

To further investigate immunoregulatory mechanisms involved in the response against SARS-CoV-2 and differential clinical outcomes, we generated correlation matrices and functional networks between the soluble immune mediators, anti-SARS-CoV-2 antibodies, leukocyte counts and biochemical indicators.

In patients with hematologic malignancies, we observed striking positive correlations regarding antibody responses in Mild patients, as well as a co-regulation of immunoregulatory cytokines, many of which were missing in those who progressed to death (Figures 6A, B). Additionally, we identified a negative correlation between the immunoregulatory cytokine IL-10 and general IgM antibody responses in patients with mild disease, which was not observed in those who progressed to death (Figure 6A). In the Mild group, network analysis also showed several hierarchical interactions, with IL-4, IL-5, IL-12A, IL-15, and IL-17A as major nodes interacting with many immune mediators (Figure 6A). The cytokine IL-15 showed positive correlations with 13 immune factors, including IL-2, IL-12A, IFN-γ, and anti-SARS-CoV-2 nucleocapsid and spike 2 IgG, classic markers of a T_H1 type immune response (Figure 6A; Supplementary Figure 4A). The anti-inflammatory cytokine IL-10 increased with increasing levels of IL-5 and D-dimer, indicating a potential coregulation of inflammatory responses. IL-10 also correlated negatively with several IgA and IgM anti-SARS-CoV-2 antibodies. In Severe-Death patients, we observed a bigger impact for interactions formed by the inflammatory cytokines TNF-alpha and IL-2, which had positive correlations with anti-SARS-CoV-2 IgG antibodies, IL-1RN, IL-4, IL-10 and FGF2 (Figure 6B). Further positive interactions were formed between the inflammatory cytokines IL-6, IL-15 and IFN-γ with different chemokines and IL-13, of which the majority had elevated concentrations in the Severe-Death as compared to the Mild group (indicated by red stars). Lastly, interactions between antibodies decreased among Severe-Death patients in comparison with Mild patients, whereas overall Spearman's rho values increased with disease severity, highlighting the

10.3389/fimmu.2022.1052104

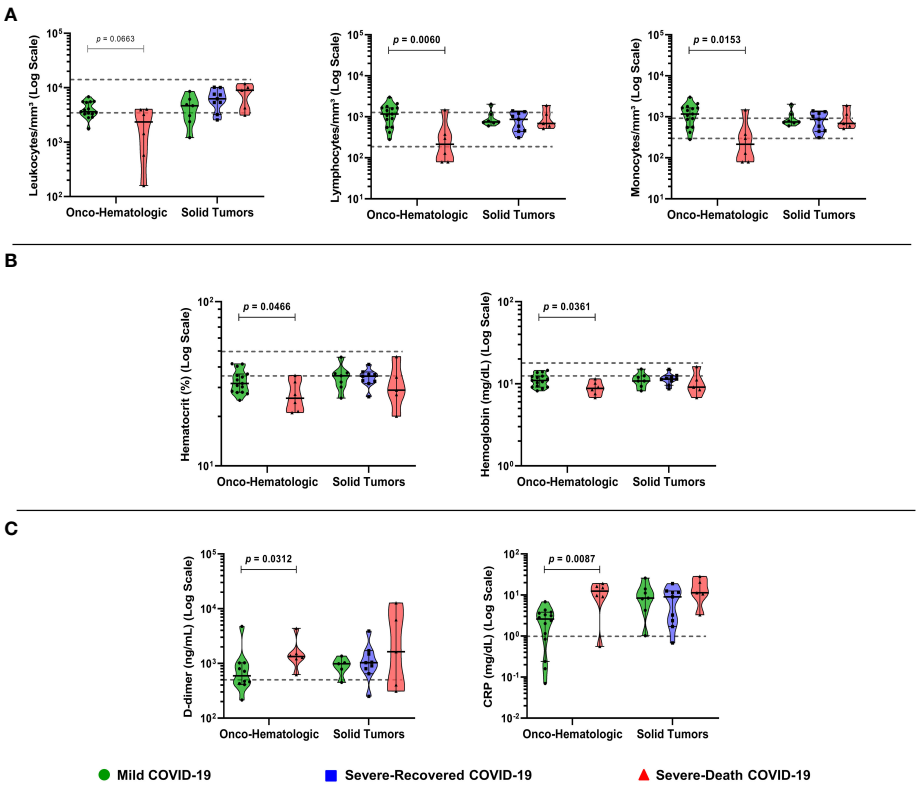

FIGURE 2
Biochemical and hematological analysis of plasma reveals that low numbers of leukocyte subpopulations are associated with death in patients with hematologic malignancies. Blood samples were collected within two days (median; 1 – 4 CI) of the positive SARS-CoV-2 diagnosis, while hemogram and biochemical exams data were gathered from electronic health records. The graphs depicts leucocytes and subpopulations **(A)**, hematologic parameters **(B)**, and biochemical parameters **(C)**. Groups were defined based on disease severity, as Mild (green), Severe-Recovered (blue), or Severe-Death (red), as described. Gray dashed lines indicate the reference value ranges for each exam. Data is presented as median plus 95% confidence intervals and was analyzed with Kruskal-Wallis adjusted for multiple comparisons followed by Dunn's *post-hoc* test or Mann-Whitney test. All exact *p*-values below 0.1 are shown. CRP, C-Reactive Protein; N = 21 for Onco-hematologic and N = 22 for Solid tumors group.

exacerbated immune response (Figures 6A, B; Supplementary Figure 4A). Overall, these findings point to a broad and regulated immune response among hematologic patients who developed mild COVID-19, whereas patients that showed early signs of cytokine-release syndrome, lack of humoral responses and poor immunoregulatory networks progressed to death.

On the other hand, the networks from solid tumor patients were distinct from those seen in patients with hematologic malignancies, highlighting different immune mechanisms behind COVID-19 progression and outcome (Figures 6 and 7). Correlation matrices indicate that patients who progressed to mild or recovered from severe COVID-19 presented several positive correlations among the immunological parameters analyzed, which were virtually lost in Severe-Death patients (Figure 7). One of those was the striking positive correlations regarding antibody responses in Mild and Severe-Recovered patients, which were not observed in Severe-Death group (Figure 7). Interestingly, a cluster of positively correlated inflammatory cytokines (IL-1β, IL-2, IFN-γ and FGF2) was present in Severe-Death patients and missing from mild and Severe-Recovered patients (Figure 7).

Mild solid tumors patients showed a complex network characterized by positive correlations between anti-SARS-CoV-2 antibodies, with IgG and IgA correlating strongly with IL-7, IL-9, IL-4 and platelet counts. In addition, they showed positive networks between anti-inflammatory factors (IL-1RN) and inflammatory factors (IFN-γ, IL-17A, CCL3, and IL-6), suggesting a coregulation of the inflammatory response (Figure 7A). Moreover, among Severe-Recovered patients, IL-4, IL-12A, IL-15 and IL-17A formed strong positively correlated interactions with one another. IL-4 correlated with other T_H2 factors, such as CCL11 and IL-9, whereas FGF2 also correlated with T_H1 factors, such as IL-15, IL-12A, and IL-7 (Figure 7B). Furthermore, Severe-Recovered patients presented positive correlations specifically between IL-10, IL-17A and TNF, indicating an important regulatory axis. Overall, these findings

10.3389/fimmu.2022.1052104

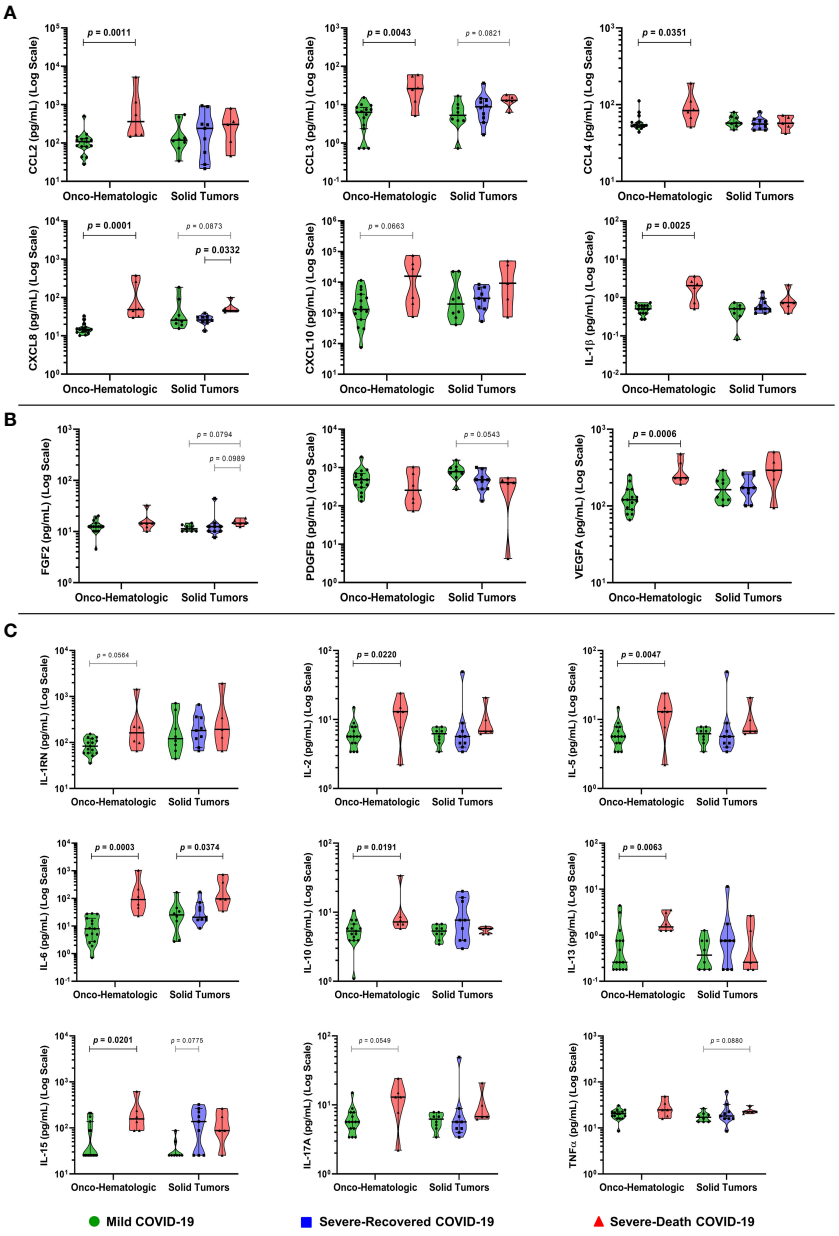

FIGURE 3
Patients with hematologic malignancies and COVID-19 that display an exacerbated soluble immune profile develop severe disease culminating in death. Blood samples were collected within two days (median; 1 – 4 CI) of the positive SARS-CoV-2 diagnostic and analyzed for 27 immune mediators, being them recruitment factors **(A)**, growth factors **(B)**, and cytokines **(C)**. Groups were defined based on disease severity, as Mild (green), Severe-Recovered (blue), or Severe-Death (red), as described. Data is presented as median plus 95% confidence intervals and was analyzed with Kruskal-Wallis adjusted for multiple comparisons followed by Dunn's *post-hoc* test or Mann-Whitney test. All exact *p*-values below 0.1 are shown. IL-1RN, Interleukin 1 Receptor Antagonist. N = 21 for Onco-hematologic and N = 22 for Solid Tumors group.

point to an active complex immunoregulatory network indicative of a balanced type I immune response in solid tumors patients that had mild COVID-19, whereas patients that recovered from severe disease presented an immune profile indicative of mixed type I and type II responses (Figures 7A, B).

In stark contrast, solid tumor patients that went on to die showed fewer interactions (Figure 7C and Supplementary Figure 4B), characterized by a node composed of CXCL8, D-dimer and monocytes, as well as an IL-15 axis characterized by both strong positive and negative correlations. Most interactions between IgG, IgM or IgA antibodies were lost in comparison

10.3389/fimmu.2022.1052104

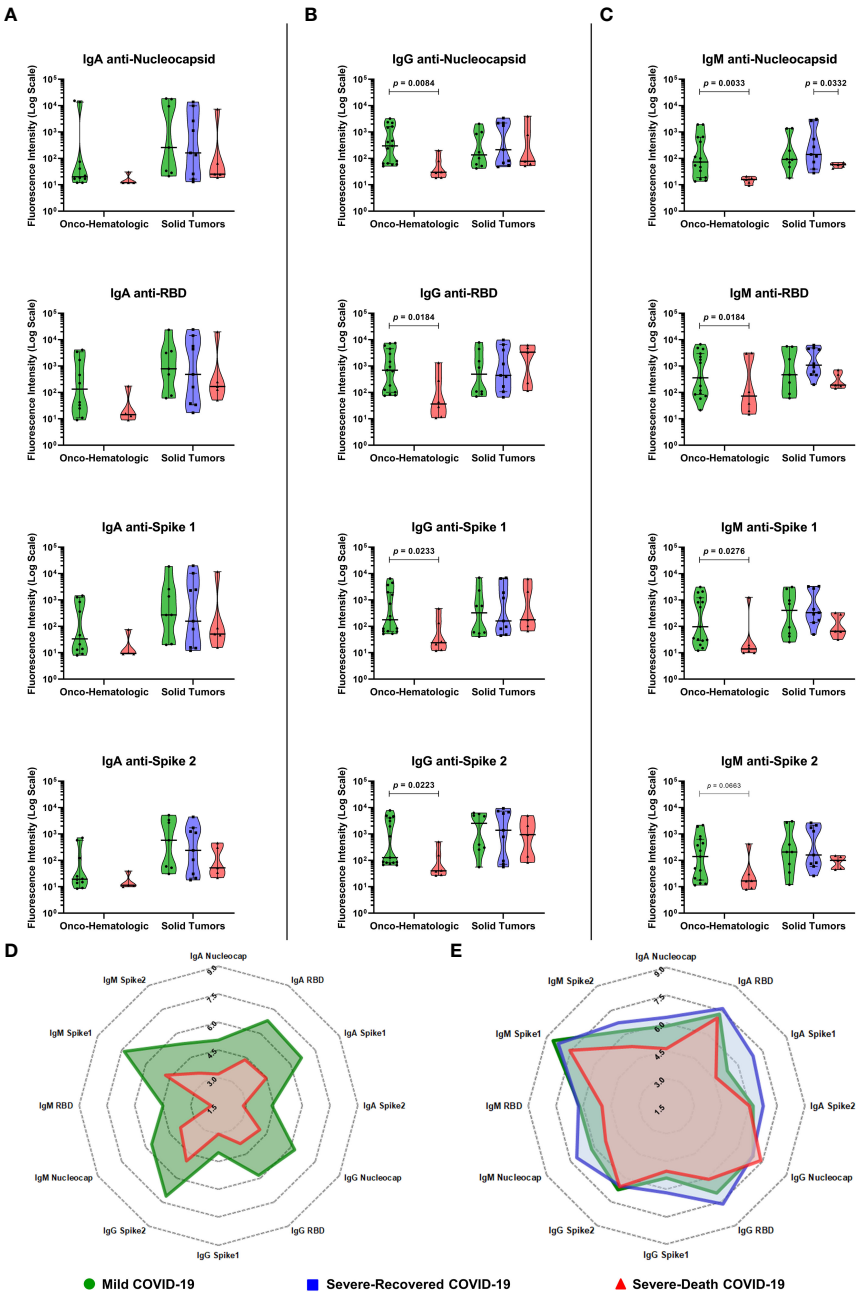

FIGURE 4
COVID-19 positive patients with hematologic malignancies that develop severe disease culminating in death display decreased IgG anti-SARS-CoV-2 antibodies before disease progression. Blood samples were collected within two days (median; 1 – 4 CI) of the positive SARS-CoV-2 diagnostic and analyzed for Immunoglobulins IgA **(A)**, IgG **(B)** and IgM **(C)** anti-SARS-CoV-2 proteins as described in Materials and Methods. Radar charts for Onco-hematologic **(D)** or Solid Tumors **(E)** patients show the mean values for each factor after fluorescence intensity data was normalized by Ln(x+1). Groups were defined based on disease severity, as Mild (green), Severe-Recovered (blue), or Severe-Death (red), as described. Data is presented as median plus 95% confidence intervals and was analyzed with Kruskal-Wallis adjusted for multiple comparisons followed by Dunn's *post-hoc* test or Mann-Whitney test. All exact *p*-values below 0.1 are shown. Nucleocapsid, RBD, Spike 1 and Spike 2 labels refers to IgG antibodies anti-SARS-CoV-2 proteins. RBD, Receptor Binding Domain. N = 21 for Onco-hematologic and N = 22 for Solid Tumors group (IgG and IgM measurements) and N = 14 for Onco-hematologic and N = 21 for Solid Tumors group (IgA measurements).

with solid tumor patients that progressed to better outcomes. Moreover, almost all interactions between IgA and IgM anti-SARS-CoV-2 proteins and other factors were negative, suggesting that increased immune activity was detrimental to antibody production in those patients (Figure 7). Lastly, the overall strength of the correlations between factors within the Severe-Death group was stronger than that in the Mild and Severe-Recovered groups (Supplementary Figure 4B).

10.3389/fimmu.2022.1052104

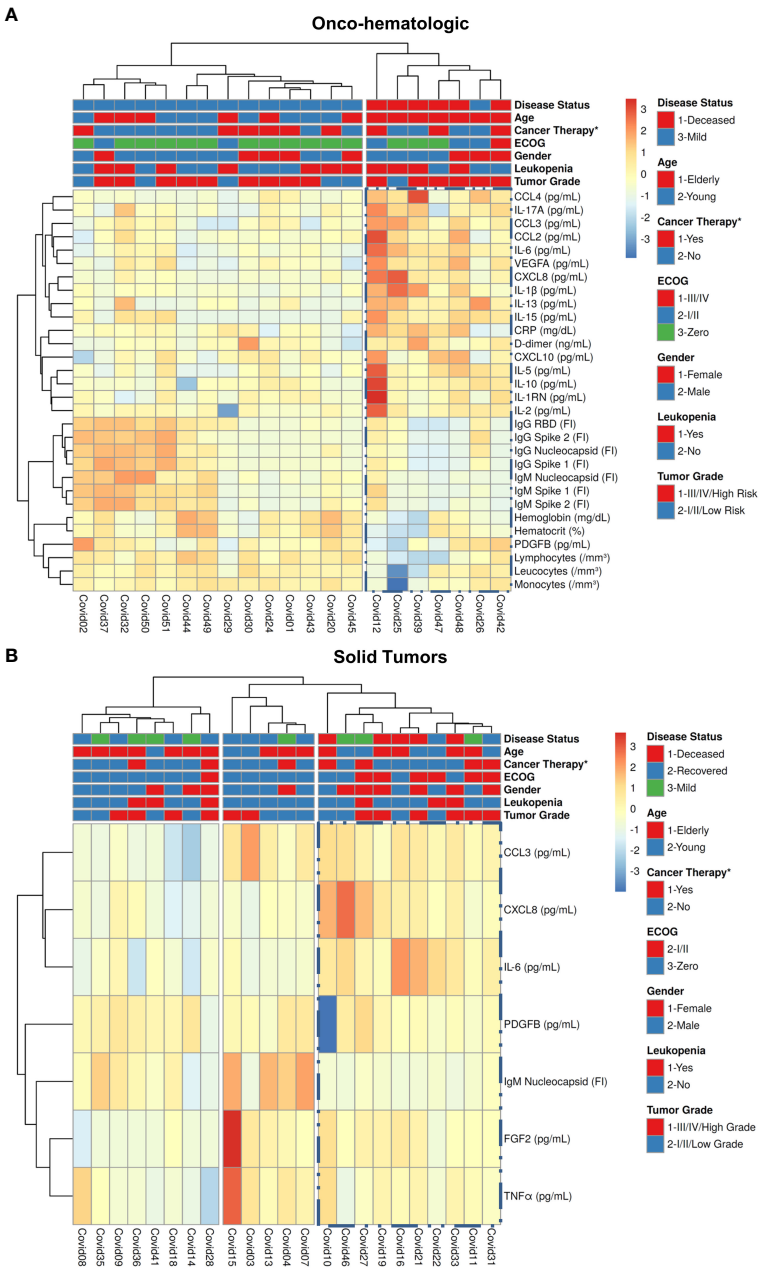

FIGURE 5
High levels of immune mediators, low IgG anti-SARS-CoV-2, and low leukocyte subpopulations segregate Severe-Death patients with hematologic malignancies from those with Mild disease outcomes. Blood samples were collected within two days (median; 1 – 4 CI) of the positive SARS-CoV-2 diagnostic and analyzed for 27 immune mediators and for immunoglobulins anti-SARS-CoV-2 proteins, as described in Materials and Methods. Groups of hematologic cancer patients **(A)** and solid tumors patients **(B)** were defined based on disease severity as described. All data was normalized by natural logarithm + 1 [ln(x +1)] before running an unsupervised cluster analysis and generation of the heatmap using ClustVis platform as described in Materials and Methods. In **(A)** both rows and columns were clustered by Manhattan distance and Complete linkage. In **(B)** both rows and columns were clustered by Euclidean distance and Ward linkage. Nucleocapsid, RBD, Spike 1 and Spike 2 labels refers to antibodies anti-SARS-CoV-2 proteins. CRP, C-Reactive Protein; RBD, Receptor Binding Domain. *Refers to active cancer therapy one month prior to COVID-19 diagnosis.

10.3389/fimmu.2022.1052104

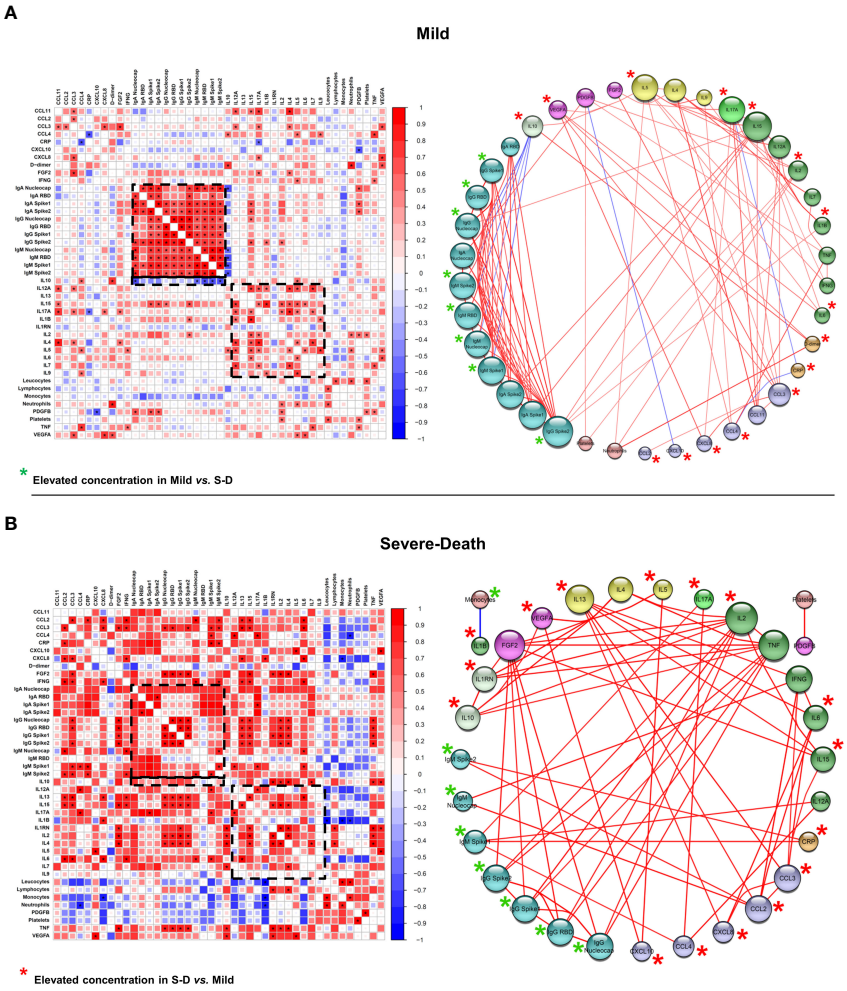

FIGURE 6
Correlation networks suggest that immune hyperactivation and an impaired antibody response are correlated with death outcome in patients with hematologic malignancies. Data from electronic health records, 27-Plex assay and anti-SARS-CoV-2 proteins' antibodies assays was used to construct a Spearman's correlation matrix with all statistically significant ($p < 0.05$, highlighted as *) Spearman's Rho values, ranging from -1 to 1. The matrix was then used to construct the correlation networks. Red lines connecting the spheres represent positive correlations, whereas line thickness and hotter colors represent correlations with Rho closer to 1. Blue lines connecting the spheres represent negative correlations, whereas line thickness and colder colors represent correlations with Rho closer to -1. Spheres' sizes correlate with the number of interactions for each factor, whereas the bigger radius represents factors with more interactions. Spheres' colors represent factors that have similar activities, characteristics or functions. Disease groups were defined as Mild (**A**; n = 15) and Severe-Death (**B**; n = 6), as described. Nucleocapsid, RBD, Spike 1 and Spike 2 labels refers to antibodies anti-SARS-CoV-2 proteins. Monocytes, Neutrophils and Platelets refers to blood counts per mm^3 of blood. CRP, C-Reactive Protein; FGF2, Fibroblast Growth Factor 2; IL-1RN, Interleukin 1 Receptor Antagonist; RBD, Receptor Binding Domain.

Cytokine levels in early stages of disease act as predictive markers for COVID-19 severity

To investigate the predictive power of soluble immune factors for identifying patients that will go on to severe disease and death (Severe-Death group) *vs*. those that will recover (Mild and Severe-Recovered groups), we performed a random forest analysis, followed by receiver operating characteristic (ROC) curve analysis.

As expected, forest plots showed that patients with hematologic neoplasms had many more segregating factors in comparison with solid tumor patients (Figures 8A, B). While CXCL8 and IL-6 were the most important factors that segregated Severe-Death solid tumors patients, CXCL8, CRP and IL-6 had important roles for segregation of patients with hematologic cancers (Figures 8A, B). Interestingly, for both groups antibodies were important factors for segregating patients that had better outcomes, whereas inflammatory factors were important for segregating individuals that went on to die (Figures 8A, B).

10.3389/fimmu.2022.1052104

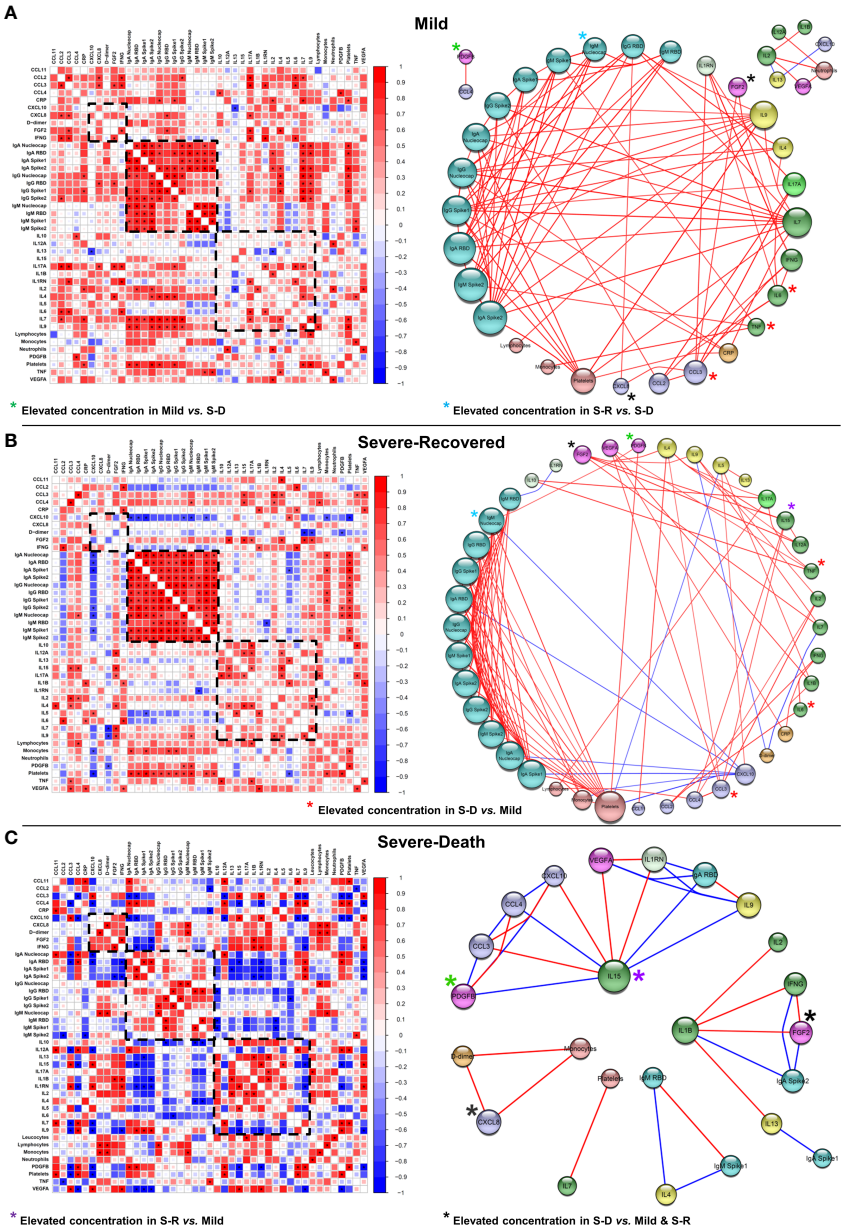

FIGURE 7
Correlation networks suggest lack of immune regulation and loss of coordinated antibody production in patients with solid tumors that went on to die from COVID-19. Data from electronic health records, 27-Plex assay and anti-SARS-CoV-2 proteins' antibodies assays was used to construct a Spearman's correlation matrix with all statistically significant ($p < 0.05$, highlighted as *) Spearman's Rho values, ranging from -1 to 1. The matrix was then used to construct the correlation networks. Red lines connecting the spheres represent positive correlations, whereas line thickness and hotter colors represent correlations with Rho closer to 1. Blue lines connecting the spheres represent negative correlations, whereas line thickness and colder colors represent correlations with Rho closer to -1. Spheres' sizes correlate with the number of interactions for each factor, whereas the bigger radius represents factors with more interactions. Spheres' colors represent factors that have similar activities, characteristics or functions. Disease groups were defined as Mild (**A**; n = 8), Severe-Recovered (**B**; n = 9) and Severe-Death (**C**; n = 5), as described. Nucleocapsid, RBD, Spike 1 and Spike 2 labels refers to antibodies anti-SARS-CoV-2 proteins. Lymphocytes, Monocytes, Neutrophils and Platelets refers to blood counts per mm^3 of blood. CRP, C-Reactive Protein; FGF2, Fibroblast Growth Factor 2; IL-1RN, Interleukin 1 Receptor Antagonist; RBD, Receptor Binding Domain.

Next, we performed predictive analysis using ROC curves with the top hits identified from the random forest analysis and identified factors that resulted in the highest AUC with clear cutoff values. We also plotted curves in an X by Y graph considering how the immune mediator concentration would influence the probability of death of an individual. Then we applied a Grompetz Growth model, which was the best to explain the data distribution (Figures 8C–E). We observed that

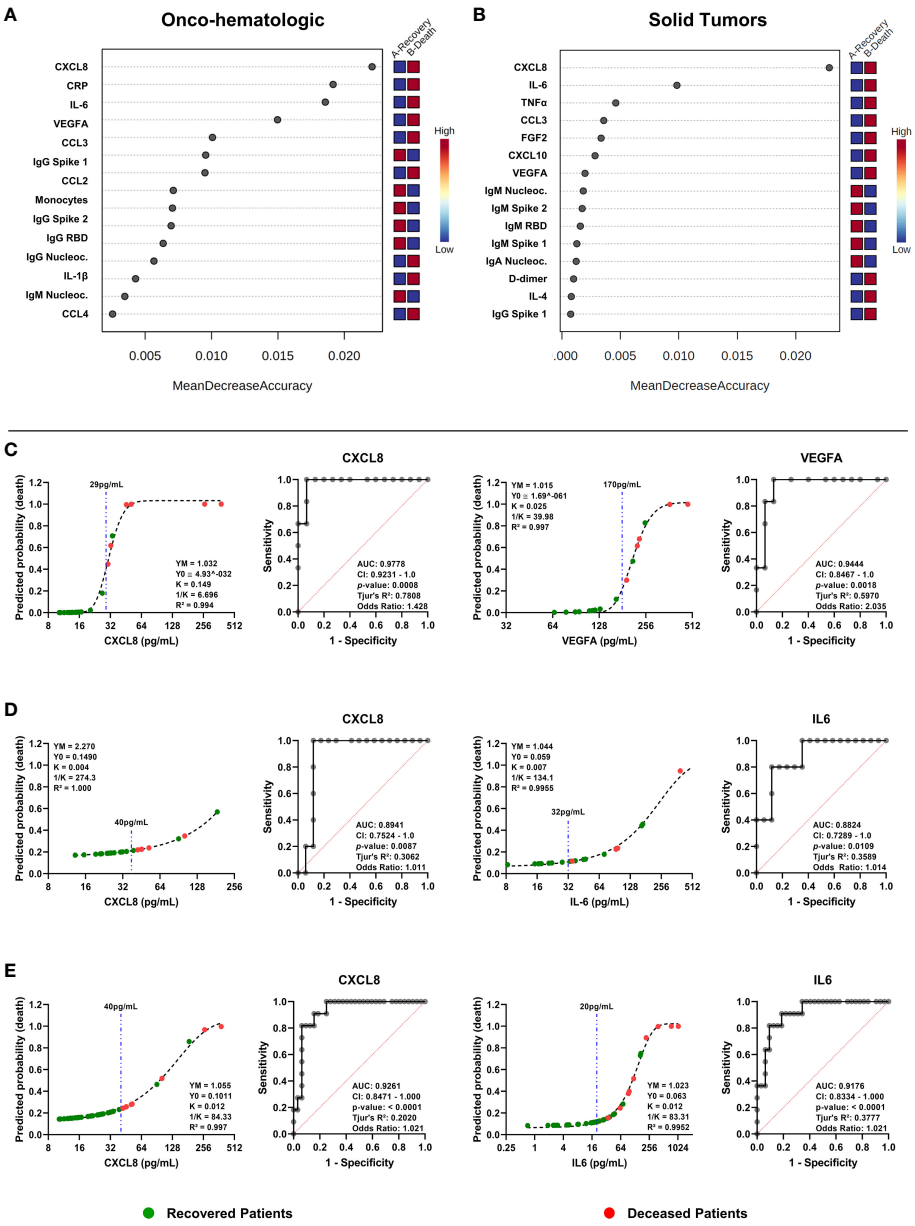

FIGURE 8
Random forests classification and receiver operating characteristic (ROC) curve analysis indicates CXCL8 as a predictor of death for oncologic patients infected by SARS-CoV-2. Data from electronic health records, 27-Plex assay and anti-SARS-CoV-2 proteins' antibodies assays was used as a base for random forests classification analysis **(A, B)** or ROC curves construction **(C–E)**. Graphs in **(A)** and **(B)** show the importance of each factor to segregate outcomes of hematologic cancer patients **(A, C)** or solid tumors patients **(B, D)**. ROC curves show area under the curve (AUC), 95% confidence interval of the AUC, *p*-value, Tjur's pseudo R^2 and odds ratio for hematologic cancer patients **(C)**, solid tumors patients **(D)**, or both **(E)**. Related line charts show predicted probability of death, R^2, and variables for the Gompertz Growth model. Dashed blue lines indicate proposed cutoffs in pg/mL. For both groups the outcomes were defined as recovery (indicating all patients that survived) versus death (all patients that went on to die). In **(A, C)**, n = 15 for "Recovery" and n = 6 for "Death"; In **(B, D)**, n = 17 for "Recovery" and n = 5 for "Death". In **(E)**, n = 22 for "Recovery" and n = 11 for "Death". Nucleocapsid, RBD, Spike 1 and Spike 2 labels refers to antibodies anti-SARS-CoV-2 proteins. CRP, C-Reactive Protein; RBD, Receptor Binding Domain.

CXCL8 (AUC 0.98) and VEGFA (AUC 0.94) were particularly good at predicting COVID-19 outcomes within hematologic cancer patients (Figure 8C), while CXCL8 (AUC 0.89) and IL-6 (AUC 0.88) were good predictors for solid tumor patients (Figure 8D). Finally, we identified both CXCL8 (AUC 0.93) and IL-6 (AUC 0.92) as excellent predictors of death for oncologic patients in general, regardless of whether they had hematologic or solid tumors (Figure 8E).

10.3389/fimmu.2022.1052104

Discussion

Our data shows that hematologic and solid tumor cancer patients display distinct systemic immune, hematological and biochemical indicators of disease following infection with SARS-CoV-2, and that these characteristics are capable of segregating patients based on disease outcome (Figure 9).

First, among blood and biochemical measurements, the hematologic cancer cohort displayed increased CRP and D-dimer concentrations and lower hematocrit and hemoglobin levels in patients that progressed to death (Severe-Death group) (Figures 2B, C). Although D-dimer evaluation, leukopenia and lymphopenia are useful markers indicative of COVID-19 severity in the general population (15, 16), only the hematologic cancer cohort displayed significant differences in D-dimer concentrations, and lymphocytes and monocyte counts (Figures 2A, C). However, it is of note that solid tumor COVID-19 patients may also suffer a reduction in specific populations of T cells (17) throughout the disease.

Regarding the systemic soluble immune molecules, the analysis revealed distinct immune networks between hematologic and solid tumor cancer patients, however, both groups displayed elevated concentrations of IL-6 and CXCL8 among individuals that progressed to death (Figure 3 and 5). The two factors are associated with cytokine-release syndrome and COVID-19 severity (12, 17, 18), and have roles in inflammation, myeloid cell recruitment and tissue damage (19). In our study, they were good early indicators of death risk (Figure 8).

Among patients with solid tumors, the analysis also showed a trend to increased concentrations of IL-15 in plasma of patients that recovered from the disease compared with patients who only presented mild COVID-19. This increased concentration was significant in patients with hematologic malignancies that would die from COVID-19 compared to individuals that would present only the mild form of the disease (Figure 3C). Given that NK cells participate in antiviral responses, and that IL-15 is a cytokine with an important role in the proliferation and biology of NK cells (20), it is of interest to determine the role of these cells as inflammatory drivers or infection-resolving agents.

Furthermore, Severe-Death hematologic cancer patients showed a trend to increased production of IL-17A, similar to what is observed in individuals from the general population infected by SARS-CoV-2 and other SARS viruses (21). The Severe-Death hematologic cancer group also had elevated concentrations of IL-5 and IL-13 (Figure 3C). These factors are associated with eosinophil activation, airway complications, pulmonary diseases, and COVID-19 severity (18, 19, 21), but their exact role in COVID-19 progression or resolution is not well understood.

We also observed increased concentrations of CCL2, CCL3, CCL4, VEGFA and IL-1β in Severe-Death hematologic cancer patients (Figures 3 and 5A). These factors are important for recruitment of myeloid cells, induction of fever and inflammation (22), and development and restructuring of blood vessels (23). VEGFA specifically is associated with virus spread (24), hypoxia, and tissue-related damage during COVID-19 (25). Overall, patients with hematologic malignancies seem to suffer from exacerbated immune responses, possibly related to the lack of leukocyte subpopulations during the initial phases of

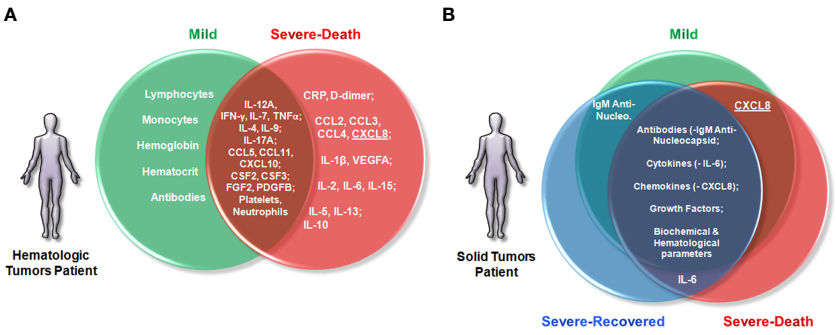

FIGURE 9
Patients with hematologic malignancies and solid tumors display distinct circulating immune profiles associated with clinical outcomes. Venn diagrams were drawn to summarize the findings of this study, highlighting factors with higher concentrations between the groups. Early increased immune cells and antibody production were associated with mild COVID-19, whereas increased concentrations of inflammatory immune markers were associated with death in the Onco-hematologic group **(A)**. On the other hand, only IL-6 was associated with death among patients with solid tumors. In fact, for those patients, death outcome was associated with a breakdown of coordinate production of antibodies and regulation of soluble factors rather than with broad differences in the concentrations of soluble mediators **(B)**. Lastly, although patients with hematologic and solid tumors display distinct profiles of soluble immune markers, CXCL8 (underlined) was an important early predictive factor of patients that would progress to death from COVID-19 across all cancers. Lymphocytes and monocytes refer to cell counts per mm^3 of blood. Antibodies refers to IgA, IgG and IgM anti-SARS-CoV-2 Nucleocapsid, Receptor Binding Domain, Spike 1 and Spike proteins. CRP, C-Reactive Protein; IL-1RN, Interleukin 1 Receptor Antagonist.

infection, since leukopenia is associated with death and the presence of $CD8^+$ T Cells with survival (10, 26). Nevertheless, this hypothesis in the oncologic context still needs further investigation.

We also found a striking decrease in the plasma levels of IgG and IgM anti-SARS-CoV-2 proteins in Severe-Death hematologic patients, which was not seen in Severe-Death solid tumor patients (Figure 4). While antibody titers may vary over the two weeks following the onset of COVID-19 symptoms (27), our findings show that initial antibody levels shortly after diagnosis among hematologic cancer patients indicate possible individuals that would have mild disease, or progress to death (Figures 4 and 5A), which was also shown in patients from the general population (28).

This lack of effective antibody-based responses among hematologic cancer patients may be associated with myeloma (29), weak T cell responses (30, 31), and oncologic treatments (32). In the COVID-19 context data on this topic is scarce and outcomes are dependent on the type of tumor, treatments, treatment timings, and individual factors (13). The few publications regarding the immune response of patients with cancer against SARS-CoV-2 infections shed light on how chemotherapy, stem cell transplant, and anti-CD20 therapies negatively impact antibody production (33, 34). Nevertheless, we could not observe a clear bias in hematologic malignancy type or cancer treatment in production of antibodies or in the outcome of COVID-19 among our patients (Figure 5, Table 1).

Regarding the multiple correlation analysis, patients with hematologic malignancies that presented only mild disease had extensive networks between a number of immune factors and antibodies, also involving cytokines associated with type I, II and III immune responses (Figures 6A, B; Supplementary Figure 4A). We observed prominent roles for type I associated factors, such as IL-2, IL-7, IL-12A, IL-15, and antibodies in general (Figure 6A), which are known for their importance for combating SARS-CoV-2 infection (25, 35, 36). We also observed a possible regulatory axis for type II responses composed of IL-4, IL-5, and IL-10, and an interesting interaction between IL-17A, CCL4 and CRP (Figure 6A). Although C-reactive protein is well known for its association with inflammation, it is important to note that this factor also display regulatory proprieties (37).

Regarding Severe-Death hematologic cancer patients, we observed a chemokine axis involving CCL2, CCL3, CXCL8 and IL-6, and an inverse correlation between IL-1β and monocytes (Figure 7C), indicating that those patients displayed an exacerbated inflammatory response as compared to patients that recovered from COVID-19. We also observed strong correlations involving IL-2, TNF-alpha and immunoglobulins, pointing to an immune response skewed toward myeloid-derived cells, which could further exacerbate the pathological process (25, 38). Supporting this possibility are previous findings indicating that high levels of TNF-alpha and IL-6 correlate negatively with T cell numbers in severe COVID-19 in the general population (30), and that B cell numbers and antibodies are reduced in COVID-19 patients with hematologic malignancies (17). Taken together these results suggest that the lack of a balanced and effective type I lymphocyte-based response, together with an exacerbated inflammatory response, are critical factors leading to death among patients with hematologic malignancies.

On the other hand, network analysis of soluble factors from patients with solid tumors showed that in mild disease IL-1RN forms a potential immunoregulatory network (Figure 7A). IL-1RN is seen in severe COVID-19 patients from the general population (18), and may have a role counterbalancing inflammatory activity (22) in patients with mild disease. Contrary to what was observed in patients with better outcomes, the Severe-Death group was marked by a negative correlation between IL-4 levels and IgM anti-SARS-CoV-2 proteins (Figure 7C). In addition, the Mild group displayed a strong correlation between anti-SARS-CoV-2 antibodies, IL-7, and IL-9 that was not seen in the severe disease groups (Figure 7). Interestingly, IL-9 shares the γ-chain receptor with other lymphocyte-proliferation cytokines, such as IL-2, IL-4 and IL-7, and aside from its effects on promoting allergic inflammation, IL-9 can also influence the effector activities of T and B lymphocytes, even enhancing the production of IgE and IgG from human cells (39, 40). Conversely, the Severe-Death group was marked by a strong positive correlation between CXCL8, D-dimer and monocytes (Figure 7C), factors associated with COVID-19 severity among the general population (7, 25, 41, 42), and in solid tumor patients specifically (17). Lastly, we also observed in the Severe-Death group an IL-15-based axis characterized by both strong positive and negative correlations with several immune mediators (Figure 7C), which highlights the need of a thorough investigation about the role of IL-15 in patients with cancer and COVID-19, given that exhausted T and NK cell populations are observed throughout the disease (17, 28, 35).

Finally, our predictive analysis showed distinctive roles for VEGFA, CXCL8, and IL-6 in segregation of patients by outcome (Figure 8). None of these factors – with the exception of IL-6 – were important predictors of mortality in studies with large numbers of markers regarding COVID-19 in the general population (18, 43). Therefore, our findings support the need of further studies to validate the use of these factors as potential clinically useful biomarkers.

However, this work has some limitations worth highlighting. The first factor is that cancer itself is a disease with broad manifestations, influenced by several factors, many of which cannot be controlled in a real-life setting. Therefore, we recognize that our cohorts are heterogeneous and that each type of cancer can influence the immune response in particular ways. The second is that cancer therapies also may affect the immune response in particular ways, a situation that depends on

several individual factors, one of which is the type of cancer itself. The last is the limited number of patients – a fact present in other studies regarding cancer and COVID-19 (17, 26, 33), and the very specific population (from a Cancer Center in Brazil with acute COVID-19 patients that were all naïve to SARS-CoV-2 vaccines). Importantly, despite these complexities, we identified immune molecules and networks associated with COVID-19 clinical outcome among our cancer patient cohorts.

To the best of our knowledge, this is the first immune-focused study comparing distinct COVID-19 outcomes in patients with cancer. Our results indicate important differences in immune responses in solid tumor and hematologic cancer individuals with COVID-19, suggesting that inflammation based on myeloid-derived cells in early phases of infection could be detrimental for the onset of severe disease and death, as indicated by other studies (25, 41, 42). Given that CXCL8 was an important predictive factor of disease outcome in oncologic patients, it will be interesting to assess if this finding is also observed in other cohorts, and how a therapeutic approach reducing neutrophil-based inflammation could help patients infected by SARS-CoV-2. In addition, investigating specific immune cell populations present in the blood could also help in understanding the different COVID-19 outcomes observed in oncologic patients, especially those with hematologic malignancies.

Materials and methods

Patient enrolment and classification

From May to November 2020, we included 43 oncologic patients with a recent diagnostic of SARS-CoV-2 from A.C.Camargo Cancer Center (Table 1). All volunteer patients received information about the project and gave written consent to participate before initiation of any procedure regarding this work. Individuals were segregated by solid tumors or hematological malignancies based on their previous diagnostic. If the individual had a history of both solid and hematologic tumors, the group selection was based on the most recent or active cancer. Severity of COVID-19 was determined based on the World Health Organization's proposed recommendations (44), as follows: Mild, no oxygen therapy; Severe-Recovered, for patients who had oxygen therapy, but recovered from the disease; and Severe-Death, for patients who had oxygen therapy and went on to die from COVID-19. For patients that received supplemental O_2, we considered a minimum of two days of therapy. All patients that received supplemental O_2 therapy also received dexamethasone treatment as recommended by the RECOVERY Collaborative Group study (45). The project was approved by A.C.Camargo Cancer Center Ethics Committee (CAE:30283220.5.0000.5432).

SARS-CoV-2 infection assessment

Patients were assessed for infection by SARS-CoV-2 using a real-time qPCR test whenever they presented symptoms for the disease (cough, dyspnea, loss of smell and/or taste, fever) or otherwise indicated by the clinical teams.

Electronic health records assessment

Biochemical evaluation (C-Reactive Protein and D-dimer concentrations), hematological data (leukocyte, lymphocyte, monocyte, neutrophil, and platelet counts, hemoglobin concentration and hematocrit), tumor classification, Eastern Cooperative Oncology Group (ECOG) performance status scale score, treatment, and other relevant information were obtained from health records available for each patient.

Blood sampling and processing

Blood samples were collected in EDTA tubes within a median of two days (95% CI: 1 – 4 days) from positive SARS-CoV-2 test result. Blood was centrifuged at 400xg, 10 minutes, 20°C for collection of plasma, which was then snap frozen in dry ice and stored at -80°C until further processing.

Quantification of plasma soluble mediators

Concentration of plasma soluble factors were determined using a 27 multiplex bead assay (Bio-Plex® Pro Human Cytokine Group I Panel 27-plex, Bio-Rad Inc., USA). Multiplex bead assays (Bio-Plex® Pro Human IgA/IgG/IgM SARS-CoV-2 N/RBD/S1/S2 4-Plex Panel, Bio-Rad Inc., USA; provided as three separate kits) were used to measure production of IgA, IgG and IgM antibodies anti-SARS-CoV-2 Nucleocapsid, Receptor Binding Domain (RBD), Spike 1 and Spike 2 proteins. Virus inactivation was performed through incubation at 56°C/30 minutes before analyte quantification. All procedures were done accordingly to the manufacturer's instructions, and plates were read in Bio-Plex platform (Bio-Plex® 200 system, Bio-Rad Inc., USA). All data is presented as pg/mL, based on standard curves provided by the kit (27-Plex), or as fluorescence intensity (4-Plex antibodies assays).

Statistical analysis

All soluble factors and hematological data were analyzed in Graph Pad Prism 8.4.2 for construction of Receiver Operator

Characteristic (ROC) curves, line plots and scatter dot plots. For scatter dot plots, data from patients with hematologic malignancies was analyzed with a two-tailed Mann-Whitney test, whereas solid tumors patient data was analyzed with a two-tailed Kruskal-Wallis adjusted test followed by Dunn's *post-hoc*. Data is presented as median and 95% confidence interval.

ROC curves were constructed using the multiple logistic regression model Logit[P(Y=1)] = Ln[(P(Y=1)/P(Y=0)] = β0 + β1*B. Related line charts show data points indicating how analyte concentration influences the probability of death of an individual, calculated based on the model aforementioned. A fitting line was drawn based on the Gompertz Growth Model given in Graph Pad Prism software, with the following equation: Y = YM*(Y0/YM)^(exp(-K*X)), where Y0 is the starting population, YM is the maximum population, K determines the lag time and 1/K is the X value of inflection point.

For radar charts, raw data (fluorescence intensity) from 4-Plex antibodies assays, including values from the positive controls, were transformed by Ln(X+1)*10. Then each measurement of antibody production for each patient was divided by the positive control value of that class of antibody. This way we could correct distinct measurements for different classes of antibodies and all measurements fit inside a scale from 1 to 10. The graphs were constructed in Microsoft Office Excel 2010.

Unsupervised cluster analysis was performed using the online tool ClustVis (46). Raw data from all parameters or parameters with a *p*-value below 0.10 were uploaded in ClustVis platform and transformed with [ln(x +1)] model. The analysis was performed using a hierarchical cluster algorithm where rows and columns were clustered by Manhattan or Euclidean distance and Ward or Complete linkage. Missing data (< 2% of total data) was estimated by imputation as per default.

Correlation matrices were done in R software version 4.0.0 and R Studio 1.4.1106, with *corrplot* and *Hmisc* packages. Briefly, raw data from each patient for each group in both cohorts was organized into a data frame, and a Spearman correlation test was run. All Spearman's coefficients are shown in the matrices, but a star indicates correlations with a *p-value* of 0.05 or below.

Networks were constructed using the Cytoscape software version 3.8.2. Data from correlation matrices was used to make the networks, considering only interactions with a *p-value* below 0.05. Line thickness and colors refers to strength and value of the interaction, while sphere radius reflects the number of interactions.

For random forests analysis, raw data was uploaded in MetaboAnalyst 5.0 platform (https://www.metaboanalyst.ca) and missing values (< 2% of total data) were estimated by Bayesian Principal Component Analysis. Forest plots were made randomly with 500 trees and 7 predictors to determine the most important factors for segregation accuracy based on outcomes, which were "Recovery" – for all patients that survived; or "Death" – for all patients that died.

Data availability statement

The raw data supporting the conclusions of this article will be made available by the authors, without undue reservation.

Ethics statement

The studies involving human participants were reviewed and approved by A.C.Carmaro Cancer Center Ethics Committee (CAE:30283220.5.0000.5432). The patients/participants provided their written informed consent to participate in this study.

Author contributions

KG and MB conceptualized and designed the study. Data collection was performed by FP-O, AF, NG and KM. Data analysis and interpretation was performed by FP-O, AF, NG, WD, MB and KG. The article was drafted by FP-O, AF, WD and KG. Critical revision of the article was performed by all authors. All authors contributed to the article and approved the submitted version.

Funding

This work was funded by FAPESP (#2020/16736-0), NIH-NCI/CNPq Brazil cooperative grant (5R01CA246368-02) and a NIVEA donation to A.C.Camargo Cancer Center. KJG and WOD are CNPq research fellows. FAPESP, CAPES and CNPq provided post-graduate fellowships. We would like to acknowledge the critical contribution of nurses and laboratory technicians in patient recruitment, care, sample collection and processing: Amanda França de Nóbrega, Amanda Stephanie Sousa, Bruna Tirapelli Gonçalves, Cassia da Silva, Fernanda Araújo Pintor, Iara Monique Messias, Lais Corsino Durant, Laís Lie Senda de Abrantes, Luciana Facure Moredo, Juliana de Oliveira Souza, Vanessa da Silva Alves, Rodrigo Reghini da Silva, Ana Paula Mitsue, Bruna Barros, Clara Maciel Cavalcanti, Gabriela Branco, Eloísa Ribeiro Olivieri, Katia Klug Oliveira, and Louise de Carvalho Mota. We also recognize the contribution of patient volunteers.

Conflict of interest

The authors declare that the research was conducted in the absence of any commercial or financial relationships that could be construed as a potential conflict of interest.

Publisher's note

All claims expressed in this article are solely those of the authors and do not necessarily represent those of their affiliated organizations, or those of the publisher, the editors and the reviewers. Any product that may be evaluated in this article, or claim that may be made by its manufacturer, is not guaranteed or endorsed by the publisher.

Supplementary material

The Supplementary Material for this article can be found online at: https://www.frontiersin.org/articles/10.3389/fimmu.2022.1052104/full#supplementary-material

References

1. Hu B. Characteristics of SARS-CoV-2 and COVID-19. *Nat Rev Microbiol* (2020) 19:141–54. doi: 10.1038/s41579-020-00459-7

2. Dhama K, Khan S, Tiwari R, Sircar S, Bhat S, Malik YS, et al. Coronavirus disease 2019 - COVID19. *Clin Microbiol Rev* (2020) 33(4):1–48. doi: 10.1128/CMR.00028-20

3. De Souza WM, Buss LF, Candido S, Carrera J, Li S, Zarebski AE, et al. Epidemiological and clinical characteristics of the COVID-19 epidemic in Brazil. *Nat Hum Behav [Internet]* (2020) 4:856–65. doi: 10.1038/s41562-020-0928-4

4. Zeiser FA, Donida B, da Costa CA, Ramos G de O, Scherer JN, Barcellos NT, et al. First and second COVID-19 waves in Brazil: A cross-sectional study of patients' characteristics related to hospitalization and in-hospital mortality. *Lancet Reg Heal - Am* (2022). doi: 10.1016/j.lana.2021.100107

5. *Brazilian Ministry of health - DATASUS. painel coronavírus [Internet]* (2022). Available at: https://covid.saude.gov.br/.

6. Croda J, Oliveira WKde, Frutuoso RL, Mandetta LH, Baia-Da-silva DC, Brito-Sousa JD, et al. Covid-19 in Brazil: Advantages of a socialized unified health system and preparation to contain cases. *Rev Soc Bras Med Trop* (2020) 53:2–7. doi: 10.1590/0037-8682-0167-2020

7. Merad M, Martin JC. Pathological inflammation in patients with COVID-19: a key role for monocytes and macrophages. *Nat Rev Immunol* (2020) 20:355–62. doi: 10.1038/s41577-020-0331-4

8. Lee LYW, Cazier JB, Starkey T, Briggs SEW, Arnold R, Bisht V, et al. COVID-19 prevalence and mortality in patients with cancer and the effect of primary tumour subtype and patient demographics: a prospective cohort study. *Lancet Oncol* (2020) 21(10):1309–16. doi: 10.1016/S1470-2045(20)30442-3

9. Robilotti EV, Babady NE, Mead PA, Rolling T, Perez-Johnston R, Bernardes M, et al. Determinants of COVID-19 disease severity in patients with cancer. *Nat Med [Internet]* (2020) 26:1218–23. doi: 10.1038/s41591-020-0979-0

10. Derosa L, Melenotte C, Griscelli F, Gachot B, Marabelle A, Kroemer G, et al. The immuno-oncological challenge of COVID-19. *Nat Cancer* (2020) 1:946–64. doi: 10.1038/s43018-020-00122-3

11. Chamilos G, Lionakis MS, Kontoyiannis DP. Are all patients with cancer at heightened risk for severe coronavirus disease 2019 (COVID-19)? *Clin Infect Dis* (2020) 72(2):351–6. doi: 10.1093/cid/ciaa1079

12. Brodin P. Immune determinants of COVID-19 disease presentation and severity. *Nat Med [Internet].* (2021) 27(1):28–33. doi: 10.1038/s41591-020-01202-8

13. Fernandes GA, Feriani D, França e Silva ILA, Mendonça e Silva DR, Arantes PE, Canteras J da S, et al. Differences in mortality of cancer patients with COVID-19 in a Brazilian cancer center. *Semin Oncol [Internet].* (2021) 48(2):171–80. doi: 10.1053/j.seminoncol.2021.01.003

14. Mehta P, McAuley DF, Brown M, Sanchez E, Tattersall RS, Manson JJ. COVID-19: consider cytokine storm syndromes and immunosuppression. *Lancet [Internet].* (2020) 395(10229):1033–4. doi: 10.1016/S0140-6736(20)30628-0

15. Pereira MAM, de Almeida Barros IC, Jacob ALV, de Assis ML, Kanaan S, Kang HC. Laboratory findings in SARS-CoV-2 infections: State of the art. *Rev Assoc Med Bras* (2020) 66(8):1152–6. doi: 10.1590/1806-9282.66.8.1152

16. Terpos E, Ntanasis-Stathopoulos I, Elalamy I, Kastritis E, Sergentanis TN, Politou M, et al. Hematological findings and complications of COVID-19. *Am J Hematol* (2020) 95(7):834–47. doi: 10.1002/ajh.25829

17. Abdul-Jawad S, Baù L, Alaguthurai T, del Molino del Barrio I, Laing AG, Hayday TS, et al. Acute immune signatures and their legacies in severe acute respiratory syndrome coronavirus-2 infected cancer patients. *Cancer Cell* (2021) 39 (2):257–275.e6. doi: 10.1016/j.ccell.2021.01.001

18. Lucas C, Wong P, Klein J, Castro TBR, Silva J, Sundaram M, et al. Longitudinal analyses reveal immunological misfiring in severe COVID-19. *Nature.* (2020) 584(7821):463–9. doi: 10.1038/s41586-020-2588-y

19. Ha H, Debnath B, Neamati N. Role of the CXCL8-CXCR1/2 axis in cancer and inflammatory diseases. *Theranostics.* (2017) 7(6):1543–88. doi: 10.7150/thno.15625

20. Carson BWE, Giri JG, Lindemann MJ, Linett ML, Ahdieh M, Paxton R, et al. Interleukin (IL) 15 is a novel cytokine that activates human natural killer cells *via* components of the IL-2 receptor. *J Exp Med* (1994) 180:(4):1395–403. doi: 10.1084/jem.180.4.1395

21. Schett G, Manger B, Simon D, Caporali R. COVID-19 revisiting inflammatory pathways of arthritis. *Nat Rev Rheumatol [Internet]* (2020) 16:465–70. doi: 10.1038/s41584-020-0451-z

22. Dinarello CA. Overview of the IL-1 family in innate inflammation and acquired immunity. *Immunol Rev* (2018) 281(1):8–27. doi: 10.1111/imr.12621

23. Presta M, Andrés G, Leali D, Dell'Era P, Ronca R. Inflammatory cells and chemokines sustain FGF2-induced angiogenesis. *Eur Cytokine Netw* (2009) 20 (2):39–50. doi: 10.1684/ecn.2009.0155

24. Polidoro RB, Hagan RS, Santiago RDS, Schmidt NW. Overview: Systemic inflammatory response derived from lung injury caused by SARS-CoV-2 infection explains severe outcomes in. *Front Immunol* (2020) 11:1626. doi: 10.3389/fimmu.2020.01626

25. Chua RL, Lukassen S, Trump S, Hennig BP, Wendisch D, Pott F, et al. COVID-19 severity correlates with airway epithelium–immune cell interactions identified by single-cell analysis. *Nat Biotechnol* (2020) 38:970–9. doi: 10.1038/s41587-020-0602-4

26. Bange EM, Han NA, Wileyto P, Kim JY, Gouma S, Robinson J, et al. CD8+ T cells contribute to survival in patients with COVID-19 and hematologic cancer. *Nat Med [Internet].* (2021) 27(7):1280–9. doi: 10.1038/s41591-021-01386-7

27. Röltgen K, Powell AE, Wirz OF, Stevens BA, Hogan CA, Najeeb J, et al. Defining the features and duration of antibody responses to SARS-CoV-2 infection associated with disease severity and outcome. *Sci Immunol* (2021) 5(54):1–20. doi: 10.1126/sciimmunol.abe0240

28. Silva J, Lucas C, Sundaram M, Israelow B, Wong P, Klein J, et al. Saliva viral load is a dynamic unifying correlate of COVID-19 severity and mortality. *medRxiv* (2021). doi: 10.1101/2021.01.04.21249236

29. Jackson DA, Elsawa SF. Factors regulating immunoglobulin production by normal and disease-associated plasma cells. *Biomolecules.* (2015) 5(1):20–40. doi: 10.3390/biom5010020

30. Diao B, Wang C, Tan Y, Chen X, Liu Y, Ning L, et al. Reduction and functional exhaustion of T cells in patients with coronavirus disease 2019 (COVID-19). *Front Immunol* (2020) 11:827. doi: 10.3389/fimmu.2020.00827

31. Grifoni A, Weiskopf D, Ramirez SI, Mateus J, Dan JM, Moderbacher CR, et al. Targets of T cell responses to SARS-CoV-2 coronavirus in humans with COVID-19 disease and unexposed individuals. *Cell [Internet].* (2020) 181(7):1489–1501.e15. doi: 10.1016/j.cell.2020.05.015

32. Mehta RS, Rezvani K. Immune reconstitution post allogeneic transplant and the impact of immune recovery on the risk of infection. *Virulence [Internet].* (2016) 7(8):901–16. doi: 10.1080/21505594.2016.1208866

33. Esperança-Martins M, Gonçalves L, Soares-Pinho I, Gomes A, Serrano M, Blankenhaus B, et al. Humoral immune response of SARS-CoV-2–infected patients with cancer: Influencing factors and mechanisms. *Oncologist [Internet].* (2021) 26 (9):e1619–32. doi: 10.1002/onco.13828

34. Thakkar A, Gonzalez-Lugo JD, Goradia N, Gali R, Shapiro LC, Pradhan K, et al. Seroconversion rates following COVID-19 vaccination among patients with cancer. *Cancer Cell [Internet].* (2021) 39(8):1081–1090.e2. doi: 10.1016/j.ccell.2021.06.002

35. Hadjadj J, Yatim N, Barnabei L, Corneau A, Breillat P, Carlier N, et al. Impaired type I interferon activity and exacerbated inflammatory responses in severe covid-19 patients. *Scient* (2020) 369(6504):718–24. doi: 10.1101/2020.04.19.20068015

36. Meffre E, Iwasaki A. Interferon deficiency can lead to severe COVID. *Nature.* (2020) 587(7834):374–6. doi: 10.1038/d41586-020-03070-1

37. Black S, Kushner I. Samols d. *C-reactive protein. J Biol Chem [Internet].* (2004) 279(47):48487–90. doi: 10.1074/jbc.R400025200

38. Channappanavar R, Perlman S. Pathogenic human coronavirus infections: causes and consequences of cytokine storm and immunopathology. *Semin Immunopathol* (2017) 39(5):529–39. doi: 10.1007/s00281-017-0629-x

39. Goswami R, Kaplan MH, Goswami R, Kaplan MH. A brief history of IL-9. *J Immunol* (2022) 186(6):3283–8. doi: 10.4049/jimmunol.1003049

40. Wan J, Wu Y, Ji X, Huang L, Cai W, Su Z, et al. IL-9 and IL-9-producing cells in tumor immunity. *Cell Communication and Signaling* (2020) 18:50. doi: 10.1186/s12964-020-00538-5

41. Bost P, Giladi A, Liu Y, Bendjelal Y, Xu G, David E, et al. Host-viral infection maps reveal signatures of severe COVID-19 patients. *Cell [Internet].* (2020) 181 (7):1475–1488.e12. doi: 10.1016/j.cell.2020.05.006

42. Grant RA, Morales-Nebreda L, Markov NS, Swaminathan S, Querrey M, Guzman ER, et al. Circuits between infected macrophages and T cells in SARS-CoV-2 pneumonia. *Nature* (2021) 590:635–41. doi: 10.1038/s41586-020-03148-w

43. Kong Y, Han J, Wu X, Zeng H, Liu J, Zhang H. VEGF-d: A novel biomarker for detection of COVID-19 progression. *Crit Care* (2020) 24(1):1–4. doi: 10.1186/s13054-020-03079-y

44. Marshall JC, Murthy S, Diaz J, Adhikari N, Angus DC, Arabi YM, et al. A minimal common outcome measure set for COVID-19 clinical research. *Lancet Infect Dis* (2020) 20(8):e192–7. doi: 10.1016/S1473-3099(20)30483-7

45. Metsalu T, Vilo J. The RECOVERY collaborative group. dexamethasone in hospitalized patients with covid-19. *N Engl J Med* (2021) 384(8):693–704. doi: 10.1056/NEJMoa2021436

46. Metsalu T, Vilo J. ClustVis: A web tool for visualizing clustering of multivariate data using principal component analysis and heatmap. *Nucleic Acids Res* (2015) 43(W1):W566–70. doi: 10.1093/nar/gkv468

frontiers | Frontiers in Immunology

TYPE Original Research
PUBLISHED 18 January 2023
DOI 10.3389/fimmu.2023.1084646

Check for updates

OPEN ACCESS

EDITED BY
E. Marion Schneider,
University of Ulm, Germany

REVIEWED BY
Lok Bahadur Shrestha,
University of New South Wales, Australia
Will Hudson,
Baylor College of Medicine, United States

*CORRESPONDENCE
Shan Zhong
zhongshan@cqmu.edu.cn
Yu Lei
leiyu_ww@aliyun.com

†These authors have contributed equally to this work and share first authorship

SPECIALTY SECTION
This article was submitted to Viral Immunology, a section of the journal Frontiers in Immunology

RECEIVED 30 October 2022
ACCEPTED 04 January 2023
PUBLISHED 18 January 2023

CITATION
Li H, Li S, Xu P, Wang X, Deng H, Lei Y and Zhong S (2023) Analysis of neutralizing antibodies to COVID-19 inactivated or subunit recombinant vaccines in hospitalized patients with liver dysfunction. *Front. Immunol.* 14:1084646. doi: 10.3389/fimmu.2023.1084646

COPYRIGHT
© 2023 Li, Li, Xu, Wang, Deng, Lei and Zhong. This is an open-access article distributed under the terms of the Creative Commons Attribution License (CC BY). The use, distribution or reproduction in other forums is permitted, provided the original author(s) and the copyright owner(s) are credited and that the original publication in this journal is cited, in accordance with accepted academic practice. No use, distribution or reproduction is permitted which does not comply with these terms.

Analysis of neutralizing antibodies to COVID-19 inactivated or subunit recombinant vaccines in hospitalized patients with liver dysfunction

Hu Li†, Shiyin Li†, Pan Xu, Xiaohao Wang, Huan Deng, Yu Lei* and Shan Zhong*

Key Laboratory of Molecular Biology for Infectious Diseases (Ministry of Education), Institute for Viral Hepatitis, Department of Infectious Diseases, The Second Affiliated Hospital of Chongqing Medical University, Chongqing, China

Background: The neutralizing antibodies (NAbs) response after COVID-19 vaccination after liver dysfunction is unclear. In this study, we evaluated the NAbs response after COVID-19 vaccination in hospitalized patients suffering from liver dysfunction.

Methods: In this cross-sectional study with longitudinal follow-up, we enrolled eligible patients with liver dysfunction and healthy volunteers with full-course COVID-19 vaccination. Blood samples were collected for the NAbs testing at the time of admission and after treatment. Multiple regression analysis to assess independent risk factors affecting NAbs response.

Results: A total of 137 patients and 134 healthy controls (HC) were enrolled. Both seropositivity (65.7% *vs* 80.6%, p<0.01) and titer (3.95 *vs* 4.94 $\log_2$ AU/ml, p<0.001) of NAbs in patients were significantly lower than that in HC. The decrease of antibody titer in patients was significantly faster than that in HC. After adjusting for potential confounding factors, males (odds ratio [OR]: 0.17; 95% confidence interval [CI]: 0.06, 0.46; p<0.001) and severe liver damage (OR: 0.30; 95% CI: 0.12, 0.71; p<0.01) were significantly associated with reduction of the probability of NAbs seropositivity in the multiple regression analysis. Males (β =-1.18; 95% CI: -1.73,-0.64) and chronic liver diseases (β =-1.45; 95% CI: -2.13, -0.76) were significantly associated with lower NAbs titers. In 26 patients with liver failure, both antibody seropositivity (53.8% *vs* 84.6%, p<0.05) and titer (3.55 *vs* 4.32 $\log_2$ AU/ml, p<0.001) did not decrease but increased after artificial liver plasmapheresis.

Conclusions: NAbs response to COVID-19 inactivated or subunit recombinant vaccines was waning in patients with liver dysfunction. Moreover, patients with male sex, severe liver injury and chronic liver diseases have an increased risk of poor antibody responses.

KEYWORDS

COVID-19, SARS-CoV-2, vaccine, neutralizing antibodies, liver dysfunction, artificial liver

1 Introduction

Coronavirus disease 2019 (COVID-19), caused by severe acute respiratory syndrome coronavirus 2 (SARS-CoV-2) infection, has been a life-threatening global health burden (1, 2). As of 23 October 2022, over 624 million confirmed cases and over 6.5 million deaths have been reported globally. Numerous studies have confirmed that SARS-CoV-2 vaccines can effectively reduce the morbidity and mortality of COVID-19 (3, 4). Vaccination against COVID-19 is currently considered the most effective, safe, and cost-effective way to prevent and control COVID-19 worldwide.

Previous studies have shown that patients with chronic liver disease are highly susceptible to COVID-19 and often have poor prognosis (5, 6). Therefore, some guidelines and expert consensus have been developed, and patients with chronic liver disease are encouraged to receive full-course SARS-CoV-2 vaccination (7, 8). Many previous studies have evaluated the safety and immunogenicity of SARS-CoV-2 vaccination in various chronic liver disease populations, including nonalcoholic fatty liver disease (9), post-liver transplant population (10), chronic hepatitis B (11), cirrhosis (12), and autoimmune liver disease (13, 14). These studies all showed the safety of SARS-CoV-2 vaccine in patients with liver disease, but the immune response to the vaccine was weaker than that in healthy people. The time after vaccination in these studies was too short for long-term observational data. In addition, some patients with chronic liver disease may experience acute liver damage due to various reasons. It is urgent for doctors to evaluate the antibody levels produced by prior COVID-19 immunizations after liver damage-caused by various reasons.

COVID-19 inactivated and receptor-binding domain (RBD) subunit recombinant vaccines are two common types of vaccines in China. However, whether the antibody responses following COVID-19 immunization is affected by liver injury is still unclear. In this study, we evaluated antibody responses in hospitalized patients with various causes of liver dysfunction after immunization with COVID-19 inactivated and RBD-subunit recombinant vaccines.

2 Patients and methods

2.1 Study design and participants

We did a cross-sectional study with longitudinal follow-up at the Second Affiliated Hospital of Chongqing Medical University from October 1, 2021, to January 30, 2022. The hospitalized patients with liver dysfunction were enrolled in the Center for Liver and Infectious diseases. At the same time, an equal number of healthy volunteers (healthy controls) who underwent annual physical examinations at the health management center were enrolled as controls. Inclusion criteria of participants were age 18 years or older, completed full-course of COVID-19 vaccination, no SARS-CoV-2 infection before receipt of the first vaccine dose (determined based on either a negative anti-SARS-CoV-2 immunoglobulin (Ig)-M/IgG test or the absence of a positive polymerase chain reaction (PCR) assay result for SARS-CoV-2, with no history of suspected clinical SARS-CoV-2 infection), and ability to understand and complete questionnaires in Chongqing, China. For healthy controls, no underlying disease history was also required. Participants with HIV co-infection, sepsis, cancers, severe extra-hepatic organ dysfunction, pregnancy during study entry, those who did not complete the full-course of vaccination, and those who provided incomplete vaccination information (including the date of their first vaccine dose and complete vaccination, and vaccine manufacturer [due to different vaccine types by manufacturers]) were excluded. All participants in this study provided about 5-10 microliters (mL) of peripheral blood samples for serological assays.

This study was approved by the Ethics Committee of the Second Affiliated Hospital of Chongqing Medical University. All participants signed an informed consent form.

2.2 Variable collection

We collected demographic characteristics (age and sex), history of SARS-CoV-2 infection (yes or no, results of anti-SARS-CoV-2 IgM/IgG and PCR assay for SARS-CoV-2 nucleic acid, and whether had clinical manifestations of SARS-CoV-2 infection), history of diseases, and vaccination-related information (the date of their first vaccine dose and complete vaccination, and vaccine types) in all participants utilizing a standardized questionnaire. Dates of vaccination and the types of vaccine were further confirmed by viewing the individual's health code which contains complete vaccination-related information. Clinical parameters including laboratory test results and comorbidities were also collected from the electronic patient files in the hospital.

Full-course COVID-19 vaccination was defined as having had two vaccinations of inactivated vaccines or three vaccinations for the RBD-subunit recombinant vaccine. The interval time was defined as the days between the final dose and the first blood sample collection for serological assays. In the longitudinal analysis, we divided the time post-vaccination into three points, M1-2 (30-60 days), M3-4 (61-120 days), and >M4 (more than 120 days), respectively.

In patients receiving artificial liver therapy for liver failure, antibody testing was performed before and after treatment to assess the effect of artificial liver therapy on antibody levels. The treatment mode of artificial liver was plasma exchange combined with plasma adsorption.

2.3 SARS-CoV-2 antibody testing

Neutralizing antibodies (NAbs) testing was performed using the commercially available Novel Coronavirus Neutralizing Antibody Detection Kit (Chemiluminescence) (Shenzhen Yahuilong Biological Technology Co., LTD, Shenzhen, China) according to the

Abbreviations: ACLF, acute on chronic liver failure; ALT, alanine aminotransferase; ALP, alkaline phosphatase; AST, aspartate aminotransferase; CI, confidence interval; COVID-19, coronavirus disease 2019; GGT, gamma-glutamyl transferase; HBV, hepatitis B virus; HC, healthy controls; HCV, hepatitis C virus; HEV, hepatitis E virus; INR, international normalized ratio; IQR, interquartile range; NAbs, neutralizing antibodies; OR, odds ratio; RBD, receptor-binding domain; SARS-CoV-2, severe acute respiratory syndrome coronavirus 2; SD, standard deviation; ULN, upper limits of normal.

manufacturer's instructions in use. The cut-off value was determined to be 5.00 AU/mL.

2.4 Statistical analysis

Continuous variables are presented as means and standard deviations (SD) or as medians and interquartile ranges (IQR) for normally and nonnormally distributed data, respectively. Categorical variables are presented as percentages (%). NAbs titers were log2-transformed due to skewed distribution. To compare the distribution of NAbs seropositivity and titers, we used analysis of chi-square tests and Student t-test tests. We used paired t-tests to analyze NAbs titers before and after artificial liver treatment.

We used multiple regression analysis to characterize the association between variables and NAbs response. We adjusted for covariates using the crude model and full adjustment models. The crude model was unadjusted. The full adjustment model was adjusted for age (continuous variable), total bilirubin (continuous variable), cirrhosis (binary variable), ACLF (binary variable), vaccine types (binary variable), and interval time (continuous variable). Data are presented as point estimates and corresponding 95% confidence intervals (CI) of the effect size estimates.

All statistical analysis was performed using SPSS (version 24.0) and R 3.0 (http://www.R-project.org, the R Foundation). All statistical tests were two-sided, and $p<0.05$ was considered statistically significant.

3 Results

3.1 Participant characteristics

A total of 137 patients and 134 healthy controls (HC) were enrolled. Table 1 presents the demographic characteristics, laboratory test results, comorbidities, and vaccination information of these participants. The mean age was 50.2 years (SD: 13.8 years) in patients and 42.6 years (SD:14.8 years) in HC. The proportions of males were 64.2% (88/137) and 38.1% (51/134) in patients and HC groups, respectively. The etiology of liver injury included 38.7% (53/137) of hepatitis B virus (HBV), 19.7% (27/137) of hepatitis C virus (HCV), 5.1% of hepatitis E virus (HEV), 9.5% (13/137) of autoimmune hepatitis, 6.6% (9/137) of alcohol, and 12.4% (17/137) of drugs. Of the 137 patients, 77.4% (106/137) had chronic liver diseases, 47.5% (65/137) had decompensated cirrhosis, and 48.2% (66/137) were diagnosed with acute-on-chronic liver failure (ACLF). The majority of patients and HC received the COVID-19 inactivated vaccine (82.5% *vs* 69.4%, respectively).

3.2 Antibody responses after COVID-19 vaccination

In the cross-sectional study, the seropositivity for NAbs in patients was significantly lower than that in the HC group (65.7% *vs* 80.6%, $p<0.01$) (Figure 1A). The mean NAbs titer in patients was also lower than in the HC group (3.95 *vs* 4.94 $\log_2$AU/ml, $p<0.001$) (Figure 1B). During longitudinal follow-up, both seropositivity and titers of NAbs decreased over time in the patient and HC groups (Figures 1C, D). Between 3 and 4 months, the NAbs seropositivity in the patients decreased from 95.0% to 66.1%, while that in the HC group decreased from 96.0% to 85.7%. Therefore, the NAbs seropositivity in the patients was significantly lower than that in the HC group at M3-4 ($p<0.05$). Over time, only half of the participants were positive for NAbs, either in patients or in HC (55.7%, and 51.4% respectively) (Figure 1C). As for NAbs titers, the rate of decrease in patients was significantly faster than that in the HC group (-2.64 *vs* -0.97 AU/ml per day, $p<0.01$) (Figure 1E). Our results showed that the NAbs responses were impaired in patients with liver dysfunction. In addition, these patients have less persistence of antibody response than the HC group within 3-4 months after vaccination.

3.3 Risk factors for poor antibody response after COVID-19 vaccination in patients with liver injury

To investigate risk factors affecting NAbs response, we compared the distribution of seropositivity and titers according to demographics, clinical parameters, and vaccine types. There were no significantly different in seropositivity and titers of NAbs between age (≤50 *vs* >50

TABLE 1 Characteristics of the participants.

Variables	Patients (n=137)	Healthy controls (n=134)
Age (years), mean (SD)	50.2 (13.8)	42.6 (14.8)
Male, n (%)	88 (64.2)	51 (38.1)
ALT (U/L), median (IQR)	86.0 (40.0-266.0)	29.0 (20.0-35.0)
Total bilirubin (μmol/L), median (IQR)	71.0 (20.0-199.7)	17.1 (11.5-22.5)
Etiology, n (%)		
HBV	53 (38.7)	0 (0)
HCV	27 (19.7)	0 (0)
HEV	7 (5.1)	0 (0)
Autoimmune	13 (9.5)	0 (0)
Alcohol	9 (6.6)	0 (0)
Drug	17 (12.4)	0 (0)
Others	11 (8.0)	0 (0)
Chronic liver diseases, n (%)	106 (77.4)	0 (0)
Cirrhosis, n (%)	65 (47.5)	0 (0)
ACLF, n (%)	66 (48.2)	0 (0)
Vaccine type, n (%)		
Inactivated	113 (82.5)	93 (69.4)
RBD-subunit recombinant	24 (17.5)	41 (30.6)
Interval time (days), mean (SD) *	118.8 (52.7)	91.7 (54.7)

Data are presented as mean (SD), median (IQR), or n (%). ACLF, acute on chronic liver failure; ALT, alanine aminotransferase; HBV, hepatitis B virus; HCV, hepatitis C virus; HEV, hepatitis E virus; IQR, interquartile range; RBD, receptor-binding domain; SD, standard deviation.
*Days between the final dose and first blood sample collection for serological assays.

10.3389/fimmu.2023.1084646

years), total bilirubin level (≤5 times the upper limits of normal [ULN] *vs* >5×ULN), albumin level (<35 *vs* ≥35 g/L), cirrhosis (*vs* noncirrhotic), international normalized ratio (INR) value (≤1.5 *vs* >1.5), ACLF (*vs* non-ACLF), and vaccine types (inactivated *vs* subunit recombinant) (all p>0.05) (Figure 2). However, both seropositivity (54.5% *vs* 85.7%, p<0.05) and titers (3.46 *vs* 4.76 log_2AU/ml, p<0.001) of NAbs in males were significantly lower than those in females (Figure 2B). Compared with the ALT ≤ 5×ULN group, the seropositivity of NAbs was significantly lower in the ALT > 5×ULN group (46.2% *vs* 73.5%, p<0.05), but there was no difference in the mean titers (3.63 *vs* 4.06 log_2AU/ml, p>0.05) between two groups (Figure 2C). In addition, patients with the chronic liver disease also had lower NAbs titers compared to those with acute liver disease (3.59 *vs* 4.78 log_2AU/ml, p<0.001) (Figure 2F).

Next, we performed multiple regression analysis to assess the association of sex, ALT levels, and liver disease status with NAbs response. After adjusting for potential confounding factors including age, total bilirubin, cirrhosis, ACLF, vaccine types, and interval time, male sex (OR: 0.17; 95% CI: 0.06, 0.46; p<0.001) and more severe liver damage (ALT > 5×ULN) (OR: 0.30; 95% CI: 0.12, 0.71; p<0.01) were significantly associated with reduction of the probability of NAbs seropositivity (Table 2). Regarding NAbs titers, male sex (β =-1.18; 95% CI: -1.73, -0.64; p<0.001) and chronic liver diseases (β =-1.45; 95% CI: -2.13, -0.76; p<0.001) were significantly associated with lower NAbs titers (Table 2). Our findings showed that male sex, severe liver injury, and chronic liver diseases have increased risk of poor antibody responses in patients with liver damage.

3.4 Impact of artificial liver therapy on seropositivity and antibody titer

The artificial liver blood purification system is an important treatment for patients with liver failure. It is unclear whether artificial liver therapy will reduce the seropositivity and titer of SARS-CoV-2 antibodies. We conducted pairwise comparisons of the NAbs seropositivity and antibody titers in 26 ACLF patients before and after artificial liver plasmapheresis. The characteristics of these patients are listed in Supplementary Table 1. Interestingly, the seropositivity and titers of NAbs in ACLF patients did not decrease but increased significantly after artificial liver therapy (before *vs* after: 53.8% *vs* 84.6%, p<0.05; 3.55 *vs* 4.32 log_2AU/ml, p<0.001) (Figure 3).

3.5 Sensitivity analysis

To eliminate the potential bias that autoimmune liver disease might introduce to investigating risk factors for NAbs response, we performed a sensitivity analysis. After excluding patients with autoimmune hepatitis, male sex (OR=0.16; 95% CI 0.06, 0.44; p<0.001) and severe liver damage (OR=0.30; 95% CI 0.12, 0.73; p<0.01) were still significantly associated with lower NAbs seropositivity. Male sex (β=-1.21; 95% CI -1.75, -0.66; p<0.001) and chronic liver disease (β=-1.40; 95% CI -2.08, -0.72; p<0.001) also remained associated with lower NAbs titers (Supplementary Table 2).

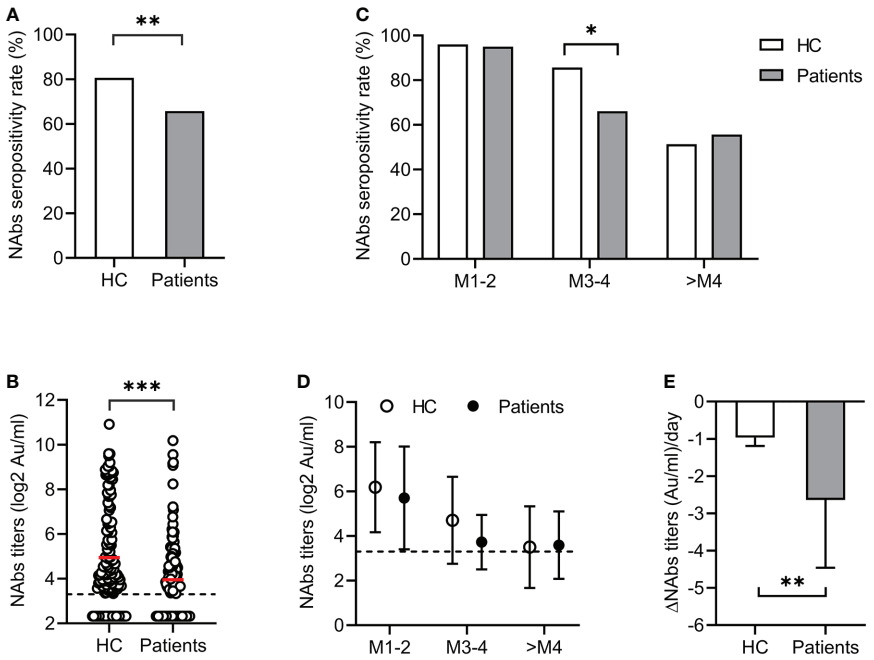

FIGURE 1
Antibody responses after COVID-19 vaccination. The seropositivity **(A)** and titers **(B)** of NAbs in patients with liver dysfunction and healthy controls (HC). Dynamic changes of NAbs seropositivity **(C)** and titers **(D)** over time during longitudinal follow-up. **(E)** Comparison of decline rate of NAbs titers in patients with liver dysfunction and HC groups. *<0.05; **<0.01; ***<0.001. AU, arbitrary units; COVID-19, coronavirus disease 2019; HC, healthy controls; NAbs, neutralizing antibodies.

10.3389/fimmu.2023.1084646

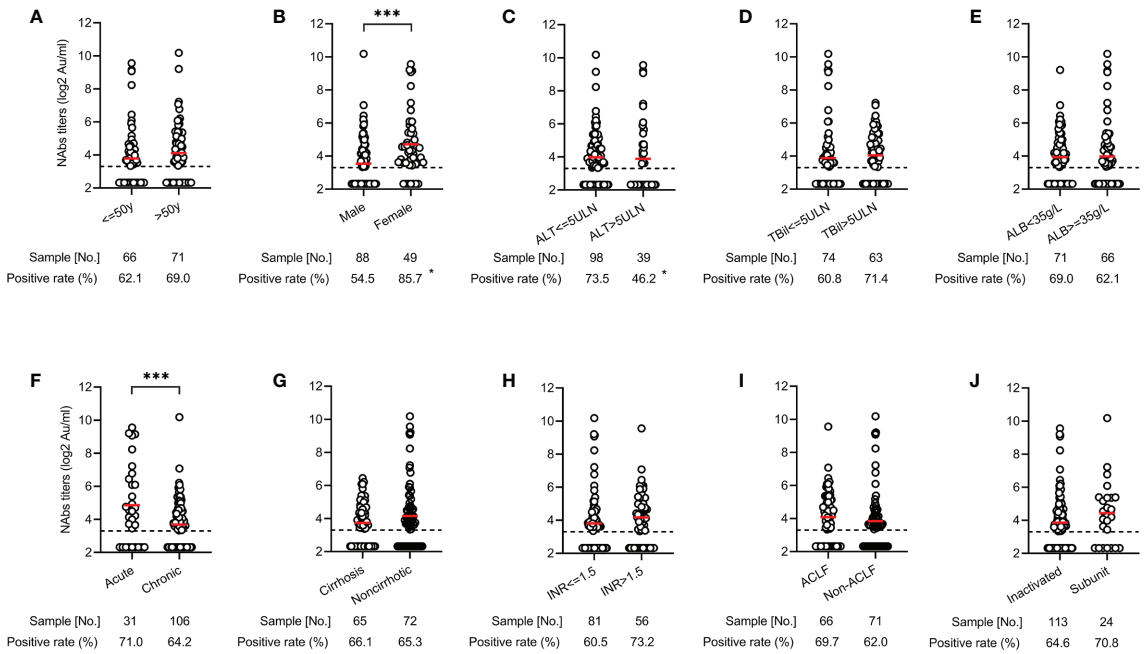

FIGURE 2
Distribution of antibody responses after COVID-19 vaccination across various clinical parameters in patients with liver dysfunction. Comparison of NAbs seropositivity and titers in the different age (≤50 vs >50 years) **(A)**, gender (male vs female) **(B)**, ALT level (≤ 5×ULN vs >5×ULN) **(C)**, total bilirubin level (≤5×ULN vs >5×ULN) **(D)**, albumin level (<35 vs ≥35 g/L) **(E)**, liver disease status (acute vs chronic) **(F)**, cirrhosis (yes vs no) **(G)**, INR value (≤1.5 vs >1.5) **(H)**, ACLF (yes vs no) **(I)**, and vaccine types (inactivated vs subunit recombinant) **(J)**. *<0.05; ***<0.001. ACLF, acute on chronic liver failure; ALT, alanine aminotransferase; COVID-19, coronavirus disease 2019; INR, international normalized ratio; NAbs, neutralizing antibodies; ULN, upper limits of normal.

4 Discussion

In this study, we investigated the effect of liver injury on antibody responses following prior COVID-19 vaccinations and reported three key findings (1): compared with healthy people, the seropositivity and titer of NAbs in patients with liver dysfunction were significantly lower and the titer decreased faster, (2) male sex, severe liver injury and chronic liver diseases have increased risk of poor antibody responses, and (3) artificial liver treatment does not reduce NAbs titers in patients with liver failure.

Most of the patients with liver damage in this study had chronic liver disease, and the study found that the seropositivity and titer of NAbs after COVID-19 vaccination in patients with liver damage were significantly lower than those in healthy subjects. Similar to the results of previous studies (9–12), our research also suggested that the antibody response rate and titer after COVID-19 vaccination in patients with chronic liver disease were reduced, which might be related to the basis of immune impairment in patients with chronic liver disease. This view is also supported by the significantly increased rates of antibody non-response in patients with immunosuppressive

TABLE 2 Multiple regression analysis of risk factors associated with NAbs response to COVID-19 vaccines in patients with liver dysfunction.

Variables	Crude model		Adjusted model	
	OR/β (95% CI)	P value	OR/β (95% CI)	P value
NAbs seropositivity (binary variable)*				
Sex (male *vs* female)	0.20 (0.08, 0.49)	<0.001	0.17 (0.06, 0.46)	<0.001
ALT level (>5×ULN *vs* ≤ 5×ULN)	0.31 (0.14, 0.67)	<0.01	0.30 (0.12, 0.71)	<0.01
Chronic liver diseases (yes *vs* no)	0.73 (0.31, 1.75)	0.48	0.39 (0.13, 1.15)	0.09
NAbs titer (continuous variable)#				
Sex (male *vs* female)	-1.17 (-1.73, -0.61)	<0.001	-1.18 (-1.73, -0.64)	<0.001
ALT level (>5×ULN *vs* ≤ 5×ULN)	-0.09 (-0.72, 0.54)	0.78	0.02 (-0.61, 0.65)	0.96
Chronic liver diseases (yes *vs* no)	-1.17 (-1.83, -0.52)	<0.001	-1.45 (-2.13, -0.76)	<0.001

*Data are presented as OR (95% CI) and p-value. #Data are presented as β (95% CI) and p-value. The crude model adjusts for none. Adjusted model adjust for age (continuous variable), total bilirubin (continuous variable), cirrhosis (binary variable), ACLF (binary variable), vaccine types (binary variable), and interval time (continuous variable). ACLF, acute on chronic liver failure; ALT, alanine aminotransferase; CI, confidence interval; NAbs, neutralizing antibodies; OR, odds ratio; ULN, upper limits of normal.

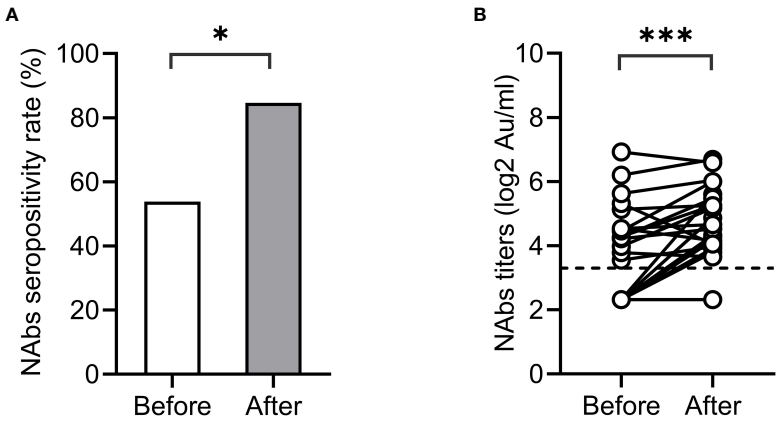

FIGURE 3
Impact of artificial liver therapy on NAbs levels. NAbs seropositivity **(A)** and titers **(B)** before and after artificial liver therapy in patients with liver failure.*<0.001.

liver transplantation, autoimmune liver disease, and patients with systemic diseases mediated by immune disorders (13–16).

In this study, male sex, severe liver injury, and chronic liver diseases were found to be risk factors for poor antibody response. In the phase 3 randomized controlled trial of an inactivated vaccine, antibody response rates were lower in healthy male volunteers than in women (17). Zheng (18) and other studies (19) also found that female participants developed higher titers of NAbs compared to the male sex. In a study of a population with cirrhosis, Zhang and his colleagues (12) found that Child-Pugh score of B and C levels is associated with hyporesponsive to COVID-19 vaccination. However, in this study, the presence of cirrhosis was not found to be associated with either seropositivity or titer of NAbs, possibly due to the relatively small number of patients with cirrhosis observed in our study.

The artificial liver system is an important treatment method for severe liver function injury, especially liver failure, among which plasma exchange and plasma adsorption are the most commonly used modes (20). In some autoimmune diseases, such as systemic lupus erythematosus, plasma exchange, and plasma adsorption can reduce the titer of circulating antibodies in patients to achieve the purpose of disease control (21–23). It is still unclear whether artificial liver therapy will reduce COVID-19 antibody titers in patients with chronic liver disease who have received the COVID-19 vaccine when liver function is severely impaired and liver failure occurs due to disease progression. In this study, in 26 patients with liver failure, the titer of NAbs in patients with artificial liver treatment did not decrease compared with that before treatment. Interestingly, most patients had significantly higher titers of NAbs than before treatment. This phenomenon may reveal that these patients received a large amount of serum from healthy volunteers, while healthy adults in China have extremely high rates of COVID-19 vaccination and antibody response. The duration of changes in antibody titers associated with artificial livers requires further follow-up studies.

Several previous studies have suggested that patients with diseases mediated by immune disorders have significantly reduced antibody responses to COVID-19 vaccines (15, 16). In a prospective observational study including patients with autoimmune liver disease, the use of immunosuppressive agents increases the risk of poor antibody response to inactivated COVID-19 vaccine in AILD patients (14). Considering the potentially negative effects of immunosuppressive agents using in patients with autoimmune hepatitis, we performed a sensitivity analysis after excluding these patients. The results showed that male sex, severe liver damage, and chronic liver disease were still associated with poor antibody responses to the COVID-19 vaccines. These results indicated that our conclusions are robust and reliable.

There are some shortcomings in this study. First, the number and duration of longitudinal follow-up of participants were relatively insufficient. Second, the effects of medications on patients were not analyzed, such as statins. Previous studies have shown that statins can reduce influenza vaccine response (24). Finally, although we adjusted for some important confounding variables (eg, age, vaccine types, interval times, etc.) to make the results reliable, it is undeniable that there are still some confounding factors that were not included.

In conclusion, this study provides evidence for poor response to the COVID-19 vaccines in patients with liver dysfunction. Especially in males, those with chronic liver disease and severe liver injury, the NAbs response will be significantly reduced, resulting in less protective effect.

Author contributions

HL, SL, YL and SZ contributed to the conception and design, analysis, interpretation of the data, and critical revision of important intellectual content. PX, XW and HD collected the data and did the analysis. All authors approved the final version and agreed to be accountable for all aspects of the work. All authors contributed to the article and approved the submitted version.

Funding

This work is supported by the National Natural Science Foundation of China (82173237, 81902068); Senior Medical Talents Program of Chongqing for Young and Middle-aged (No. [2022]15); Program for Youth Innovation in Future Medicine, Chongqing

Medical University (W0082); Kuanren Talents Program of the Second Affiliated Hospital of Chongqing Medical University (SZ, HL).

Acknowledgments

We wish to acknowledge Professor Zhi Zhou of Chongqing Medical University for his full support of our team in completing this study.

Conflict of interest

The authors declare that the research was conducted in the absence of any commercial or financial relationships that could be construed as a potential conflict of interest.

Publisher's note

All claims expressed in this article are solely those of the authors and do not necessarily represent those of their affiliated organizations, or those of the publisher, the editors and the reviewers. Any product that may be evaluated in this article, or claim that may be made by its manufacturer, is not guaranteed or endorsed by the publisher.

Supplementary material

The Supplementary Material for this article can be found online at: https://www.frontiersin.org/articles/10.3389/fimmu.2023.1084646/full#supplementary-material

References

1. Whittaker C, Walker PGT, Alhaffar M, Hamlet A, Djaafara BA, Ghani A, et al. Under-reporting of deaths limits our understanding of true burden of covid-19. *BMJ* (2021) 12:375:n2239. doi: 10.1136/bmj.n2239

2. Shang W, Wang Y, Yuan J, Guo Z, Liu J, Liu M. Global excess mortality during COVID-19 pandemic: A systematic review and meta-analysis. vaccines. *(Basel)* (2022) 12;10(10):1702. doi: 10.3390/vaccines10101702

3. Tulimilli SV, Dallavalasa S, Basavaraju CG, Rao VK, Chikkahonnaiah P, Madhunapantula SV, et al. Variants of severe acute respiratory syndrome coronavirus 2 (SARS-CoV-2) and vaccine effectiveness. vaccines. *(Basel)* (2022) 19;10(10):1751. doi: 10.3390/vaccines10101751

4. Steele MK, Couture A, Reed C, Iuliano D, Whitaker M, Fast H, et al. Estimated number of COVID-19 infections, hospitalizations, and deaths prevented among vaccinated persons in the US, December 2020 to September 2021. *JAMA Netw Open* (2022) 5(7):e2220385. doi: 10.1001/jamanetworkopen.2022.20385

5. Alqahtani SA, Aljumah AA, Hashim A, Alenazi TH, AlJawad M, Al Hamoudi WK, et al. Principles of care for patients with liver disease during the coronavirus disease 2019 (COVID-19) pandemic: Position statement of the Saudi association for the study of liver disease and transplantation. *Ann Saudi Med* (2020) 40(4):273–80. doi: 10.5144/0256-4947.2020.273

6. Boettler T, Marjot T, Newsome PN, Mondelli MU, Maticic M, Cordero E, et al. Impact of COVID-19 on the care of patients with liver disease: EASL-ESCMID position paper after 6 months of the pandemic. *JHEP Rep* (2020) 2(5):100169. doi: 10.1016/j.jhepr.2020.100169

7. C.M.A. Chinese Society of Hepatology. Rapid guideline for COVID-19 vaccination in patients with chronic liver diseases, hepatolbiliary malignancy and liver transplant. *Zhonghua Gan Zang Bing Za Zhi* (2021) 29:523–6. doi: 10.3760/cma.j.cn501113-20210612-00278

8. Cornberg M, Buti M, Eberhardt CS, Grossi PA, Shouval D. EASL position paper on the use of COVID-19 vaccines in patients with chronic liver diseases, hepatobiliary cancer and liver transplant recipients. *J Hepatol* (2021) 74(4):944–51. doi: 10.1016/j.jhep.2021.01.032

9. Wang J, Hou Z, Liu J, Gu Ye, Wu Y, Chen Z, et al. Safety and immunogenicity of COVID-19 vaccination in patients with non-alcoholic fatty liver disease (CHESS2101): A multicenter study. *J Hepatol* (2021) 75(2):439–41. doi: 10.1016/j.jhep.2021.04.026

10. Sripongpun P, Pinpathomrat N, Bruminhent J, Kaewdech A. Coronavirus disease 2019 vaccinations in patients with chronic liver disease and liver transplant recipients: An update. *Front Med* (2022) 9:924454. doi: 10.3389/fmed.2022.924454

11. He T, Zhou Y, Xu P, Ling N, Chen M, Huang T, et al. Safety and antibody response to inactivated COVID-19 vaccine in patients with chronic hepatitis b virus infection. *Liver Int* (2022) 42(6):1287–96. doi: 10.1111/liv.15173

12. Wang J, Zhang Q, Ai J, Liu D, Liu C, Xiang H, et al. Safety and immunogenicity of SARS-CoV-2 vaccines in Chinese patients with cirrhosis: a prospective multicenter study. *Hepatol Int* (2022) 16(3):691–701. doi: 10.1007/s12072-022-10332-9

13. Efe C, Taşçılar K, Gerussi A, Bolis F, Lammert C, Ebik B, et al. SARS-CoV-2 vaccination and risk of severe COVID-19 outcomes in patients with autoimmune hepatitis. *J Autoimmun* (2022) 7:132:102906. doi: 10.1016/j.jaut.2022.102906

14. Li Hu, Wang Y, Ao L, Ke M, Chen Z, Chen M, et al. Association between immunosuppressants and poor antibody responses to SARS-CoV-2 vaccines in patients with autoimmune liver diseases. *Front Immunol* (2022) 5:988004(13). doi: 10.3389/fimmu.2022.988004

15. Boekel L, Steenhuis M, Hooijberg F, Hooijberg F, van Dam KPJ, Besten YR, et al. Antibody development after COVID-19 vaccination in patients with autoimmune diseases in the Netherlands: A substudy of data from two prospective cohort studies. *Lancet Rheumatol* (2021) 3(11):e778–88. doi: 10.1016/S2665-9913(21)00222-8

16. Furer V, Eviatar T, Zisman D, Peleg H, Paran D, Levartovsky D, et al. Immunogenicity and safety of the BNT162b2 mRNA COVID-19 vaccine in adult patients with autoimmune inflammatory rheumatic diseases and in the general population: A multicentre study. *Ann Rheum Dis* (2021) 10:1–9. doi: 10.1136/annrheumdis-2021-220647

17. Tanriover MD, Doğanay HL, Akova M, Güner HR, Azap A, Akhan Sıla, et al. Efficacy and safety of an inactivated whole-virion SARS-CoV-2 vaccine (CoronaVac): interim results of a double-blind, randomised, placebo-controlled, phase 3 trial in Turkey. *Lancet* (2021) 398:213–22. doi: 10.1016/S0140-6736(21)01429-X

18. Xiang T, Liang B, Wang H, Quan X, He S, Zhou H, et al. Safety and immunogenicity of a SARS-CoV-2 inactivated vaccine in patients with chronic hepatitis b virus infection. *Cell Mol Immunol* (2021) 18(12):2679–81. doi: 10.1038/s41423-021-00795-5

19. Li Z, Xiang T, Liang B, Deng H, Wang H, Fenget X, et al. Characterization of SARS-CoV-2-Specific humoral and cellular immune responses induced by inactivated COVID-19 vaccines in a real-world setting. *Front Immunol* (2021) 12:802858. doi: 10.3389/fimmu.2021.802858

20. Li LJ, Zhang YM, Liu XL, Du WB, Huang JR, Yang Q, et al. Artificial liver support system in China: a review over the last 30 years. *Ther Apher Dial* (2006) 10(2):160–7. doi: 10.1111/j.1744-9987.2006.00358.x

21. Kronbichler A, Brezina B, Quintana LF, Jayne DRW. Efficacy of plasma exchange and immunoadsorption in systemic lupus erythematosus and antiphospholipid syndrome: A systematic review. *Autoimmun Rev* (2016) 15(1):38–49. doi: 10.1016/j.autrev.2015.08.010

22. Zanatta E, Cozzi M, Marson P, Cozzi F. The role of plasma exchange in the management of autoimmune disorders. *Br J Haematol* (2019) 186(2):207–19. doi: 10.1111/bjh.15903

23. Hohenstein B, Bornstein SR, Aringer M. Immunoadsorption for connective tissue disease. *Atheroscler Suppl* (2013) 14(1):185–9. doi: 10.1016/j.atherosclerosissup.2012.10.034

24. Chiu H-T, Shen L-J, Chen Y-C, Lin J-H, Wang C-C. Effect of statin use on the risk of medically attended acute respiratory illness among influenza vaccinated elderly. *Vaccine* (2018) 36(41):6133–7. doi: 10.1016/j.vaccine.2018.08.067

frontiers | Frontiers in Immunology

TYPE Review
PUBLISHED 30 January 2023
DOI 10.3389/fimmu.2023.1077236

Check for updates

OPEN ACCESS

EDITED BY
Edwin Bölke,
Heinrich Heine University of Düsseldorf, Germany

REVIEWED BY
Chang Li,
Chinese Academy of Agricultural Sciences (CAAS), China
Zhanbo Zhu,
Heilongjiang Bayi Agricultural University, China

*CORRESPONDENCE
Kurosh Kalantar
Kalantark@sums.ac.ir
Seppo Meri
seppo.meri@helsinki.fi

SPECIALTY SECTION
This article was submitted to Viral Immunology, a section of the journal Frontiers in Immunology

RECEIVED 22 October 2022
ACCEPTED 12 January 2023
PUBLISHED 30 January 2023

CITATION
Nasrollahi H, Talepoor AG, Saleh Z, Eshkevar Vakili M, Heydarinezhad P, Karami N, Noroozi M, Meri S and Kalantar K (2023) Immune responses in mildly versus critically ill COVID-19 patients. *Front. Immunol.* 14:1077236. doi: 10.3389/fimmu.2023.1077236

COPYRIGHT
© 2023 Nasrollahi, Talepoor, Saleh, Eshkevar Vakili, Heydarinezhad, Karami, Noroozi, Meri and Kalantar. This is an open-access article distributed under the terms of the Creative Commons Attribution License (CC BY). The use, distribution or reproduction in other forums is permitted, provided the original author(s) and the copyright owner(s) are credited and that the original publication in this journal is cited, in accordance with accepted academic practice. No use, distribution or reproduction is permitted which does not comply with these terms.

Immune responses in mildly versus critically ill COVID-19 patients

Hamid Nasrollahi[1], Atefe Ghamar Talepoor[2], Zahra Saleh[2], Mahsa Eshkevar Vakili[2], Paria Heydarinezhad[2], Narges Karami[2], Maryam Noroozi[2], Seppo Meri[3]* and Kurosh Kalantar[2,4]*

[1]Radio-Oncology Department, School of Medicine, Shiraz University of Medical Sciences, Shiraz, Iran, [2]Department of Immunology, School of Medicine, Shiraz University of Medical Sciences, Shiraz, Iran, [3]Department of Bacteriology and Immunology, University of Helsinki and Diagnostic Center of the Helsinki University Hospital, Helsinki, Finland, [4]Autoimmune Diseases Research Center, Shiraz University of Medical Sciences, Shiraz, Iran

The current coronavirus pandemic (COVID-19), caused by SARS-CoV-2, has had devastating effects on the global health and economic system. The cellular and molecular mediators of both the innate and adaptive immune systems are critical in controlling SARS-CoV-2 infections. However, dysregulated inflammatory responses and imbalanced adaptive immunity may contribute to tissue destruction and pathogenesis of the disease. Important mechanisms in severe forms of COVID-19 include overproduction of inflammatory cytokines, impairment of type I IFN response, overactivation of neutrophils and macrophages, decreased frequencies of DC cells, NK cells and ILCs, complement activation, lymphopenia, Th1 and Treg hypoactivation, Th2 and Th17 hyperactivation, as well as decreased clonal diversity and dysregulated B lymphocyte function. Given the relationship between disease severity and an imbalanced immune system, scientists have been led to manipulate the immune system as a therapeutic approach. For example, anti-cytokine, cell, and IVIG therapies have received attention in the treatment of severe COVID-19. In this review, the role of immunity in the development and progression of COVID-19 is discussed, focusing on molecular and cellular aspects of the immune system in mild vs. severe forms of the disease. Moreover, some immune- based therapeutic approaches to COVID-19 are being investigated. Understanding key processes involved in the disease progression is critical in developing therapeutic agents and optimizing related strategies.

KEYWORDS

SARS-CoV-2, COVID-19, immune response, cytokine storm, T cells, antibodies, inflammation, therapeutic targets

1 Background

The coronavirus disease 2019 (COVID-19), caused by the severe acute respiratory syndrome- coronavirus- 2 (SARS-CoV-2), is a viral infectious disease spread worldwide (1). The outbreak of COVID-19 has led to extensive global morbidity and mortality (2). The Coronaviridae family contains α and β coronaviruses capable of causing both mild and severe respiratory diseases in wild animals and humans. SARS-CoV, MERS-CoV and SARS-CoV-2 are positive-sense single-stranded RNA β-coronaviruses causing severe respiratory tract infections in humans (3, 4).

SARS-CoV-2 infection can have a variable clinical picture ranging from asymptomatic to severe. In about 5% of patients, there is a risk of death, while the overall mortality is about 1% (5). With increasing vaccine coverage the numbers are getting smaller. SARS-CoV-2 can enter and infect epithelial, and possibly endothelial cells expressing the receptor angiotensin- converting enzyme 2 receptor (ACE2) and, in certain cells, neuropilin-1 (6, 7).

During the initial exposure, the virus infects epithelial cells in the upper respiratory tract through the ACE2 receptor. At this stage, the innate and adaptive immunity try to inhibit the virus at the mucosal sites and prevent the progression of the disease by various mechanisms. These include the production of mucus and antiviral metabolites, interferons and other cytokines, as well as IgA, when there is preexisting immunity to the virus.

SARS-CoV-2 is able to inhibit innate and adaptive immune responses in various ways. It can replicate unchecked in the respiratory tract and eventually spread to the lungs (8, 9). COVID-19 patients may develop a systemic disease with extrapulmonary manifestations. Systemic manifestations during a later stage of COVID-19 are linked to lymphopenia, increased amounts of neutrophils, cytokine release syndrome (CRS) or cytokine storm, activation of complement and coagulation cascades and elevated levels of inflammatory chemokines and alarmins (10, 11). Several studies have shown that male gender, higher age, obesity, diabetes, hematological cancer, autoimmune diseases (e.g., psoriasis), hypertension (especially pulmonary arterial hypertension), and cardiovascular, cerebrovascular and chronic kidney diseases are risk factors closely related to the severity and outcomes of COVID-19 infection (12–16).

Although innate and adaptive immunities are linked, they both also have different cell types with varying functions (17). The innate immune system includes monocytes, macrophages, dendritic cells (DC), myeloid-derived suppressor cells (MDSC) and innate lymphoid cells (ILCs). ILCs can be divided into different groups: natural killer (NK) cells, 3 subsets of helper like ILCs (ILC1, 2 and 3), fetal lymphoid tissue- inducer (LTi) cells and a population of innate intraepithelial lymphocytes (IELs) in the intestine that express T cell markers (18). In addition, the innate response includes a number of molecules, e.g. the entire complement system with more than 40 different soluble or cell-bound components. Innate immune cells expressing pattern-recognition receptors (PRRs) can detect pathogen-associated molecular patterns (PAMPs) of invading viruses to develop and maintain innate immune responses by secreting interferons (IFNs) of type I (IFN-α and IFN-β) and type III (IFN-λ), as well as pro-inflammatory cytokines and chemokines (19, 20). The adaptive immune system comprises B cells, $CD4^+$ T helper and $CD8^+$ cytotoxic T cells. $CD4^+$ T cells orchestrate the immune response by producing cytokines and providing help to other immune cells. $CD8^+$ T cells kill virally infected cells, and B cells develop and produce antigen-specific IgM, IgG and IgA antibodies (21). Larger amounts of specific antibodies are produced by plasma cells that locate themselves into niches in the bone marrow.

Given that appropriate innate and adaptive immune responses are required to control and contain COVID-19 infection and prevent the disease in the long term, it is critical to recognize both types of responses to SARS-CoV-2. This review aims to shed light on the molecular and cellular players of the immune system in COVID-19 pathogenesis. Accordingly, the molecular and cellular compartments involved in the innate and adaptive immune responses to SARS-CoV-2 are thoroughly reviewed (A brief comparison of immune responses in mildly versus critically ill COVID-19 patients has been provided in Table 2). Special emphasis is on delineating differences that distinguish severe disease forms from those of milder forms. Why do certain individuals suffer from serious lung complications and systemic effects, and what is the contribution of the immune system itself in a vicious circle of inflammation in response to a viral infection?.

2 The relationship between the innate immune system and the progression of COVID-19

2.1 Neutrophils

SARS-CoV-2 infection is marked by neutrophil migration into pulmonary capillaries and alveolar spaces, leading to acute capillaritis, fibrin deposition and neutrophilic mucositis (22). Neutrophils display antiviral activity through different mechanisms, including direct, antibody or complement-mediated recognition of the virus and phagocytosis and secretion of cytokines, myeloperoxidase (MPO), elastase and defensins. They can also form neutrophil extracellular traps (NET) and modulate adaptive antiviral immunity (23–25). Recent studies have found increased neutrophil counts in the peripheral blood of non-surviving and severely ill COVID-19 patients compared to mildly ill cases. In addition, increased numbers of low-density neutrophils have been found in the blood of acute COVID-19 patients (26, 27). Different populations of granulocytes in the blood could reflect emergency myelopoiesis. Some of the granulocytes (N2-type) could be immunosuppressive and cause impaired lymphocyte responses during acute disease (28). Previous studies have also observed a high neutrophil- to- lymphocyte ratio (NLR) in critically ill COVID-19 patients compared to cases with mild disease. Therefore, NLR has been introduced as an independent risk factor for severe disease (27, 29, 30). High levels of MPO and citrullinated histone H3 (Cit-H3), serum markers of NETs and indicators of neutrophil activation have also been described in severe COVID-19 (31–33). It has thus been concluded that neutrophilia and excessive formation of NETs, as well as the release of reactive oxygen species (ROS), in severe COVID-19 trigger cytokine release and respiratory failure, contributing to disease severity (22, 34, 35). The changes in innate immune cells in COVID-19 are summarized in Figure 1.

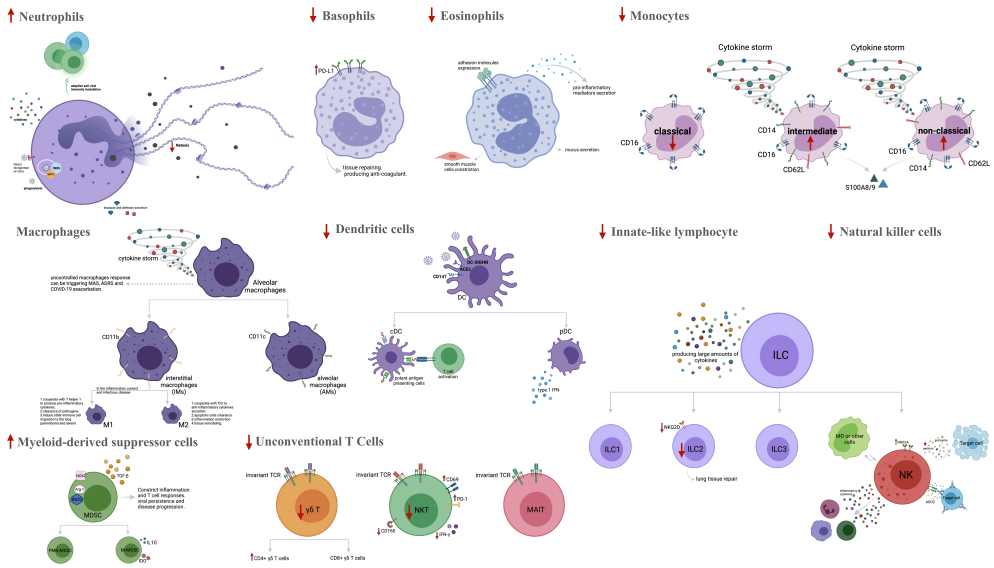

FIGURE 1
The frequency and function of innate immune cells in severe COVID-19. SARS-CoV-2 infects cells that present the surface receptor ACE2. It is recognized by tissue-resident immune cells in the lungs, which provoke a local immune response. More innate immune cells are recruited from the blood by chemokines and complement activation products. The amounts of neutrophils, $CD16^+$ monocytes, M1 macrophages and MDSCs are bigger in severe COVID-19 patients, while the percentages of basophils, eosinophils, M2 macrophages, classical monocytes, DCs, ILCs, NK cells and unconventional T cells are reduced. Activated neutrophils can amplify inflammation by secretion of pro-inflammatory cytokines, MPO, elastase and defensins. They can also promote NET formation and Th17 cell differentiation. Activated basophils and eosinophils appear to predispose the development of ARDS by releasing inflammatory and vasoactive substances. Peripheral $CD16^+$ monocytes and M1 macrophages are involved in a hyper-inflammatory response and cytokine storm during the inflammatory phase in severe COVID-19. Significant decrease in viral sensing and IFN signaling as well as suppressed antigen presentation by both pDC and cDC have been reported in severe COVID-19. Aberrant or ineffective responses of ILCs (ILC1, ILC2, ILC3 and NK cells), MDSCs and unconventional T cells (MAIT cells, γδ T cells) also have role in promoting inflammation in severe COVID-19. ACE2, Angiotensin-converting enzyme 2; MDSCs, Myeloid-derived suppressor cells; DC, Dendritic cell; ILCs, Innate-like lymphocyte; NK cell, Natural killer cell; MPO, Myeloperoxidase; NET, Neutrophil extracellular trap; Th, T helper; ARDS, Acute respiratory distress syndrome; MAS, Macrophage activation syndrome; PD-L1, Programmed cell death ligand 1; IFN: Interferon; cDC, Classical DC; pDC, Plasmacytoid DCiNOS, Inducible nitric oxide synthase; PMN-MDSCs, Polymorphonuclear-MDSCs; M-MDSCs, Monocytic-MDSCs; ADCC, antibody-dependent cellular cytotoxicity; NKG2A, NK cell lectin-like receptor subfamily C member 1. Figure was created by BioRender (Toronto, ON, Canada).

2.2 Monocytes

Monocytes are a pivotal component of the innate immune response. They participate in inflammatory responses, phagocytosis, antigen presentation and other immune functions (36, 37). Human monocytes are classified into classical ($CD14^{high}$ $CD16^-$), intermediate ($CD14^{high}CD16^+$) and non-classical ($CD14^{low}$ $CD16^+$) subsets (38). Intermediate and non-classical monocytes are known as the "inflammatory" subsets due to their potent pro-inflammatory activity. They contribute to various conditions such as asthma, coronary artery disease, Crohn's disease, sepsis and hepatitis B (39). Recent studies have demonstrated that inflammatory monocytes are involved in the hyper-inflammatory response and cytokine storm observed during the infectious and inflammatory phases of severe COVID-19 (40). The results indicate that the absolute numbers of all blood and $CD16^-$ classical monocytes decrease in severely ill COVID-19 patients, while the levels of the inflammatory subsets increase in patients in comparison to the healthy controls (41). One study showed an increased percentage of inflammatory monocytes expressing S100A8+ S100A9 (calprotectin), CD14 and CD62L, possibly correlating with a profibrotic differentiation pattern in severe COVID-19 as compared to mild disease (42). Furthermore, a significant increase in the frequency of $CD14^{high}$ $CD16^+$ monocytes producing IL-6 was reported in the peripheral blood of COVID-19 patients in the ICU compared to those without ICU hospitalization (43, 44). An increased number of inflammatory monocytes in patients with mild disease has also been reported in several studies. This could be considered as an indicator of viral control in such patients (45, 46).

2.3 Macrophages

The function of alveolar macrophages in the lungs is to preserve homeostasis by removing dead cells and invading pathogens (47). Under steady-state, two distinct populations of macrophages, the interstitial macrophages (IMs) and alveolar macrophages (AMs), are present in the lungs (48, 49). Interstitial macrophages are characterized as $CD11b^+CD11c^-$ cells localized in the parenchyma, while AMs are identified as $CD11b^-CD11c^+$ macrophages residing in the air space lumen (50). In inflammation and infectious diseases, alveolar macrophages are polarized into the M1 or M2 subgroup (47). M1 macrophages cooperate with T helper (Th) 1 cell to produce pro-inflammatory cytokines and clear pathogens. They also induce the migration of other immune cells to the lung parenchyma and alveoli. M2 macrophages are associated with Th2 cells to increase the secretion of anti-inflammatory cytokines and clearance of apoptotic or senescent cells. Thus, the M2 cells restrict inflammation and promote tissue remodeling (47, 51).

Based on recent data, macrophages are considered promoters of the cytokine storm during infection by SARS-CoV-2. They are

associated with severe COVID-19 with a high risk of death (52, 53). Moreover, the cytokine storm, mainly macrophage activation syndrome (MAS), in addition to complement and neutrophil activation, contributes to COVID-19-associated adult respiratory distress syndrome (ARDS) and its exacerbation (54, 55). Another study reported a significant correlation between SARS-CoV-2 infection of macrophages in the spleen and lymph nodes and severe lymphocyte apoptosis in COVID-19 patients (27). Recent studies by single-cell RNA sequencing of samples recovered from bronchoalveolar lavage fluid of mildly and severely ill COVID-19 patients have revealed that SARS-CoV-2 infection leads to the recruitment of an inflammatory macrophage subset with down-regulation of type I IFN genes, which is related to disease severity (56–58). In conclusion, macrophages sense SARS-CoV-2 and respond to its threat by secreting pro-inflammatory cytokines and chemokines. However, an uncontrolled macrophage response could trigger MAS, ARDS and an exacerbation of COVID-19 (42).

2.4 Dendritic cells

Among other places, DCs are distributed in the respiratory tract, where they can recognize invading microbes. SARS-CoV-2 can gain entry into DCs, particularly into interstitial lung DCs, *via* ACE2, CD147 and dendritic cell-specific intracellular adhesion molecule-grabbing non-integrin (DC-SIGN) receptors (59). Classical myeloid DCs (cDCs) and plasmacytoid DCs (pDCs) are two distinct DC subsets in humans. The former serve as potent antigen- presenting cells (APCs), while the latter is a specialized subset that can produce type 1 IFN (60, 61). It has been found that pDC along with viral sensing, interferon signaling and antigen presentation are more defective in severe versus mild COVID-19 (62–68). Further impairment in DC maturation and function in severe vs. mild disease may be associated with a worse disease (69). In addition, another study reported that the frequency of DCs in the blood of COVID-19 patients decreased compared to healthy controls. It was found that DCs from individuals with acute COVID-19 were functionally impaired in maturation and in the ability to activate T cells (43, 70). Two recent studies found both types of DCs (cDCs and pDCs) to be much less abundant in the blood samples of people with severe COVID-19 than in those with mild COVID-19 (71, 72).

2.5 Innate-like lymphocytes

ILCs are effector cells that detect environmental stimuli and contribute to early immune responses by producing large amounts of cytokines (73). They are categorized into four main groups: NK cells, ILC1, ILC2, and ILC3 (74, 75). Transcriptionally and functionally, the ILC1, ILC2, and ILC3 resemble Th1, Th2, and Th17 cells, respectively, while NK cells resemble $CD8^+$ T cells (73). However, little is known about the distribution and function of different ILC subsets in COVID-19. Recent studies have reported a reduced percentage and lower absolute counts of ILCs in the blood of COVID-19 patients (73). Accordingly, results have shown a significant decrease in the frequency of ILC2 in severe compared to moderate COVID-19 (73). Furthermore, previous studies have observed that the frequency of ILC2s in COVID-19 patients negatively correlates with the level of the coagulation factor fibrinogen-derived D-dimer and the development of severe disease (76, 77). ILC2s could thus have a protective role in the disease.

Previously, it has been shown that ILC2 plays an important role in lung tissue repair during *influenza A* infection in mice (78). Therefore, it can be hypothesized that low ILC2 levels in COVID-19 patients correlate with a more severe disease outcome. One further investigation reported a decreased frequency of all ILCs, and particularly of the ILC2 subpopulation, in severe COVID-19. Also, compared to mildly diseased patients, it was observed that the expression of $NKG2D^+$, the activating C-type lectin-like molecule, on ILC2s was significantly reduced in patients requiring mechanical ventilation (79). Therefore, an increase in $NKG2D^+$ ILC2s, along with elevated levels of anti-inflammatory mediators, might be related to a better prognosis in severe COVID-19 (Figure 1).

2.6 Natural killer cells

NK cells are the most important innate immune cells in fighting viral infection. This is because they can induce direct lysis of target cells by producing perforin and granzyme B, secrete inflammatory cytokines, contribute to antibody-dependent cell cytotoxicity (ADCC) and interact with other immune cells such as monocytes (80). A significant decrease in the absolute number of NK cells in the peripheral blood of patients with severe COVID-19, as well as in those admitted to ICU, has been reported recently (81–83). According to Leem et al., unconventional $CD56^{dim}CD16^{neg}$ NK cells, associated with decreased cytotoxic activity, expanded in both severe and mild forms of the disease. These changes were reversed more rapidly in mild vs. severe COVID-19 (84). Another study showed that the percentage of $perforin^+$ NK cells in COVID-19 patients, who were in the ICU, was reduced as compared with non-ICU patients and healthy controls (85). Previous studies have shown an increased expression of the inhibitory receptor NKG2A on NK cells in severely ill COVID-19 patients, as compared to mildly ill patients and healthy subjects (86). NKG2A expression along with decreased IFN-γ, granzyme B, and TNF-α production is associated with NK cell exhaustion and disease progression in COVID-19 patients. Further, the percentage of NK cells expressing NKG2A is reduced in COVID-19 patients, who recovered after receiving proper therapy (27, 87). Hajeer et al. found an association between two NK cell immunoglobulin-like receptors (KIR), named KIR2DS4 and KIR3DL1, with an inhibitory and activating function, respectively, and an increased risk of severe disease (88). Another study reported a significant decrease in the inhibitory KIR receptors in COVID-19 patients compared to healthy controls and a considerable increase in activating KIR receptors in patients with a severe disease (89) (Figure 1).

2.7 Basophils

Basophils are a type of granulocyte representing less than 1% of peripheral blood leukocytes (90). As they are involved in tissue repair and production of anti-coagulant factors, their depletion results in

increased pneumonitis in COVID-19 (91). In recent studies, a significant decrease has been observed in the frequency and the absolute numbers of basophils in patients with severe COVID-19 (82, 92, 93). Moreover, a stronger expression of programmed cell death ligand 1 (PD-L1), an inhibitor of T cell activation, has been found on basophils in severe vs. mild COVID-19, correlating with poor disease outcomes (89).

2.8 Eosinophils

Eosinophils are multifunctional granulocytes involved in various inflammatory contexts, including helminth, bacterial and viral infections, tissue injury, tumor immunity and allergic diseases. They secrete pro-inflammatory mediators, express adhesion molecules and support smooth muscle cells (94, 95). Significantly decreased eosinophil counts have been found in COVID-19 patients compared to healthy controls or patients with mild disease (82, 96). A decrease in eosinophil counts is related to fever, fatigue, shortness of breath and poor outcome in COVID-19 patients (96, 97).

2.9 Myeloid-derived suppressor cells

In humans, MDSCs are classified into polymorphonuclear-MDSCs (PMN-MDSCs) and monocytic-MDSCs (M-MDSCs), which control inflammation and T cell responses through a high-level expression of inducible nitric oxide synthase (iNOS), arginase-1 (Arg-1), nicotinamide adenine dinucleotide phosphate oxidase (NOX2) and transforming growth factor-beta (TGF-β) (98). In viral infections, MDSC-mediated immunosuppression causes viral persistence and disease progression (99). A recent study showed a significantly higher frequency of PMN-MDSCs in the peripheral blood of patients with severe COVID-19 and in those who required ICU compared to healthy blood donors (98). This correlated with decreased antigen-specific T cell responses and poor disease outcomes (98). Another study demonstrated an increased frequency of MDSCs in both mild and severe COVID-19. According to this study, MDSC expansion during the early phase of acute infection was protective by reducing T cell hyperactivation and inflammation but could also decrease the protective immune response (100). The percentage of M-MDSCs correlated positively with neutrophil count, C-reactive protein (CRP) and D-dimer levels, hospital stay and viral RNA load and negatively with lymphocyte count and serum albumin in COVID-19 patients admitted to ICU compared to healthy controls and non-ICU patients (101). An increase in MDSC recruitment and expansion along with impaired T cell function was observed in severe COVID-19. This was related to IL-10, arginase-1 and indoleamine 2,3-dioxygenase (IDO) production by MDSCs (102, 103).

2.10 Unconventional T cells

Unconventional T or innate-like T cells, such as natural killer T (NKT), mucosa-associated invariant T (MAIT) and γδ T cells, exhibit characteristics of both innate and adaptive cells. They express T cell receptors (TCRs) with limited diversity and recognize alternative microbial antigens in major histocompatibility complex (MHC)-unrestricted compartments (74). Most responses of NKT and γδ T cells seem to be stimulated against pathogenic agents. In particular, the potent cytotoxic responses of these cells in patients infected with influenza A viruses, herpes viruses or lentiviruses may be essential for suppressing viral replication and regulating immunosuppressive MDSCs (104–110). Recent studies have shown a reduced frequency of NKT cells in patients with severe COVID-19 and a small PaO2/FiO2 (P/F) ratio (82, 111). An increased expansion of $CD160^+$ NKT cells has been reported in mild COVID-19, possibly supporting recovery from infection by direct cytotoxicity (112). Furthermore, decreases in the levels of circulating NKT cells and IFN-γ production are observed in severe COVID-19. However, the expression levels of CD69 and PD-1 are increased in NKT cells, and a strong PD-1 expression in NKT cells continues in patients in ICU on day 15 (113). Another study showed that while the total percentage of γδ T cells decreased in COVID-19 patients, the percentage of $CD4^+$γδ T cells significantly increased (114). It was suggested that the latter subset might be associated with antigen presentation and activation of adaptive immune cells (114). Based on another investigation, increased frequencies and absolute numbers of naïve-like ($CD45RA^+CD62L^+$) γδ T cells and a decreased frequency of effector-like ($CD45RA^-CD62L^-$) γδT cells were observed both in mild and severe COVID-19. This study suggested that effector-like γδ T cells might be localized in the lungs of COVID-19 patients to contribute to the immune response against the infecting virus (115) (Figure 1).

2.11 Complement system

The complement system belongs mostly to innate immunity. It can respond to invading microbes and other foreign materials (22, 116). It may recognize SARS-CoV-2 directly or with the help of antibodies. Additionally, tissue damage caused by the virus can activate complement. Complement activation can lead to acute or chronic inflammation, thrombus formation, endothelial cell dysfunction and intravascular coagulation, thus ultimately contributing to multiple organ failure (MOF) and death (117). A recent study showed prominent complement activation in the lungs, skin and blood of severely ill COVID-19 patients compared to cases with mild disease. Some individuals treated with a complement inhibitor recovered with no adverse reactions (118). Complement activation generates the pro-inflammatory polypeptides, C3a and C5a, which can recruit and activate neutrophils and monocytes. Mannose-binding lectin (MBL) interacts with SARS-CoV-2 and could consequently activate complement C3 *via* the lectin pathway (119). Through neutrophil extracellular trap (NETs) formation, neutrophils activate the alternative complement pathway and may engage an inflammatory feedback loop. Recently, a significant correlation has been found between the activation of complement component C3 and COVID-19 severity (120, 121). Similarly, an investigation showed higher levels of C3a and C5a as well as C3-fragment deposition in the lung biopsy samples of severe COVID-19 patients (122). Furthermore, in a further study, high levels of soluble C5a and an increased expression of the C5a receptor in blood and pulmonary myeloid cells were found in severe COVID-19 with acute

respiratory distress syndrome compared to mildly diseased patients and controls (123). Thus, multiple features of severe COVID-19 point to the importance of complement activation in its pathogenesis, mainly during inflated inflammatory responses and effects on vascular endothelial cells, including promotion of blood coagulation and increased capillary permeability.

3 The relationship between the adaptive immune system and the progression of COVID-19

3.1 Cell-mediated immunity

$CD4^+$ and $CD8^+$ T cells play important roles in resolving acute viral infections and providing subsequent protection against reinfection. DCs induce polarization and maturation of naive T cells *via* the presentation of peptides in the context of MHC along with the secretion of chemokines and cytokines. Subsequently, activated T cells migrate to the site of infection, producing antiviral cytokines, chemokines and cytotoxic molecules (124). Acute and severe SARS-CoV-2 infections are associated with lymphopenia and remarkable loss of $CD4^+$ and $CD8^+$ T cells, which is reversed by disease recovery (125–127). Transient lymphopenia may be associated with a direct effect of SARS-CoV-2 infection on the production and/or differentiation of lymphocytes in primary lymphoid organs and their release into the circulation (115, 128). High levels of IL-6, IL-10 or TNF-alpha directly promote thymic dysfunction and indirectly promote T cell apoptosis (127, 129–132). In early studies on COVID-19, impairment in function and increased expression of markers, which are hallmarks for activation and/or exhaustion of $CD4^+$ and $CD8^+$ T cells, were observed in patients. The expression levels of Ki-67, PD-1, perforin and granzyme B in $CD4^+$ or $CD8^+$ T cells were found to be high in patients with severe disease (133, 134). Some studies have considered the PD-1/PDL-1 axis as a severity-associated biomarker that can inform about lymphocyte depletion/exhaustion (135, 136). However, it seems that the stronger expression of T cell inhibitory molecules (PD-1 and Tim-3) in severe vs. mild COVID-19 might not only indicate T cell exhaustion but could also suggest the existence of antigen-specific T cells (77, 137, 138). Recent studies, including more than 1000 COVID-19 cases, have indicated that a reduced frequency of $CD4^+$ T cells is related to disease severity (139, 140). The lower proportion of SARS-CoV-2-specific $CD4^+$ $CD154^+$ T cells, which are unable to secrete IL-2 and IFN-γ following stimulation with S- protein, and weaker humoral immune responses have been reported in asymptomatic individuals with SARS-CoV-2 infection. In the symptomatic group, the higher frequency of SARS-CoV-2-specific $CD4^+$ $CD154^+$ T cells was significantly correlated with higher serum levels of SARS-CoV-2-specific IgA, IgG and IgM antibodies (141). Different subpopulations of $CD4^+$ T cells, such as Th1, Th2, Th17 and regulatory T cells (Treg), have been found to accumulate in COVID-19 patients. In the following, the subpopulations of $CD4^+$T cells, as well as $CD8^+$ T cells and memory T cell subsets in COVID-19 inflammatory conditions, will be discussed.

3.2 Th1 cells

Previous studies have indicated that Th1 responses could play protective roles in the early phase of SARS-CoV-2 infection (142). Indeed, highly functional and terminally differentiated effector Th1 cells that eliminate infected target cells have been identified in the early phase of COVID-19 (143, 144). A decreased expression of IFN-γ on $CD4^+$ T cells has also been shown in severe COVID-19 cases (145). Moreover, Th1 hypo-activation is associated with a poor prognosis of the disease, and a lower percentage of Th1 cells is observed in severe COVID-19 patients compared to mild patients (146, 147). Earlier investigations suggested that in comparison to mild COVID-19, increased expansion of peripheral neutrophils in severe COVID-19 potentially suppresses Th1 cell differentiation and triggers Th17 cell polarization (148) (Figure 2).

3.3 Th2 cells

Th2 cells usually mount an appropriate immune response against extracellular pathogens. A recent study showed that Th2 hyper-activation and higher plasma levels of Th2-produced cytokines, including IL-4, -5, -10, and -13, significantly correlated with COVID-19 severity and its related mortality (146, 147). Some studies have highlighted the possible role of Th2 responses in immune-driven lung injury and ARDS progression (142, 143). The association between an increased percentage of Th2 cells and critical care, as well as the poor prognosis, is reported in COVID-19 patients (149) (Figure 2).

Th17 cells secrete IL-17 and induce effector cells and inflammatory cytokine production that amplifies uncontrolled systemic inflammation and triggers tissue injury as well as multi-organ failure and death. Several studies have demonstrated that increased frequency and hyper-activation of Th17 cells and subsequent production of pro-inflammatory cytokines are related to the poor outcomes of COVID-19 (35, 142, 145, 148, 150–156). Recently, a higher percentage of $GM\text{-}CSF^+$ $IL\text{-}6^+$ $CCR6^+$ Th17 cells has been detected in the blood circulation of COVID-19 patients (43). According to new research, Th17 hyperactivation and signaling are significantly correlated with a critical form of COVID-19 (148, 153).

3.4 Treg cells

Current evidence indicates smaller amounts of Treg cells in correlation with disease severity in the peripheral blood of COVID-19 patients (115, 157, 158). The frequency of this subset increases during the recovery phase of the disease (159). The decrease in the frequency of Tregs in the peripheral blood of COVID-19 cases might be related to Treg migration into the lungs to resolve lung injury. Besides, there is some evidence of enhanced apoptosis of Tregs due to reduced IL-2 levels in severe compared to mild cases (139, 154, 160–162). A higher frequency of Treg cells in the early phase and a lower frequency in the late phase of SARS-CoV-2 infection could be associated with poor outcomes of COVID-19 (139, 154, 160–162). Accordingly, a decrease in Treg cells along with an increase in Th17 cells is associated with the deregulated pro-inflammatory cytokine secretion in COVID-19 patients (163) (Figure 2).

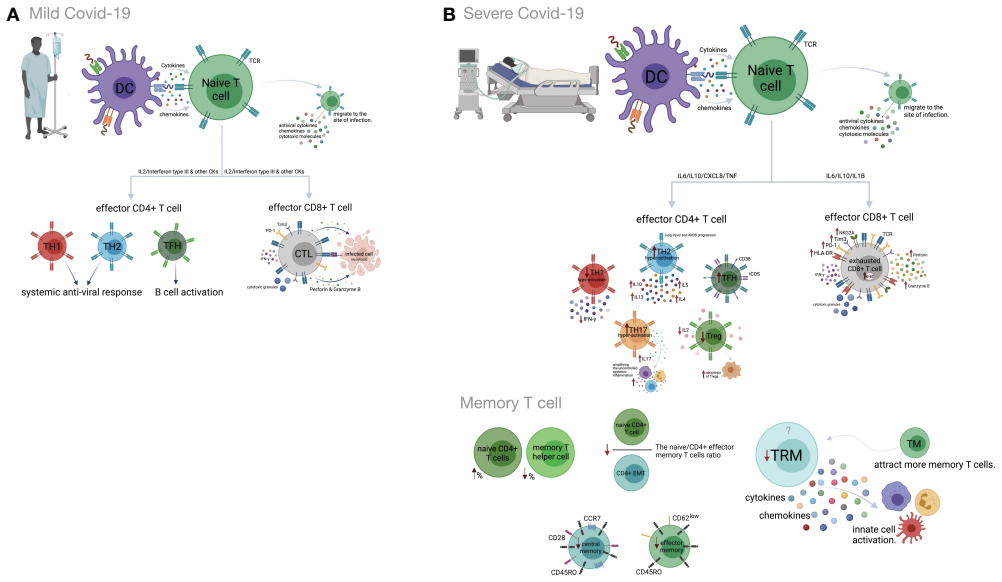

FIGURE 2
Cell-mediated immune responses during COVID-19 progression in mild versus severe disease. **(A)** Dendritic cells (DCs) promote activation of T cell responses by presentation of SARS-CoV-2 antigenic peptides in major histocompatibility complex (MHC) molecules along with costimulatory interactions and the secretion of chemokines and cytokines. T cell responses can mainly be polarized into T helper (Th) cells and effector cytotoxic cells (CTLs). In mild COVID-19, a higher proportion of Th1 cells plays an important role in defense against the virus by producing interleukin-2 (IL-2) and interferon-gamma (IFN-γ). Th1 cells and the cytokines they secrete activate macrophages, CTLs and natural killer (NK) cells. The Th2 cells stimulate the humoral response and activate eosinophils, basophils and mast cells through IL-4 and IL-5 secretion. The T follicular helper (Tfh) cells are essential for the formation of germinal centers (GCs), B cell maturation and immunoglobulin (Ig) production. $CD8^+$ T cells, which coordinate the protective antiviral activities in COVID-19, secrete cytotoxic granules containing perforin and granzyme B as well as IFN-γ in patients who developed mild disease. **(B)** Lymphopenia is a hallmark feature of patients with severe COVID-19. This may be the result of the migration of enormous numbers of T cells to the lungs and other sites of inflammation. Both $CD4^+$ and $CD8^+$ T cells express strongly CD69, CD38, CD45RO, CD44, HLA-DR, programmed cell death protein-1 (PD-1), T cell immunoglobulin domain and mucin domain-3 (TIM-3) and killer cell lectin-like receptor subfamily C member 1 (NKG2A), which can represent hyperactivated, exhausted or a hypoactivated state of T cells in severe patients. Furthermore, the numbers and functions of regulatory T cells (Treg) are significantly reduced in these patients. Smaller proportions of $CD4^+$ and/or $CD8^+$ effector cells ($CD45RO^+$ $CD45RA^-$ $CCR7^-CD28^-$ $CD62L^{low}$), central memory cells ($CD45RO^+$ $CD45RA^-$ $CCR7^+$ $CD28^+$) and tissue-resident memory ($CD69^+$ $CD103^+$ $CD49a^+$) T cells were demonstrated in severe COVID-19 patients. Figure was created by BioRender (Toronto, ON, Canada).

3.5 CD8+ T cells

$CD8^+$ T cells exert their antiviral activity by killing or inducing apoptosis of infected cells. This occurs by release of cytotoxic granules (154) and secretion of cytokines (164). Several studies reported lower $CD8^+$ T cell counts in patients, even with mild or moderate, but especially with severe or critical COVID-19 (160, 165–168). A decreased frequency of $CD8^+$ T cells in non-survivors was reported until death (169). The percentage of $HLA\text{-}DR^+$ $PD\text{-}1^+$ $Tim\text{-}3^+$ $NKG2A^+$ activated $CD8^+$ T cells has been reported to be higher in patients with severe than mild COVID-19 (154, 170, 171). These findings suggest that hyper-active $CD8^+$ T cells may play a protective role in the early phase of COVID-19, but rather a pathogenic role in the late phases of the disease due to reduced cytotoxic function and increased cytokine production (160).

3.6 Memory T cells

Memory T cells display rapid responses against subsequent infection with similar or related pathogens (172). SARS-CoV-2-specific memory T cell responses in the early recovery phase have been reported recently (138). Compared to mild disease, an increased percentage of naïve $CD4^+$T cells and a decreased percentage of memory T helper cells are observed in severe COVID-19 (173). Also, reduced frequencies of $CD4^+$ and/or $CD8^+$ effector and central memory T cells have been observed in severe compared to mild COVID-19. The naive/effector $CD4^+$ memory T cell ratio, an indicator of the differentiation from naive to memory T cells, is reduced in severe cases due to severe impairment of adaptive immunity (14, 174). Tissue-resident memory T cells secrete cytokines and chemokines, resulting in the activation of innate cells and an increase in the recruitment of memory T cells from the periphery (175, 176). Although airway-resident memory T cells mediate protective immune responses against emerging respiratory coronaviruses, the role of this memory subset in the immunopathogenesis of SARS-Cov2 infection should be analyzed further (177). Accordingly, studies on COVID-19 patients, who required ICU treatment, have revealed a lower frequency of tissue-resident memory T cells than effector-memory T cells (178). Likewise, tissue-resident memory-like Th17 cells (TRM17 cells), characterized by an aberrant cytokine profile, are found in the lungs of recovered cases (179). Despite these findings, some studies state that the enrichment of virus-specific $CD8^+$ TRM cells in the patients´

respiratory system is positively correlated with the degree of lung damage and even contributes to damage after the recovery (180) (Figure 2).

3.7 Humoral immunity

In addition to antibody production, B cells display antiviral immune responses through the secretion of inflammatory mediators and T cell activation through antigen presentation (181–183). These cells are a pivotal source of neutralizing antibodies (Abs) that interfere with viral infections, including SARS, MERS, HIV and Ebola. They bind to the virions and prevent their entry into the host cells. Antibodies may activate the complement system and kill infected cells through antibody-dependent cellular cytotoxicity (ADCC) (126, 184, 185). On the other hand, antibodies could also facilitate viral infections by increasing virion uptake *via* Fc or complement receptors. The former is referred to as antibody-dependent enhancement (ADE). ADE has been observed in dengue virus, HIV, influenza, RSV and Ebola, as well as SARS-CoV-2 infections (181, 186–188).

Impaired cellular and humoral immune responses have been reported in COVID-19 patients (5, 189). B cell immune responses to SARS-CoV-2 infection have been found to be stronger in severe than in mild COVID-19. Accordingly, increased clonal expansion of B cells, and frequencies of plasmablasts, complement activation and phagocytosis have been reported in severe cases (190, 191). Similarly to chronic hepatitis B infection, the overall amounts of B cells are large in severe COVID-19 cases. However, the B cell responses are deficient due to decreased clonal diversity. In addition to decreased T cell activity, this is another cause for improper immune responses against infectious agents in elderly individuals (192, 193). Conversely, several studies have reported decreased absolute numbers and frequencies of B cells, as well as lower expression of genes associated with BCR activation signaling, in severe vs. mild COVID-19. This might be due to the consumption of B cells by SARS-CoV-2 in order to inhibit immune activity (2, 83, 154, 194–198).

Also memory B cells are produced after infection with SARS-CoV-2. They include classical $CD24^+$ class-switched memory B cells, activated $CD24^-$ and natural unswitched $CD27^+$ IgD^+ IgM^+ subsets. Recently, reduced frequencies of switched and unswitched memory B cells have been observed in severe COVID-19 patients (83, 190, 197, 199–201). In contrast, some studies have reported higher percentages of SARS-CoV2-S-specific memory B cells in severely ill compared to mildly ill patients. The memory B cell levels remain stable several months after disease resolution and provide protection against future exposure (202–206). In one study, a higher proportion of double-negative B cells (IgD^- $CD27^-$) was reported in severe COVID-19 (199, 207, 208). These cells exacerbate disease progression, possibly by cytokine secretion (209–212). Increased frequencies of $CD21^+$and $CD21^{low/-}$ transitional B cells have also been observed in mild to moderate and severe forms of COVID-19 (190, 199).

Many studies have shown high titers of antibodies in severe COVID-19 that do not correlate to disease resolution (83, 154, 178, 191, 213–216). Indeed, it has been shown that anti-spike IgG could promote pro-inflammatory responses in M1 macrophages, disruption of endothelial barriers, and microvascular thrombosis (217). This type of thrombotic microangiopathy could be mediated by complement activation. Moreover, anti-SARS-CoV-2 antibodies could enhance virus entry into immune cells through the ADE mechanism (166, 218, 219). In severely ill patients, increased production of autoantibodies, such as antinuclear (ANAs), anti-phospholipid and anti-cardiolipin antibodies, have been associated with poor outcomes (219, 220). They could be due to polyclonal B cell activation or be induced by tissue damage. Also, several studies have reported higher titers of anti-S1- and anti-N- specific IgG and IgM antibodies, as well as neutralizing antibodies (nAbs) in severe vs. mild COVID-19 (199, 221–223). High titers of anti-N Abs have been found to be related to increased virus replication and more severe disease (221) (Figure 3).

4 Cytokines, interferons and the progression of COVID-19

Cytokines play a major role in many physiological and pathological processes. In the inflammatory context, different immune and non-immune cells, such as monocytes, macrophages, T cells and platelets, as well as endothelial cells, epithelial cells and fibroblasts, produce various cytokines. A cytokine storm, CRS, is defined as an overproduction of cytokines due to an uncontrolled host inflammatory response to different triggers. The triggers could include infections, tissue damage, malignancy, rheumatic disorders and certain drugs. Several studies on severely ill COVID-19 patients have identified significant variations in the serum or plasma levels of cytokines associated with COVID-19 pathogenicity (224, 225). It has been demonstrated that cytokine storm plays an important role in the severity of SARS-CoV-2 infection and lung damage, possibly resulting in ARDS and patient referral to ICU (226, 227). Overproduction of cytokines, including IL-17, IL-7, IL-1β, IL-9, IL-2, IL-10, TNF-α, GM-CSF, G-CSF, IFN-γ, MCP1, MIP1A, MIP1B, CXCL10 and CXCL8, by monocytes and macrophages has been reported in severe COVID-19 cases (182, 228, 229). Moreover, in a study conducted in a group of 52 patients with severe conditions, high plasma concentrations of GM-CSF were reported in COVID-19 patients who required ICU, suggesting a role for GM-CSF in disease severity (182). A study conducted in Taiwan in 2021 compared 40 cytokines in COVID-19 patients with mild, moderate, severe or critical diseases. It was found that the levels of 22 cytokines gradually increased in critical and severe cases compared to moderate ones (230). Evidence indicates that macrophages are the main promoters of cytokine storm during SARS-CoV-2 infection, leading to deleterious clinical manifestations and acute mortality in critically ill patients with COVID-19 (37, 231).

As a broad class of cytokines, interferons (IFNs) are a group of related proteins produced by a variety of cells against viral infection (232). IFNs are classified into three types: type I, type II, and type III. Plasmacytoid dendritic cells (pDC) are the main producers of type I IFNs. By binding to their receptors, the interferons induce the expression of IFN-stimulated genes (ISGs), thereby generating an antiviral state by inhibiting virus replication in cells under infection threat (233–235). Several studies have reported that both IFN-β1b and IFN-β1a exert an inhibitory effect on SARS-CoV-2 (236–239). In this regard, an impaired type I IFN response is reported in patients

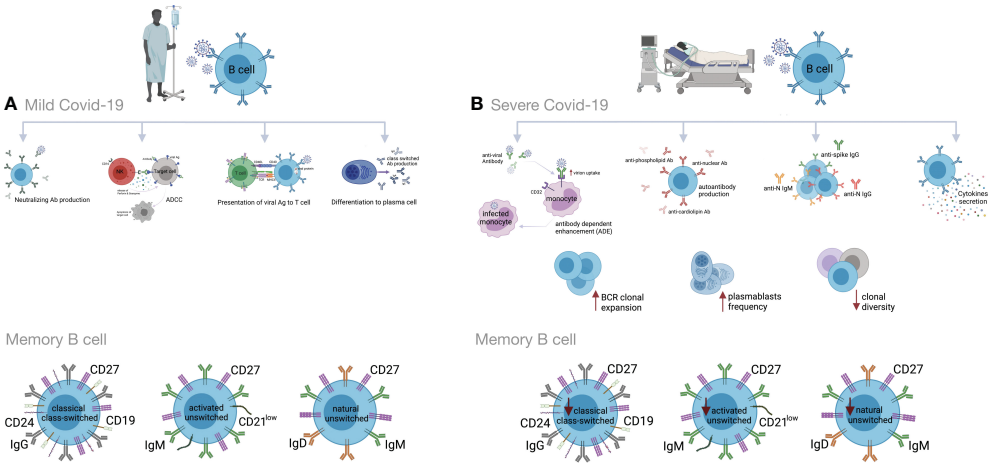

FIGURE 3
Humoral immune responses during COVID-19 progression in mild versus severe disease. **(A)** During mild COVID-19, B cells contribute to antiviral immune responses in many ways. The first is through production of neutralizing antibodies (Abs), which will bind to the virion and block its entry to the host cells, thus impeding further infection. The second is through a process called antibody-dependent cellular cytotoxicity (ADCC), in which Fc receptor-bearing effector cells can recognize and kill antibody-coated target cells expressing pathogen-derived antigens. The third is through antigen presentation to T cells and activation of cell-mediated immunity. B cells also produce some cytokines to regulate inflammation and activation of adaptive responses. Lastly, B cells can differentiate into antibody-secreting plasma cells, which produce high affinity and class-switched Abs. **(B)** B cell immune responses in severe COVID-19 may exacerbate disease progression by excessive secretion of cytokines and production of autoantibodies. As an adverse effect anti-viral antibodies can facilitate the entry of virus into monocytes/macrophages and granulocytic cells through interaction with Fc and/or complement receptors in a process that is called antibody dependent enhancement (ADE). In addition, increased clonal expansion of B cells, higher frequency of plasmablasts as well as reduced frequency of $CD24^{+}$ switched and $CD24^{-}CD27^{+}$ IgD^{+} IgM^{+} unswitched memory B cells have been reported in severe COVID-19 cases. Figure was created by BioRender (Toronto, ON, Canada).

with severely and critically ill COVID-19 compared to those with mild infections. Indeed, patients with lower plasma levels of type I IFN have higher levels of TNF- α and IL-6, increased viral load, and extensive NFκB-driven inflammatory responses (240). A recent study showed that SARS-CoV-2 mRNA-encoded proteins, ORF3b and ORF6, inhibit IFN production and signaling (241). Another study found that high IFN-λ levels during the early stages of SARS-CoV-2 infection were associated with a lower viral load in bronchial aspirates and a better outcome in severely ill COVID-19 patients. In late stages in critically ill COVID-19 patients, however, the serum levels of IFN-α and IFN-λ were found to be decreased compared to those with mild disease (242).

5 Therapeutic approaches to COVID-19

Considering that SARS-CoV-2 infection and imbalanced immune responses are the two main drivers of COVID-19 pathogenesis, glucocorticoids and antiviral drugs have been the most commonly used treatments to treat COVID-19 and its complications (243, 244). Safe strategies to limit morbidity and mortality and to improve the efficacy of treatments by finding new therapeutic targets are still urgently required. Current studies have focused on specific means to interfere with SARS-CoV-2 infection (245, 246). Nowadays, several approaches are followed to explore candidates to decrease or subvert inflammatory responses against primary SARS-CoV-2 and mutant strains. Below, the most promising potential targets are reviewed, and an update on the progress of treatments for COVID-19 is provided (Table 1).

5.1 Anti-cytokine therapy

One approach to treat cytokine storm in COVID-19 is to use traditional anti-inflammatory drugs such as corticosteroids, chloroquine and colchicine (258, 259). However, except for corticosteroids, their use has remained limited. Recently, recombinant cytokines and antibodies or inhibitor molecules against different cytokines and their signaling pathways have been tried or are in the pipeline for production. Below, some of the approaches that are currently or could potentially be applied to manage more serious forms of COVID-19 are described. For the less serious, flu-like illnesses, rest and symptomatic treatment are usually sufficient.

Recombinant human IL-7 (rhIL-7). According to a recent study, recombinant human IL-7 (rhIL-7) administration significantly rescued the immune function in a 74-year-old ICU patient with severe COVID-19 (260). In another study, higher lymphocyte counts without widespread inflammation or pulmonary injury were observed in COVID-19 cases who received IL-7 (247). It has been found that administration of dexamethasone with IL-7 leads to IL7 receptor (IL-7Rα) upregulation and increased IL-7 activity in the more severe stage of COVID-19 (261–263). Another clinical trial (NCT04379076) is currently investigating the effect of CYT107, a commercial derivative of rhIL-7, on the clinical picture and immune reconstitution in severe COVID-19 patients. Accordingly, these results suggest that appropriate administration of IL-7 with or without other agents could be applied to critically ill COVID-19 patients with severe lymphopenia. Because of its lymphopoiesis- stimulating effect, IL-7 has also been suggested as a potential vaccine adjuvant.

TABLE 1 Therapeutic approaches in COVID-19.

Therapeutic approaches	Mechanism of action	References
Target for anti-cytokine therapy		
IL-7	Immune reconstitution Increased lymphocyte counts	(247, 248)
IL-6	Reduced oxygen requirement Reduced CRP level Reduced risk of mortality in ICU Improved lymphocyte production and activity Improved clinical outcomes	(217, 249)
IL-1	Reduced oxygen requirement and reduced CRP level Improved clinical condition Reduced white blood cell counts Reduced ferritin, creatinine, procalcitonin and bilirubin levels Increased the PaO2/FiO2 ratio	(250, 251)
TNF-α	Reduced inflammatory cytokine production Reduced hyperinflammation	(252, 253)
Interferon therapy		
	Reduced inflammatory cytokine production Improved clinical outcomes	(254, 255)
Cell therapy		
	Reduced inflammatory cytokine production Improved clinical outcomes	(256)
Intravenous immunoglobulin therapy		
	Reduced mortality Improved clinical outcomes	(257)

5.2 Targeting IL-6 signaling

A high concentration of the acute phase response stimulating cytokine IL-6 is related to an increased risk for severe COVID-19. Thus, targeting IL-6 signaling may provide a therapeutic approach for the prevention of aggravated inflammation in SARS-CoV-2 infection (264–266). A retrospective clinical trial showed that treatment with tocilizumab, a monoclonal antibody against IL-6R, reduced oxygen requirements, serum level of CRP, and hospital stays, as well as improving lymphocyte recovery and clinical outcomes in severe or critical COVID-19 (217). Another cohort study demonstrated a decreased mortality in ICU COVID-19 patients who received tocilizumab immediately after ICU admission as compared to those who did not receive early tocilizumab intervention (249). A recent study showed that the treatment of severe COVID-19 patients with sarilumab, a monoclonal antibody against IL-6R, promoted the recovery of cases with mild lung disease (267). In addition, according to a retrospective clinical trial, sarilumab treatment improved clinical symptoms and reduced serum CRP concentrations in most COVID-19 patients (268). A controlled cohort study (NCT04322188) evaluated the impact of siltuximab, a monoclonal antibody against IL-6, on the mortality rate of 30 COVID-19 patients requiring ventilator support. The results showed that siltuximab treatment, in combination with optimal supportive care, reduced the mortality rate of COVID-19 cases as compared to control patients who received only optimal supportive care (269).

5.3 Targeting IL-1 signaling

Given the important role of IL-1β in the cytokine storm, several agents targeting IL-1β signaling, including canakinumab and anakinra, have been introduced to clinical COVID-19 treatment trials (250, 270, 271). A retrospective clinical trial among 22 severe/critical COVID-19 patients indicated that >8 days of treatment with anakinra (IL-1 receptor antagonist) led to a reduced requirement for mechanical ventilation, decreased serum CRP levels, and improved clinical conditions in patients compared to the control group (251). Another cohort study found that anakinra treatment reduced several clinical parameters, including temperature, white blood cell count, and plasma levels of ferritin, creatinine, procalcitonin, and bilirubin in COVID-19 patients (272). According to a retrospective study, subcutaneous administration of canakinumab (anti-IL-1β) decreased hyperinflammation and improved PaO2/FiO2 ratio in COVID-19 patients (250). Another cohort study on non-ICU patients with mild or severe COVID-19 who received subcutaneous canakinumab showed that canakinumab treatment significantly increased the PaO2/FiO2 ratio and reduced inflammation (273). Furthermore, other studies have reported the positive effects of canakinumab during SARS-CoV-2 infection (274–276), and six other clinical trials (NCT04348448, NCT04476706, NCT04362813, NCT04365153, NCT04510493, NCT04278404) have been registered to evaluate their potential therapeutic effects in SARS-CoV-2 infection (252).

5.4 Targeting TNF-α

Since TNF-α is an initial driver of NF-κB activation and involved in the expression of several pro-inflammatory and anti-apoptotic genes in SARS-CoV-2 infection, its inhibition can attenuate excessive cytokine release and hyperinflammation in COVID-19 (28, 197, 277, 278). Recently, it has been observed that the temporary use of etanercept, a soluble TNF-α receptor fusion protein, reduces hyperinflammation in severe COVID-19 (28). A case report study demonstrated that subcutaneous etanercept administration in a 60-year-old man induced a rapid recovery from COVID-19 and did not cause any signs of respiratory failure (279). A total of four clinical trials of infliximab (anti-TNF-α) (NCT04425538, NCT04734678, NCT04593940, NCT04344249) and two clinical trials with adalimumab, another anti-TNF-α antibody (ChiCTR2000030089, NCT04705844) are ongoing to evaluate its effects in COVID-19 (252).

Interferon therapy: Some patients with life-threatening COVID-19 have been shown to have IgG autoantibodies against type I interferon. Defects, both genetic and acquired, within the IFN pathways have also been shown to predispose to severe COVID-19. Therefore, IFNs have been introduced into clinical trials in an attempt to decrease COVID-19 morbidity and mortality (280). The results of a clinical trial demonstrated that the early triple combination of IFN-1β + lopinavir/ritonavir + ribavirin could reduce clinical symptoms and hospital stay in patients with mild-to-moderate COVID-19 (238). A previous study in China found that lopinavir/ritonavir in combination with IFN-1α reduced the duration of SARS-CoV-2 shedding (281). Other clinical trials and case reports have shown that IFN-α1b and -α2b positively affect cytokine levels in the blood, virus clearance, and clinical symptoms (254, 255). On the other hand, IFNs can also induce adverse effects such as flu-like symptoms, headaches, gastrointestinal reactions, and rashes. In addition, the sustained presence of IFNs could be involved in maintaining local and systemic inflammation and causing tissue damage. The results described above suggest that interferon therapy with antiviral drugs early in the course of infection could help people with mild COVID-19; however, its practicality still remains to be seen.

TABLE 2 Key features of immune responses in mildly versus critically ill COVID-19 patients.

Immune Response Players	Key Features	References
Innate Immune Response Players		
Cytokines	Overproduction of cytokines in severe compared to mild patients can result in detrimental manifestations and mortality	(22, 122)
Interferons	Impaired type I IFN response in patients with severely ill COVID-19 compared to patients with a mild infection	(32)
Complement system	More intense complement activation and inflammatory responses in severely compared to mildly ill patients	(38, 39)
Neutrophils	Higher number of neutrophils, excessive NET formation and ROS production in severely compared to mildly ill patients	(44, 48, 56)
Monocytes	Increased percentage of inflammatory monocytes in severe COVID-19 compared with mild disease	(63)
Macrophages	Macrophages are considered as promoters of cytokine storm and are associated with a high risk of death in severe COVID-19 patients	(73, 74)
Dendritic cells	Decreased number and further impairment in maturation and function of DC in severe compared with mild disease	(83, 84)
ILCs	Decreased frequency of ILC2 in severe COVID-19 in comparison to moderate disease	(89)
Natural killer cells	Decreased number and cytotoxicity of NK cells in severely ill COVID-19 patients	(97, 100)
Basophils	Decreased number and increased expression of PD-L1 on basophils in severe vs. mild COVID-19	(104)
Eosinophils	Decreased number of eosinophils in severe vs. mild disease	(106)
MDSCs	Higher frequency of MDSCs in severely ill COVID-19 patients correlated with decreased specific T cell responses and poor disease outcomes	(107)
NKT cells	Reduced frequency of NKT cells as well as of IFN-γ production in severely ill COVID-19 patients	(129)
Adaptive Immune Response Players		
Th1 cells	Lower percentage of Th1 cells and decreased production of IFN-γ in severe COVID-19	(147, 148)
Th2 cells	Th2 hyper-activation and higher plasma levels of Th2-produced cytokines correlated with disease severity and mortality	(148)
Th17 cells	Increased frequency and hyper-activation of Th17 cells and subsequent production of pro-inflammatory cytokines in critical forms of COVID-19	(149, 151)
Treg cells	Decreased frequency and enhanced apoptosis of Tregs in severe cases compared to mild ones	(156, 158)
CD8+ T cells	Decreased frequency and cytotoxic function of CD8+ T cells in critically ill patients	(166, 167)
Memory T cells	Decreased percentage of memory T helper cells in severe COVID-19	(170)
B cells	Decreased number of B cells and deficient humoral immune responses in severe cases	(185, 186)
Antibodies	Higher titers of antibodies in severe vs. mild patients associated with increased virus replication and a more severe disease	(209)

5.5 Cell therapy

While current treatment options for COVID-19 are mainly nonspecific, e.g., the use of dexamethasone or anti-inflammatory agents with significant side effects, the accessibility of other approaches such as remdesivir and tocilizumab (anti-IL-6 receptor) is limited (282). These therapeutic agents have no effects on regenerating damaged tissue structures or functions. Thus, the relevance of cell therapies in the treatment of COVID-19 has received considerable attention (283). Although, particular cell types used in cell therapy for COVID-19 are mesenchymal stem cells (MSCs), NK cells, and T cells, early apoptotic cells, and other cell types are being investigated (284). MSCs exhibit strong immunomodulatory and pluripotential properties that can suppress CD3, CD8, and CD4 T cells and attenuate cytokine secretion (285, 286). MSCs have been used in several clinical trials, including graft vs. host disease (GvHD) (287), type 2 diabetes (288), autoimmune diseases (289), and spinal cord injury (290). Considering that MSCs do not express ACE2 receptors, MSC therapy can accomplish immunomodulatory effects in SARS-CoV-2 infection (291). Previous clinical trials have shown that the intravenous injection of human umbilical cord-derived MSCs is related to an attenuated cytokine storm and improves outcomes in severely ill COVID-19 patients (256). Treatment of severely ill patients who were refractory to steroids with human umbilical cord MSCs results in the healing of pulmonary lesions (292). It has also been reported that a single- dose injection of MSCs in mild, severe, and critical COVID-19 leads to improved clinical outcomes (256). A recent study indicated that COVID-19 patients were extubated approximately 7 days after injection of adipose-derived MSCs (293). Furthermore, a phase 1/2a randomized trial (NCT04355728) found that administration of umbilical cord derived-MSCs for COVID-19 patients with ARDS improved survival following therapy (294).

5.6 Intravenous immunoglobulin therapy

IVIG is a natural immunoglobulin pool prepared from the sera of healthy donors. The major component of IVIG is the serum IgG fraction, mainly IgG1 and IgG2 subclasses (295). It is well known that anti-cytokine autoantibodies, including IL-1, IL-6, and IFN-γ autoantibodies, are present in the IVIG of healthy individuals. These antibodies may be related to the anti-inflammatory effects of IVIG in inflammatory and autoimmune disorders (296–298). Previously, the promising effect of IVIG therapy has been reported in SARS and the 2009 H1N1 influenza pandemic (299, 300). Recently, the possible positive effects of IVIG administration during the early phase of COVID-19 have been reported (301). A meta-analysis in three groups of patients with non-severe, severe, or critical illness, including 825 hospitalized COVID-19 patients, indicated that IVIG might be associated with a reduced mortality rate in critically ill patients (302). Further, a significant correlation between IVIG treatment and increased survival rate and decreased COVID-19 progression has been shown (283). Moreover, the potential benefit of IVIG administration along with antiviral drugs and mechanical ventilation in severe COVID-19 patients has been reported (257). Conversely, IVIG administration, along with hydroxychloroquine and lopinavir/ritonavir, in the treatment of severe COVID-19 cases, has not been supported by recent findings (301).

6 Conclusion

At this point in the pandemic, further understanding of the SARS-CoV-2 biology and systemic host immune responses can provide information on the processes and mechanisms involved in immune-mediated viral clearance and define specific targets for the treatment of COVID-19. Recent research on the immune mechanisms in COVID-19 refer to the initiation of infection by SARS-CoV-2 accompanied by cellular immune responses, including specifically poly-functional $CD4^+$ and $CD8^+$ T cell responses, which may become chronic along with immune inflammation. Recovery from tissue injury, prolonged inflammation and deviations in adaptive immune activity may play a role in the postinfectious complications, termed post-COVID. The consequences of deviated immune processes also depend on genetic make-up and environmental risk factors. Due to the SARS-CoV-2 contagiousness, the increased risk of death and the need for an ICU in severe cases of the disease, there is an urgent need for long-term follow-up of the molecular and cellular mechanisms in virus-host communication at all stages of the disease. This information is needed for delineating the optimal management of infected patients in order to prevent the progression to severe forms of the disease. Currently, ongoing large clinical trials based on antiviral and immune-based treatments may soon provide efficient therapeutic agents for COVID-19 patients. In any case, vaccination still remains the best means for preventing severe illness.

Author contributions

HN, SM and KK conceived the study and wrote the manuscript. HN contributed to the final revision of the manuscript. AT, ZS, MV, PH, NK and MN participated in preparing the first draft and were involved in the final revision of the manuscript. All authors contributed to the article and approved the submitted version.

Funding

This work was supported by Academy of Finland (Grant No 336431), the Helsinki University Hospital Funds (TYH2022315, TYH2023322) and Sigrid Jusélius Foundation.

Conflict of interest

The authors declare that the research was conducted in the absence of any commercial or financial relationships that could be construed as a potential conflict of interest.

Publisher's note

All claims expressed in this article are solely those of the authors and do not necessarily represent those of their affiliated organizations, or those of the publisher, the editors and the reviewers. Any product that may be evaluated in this article, or claim that may be made by its manufacturer, is not guaranteed or endorsed by the publisher.

References

1. Jesenak M, Brndiarova M, Urbancikova I, Rennerova Z, Vojtkova J, Bobcakova A, et al. Immune parameters and covid-19 infection – associations with clinical severity and disease prognosis. *Front Cell Infect Microbiol* (2020) 10:364(364). doi: 10.3389/fcimb.2020.00364

2. Yang L, Liu S, Liu J, Zhang Z, Wan X, Huang B, et al. Covid-19: Immunopathogenesis and immunotherapeutics. *Signal Transduct Target Ther* (2020) 5 (1):1–8. doi: 10.1038/s41392-020-00243-2

3. Wartecki A, Rzymski P. On the coronaviruses and their associations with the aquatic environment and wastewater. *Water* (2020) 12(6):1598. doi: 10.3390/w12061598

4. Roussel Y, Giraud-Gatineau A, Jimeno M-T, Rolain J-M, Zandotti C, Colson P, et al. Sars-Cov-2: Fear versus data. *Int J Antimicrob Agents* (2020) 55(5):105947. doi: 10.1016/j.ijantimicag.2020.105947

5. Guan W-j, Ni Z-y, Hu Y, Liang W-h, Ou C-q, He J-x, et al. Clinical characteristics of coronavirus disease 2019 in China. *N Engl J Med* (2020) 382(18):1708–20. doi: 10.1056/NEJMoa2002032

6. Daly JL, Simonetti B, Klein K, Chen K-E, Williamson MK, Antón-Plágaro C, et al. Neuropilin-1 is a host factor for sars-Cov-2 infection. *Science* (2020) 370(6518):861–5. doi: 10.1126/science.abd3072

7. Cantuti-Castelvetri L, Ojha R, Pedro LD, Djannatian M, Franz J, Kuivanen S, et al. Neuropilin-1 facilitates sars-Cov-2 cell entry and infectivity. *Science* (2020) 370 (6518):856–60. doi: 10.1126/science.abd2985

8. Smith N, Goncalves P, Charbit B, Grzelak L, Beretta M, Planchais C, et al. Distinct systemic and mucosal immune responses during acute sars-Cov-2 infection. *Nat Immunol* (2021) 22(11):1428–39. doi: 10.1038/s41590-021-01028-7

9. Ziegler CGK, Miao VN, Owings AH, Navia AW, Tang Y, Bromley JD, et al. Impaired local intrinsic immunity to sars-Cov-2 infection in severe covid-19. *Cell* (2021) 184(18):4713–33.e22. doi: 10.1016/j.cell.2021.07.023

10. Zhou Z, Zhao Z, Shi S, Wu J, Li D, Li J, et al. Model-based cellular kinetic analysis of sars-Cov-2 infection: Different immune response modes and treatment strategies. *arXiv preprint arXiv:210104477* (2021), Available at: https://arxiv.org/abs/2101.04477v1

11. Mahler M, Meroni PL, Infantino M, Buhler KA, Fritzler MJ. Circulating calprotectin as a biomarker of covid-19 severity. *Expert Rev Clin Immunol* (2021) 17 (5):431–43. doi: 10.1080/1744666x.2021.1905526

12. Chen T, Wu D, Chen H, Yan W, Yang D, Chen G, et al. Clinical characteristics of 113 deceased patients with coronavirus disease 2019: Retrospective study. *BMJ* (2020) 368:m1091. doi: 10.1136/bmj.m1091

13. Wu C, Chen X, Cai Y, Xia J, Zhou X, Xu S, et al. Risk factors associated with acute respiratory distress syndrome and death in patients with coronavirus disease 2019 pneumonia in wuhan, China. *JAMA Internal Med* (2020) 180(7):934–43. doi: 10.1001/jamainternmed.2020.0994

14. Kalpakci Y, Hacibekiroglu T, Trak G, Karacaer C, Demirci T, Kocayigit H, et al. Comparative evaluation of memory T cells in covid-19 patients and the predictive role of Cd4+ Cd8+ double positive T lymphocytes as a new marker. *Rev Assoc Med Bras* (2020) 66:1666–72. doi: 10.1590/1806-9282.66.12.1666

15. Zhang H, Zhou P, Wei Y, Yue H, Wang Y, Hu M, et al. Histopathologic changes and sars-Cov-2 immunostaining in the lung of a patient with covid-19. *Ann Internal Med* (2020) 172(9):629–32. doi: 10.7326/m20-0533

16. Zhang JJ, Dong X, Liu GH, Gao YD. Risk and protective factors for covid-19 morbidity, severity, and mortality. *Clin Rev Allergy Immunol* (2022), 1–18. doi: 10.1007/s12016-022-08921-5

17. Sette A, Crotty S. Adaptive immunity to sars-Cov-2 and covid-19. *Cell* (2021) 184 (4):861–80. doi: 10.1016/j.cell.2021.01.007

18. Guia S, Narni-Mancinelli E. Helper-like innate lymphoid cells in humans and mice. *Trends Immunol* (2020) 41(5):436–52. doi: 10.1016/j.it.2020.03.002

19. Kawai T, Akira S. The role of pattern-recognition receptors in innate immunity: Update on toll-like receptors. *Nat Immunol* (2010) 11(5):373–84. doi: 10.1038/ni.1863

20. Amigues I, Pearlman AH, Patel A, Reid P, Robinson PC. Coronavirus disease 2019: Investigational therapies in the prevention and treatment of hyperinflammation. *Expert Rev Clin Immunol* (2020) 16(12):1185–204. doi: 10.1080/1744666x.2021.1847084

21. Newton AH, Cardani A, Braciale TJ. The host immune response in respiratory virus infection: Balancing virus clearance and immunopathology. *Semin immunopathol* (2016) 38(4):471–82. doi: 10.1007/s00281-016-0558-0

22. Zuo Y, Estes SK, Ali RA, Gandhi AA, Yalavarthi S, Shi H, et al. Prothrombotic antiphospholipid antibodies in covid-19. *medRxiv preprint server Health Sci* (2020) 2020.06.15.20131607. doi: 10.1101/2020.06.15.20131607

23. Naumenko V, Turk M, Jenne CN, Kim S-J. Neutrophils in viral infection. *Cell Tissue Res* (2018) 371(3):505–16. doi: 10.1007/s00441-017-2763-0

24. Mohamadzadeh M, Coberley SS, Olinger GG, Kalina WV, Ruthel G, Fuller CL, et al. Activation of triggering receptor expressed on myeloid cells-1 on human neutrophils by marburg and Ebola viruses. *J Virol* (2006) 80(14):7235–44. doi: 10.1128/JVI.00543-06

25. Hashimoto Y, Moki T, Takizawa T, Shiratsuchi A, Nakanishi Y. Evidence for phagocytosis of influenza virus-infected, apoptotic cells by neutrophils and macrophages in mice. *J Immunol* (2007) 178(4):2448–57. doi: 10.4049/jimmunol.178.4.2448

26. Wang D, Hu B, Hu C, Zhu F, Liu X, Zhang J, et al. Clinical characteristics of 138 hospitalized patients with 2019 novel coronavirus-infected pneumonia in wuhan, China. *Jama* (2020) 323(11):1061–9. doi: 10.1001/jama.2020.1585

27. Du RH, Liang LR, Yang CQ, Wang W, Cao TZ, Li M, et al. Predictors of mortality for patients with covid-19 pneumonia caused by sars-Cov-2: A prospective cohort study. *Eur Respir J* (2020) 55(5); 2000524. doi: 10.1183/13993003.00524-2020

28. Schulte-Schrepping J, Reusch N, Paclik D, Baßler K, Schlickeiser S, Zhang B, et al. Severe covid-19 is marked by a dysregulated myeloid cell compartment. *Cell* (2020) 182 (6):1419–40.e23. doi: 10.1016/j.cell.2020.08.001

29. Liu J, Li S, Liu J, Liang B, Wang X, Wang H, et al. Longitudinal characteristics of lymphocyte responses and cytokine profiles in the peripheral blood of sars-Cov-2 infected patients. *EBioMedicine* (2020) 55:102763. doi: 10.1016/j.ebiom.2020.102763

30. Fu J, Kong J, Wang W, Wu M, Yao L, Wang Z, et al. The clinical implication of dynamic neutrophil to lymphocyte ratio and d-dimer in covid-19: A retrospective study in suzhou China. *Thromb Res* (2020) 192:3–8. doi: 10.1016/j.thromres.2020.05.006

31. Middleton EA, He XY, Denorme F, Campbell RA, Ng D, Salvatore SP, et al. Neutrophil extracellular traps contribute to immunothrombosis in covid-19 acute respiratory distress syndrome. *Blood* (2020) 136(10):1169–79. doi: 10.1182/blood.2020007008

32. Zuo Y, Yalavarthi S, Shi H, Gockman K, Zuo M, Madison JA, et al. Neutrophil extracellular traps in covid-19. *JCI Insight* (2020) 5(11): e138999. doi: 10.1172/jci.insight.138999

33. Saheb Sharif-Askari N, Saheb Sharif-Askari F, Mdkhana B, Hussain Alsayed HA, Alsafar H, Alrais ZF, et al. Upregulation of oxidative stress gene markers during sars-Cov-2 viral infection. *Free Radical Biol Med* (2021) 172:688–98. doi: 10.1016/j.freeradbiomed.2021.06.018

34. Laforge M, Elbim C, Frère C. Tissue damage from neutrophil-induced oxidative stress in covid-19. *Nat Rev Immunol* (2020) 20(9):515–6. doi: 10.1038/s41577-020-0407-1

35. Shibabaw T. Inflammatory cytokine: Il-17a signaling pathway in patients present with covid-19 and current treatment strategy. *J Inflammation Res* (2020) 13:673–80. doi: 10.2147/jir.s278335

36. Sampath P, Moideen K, Ranganathan UD, Bethunaickan R. Monocyte subsets: Phenotypes and function in tuberculosis infection. *Front Immunol* (2018) 9:1726. doi: 10.3389/fimmu.2018.01726

37. Pence BD. Severe covid-19 and aging: Are monocytes the key? *GeroScience* (2020) 42(4):1051–61. doi: 10.1007/s11357-020-00213-0

38. Boyette LB, Macedo C, Hadi K, Elinoff BD, Walters JT, Ramaswami B, et al. Phenotype, function, and differentiation potential of human monocyte subsets. *PloS One* (2017) 12(4):e0176460. doi: 10.1371/journal.pone.0176460

39. Ong S-M, Hadadi E, Dang T-M, Yeap W-H, Tan CT-Y, Ng T-P, et al. The pro-inflammatory phenotype of the human non-classical monocyte subset is attributed to senescence. *Cell Death Dis* (2018) 9(3):1–12. doi: 10.1038/s41419-018-0327-1

40. Martinez FO, Combes TW, Orsenigo F, Gordon S. Monocyte activation in systemic covid-19 infection: Assay and rationale. *EBioMedicine* (2020) 59:102964. doi: 10.1016/j.ebiom.2020.102964

41. Qin S, Jiang Y, Wei X, Liu X, Guan J, Chen Y, et al. Dynamic changes in monocytes subsets in covid-19 patients. *Hum Immunol* (2021) 82(3):170–6. doi: 10.1016/j.humimm.2020.12.010

42. Liao M, Liu Y, Yuan J, Wen Y, Xu G, Zhao J, et al. Single-cell landscape of bronchoalveolar immune cells in patients with covid-19. *Nat Med* (2020) 26(6):842–4. doi: 10.1038/s41591-020-0901-9

43. Zhou Y, Fu B, Zheng X, Wang D, Zhao C, Qi Y, et al. Pathogenic T-cells and inflammatory monocytes incite inflammatory storms in severe covid-19 patients. *Natl Sci Rev* (2020) 7(6):998–1002. doi: 10.1093/nsr/nwaa041

44. Zhang D, Guo R, Lei L, Liu H, Wang Y, Wang Y, et al. Covid-19 infection induces readily detectable morphologic and inflammation-related phenotypic changes in peripheral blood monocytes. *J Leukoc Biol* (2020) 109 (1):13–22. doi: 10.1002/JLB.4HI0720-470R

45. Silvin A, Chapuis N, Dunsmore G, Goubet AG, Dubuisson A, Derosa L, et al. Elevated calprotectin and abnormal myeloid cell subsets discriminate severe from mild covid-19. *Cell* (2020) 182(6):1401–18.e18. doi: 10.1016/j.cell.2020.08.002

46. Sanchez-Cerrillo I, Landete P, Aldave B, Sanchez-Alonso S, Sanchez-Azofra A, Marcos-Jimenez A, et al. Differential redistribution of activated monocyte and dendritic cell subsets to the lung associates with severity of covid-19. *medRxiv preprint server Health Sci* (2020) 2020.05.13.20100925. doi: 10.1101/2020.05.13.20100925

47. Meidaninikjeh S, Sabouni N, Marzouni HZ, Bengar S, Khalili A, Jafari R. Monocytes and macrophages in covid-19: Friends and foes. *Life Sci* (2021), 269:119010. doi: 10.1016/j.lfs.2020.119010

48. Hussell T, Bell TJ. Alveolar macrophages: Plasticity in a tissue-specific context. *Nat Rev Immunol* (2014) 14(2):81–93. doi: 10.1038/nri3600

49. Franke-Ullmann G, Pförtner C, Walter P, Steinmüller C, Lohmann-Matthes ML, Kobzik L. Characterization of murine lung interstitial macrophages in comparison with alveolar macrophages in vitro. *J Immunol* (1996) 157(7):3097–104. doi: 10.4049/jimmunol.157.7.3097

50. Helms J, Kremer S, Merdji H. Neurologic features in severe sars-Cov-2 infection. *N Engl J Med* (2020) 382(23):2268–70. doi: 10.1056/NEJMc2008597

51. Nemati M, Malla N, Yadav M, Khorramdelazad H, Jafarzadeh A. Humoral and T cell–mediated immune response against trichomoniasis. *Parasite Immunol* (2018) 40(3): e12510. doi: 10.1111/pim.12510

52. Wu A, Peng Y, Huang B, Ding X, Wang X, Niu P, et al. Genome composition and divergence of the novel coronavirus (2019-ncov) originating in China. *Cell Host Microbe* (2020) 27(3):325–8. doi: 10.1016/j.chom.2020.02.001

53. Kosyreva A, Dzhalilova D, Lokhonina A, Vishnyakova P, Fatkhudinov T. The role of macrophages in the pathogenesis of sars-Cov-2-Associated acute respiratory distress syndrome. *Front Immunol* (2021) 12:682871. doi: 10.3389/fimmu.2021.682871

54. Jafarzadeh A, Chauhan P, Saha B, Jafarzadeh S, Nemati M. Contribution of monocytes and macrophages to the local tissue inflammation and cytokine storm in covid-19: Lessons from sars and mers, and potential therapeutic interventions. *Life Sci* (2020), 257:118102. doi: 10.1016/j.lfs.2020.118102

55. Tay MZ, Poh CM, Rénia L, MacAry PA, Ng LF. The trinity of covid-19: Immunity, inflammation and intervention. *Nat Rev Immunol* (2020) 20(6):363–74. doi: 10.1038/s41577-020-0311-8

56. Wang Y, Ding Q, Lu YC, Cao SY, Liu QX, Zhang L. Interferon-stimulated gene 15 enters posttranslational modifications of P53. *J Cell Physiol* (2019) 234(5):5507–18. doi: 10.1002/jcp.27347

57. Nile SH, Nile A, Qiu J, Li L, Jia X, Kai G. Covid-19: Pathogenesis, cytokine storm and therapeutic potential of interferons. *Cytokine Growth factor Rev* (2020) 53:66–70. doi: 10.1016/j.cytogfr.2020.05.002

58. Bost P, Giladi A, Liu Y, Bendjelal Y, Xu G, David E, et al. Host-viral infection maps reveal signatures of severe covid-19 patients. *Cell* (2020) 181(7):1475–88.e12. doi: 10.1016/j.cell.2020.05.006

59. Borges RC, Hohmann MS, Borghi SM. Dendritic cells in covid-19 immunopathogenesis: Insights for a possible role in determining disease outcome. *Int Rev Immunol* (2021) 40(1-2):108–25. doi: 10.1080/08830185.2020.1844195

60. Banchereau J, Steinman RM. Dendritic cells and the control of immunity. *Nature* (1998) 392(6673):245–52. doi: 10.1038/32588

61. Pollara G, Kwan A, Newton PJ, Handley ME, Chain BM, Katz DR. Dendritic cells in viral pathogenesis: Protective or defective? *Int J Exp Pathol* (2005) 86(4):187–204. doi: 10.1111/j.0959-9673.2005.00440.x

62. Wack A. Monocyte and dendritic cell defects in covid-19. *Nat Cell Biol* (2021) 23 (5):445–7. doi: 10.1038/s41556-021-00685-y

63. Bencze D, Fekete T, Pázmándi K. Correlation between type I interferon associated factors and covid-19 severity. *Int J Mol Sci* (2022) 23(18): 10968. doi: 10.3390/ijms231810968

64. Wang X, Bai H, Ma J, Qin H, Zeng Q, Hu F, et al. Identification of distinct immune cell subsets associated with asymptomatic infection, disease severity, and viral persistence in covid-19 patients. *Front Immunol* (2022) 13:812514. doi: 10.3389/fimmu.2022.812514

65. Rajamanickam A, Kumar NP, Pandiaraj AN, Selvaraj N, Munisankar S, Renji RM, et al. Restoration of dendritic cell homeostasis and type I/Type iii interferon levels in convalescent covid-19 individuals. *BMC Immunol* (2022) 23(1):51. doi: 10.1186/s12865-022-00526-z

66. Falck-Jones S, Österberg B, Smed-Sörensen A. Respiratory and systemic monocytes, dendritic cells, and myeloid-derived suppressor cells in covid-19: Implications for disease severity. *J Internal Med* (2022) 293 (2):130–143. doi: 10.1111/joim.13559

67. Winheim E, Rinke L, Lutz K, Reischer A, Leutbecher A, Wolfram L, et al. Impaired function and delayed regeneration of dendritic cells in covid-19. *PloS Pathog* (2021) 17 (10):e1009742. doi: 10.1371/journal.ppat.1009742

68. Marongiu L, Protti G, Facchini FA, Valache M, Mingozzi F, Ranzani V, et al. Maturation signatures of conventional dendritic cell subtypes in covid-19 reflect direct viral sensing. *bioRxiv* (2021) 52 (1):109–122. doi: 10.1101/2021.03.03.433597

69. Marongiu L, Protti G, Facchini FA, Valache M, Mingozzi F, Ranzani V, et al. Maturation signatures of conventional dendritic cell subtypes in covid-19 suggest direct viral sensing. *Eur J Immunol* (2022) 52(1):109–22. doi: 10.1002/eji.202149298

70. Borcherding L, Teksen AS, Grosser B, Schaller T, Hirschbühl K, Claus R, et al. Impaired dendritic cell homing in covid-19. *Front Med* (2021) 8:761372. doi: 10.3389/fmed.2021.761372

71. Kulkarni-Munje A, Palkar S, Shrivastava S, Lalwani S, Mishra AC, Arankalle VA. Disease-duration based comparison of subsets of immune cells in sars cov-2 infected patients presenting with mild or severe symptoms identifies prognostic markers for severity. *Immun Inflammation Dis* (2021); 9 (2):419–434. doi: 10.1002/iid3.402

72. Matic S, Popovic S, Djurdjevic P, Todorovic D, Djordjevic N, Mijailovic Z, et al. Sars-Cov-2 infection induces mixed M1/M2 phenotype in circulating monocytes and alterations in both dendritic cell and monocyte subsets. *PloS One* (2020) 15(12):e0241097. doi: 10.1371/journal.pone.0241097

73. García M, Kokkinou E, Carrasco García A, Parrot T, Palma Medina LM, Maleki KT, et al. Innate lymphoid cell composition associates with covid-19 disease severity. *Clin Trans Immunol* (2020) 9(12):e1224. doi: 10.1002/cti2.1224

74. Hildreth AD, O'Sullivan TE. Tissue-resident innate and innate-like lymphocyte responses to viral infection. *Viruses* (2019) 11(3):272. doi: 10.3390/v11030272

75. Vabret N, Britton GJ, Gruber C, Hegde S, Kim J, Kuksin M, et al. Immunology of covid-19: Current state of the science. *Immunity* (2020) 52 (6):910–941. doi: 10.1016/j.immuni.2020.05.002

76. Velavan TP, Meyer CG. Mild versus severe covid-19: Laboratory markers. *Int J Infect Dis* (2020) 95:304–7. doi: 10.1016/j.ijid.2020.04.061

77. Zhou F, Yu T, Du R, Fan G, Liu Y, Liu Z, et al. Clinical course and risk factors for mortality of adult inpatients with covid-19 in wuhan, China: A retrospective cohort study. *Lancet* (2020) 395(10229):1054–62. doi: 10.1016/S0140-6736(20)30566-3

78. Monticelli LA, Sonnenberg GF, Abt MC, Alenghat T, Ziegler CG, Doering TA, et al. Innate lymphoid cells promote lung-tissue homeostasis after infection with influenza virus. *Nat Immunol* (2011) 12(11):1045–54. doi: 10.1031/ni.2131

79. Gomez-Cadena A, Spehner L, Kroemer M, Khelil MB, Bouiller K, Verdeil G, et al. Severe covid-19 patients exhibit an Ilc2 Nkg2d+ population in their impaired ilc compartment. *Cell Mol Immunol* (2021) 18(2):484–6. doi: 10.1038/s41423-020-00596-2

80. van Eeden C, Khan L, Osman MS, Cohen Tervaert JW. Natural killer cell dysfunction and its role in covid-19. *Int J Mol Sci* (2020) 21(17): 6351. doi: 10.3390/ijms21176351

81. Song J-W, Zhang C, Fan X, Meng F-P, Xu Z, Xia P, et al. Immunological and inflammatory profiles in mild and severe cases of covid-19. *Nat Commun* (2020) 11(1):1–10. doi: 10.1038/s41467-020-17240-2

82. Mazzoni A, Salvati L, Maggi L, Capone M, Vanni A, Spinicci M, et al. Impaired immune cell cytotoxicity in severe covid-19 is il-6 dependent. *J Clin Invest* (2020) 130 (9):4694–703. doi: 10.1172/jci138554

83. Carsetti R, Zaffina S, Piano Mortari E, Terreri S, Corrente F, Capponi C, et al. Different innate and adaptive immune responses to sars-Cov-2 infection of asymptomatic, mild, and severe cases. *Front Immunol* (2020) 11:610300. doi: 10.3389/fimmu.2020.610300

84. Leem G, Cheon S, Lee H, Choi SJ, Jeong S, Kim ES, et al. Abnormality in the nk-cell population is prolonged in severe covid-19 patients. *J Allergy Clin Immunol* (2021) 148 (4):996–1006.e18. doi: 10.1016/j.jaci.2021.07.022

85. Bordoni V, Sacchi A, Cimini E, Notari S, Grassi G, Tartaglia E, et al. An inflammatory profile correlates with decreased frequency of cytotoxic cells in coronavirus disease 2019. *Clin Infect Dis* (2020) 71(16):2272–5. doi: 10.1093/cid/ciaa577

86. Malengier-Devlies B, Filtjens J, Ahmadzadeh K, Boeckx B, Vandenhaute J, De Visscher A, et al. Severe covid-19 patients display hyper-activated nk cells and nk cell-platelet aggregates. *Front Immunol* (2022), 13:5004. doi: 10.3389/fimmu.2022.861251

87. Di Vito C, Calcaterra F, Coianiz N, Terzoli S, Voza A, Mikulak J, et al. Natural killer cells in sars-Cov-2 infection: Pathophysiology and therapeutic implications. *Front Immunol* (2022) 13:888248. doi: 10.3389/fimmu.2022.888248

88. Hajeer A, Jawdat D, Massadeh S, Aljawini N, Abedalthagafi MS, Arabi YM, et al. Association of kir gene polymorphisms with covid-19 disease. *Clin Immunol* (2022) 234:108911. doi: 10.1016/j.clim.2021.108911

89. Maruthamuthu S, Rajalingam K, Kaur N, Morvan MG, Soto J, Lee N, et al. Individualized constellation of killer cell immunoglobulin-like receptors and cognate hla class I ligands that controls natural killer cell antiviral immunity predisposes covid-19. *Front Genet* (2022) 13. doi: 10.3389/fgene.2022.845474

90. Siracusa MC, Kim BS, Spergel JM, Artis D. Basophils and allergic inflammation. *J Allergy Clin Immunol* (2013) 132(4):789–801. doi: 10.1016/j.jaci.2013.07.046

91. Negro F. Facts and fictions of hcv and comorbidities: Steatosis, diabetes mellitus, and cardiovascular diseases. *J Hepatol* (2014) 61(1 Suppl):S69–78. doi: 10.1016/j.jhep.2014.08.003

92. Kazancioglu S, Bastug A, Ozbay BO, Kemirtlek N, Bodur H. The role of haematological parameters in patients with covid-19 and influenza virus infection. *Epidemiol Infect* (2020) 148: e272. doi: 10.1017/S095026882000271X

93. Vitte J, Diallo AB, Boumaza A, Lopez A, Michel M, Allardet-Servent J, et al. A granulocytic signature identifies covid-19 and its severity. *J Infect Dis* (2020) 222 (12):1985–96. doi: 10.1093/infdis/jiaa591

94. Hogan SP, Rosenberg HF, Moqbel R, Phipps S, Foster PS, Lacy P, et al. Eosinophils: Biological properties and role in health and disease. *Clin Exp Allergy* (2008) 38(5):709–50. doi: 10.1111/j.1365-2222.2008.02958.x

95. Gao Y-d, Agache I, Akdis M, Nadeau K, Klimek L, Jutel M, et al. The effect of allergy and asthma as a comorbidity on the susceptibility and outcomes of covid-19. *Int Immunol* (2022) 34(4):177–88. doi: 10.1093/intimm/dxab107

96. Xie G, Ding F, Han L, Yin D, Lu H, Zhang M. The role of peripheral blood eosinophil counts in covid-19 patients. *Allergy* (2021) 76(2):471–82. doi: 10.1111/all.14465

97. Eggert LE, He Z, Collins W, Lee AS, Dhondalay G, Jiang SY, et al. Asthma phenotypes, associated comorbidities, and long-term symptoms in covid-19. *Allergy* (2022) 77(1):173–85. doi: 10.1111/all.14972

98. Sacchi A, Grassi G, Bordoni V, Lorenzini P, Cimini E, Casetti R, et al. Early expansion of myeloid-derived suppressor cells inhibits sars-Cov-2 specific T-cell response and may predict fatal covid-19 outcome. *Cell Death Dis* (2020) 11(10):1–9. doi: 10.1038/s41419-020-03125-1

99. Wang C, Zhang N, Qi L, Yuan J, Wang K, Wang K, et al. Myeloid-derived suppressor cells inhibit T follicular helper cell immune response in Japanese encephalitis virus infection. *J Immunol* (2017) 199(9):3094–105. doi: 10.4049/jimmunol.1700671

100. Agrati C, Sacchi A, Bordoni V, Cimini E, Notari S, Grassi G, et al. Expansion of myeloid-derived suppressor cells in patients with severe coronavirus disease (Covid-19). *Cell Death Differ* (2020) 27(11):3196–207. doi: 10.1038/s41418-020-0572-6

101. Xue G, Jiang M, Zhao R, Le A, Li J. Elevated frequencies of Cd14(+)Hla-Dr(Lo/Neg) mdscs in covid-19 patients. *Aging* (2021) 13(5):6236–46. doi: 10.18632/aging.202571

102. Reizine F, Lesouhaitier M, Gregoire M, Pinceaux K, Gacouin A, Maamar A, et al. Sars-Cov-2-Induced Ards associates with mdsc expansion, lymphocyte dysfunction, and arginine shortage. *J Clin Immunol*, 41(3):1–11. doi: 10.1007/s10875-020-00920-5

103. Dean MJ, Ochoa JB, Sanchez-Pino MD, Zabaleta J, Garai J, Del Valle L, et al. Severe covid-19 is characterized by an impaired type I interferon response and elevated levels of arginase producing granulocytic myeloid derived suppressor cells. *Front Immunol* (2021) 12:695972. doi: 10.3389/fimmu.2021.695972

104. De Santo C, Salio M, Masri SH, Lee LY-H, Dong T, Speak AO, et al. Invariant nkt cells reduce the immunosuppressive activity of influenza a virus–induced myeloid-derived suppressor cells in mice and humans. *J Clin Invest* (2008) 118(12):4036–48. doi: 10.1172/JCI36264

105. Johnson TR, Hong S, Van Kaer L, Koezuka Y, Graham BS. Nk T cells contribute to expansion of Cd8+ T cells and amplification of antiviral immune responses to respiratory syncytial virus. *J Virol* (2002) 76(9):4294–303. doi: 10.1128/jvi.76.9.4294-4303.2002

106. Chen N, McCarthy C, Drakesmith H, Li D, Cerundolo V, McMichael AJ, et al. Hiv-1 down-regulates the expression of Cd1d *Via* nef. *Eur J Immunol* (2006) 36(2):278–86. doi: 10.1002/eji.200535487

107. Miura S, Kawana K, Schust DJ, Fujii T, Yokoyama T, Iwasawa Y, et al. Cd1d, a sentinel molecule bridging innate and adaptive immunity, is downregulated by the human papillomavirus (Hpv) E5 protein: A possible mechanism for immune evasion by hpv. *J Virol* (2010) 84(22):11614–23. doi: 10.1128/JVI.01053-10

108. Rao P, Pham HT, Kulkarni A, Yang Y, Liu X, Knipe DM, et al. Herpes simplex virus 1 glycoprotein b and Us3 collaborate to inhibit Cd1d antigen presentation and nkt cell function. *J Virol* (2011) 85(16):8093–104. doi: 10.1128/JVI.02689-10

109. Sanchez DJ, Gumperz JE, Ganem D. Regulation of Cd1d expression and function by a herpesvirus infection. *J Clin Invest* (2005) 115(5):1369–78. doi: 10.1172/JCI24041

110. Webb TJR, Litavecz RA, Khan MA, Du W, Gervay-Hague J, Renukaradhya GJ, et al. Inhibition of Cd1d1-mediated antigen presentation by the vaccinia virus B1r and H5r molecules. *Eur J Immunol* (2006) 36(10):2595–600. doi: 10.1002/eji.200636024

111. Zingaropoli MA, Perri V, Pasculli P, Dezza FC, Nijhawan P, Savelloni G, et al. Major reduction of nkt cells in patients with severe covid-19 pneumonia. *Clin Immunol* (2021) 222:108630. doi: 10.1016/j.clim.2020.108630

112. Zhang JY, Wang XM, Xing X, Xu Z, Zhang C. Single-cell landscape of immunological responses in patients with covid-19. *Nat Immunol* (2020) 21(9):1107–18. doi: 10.1038/s41590-020-0762-x

113. Jouan Y, Guillon A, Gonzalez L, Perez Y, Boisseau C, Ehrmann S, et al. Phenotypical and functional alteration of unconventional T cells in severe covid-19 patients. *J Exp Med* (2020) 217(12):e20200872. doi: 10.1084/jem.20200872

114. Lei L, Qian H, Yang X, Zhang X, Zhang D, Dai T, et al. The phenotypic changes of Γδ T cells in covid-19 patients. *J Cell Mol Med* (2020) 24(19):11603–6. doi: 10.1111/jcmm.15620

115. Odak I, Barros-Martins J, Bošnjak B, Stahl K, David S, Wiesner O, et al. Reappearance of effector T cells is associated with recovery from covid-19. *EBioMedicine* (2020) 57:102885. doi: 10.1016/j.ebiom.2020.102885

116. Mastellos DC, Ricklin D, Lambris JD. Clinical promise of next-generation complement therapeutics. *Nat Rev Drug Discovery* (2019) 18(9):707–29. doi: 10.1038/s41573-019-0031-6

117. Noris M, Benigni A, Remuzzi G. The case of complement activation in covid-19 multiorgan impact. *Kidney Int* (2020) 98(2):314–322. doi: 10.1016/j.kint.2020.05.013

118. Lo MW, Kemper C, Woodruff TM. Covid-19: Complement, coagulation, and collateral damage. *J Immunol* (2020) 205(6):1488–95. doi: 10.4049/jimmunol.2000644

119. Ip WK, Chan KH, Law HK, Tso GH, Kong EK, Wong WH, et al. Mannose-binding lectin in severe acute respiratory syndrome coronavirus infection. *J Infect Dis* (2005) 191(10):1697–704. doi: 10.1086/429631

120. Java A, Apicelli AJ, Liszewski MK, Coler-Reilly A, Atkinson JP, Kim AH, et al. The complement system in covid-19: Friend and foe? *JCI Insight* (2020) 5(15):e140711. doi: 10.1172/jci.insight.140711

121. Zinellu A, Mangoni AA. Serum complement C3 and C4 and covid-19 severity and mortality: A systematic review and meta-analysis with meta-regression. *Front Immunol* (2021) 12:696085. doi: 10.3389/fimmu.2021.696085

122. Risitano AM, Mastellos DC, Huber-Lang M, Yancopoulou D, Garlanda C, Ciceri F, et al. Complement as a target in covid-19? *Nat Rev Immunol* (2020) 20(6):343–4. doi: 10.1038/s41577-020-0320-7

123. Carvelli J, Demaria O, Vély F, Batista L, Benmansour NC, Fares J, et al. Association of covid-19 inflammation with activation of the C5a–C5ar1 axis. *Nature* (2020), 588(7836): 1–5. doi: 10.1038/s41586-020-2600-6

124. Channappanavar R, Zhao J, Perlman S. T Cell-mediated immune response to respiratory coronaviruses. *Immunol Res* (2014) 59(1):118–28. doi: 10.1007/s12026-014-8534-z

125. Xie L-X. Interpretation of the 7th edition of the "Diagnosis and treatment guidelines of coronavirus disease 2019 in china": Progress and challenges. *Chronic Dis Transl Med* (2020) 6(2):75. doi: 10.1016/j.cdtm.2020.04.001

126. Yan L, Zhang H-T, Goncalves J, Xiao Y, Wang M, Guo Y, et al. An interpretable mortality prediction model for covid-19 patients. *Nat Mach Intell* (2020) 2(5):283–8. doi: 10.1038/s42256-020-0180-7

127. Dai W, Zhong A, Qiao Q, Wu J, Li W, Wu Q, et al. Characteristics of lymphocyte subset alterations in covid-19 patients with different levels of disease severity. *Virol J* (2022) 19(1):1–14. doi: 10.1186/s12985-022-01926-8

128. Rahimmanesh I, Kouhpayeh S, Azizi Y, Khanahmad H. Conceptual framework for Sars-Cov-2–related lymphopenia. *Adv Biomed Res* (2022), 11:16. doi: 10.4103/abr.abr_303_20

129. Carbajosa S, Gea S, Chillón-arinas C, Poveda C, del Carmen Maza M, Fresno M, et al. Altered bone marrow lymphopoiesis and interleukin-6-Dependent inhibition of thymocyte differentiation contribute to thymic atrophy during trypanosoma cruzi infection. *Oncotarget* (2017) 8(11):17551. doi: 10.18632/oncotarget.14886

130. Diao B, Wang C, Tan Y, Chen X, Liu Y, Ning L, et al. Reduction and functional exhaustion of T cells in patients with coronavirus disease 2019 (Covid-19). *Front Immunol* (2020) 11:827. doi: 10.3389/fimmu.2020.00827

131. Urra J, Cabrera C, Porras L, Ródenas I. Selective Cd8 cell reduction by sars-Cov-2 is associated with a worse prognosis and systemic inflammation in covid-19 patients. *Clin Immunol* (2020) 217:108486. doi: 10.1016/j.clim.2020.108486

132. Niedźwiedzka-Rystwej P, Majchrzak A, Kurkowska S, Małkowska P, Sierawska O, Hrynkiewicz R, et al. Immune signature of covid-19: In-depth reasons and consequences of the cytokine storm. *Int J Mol Sci* (2022) 23(9):4545. doi: 10.3390/ijms23094545

133. Kang CK, Han G-C, Kim M, Kim G, Shin HM, Song K-H, et al. Aberrant hyperactivation of cytotoxic T-cell as a potential determinant of covid-19 severity. *Int J Infect Dis* (2020) 97:313–21. doi: 10.1016/j.ijid.2020.05.106

134. Georg P, Astaburuaga-García R, Bonaguro L, Brumhard S, Michalick L, Lippert LJ, et al. Complement activation induces excessive T cell cytotoxicity in severe covid-19. *Cell* (2022) 185(3):493–512.e25. doi: 10.1016/j.cell.2021.12.040

135. Beserra DR, Alberca RW, Branco ACCC, Oliveira LM, de Souza Andrade MM, Gozzi-Silva SC, et al. Upregulation of pd-1 expression and high spd-L1 levels associated with covid-19 severity. *J Immunol Res* (2022) 2022: 9764002. doi: 10.1155/2022/9764002

136. BenMohamed L, Srivastava R, Dhanushkodi N, Prakash S, Coulon P-G, Vahed H, et al. High frequencies of phenotypically and functionally senescent and exhausted Cd56+ Cd57+ pd-1+ natural killer cells, sars-Cov-2-Specific memory Cd4+ and Cd8+ T cells associated with severe disease in unvaccinated covid-19 patients. *bioRxiv* (2022) 2022.07.26.501655. doi: 10.1101/2022.07.26.501655

137. Ronit A, Berg RM, Bay JT, Haugaard AK, Ahlström MG, Burgdorf KS, et al. Compartmental immunophenotyping in covid-19 Ards: A case series. *J Allergy Clin Immunol* (2021) 147(1):81–91. doi: 10.1016/j.jaci.2020.09.009

138. Sekine T, Perez-Potti A, Rivera-Ballesteros O, Strålin K, Gorin J-B, Olsson A, et al. Robust T cell immunity in convalescent individuals with asymptomatic or mild covid-19. *Cell* (2020) 183(1):158–68. e14. doi: 10.1016/j.cell.2020.08.017

139. Qin C, Zhou L, Hu Z, Zhang S, Yang S, Tao Y, et al. Dysregulation of immune response in patients with coronavirus 2019 (Covid-19) in wuhan, China. *Clin Infect Dis* (2020) 71(15):762–8. doi: 10.1093/cid/ciaa248

140. Liu Z, Long W, Tu M, Chen S, Huang Y, Wang S, et al. Lymphocyte subset (Cd4+, Cd8+) counts reflect the severity of infection and predict the clinical outcomes in patients with covid-19. *J infect* (2020) 81(2):318–56. doi: 10.1016/j.jinf.2020.03.054

141. Mazzoni A, Maggi L, Capone M, Spinicci M, Salvati L, Colao MG, et al. Cell-mediated and humoral adaptive immune responses to sars-Cov-2 are lower in asymptomatic than symptomatic covid-19 patients. *Eur J Immunol* (2020) 50 (12):2013–24. doi: 10.1002/eji.202048915

142. Martonik D, Parfieniuk-Kowerda A, Rogalska M, Flisiak R. The role of Th17 response in covid-19. *Cells* (2021) 10(6):1550. doi: 10.3390/cells10061550

143. Neidleman J, Luo X, Frouard J, Xie G, Gill G, Stein ES, et al. Sars-Cov-2-Specific T cells exhibit phenotypic features of helper function, lack of terminal differentiation, and high proliferation potential. *Cell Rep Med* (2020) 1(6):100081. doi: 10.1016/j.xcrm.2020.100081

144. Verhagen J, van der Meijden ED, Lang V, Kremer AE, Völkl S, Mackensen A, et al. Human Cd4+ T cells specific for dominant epitopes of sars-Cov-2 spike and nucleocapsid proteins with therapeutic potential. *Clin Exp Immunol* (2021) 205 (3):363–378. doi: 10.1111/cei.13627

145. Sadeghi A, Tahmasebi S, Mahmood A, Kuznetsova M, Valizadeh H, Taghizadieh A, et al. Th17 and treg cells function in sars-Cov2 patients compared with healthy controls. *J Cell Physiol* (2021) 236(4):2829–39. doi: 10.1002/jcp.30047

146. Gil-Etayo FJ, Suàrez-Fernández P, Cabrera-Marante O, Arroyo D, Garcinuño S, Naranjo L, et al. T-Helper cell subset response is a determining factor in covid-19 progression. *Front Cell Infect Microbiol* (2021) 11:624483. doi: 10.3389/fcimb.2021.624483

147. Aleebrahim-Dehkordi E, Molavi B, Mokhtari M, Deravi N, Fathi M, Fazel T, et al. T Helper type (Th1/Th2) responses to sars-Cov-2 and influenza a (H1n1) virus: From cytokines produced to immune responses. *Transplant Immunol* (2022) 70:101495. doi: 10.1016/j.trim.2021.101495

148. Parackova Z, Bloomfield M, Klocperk A, Sediva A. Neutrophils mediate Th17 promotion in covid-19 patients. *J Leukoc Biol* (2021) 109(1):73–6. doi: 10.1002/JLB.4COVCRA0820-481RRR

149. Wei Ll, Wang Wj, Chen Dx, Xu B. Dysregulation of the immune response affects the outcome of critical covid-19 patients. *J Med Virol* (2020) 92(11):2768–76. doi: 10.1002/jmv.26181

150. Muyayalo KP, Huang DH, Zhao SJ, Xie T, Mor G, Liao AH. Covid-19 and Treg/Th17 imbalance: Potential relationship to pregnancy outcomes. *Am J Reprod Immunol* (2020) 84(5):e13304. doi: 10.1111/aji.13304

151. Wu D, Yang XO. Th17 responses in cytokine storm of covid-19: An emerging target of Jak2 inhibitor fedratinib. *J Microbiol Immunol Infect* (2020) 53(3):368–70. doi: 10.1016/j.jmii.2020.03.005

152. Tahmasebi S, El-Esawi MA, Mahmoud ZH, Timoshin A, Valizadeh H, Roshangar L, et al. Immunomodulatory effects of nanocurcumin on Th17 cell responses in mild and severe covid-19 patients. *J Cell Physiol* (2021) 236(7):5325–38. doi: 10.1002/jcp.30233

153. Orlov M, Wander PL, Morrell ED, Mikacenic C, Wurfel MM. A case for targeting Th17 cells and il-17a in sars-Cov-2 infections. *J Immunol* (2020) 205(4):892–8. doi: 10.4049/jimmunol.2000554

154. Zheng M, Gao Y, Wang G, Song G, Liu S, Sun D, et al. Functional exhaustion of antiviral lymphocytes in covid-19 patients. *Cell Mol Immunol* (2020) 17(5):533–5. doi: 10.1038/s41423-020-0402-2

155. Wang J, Li Q, Qiu Y, Lu H. Covid-19: Imbalanced cell-mediated immune response drives to immunopathology. *Emerg Microbes Infect* (2022) 11(1):2393–404. doi: 10.1080/22221751.2022.2122579

156. Choto TA, Makupe I, Cakana AZ, Sibanda EN, Mduluza T. Excessive neutrophil recruitment promotes typical T-helper 17 responses in coronavirus disease 2019 patients. *PloS One* (2022) 17(8):e0273186. doi: 10.1371/journal.pone.0273186

157. Tahmasebi S, Saeed BQ, Temirgalieva E, Yumashev AV, El-Esawi MA, Navashenaq JG, et al. Nanocurcumin improves treg cell responses in patients with mild and severe sars-Cov2. *Life Sci* (2021) 276:119437. doi: 10.1016/j.lfs.2021.119437

158. Alahyari S, Rajaeinejad M, Jalaeikhoo H, Amani D. Regulatory T cells in immunopathogenesis and severity of covid-19: A systematic review. *Arch Iranian Med* (2022) 25(2):127–32. doi: 10.34172/aim.2022.22

159. Carissimo G, Xu W, Kwok I, Abdad MY, Chan Y-H, Fong S-W, et al. Whole blood immunophenotyping uncovers immature neutrophil-to-Vd2 T-cell ratio as an early marker for severe covid-19. *Nat Commun* (2020) 11(1):1–12. doi: 10.1038/s41467-020-19080-6

160. Chen G, Wu D, Guo W, Cao Y, Huang D, Wang H, et al. Clinical and immunological features of severe and moderate coronavirus disease 2019. *J Clin Invest* (2020) 130(5):2620–9. doi: 10.1172/JCI137244

161. Kalfaoglu B, Almeida-Santos J, Tye CA, Satou Y, Ono M. T-Cell hyperactivation and paralysis in severe covid-19 infection revealed by single-cell analysis. *Front Immunol* (2020) 11:589380. doi: 10.3389/fimmu.2020.589380

162. Chu H, Zhou J, Wong BH-Y, Li C, Chan JF-W, Cheng Z-S, et al. Middle East respiratory syndrome coronavirus efficiently infects human primary T lymphocytes and activates the extrinsic and intrinsic apoptosis pathways. *J Infect Dis* (2016) 213(6):904–14. doi: 10.1093/infdis/jiv380

163. Neurath MF. Covid-19 and immunomodulation in ibd. *Gut* (2020) 69(7):1335–42. doi: 10.1136/gutjnl-2020-321269

164. Taylor GA, Feng CG, Sher A. P47 gtpases: Regulators of immunity to intracellular pathogens. *Nat Rev Immunol* (2004) 4(2):100–9. doi: 10.1038/nri1270

165. Peng Y, Mentzer AJ, Liu G, Yao X, Yin Z, Dong D, et al. Broad and strong memory Cd4+ and Cd8+ T cells induced by sars-Cov-2 in uk convalescent individuals following covid-19. *Nat Immunol* (2020) 21(11):1336–45. doi: 10.1038/s41590-020-0782-6

166. Cao X. Covid-19: Immunopathology and its implications for therapy. *Nat Rev Immunol* (2020) 20(5):269–70. doi: 10.1038/s41577-020-0308-3

167. Zhang W, Zhao Y, Zhang F, Wang Q, Li T, Liu Z, et al. The use of anti-inflammatory drugs in the treatment of people with severe coronavirus disease 2019 (Covid-19): The perspectives of clinical immunologists from China. *Clin Immunol* (2020) 214:108393. doi: 10.1016/j.clim.2020.108393

168. Ma Y, Qiu F, Deng C, Li J, Huang Y, Wu Z, et al. Integrating single-cell sequencing data with gwas summary statistics reveals Cd16+ monocytes and memory Cd8+ T cells involved in severe covid-19. *Genome Med* (2022) 14(1):1–21. doi: 10.1186/s13073-022-01021-1

169. Heeb LE, Egholm C, Boyman O. Evolution and function of interleukin-4 receptor signaling in adaptive immunity and neutrophils. *Genes Immun* (2020) 21(3):143–9. doi: 10.1038/s41435-020-0095-7

170. Moon C. Fighting covid-19 exhausts T cells. *Nat Rev Immunol* (2020) 20(5):277–8. doi: 10.1038/s41577-020-0304-7

171. Kaneko N, Boucau J, Kuo H-H, Perugino C, Mahajan VS, Farmer JR, et al. Temporal changes in T cell subsets and expansion of cytotoxic Cd4+ T cells in the lungs in severe covid-19. *Clin Immunol* (2022) 237:108991. doi: 10.1016/j.clim.2022.108991

172. Wherry EJ, Ahmed R. Memory Cd8 T-cell differentiation during viral infection. *J Virol* (2004) 78(11):5535–45. doi: 10.1128/JVI.78.11.5535-5545.2004

173. Qin C, Zhou L, Hu Z, Zhang S, Yang S, Tao Y, et al. Dysregulation of immune response in patients with covid-19 in wuhan, China. *Clin Infect Dis* (2020) 71 (15):762–768. doi: 10.1093/cid/ciaa248

174. Zuin J, Fogar P, Musso G, Padoan A, Piva E, Pelloso M, et al. T Cell senescence by extensive phenotyping: An emerging feature of covid-19 severity. *Lab Med* (2022) 53 (6):609–13. doi: 10.1093/labmed/lmac048

175. Strutt TM, McKinstry KK, Dibble JP, Winchell C, Kuang Y, Curtis JD, et al. Memory Cd4+ T cells induce innate responses independently of pathogen. *Nat Med* (2010) 16(5):558–64. doi: 10.1038/nm.2142

176. Schenkel JM, Fraser KA, Vezys V, Masopust D. Sensing and alarm function of resident memory Cd8+ T cells. *Nat Immunol* (2013) 14(5):509–13. doi: 10.1038/ni.2568

177. Zhao J, Zhao J, Mangalam AK, Channappanavar R, Fett C, Meyerholz DK, et al. Airway memory Cd4+ T cells mediate protective immunity against emerging respiratory coronaviruses. *Immunity* (2016) 44(6):1379–91. doi: 10.1016/j.immuni.2016.05.006

178. Oja AE, Saris A, Ghandour CA, Kragten NA, Hogema BM, Nossent EJ, et al. Divergent sars-Cov-2-Specific T-and b-cell responses in severe but not mild covid-19 patients. *Eur J Immunol* (2020) 50(12):1998–2012. doi: 10.1002/eji.202048908

179. Zhao Y, Kilian C, Turner J-E, Bosurgi L, Roedl K, Bartsch P, et al. Clonal expansion and activation of tissue-resident memory-like Th17 cells expressing gm-csf in the lungs of severe covid-19 patients. *Sci Immunol* (2021) 6(56): eabf6692. doi: 10.1126/sciimmunol.abf6692

180. Chen L, Wei B, Di D. A narrative review of tissue-resident memory T cells and their role in immune surveillance and covid-19. *Eur Rev Med Pharmacol Sci* (2022) 26 (12):4486–96. doi: 10.26355/eurrev_202206_29088

181. Lam JH, Smith FL, Baumgarth N. B cell activation and response regulation during viral infections. *Viral Immunol* (2020) 33(4):294–306. doi: 10.1089/vim.2019.0207

182. Jin Y, Yang H, Ji W, Wu W, Chen S, Zhang W, et al. Virology, epidemiology, pathogenesis, and control of covid-19. *Viruses* (2020) 12(4):372. doi: 10.3390/v12040372

183. Wildner NH, Ahmadi P, Schulte S, Brauneck F, Kohsar M, Lütgehetmann M, et al. B cell analysis in sars-Cov-2 versus malaria: Increased frequencies of plasmablasts and atypical memory b cells in covid-19. *J Leukoc Biol* (2021) 109(1):77–90. doi: 10.1002/JLB.5COVA0620-370RR

184. Davis CW, Jackson KJ, McElroy AK, Halfmann P, Huang J, Chennareddy C, et al. Longitudinal analysis of the human b cell response to Ebola virus infection. *Cell* (2019) 177(6):1566–82. e17. doi: 10.1016/j.cell.2019.04.036

185. Butler AL, Fischinger S, Alter G. The antibodiome–mapping the humoral immune response to hiv. *Curr HIV/AIDS Rep* (2019) 16(2):169–79. doi: 10.1007/s11904-019-00432-x

186. Siracusano G, Pastori C, Lopalco L. Humoral immune responses in covid-19 patients: A window on the state of the art. *Front Immunol* (2020) 11:1049. doi: 10.3389/fimmu.2020.01049

187. Kulkarni R. Antibody-dependent enhancement of viral infections. *Dyn Immune Activation Viral Dis* Ed Bramhachari P (2020), (Springer, Singapore). doi: 10.1007/978-981-15-1045-8_2

188. Yang Y, Xu F. Evolving understanding of antibody-dependent enhancement (ADE) of SARS-CoV-2. *Front Immunol* (2022), 13: 1008285. doi: 10.3389/fimmu.2022.1008285

189. Yao C, Bora SA, Parimon T, Zaman T, Friedman OA, Palatinus JA, et al. Cell-Type-Specific immune dysregulation in severely ill covid-19 patients. *Cell Rep* (2021) 34 (1):108590. doi: 10.1016/j.celrep.2020.108590

190. Sosa-Hernández VA, Torres-Ruíz J, Cervantes-Díaz R, Romero-Ramírez S, Páez-Franco JC, Meza-Sánchez DE, et al. B cell subsets as severity-associated signatures in covid-19 patients. *Front Immunol* (2020) 11:611004. doi: 10.3389/fimmu.2020.611004

191. Bastard P, Rosen LB, Zhang Q, Michailidis E, Hoffmann H-H, Zhang Y, et al. Autoantibodies against type I ifns in patients with life-threatening covid-19. *Science* (2020) 370(6515): eabd4585. doi: 10.1126/science.abd4585

192. Tabibian-Keissar H, Hazanov L, Schiby G, Rosenthal N, Rakovsky A, Michaeli M, et al. Aging affects b-cell antigen receptor repertoire diversity in primary and secondary lymphoid tissues. *Eur J Immunol* (2016) 46(2):480–92. doi: 10.1002/eji.201545586

193. Hong B, Wang L, Huang C, Hong X, Liu A, Li Q, et al. Decrease of clone diversity in igm repertoires of hbv chronically infected individuals with high level of viral replication. *Front Immunol* (2021) 11:615669. doi: 10.3389/fmicb.2020.615669

194. Kaneko N, Kuo H-H, Boucau J, Farmer JR, Allard-Chamard H, Mahajan VS, et al. Loss of bcl-6-Expressing T follicular helper cells and germinal centers in covid-19. *Cell* (2020) 183(1):143–57.e13. doi: 10.1016/j.cell.2020.08.025

195. Wang F, Nie J, Wang H, Zhao Q, Xiong Y, Deng L, et al. Characteristics of peripheral lymphocyte subset alteration in covid-19 pneumonia. *J Infect Dis* (2020) 221 (11):1762–9. doi: 10.1093/infdis/jiaa150

196. Shuwa HA, Shaw TN, Knight S, McClure FA, Wemyss K, Prise I, et al. Long-lasting alterations in T and b cell function in convalescent covid-19 patients. (2020). doi: 10.2139/ssrn.3720301

197. Feldmann M, Maini RN, Woody JN, Holgate ST, Winter G, Rowland M, et al. Trials of anti-tumour necrosis factor therapy for covid-19 are urgently needed. *Lancet (London England)* (2020) 395(10234):1407–9. doi: 10.1016/s0140-6736(20)30858-8

198. Stephenson E, Reynolds G, Botting RA, Calero-Nieto FJ, Morgan MD, Tuong ZK, et al. Single-cell multi-omics analysis of the immune response in covid-19. *Nat Med* (2021) 27(5):904–16. doi: 10.1038/s41591-021-01329-2

199. Woodruff MC, Ramonell RP, Nguyen DC, Cashman KS, Saini AS, Haddad NS, et al. Extrafollicular b cell responses correlate with neutralizing antibodies and morbidity in covid-19. *Nat Immunol* (2020) 21(12):1506–16. doi: 10.1038/s41590-020-00814-z

200. Woodruff M, Ramonell R, Cashman K, Nguyen D, Saini A, Haddad N, et al. Dominant extrafollicular b cell responses in severe covid-19 disease correlate with robust viral-specific antibody production but poor clinical outcomes. *medRxiv preprint server Health Sci* (2020) 21 (12):1506–1516. doi: 10.1101/2020.04.29.20083717

201. Hoehn KB, Ramanathan P, Unterman A, Sumida TS, Asashima H, Hafler DA, et al. Cutting edge: Distinct b cell repertoires characterize patients with mild and severe covid-19. *J Immunol* (2021) 206(12):2785–90. doi: 10.4049/jimmunol.2100135

202. Gao L, Zhou J, Yang S, Wang L, Chen X, Yang Y, et al. The dichotomous and incomplete adaptive immunity in covid-19 patients with different disease severity. *Signal Transduct Target Ther* (2021) 6(1):1–10. doi: 10.1038/s41392-021-00525-3

203. Sakharkar M, Rappazzo CG, Wieland-Alter WF, Hsieh C-L, Wrapp D, Esterman ES, et al. Prolonged evolution of the human b cell response to sars-Cov-2 infection. *Sci Immunol* (2021) 6(56): eabg6916. doi: 10.1126/sciimmunol.abg6916

204. Rodda LB, Netland J, Shehata L, Pruner KB, Morawski PA, Thouvenel CD, et al. Functional sars-Cov-2-Specific immune memory persists after mild covid-19. *Cell* (2021) 184(1):169–83.e17. doi: 10.1016/j.cell.2020.11.029

205. Golovkin A, Kalinina O, Bezrukikh V, Aquino A, Zaikova E, Karonova T, et al. Imbalanced immune response of T-cell and b-cell subsets in patients with moderate and severe covid-19. *Viruses* (2021) 13(10):1966. doi: 10.3390/v13101966

206. Laidlaw BJ, Ellebedy AH. The germinal centre b cell response to sars-Cov-2. *Nat Rev Immunol* (2022) 22(1):7–18. doi: 10.1038/s41577-021-00657-1

207. Hasan A, Al-Ozairi E, Al-Baqsumi Z, Ahmad R, Al-Mulla F. Cellular and humoral immune responses in covid-19 and immunotherapeutic approaches. *ImmunoTargets Ther* (2021) 10:63. doi: 10.2147/ITT.S280706

208. Röltgen K, Boyd SD. Antibody and b cell responses to sars-Cov-2 infection and vaccination. *Cell Host Microbe* (2021) 29(7):1063–75. doi: 10.1016/j.chom.2021.06.009

209. Bulati M, Buffa S, Martorana A, Gervasi F, Camarda C, Azzarello DM, et al. Double negative (Igg+ igd– Cd27–) b cells are increased in a cohort of moderate-severe alzheimer's disease patients and show a pro-inflammatory trafficking receptor phenotype. *J Alzheimers Dis* (2015) 44(4):1241–51. doi: 10.3233/JAD-142412

210. You X, Zhang R, Shao M, He J, Chen J, Liu J, et al. Double negative b cell is associated with renal impairment in systemic lupus erythematosus and acts as a marker for nephritis remission. *Front Med (Lausanne)* (2020) 7:85. doi: 10.3389/fmed.2020.00085

211. Taefehshokr N, Taefehshokr S, Heit B. Mechanisms of dysregulated humoral and cellular immunity by sars-Cov-2. *Pathogens* (2020) 9(12):1027. doi: 10.3390/pathogens9121027

212. Ruschil C, Gabernet G, Lepennetier G, Heumos S, Kaminski M, Hracsko Z, et al. Specific induction of double negative b cells during protective and pathogenic immune responses. *Front Immunol* (2020) 11:606338. doi: 10.3389/fimmu.2020.606338

213. Kuri-Cervantes L, Pampena MB, Meng W, Rosenfeld AM, Ittner CA, Weisman AR, et al. Comprehensive mapping of immune perturbations associated with severe covid-19. *Sci Immunol* (2020) 5(49): eabd7114. doi: 10.1126/sciimmunol.abd7114

214. Zhao J, Yuan Q, Wang H, Liu W, Liao X, Su Y, et al. Antibody responses to sars-Cov-2 in patients with novel coronavirus disease 2019. *Clin Infect Dis* (2020) 71(16):2027–34. doi: 10.1093/cid/ciaa344

215. Farris AD, Guthridge JM. Overlapping b cell pathways in severe covid-19 and lupus. *Nat Immunol* (2020) 21(12):1478–80. doi: 10.1038/s41590-020-00822-z

216. Guthmiller JJ, Stovicek O, Wang J, Changrob S, Li L, Halfmann P, et al. Sars-Cov-2 infection severity is linked to superior humoral immunity against the spike. *Mbio* (2021) 12(1): e02940-20. doi: 10.1128/mBio.02940-20

217. Hoepel W, Chen H-J, Allahverdiyeva S, Manz X, Aman J, Bonta P, et al. Anti-Sars-Cov-2 igg from severely ill covid-19 patients promotes macrophage hyper-inflammatory responses. *BioRxiv* (2020). doi: 10.1101/2020.07.13.190140

218. Karthik K, Senthilkumar TMA, Udhayavel S, Raj GD. Role of antibody-dependent enhancement (Ade) in the virulence of sars-Cov-2 and its mitigation strategies for the development of vaccines and immunotherapies to counter covid-19. *Hum Vaccin Immunother* (2020) 16(12):3055–60. doi: 10.1080/21645515.2020.1796425

219. Lu L, Zhang H, Zhan M, Jiang J, Yin H, Dauphars DJ, et al. Antibody response and therapy in covid-19 patients: What can be learned for vaccine development? *Sci China Life Sci* (2020), 63 (12):1833–1849. doi: 10.1007/s11427-020-1859-y

220. Pascolini S, Vannini A, Deleonardi G, Ciordinik M, Sensoli A, Carletti I, et al. Covid-19 and immunological dysregulation: Can autoantibodies be useful? *Clin Transl Sci* (2020); 14 (2):502–508. doi: 10.1111/cts.12908

221. Hashem AM, Algaissi A, Almahboub SA, Alfaleh MA, Abujamel TS, Alamri SS, et al. Early humoral response correlates with disease severity and outcomes in covid-19 patients. *Viruses* (2020) 12(12):1390. doi: 10.3390/v12121390

222. Chakraborty S, Gonzalez J, Edwards K, Mallajosyula V, Buzzanco AS, Sherwood R, et al. Proinflammatory igg fc structures in patients with severe covid-19. *Nat Immunol* (2021) 22(1):67–73. doi: 10.1038/s41590-020-00828-7

223. Yang Y, Yang M, Peng Y, Liang Y, Wei J, Xing L, et al. Longitudinal analysis of antibody dynamics in covid-19 convalescents reveals neutralizing responses up to 16 months after infection. *Nat Microbiol* (2022) 7(3):423–33. doi: 10.1038/s41564-021-01051-2

224. Ye Q, Wang B, Mao J. The pathogenesis and treatment of the `Cytokine Storm' in COVID-19. *J Infect* (2020); 80(6):607–613. doi: 10.1016/j.jinf.2020.03.037

225. Mistry P, Barmania F, Mellet J, Peta K, Strydom A, Viljoen IM, et al. Sars-Cov-2 variants, vaccines, and host immunity. *Front Immunol* (2021) 12:809244. doi: 10.3389/fimmu.2021.809244

226. Wiersinga WJ, Rhodes A, Cheng AC, Peacock SJ, Prescott HC. Pathophysiology, transmission, diagnosis, and treatment of coronavirus disease 2019 (Covid-19): A review. *Jama* (2020) 324(8):782–93. doi: 10.1001/jama.2020.12839

227. İnandıklıoğlu N, Akkoc T. Immune Responses to SARS-CoV, MERS-CoV and SARS-CoV-2. *Cell Biol Trans Med Vol 9: Adv Exp Med Biol* (2020), 1288:5–12. doi: 10.1007/5584_2020_549

228. Yang X, Yu Y, Xu J, Shu H, Liu H, Wu Y, et al. Clinical course and outcomes of critically ill patients with sars-Cov-2 pneumonia in wuhan, China: A single-centered, retrospective, observational study. *Lancet Respir Med* (2020) 8(5):475–81. doi: 10.1016/S2213-2600(20)30079-5

229. Eskilsson A, Mirrasekhian E, Dufour S, Schwaninger M, Engblom D, Blomqvist A. Immune-induced fever is mediated by il-6 receptors on brain endothelial cells coupled to Stat3-dependent induction of brain endothelial prostaglandin synthesis. *J Neurosci* (2014) 34(48):15957–61. doi: 10.1523/JNEUROSCI.3520-14.2014

230. Hsu RJ, Yu WC, Peng GR, Ye CH, Hu S, Chong PCT, et al. The role of cytokines and chemokines in severe acute respiratory syndrome coronavirus 2 infections. *Front Immunol* (2022) 13:832394. doi: 10.3389/fimmu.2022.832394

231. Bhaskar S, Sinha A, Banach M, Mittoo S, Weissert R, Kass JS, et al. Cytokine storm in Covid-19–immunopathological mechanisms, clinical considerations, and therapeutic approaches: The reprogram consortium position paper. *Front Immunol* (2020) 11:1648. doi: 10.3389/fimmu.2020.01648

232. Samuel CE. Antiviral actions of interferons. *Clin Microbiol Rev* (2001) 14(4):778–809. doi: 10.1128/CMR.14.4.778-809.2001

233. Takeuchi O, Akira S. Innate immunity to virus infection. *Immunol Rev* (2009) 227 (1):75–86. doi: 10.1111/j.1600-065X.2008.00737.x

234. Katze MG, He Y, Gale M. Viruses and interferon: A fight for supremacy. *Nat Rev Immunol* (2002) 2(9):675–87. doi: 10.1038/nri888

235. Tang F, Du Q, Liu Y-J. Plasmacytoid dendritic cells in antiviral immunity and autoimmunity. *Sci China Life Sci* (2010) 53(2):172–82. doi: 10.1007/s11427-010-0045-0

236. Felgenhauer U, Schoen A, Gad HH, Hartmann R, Schaubmar AR, Failing K, et al. Inhibition of sars-Cov-2 by type I and type iii interferons. *J Biol Chem* (2020) 295 (41):13958–64. doi: 10.1074/jbc.AC120.013788

237. Huang CT, Chao TL, Kao HC, Pang YH, Lee WH, Hsieh CH, et al. Enhancement of the ifn-B-Induced host signature informs repurposed drugs for covid-19. *Heliyon* (2020) 6(12):e05646. doi: 10.1016/j.heliyon.2020.e05646

238. Hung IF, Lung KC, Tso EY, Liu R, Chung TW, Chu MY, et al. Triple combination of interferon beta-1b, lopinavir-ritonavir, and ribavirin in the treatment of patients admitted to hospital with covid-19: An open-label, randomised, phase 2 trial. *Lancet (London England)* (2020) 395(10238):1695–704. doi: 10.1016/s0140-6736(20)31042-4

239. Khamis F, Al Naabi H, Al Lawati A, Ambusaidi Z, Al Sharji M, Al Barwani U, et al. Randomized controlled open label trial on the use of favipiravir combined with inhaled interferon beta-1b in hospitalized patients with moderate to severe covid-19 pneumonia. *Int J Infect Dis* (2021) 102:538–43. doi: 10.1016/j.ijid.2020.11.008

240. Hadjadj J, Yatim N, Barnabei L, Corneau A, Boussier J, Smith N, et al. Impaired type I interferon activity and inflammatory responses in severe covid-19 patients. *Science* (2020) 369(6504):718–24. doi: 10.1126/science.abc6027

241. Kopecky-Bromberg SA, Martínez-Sobrido L, Frieman M, Baric RA, Palese P. Severe acute respiratory syndrome coronavirus open reading frame (Orf) 3b, orf 6, and nucleocapsid proteins function as interferon antagonists. *J Virol* (2007) 81(2):548–57. doi: 10.1128/JVI.01782-06

242. Galani I-E, Rovina N, Lampropoulou V, Triantafyllia V, Manioudaki M, Pavlos E, et al. Untuned antiviral immunity in covid-19 revealed by temporal type I/Iii interferon patterns and flu comparison. *Nat Immunol* (2021) 22(1):32–40. doi: 10.1038/s41590-020-00840-x

243. Yousefifard M, Zali A, Mohamed Ali K, Madani Neishaboori A, Zarghi A, Hosseini M, et al. Antiviral therapy in management of covid-19: A systematic review on current evidence. *Arch Acad Emergency Med* (2020) 8(1):e45.

244. Mattos-Silva P, Felix NS, Silva PL, Robba C, Battaglini D, Pelosi P, et al. Pros and cons of corticosteroid therapy for covid-19 patients. *Respir Physiol Neurobiol* (2020) 280:103492. doi: 10.1016/j.resp.2020.103492

245. Krumm ZA, Lloyd GM, Francis CP, Nasif LH, Mitchell DA, Golde TE, et al. Precision therapeutic targets for covid-19. *Virol J* (2021) 18(1):66. doi: 10.1186/s12985-021-01526-y

246. Zhou YW, Xie Y. Therapeutic targets and interventional strategies in covid-19: Mechanisms and clinical studies. *Signal Transduct Target Ther* (2021) 6(1):317. doi: 10.1038/s41392-021-00733-x

247. Laterre PF, François B, Collienne C, Hantson P, Jeannet R, Remy KE, et al. Association of interleukin 7 immunotherapy with lymphocyte counts among patients with severe coronavirus disease 2019 (Covid-19). *JAMA netw Open* (2020) 3(7):e2016485. doi: 10.1001/jamanetworkopen.2020.16485

248. Monneret G, de Marignan D, Coudereau R, Bernet C, Ader F, Frobert E, et al. Immune monitoring of interleukin-7 compassionate use in a critically ill covid-19 patient. *Cell Mol Immunol* (2020) 17(9):1001–3. doi: 10.1038/s41423-020-0516-6

249. Gupta S, Wang W, Hayek SS, Chan L, Mathews KS, Melamed ML, et al. Association between early treatment with tocilizumab and mortality among critically ill patients with covid-19. *JAMA Internal Med* (2021) 181(1):41–51. doi: 10.1001/jamainternmed.2020.6252

250. Ucciferri C, Auricchio A, Di Nicola M, Potere N, Abbate A, Cipollone F, et al. Canakinumab in a subgroup of patients with covid-19. *Lancet Rheumatol* (2020) 2(8): e457–ee8. doi: 10.1016/s2665-9913(20)30167-3

251. Cauchois R, Koubi M. Early il-1 receptor blockade in severe inflammatory respiratory failure complicating covid-19. *Proc Natl Acad Sci U.S.A.* (2020) 117 (32):18951–3. doi: 10.1073/pnas.2009017117

252. Yang L, Xie X, Tu Z, Fu J, Xu D, Zhou Y. The signal pathways and treatment of cytokine storm in covid-19. *Signal Transduct Target Ther* (2021) 6(1):255. doi: 10.1038/s41392-021-00679-0

253. Duret PM, Spielmann L, Messer L. Response to: 'Correspondence on recovery from covid-19 in a patient with spondyloarthritis treated with tnf-alpha inhibitor etanercept. a report on a covid-19 patient with psoriatic arthritis receiving ustekinumab' by Messina et al. *Ann Rheum Dis* (2021) 80(5):e80. doi: 10.1136/annrheumdis-2020-218147

254. Zhou Q, Chen V, Shannon CP, Wei XS, Xiang X, Wang X, et al. Interferon-A2b treatment for covid-19. *Front Immunol* (2020) 11:1061. doi: 10.3389/fimmu.2020.01061

255. Xie X, Jiang Y, Zeng Y, Liu H. Combination antiviral therapy with Lopinavir/Ritonavir, arbidol and interferon-A1b for covid-19. *Antiviral Ther* (2020) 25(4):233–9. doi: 10.3851/imp3362

256. Leng Z, Zhu R, Hou W, Feng Y, Yang Y, Han Q, et al. Transplantation of Ace2(-) mesenchymal stem cells improves the outcome of patients with covid-19 pneumonia. *Aging Dis* (2020) 11(2):216–28. doi: 10.14336/ad.2020.0228

257. Suzuki Y, Tanino Y, Nikaido T, Minemura H, Umeda T, Rikimaru M, et al. Severe coronavirus disease 2019 that recovered from respiratory failure by treatment that included high-dose intravenous immunoglobulin. *Internal Med (Tokyo Japan)* (2021) 60(3):457–61. doi: 10.2169/internalmedicine.6326-20

258. Liu Q, Zhou YH, Yang ZQ. The cytokine storm of severe influenza and development of immunomodulatory therapy. *Cell Mol Immunol* (2016) 13(1):3–10. doi: 10.1038/cmi.2015.74

259. Lee DW, Gardner R, Porter DL, Louis CU, Ahmed N, Jensen M, et al. Current concepts in the diagnosis and management of cytokine release syndrome. *Blood* (2014) 124(2):188–95. doi: 10.1182/blood-2014-05-552729

260. Kaplon H, Reichert JM. Antibodies to watch in 2021. *MAbs* (2021) 13(1):1860476. doi: 10.1080/19420862.2020.1860476

261. Clark IA. Background to new treatments for COVID-19, including its chronicity, through altering elements of the cytokine storm. *Rev Med Virol* (2020); 31 (5):1–13. doi: 10.1002/rmv.2210

262. Sterne JAC, Murthy S, Diaz JV, Slutsky AS, Villar J, Angus DC, et al. Association between administration of systemic corticosteroids and mortality among critically ill patients with covid-19: A meta-analysis. *Jama* (2020) 324(13):1330–41. doi: 10.1001/jama.2020.17023

263. Johnson RM, Vinetz JM. Dexamethasone in the management of covid -19. *Bmj* (2020) 370:m2648. doi: 10.1136/bmj.m2648

264. Lin P. Targeting interleukin-6 for noninfectious uveitis. *Clin Ophthalmol (Auckland NZ)* (2015) 9:1697–702. doi: 10.2147/opth.s68595

265. Karkhur S, Hasanreisoglu M, Vigil E, Halim MS, Hassan M, Plaza C, et al. Interleukin-6 inhibition in the management of non-infectious uveitis and beyond. *J ophthal Inflammation infect* (2019) 9(1):17. doi: 10.1186/s12348-019-0182-y

266. Tang L, Yin Z, Hu Y, Mei H. Controlling cytokine storm is vital in covid-19. *Front Immunol* (2020) 11:570993. doi: 10.3389/fimmu.2020.570993

267. Della-Torre E, Campochiaro C. Interleukin-6 blockade with sarilumab in severe covid-19 pneumonia with systemic hyperinflammation: An open-label cohort study. *Ann Rheum Dis* (2020) 79(10):1277–85. doi: 10.1136/annrheumdis-2020-218122

268. Benucci M, Giannasi G, Cecchini P, Gobbi FL, Damiani A, Grossi V, et al. Covid-19 pneumonia treated with sarilumab: A clinical series of eight patients. *J Med Virol* (2020) 92(11):2368–70. doi: 10.1002/jmv.26062

269. Gritti G, Raimondi F, Ripamonti D, Riva I, Landi F, Alborghetti L, et al. Il-6 signalling pathway inactivation with siltuximab in patients with covid-19 respiratory failure: An observational cohort study. *medRxiv preprint server Health Sci* (2020). doi: 10.1101/2020.04.01.20048561

270. Cavalli G, De Luca G, Campochiaro C, Della-Torre E, Ripa M, Canetti D, et al. Interleukin-1 blockade with high-dose anakinra in patients with covid-19, acute respiratory distress syndrome, and hyperinflammation: A retrospective cohort study. *Lancet Rheumatol* (2020) 2(6):e325–e31. doi: 10.1016/s2665-9913(20)30127-2

271. Dimopoulos G, de Mast Q, Markou N, Theodorakopoulou M, Komnos A, Mouktaroudi M, et al. Favorable anakinra responses in severe covid-19 patients with secondary hemophagocytic lymphohistiocytosis. *Cell Host Microbe* (2020) 28(1):117–23.e1. doi: 10.1016/j.chom.2020.05.007

272. Kooistra EJ, Waalders NJB, Grondman I, Janssen NAF, de Nooijer AH, Netea MG, et al. Anakinra treatment in critically ill covid-19 patients: A prospective cohort study. *Crit Care* (2020) 24(1):688. doi: 10.1186/s13054-020-03364-w

273. Katia F, Myriam DP, Ucciferri C. Efficacy of canakinumab in mild or severe covid-19 pneumonia. *Immun Inflammation Dis* (2021) 9(2):399–405. doi: 10.1002/iid3.400

274. Generali D, Bosio G, Malberti F, Cuzzoli A, Testa S, Romanini L, et al. Canakinumab as treatment for covid-19-Related pneumonia: A prospective case-control study. *Int J Infect Dis* (2021) 104:433–40. doi: 10.1016/j.ijid.2020.12.073

275. Sheng CC, Sahoo D, Dugar S, Prada RA, Wang TKM, Abou Hassan OK, et al. Canakinumab to reduce deterioration of cardiac and respiratory function in sars-Cov-2 associated myocardial injury with heightened inflammation (Canakinumab in covid-19 cardiac injury: The three c study). *Clin Cardiol* (2020) 43(10):1055–63. doi: 10.1002/clc.23451

276. Landi L, Ravaglia C, Russo E, Cataleta P, Fusari M, Boschi A, et al. Blockage of interleukin-1β with canakinumab in patients with covid-19. *Sci Rep* (2020) 10(1):21775. doi: 10.1038/s41598-020-78492-y

277. Kunisaki R, Tsukiji J, Kudo M. Potential inhibition of covid-19-Driven pneumonia by immunosuppressive therapy and anti-tnfα antibodies: A case report. *J Crohn's colitis* (2020) 14 (12):1786–1787. doi: 10.1093/ecco-jcc/jjaa105

278. Guo Y, Hu K, Li Y, Lu C, Ling K, Cai C, et al. Targeting tnf-A for covid-19: Recent advanced and controversies. *Front Public Health* (2022) 10:833967. doi: 10.3389/fpubh.2022.833967

279. Duret PM, Sebbag E, Mallick A, Gravier S, Spielmann L. Recovery from covid-19 in a patient with spondyloarthritis treated with tnf-alpha inhibitor etanercept. *Ann Rheum Dis* (2020) 79(9):1251–2. doi: 10.1136/annrheumdis-2020-217362

280. Calabrese LH, Lenfant T, Calabrese C. Interferon therapy for covid-19 and emerging infections: Prospects and concerns. *Cleveland Clinic J Med* (2020). doi: 10.3949/ccjm.87a.ccc066

281. Zuo Y, Liu Y, Zhong Q, Zhang K, Xu Y, Wang Z. Lopinavir/Ritonavir and interferon combination therapy may help shorten the duration of viral shedding in patients with covid-19: A retrospective study in two designated hospitals in anhui, China. *J Med Virol* (2020) 92(11):2666–74. doi: 10.1002/jmv.26127

282. Mehta N, Mazer-Amirshahi M, Alkindi N, Pourmand A. Pharmacotherapy in covid-19; a narrative review for emergency providers. *Am J Emergency Med* (2020) 38 (7):1488–93. doi: 10.1016/j.ajem.2020.04.035

283. Saleh M, Vaezi AA, Aliannejad R, Sohrabpour AA, Kiaei SZF, Shadnoush M, et al. Cell therapy in patients with covid-19 using wharton's jelly mesenchymal stem cells: A phase 1 clinical trial. *Stem Cell Res Ther* (2021) 12(1):410. doi: 10.1186/s13287-021-02483-7

284. Zaki MM, Lesha E. Cell therapy strategies for covid-19: Current approaches and potential applications. *Sci Adv* (2021) 7(33): eabg5995. doi: 10.1126/sciadv.abg5995

285. Hashmi S, Ahmed M, Murad MH, Litzow MR, Adams RH, Ball LM, et al. Survival after mesenchymal stromal cell therapy in steroid-refractory acute graft-Versus-Host disease: Systematic review and meta-analysis. *Lancet Haematol* (2016) 3(1):e45–52. doi: 10.1016/s2352-3026(15)00224-0

286. Aggarwal S, Pittenger MF. Human mesenchymal stem cells modulate allogeneic immune cell responses. *Blood* (2005) 105(4):1815–22. doi: 10.1182/blood-2004-04-1559

287. Fisher SA, Cutler A, Doree C, Brunskill SJ, Stanworth SJ, Navarrete C, et al. Mesenchymal stromal cells as treatment or prophylaxis for acute or chronic graft-Versus-Host disease in haematopoietic stem cell transplant (Hsct) recipients with a haematological condition. *Cochrane Database syst Rev* (2019) 1(1):Cd009768. doi: 10.1002/14651858.CD009768.pub2

288. Päth G, Perakakis N, Mantzoros CS, Seufert J. Stem cells in the treatment of diabetes mellitus - focus on mesenchymal stem cells. *Metab: Clin Exp* (2019) 90:1–15. doi: 10.1016/j.metabol.2018.10.005

289. Weiss ARR, Dahlke MH. Immunomodulation by mesenchymal stem cells (Mscs): Mechanisms of action of living, apoptotic, and dead mscs. *Front Immunol* (2019) 10:1191. doi: 10.3389/fimmu.2019.01191

290. Shende P, Subedi M. Pathophysiology, mechanisms and applications of mesenchymal stem cells for the treatment of spinal cord injury. *Biomed pharmacother = Biomed pharmacother* (2017) 91:693–706. doi: 10.1016/j.biopha.2017.04.126

291. Wang SH, Shetty AK, Jin K, Chunhua Zhao R. Combating covid-19 with mesenchymal Stem/Stromal cell therapy: Promise and challenges. *Front Cell Dev Biol* (2020) 8:627414. doi: 10.3389/fcell.2020.627414

292. Liang B, Chen J, Li T, Wu H, Yang W, Li Y, et al. Clinical remission of a critically ill covid-19 patient treated by human umbilical cord mesenchymal stem cells: A case report. *Med (Baltimore)* (2020) 99(31):e21429. doi: 10.1097/md.0000000000021429

293. Sánchez-Guijo F, García-Arranz M, López-Parra M, Monedero P, Mata-Martínez C, Santos A, et al. Adipose-derived mesenchymal stromal cells for the treatment of patients with severe sars-Cov-2 pneumonia requiring mechanical ventilation. *A Proof Concept Study EClinicalMed* (2020) 25:100454. doi: 10.1016/j.eclinm.2020.100454

294. Lanzoni G, Linetsky E, Correa D, Messinger Cayetano S, Alvarez RA, Kouroupis D. Umbilical cord mesenchymal stem cells for covid-19 acute respiratory distress syndrome: A double-blind, phase 1/2a, randomized controlled trial. *Stem Cells Transl Med* (2021) 10(5):660–73. doi: 10.1002/sctm.20-0472

295. Schwab I, Nimmerjahn F. Intravenous immunoglobulin therapy: How does igg modulate the immune system? *Nat Rev Immunol* (2013) 13(3):176–89. doi: 10.1038/nri3401

296. Ross C, Svenson M, Hansen MB, Vejlsgaard GL, Bendtzen K. High avidity ifn-neutralizing antibodies in pharmaceutically prepared human igg. *J Clin Invest* (1995) 95 (5):1974–8. doi: 10.1172/jci117881

297. Mohan PV, Tarnow-Mordi W, Stenson B, Brocklehurst P, Haque K, Cavendish V, et al. Can polyclonal intravenous immunoglobulin limit cytokine mediated cerebral damage and chronic lung disease in preterm infants? *Arch Dis childhood Fetal neonatal edition* (2004) 89(1):F5–8. doi: 10.1136/fn.89.1.f5

298. Watanabe M, Uchida K, Nakagaki K, Trapnell BC, Nakata K. High avidity cytokine autoantibodies in health and disease: Pathogenesis and mechanisms. *Cytokine Growth factor Rev* (2010) 21(4):263–73. doi: 10.1016/j.cytogfr.2010.03.003

299. Hung IFN, To KKW, Lee CK, Lee KL, Yan WW, Chan K, et al. Hyperimmune iv immunoglobulin treatment: A multicenter double-blind randomized controlled trial for patients with severe 2009 influenza a(H1n1) infection. *Chest* (2013) 144(2):464–73. doi: 10.1378/chest.12-2907

300. Chong PY, Chui P, Ling AE, Franks TJ, Tai DY, Leo YS, et al. Analysis of deaths during the severe acute respiratory syndrome (Sars) epidemic in Singapore: Challenges in determining a sars diagnosis. *Arch Pathol Lab Med* (2004) 128(2):195–204. doi: 10.5858/2004-128-195-aoddts

301. Tabarsi P, Barati S, Jamaati H, Haseli S, Marjani M, Moniri A, et al. Evaluating the effects of intravenous immunoglobulin (Ivig) on the management of severe covid-19 cases: A randomized controlled trial. *Int Immunopharmacol* (2021) 90:107205. doi: 10.1016/j.intimp.2020.107205

302. Xiang HR, Cheng X, Li Y, Luo WW, Zhang QZ, Peng WX. Efficacy of ivig (Intravenous immunoglobulin) for corona virus disease 2019 (Covid-19): A meta-analysis. *Int Immunopharmacol* (2021) 96:107732. doi: 10.1016/j.intimp.2021.107732

frontiers | Frontiers in Immunology

TYPE Original Research
PUBLISHED 09 February 2023
DOI 10.3389/fimmu.2023.971277

Check for updates

OPEN ACCESS

EDITED BY
Edwin Bölke,
Heinrich Heine University of Düsseldorf, Germany

REVIEWED BY
Gualberto Ruaño,
Hartford Hospital, United States
Karin Neukam,
Virgen del Rocío University Hospital, Spain

*CORRESPONDENCE
Savita Pahwa
spahwa@med.miami.edu

SPECIALTY SECTION
This article was submitted to Viral Immunology, a section of the journal Frontiers in Immunology

RECEIVED 16 June 2022
ACCEPTED 27 January 2023
PUBLISHED 09 February 2023

CITATION
Williams EC, Kizhner A, Stark VS, Nawab A, Muniz DD, Echeverri Tribin F, Carreño JM, Bielak D, Singh G, Hoffer ME, Krammer F, Pallikkuth S and Pahwa S (2023) Predictors for reactogenicity and humoral immunity to SARS-CoV-2 following infection and mRNA vaccination: A regularized, mixed-effects modelling approach. *Front. Immunol.* 14:971277. doi: 10.3389/fimmu.2023.971277

COPYRIGHT
© 2023 Williams, Kizhner, Stark, Nawab, Muniz, Echeverri Tribin, Carreño, Bielak, Singh, Hoffer, Krammer, Pallikkuth and Pahwa. This is an open-access article distributed under the terms of the Creative Commons Attribution License (CC BY). The use, distribution or reproduction in other forums is permitted, provided the original author(s) and the copyright owner(s) are credited and that the original publication in this journal is cited, in accordance with accepted academic practice. No use, distribution or reproduction is permitted which does not comply with these terms.

Predictors for reactogenicity and humoral immunity to SARS-CoV-2 following infection and mRNA vaccination: A regularized, mixed-effects modelling approach

Erin C. Williams[1], Alexander Kizhner[2], Valerie S. Stark[1], Aria Nawab[1], Daniel D. Muniz[1], Felipe Echeverri Tribin[3], Juan Manuel Carreño[4], Dominika Bielak[4], Gagandeep Singh[4], Michael E. Hoffer[1,5], Florian Krammer[3,6], Suresh Pallikkuth[2] and Savita Pahwa[2*]

[1]Department of Otolaryngology, University of Miami Miller School of Medicine, Miami, FL, United States, [2]Department of Microbiology and Immunology, University of Miami Miller School of Medicine, Miami, FL, United States, [3]Department of Biomedical Engineering, University of Miami, Miami, FL, United States, [4]Department of Microbiology, Icahn School of Medicine at Mount Sinai, New York, NY, United States, [5]Department of Neurological Surgery, University of Miami, Miller School of Medicine, Miami, FL, United States, [6]Department of Pathology, Molecular and Cell-based Medicine, Icahn School of Medicine at Mount Sinai, New York, NY, United States

Introduction: The influence of pre-existing humoral immunity, inter-individual demographic factors, and vaccine-associated reactogenicity on immunogenicity following COVID vaccination remains poorly understood.

Methods: Ten-fold cross-validated least absolute shrinkage and selection operator (LASSO) and linear mixed effects models were used to evaluate symptoms experienced by COVID+ participants during natural infection and following SARS-CoV-2 mRNA vaccination along with demographics as predictors for antibody (AB) responses to recombinant spike protein in a longitudinal cohort study.

Results: In previously infected individuals (n=33), AB were more durable and robust following primary vaccination when compared to natural infection alone. Higher AB were associated with experiencing dyspnea during natural infection, as was the total number of symptoms reported during the COVID-19 disease course. Both local and systemic symptoms following 1st and 2nd dose (n=49 and 48, respectively) of SARS-CoV-2 mRNA vaccines were predictive of higher AB after vaccination. Lastly, there was a significant temporal relationship between AB and days since infection or vaccination, suggesting that vaccination in COVID+ individuals is associated with a more robust immune response.

Discussion: Experiencing systemic and local symptoms post-vaccine was suggestive of higher AB, which may confer greater protection.

KEYWORDS

vaccine reactogenicity, infection, protective antibodies, COVID-19, SARS-CoV-2

1 Introduction

The heterogeneous presentation of SARS-CoV-2 infection is associated with inter-individual factors (1, 2) including age, biological sex, comorbidities, susceptibility to the virus, exposure load, viral shedding, pre-existing binding or neutralizing antibodies (3, 4), and pre-existing cross-reactive T cells (5–7). Variability in these factors and their distinct contributions to the individual immune response has made it difficult to generalize the disease course in SARS-CoV-2-infected individuals (1, 8). Immunoassays (i.e., virus-specific serologic assays) have been used extensively throughout the COVID-19 pandemic (9). Primarily used to characterize the immune response following vaccination, assessing viability for convalescent plasma donation, and acting as a population surveillance tool (10, 11), the most pressing work remains developing correlates for protection. Neutralizing and binding titers remain well supported as protective markers (3, 12) regardless of natural infection or vaccination, including a recent study (13) which associated increased binding and neutralizing antibodies with an inverse risk for SARS-CoV-2 infection following mRNA-1273 (Moderna) vaccination.

Previous studies have evaluated change in peak post-vaccination antibody titers as a function of time (14) and the relationship between lower quantitative antibodies and disease severity (15). Additionally, evidence suggests that higher antibody titers in vaccinated, previously coronavirus disease 2019 positive (COVID+) individuals are associated with an increased degree of immune protection (16–18). Studies have also shown that vaccination with mRNA vaccines results in rapid, robust antibody production and associated reactogenicity after the first vaccine dose (19, 20) as well as following heterologous booster doses (21). Here, we investigated relationships between sociodemographic factors, reactogenicity, and immunogenicity following SARS-CoV-2 mRNA vaccination among previously SARS-CoV-2 infected (COVID+) individuals participating in our longitudinal cohort study (COVID-19 ImmuniTY study, or "CITY"). This analysis may help elucidate how underlying immunologic determinants, pre-existing immunity, and vaccine reactogenicity are associated with post-vaccination antibody titers (i.e., humoral immunogenicity) in an ethnically diverse cohort. Conclusions drawn from this study may contribute to a more personalized public health approach to future COVID-19 vaccine strategies, which could account for an individual's demographics (e.g., age, gender, or race) or existing immunity prior to vaccination or booster receipt (22).

2 Methods

2.1 Study design and participants

2.1.1 "CITY" cohort

Participants were enrolled in our Institutional Review Board (IRB) approved (#20201026), longitudinal, observational SARS-CoV-2 immunity study (n=228) known as "CITY" (COVID-19 ImmuniTY study). The study began in October 2020 at the University of Miami Miller School of Medicine, and study subjects participated in visits every 3 months for a total of 2 years from the time of enrollment. The primary objective of the CITY study is to characterize differential antibody kinetics among SARS-CoV-2 uninfected and infected individuals in a high-risk, ethnically diverse cohort. The "high-risk" designation for inclusion referred to hazardous occupational exposure (e.g., healthcare workers) but also to advanced age or other sociodemographic characteristics known to increase risk of SARS-CoV-2 morbidity and mortality. Following written informed consent, participants provided demographic details to include lifestyle habits and relevant past medical history that would preclude them to more severe SARS-CoV-2 infection-related outcomes. Those who suffered from SARS-CoV-2 infection with a documented positive nucleic acid amplification test (NAAT+) prior to entry provided evidence details regarding their past COVID-19 infection symptoms during the baseline visit to the study team.

At all regularly scheduled visits, participants prospectively answered symptom questionnaires to screen for new or recent SARS-CoV-2 infection, and blood samples were collected for serum and peripheral blood mononuclear cell (PBMC) processing. Plasma was stored at -80°C and PBMCs were cryopreserved in liquid N_2 (23). All participants agreed to sample banking for future research use. Those who received vaccines were asked to return for two optional, additional visits at 1 week and 1 month following vaccine receipt, where they answered binary "Yes/No" questions in a survey about their symptoms following vaccination. Vaccine-related symptoms were rated on a Likert scale, where a "0" indicated no symptoms and a "10" indicated the highest symptom severity. Blood samples were collected and processed as described above.

2.1.2 CITY sub-cohort analysis (COVID+ unvaccinated and COVID+ vaccinated participants)

For this study, we included three groups, comprising of CITY participants enrolled between October 2020 – June 2021 with a history of COVID-19 prior to vaccination (i.e., natural infection (NI)), COVID-19+ participants who received Dose 1 (NI + dose 1 (D1)) of an mRNA vaccine, and fully vaccinated COVID-19+ participants who received Dose 1 and Dose 2 (NI + dose 2 (D2); deemed "fully vaccinated") of an mRNA vaccine. Pfizer (BNT162b2) and Moderna (mRNA-1273) were the primary options available (9) during the enrollment period; thus, participants who only received one dose or received Johnson & Johnson (n=4 across the entire cohort) were excluded from this analysis. Additionally, participants who were administered their second dose of an mRNA vaccine >7 days after or <4 days before the recommended (24) number of days after the first dose (21 days for Pfizer; 28 days for Moderna) were excluded as well in order to account for the temporal, transient nature of post-vaccine reactogenicity and the subsequent immune response to best reflect the general population. Individuals with suspected (>2-fold increase in Ab) or confirmed (with a NAAT+ test) reinfection or breakthrough infection were also excluded. Individuals infected with SARS-CoV-2 after June 2021 were also excluded in order to control for changes in variant-specific antigenic profiles and related changes in disease presentation (i.e., the Delta VOC). Further, limited symptomatic primary infections occurred after this June 2021 as most individuals were vaccinated during this period.

In total, 32 participants overlap between the naturally infected, pre-vaccine (NI) and post-vaccination (NI + D1; NI + D2) groups.

Among those who met criteria for inclusion in the sub-analysis, all samples provided during the baseline visit and thereafter were included. Of note, participants were considered "fully vaccinated" 14 days after they received Dose 2.

2.2 Enzyme-linked immunosorbent assay

SARS-CoV-2 ELISAs were performed using a well-described assay developed by the Icahn School of Medicine at Mount Sinai (10, 11). Discrete titers were reported in values of 1:100, 1:200, 1:400, 1:800, 1:1600, 1:3200, 1:6400, 1:12800, 1:25600, 1:51200, 1:102400, and 1:204800. The limit of detection was set at 1:100.

2.3 Statistical analysis

SARS-CoV-2 antibody titers were $\log_2$-transformed before all statistical analyses. To model the bi-phasic change in antibodies over time, we utilized a generalized additive model (GAM) incorporating the rate of both antibody decay following natural infection (following COVID+ participants' last positive SARS-CoV-2 test [LPT] result) and full vaccination (≥14 days after the second mRNA vaccine dose) [24]. The GAM modelled antibody titers with a smoothed function for number of days elapsed using a cubic regression with 3 knots as well as the fixed effect of vaccination status (NI and NI + D2). We then replicated the above as a linear mixed-effects model (LMM), where we incorporated the same fixed effects but included participants as a random-intercepts effect to control for individual differences. The rates of log-transformed antibody titer decay along with the limit of detection of our assay were used to estimate the number of days that the antibodies remain detectable after both natural infection and full vaccination.

Ten-fold cross-validated least absolute shrinkage and selection operator (LASSO) models were employed as a feature-selection and regularization technique. LASSO models were tuned to select the simplest model within one standard error of the lowest value root-mean-square error accuracy metric that included at least two predictors (Supplementary Table 1). Four models with identical demographic variables were constructed while controlling for time or days since LPT, 1st dose, or 2nd dose, respectively, including: 1) the effect of infection symptoms on the antibody response post-infection, 2) the effect of infection symptoms on the antibody response post full vaccination, 3) the effect of dose 1 vaccine symptoms on the antibody response post full vaccination, and 4) the effect of dose 2 vaccine symptoms on the antibody response post full vaccination. The selected predictors from each of the best-fitting cross-validated LASSO models were then included as fixed effects in follow-up LMMs with by-participant random intercepts, allowing us to control for individual differences. For significant categorical fixed effects from the LMMs, we conducted *post-hoc* Tukey tests to confirm directionality and to correct for multiple comparisons.

Additional linear regressions were used to investigate effects of each symptom following natural infection alone (NI), natural infection and the 1st dose of SARS-CoV-2 mRNA vaccination (NI + D1), and natural infection and the 2nd dose of vaccination (NI + D2) and explore possible relationships between demographics factors on peak antibody titer levels following full vaccination. Analyses were performed using R statistical software Version 4.1.1 (25). Generalized additive modeling, cross-validation, LASSO modelling, LMM, and *post-hoc* Tukey tests were conducted with the R packages *mgcv* (26), *caret* (27), *glmnet* (28), *nlme* (29), and *glht* (30), respectively, while the linear modelling, Mann-Whitney U tests, and Kruskal-Wallace tests were performed using the R package *stats* (25). Plots were produced using the *ggplot2* (31).

3 Results

3.1 Characteristics of the study population

Demographic characteristics are detailed in Table 1. Thirty-three participants with a history of COVID-19 were included in our post infection cohort (NI [natural infection alone]). Following natural infection (prior to mRNA vaccine receipt), the median number of days since last PCR-positive SARS-CoV-2 test to the baseline study visit was 101 days. For the post dose 1 (NI + D1 [natural infection and primary vaccine dose 1]) and post dose 2 (NI + D2 [natural infection and primary vaccine dose 2]) analysis, we included 49 and 48 participants, respectively. Median days from LPT to Dose 1 and Dose 2 were 99 and 127 days, respectively. No participants were known to be immunocompromised. All infections were deemed to be mild, with none requiring hospitalization.

3.2 Symptoms reported following infection and vaccination

The highest reported symptom during the vaccine-naïve COVID-19 course was fatigue (63%) (Table 2). Other highly reported symptoms included anosmia (55%), congestion (53%), and myalgias/muscle aches (57%). Following dose 1, the most common symptoms were injection site pain (51%), headache (29%), and fatigue (29%). Similarly, the most common symptoms reported following the second mRNA vaccination (dose 2) were injection site pain (53%), fatigue (39%), and myalgias (29%) (Table 2).

3.3 In previously infected individuals, antibody titers are more robust following full-vaccination as compared to post natural infection

There was a more robust antibody response immediately following full vaccination (Figure 1C) when compared to the antibody response following natural infection (estimate = 4.117, t = 12.950, p = < 0.001) (Figure 1B), where peak $\log_2$ antibody titers were greater in the vaccination with prior infection (14.517) than in natural infection (9.217). This is illustrated in Figure 1A, where natural infection and post-full vaccination titers were included in a bi-phasic model to show longitudinal antibody responses. Infected individuals had a slower rate of antibody titer decay (-0.010 *vs* -0.015 log per day), though this effect was small (estimate = -0.005, t = 2.351, p = 0.020).

10.3389/fimmu.2023.971277

TABLE 1 Characteristics of the study population following natural infection, 1st dose of vaccine, and 2nd dose of vaccine.

	Natural Infection (NI)	Natural Infection + Vaccine Dose 1 (NI + D1)	Natural Infection + Vaccine Dose 2 (NI + D2)
n	33	49	48
Gender, M/F	14/19	17/32	16/32
Race	White [25 (76%)] Black/African American [2 (6%)] Asian [1 (3%)] Other [5 (15%)]	White [39 (80%)] Black/African American [2 (4%)] Asian [2 (4%)] Other [6 (12%)]	White [(39 (81%)] Black/African American [2 (4%)] Asian [2 (4%)] Other [5 (110%)]
Ethnicity, Hispanic/Not Hispanic	14/19 (42%/58%)	22/27 (45%/55%)	21/27 (44%/56%)
Median age [Range]	39 [20-76]	39 [20-78]	39 [20-78]
Vaccine manufacturer, Pfizer/Moderna	–	31/18 (63%/37%)	30/18 (62.5%/37.5%)
Median days since COVID diagnosis by PCR to entry SD Range	101 74.87 8 - 292	–	–
Median days since COVID diagnosis by PCR to vaccination 95% CI	–	99 72 – 159	127 102-180

LMMs confirmed our findings that antibody titer declined faster following full vaccination than in natural infection (estimate = -0.006, F =11.238, p <0.001). Of note, the combination of natural infection followed by vaccination, or so-called "hybrid immunity", elicits a more durable antibody response than natural infection alone (estimate = 4.138, F = 794.623, p < 0.0001), as $\log_2$ antibody titers were predicted to remain detectable for a longer period of time following natural infection and full vaccination (550 days) than natural infection alone (464 days).

3.4 Days elapsed and symptoms reported during infection influence antibody titers

As shown in Table 3, difficulty breathing during infection (estimate = 1.590, F = 5.684, p = 0.024) and days elapsed since LPT (estimate = -0.006, F = 9.912, p = .004) were significant main effects in predicting antibody titers following natural infection. *Post-hoc* testing confirmed that antibody titers were elevated in individuals who experienced difficulty breathing (z = 2.612; p = 0.009).

When modeling demographics and symptoms at infection to predict the antibody response after full vaccination, we found that days elapsed since full vaccination (estimate = -0.014; F = 258.176; p < 0.0001), increased age (estimate = 0.018; F = 6.000; p = 0.019), and ethnicity (Hispanic) (estimate = 0.456; F = 5.265; p = 0.018) were significant main effects, though no categorical variables were significant after *post-hoc* testing.

3.5 Symptoms following vaccination are predictive of higher antibody titers after full vaccination

Local and systemic symptoms following the 1st dose of SARS-CoV-2 mRNA vaccines were predictive of higher antibody titers after full vaccination. As seen in Table 3, the results of the LMM show that days elapsed since full vaccination (estimate = -0.014, F = 262.855, p < 0.0001), chills (estimate = 0.541; F = 4.915; p = 0.032), injection site redness (estimate = 1.243; F = 4.330; p = 0.044), age (estimate = 0.021; F = 6.960; p = 0.012), and ethnicity (estimate = 0.562, F = 4.583, p = 0.038) were significant. Following *post-hoc* Tukey testing on the significant categorical main effects, we found that injection site redness (z = 2.081, p = 0.038) and ethnicity (Hispanic) (z = 2.382, p = 0.017) were significant, while the main effect of chills was not.

We also examined demographics and symptoms reported during the 2nd dose of SARS-CoV-2 mRNA vaccination and their effect on the antibody response after full vaccination. Days since full vaccination (estimate = -0.014; F = 259.745; p < 0.0001), age (estimate = 0.023; F = 7.652; p = 0.009), identifying as Hispanic (estimate = 0.609; F = 6.683; p = 0.013), fever (estimate = 0.839; F = 11.154, p = 0.002), and influenza vaccination (estimate = -0.475; F = 4.405; p = 0.042) were observed to be significant. Fever and ethnicity (Hispanic) were found to be statistically significant (z = 3.016, p = 0.003; z = 2.735, p = 0.006, respectively) following *post-hoc* testing, though influenza vaccination was not.

3.6 The number of symptoms observed during infection are associated with higher peak antibody titers post full-vaccination

The number of symptoms self-reported during infection significantly predicted peak antibody titers after full vaccination (estimate = 0.10, t = 2.10, Pearson's r = 0.296; p = .041). Additional linear models were conducted for the number of symptoms reported as a function of demographics, where we found that the number of symptoms self-reported during infection was significantly influenced by self-identifying as White (estimate = 4.679, t = 2.153, p = 0.037). No other demographic factors was significant.

4 Discussion

The goal of this study was to investigate the role of demographics, pre-existing immunity, and symptomatology following infection and vaccination to ascertain whether they independently or collectively are associated with immunogenicity following mRNA vaccination against SARS-CoV-2 infection in individuals previously infected with SARS-CoV-2. Our results demonstrate higher durability and robustness of antibody titers despite a faster rate of antibody decay following vaccination, which supports previously reported findings (32) for SARS-CoV-2 mRNA vaccines. Unsurprisingly, our results also demonstrate that a larger temporal gap between an individual's LPT and antigen testing predicts decline of antibody titers over time. We also found that in previously infected individuals, SARS-CoV-2 mRNA vaccines result in a more robust antibody response than that following infection alone.

Following infection alone, the number of symptoms reported and difficulty breathing during the COVID-19 course were predictive of higher antibody titers. This result supports existing evidence (33, 34) that individuals who report a more severe or symptomatic SARS-CoV-2 infection have higher peak titers than asymptomatic individuals. After receiving dose 1, injection site redness was found to be significantly predictive for higher antibody titers following full vaccination. Interestingly, after dose 2 we found that fever was significantly predictive for higher antibody titers following full vaccination. It should be noted that asymptomatic individuals mounted robust immune responses as well.

In previously infected individuals, SARS-CoV-2 mRNA vaccines result in a more robust antibody response than that following infection alone. Indeed, in individuals with "hybrid immunity", antibody titers following full vaccination peak at 4-fold higher than those following naturally acquired immunity and appear to persist at

TABLE 2 Symptoms experienced by the study cohort following natural infection, 1st dose of vaccine, and 2nd dose of vaccine.

	Natural Infection (NI)[b]	Natural Infection + Vaccine Dose 1 (NI + D1)	Natural Infection + Vaccine Dose 2 (NI + D2)
Symptoms Reported During SARS-CoV-2 Infection[a]			
Asymptomatic	10 (20%)	–	–
Anosmia	27 (55%)	–	–
Congestion/ rhinorrhea	26 (53%)	–	–
Cough	23 (47%)	–	–
Difficulty breathing	12 (24%)	–	–
Dysgeusia	26 (53%)	–	–
Fatigue	31 (63%)	–	–
Fever	18 (37%)	–	–
Myalgias	28 (57%)	–	–
Nausea or vomiting	5 (10%)	–	–
Sore Throat	15 (31%)	–	–
Upset Stomach	14 (29%)	–	–
Local Symptoms Reported Following Vaccination[a]			
Injection site pain	–	25 (51%)	26 (53%)
Injection site redness	–	2 (4%)	4 (8%)
Injection site swelling	–	4 (8%)	5 (10%)
Systemic Symptoms Reported Following Vaccination[a]			
Asymptomatic	–	22 (45%)	20 (41%)
Chills	–	9 (18%)	11 (22%)
Fatigue	–	14 (29%)	19 (39%)
Fever	–	10 (20%)	10 (20%)
Headache	–	14 (29%)	12 (24%)
Myalgias/Muscle Aches	–	12 (24%)	14 (29%)

Each count is the number of individuals who self-reported each symptom at the timepoint listed in each column. Percentages are based on the total n for each column.
[a]All symptoms reported during SARS-CoV-2 Infection, as well as local and systemic symptoms following vaccination were included in LASSO modeling as shown in Supplementary Table 1.
[b]All samples collected following natural infection were included for analysis.

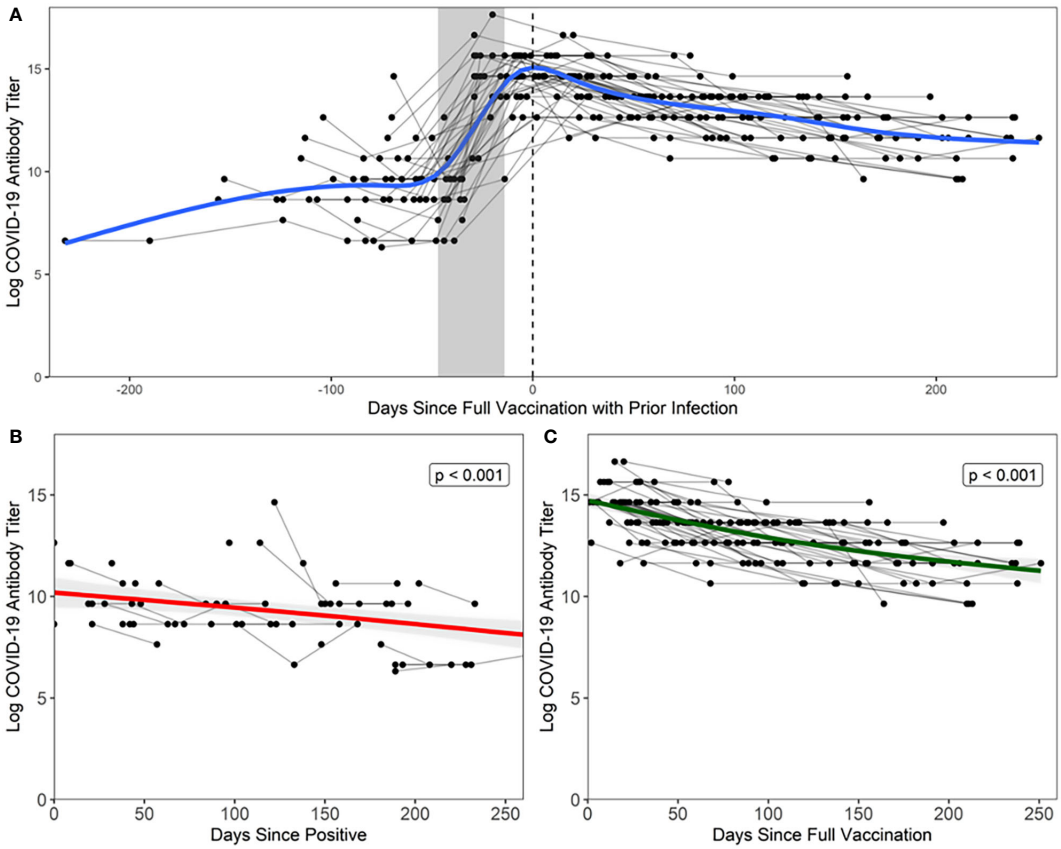

FIGURE 1
Antibody response following natural infection and vaccination Each black point represents a sample from a participant, grey lines connect points from the same participant, and the grey shaded area represents the maximum number of days between doses relative to date of full vaccination (14 days after second dose, regardless of vaccine manufacturer). **(A)** Days since full vaccination *vs*. log titers over time. t=0 on the x-axis represents the day when COVID+ participants became fully vaccinated (2 weeks after second vaccination). Bi-phasic, generalized additive model (GAM) is visualized by a blue line. **(B)** In unvaccinated COVID+ participants, log_2 antibody titers decay at a rate of -0.010 per day after last positive COVID-19 test result. Fitted linear model is visualized by a red line. Note that three points were excluded from the above figure due to the temporal scale used to graphically depict the data but are included in the analyses herein. **(C)** In vaccinated COVID+ participants, log2 antibody titers decay at a rate of -0.015 per day after full vaccination. Fitted linear model is visualized by a green line.

detectable levels for >500 days following vaccination. One explanation for this increased response could be the presence of pre-existing memory T and B cell responses developed during natural infection. These cells might enhance a secondary immune response following vaccination similar to that of a booster immunization. In addition to bolstering the current CDC recommendations (35) that individuals previously infected with SARS-CoV-2 receive vaccination, our results provide additional, longitudinal support for this measure.

Intrinsic factors, such as age and gender are thought to influence immunogenicity (36). Though our data support higher peak antibody titers following infection and vaccination with increasing age (33, 37) it should be noted that the median age across all groups included in this analysis was 39 years with no participant above 80 years of age and therefore should not be interpreted as a superior post-infection or post-vaccine antibody responses in the elderly. We expect that old age will be associated with poorer vaccine responses as has been described previously (38) but this was not evaluated here. Notably, our study was conducted in Miami-Dade County, an international, multi-cultural hub with a largely Hispanic and bilingual population. Our analysis demonstrated a significant relationship between Hispanic ethnicity and higher antibody titers over time at nearly every time point of interest, including infection where the analysis approached significance (p = 0.0624). Other groups have demonstrated higher rates of Hispanic SARS-CoV-2 seroconversion when compared to other ethnicities (39, 40) and have found that Hispanic ethnicity is linked to higher rates of seroprotection and seroconversion following H1N1 monovalent vaccination (41, 42), but future studies with a large number of participants are needed to support a generalizable trend for antibody magnitude over time in this population. Related, we also found that influenza vaccination was associated with higher antibody titers, though it was not significant following *post-hoc* testing. Though the biological relevance of this finding is unknown, we previously showed that specific CD4 responses to influenza A(H1N1) correlate with SARS-CoV-2 specific CD4 T-cells, suggesting a protective effect of pre-existing influenza specific T-cells (7). We speculate that this provides evidence of healthy and "trained" immune systems within our cohort, wherein epigenetic and metabolic reprogramming have augmented innate immune cells that enhance adaptive immunity to

10.3389/fimmu.2023.971277

TABLE 3 Symptoms and demographic factors influence antibody responses following natural infection and full vaccination.

Category	Predictor	Coefficient[a]	F-value[a]	p-value[a]	Pr(>|z|)[b]
Demographics, symptoms reported during infection and titers following natural infection					
Days elapsed	Days since positive test	-0.01	9.991	**0.004***	–
Symptoms reported during infection	Difficulty breathing	0.58	5.684	0.024*	**0.020***
	Subjective symptom severity	0.00	2.524	0.123	–
Demographics, symptoms reported during infection and titers following full vaccination					
Days elapsed	Days since full vaccination	-0.01	258.176	**<0.0001***	–
Symptoms reported during infection	Anosmia during infection	0.31	2.910	0.096	–
Demographics	Age	0.01	6.000	**0.019***	–
	Ethnicity (Hispanic)	0.20	5.265	0.027*	0.062
	Flu vaccinated	-0.37	3.612	0.064	–
	Gender (Male)	-0.09	2.402	0.129	–
	Vaccine manufacturer (Pfizer)	-0.16	0.306	0.583	–
Demographics, symptoms reported following Dose 1, and titers following full vaccination					
Days elapsed	Days since full vaccination	-0.01	262.855	**<0.0001***	–
Symptoms reported after 1st vaccine dose	Chills after 1st dose	0.34	4.915	0.032*	0.085
	Injection site redness after 1st dose	0.91	4.330	0.044*	**0.038***
Demographics	Age	0.01	6.960	**0.012***	–
	Ethnicity (Hispanic)	0.28	4.583	0.038*	**0.017***
	Flu vaccinated	-0.15	1.771	0.191	–
	Gender (Male)	-0.08	2.288	0.138	–
Demographics, symptoms reported following Dose 2, and titers following full vaccination					
Days elapsed	Days since full vaccination	-0.01	259.745	**<0.0001***	–
Symptoms reported after 2nd dose	Fever	0.61	11.154	0.002*	**0.003***
	Injection site swelling after 2nd dose	0.31	1.579	0.216	–
	Subjective symptom severity	-0.03	3.064	0.088	–
Demographics	Age	0.01	7.652	**0.009***	–
	Ethnicity (Hispanic)	0.32	6.683	0.013*	**0.006***
	Flu vaccinated	-0.29	4.405	0.042*	0.166
	Gender (Male)	-0.05	3.452	0.071	–

Four LASSO models and linear mixed-effects (LME) p-values were generated to assess the predictive value of categorical and discrete variables while controlling for between-subjects' differences. Significant categorical LASSO-generated variables underwent additional post-hoc Tukey to test for directionality and to correct for multiple comparisons. A p-value <0.05 was considered statistically significant.

[a]LME for predictors of main effects.

[b]Post-hoc Tukey test for directionality of categorical variables due to significant main effects.

increase SARS-CoV-2 specific responses (7, 43).

Our study has several limitations, namely that sample sizes for each cohort examined were small due to variability in vaccination timelines and participant scheduling. Some individuals were excluded due to a confounding effect on our predictive modeling, which is controlled for by the fixed effect of time relative to desired endpoints (i.e.: infection and vaccination). The natural infection group was further limited by the study timeline, as the first SARS-CoV-2 vaccination became available shortly after enrollment began and therefore limited the number of naturally infected individuals, we were able to follow longitudinally. Additionally, our analysis only included quantitative binding antibody titers. Though recent work has demonstrated that higher binding antibodies correlate to higher neutralizing antibodies (13), expansive, multi-center longitudinal studies profiling the cellular and humoral response are needed. Comprehensive future work would benefit from characterizing immunogenetic determinants for SARS-CoV-2 vaccine effectiveness (44, 45) *via* a so-called "Adversomics" approach (46) and should include profiling of quantitative binding antibodies, neutralizing and non-neutralizing antibodies, memory B-cells, and T-cell responses, as

immune protection appears to be contingent on all three tiers of the immune response (47, 48).

Finally, some of the predictors used in our statistical analysis were found to be significant in one test but not in *post-hoc* tests. Large, longitudinal studies are required to confirm a significant group difference, but the predictors utilized herein should be included in future analyses. Our bivariate analysis of symptoms experienced following the 1st and 2nd doses failed to demonstrate that individual symptoms can influence peak antibody titers following full vaccination. The same was true for race and ethnicity, which were not found to be significantly predictive for peak titers, though we contend that this is because these models failed to control for individual differences, or intercepts, to account for between-subjects' variability.

In conclusion, this study demonstrates that a combination of systemic and local symptoms is predictive of higher antibody titers, which may correlate to a higher degree of protection. Additional studies are needed to understand the role of immunologic determinants (including underlying genetic polymorphisms that influence immune cell activation/differentiation, etc.) for protection against SARS-CoV-2 infection and breakthrough infection in the age of boosters and variants capable of immune escape, as symptom profiles seem to be variant-specific (49, 50). Repeating this type of analysis at the population level along with fully characterized adaptive cellular responses will be critical in providing personalized recommendations for future vaccine measures, including recommendations for optimal booster timing.

Data availability statement

The raw data supporting the conclusions of this article will be made available by the authors, without undue reservation.

Ethics statement

The studies involving human participants were reviewed and approved by University of Miami Institutional Review Board. The patients/participants provided their written informed consent to participate in this study.

Author contributions

SaP conceived the Miami cohort study and EW, AK, SuP contributed to conception and design of the manuscript. VS, FT, DM organized the database. AK performed the statistical analysis and generated data visualizations. EW, VS, AN, DM wrote sections of the manuscript. EW, AN, DM, FT, JMC, DB, and GS provided technical assistance or collected data for this manuscript. MH, FK, JMC, SaP, and SuP provided oversight of the study and edited the manuscript. All authors contributed to manuscript revision, read, and approved the submitted version.

Funding

This work is part of the PARIS /SPARTA studies funded by the NIAID Collaborative Influenza Vaccine Innovation Centers (CIVIC) contract 75N93019C00051 (PI F Krammer) with SaP as PI of the University of Miami site and by R01DA051202S1 to SaP.

Acknowledgments

We express our sincerest gratitude to our intellectually curious and willing study participants for donating their blood and time to this study. We also thank the core research team that have made this study logistically possible, including Margaret Roach, Elizabeth Varghese, Celeste Sanchez, Ailet Reyes, and the entire team of phlebotomists at the University of Miami's Clinical Translational Research Site. This work has been previously published (51) on the pre-print server, medRxiv.

Conflict of interest

The Icahn School of Medicine at Mount Sinai has filed patent applications relating to SARS-CoV-2 serological assays U.S. Provisional Application Numbers: 62/994,252, 63/018,457, 63/020,503 and 63/024,436 and NDV-based SARS-CoV-2 vaccines U.S. Provisional Application Number: 63/251,020 which list Florian Krammer as co-inventor. Patent applications were submitted by the Icahn School of Medicine at Mount Sinai. Mount Sinai has spun out a company, Kantaro, to market serological tests for SARS-CoV-2. FK has consulted for Merck and Pfizer before 2020, and is currently consulting for Pfizer, Third Rock Ventures, Seqirus and Avimex. The Krammer laboratory is also collaborating with Pfizer on animal models of SARS-CoV-2.

The remaining authors declare that the research was conducted in the absence of any commercial or financial relationships that could be construed as a potential conflict of interest.

Publisher's note

All claims expressed in this article are solely those of the authors and do not necessarily represent those of their affiliated organizations, or those of the publisher, the editors and the reviewers. Any product that may be evaluated in this article, or claim that may be made by its manufacturer, is not guaranteed or endorsed by the publisher.

Supplementary material

The Supplementary Material for this article can be found online at: https://www.frontiersin.org/articles/10.3389/fimmu.2023.971277/full#supplementary-material

References

1. Rodebaugh TL, Frumkin MR, Reiersen AM, Lenze EJ, Avidan MS, Miller JP, et al. Acute symptoms of mild to moderate COVID-19 are highly heterogeneous across individuals and over time. *Open Forum Infect Dis* (2021) 8(3):ofab090. doi: 10.1093/ofid/ofab090

2. Zimmermann P, Curtis N. Factors that influence the immune response to vaccination. *Clin Microbiol Rev* (2019) 32(2):e00084–18. doi: 10.1128/CMR.00084-18

3. Khoury DS, Cromer D, Reynaldi A, Schlub TE, Wheatley AK, Juno JA, et al. Neutralizing antibody levels are highly predictive of immune protection from symptomatic SARS-CoV-2 infection. *Nat Med* (2021) 27(7):1205–11. doi: 10.1038/s41591-021-01377-8

4. Garcia-Beltran WF, Lam EC, Astudillo MG, Yang D, Miller TE, Feldman J, et al. COVID-19-neutralizing antibodies predict disease severity and survival. *Cell* (2021) 184 (2):476–88.e11. doi: 10.1016/j.cell.2020.12.015

5. da Silva Antunes R, Pallikkuth S, Williams E, Dawen Yu E, Mateus J, Quiambao L, et al. Differential T-cell reactivity to endemic coronaviruses and SARS-CoV-2 in community and health care workers. *J Infect Dis* (2021) 224(1):70–80. doi: 10.1093/infdis/jiab176

6. Mateus J, Grifoni A, Tarke A, Sidney J, Ramirez SI, Dan JM, et al. Selective and cross-reactive SARS-CoV-2 T cell epitopes in unexposed humans. *Science* (2020) 370 (6512):89–94. doi: 10.1126/science.abd3871

7. Pallikkuth S, Williams E, Pahwa R, Hoffer M, Pahwa S. Association of flu specific and SARS-CoV-2 specific CD4 T cell responses in SARS-CoV-2 infected asymptomatic heath care workers. *Vaccine* (2021) 39:6019–24. doi: 10.1016/j.vaccine.2021.08.092

8. Thevarajan I, Buising KL, Cowie BC. Clinical presentation and management of COVID-19. *Med J Aust* (2020) 213(3):134–9. doi: 10.5694/mja2.50698

9. FDA. *Coronavirus disease 2019 (COVID-19)*. EUA Informatin (2022). Available at: https://www.fda.gov/emergency-preparedness-and-response/mcm-legal-regulatory-and-policy-framework/emergency-use-authorizationvaccines.

10. Amanat F, Stadlbauer D, Strohmeier S, Nguyen THO, Chromikova V, McMahon M, et al. A serological assay to detect SARS-CoV-2 seroconversion in humans. *Nat Med* (2020) 26(7):1033–6. doi: 10.1038/s41591-020-0913-5

11. Stadlbauer D, Amanat F, Chromikova V, Jiang K, Strohmeier S, Arunkumar GA, et al. SARS-CoV-2 seroconversion in humans: A detailed protocol for a serological assay, antigen production, and test setup. *Curr Protoc Microbiol* (2020) 57(1):e100. doi: 10.1002/cpmc.100

12. Feng S, Phillips DJ, White T, Sayal H, Aley PK, Bibi S, et al. Correlates of protection against symptomatic and asymptomatic SARS-CoV-2 infection. *Nat Med* (2021) 27 (11):2032–40. doi: 10.1038/s41591-021-01540-1

13. Gilbert PB, Montefiori DC, McDermott AB, Fong Y, Benkeser D, Deng W, et al. Immune correlates analysis of the mRNA-1273 COVID-19 vaccine efficacy clinical trial. *Science* (2022) 375(6576):43–50. doi: 10.1126/science.abm3425

14. Crawford KHD, Dingens AS, Eguia R, Wolf CR, Wilcox N, Logue JK, et al. Dynamics of neutralizing antibody titers in the months after severe acute respiratory syndrome coronavirus 2 infection. *J Infect Dis* (2021) 223(2):197–205. doi: 10.1093/infdis/jiaa618

15. Nagura-Ikeda M, Imai K, Kubota K, Noguchi S, Kitagawa Y, Matsuoka M, et al. Clinical characteristics and antibody response to SARS-CoV-2 spike 1 protein using VITROS anti-SARS-CoV-2 antibody tests in COVID-19 patients in Japan. *J Med Microbiol* (2021) 70(4):001291. doi: 10.1099/jmm.0.001291

16. Callegaro A, Borleri D, Farina C, Napolitano G, Valenti D, Rizzi M, et al. Antibody response to SARS-CoV-2 vaccination is extremely vivacious in subjects with previous SARS-CoV-2 infection. *J Med Virol* (2021) 93(7):4612–5. doi: 10.1002/jmv.26982

17. Lozano-Ojalvo D, Camara C, Lopez-Granados E, Nozal P, Del Pino-Molina L, Bravo-Gallego LY, et al. Differential effects of the second SARS-CoV-2 mRNA vaccine dose on T cell immunity in naive and COVID-19 recovered individuals. *Cell Rep* (2021) 36(8):109570. doi: 10.1016/j.celrep.2021.109570

18. Mungmunpuntipantip R, Wiwanitkit V. Antibody response to SARS-CoV-2 vaccination, previous SARS-CoV-2 infection, and change to single-dose vaccination. *J Med Virol* (2021) 93(12):6474. doi: 10.1002/jmv.27263

19. Kelsen SG, Braverman AS, Aksoy MO, Hayman JA, Patel PS, Rajput C, et al. SARS-CoV-2 BNT162b2 vaccine–induced humoral response and reactogenicity in individuals with prior COVID-19 disease. *JCI Insight* (2022) 7(4). doi: 10.1172/jci.insight.155889

20. Ontañón J, Blas J, de Cabo C, Santos C, Ruiz-Escribano E, García A, et al. Influence of past infection with SARS-CoV-2 on the response to the BNT162b2 mRNA vaccine in health care workers: Kinetics and durability of the humoral immune response. *EBioMedicine* (2021) 73:103656. doi: 10.1016/j.ebiom.2021.103656

21. Pereson MJ, Amaya L, Neukam K, Baré P, Echegoyen N, Badano MN, et al. Heterologous gam-COVID-vac (sputnik V)/mRNA-1273 (moderna) vaccination induces a stronger humoral response than homologous sputnik V in a real-world data analysis. *Clin Microbiol Infection* (2022) 28(10):1382–8. doi: 10.1016/j.cmi.2022.05.009

22. Tsang JS, Dobaño C, VanDamme P, Moncunill G, Marchant A, Othman RB, et al. Improving vaccine-induced immunity: Can baseline predict outcome? *Trends Immunol* (2020) 41(6):457–65. doi: 10.1016/j.it.2020.04.001

23. HANC. *Cross-network PBMC processing standard operating procedure*. HIV/AIDS Network Coordination (2018). pp. 1–45. Available at: https://www.hanc.info/content/dam/hanc/documents/laboratory/cross-network-procedures-sops/HANC-LAB-P0001_v6.0_2018-04-26_PBMC_SOP.pdf

24. CDC. *Interim clinical considerations for use of COVID-19 vaccines currently approved or authorized in the united states*. Centers for Disease Control and Prevention (2022). Available at: https://www.cdc.gov/vaccines/covid-19/clinical-considerations/covid-19-vaccines-us.html

25. R Development Core Team. *R: A language and environment for statistical computing*. R Core Team (2021). Availabe at: https://www.R-project.org

26. Wood SN. Stable and efficient multiple smoothing parameter estimation for generalized additive models. *J Am Stat Assoc* (2022) 99:673–86. doi: 10.1198/016214504000000980 https://cran.r-project.org/web/packages/nlme/nlme.pdf

27. Kuhn M. *Caret: Classification and regression training*. Springer: Verlag New York (2021). Availabe at: https://github.com/topepo/caret/

28. Friedman J, Hastie T, Tibshirani R. Regularization paths for generalized linear models *via* coordinate descent. *J Stat Software* (2010) 33(1):1–22. doi: 10.18637/jss.v033.i01

29. Pinheiro J, Bates D, DebRoy S, Sarkar DR Core Team. *Nlme: Linear and nonlear mixed effects models*. R package version 31-1522021. (2022). Available at: https://cran.r-project.org/web/packages/nlme/nlme.pdf

30. Hothorn T, Bretz F, Westfall P. Simultaneous inference in general parametric models. *Biometric J* (2008) 50(3):346–63. doi: 10.1002/bimj.200810425

31. Wickham H. *ggplot2: Elegant graphics for data analysis*. New York: Springer-Verlag (2016).

32. Levin EG, Lustig Y, Cohen C, Fluss R, Indenbaum V, Amit S, et al. Waning immune humoral response to BNT162b2 covid-19 vaccine over 6 months. *New Engl J Med* (2021) 385(24):e84. doi: 10.1056/NEJMoa2114583

33. Röltgen K, Powell AE, Wirz OF, Stevens BA, Hogan CA, Najeeb J, et al. Defining the features and duration of antibody responses to SARS-CoV-2 infection associated with disease severity and outcome. *Sci Immunol* (2020) 5(54). doi: 10.1126/sciimmunol.abe0240

34. Gudbjartsson DF, Norddahl GL, Melsted P, Gunnarsdottir K, Holm H, Eythorsson E, et al. Humoral immune response to SARS-CoV-2 in Iceland. *New Engl J Med* (2020) 383(18):1724–34. doi: 10.1056/NEJMoa2026116

35. CDC. *Science brief: SARS-CoV-2 infection-induced and vaccine-induced immunity*. (2021).

36. Hervé C, Laupèze B, Del Giudice G, Didierlaurent AM, Tavares Da Silva F. The how's and what's of vaccine reactogenicity. *NPJ Vaccines* (2019) 4(1):39. doi: 10.1038/s41541-019-0132-6

37. Dan JM, Mateus J, Kato Y, Hastie KM, Yu ED, Faliti CE, et al. Immunological memory to SARS-CoV-2 assessed for up to 8 months after infection. *Science* (2021) 371 (6529). doi: 10.1126/science.abf4063

38. Müller L, Andrée M, Moskorz W, Drexler I, Walotka L, Grothmann R, et al. Age-dependent immune response to the Biontech/Pfizer BNT162b2 coronavirus disease 2019 vaccination. *Clin Infect Dis* (2021) 73(11):2065–72. doi: 10.1093/cid/ciab381

39. Kennedy JL, Forrest JC, Young SG, Amick B, Williams M, James L, et al. Temporal variations in seroprevalence of SARS-CoV-2 infections by race and ethnicity in Arkansas. *medRxiv* (2021). doi: 10.1101/2021.07.15.21260213

40. Rogawski McQuade ET, Guertin KA, Becker L, Operario D, Gratz J, Guan D, et al. Assessment of seroprevalence of SARS-CoV-2 and risk factors associated with COVID-19 infection among outpatients in Virginia. *JAMA Network Open* (2021) 4(2):e2035234–e. doi: 10.1001/jamanetworkopen.2020.35234

41. Pass RF, Nachman S, Flynn PM, Muresan P, Fenton T, Cunningham CK, et al. Immunogenicity of licensed influenza a (H1N1) 2009 monovalent vaccines in HIV-infected children and youth. *J Pediatr Infect Dis Soc* (2013) 2(4):352–60. doi: 10.1093/jpids/pit040

42. Arguedas A, Soley C, Lindert K. Responses to 2009 H1N1 vaccine in children 3 to 17 years of age. *New Engl J Med* (2010) 362(4):370–2. doi: 10.1056/NEJMc0909988

43. Netea MG, Domínguez-Andrés J, Barreiro LB, Chavakis T, Divangahi M, Fuchs E, et al. Defining trained immunity and its role in health and disease. *Nat Rev Immunol* (2020) 20(6):375–88. doi: 10.1038/s41577-020-0285-6

44. Smatti MK, Alkhatib HA, Al Thani AA, Yassine HM. Will host genetics affect the response to SARS-CoV-2 vaccines? historical precedents. *Front Med* (2022) 9. doi: 10.3389/fmed.2022.802312

45. Valdés-Fernández BN, Duconge J, Espino AM, Ruaño G. Personalized health and the coronavirus vaccines-do individual genetics matter? *Bioessays* (2021) 43(9):e2100087. doi: 10.1002/bies.202100087

46. Whitaker JA, Ovsyannikova IG, Poland GA. Adversomics: A new paradigm for vaccine safety and design. *Expert Rev Vaccines* (2015) 14(7):935–47. doi: 10.1586/14760584.2015.1038249

47. Rydyznski Moderbacher C, Ramirez SI, Dan JM, Grifoni A, Hastie KM, Weiskopf D, et al. Antigen-specific adaptive immunity to SARS-CoV-2 in acute COVID-19 and associations with age and disease severity. *Cell* (2020) 183(4):996–1012.e19. doi: 10.1016/j.cell.2020.09.038

48. Vardhana S, Baldo L, Morice WG2nd, Wherry EJ. Understanding T cell responses to COVID-19 is essential for informing public health strategies. *Sci Immunol* (2022) 7(71): eabo1303. doi: 10.1126/sciimmunol.abo1303

49. Graham MS, Sudre CH, May A, Antonelli M, Murray B, Varsavsky T, et al. Changes in symptomatology, reinfection, and transmissibility associated with the SARS-CoV-2 variant B.1.1.7: An ecological study. *Lancet Public Health* (2021) 6(5):e335–e45. doi: 10.1016/S2468-2667(21)00055-4

50. Whitaker M, Elliott J, Bodinier B, Barclay W, Ward H, Cooke G, et al. Variant-specific symptoms of COVID-19 in a study of 1,542,510 adults in England. *Nat Commun* (2022) 13(1):6856. doi: 10.1038/s41467-022-34244-2

51. Williams EC, Kizhner A, Stark VS, Nawab A, Muniz DD, Tribin FE, et al. Predictors for reactogenicity and humoral immunity to SARS-CoV-2 following infection and mRNA vaccination: A regularized mixed-effects modelling approach. *medRxiv* (2022). doi: 10.1101/2022.04.05.22273450

frontiers | Frontiers in Immunology

TYPE Original Research
PUBLISHED 20 February 2023
DOI 10.3389/fimmu.2023.1064293

Check for updates

OPEN ACCESS

EDITED BY
Martijn van Griensven,
Maastricht University, Netherlands

REVIEWED BY
Rod Russell,
Memorial University of Newfoundland, Canada
Javier Traba,
Autonomous University of Madrid, Spain

*CORRESPONDENCE
Douglas C. Wallace
wallaced1@email.chop.edu

SPECIALTY SECTION
This article was submitted to Viral Immunology, a section of the journal Frontiers in Immunology

RECEIVED 08 October 2022
ACCEPTED 30 January 2023
PUBLISHED 20 February 2023

CITATION
Guarnieri JW, Angelin A, Murdock DG, Schaefer P, Portluri P, Lie T, Huang J and Wallace DC (2023) SARS-COV-2 viroporins activate the NLRP3-inflammasome by the mitochondrial permeability transition pore. *Front. Immunol.* 14:1064293. doi: 10.3389/fimmu.2023.1064293

COPYRIGHT
© 2023 Guarnieri, Angelin, Murdock, Schaefer, Portluri, Lie, Huang and Wallace. This is an open-access article distributed under the terms of the Creative Commons Attribution License (CC BY). The use, distribution or reproduction in other forums is permitted, provided the original author(s) and the copyright owner(s) are credited and that the original publication in this journal is cited, in accordance with accepted academic practice. No use, distribution or reproduction is permitted which does not comply with these terms.

SARS-COV-2 viroporins activate the NLRP3-inflammasome by the mitochondrial permeability transition pore

Joseph W. Guarnieri[1], Alessia Angelin[1], Deborah G. Murdock[1], Patrick Schaefer[1], Prasanth Portluri[1], Timothy Lie[1,2], Jessica Huang[1] and Douglas C. Wallace[1,3]*

[1]Center for Mitochondrial and Epigenomic Medicine, Division of Human Genetics, The Children's Hospital of Philadelphia, Philadelphia, PA, United States, [2]Department of biology, University of Pennsylvania, Philadelphia, PA, United States, [3]Department of Pediatrics, Division of Human Genetics, Perelman School of Medicine, University of Pennsylvania, Philadelphia, PA, United States

Background: Compared to healthy controls, severe COVID19 patients display increased levels of activated NLRP3-inflammasome (NLRP3-I) and interleukin (IL)-1β. SARS-CoV-2 encodes viroporin proteins E and Orf3a(2-E+2-3a) with homologs to SARS-CoV-1, 1-E+1-3a, which elevate NLRP3-I activation; by an unknown mechanism. Thus, we investigated how 2-E+2-3a activates the NLRP3-I to better understand the pathophysiology of severe COVID-19.

Methods: We generated a polycistronic expression-vector co-expressing 2-E+2-3a from a single transcript. To elucidate how 2-E+2-3a activates the NLRP3-I, we reconstituted the NLRP3-I in 293T cells and used THP1-derived macrophages to monitor the secretion of mature IL-1β. Mitochondrial physiology was assessed using fluorescent microscopy and plate reader assays, and the release of mitochondrial DNA (mtDNA) was detected from cytosolic-enriched fractions using Real-Time PCR.

Results: Expression of 2-E+2-3a in 293T cells increased cytosolic Ca++ and elevated mitochondrial Ca++, taken up through the MCUi11-sensitive mitochondrial calcium uniporter. Increased mitochondrial Ca++ stimulated NADH, mitochondrial reactive oxygen species (mROS) production and the release of mtDNA into the cytosol. Expression of 2-E+2-3a in NLRP3-I reconstituted 293T cells and THP1-derived macrophages displayed increased secretion of IL-1β. Increasing mitochondrial antioxidant defenses via treatment with MnTBAP or genetic expression of mCAT abolished 2-E+2-3a elevation of mROS, cytosolic mtDNA levels, and secretion of NLRP3-activated-IL-1β. The 2-E+2-3a-induced release of mtDNA and the secretion of NLRP3-activated-IL-1β were absent in cells lacking mtDNA and blocked in cells treated with the mitochondrial-permeability-pore(mtPTP)-specific inhibitor NIM811.

Conclusion: Our findings revealed that mROS activates the release of mitochondrial DNA via the NIM811-sensitive mitochondrial-permeability-pore (mtPTP), activating the inflammasome. Hence, interventions targeting mROS and the mtPTP may mitigate the severity of COVID-19 cytokine storms.

KEYWORDS

COVID-19, NLRP3-inflammasome, viroporin, mitochondrial permeability transition pore, mitochondria in innate immune responses

10.3389/fimmu.2023.1064293

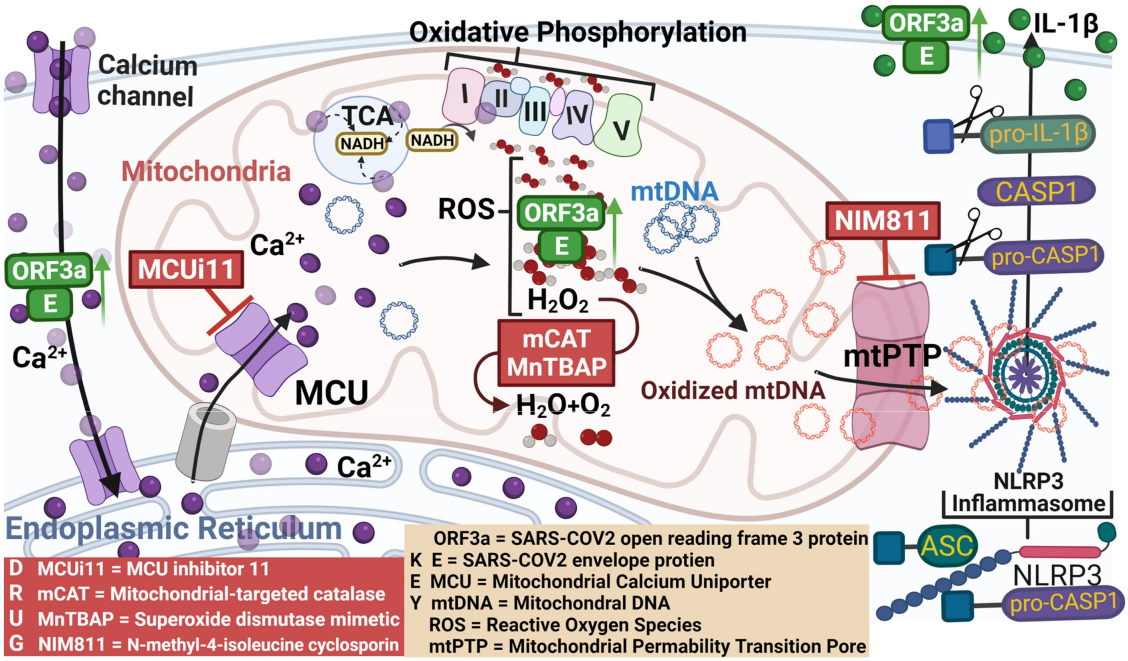

GRAPHICAL ABSTRACT

Introduction

Approximately 609 million cases of COVID-19 have been reported globally, resulting in over 6.5 million deaths (1). COVID-19 is caused by SARS-CoV-2 whose genome structure encodes a polyprotein that is cleaved into 16 non-structural proteins as well as the structural proteins S (Spike), E (Envelope), M (Membrane), and N (Nucleocapsid), plus seven open reading frames (Orfs) 3a, 6, 7a/b, 8, 9b, and 10. Severe COVID-19 manifests as pneumonia, acute respiratory distress syndrome, respiratory failure, and cytokine storm resulting in multiple organ failure (2–4). The cytokine storm results from the elaboration of pro-inflammatory cytokines such as IL-1β (5–7).

The production of mature IL-1β requires the activation of the mitochondrially-bound NLRP3-inflammasome (NLRP3-I), which encompasses the NLR family pyrin domain containing 3 (NLRP3) receptor; the adaptor molecule apoptosis-associated speck-like protein containing a caspase activation and recruitment domain (ASC); and the pro-IL-1β-converting enzyme pro-caspase-1 (CASP1). Upon activation, the NLRP3-I triggers the proteolytic cleavage of pro-caspase-1 (pro-CASP1), and CASP1 cleaves pro-IL-1β and pro-IL-18 to generate IL-1β and IL-18 which are secreted from the cell (8). Autopsy samples from severe COVID-19 patients display increased NLRP3-I activation in lung tissues and peripheral blood mononuclear cells (2), and monocytes isolated from severe COVID-19 patients have increased levels of activated NLRP3-I and IL-1β (4). Thus, understanding the mechanism by which SARS-CoV-2 activates the NLRP3-I is imperative for understanding the pathophysiology of severe COVID-19.

Recently, mitochondrial dysfunction has been shown to activate the innate immune system *via* mROS production and oxidation of the mitochondrial DNA (mtDNA) during replication. mtDNA replication is induced by the expression of the rate-limiting enzyme cytosine monophosphate kinase 2 (CMPK2). The oxidized mtDNA (Ox-mtDNA) is released from the mitochondrion to bind and activate the NLRP3-I (9, 10). While the mechanism by which SARS-CoV-2 activates the NLRP3-I is unknown, expression of the SARS-CoV-1/2 viroporins have been associated with activation of NLRP3-I (11–15) and are known to be membrane ion channels (16, 17).

SARS-CoV-2 encodes two viroporins E (2-E) and ORF3a (2-3a), with homologues to SARS-CoV-1 proteins (18). SARS-CoV-1/2 E and 3a viroporins localize to the endoplasmic reticulum (ER), Golgi apparatus, and plasma membrane (18) where they increase the permeability to cations such as Ca^{++} (19, 20). For SARS-CoV-1, the 1-E and 1-3a have been shown to activate the NLRP3-I in human monocyte-derived macrophages (11, 13, 15). In LPS-primed macrophages, co-expression of 1-E plus 1-3a resulted in higher levels of IL-1β secretion than either viroporin alone (11). 1-E has been reported to activate NLRP3-I through disrupting Ca^{++} homeostasis in cells (12, 14), and activation of the NLRP3-I and secretion of IL-1β by 1-E and 1-3a is mitigated by treatment with the mROS scavenger MitoQ (11). However, the mechanism by which SARS-CoV-2 activates the NLRP3-I has yet to be elucidated.

We hypothesized that expression of 2-E plus 2-3a results in increased Ca^{++} flux into the cytosol where it is taken up by the mitochondrion through the mitochondrial Ca^{++} uniporter (MCU). Within the mitochondrion, the Ca^{++} activates the pyruvate and α-ketoglutarate dehydrogenases to generate excessive NADH (21). The increased NADH overloads the mitochondrial electron transport chain producing increased mROS. The mROS oxidizes the mtDNA, and the Ox-mtDNA is released through the mtPTP to bind to the NLRP3 inflammasome. This activates caspase-1 to cleave pro-IL-1β and pro-IL-18 resulting in the secretion of active IL-1β and IL-18 (10, 22). Our current results support this scenario, thus placing mitochondrial function at the nexus between SARS-CoV-2 infection and the cytokine storm.

Methods

Cells, infections, and reagents

293T & THP1 cells were obtained from the American Type Culture Collection (ATCC). Cells were grown at 37°C with an atmosphere of 98% humidity and 5% CO_2. 293T cells were maintained in Dulbecco's modified Eagle's medium + GlutaMAX™ supplement with pyruvate (GIBCO), 1% non-essential amino acids (SIGMA), and 10% fetal bovine serum (FBS) (Takara Bio). 293T-ρ^0 were generate as previously described in (23). 293T-ρ^0 cells were maintained in the same media used to maintain 293T cells with the addition of 100 ug/mL of Uridine (SIGMA). THP1 cells were grown in RPMI 1640 Medium (GIBCO) supplemented with 10% FBS (Takara Bio). 293T and 293T-ρ^0 cells were infected with lenti viruses (MOI 4) as previously described (24). THP1 cells were infected with lenti viruses (MOI 8) with the addition of 10 μg/ml polybrene (VectorBuilder) and spin-inoculated at 700×g for 25min.

Plasmids, viral vectors, THP1 stable-transformants

Plasmid vectors

To express the components of the NLRP3-inflammasome (NLFP3-I), we utilized four plasmids expressing mouse NLRP3 (pcDNA3-N-Flag-NLRP3, Addgene plasmid # 75127), ASC (pcDNA3-N-Flag-ASC1, Addgene plasmid # 75134), CASP1 (pcDNA3-N-Flag-Caspase-1, Addgene plasmid # 75128) and pro-IL-1B (pCMV-pro-Il1b-C-Flag, Addgene plasmid # 75131). The use and construction of the NLRP3-I expression plasmids were previously described (25).

The plasmid vector used to express mitochondrial-targeted catalase (mCAT) and its respective control vector were p-mCAT (VectorBuilder ID VB170403-1078nzg) and p-EV (VectorBuilder ID VB210726-1273jte). The p-mCAT transgene cassette was transcribed from the 212 nucleotide elongation factor α1 "short" (EFS) promoter. The EFS promoter transcribes a polycistronic transcript encoding EGFP (enhanced green fluorescent protein), a self-cleaving 2A peptide site, followed by mCAT cDNA, and terminated by a simian virus 40 (SV40) late polyA sequence. p-EV is identical to the p-mCAT construct, except lacking the EGFP and mCAT sequences.

Lentiviral vectors

The lentiviral vector used to co-express 2-E+2-3a was LV-E3a (Vectorbuilder ID VB210112-1153ufz) and its respective control vector LV-EV (Vectorbuilder ID VB210112-1153ufz). The LV-E3a vector contains the *cytomegalovirus* (CMV) promoter, the 2-E+2-3a viroporins obtained from Gordon et al., 2020 (18) separated by a 2A peptide site, and terminated by a SV40 late polyA sequence cloned into the LV-EV vector. The viroporin sequences deduced from the protein sequences were modified by adding an ATG codon 5' and three N-terminal FLAG-tags added to the 3' end of each viral protein. LV-EV is an empty vector.

The lentiviral vector expressing our mCAT and its respective control vector were LV-mCAT (VectorBuilder 210909-1242kdf) and LV-EV (VectorBuilder 900122-0484ubz). The LV-mCAT vector includes the EFS promoter, EGFP, 2A peptide site, mCAT, and SV40 late polyA sequence. The LV-EVcontrol vector lacks the EGFP and mCAT sequences.

THP1 mCAT stable-transformants

THP1 cells were transduced with LV-mCAT or empty vector and selected with puromycin. Expression of stable-transformants of mCAT were validated by EGFP fluorescence.

Method details

Cell staining

293T cells were plated at a density of 45×10^3 in 0.2% gelatin-coated (ScienCell) 96-well glass-bottom plates with high-performance #1.5 mm cover glass (Cellvis). Twenty-four hours post-plating, sub-confluent monolayers of 293T cells were transduced with LV-EV or LV-E3a. Twenty-four hours post-transduction, cells were washed two times with phosphate-buffered saline (PBS), then stained. For determination of mROS levels, cells were co-stained with 3 μM MitoSOX™ Red (MitoSOX, mitochondrial superoxide indicator) and 50 nM MitoTracker™ Deep Red FM (MTDR) for 30 min at 37°C. For assaying mROS levels after treatment with Thapsigargin (TG) using the plate reader, cells were stained with 3 μM MitoSOX for 30 min at 37° C.To quantify mROS after staining, cells were washed three times in PBS, maintained in FluoroBrite™ DMEM (GIBCO) supplemented with 12.5 mM HEPES (SIGMA) and 1% non-essential amino acids (SIGMA), and the fluorescence measured.

To determine cytosolic Ca^{++} levels, cells were washed three times with Tyrode's Salts (Sigma-Aldrich), stained for 40 min with 2 μM Fura Red™, acetoxymethyl ester (AM), cell-permeant (Fura-Red) in 0.02% pluronic F127 (Pluronic® F-127) detergent. To determine mitochondrial Ca^{++} levels, cells were washed three times with Tyrode's Salts, stained for 40 min with 10 μM Rhod-2, AM, cell-permeant (Rhod2) and 50 nM MTDR in 0.02% pluronic F127. After staining cells were washed three times, maintained in Tyrode's Salts, and the florescence measured. To determine mitochondrial Ca^{++} levels after treating with TG, cells were stained for 40 min with 10 μM Rhod2, washed three times, maintained in Tyrode's Salts, and the florescence measured.

SpectraMax plate reader assay

Measurement of mROS and cytosolic and mitochondrial Ca^{++} levels

After staining cells (see "Cell Staining"), mean fluorescence was assessed using the *SpectraMax® Paradigm® Multi-mode Detection Platform*, equipped with *a* Tunable Wavelength (TUNE) Detection Cartridge (Molecular Devices). mROS was quantified by MitoSOX fluorescence (ex:540 nm, em:590 nm) and MTDR (ex:633 nm, em:680 nm) and MitoSOX/MTDR calculated. Rhod2 fluorescence for mitochondrial Ca^{++} level (ex:540 nm, em:590 nm) and MTDR (ex:633 nm, em:680 nm), and Rhod2/MTDR calculated. Fura-Red fluorescence was measured for cytosolic bound-Ca^{++} level using ex:405 nm, em:637 nm and unbound-Ca^{++} level using ex:514 nm, em:672 nm. The ratio of bound-Ca^{++}/unbound-Ca^{++} was calculated.

Measurement of mitochondrial Ca^{++} and mROS after treating with TG

After staining cells with Rhod2 or MitoSOX ("Cell Staining"), cells were treated for 10 min with or without 10 µM mitochondria channel uniporter inhibitor 11 (MCUi11), or dimethylsulfoxide (DMSO) as a negative control. Mitochondrial Ca^{++} determined from Rhod2 was measured using ex:540 nm, em:590 nm and mROS from MitoSOX using ex:540 nm, em:590 nm. Cells were then treated with 2.5 µM TG and changes in mitochondrial Ca^{++} or mROS recorded every 15 seconds for 180 seconds. Relative change in mitochondrial Ca^{++} was calculated by dividing the average change in Rhod2 fluorescence after treatment with TG by Rhod2 fluorescence before treatment with TG. Relative change in mROS levels were calculated by dividing the average change in MitoSOX fluorescence after treatment with TG by MitoSOX fluorescence before treatment with TG.

Confocal microscopy

Live-cell fluorescence imaging was performed using a Zeiss 710 LSM confocal microscope with an environmental chamber maintained at 37°C and 5% CO2. Laser lines used: diode 405 nm, Argon 514 nm, HeNe lasers 543 nm and 633 nm excitation wavelengths. Fluorescence was analyzed using ImageJ. Fluorescence intensities of stained cells were normalized to the unstained negative cells. A minimum of 60 images was taken for each condition across at least three independent experiments.

Fluorescence lifetime imaging microscopy (FLIM) of NADH autofluorescence

Fluorescence lifetime imaging microscopy (FLIM) of NADH autofluorescence was performed according to Schaefer et al. (26). Using FLIM, NADH was measured on a Zeiss LSM 710 Laser Scanning Microscope equipped with a pulsed, two-photon titanium-sapphire laser (80 MHz, 100 fs pulse width). NADH was excited at 730 nm and emission was recorded through a 460/60 nm bandpass filter using the hybrid detector HPM-100-40, mounted on the NDD port of the LSM710. Time-correlated single photon counting (TCSPC) was performed with a temporal resolution of 256 time channels within a pulse period of 12.5 ns, resulting in FLIM images of 512 × 512 pixel. The final measurement settings were 60 sec collection time; ≈ 15 µsec pixel dwell time; 135 × 135 μm^2 scanning area using a Plan-Apochromat 63x/1.40 Oil DIC M27 lens. SPCM 9.8 was used to record the data, which were subsequently analyzed using SPCImage 8.0 by fitting (WLS method) of a biexponential decay with lifetime components fixed to 400 ps and 2500 ps for free and protein-bound NADH, respectively. Final analysis settings were square binning of 2, peak threshold adapted to background, and shift fixed at a pixel with clear NADH signal. The mean NADH lifetime (t_{mean}) was calculated and is depicted in false-color coding with red indicating a shorter and blue a longer NADH lifetime. For subcellular analysis, region of interests (ROIs) of similar size were drawn for five nuclei across each image. For the mitochondria-rich region, the peak threshold was increased to remove nuclear and cytosolic NADH signal, averaging only the t_{mean} of the mitochondrial NADH.

Catalase assay

Catalase activity was assessed through cleavage of H_2O_2 in 293T cell lysates collected twenty-four hours post-transfection with p-mCAT or p-EV, using a Catalysis Activity Kit (Abcam, ab83464).

Western blot analysis

Twenty-four hours post-transduction, cells were washed with cold PBS and then lysed with 2.5% n-Dodecyl-B-D-Maltoside in 20 mM HEPES (pH 7.4), 50 mM β-glycerophosphate, 2 mM EGTA, 10% (v/v) glycerol, and 0.01% Bromophenol blue. Lysates were electrophoresed on 4 to 12%, Bis-Tris gels (Invitrogen) SDS-polyacrylamide NuPAGE™ gels. Gels were transferred to a nitrocellulose membrane by the iBlot Gel Transfer System (Invitrogen), membranes blocked for one hour in 5% nonfat milk in 150 mM NaCl and 25 mM Tris-buffered saline in 0.1% Tween® 20 Detergent (TBST) then incubated overnight at 4°C with shaking. The primary antibody was diluted 1:1000 in TBST. Membranes were then washed three times with TBST and incubated with Alexa Fluor-conjugated secondary antibodies for one hour at room temperature. Protein levels were quantified using the Odyssey imaging system (LiCOR Biosciences). GAPDH as a loading control.

Detection of secreted IL-1β in 293T cells with reconstituted NLRP3-I and THP1 macrophages

293T cells were plated at a density of 100 × 10^3 in 24-well plates. Twenty-four hours post-plating sub-confluent monolayers of 293T cells were infected with LV-EV or LV-E3a. Six hours post-infection cells were co-transfected using the TransIT-X2® Dynamic Delivery System (Mirus Bio) with the plasmids encoding the components of the NLRP3-I (25), followed by p-mCAT or p-EV transduction. Twenty-four hours post-transfection, cells were washed two times

with PBS, then cultured with or without the addition of 50 uM MnTBAP. Cell lysates and culture supernatants were collected twelve hours post-treatment and centrifuged to remove cell debris. Supernatant IL-1β was quantified by ELISA (Abcam, ab197742).

THP-1 cells were plated at a density of 100×10^3 in 96-well plates. THP1 cells were infected with LV-EV or LV-E3a. Six hours post-infection, THP1 cells were differentiated into macrophages with 50 ng/ml Phorbol 12-myristate 13-acetate (PMA) overnight. After differentiation, cells were washed two times with PBS, and fresh media was added with the addition of 100 μM MnTBAP, 5 μM MCC950, or 10 μM N-methyl-4-isoleucine-cyclosporin (NIM811). Nine hours post-treatment with MnTBAP or MCC950 or one-hour post-treatment with NIM811, THP1 macrophages were stimulated with 100 ng/ml Lipopolysaccharides (LPS) and 2.5 μM of nigericin for nine hours. Supernatants were collected, centrifuged, and the amount of IL-1β in the supernatants measured by ELISA (Abcam, ab46052). THP1 cells stably expressing LV-mCAT or control vector, were infected with LV-EV or LV-E3a, and 6 hours post-infection the THP1 cells were differentiated into macrophages, and supernatant IL-1β quantified *via* ELISA.

Detection of mtDNA from cytosolic-enriched fractions in 293T cells

Twenty-four hours post-plating, sub-confluent monolayers of 293T cells were infected with LV-EV or LV-E3a. Six hours post-infection, cells were transfected with the plasmids encoding p-mCAT or p-EV, or twenty-four hours post-infection cells were treated with or without the addition of 50 uM MnTBAP or 10 uM NIM811. Twenty-four hours post-transfection or ten hours post-treatment, cells were washed with PBS, then dissociated from the plate with Trypsin. The dissociated cells were then pelleted *via* centrifugation and lysed with hypertonic buffer consisting of 20 mM Tris-HCl (pH 7.4), 10 mM NaCl, and 3 mM MgCl2 for fifteen minutes on ice, then treated with Non-Ionic Detergent P-40 (NP-40) 0.05% (v/v) and vortexed at max speed. Cell lysates were centrifuged for 15 minutes at 1,000 g, and the resulting supernatants were centrifuged for 1 hour at 200,000 g to isolate a cytosolic enriched fraction. After centrifugation, protein concentrations were determined from the resulting supernatants by Bradford assay using the Bio-Rad protein assay (Bio-Rad, Hercules, CA). DNA was isolated from equal amounts of protein using the DNA Clean & Concentrator-5 (Zymo Research, 11-303). Levels of mitochondrial DNA in the cytosolic enriched fraction were then determined *via* TaqMan Real-Time PCR assays to detect mitochondrial NADH dehydrogenase subunit 5 (*MT-ND5*) using the TaqMan probe (*MT-ND5* Hs02596878_g1).

Statistical and reproducibility

For quantitative analyses, a minimum of 3 biological replicates were analyzed. Western blot data are from the respective experiment, processed in parallel, and represent at least three independent experiments. One-way ANOVA was performed for statistical differences between three or more groups, followed by a *post hoc* Tukey's HSD test to test for statistical differences. For studies that require a quantitative evaluation between two groups, statistical significance was determined using unpaired two-tail Student's t-test. All data bar graphs, data are reported as mean ± standard error of the mean (SEM). All statistical analysis was done on GraphPad Prism 9.01. For student's t-test * = p < value 0.05, ** = p < value 0.01, *** = p < value 0.001, **** = p < value 0.0001).

Results

Expression of 2-E+2-3a increases Ca^{++} leakage into the cytosol, elevates mitochondrial Ca^{++} levels, and increases mROS production

A major unanswered question is how 2-E and 2-3a activate the NLRP3-I. We hypothesized that expression of 2-E and 2-3a results in increased Ca^{++} flux into the cytosol where it is taken up by the mitochondrion through the MCU. Within the mitochondrion, the Ca^{++} activates the pyruvate and α-ketoglutarate dehydrogenases to generate excessive NADH. The increased NADH overloads the electron transport chain producing increased mROS. The mROS oxidizes the mtDNA which is released through the mtPTP to bind to the NLRP3-I. This activates caspase 1 to cleave pro-IL-1β and pro-IL-18 resulting in the secretion of active IL-1β and IL-18 (10, 22).

To test this hypothesis, we constructed a polycistronic expression vector combining 2-E+2-3a (LV-E3a) to determine how these viroporins function synergistically to engage the NLRP3-I (Figures 1A, B). In this vector the 2-E+2-3a sequences were separated by the self-cleaving 2A peptide site (27) to allow co-expression from a single transcript. The expression of 2-E+2-3a in LV-E3a transduced 293T cells was confirmed by Western blot (Figure 1C). We then demonstrated that LV-E3a transduced 293T cells experience increased cytosolic Ca^{++} with Fura-Red by plate reader assay (Figures 1D, J) and confocal microscopy (Figure 1E). Additionally, we demonstrated that LV-E3a transduced 293T cells experience increased mitochondrial Ca++ with Rhod2 by plate reader assay (Figures 1F, J) and confocal microscopy (Figure 1G). The LV-E3a transduced 293T cells had elevated levels of both cytosolic and mitochondrial Ca^{++}.

Treating with thapsigargin (TG) triggers Ca^{++} flux into the cytosol resulting in increased mitochondrial Ca^{++} uptake (28, 29). Treatment with the mitochondrial calcium uniporter inhibitor 11 (MCUi11) blocks Ca^{++} entry into the mitochondrion (30, 31). Treatment with MCUi11 abolished mitochondrial calcium uptake in LV-E3a transduced cells (Figure 1H) following TG treatment. Thus, expression of 2-E+2-3a in 293T cells results in increased Ca^{++} flux into the cytosol resulting in an elevation of cytosolic Ca^{++}. The cytosolic Ca^{++} is then taken up by the mitochondrial calcium uniporter resulting in elevated mitochondrial Ca^{++} (Figure 1H).

Elevated mitochondrial Ca^{++} activates the tricarboxylic acid cycle dehydrogenases generating excess NADH (21). Expression of 2-E+2-3a in 293T cells resulted in increased mitochondrial NADH levels detected *via* NADH fluorescence lifetime imaging (FLIM) (NAD^+/NADH) mean (ps) (Figures 1I, J).

Excessive NADH levels can overload the electron transport chain producing increased mROS. The increased NDAH in 2-E+2-3a

10.3389/fimmu.2023.1064293

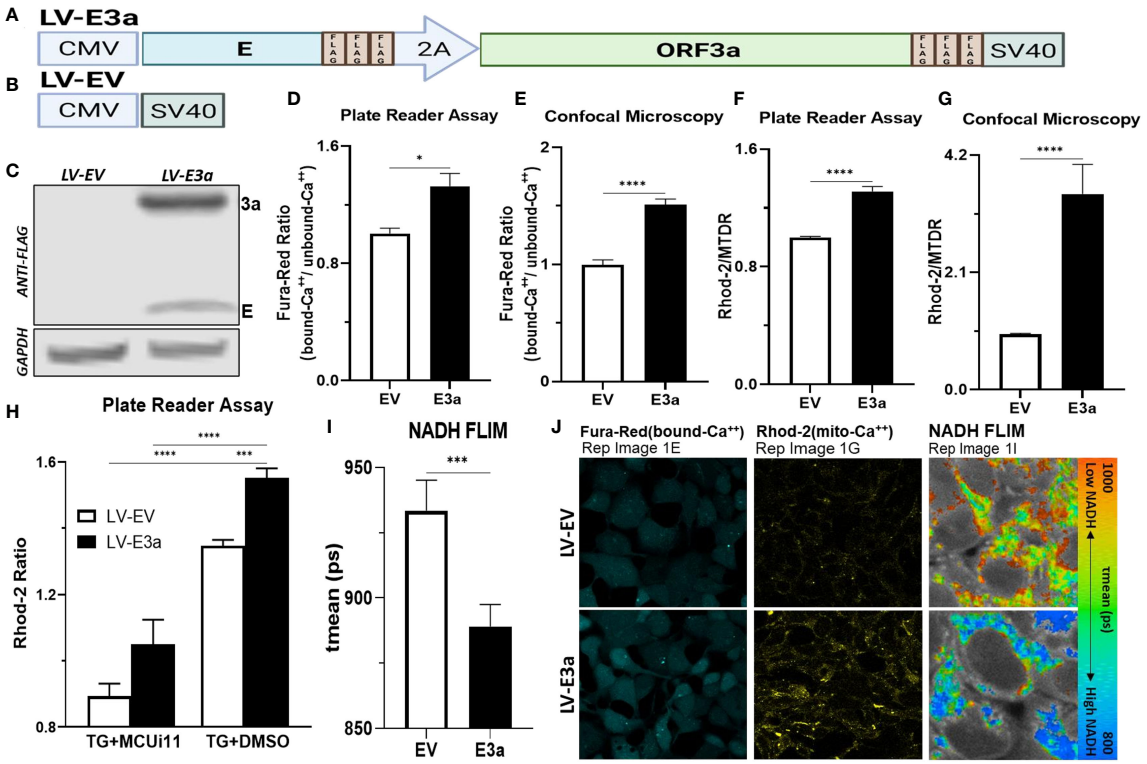

FIGURE 1
Expression of 2-E+2-3a induces mROS production by elevating mitochondrial Ca^{++} levels. **(A, B)** Schematics of our LV-EV and LV-E3a vectors. **(C)** 293T cells were transduced with LV-EV or LV-E3a, and samples analyzed by immunoblot with a mouse monoclonal antibody against FLAG-Tag, to detect the FLAG-tagged 2-E+2-3a viroporins. GAPDH was a loading control. **(D, E)** 24 hrs post-transduction cells were stained with Fura-Red to measure cytosolic Ca^{++} levels, **(F, G)** and with Rhod2 & Mitotracker Deep Red (MTDR) to measure mitochondrial Ca^{++} levels. **(E, G, J)** data from confocal microscopy or **(D, F)** data from plate reader assays. **(H)** 24 hrs post-transduction with LV-EV or LV-E3a 293T cells were treated with or without 10 μM MCUi11, and then 2.5 μM TG and stained with Rhod2 to measure mitochondrial Ca^{++} levels by plate reader assays. **(I)** Cells, 24 hrs post-transduction with LV-EV or LV-E3a, were analyzed for mean mitochondrial NADH lifetime (t_{mean}) indicating (NAD^+/NADH ratio) using FLIM. **(J)** Representative images of Fura-Red, Rhod2-stained, and NADH lifetime imaged cells. Scale bar = 30 μm. Error bars represent SEM from 3 independent experiments; statistically significant data is indicated with asterisks (*).

expressing 293T cells was associated with increased mROS production detected by staining transduced cells with MitoSOX, which detects mitochondrial superoxide anion production (Figures 2A–C). To determine if the increased mROS was due to the entry of Ca^{++} into the mitochondrion, we treated the cells with MCUi11 which blocked the increased mROS production (Figure 2D). As predicted MCUi11 blocked the increased mROS production. Hence the increased mROS production in 2-E+2-3a cells was dependent on elevated mitochondrial Ca^{++}.

To confirm that the 2-E+2-3a induced ROS production was mROS, we transfected the 2-E+2-3a expressing 293T cells with a vector expressing mitochondrially-targeted catalase (mCAT) (Figures 2E–I, L) which removes mitochondrial H_2O_2 (32). We also treated the cells with the mitochondrially targeted catalytic metalloporphyrin anti-oxidant, MnTBAP (Figures 2J, K, M) (33). Treatment with either MnTBAP or mCAT extinguished the 2-E+2-3a activated ROS product, confirming that the ROS was generated by the mitochondrion.

2-E+2-3a induced mROS is involved in NLRP3-activation and IL-1β production. SARS-CoV-1, activation of the NLRP3-I and associated pathogenicity were observed for both viroporins 1-E+1-3a (11, 14, 34, 35). To determine if this is the case for SARS-CoV-2, we used two model systems to determine if 2-E+2-3a expression activates the NLRP3-I *via* the mitochondrion. In the first, we reconstituted the inflammasome in 293T cells by transforming with plasmids encoding the components of the NLRP3-I (Figure 3A) (25). In the second, we employed the human acute monocytic leukemia derived cell line, THP1, which can be converted to macrophages by treatment with phorbol ester (PMA) and the macrophages treated with LPS + nigericin (Figure 3B) (36). The reconstituted NLRP3-I 293T cells were transduced with the 2-E+2-3a expression vector (Figure 3A). The THP-1 cells were first transduced with the 2-E+2-3a expression vector and then treated with PMA and LPS + nigericin (Figure 3B). The expression of 2-E+2-3a in both cell systems, 293T (Figure 3C) and THP1 macrophages (Figures 3D–F) resulted in enhanced secretion of NLRP3-activated IL-1β in 293T-NLRP3-I (Figure 3E) and THP1 macrophages (Figures 3D, E).

We then confirmed that 2-E+2-3a expression activates the NLRP3-I and IL-1β secretion *via* increased mROS production. 293T cells expressing the inflammasome proteins (Figure 3C) and LPS-nigericin treated THP1 macrophages (Figures 3D, E) were treated with mitochondrially targeted antioxidants: transformation with mCAT or treatment with MnTBAP. Both mCAT expression and MnTBAP treatment impaired IL-1β secretion.

We then determined if mROS activation of the NLRP3-I was mediated by release of a mitochondrial component *via* the mtPTP,

10.3389/fimmu.2023.1064293

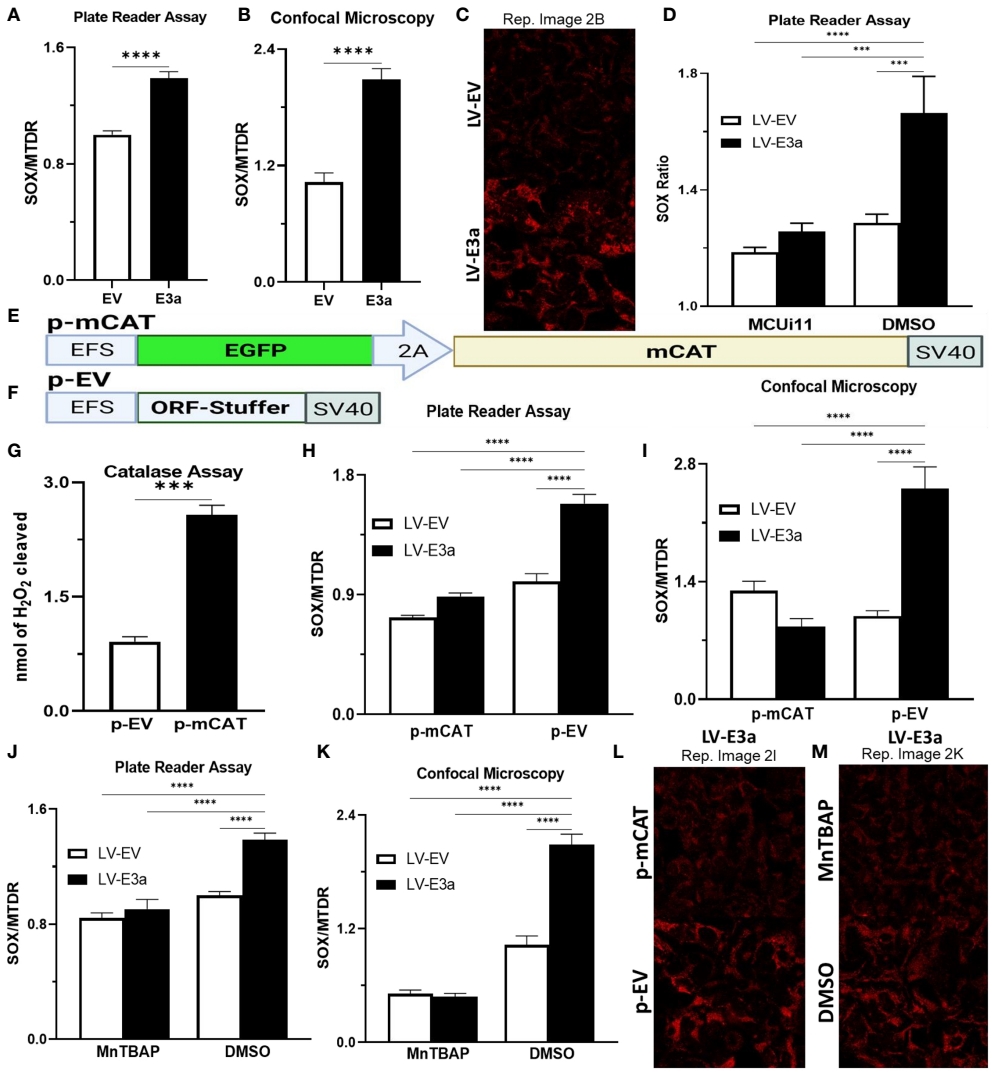

FIGURE 2
Expression of mCAT or treatment with the mROS scavenger MnTBAP antioxidant defenses blocks 2-E+2-3a induced mROS. **(A–C)** 24 hrs post-transduction cells were stained with MitoSOX and MTDR to measure mROS levels *via* **(A)** data from plate reader assays or **(B, C)** data from confocal microscopy. **(D)** 24 hrs post-transduction with LV-EV or LV-E3a 293T, cells were treated with or without 10 μM MCUi11, and then 2.5 μM TG and stained with MitoSOX to measure mROS levels by plate reader assays. **(E, F)** Schematics of p- p-mCAT and EV vectors. **(G)** Catalase assay through cleavage of H_2O_2 in 293T cell lysates collected 24 hrs post-transfection with p-EV or p-mCAT. **(H-M)** 24 hrs post-transfection levels of mROS assessed using MitoSOX and MTDR fluorescence 293T cells transduced with LV-EV or LV-E3a and transfected **(H, I, L)** with p-mCAT or its respective control p-EV or **(J, K, M)** cultured in the presence or absence of 50 μM MnTBAP, DMSO used as a negative control. MTDR fluorescence was used to normalize for mitochondrial content with mROS expressed as the ratio of MitoSOX/MTDR, by **(H, J)** plate reader assays or **(I, K, L, M)** confocal microscopy. **(C, L, M)** Representative images of MitoSOX-stained cells. Scale bar = 30 μm. Error bars represent SEM from 3 independent experiments; statistically significant data is indicated with asterisks (*).

which has been conjectured but not proven. We treated 2-E+2-3a transduced THP1 macrophages with the specific mtPTP inhibitor N-methyl-4-isoleucine-cyclosporin (NIM811). NIM811 blocks the mtPTP by binding to cyclophilin D, analogous to cyclosporin A (CsA), but without calcineurin inactivation (37–39). NIM811 treatment suppressed the secretion of IL-1β following LPS + nigericin activation of the THP1 macrophages (Figure 3F) demonstrating for the first time the mtPTP is the route by which a mitochondrial factor, presumably mtDNA, reaches the NRLP3-I. Finally, to confirm that 2-E+2-3a secretion of IL-1β occurred through NRLP3-I, we treated THP1 macrophages with MCC950, a selective small molecule inhibitor that binds to the NACHT domain of NLRP3 (40). MCC950 blocked IL-1β secretion in 2-E+2-3a expressing THP1 macrophages, demonstrating that E3a secretion of IL-1β, was mainly through the activation of the NLRP3-I (Figure 3G).

We next demonstrated that LV-E3a transduced 293T cells increased levels of cytosolic mtDNA *via* Real-Time PCR quantification of mitochondrial NADH dehydrogenase subunit 5 (*MT-ND5*) in cytosolic-enriched supernatants (Figures 4A–C). To confirm that 2-E+2-3a increased the levels of cytosolic mtDNA *via* efflux through the mtPTP, we treated 2-E+2-3a expressing 293T cells with NIM811, which extinguished the 2-E+2-3a elevation of cytosolic mtDNA. This confirms that mtPTP opening contributes to 2-E+2-3a elevation of cytosolic mtDNA (Figure 4B). To determine if mROS contributed to 2-E+2-3a release of mtDNA we transduced 293T cell expressing 2-E+2-3a cells with mCAT or treated the cells with

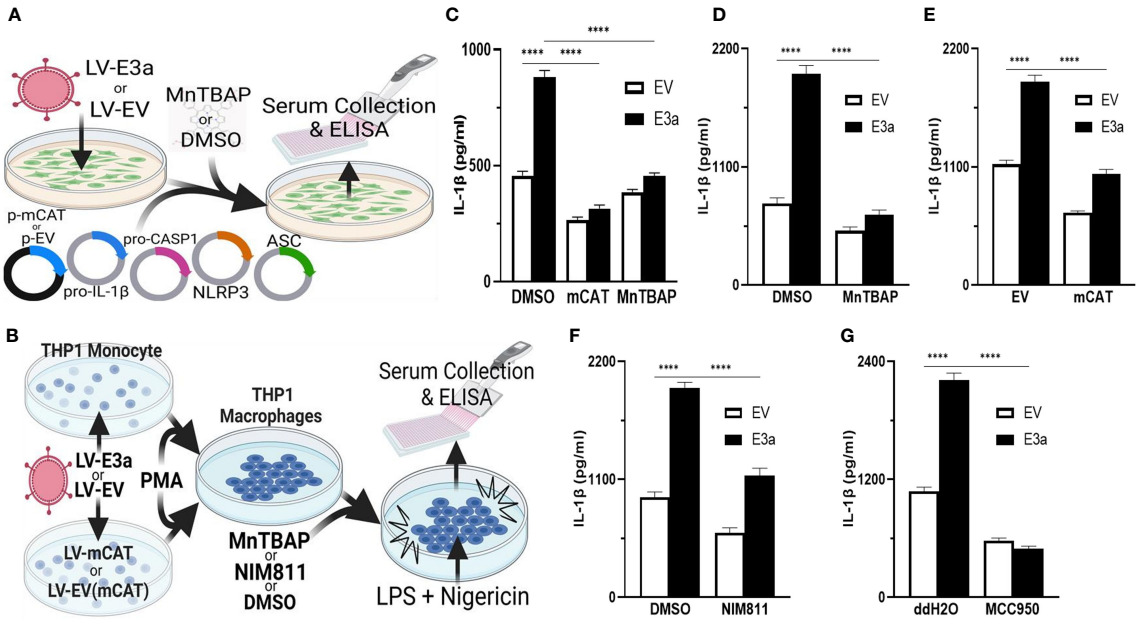

FIGURE 3
mROS and the mtPTP are required for activation of the NLRP3-I by the 2-E+2-3a viroporins. **(A, B)** Experimental design used to assess NLRP3-activated by IL-1β in cell-free supernatants quantified by ELISA. **(A)** 293T cells with an NLRP3-I reconstitution system (NLRP3, ASC, pro-CASP1, pro-IL-1β) and **(B)** THP1 differentiated into macrophages and primed with LPS + nigericin. **(C)** 293T cells transfected with LV-EV or LV-E3a were transfected with the NLRP3-I plasmids and p-mCAT or its control plasmid p-EV, or cultured in the presence or absence of 50 μM MnTBAP. **(D, F, G)** THP1 cells were transduced with LV-EV or LV-E3a, differentiated into macrophages, treated with LPS + nigericin, and treated with 5 μM MCC950, 100 μM MnTBAP or 10 μM NIM811, the supernatants analyzed for IL-1β by ELISA. **(E)** THP1 cells stably expressing LV-mCAT or control plasmid were infected with LV-EV or LV-E3a, differentiated into macrophages, and supernatant IL-1β levels determined *via* ELISA. Error bars represent SEM from 3 independent experiments; statistically significant data is indicated with asterisks (*).

MnTBAP. Both mitochondrial catalytic antioxidants impaired 2-E+2-3a elevation of cytosolic mtDNA (Figures 4B, C). Finally, to confirm that 2-E+2-3a activation of the NRLP3-I, was dependent on mtDNA we showed that secretion of the IL-1β was lost in 293T cells with a reconstituted inflammasome (Figure 4D) that had been cured of their resident mtDNA (ρ^0 cells). The presence of mtDNA is thus an absolute requirement for 2-E+2-3a activation of the NRLP3-I.

Thus, we have demonstrated that co-expression of 2-E+2-3a enhances Ca^{++} leakage into the cytosol, increasing levels of cytosolic and mitochondrial Ca^{++}. This 2-E+2-3a mediated increase in mitochondrial Ca^{++} increases mitochondrial NADH in association with increased mROS. mtDNA is then released into the cytosol *via* the mtPTP which activates the NLRP3-I stimulating the secretion of IL-1β. Increasing mitochondrial antioxidant defenses through treatment with the pharmacological mROS scavenger MnTBAP or genetic expression of mCAT blocks 2-E+2-3a induced activation of the NLRP3-I, which is absolutely dependent on the presence of mtDNA. Together these findings reveal that the mechanism by which 2-E+2-3a engage the NLRP3-I is *via* viroporin manipulation of mitochondrial physiology causing release of mtDNA to bind to the NLRP3-I.

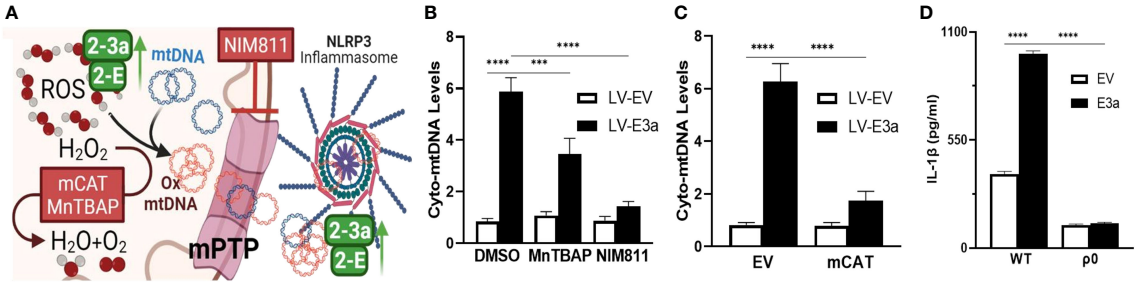

FIGURE 4
2-E+2-3a viroporins induced mROS is required for the release of mtDNA from the mitochondrion into the cytosol *via* the mtPTP. **(A)** Representative Figure. **(B, C)** 293T cells were transduced with LV-EV or LV-E3a. **(B)** 24 hrs post-transduction cells were treated with or without 50 uM MnTBAP or 10 μM NIM811. 10 hrs post-treatment, cells were lysed, cytosolic-enriched fractions collected, DNA isolated from the cytosolic-enriched fractions, and levels of cytosolic mtDNA determined by RT-PCR with a probe specific for *MT-ND5*. **(C)** 6 hrs post-transduction with LV-EV or LV-E3a, 293T cells were transfected with p-mCAT or its control plasmid p-EV. 24 hrs post-transfection, levels of cytosolic mtDNA were determined as described above. **(D)** 293T or 293T-ρ^0 cells transduced with LV-EV or LV-E3a were transfected with the NLRP3-I plasmids the supernatants analyzed for IL-1β by ELISA. Error bars represent SEM from 3 independent experiments; statistically significant data is indicated with asterisks (*).

Discussion

A variety of mechanisms have been proposed to activate the NLRP3-I. These include interferon antagonism, organelle stress, mROS production, direct binding to inflammasome components (9, 10), and cellular expression of viroporins (16, 17). SARS-CoV-1/2 have been shown to agonizes the NLRP3-I by three mechanisms. First, through direct viral protein interaction with components or regulatory proteins of the NLRP3-I, *via* 2-N interaction with the NLRP3 receptor, and 1-3a interaction with CASP1 & TNF Receptor Associated Factor 3 (TRAF3) (13, 15, 36). Second, by increasing NF-κB-dependent target gene transcription of pro-inflammatory cytokines such as IL-18 and IL-1β through the 2-N, 2-S, 2-7a, 1-3a & 2-3a proteins (15, 36, 41, 42). Third, by distress or cellular damage caused by SARS-CoV-1/2 viroporins (11–13, 15, 43), which are transmembrane pore-forming proteins that localize to membranes and augment cell permeability to ions.

All human coronaviruses encode one or more viroporins that antagonize the NLRP3-I (44–47). SARS-CoV-1 encodes for three viroporins 1-E, 1-3a, and 1-8b. Several studies have shown that 1-E & 1-3a activate the NLRP3-I in various human cell lines transduced with the components of the NLRP3-I or LPS-primed macrophages and monocyte-derived macrophages (11, 13, 15). The 1-E viroporin has been reported to engage the NLRP3-I and elicit production of chemokines and cytokines through disrupting cellular Ca^{++} homeostasis (12, 14). Treatment of LPS-primed macrophages with the mROS scavenger MitoQ decreased 1-E or 1-3a activation of the NLRP3-I and secretion of IL-1β and co-expression of 1-E and 1-3a significantly increased levels of IL-1β secretion demonstrating a synergistic effect between the two viroporins (11).

SARS-CoV-2 encodes two viroporins 2-E & 2-3a, which share high sequence homology with their SARS-CoV-1 counterparts and function as cation-selective ion channels (19, 48). Both 1-3a & 2-3a stimulate NF-κB-dependent gene transcription and that 2-E increases the transcription of pro-inflammatory cytokines and chemokines, including IL-1β (13, 14, 42). However, the central role of the mitochondrion in viroporin activation of the NLRP3-I and the central role of mitochondrial Ca^{++}, mROS, and mtDNA in viroporin-induced inflammation had not been determined. Our paper now demonstrates that the activation of the NLRP3-I *via* the 2-E and 2-3a proteins requires mitochondrial signaling *via* mitochondrial uptake of Ca^{++}, increased NADH and mROS levels, the presence of mtDNA, and the release of mtDNA through the mtPTP. By inducing Ca^{++} release into the cytosol, 2-E+2-3a likely activates the tricarboxylic acid cycle dehydrogenases generating the excess NADH (21). The resulting excessive reducing equivalents likely then overloads the electron transport chain producing increased mROS. Presumably, the increased mROS damages the mtDNA and activates mtPTP opening. This increases cytosolic mtDNA, which can bind to and activate the NLRP3-I.

While our experiments did not confirm that the mtDNA released through the mtPTP was oxidized, other studies have shown that oxidized mtDNA is a ligand of NLRP3-I (10, 22). Thus, we complete the mitochondrial innate immune activation pathway by showing that the presence of mtDNA is required for activation of the NLRP3-I and that release of mtDNA is *via* the mtPTP.

Demonstration that SARS-CoV-2 activated the inflammasome *via* the mitochondria provides new approaches to mitigating the severity of the cytokine storm. Previous studies have indicated that generalized antioxidants such as N-acetyl cysteine (49), glutathione (50), and catalase (51) can reduce viral propagation and pathology. Our data extend these observations by identifying the sequence of events by which SARS-CoV-2 activates the NLRP3-I, thus demonstrating that mROS and the mtPTP are critical steps in NLRP3-I activation. Therefore more effective therapies may be obtained using mitochondrially targeted catalytic antioxidants such as MnTBAP (33), EUK-8, and EUK-134 (52) and also inhibitors of the mtPTP such as NIM811 (37, 38).

Data availability statement

The original contributions presented in the study are included in the article/supplementary material. Further inquiries can be directed to the corresponding author.

Author contributions

Conceptualization: JG, DW. Methodology: JG, PP, PS, DW, AA, DM. Literature and concept integration: JG, PP, DW, AA, DM. Formal Analysis: JG, PS, DW, AA, DM. Literature and concept integration: JG, P.P, DW, AA, DM, AA, DM, DW. Writing – Original Draft: JG. Investigation: JG, AA, DM, DW, TL, JH. Sample Collection: JG, T.L. Writing – Review & Editing: JG, DW, AA, DM, PS, TL. Visualization: JG, DW, AA, DM. Supervision: JG, P.P, DW, AA, DM. Funding Acquisition: DW. All authors contributed to the article and approved the submitted version.

Funding

This work was supported by DOD grant W81XWH-21-1-0128 awarded to D.C.W.

Acknowledgments

The authors thank Dr. Bruce Beutler for gifts of expression plasmids and Dr. Cristina Mammucari (Department of Biomedical Sciences, University of Padua, 35131 Padua, Italy) and Dr. Kevin Foskett (Department of Cell and Developmental Biology, University of Pennsylvania, 19104 Philadelphia, Pennsylvania) and Dr. Diego De Stefani (Department of Biomedical Sciences, University of Padua, Padua, Italy) for gifting MCUi11, which they purchased from AKos Consulting & Solutions GmbH.

Conflict of interest

DW serves of the advisory boards of Plano Therapeutics, Medical Excellent Capital, and has a grant from March Therapeutics.

The remaining authors declare that the research was conducted in the absence of any commercial or financial relationships that could be construed as a potential conflict of interest.

Publisher's note

All claims expressed in this article are solely those of the authors and do not necessarily represent those of their affiliated organizations, or those of the publisher, the editors and the reviewers. Any product that may be evaluated in this article, or claim that may be made by its manufacturer, is not guaranteed or endorsed by the publisher.

References

1. Dong E, Du H, Gardner L. An interactive web-based dashboard to track COVID-19 in real time. *Lancet Infect Dis* (2020) 20(5):533–4. doi: 10.1016/S1473-3099(20)30120-1

2. Rodrigues TS, de Sá KSG, Ishimoto AY, Becerra A, Oliveira S, Almeida L, et al. Inflammasomes are activated in response to SARS-CoV-2 infection and are associated with COVID-19 severity in patients. *J Exp Med* (2021) 218(3). doi: 10.1084/jem.20201707

3. Yang L, Xie X, Tu Z, Fu J, Xu D, Zhou Y. The signal pathways and treatment of cytokine storm in COVID-19. *Signal transduction targeted Ther* (2021) 6(1):255. doi: 10.1038/s41392-021-00679-0

4. Ferreira AC, Soares VC, de Azevedo-Quintanilha IG, Dias S, Fintelman-Rodrigues N, Sacramento CQ, et al. SARS-CoV-2 engages inflammasome and pyroptosis in human primary monocytes. *Cell Death Discovery* (2021) 7(1):43. doi: 10.1038/s41420-021-00428-w

5. Ajaz S, McPhail MJ, Singh KK, Mujib S, Trovato FM, Napoli S, et al. Mitochondrial metabolic manipulation by SARS-CoV-2 in peripheral blood mononuclear cells of patients with COVID-19. *Am J Physiol Cell Physiol* (2021) 320(1):C57–65. doi: 10.1152/ajpcell.00426.2020

6. Wen W, Su W, Tang H, Le W, Zhang X, Zheng Y, et al. Immune cell profiling of COVID-19 patients in the recovery stage by single-cell sequencing. *Cell discov* (2020) 6:31. doi: 10.1038/s41421-020-0168-9

7. Lucas C, Wong P, Klein J, Castro TBR, Silva J, Sundaram M, et al. Longitudinal analyses reveal immunological misfiring in severe COVID-19. *Nature* (2020) 584 (7821):463–9. doi: 10.1038/s41586-020-2588-y

8. Broz P, Dixit VM. Inflammasomes: Mechanism of assembly, regulation and signalling. *Nat Rev Immunol* (2016) 16(7):407–20. doi: 10.1038/nri.2016.58

9. West AP, Shadel GS. Mitochondrial DNA in innate immune responses and inflammatory pathology. *Nat Rev Immunol* (2017) 17(6):363–75. doi: 10.1038/nri.2017.21

10. Zhong Z, Liang S, Sanchez-Lopez E, He F, Shalapour S, Lin XJ, et al. New mitochondrial DNA synthesis enables NLRP3 inflammasome activation. *Nature* (2018) 560(7717):198–203. doi: 10.1038/s41586-018-0372-z

11. Chen IY, Moriyama M, Chang MF, Ichinohe T. Severe acute respiratory syndrome coronavirus viroporin 3a activates the NLRP3 inflammasome. *Front Microbiol* (2019) 10:50. doi: 10.3389/fmicb.2019.00050

12. Nieto-Torres JL, Verdiá-Báguena C, Jimenez-Guardeño JM, Regla-Nava JA, Castaño-Rodriguez C, Fernandez-Delgado R, et al. Severe acute respiratory syndrome coronavirus e protein transports calcium ions and activates the NLRP3 inflammasome. *Virology* (2015) 485:330–9. doi: 10.1016/j.virol.2015.08.010

13. Siu KL, Yuen KS, Castano-Rodriguez C, Ye ZW, Yeung ML, Fung SY, et al. Severe acute respiratory syndrome coronavirus ORF3a protein activates the NLRP3 inflammasome by promoting TRAF3-dependent ubiquitination of ASC. *FASEB J* (2019) 33(8):8865–77. doi: 10.1096/fj.201802418R

14. Xia B, Shen X, He Y, Pan X, Liu FL, Wang Y, et al. SARS-CoV-2 envelope protein causes acute respiratory distress syndrome (ARDS)-like pathological damages and constitutes an antiviral target. *Cell Res* (2021) 31(8):847–60. doi: 10.1038/s41422-021-00519-4

15. Yue Y, Nabar NR, Shi CS, Kamenyeva O, Xiao X, Hwang IY, et al. SARS-coronavirus open reading frame-3a drives multimodal necrotic cell death. *Cell Death Dis* (2018) 9(9):904. doi: 10.1038/s41419-018-0917-y

16. Hover S, Foster B, Barr JN, Mankouri J. Viral dependence on cellular ion channels - an emerging anti-viral target? *J Gen Virol* (2017) 98(3):345–51. doi: 10.1099/jgv.0.000712

17. Nieva JL, Madan V, Carrasco L. Viroporins: Structure and biological functions. *Nat Rev Microbiol* (2012) 10(8):563–74. doi: 10.1038/nrmicro2820

18. Gordon DE, Hiatt J, Bouhaddou M, Rezelj VV, Ulferts S, Braberg H, et al. Comparative host-coronavirus protein interaction networks reveal pan-viral disease mechanisms. *Science* (2020) 370(6521):eabe9403. doi: 10.1126/science.abe9403

19. Kern DM, Sorum B, Mali SS, Hoel CM, Sridharan S, Remis JP, et al. Cryo-EM structure of SARS-CoV-2 ORF3a in lipid nanodiscs. *Nat Struct Mol Biol* (2021) 28 (7):573–82. doi: 10.1038/s41594-021-00619-0

20. Verdiá-Báguena C, Aguilella VM, Queralt-Martín M, Alcaraz A. Transport mechanisms of SARS-CoV-E viroporin in calcium solutions: Lipid-dependent anomalous mole fraction effect and regulation of pore conductance. *Biochim Biophys Acta Biomembranes.* (2021) 1863(6):183590. doi: 10.1016/j.bbamem.2021.183590

21. Denton RM. Regulation of mitochondrial dehydrogenases by calcium ions. *Biochim Biophys Acta* (2009) 1787(11):1309–16. doi: 10.1016/j.bbabio.2009.01.005

22. Xian H, Liu Y, Rundberg Nilsson A, Gatchalian R, Crother TR, Tourtellotte WG, et al. Metformin inhibition of mitochondrial ATP and DNA synthesis abrogates NLRP3 inflammasome activation and pulmonary inflammation. *Immunity* (2021) 54(7):1463–77.e11. doi: 10.1016/j.immuni.2021.05.004

23. Mueller EE, Mayr JA, Zimmermann FA, Feichtinger RG, Stanger O, Sperl W, et al. Reduction of nuclear encoded enzymes of mitochondrial energy metabolism in cells devoid of mitochondrial DNA. *Biochem Biophys Res Commun* (2012) 417(3):1052–7. doi: 10.1016/j.bbrc.2011.12.093

24. Potluri P, Procaccio V, Scheffler IE, Wallace DC. High throughput gene complementation screening permits identification of a mammalian mitochondrial protein synthesis (ρ-) mutant. *Biochim Biophys Acta* (2016) 1857(8):1336–43. doi: 10.1016/j.bbabio.2016.02.021

25. Shi H, Wang Y, Li X, Zhan X, Tang M, Fina M, et al. NLRP3 activation and mitosis are mutually exclusive events coordinated by NEK7, a new inflammasome component. *Nat Immunol* (2016) 17(3):250–8. doi: 10.1038/ni.3333

26. Schaefer PM, Hilpert D, Niederschweiberer M, Neuhauser L, Kalinina S, Calzia E, et al. Mitochondrial matrix pH as a decisive factor in neurometabolic imaging. *Neurophotonics* (2017) 4(4):045004. doi: 10.1117/1.NPh.4.4.045004

27. Szymczak-Workman AL, Vignali KM, Vignali DA. Verification of 2A peptide cleavage. *Cold Spring Harb Protoc* (2012) 2012(2):255–7. doi: 10.1101/pdb.prot067892

28. Csordás G, Weaver D, Hajnóczky G. Endoplasmic reticulum-mitochondrial contactology: Structure and signaling functions. *Trends Cell Biol* (2018) 28(7):523–40. doi: 10.1016/j.tcb.2018.02.009

29. Bagur R, Hajnóczky G. Intracellular Ca(2+) sensing: Its role in calcium homeostasis and signaling. *Mol Cell* (2017) 66(6):780–8. doi: 10.1016/j.molcel.2017.05.028

30. Di Marco G, Vallese F, Jourde B, Bergsdorf C, Sturlese M, De Mario A, et al. A high-throughput screening identifies MICU1 targeting compounds. *Cell Rep* (2020) 30 (7):2321–31.e6. doi: 10.1016/j.celrep.2020.01.081

31. Márta K, Hasan P, Rodríguez-Prados M, Paillard M, Hajnóczky G. Pharmacological inhibition of the mitochondrial Ca(2+) uniporter: Relevance for pathophysiology and human therapy. *J Mol Cell Cardiol* (2021) 151:135–44. doi: 10.1016/j.yjmcc.2020.09.014

32. Schriner SE, Linford NJ, Martin GM, Treuting P, Ogburn CE, Emond M, et al. Extension of murine life span by overexpression of catalase targeted to mitochondria. *Science* (2005) 308(5730):1909–11. doi: 10.1126/science.1106653

33. Melov S, Schneider JA, Day BJ, Hinerfeld D, Coskun P, Mirra SS, et al. A novel neurological phenotype in mice lacking mitochondrial manganese superoxide dismutase. *Nat Genet* (1998) 18(2):159–63. doi: 10.1038/ng0298-159

34. Nieto-Torres JL, DeDiego ML, Verdiá-Báguena C, Jimenez-Guardeño JM, Regla-Nava JA, Fernandez-Delgado R, et al. Severe acute respiratory syndrome coronavirus envelope protein ion channel activity promotes virus fitness and pathogenesis. *PloS pathogens.* (2014) 10(5):e1004077. doi: 10.1371/journal.ppat.1004077

35. Zhang X, Liu Y, Liu J, Bailey AL, Plante KS, Plante JA, et al. A trans-complementation system for SARS-CoV-2 recapitulates authentic viral replication without virulence. *Cell* (2021) 84(8):2229–38.e13. doi: 10.1016/j.cell.2021.02.044

36. Pan P, Shen M, Yu Z, Ge W, Chen K, Tian M, et al. SARS-CoV-2 n protein promotes NLRP3 inflammasome activation to induce hyperinflammation. *Nat Commun* (2021) 12(1):4664. doi: 10.1038/s41467-021-25015-6

37. Dittmar M, Lee JS, Whig K, Segrist E, Li M, Kamalia B, et al. Drug repurposing screens reveal cell-type-specific entry pathways and FDA-approved drugs active against SARS-Cov-2. *Cell Rep* (2021) 35(1):108959. doi: 10.1016/j.celrep.2021.108959

38. Tóth E, Maléth J, Závogyán N, Fanczal J, Grassalkovich A, Erdős R, et al. Novel mitochondrial transition pore inhibitor n-methyl-4-isoleucine cyclosporin is a new therapeutic option in acute pancreatitis. *J Physiol* (2019) 597(24):5879–98. doi: 10.1113/JP278517

39. Zhang M, He Q, Chen G, Li PA. Suppression of NLRP3 inflammasome, pyroptosis, and cell death by NIM811 in rotenone-exposed cells as an *in vitro* model of parkinson's disease. *Neuro-degenerative Dis* (2020) 20(2-3):73–83. doi: 10.1159/000511207

40. Coll RC, Hill JR, Day CJ, Zamoshnikova A, Boucher D, Massey NL, et al. MCC950 directly targets the NLRP3 ATP-hydrolysis motif for inflammasome inhibition. *Nat Chem Biol* (2019) 15(6):556–9. doi: 10.1038/s41589-019-0277-7

41. Albornoz EA, Amarilla AA, Modhiran N, Parker S, Li XX, Wijesundara DK, et al. SARS-CoV-2 drives NLRP3 inflammasome activation in human microglia through spike protein. *Mol Psychiatry* (2022). doi: 10.1101/2022.01.11.475947

42. Su CM, Wang L, Yoo D. Activation of NF-κB and induction of proinflammatory cytokine expressions mediated by ORF7a protein of SARS-CoV-2. *Sci Rep* (2021) 11 (1):13464. doi: 10.1038/s41598-021-92941-2

43. Shi CS, Nabar NR, Huang NN, Kehrl JH. SARS-coronavirus open reading frame-8b triggers intracellular stress pathways and activates NLRP3 inflammasomes. *Cell Death Discovery* (2019) 5:101. doi: 10.1038/s41420-019-0181-7

44. Zhang R, Wang K, Ping X, Yu W, Qian Z, Xiong S, et al. The ns12.9 accessory protein of human coronavirus OC43 is a viroporin involved in virion morphogenesis and pathogenesis. *J Virol* (2015) 89(22):11383–95. doi: 10.1128/JVI.01986-15

45. Zhang R, Wang K, Lv W, Yu W, Xie S, Xu K, et al. The ORF4a protein of human coronavirus 229E functions as a viroporin that regulates viral production. *Biochim Biophys Acta* (2014) 1838(4):1088–95. doi: 10.1016/j.bbamem.2013.07.025

46. Surya W, Li Y, Verdià-Bàguena C, Aguilella VM, Torres J. MERS coronavirus envelope protein has a single transmembrane domain that forms pentameric ion channels. *Virus Res* (2015) 201:61–6. doi: 10.1016/j.virusres.2015.02.023

47. Abdul-Rasool S, Fielding BC. Understanding human coronavirus HCoV-NL63. *Open Virol J* (2010) 4:76–84. doi: 10.2174/1874357901004010076

48. Mandala VS, McKay MJ, Shcherbakov AA, Dregni AJ, Kolocouris A, Hong M. Structure and drug binding of the SARS-CoV-2 envelope protein transmembrane domain in lipid bilayers. *Nat Struct Mol Biol* (2020) 27(12):1202–8. doi: 10.1038/s41594-020-00536-8

49. Geiler J, Michaelis M, Naczk P, Leutz A, Langer K, Doerr HW, et al. N-acetyl-L-cysteine (NAC) inhibits virus replication and expression of pro-inflammatory molecules in A549 cells infected with highly pathogenic H5N1 influenza a virus. *Biochem Pharmacol* (2010) 79(3):413–20. doi: 10.1016/j.bcp.2009.08.025

50. Cai J, Chen Y, Seth S, Furukawa S, Compans RW, Jones DP. Inhibition of influenza infection by glutathione. *Free Radical Biol Med* (2003) 34(7):928–36. doi: 10.1016/S0891-5849(03)00023-6

51. Shi X, Shi Z, Huang H, Zhu H, Zhou P, Zhu H, et al. Ability of recombinant human catalase to suppress inflammation of the murine lung induced by influenza a. *Inflammation* (2014) 37(3):809–17. doi: 10.1007/s10753-013-9800-2

52. Melov S, Doctrow SR, Schneider JA, Haberson J, Patel M, Coskun PE, et al. Lifespan extension and rescue of spongiform encephalopathy in superoxide dismutase 2 nullizygous mice treated with superoxide dismutase-catalase mimetics. *J Neurosci* (2001) 21(21):8348–53. doi: 10.1523/JNEUROSCI.21-21-08348.2001

frontiers | Frontiers in Immunology

TYPE Original Research
PUBLISHED 08 March 2023
DOI 10.3389/fimmu.2023.1078922

Check for updates

OPEN ACCESS

EDITED BY
Edwin Bölke,
Heinrich Heine University of Düsseldorf, Germany

REVIEWED BY
Antonio C. R. Vallinoto,
Federal University of Pará, Brazil
Devendra Kumar,
University of Nebraska Medical Center, United States

*CORRESPONDENCE
Tatjana Souza Lima Keesen
tat.keesen@cbiotec.ufpb.br

SPECIALTY SECTION
This article was submitted to Viral Immunology, a section of the journal Frontiers in Immunology

RECEIVED 24 October 2022
ACCEPTED 22 February 2023
PUBLISHED 08 March 2023

CITATION
de Sousa Palmeira PH, Peixoto RF, Csordas BG, de Medeiros IA, de Azevedo FdLAA, Veras RC, Janebro DI, Amaral IPG and Keesen TSL (2023) Differential regulatory T cell signature after recovery from mild COVID-19. *Front. Immunol.* 14:1078922. doi: 10.3389/fimmu.2023.1078922

COPYRIGHT
© 2023 de Sousa Palmeira, Peixoto, Csordas, de Medeiros, de Azevedo, Veras, Janebro, Amaral and Keesen. This is an open-access article distributed under the terms of the Creative Commons Attribution License (CC BY). The use, distribution or reproduction in other forums is permitted, provided the original author(s) and the copyright owner(s) are credited and that the original publication in this journal is cited, in accordance with accepted academic practice. No use, distribution or reproduction is permitted which does not comply with these terms.

Differential regulatory T cell signature after recovery from mild COVID-19

Pedro Henrique de Sousa Palmeira[1], Rephany Fonseca Peixoto[1], Bárbara Guimarães Csordas[2], Isac Almeida de Medeiros[3], Fátima de Lourdes Assunção Araújo de Azevedo[3], Robson Cavalcante Veras[3], Daniele Idalino Janebro[3], Ian P.G. Amaral[4] and Tatjana Souza Lima Keesen[5]*

[1]Postgraduate program in Physiology Science, Immunology Laboratory of Infectious Diseases, Department of Cellular and Molecular Biology, Federal University of Paraiba, João Pessoa, Paraíba, Brazil, [2]Postgraduate program in Natural and Synthetic Bioactive Products, Immunology Laboratory of Infectious Diseases, Federal University of Paraiba, João Pessoa, Paraíba, Brazil, [3]Research Institute for Drugs and Medicines, Federal University of Paraiba, João Pessoa, Paraíba, Brazil, [4]Biotechnology Graduation Program, Immunology Laboratory of Infectious Diseases, Federal University of Paraiba, João Pessoa, Paraíba, Brazil, [5]Immunology Laboratory of Infectious Diseases, Department of Cellular and Molecular Biology, Federal University of Paraiba, João Pessoa, Paraíba, Brazil

Severe acute respiratory syndrome coronavirus 2 (SARS-CoV-2) is characterized by a range of symptoms in which host immune response have been associated with disease progression. However, the putative role of regulatory T cells (Tregs) in determining COVID-19 outcomes has not been thoroughly investigated. Here, we compared peripheral Tregs between volunteers not previously infected with SARS-CoV-2 (healthy control [HC]) and volunteers who recovered from mild (Mild Recovered) and severe (Severe Recovered) COVID-19. Peripheral blood mononuclear cells (PBMC) were stimulated with SARS-CoV-2 synthetic peptides (Pool Spike CoV-2 and Pool CoV-2) or staphylococcal enterotoxin B (SEB). Results of a multicolor flow cytometric assay showed higher Treg frequency and expression of IL-10, IL-17, perforin, granzyme B, PD-1, and CD39/CD73 co-expression in Treg among the PBMC from the Mild Recovered group than in the Severe Recovered or HC groups for certain SARS-CoV-2 related stimulus. Moreover, Mild Recovered unstimulated samples presented a higher Tregs frequency and expression of IL-10 and granzyme B than did that of HC. Compared with Pool CoV-2 stimuli, Pool Spike CoV-2 reduced IL-10 expression and improved PD-1 expression in Tregs from volunteers in the Mild Recovered group. Interestingly, Pool Spike CoV-2 elicited a decrease in Treg IL-17$^+$ frequency in the Severe Recovered group. In HC, the expression of latency-associated peptide (LAP) and cytotoxic granule co-expression by Tregs was higher in Pool CoV-2 stimulated samples. While Pool Spike CoV-2 stimulation reduced the frequency of IL-10$^+$ and CTLA-4$^+$ Tregs in PBMC from volunteers in the Mild Recovered group who had not experienced certain symptoms, higher levels of perforin and perforin$^+$granzyme B$^+$ co-expression by Tregs were found in the Mild Recovered group in volunteers who had experienced dyspnea. Finally, we found differential expression of CD39 and CD73 among volunteers in the Mild Recovered group between those who had and had not experienced musculoskeletal pain. Collectively, our study suggests that changes in

the immunosuppressive repertoire of Tregs can influence the development of a distinct COVID-19 clinical profile, revealing that a possible modulation of Tregs exists among volunteers of the Mild Recovered group between those who did and did not develop certain symptoms, leading to mild disease.

KEYWORDS

regulatory T cells, mild symptoms, immunomodulation, SARS-CoV-2, immune response, recovered COVID-19

1 Introduction

In December 2019, pneumonia of unknown etiology was observed in Wuhan, China, and was later associated with a new betacoronavirus (1). Named Coronavirus of Severe Acute Respiratory Syndrome 2 (SARS-CoV-2), this new pathogen is the causative agent of Coronavirus Disease 2019 (COVID-19) and is responsible for the current pandemic announced by the World Health Organization (WHO) on 11 March 2020 (1–3). Although the disease may present with a broad spectrum of manifestations, including asymptomatic cases and severe symptoms that may result in death, most affected individuals develop a non-severe condition (3, 4).

The public health emergency caused by the SARS-CoV-2 infection has prompted the scientific community to evaluate immune response, revealing the significant contribution of the immune system to disease progression (5). In this context, factors such as viral load and the efficacy of innate immunity, especially those mediated by type I interferons, seem to be pivotal to adaptive responsiveness and clinical outcomes (6). For example, the time of action of $CD4^+$ T lymphocytes has been associated with different clinical conditions (7). Additionally, lymphopenia and defects in Th1 immune profile have been associated with increased severity in COVID-19 cases (8).

Regulatory T cells (Tregs), a $CD4^+$ T lymphocyte subpopulation with regulatory functions, develop a pivotal role in self-tolerance and immune homeostasis in some diseases (9, 10). In the context of COVID-19, alterations in IL-10^+ and $CD39^+$ Treg subpopulations or an imbalance between Tregs/Th17 can be associated with disease severity (10–13). However, divergent results regarding the frequency of these lymphocytes raise questions regarding the role of Tregs in disease progression (10, 14–16).

Thus, to better understand the role of Tregs in the context of SARS-CoV-2 infection, we evaluated Tregs ($CD3^+CD4^+CD25^+FOXP3^+$) based on their frequency and expression of cytokines, cytotoxic granules, inhibitory receptors, and ectonucleotidases in the peripheral blood mononuclear cells (PBMC) from volunteers recovered from mild and severe forms of COVID-19. Among the volunteers who recovered from mild disease, we compared the immune parameters between those who did and did not experience certain symptoms. We observed a differential Treg immune profile after disease resolution particularly in the group of volunteers who recovered from mild SARS-CoV-2 infection. This study points to a pivotal change in the Treg profile that could help the scientific community understand the role of this subpopulation of lymphocytes in the course of different clinical forms of COVID-19.

2 Materials and methods

2.1 Ethics statement

This study was approved by the National Commission of Ethics in Research (certificate CAAE: 31354720.0.0000.5188). All experiments were performed in compliance with the relevant regulations, institutional guidelines, and ethical standards of the Declaration of Helsinki. Informed consent was obtained from all the enrolled volunteers.

2.2 Patient recruitment

This study was conducted from May 2020 to May 2021 in Brazil. The study began around the time when the SARS-CoV-2 virus of the original lineage was still circulating and continued with the alpha and gamma variants being first detected in the end of 2020 (between October and December). These studies ended in May 2021, a few days after the delta variant was identified for the first time in Brazil (April 26, 2021) (17, 18). Sixteen nonvaccinated volunteers who presented COVID-19 symptoms between May 2020 and May 2021 and had subsequently recovered were recruited. The SARS-CoV-2 diagnosis was based on RT qPCR for COVID-19 during the acute phase and IgG serological tests (Euroimmun Anti-SARS-CoV-2 assay, Perkin Elmer Company) after recovery. The recovered COVID-19 volunteers were assigned to either the Mild Recovered (did not need hospitalization, n = 9) or Severe Recovered (presented pulmonary symptoms requiring hospitalization, n = 7) group. For epidemiologic purposes, severe dyspnea, a respiratory rate of 30 or more breaths per minute, a blood oxygen saturation of 93% or less, and infiltrates in more than 50% of the lung were considered severe symptoms of COVID-19 (19). In addition, a healthy control group (HC, n = 8) was included. Volunteers in the HC group were not previously vaccinated against COVID-19, were reportedly asymptomatic for the last 10 weeks, were negative by

certified SARS-CoV-2 antibody test (Euroimmun Anti-SARS-CoV-2 assay Perkin Elmer Company), and had a negative RT qPCR test for SARS-CoV-2. Whole blood for flow cytometry analysis was collected in sodium heparin-coated vacutainers and gently agitated until processing. The blood samples were processed on the day of collection.

2.3 RT qPCR assay

Quantitative real-time PCR (RT qPCR) was performed as described previously (20) at the time of sample collection for flow cytometry experiments. This procedure was essential to ensure that no SARS-CoV-2 infection or reinfection occurred in the HC and recovered volunteers. The RNA isolated from nasopharyngeal or oropharyngeal swabs was extracted (QIAprep&amp Viral RNA UM Kit, QIAGEN, USA) and amplified by one-step RT qPCR (SARS-CoV-2 N1+N2 Assay Kits, QIAGEN, USA).

2.4 Design and preparation of SARS-CoV-2 epitope pools

For peptide design, we identify the most frequent HLA-class I/II alleles among the Brazilian population and most frequently in the world in the IEDB tools. We then performed MHC-I and II binding affinity and antigenicity predictions and analyzed the peptide molecular dynamics of the best-fitted MHC-I and II/protein of SARS-CoV-2 complexes. SARS-CoV-2 virus-specific CD4 and CD8 peptides (Table 1) (patent number: BR 10 2022 005518 1) were synthesized (GenOne Biotechnologies, Rio de Janeiro, Brazil), lyophilized, and stored at -20°C for subsequent analysis. Subsequently, the peptides were resuspended in H_2O (MiliQ) and pooled into groups (Pool CoV-2 contained peptides from the spike protein and non-spike proteins, whereas Pool Spike CoV-2 contained peptides from the spike protein only, Table 1).

SARS-CoV-2 epitopes were predicted using protein sequences derived from the Brazilian SARS-CoV-2 sequences deposited in GenBank and IEDB analysis resources. CD4 SARS-CoV-2 epitope prediction was performed as previously reported, using the NetMHCIIpan 4.0 algorithm and CD4 immunogenicity prediction (IEDB), HLA-DRB*1:03:01, HLA-DRB*1:07:01, HLA-DRB*1:15:01, HLA-DRB*3:01:01, HLA-DRB*3:02:02, HLA-DR*4:01:01, and HLA-DRB*5:01:01. Due to extremely high heterogenicity of the Brazilian population, we carefully included the frequently identified HLA I and II in the Brazilian population along with the most frequently identified HLA populations in the world. CD8 SARS-CoV-2 epitope prediction was performed as previously reported using the NetMHCpan4.0 algorithm (HLA-A* 01: 01; HLA-A* 02: 01; HLA-A* 11: 01; HLA-A* 24: 02; HLA-A* 68: 01; HLA-A* 23: 01; HLA-A* 26: 01; HLA-A* 30: 02; HLA-A* 31: 01; HLA-B* 07: 02; HLA-B* 51: 01; HLA-B* 35: 01; HLA-B* 44: 02; HLA-B* 35: 03; HLA-C* 05: 01; HLA- C* 07: 01 e HLA-C* 15: 02). Despite inferring cellular populations of T lymphocytes, this strategy extrapolates to lymphocyte-like cells, such as natural killer (NK) cells, because a specific prediction program for NK cell populations is not yet available.

2.5 Isolation of plasma

Plasma samples were collected after centrifugation of whole blood at 400 × *g* for 10 min at room temperature (25°C). The undiluted plasma was then transferred to cryotubes, aliquoted, and stored at -80°C for subsequent analysis.

2.6 Isolation of PBMC

PBMC from volunteers inserted in the HC and volunteers who had recovered from mild and severe COVID-19 (Mild Recovered and Severe Recovered groups, respectively) were obtained from

TABLE 1 List of peptides chosen in this study through prediction studies and Spike peptide pool.

		Name	Peptide	a.a.* position	Source
Pool CoV-2		ORF1a	ILASFSASTSAFVET	476-490	This study
		ORF1a	FLHFLPRVFSAVGNICYTP	2880-2890	This study
		ORF1b	FVDGVPFVVSTGYHFR	4726-4741	This study
	Pool Spike CoV-2	SPIKE_NTD	NIDGYFKIYSKHTPINLV	196-210	(21)
		SPIKE_RBD	ATRFASVYAWNRKRI	344-358	(21)
		SPIKE_S2	ALQIPFAMQMAYRFN	893-907	(21)
		ORF3	KKRWQLALSKGVHFV	66-80	This study
		E	FYVYSRVKNLNSSRV	56-70	This study
		M	LYLYALVYFLQSINFVRIIM	114-123	This study
		M	KEITVATSRTLSYYK	166-180	This study
		ORF8	FYSKWYIRVGARKSA	41-55	This study

*a.a, amino acid.

heparinized venous blood using density gradient centrifugation (Ficoll-Paque ™ Plus, GE Healthcare, Life Sciences, Pittsburgh, PA, USA). PBMC were centrifuged for 40 min at 400 × *g* and washed three times with phosphate-buffered saline (PBS) before counting. PBMC were maintained in RPMI-1640 (Sigma-Aldrich) supplemented with antibiotics (penicillin, 200 U/mL; streptomycin, 0.1 mg/mL), 1 mM L-glutamine (1 mM), and 10% heat-inactivated AB Rh+ human serum (Sigma-Aldrich), hereafter referred to as medium. Cultures were set up at a concentration of 2.5 X 10^5 cells in 96-well plates in the presence or absence of SARS-CoV-2 antigens and Staphylococcal enterotoxin B from *Staphylococcus aureus* (SEB, Sigma-Aldrich). PBMC were subjected to four different conditions: unstimulated (medium), stimulated with SARS-CoV-2 antigens (Pool Spike Cov-2 and Pool Cov-2, each at 1 µg/well), and stimulated with SEB (1 ug/well). The cells were incubated under 5% CO_2 in an incubator at 37°C for 16 h. Next, brefeldin-A (1 mg/mL, Sigma-Aldrich) was added and the samples were incubated under 5% CO_2 in an incubator at 37°C for 4 h.

2.7 Flow cytometry assay

Briefly, freshly isolated PBMC were plated at a concentration of 2.5 x 10^5 cells per well in a 96-well U-bottom plate. Cocktails of Antibodies for extracellular staining were added and incubated for 30 min at 4°C. For extracellular staining, the following antibodies from BD Biosciences were used: extracellular PE-Cy5 conjugated anti-CD3 (clone UCHT1, isotype. Mouse BALB/c IgG1, κ, cat. 555334, specie. mouse), APC-Cy7 conjugated anti-CD4 (clone RPA-T4, isotype. Mouse IgG1, κ, cat. 557871, specie. mouse), PE-Cy7 conjugated anti-CD25 (clone M-A251, isotype. Mouse BALB/c IgG1, κ, cat. 557741, specie. mouse), PE-conjugated anti-CD39 (clone TU66, Isotype: Mouse IgG2b, κ, cat. 555464, specie. mouse), APC-conjugated anti-CD73 (clone AD2, isotype: Mouse IgG1, κ, cat. 560847, specie. mouse), PE-conjugated anti-PD1 (clone MIH4, isotype. Mouse IgG1, κ, cat. 557946, specie. mouse), PE-conjugated anti-LAP (clone TW4-2F8, isotype. Mouse BALB/c IgG1, κ, cat. 562260, specie. mouse), IgG isotypes control antibodies such as IgG3-FITC (clone J606, isotype. Mouse BALB/c IgG3, κ, cat. 555578, specie. mouse), IgG3-Alexa Fluor 647 (clone J606, isotype. Mouse BALB/c IgG3, κ, cat. 560803, specie. mouse), IgG1-APC-H7 (clone MOPC-21, isotype. Mouse IgG1, κ, cat. 560167, specie. mouse), IgG1-PE-Cy-5 (clone MOPC-21, isotype. Mouse IgG1, κ, cat. 555750, specie. mouse), and IgG1-PE-Cy-7 (clone MOPC-21, isotype. Mouse IgG1, κ, cat. 557872, specie. mouse). After incubation with antibodies for 30 min at 4°C, the cells were washed with 150 µL of PBS. The plate was centrifuged (8 min, 244 × *g*, 4°C), the supernatant was removed, and 100 µL of 4% formaldehyde and 100 µL of PBS were added to the wells. The plate was incubated at room temperature (25°C) for 20 min to fix the extracellular staining. After centrifugation (8 min, 244 × *g*, 4°C), the supernatant was discarded and the samples were washed with 150 µL of PBS. The plate was centrifuged yet again (8 min, 244 × *g*, 4°C) and the supernatant was discarded. For intracellular staining, the cells were permeabilized with 150 µL of permeabilization buffer (0.5% bovine serum albumin (BSA), w/v and 0.5% saponin, w/v in PBS) for 10 min at room temperature (25°C). After centrifugation (8 min, 244 × *g*, 4°C), the supernatant was removed, and intracellular staining was performed. The following conjugated antibodies from BD Biosciences were used to detect intracellular molecules: Alexa Fluor 647 conjugated anti-perforin (clone δG9, isotype. Mouse BALB/c IgG2b, κ, cat. 563576, specie. mouse), PE-conjugated anti-granzyme B (clone GB11, isotype. Mouse BALB/c IgG1, κ, cat. 561142, specie. mouse), PE-conjugated anti-CTLA-4 (clone BNI3, isotype. Mouse BALB/c IgG2a, κ, cat. 555853, specie. mouse), APC-conjugated anti-IL10 (clone JES3-19F1, isotype. Rat IgG2a, κ, cat. 554707, specie. rat), PE-conjugated anti-IL-17 (clone SCPL1362, isotype. Mouse IgG1, κ, cat. 560436, specie. mouse), Alexa Fluor 488 conjugated anti-FOXP3 (clone 236A/E7, isotype. Mouse BALB/c IgG1, κ, cat. 561181, specie. mouse), and IgG isotype control antibodies IgG1-PE (clone MOPC-21, isotype. Mouse IgG1, κ, cat. 559320, specie. mouse). All antibodies were used according to the manufacturer's instructions. The plate was then incubated for 45 min at room temperature (25°C), and 150 µL of permeabilization buffer was added. After centrifugation, the supernatant was removed (8 min, 244 × *g*, 4°C). Finally, 200 µL of wash B (PBS/BSA) was added, and the samples were transferred to fluorescence-activated cell sorting (FACS) tubes and maintained at 4°C. At least 70,000 gated events were acquired using FACS CANTO II (BD Biosciences) and analyzed using the FlowJo v.10.8 software (BD, Ashland - USA).

2.8 Flow cytometry data analysis

All parameters evaluated in Tregs were analyzed using FlowJo software v.10.8 (BD, Ashland, USA). Limits for quadrant markers were set based on negative populations (cells), isotype controls, and fluorescence minus one (FMO), when appropriate. Five or six different fluorochromes were identified in each analysis. Four fluorochromes, anti-CD3 PE-Cy5, anti-CD4 APC-Cy7, anti-CD25 PE-Cy7, and anti-FOXP3 Alexa Fluor 488, were used to identify Tregs ($CD3^+CD4^+CD25^+FOXP3^+$). We first selected the total lymphocyte gate through size-FSC-A and granularity-SSC-A profiles, followed by singlet separation using the FSC-A × FSC-H parameters. Next, we set the $CD3^+CD4^+$ cells and identified CD25 + T cells within this subpopulation. Subsequently, $CD3^+CD4^+CD25^+FOXP3^+$ T-cells were detected. Two fluorochromes, anti-X PE and anti-Y APC (or Alexa Fluor 647), were used to assess the intracellular or surface markers. The following markers were used: IL-10, IL-17, latency-associated peptide (LAP), perforin, granzyme B, CTLA-4, PD-1, CD39, and CD73. The analytical strategy is shown in Supplementary Figures 1–5.

2.9 Statistical analysis

The Shapiro–Wilk normality test was performed for all parameters evaluated using flow cytometry. If normally distributed, multiple comparisons were performed using two-way ANOVA and Tukey's *post-hoc* test or one-way ANOVA and

Tukey's *post-hoc* test. Kruskal-Wallis with Dunn's multiple comparisons test was performed if the data were not normally distributed. The immunological data between volunteers who had and had not developed certain symptoms in the Mild Recovered group was compared and analyzed based on the following clinical data: dyspnea, sore throat, nasal obstruction, myalgia, arthralgia, fatigue, diarrhea, anosmia, and ageusia. These comparisons were performed using one-way ANOVA and Tukey's *post hoc* test or Kruskal-Wallis with Dunn's multiple comparisons tests. Differences were considered statistically significant at $p < 0.05$. Statistical analyses were performed using GraphPad Prism 8.4.3. To create a heat map matrix regarding immunological marker expression in the HC, mild recovered, and severe recovered groups, we used Morpheus software and adjusted it to Z-score (22).

3 Results

3.1 Characteristics of HC, mild recovered, and severe recovered volunteers

For this study, we recruited 24 volunteers and distributed them into three groups. In the HC group, 8 volunteers (4 male and 4 female) with a mean age of 35.62 (± 8.63) were enrolled. The Mild Recovered group included 9 volunteers (5 male and 4 female) with a mean age of 33.22 (± 6.70). Finally, 7 volunteers were enrolled in the Severe Recovered group (4 male and 3 female) with a mean age of 36.85 (± 7.64) (Tables 2–4). No significant differences in age were found between the groups.

Most volunteers who experienced mild COVID-19 reported headache, runny nose, and fatigue (Table 3). All volunteers in the severe recovery group experienced pulmonary infiltration, low oxygen saturation, and headache, whereas almost all had high fever, tachypnea, and fatigue (Table 4). Regarding comorbidities, obesity was a significant chronic disease observed among 56% of the recovered COVID-19 cases.

Finally, volunteers were asked to self-identify themselves among the following ethnic–racial classifications: white, brown, black, yellow (Asian), and indigenous (Native American). Volunteers who self-classified themselves as brown and white comprised 58.33% and 33.33%, respectively, whereas those of black and indigenous self-classification comprised 4.1% each. Thus, the demographic of the HC group was white (62.5%), brown (25%), and indigenous (12.5%); that of Mild Recovered group was brown (88.88%) and white (11.11%), whereas that of Severe Recovered group was brown (57.14%), white (28.57%), and black (14.28%). The demographic and clinical details of the volunteers are shown in Tables 2–4.

3.2 Mild-recovered volunteers have elevated levels of Tregs

Analysis of PBMC from volunteers recovered from COVID-19 revealed a higher frequency of occurrence of Tregs in Mild Recovered group than in HC for non-stimulated samples (Figure 1A). In addition, pool CoV-2-stimulated samples from Mild Recovered and Severe Recovered groups presented more Tregs than did HC (Figure 1A). We also compared the frequency of occurrence of the studied lymphocyte subset among the Mild Recovered volunteers between those who had and had not experienced the following symptoms during acute COVID-19: dyspnea, myalgia, sore throat, arthralgia, fatigue, nasal obstruction, diarrhea, anosmia, and ageusia. Our data showed that those who did not experience nasal obstruction had more Tregs among the non-stimulated and Pool Spike CoV-2 stimulated PBMC than in those with this symptom (Figure 1B). A comparison of the frequency of occurrence of Treg among the Mild Recovered volunteers between those who had and had not experienced the other symptoms was also analyzed, but no significant results were found (Supplementary Figure 1).

3.3 Expression of IL-10 and IL-17 by Tregs is higher in volunteers who recovered from mild COVID-19

We also evaluated cytokine expression by Tregs in all the groups. Mild Recovered non-stimulated samples had higher levels

TABLE 2 Gender, age, and ethnic-racial self-classification of healthy control volunteers (HC).

#Code	Gender	Age	Ethnic-racial self-classification
CTL 1	Female	46	White
CLT 3	Male	47	White
CLT 4	Female	28	White
CLT 5	Male	35	White
CLT 6	Male	22	Brown
CLT 7	Female	36	Indigenous
CLT 8	Male	40	White
CLT 9	Female	31	Brown
MEAN	***4F:4M**	**35.62 (± 8.63)**	

*F, Female; M, Male. The bold value represents the mean and standard deviation (in brackets) of the Age regarding HC volunteers.

10.3389/fimmu.2023.1078922

TABLE 3 Gender, age, ethnic-racial self-classification, comorbidities, and symptoms of mild recovered volunteers (Mild Recovered).

#Code	Gender	Age	Blood collection after recovery of COVID-19 (days)	Ethnic-racial self-classification	Comorbidities	Symptoms
COV3	Male	21	194	Brown	Guillain-Barré	Headache, Runny nose, cough with phlegm, Nasal obstruction, Chills, and Fatigue
COV5	Female	33	204	Brown	Obesity	Fever, Headache, Dry cough, Myalgia, Chills, Fatigue, and Anosmia
COV6	Male	24	214	Brown		Fever, Headache, Runny nose, Sore throat, Dyspnea, Diarrhea, Fatigue, Anosmia, and Ageusia
COV7	Male	39	211	Brown		Fever and Dry cough
COV8	Male	32	195	Brown	Obesity	Runny nose, Sore throat, Nasal obstruction, Myalgia, Diarrhea, and Fatigue
COV9	Male	40	56	Brown		Headache, Runny nose, and Dyspnea
COV10	Female	36	16	White	Obesity	Arthralgia
COV11	Female	39	196	Brown		Fever, Headache, Runny nose, Sore throat, Dry cough, Dyspnea, Tachypnea, Arthralgia, Myalgia, Nausea, Vomiting, Diarrhea, Chills, Fatigue, Anosmia, and Ageusia
COV15	Female	35	50	Brown	Obesity	Headache, Runny nose, Sore throat, Dry cough, Cough with phlegm, Nasal obstruction, and Fatigue
MEAN	***4F:5M**	**33.22 (± 6.70)**	**148.44 (± 81.83)**			

*F, Female; M, Male. The bold value represents the mean and standard deviation (in brackets) of the Age and Blood collection after recovery of COVID-19 (days) regarding mild recovered volunteers.

TABLE 4 Gender, age, ethnic-racial self-classification, comorbidities, and symptoms of severe recovered volunteers (Severe Recovered).

#Code	Gender	Age	Blood collection after recovery of COVID-19 (days)	Ethnic-racial self-classification	Comorbidities	Symptoms
COV1	Female	27	73	Brown		Low blood oxygen saturation, Headache, Lung infiltrate, Sore throat, Dry cough, Dyspnea, Nasal obstruction, Tachypnea, Diarrhea, and Fatigue.
COV2	Male	43	182	Brown	Hypertension and Obesity	Fever, Low blood oxygen saturation, Headache, Arthralgia, Myalgia, Lung infiltrate, Nausea, Diarrhea, Fatigue, Tachypnea, Eye swelling, Anosmia, and Ageusia
COV4	Female	38	138	White	Hypertension and Obesity	Fever, Low blood oxygen saturation, Headache, Dry cough, Cough with phlegm, Dyspnea, Tachypnea, Myalgia, Vomiting, Lung infiltrate, Chills, and Fatigue
COV14	Male	25	301	Black	Obesity	Low blood oxygen saturation, Fever, Headache, Lung infiltrates, Runny nose, Sore throat, Dry cough, Dyspnea, Nausea, Fatigue, Eye swelling, and Anosmia
COV16	Male	43	40	Brown	Asthma and Obesity	Low blood oxygen saturation, Fever, Headache, Sore throat, Cough with blood, Lung infiltrates, dyspnea, and Tachypnea
COV17	Female	40	62	Brown		Fever, Headache, Sore throat, Low blood oxygen saturation, Arthralgia, Myalgia, Lung infiltrate, Chills, Fatigue, Anosmia, Ageusia, and Tachypnea
COV18	Male	42	61	White	Obesity (IMC 38.5)	Low blood oxygen saturation, Fever, Headache, Runny nose, Sore throat, Lung infiltrates, Dry cough, Dyspnea, Nasal obstruction, Tachypnea, Myalgia, Diarrhea, Chills, Fatigue, Anosmia, and Ageusia.
MEAN	***3F:4M**	**36.85 (± 7.64)**	**122.42 (± 93.40)**			

*F, Female; M, Male. The bold value represents the mean and standard deviation (in brackets) of the Age and Blood collection after recovery of COVID-19 (days) regarding severe recovered volunteers.

10.3389/fimmu.2023.1078922

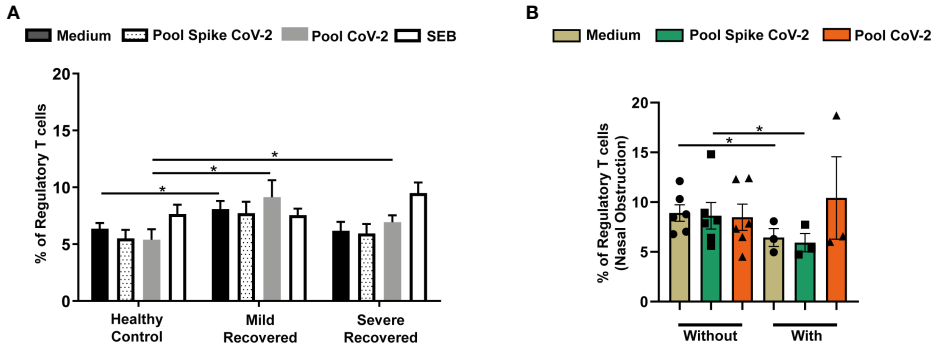

FIGURE 1
Frequency of regulatory T cells in peripheral blood from volunteers. Peripheral blood mononuclear cells (PBMC) were collected from volunteers not previously affected with SARS-CoV-2 infection (Healthy Control - HC, n = 8) and volunteers who had recovered from mild (Mild Recovered, n = 9) and severe (Severe Recovered, n = 7) COVID-19. The samples were incubated for 20 hours under four conditions: unstimulated (medium), stimulated with SARS-CoV-2 peptides (Pool Spike CoV-2 and Pool CoV-2 peptide), and stimulated with SEB. Unstimulated and SEB-stimulated PBMC were used as a negative and positive control, respectively. **(A)** Frequency of regulatory T cells in HC, Mild Recovered, and Severe Recovered. **(B)** Comparison of the frequency of regulatory T cells among Mild Recovered volunteers who had and had not experienced nasal obstruction during acute COVID-19. The symbols ●, ■, and ▲ represent each sample from Mild Recovered volunteer that was unstimulated (medium condition only) or stimulated with Pool Spike CoV-2 peptides or Pool CoV-2 peptides, respectively. Multiple comparisons were performed using two-way ANOVA and Tukey's *post hoc* test, one-way ANOVA and Tukey's *post hoc* test, and Kruskal-Wallis with Dunn's multiple comparisons test when appropriate. The bars represent the mean values, and the error bars show the standard error of the mean (SEM) for each group. The lines above the bars indicate statistically significant differences between the two groups. *p < 0.05. SEB, staphylococcal enterotoxin B.

of IL-10-producing Tregs than did the HC group (Figure 2A). Moreover, in Pool CoV-2-stimulated cells, the frequency of $CD3^+CD4^+CD25^+FOXP3^+IL\text{-}10^+$ was lower in the Severe Recovered group than in the Mild Recovered group (Figure 2A). In the Mild Recovered group, the IL-10 expression by Tregs due to Pool CoV-2 peptide stimulus was higher compared with that due to Pool Spike CoV-2 stimulus (Figure 2A).

We also detected an elevated $IL\text{-}17^+$ Treg frequency in PBMC from volunteers in the Mild Recovered group stimulated with SARS-CoV-2 related peptides compared with those from HC and Severe Recovered volunteers (Figure 2B). Severe Recovered group also presented higher IL-17 expression by Tregs than did the Pool CoV-2-stimulated PBMC in HC (Figure 2B). In addition, in HC samples incubated with SEB, $IL\text{-}17^+$ Treg expression was more pronounced than in PBMC incubated with SARS-CoV-2-related peptides (Figure 2B). In contrast, Pool Spike CoV-2 reduced IL-17 expression by Tregs in the Severe Recovered group (Figure 2B). Finally, the levels of LAP^+ Tregs did not differ between the HC, Mild Recovered, and Severe Recovered groups (Figure 2C). However, in the Pool CoV-2-stimulated PBMC, the frequency of Tregs expressing LAP was more accentuated than in Pool Spike CoV-2-stimulated samples (Figure 2C).

We also compared cytokine expression by Tregs among Mild Recovered volunteers between those who had and had not experienced certain symptoms of acute COVID-19. The Pool Spike CoV-2-stimulated samples of Mild Recovered volunteers who had not developed myalgia, fatigue, or nasal obstruction presented lower $IL\text{-}10^+$ Treg frequency than did the unstimulated cells (Figure 2D). Diminished levels of IL-10 expression were observed in Pool Spike CoV-2-stimulated-Tregs compared with that of Pool CoV-2-stimulated Tregs in volunteers who had not developed myalgia, diarrhea, or anosmia during acute disease (Figure 2D). Finally, in unstimulated samples, the expression of IL-10 by Tregs was higher and lower in volunteers with arthralgia and fatigue, respectively, than in those who had not developed these symptoms (Figure 2D).

Interestingly, compared to unstimulated samples, Pool CoV-2 elicited the expression of IL-17 by Tregs in the Mild Recovered volunteers who did not present with myalgia and diminished the frequency of $IL\text{-}17^+$ Treg in those who developed this symptom (Figure 2E). In the unstimulated samples, expression of IL-17 by Tregs from volunteers who did not have myalgia was lower than that by Tregs from those with this symptom (Figure 2E). Our data showed that IL-17 expression was less prevalent in volunteers with fatigue than in those without fatigue in samples stimulated with Pool CoV-2 (Figure 2E). For volunteers who experienced anosmia, the Pool Spike CoV-2 stimulus reduced the expression of IL-17 in Tregs compared with that of unstimulated samples (Figure 2E).

We also found elevated LAP^+ Treg levels in Pool CoV-2-stimulated samples from Mild Recovered volunteers with dyspnea, whereas the opposite was observed in nasal obstruction (Figure 2F). In addition, unstimulated PBMC from Mild Recovered volunteers who had not experienced sore throat expressed a higher frequency of LAP-expressing Tregs than did the PBMC from those who had this symptom (Figure 2F). A comparison of cytokine expression among Mild Recovered volunteers between those who had and had not experienced the other symptoms was also analyzed, but no significant results were found (Supplementary Figure 2).

3.4 Production of cytotoxic granules by Tregs was higher in mild recovered volunteers who experienced dyspnea

The present study also analyzed the production of cytotoxic granules by Tregs. Pool CoV-2-stimulated samples presented a

10.3389/fimmu.2023.1078922

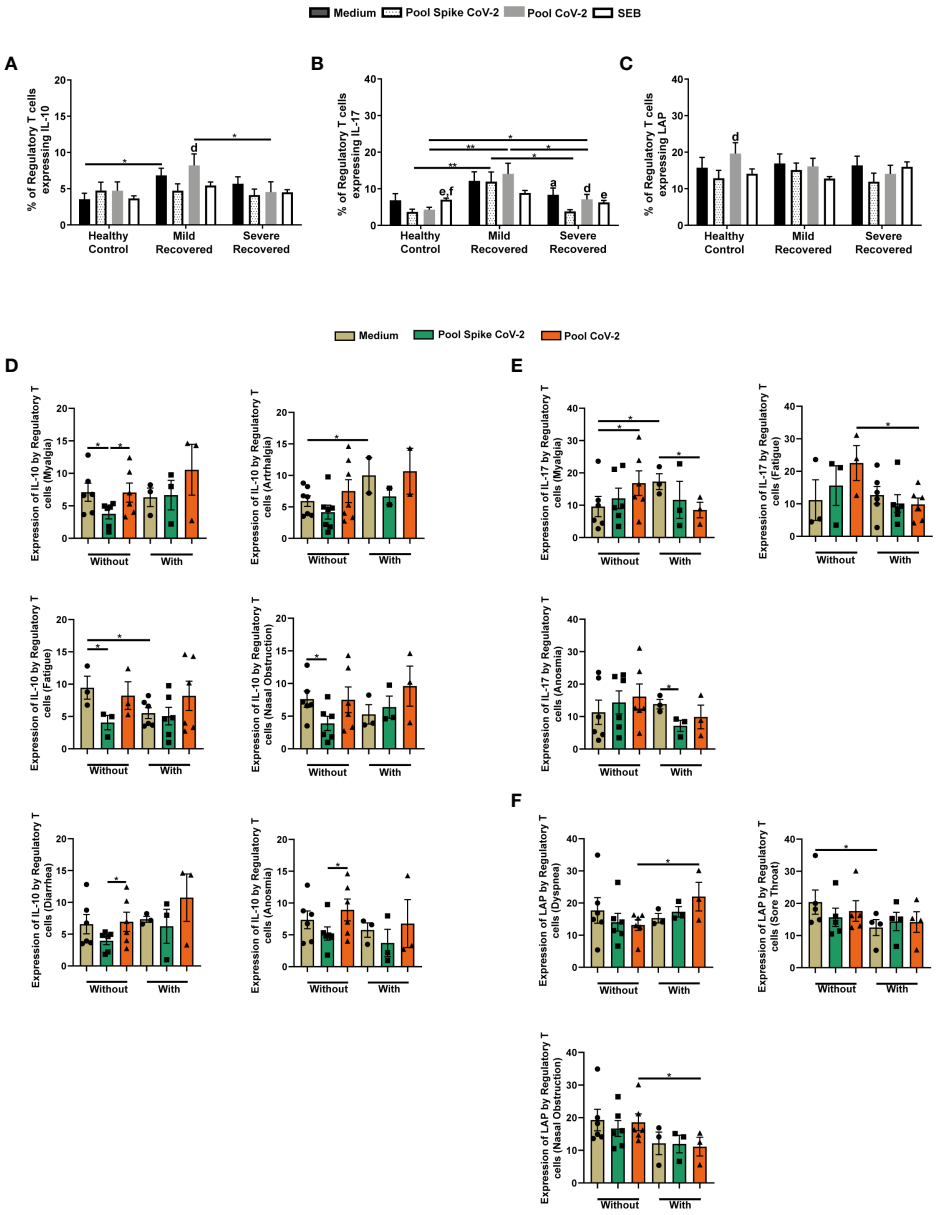

FIGURE 2
Regulatory T cells expressing IL-10, IL-17, and latency-associated peptide (LAP) in peripheral blood from volunteers. Peripheral blood mononuclear cells (PBMC) were collected from volunteers not previously affected by SARS-CoV-2 infection (Healthy Control – HC, n = 8) and volunteers who recovered from mild (Mild Recovered, n = 9) and severe (Severe Recovered, n = 7) COVID-19. The samples were incubated for 20 hours under four conditions: unstimulated (medium), stimulated with SARS-CoV-2 peptides (Pool Spike CoV-2 and Pool CoV-2 peptide), and stimulated with SEB. Unstimulated and SEB-stimulated PBMC were used as a negative and positive control, respectively. Frequency of regulatory T cells expressing IL-10 **(A)**, IL-17 **(B)**, and LAP **(C)** in HC, Mild Recovered, and Severe Recovered. Lowercase letters represent statistical differences ($p < 0.05$) between conditions within each group: (a) (medium × Pool Spike CoV-2), (d) (Pool Spike CoV-2 × Pool CoV-2), (e) (Pool Spike CoV-2 × SEB), and (f) (pool CoV-2 × SEB). **(D)** Comparison of the frequency of regulatory T cells expressing IL-10 among Mild Recovered volunteers who had and had not experienced the following symptoms: myalgia, arthralgia, fatigue, nasal obstruction, diarrhea, and anosmia during acute COVID-19. **(E)** Comparison of the frequency of regulatory T cells expressing IL-17 among Mild Recovered volunteers who had and had not experienced the following symptoms: myalgia, fatigue, and anosmia during acute COVID-19. **(F)** Comparison of the frequency of regulatory T cells expressing LAP among Mild Recovered volunteers who had and had not experienced the following symptoms: dyspnea, sore throat, and nasal obstruction during acute COVID-19. The symbols ●, ■, and ▲ represent each sample from Mild Recovered volunteer that was unstimulated (medium condition only) or stimulated with Pool Spike CoV-2 peptides or Pool CoV-2 peptides, respectively. Multiple comparisons were performed using two-way ANOVA and Tukey's *post hoc* test, one-way ANOVA and Tukey's *post hoc* test, and Kruskal-Wallis with Dunn's multiple comparisons test when appropriate. The bars represent the mean values, and the error bars show the standard error of the mean (SEM) for each group. The lines above the bars indicate statistically significant differences between the two groups. *$p < 0.05$; **$p < 0.01$. SEB, staphylococcal enterotoxin B.

10.3389/fimmu.2023.1078922

higher Perforin^{+} Treg frequency in the Mild Recovered group than in the other groups (Figure 3A). In contrast, in Pool Spike CoV-2 stimulus Tregs in the Mild Recovered group produced more perforin than that in the Severe Recovered group (Figure 3A). In addition, SEB-incubated PBMC from HC presented higher levels of Perforin^{+} Tregs than in cells from Severe Recovered group (Figure 3A). Finally, in the Mild Recovered group, the frequency of Tregs that produced perforin was lower in the SEB-stimulated cells than in the Pool CoV-2-stimulated samples (Figure 3A).

We also found elevated levels of granzyme B producing Treg in Mild Recovered group than in the HC in unstimulated or SARS-CoV-2-related peptide-stimulated samples (Figure 3B). When perforin and granzyme B co-expression was analyzed, we observed that SEB-stimulated PBMC from HC presented higher levels of Tregs co-expressing both granules than did the cells from the Severe Recovered group (Figure 3C). In the HC, Pool CoV-2 stimulus induced a higher frequency of perforin^{+}granzyme B^{+} Tregs compared to that in the unstimulated samples (Figure 3C). In contrast, in the Severe Recovered group, the SEB-incubated samples presented lower perforin and granzyme B co-expression by Tregs than in the other conditions (Figure 3C).

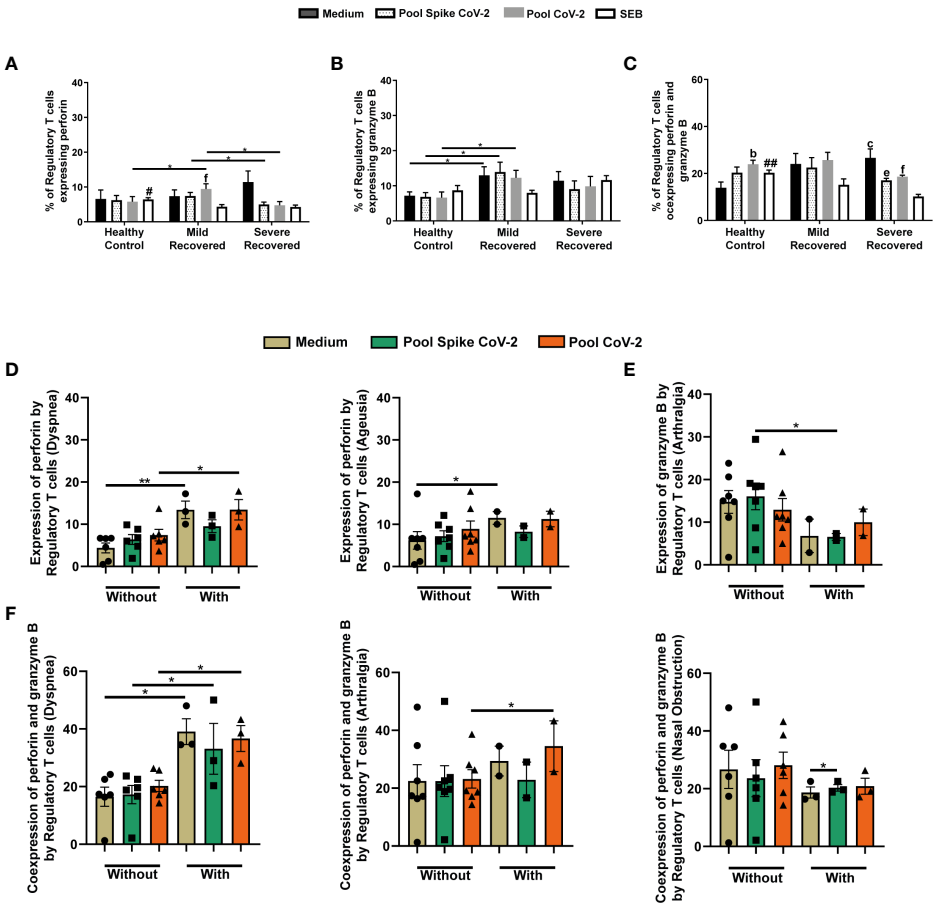

FIGURE 3
Regulatory T cells expressing perforin and granzyme B in peripheral blood from volunteers. Peripheral blood mononuclear cells (PBMC) were collected from volunteers not previously affected by SARS-CoV-2 infection (Healthy Control - HC, n = 8) and volunteers who recovered from mild (Mild Recovered, n = 9) and severe (Severe Recovered, n = 7) COVID-19. The samples were incubated for 20 hours under four conditions: unstimulated (medium), stimulated with SARS-CoV-2 peptides (Pool Spike CoV-2 and Pool CoV-2 peptide), and stimulated with SEB. Unstimulated and SEB-stimulated PBMC were used as a negative and positive control, respectively. Frequency of regulatory T cells expressing perforin **(A)**, granzyme **(B)**, and co-expressing perforin and granzyme B **(C)** in HC, Mild Recovered, and Severe Recovered. Lowercase letters represent statistical differences ($p < 0.05$) between the conditions within each group: (b) (medium × Pool CoV-2), (c) (medium × SEB), (e) (Pool Spike CoV-2 × SEB), and (f) (Pool CoV-2 × SEB). Symbol **#** represents statistically significant differences between the HC and Severe Recovered groups in the SEB conditions. The bars with **#** above depict the higher expression of the analyzed marker compared with that in the other group. **(D)** Comparison of the frequency of regulatory T cells expressing perforin among Mild Recovered volunteers who had and had not experienced the following symptoms: dyspnea and ageusia during acute COVID-19. **(E)** Comparison of the frequency of regulatory T cells expressing granzyme B among Mild Recovered volunteers who had and had not experienced arthralgia during acute COVID-19. **(F)** Comparison of the frequency of regulatory T cells coexpressing perforin and granzyme B among Mild Recovered volunteers who had and had not experienced the following symptoms: dyspnea, arthralgia, and nasal obstruction during acute COVID-19. The symbols ●, ■, and ▲ represent each sample from Mild Recovered volunteer, that was unstimulated (medium condition only) or stimulated with Pool Spike CoV-2 peptides or Pool CoV-2 peptides, respectively. Multiple comparisons were performed using two-way ANOVA and Tukey's *post hoc* test, one-way ANOVA and Tukey's *post hoc* test, and Kruskal-Wallis with Dunn's multiple comparisons test when appropriate. The bars represent the mean values, and the error bars show the standard error of the mean (SEM) for each group. The lines above the bars indicate statistically significant differences between the two groups. *$p < 0.05$; **$p < 0.01$; $^{\#}p < 0,05$; $^{\#\#}p < 0.01$. SEB, staphylococcal enterotoxin B.

We compared and analyzed the expression of perforin by Tregs among Mild Recovered volunteers between those who had and had not experienced certain symptoms and found higher Perforin$^+$ Treg levels in unstimulated and Pool CoV-2-stimulated PBMC from volunteers who presented with dyspnea during acute COVID-19 than in those who did not (Figure 3D). We also detected higher levels of perforin produced by unstimulated Tregs from volunteers who had ageusia than in those who did not (Figure 3D). Elevated granzyme B expression was observed in Tregs in samples stimulated with Pool Spike CoV-2 in Mild Recovered volunteers who did not have arthralgia during acute COVID-19 than in those who did (Figure 3E).

In samples unstimulated and stimulated with peptides related to SARS CoV-2, the co-expression of cytotoxic granules by Tregs was higher in Mild Recovered volunteers who experienced dyspnea than in those who did not (Figure 3F). Higher levels of Tregs Perforin$^+$Granzyme B$^+$ cells were detected in Pool CoV-2-stimulated PBMC from volunteers who had arthralgia than in those who did not (Figure 3F). However, for those who developed nasal obstruction during acute COVID-19, we observed a mild Pool Spike CoV-2-induced co-expression of cytotoxic granules by Tregs (Figure 3F). Comparison of the cytotoxic granule expression among Mild Recovered volunteers between those who had and had not experienced other symptoms were also analyzed, but no significant results were found (Supplementary Figure 3).

3.5 Pool spike CoV-2 stimulus reduces CTLA-4 expression by Tregs in mild recovered volunteers who did not experience certain symptoms

This study evaluated the expression of inhibitory receptors such as PD-1 and CTLA-4. Although CTLA-4 did not show significant changes in any of the studied groups (Supplementary Table 1), the frequency of Tregs expressing PD-1 was lower in the Severe Recovered group than in the Mild Recovered group in PBMC stimulated with Pool Spike CoV-2 (Supplementary Table 1). The Pool Spike CoV-2-stimulated samples in the Mild Recovered group presented a higher frequency of PD-1-producing Tregs than did those incubated with Pool CoV-2 peptide (Supplementary Table 1).

Analyzing the PD-1$^+$ Treg frequency between Mild Recovered volunteers with or without certain symptoms revealed that those who experienced dyspnea presented lower levels of PD-1$^+$ Tregs in PBMC stimulated with Pool CoV-2 than with Pool Spike CoV-2 (Figure 4A). In addition, the volunteers who did not develop sore throat or nasal obstruction presented a higher frequency of PD-1$^+$ Treg in unstimulated PBMC than in those stimulated with Pool CoV-2 (Figure 4A). Finally, unstimulated samples from volunteers who did not experience sore throat or fatigue presented a higher frequency of PD-1 producing Tregs than the cells from volunteers who developed these symptoms (Figure 4A).

The frequency of CTLA-4$^+$ Treg among Mild Recovered volunteers between those who had and had not experienced certain symptoms during acute COVID-19 was compared, and we observed that those who had not experienced sore throat, nasal obstruction, diarrhea, and ageusia had a lower Pool Spike CoV-2 peptide-induced CTLA-4 expression in Tregs compared with that in unstimulated cells (Figure 4B). We observed higher levels of CTLA-4$^+$ Tregs in PBMC stimulated with Pool CoV-2 than with Pool Spike CoV-2 among Mild Recovered volunteers who had not experienced fatigue (Figure 4B). Pool CoV-2-stimulated PBMC presented fewer Tregs expressing CTLA-4 in those who had developed anosmia when compared with that of the unstimulated samples (Figure 4B). We also observed a lower Treg CTLA-4$^+$ frequency in Pool CoV-2-stimulated PBMC from Mild Recovered volunteers who had experienced fatigue, anosmia, and ageusia than in those who had not developed these symptoms (Figure 4B). The Treg CTLA-4$^+$ levels in the Pool Spike CoV-2-stimulated PBMC were higher in volunteers who had developed diarrhea than in those who had not (Figure 4B). A comparison of the expression of the inhibitory receptors among Mild Recovered volunteers between those who had and had not experienced other symptoms was also analyzed, but no significant results were found (Supplementary Figure 4).

3.6 Contrary CD39 and CD73 expression patterns are observed among mild recovered volunteers between those who had and had not experienced certain symptoms

Finally, the expression of CD39 and CD73 by Tregs was analyzed. As shown in Figures 5A, B), no significant changes in the levels of Tregs expressing CD39 or CD73 were observed between the studied groups. However, when the co-expression of CD39$^+$CD73$^+$ was analyzed, Mild Recovered samples incubated with Pool CoV-2 had a higher frequency of CD39$^+$CD73$^+$ Treg expression than did the HC (Figure 5C). In the HC group, we also observed the high co-expression by Tregs in samples stimulated with SEB that with Pool CoV-2 (Figure 5C).

The comparison of ectonucleotidase expression among Mild Recovered volunteers between those who had and had not experienced certain symptoms showed a higher CD39$^+$ Treg frequency in unstimulated PBMC from volunteers who had not developed myalgia and arthralgia than in those who had (Figure 5D). In addition, the levels of CD39 expression by Tregs in volunteers who had presented with fatigue and anosmia were more prevalent in the unstimulated samples than in Pool Spike CoV-2-stimulated samples (Figure 5D). The anosmia-positive volunteers were also marked by a lower expression of CD39 by Tregs in Pool CoV-2 stimulus compared to those that had not experienced this symptom (Figure 5D).

In Pool Spike CoV-2-incubated samples from Mild Recovered volunteers who had myalgia, arthralgia, and diarrhea, we observed a higher level of CD73$^+$ Treg frequency than in those who had not presented these symptoms (Figure 5E). Volunteers who experienced arthralgia also presented higher CD73 expression by Tregs in unstimulated samples than in those without arthralgia

10.3389/fimmu.2023.1078922

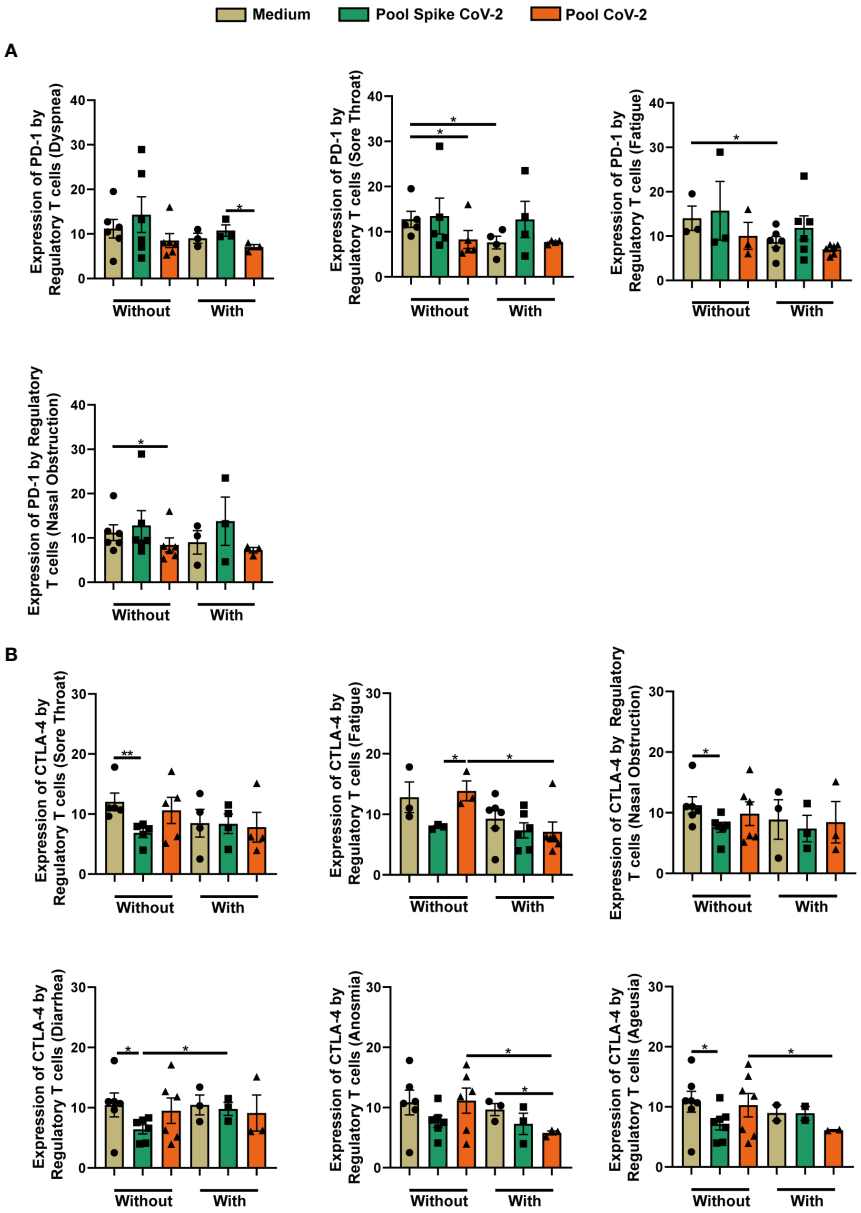

FIGURE 4
Comparison of the frequency of regulatory T cells expressing PD-1 and CTLA-4 among Mild Recovered volunteers who had and had not developed some symptoms. Peripheral blood mononuclear cells (PBMC) were collected from volunteers and the samples were incubated for 20 hours under four conditions: unstimulated (medium), stimulated with SARS-CoV-2 peptides (Pool Spike CoV-2 and Pool CoV-2 peptide), and stimulated with SEB (did not show in this figure). **(A)** Comparison of the frequency of regulatory T cells expressing PD-1 among Mild Recovered volunteers who had and had not developed the following symptoms: dyspnea, sore throat, fatigue, and nasal obstruction during acute COVID-19. **(B)** Comparison of the frequency of regulatory T cells expressing CTLA-4 among Mild Recovered volunteers who had and had not experienced the following symptoms: sore throat, fatigue, nasal obstruction, diarrhea, anosmia, and ageusia during acute COVID-19. The symbols ●, ■, and ▲ represent each sample from Mild Recovered volunteer that was unstimulated (medium condition only) or stimulated with Pool Spike CoV-2 peptides or Pool CoV-2 peptides, respectively. Multiple comparisons were performed using one-way ANOVA and Tukey's *post hoc* test, and Kruskal-Wallis with Dunn's multiple comparisons test when appropriate. The bars represent the mean values, and the error bars show the standard error of the mean (SEM) for each group. The lines above the bars indicate statistically significant differences between the two groups. *$p < 0.05$; **$p < 0.01$. SEB, staphylococcal enterotoxin B.

(Figure 5E). Interestingly, $CD39^{+}CD73^{+}$ Tregs were more prevalent in all conditions for volunteers who had developed myalgia than for those who had not (Figure 5F). A similar result was observed for diarrhea with the exception of unstimulated samples; no significant differences were found among volunteers between those who had and had not developed this symptom (Figure 5F). No significant results were found in the comparison of ectonucleotidase expression among Mild Recovered volunteers between those who had and had not experienced other symptoms (Supplementary Figure 5).

10.3389/fimmu.2023.1078922

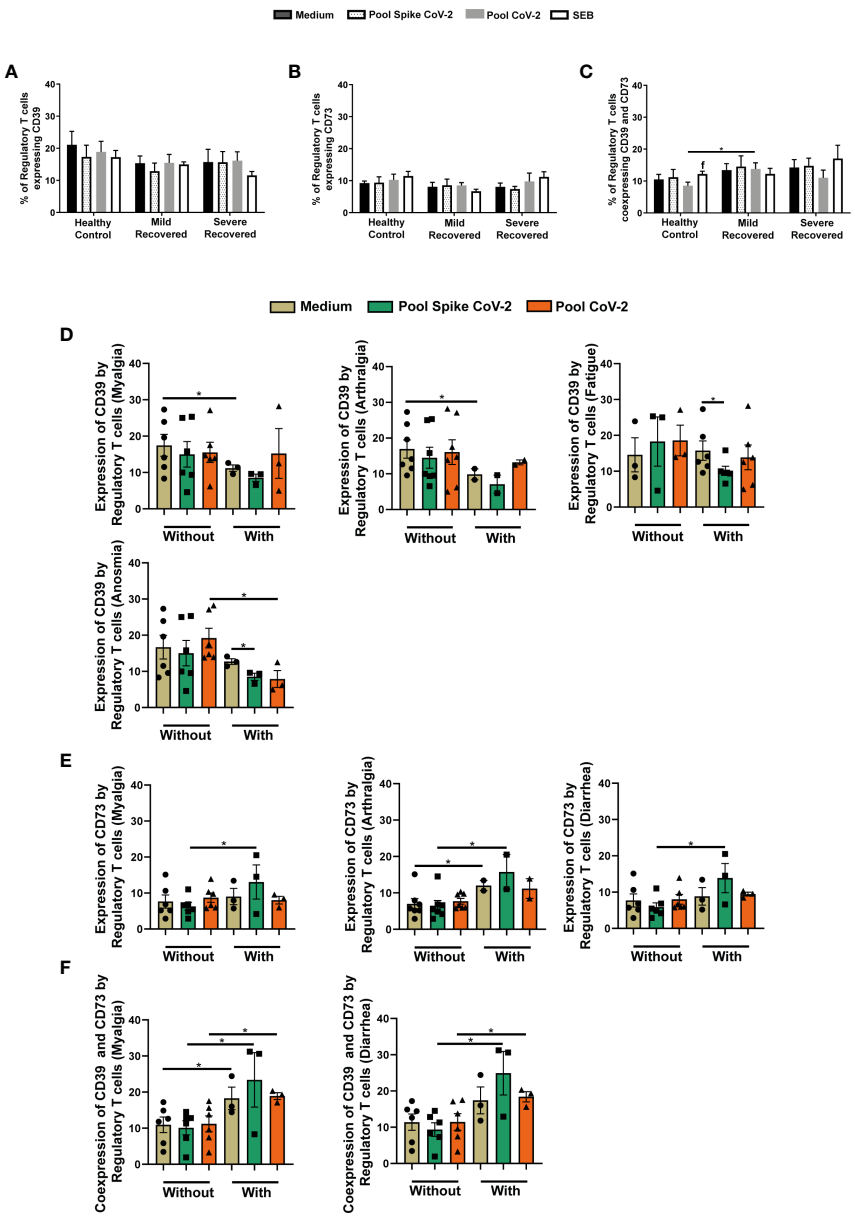

FIGURE 5
Regulatory T cells expressing CD39 and CD73 in peripheral blood from volunteers. Peripheral blood mononuclear cells (PBMC) were collected from volunteers not previously affected by SARS-CoV-2 infection (Healthy Control - HC, n = 8) and volunteers who recovered from mild (Mild Recovered, n = 9) and severe (Severe Recovered, n = 7) COVID-19. The samples were incubated for 20 hours under four conditions: unstimulated (medium), stimulated with SARS-CoV-2 peptides (Pool Spike CoV-2 and Pool CoV-2 peptide), and stimulated with SEB. Unstimulated and SEB-stimulated PBMC were used as a negative and positive control, respectively. Frequency of regulatory T cells expressing CD39 **(A)**, CD73 **(B)**, and co-expressing CD39 and CD73 **(C)** in HC, Mild Recovered, and Severe Recovered. Lowercase letters represent statistical differences ($p < 0.05$) between the conditions within each group: (f) (Pool CoV-2 × SEB). **(D)** Comparison of the frequency of regulatory T cells expressing CD39 among Mild Recovered volunteers who had and had not experienced the following symptoms: myalgia, arthralgia, fatigue, and anosmia during acute COVID-19. **(E)** Comparison of the frequency of regulatory T cells expressing CD73 among Mild Recovered volunteers who had and had not experienced the following symptoms: myalgia, arthralgia, and diarrhea during acute COVID-19. **(F)** Comparison of the frequency of regulatory T cells coexpressing CD39 and CD73 among Mild Recovered volunteers who had and had not experienced the following symptoms: myalgia and diarrhea during acute COVID-19. The symbols ●, ■, and ▲ represent each sample from Mild Recovered volunteer that was unstimulated (medium condition only) or stimulated with Pool Spike CoV-2 peptides or Pool CoV-2 peptides, respectively. Multiple comparisons were performed using two-way ANOVA and Tukey's *post hoc* test, one-way ANOVA and Tukey's *post hoc* test, and Kruskal-Wallis with Dunn's multiple comparisons test when appropriate. The bars represent the mean values, and the error bars show the standard error of the mean (SEM) for each group. The lines above the bars indicate statistically significant differences between the two groups. *$p < 0.05$. SEB, staphylococcal enterotoxin B.

10.3389/fimmu.2023.1078922

4 Discussion

The worldwide emergency caused by the current COVID-19 pandemic has led to significant efforts by the scientific community to understand the host immune response to SARS-CoV-2 infection (5). Although most infected individuals develop mild COVID-19, the severity was high in some people, and excessive inflammation is usually associated with the worsening of the illness (23, 24). To better understand the impact of SARS-CoV-2 infection on adaptive immunity after infection resolution, we evaluated the peripheral Tregs of volunteers who had recovered from mild and severe COVID-19. Compared to HC, we report higher levels of Tregs in Pool CoV-2-stimulated samples from Mild and Severe Recovered volunteers. In addition, unstimulated PBMC from the Mild Recovered group presented a higher frequency of Tregs than did HC, suggesting long-term immune changes after SARS-CoV-2 infection as previously reported by Liu et al. (2021) (25). The absence of statistical differences between the Mild and Severe Recovered groups could indicate no correlation between Treg frequency and the course of COVID-19.

However, it is interesting to consider the possibility that after recovery from COVID-19, the Treg levels were downregulated. This raises questions regarding the parameters and their actual impact on distinct forms of the disease. However, the higher Treg frequency in unstimulated PBMC from the Mild Recovered group than in HC suggests improved activity during the acute stage that was partially sustained after the cure. In this case, no differences were found between the Mild Recovery volunteers who did and did not have the evaluated symptoms during acute disease, nasal obstruction being an exception. Volunteers without nasal obstruction had more Tregs than in those with this clinical sign, indicating that these cells participate in the development of an attenuated form of COVID-19. However, the analysis of cell frequency alone does not provide details on the impact of long-term SARS-CoV-2 infection on Tregs from recovered volunteers. Thus, we analyzed the expression of some proteins related to Treg activity in all the evaluated groups.

IL-10 is a cytokine with anti-inflammatory properties used by Tregs as a direct tool for immune response modulation during immunosuppressive activity (26). We found a higher frequency of IL-10$^+$ Treg in unstimulated or Pool CoV-2-stimulated Mild Recovered PBMC compared to that in HC and Severe Recovered groups, strengthening the hypothesis of persistent immune changes after the resolution of infection (27, 28). Although some studies correlate cytokines such as IL-6 and IL-10 as predictors of COVID-19 severity, elevated IL-10 levels could act to moderate excessive inflammation even though it is not able to do so (29–31).

Considering that acute COVID-19 induced higher expression levels of Treg IL-10$^+$ in Mild Recovered volunteers, these results may indicate an improved regulatory activity to aid in an adequate antiviral response leading to the resolution of infection with little tissue injury. Consistent with this, Shuwa et al. (2021) (27) showed that GcPC-stimulated PBMC from convalescent patients with chest X-ray abnormalities manifested a reduced frequency of IL-10-producing B cells compared with that in those without the abnormalities, suggesting a correlation between pulmonary pathology resolution and B IL-10$^+$ cell expansion. Volunteers who recovered from mild COVID-19 presented elevated levels of IL-10 producing Tregs, which points to a sustained immunosuppressive microenvironment that can attenuate inflammation upon reinfection. Our data showed that Pool CoV-2 stimulation elicited more IL-10 expression than did Pool Spike CoV-2 stimulus in the Mild Recovered group. This result points to increased suppressive capacity in reactive Tregs because Mild Recovered IL-10$^+$ Tregs levels were also higher than that in the cells from Pool CoV-2 stimulated Severe Recovered group. Meckiff et al. (2020) (32) suggested a potentially impaired Treg response in hospitalized COVID-19 patients, corroborating our findings.

Analyzing the expression of IL-17 by Tregs (33–37), we observed a more pronounced level of cytokine synthesis in Mild Recovered volunteers. Some studies point to the contribution of this interleukin into the severity of COVID-19, also showing that the activation of IL-17 signaling pathways due to the interaction of SARS-CoV-2 ORF8 with IL-17 receptor could induce the expression of pro-inflammatory factor, contributing to cytokine storm (38, 39). However, Ghazavi et al. (2021) (40) found higher IL-17 plasma levels in patients with mild COVID-19, whereas Shuwa et al. (2021) (27) observed the expression of IL-17 among CD4+ T cells in a population of stimulated PBMC during acute disease, and it was maintained in the convalescent stage regardless of the clinical profile. Hence, it might be possible that SARS-CoV-2 infection elicited a greater IL-17 expression in Tregs from Mild Recovered volunteers during the acute stage and the levels were maintained after disease resolution. This could be why statistically significant differences were detected only after stimulation by SARS-CoV-2-related peptides. The similarity in IL-17 production between unstimulated, Pool Spike CoV-2-stimulated, and Pool CoV-2-stimulated cells supports the above-mentioned hypothesis.

The elevated levels of IL-17 synthesis by Tregs in Mild Recovered volunteers could also indicate a high level of expression of transcription factor (TF) RORγt. RORγt$^+$ Tregs could possibly impede Th17 differentiation, thus attenuating the production of inflammatory mediators. Previous studies have suggested that Tregs expressing TF of other CD4$^+$ T subpopulations help in the immunosuppression of distinct inflammatory profiles (36, 41–44). However, SARS-CoV-2 peptides appear to elicit a higher Th1 response profile in T cells (45–47). Hence, the decreased IL-17 expression by Tregs under Spike stimulus may point to an appropriate assembly of the antiviral immune response during reinfection in Severe Recovered volunteers, contributing to a faster infection resolution. However, both hypotheses suggest a distinct Treg profile between Mild and Severe Recovered volunteers with the potential to fight SARS-CoV-2 reinfection appropriately.

The contribution of IL-17 to proper disease resolution upon first exposure to or reinfection with SARS-CoV-2 could aid in understanding other potential favorable properties of IL-17$^+$ Tregs. A study by Schnoeller et al. (2014) (48) demonstrated a protective role of IL-17 in respiratory syncytial virus (RSV) infection following vaccination with attenuated *Bordetella pertussis*. Wang et al. (2011) (49) also reported a beneficial role of IL-17 against the H5N1 virus,

possibly through migratory modulation of B lymphocytes. Under certain conditions, Treg subpopulations express IL-17 displaying considerable and expressive immunosuppressive activity (35, 50, 51). Interestingly, *in vitro* studies by Li et al. (2012) (51) demonstrated that IL-17-producing Tregs, named Tr17, expressed higher amounts of perforin, granzyme B, and CD107a, suggesting a greater degranulation capacity compared with that of IL-17$^-$ Tregs. Taken together, our data indicate that the Treg subpopulation may improve the immunomodulatory profile in volunteers who recovered from mild COVID-19.

Consistent with Li et al. (2012) (51), IL-17$^+$ Tregs may have been partially responsible for the higher expression of perforin and granzyme B found in the Mild Recovered group and probably contributed to the mildness of the disease in these volunteers during acute COVID-19. Interestingly, comparative analysis of data in the Mild Recovered group showed higher perforin levels or co-production of perforin and granzyme B by Tregs from those who experienced certain symptoms, especially dyspnea. Although cytotoxic granule expression may correlate with COVID-19 severity, perforin and granzyme production by Tregs is essential for its immunosuppressive properties (52–55). Considering the immunomodulatory roles of Tregs, the differential expression of cytotoxic granules in Mild Recovered volunteers affected mainly by dyspnea suggests a partial contribution of Tregs to inflammation control through this mechanism, resulting in milder forms of COVID-19. Loebbermann et al. (2012) (53) demonstrated the essential role of granzyme B-producing Treg cells in controlling pulmonary inflammation during acute viral infection. Hence, cytotoxic granule producing Tregs could exert an immunomodulatory effect through targeted immune cell death and prevent exacerbated inflammatory activity. The importance attributed to the Treg-secreted granules in inducing cell death (or suppression) in dendritic cells (DC), NK cells, and CD8+ T cells, raises the possibility of immunomodulation at the level of innate and adaptive immunity (52, 56, 57).

Interestingly, our data also showed a significant increase in Tregs expressing LAP and co-expressing perforin and granzyme B in Pool CoV-2-stimulated PBMC from HC. Samples of patients not previously exposed to the virus showed the presence of reactive T cells to SARS-CoV-2, probably due to exposure to other endemic coronaviruses (58). Therefore, our findings may point to immunological cross-reactivity caused by prior infections by other pathogens.

Modulation of costimulatory (such as CD28 and ICOS) or inhibitory (such as CTLA-4 and PD-1) receptors is a valuable mechanism for T lymphocyte responsiveness control (59, 60). Tregs express inhibitory receptors responsible for the modulation of the immune response through cell–cell contact mechanisms (55, 61). Despite similar CTLA-4 production levels among the evaluated groups, comparative analysis of the data of the Mild Recovered group demonstrated a decreased expression pattern of IL-10$^+$ and CTLA-4$^+$ Tregs in Pool Spike CoV-2-stimulated samples from volunteers who had not experienced specific symptoms. This result suggests a distinct modulation of immunosuppressive Treg tools among Mild Recovered volunteers who had and did not develop certain clinical signs during acute COVID-19. Some studies have indicated that SARS-CoV-2 peptides elicit a stronger Th1 response (45–47). Based on the differential Treg profile data, it seems possible that Mild Recovered volunteers experience a well-coordinated immune response, partially because of attenuated Treg immunosuppressive mechanisms, which elicited a faster antiviral signature. Considering the highly functional and balanced T cell responsiveness in asymptomatic individuals (62), our data suggest that immunomodulation at Treg levels aids in better infection resolution.

We also demonstrated that Pool Spike CoV-2 induced a higher frequency of PD-1$^+$ Tregs than did Pool CoV-2 in Mild Recovered volunteers, similar to that observed in volunteers from the same group who had experienced dyspnea during acute COVID-19. Kamada et al. (2019) (63) reported an improvement in cell-mediated immunosuppression after blocking PD-1 on Tregs. Since the frequency of Tregs expressing PD-1 was more pronounced in Mild than in Severe Recovered samples with Pool Spike CoV-2 stimulation, these results indicate a possible limiting immunosuppressive activity that favors antiviral responsiveness.

Finally, we evaluated the expression of ectonucleotidases CD39 (NTPDase1) and CD73 (5′-ribonucleotide phosphohydrolase), which is another immunosuppressive mechanism exerted by Tregs through purinergic signaling modulation by hydrolysis of extracellular ATP (pro-inflammatory) and generation of adenosine (immunosuppressive) (55, 64–66). Even without significant differences in CD39 or CD73 expression among the recovered groups, the Pool CoV-2-stimulated PBMC from Mild Recovered volunteers presented more CD39$^+$CD73$^+$ Tregs than did the HC, suggesting greater adenosine synthesis capacity upon reinfection.

Interestingly, we found higher CD3$^+$CD4$^+$CD25$^+$FOXP3$^+$CD39$^+$ T cell frequency in unstimulated conditions in Mild Recovered volunteers who had not experienced musculoskeletal symptoms (arthralgia and myalgia) during acute COVID-19. Past studies have shown an overall correlation between CD39 expression in some lymphocytes and excellent responsiveness to rheumatoid arthritis (RA)-associated treatments or between reduced RA activity and rheumatoid factor (RF) levels (67–69). In contrast, Gu et al. (2017) (70) showed that CD39^{high} Tregs may have more stability and protective roles compared with that CD39^{low} Tregs. This partially explains the higher frequency of CD39$^+$ Tregs in Mild Recovered volunteers who had not experienced musculoskeletal pain during active disease. Based on these observations by Gu et al. (2017) (70), CD39$^+$ Tregs could be evaluated to validate whether these cells are endowed with higher immunosuppressive capacity in volunteers without arthralgia and myalgia than in those who had developed these symptoms. This is a possibility considering that in Mild Recovered volunteers who had experienced anosmia and fatigue, Pool Spike CoV-2 elicited a downregulation in CD39$^+$ Tregs. At the same time, a lower frequency of this subpopulation was found post Pool CoV-2 stimulation in samples of Mild Recovered volunteers who had experienced anosmia compared with those who had not.

The frequency of CD73$^+$ Tregs, in contrast to that of CD39, was higher in Mild Recovered volunteers who had developed myalgia and arthralgia in the acute phase of the disease, suggesting differential ectonucleotidase modulation in the face of musculoskeletal symptoms. A correlation exists between low

CD73 expression and the severity of juvenile idiopathic arthritis (JIA) (71). CD73 also plays a protective role in collagen-induced arthritis (CIA) in a mouse model for the study of RA (72). Thus, Mild Recovered COVID-19 volunteers who had experienced musculoskeletal symptoms possibly had better adenosine production mediated by Tregs. These results suggest a protective role of this subpopulation in this group, partially explaining the greater $CD39^+CD73^+$ Treg frequency in Mild Recovered volunteers who had developed myalgia.

Unfortunately, due to the lack of a longitudinal study, we could not determine whether the lower levels of $CD39^+$ Tregs and higher levels of $CD73^+$ and $CD39^+$ $CD73^+$ Tregs in volunteers who had musculoskeletal symptoms occurred before, during, or after the first infection. Since similar levels of $CD39^+$ Tregs were observed in both stimulated and unstimulated PBMC, the frequency of this subpopulation in Mild Recovered volunteers without musculoskeletal symptoms could have been high even before the infection, leading to the absence of these clinical signs. This raises the possibility of a correlation between CD39 expression by Tregs and the course of COVID-19. We, however, suggest that Mild Recovered volunteers who had and had not experienced certain symptoms are endowed with distinct immunosuppressive components that can converge to aid in host protection in case of reinfection. The lower $CD39^+$ and higher $CD73^+$ Treg expression in Mild Recovered volunteers who had experienced certain symptoms suggests that the opposite expression of both enzymes possibly elicited by SARS-CoV-2 infection in the Mild Recovered group can persist for long periods after disease resolution.

5 Conclusion

In the present study, we observed higher frequencies of Tregs and expression of IL-10, IL-17, perforin, granzyme B, PD-1, and $CD39^+CD73^+$ co-expression by Tregs in the Mild Recovered group compared with that in HC or Severe Recovered group under certain conditions. We also observed a differential frequency of Tregs expressing immunological markers between cells from Mild Recovered volunteers among those who had and had not developed certain symptoms during acute COVID-19. Hence, we arrived at a few inferences. In Mild Recovered volunteers who had not experienced certain clinical signs, Pool Spike CoV-2 stimulus elicited a downregulation of $CTLA\text{-}4^+$ and $IL\text{-}10^+$ Tregs frequency, indicating attenuation of specific immunosuppressive mechanisms that possibly contributed to the effective antiviral response. A differential expression between CD39 and CD73 by Tregs was also observed. Dyspnea was associated with high levels of perforin and cytotoxic granule co-expression by the studied lymphocytes. Finally, the SARS-CoV-2-related peptides (Pool Spike CoV-2 and/or Pool CoV-2) induced changes in the expression of IL-10 and PD-1 in volunteers who recovered from mild COVID-19, IL-17 in volunteers who recovered from Severe COVID-19, and LAP and co-expression of cytotoxic granules in HC.

Our study has some limitations, including the small number of volunteers, mainly in the Severe Recovered group. This work does not encompass the full scale of heterogeneity in the Brazilian population. Hence, we were not able to explore genetics and age as factors that may affect the immune response to infections (73, 74). However, despite these limitations, our study reveals important data about the participation of Tregs in COVID-19, suggesting that modulation of immunosuppressive markers could partially drive a mild disease, and these alterations that possibly occur during the acute disease can persist for months. It is noteworthy to highlight that this study enrolled just unvaccinated volunteers. Thus, we believe that this study would greatly aid the scientific community to make further advancements and gain knowledge regarding the contribution of immunological changes at the level of Tregs to the development of distinct clinical profiles in COVID-19.

Data availability statement

The original contributions presented in the study are included in the article/Supplementary Material. Further inquiries can be directed to the corresponding author.

Ethics statement

The studies involving human participants were reviewed and approved by National Commission of Ethics in Research (certificate CAAE: 31354720.0.0000.5188). The patients/participants provided their written informed consent to participate in this study.

Author contributions

PP: Investigation, data curation, formal analysis, visualization, and writing of the original draft. RP: Investigation and data curation. BC: Investigation and data curation. IM: Formal analysis and resources provided. FA: Formal analysis and resources provided. RV: Formal analysis. DJ: Formal analysis. IA: Writing, review, and editing. TK: Conceptualization, methodology, validation, resources provision, supervision, project administration, funding acquisition, writing of the original draft, review, and editing. All authors contributed to the article and approved the submitted version.

Funding

This work was supported by the Conselho Nacional de Desenvolvimento Científico e Tecnológico- CNPq CHAMADA 4 BRICS STI COVID- 19 (Number 440939/2020-8) and Coordenação de Aperfeiçoamento de Pessoal de Nível Superior-CAPES by fellowships support. The funding sources were not involved in the study design, collection, analysis, and interpretation of data, writing of the report, or in the decision to submit the article for publication.

Acknowledgments

The authors are grateful to all the volunteers who enrolled in this study and the Federal University of Paraiba, Brazil, for providing the structure to perform this work. We would like to thank Editage (www.editage.com) for English language editing.

Conflict of interest

The authors declare that the research was conducted in the absence of any commercial or financial relationships that could be construed as a potential conflict of interest.

Publisher's note

All claims expressed in this article are solely those of the authors and do not necessarily represent those of their affiliated organizations, or those of the publisher, the editors and the reviewers. Any product that may be evaluated in this article, or claim that may be made by its manufacturer, is not guaranteed or endorsed by the publisher.

Supplementary material

The Supplementary Material for this article can be found online at: https://www.frontiersin.org/articles/10.3389/fimmu.2023.1078922/full#supplementary-material

References

1. Hu B, Guo H, Zhou P, Shi ZL. Characteristics of SARS-CoV-2 and COVID-19. *Nat Rev Microbiol* (2021) 19:141–54. doi: 10.1038/s41579-020-00459-7

2. Lafon E, Diem G, Witting C, Zaderer V, Bellmann-Weiler RM, Reindl M, et al. Potent SARS-CoV-2-specific T cell immunity and low anaphylatoxin levels correlate with mild disease progression in COVID-19 patients. *Front Immunol* (2021) 12:684014. doi: 10.3389/fimmu.2021.684014

3. Merad M, Blish CA, Sallusto F, Iwasaki A. The immunology and immunopathology of COVID-19. *Science* (2022) 375:1122–7. doi: 10.1126/science.abm8108

4. Zhai W, Luo Z, Zheng Y, Dong D, Wu E, Wang Z, et al. Moderate vs. mild cases of overseas-imported COVID-19 in Beijing: a retrospective cohort study. *Sci Rep* (2021) 11:1–11. doi: 10.1038/s41598-021-85869-0

5. Caldrer S, Mazzi C, Bernardi M, Prato M, Ronzoni N, Rodari P, et al. Regulatory T cells as predictors of clinical course in hospitalised COVID-19 patients. *Front Immunol* (2021) 12:789735. doi: 10.3389/fimmu.2021.789735

6. Moss P. The T cell immune response against SARS-CoV-2. *Nat Immunol* (2022) 23:186–93. doi: 10.1038/s41590-021-01122-w

7. Sette A, Crotty S. Adaptive immunity to SARS-CoV-2 and COVID-19. *Cell* (2021) 184:861–80. doi: 10.1016/j.cell.2021.01.007

8. André S, Picard M, Cezar R, Roux-Dalvai F, Alleaume-Butaux A, Soundaramourty C, et al. T Cell apoptosis characterize severe covid-19 disease. *Cell Death Differ* (2022) 29:1486–99. doi: 10.1038/s41418-022-00936-x

9. Bayati F, Mohammadi M, Valadi M, Jamshidi S, Foma AM, Sharif-Paghaleh E. The therapeutic potential of regulatory T cells: challenges and opportunities. *Front Immunol* (2021) 11:585819. doi: 10.3389/fimmu.2020.585819

10. Simsek A, Kizmaz MA, Cagan E, Dombaz F, Tezcan G, Asan A, et al. Assessment of CD39 expression in regulatory T-cell subsets by disease severity in adult and juvenile COVID-19 cases. *J Med Virol* (2022) 94:2089–101. doi: 10.1002/jmv.27593

11. Neumann J, Prezzemolo T, Vanderbeke L, Roca CP, Gerbaux M, Janssens S, et al. Increased IL-10-producing regulatory T cells are characteristic of severe cases of COVID-19. *Cli Transl Immunol* (2020) 9:1–13. doi: 10.1002/cti2.1204

12. Sadeghi A, Tahmasebi S, Mahmood A, Kuznetsova M, Valizadeh H, Taghizadieh A, et al. Th17 and treg cells function in SARS-CoV2 patients compared with healthy controls. *J Cell Physiol* (2021) 236:2829–39. doi: 10.1002/jcp.30047

13. Vick SC, Frutoso M, Mair F, Konecny AJ, Greene E, Wolf CR, et al. A regulatory T cell signature distinguishes the immune landscape of COVID-19 patients from those with other respiratory infections. *Sci Adv* (2021) 7:1–17. doi: 10.1126/sciadv.abj0274

14. Rahimzadeh M, Naderi N. Toward an understanding of regulatory T cells in COVID-19: A systematic review. *J Med Virol* (2021) 93:4167–81. doi: 10.1002/jmv.26891

15. Wang H, Wang Z, Cao W, Wu Q, Yuan Y, Zhang X. Regulatory T cells in COVID-19. *Aging Dis* (2021) 12:1545–53. doi: 10.14336/AD.2021.0709

16. Wang Y, Zheng J, Islam MS, Yang Y, Hu Y, Chen X. The role of CD4+ FoxP3+ regulatory T cells in the immunopathogenesis of COVID-19: implications for treatment. *Int J Biol Sci* (2021) 17:1507–20. doi: 10.7150/ijbs.59534

17. BRASIL. Ministério da Saúde. *Informe semanal n° 37 de evidências sobre variantes de atenção de SARS-CoV-2* (2021). Available at: https://www.gov.br/saude/pt-br/coronavirus/publicacoes-tecnicas/informes-de-variantes/informe_s37.pdf/view (Accessed September 21, 2022).

18. Adamoski D, Baura VA, Rodrigues AC, Royer CA, Aoki MN, Tschá MK, et al. SARS-CoV-2 delta and omicron variants surge in curitiba, southern Brazil, and its impact on overall COVID-19 lethality. *Viruses* (2022) 14:1–8. doi: 10.3390/v14040809

19. Wu Z, Mcgoogan JM. Characteristics of and important lessons from the coronavirus disease 2019 (COVID-19) outbreak in China: Summary of a report of 72 314 cases from the Chinese center for disease control and prevention. *JAMA* (2020) 323:1239–42. doi: 10.1001/jama.2020.2648

20. Guerra-Gomes IC, Gois BM, Peixoto RF, Palmeira PHS, Dias CNS, Csordas BG, et al. Phenotypical characterization of regulatory T cells in acute zika infection. *Cytokine* (2021) 146:1–7. doi: 10.1016/j.cyto.2021.155651

21. Steinhagen K, Messing C, Lattwein E, Stiba K, Lindhorst F, Neugebauer E, et al. Applicants: Eurimmun medizinische labordagnostika AG, charité - universitätsmedizin berlin. a method and reagents for the diagnosis of SARS-COV-2. (2021). N. EP20158626A.-Date of filing: 20 Feb. 2020. Date of publication: 25 Ago.

22. Morpheus. (2022). Available at: https://software.broadinstitute.org/morpheus/.

23. Merad M, Subramanian A, Wang TT. An aberrant inflammatory response in severe COVID-19. *Cell Host Microbe* (2021) 29:1043–7. doi: 10.1016/j.chom.2021.06.018

24. Li Q, Wang Y, Sun Q, Knopf J, Herrmann M, Lin L, et al. Immune response in COVID-19: what is next? *Cell Death Differ* (2022) 29:1107–22. doi: 10.1038/s41418-022-01015-x

25. Liu J, Yang X, Wang W, Li Z, Deng H, Liu J, et al. Analysis of the long-term impact on cellular immunity in COVID-19-recovered individuals reveals a profound NKT cell impairment. *Mbio* (2021) 12:1–14. doi: 10.1128/mBio.00085-21

26. Rocamora-Reverte L, Melzer FL, Würzner R, Weinberger B. The complex role of regulatory T cells in immunity and aging. *Front Immunol* (2021) 11:616949. doi: 10.3389/fimmu.2020.616949

27. Shuwa HA, Shaw TN, Knight SB, Wemyss K, McClure FA, Pearmain L, et al. Alterations in T and b cell function persist in convalescent COVID-19 patients. *Med* (2021) 2:720–35. doi: 10.1016/j.medj.2021.03.013

28. Singh R, Hemati H, Bajpai M, Yadav P, Maheshwari A, Kumar S, et al. Sustained expression of inflammatory monocytes and activated T cells in COVID-19 patients and recovered convalescent plasma donors. *Immuni Inflammation Dis* (2021) 9:1279–90. doi: 10.1002/iid3.476

29. Han H, Ma Q, Li C, Liu R, Zhao L, Wang W, et al. Profiling serum cytokines in COVID-19 patients reveals IL-6 and IL-10 are disease severity predictors. *Emerg Microbes Infect* (2020) 9:1123–30. doi: 10.1080/22221751.2020.1770129

30. Islam H, Chamberlain TC, Mui AL, Little JP. Elevated interleukin-10 levels in COVID-19: potentiation of pro-inflammatory responses or impaired anti-inflammatory action. *Front Immunol* (2021) 12:6770. doi: 10.3389/fimmu.2021.6770

31. de-Oliveira-Pinto LM, Solórzano VEF, Martins ML, Fernandes-Santos C, Damasco PH, Siqueira MAMT, et al. Comparative analysis of circulating levels of SARS-CoV-2 antibodies and inflammatory mediators in healthcare workers and COVID-19 patients. *Viruses* (2022) 14:1–19. doi: 10.3390/v14030455

32. Meckiff BJ, Ramírez-Suástegui C, Fajardo V, Chee SJ, Kusnadi A, Simon H, et al. Imbalance of regulatory and cytotoxic SARS-CoV-2-reactive CD4+ T cells in COVID-19. *Cell* (2020) 183:1340–1353.e16. doi: 10.1016/j.cell.2020.10.001

33. Beriou G, Costantino CM, Ashley CW, Yang L, Kuchroo VK, Baecher-Allan C, et al. IL-17–producing human peripheral regulatory T cells retain suppressive function. *Blood* (2009) 113:4240–9. doi: 10.1182/blood-2008-10-183251

34. Kryczek I, Wu K, Zhao E, Wei S, Vatan L, Szeliga W, et al. IL-17+ regulatory T cells in the microenvironments of chronic inflammation and cancer. *J Immunol* (2011) 186:4388–95. doi: 10.4049/jimmunol.1003251

35. Afzali B, Mitchell PJ, Edozie FC, Povoleri GAM, Dowson SE, Demandt L, et al. CD 161 expression characterize a subpopulation of human regulatory T cells that produces IL-17 in a STAT 3-dependent manner. *Eur J Immunol* (2013) 43:2043–54. doi: 10.1002/eji.201243296

36. Sefik E, Geva-Zatorsky N, Oh S, Konnikova L, Zemmour D, McGuire AM, et al. Individual intestinal symbionts induce a distinct population of RORγ+ regulatory T cells. *Science* (2015) 349:993–7. doi: 10.1126/science.aaa9420

37. Jung MK, Kwak J, Shin E. IL-17A-producing Foxp3+ regulatory T cells and human diseases. *Immune Netw* (2017) 17:276–86. doi: 10.4110/in.2017.17.5.276

38. Darif D, Hammi I, Kihel A, Saik IEI, Guessous F, Akarid K. The pro-inflammatory cytokines in COVID-19 pathogenesis: What goes wrong? *Microb Pathog* (2021) 153:1–10. doi: 10.1016/j.micpath.2021.104799

39. Lin X, Fu B, Yin S, Li Z, Liu H, Zhang H, et al. ORF8 contributes to cytokine storm during SARS-CoV-2 infection by activating IL-17 pathway. *Iscience* (2021) 24:1–24. doi: 10.1016/j.isci.2021.102293

40. Ghazavi A, Ganji A, Keshavarzian N, Rabiemajd S, Mosayebi G. Cytokine profile and disease severity in patients with COVID-19. *Cytokine* (2021) 137:1–5. doi: 10.1016/j.cyto.2020.155323

41. Chaudhry A, Rudra D, Treuting P, Samstein RM, Liang Y, Kas A, et al. CD4+ regulatory T cells control TH17 responses in a Stat3-dependent manner. *Science* (2009) 326:986–91. doi: 10.1126/science.1172702

42. Koch MA, Tucker-Heard G, Perdue NR, Killebrew JR, Urdahl KB, Campbell DJ. The transcription factor T-bet controls regulatory T cell homeostasis and function during type 1 inflammation. *Nat Immunol* (2009) 10:595–602. doi: 10.1038/ni.1731

43. Levine AG, Mendoza A, Hemmers S, Moltedo B, Niec RE, Schizas M, et al. Stability and function of regulatory T cells expressing the transcription factor T-bet. *Nature* (2017) 546:421–5. doi: 10.1038/nature22360

44. Clay SL, Bravo-Blas A, Wall DM, MacLeod MKL, Milling SWF. Regulatory T cells control the dynamic and site-specific polarization of total CD4 T cells following salmonella infection. *Mucosal Immunol* (2020) 13:946–57. doi: 10.1038/s41385-020-0299-1

45. Grifoni A, Weiskopf D, Ramirez SI, Mateus J, Dan JM, Moderbacher CR, et al. Targets of T cell responses to SARS-CoV-2 coronavirus in humans with COVID-19 disease and unexposed individuals. *Cell* (2020) 181:1489–1501.e15. doi: 10.1016/j.cell.2020.05.015

46. Neidleman J, Luo X, Frouard J, Xie G, Gill G, Stein ES, et al. SARS-CoV-2-specific T cells exhibit phenotypic features of helper function, lack of terminal differentiation, and high proliferation potential. *Cell Rep Med* (2020) 1:1–30. doi: 10.1016/j.xcrm.2020.100081

47. Weiskopf D, Schmitz KS, Raadsen MP, Grifoni A, Okba NMA, Endeman H, et al. Phenotype and kinetics of SARS-CoV-2–specific T cells in COVID-19 patients with acute respiratory distress syndrome. *Sci Immunol* (2020) 5:1–11. doi: 10.1126/sciimmunol.abd2071

48. Schnoeller C, Roux X, Sawant D, Raze D, Olszewska W, Locht C, et al. Attenuated bordetella pertussis vaccine protects against respiratory syncytial virus disease *via* an IL-17–dependent mechanism. *Am J Respir Crit Care Med* (2014) 189:194–202. doi: 10.1164/rccm.201307-1227OC

49. Wang X, Chan CCS, Yang M, Deng J, Poon VKM, Leung VHC, et al. A critical role of IL-17 in modulating the b-cell response during H5N1 influenza virus infection. *Cell Mol Immunol* (2011) 8:462–8. doi: 10.1038/cmi.2011.38

50. Voo KS, Wang YH, Santori FR, Boggiano C, Wang YH, Arima K, et al. Identification of IL-17-producing FOXP3+ regulatory T cells in humans. *Proc Natl Acad Sci U.S.A.* (2009) 106:4793–8. doi: 10.1073/pnas.0900408106

51. Li L, Patsoukis N, Petkova V, Boussiotis VA. Runx1 and Runx3 are involved in the generation and function of highly suppressive IL-17-producing T regulatory cells. *PLos One* (2012) 7:1–7. doi: 10.1371/journal.pone.0045115

52. Cao X, Cai SF, Fehniger TA, Song J, Collins LI, Piwnica-Worm DR, et al. Granzyme b and perforin are important for regulatory T cell-mediated suppression of tumor clearance. *Immunity* (2007) 27:635–46. doi: 10.1016/j.immuni.2007.08.014

53. Loebbermann J, Thornton H, Durant L, Sparwasser T, Webster KE, Sprent J, et al. Regulatory T cells expressing granzyme b play a critical role in controlling lung inflammation during acute viral infection. *Mucosal Immunol* (2012) 5:161–72. doi: 10.1038/mi.2011.62

54. Kang CK, Han GC, Kim M, Kim G, Shin HM, Song KH, et al. Aberrant hyperactivation of cytotoxic T-cell as a potential determinant of COVID-19 severity. *Int J Infect Dis* (2020) 97:313–21. doi: 10.1016/j.ijid.2020.05.106

55. Grover P, Goel PN, Greene MI. Regulatory T cells: regulation of identity and function. *Front Immunol* (2021) 12:750542. doi: 10.3389/fimmu.2021.750542

56. Boissonnas A, Scholer-Dahirel A, Simon-Blancal V, Pace L, Valet F, Kissenpfennig A, et al. Foxp3+ T cells induce perforin-dependent dendritic cell death in tumor-draining lymph nodes. *Immunity* (2010) 32:266–78. doi: 10.1016/j.immuni.2009.11.015

57. Salti SM, Hammelev EM, Grewal JL, Reddy ST, Zemple SJ, Grossman WJ, et al. Granzyme b regulates antiviral CD8+ T cell responses. *J Immunol* (2011) 187:6301–9. doi: 10.4049/jimmunol.1100891

58. Anft M, Blazquez-Navarro A, Stervbo U, Skrzypczyk S, Witzke O, Wirth R, et al. Detection of pre-existing SARS-CoV-2-reactive T cells in unexposed renal transplant patients. *J Nephrol* (2021) 34:1025–37. doi: 10.1007/s40620-021-01092-0

59. Chikuma S. CTLA-4, an essential immune-checkpoint for T-cell activation. *Curr Topics Microbiol Immunol* (2017) 410:99-126. doi: 10.1007/82_2017_61

60. Rowshanravan B, Halliday N, Sansom DM. CTLA-4: a moving target in immunotherapy. *Blood* (2018) 131:58–67. doi: 10.1182/blood-2017-06-741033

61. Koyama S, Nishikawa H. Mechanisms of regulatory T cell infiltration in tumors: implications for innovative immune precision therapies. *J Immunother Cancer* (2021) 9:1–13. doi: 10.1136/jitc-2021-002591

62. Le Bert N, Clapham HE, Tan AT, Chia WN, Tham CYL, Lim JM, et al. Highly functional virus-specific cellular immune response in asymptomatic SARS-CoV-2 infection. *J Exp Med* (2021) 218:1–13. doi: 10.1084/jem.20202617

63. Kamada T, Togashi Y, Tay C, Ha D, Sasaki A, Nakamura Y, et al. PD-1+ regulatory T cells amplified by PD-1 blockade promote hyperprogression of cancer. *Proc Natl Acad Sci U.S.A.* (2019) 116:9999–10008. doi: 10.1073/pnas.1822001116

64. Antonioli L, Pacher P, Vizi ES. Haskó G CD39 and CD73 in immunity and inflammation. *Trends Mol Med* (2013) 19:355–67. doi: 10.1016/j.molmed.2013.03.005

65. Allard B, Longhi MS, Robson SC, Stagg J. The ectonucleotidases CD39 and CD73: novel checkpoint inhibitor targets. *Immunol Rev* (2017) 276:121–44. doi: 10.1111/imr.12528

66. Battastini AMO, Figueiró F, Leal DBR, Doleski PH, Schetinger MRC. CD39 and CD73 as promising therapeutic targets: What could be the limitations? *Fron Pharmacol* (2021) 12:633603. doi: 10.3389/fphar.2021.633603

67. Peres RS, Liew FY, Talbot J, Carregaro V, Oliveira RD, Almeida SL, et al. Low expression of CD39 on regulatory T cells as a biomarker for resistance to methotrexate therapy in rheumatoid arthritis. *Proc Natl Acad Sci U.S.A.* (2015) 112:2509–14. doi: 10.1073/pnas.1424792112

68. Gupta V, Katiyar S, Singh A, Misra R, Aggarwal A. CD39 positive regulatory T cell frequency as a biomarker of treatment response to methotrexate in rheumatoid arthritis. *Int J Rheum Dis* (2018) 21:1548–56. doi: 10.1111/1756-185X.13333

69. Zacca ER, Vesely MCA, Ferrero PV, Acosta CDV, Ponce NE, Bossio SN, et al. B cells from patients with rheumatoid arthritis show conserved CD39-mediated regulatory function and increased CD39 expression after positive response to therapy. *J Mol Biol* (2021) 433:1–11. doi: 10.1016/j.jmb.2020.10.021

70. Gu J, Ni X, Pan X, Lu H, Lu Y, Zhao J, et al. Human CD39^{hi} regulatory T cells present stronger stability and function under inflammatory conditions. *Cell Mol Immunol* (2017) 14:521–8. doi: 10.1038/cmi.2016.30

71. Gordon-Smith SB, Ursu S, Eaton S, Moncrieffe H, Wedderburn LR. Correlation of low CD73 expression on synovial lymphocytes with reduced adenosine generation and higher disease severity in juvenile idiopathic arthritis. *Arthritis Rheumatol* (2015) 67:545–54. doi: 10.1002/art.38959

72. Chrobak P, Charlebois R, Rejtar P, Bikai RE, Allard B, Stagg J. CD73 plays a protective role in collagen-induced arthritis. *J Immunol* (2015) 194:2487–92. doi: 10.4049/jimmunol.1401416

73. Bartleson JM, Radenkovic D, Covarrubias AJ, Furman D, Winer DA, Verdin E. SARS-CoV-2, COVID-19, and the ageing immune system. *Nat Aging* (2021) 1:769–82. doi: 10.1038/s43587-021-00114-7

74. Secolin R, Araujo TK, Gonsales MC, Rocha CS, Naslavsky M, Marco L, et al. Genetic variability in COVID-19-related genes in the Brazilian population. *Hum Genome Var* (2021) 8:1–9. doi: 10.1038/s41439-021-00146-w

frontiers | Frontiers in Immunology

TYPE Review
PUBLISHED 20 March 2023
DOI 10.3389/fimmu.2023.1070077

Check for updates

OPEN ACCESS

EDITED BY
Martijn van Griensven,
Maastricht University, Netherlands

REVIEWED BY
Yu Nee Lee,
Sheba Medical Center, Israel
Paul Goepfert,
University of Alabama at Birmingham,
United States

*CORRESPONDENCE
Apollinariya V. Bogolyubova
apollinariya.bogolyubova@gmail.com

SPECIALTY SECTION
This article was submitted to
Viral Immunology,
a section of the journal
Frontiers in Immunology

RECEIVED 14 October 2022
ACCEPTED 08 March 2023
PUBLISHED 20 March 2023

CITATION
Zornikova KV, Sheetikov SA, Rusinov AY, Iskhakov RN and Bogolyubova AV (2023) Architecture of the SARS-CoV-2-specific T cell repertoire.
Front. Immunol. 14:1070077.
doi: 10.3389/fimmu.2023.1070077

COPYRIGHT
© 2023 Zornikova, Sheetikov, Rusinov, Iskhakov and Bogolyubova. This is an open-access article distributed under the terms of the Creative Commons Attribution License (CC BY). The use, distribution or reproduction in other forums is permitted, provided the original author(s) and the copyright owner(s) are credited and that the original publication in this journal is cited, in accordance with accepted academic practice. No use, distribution or reproduction is permitted which does not comply with these terms.

Architecture of the SARS-CoV-2-specific T cell repertoire

Ksenia V. Zornikova[1], Saveliy A. Sheetikov[1,2], Alexander Yu Rusinov[1,2], Rustam N. Iskhakov[1,2] and Apollinariya V. Bogolyubova[1]*

[1]Laboratory of Transplantation Immunology, National Medical Research Center for Hematology, Moscow, Russia, [2]Faculty of Biology, Lomonosov Moscow State University, Moscow, Russia

The T cell response plays an indispensable role in the early control and successful clearance of SARS-CoV-2 infection. However, several important questions remain about the role of cellular immunity in COVID-19, including the shape and composition of disease-specific T cell repertoires across convalescent patients and vaccinated individuals, and how pre-existing T cell responses to other pathogens—in particular, common cold coronaviruses—impact susceptibility to SARS-CoV-2 infection and the subsequent course of disease. This review focuses on how the repertoire of T cell receptors (TCR) is shaped by natural infection and vaccination over time. We also summarize current knowledge regarding cross-reactive T cell responses and their protective role, and examine the implications of TCR repertoire diversity and cross-reactivity with regard to the design of vaccines that confer broader protection against SARS-CoV-2 variants.

KEYWORDS

T cell receptors, T cell immune response, SARS-CoV-2, T cell repertoire, T cell repertoire dynamic

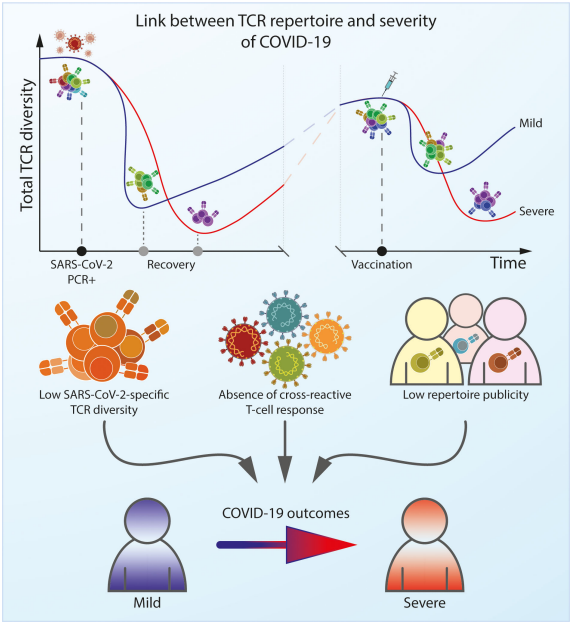

GRAPHICAL ABSTRACT

1 Introduction

The clinical manifestations and subsequent immune response to SARS-CoV-2 infection are diverse, with patients exhibiting a wide range of disease severity and susceptibility to future reinfections. T cells are crucial for early control and successful clearance of viral infections alongside the humoral response. The involvement of $CD4^+$ and $CD8^+$ T cells in the immune response reduces the severity of disease (1–3), and the presence of pre-existing SARS-CoV-2-specific T cells can prevent the development of COVID-19 (4, 5) and decrease the risk of reinfection (6). Accordingly, it has been shown that a subgroup of seronegative patients was partially protected from infection by T cells (7, 8). On the other hand, anergy of T cells is associated with a poor prognosis (9).

However, it is not only the magnitude of the T cell response but also its diversity that ultimately influences the outcome of infection (10, 11). Recently, researchers have focused on analyzing the dynamics of the TCR repertoire as an indicator of the immune response in autoimmune diseases such as multiple sclerosis (12) and rheumatoid arthritis (10), viral infections (13), and cancer (14). TCR repertoire analysis is also proving useful as a biomarker of the response to immunotherapy (15). The TCR repertoire can provide insights into immunodominance, functionality, and the protective effects of the T cell response (16, 17). Even though some conclusions may be ambiguous due to different approaches and consideration of both antigen-specific and non-antigen-specific data such as characteristics of overall TCR repertoire, TCR repertoire analysis offers a valuable tool for understanding the parameters of T cell-mediated immune responses to SARS-CoV-2 and the impact of viral mutations on immunological protection against newly-emerging SARS-CoV-2 variants.

2 Structure of the T cell repertoire and COVID-19 infection

The ability of the adaptive immune system to protect host organisms from a wide variety of pathogens is facilitated by the production of T cells that collectively express a large and diverse repertoire of unique TCRs. Naïve TCR diversity is generated by random rearrangement of the V and J segments of the TCR alpha (TCRα) genes and V, D, and J segments of the TCR beta (TCRβ) genes in maturing T cells within the thymus. But the ultimate structure of memory repertoire is shaped by interactions of these naïve cells with various pathogens over the course of a lifetime. The size, frequency, and publicity of individual clonotypes within a TCR repertoire can reveal both successful and failed immune responses, and recent studies have shown that the SARS-CoV-2-specific repertoire not only has its own architecture (18), but also differs depending on the severity of the disease and can change over time (19).

The SARS-CoV-2 proteome comprises at least 29 proteins (20), and as such, the number of potential epitopes is huge. However, the immunogenic regions of this proteome are unevenly distributed. ORF1 is the largest SARS-CoV-2 protein, and makes the largest contribution to T cell recognition, although the much-smaller ORF3 and Spike (S) proteins have a higher density of immunogenic epitopes compared to ORF1 (21). About 25% of the overall antigen-specific T cell response is accounted for S

protein response (22). Other structural proteins are highly recognized as well and accounted for roughly 55% of CD4+ and CD8+ T cell response (22, 23). Many immunogenic epitopes in SARS-CoV-2 have been identified (24–27). However, most of these do not achieve 100% immunogenicity in convalescent donors (5) and T cells of each individual recognize 30 to 40 different CD4+ and CD8+ epitopes (22). This can be explained by the fact that the structure of the TCR repertoire is mostly determined by the presence of specific HLA alleles (28, 29), as well as the fact that epitopes compete for antigen presentation (30). Moreover, different TCRs have different probabilities of formation during the recombination process, such that the frequency of naïve cells with such TCRs may vary (28, 31). Lastly, methods of assessing immunogenicity can differ in their sensitivity and specificity, and the structure of the repertoire may vary in different studies. One particularly important factor is the time of sampling: at the peak of infection, more than 10% of total $CD8^+$ T cells may be specific to a single SARS-CoV-2 epitope (21, 26). A month after infection, the frequency of most epitope-specific T cell populations is typically < 1% of total $CD8^+$ T cells (24, 32–35).

The abundance of a given memory T cell clonotype in blood does not correlate with the immunodominance of its corresponding epitope (32, 35, 36). For example, studies have shown that $CD8^+$ T cells specific to the highly immunogenic epitope YLQ are present at very low levels in the blood of convalescent donors (36, 37).

Limited diversity of T cell repertoire seems to be associated with severe disease (38, 39), whereas higher diversity is more likely to result in successful elimination of the virus. Multiple studies have found that the overall diversity of non-antigen-specific TCRs in blood samples taken from patients with COVID-19 is lower than that of healthy donors (40, 41), and is even lower in patients with severe disease. For example, a cohort of patients with pneumonia had a slightly less diverse overall TCR repertoire compared to those with mild disease (38) presumably due to expansion of SARS-CoV-2 specific T to defend against the infection cells in symptomatic and hospitalized individuals (42) On the other hand, low repertoire diversity may be a prognostic factor and explain the higher risk of serious illness and death in elderly patients (43–47), as it is well known that TCR repertoire diversity declines with aging, and this is also known to affect the antiviral response to other pathogens, such as the human influenza A virus (48, 49).

In general, peripheral selection and expansion of antigen-specific clonotypes driven by persistent pathogens leads to a higher proportion of shared clones among abundant clonotypes (50). The overlap of the overall non-antigen specific TCR repertoire between individuals is significantly higher in COVID-19 patients than in healthy individuals (41), and this is primarily because some epitopes of SARS-CoV-2 tend to give rise to shared, public clonotypes (35, 36, 51). Public clonotypes tend to have short CDR3 regions and arise from specific V(D)J-rearrangement events that occur with higher probability (28). Such clonotypes are thought to play a crucial role in establishing an effective pathogen-specific response and infection control of other pathogens like Cytomegalovirus (CMV), Epstein-Barr virus (EBV) and Adenovirus (52, 53).

Numerous studies have shown that the TCR repertoire in patients with mild COVID-19 infection remains relatively diverse within CDR3 central region, with high generation probability compare to severe patients (38). This leads to a broad range of SARS-CoV-2-specific sequences observed in mild disease, with many public CDR3 sequences (19, 36, 38, 54) This potentially explains why pneumonia patients have TCRs with longer CDR3 regions arising from lower-probability V(D)J-rearrangement events relative to the SARS-CoV-2-associated TCR repertoires in patients with mild disease, which also tend to prominently feature public clonotypes (38, 40). TCR repertoire profiles in asymptomatic infection is similar to mild disease (36).

It was demonstrated that preferential usage of V-, D-, and J- genes is significantly different in different viral infections including COVID-19 (55). Moreover, few studies demonstrated overrepresentation or underrepresentation of particular V-, D- and J-segments in patients with different COVID-19 clinical picture (55). Asymptomatic patients had overrepresentation of TRAV (TRAV17, TRAV12-1, TRAV19, TRAV35, and TRAV41), TRBV (TRBV12-5 and TRBV19) (56), TRAJ16 and TRBJ2-1 (57) genes compared to patients with symptoms. Frequency of TRAV2, TRAJ8, TRAJ40, TRBV3-1 and TRBV5-1 were the highest in symptomatic patients (57) while four TCBV gene segments (TRBV5-6, TRBV14, TRBV13 and TRBV24-1) were found to be overrepresented in severe patients with little Jβ gene-segment skewing (58). Another 25 sequences of the central part of the CDR3 region were found predictive for severe infection (54). The data suggest distinct clonal expansion influence on the disease progression.

3 Dynamics of the TCR repertoire after COVID-19 infection

During SARS-CoV-2 infection, the diversity and clonality of the antigen-specific TCR repertoire peaks within 8–14 days, then contracts slightly (25, 59) before returning to basal levels within one week after virus elimination (60). A SARS-CoV-2 specific TCR repertoire can be detected in the vast majority of convalescent patients, persisting for up to 15 months after viral clearance with a slight decrease (35, 42, 59) or even increase of clonal diversity (61). Moreover, SARS-CoV-2 epitope-specific T cells are able to proliferate in individuals who were vaccinated after infection (42) or in the re-detectable positive cases (Y. 62). Notably, SARS-CoV-1 specific T cells have demonstrated an impressive ability to persist for long periods of time, with one study detecting such clones up to 17 years after infection (63).

The durability of an antigen-specific response is determined by characteristics such as the publicity, diversity, and clonality of clonotypes recognizing that antigen (35, 51). It has been shown that long-term immunity is principally mediated by the clonal diversity of the antigen-specific T cell response (35, 61), whereas clonality does not appear to play a significant role (35). In some cases, however, dominant clones in the acute phase coincide with those found in the recovery phase (59). Numerous studies offer clear evidence that a highly diverse repertoire protects against a wide range of antigens of CMV, EBV and Human Immunodeficiency Virus-1 (HIV-1) (64, 65), and it is quite likely that such repertoires are associated with a higher level of avidity, affinity, and overall functionality (66, 67).

Despite numerous attempts to predict the longevity of virus-specific T cell immune response based on repertoire characteristics (35, 51, 68, 69), Bensouda Koraichi et al. study surmised that TCR clonotypes dynamic can be described by geometric Brownian motion. The model includes random unstimulated T cell proliferation and death, as well as asymptomatic or weakly symptomatic antigenic stimulation. However, the actual longevity of response varies from individual to individual, and in young individuals, the repertoire changes faster than in older individuals (70). Thus, at the moment, TCR clonotypes cannot be considered as the sole reliable predictor of the strength and effectiveness of the immune response.

4 Vaccine-induced T cell response and TCR repertoire

The high levels of mortality and morbidity associated with COVID-19 have prompted a massive, global vaccine development effort. At the time of writing this review, more than 170 vaccines have been developed, according to the World Health Organization (WHO) (https://www.who.int/publications/m/item/draft-landscape-of-covid-19-candidate-vaccines). Nearly a dozen of these are now in clinical use, and most demonstrate high efficiency in terms of protection (71, 72) and induce an immune response closely resembling that induced by infection in terms of immunophenotype, magnitude of $CD4^+$ response and antibody levels (73–75). However, vaccine-induced $CD8^+$ T cell expansion seems to be relatively weaker and with fewer distinct clonotype clusters compared to those induced by natural infection (76).

Only a small subset of vaccines consists of inactivated viral particles or mixtures of different viral proteins. Instead, the vast majority are aimed at inducing an immune response to the S protein (77). This approach produces a skewed T cell response that is enhanced against immunodominant epitopes (51) while also being targeted at less-dominant S-derived epitopes in vaccine recipients compared to convalescent individuals (78). In the aftermath of natural infection, the resulting $CD8^+$ T cell clones are likely to recognize a broader set of viral epitopes that are not encountered in vaccines (76), and this T cell repertoire also demonstrates a higher rate of cross-recognition of epitopes from common-cold coronaviruses (79). Nevertheless, the repertoire induced by S protein-based vaccines is generally capable of protecting against existing variants as well as emerging variants of concern (VOCs) (80–82).

The antigen-specific TCR repertoire induced by both the virus and vaccines undergoes significant clonal contraction over time (79), along with an overall decrease in immune response (35), and the only way to increase protection over the long term may be booster vaccination (78).

5 Changes in the previously primed TCR repertoire after vaccination

Over time, SARS-CoV-2-primed T cells transition to a memory phenotype, and the diversity of the SARS-CoV-2-specific TCR repertoire decreases alongside the humoral response in convalescent individuals (35). Since T cells and antibodies provide effective antiviral protection, the exhaustion of any of them leads to a decrease in protection properties, which was shown in the large-scale prospective study (8). However, the existence of a pool of memory cells is important for fending off the virus in future encounters, and the complete absence of SARS-CoV-2-specific antibodies and T cells may lead to reinfection, although neutralizing antibodies play more important role in protection from reinfection (83)

Vaccination offers a way to boost previously primed immunity, and it has been shown that the vaccine-induced cellular response is more robust in convalescent donors. Most convalescent individuals demonstrate the same level of T cell and humoral response as previously-unexposed individuals after one shot of mRNA vaccine (84). Because the antigen-specific $CD8^+$ T cell response develops more slowly than the $CD4^+$ T cell response after natural infection and primary vaccination (5), it reaches its maximum only after administration of the second vaccine dose (84).

Vaccine response patterns may differ due to the difficulty of involving naïve $CD8^+$ precursors in the immune response. While the vaccine-induced response of $CD4^+$ T cells includes both the recruitment of memory cells and the proliferation of new, unique S protein-specific $CD4^+$ T cells (79) in convalescent individuals, a rapid boost of S protein-specific $CD8^+$ T cells is predominantly provided by persisting early memory S protein-specific $CD38^-CD8^+$ T cells (85, 86). Moreover, the overall magnitude of the S protein-specific $CD8^+$ T cell response to vaccination in convalescent individuals is the same as in previously unexposed individuals due to the involvement of the memory compartment. However, it has been shown that vaccination selectively stimulates the expansion of S protein-specific clones and the contraction of clonotypes with non-S-protein specificity in convalescent donors (51).

SARS-CoV-2 mutations can reduce recognition of the virus by the $CD8^+$ T cell compartment, possibly due to escape from HLA binding (87), although the T cell response is generally capable of effectively responding to mutant viral strains (88, 89). Vaccine-induced T cell response was also preserved across different SARS-CoV-2 variants while B cell and neutralizing antibodies recognition was significantly reduced (90). Moreover T cell response may be enhanced with booster vaccination (78, 91). which substantially increase effectiveness of protection against reinfection from 24.7% with previous infection up to 41.8% with combination of infection and vaccination. However, the most important thing is that vaccination after infection is much more effective against hospital admission or severe disease than infection alone: the effectiveness of protection increased from 74.6% to 97.4% with vaccination (92).

Nevertheless, there remains a need for further vaccine optimization and the incorporation of more immunogenic epitopes (93) that can elicit more broadly protective T cell responses (81) even in the face of the emergence of new SARS-CoV-2 variants. This is especially important for the protection of immunocompromised individuals and elderly people, and despite a greater proportion of pre-existing memory T cells in the elderly compared to the young, booster vaccination has been shown to be

less effective in older individuals due to the minimal contribution of memory clonotypes in supporting high-quality T cell responses (94).

6 Cross-reactiveness of T cell repertoire

A more robust T cell response is also conferred by their capacity for cross-reactivity. A single T cell can cross-react to up to 10^6–10^7 foreign peptides (95), and this has been shown to be an essential feature of the T cell response (96–98). For some individuals who remain asymptomatic and seronegative even after close contact with COVID-19 patients (5), it has been shown that T cell-mediated protection may arise from cross-reactivity to T cells that target self-antigens and epitopes derived from various other pathogens including CMV, influenza A, EBV and HIV-1 (99, 100). Some parts of SARS-CoV-2 are very highly conserved relative to other 'common cold' human coronaviruses (HCoVs) (101, 102), and pre-existing protective T cells most likely originate from memory T cells derived after exposure to viruses such as HCoV-OC43, HCoV-HKU1, HCoV-NL63 and HCoV-229E (4), which circulate widely in the human population (63, 103, 104).

Some studies have shown that more than 20% of pre-pandemic samples contained SARS-CoV-2-reactive T cells (63, 103, 104), which protect patients from developing severe illness (105). But other research has failed to confirm such strong cross-reactivity, and has instead revealed that these cross-reactive T cells from pre-pandemic samples have a predominantly naïve phenotype, which means that they did not develop from an immune response to HCoVs (32, 77). This difference in results may be attributable to the choice of peptides used in the study. T cells specific to peptides that are conserved among coronaviruses are more abundant and tend to have a memory phenotype compared to those which recognize unique SARS-CoV-2 peptides. Notably, $CD8^+$ T cells that cross-react to these conserved epitopes are much more plentiful in patients with mild COVID-19 versus those with severe illness, suggesting a protective role (105). Moreover, TCR repertoires that recognize the same conserved peptides were similar in unexposed donors and convalescent individuals (106). Other studies have suggested that pre-existing T cells that react to SARS-CoV-2 RNA polymerase may also be associated with asymptomatic disease (4, 107).

One of the most cross-reactive epitopes in unexposed individuals is $SPRWYFYYL_{N105\text{-}113}$ (SPR) restricted in HLA-B*07:02 (77, 108). The immunodominance of SPR originates from a high frequency of naïve precursors in pre-pandemic samples. Many naïve SPR progenitors arise from a highly diverse TCRαß repertoire (77, 109), and a diverse SPR-specific $CD8^+$ T cell response with high functional avidity and antiviral effector functions has been detected in patients with mild disease compared to individuals with severe COVID-19 (108). Interestingly to note that only one SPR homologous epitope from HCoVs, LPRWYFYYL, has also demonstrated the ability to elicit a cross-reactive response (109). Other highly immunodominant epitopes, like $KPRQKRTAT_{N257\text{-}265}$ (KPR), $YLQPRTFLL_{S269\text{-}277}$ (YLQ), and $QYIKWPWYI_{S1208\text{-}1217}$ (QYI), have been shown to be abundant in pre-existing naïve T cell repertoires (32, 77, 108).

The importance of cross-reactive T cell response for protection against newly-emerging mutant strains is well established (110). New VOCs may be less susceptible to neutralizing antibodies (80, 111, 112), while T cells retain their protective capabilities (89, 113, 114). This protective capacity is shaped by the wide variety of epitopes recognized in different people (21). Nevertheless, the emergence of non-synonymous mutations in some T cell epitopes can lead to a decrease in peptide and MHC binding or a reduced ability to activate T cells (115, 116). However, such mutations are rarely found in VOCs, and it is likely that an epitope that evades presentation by one HLA allele will become presentable by the other (87). This mechanism may explain why the magnitude of T cell response to new variants is typically decreased by only 20–30% (89, 117).

It should also be noted that cross-recognition does not always provide protection, and can also be associated with worse disease outcomes; this suggests that other mechanisms are coming into play, including age-related differences in the involvement of different cell populations in the immune response (118). Several studies have examined the potential protective effects of Bacille Calmette–Guérin (BCG) immunization due to the presence of epitopes that resemble epitopes from SARS-CoV-2 (119, 120), but clinical trials have offered no evidence for such protection (121).

7 Conclusion

The severity of COVID-19 can vary from asymptomatic to lethal disease, and many different factors contribute to the outcome of infection, most notably including gender, ethnicity, health, and age (46, 47). However, demographics only partially explain the differences in mortality rates between countries (122), and numerous studies strongly point to the influence of the TCR repertoire on the ultimate course of infection. It has been shown that TCR repertoire diversity and clonality might determine the success of the immune response to both the virus and the vaccine, and several machine learning-based tools have been developed and applied in order to distinguish between convalescent and naive individuals (18) and predict disease outcomes (19, 54, 123) based on TCR repertoire. Despite high hopes and numerous studies of cross-reactive responses from pre-existing immunity to other HCoVs and other pathogens, protectiveness of cross-recognition is still debating (124). The studies to date have shown that protectiveness of cross-recognition in the context of prior infection with SARS-CoV-2 against reinfection is relatively low and waned to 24·7% at 12 months, but may be significantly improved with vaccination (92). Against this backdrop, the ongoing spread of SARS-CoV-2 and emergence of new, potentially immune-escaping VOCs reinforces the urgency of further optimizing the composition of vaccines based on insights derived from research into the T cell response against SARS-CoV-2.

Author contributions

AB, and KZ contributed to conception of the review. KZ wrote the first draft of the manuscript. KZ, SS, AR, and RI wrote sections of the manuscript. SS drew the graphical abstract. All authors contributed to manuscript revision, read, and approved the submitted version. All authors contributed to the article and approved the submitted version.

Funding

Russian Science Foundation grant 20-15-00395.

Conflict of interest

The authors declare that the research was conducted in the absence of any commercial or financial relationships that could be construed as a potential conflict of interest.

Publisher's note

All claims expressed in this article are solely those of the authors and do not necessarily represent those of their affiliated organizations, or those of the publisher, the editors and the reviewers. Any product that may be evaluated in this article, or claim that may be made by its manufacturer, is not guaranteed or endorsed by the publisher.

References

1. Liao M, Liu Y, Yuan J, Wen Y, Xu G, Zhao J, et al. Single-cell landscape of bronchoalveolar immune cells in patients with COVID-19. *Nat Med* (2020) 26(6):842–4. doi: 10.1038/s41591-020-0901-9

2. Rydyznski Moderbacher C, Ramirez SI, Dan JM, Grifoni A, Hastie KM, Weiskopf D, et al. Antigen-specific adaptive immunity to SARS-CoV-2 in acute COVID-19 and associations with age and disease severity. *Cell* (2020) 183(4):996–1012.e19. doi: 10.1016/j.cell.2020.09.038

3. Tan M, Liu Y, Zhou R, Deng X, Li F, Liang K, et al. Immunopathological characteristics of coronavirus disease 2019 cases in guangzhou, China. *Immunology* (2020) 160(3):261–8. doi: 10.1111/imm.13223

4. Swadling L, Diniz MO, Schmidt NM, Amin OE, Chandran A, Shaw E, et al. Pre-existing polymerase-specific T cells expand in abortive seronegative SARS-CoV-2. *Nature* (2022) 601(7891):110–7. doi: 10.1038/s41586-021-04186-8

5. Titov A, Shaykhutdinova R, Shcherbakova OV, Serdyuk YV, Sheetikov SA, Zornikova KV, et al. Immunogenic epitope panel for accurate detection of non-cross-reactive T cell response to SARS-CoV-2. *JCI Insight* (2022) 7(9). doi: 10.1172/jci.insight.157699

6. Wyllie D, Jones HE, Mulchandani R, Trickey A, Taylor-Phillips S, Brooks T, et al. SARS-CoV-2 responsive T cell numbers and anti-Spike IgG levels are both associated with protection from COVID-19: A prospective cohort study in keyworkers. *MedRxiv* (2021). doi: 10.1101/2020.11.02.20222778

7. Marasco V, Carniti C, Guidetti A, Farina L, Magni M, Miceli R, et al. T-Cell immune response after mRNA SARS-CoV-2 vaccines is frequently detected also in the absence of seroconversion in patients with lymphoid malignancies. *Br J Haematol* (2022) 196(3):548–58. doi: 10.1111/bjh.17877

8. Molodtsov IA, Kegeles E, Mitin AN, Mityaeva O, Musatova OE, Panova AE, et al. Severe acute respiratory syndrome coronavirus 2 (SARS-CoV-2)–specific T cells and antibodies in coronavirus disease 2019 (COVID-19) protection: A prospective study. *Clin Infect Dis* (2022) 75(1):e1–9. doi: 10.1093/cid/ciac278

9. Renner K, Schwittay T, Chaabane S, Gottschling J, Müller C, Tiefenböck C, et al. Severe T cell hyporeactivity in ventilated COVID-19 patients correlates with prolonged virus persistence and poor outcomes. *Nat Commun* (2021) 12(1):3006. doi: 10.1038/s41467-021-23334-2

10. Chang C-M, Hsu Y-W, Wong HS-C, Wei JC-C, Liu X, Liao H-T, et al. Characterization of T-cell receptor repertoire in patients with rheumatoid arthritis receiving biologic therapies. *Dis Markers* (2019) 2019:1–12. doi: 10.1155/2019/2364943

11. Wang F, Hou H, Yao Y, Wu S, Huang M, Ran X, et al. Systemically comparing host immunity between survived and deceased COVID-19 patients. *Cellular & Molecular Immunology* (2020) 17(8):875–7. doi: 10.1038/s41423-020-0483-y

12. Alves Sousa A, de P, Johnson KR, Ohayon J, Zhu J, Muraro PA, et al. Comprehensive analysis of TCR-β repertoire in patients with neurological immune-mediated disorders. *Sci Rep* (2019) 9(1):344. doi: 10.1038/s41598-018-36274-7

13. Krummey SM, Morris AB, Jacobs JR, McGuire DJ, Ando S, Tong KP, et al. CD45RB status of CD8+ T cell memory defines T cell receptor affinity and persistence. *Cell Rep* (2020) 30(5):1282–1291.e5. doi: 10.1016/j.celrep.2020.01.016

14. Reuben A, Zhang J, Chiou S-H, Gittelman RM, Li J, Lee W-C, et al. Comprehensive T cell repertoire characterization of non-small cell lung cancer. *Nat Commun* (2020) 11(1):603. doi: 10.1038/s41467-019-14273-0

15. Valpione S, Galvani E, Tweedy J, Mundra PA, Banyard A, Middlehurst P, et al. Immune awakening revealed by peripheral T cell dynamics after one cycle of immunotherapy. *Nat Cancer* (2020) 1(2):210–21. doi: 10.1038/s43018-019-0022-x

16. Messaoudi I, Patiño JAG, Dyall R, LeMaoult J, Nikolich-Žugich J. Direct link between *mhc* polymorphism, T cell avidity, and diversity in immune defense. *Science* (2002) 298(5599):1797–800. doi: 10.1126/science.1076064

17. Ndhlovu ZM, Kamya P, Mewalal N, Kløverpris HN, Nkosi T, Pretorius K, et al. Magnitude and kinetics of CD8+ T cell activation during hyperacute HIV infection impact viral set point. *Immunity* (2015) 43(3):591–604. doi: 10.1016/j.immuni.2015.08.012

18. Shoukat MS, Foers AD, Woodmansey S, Evans SC, Fowler A, Soilleux EJ. Use of machine learning to identify a T cell response to SARS-CoV-2. *Cell Rep Med* (2021) 2(2):100192. doi: 10.1016/j.xcrm.2021.100192

19. Schultheiß C, Paschold L, Simnica D, Mohme M, Willscher E, von Wenserski L, et al. Next-generation sequencing of T and b cell receptor repertoires from COVID-19 patients showed signatures associated with severity of disease. *Immunity* (2020) 53(2):442–455.e4. doi: 10.1016/j.immuni.2020.06.024

20. Rauti R, Shahoha M, Leichtmann-Bardoogo Y, Nasser R, Paz E, Tamir R, et al. Effect of SARS-CoV-2 proteins on vascular permeability. *ELife* (2021) 10. doi: 10.7554/eLife.69314

21. Saini SK, Hersby DS, Tamhane T, Povlsen HR, Hernandez SPA, Nielsen M, et al. SARS-CoV-2 genome-wide T cell epitope mapping reveals immunodominance and substantial CD8 $^{+}$ T cell activation in COVID-19 patients. *Sci Immunol* (2021) 6(58). doi: 10.1126/sciimmunol.abf7550

22. Tarke A, Sidney J, Kidd CK, Dan JM, Ramirez SI, Yu ED, et al. Comprehensive analysis of T cell immunodominance and immunoprevalence of SARS-CoV-2 epitopes in COVID-19 cases. *Cell Rep Med* (2021) 2(2):100204. doi: 10.1016/j.xcrm.2021.100204

23. Li L, Chen Q, Han X, Shen M, Hu C, Chen S, et al. T Cell immunity evaluation and immunodominant epitope T cell receptor identification of severe acute respiratory syndrome coronavirus 2 spike glycoprotein in COVID-19 convalescent patients. *Front Cell Dev Biol* (2021) 9:696662. doi: 10.3389/fcell.2021.696662

24. Ferretti AP, Kula T, Wang Y, Nguyen DMV, Weinheimer A, Dunlap GS, et al. Unbiased screens show CD8+ T cells of COVID-19 patients recognize shared epitopes in SARS-CoV-2 that largely reside outside the spike protein. *Immunity* (2020) 53(5):1095–1107.e3. doi: 10.1016/j.immuni.2020.10.006

25. Snyder TM, Gittelman RM, Klinger M, May DH, Osborne EJ, Taniguchi R, et al. Magnitude and dynamics of the T-cell response to SARS-CoV-2 infection at both individual and population levels. *MedRxiv* (2020). doi: 10.1101/2020.07.31.20165647

26. Gangaev A, Ketelaars SLC, Isaeva OI, Patiwael S, Dopler A, Hoefakker K, et al. Identification and characterization of a SARS-CoV-2 specific CD8+ T cell response with immunodominant features. *Nat Commun* (2021) 12(1):2593. doi: 10.1038/s41467-021-22811-y

27. Schulien I, Kemming J, Oberhardt V, Wild K, Seidel LM, Killmer S, et al. Characterization of pre-existing and induced SARS-CoV-2-specific CD8+ T cells. *Nat Med* (2021) 27(1):78–85. doi: 10.1038/s41591-020-01143-2

28. Pogorelyy MV, Fedorova AD, McLaren JE, Ladell K, Bagaev DV, Eliseev AV, et al. Exploring the pre-immune landscape of antigen-specific T cells. *Genome Med* (2018) 10(1):68. doi: 10.1186/s13073-018-0577-7

29. Fischer JC, Schmidt AG, Bölke E, Uhrberg M, Keitel V, Feldt T, et al. Association of HLA genotypes, AB0 blood type and chemokine receptor 5 mutant CD195 with the clinical course of COVID-19. *Eur J Med Res* (2021) 26(1):107. doi: 10.1186/s40001-021-00560-4

30. Adorini L, Nagy ZA. Peptide competition for antigen presentation. *Immunol Today* (1990) 11:21–4. doi: 10.1016/0167-5699(90)90006-U

31. Jackson KJL, Kidd MJ, Wang Y, Collins AM. The shape of the lymphocyte receptor repertoire: Lessons from the b cell receptor. *Front Immunol* (2013) 4:263. doi: 10.3389/fimmu.2013.00263

32. Habel JR, Nguyen THO, van de Sandt CE, Juno JA, Chaurasia P, Wragg K, et al. Suboptimal SARS-CoV-2–specific CD8 $^{+}$ T cell response associated with the prominent HLA-A*02:01 phenotype. *Proc Natl Acad Sci* (2020) 117(39):24384–91. doi: 10.1073/pnas.2015486117

33. Peng Y, Mentzer AJ, Liu G, Yao X, Yin Z, Dong D, et al. Broad and strong memory CD4+ and CD8+ T cells induced by SARS-CoV-2 in UK convalescent individuals following COVID-19. *Nat Immunol* (2020) 21(11):1336–45. doi: 10.1038/s41590-020-0782-6

34. Kared H, Redd AD, Bloch EM, Bonny TS, Sumatoh H, Kairi F, et al. SARS-CoV-2–specific CD8+ T cell responses in convalescent COVID-19 individuals. *J Clin Invest* (2021) 131(5). doi: 10.1172/JCI145476

35. Zornikova KV, Khmelevskaya A, Sheetikov SA, Kiryukhin DO, Shcherbakova OV, Titov A, et al. Clonal diversity predicts persistence of SARS-CoV-2 epitope-specific T-cell response. *Commun Biol* (2022) 5(1):1351. doi: 10.1038/s42003-022-04250-7

36. Shomuradova AS, Vagida MS, Sheetikov SA, Zornikova K, Kiryukhin D, Titov A, et al. SARS-CoV-2 epitopes are recognized by a public and diverse repertoire of human T cell receptors. *Immunity* (2020) 53(6):1245–1257.e5. doi: 10.1016/j.immuni.2020.11.004

37. Nguyen THO, Rowntree LC, Petersen J, Chua BY, Hensen L, Kedzierski L, et al. CD8+ T cells specific for an immunodominant SARS-CoV-2 nucleocapsid epitope display high naive precursor frequency and TCR promiscuity. *Immunity* (2021) 54 (5):1066–1082.e5. doi: 10.1016/j.immuni.2021.04.009

38. Chang C-M, Feng P, Wu T-H, Alachkar H, Lee K-Y, Chang W-C. Profiling of T cell repertoire in SARS-CoV-2-Infected COVID-19 patients between mild disease and pneumonia. *J Clin Immunol* (2021) 41(6):1131–45. doi: 10.1007/s10875-021-01045-z

39. Salomé B, Horowitz A. Impaired CD4 T-cell response to SARS-CoV-2: Rationale for PD-1 blockade in patients with cancer and COVID-19? *Cancer Discovery* (2021) 11(8):1877–8. doi: 10.1158/2159-8290.CD-21-0613

40. Park JJ, Lee KA, Lam SZ, Moon KS, Fang Z, Chen S. Machine learning identifies T cell receptor repertoire signatures associated with COVID-19 severity. *Commun Biol* (2023) 6(1):76. doi: 10.1038/s42003-023-04447-4

41. Wang G, Wang Y, Jiang S, Fan W, Mo C, Gong W, et al. Comprehensive analysis of TCR repertoire of COVID-19 patients in different infected stage. *Genes Genomics* (2022) 44(7):813–22. doi: 10.1007/s13258-022-01261-w

42. Gittelman RM, Lavezzo E, Snyder TM, Zahid HJ, Carty CL, Elyanow R, et al. Longitudinal analysis of T cell receptor repertoires reveals shared patterns of antigen-specific response to SARS-CoV-2 infection. *JCI Insight* (2022) 7(10). doi: 10.1172/jci.insight.151849

43. Grasselli G, Zangrillo A, Zanella A, Antonelli M, Cabrini L, Castelli A, et al. Baseline characteristics and outcomes of 1591 patients infected with SARS-CoV-2 admitted to ICUs of the Lombardy region, Italy. *JAMA* (2020) 323(16):1574. doi: 10.1001/jama.2020.5394

44. Gutierrez L, Beckford J, Alachkar H. Deciphering the TCR repertoire to solve the COVID-19 mystery. *Trends Pharmacol Sci* (2020) 41(8):518–30. doi: 10.1016/j.tips.2020.06.001

45. Ruan Q, Yang K, Wang W, Jiang L, Song J. Clinical predictors of mortality due to COVID-19 based on an analysis of data of 150 patients from wuhan, China. *Intensive Care Med* (2020) 46(5):846–8. doi: 10.1007/s00134-020-05991-x

46. Wu Z, McGoogan JM. Characteristics of and important lessons from the coronavirus disease 2019 (COVID-19) outbreak in China. *JAMA* (2020) 323 (13):1239. doi: 10.1001/jama.2020.2648

47. Zhou F, Yu T, Du R, Fan G, Liu Y, Liu Z, et al. Clinical course and risk factors for mortality of adult inpatients with COVID-19 in wuhan, China: a retrospective cohort study. *Lancet* (2020) 395(10229):1054–62. doi: 10.1016/S0140-6736(20)30566-3

48. Gil A, Yassai MB, Naumov YN, Selin LK. Narrowing of human influenza a virus-specific T cell receptor α and β repertoires with increasing age. *J Virol* (2015) 89 (8):4102–16. doi: 10.1128/JVI.03020-14

49. Nguyen THO, Sant S, Bird NL, Grant EJ, Clemens EB, Koutsakos M, et al. Perturbed CD8+ T cell immunity across universal influenza epitopes in the elderly. *J Leukocyte Biol* (2018) 103(2):321–39. doi: 10.1189/jlb.5MA0517-207R

50. Chandran SS, Paria BC, Srivastava AK, Rothermel LD, Stephens DJ, Dudley ME, et al. Persistence of CTL clones targeting melanocyte differentiation antigens was insufficient to mediate significant melanoma regression in humans. *Clin Cancer Res* (2015) 21(3):534–43. doi: 10.1158/1078-0432.CCR-14-2208

51. Minervina AA, Pogorelyy MV, Kirk AM, Crawford JC, Allen EK, Chou C-H, et al. SARS-CoV-2 antigen exposure history shapes phenotypes and specificity of memory CD8+ T cells. *Nat Immunol* (2022) 23(5):781–90. doi: 10.1038/s41590-022-01184-4

52. Zhao Y, Nguyen P, Ma J, Wu T, Jones LL, Pei D, et al. Preferential use of public TCR during autoimmune encephalomyelitis. *J Immunol* (2016) 196(12):4905–14. doi: 10.4049/jimmunol.1501029

53. Huisman W, Hageman L, Leboux DAT, Khmelevskaya A, Efimov GA, Roex MCJ, et al. Public T-cell receptors (TCRs) revisited by analysis of the magnitude of identical and highly-similar TCRs in virus-specific T-cell repertoires of healthy individuals. *Front Immunol* (2022) 13:851868. doi: 10.3389/fimmu.2022.851868

54. Sidhom J-W, Baras AS. Deep learning identifies antigenic determinants of severe SARS-CoV-2 infection within T-cell repertoires. *Sci Rep* (2021) 11(1):14275. doi: 10.1038/s41598-021-93608-8

55. Wang P, Jin X, Zhou W, Luo M, Xu Z, Xu C, et al. Comprehensive analysis of TCR repertoire in COVID-19 using single cell sequencing. *Genomics* (2021) 113 (2):456–62. doi: 10.1016/j.ygeno.2020.12.036

56. Sen K, Datta S, Ghosh A, Jha A, Ahad A, Chatterjee S, et al. Single-cell immunogenomic approach identified SARS-CoV-2 protective immune signatures in asymptomatic direct contacts of COVID-19 cases. *Front Immunol* (2021) 12:733539. doi: 10.3389/fimmu.2021.733539

57. Bai H, Ma J, Mao W, Zhang X, Nie Y, Hao J, et al. Identification of TCR repertoires in asymptomatic COVID-19 patients by single-cell T-cell receptor sequencing. *Blood Cells Molecules Dis* (2022) 97:102678. doi: 10.1016/j.bcmd.2022.102678

58. Cheng MH, Zhang S, Porritt RA, Noval Rivas M, Paschold L, Willscher E, et al. Superantigenic character of an insert unique to SARS-CoV-2 spike supported by skewed TCR repertoire in patients with hyperinflammation. *Proc Natl Acad Sci* (2020) 117(41):25254–62. doi: 10.1073/pnas.2010722117

59. Adamo S, Michler J, Zurbuchen Y, Cervia C, Taeschler P, Raeber ME, et al. Signature of long-lived memory CD8+ T cells in acute SARS-CoV-2 infection. *Nature* (2022) 602(7895):148–55. doi: 10.1038/s41586-021-04280-x

60. Luo L, Liang W, Pang J, Xu G, Chen Y, Guo X, et al. Dynamics of TCR repertoire and T cell function in COVID-19 convalescent individuals. *Cell Discovery* (2021) 7 (1):89. doi: 10.1038/s41421-021-00321-x

61. Bilich T, Nelde A, Heitmann JS, Maringer Y, Roerden M, Bauer J, et al. T Cell and antibody kinetics delineate SARS-CoV-2 peptides mediating long-term immune responses in COVID-19 convalescent individuals. *Sci Trans Med* (2021) 13(590). doi: 10.1126/scitranslmed.abf7517

62. Li Y, Hu J, Wang Y, Liu D, Shi Y, Zhang J, et al. T-Cell repertoire characteristics of asymptomatic and re-detectable positive COVID-19 patients. *Front Immunol* (2022) 12:769442. doi: 10.3389/fimmu.2021.769442

63. le Bert N, Tan AT, Kunasegaran K, Tham CYL, Hafezi M, Chia A, et al. SARS-CoV-2-specific T cell immunity in cases of COVID-19 and SARS, and uninfected controls. *Nature* (2020) 584(7821):457–62. doi: 10.1038/s41586-020-2550-z

64. Miconnet I, Marrau A, Farina A, Taffé P, Vigano S, Harari A, et al. Large TCR diversity of virus-specific CD8 T cells provides the mechanistic basis for massive TCR renewal after antigen exposure. *J Immunol* (2011) 186(12):7039–49. doi: 10.4049/jimmunol.1003309

65. Dash P, Fiore-Gartland AJ, Hertz T, Wang GC, Sharma S, Souquette A, et al. Quantifiable predictive features define epitope-specific T cell receptor repertoires. *Nature* (2017) 547(7661):89–93. doi: 10.1038/nature22383

66. Price DA, Brenchley JM, Ruff LE, Betts MR, Hill BJ, Roederer M, et al. Avidity for antigen shapes clonal dominance in CD8+ T cell populations specific for persistent DNA viruses. *J Exp Med* (2005) 202(10):1349–61. doi: 10.1084/jem.20051357

67. Zehn D, Lee SY, Bevan MJ. Complete but curtailed T-cell response to very low-affinity antigen. *Nature* (2009) 458(7235):211–4. doi: 10.1038/nature07657

68. Sant S, Grzelak L, Wang Z, Pizzolla A, Koutsakos M, Crowe J, et al. Single-cell approach to influenza-specific CD8+ T cell receptor repertoires across different age groups, tissues, and following influenza virus infection. *Front Immunol* (2018) 9:1453. doi: 10.3389/fimmu.2018.01453

69. Attaf M, Roider J, Malik A, Rius Rafael C, Dolton G, Prendergast AJ, et al. Cytomegalovirus-mediated T cell receptor repertoire perturbation is present in early life. *Front Immunol* (2020) 11:1587. doi: 10.3389/fimmu.2020.01587

70. Bensouda Koraichi M, Ferri S, Walczak AM, Mora T. Inferring the T cell repertoire dynamics of healthy individuals. *Proc Natl Acad Sci* (2023) 120(4). doi: 10.1073/pnas.2207516120

71. Fiolet T, Kherabi Y, MacDonald C-J, Ghosn J, Peiffer-Smadja N. Comparing COVID-19 vaccines for their characteristics, efficacy and effectiveness against SARS-CoV-2 and variants of concern: a narrative review. *Clin Microbiol Infection* (2022) 28 (2):202–21. doi: 10.1016/j.cmi.2021.10.005

72. Ssentongo P, Ssentongo AE, Voleti N, Groff D, Sun A, Ba DM, et al. SARS-CoV-2 vaccine effectiveness against infection, symptomatic and severe COVID-19: a systematic review and meta-analysis. *BMC Infect Dis* (2022) 22(1):439. doi: 10.1186/s12879-022-07418-y

73. Keech C, Albert G, Cho I, Robertson A, Reed P, Neal S, et al. Phase 1–2 trial of a SARS-CoV-2 recombinant spike protein nanoparticle vaccine. *New Engl J Med* (2020) 383(24):2320–32. doi: 10.1056/NEJMoa2026920

74. Krammer F. SARS-CoV-2 vaccines in development. *Nature* (2020) 586 (7830):516–27. doi: 10.1038/s41586-020-2798-3

75. Ewer KJ, Barrett JR, Belij-Rammerstorfer S, Sharpe H, Makinson R, Morter R, et al. T Cell and antibody responses induced by a single dose of ChAdOx1 nCoV-19 (AZD1222) vaccine in a phase 1/2 clinical trial. *Nat Med* (2021) 27(2):270–8. doi: 10.1038/s41591-020-01194-5

76. Sureshchandra S, Lewis SA, Doratt BM, Jankeel A, Coimbra Ibraim I, Messaoudi I. Single-cell profiling of T and b cell repertoires following SARS-CoV-2 mRNA vaccine. *JCI Insight* (2021) 6(24). doi: 10.1172/jci.insight.153201

77. Nguyen THO, Cohen CA, Rowntree LC, Bull MB, Hachim A, Kedzierska K, et al. T Cells targeting SARS-CoV-2: By infection, vaccination, and against future variants. *Front Med* (2021) 8:793102. doi: 10.3389/fmed.2021.793102

78. Lang-Meli J, Luxenburger H, Wild K, Karl V, Oberhardt V, Salimi Alizei E, et al. SARS-CoV-2-specific T-cell epitope repertoire in convalescent and mRNA-vaccinated individuals. *Nat Microbiol* (2022) 7(5):675–9. doi: 10.1038/s41564-022-01106-y

79. Dykema AG, Zhang B, Woldemeskel BA, Garliss CC, Rashid R, Westlake T, et al. SARS-CoV-2 vaccination diversifies the CD4+ spike-reactive T cell repertoire in patients with prior SARS-CoV-2 infection. *EBioMedicine* (2022) 80:104048. doi: 10.1016/j.ebiom.2022.104048

80. Alter G, Yu J, Liu J, Chandrashekar A, Borducchi EN, Tostanoski LH, et al. Immunogenicity of Ad26.COV2.S vaccine against SARS-CoV-2 variants in humans. *Nature* (2021) 596(7871):268–72. doi: 10.1038/s41586-021-03681-2

81. Tarke A, Sidney J, Methot N, Yu ED, Zhang Y, Dan JM, et al. Impact of SARS-CoV-2 variants on the total CD4+ and CD8+ T cell reactivity in infected or vaccinated individuals. *Cell Rep Med* (2021) 2(7):100355. doi: 10.1016/j.xcrm.2021.100355

82. Ballesteros-Sanabria L, Pelaez-Prestel HF, Ras-Carmona A, Reche PA. Resilience of spike-specific immunity induced by COVID-19 vaccines against SARS-CoV-2 variants. *Biomedicines* (2022) 10(5):996. doi: 10.3390/biomedicines10050996

83. Cromer D, Steain M, Reynaldi A, Schlub TE, Wheatley AK, Juno JA, et al. Neutralising antibody titres as predictors of protection against SARS-CoV-2 variants and the impact of boosting: a meta-analysis. *Lancet Microbe* (2022) 3(1):e52–61. doi: 10.1016/S2666-5247(21)00267-6

84. Painter MM, Mathew D, Goel RR, Apostolidis SA, Pattekar A, Kuthuru O, et al. Rapid induction of antigen-specific CD4+ T cells is associated with coordinated humoral and cellular immunity to SARS-CoV-2 mRNA vaccination. *Immunity* (2021) 54(9):2133–2142.e3. doi: 10.1016/j.immuni.2021.08.001

85. Mazzoni A, di Lauria N, Maggi L, Salvati L, Vanni A, Capone M, et al. First-dose mRNA vaccination is sufficient to reactivate immunological memory to SARS-CoV-2 in subjects who have recovered from COVID-19. *J Clin Invest* (2021) 131(12). doi: 10.1172/JCI149150

86. Oberhardt V, Luxenburger H, Kemming J, Schulien I, Ciminski K, Giese S, et al. Rapid and stable mobilization of CD8+ T cells by SARS-CoV-2 mRNA vaccine. *Nature* (2021) 597(7875):268–73. doi: 10.1038/s41586-021-03841-4

87. Nersisyan S, Zhiyanov A, Shkurnikov M, Tonevitsky A. T-CoV: a comprehensive portal of HLA-peptide interactions affected by SARS-CoV-2 mutations. *Nucleic Acids Res* (2022) 50(D1):D883–7. doi: 10.1093/nar/gkab701

88. GeurtsvanKessel CH, Geers D, Schmitz KS, Mykytyn AZ, Lamers MM, Bogers S, et al. Divergent SARS-CoV-2 omicron–reactive T and b cell responses in COVID-19 vaccine recipients. *Sci Immunol* (2022) 7(69). doi: 10.1126/sciimmunol.abo2202

89. Keeton R, Tincho MB, Ngomti A, Baguma R, Benede N, Suzuki A, et al. T Cell responses to SARS-CoV-2 spike cross-recognize omicron. *Nature* (2022) 603 (7901):488–92. doi: 10.1038/s41586-022-04460-3

90. Tarke A, Coelho CH, Zhang Z, Dan JM, Yu ED, Methot N, et al. SARS-CoV-2 vaccination induces immunological T cell memory able to cross-recognize variants from alpha to omicron. *Cell* (2022) 185(5):847–859.e11. doi: 10.1016/j.cell.2022.01.015

91. Naranbhai V, Nathan A, Kaseke C, Berrios C, Khatri A, Choi S, et al. T Cell reactivity to the SARS-CoV-2 omicron variant is preserved in most but not all individuals. *Cell* (2022) 185(6):1041–1051.e6. doi: 10.1016/j.cell.2022.01.029

92. Bobrovitz N, Ware H, Ma X, Li Z, Hosseini R, Cao C, et al. Protective effectiveness of previous SARS-CoV-2 infection and hybrid immunity against the omicron variant and severe disease: a systematic review and meta-regression. *Lancet Infect Dis* (2023). doi: 10.1016/S1473-3099(22)00801-5

93. Nathan A, Rossin EJ, Kaseke C, Park RJ, Khatri A, Koundakjian D, et al. Structure-guided T cell vaccine design for SARS-CoV-2 variants and sarbecoviruses. *Cell* (2021) 184(17):4401–4413.e10. doi: 10.1016/j.cell.2021.06.029

94. Saggau C, Martini GR, Rosati E, Meise S, Messner B, Kamps A-K, et al. The pre-exposure SARS-CoV-2-specific T cell repertoire determines the quality of the immune response to vaccination. *Immunity* (2022) 55(10):1924–39.e5. doi: 10.1016/j.immuni.2022.08.003

95. Mason D. A very high level of crossreactivity is an essential feature of the T-cell receptor. *Immunol Today* (1998) 19(9):395–404. doi: 10.1016/S0167-5699(98)01299-7

96. Sewell AK. Why must T cells be cross-reactive? *Nat Rev Immunol* (2012) 12 (9):669–77. doi: 10.1038/nri3279

97. Wooldridge L, Ekeruche-Makinde J, van den Berg HA, Skowera A, Miles JJ, Tan MP, et al. A single autoimmune T cell receptor recognizes more than a million different peptides. *J Biol Chem* (2012) 287(2):1168–77. doi: 10.1074/jbc.M111.289488

98. Lee CH, Salio M, Napolitani G, Ogg G, Simmons A, Koohy H. Predicting cross-reactivity and antigen specificity of T cell receptors. *Front Immunol* (2020) 11:565096. doi: 10.3389/fimmu.2020.565096

99. Mahajan S, Kode V, Bhojak K, Karunakaran C, Lee K, Manoharan M, et al. Immunodominant T-cell epitopes from the SARS-CoV-2 spike antigen reveal robust pre-existing T-cell immunity in unexposed individuals. *Sci Rep* (2021) 11(1):13164. doi: 10.1038/s41598-021-92521-4

100. Buckley PR, Lee CH, Pereira Pinho M, Ottakandathil Babu R, Woo J, Antanaviciute A, et al. HLA-dependent variation in SARS-CoV-2 CD8 $^+$ T cell cross-reactivity with human coronaviruses. *Immunology* (2022) 166(1):78–103. doi: 10.1111/imm.13451

101. Tan CCS, Owen CJ, Tham CYL, Bertoletti A, van Dorp L, Balloux F. Pre-existing T cell-mediated cross-reactivity to SARS-CoV-2 cannot solely be explained by prior exposure to endemic human coronaviruses. *Infection Genet Evol* (2021) 95:105075. doi: 10.1016/j.meegid.2021.105075

102. Zhang B, Tian J, Zhang Q, Xie Y, Wang K, Qiu S, et al. Comparing the nucleocapsid proteins of human coronaviruses: Structure, immunoregulation, vaccine, and targeted drug. *Front Mol Biosci* (2022) 9:761173. doi: 10.3389/fmolb.2022.761173

103. Grifoni A, Weiskopf D, Ramirez SI, Mateus J, Dan JM, Moderbacher CR, et al. Targets of T cell responses to SARS-CoV-2 coronavirus in humans with COVID-19 disease and unexposed individuals. *Cell* (2020) 181(7):1489–1501.e15. doi: 10.1016/j.cell.2020.05.015

104. Weiskopf D, Schmitz KS, Raadsen MP, Grifoni A, Okba NMA, Endeman H, et al. Phenotype and kinetics of SARS-CoV-2–specific T cells in COVID-19 patients with acute respiratory distress syndrome. *Sci Immunol* (2020) 5(48). doi: 10.1126/sciimmunol.abd2071

105. Mallajosyula V, Ganjavi C, Chakraborty S, McSween AM, Pavlovitch-Bedzyk AJ, Wilhelmy J, et al. CD8 $^+$ T cells specific for conserved coronavirus epitopes correlate with milder disease in patients with COVID-19. *Sci Immunol* (2021) 6(61). doi: 10.1126/sciimmunol.abg5669

106. Hu W, He M, Wang X, Sun Q, Kuang M. Specific CD8+ TCR repertoire recognizing conserved antigens of SARS-CoV-2 in unexposed population: A prerequisite for broad-spectrum CD8+ T cell immunity. *Vaccines* (2021) 9(10):1093. doi: 10.3390/vaccines9101093

107. Nesterenko PA, McLaughlin J, Tsai BL, Burton Sojo G, Cheng D, Zhao D, et al. HLA-A*02:01 restricted T cell receptors against the highly conserved SARS-CoV-2 polymerase cross-react with human coronaviruses. *Cell Rep* (2021) 37(13):110167. doi: 10.1016/j.celrep.2021.110167

108. Peng Y, Felce SL, Dong D, Penkava F, Mentzer AJ, Yao X, et al. An immunodominant NP105–113-B*07:02 cytotoxic T cell response controls viral replication and is associated with less severe COVID-19 disease. *Nat Immunol* (2022) 23(1):50–61. doi: 10.1038/s41590-021-01084-z

109. Lineburg KE, Grant EJ, Swaminathan S, Chatzileontiadou DSM, Szeto C, Sloane H, et al. CD8+ T cells specific for an immunodominant SARS-CoV-2 nucleocapsid epitope cross-react with selective seasonal coronaviruses. *Immunity* (2021) 54(5):1055–1065.e5. doi: 10.1016/j.immuni.2021.04.006

110. Goel RR, Painter MM, Apostolidis SA, Mathew D, Meng W, Rosenfeld AM, et al. mRNA vaccines induce durable immune memory to SARS-CoV-2 and variants of concern. *Science* (2021) 374(6572). doi: 10.1126/science.abm0829

111. Cele S, Gazy I, Jackson L, Hwa S-H, Tegally H, Lustig G, et al. Escape of SARS-CoV-2 501Y.V2 from neutralization by convalescent plasma. *Nature* (2021) 593 (7857):142–6. doi: 10.1038/s41586-021-03471-w

112. Tegally H, Wilkinson E, Giovanetti M, Iranzadeh A, Fonseca V, Giandhari J, et al. Detection of a SARS-CoV-2 variant of concern in south Africa. *Nature* (2021) 592 (7854):438–43. doi: 10.1038/s41586-021-03402-9

113. Geers D, Shamier MC, Bogers S, den Hartog G, Gommers L, Nieuwkoop NN, et al. SARS-CoV-2 variants of concern partially escape humoral but not T cell responses in COVID-19 convalescent donors and vaccine recipients. *Sci Immunol* (2021) 6(59). doi: 10.1126/sciimmunol.abj1750

114. Riou C, Keeton R, Moyo-Gwete T, Hermanus T, Kgagudi P, Baguma R, et al. Escape from recognition of SARS-CoV-2 variant spike epitopes but overall preservation of T cell immunity. *Sci Trans Med* (2022) 14(631). doi: 10.1126/scitranslmed.abj6824

115. Agerer B, Koblischke M, Gudipati V, Montaño-Gutierrez LF, Smyth M, Popa A, et al. SARS-CoV-2 mutations in MHC-i-restricted epitopes evade CD8 $^+$ T cell responses. *Sci Immunol* (2021) 6(57). doi: 10.1126/sciimmunol.abg6461

116. Wu D, Kolesnikov A, Yin R, Guest JD, Gowthaman R, Shmelev A, et al. Structural assessment of HLA-A2-restricted SARS-CoV-2 spike epitopes recognized by public and private T-cell receptors. *Nat Commun* (2022) 13(1):19. doi: 10.1038/s41467-021-27669-8

117. Gao Y, Cai C, Grifoni A, Müller TR, Niessl J, Olofsson A, et al. Ancestral SARS-CoV-2-specific T cells cross-recognize the omicron variant. *Nat Med* (2022) 28(3):472–6. doi: 10.1038/s41591-022-01700-x

118. Jo N, Zhang R, Ueno H, Yamamoto T, Weiskopf D, Nagao M, et al. Aging and CMV infection affect pre-existing SARS-CoV-2-Reactive CD8+ T cells in unexposed individuals. *Front Aging* (2021) 2:719342. doi: 10.3389/fragi.2021.719342

119. Tomita Y, Sato R, Ikeda T, Sakagami T. BCG Vaccine may generate cross-reactive T cells against SARS-CoV-2: In silico analyses and a hypothesis. *Vaccine* (2020) 38(41):6352–6. doi: 10.1016/j.vaccine.2020.08.045

120. Eggenhuizen PJ, Ng BH, Chang J, Fell AL, Cheong RMY, Wong WY, et al. BCG Vaccine derived peptides induce SARS-CoV-2 T cell cross-reactivity. *Front Immunol* (2021) 12:692729. doi: 10.3389/fimmu.2021.692729

121. Upton CM, van Wijk RC, Mockeliunas L, Simonsson USH, McHarry K, van den Hoogen G, et al. Safety and efficacy of BCG re-vaccination in relation to COVID-19 morbidity in healthcare workers: A double-blind, randomised, controlled, phase 3 trial. *EClinicalMedicine* (2022) 48:101414. doi: 10.1016/j.eclinm.2022.101414

122. O'Driscoll M, Ribeiro Dos Santos G, Wang L, Cummings DAT, Azman AS, Paireau J, et al. Age-specific mortality and immunity patterns of SARS-CoV-2. *Nature* (2021) 590(7844):140–5. doi: 10.1038/s41586-020-2918-0

123. Liu Y, Wu Y, Liu B, Zhang Y, San D, Chen Y, et al. Biomarkers and immune repertoire metrics identified by peripheral blood transcriptomic sequencing reveal the pathogenesis of COVID-19. *Front Immunol* (2021) 12:677025. doi: 10.3389/fimmu.2021.677025

124. Murray SM, Ansari AM, Frater J, Klenerman P, Dunachie S, Barnes E, et al. The impact of pre-existing cross-reactive immunity on SARS-CoV-2 infection and vaccine responses. *Nat Rev Immunol* (2022), 1–13. doi: 10.1038/s41577-022-00809-x

frontiers | Frontiers in Immunology

TYPE Original Research
PUBLISHED 21 March 2023
DOI 10.3389/fimmu.2023.1031336

Check for updates

OPEN ACCESS

EDITED BY
Martijn van Griensven,
Maastricht University, Netherlands

REVIEWED BY
Minhui Guan,
University of Missouri, United States
Meihong Deng,
Feinstein Institute for Medical Research, United States

*CORRESPONDENCE
Christine McDonald
mcdonac2@ccf.org

†These authors have contributed equally to this work and share first authorship

‡These authors have contributed equally to this work and share senior authorship

SPECIALTY SECTION
This article was submitted to Viral Immunology, a section of the journal Frontiers in Immunology

RECEIVED 29 August 2022
ACCEPTED 08 March 2023
PUBLISHED 21 March 2023

CITATION
Narang J, Jatana S, Ponti AK, Musich R, Gallop J, Wei AH, Seck S, Johnson J, Kokoczka L, Nowacki AS, McBride JD, Mireles-Cabodevila E, Gordon S, Cooper K, Fernandez AP and McDonald C (2023) Abnormal thrombosis and neutrophil activation increase hospital-acquired sacral pressure injuries and morbidity in COVID-19 patients.
Front. Immunol. 14:1031336.
doi: 10.3389/fimmu.2023.1031336

COPYRIGHT
© 2023 Narang, Jatana, Ponti, Musich, Gallop, Wei, Seck, Johnson, Kokoczka, Nowacki, McBride, Mireles-Cabodevila, Gordon, Cooper, Fernandez and McDonald. This is an open-access article distributed under the terms of the Creative Commons Attribution License (CC BY). The use, distribution or reproduction in other forums is permitted, provided the original author(s) and the copyright owner(s) are credited and that the original publication in this journal is cited, in accordance with accepted academic practice. No use, distribution or reproduction is permitted which does not comply with these terms.

Abnormal thrombosis and neutrophil activation increase hospital-acquired sacral pressure injuries and morbidity in COVID-19 patients

Jatin Narang[1†], Samreen Jatana[2†], András K. Ponti[2], Ryan Musich[2], Joshua Gallop[1], Angela H. Wei[1], Sokhna Seck[1], Jessica Johnson[1], Lynne Kokoczka[3], Amy S. Nowacki[1,4], Jeffrey D. McBride[5], Eduardo Mireles-Cabodevila[3], Steven Gordon[6], Kevin Cooper[7], Anthony P. Fernandez[8,9‡] and Christine McDonald[1,2,10*‡]

[1]Cleveland Clinic Lerner College of Medicine, Case Western Reserve University, Cleveland, OH, United States, [2]Department of Inflammation and Immunity, Lerner Research Institute, Cleveland Clinic, Cleveland, OH, United States, [3]Medical Intensive Care Unit, Cleveland Clinic, Cleveland, OH, United States, [4]Department of Quantitative Health Sciences, Cleveland Clinic, Cleveland, OH, United States, [5]Department of Dermatology, The University of Oklahoma College of Medicine, Oklahoma City, OK, United States, [6]Department of Infectious Disease, Cleveland Clinic, Cleveland, OH, United States, [7]Department of Dermatology, University Hospitals Cleveland Medical Center, Cleveland, OH, United States, [8]Department of Dermatology, Dermatology and Plastic Surgery Institute, Cleveland Clinic, Cleveland, OH, United States, [9]Department of Anatomic Pathology, Pathology and Lab Medicine, Cleveland Clinic, Cleveland, OH, United States, [10]Department of Molecular Medicine, Cleveland Clinic Lerner College of Medicine, Case Western Reserve University, Cleveland, OH, United States

Hospitalized patients have an increased risk of developing hospital-acquired sacral pressure injury (HASPI). However, it is unknown whether SARS-CoV-2 infection affects HASPI development. To explore the role of SARS-CoV-2 infection in HASPI development, we conducted a single institution, multi-hospital, retrospective study of all patients hospitalized for ≥5 days from March 1, 2020 to December 31, 2020. Patient demographics, hospitalization information, ulcer characteristics, and 30-day-related morbidity were collected for all patients with HASPIs, and intact skin was collected from HASPI borders in a patient subset. We determined the incidence, disease course, and short-term morbidity of HASPIs in COVID-19(+) patients, and characterized the skin histopathology and tissue gene signatures associated with HASPIs in COVID-19 disease. COVID-19(+) patients had a 63% increased HASPI incidence rate, HASPIs of more severe ulcer stage (OR 2.0, p<0.001), and HASPIs more likely to require debridement (OR 3.1, p=0.04) compared to COVID-19(-) patients. Furthermore, COVID-19(+) patients with HASPIs had 2.2x increased odds of a more severe hospitalization course compared to COVID-19(+) patients without HASPIs. HASPI skin histology from COVID-19(+) patients predominantly showed thrombotic vasculopathy, with the number of thrombosed vessels being significantly greater than HASPIs from COVID-19(-) patients. Transcriptional signatures of a COVID-19(+) sample subset were enriched for innate immune responses, thrombosis, and neutrophil activation genes. Overall, our results

suggest that immunologic dysregulation secondary to SARS-CoV-2 infection, including neutrophil dysfunction and abnormal thrombosis, may play a pathogenic role in development of HASPIs in patients with severe COVID-19.

KEYWORDS

COVID-19, SARS-CoV-2, sacral ulcer, pressure ulcer, thrombotic vasculopathy, thrombosis, immune activation, neutrophil extracellular trap

Introduction

Patients with coronavirus disease 2019 (COVID-19) develop multi-organ manifestations and tissue damage secondary to both intrinsic properties of the SARS-CoV-2 virus and the resultant host immune response. The skin is among the organs affected by COVID-19, with manifestations including various localized or diffuse exanthems and retiform or acral purpura associated with thrombotic vasculopathy (1–5). Skin manifestations in COVID-19 disease may contribute to adverse symptoms and exacerbate patient morbidity, but significant skin necrosis leading to permanent damage in the form of scarring is rarely reported. Although several groups have reported challenges detecting SARS-CoV-2 virus in the skin; some studies have demonstrated the presence of viral Spike protein *via* immunohistochemistry (6–8).

Sacral ulcers are a leading cause of cutaneous-related patient morbidity in hospitalized patients (9, 10). The most common cause of sacral ulcers in hospitalized patients are hospital-acquired sacral pressure injuries (HASPIs), which occur secondary to unremitting pressure on the sacral and/or buttocks region (11, 12). Given the significant risk of HASPIs in hospitalized patients, most hospitals have developed protocols involving monitoring for early pressure-induced changes and routine off-loading measures in attempts to prevent them. Risk factors for HASPI formation include prolonged periods of immobility, decreased sensory perception, decreased mobility, increased moisture, and poor nutrition, many of which are typically present in hospitalized COVID-19 patients (11). Although small case series have reported the development of sacral ulcers in hospitalized COVID-19 patients, detailed analyses concerning incidence and prevalence of such ulcers, as well as risk factors associated with their development, are lacking (13, 14).

Despite the frequent presence of common HASPI risk factors, our clinical experience is that some COVID-19 patients acquire HASPIs that develop and progress more rapidly than usual, which may be associated with retiform purpura (13, 15). Based on these observations, we hypothesized that factors inherent to SARS-CoV-2 infection contribute to formation of HASPIs in some COVID-19 patients. This study explored the pathogenesis and determined the risk and associated morbidity of HASPIs in hospitalized COVID-19 patients. In addition to characterizing the clinical features of COVID-19(+) patients with HASPIs, histologic features of sacral skin biopsies acquired from COVID-19(+) patients with HASPIs were compared to sacral skin samples from pressure ulcers (PU) in COVID-19(-) patients. Furthermore, the transcriptional landscapes of sacral skin samples from COVID-19(+) and COVID-19(-) patients were analyzed to identify SARS-CoV-2-associated contributions.

We found that COVID-19(+) patients are at an increased risk of developing HASPIs and HASPI-associated morbidity compared to COVID-19(-) patients, even when controlling for baseline risk factors for ulceration. A large percentage of sacral skin biopsies from the borders of HASPIs of COVID-19(+) patients displayed thrombotic vasculopathy (TV), with significantly more thrombosed vessels per tissue section compared to sacral skin samples from PU in COVID-19(-) patients. Furthermore, the transcriptional profile differences in sacral biopsies from COVID-19(+) patients with TV support abnormal thrombosis and enhanced neutrophil extracellular trap (NET)-driven inflammation in sacral skin of COVID-19(+) patients compared to sacral skin specimens from PU in COVID-19(-) patients. These findings implicate thrombotic and inflammatory responses to SARS-CoV-2 infection in the promotion of cutaneous vascular thromboses, tissue ischemia, and eventual cutaneous ulceration.

Results

Risk of HASPI development and severity is increased in hospitalized COVID-19 patients

To understand the risk of HASPI development in COVID-19 disease, the incidence of sacral ulcers was compared between COVID-19(+) and COVID-19(-) patients in our study cohort (Supplementary Figure 1). Clinical and demographic characteristics of hospitalized patients during the study period were compared based on COVID-19 status, regardless of HASPI status. On average, COVID-19(+) patients were significantly older ($p<0.001$), with an increased percentage of males ($p=0.003$) and non-whites ($p<0.001$) compared to COVID-19(-) patients (Supplementary Table 1). COVID-19(+) patients had a significantly higher baseline risk of ulcer formation, longer length of hospitalization, higher rate of intensive care unit (ICU) admission, and a higher rate of mechanical ventilation compared to COVID-19(-) patients (Supplementary Table 1; $p<0.001$ for all 3 outcomes). Of 293 patients with HASPIs, COVID-19(+) patients had a HASPI occurrence of 7.5 per 10,000 days (49 patients; 16.7%), while

HASPIs occurred in COVID-19(-) patients at 4.6 per 10,000 days (244 patients; 83.3%) (Supplementary Table 1). This translated to a 63% increased incidence and a 2-fold higher relative risk for HASPIs in COVID-19(+) patients compared to COVID-19(-) patients.

COVID-19 severity is associated with HASPI risk and morbidity in relation to co-morbidities

Next, the hospitalization course of COVID-19(+) patients with and without HASPIs were compared in relation to their comorbidities (Supplementary Table 2). COVID-19(+) patients with HASPIs had a higher risk of ulcer formation at admission (Braden score of 14 *vs.* 19, p<0.001), longer hospitalization length (29 *vs.* 8 days, p<0.001), and more severe COVID-19 disease course, including increased requirement of mechanical ventilation or death (p<0.001) as compared to COVID-19(+) patients without HASPIs (Supplementary Table 2).

Multivariable regression analysis controlling for age at admission and patient co-morbidities (hypertension, chronic obstructive pulmonary disease (COPD), congestive heart failure and diabetes) was performed to assess impact of co-morbidities on HASPI development and hospitalization course (Supplementary Table 3). When controlling for age and comorbidities, COVID-19(+) patients who developed HASPIs were 2.2-fold more likely to have a severe COVID-19 hospitalization course compared to COVID-19(+) patients without HASPIs.

In patients that developed HASPIs, COVID-19(+) patients are more likely to develop severe HASPIs that require debridement

Clinical and demographic characteristics in the subset of COVID-19(+) (49 patients) and COVID-19(-) (244 patients) hospitalized patients who developed HASPIs were compared to examine the impact of COVID-19 on disease course and ulcer phenotypes (Table 1). Amongst patients who developed HASPIs, COVID-19(+) patients had a higher baseline risk of ulcer formation at hospital admission (Braden score of 14 *vs.* 18, p<0.001) and a higher frequency of requiring intubation (20.4% *vs* 3.3%, p<0.001) compared to COVID-19(-) patients (Table 1). On the other hand, gender, hospitalization length, and ICU admission rate did not differ between the two groups. A larger percentage of COVID-19(+) patients with HASPIs were black (p=0.03) (Table 1). Time to HASPI and HASPI size did not differ between COVID-19(+) and COVID-19(-) patients; however, COVID-19(+) patients were more likely to have a severe HASPI stage compared to COVID-19(-) patients (24.9% *vs.* 9.0% Stage 3 or 4 ulcer p=0.003).

We also compared laboratory parameters for patients who developed HASPIs to determine if there were differences among COVID-19(+) and COVID-19(-) patients. COVID-19(+) patients had significantly higher maximum ferritin concentrations compared to COVID-19(-) patients (1,303 *vs.* 813 ng/mL, p=0.007). Other laboratory parameters, including maximum D-dimer concentration, maximum white blood cell (WBC) count, and neutrophil-to-lymphocyte ratio did not significantly differ between the two groups (Table 1).

We performed multivariable regression modeling, controlling for Braden ulcer risk at admission, hypertension, congestive heart failure, chronic obstructive pulmonary disease, diabetes mellitus, age at admission, hospitalization length, requirement for ICU admission, and requirement for intubation to assess the impact of SARS-CoV-2 infection on HASPI development and characteristics (Table 2). Within our cohort, COVID-19 positivity was associated with 40% increased odds of developing a HASPI (p=0.03) even after controlling for Braden ulcer risk score at admission and other variables. Additionally, COVID-19(+) patients were 2.1-fold more likely to develop a HASPI of more severe stage (p<0.001) and 3.1-fold more likely to require debridement (p=0.045) compared to COVID-19(-) patients. Time to HASPI development and wound size were not significantly associated with COVID-19 status based on multivariable regression (Table 2). Overall, 30-day morbidity did not differ amongst the two groups (Supplementary Table 4). However, a greater percentage of COVID-19(+) patients required surgical debridement compared to COVID-19(-) patients (14.3% *vs.* 5.7%, p=0.047; Supplementary Table 4).

Thrombotic vasculopathy is a prominent histopathologic feature in a significant percentage of COVID-19(+) patient HASPIs

The histopathological features of skin biopsies from the edges of HASPIs in COVID-19(+) patients were compared to similar tissue specimens from COVID-19(-) patients with PUs. Qualitative assessments revealed that biopsies of COVID-19(+) patients with HASPIs could be broadly categorized into 2 groups: histologic features consistent with thrombotic vasculopathy (TV; 67%) or histologic features consistent with PUs (33%); (Figure 1; Table 3). In our study, PU is defined to be a cutaneous ulceration secondary to tissue ischemia caused entirely by unremitting pressure on the involved anatomic location, without important contributions from other pathologic processes. Whereas specimens with a TV pattern displayed diffuse fibrin thrombi within superficial and deep dermal and subcutaneous blood vessels, in addition to dermal neutrophils with occasional leukocytoclasis, specimens with a PU pattern displayed only occasional vascular thromboses with a sparse superficial dermal inflammatory infiltrate, but also displayed dermal neutrophils with occasional leukocytoclasis (Figures 1A, B; Supplementary Figures 2A, B, 3A, B, 4A, B; Table 3). Specimens in the COVID-19(-) PU control group typically displayed mixed dermal inflammation and dilated vascular spaces with congestion and only occasional fibrin thrombi (Figure 1C; Supplementary Figures 2C, 3C, 4C; Table 3). Most specimens had an intact epidermis, but two COVID-19(-) PU control specimens had at least partial epidermal ulceration (20%). Additionally, COVID-19 (-) PU specimens lacked leukocytoclasis and typically had eosinophils within the dermal inflammatory infiltrate or within vascular lumina (Figure 1C; Supplementary Figure 2C).

10.3389/fimmu.2023.1031336

TABLE 1 Clinical and Demographic characteristics of hospitalized patients who developed HASPIs.

			COVID (+)	COVID (-)	p-value[a]
N			49	244	–
Pressure Ulcer Risk at Admission[b]			14 (12-16.5)	18 (14-20)	**0.001**
Female Sex			17 (34.7%)	90 (36.9%)	0.77
Age (Years)			66.3 (56.7-73.6)	65.3 (55.0-73.6)	0.31
Race	White		29 (59.2%)	184 (75.4%)	
	Black		19 (38.8%)	50 (20.5%)	**0.03**
	Other		1 (2.0%)	10 (4.1%)	
Hospitalization Length (Days)			29 (19.5-35)	27 (16-41)	0.75
ICU Admission: Yes			45 (91.8%)	216 (88.5%)	0.5
Intubation: Yes			10 (20.4%)	8 (3.3%)	**<0.001**
Time to HASPI (Days)			12 (8-20)	14 (8-22)	0.5
HASPI Stage[c]		2	37	222	**0.003**
		3	7	17	
		4	5	5	
HASPI Size (cm^2)			12 (2.3-55.5)	6 (1.2-29.0)	0.06
Max D-Dimer (ng/mL)[d]			8,330	5,490	0.13
			(3,820-18,370)	(2,428-15,555)	
Max Ferritin (ng/mL)[d]			1,303	813	**0.007**
			(909-3,582)	(422-1,938)	
Max White Blood Cell Count (K/uL)[d]			18.5 (13.6-28.5)	21.3 (14.9-29.7)	0.33
Max Neutrophil to Lymphocyte Ratio			8.4 (4.6-12)	9.6 (4.6-15)	0.31

Bolded values denote statistically significant p-values.
[a]Based on Wilcoxon-rank sum test for continuous variable comparisons and Chi-squared test for categorical variables comparisons.
[b]Based on Braden risk assessment score closest to admission.
[c]Three COVID (+) and thirteen COVID (-) patients had unstageable HASPIs and were excluded from this analysis. P-value based on Cochrane-Armitage trend test.
[d]COVID (+): 6/49 (12.2%) patients had no recorded D-dimer concentration, 12/49 (24.5%) had no recorded ferritin concentration, 3/49 (6.1%) had no recorded white blood cell count. COVID (-): 174/244 (71.3%) patients had no recorded D-dimer concentration, 148/244 (60.7%) had no recorded ferritin concentration, and 12/244 (4.9%) had no recorded white blood cell count.

TABLE 2 Multivariable logistic regression model assessing the impact of COVID-19 status (positive *vs.* negative) on HASPI development and characteristics.

Outcome	Regression Estimate (95% CI)	p-value[a]
Developing a HASPI[b,c]	1.4 (1.01-1.9)	**0.03**
Time to HASPI[d]	1.3 (0.89-1.8)	0.2
Stage of HASPI[e]	2.1 (1.4-3.3)	**<0.001**
Need for Debridement[c]	3.1 (1.02-9.4)	**0.045**
Wound Size[f]	8.1 (-0.4-16.5)	0.06

Bolded values denote statistically significant p-values.
[a]P-values are representative of 5 different multivariable regression analysis all controlling for Braden ulcer risk at admission, medical comorbidities (hypertension, congestive heart failure, chronic obstructive pulmonary disease, and diabetes mellitus), age at admission, length of hospital stay, requirement for ICU admission, and requirement for intubation with COVID-19 status (positive vs. negative) as the predictor variable.
[b]HASPI: Hospital-acquired sacral pressure injury.
[c]P-value based on odds ratio from multivariable logistic regression results.
[d]P-value based on hazard ratio from multivariable Cox proportional hazards model.
[e]P-value based on odds ratio from multivariable ordinal regression.
[f]P-value based on parameter estimate from multivariable linear regression.

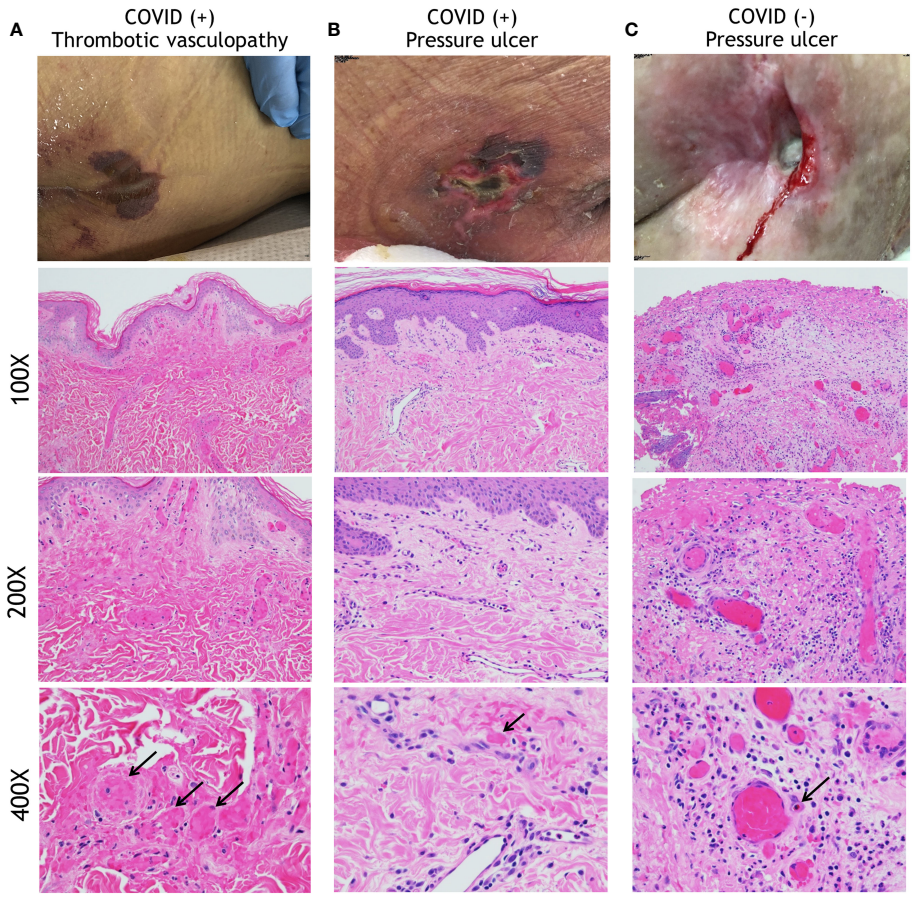

FIGURE 1
Histopathology analysis of HASPIs. **(A)** COVID-19-related Thrombotic Vasculopathy. A man in his 30s was intubated in the ICU due to severe COVID-19 with an acute purpuric rash on the buttocks that subsequently ulcerated. A low-power photomicrograph (100X) reveals a relatively normal and intact epidermis with diffuse fibrin thrombi involving superficial and deep dermal vessels. A higher power image (200X) further highlights diffuse fibrin thrombi and occasional inflammatory cells within the dermis. At even higher power (400X) occasional neutrophils and leukocytoclasis can be seen. **(B)** A woman in her 80s who developed a sacral ulcer with surrounding purpura in the setting of COVID-19 after 6 weeks of intubation. At low power (100X), a photomicrograph displays an intact epidermis with mostly patent vascular spaces in the dermis. At higher power (200X), a sparse superficial dermal inflammatory infiltrate with occasional neutrophils is noted. A 400X image reveals a rare vascular thrombosis. Other vessels display intact neutrophils within their lumens. **(C)** A pressure ulcer in a COVID-19(-), wheelchair-bound man in his 70s. A low-power (100X) image reveals an ulcer with superficial fibrin necrosis, mixed inflammation, and dilated vascular spaces with congestion and occasional fibrin thrombi. A higher power (200X) image reveals centrally located vessels with congestion and peripheral vessels with fibrin thrombi. At 400X magnification, a mixed inflammatory infiltrate is seen surrounding vessels that are either congested or with contained fibrin thrombi. Neutrophils are intact, without obvious leukocytoclasis. An eosinophil is present within a vascular lumen (arrow, (400X)). Eosinophils were often seen in COVID-19(-)-associated ulcer specimens, either within vascular lumina or in the dermis.

The clinical and histological characteristics of biopsied patients were further analyzed in a quantitative manner (Table 3). Age and sex of patients with sacral tissue specimens did not differ, however average hospitalization length and severity of disease course of biopsied COVID-19(+) patients (both TV and PU) was significantly greater than in COVID(-) patients ($p=0.02$ and $p<0.001$, respectively). COVID-19(-) patients with tissue specimens available had ulcers of more severe stage compared to the two COVID-19(+) groups. Additionally, due to frequent consultation to evaluate unusual purpuric sacral rashes in COVID-19(+) patients, skin tissue specimens were taken from COVID-19(+) patients at time points closer to onset of ulceration compared to the COVID-19(-) patients (19.5 *vs.* 59.5 days). There were no significant differences observed in the maximum D-dimer levels and the absolute neutrophil counts between the three groups; however, not all subjects had D-dimer levels reported, especially in COVID-19(-) patients. Histologically, COVID-19(+) TV biopsies had a significantly greater number of vascular thromboses in the superficial and deep dermis, but not in the subcutis, and significantly more leukocytoclasis in the upper dermis, compared to COVID-19(+) PU and COVID-19 (-) PU histologic sections (Table 3).

Genes involved in interferon-related viral responses and neutrophil extracellular trap formation are uniquely upregulated in COVID-19(+) TV skin

The combination of clinical retiform purpura and histologic thrombotic vasculopathy in the majority of the COVID-19(+)

10.3389/fimmu.2023.1031336

TABLE 3 Clinical and pathological characteristics of biopsied patients.

		COVID (+) TV	COVID (+) PU	COVID (-) PU	p
N		10	5	10	
Age		67 (63-70)	64 (57-78)	55 (44-64)	0.17
% Male		5 (50%)	4 (80%)	5 (50%)	0.66
Hospitalization Length (Days)		20 (16-34)	33 (28-66)	15 (12-28)	**0.02**
Ulcer Stage[a]	2	2 (67%)	2 (40%)	0 (0%)	**0.04**
	3	0 (0%)	1 (20%)	1 (11%)	
	4	1 (33%)	2 (40%)	8 (89%)	
Disease Course	Hospitalization Only	1 (10%)	0 (0%)	9 (100%)	**<0.001**
	ICU	0 (0%)	1 (20%)	0 (0%)	
	Ventilation	4 (40%)	3 (60%)	0 (0%)	
	Death	5 (50%)	1 (20%)	0 (0%)	
Max D-Dimer		7,660	5,070	3,880	0.39[b]
		(5,465-32,580)	(3,730-24,575)	(3,880-3,880)	
Max Absolute Neutrophil Count		9.9 (4.7-17.4)	13 (10-22)	7.4 (3.7-15)	0.14
Pathology Features					
Epidermis	**Neutrophil Infiltrate**	3 (30%)	4 (80%)	1 (10%)	**0.031**
Upper Dermis	**Vascular Thrombosis**	10 (100%)	5 (100%)	5 (50%)	**0.01**
	# of Thromboses	53 (26-99)	12 (7-26)	1 (0-12)	**0.0006**
	Intraluminal Neutrophils	8 (80%)	4 (80%)	9 (90%)	0.99
	Leukocytoclasis	9 (90%)	4 (80%)	1 (10%)	**0.001**
Deep Dermis	**Vascular Thrombosis**	10 (100%)	2 (40%)	6 (60%)	**0.02**
	# of Thromboses	15 (6-20)	0 (0-3)	2 (0-6)	**0.001**
	Intraluminal Neutrophils	9 (90%)	3 (60%)	9 (90%)	0.47
	Leukocytoclasis	9 (90%)	3 (60%)	3 (30%)	0.07
Subcutis	**Vascular Thrombosis**	8 (80%)	1 (20%)	2 (20%)	0.2
	# of Thromboses	4 (1-11)	0 (0-2)	2 (0-3)	0.13
	Intraluminal Neutrophils	7 (70%)	1 (20%)	2 (20%)	0.32
	Leukocytoclasis	5 (50%)	0 (0%)	1 (20%)	0.29

Bolded values denotes statistically significant p-value.
[a]3 patients had unstageable ulcers and 1 had DTI.
[b]Comparison between COVID(+) groups only as only 1 patient in COVID(-) had D-dimer value.

patients with HASPIs led us to hypothesize that immunologic dysregulation due to SARS-CoV-2 infection may contribute to the pathogenesis of HASPIs in these patients. To explore this, the differentially expressed gene (DEG) profile of the tissue specimens from the TV and PU COVID-19(+) groups were compared to the COVID-19(-) PU controls. Dimensionality reduction using principal component analysis (PCA) revealed that the COVID-19 (+) TV and PU groups segregated into separate clusters that were distinct from the COVID-19(-) PU control group (Figure 2A).

Among 44 DEGs that were unique to the COVID-19(+) TV group (Figure 2B), genes involved in responses to viral infection, such as the interferon regulatory factor 7 (IRF7) transcription factor and interferon-induced with helicase C domain 1 (IFIH1) that encodes the cytosolic nucleic acid sensor MDA-5, were identified among the top TV-specific up-regulated genes compared to COVID-19(+) PU and COVID-19(-) PU groups. CD274 (PD-L1), which has been implicated in dysregulated neutrophil responses in severe COVID-19, and PADI2, an enzyme involved in the citrullination of arginine residues and neutrophil extracellular trap (NET) formation, were also highly expressed in the TV group compared to the other two groups (16).

HLA-DRB3, CXCL13, PTPN22 and AHR were identified as genes that were commonly down-regulated in both COVID-19(+) TV and COVID-19(+) PU groups compared to the COVID-19(-)

10.3389/fimmu.2023.1031336

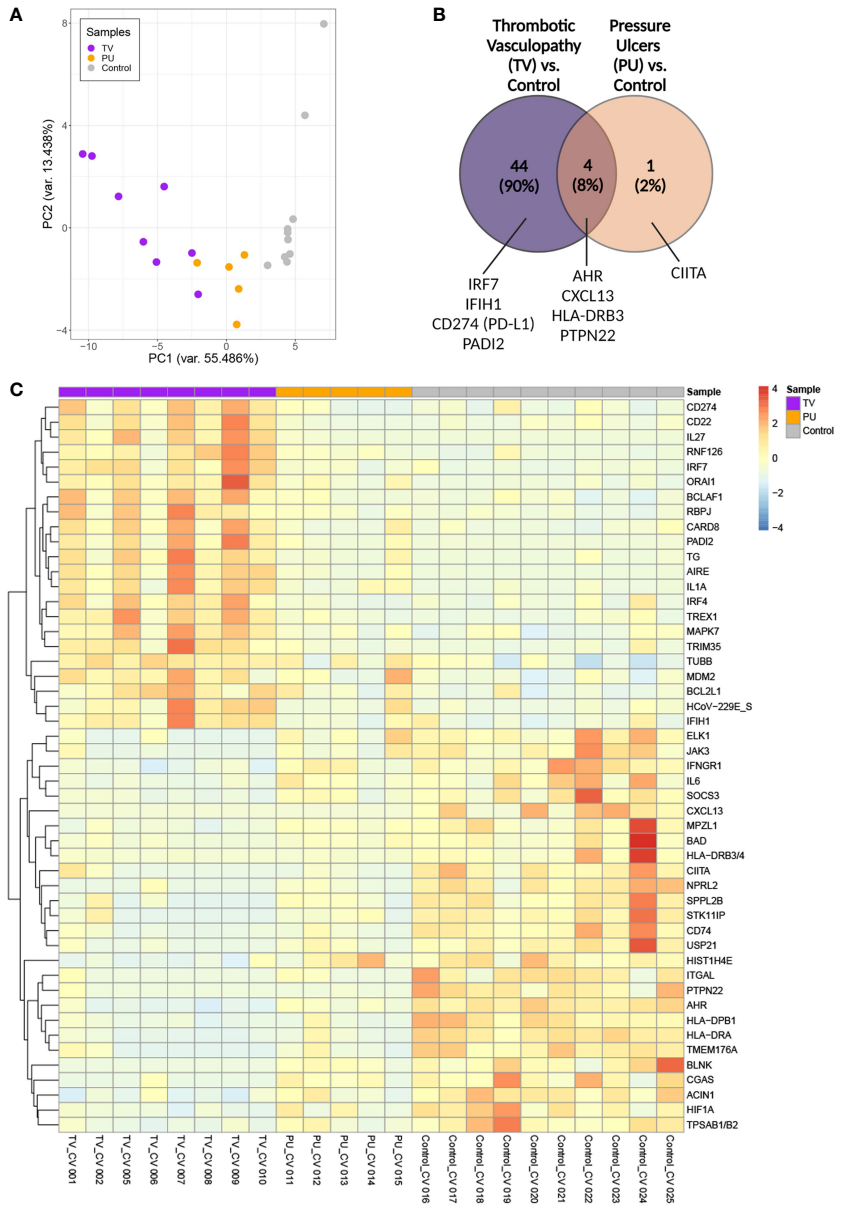

FIGURE 2
Transcriptomic analysis of sacral ulcer biopsies from COVID-19(+) patients reveals distinct signatures between TV and PU groups relative to COVID-19(-) PU control ulcers. **(A)** Principal component analysis of all patient samples using normalized counts from the differentially expressed genes with FDR adjusted *p*-value of < 0.05 indicates the distance between COVID-19(+) TV (TV), COVID-19(+) PU (PU), and COVID-19(-) PU (Control) samples. **(B)** Venn diagram showing differentially expressed genes (FDR adjusted *p*-value of < 0.05) in COVID-19(+) patients with TV and PU compared with COVID-19(-) PU control. Representative genes are indicated. **(C)** Supervised two-dimensional Hierarchical clustering of the 49 genes whose average normalized counts were significantly different in COVID-19(+) TV and PU groups compared to COVID-19(-) PU control samples (FDR adjusted *p*-value of < 0.05).

PU control group. These genes are key players in antigen processing and T and B cell homeostasis. Only CIITA, a master regulator of MHC class II genes, was differentially expressed and down-regulated in the COVID-19(+) PU group compared to the COVID-19(-) PU controls. Taken together, this data suggests that innate immune responses are primarily dysregulated in COVID-19 (+) TV pathology in comparison to COVID-19(-) PUs. In contrast, antigen processing and T and B cell signaling mechanisms are potentially downregulated in both COVID-19(+) TV and PU groups.

Hierarchical clustering of differentially-expressed genes reveals unique immunologic pathway dysregulation in COVID-19(+) TV skin compared to COVID-19(+) and (-) PU skin

To better characterize the transcriptional signatures in skin tissue from the three ulcer groups, hierarchical clustering of the top up- and down-regulated genes in each disease category was performed (Figure 2C). The signatures associated with the

COVID-19(+) TV and COVID-19(-) PU group were distinct from one another, supporting unique biological mechanisms of disease pathogenesis in sacral skin as a result of severe SARS-CoV-2 infection. In comparison to the COVID-19(-) PU controls, genes highly expressed in the TV group fell into categories that included neutrophil dysfunction (CD274, PADI2), inhibition of B and T cell responses (CD22, IRF4, ORAI1), and upregulation of pro-inflammatory response pathways (CARD8, MAPK7, IRF7, IFIH1). In contrast to COVID-19(+) TV, highly expressed in the COVID-19(-) PU control group included MHC class II antigen processing (HLA-DRB3/4, HLA-DPB1, HLA-DRA, CIITA, and CD74), mast cell degranulation (TPSAB1/B2), B cell activation (CXCL13, BLNK, IL-6) and histone modification (USP21, HIST1H4E). An apoptotic gene signature was found in both COVID-19(+) TV and COVID-19(-) PU control groups but not in the COVID-19(+) PU samples, consistent with the level of tissue necrosis in these tissue specimens. However, these apoptotic gene signatures were characterized by distinct DEGs expressed in the COVID-19(+) TV (BCLAF1, BCL2L1) and COVID-19(-) PU control groups (BAD, ACIN1, HIF1A) (Figure 2C).

SARS-CoV-2-specific transcripts were also measured to determine whether transcriptional profiles and immune responses in the skin of COVID-19(+) patients may be a direct, local response to viral infection or a result of systemic immune responses. Although a majority of the COVID-19(+) TV tissue samples were positive for the presence of a limited set of SARS-CoV-2 transcripts (Supplementary Figure 5), these differences in transcript level do not persist as significant when false discovery rate (FDR) testing was performed on the entire Nanostring panel. Therefore, it is unclear from this limited sample set whether local SARS-CoV-2 infection contributes to HASPI pathology.

Taken together, these results indicate distinct transcriptional differences in HASPI skin of COVID-19(+) TV patients compared to COVID-19(+) PU and COVID-19(-) PU controls. Genes that were highly upregulated in COVID-19(+) TV were downregulated in both PU groups indicative of similar mechanisms of pathogenesis in PU. Upregulation of genes involved in neutrophil dysfunction and pro-inflammatory response mechanisms, specifically genes involved in response to viral infection, suggests that transcriptional differences observed in the COVID-19(+) TV group might be a result of SARS-CoV-2 infection (either locally or systemically) and account for the unique histopathological findings of thrombotic vasculopathy (Figure 1A).

COVID-19(+) TV skin displays upregulation of unique biologic pathways compared to COVID-19(-) PU control skin

To understand the effect of infection and thrombotic vasculopathy in the COVID-19(+) TV group compared to the COVID-19(-) PU control group, the top 10 enriched Gene Ontology (GO) biological pathways in the COVID-19(+) TV and COVID-19(-) PU control groups were identified, followed by a sub-analysis to determine the significantly altered transcripts within these pathways (Figure 3). Both distinct and common biological mechanisms were identified in each set of analyses (Figures 3A, B). Top biological pathways in the COVID-19(+) TV group up-regulated in comparison to COVID-19(-) PU controls included positive regulation of pro-inflammatory cytokine production, defense response to virus, and the innate immune response pathway (Figure 3A). Hematopoietic or lymphoid organ development and T cell activation involved in immune response represented top down-regulated pathways in the COVID-19(+) TV group compared to the COVID-19(-) PU control group (Figure 3B). Antigen processing and presentation of exogenous peptide antigen *via* MHC class II biological pathway was also down-regulated in the COVID-19(+) TV group compared to the COVID-19(-) PU control group, indicating hampered adaptive immune responses in the COVID-19(+) TV group (Figure 3B). Pathway analysis did not reveal major pathways that were distinctly up- or down-regulated in the COVID-19(+) PU group compared to the COVID-19(-) PU group, suggesting similar biological mechanisms contribute to disease pathology of PU regardless of infection status.

The analysis was expanded to uncover transcriptional signatures in the above three biological pathways up-regulated in COVID-19(+) TV specimens compared to COVID-19(-) PU control specimens (Figure 3C). Select genes that were highly expressed in COVID-19 (+) TV specimens compared to COVID-19(+) PU and COVID-19(-) PU control groups play a central role in regulation of innate immune responses and defense to viral infection, including CARD8, IL1A, CD274, TRIM35, IRF7, and IFIH1 (Figure 3C). Both PU groups displayed similar trends in gene expression in the subset of genes that were upregulated in the COVID-19(+) TV group.

As several of the GO pathways altered in COVID-19(+) TV samples relate to regulation of immune cell populations, cell type scores were calculated to identify differences in the skin immune cell landscape in the tissue specimens from the three HASPI groups. Neutrophils and $CD56^{+dim}$ natural killer (NK) cells were significantly higher in the COVID-19(+) TV group compared to the other disease groups (Figure 3D). The identification of a neutrophil gene signature in the COVID-19(+) TV samples is consistent with results of our DEG and GO biological pathway analyses supporting involvement of innate immune response (CD274, PADI2), as well as histologic differences in the inflammatory cell infiltrates observed in the disease groups (Figure 3D and Figure 2, Table 3). Taken together, these results demonstrate that HASPI tissue from the COVID-19(+) TV group displays upregulation of unique biologic pathways, including defense response to virus and innate immune responses, and a differential immune cell signature, compared to the COVID-19 (+) PU and COVID-19(-) PU groups, suggesting differing HASPI pathogeneses. It also reinforces the histologic observations that neutrophils might be key players in COVID-19(+) TV pathology.

Genes associated with thrombosis, PADI2-associated NET formation, and exacerbated inflammatory responses are specifically up-regulated in COVID-19(+) TV skin

Neutrophils have been implicated as key players in mechanisms contributing to immunothrombosis in COVID-19 disease (17–19).

10.3389/fimmu.2023.1031336

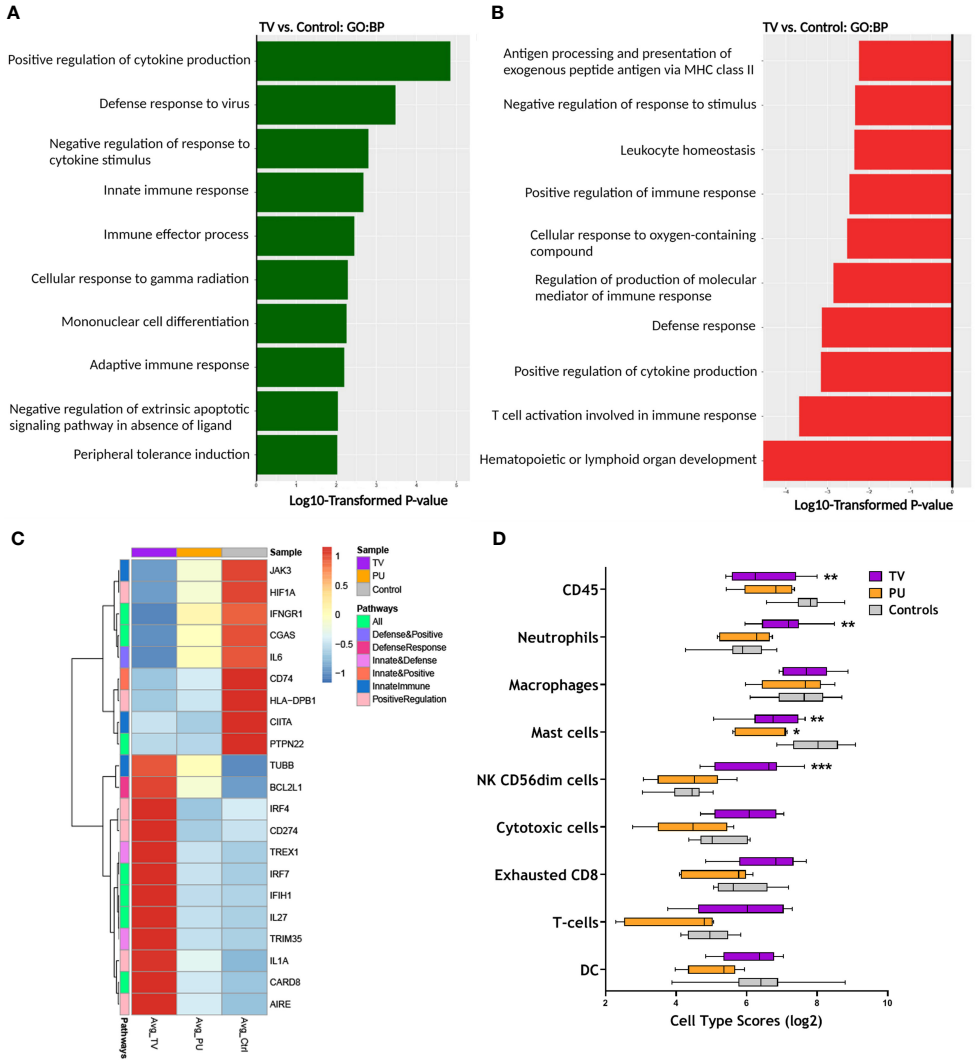

FIGURE 3
RNA expression reveals distinct immune responses in TV ulcers. **(A)** Top enriched GO biological pathways (N=10) in COVID-19(+) TV (TV) samples compared with COVID-19(-) PU (Control). **(B)** Top GO biological pathways (N=10) downregulated in TV samples relative to controls. **(C)** Clustered heatmap comparing average normalized counts of COVID-19(+) TV and COVID-19(+) PU (PU) groups with COVID-19(-) PU Control samples depicts differentially expressed genes (FDR adjusted *p*-value of <0.05) involved in positive regulation of cytokine production, defense response to virus, and innate immune response pathways. Genes involved in pathways were identified from GO biological pathways **(D)** Box and whisker plot shows the relative immune cell type scores of TV, PU, and Control samples. Cell type scores were determined using NanoString Advanced Analysis.

Given this and our above results, gene-set enrichment analysis (GSEA) was utilized to more completely characterize transcriptional signatures associated with thrombosis, immune cell chemotaxis, and neutrophil-specific biological functions in our HASPI groups. First, examined were genes involved in thrombosis and complement genes that may contribute to enhanced thrombosis. Notably, CXCL10, a cytokine that is implicated among the three key players contributing to COVID-19 cytokine storm and increased fatal COVID-19 outcomes (20), was highly expressed in the COVID-19(+) TV group compared to the other disease groups. Additionally, genes associated with thrombotic mechanisms, including MEFV, STAT5B, CD55, CRP, CTLA4, TLR4, CCR1, CFP, C4A/B and IL23R, were only upregulated in the COVID-19(+) TV group (Figure 4A). Alternatively, complement activation genes were similarly expressed in all three ulcer groups (Figure 4A). These findings suggest that COVID-19(+) TV HASPIs may have abnormal thrombosis without enhanced complement activation due to upregulation of genes that mediate thrombosis.

Next, the dataset was surveyed for all genes that are involved in immune cell chemotaxis and extravasation (Figure 4B). In both COVID-19(+) TV and COVID-19(-) PU control groups a gene expression signature associated with neutrophil activation and chemotaxis was expressed; however, these signatures were characterized by unique subsets of genes in COVID-19(+) TV (TREM1, CXCR1, CXCL8, and S100A12) and COVID-19(-) PU control (CXCL1, CXCL2, and CD177) groups (Figure 4B). A small subset of genes involved in neutrophil and T cell activation (CXCL5, CXCL9, CCL21) were expressed in both COVID-19(+) TV and COVID-19(-) PU groups. Additionally, genes associated with

10.3389/fimmu.2023.1031336

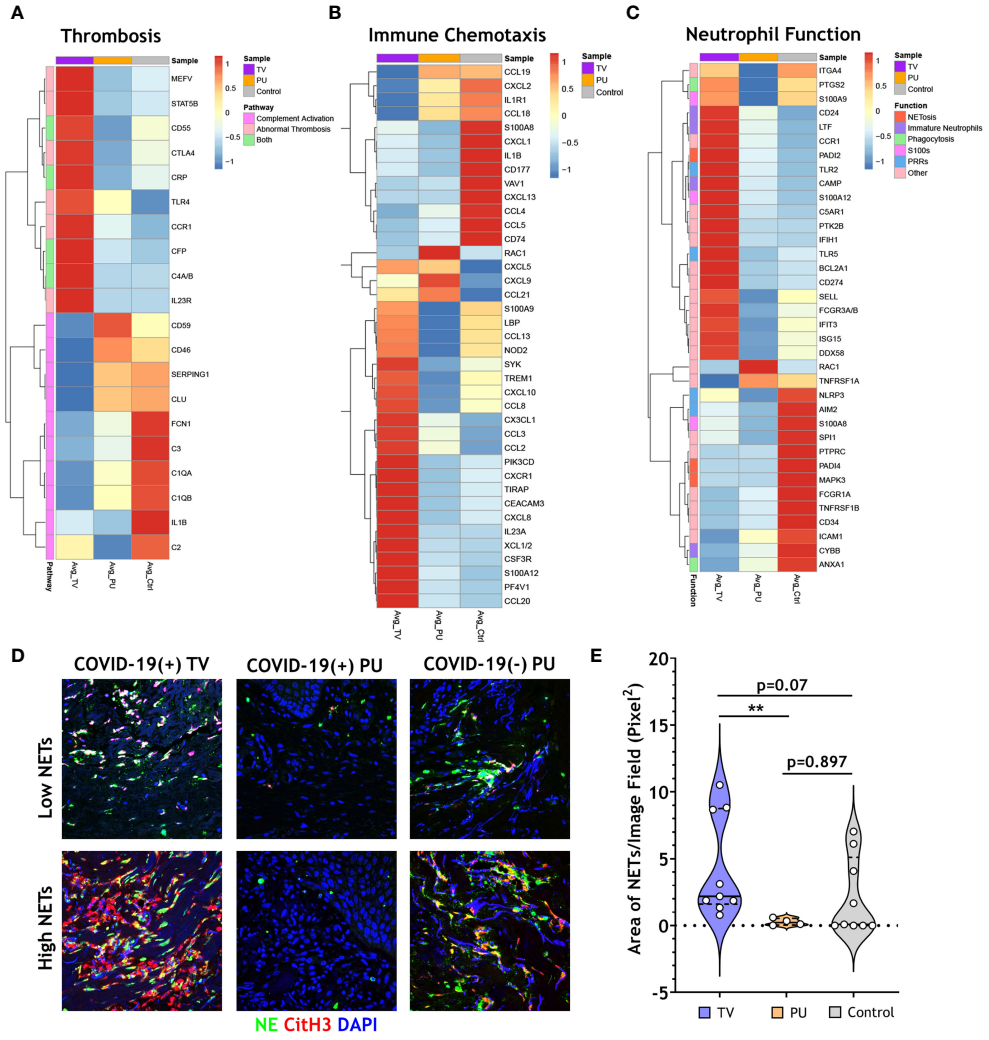

FIGURE 4
COVID-19 thrombotic vasculopathy is characterized by abnormal thrombosis and neutrophil extracellular trap formation. **(A)** Clustered heatmap shows the average normalized counts of genes involved in thrombosis and complement activation for COVID-19(+) TV (TV) and COVID-19(+) PU (PU) samples compared to COVID-19(-) PU (Control). Pathway specific genes were selected based on GO biological pathways. **(B)** Clustered heatmap illustrates the average normalized counts of genes involved in immune cell chemotaxis and extravasation for COVID-19(+)TV and PU samples compared to COVID-19(-) PU Controls. Genes were selected based on GO biological pathways. **(C)** Neutrophil specific genes arranged by function (NETosis, Immature Neutrophils, Phagocytosis, S100s, PRRs, or Other) represented in a clustered heatmap comparing the average normalized counts of DEGs in COVID-19(+) TV and PU groups relative to COVID-19(-) PU Controls. **(D)** Immunofluorescence staining of NETs in skin tissue sections. Markers of NETs used include NE (green), CitH3 (red) and nuclei (blue). Images acquired using confocal microscopy, 40X oil objective **(E)** Quantification of tissue NETs in the skin using Image J analysis.

antimicrobial defense mechanisms, including alarmins (S100A9, S100A12) and pattern recognition receptors (LBP, and NOD2), were up-regulated in the COVID-19(+) TV group compared to the COVID-19(-) PU control group, while suppressed in the COVID-19(+) PU group. While some genes involved in monocyte and lymphocyte migration and function were expressed in the COVID-19(+) TV group (CCL13, CCL8, and CCL20), a greater number of these genes were expressed in the COVID-19(-) PU control group (CCL19, CCL18, CXCL13, CCL4, CCL5, CXCL9). Only two genes (RAC1, CXCL9) were upregulated in COVID-19(+) PU compared to the other two disease groups. These genes are involved in the control of cell growth and lymphocyte chemoattraction, respectively. These findings support the histologic findings of different immune cell populations present in the HASPI groups. Taken together, these results demonstrate that while neutrophil activation and dysfunction may play a role in HASPI skin of both COVID-19(+) TV and COVID-19(-) PU groups, abnormal thrombosis and exacerbated inflammatory responses appear to be unique to HASPI skin in the COVID-19(+) TV group.

NET formation and upregulation of genes associated with the immature neutrophil subset are significantly elevated in COVID-19(+) TV skin

Schulte-Schrepping et al., utilized single-cell RNA sequencing of whole blood and peripheral blood mononuclear cells from COVID-

19(+) patients to study the role of mature and immature neutrophil subsets in COVID-19 disease pathogenesis (16). We utilized this published dataset of neutrophil function-related genes that contribute to systemic inflammation in COVID-19 disease and compared them to the transcriptional signatures in our HASPI skin tissue dataset. Genes contributing to dysregulated NET formation were highly expressed in both COVID-19(+) TV and COVID-19(-) PU groups, but not in the COVID-19(+) PU group (Figure 4C). However, genes related to distinct mechanisms of NET induction were differentially expressed in the COVID-19(+) TV and COVID-19(-) PU control groups, with COVID-19(+) TV samples expressing PADI2 versus PADI4 expression in COVID-19(-) PU controls.

Immature neutrophils, or low-density granulocytes, have been shown to undergo uncontrolled NET formation in several autoinflammatory and autoimmune diseases, contributing to disease pathology (21). Genes associated with the immature neutrophil subset (CD24, LTF, CAMP) were up-regulated in COVID-19(+) TV skin, but not in COVID-19(+) PU or COVID-19(-) PU skin tissue (Figure 4C). Several other neutrophil function-related genes were also uniquely expressed in the COVID-19(+) TV group, including those related to antiviral response (IFIT3, DDX58, PTGS2, and IFIH1) and Toll-like receptor (TLR)-mediated signaling (TLR2, TLR5). Finally, CD274 (PD-L1), a known inhibitor of T cell activation, was highly expressed in COVID-19 (+) TV skin tissue compared to the other 2 groups. These results reveal that while certain neutrophil chemotactic genes are expressed in both COVID-19(+) TV and COVID-19(-) PU control groups, expression of genes associated with the immature neutrophil subset is a distinct characteristic of the COVID-19(+) TV group, suggesting this neutrophil subset might contribute to enhanced vascular thrombosis at the local skin tissue level.

Finally, NETs in skin tissue from all three HASPI groups were visualized by immunofluorescent staining. Rare NETs were detected in the COVID-19(+) PU group (Figure 4D), which is consistent with the low NET-specific DEGs detected in this group (Figure 4C). This is in contrast to the visualization of NETs mainly in the dermis in all of the COVID-19(+) TV samples, which ranged from relatively low to extensive NETosis (Figure 4D). NETs were also variably detected in COVID-19(-) PU control tissue specimens, with five of nine COVID-19(-) PU skin specimens (~55%) demonstrating a lack of detectable NETs (Figure 4D). This was supported by image analysis to quantify the area of NETs within the tissue, which demonstrated the median total NET area in the COVID-19(+) TV group was modestly elevated compared to COVID-19(-) PU controls ($p=0.07$) (Figure 4E). Total area of NETs in the COVID-19(+) TV tissue was significantly higher than in the COVID-19(+) PU group ($p<0.01$), indicating a potential role for neutrophils in abnormal thrombosis-mediated biological mechanisms. These results demonstrate that while NETs may contribute to pathology in both COVID-19(+) TV and COVID-19(-) PU groups, mechanisms of NET induction (PADI2 *vs.* PADI4) and neutrophil subsets that potentially contribute to disease pathology (immature *vs.* mature neutrophil subsets) differ, possibly due to local SARS-CoV-2 infection.

Discussion

Although the hallmark of COVID-19 disease is acute respiratory distress syndrome and respiratory failure, manifestations are known to occur in many organ systems (22). Inflammation related to COVID-19 can cause transient or permanent organ damage, adding considerable morbidity to patients who survive their COVID-19 disease course. Numerous cutaneous eruptions have been described in the setting of COVID-19, but the peer-reviewed literature has focused mainly on outbreaks that resolve without significant tissue damage. Alternatively, HASPIs represent localized areas of significant and often permanent skin damage. HASPIs occur mainly in hospitalized patients and are associated with substantial patient morbidity and healthcare costs, with estimates ranging from $10 billion to >$26 billion annually (23). Given the significant impact of HASPIs and requirement for hospitalization in a substantial percentage of patients with COVID-19, we explored the incidence of HASPIs and risk factors for their development in a large cohort at a single tertiary care, multi-hospital institution.

This study revealed a number of important findings surrounding HASPIs in COVID-19(+) patients. Overall, COVID-19(+) patients had a 63% increased incidence of developing a HASPI compared to COVID-19(-) patients (Supplementary Table 1). Additionally, COVID-19(+) hospitalized patients have a 40% increased odds of developing HASPIs compared to COVID-19 (-) patients, even when controlling for baseline ulceration risk at admission, ICU admission, and other variables (Table 2). Although the overall etiology of HASPIs in COVID-19 patients is likely multifactorial, there are numerous possible explanations for the increased risk we found in these patients. One obvious possibility is that COVID-19(+) patients have increased risk of ulceration at time of admission. However, the elevated risk of HASPIs in COVID-19(+) patients persisted compared to COVID-19(-) patients when controlling for risk of ulceration in a multivariable model. Another possibility is that meticulous routine care for these patients was compromised to protect caregivers from excess exposure to COVID-19(+) patients. However, protocols for frequent skin checks for HASPIs were not changed at our institution during the COVID-19 pandemic. This makes lack of adequate care an unlikely cause of increased HASPIs in our COVID-19(+) patient population and suggests other factors contribute to this increased risk, potentially including factors inherently related to SARS-CoV-2 infection.

This study identified that COVID-19(+) patients are at risk of more severe HASPIs and more often require surgical debridement compared to COVID-19(-) patients (Tables 1, 2). In particular, the finding that almost 25% of the COVID-19(+) HASPIs were Stage 3 or Stage 4 (compared to <10% in the COVID-19(-) cohort) is important, as these stages of pressure injuries are considered hospital 'never events'. These 'never events' were defined by the National Quality Forum as events that are measurable and preventable, and that may lead to severe patient morbidity and mortality. The increased incidence of these severe ulcerations, despite continuing standard clinical monitoring protocols during COVID-19 to prevent them, is concerning.

Importantly, when controlling for age, co-morbidities, and other variables COVID-19(+) patients with HASPIs were more likely to have a severe hospitalization course compared to COVID-19(+) patients without HASPI. These results support that development of a HASPI is a poor prognostic sign in the setting of COVID-19. However, it is unclear whether a severe hospitalization course increases risk of HASPI development, or vice versa. Regardless, this finding aligns with the hypothesis that HASPIs in COVID-19 (+) patients likely arise as a result of both intrinsic and extrinsic disease factors.

A comparison of laboratory parameters revealed COVID-19(+) HASPI patients had significantly higher maximum levels of serum ferritin compared to COVID-19(-) HASPI patients (Table 1). Hyperferritinemia has been associated with poor prognosis in COVID-19 patients and has been implicated to have a pathogenic role in cytokine storm (24). In the setting of an inflammatory state, ferritin has also been hypothesized to be a marker of cellular damage. Thus, COVID-19-associated inflammation may result in more significant cellular damage compared to other medical conditions leading to hospitalization, resulting in an overall catabolic state that promotes HASPI ulceration.

Surprisingly, maximum D-dimer levels were not significantly higher in COVID-19(+) patients with HASPIs compared to COVID-19(-) patients with HASPIs in our cohort. However, a high percentage of COVID-19(-) patients had no D-dimer levels drawn, suggesting a selection bias towards evaluating D-dimer levels in those patients who may have had clinical features supporting a thrombotic state (Table 1). Elevated D-dimer levels strongly correlate with an increased risk of thrombotic events in COVID-19 patients and, importantly, all COVID-19(+) HASPI patients in our cohort had elevated D-dimer levels (25). Factors other than elevated D-dimer levels, such as elevated expression of thrombotic genes or heightened triggering of complement pathway activation, may also contribute to thrombotic pathology in COVID-19 patients.

SARS-CoV-2-induced thrombotic events in the skin microcirculation represent another possible contributor to increased HASPI risk in COVID-19 patients. Thrombotic events in the skin and other organs of patients with COVID-19 are well-described (2, 3). Although these events typically do not appear to result in significant skin damage, they may promote eventual ulceration in areas like the sacrum that are additionally affected by pressure. In support of this, we have previously seen and reported several patients with severe COVID-19 who developed unusual retiform purpura on the buttocks associated with histologic thrombotic vasculopathy and subsequent development of sacral ulcers (13, 15).

In our cohort, 25 patients had skin specimens of their HASPIs available, 15 of which were biopsies performed on COVID-19(+) patients (TV and PU). We compared the histologic, cellular and molecular characteristics of these specimens in detail to each other and to those in COVID-19(-) PU control skin tissue. Significantly higher numbers of vascular thromboses and leukocytoclasis were observed in skin tissue from the COVID-19(+) TV group compared to the other groups, supporting the role of thrombotic vasculopathy as a potential contributor to subsequent ulceration in some COVID-19(+) patients.

Interestingly, vascular thromboses were detected occasionally in our COVID-19(-) PU control specimens. In fact, vascular thromboses have been described in skin biopsies of HASPIs in COVID-19(-) patients, and vascular occlusion has long been hypothesized to play an important pathogenic role in the development of PUs (26, 27). However, vascular thromboses were far more numerous and prominent in COVID-19(+) TV tissue compared to what we found in COVID-19(-) PU skin and compared to what has been described in prior histologic studies of PUs, suggesting additional pathogenic contributors to thrombotic vasculopathy in the COVID-19(+) TV group, such as factors inherent to COVID-19 (17, 28, 29). Additionally, some prior histologic studies of PUs describe vascular thromboses underlying ulcerated skin, suggesting they may represent secondary phenomena related to inflammation in areas of ulcer, whereas our COVID-19(+) TV tissue contained diffuse vascular thromboses in skin with intact epidermis, prior to ulceration (30, 31).

Although the majority of skin specimens from COVID-19(+) patients showed a TV pattern, one-third showed a PU histologic pattern with far less vascular thromboses compared to TV skin tissue. Although not statistically significant, mean maximum D-dimer levels were higher in the COVID-19(+) TV group compared to the COVID-19(+) PU group. This raises the possibility that there may also be a threshold D-dimer level, above which there is increased risk of vascular thrombosis in cutaneous vessels under pressure during viral infection, which might contribute to the unique histologic observations in this study.

Transcriptional analyses on skin specimens from the sites of sacral ulcer formation evaluated the inflammatory landscape in skin tissue during SARS-CoV-2 infection in comparison to sacral ulcers obtained from uninfected patients. This type of analysis has not been previously performed. Our results showed that COVID-19(+) TV skin is associated with up-regulation of genes related to innate immune responses and viral defense responses, and down-regulation of T-cell mediated immune responses (Figures 3A, B). Importantly, biological pathways and DEGs upregulated in COVID-19(+) TV skin were mainly categorized as genes that would potentially contribute to abnormal thromboses and immunothrombosis, consistent with our histopathology results (Figure 4). Analysis of DEGs showed that while interferon response genes and neutrophil-associated genes were highly expressed in COVID-19(+) TV skin, genes associated with MHC class II antigen presentation were down-regulated, indicative of stunted adaptive immune responses in COVID-19(+) TV (Figure 2C). Consistent with results of histopathological observations (Table 3), we also observed that genes associated with mechanisms of dysregulated immature neutrophil responses were highly expressed in COVID-19(+) TV skin compared to COVID-19(-) PU skin (Figures 4B, C). Given the known association between SARS-CoV-2 infection and immature neutrophil responses, this result further implicates SARS-CoV-2 infection itself with augmentation of ischemia in these areas and contribution to eventual tissue necrosis and ulceration. Although

trending higher, we were unable to detect significant presence of SARS-CoV-2 transcripts in the COVID-19(+) TV samples in our limited dataset, so are unable to conclusively determine whether the immune dysregulation and enhanced thrombosis observed is a direct, local response to virus present in the skin or a more systemic response to SARS-CoV-2 infection. Interestingly, genes related to complement activation were upregulated in all disease groups, indicating that the alternative complement activation pathway was triggered in infected as well as uninfected skin tissue. Overall, our results suggest SARS-CoV-2 infection may amplify ischemia and eventual tissue necrosis and ulceration in skin under pressure by increasing thrombosis and neutrophil dysregulation, and not complement activation.

Recently, Yang et al. (32) examined the importance of CXCL10 plasma levels (interferon γ-inducible protein 10; IP-10) in COVID-19 disease severity and progression of COVID-19 disease. They reported that 5 cytokines, including CXCL10, were associated with fatal outcomes during infection (32). Several other studies have also shown the prognostic value of CXCL10 in determining COVID-19 disease course (33, 34). CXCL10 was found to be up-regulated in COVID-19(+) TV skin in comparison to COVID-19(+) PU and COVID-19(-) PU skin in our study (Figure 4A). These results suggest COVID-19 severity may be important for precipitating cutaneous vasculopathy in skin under pressure, which would further support a threshold is needed for SARS-CoV-2-associated contributions to cutaneous thrombosis.

Cytokines, such as IL1A and IL27, which have been shown to be higher in patients with more severe COVID-19 disease (35–37), were highly expressed in COVID-19(+) TV skin in comparison to the other groups. We also found that alarmins (S100A9, S100A12) and pattern-recognition receptors (PRRs) including TLR2, TLR4, TLR5, IFIH1, and NOD2 had higher expression in COVID-19(+) TV skin. It has been shown that SARS-CoV-2 spike protein binds TLR4 to increase the cell surface expression of ACE2 and facilitate viral entry (38, 39) exacerbating innate immune responses during infection. Expression of SARS-CoV-2-specific genes and higher transcript levels of PRRs in COVID-19(+) TV skin could potentially explain the enhanced innate immune responses observed with examination of GO biological pathways, and a contribution of neutrophil dysfunction in promoting cutaneous vascular thromboses.

Cell type scoring demonstrated that neutrophils were enriched in COVID-19(+) TV skin compared to COVID-19(+) PU and COVID-19(-) PU skin. While we also observed changes in $CD56^{+dim}$ NK cell, $CD45^{+}$ cell, and mast cell signatures, we focused our subsequent efforts on specifically understanding the role of neutrophils in the ulcer phenotypes with and without SARS-CoV-2 infection since neutrophils have been shown to play an important role in COVID-19 disease pathogenesis, particularly in relation to thromboses and multi-organ damage (19, 40, 41). A study of dysregulated myeloid cell responses in COVID-19 revealed that presence of CD274 and ARG1 expressing dysfunctional mature neutrophils contributed to severe COVID-19 disease (16). In our dataset, the expression of CD274 was significantly higher in TV skin compared to skin in the other groups. Given that T cell mediated immune responses were down-regulated in COVID-19(+) TV skin, it is possible that presence of $CD274^{high}$ ($PD\text{-}L1^{+}$) mature neutrophils in TV skin tissue suppress T cell responses due to the inhibitory interaction between PD-L1 and PD-1, resulting in stunted adaptive immune responses. In support of this, mature CD274 ($PD\text{-}L1^{+}$) neutrophils have been shown to exert suppressive effects on T cell function in various other diseases like cancer and HIV infection (42, 43).

The presence of NETs in skin tissue was directly evaluated to understand whether exacerbated NET formation contributed to inflammation in the skin. Results showed that NETs were significantly higher in COVID-19(+) TV *vs*. PU skin, indicating that neutrophils and NETs potentially contribute to cutaneous thrombotic vasculopathy during severe COVID-19 infection. While NETs were also observed in COVID-19(-) PU (controls), the baseline levels in 5 patients were nearly zero, indicating that exacerbated NET formation might be a consistent feature of TV in COVID-19(+) patients. In addition to significantly higher NETs in COVID-19(+) TV *vs*. COVID-19(+) PU skin, COVID-19(+) TV skin also had more intense neutrophil elastase and CD61 staining than COVID-19(+) PU skin, correlating with the known ability of NETs to propagate inflammation and thrombosis (Figure 4D and Supplementary Figure 3). The reason for the difference in NETs in COVID-19(+) TV and PU skin is not entirely clear. However, previous work has supported that COVID-19 is a pro-NETotic state that is influenced by disease severity and levels of certain clinical biomarkers (44). The degree of NETosis is likely influenced by many factors in a given COVID-19 patient, including genetic factors, amount of viral-damaged epithelial cells, levels of various inflammatory cytokines, extent of platelet and endothelial cell activation and others. Although details concerning how NETosis is triggered in the setting of severe COVID-19 requires additional work, our results support that presence of significant cutaneous NETosis correlates with increased cutaneous thromboses, and likely contributes to development of HASPIs in this particular population of severe COVID-19 patients.

Our study has several advantages and limitations. Advantages include the establishment of a comprehensive COVID-19 registry at our institution that allowed identification of all COVID-19(+) patients admitted to our institutional hospitals, as well as a relatively large cohort utilized for analysis. Additionally, the standard protocol to photograph ulcers allowed objective confirmation that patients were accurately labeled as having HASPIs. More importantly, our results correlate clinical findings with histopathologic and molecular results. The comparison of COVID-19(+) patients with HASPIs to both COVID-19(+) patients without HASPIs and COVID-19(-) patients with HASPIs has not previously been done, especially with quantification of genes in sacral skin under pressure in all 3 groups. We were also able to corroborate the contribution of NETs to local tissue inflammation indicated by our transcript analyses using immunofluorescence imaging.

Limitations include the retrospective nature of our study and possibility that electronic medical records did not always contain accurate documentation of data points (i.e. date of ulcer onset). One important data point that we could not completely characterize was skin color due to absence of images and/or incomplete disclosure of ethnicity for several patients in our cohort. However, we believe it is

notable that our COVID-19(+) HASPI cohort had a large number of black patients. As black patients have been found to be at increased risk for severe COVID-19 compared to other ethnic groups, our ethnicity data further supports a link between severe COVID-19 and HASPI development, and suggests clinicians should be particularly meticulous in monitoring black COVID-19(+) patients for HASPI development (45, 46). Additionally, laboratory data points and skin tissue specimens were not always captured on similar days during hospitalizations or in all patients to allow precise comparison. The number of biopsies evaluated in each cohort was relatively small with only limited amounts of tissue available for research. However, given HASPIs are typically diagnosed clinically and patients with severe COVID-19 can be difficult to biopsy for various reasons, we believe our biopsy sample numbers are adequate to gain insights into central pathways altered in these patients. These limitations impacted our ability to conclusively determine whether these dysregulated pathways are altered in response to local or systemic SARS-CoV-2 infection and will need to be explored further in a larger study cohort with a secondary method to confirm presence of virus in cutaneous tissue. We were unable to utilize fresh biopsies for transcript-level analyses and corroborate with systemic markers due to the unavailability of these resources in severely ill patients during the initial months of the outbreak. Therefore, the transcriptional analyses were limited to bulk tissue digests of paraffin-embedded tissue, precluding single cell transcriptomic analyses. Furthermore, as this study consists of a cohort from a single institution, our results are not necessarily generalizable. This study also focused specifically on the role of neutrophils and NETs in disease pathology; however, future studies will explore the role of other cells types, including platelets that were significantly altered in the three disease groups.

In conclusion, we show that COVID-19(+) patients are at an increased risk of HASPIs compared to COVID-19(-) patients, and COVID-19(+) patients with HASPIs develop ulcerations of more severe stage that more often require debridement than COVID-19(-) patients. Furthermore, we show that thrombotic vasculopathy was prominent in sacral skin of COVID-19(+) patients with HASPIs compared to controls, and TV tissue displayed increased expression of DEGs known to contribute to abnormal thrombosis and ischemia. Overall, our results implicate SARS-CoV-2 infection as a contributing factor to HASPIs in at least some COVID-19 patients.

Unlike other reports of skin manifestations in COVID-19 patients, our overall findings support the skin is yet another organ system that may sustain significant damage secondary to COVID-19. Recognizing risk of HASPIs and the potential role of SARS-CoV-2 infection in COVID-19 patients is important, as they may contribute to significant future morbidity, healthcare expenditure, and even mortality in patients who recover from COVID-19. Further research is needed to uncover detailed pathogenic factors leading to increased HASPI risk in COVID-19 (+) patients, as well as how to optimally prevent them from occurring. For now, healthcare workers should be especially attentive to potential early signs of HASPI development in patients hospitalized with COVID-19, especially those with serious disease, and be meticulous with currently proven preventative clinical interventions.

Materials and methods

Patient identification

Patients with HASPIs were identified as having been hospitalized for greater than 5 days within our institution between March 1 and December 31, 2020, with an ICD-10 diagnosis of sacral ulcer or photographic documentation of sacral ulceration at some point during hospitalization (Supplementary Table 5). We defined a sacral ulcer as any new onset ulceration involving the sacral and/or buttocks areas acquired during an inpatient hospital admission at one of our facilities within the above time period. The decision to utilize an image search was made because nursing staff at our institution are instructed to image all potential HASPIs for documentation and clinical improvement purposes, and because photographs provide objective proof of ulceration. Based on our search criteria, we assumed all sacral ulcers that developed during hospitalization represented HASPIs unless otherwise stated in clinical notes and will refer to them as such from this point forward.

Patients that did not undergo a polymerase chain reaction (PCR)-based COVID-19 test at admission or during hospitalization, those hospitalized for <5 days, and those with sacral ulcers already present at hospital admission were excluded from our study. Additionally, stage 1 ulcer patients were excluded as these types of ulcers are difficult to reliably detect and are not routinely documented by our wound care teams. Some patients were hospitalized more than once during our defined study period. However, only the hospitalization associated with an initial development of a HASPI was included for our study purposes.

Among the 143,223 patients hospitalized at our institution during our defined study period (March 2020-December 2020), 58,766 patients met our inclusion/exclusion criteria and comprised our study cohort (Supplementary Figure 1). These patients were hospitalized for a total 591,763 days. Of our 58,766 patients, 5,531 (9.4%) were COVID-19(+) patients (total hospitalization days = 64,980; average 11.8 days) and 53,528 (89.6%) were COVID-19(-) patients (total hospitalization days=526,783; average 9.8 days). A total of 3,352 patients had a diagnosis of sacral ulcer during their hospitalization with or without an image of their sacral region in their electronic medical records. Of these patients, 2,992 had their sacral ulcers documented prior to or upon admission and 67 were seen at an outside hospital and were excluded from our study. Thus, our final study cohort consisted of 293 patients with HASPIs (Supplementary Figure 1).

Patient and ulcer characteristics

For all patients who met our inclusion/exclusion criteria, we thoroughly reviewed electronic medical records to obtain detailed clinical information. Clinical data acquired included demographic information (age, gender, race), HASPI ulceration risk (based on Braden risk assessment at hospital admission), presence of specific medical comorbidities (obesity, hypertension, diabetes mellitus, and

chronic obstructive pulmonary disease (COPD)) index hospitalization information (COVID-19 status, length of stay, intensive care unit (ICU) admission, intubation/mechanical ventilation requirements), laboratory results (including maximum D-dimer concentration, maximum ferritin concentration, and maximum white blood cell count (WBC)), HASPI characteristics (time from admission to ulcer formation, ulcer stage, and ulcer size), and 30-day HASPI-related morbidity information (defined as either need for surgical debridement or subsequent ulcer-related infection within 30-days of discharge).

The Braden risk assessment score is a validated clinical tool calculated by nursing staff throughout our institution as part of routine patient skin assessments at admission and every 12 hours thereafter. This standardized risk scale assigns numerical ratings (ranging from 1-4) to six domains, including sensory perception, moisture, activity, mobility, nutrition, and friction/shear forces (47). The sum of these domains is used to risk stratify patients for HASPI formation; a lower score is correlated with increased risk of HASPI development (48). The primary outcome of our study was development of HASPI during the indexed hospitalization. Our secondary outcome was severity of hospitalization course, which was an ordinal categorical variable defined as either (1) hospitalization only, (2) hospitalization requiring ICU admission, (3) hospitalization requiring ICU admission and need for mechanical ventilation, and (4) hospitalization leading to death.

COVID-19 status was determined by nasal swab and PCR-based diagnostic testing. If a patient tested positive for COVID-19 at least once during the index hospitalization, they were classified as COVID-19(+). Time to ulcer formation was measured in days from admission to first mention and/or photographic documentation of HAPSI in the patient's EMR, whichever occurred first. Ulcer size was defined as the largest recorded area (measured in cm^2) of sacral ulceration during the index hospitalization. Ulcer stage was defined as most severe stage of ulcer (2, 3, 4, or unstageable) recorded during hospitalization according to National Pressure Injury Advisory Panel (NPIAP) classifications. Severe stage of HASPI was defined as either Stage 3 or Stage 4 HASPI according to NPIAP staging criteria. These specific stages were selected as they are considered hospital 'never events' by the NPIAP due to their associated, independent risk of increased morbidity and mortality (49).

Histopathology analysis of tissue specimens

Histopathologic characteristics of biopsied patients were qualitatively and quantitatively assessed using hematoxylin and eosin (H&E) stained tissue specimens by a board-certified dermatopathologists (APF and JDM). For COVID-19(+) patients, 4mm biopsies from (typically) areas of sacral purpura were obtained. For control COVID-19(-) specimens, which were typically submitted to pathology during debridement, a search of Cleveland Clinic pathology archives was performed to find specimens from PUs. H&E sections of all available specimens were reviewed to identify those appropriate to use as control specimens. Any specimens with histologic features suggestive of secondary infection, extensive epidermal ulceration, or prominent fibrosis (supporting significant chronicity) were excluded. Ten specimens were found to have histologic features suggestive of inherent pressure-induced changes. For these, a 4mm wide area was demarcated and examined to be consistent with the area examined in COVID-19(+) tissue. When possible, areas with intact epidermis were chosen in COVID-19(-) specimens to also reduce variability with tissue examined from COVID-19(+) patients. Histopathologic features that were evaluated included neutrophil infiltrate, vascular thrombosis, total number of thromboses, intraluminal neutrophils and leukocytoclasis (Table 3). These features were scored for their presence or absence, in addition to quantitating them if present. Phosphotungstic Acid Hematoxylin (PTAH/fibrin) and CD61 staining to evaluate microthrombi formation was performed on biopsied tissues samples obtained from the cases highlighted in Figure 1.

NanoString analysis

RNA was extracted from Formalin-Fixed and Paraffin Embedded (FFPE) tissue biopsies, using the RNeasy FFPE kit (Qiagen) with deparaffinization solution (Qiagen). Total RNA concentrations were determined using a Nanodrop ND-1000 spectrophotometer (Thermo Fisher Scientific). One-hundred nanograms of RNA was then hybridized with the NanoString Human Autoimmune Profiling Panel and spike in Coronavirus Panel Plus probe sets (NanoString Technologies). Transcriptional analysis of immune related genes and SARS-CoV-2 genes in tissue biopsies was conducted using the NanoString nCounter Pro Analysis System (NanoString Technologies). Raw data was initially processed using the nSolver Analysis Software (V.4.0). Quality control and normalization was performed using the 6 positive control, 8 negative control, and 20 housekeeping probes. Samples flagged for failing quality control were removed. Remaining data was assessed for cell type scoring using nSolver Advanced Analysis (V.2.0) and exported for subsequent analysis in R software.

Bioinformatics analysis

Analysis was performed using R (version 4.1.0). Venn diagram was generated utilizing DEGs from TV *vs* Control results against PU *vs* Control. Resulting residuals for principal component analysis (PC1 and PC2) were plotted using 'ggplot2' package (version 3.3.5). For pathway analysis, DEGs were separated into up- and down-regulated gene lists (fold change > 0 and fold change < 0 respectively). Package 'gprofiler2' (version 0.2.1) to find up- and down-regulated pathways. GO pathways were filtered to remove redundant pathways to generate the data by GO's hierarchically structured database. Using ordered p-values from pathway analysis, the top 10 up-regulated and down-regulated pathways were obtained and p-values were log10-transformed for Figures 3A, B.

Heatmaps were generated using normalized counts for specific gene sets (pheatmap version 1.0.12). Gene set enrichment analysis (GSEA) was utilized to identify genes involved in specific biological functions like neutrophil activation, abnormal thrombosis and complement activation. COVID-19-specific neutrophil genes (Figure 4C) were analyzed using published single-cell sequencing data. The p-value cutoffs that were used to determine significant genes from the NanoString data was FDR adjusted p-values < 0.05.

Neutrophil extracellular traps immunofluorescence staining and confocal imaging

Paraffin embedded 5 µm tissue sections were sectioned by the Cleveland Clinic Histology Core. Sections were deparaffinized and blocked using blocking buffer (Hank's balanced salt solution containing 2% bovine serum albumin and 2% goat serum) for 1 hour at room temperature. Qualitative evaluation of presence of NETs in the tissue was performed using antibodies for anti-neutrophil elastase (NE/ELA2; R&D Systems, Catalogue# MAB91671-100; monoclonal mouse IgG; RRID : AB_2923234) and Anti-Histone H3 (citrulline R2 + R8 + R17; Abcam, Catalogue# ab5103; Rabbit polyclonal IgG; RRID : AB_304752). Primary antibody dilutions were made in the blocking buffer (NE, CitH3; used at 1:100 dilution) and added to the sections for an overnight incubation at 4°CC. Next day, slides were washed in 1X PBS (3X) and secondary antibodies were added to the sections for 1 hour at room temperature (1:1000 dilution in blocking buffer, Goat anti-Mouse 633 and Goat anti-Rabbit 568). After the 1 hour incubation, slides were washed in 1X PBS (3X) and mounted with DAPI (ProLong™ Gold Antifade Mountant with DAPI, ThermoFisher Scientific, Catalogue# P36931). Images were obtained using an inverted Leica SP8 confocal microscope using objective lens 40X oil/1X zoom factor. Five fields/tissue section were imaged for the purpose of quantitative assessment of presence of tissue NETs in the epidermis as well as the dermis. Images obtained from various disease groups were qualitatively assessed for presence of high, medium-low and no tissue NETs. Area of NETs was quantified using Image J software (version 1.53r 21).

Statistical analysis

Categorical variables are presented as count (percentage) and continuous variables as median (interquartile range). Wilcoxon rank-sum was utilized for two-sample continuous variable comparisons. Chi-square and Fisher's Exact tests were utilized to compare nominal categorical data across groups. Cochrane-Armitage exact trend test was utilized to compare univariate ordinal categorical data. Multivariable logistic and multivariable Cox proportional hazards regression were used to model binary and time-to-event outcomes, respectively. Multivariable linear regression was used to model wound size. Potential for multicollinearity was explored using variance inflation factor analysis. One-way ANOVA was utilized for analysis of tissue NETs with post-hoc Tukey analysis. An a level of 5% (two-sided) was utilized for all comparisons. Statistical analysis was performed using SAS JMP Pro (version 15) and Prism (version 9.3.1).

Data availability statement

The datasets presented in this study can be found in online repositories. The names of the repository/repositories and accession number(s) can be found below: www.ncbi.nlm.nih.gov/geo/, GSE214647.

Ethics statement

The studies involving human participants were reviewed and approved by Cleveland Clinic Institutional Review Board. The patients/participants provided their written informed consent to participate in this study.

Author contributions

JN, SJ, AF and CM conceptualized and designed the study. JN, SJ, KC, AF and CM acquired funding for the study. JN, SJ and AP carried out laboratory-based investigations. JN, SJ, AP, RM, JG, AW, SS, JJ, LK, AN, JM, EM-C, SG, KC, AF, CM carried out clinical-based investigations and analysis of data including statistical analysis. AF and CM supervised the study. JN, SJ, AP and RM created the original figures and tables. AP and RM performed analysis of the Nanostring data. JN and SJ wrote the original draft of the manuscript. JN, SJ, AP, AF and CM wrote, reviewed and edited the manuscript. The order of authors was based on their sequential roles in the study. All authors contributed to the article and approved the submitted version.

Funding

This publication was made possible by a COVID-19 Themed Pilot Grant Award (to AF and CM) from the Clinical and Translational Science Collaborative (CTSC) of Cleveland from the National Center for Advancing Translational Sciences (NCATS) component of the National Institutes of Health and NIH roadmap for Medical Research (UL1TR002548). This work was also funded by the Office of the Assistant Secretary of Defense for Health Affairs through the Congressionally Directed Medical Research Programs Peer Reviewed Medical Research Program (W81XWH-16-0439/PR150299 to CM). This study was also supported by the Crohn's & Colitis Foundation (#662997 to SJ). JN was supported by the Case Investigative and Translational Dermatology Training Program funded by the National Institute of Arthritis and Musculoskeletal and Skin Diseases of the National Institutes of Health (T32AR007569 to KC). This work utilized the Leica SP8 confocal microscope that was purchased with funding from the National Institutes of Health Shared Instrumentation Grant 1S10OD019972-01. Opinions, interpretations,

conclusions, and recommendations are those of the authors and are not necessarily endorsed by the funders.

Acknowledgments

We would like to thank Emily Jiang from the Cleveland Clinic Department of Business Intelligence; Greg Strnad from the Cleveland Clinic COVID-19 Registry; and Janine Sot from the Cleveland Clinic Department of Dermatology.

Conflict of interest

The authors declare that the research was conducted in the absence of any commercial or financial relationships that could be construed as a potential conflict of interest.

Publisher's note

All claims expressed in this article are solely those of the authors and do not necessarily represent those of their affiliated organizations, or those of the publisher, the editors and the reviewers. Any product that may be evaluated in this article, or claim that may be made by its manufacturer, is not guaranteed or endorsed by the publisher.

Supplementary material

The Supplementary Material for this article can be found online at: https://www.frontiersin.org/articles/10.3389/fimmu.2023.1031336/full#supplementary-material

References

1. Galvan Casas C, Catala A, Carretero Hernandez G, Rodriguez-Jimenez P, Fernandez-Nieto D, Rodriguez-Villa Lario A, et al. Classification of the cutaneous manifestations of COVID-19: A rapid prospective nationwide consensus study in Spain with 375 cases. *Br J Dermatol* (2020) 183(1):71–7. doi: 10.1111/bjd.19163

2. Magro C, Mulvey JJ, Berlin D, Nuovo G, Salvatore S, Harp J, et al. Complement associated microvascular injury and thrombosis in the pathogenesis of severe COVID-19 infection: A report of five cases. *Transl Res* (2020) 220:1–13. doi: 10.1016/j.trsl.2020.04.007

3. Magro CM, Mulvey JJ, Laurence J, Sanders S, Crowson AN, Grossman M, et al. The differing pathophysiologies that underlie COVID-19-associated perniosis and thrombotic retiform purpura: A case series. *Br J Dermatol* (2021) 184(1):141–50. doi: 10.1111/bjd.19415

4. Droesch C, Do MH, DeSancho M, Lee EJ, Magro C, Harp J. Livedoid and purpuric skin eruptions associated with coagulopathy in severe COVID-19. *JAMA Dermatol* (2020) 156(9):1–3. doi: 10.1001/jamadermatol.2020.2800

5. Freeman EE, McMahon DE, Lipoff JB, Rosenbach M, Kovarik C, Desai SR, et al. The spectrum of COVID-19-associated dermatologic manifestations: An international registry of 716 patients from 31 countries. *J Am Acad Dermatol* (2020) 83(4):1118–29. doi: 10.1016/j.jaad.2020.06.1016

6. Gehlhausen JR, Little AJ, Ko CJ, Emmenegger M, Lucas C, Wong P, et al. Lack of association between pandemic chilblains and SARS-CoV-2 infection. *Proc Natl Acad Sci USA* (2022) 119(9):e2122090119. doi: 10.1073/pnas.2122090119

7. Liu J, Li Y, Liu L, Hu X, Wang X, Hu H, et al. Infection of human sweat glands by SARS-CoV-2. *Cell Discov* (2020) 6(1):84. doi: 10.1038/s41421-020-00229-y

8. Magro C, Nuovo G, Mulvey JJ, Laurence J, Harp J, Crowson AN. The skin as a critical window in unveiling the pathophysiologic principles of COVID-19. *Clin Dermatol* (2021) 39(6):934–65. doi: 10.1016/j.clindermatol.2021.07.001

9. Avsar P, Moore Z, Patton D, O'Connor T, Budri AM, Nugent L. Repositioning for preventing pressure ulcers: a systematic review and meta-analysis. *J Wound Care* (2020) 29(9):496–508. doi: 10.12968/jowc.2020.29.9.496

10. Reddy M, Gill SS, Rochon PA. Preventing pressure ulcers: A systematic review. *JAMA* (2006) 296(8):974–84. doi: 10.1001/jama.296.8.974

11. Lyder CH. Pressure ulcer prevention and management. *JAMA* (2003) 289 (2):223–6. doi: 10.1001/jama.289.2.223

12. Thomas DR. Does pressure cause pressure ulcers? An inquiry into the etiology of pressure ulcers. *J Am Med Dir Assoc* (2010) 11(6):397–405. doi: 10.1016/j.jamda.2010.03.007

13. Young S, Narang J, Kumar S, Kwizera E, Malik P, Billings SD, et al. Large Sacral/buttocks ulcerations in the setting of coagulopathy: A case series establishing the skin as a target organ of significant damage and potential morbidity in patients with severe COVID-19. *Int Wound J* (2020) 17(6):2033–7. doi: 10.1111/iwj.13457

14. Rrapi R, Chand S, Lo JA, Gabel CK, Song S, Holcomb Z, et al. The significance of pressure injuries and purpura in COVID-19 patients hospitalized at a large urban academic medical center: A retrospective cohort study. *J Am Acad Dermatol* (2021) 85 (2):462–4. doi: 10.1016/j.jaad.2021.03.051

15. McBride JD, Narang J, Simonds R, Agrawal S, Rodriguez ER, Tan CD, et al. Development of sacral/buttock retiform purpura as an ominous presenting sign of COVID-19 and clinical and histopathologic evolution during severe disease course. *J Cutan Pathol* (2021) 48(9):1166–72. doi: 10.1111/cup.14038

16. Schulte-Schrepping J, Reusch N, Paclik D, Bassler K, Schlickeiser S, Zhang B, et al. Severe COVID-19 is marked by a dysregulated myeloid cell compartment. *Cell* (2020) 182(6):1419–40 e23. doi: 10.1016/j.cell.2020.08.001

17. Bonaventura A, Vecchie A, Dagna L, Martinod K, Dixon DL, Van Tassell BW, et al. Endothelial dysfunction and immunothrombosis as key pathogenic mechanisms in COVID-19. *Nat Rev Immunol* (2021) 21(5):319–29. doi: 10.1038/s41577-021-00536-9

18. Reusch N, De Domenico E, Bonaguro L, Schulte-Schrepping J, Bassler K, Schultze JL, et al. Neutrophils in COVID-19. *Front Immunol* (2021) 12:652470. doi: 10.3389/fimmu.2021.652470

19. Ackermann M, Anders HJ, Bilyy R, Bowlin GL, Daniel C, De Lorenzo R, et al. Patients with COVID-19: in the dark-NETs of neutrophils. *Cell Death Differ* (2021) 28 (11):3125–39. doi: 10.1038/s41418-021-00805-z

20. Vaninov N. In the eye of the COVID-19 cytokine storm. *Nat Rev Immunol* (2020) 20(5):277. doi: 10.1038/s41577-020-0305-6

21. Papayannopoulos V. Neutrophil extracellular traps in immunity and disease. *Nat Rev Immunol* (2018) 18(2):134–47. doi: 10.1038/nri.2017.105

22. Gupta A, Madhavan MV, Sehgal K, Nair N, Mahajan S, Sehrawat TS, et al. Extrapulmonary manifestations of COVID-19. *Nat Med* (2020) 26(7):1017–32. doi: 10.1038/s41591-020-0968-3

23. Wassel CL, Delhougne G, Gayle JA, Dreyfus J, Larson B. Risk of readmissions, mortality, and hospital-acquired conditions across hospital-acquired pressure injury (HAPI) stages in a US national hospital discharge database. *Int Wound J* (2020) 17 (6):1924–34. doi: 10.1111/iwj.13482

24. Terpos E, Ntanasis-Stathopoulos I, Elalamy I, Kastritis E, Sergentanis TN, Politou M, et al. Hematological findings and complications of COVID-19. *Am J Hematol* (2020) 95(7):834–47. doi: 10.1002/ajh.25829

25. Zhan H, Chen H, Liu C, Cheng L, Yan S, Li H, et al. Diagnostic value of d-dimer in COVID-19: A meta-analysis and meta-regression. *Clin Appl Thromb Hemost* (2021) 27:10760296211010976. doi: 10.1177/10760296211010976

26. Parish LC, Lowthian P, Witkowski JA. The decubitus ulcer: many questions but few definitive answers. *Clin Dermatol* (2007) 25(1):101–8. doi: 10.1016/j.clindermatol.2006.09.013

27. Lowthian PT. Trauma and thrombosis in the pathogenesis of pressure ulcers. *Clin Dermatol* (2005) 23(1):116–23. doi: 10.1016/j.clindermatol.2004.10.001

28. Witkowski JA, Parish LC. Histopathology of the decubitus ulcer. *J Am Acad Dermatol* (1982) 6(6):1014–21. doi: 10.1016/S0190-9622(82)70085-4

29. Salcido R, Donofrio JC, Fisher SB, LeGrand EK, Dickey K, Carney JM, et al. Histopathology of pressure ulcers as a result of sequential computer-controlled pressure sessions in a fuzzy rat model. *Adv Wound Care* (1994) 7(5):23–4,26,28 passim.

30. Vande Berg JS, Rudolph R. Pressure (decubitus) ulcer: variation in histopathology–a light and electron microscope study. *Hum Pathol* (1995) 26 (2):195–200. doi: 10.1016/0046-8177(95)90037-3

31. Kitagawa HS A, Nakatani T, Sugama J, Konya C, Okuwa M, Nagakawa T. Histological examination of pressure ulcer tissue in terminally ill cancer patients. *Japan J Nurs Sci* (2004) 1:35–46. doi: 10.1111/j.1742-7924.2004.00008.x

32. Yang Y, Shen C, Li J, Yuan J, Wei J, Huang F, et al. Plasma IP-10 and MCP-3 levels are highly associated with disease severity and predict the progression of COVID-19. *J Allergy Clin Immunol* (2020) 146(1):119–27 e4. doi: 10.1016/j.jaci.2020.04.027

33. Chen Y, Wang J, Liu C, Su L, Zhang D, Fan J, et al. IP-10 and MCP-1 as biomarkers associated with disease severity of COVID-19. *Mol Med* (2020) 26(1):97. doi: 10.1186/s10020-020-00230-x

34. Lev S, Gottesman T, Sahaf Levin G, Lederfein D, Berkov E, Diker D, et al. Observational cohort study of IP-10's potential as a biomarker to aid in inflammation regulation within a clinical decision support protocol for patients with severe COVID-19. *PloS One* (2021) 16(1):e0245296. doi: 10.1371/journal.pone.0245296

35. Angioni R, Sanchez-Rodriguez R, Munari F, Bertoldi N, Arcidiacono D, Cavinato S, et al. Age-severity matched cytokine profiling reveals specific signatures in covid-19 patients. *Cell Death Dis* (2020) 11(11):957. doi: 10.1038/s41419-020-03151-z

36. Tamayo-Velasco A, Martinez-Paz P, Penarrubia-Ponce MJ, de la Fuente I, Perez-Gonzalez S, Fernandez I, et al. HGF, IL-1alpha, and IL-27 are robust biomarkers in early severity stratification of COVID-19 patients. *J Clin Med* (2021) 10(9):2017. doi: 10.3390/jcm10092017

37. Kleymenov DA, Bykonia EN, Popova LI, Mazunina EP, Gushchin VA, Kolobukhina LV, et al. A deep look into COVID-19 severity through dynamic changes in blood cytokine levels. *Front Immunol* (2021) 12:771609. doi: 10.3389/fimmu.2021.771609

38. Aboudounya MM, Heads RJ. COVID-19 and toll-like receptor 4 (TLR4): SARS-CoV-2 may bind and activate TLR4 to increase ACE2 expression, facilitating entry and causing hyperinflammation. *Med Inflamm* (2021) 2021:8874339. doi: 10.1155/2021/8874339

39. Zhao Y, Kuang M, Li J, Zhu L, Jia Z, Guo X, et al. SARS-CoV-2 spike protein interacts with and activates TLR41. *Cell Res* (2021) 31(7):818–20. doi: 10.1038/s41422-021-00495-9

40. Meizlish ML, Pine AB, Bishai JD, Goshua G, Nadelmann ER, Simonov M, et al. A neutrophil activation signature predicts critical illness and mortality in COVID-19. *Blood Adv* (2021) 5(5):1164–77. doi: 10.1182/bloodadvances.2020003568

41. Szturmowicz M, Demkow U. Neutrophil extracellular traps (NETs) in severe SARS-CoV-2 lung disease. *Int J Mol Sci* (2021) 22(16):8854. doi: 10.3390/ijms22168854

42. Wang TT, Zhao YL, Peng LS, Chen N, Chen W, Lv YP, et al. Tumour-activated neutrophils in gastric cancer foster immune suppression and disease progression through GM-CSF-PD-L1 pathway. *Gut* (2017) 66(11):1900–11. doi: 10.1136/gutjnl-2016-313075

43. Bowers NL, Helton ES, Huijbregts RP, Goepfert PA, Heath SL, Hel Z. Immune suppression by neutrophils in HIV-1 infection: role of PD-L1/PD-1 pathway. *PloS Pathog* (2014) 10(3):e1003993. doi: 10.1371/journal.ppat.1003993

44. Zuo Y, Yalavarthi S, Shi H, Gockman K, Zuo M, Madison JA, et al. Neutrophil extracellular traps in COVID-19. *JCI Insight* (2020) 5(11):e138999. doi: 10.1172/jci.insight.138999

45. Yancy CW. COVID-19 and African americans. *JAMA* (2020) 323(19):1891–2. doi: 10.1001/jama.2020.6548

46. Mackey K, Ayers CK, Kondo KK, Saha S, Advani SM, Young S, et al. Racial and ethnic disparities in COVID-19-Related infections, hospitalizations, and deaths : A systematic review. *Ann Intern Med* (2021) 174(3):362–73. doi: 10.7326/M20-6306

47. Braden BJ. The braden scale for predicting pressure sore risk: reflections after 25 years. *Adv Skin Wound Care* (2012) 25(2):61. doi: 10.1097/01.ASW.0000411403.11392.10

48. Moore ZE, Patton D. Risk assessment tools for the prevention of pressure ulcers. *Cochrane Database Syst Rev* (2019) 1:CD006471. doi: 10.1002/14651858.CD006471.pub4

49. Zaratkiewicz S, Whitney JD, Lowe JR, Taylor S, O'Donnell F, Minton-Foltz P. Development and implementation of a hospital-acquired pressure ulcer incidence tracking system and algorithm. *J Healthc Qual* (2010) 32(6):44–51. doi: 10.1111/j.1945-1474.2010.00076.x

Frontiers in Immunology

Explores novel approaches and diagnoses to treat immune disorders.

The official journal of the International Union of Immunological Societies (IUIS) and the most cited in its field, leading the way for research across basic, translational and clinical immunology.

Discover the latest Research Topics

See more →

Frontiers

Avenue du Tribunal-Fédéral 34
1005 Lausanne, Switzerland
frontiersin.org

Contact us

+41 (0)21 510 17 00
frontiersin.org/about/contact